Mala Sibal

Ultrasound in Gynecology

An Atlas and Guide

Springer

Mala Sibal

Ultrasound in Gynecology

An Atlas and Guide

Springer

Mala Sibal
Department of Fetal Medicine and Obstetric & Gynecological Ultrasound
Manipal Hospital
Bangalore
Karnataka
India

ISBN 978-981-10-2713-0 ISBN 978-981-10-2714-7 (eBook)
DOI 10.1007/978-981-10-2714-7

Library of Congress Control Number: 2017930417

Printed on acid-free paper

This Springer imprint is published by Springer Nature
The registered company is Springer Nature Singapore Pte Ltd.
The registered company address is 152 Beach Road, #21-01/04 Gateway East, Singapore 189721, Singapore

This book is dedicated to my patients, in whose service I learnt medicine, and to my husband, Abbas Shad, for his unstinting love and support.

Foreword by Suresh Seshadri

It is indeed a pleasure to pen a few words about this book, which is a felt need in the field of gynecological ultrasound. This book is the culmination of decades of the author's experience and a strong commitment to share the knowledge to the fraternity. The chapters have been well thought out and give several practice points which can be easily adapted to improve quality of imaging and reporting. The initial chapters of the book describe not only the basic techniques in imaging but also advanced techniques like 3D and other innovative methods like gel sonovaginography. Each chapter has been structured in a simple, comprehendible fashion. The flow of information has been well thought out which not only makes for easy reading but also for easy recall. The illustrations are of high quality from the author's own body of work. The summary boxes at the end of each chapter give the key points in a nutshell, which are a 'must know'.

When any book is written, the one important question that comes to the mind is 'who is this book meant for?' I remember asking the author the same question when she embarked on this journey. Her answer was 'to everyone who wants to know about gynecological ultrasound!' I'm very happy to note that this book has fulfilled her desire as it is written in a way that will be useful for students, clinicians and imaging specialists alike. This indeed is one of the best books written on the subject with an international appeal and a 'must possess' for any practitioner.

Mediscan Systems
Chennai, India

Suresh Seshadri
07.07.2016

Foreword by Lil Valentin

It is a great privilege for me to have been given the possibility to read this book on gynecological ultrasound written by Mala Sibal. It is a book that fulfils the needs of those practicing gynecological ultrasound and wanting to improve their skills, as well as the needs of those planning to practice gynecological ultrasound and wishing to learn how to do it and how to interpret the images.

This book is full of tips and tricks that help improve visualisation of both simple and complex structures. It presents clinically important facts about each type of pathology, and facts are presented in a concise and structured manner – the structure being the same in all chapters. No information is redundant. The structured and concise format makes this book very easy to read and to digest. Last, but not least, there are hundreds of beautiful and instructive ultrasound images illustrating the typical ultrasound features of each type of pathology. Images are essential, because one image tells us more than 1000 words.

Lund University
Lund, Sweden

Lil Valentin
02.10.2016

Preface

In recent years, gynecological ultrasound has seen rapid advances in new investigative techniques, primarily owing to improved ultrasound technology, imaging equipment and expanding research in the field. There is a need to provide a practical guide and comprehensive atlas that covers new-found knowledge and novel diagnostic techniques to update and supplement the limited literature that is currently available. The literature in this field is limited partly because gynecological ultrasound has historically been in the shadow of obstetric and fetal ultrasound. There is often a lack of focused effort to follow-up on gynecological cases to validate diagnoses through either surgery or histopathology, due to which definitive developments have not been rapid enough and quality literature relatively sparse. Further, since a typical medical residency provides precious little exposure in the use of ultrasound to diagnose gynecological pathologies, it is not uncommon for clinicians and radiologists to lack an in-depth knowledge of gynecological ultrasound.

This book is intended to fill these gaps. It is a comprehensive atlas and guidebook which is accompanied by abundant illustrations of classical and new ultrasound features and gynecological pathologies. The text and images contained in this book are primarily based on my work as an instructor, researcher and practitioner, having personally performed detailed scans and thorough investigations in numerous complex gynecological cases over my career, some of which have resulted in novel biomarkers for early detection of pathologies which I have reported in research journals and have included in this book.

This atlas and guide has been written to cater to practicing sonologists, gynaecologists and radiologists and those who are training to become practitioners in these fields, as well as postgraduate medical students in these fields. It will be useful not only for the routine diagnosis of gynecological pathologies but also in cases of emergencies like ovarian torsion, where a delay in diagnosis can cause infarction and loss of the ovaries, or where a wrong diagnosis can lead to unnecessary surgery with added risks and cost. It will also help practitioners differentiate between multiple conditions that are often lumped together as a single diagnosis, like the commonly used ambiguous term ‘complex adnexal cyst’, which provides no information on whether the cyst may be physiological, malignant or benign. Specificity is the key to an effective diagnosis, determination of specialists who need to be consulted, surgeries that may need to be performed and, more generally, proper disease management. This is particularly relevant in today’s world where medical litigations are on the rise.

A frustrating challenge in gynecological ultrasound has been the lack of a global consensus in the use and meaning of terminologies employed in the field. Of late, the International

Endometrial Tumor Analysis (IETA), Morphological Uterus Sonographic Assessment (MUSA) and International Ovarian Tumour Analysis (IOTA) groups have arrived at a consensus to describe various sonographic features and gynecological pathologies. I am a primary researcher of the ongoing IOTA study, and this book uses and provides an explanation of these terminologies, thereby encouraging the reader to use standard terms for evaluation and reporting.

This book has been organised into chapters, based on the origin of pathologies in various gynecological organs and structures of the female pelvis, with a summary of key points in each chapter for quick reference. The chapters include drawings and a rich set of comprehensive single and composite images to illustrate key concepts and pinpoint various features and pathologies. In addition to basic greyscale images of two-dimensional scans, there are also relevant images of Doppler and three-dimensional ultrasound scans.

I sincerely hope the reader uses this book as an essential guide, lucid atlas and a reliable reference for accurate diagnosis and research of gynecological pathologies, and in turn helps further this important and fascinating field.

Bangalore, India Mala Sibal

Acknowledgements

The compiling of knowledge, examination of cases and follow-up over the years that led to this book have been due to the support and help of many colleagues, friends and family members.

The first among them is Dr. Priti Venkatesh who is my senior, friend, mentor and the head of our department at Manipal Hospital. It was by observing her scans that I developed an enduring fascination for the field of gynecological ultrasound. I shall remain indebted to her for the support she provided me, especially during my initial years, when literature in this field was sparse. I am also grateful to Dr. Jaya Bhat, the head of the Obstetrics and Gynecology Department when I first began, who encouraged me to focus on ultrasound and supported my work. In addition I would like to acknowledge the support I have received from my colleague Dr. Thankam Rathinaswami for her critical review of my research and academic work over the years.

I would also like to thank Manipal Hospital, a large multi-speciality hospital in Bangalore, where I have the opportunity to investigate a variety of cases and also gain access to information from follow-up visits of patients, which has helped my learning process tremendously.

I would like to thank my referring clinicians who keep me posted and provide an excellent feedback and follow-up of cases evaluated using ultrasound. I would like to especially thank Dr. Gayathri Karthik who has supported my professional endeavours with great interest.

I also thank the pathologists of our hospital with whom I interact on the pathology of complex cases. A special thanks to Dr. Mahesha Vankalakunti who helped with the pathological correlation of the 'follicular ring sign', a new ultrasound feature for early diagnosis of ovarian torsion, which is included in this book.

I would like to thank the staff and nurses of our department as well, who support not only my clinical work but also help with the follow-up of cases.

I also thank the postgraduates of the Obstetrics and Gynecology Department at Manipal Hospital who assisted me through the process of writing this book. These include Dr. Supriya Preman, Dr. Bharti Singh, Dr. Vasumathi Pasupaleti and Dr. Spurthi Janney.

A special word of thanks goes out to Padmini Baruah, a bright young law school graduate, who played a significant role in helping me write and proofread various parts of this book. I am also thankful to Shibani Timothy and Nomita Singh for helping me with the final proof-reading of this book.

I would also like to specially thank Dr. Rajesh Uppal, a distinguished radiologist, who critically evaluated and proofread the chapters.

I also thank Dr. Suresh Seshadri for encouraging me to write this book and for authoring the foreword. I would also like to thank Springer for their effort and support in the publication of this book.

Finally, I would like to thank my family. A special thanks to my parents Pushpa Sibal and Anil Sibal, for their support and for the interest in science that they inculcated in their children. I also wish to thank my aunt Shashi Sibal, an amazing teacher, who taught me biology and got me interested in pursuing medicine. A big thanks to my brother, Dr. Sandeep Sibal, for stepping in at various points to help solve challenges I faced during the writing of this book. Lastly, I would like to thank my children Sohail Shad and Sonia Shad for completing my life, helping me structure chapters and encouraging me to write this book.

Contents

List of Abbreviations

2D	Two-dimensional
3D	Three-dimensional
AF	Anteflexed
AFC	Antral follicle count
AV	Anteverted
AVC	Automated volume calculation
AVM	Arteriovenous Malformation
B hCG	Beta human chorionic gonadotropin
BMI	Body mass index
CL	Corpus luteum
CS	Caesarean section
CSD	Caesarean scar defect
CT	Chemotherapy
D&C	Dilation and curettage
DIE	Deep infiltrating endometriosis
EMJ	Endomyometrial junction
EP	Early pregnancy
ESHRE	European Society of Human Reproduction and Embryology
ET	Endometrial thickness
ETT	Epithelioid Trophoblastic Tumour
F	French
FHR	Fetal heart rate
FI	Flow index
FIGO	International Federation of Gynecology and Obstetrics
FP	Fetal pole
FSH	Follicle-stimulating hormone
GS	Gestational sac
GSV	Gel sonovaginography
GTD	Gestational trophoblastic disease
GTN	Gestational trophoblastic neoplasia
hCG	Human chorionic gonadotropin
HD flow	High-definition flow
HDI	High-definition imaging
HPE	Histopathological examination
IDEA	International Deep Endometriosis Analysis
IETA	International Endometrial Tumor Analysis
IMB	Intermenstrual bleeding
IOTA	International Ovarian Tumour Analysis
IU	International units
IUCD	Intrauterine contraceptive device

IVF	In vitro fertilisation
JZ	Junctional zone
LH	Luteinising hormone
LIF	Left iliac fossa
LS	Longitudinal section
LSCS	Lower segment caesarean section
LUF	Luteinised unruptured follicle
ML	Midline
MP	Mid-positioned
MRI	Magnetic resonance imaging
MRP	Manual removal of placenta
MTP	Medical termination of pregnancy
MUSA	Morphological Uterus Sonographic Assessment
NSAID	Non-steroidal anti-inflammatory drug
OHSS	Ovarian hyperstimulation syndrome
PCB	Post-coital bleeding
PCO	Polycystic ovaries
PCOD	Polycystic ovarian disease
PI	Pulsatility index
PID	Pelvic inflammatory disease
PO	Paraovarian
POD	Pouch of Douglas
PPH	Post-partum haemorrhage
PRF	Pulse repetition frequency
PS	Per speculum
PSTT	Placental site trophoblastic tumour
PSV	Peak systolic velocity
PUL	Pregnancy of unknown location
PV	Per vagina
RF	Retroflexed
RI	Resistance index
RIF	Right iliac fossa
ROI	Region of interest
RPOC	Retained products of conception
RT	Radiotherapy
RV	Retroverted
SHG	Sonohysterogram
SIS	Saline infusion sonohysterogram
SLT	Single-layer thickness
TAH	Total abdominal hysterectomy
TAS	Transabdominal scan
TO	Tubo-ovarian
TOP	Termination of pregnancy
TS	Transverse section
TSH	Thyroid-stimulating hormone
TUI	Tomographic ultrasound imaging
TVS	Transvaginal scan
UPT	Urinary pregnancy test
UPT	Urine pregnancy test
USG	Ultrasonography
UV	Uterovesical
VFI	Vascularisation flow index
VI	Vascularisation index
VOCAL	Virtual organ computer-aided analysis
YS	Yolk sac

About the Author

Dr. Mala Sibal is a consultant physician in the Department of Fetal Medicine and Obstetric and Gynecological Ultrasound at Manipal Hospital, Bangalore. She has fourteen years of experience in the field of gynecological ultrasound prior to which she practiced clinical obstetrics and gynecology for 7 years.

Dr. Sibal has been an invited speaker at numerous national and international conferences on this subject and has authored peer-reviewed journal articles on novel diagnostic ultrasound techniques in the American *Journal of Ultrasound in Medicine*. She has also trained and taught several practitioners and medical students in the field of gynecological ultrasound. Dr. Sibal is also a principal investigator in the ongoing International Ovarian Tumour Analysis (IOTA-5) International Research Programme. She has also begun an online portal, 'Gynecology Academy' (www.gynac.org), for training and skill enhancement in gynecological ultrasound.

She has a DNB postgraduate degree in obstetrics and gynecology and an MBBS graduate degree from Jawaharlal Nehru Medical College, Belgaum, where she stood first in gynecology.

Introduction

1

Before the advent of ultrasound, diagnosis in gynecology was difficult and inaccurate, since it had to be made with the use of bimanual vaginal examination, wherein one would physically feel various pelvic structures and make an attempt to diagnose the pathology. Ultrasound, specifically transabdominal ultrasound (TAS), revolutionised gynecology and for the first time allowed the clinical practitioner to visualise the structures in the pelvis in addition to feeling them bimanually. Today, with the advent of transvaginal ultrasound (TVS), we can not only see the pathology at close range with better resolution, but also simultaneously touch the various structures with the probe and identify whether they are tender, fixed, etc. This interactive component of TVS has further increased the accuracy of diagnosis, giving it in many cases an edge over CT or MRI. Ultrasound for evaluation is also easily available and more affordable. Since TVS accesses many of the pelvic structures at closer range, it also enhances tissue resolution and Doppler evaluation. The addition of Doppler to ultrasound examination, and in particular 'Power Doppler' that studies low-velocity flows, helps visualise the presence of flow within tissues and vascular patterns that further enhances the accuracy of diagnosis and also helps in differentiating between pathologies. Images generated by using all these three techniques have been extensively used in the chapters that follow.

In addition to 2D ultrasound (TAS and TVS) and Doppler, 3D ultrasound is also a useful adjunct and is indispensable in the diagnosis of certain conditions like uterine anomalies or the location of intrauterine contraceptive devices (IUCDs). 3D ultrasound has also contributed to accurate volume estimations, as well as reproducibility and storage of data, which is important in the research and study of pathologies. There has also been further progress in ultrasound diagnosis with sonohysterogram (SHG) and gel sonovaginography (GSV), which is resorted to in special cases. All of the above techniques of gynecological ultrasound have been described and employed to identify features and gynecological pathologies in the chapters ahead, and accordingly, images generated using these techniques can be found across various chapters of this book.

There are13 chapters that follow. Chapter 2 is based on basic methods of 2D, 3D and Doppler ultrasound along with newer available techniques in ultrasound examination, applicable to all pathologies. It also includes a few 'tips and tricks' that can make a significant difference in gynecological ultrasound diagnosis. The bulk of the remaining chapters (Chaps. 3, 4, 5, 6, 7, 8, 9, 10, 11 and 12) describe features and pathologies that are categorised by the various gynecological organs and structures in the female pelvis where these pathologies originate. Some topics that are better dealt with individually or require special focus have been discussed separately as well. Chapter 13 has a mix of miscellaneous topics of interest that don't fit in too well into the themes of other chapters but are nonetheless important in practice. Chapter 14 explores pathologies based on four common clinical situations: abnormal uterine bleeding, pelvic/adnexal masses, acute pelvic pain and scans to locate the pregnancy – including pregnancies of unknown location (PUL).

In most of the chapters, the first subsection typically discusses how to evaluate and report on the region of interest using ultrasound. These are based primarily on the consensus statement of the International Ovarian Tumour Analysis (IOTA), International Endometrial Tumor Analysis (IETA) and Morphological Uterus Sonographic Assessment (MUSA) groups. This subsection is usually followed by normal findings in that region, including variations with age and variations across phases of the menstrual cycle. This is followed by subsections of the chapter that are devoted to various pathologies. Each of the pathologies has some basic information on the pathology, along with the classification and clinical presentations mentioned briefly upfront. This is followed by ultrasound features that are captured in succinct itemised points. This, in turn, is followed by a large number of images – many of which are

M. Sibal, *Ultrasound in Gynecology*, DOI 10.1007/978-981-10-2714-7_1

composite images of a single case showing various aspects of ultrasound imaging that aid in the diagnosis. These figures have legends below that highlight the ultrasound findings and, in some cases, additional clinical information of the patient that is relevant.

All the images shown in the chapters are of patients that the author has personally scanned using multiple ultrasound techniques that were curated over a period of 14 years. Further, most of the patients have been followed up clinically, with operation notes, discharge summaries and histopathology reports. This is particularly important so that the reader sees ultrasound images of cases with confirmed pathologies, as opposed to images where the diagnosis of the pathology has been presumed but not confirmed.

General Techniques in Gynecological Ultrasound

2

Today, with ultrasound, we can actually see pathology, and with a transvaginal ultrasound (TVS), one can not only see the pathology at close range, but also simultaneously touch the various structures that are seen, making it a dynamic and interactive examination (Fig. 2.1). This is a distinct advantage of TVS over CT and MRI. Presently, ultrasound technology has advanced to such an extent that one can see on ultrasound almost as much as a pathologist can see on gross examination of a specimen (both the external surface and cut sections). Not only that, one can in addition see flow patterns within the mass which cannot be ascertained by gross examination of the specimen.

Ideally a transabdominal scan (TAS) is done first with a full bladder, followed by a transvaginal scan (TVS) after having emptied the bladder. It is important that the technique is standardised, fixed and predetermined.

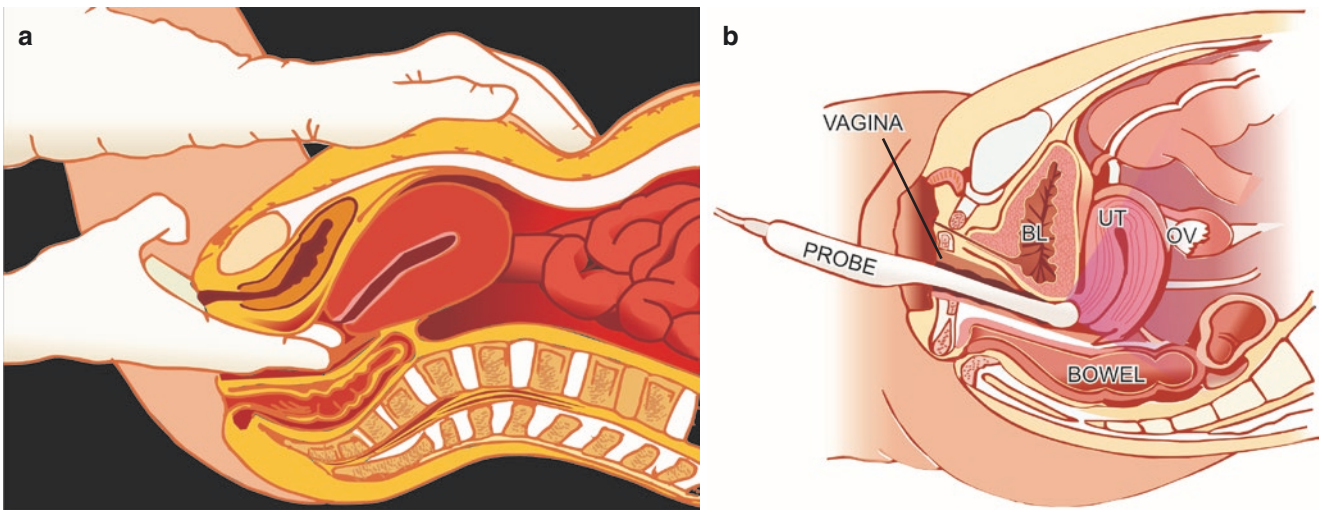

Fig. 2.1 (**a**) Bimanual per vaginal examination which uses touch sensation to assess pathology of pelvic structures; (**b**) with TVS, which allows one to see pathology while touching the various structures simultaneously

M. Sibal, *Ultrasound in Gynecology*, DOI 10.1007/978-981-10-2714-7_2

2.1 Transabdominal Scan

Filling the Bladder

For a good transabdominal scan, the bladder should be sufficiently filled, so as to push the bowels that lie in front of the pelvic organs towards the upper abdomen. Another advantage of a full bladder is that urine, being fluid, enhances the sound waves of the ultrasound beam, resulting in better visualisation. The bladder should not be over-distended because that would cause discomfort to the patient. In addition, a very full bladder increases the distance of the uterus and ovaries from the probe, decreasing resolution and resulting in suboptimal visualisation. A few points to be kept in mind here are:

1. Very often one may be able to see sufficiently well on TAS even with a suboptimally filled bladder. Especially in cases that are to be followed by TVS, there is no need to insist that the bladder should be further filled.
2. In emergency cases (like a case of a ruptured ectopic pregnancy), waiting for the bladder to fill may not be justified.
3. In cases with a previous caesarean, the bladder may be adherent to the uterus at the site of the LSCS scar, and filling the bladder so as to visualise the upper uterus may not be possible. Instead, the more the patient fills her bladder, the more the lower uterine body and cervix get stretched, causing discomfort.
4. With a very large and bulky uterus, a full bladder may not be able to overlie the entire uterus. Very often in these cases, the bulky uterus itself pushes the intestines out of the pelvis into the upper abdomen.

Scanning Technique for TAS (Figs. 2.2 and 2.3)

For a transabdominal scan, typically a 3.5–5 MHz transducer is used. The transducer is placed longitudinally on the patient's abdomen in the midline. It has a groove on one side and it is placed such that this groove lies facing the superior end of the patient. This produces a sagittal section of the uterus, and the area corresponding to the groove is highlighted on the screen by a 'GE' mark which is green on the active screen and white on the adjacent frozen image. This corresponds to the upper end of the uterine body. That is, basically, structures that are in the superior part of the patient's body are seen on the right of the screen, and structures in the inferior part are seen on the left of the screen.

After studying the LS, the probe is rotated in an anticlockwise direction, such that the groove now lies on the right of the patient. The area corresponding to the groove is highlighted by the 'GE' mark and is seen on the right side of the screen. Thus, structures on the right side of the patient are seen on the right side of the screen, and those on the left side of the patient are seen on the left side of the screen.

Ovaries and Adnexa

To visualise the ovaries and adnexa, one can move and/or angulate the probe to one side. Regardless of whether one is examining structures on the left or the right, the rotation from LS to TS is always anticlockwise.

Advantages of a Transabdominal Scan

- TAS provides a panoramic view and thus furnishes a global survey of pelvic anatomy. One is, therefore, less likely to miss any small pathology (like an ectopic pregnancy mass or a pedicle of a torsed ovary), and while doing TVS, one would know exactly where to look in order to study the pathology.
- Large masses extending into the upper abdomen are better assessed on TAS and may be missed with TVS alone, as those structures lie too far away from the transvaginal probe (e.g. a subserous or pedunculated fundal fibroid).
- The endometrium of mid-positioned uterus is better seen on TAS than TVS. Endometrial polyps can thus be missed on a TVS in a patient with a mid-positioned uterus.
- Masses like fibroids in the lower corpus or cervix can cause shadowing resulting in suboptimal visualisation of structures above it, like other fibroids, ovaries, etc. on TVS. In such cases, the structures lying above are best seen on TAS.
- In dermoids (particularly large ones) one may not be able to see its superior parts and margins due to shadowing on TVS. Measuring such dermoids is easier on TAS (Fig. 2.4).
- TAS in most cases is not time consuming.
- Sometimes TAS is the only method to scan a patient who declines a TVS (as is sometimes the case with virgins/unmarried patients). Transrectal scan is another option, provided the patient consents and facilities are available for the same.

Most sonologists measure the uterus and take a cursory look at the rest of the pelvis prior to a TVS. The author, however, prefers to measure the uterus and endometrium and also to study the endometrium qualitatively as in many cases the endometrium of a mid-positioned uterus is not clearly seen on TVS. In addition, large masses extending beyond the pelvis and fibroids high up in the uterine body can be studied in greater detail on TAS. Furthermore, in cases with uterine anomalies, it is preferable to execute the 3D rendering of the uterus on TAS as well, prior to carrying out a TVS. This is recommended because with a full bladder, the uterus is most often stretched, more linear and perpendicular to the probe, which makes 3D rendering of the uterus simpler to obtain and assess.

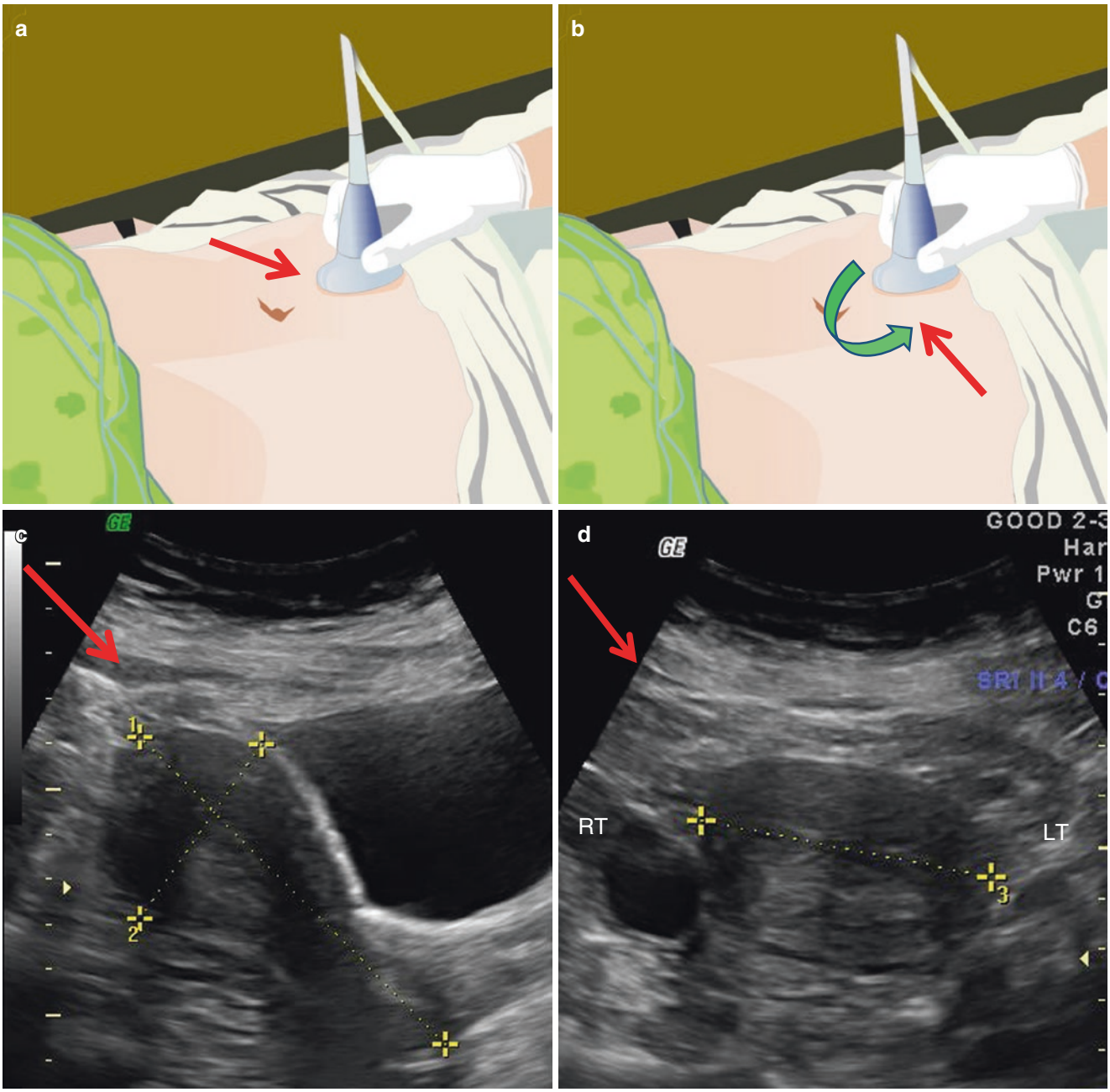

Fig. 2.2 TAS for uterus. (**a**) Placement of probe for LS scan. *Arrow* indicative of marker on the probe. (**b**) Placement of probe for TS scan (after 90° anticlockwise rotation). *Arrow* indicative of the marker on the probe, now to the right of the patient. (**c**) Midsagittal section of uterus. *Arrow*, showing upper end of the uterus, corresponds to the marker on the probe in the image (a). (**d**) TS of uterus – *arrow*, showing right side of the uterus, corresponds to the marker on the probe in the image (b). Structures on the right side of the patient are seen on the right side of the screen and, similarly, those on the left side of the patient are observed on the left of the screen

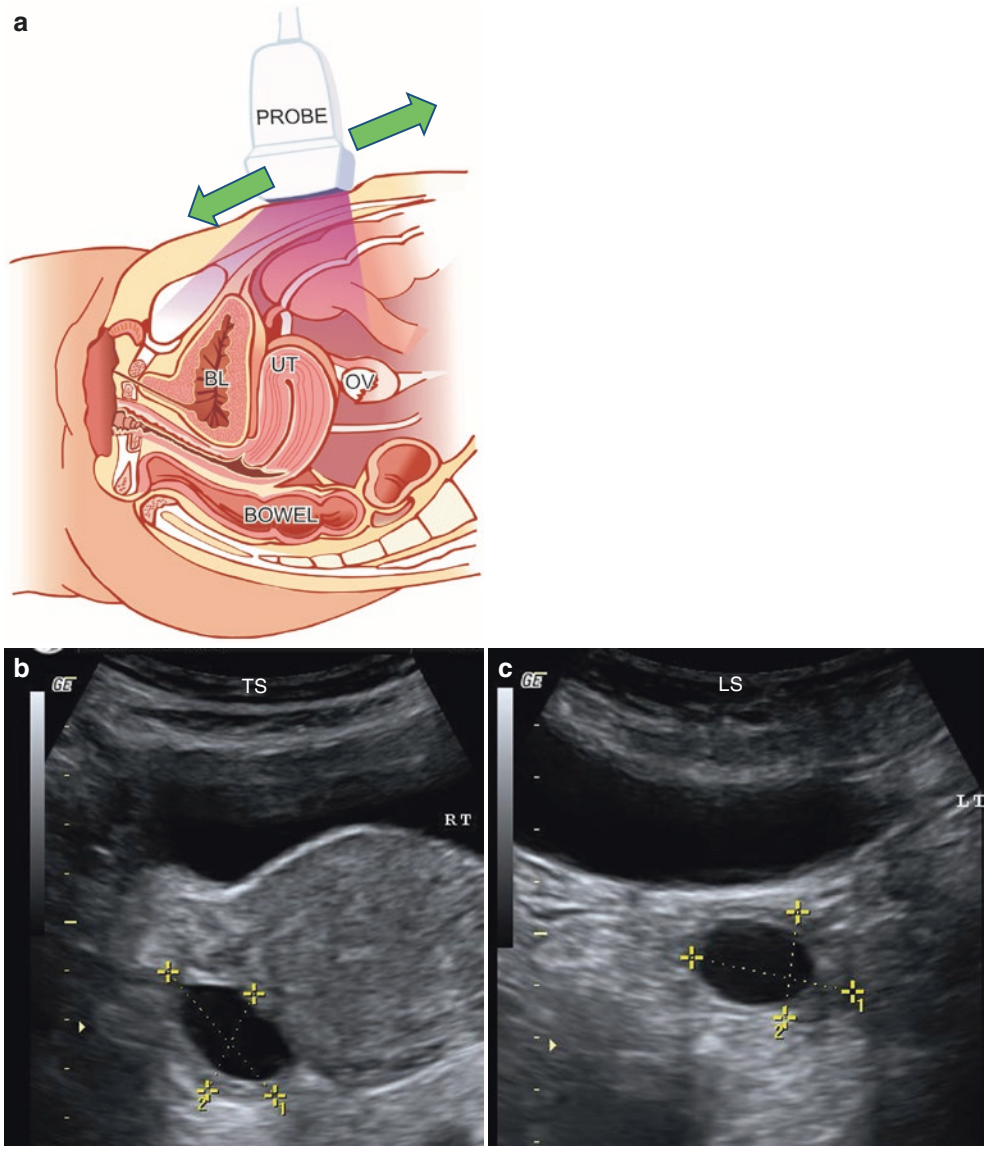

Fig. 2.3 TAS for examining the adnexa. (**a**) The probe can be placed on either side of the midline and the rotation should be anticlockwise from LS to TS. (**b**, **c**) Right ovary seen in TS and LS

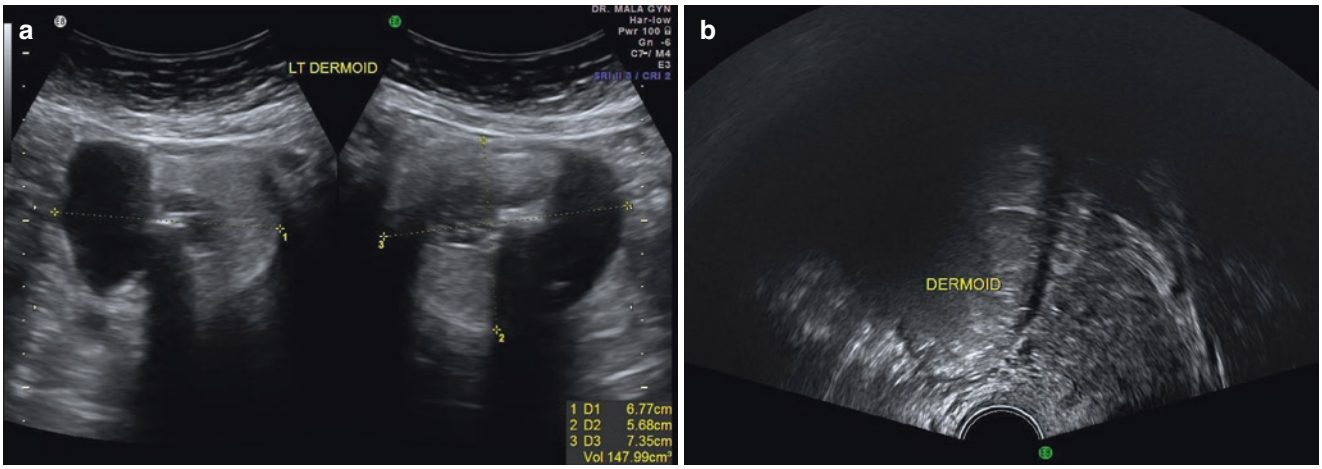

Fig. 2.4 Case with a large dermoid. (**a**) TAS – the entire dermoid seen. (**b**) TVS – Dermoid was not seen. Due to significant acoustic shadowing by the dermoid, only its lower end which resembles the bowel is seen, making it difficult to visualise the dermoid

2.2 Transvaginal Scan

The patient's bladder should be empty for a TVS.

Scanning Technique for TVS (Figs. 2.5, 2.6 and 2.7)
For a transvaginal scan, typically a 5–9 MHz transducer is used.

The ideal position in such cases is the lithotomy position. This facilitates downward movement of the hand with the probe, so that structures placed anteriorly in the pelvis are clearly seen.

The probe is always covered with a probe cover, with jelly between the two. Air bubbles should be avoided. Jelly is applied to the tip of the probe and then the probe is gently introduced into the vagina.

The transducer has a groove which should face upwards (anterior part of patient's abdomen) at insertion. This produces a sagittal section of the uterus, and the area corresponding to the groove is highlighted by a 'GE' mark on the screen. This corresponds to the anterior part of the uterine body at the UV fold.

The probe is angulated and rotated a little so as to obtain the midsagittal (LS) section of the uterus.

There are two commonly used methods of observing the image on the screen (Fig. 2.5b, c). The first with the TVS probe footprint below is generally considered ideal because of two reasons:

- The image orientation is more natural, with superior structures seen in the upper part of the screen and inferior structures in the lower part. In the alternative method, structures higher up are seen lower down on the screen and vice versa.
- There is a clear-cut difference in images that are TAS versus TVS because in the former, the footprint lies above and in the latter the footprint of the probe lies below.

In this book, the images will be seen in the orientation that is considered ideal (that is with the footprint below), as the author has been following that orientation over the years. It is now suggested that students and those learning gynecological ultrasound for the first time should follow the ideal orientation with the footprint at the lower end of the screen. Standardisation of orientation on screen is important. It does not really matter how one is used to observing the image on the screen, provided it is consistently done in the same manner.

The following methodology is one with the footprint of the probe lying in the lower part of the screen, which is considered ideal.

Uterus
To obtain TS of the uterus after LS, on TVS, rotation is done in a clockwise direction. The groove which lay anteriorly now lies on the patient's left. This produces a transverse section (TS) of the uterus, and the area corresponding to the groove is highlighted by a 'GE' mark on the screen. This corresponds to the left side of the uterine body. Structures on the left of the patient are seen on the left of the screen and, similarly, those on the right are seen on the right of the screen.

Ovaries and Adnexa
To assess the ovaries and adnexa on either side of the uterus, one can either angulate the probe from the LS section of the uterus to obtain the LS of any adnexa/ovary, or, as is more frequently done, the probe can be angulated from the TS of the uterus to obtain the TS of any adnexa/ovary. On TS, the ovaries are typically seen lying just medial to the external iliac vessels.

Rotation from LS to TS is to be done in a clockwise direction. It is imperative to keep in mind that rotation from LS to TS must always be standardised, regardless of which structure or which side is being studied.

A transvaginal probe offers a combination of touch along with simultaneous visualisation of pelvic structures, making TVS dynamic and interactive. TVS should include the following:

- Measurement and morphological evaluation of the myometrium, endometrium and ovary (including adnexa) for normal and pathological conditions. The evaluation of the uterus (myometrium and endometrium) is discussed in Chaps. 3 and 4. The ovary and adnexal masses are evaluated as given in Chap. 7.
- Assessment of the cervix and vagina has been discussed in Chaps. 5 and 6. These structures are often not given attention during an ultrasound examination because pathologies of these structures are infrequent and visualising them is often challenging. Currently, ultrasound machines provide better resolution, and there is increasing literature available on cervical and vaginal pathologies. This has facilitated diagnosis of vaginal and cervical pathology on ultrasound, and their examination is now considered an integral part of routine pelvic examination.
- Assessment of uterine version and flexion – which may serve as a marker to pathology and a guide for possible intrauterine procedures (details provided later in this chapter).
- Looking for fixity of ovaries by applying pressure with the probe. By doing this, one can assess whether the ovaries are adherent to the uterus and/or the pelvic walls.
- Assessing the fixity of the uterus. In cases where the uterus is adherent posteriorly, a typical 'ear'- or 'question mark'-shaped uterus is often noted (details in Chap. 8).
- Looking for any tenderness, and if present, that should serve as a guide for a detailed search in that area for any

pathology. This 'pain-guided approach' is useful in diagnosing conditions like DIE and ectopic pregnancy. In patients presenting with pain, TVS is useful in assessing whether the pathology being observed is the cause for pain. The tender organ will elicit the same pain that the patient complains of.

- Assessing whether the bowels are adherent to the posterior wall of the uterus. Normally the large bowel (rectosigmoid), on applying pressure on the cervix and uterus with the probe, is seen to slide smoothly over the posterior cervix and vagina ('low sliding sign') and the uterine body and fundus ('high sliding sign'). The absence of sliding sign indicates that the bowels are adherent to the posterior wall of the uterus and raises a high suspicion of bowel DIE.
- Ideally, specific search for DIE nodules (described in Chap. 8) should also be done. This is particularly so in women with pain, endometriomas or any tenderness. The bladder wall and mucosa should also be examined for possible DIE. Since visualisation of bladder DIE requires a partially filled bladder, it is best done towards the end of the TVS evaluation.

Advantages of Transvaginal Scan

- Because of the close proximity of the various structures to the probe, a higher frequency probe is used for TVS, which provides a close-up view of pelvic structures with high resolution. Thus:
  1. Small lesions not seen on TAS may be observed on TVS (e.g. small endometriotic cysts).
  2. There is better characterisation of pathology (e.g. fibroid or adenomyoma).
  3. Doppler studies are also better because of proximity of structures to probe.
- The transvaginal probe offers a superb combination of *visualisation of pelvic structures with a simultaneous possibility of touching them*. This is analogous to performing an internal physical pelvic examination and simultaneously seeing the structures. This helps us identify which structures are tender or adherent.

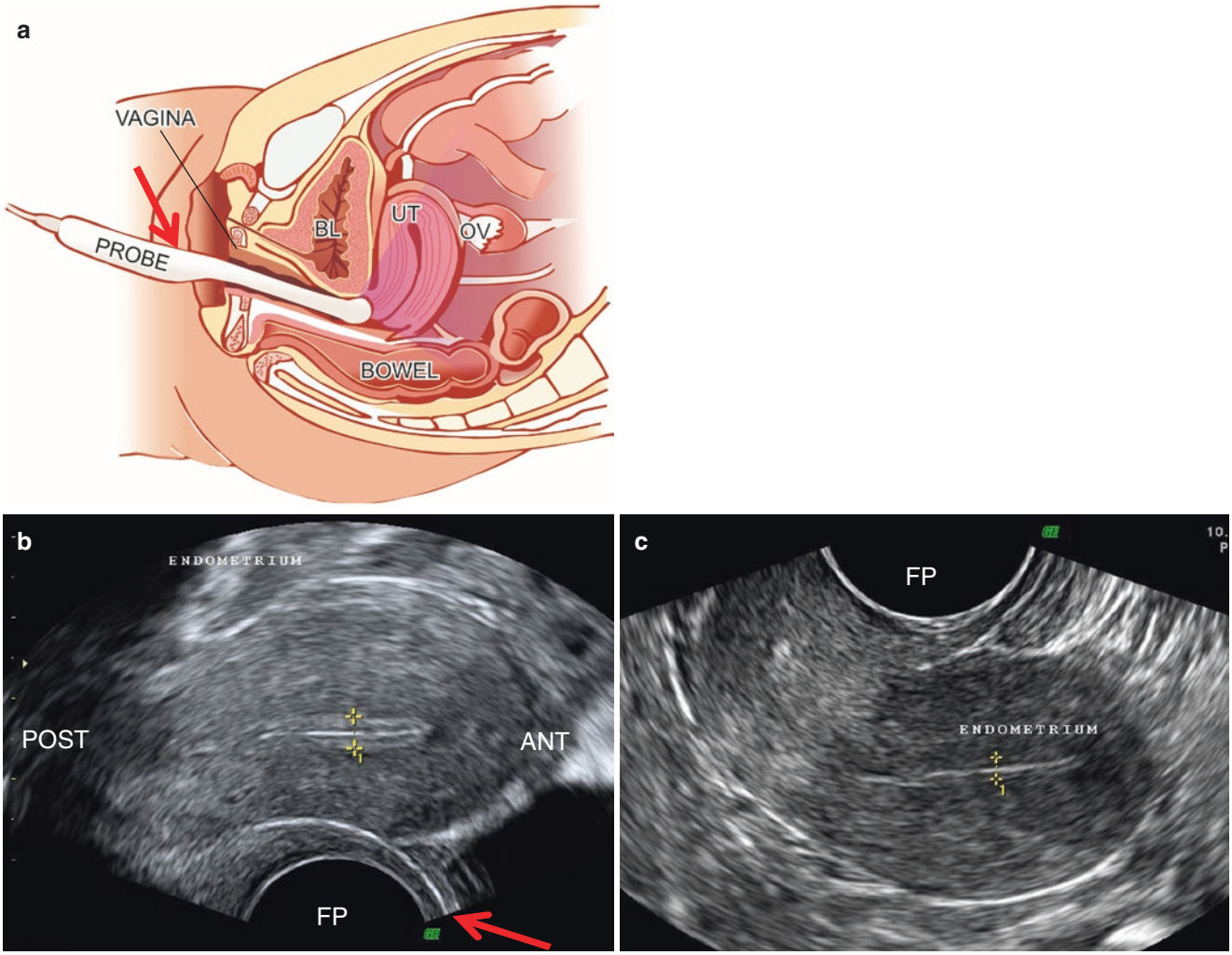

Fig. 2.5 Orientation for TVS. (**a**) Placement of probe for LS view of uterus. *Arrow* indicative of marker on the probe seen anteriorly. (**b**) Midsagittal section of the uterus with footprint (*FP*) of the probe lying in the lower part of the image. *Arrow*, showing anterior margin of the uterus (in the UV fold), corresponds to the marker on the probe. (**c**) Footprint (*FP*) of the probe lying in the upper part of the image, which is an alternate acceptable method of observing the image on the screen

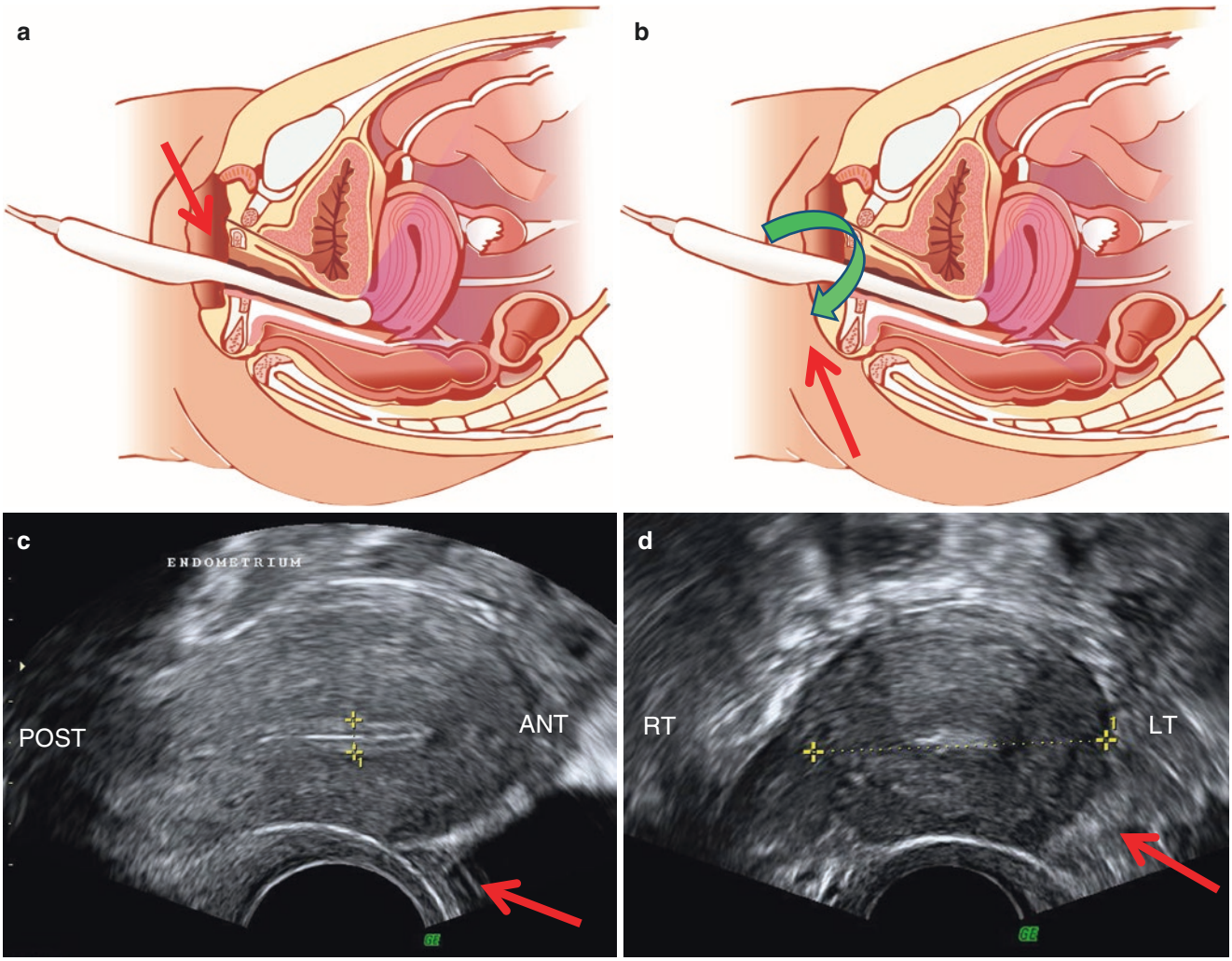

Fig. 2.6 TVS for uterus. (**a**) Placement of probe for LS scan. *Arrow* indicative of marker on the probe. (**b**) Placement of probe for TS scan (after 90° clockwise rotation). *Arrow* indicative of the marker on the probe, now to the left of the patient. (**c**) Midsagittal section of the uterus. *Arrow*, showing anterior margin of the uterus and UV fold which corresponds to the marker on the probe in (a). (**d**) TS of uterus. *Arrow*, showing left side of the uterus which corresponds to the marker on the probe in (b). Structures on the left of the patient are seen on the left of the screen and similarly, those on the right of the patient are observed on the right of the screen

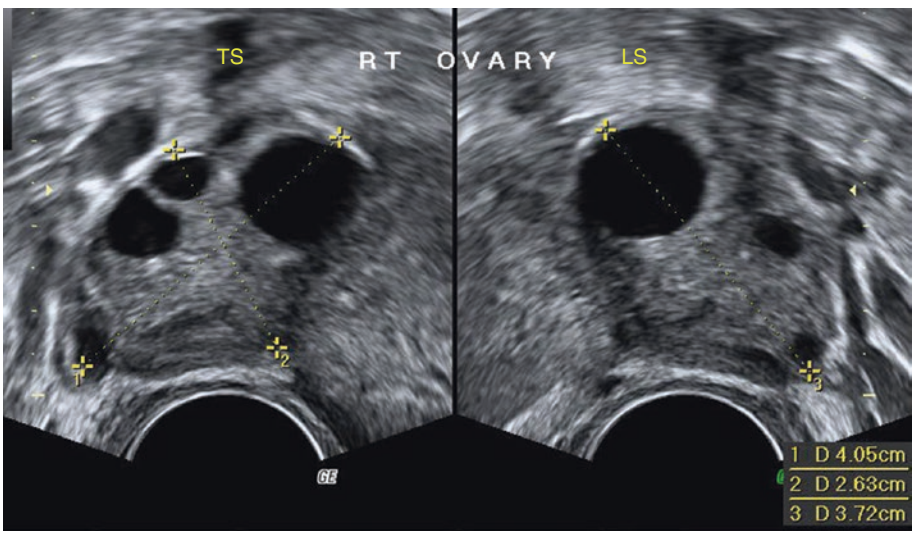

Fig. 2.7 Right ovary TS and LS view. Rotation from LS to TS is done in a clockwise direction and vice versa

Version–Flexion (Figs. 2.8 and 2.9)
Version is the angle between the vagina and the cervix, and flexion is the angle between the cervix and the uterine body. The prefix 'ante' is used to denote forward or anterior (i.e. towards the bladder) and the prefix 'retro' to denote backward or posterior (i.e. away from the bladder).

In comparison to the vaginal axis (i.e., the direction of the TVS probe), if the cervix is directed towards the bladder, it is termed an 'anteverted uterus', and if it is directed away from the bladder, it is termed a 'retroverted uterus'. Similarly, in comparison with the cervix, if the uterus is directed towards the bladder, it is termed an 'anteflexed uterus', and if it is directed away from the bladder, it is termed a 'retroflexed uterus'. Thus, based on the angle of version and flexion, various uterine positions are possible.

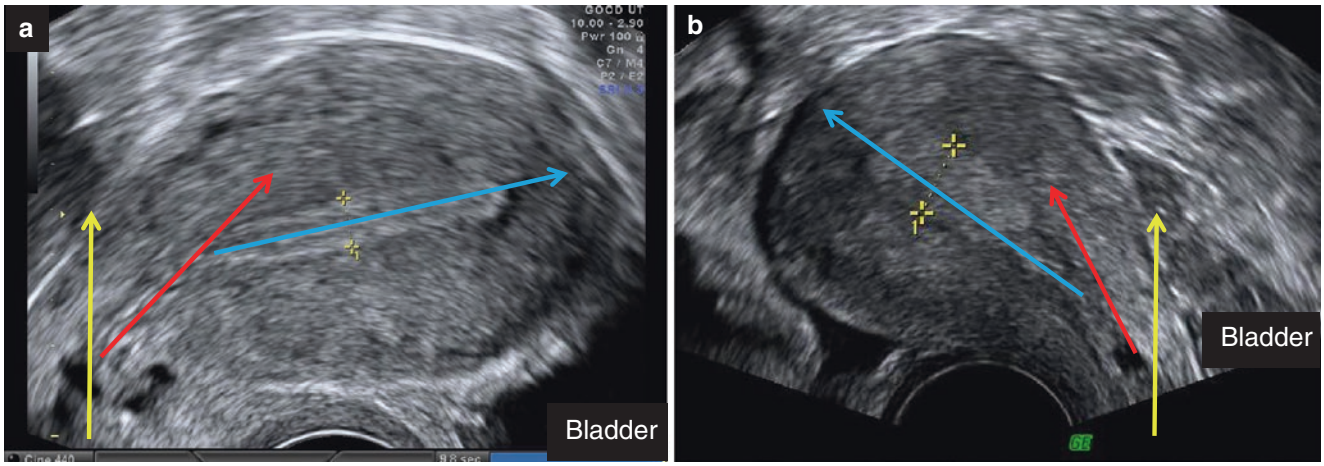

Fig. 2.8 Uterine version and flexion. *Yellow/lowest arrows* indicate angle of the vaginal axis, *red/middle arrows* indicate the cervical axis and *blue/highest*, the axis of the uterine cavity. (**a**) AVAF uterus. Cervix directed towards the bladder (anteriorly) as compared to the vagina (anteversion). Endometrial axis directed towards the bladder (anteriorly) as compared to the cervix (anteflexed). (**b**) RVRF uterus. Cervix directed away from the bladder (posteriorly) as compared to the vagina (retroversion). Endometrial axis directed away from the bladder (posteriorly) as compared to the cervix (retroflexed)

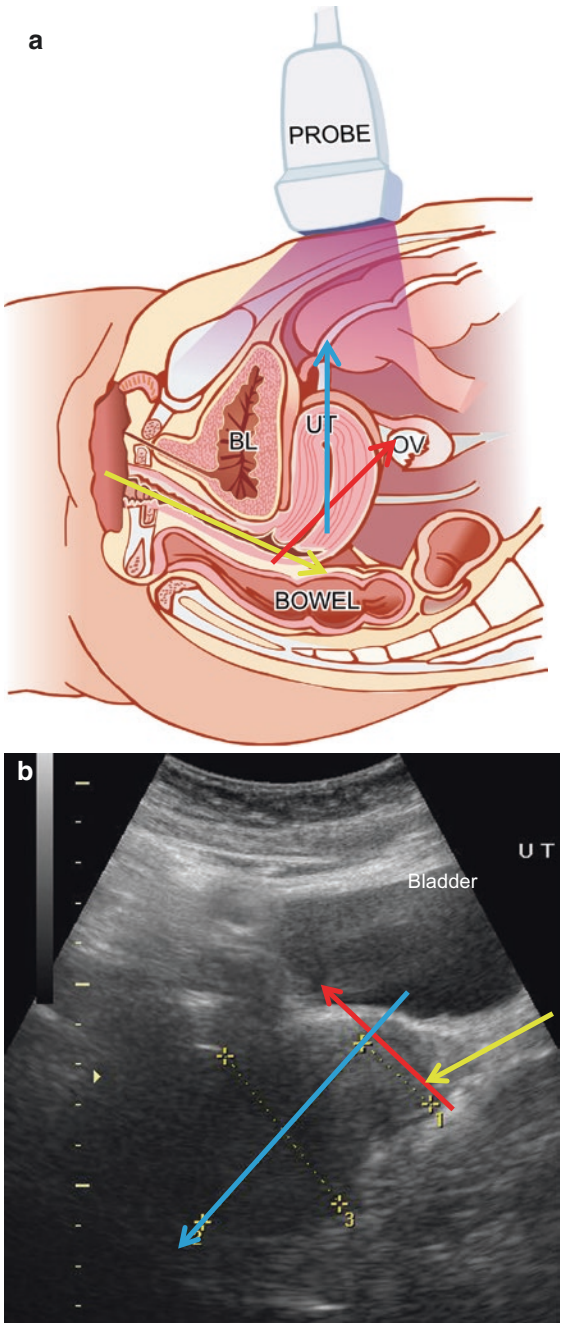

Fig. 2.9 Version and flexion. *Yellow/lowest arrows* indicate angle of the vaginal axis, *red/middle arrows* indicate the cervical axis and *blue/highest*, the axis of the uterine cavity. (**a**) Diagrammatic representation of an AVAF uterus. (**b**) TAS of an AVRF uterus

2.3 Three-Dimensional Ultrasound

(Figs. 2.10, 2.11, 2.12, 2.13, 2.14, 2.15, 2.16, 2.17, 2.18, 2.19, 2.20, 2.21, 2.22, 2.23 and 2.24)

The addition of three-dimensional (3D) ultrasound to transvaginal scan has improved the diagnostic utility of ultrasound in gynecological imaging to a great extent. In 3D ultrasound, the entire volume of a tissue block is acquired, from which sections along multiple planes can be displayed and analysed for better assessment. The addition of Doppler to 3D has further enhanced its utility. This means that, in 3D ultrasound, three-dimensional information of the entire volume of the region of interest can be obtained for analysis. This data can even be stored for manipulation at a later time. Four-dimensional ultrasound is useful to assess moving structures (where the fourth dimension is time) like the fetal face and cardia in obstetric ultrasound, but in gynecological ultrasound, since these structures are stationary, 3D is preferred.

In some gynecological conditions 3D ultrasound is essential for proper diagnosis. These include uterine anomalies and pelvic floor studies. In many other conditions, however, it is a value-added modality that increases the clarity and accuracy of the 2D ultrasound findings. The advantages of 3D in gynecological ultrasound are mentioned in the following paragraphs. However, their utility in various gynecological pathologies will be discussed in the relevant chapters.

Rendering (Fig. 2.10) This is viewing the block along a cut section. Here, masses with different echo densities are well outlined. One of the greatest advantages of 3D ultrasound is the capacity to render an image in various planes, particularly the coronal plane. On 2D, the uterus is generally clearly seen on sagittal and transverse planes both on TAS and TVS. However, 3D is able to provide a coronal section of the uterus, which cannot be visualised on 2D. This is very useful in assessing the shape of the uterine cavity, which is clearly visualised on 3D because of the difference in echo densities between the endometrium and myometrium. 3D can also be used in cases where delineation of masses is difficult on 2D.

Volume Contrast Imaging (VCI) (Fig. 2.11) This feature allows the addition of slices of different thickness onto the rendered section, for better contrast differentiation. This provides a better outline of structures and is useful in gynecology to outline a poorly circumscribed fibroid or to assess the endomyometrial junction in cases with adenomyosis or endometrial malignancy (to look for myometrial invasion).

Multiplanar Imaging (Fig. 2.12) Here, a structure/tissue block can be visualised in all three dimensions simultaneously. There is a dot provided at the intersection of three planes so that one can see the same anatomical landmark in all three planes at the same time. While walking through one plane with the dot, the dot moves to the corresponding spot in the other two planes. This is very helpful when the anatomy is confusing.

Depth Perception (Fig. 2.13) 3D rendered images, particularly of cystic areas, are able to provide a sense of depth which is useful for a subjective assessment of depth. This helps not only the sonologist but also the patient and referring clinician to understand the pathology better. The addition of cine loop, by which the 3D rendered image can be rotated, and editing the direction of the light source in rendered images further add to this perception.

Volume Calculation (Figs. 2.14, 2.15 and 2.16) Volume calculation is more accurate with 3D ultrasound using virtual organ computer-aided analysis (VOCAL) software, particularly for masses with irregular outline. This can be done for both solid structures like the endometrium and for cystic spaces. In addition, when there are both solid and cystic components in a mass, the percentage of cystic versus solid can also be calculated. This software can also be used for quick and more accurate assessment of antral follicle count.

Assessing Flows (Figs. 2.17 and 2.18) The vascular pattern of flow indices of the region of interest (ROI) can also be done by a combination of Doppler with 3D (discussed in greater detail later in this chapter, in the section on Dopplers). Flow indices of the ROI can also be obtained.

Working Offline The advantage of storing 3D volumes is that they can be used to assess the pathology at a later time. This is particularly useful in a busy ultrasound clinic and also when a patient is in pain and one cannot toggle with the probe and knobs for a long time. It has also been used for assessing subjective reproducibility of ultrasound findings in various studies. In difficult cases, these stored volumes may facilitate access to a second opinion from an expert examiner.

Steps in 3D Ultrasound

It is out of the scope of this book to explain in detail the steps involved in 3D ultrasound. This has been briefly discussed as follows:

1. *Data acquisition:*
   (a) *Orientation of 2D image* – The 2D image of the region of interest should be well visualised for a proper 3D assessment. The best 2D plane for acquisition of the volume may depend on the structure being assessed, for example, in order to acquire a volume in cases of uterine anomalies, the most commonly used plane is the mid sagittal plane of the uterus.
   (b) *Defining the region of interest (ROI)* – The region of interest should be completely included within the 3D box, and the angle of acquisition should be such that the entire volume of ROI is included in the 3D sweep.
   (c) *Volume acquisition* – Once the ROI and angle of acquisition have been decided, a volume sweep is taken so that the entire volume of ROI is now available for analysis.
2. *3D/4D Visualisation (Display Mode)* (Figs. 2.19, 2.20, 2.21, and 2.22) – Once the volume has been acquired, it is possible to display and study it in various ways:
   (a) *Multiplanar display* – This basically displays the region of interest in three different orthogonal planes simultaneously. The utility of this has been explained earlier in this section.
   (b) *Surface-rendered image (including high-density imaging or HDI)* – In this, the ROI can be visualised in any cut section desired, the utility of which has been discussed earlier in this section. The addition of cine loop, where the image can be rotated, and the capacity to edit the direction of the source of light on the rendered image further enhance the image quality and assessment.
   (c) *Tomographic display (TUI)* – In this, the volume can be imaged in multiple parallel sections similar what is done in a CT scan.
   (d) *Glass body display* – This is a combination of surface or transparent rendering with colour/power Doppler. The pattern of vascular flow to the ROI can be well assessed. This is even better appreciated with the help of a cine loop by which the image can be rotated.
   (e) *OmniView* (GE Healthcare, Zipf, Austria) – In OmniView the software helps to obtain sections in various non-linear planes. Planes of interest are often not geometrically uniform, and the polyline option is particularly useful in assessing uterine anomalies where the cervix and uterine body are not in the same plane.
   (f) *Inversion mode* – This is used to obtain a solid outline of a cystic structure, for example, a hydrosalpinx. Its

diagnostic utility in gynecological ultrasound is limited.

(g) *Volume analysis (VOCAL and SonoAVC)* – Volume calculations are very accurate with 3D ultrasound, using VOCAL software. After the volume has been acquired, one section is selected and is rotated through 180 degrees, step by step. The angle selected for each step can be 6°, 12°, 15° or 30°. At each step the margin of the structure whose volume is to be calculated is outlined. After 180° of rotation is completed, the calculated volume is displayed on the screen.

The SonoAVC software calculates the volume of all fluid-filled structures and colour codes them, which is of great help in calculating the number and size of antral follicles when an antral follicle count is required.

3. *Volume/image processing* (Figs. 2.23 and 2.24) – These are various tools used to enhance the displayed image:
   (a) *Electronic scalpel* – This helps to cut out and visualise just the region of interest; the structures outside the ROI can be cut away.
   (b) *Contrast and brightness control* – This can be used to enhance the image.
   (c) *Colour selection* – The images displayed can be shown in various colours like grey, sepia, ice blue, etc., depending on the choice of the sonologist. It is believed that colour enhances visual perception by the human eye.
   (d) *Edit light* – This facility is useful particularly when there are structures projecting into a cavity, like papillae in a cyst. Many machines now have multiple options of directions of light source for the given image displayed on the panel. This helps to quickly choose the best image.
4. *Storage of volumes* – This feature is of great advantage as it allows the sonologist to assess structures at a later, convenient time. The acquired volume can be stored immediately. However, it is most often done after working on the volume to some extent, so as to ensure that the volume acquired is appropriate in quantity and quality.

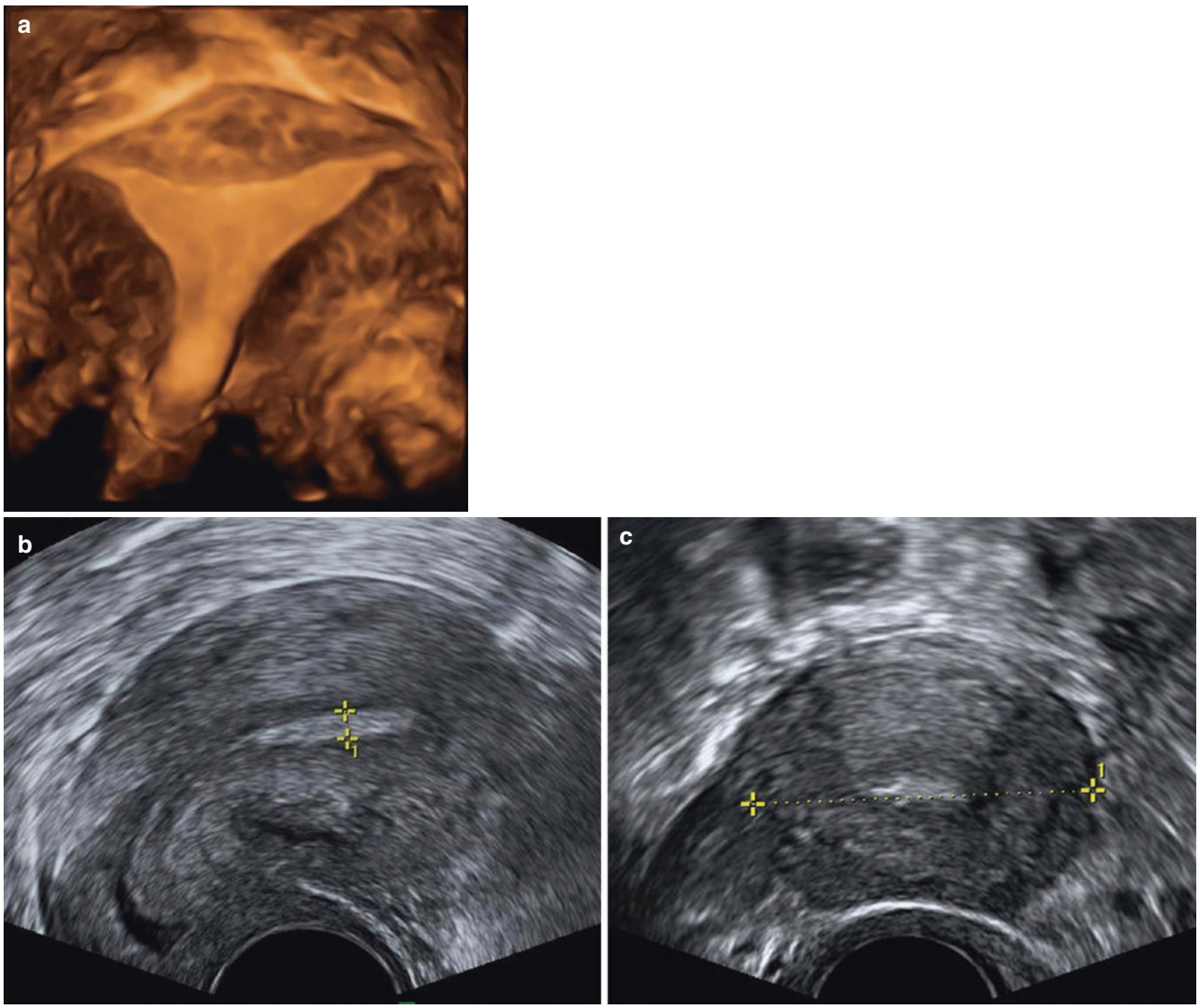

Fig. 2.10 Sections of the uterus. (**a**) Coronal section of the uterus on a 3D rendered image. (**b**) Sagittal section of the uterus on regular TVS. (**c**) Transverse section of the uterus on regular TVS

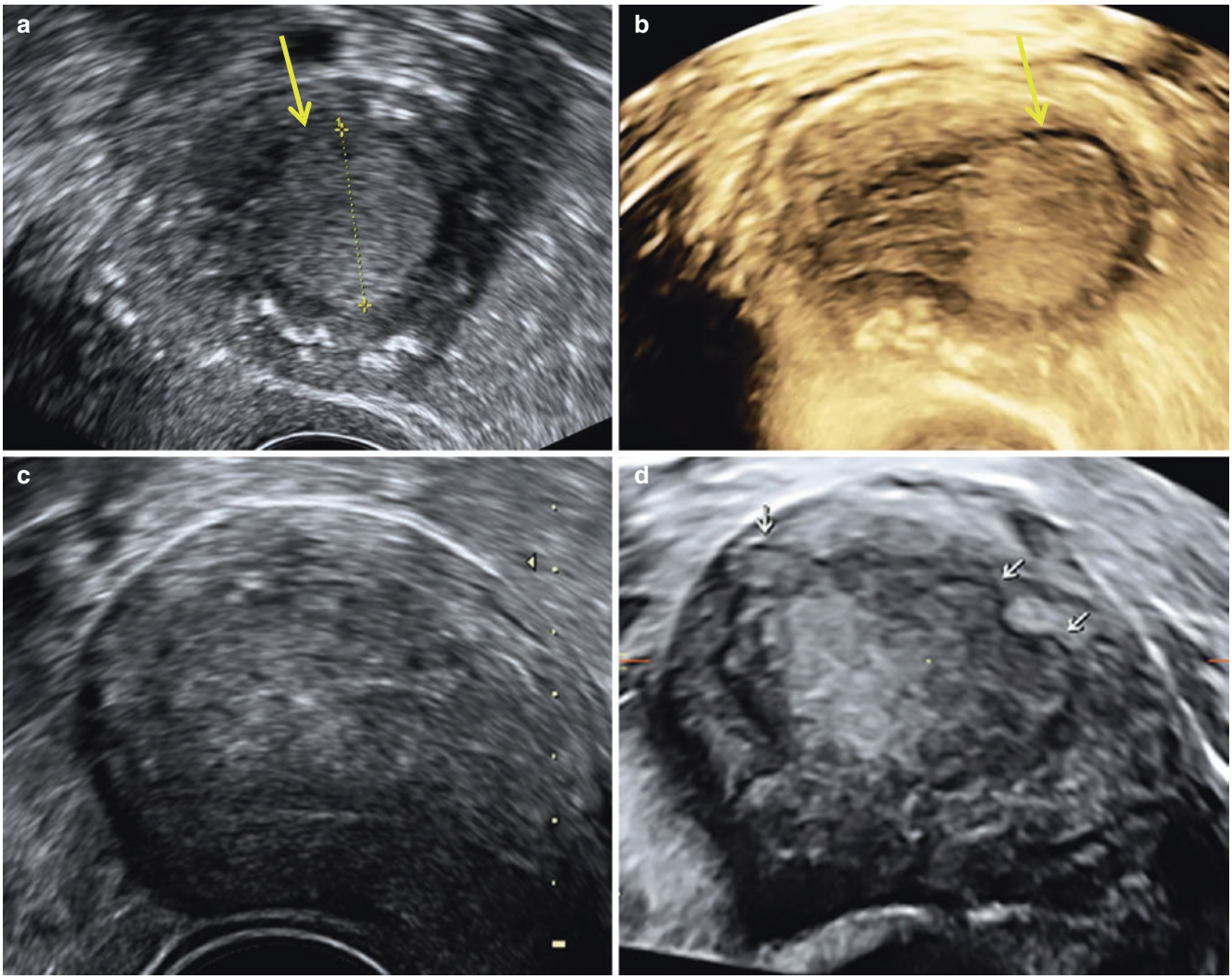

Fig. 2.11 Sagittal section of the uterus showing EMJ. (**a**, **b**) Postmenopausal lady with an endometrial polyp, (**a**) on 2D greyscale, EMJ is seen but not well defined (*arrow*). (b) 3D image of the same section of the uterus as in (a) with VCI showing a very well-defined EMJ (*arrow*), as compared to (a). (**c**, **d**) Postmenopausal lady with endometrial cancer (c) on 2D greyscale. EMJ not well defined. (d) 3D image of the same section of the uterus as in (a) with VCI showing an irregular EMJ with myometrial invasion (*small arrows*)

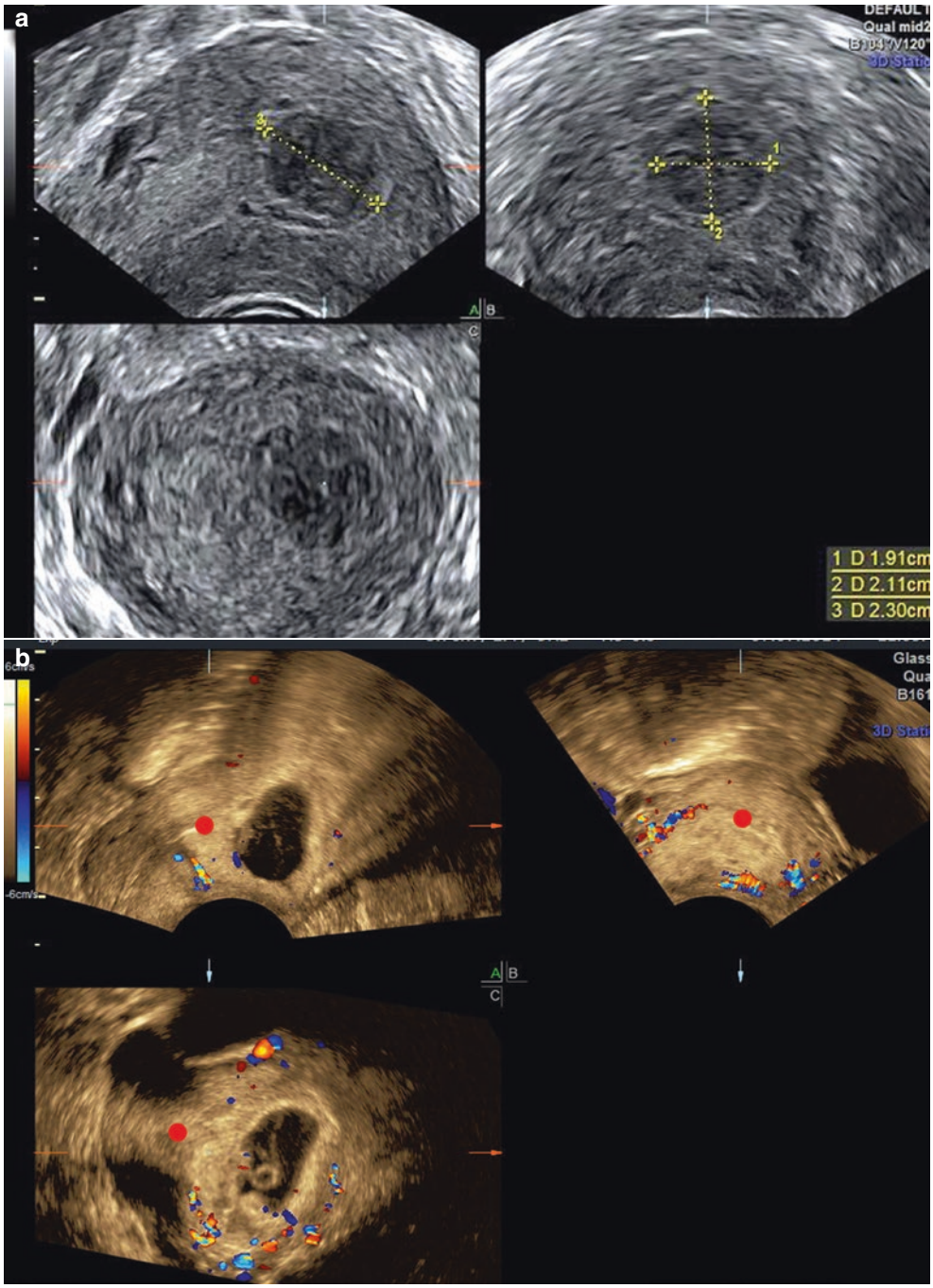

Fig. 2.12 Multiplanar imaging. (**a**) Fibroid seen in all three perpendicular planes of the uterus (LS/TS/coronal). (**b**) Multiplanar view with all three-dimensional planes visualised simultaneously. Dot (here enlarged and in *red*) of intersection of the three planes is visualised, which helps in observing the corresponding point in the two other planes

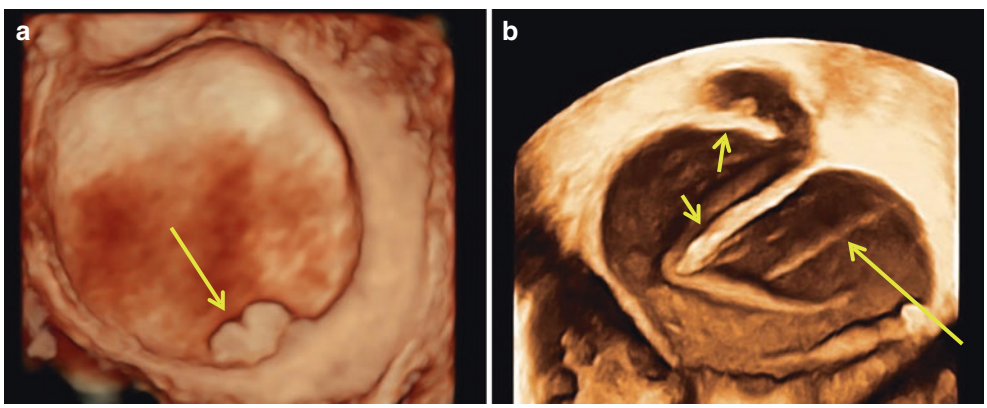

Fig. 2.13 3D rendered image. (**a**) HDI view of a papillary cyst (*arrow* showing papilla). (**b**) 3D rendered image of a hydrosalpinx showing incomplete septae (*short arrows*) and compressed mucosal folds (*long arrow*)

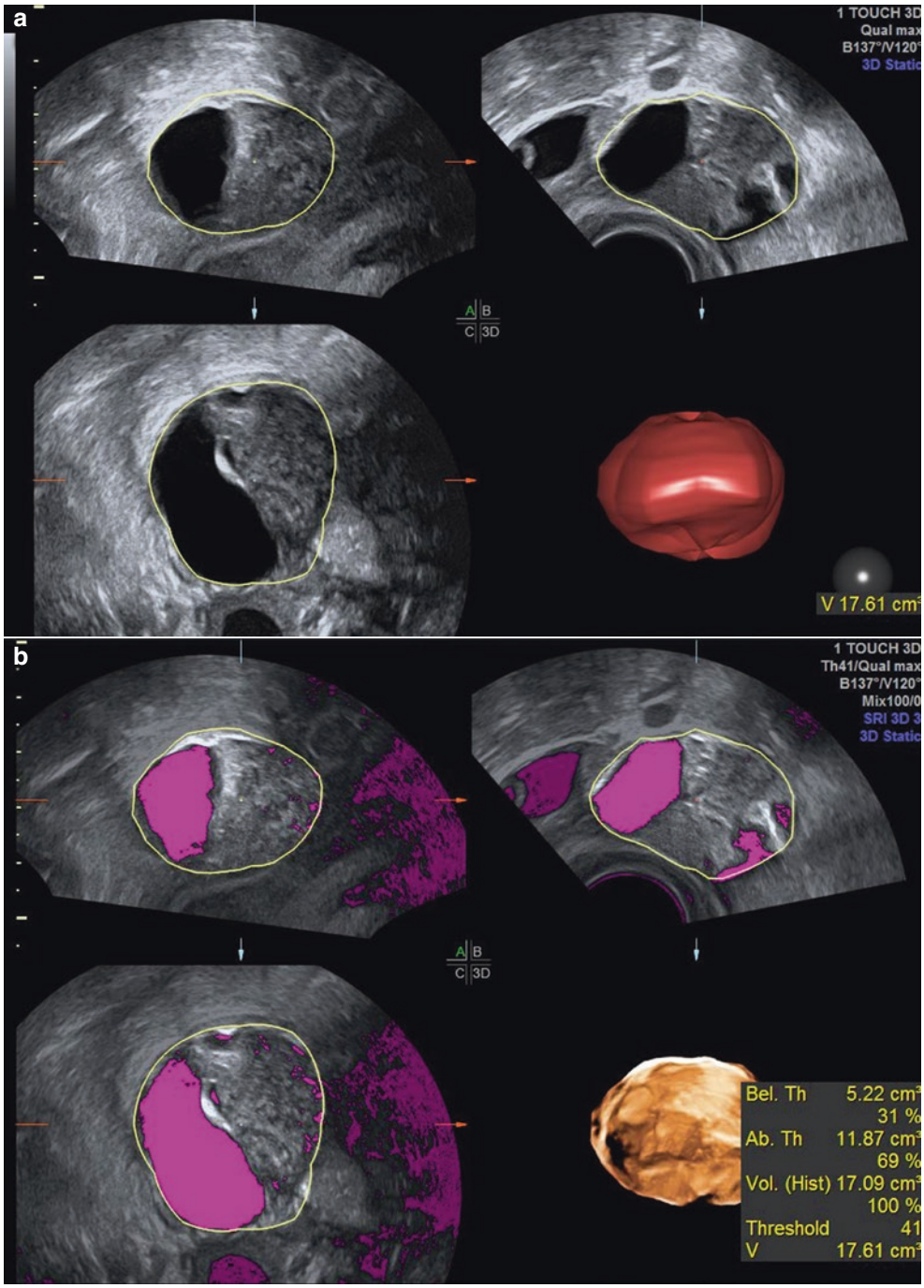

Fig. 2.14 3D volume of an adnexal mass with solid and cystic components. (**a**) VOCAL software used to calculate Volume of the mass. (**b**) Volume of cystic ('below threshold') and the solid components ('above threshold') can be assessed separately

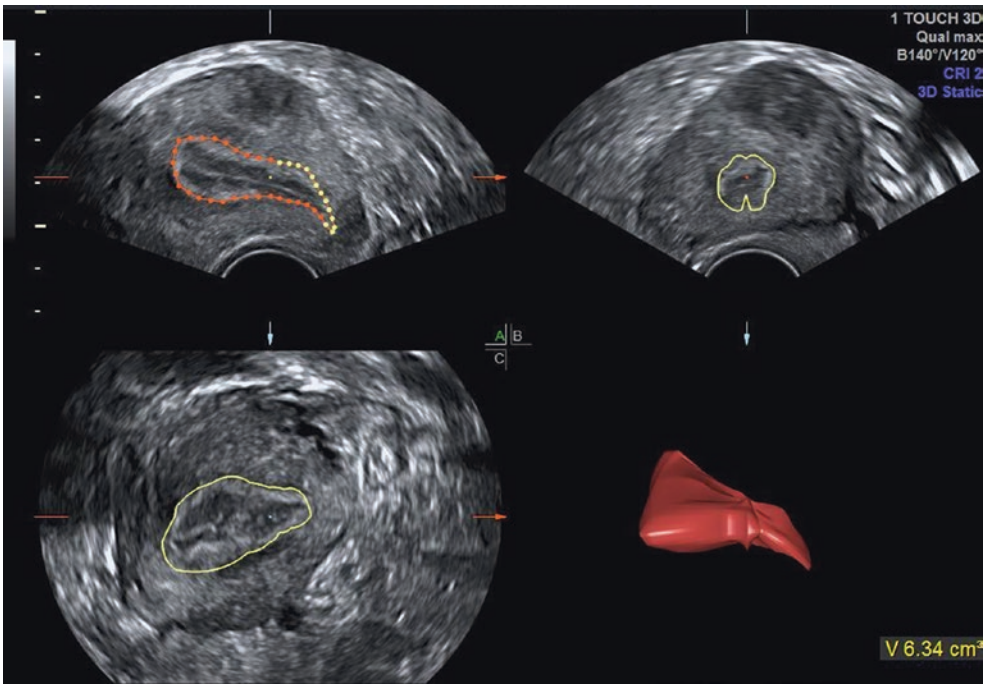

Fig. 2.15 Volume assessment of endometrium. VOCAL is especially useful in volume calculation of masses which are not regular in shape, like the endometrium

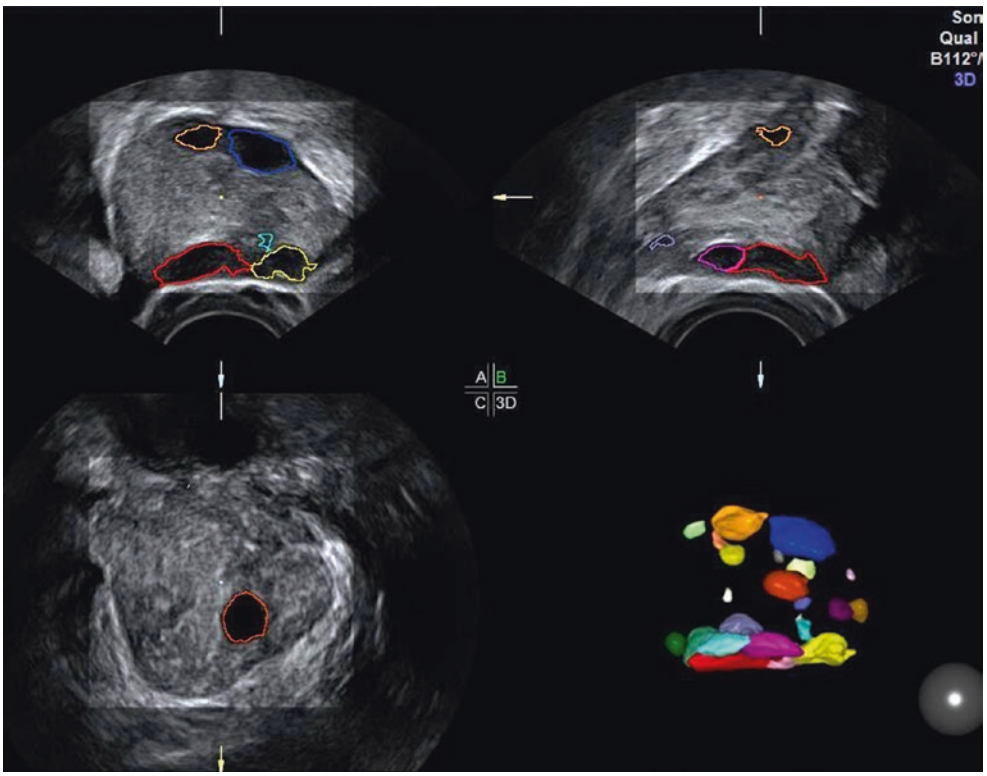

Fig. 2.16 Antral follicle count with SonoAVC

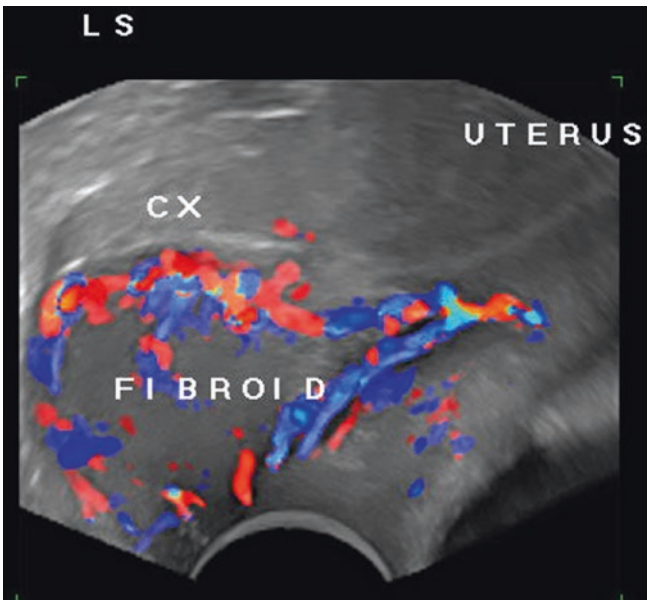

Fig. 2.17 Fibroid polyp with its vascular morphology using 3D Doppler with glass body display

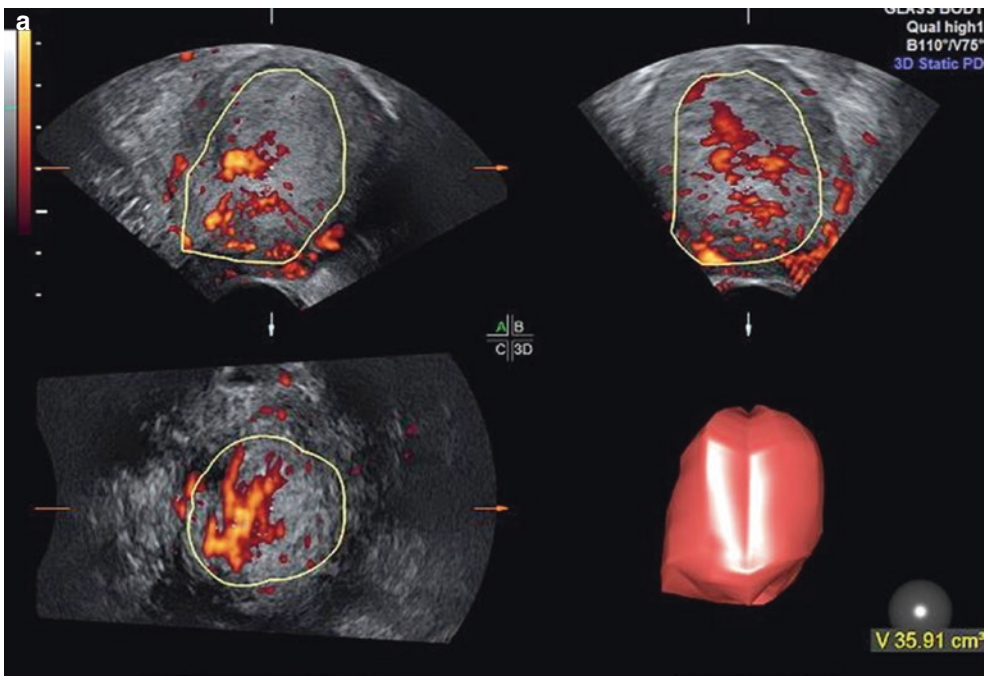

Fig. 2.18 3D flow assessment in a case of carcinoma endometrium. (**a**) Volume of endometrium is calculated. (**b**) VI, FI and VFI of the region of interest (endometrium) are calculated

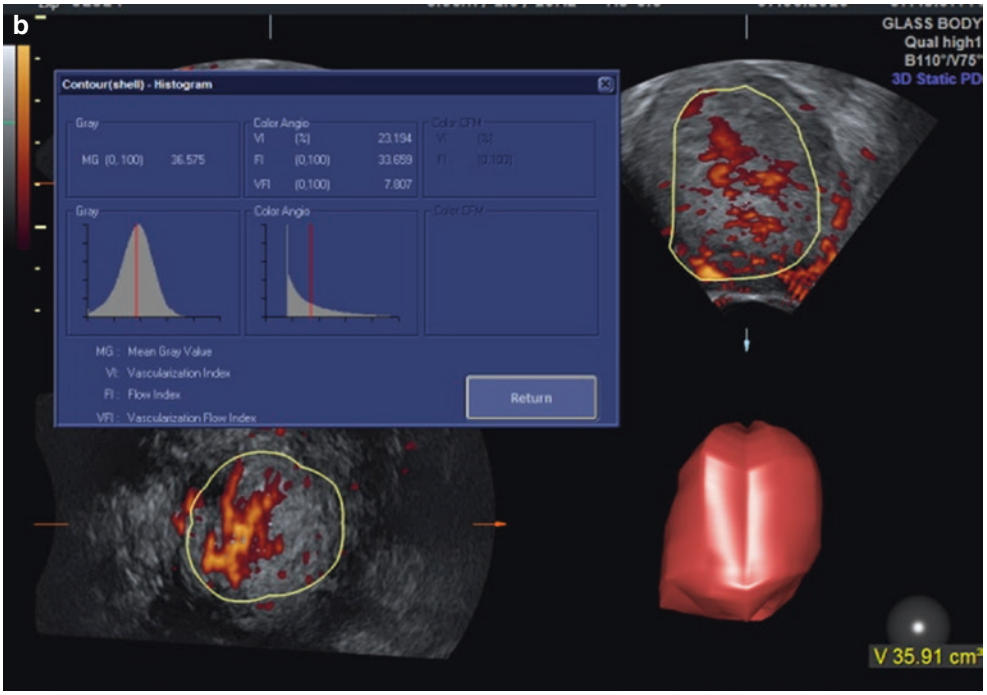

Fig. 2.18 (continued)

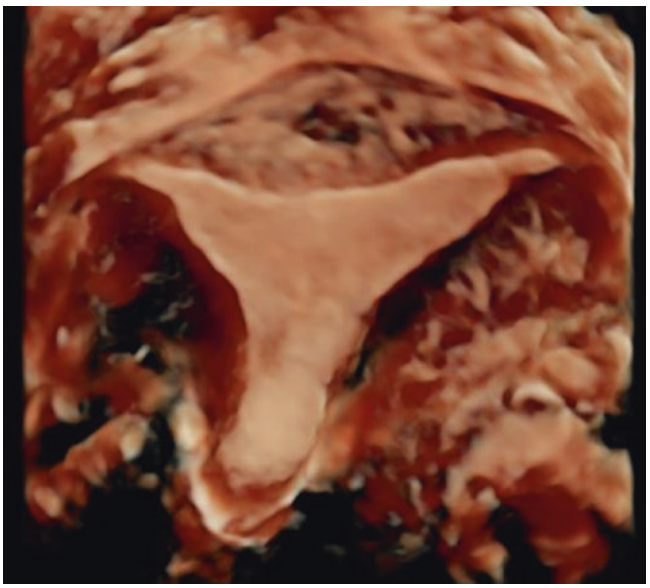

Fig. 2.19 Coronal section of uterus – rendering with high-definition imaging (HDI)

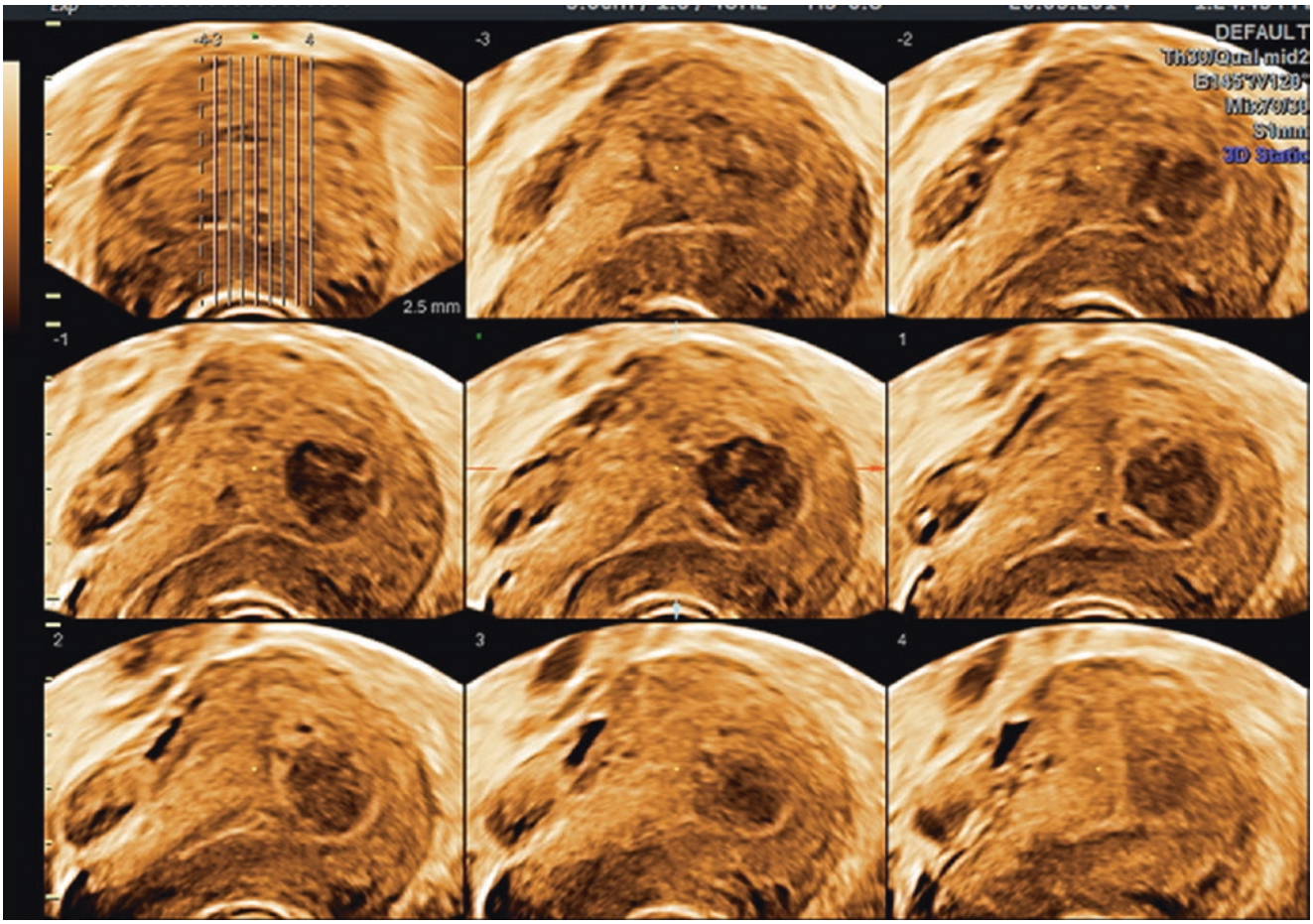

Fig. 2.20 Tomographic display of a submucous fibroid

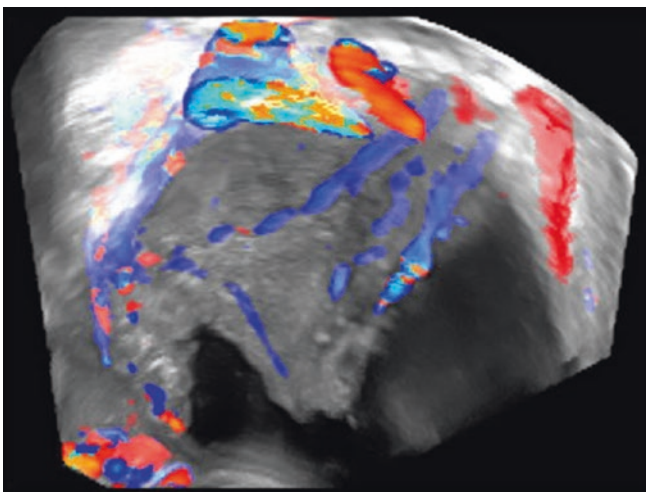

Fig. 2.21 Glass body display showing vessels in the septum of a cyst

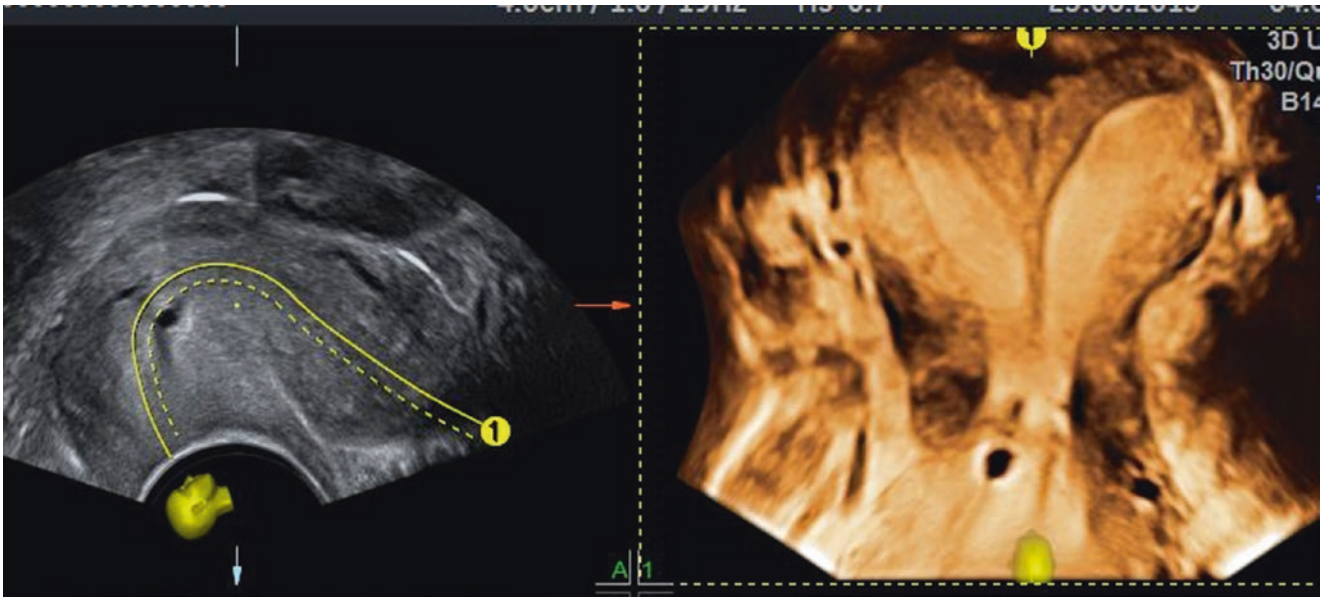

Fig. 2.22 OmniView (*polyline*) showing a coronal section of the uterus along with the cervix in a patient with septate uterus

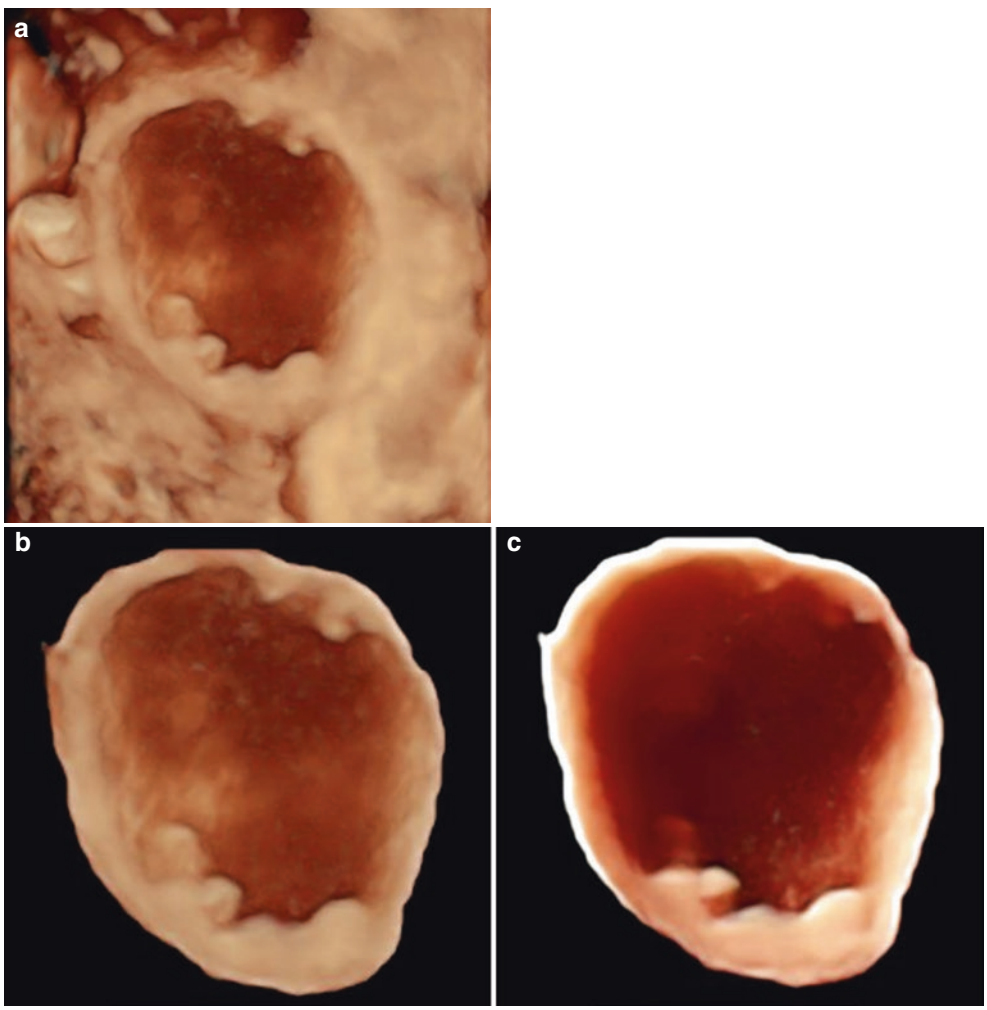

Fig. 2.23 (**a**) 3D rendered HDI image of a papillary cyst. (**b**) 'Magic cut' with electronic scalpel showing only the ROI (cyst) with its papillae. Surrounding structures have been cut out. (**c**) 'Edit light' facility provides various options of directions of the light source from which the best rendered image can be selected

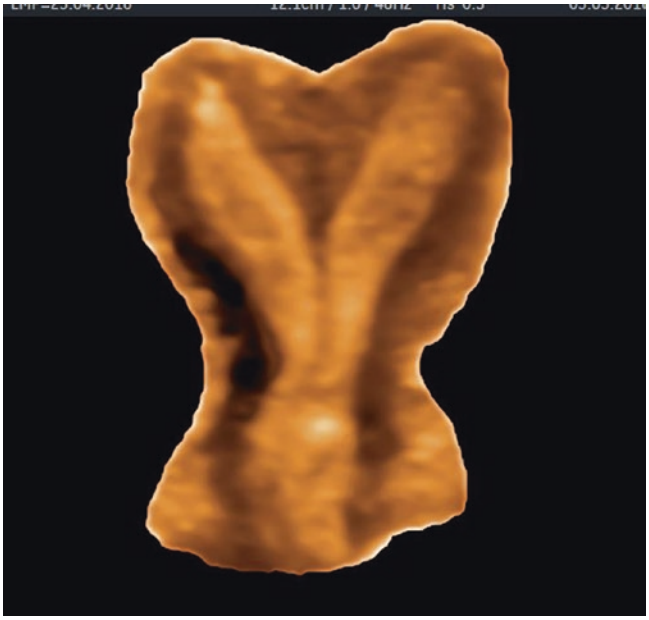

Fig. 2.24 'Magic cut' with electronic scalpel showing only the ROI (uterus and uterine cavity). Other surrounding structures that are not relevant can be cut away. It is important to cut just beyond the ROI (here, the serosal surface of the uterus which is seen as white margins in the image above), so that the shape or outline of the structure does not get altered by the 'magic cut'

2.4 Doppler (Figs. 2.25, 2.26, 2.27, 2.28, 2.29, 2.30, 2.31 and 2.32)

Doppler helps pick up blood flow in various tissues and is therefore a very useful adjunct to greyscale imaging for ultrasound diagnosis in gynecology. When sound is reflected from a moving object, the returning wave has a different frequency, and this change in frequency is called 'Doppler shift'. There are various types of Doppler studies that are used for ultrasound diagnosis (Fig. 2.25):

- *Colour Doppler*: This provides a directional semi-quantitative flow assessment. Flow towards the probe is seen in red and flow away from the probe is seen in blue. The intensity of the flow affects the brightness of colour and turbulent flows show mosaic patterns.
- *Power Doppler*: This is a non-directional Doppler that can pick up low-velocity blood flows. It is useful in gynecology, where often the quantity of flow is important rather than the direction.
- *High-Definition Doppler*: This is a combination of the above two, where low-velocity flows are picked up and the direction can also be assessed with red flows towards the probe and blue flows away from the probe.
- *Pulsed Wave Doppler or Spectral Doppler*: This provides a quantitative assessment of flow, by obtaining a continuous tracing of flow from a vessel. Flow towards the probe is seen above the baseline and flow away from the probe is seen below the baseline.

  The pulse wave gate should generally be equal to the diameter of the vessel being sampled. The sample angle is best when it is parallel to the flow. However, this may not always be possible, and therefore, there is a provision to correct the sample angle, which should be less than 60°. Various flow indices like RI, PI and PSV can be calculated using the traced spectral waveforms. The resistance index (RI) and the pulsatility index (PI) depict resistance to flow. The peak systolic velocity (PSV) shows the velocity (PSV) of flow in the vessel. Angle correction may result in incorrect PSV values.
- *3D Colour Doppler or Power Doppler*: Here, 3D acquisition is done with power Doppler in glass body or angio mode. This helps in assessing soft tissue details with its vascular anatomy (in the glass body mode) or only blood vessel morphology (in the angio mode). In glass body mode, the greyscale morphology is seen simultaneously (though it is not very distinct) in the background, providing additional information of the relationship of vessels to the anatomy seen on greyscale.

With volume histogram, quantitative assessment of vascular flow is possible in the region of interest within the acquired volume.

Doppler is a useful add-on to greyscale imaging as it increases the accuracy of diagnosis either by providing additional information or confirming greyscale diagnosis.

The advantages of using Doppler in gynecology include the assessment of:

- Presence or absence of flow (Fig. 2.26): Live tissue shows flow, whereas avascular tissues (like clots) do not show flow. To assess this, it is important that Doppler settings are optimised.
- Abundance of flow (Fig. 2.27): The quantity of flow can be assessed subjectively (by use of colour score which is explained in the following table) or with the help of 3D power Doppler with volume histogram, which is objective and quantitative.

Colour score	Vascularity
1	No flow
2	Minimal flow (few colour spots)
3	Moderate flow
4	Abundant flow

The absence of flow or a colour score of 1 increases the likelihood of the mass being benign. A colour score of 3–4 increases the likelihood of malignancy, but may also be seen in benign masses, infections, corpora lutea and trophoblastic tissue.

- Vascular morphology (Figs. 2.28 and 2.29): This can help in assessing the nature of a mass (benign or malignant). With 2D Doppler, vessels can be seen only in a given plane, therefore, one may see the path of linear vessels. But to visualise the entire vascular tree/pattern, 3D Doppler is essential (especially when vessels are non-linear and follow tortuous paths). Subjective evaluation of the morphology of the vessel is best seen on 3D power Doppler with glass body display. This can be further enhanced by cine rotation for views from different angles. This vascular morphology is best studied in bulky solid tissue. If the tissue is scant or has multiple cystic areas, the vascular tree cannot be evaluated either because the tissue is minimal in amount or because of distortion of the tissue and its vessels, secondary to pressure and displacement by the cysts.

  After completion of the greyscale ultrasound examination, the power Doppler mode and then the 3D mode are turned on. One must try to include the whole ROI in the 3D volume. The patient is asked to remain still during volume acquisition. Then the glass body display is selected.

  Abnormal features in vascular morphology that suggest malignancy include:
  - High density of vessels.
  - Multiple and frequent branching.
  - Randomly dispersed vessels (no uniformity in distribution).
  - Tortuous and coiled vessels – in contrast to the straight or gently curved paths of vessels in benign masses.
  - Vessels of varying calibre are seen.
  - In a single vessel itself the calibre varies. Segments with microaneurysms and stenotic areas may be seen.
  - Looping and bridging of vessels.
- Direction of flow (Fig. 2.30): For this, other than appropriate settings, it is important to know that any flow perpendicular to the ultrasound beam will not be picked up on Doppler. It may, therefore, be required to angulate the probe or move structures around to pick up flows or trace vessels. By tracing vessels, the site of origin of the pathology can often be deciphered.
- Location of flow (Fig. 2.31): Doppler helps to assess whether flow is in the periphery or the centre of a lesion.
- Flow impedance and velocities (Fig. 2.32): These can be assessed with flow indices like RI, PI and PSV. They are helpful as high-velocity and low-resistance flows are more indicative of malignancy, inflammation and trophoblastic tissue. Flow indices typically show low resistance (RI less than 0.45) in these cases, but often it is not so. In addition, variable values may be obtained in a given case. It is, therefore, recommended that in assessing flow in tissues, particularly tumours, multiple values should be obtained from various sites. If variable values are obtained, one can either provide the range of values, or it is recommended that one selects the tracing with the highest peak systolic value and the corresponding RI of that tracing is reported. Pressure from probe should also be avoided as it can alter Doppler flow indices.

  For proper evaluation of flows, Doppler settings must be optimised. A few tips have been briefly mentioned. (Details of this are beyond the scope of this book.) Generally the application specialist provides presets for gynecology and also explains how these can be altered in various cases. Points that need attention during Doppler studies include:
  - Colour box size – Like in greyscale the size of the colour box should be kept minimal.
  - Pulse repetition frequency (PRF) – PRF should be set at high for high-velocity flows; however, for low-velocity flows, as is commonly required in assessing masses in gynecology, low PRF values of 0.3 to 0.9 are ideal.
  - Wall filter – This should be set at low for low-velocity flows and smaller vessels (for most masses in gynecology it should be set at L1).
  - Gain – Doppler gain should be stepped up till artefacts appear and then gradually brought down till the artefacts just disappear.

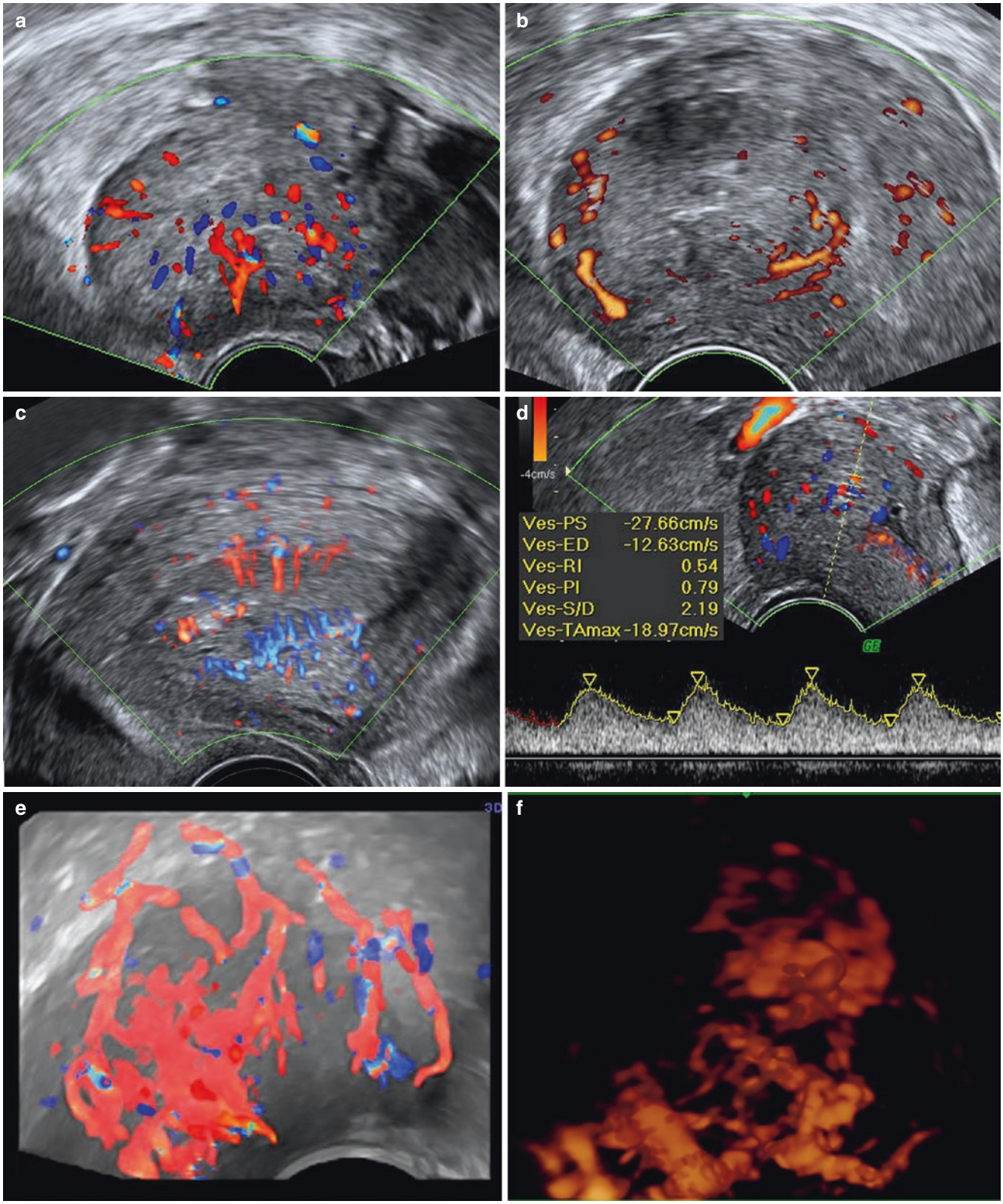

Fig. 2.25 Various types of Dopplers: (**a**) Colour Doppler; (**b**) Power Doppler; (**c**) High-definition Doppler; (**d**) Pulse wave or spectral Doppler; (**e**) 3D colour Doppler with glass body display mode (showing greyscale image of the tissue studied in background); (**f**) 3D power Doppler with angio display mode (the vascular tree morphology is seen, but greyscale tissue display to correlate is absent); (**g**) Volume histogram for flow indices (VI, FI, VFI)

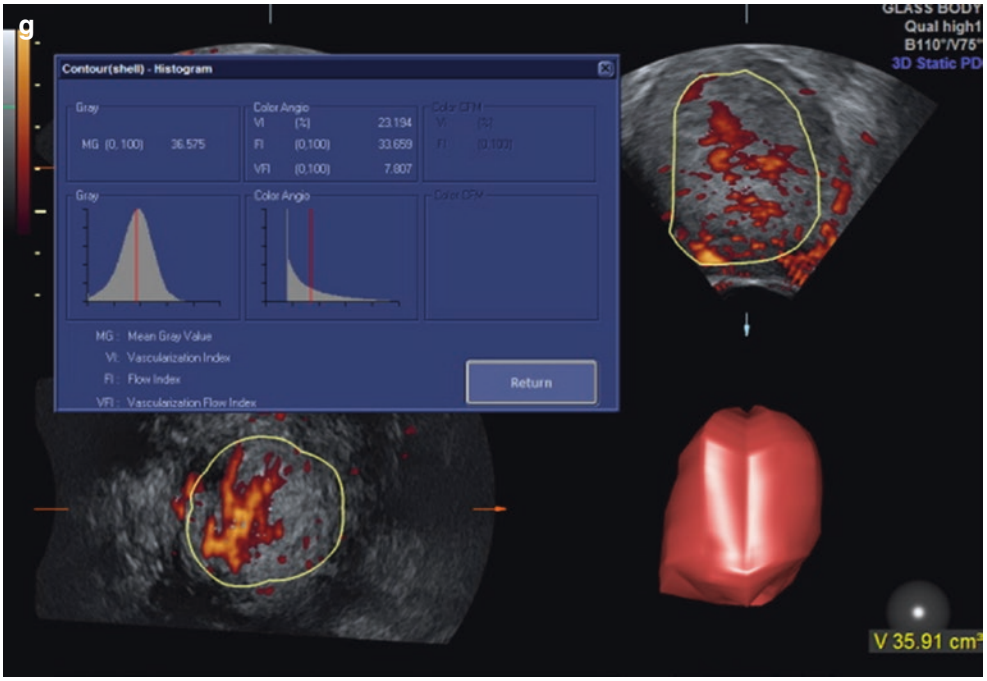

Fig. 2.25 (continued)

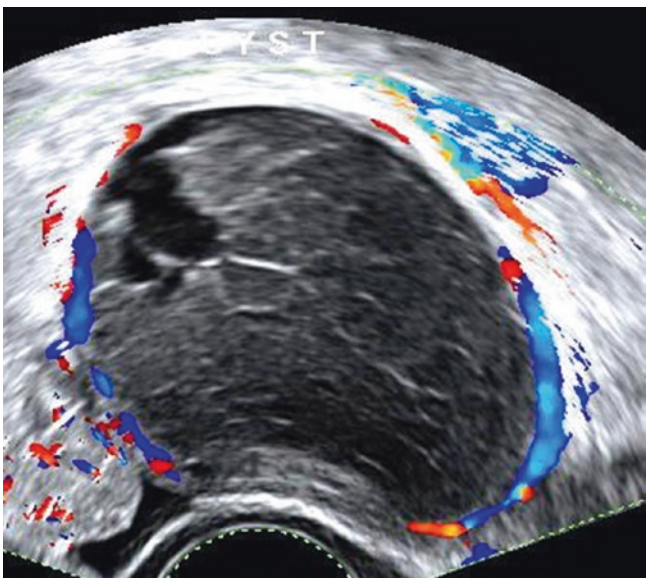

Fig. 2.26 No flow seen within the clot of a hemorrhagic cyst

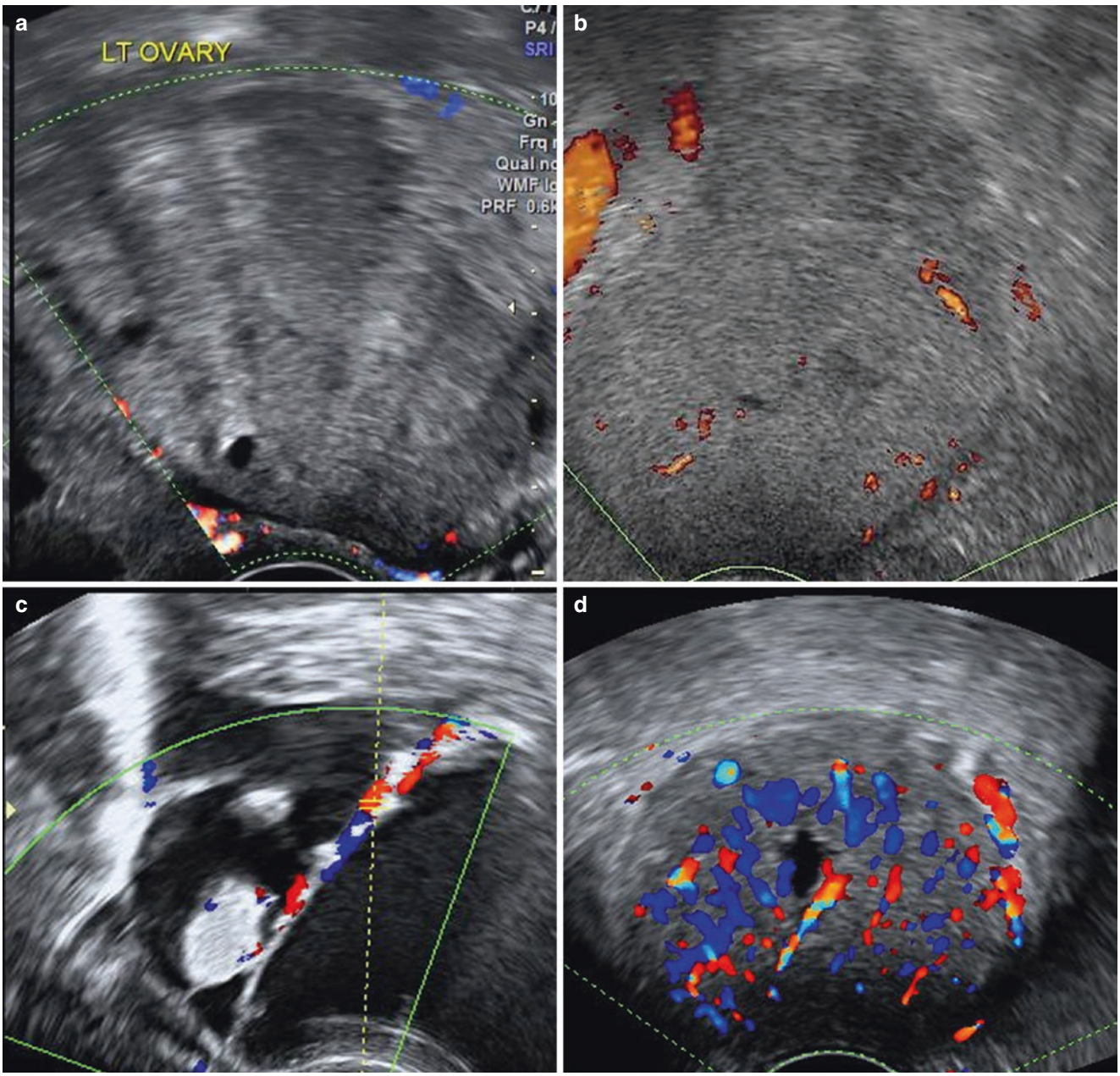

Fig. 2.27 Colour score: (**a**) 1 – no flow; (**b**) 2 – minimal flow; (**c**) 3 – moderate flow; (**d**) 4 – abundant flow

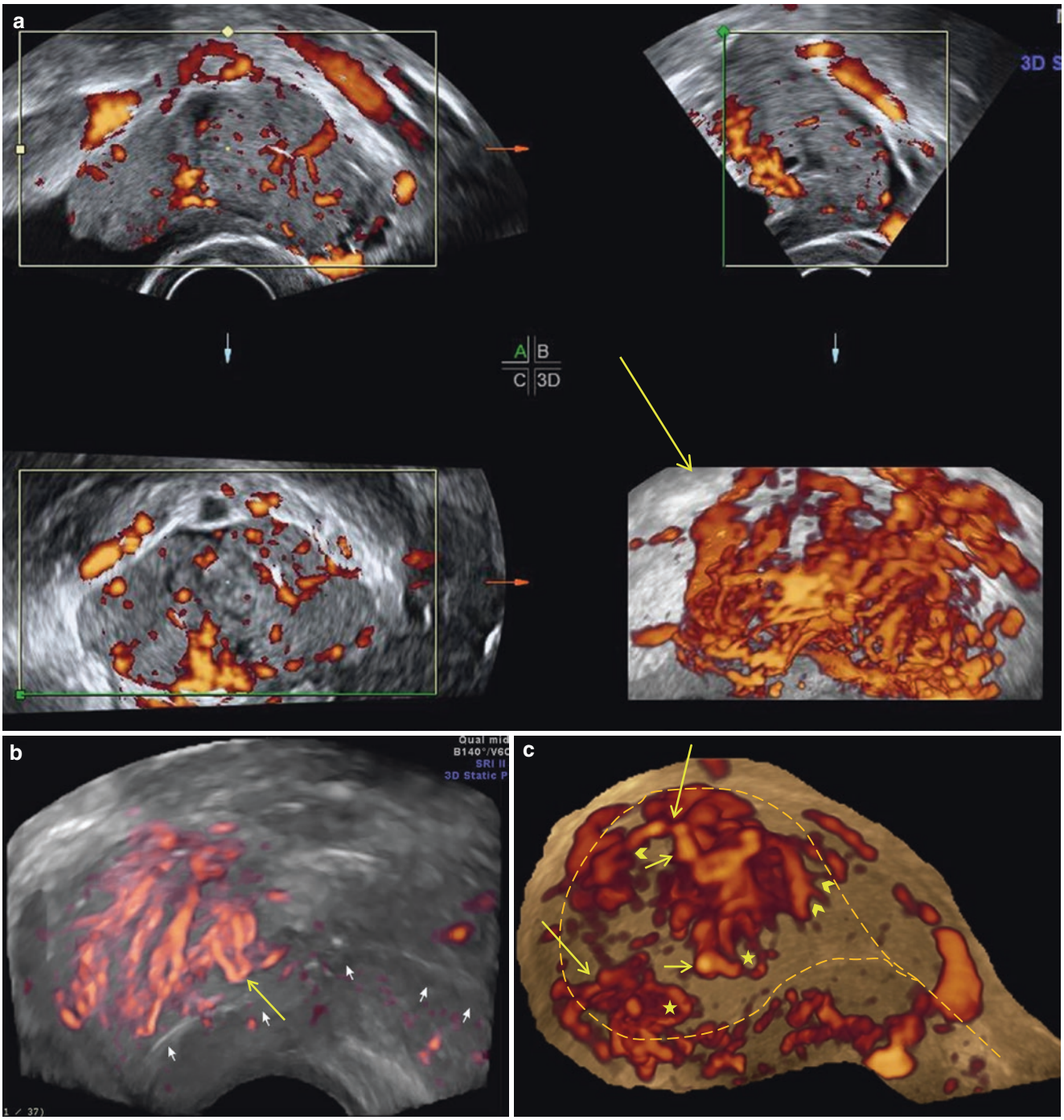

Fig. 2.28 Abnormal vascular morphology well seen with glass body mode (TVS) in a patient with (**a**) ovarian cancer. In the image, three multiplanar sections are seen which show colour signals and splashes, but for most part the vessel pathway cannot be seen. In contrast the entire vascular network of vessels is seen in the 3D rendered image (*arrow*). (**b**) Cervical cancer showing increased vascularity in the thickened posterior wall of the cervix. *Arrow* shows a tortuous, looped vessel. *Short arrows* highlighting cervical canal and lower endometrial cavity. (**c**) Endometrial cancer (LS of uterus with endometrial cavity outlined). Vessels are randomly dispersed and vary from each other in calibre. Vessels show dilated segments (*short arrows*) and stenotic segments (*long arrows*). Looping (*stars*) and branching (*arrowheads*) can also be seen

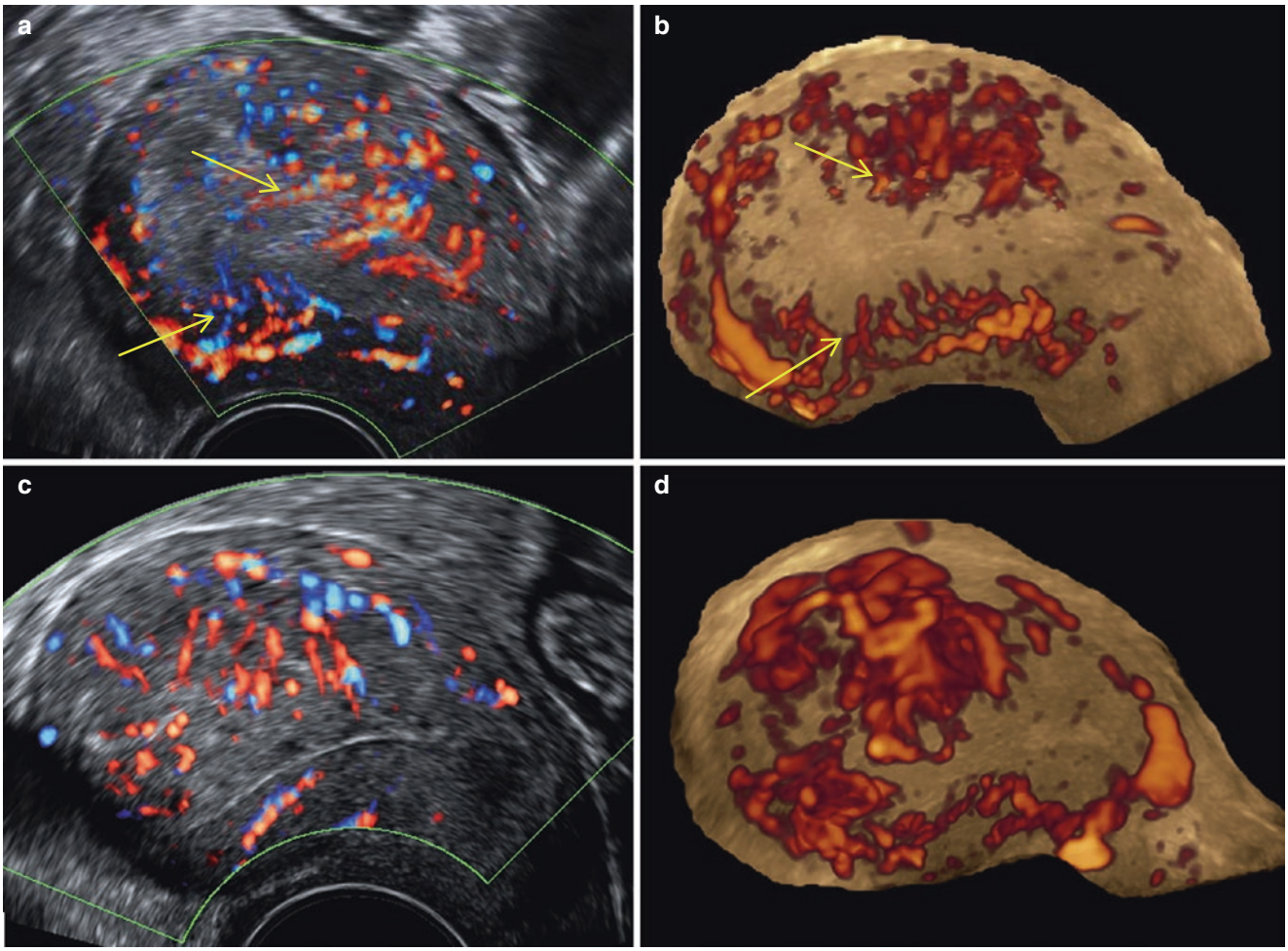

Fig. 2.29 Benefit of 3D power Doppler with glass body display is primarily to detect vascular morphology of tortuous vessels that don't flow along a single plane. Linear vessel flowing along a single plane and can be seen pretty well even on 2D Doppler. (**a**, **b**) Flow in normal secretory endometrium (a) regular 2D Doppler showing linear vessels crossing the EMJ (*arrows*), (b) 3D – glass body display shows the same linear vessels crossing the EMJ (*arrows*). (**c**, **d**) Case of endometrial malignancy (c) regular 2D Doppler showing colour signal dispersed in the endometrium (most of the vessels could not be traced along their length). Only a few linear vessels crossing the anterior EMJ can be traced. (d) 3D – glass body display shows the tortuous path of the endometrial vessels and the abnormal vascular tree. The few linear vessels crossing the EMJ seen in (c) are also seen

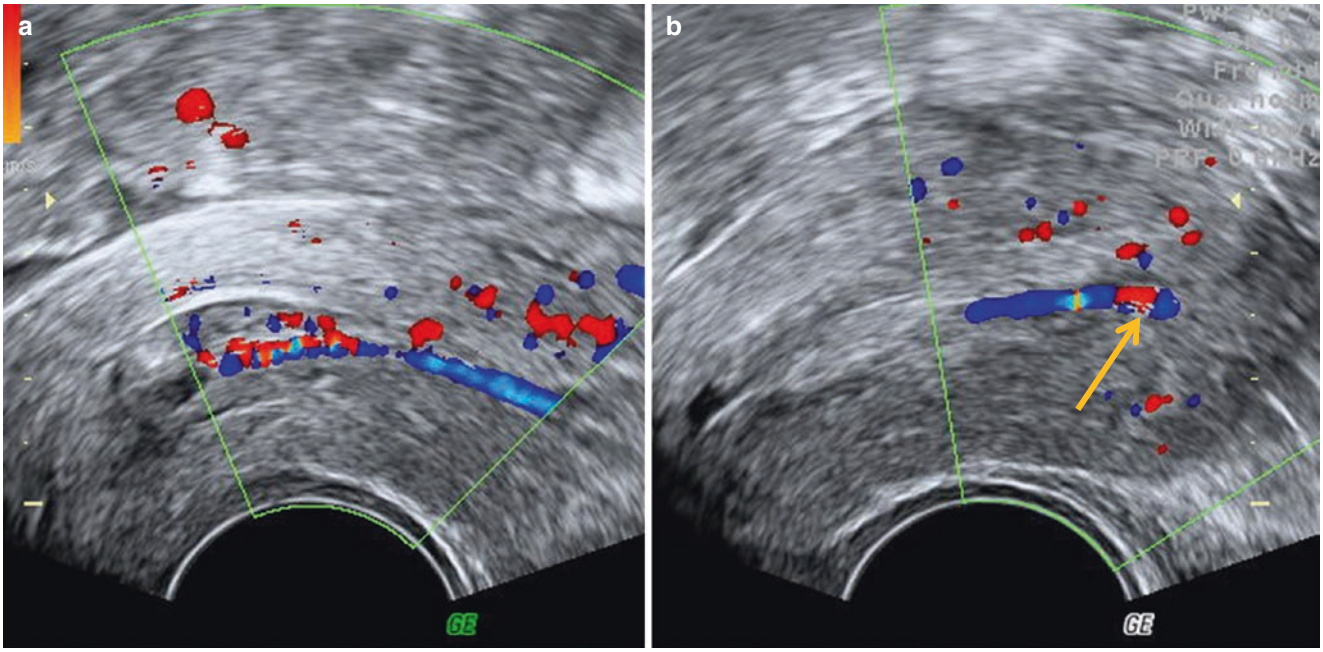

Fig. 2.30 Direction and origin of flow in a case with a polyp in the cervix. (**a**) The flow to the polyp was seen approaching it from higher up in the endometrial cavity. (**b**) The origin of the feeder vessel (*arrow*) is seen at the upper end of the endometrial cavity after angulation of the probe so as to pick up Doppler signals

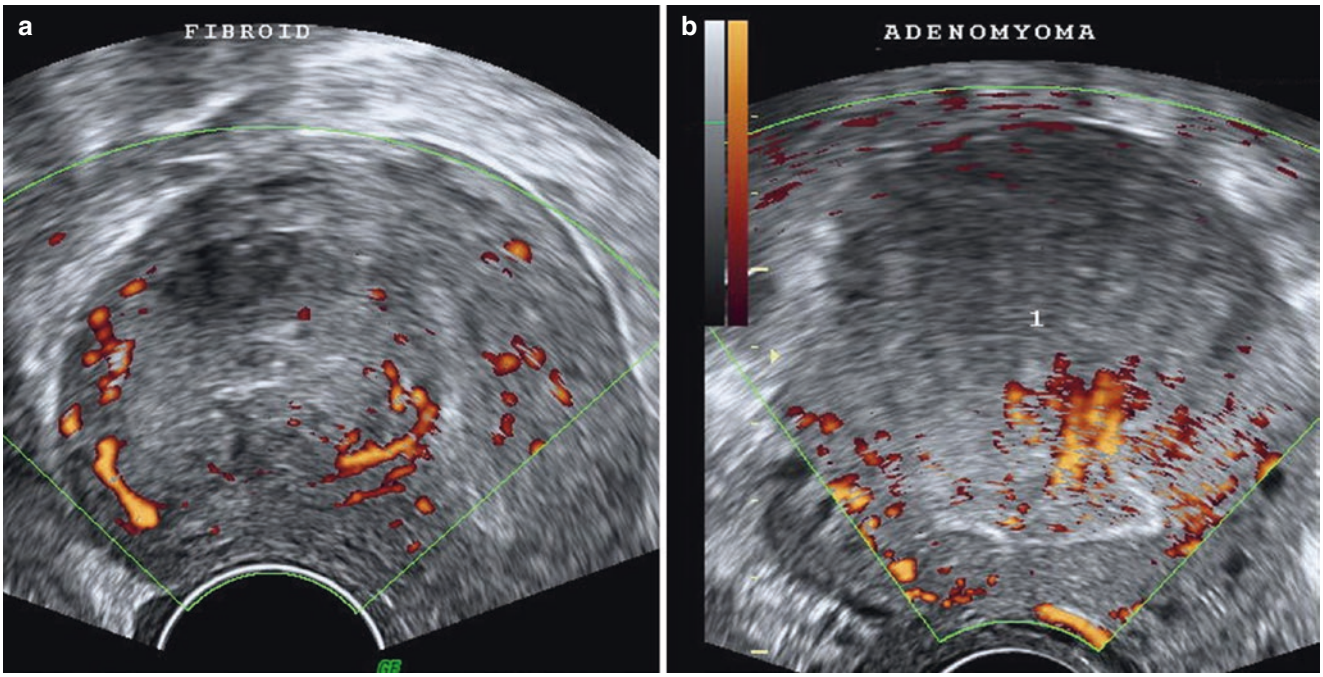

Fig. 2.31 Location of flow. (**a**) Fibroid showing peripheral flow. (**b**) Adenomyoma showing central flow

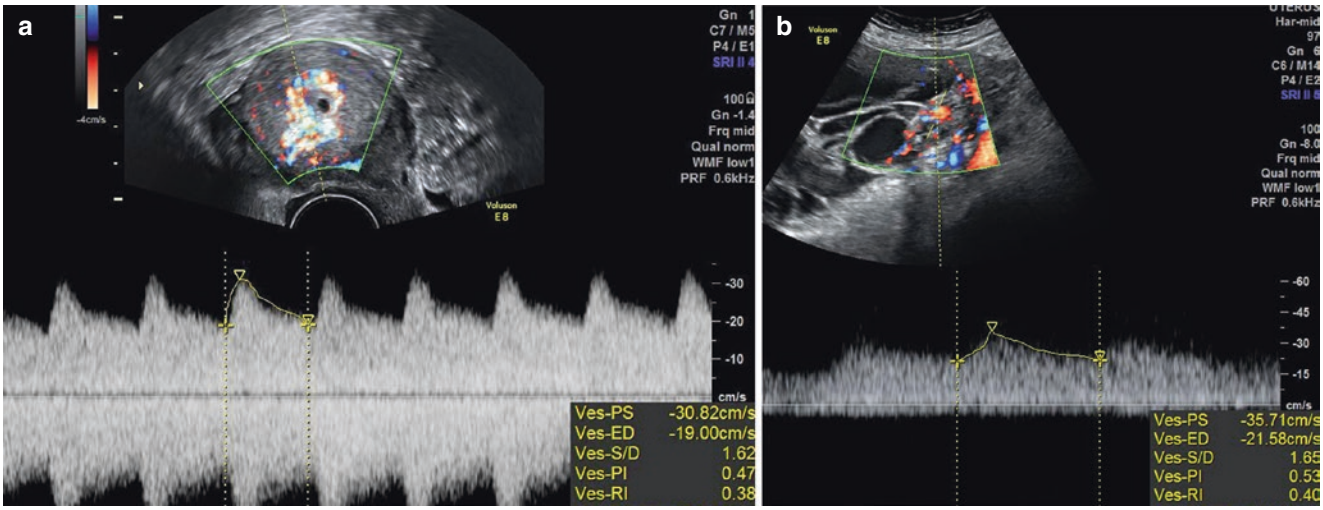

Fig. 2.32 Flow indices: Low-resistance, high-velocity flows seen in (**a**) RPOC and (**b**) ovarian carcinoma

2.5 Tips and Tricks of Pelvic Ultrasound

This section provides a few practical tips on how ultrasound evaluation in gynecology is done and also how it can be optimised to the investigator's advantage.

- *Adjustment of scan parameters*: The details of the physics of ultrasound are beyond the scope of this book. A few important adjustments for enhanced resolution are:
  - *Depth*: Scan depth should be adjusted so as to only include the region of interest.
  - *Focus*: Focal zone is the level at which the image is the sharpest, and therefore, it should be adjusted to the level of the area of interest.
  - *Scan angle*: Large scan angle is useful to obtain a panoramic view, but for a higher resolution, the angle should be reduced to cover only the region of interest.
  - *Zoom*: The image should be zoomed such that the ROI occupies about three fourths of the screen.
- *Fixing TS and LS on a split image screen* (Fig. 2.33): It is a good idea to follow a consistent protocol of fixing the transverse sections (TS) and long sections (LS) of structures on the screen, so that we do not have to label each image. This helps save time. For example, the left half of the screen can be fixed for transverse sections and the right half for longitudinal sections.
- *Use of sepia or other colour tints* (Fig. 2.34): This is believed to enhance visual perception by the human eye, which has a greater accuracy for colour vision than for black and white.
- *Enhancing the image resolution, by altering the angle of the ultrasound beam, to the structure being assessed* (Figs. 2.35 and 2.36)

  On TAS, sometimes the bladder is not optimally filled or the uterus is large and bulky. In such cases, the TAS probe is moved a little lower down and tilted (or angulated) superiorly so that the entire length of the uterus can be seen through the partially filled bladder.

  Structures that lie perpendicular to the ultrasound beam are well seen. Therefore, on TVS, in a mid-positioned uterus, (which lies parallel to the ultrasound beam on TVS), the assessment of structures, particularly the endometrium, becomes difficult. To overcome this difficulty, one can place the probe in the anterior or posterior fornix and push on the cervix to retrovert or antevert the uterus further, to try and make the endometrium as perpendicular to the beam as possible. Alternatively one can push the uterine fundus manually from the abdomen towards the probe. In cases with a midpositioned uterus, a TAS may be more informative. If it is still not possible to assess or measure the endometrium accurately, it should be mentioned so in the report.
- *Calculating the volume of any mass (cystic or solid)* (Fig. 2.37): For volume calculation of any structure (cystic or solid) on 2D greyscale imaging, the dimensions of the mass in three orthogonal (perpendicular) planes are required. One half of the screen should preferably have an image of the transverse section of the structure while the other should have an image of the longitudinal section of the strutures (at right angles to the first). One must try and ensure that the maximum dimension of the mass has been included in one of the two images, for which the probe may have to be angulated a little from a pure transverse or a pure longitudinal section. One must, however, ensure that even if the probe has been angulated for the above reason, the two images on both sides of the screen are taken in planes perpendicular to each other, by rotating the probe through 90°. One measurement is taken transversely across the structure in one image, the second transversely across the second image and the third perpendicular to either the first or the second measurement. The volume can be calculated with the formula – $x \times y \times z \times 0.523$, where x, y and z are the three dimensions of the mass measured as mentioned earlier. Most ultrasound machines calculate the volume automatically from the three measurements of the structure. This automated calculation is what is most often resorted to, instead of manual calculation of volume with the formula given above. Volume analysis is very important not only for assessing the present size that may help in diagnosis, but also for assessing regression or growth of cysts and masses during follow-up. Two-dimensional measurements in a single plane are not acceptable for evaluation of the size of any mass. With 3D ultrasound, assessment of volume is even more accurate, particularly for structures that are not uniform in shape, as mentioned in the section on 3D ultrasound earlier in this chapter.
- *Assessing the echogenicity of a structure/mass* (Fig. 2.38):

  On ultrasound, echogenicity is compared typically using the liver as a yardstick. In gynecological ultrasound, the echogenicity of the normal myometrium is used as the standard for assessment of the echogenicity of other structures. Myometrium and structures with echogenicity similar to that of the myometrium are considered isoechoic. The structures that are less echoic (darker grey) than the normal myometrium are considered hypoechoic, e.g. a cyst with turbid contents. Structures that are more echoic (whiter) than the myometrium are considered hyperechoic, e.g. endometrium. Structures which show no echoes (black) are considered anechoic, e.g. a follicle with clear fluid. The echogenicity of a structure on ultrasound can be altered by altering the gain settings. The gain setting should be such that the myometrium appears grey in colour and normal urine in the bladder, black. This is helpful in adjusting the gain settings, especially for beginners. Often cystic masses that appear anechoic on TAS (because of the increased distance of the cystic mass from the probe) may, on TVS, be found to show internal echoes suggestive of turbid fluid (because of close proximity of the mass to the probe, resulting in improved resolution).

- *Cystic or solid* (Fig. 2.39): We know that on ultrasound, the denser the structure, the whiter it appears. Clear fluid is therefore anechoic. Many cysts, however, have dense or thick contents which may give them a solid appearance. Factors that assist in differentiating a solid mass from a cyst with turbid contents are outlined as follows.
  - A cystic structure generally shows acoustic enhancement distal to the cyst.
  - A cystic structure does not show any flow in the fluid contents within it on Doppler. However, most solid structures with live tissue will show some flow within. For Doppler evaluation, it is very important that Doppler settings be optimised, as mentioned in the section on Doppler earlier in this chapter.
  - Cystic structures, particularly with thick contents, show movement of fluid particles on release of pressure by the TVS probe. Streaming is another phenomenon seen in cystic structures with hyperechoic internal echoes on ultrasound. Streaming is nothing but movement of particles (echoes) within the cyst during ultrasound examination when the probe is held still.
- *Evaluation of hyperechoic areas within a cyst* (Fig. 2.40): Hyperechoic areas within a cyst could either be clots or solid tissue. Factors that help differentiate between the two are outlined as follows.
  - Clots often show jelly-like movement on release of pressure.
  - Typically, clots have concave margins facing the lumen.
  - Clots are usually not attached to the cyst wall along their entire length, and part of the outer margins of the clot are usually some distance away from the cyst wall.
  - Clots are avascular, and this feature is very important in distinguishing these areas of haemorrhage from solid tissue within a cyst that could have a similar appearance. For this, however, the Doppler settings must be optimised.

Debris within a cyst may be seen as a relatively hyperechoic avascular area in the dependent portion of the cyst usually along the posterior/inferior margins. Denser fluid (more hyperechoic) with debris may collect in the dependent portion of the cyst as a result of which a fluid–fluid level may be seen within the cyst. In cysts with thicker contents, however, this fluid–fluid level may be less regular and well defined. In cysts with debris, changing the position of the patient will show the debris gradually moving into a different location (the new dependent part of the cyst).

- *Evaluating Doppler flows* (for the presence of flow and for flow indices):
  - Avoid applying pressure with the probe, as this can alter (decrease) flow in vessels.
  - Uterine contractions can transiently diminish flows in the endometrium and myometrium – and so while assessing vascularity in conditions like AV malformations, RPOC or polyps, it is prudent to wait for a few seconds, if flow is not initially seen.
- *Complex masses with blood and clots* (Fig. 2.41): At times, there may be a complex mass seen in the adnexa or POD with no well-defined structure made out within. This is usually because of blood and clots surrounding the structure. In such cases, Doppler helps to detect live tissues like the margins of the fallopian tube, cyst wall or ectopic tissue, which are not clear on greyscale, because Doppler is able to pick up colour flow in these live tissues.
- *Sliding sign and splitting sign*: The sliding sign is nothing but the movement of one structure/mass along another when the TVS probe is used to push any one of these structures. The splitting sign is the moving away of two structures from one another when the TVS probe is pushed between the two. These signs basically tell us that these two structures are not adherent to one another and also that they are not of common origin (unless there is a pedicle connecting the two, e.g. a subserous pedunculated fibroid sliding along the uterine wall). This sliding sign is often used to assess whether structures like the ovary and bowel are adherent to the uterus.
- *Detecting the presence of adhesions* (Fig. 2.42): Structures are assessed as adherent
  - If there is no sliding or splitting sign between two different structures, they are either adherent or of common origin.
  - When an attempt is made to move fixed structures, the patient will complain of pain or one may see the two structures move en masse.
  - Adhesions and loculated fluid between structures suggest they are adherent to each other, for example, between the ovary and the uterine wall.
  - Sudden angulation in one part of the circumscribed margin of a cyst is indicative of the cyst being adherent in that area.
- *Structure of origin* (Figs. 2.43, 2.44, 2.45, 2.46, and 2.47):
  - A common problem faced, particularly when one sees an adnexal mass, is to know whether it is of ovarian origin or not. Points that assist in this identification are detailed as follows:
    1. Visualisation of the ovaries away and separate from the mass clearly tells us that the mass is not of ovarian origin.
    2. The splitting and sliding sign can also be used to push the mass away from the ovaries, if the mass is not of ovarian origin.
    3. If ovarian tissue is seen stretched along the walls of a mass or a cyst as if it were hugging the cyst, the so-called crescent sign, the mass is likely to be of ovarian origin.

4. If the contour/outline of the ovarian tissue is continuous with that of the mass, the mass is likely to be of ovarian origin. However, if there is any other tissue invaginating between the ovarian tissue and the mass, it could be an extra ovarian mass.

– The presence of a *pedicle* and the *source of blood supply* to a structure helps not only in identifying the structure of origin, but also in locating the site of origin. For example, a solid mass with coarse striated echoes could be either a subserous pedunculated fibroid or an ovarian fibroma. In case ovarian tissue is not seen separately or along the mass, it may be difficult to ascertain the diagnosis. The presence of a pedicle connecting the mass to the uterus will tell us not only that it is a subserous pedunculated fibroid, but also the exact location from where the fibroid is arising from the uterus. The pedicle can be seen both on greyscale and colour Doppler and is particularly well visualised if there is fluid surrounding it. Another example is a polyp at the cervix, the site of origin of which is assessed on Doppler, when it is often found to be arising from high up in the endometrial cavity.
– When two structures move en masse on pressure from the probe or manually, it indicates that the two are of common origin or adherent to each other.
– The shape and appearance of a structure often helps in deciding the structure of origin. For example, ovarian tissue is identified by the presence of antral follicles in a premenopausal woman; a cystic structure with an incomplete septum is of tubal origin, and an elongated tortuous mass in the adnexa is likely to be the fallopian tube.
– Very often, antral follicles of the ovary are seen along its periphery. This helps in delineating the margins of the ovary, which is helpful when the ovary forms a part of a complex mass, like a TO mass.
– Carefully visualising the outer contour and surroundings also helps in assessing the origin and the nature of the mass. The presence of fluid at the lower end of a large endometrial polyp, for example, indicates that thickened endometrium is really a bulky polyp within the endometrial cavity.
– Loculated fluid within adhesions is generally not of smooth contour, and the presence of narrow beak-like extensions between tissue planes indicates that this is cystic fluid encompassed between tissue planes, and not an ovarian or a paraovarian cyst.

- *Fibroid mapping* (Fig. 2.48): In order to study the location of any mass like a fibroid in the uterus, one must be able to assess the uterine midline (which is the endometrial cavity). Every now and then, when the architecture of the uterus is distorted by multiple fibroids, locating the endometrium may become challenging. One must, however, move the probe in various directions to try one's best to trace the endometrium. Sometimes, tracing the endometrium is facilitated by visualising the cervical canal and tracing it upwards. This is important because the location of a fibroid is typically defined by four parameters:
  1. Whether it is in the anterior or posterior wall
  2. Whether it is in the midline or to the left or right
  3. Whether it lies in the uterine fundus, upper corpus, mid corpus, lower corpus or cervix
  4. Its relationship to the serosa and endometrial mucosa, that is, whether it is submucous, intramural or subserous

  Diagrams of fibroid mapping showing the uterus with fibroids, in one or more planes, are very useful to the clinician to assess how best to manage the fibroids.
- *Delineating the margins of a dermoid*: The margins of a dermoid are not well defined because of acoustic shadowing and its resemblance to the bowel. The method used to delineate the entire margin of a dermoid (particularly a large dermoid) is to move the dermoid by applying pressure with the TVS probe. The entire part that moves en masse is the dermoid.
- *The 'hyperechoic line'* (Fig. 2.49): On ultrasound the interface between two smooth surfaces appears as a hyperechoic line. Examples of this include the midline of the endometrium, margins of a polyp and the lumen of the opposite half of a septate vagina with the TVS probe in one hemivagina.
- *Special manoeuvres with the probe:*

  In torsion, gradual movement of the probe along the long axis of the pedicle showing the transverse section of the twisted pedicle produces a whirlpool pattern both on greyscale and Doppler, namely, the whirlpool sign. This is a very specific sign for the diagnosis of torsion of any structure (ovary, paraovarian cyst or hydrosalpinx).

  In a hydrosalpinx, on moving the probe, one can see the cystic spaces communicating with each other, which may not be obvious without the movement of the probe.
- *Tenderness:*

  Since TVS provides us with the ability to simultaneously see and touch structures with the probe, it is possible to identify which structure is tender and the cause of pain. Also, at times the lesion causing pain may be small and difficult to visualise, but a pain-guided approach may help locate the lesion, e.g. an ectopic mass or a focus of deep infiltrating endometriosis. The patient usually acknowledges that the pain she is experiencing during TVS is the same pain that she has been suffering from.
- *Reproducibility in multiple planes and with multiple modalities* (Figs. 2.50 and 2.51):

  When a structure is visualised in one plane, assessment may sometimes be challenging, and rotating the probe by 90° and revaluating the same area provides a better impression of the structure/pathology. There are lesser chances of error or artefact if the structure one is suspecting is seen even after a 90° rotation, i.e. if it is reproducible in multiple planes.

  Similarly, reproducing the pathology/lesion with multiple modalities also enhances diagnostic accuracy. For example, a polyp may be seen on 2D greyscale imaging and

with 3D rendering. In addition, a Doppler evaluation will show us its feeder vessel, which further helps to confirm the diagnosis.

- *Importance of previous scan reports and images*

  Availability of previous scan reports and images is useful in making a diagnosis and assessing the effectiveness of management. For example, a physiological ovarian cyst does not persist at follow-up scans, while an endometriotic or neoplastic cyst continues to increase in size. Similarly, if one is aware that a patient has an endometriotic cyst documented at a previous scan, the presence of solid vascular areas along its cyst walls during pregnancy, due to decidualisation of the endometriotic cyst, will not be misinterpreted as a neoplastic malignant mass. Along the same lines, in patients on medical treatment for chronic infection like pelvic tuberculosis or endometriosis, the efficacy of management can be assessed only if previous reports are available.
- *Timing of ultrasound*

  Baseline assessment of the ovary for antral follicle count and ovarian reserve in patients with infertility is done on Day 2 or 3* of the menstrual cycle.

  For Doppler evaluation of the ovaries, particularly in the presence of small masses, Day 2 to Day 6* of menstrual cycle is ideal.

  For assessment of endometrial pathology like polyps, the preovulatory phase (Day 10 to Day 12*) is ideal.

  For 3D evaluation of the endometrial cavity, the secretory phase (Day 18 to Day 23*) is ideal as the endometrium is fluffy and edematous at that time and therefore is visualised well on a 3D rendered image.

  For evaluation of cervix (as in uterine anomalies or cervical polyps), mid-cycle (Day 12 to Day 14*) is ideal as the cervical mucous present helps to delineate better the cervical canal or any pathology within.

  * (This is applicable in women with regular menstrual cycles of 28–30 days.)
- *Reporting of ultrasound in gynecology*

  After a good ultrasound evaluation of the pelvis, it is important that reporting is done systematically to ensure that nothing is missed. Reporting should therefore include:

  – Relevant history and indication of ultrasound. This should be mentioned in the report.
  – Uterus – The size and position should be mentioned.
  – Endometrium – The appearance and thickness should be mentioned. Any pathology seen within should be described (in terms of size, location, greyscale morphology and Doppler flows).
  – Myometrium – If the myometrium is homogeneous and shows no pathology, it should be reported as normal. If any pathology is present, it should be described (in terms of size, location, greyscale morphology and Doppler flows).
  – Ovaries – Their size and mobility should be mentioned. The presence of developing follicles or corpus luteum should also be reported. Any pathology in the ovary should be described (in terms of size, location, greyscale morphology and Doppler flows).
  – Adnexa – The presence or absence of any pathology should be mentioned. If present, it should be described (in terms of size, location, greyscale morphology and Doppler flows).
  – Cervix and vagina – The presence or absence of any pathology should be mentioned, if present.
  – Pouch of Douglas – the presence of any fluid, adhesions or any other pathology, if present, should be mentioned.
  – High and low sliding sign – This (i.e. the sliding of the bowels along the upper and lower posterior wall of the uterus) should be mentioned in the report.
  – Tenderness – If tenderness is present during TVS, it should be mentioned. DIE nodules if present should be described (size and location).
  – Kidneys – Many sonologists include evaluation of the kidneys as a part of routine examination. This is because hydronephrosis may be seen secondary to some gynecological pathologies, and in patients with uterine anomalies there may be associated renal anomalies.

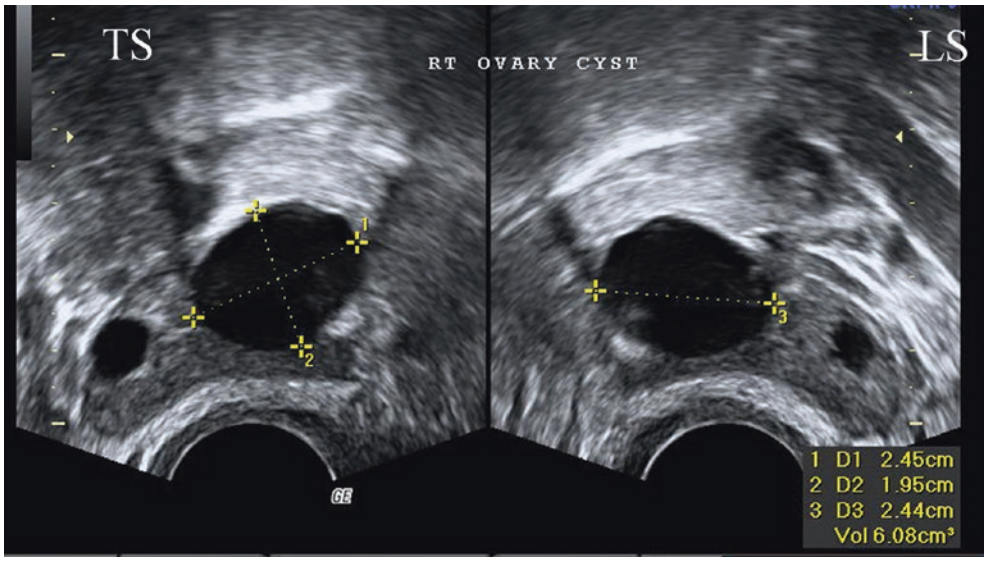

Fig. 2.33 Ovaries seen in TS and LS views

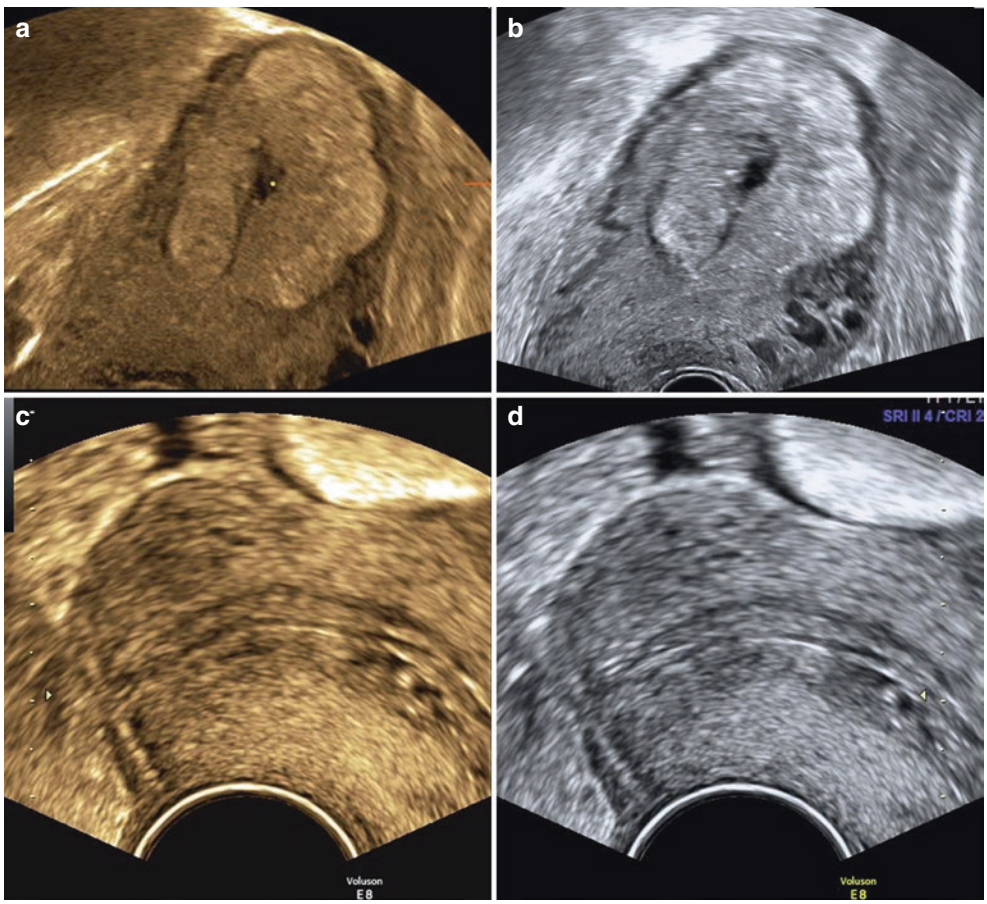

Fig. 2.34 Sepia and greyscale images in two different patients – for comparison. (**a**, **b**) Retained placenta. (**c**, **d**) Normal cervix

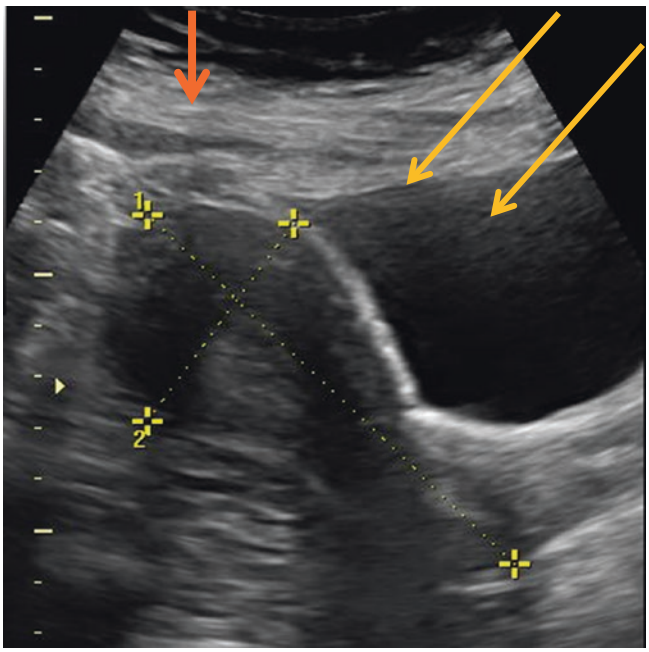

Fig. 2.35 Imaging the uterus with a partially filled bladder. Changing the angle of the ultrasound beam from above the uterus (*short arrow*), by moving the probe downwards on the patient's abdomen and tilting it upwards, provides better visualisation of the uterus as the angle of the beam passes through the fluid-filled bladder (*long arrows*)

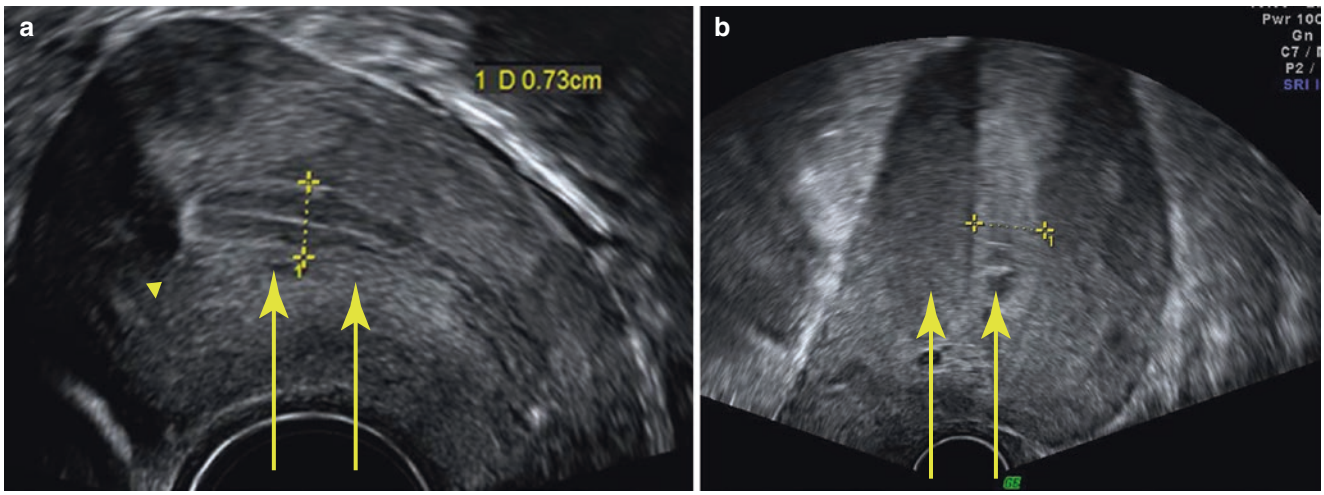

Fig. 2.36 Visualisation of endometrium. (**a**) In an RF uterus with the endometrium perpendicular to the ultrasound beam (*arrows*). The endometrium is clearly visualised. (**b**) In a mid-positioned (axial) uterus, with endometrium parallel to the ultrasound beam (*arrows*). The endometrium is not well seen

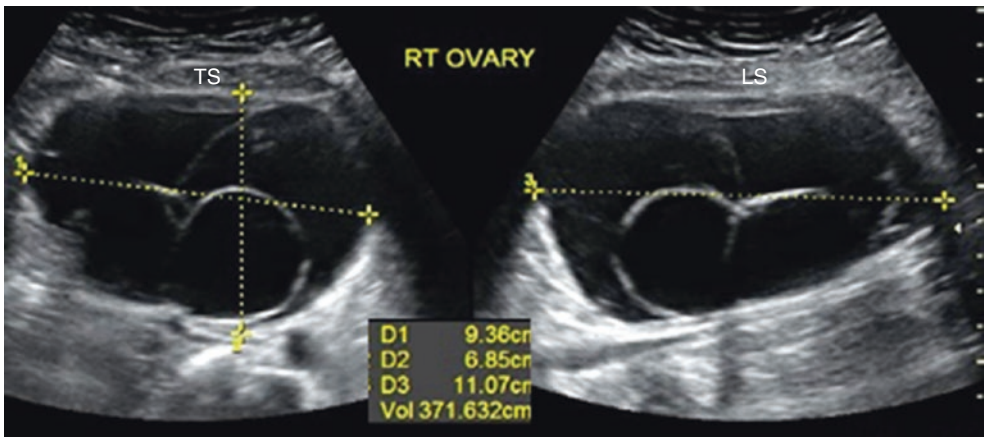

Fig. 2.37 Calculating the volume of a right ovarian neoplastic mass by measuring its three dimensions in two perpendicular planes (TS and LS)

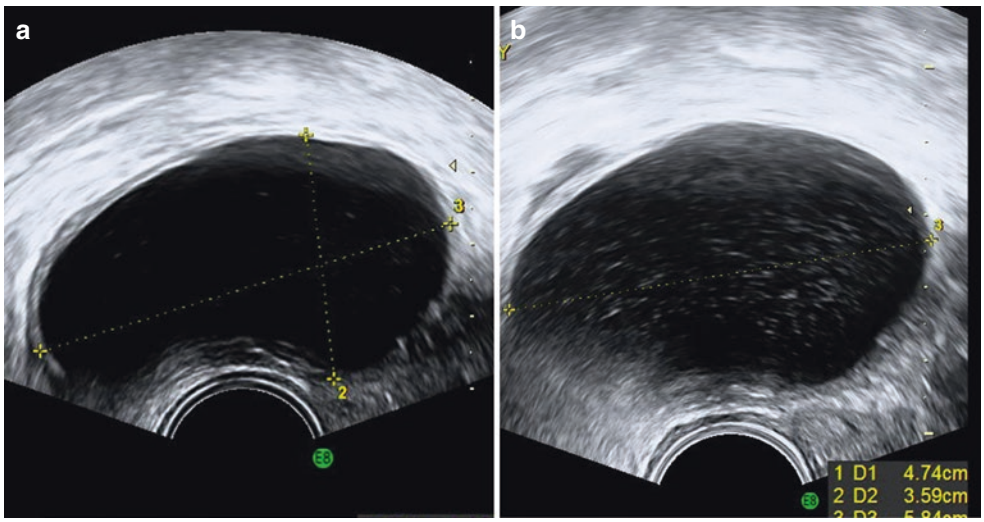

Fig. 2.38 Cyst echogenicity can be altered by changing the 2D gain settings. (**a**) Appears anechoic with low gain settings. (**b**) Shows low-grade internal echoes with high gain settings

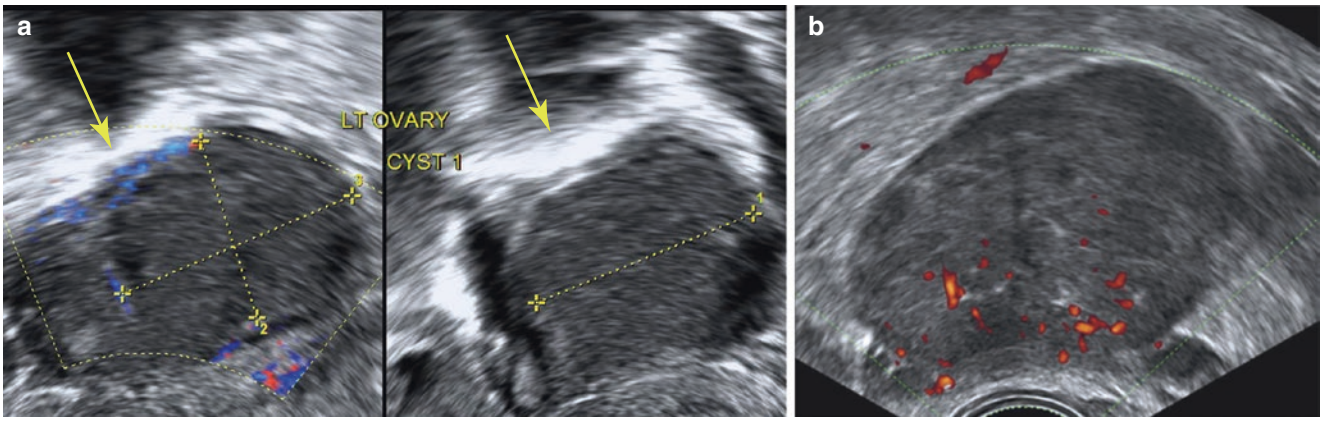

Fig. 2.39 Differentiation between cystic and solid masses. (**a**) Cystic mass with turbid contents showing acoustic enhancement (*arrows*) and no flow on Doppler within. (**b**) Solid mass showing flow within on Doppler and no acoustic enhancement

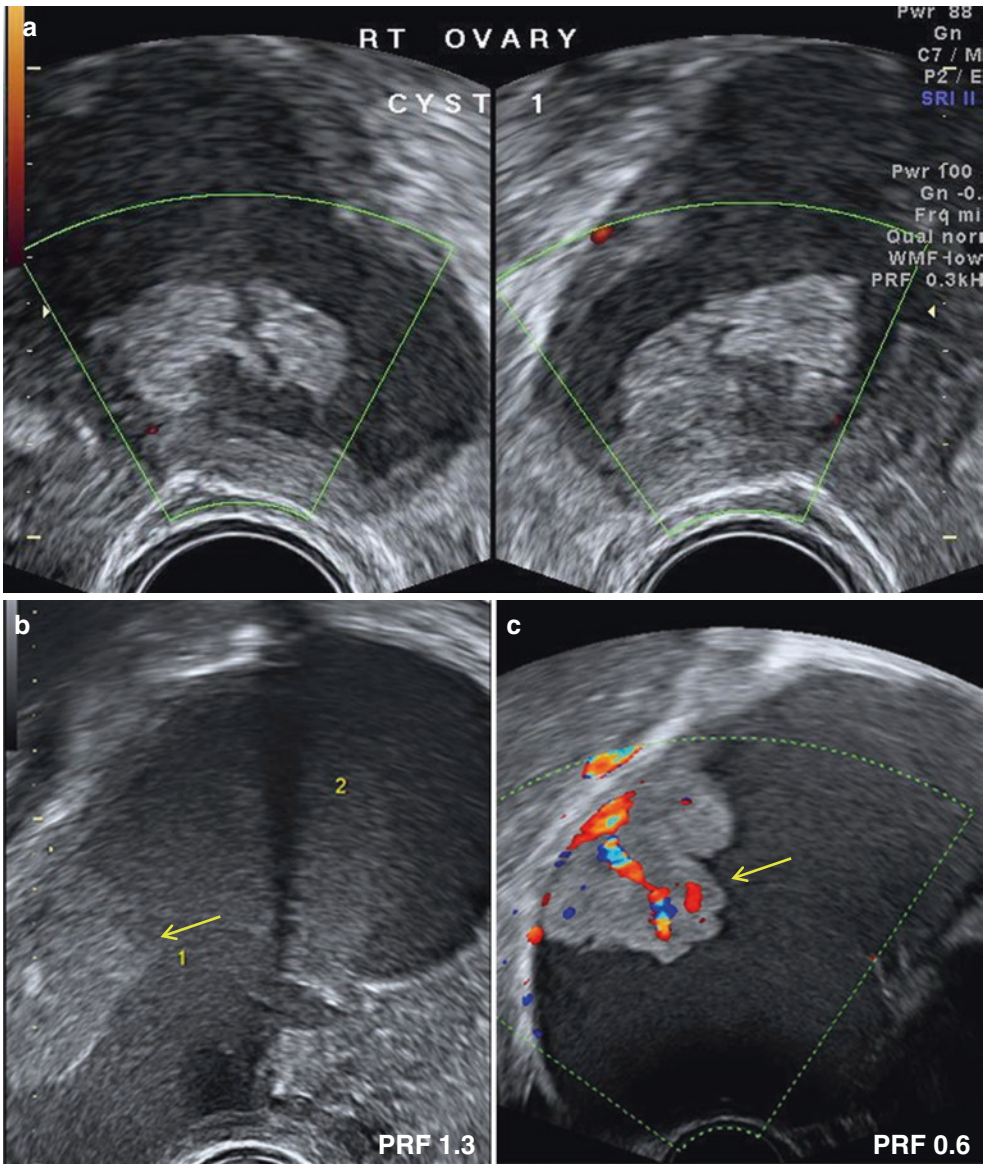

Fig. 2.40 Hyperechoic areas within a cyst. (**a**) Clot in an endometriotic cyst showing no flow on Doppler. (**b**) Cyst with a hyperechoic solid area (*arrow*) showing no flow on Doppler because of a high PRF setting of 1.3. (**c**) The same cyst seen a few months later, with the solid area (*arrow*) showing flow within on Doppler, because of an optimally low PRF of 0.6

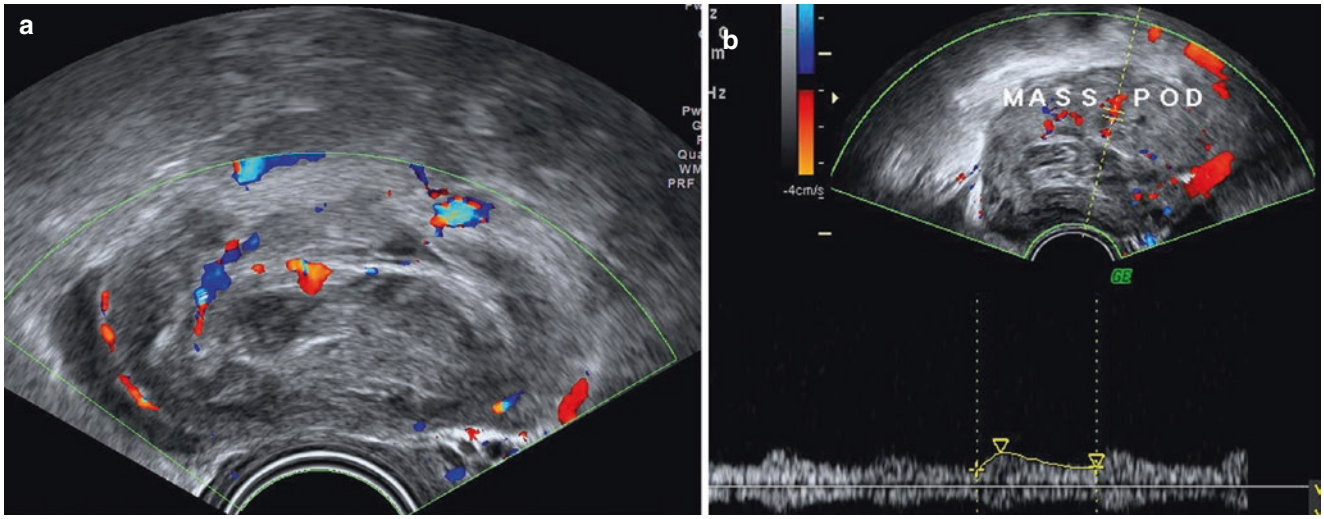

Fig. 2.41 Doppler in complex adnexal masses containing clots in two different patients with ectopic pregnancy. (**a**) Flow is seen in the tubal walls of the hematosalpinx. (**b**) Spectral tracing of flow around ectopic tissue in a hematosalpinx

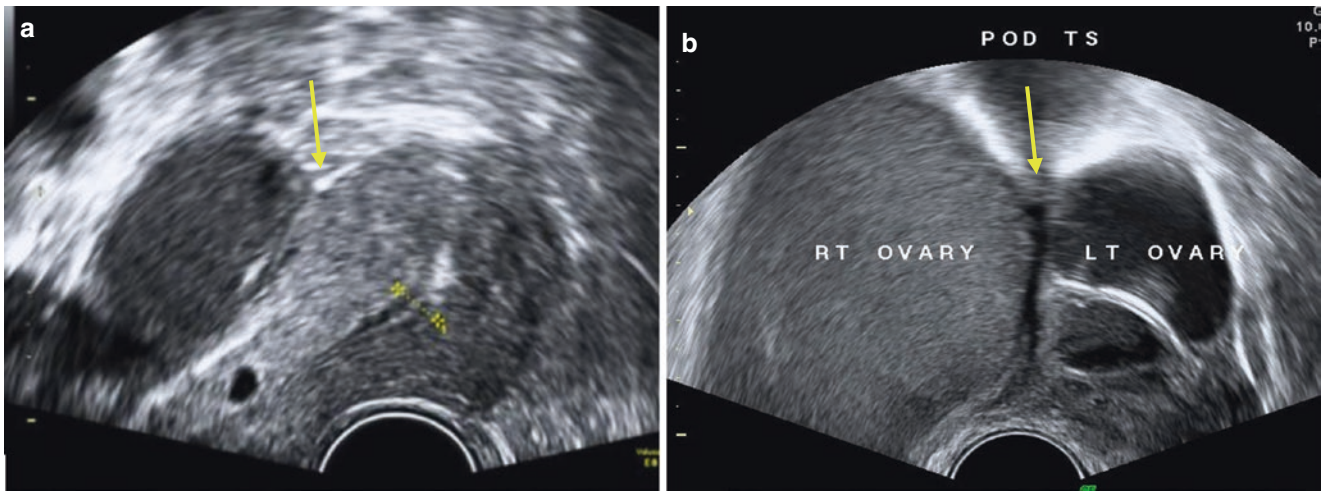

Fig. 2.42 Adherent ovaries in two different patients with endometriosis. (**a**) Ovary is adherent to the posterior wall of the uterus showing a sudden angulation (*arrow*) of its otherwise regular circumscribed margin. (**b**) Both ovaries adherent to each other with a sudden angulation seen in their contour (*arrow*)

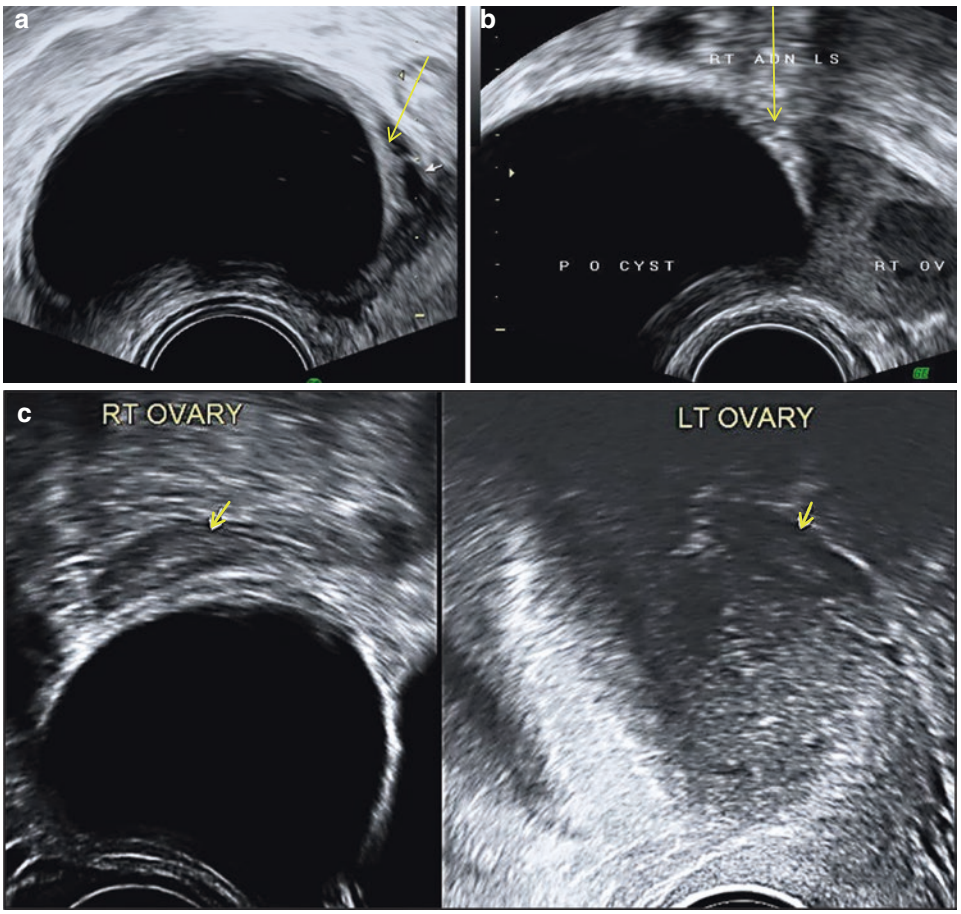

Fig. 2.43 To assess ovarian origin of a mass. (**a**) Cyst of ovarian origin showing 'crescent sign' (ovarian tissue stretched out and hugging the cyst, denoted by the *arrow*). (**b**) Paraovarian cyst with a wedge of tissue (*arrows*) intervening between the ovary and paraovarian cyst. (**c**) Atrophic ovaries (*small arrows*) seen separate from the cyst

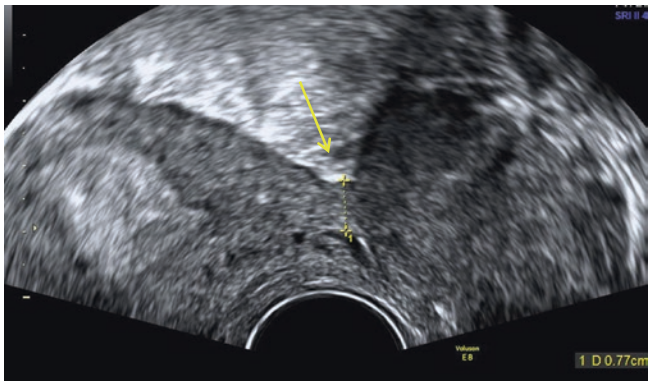

Fig. 2.44 Subserous pedunculated fibroid seen attached to the uterus by a pedicle (*arrow*)

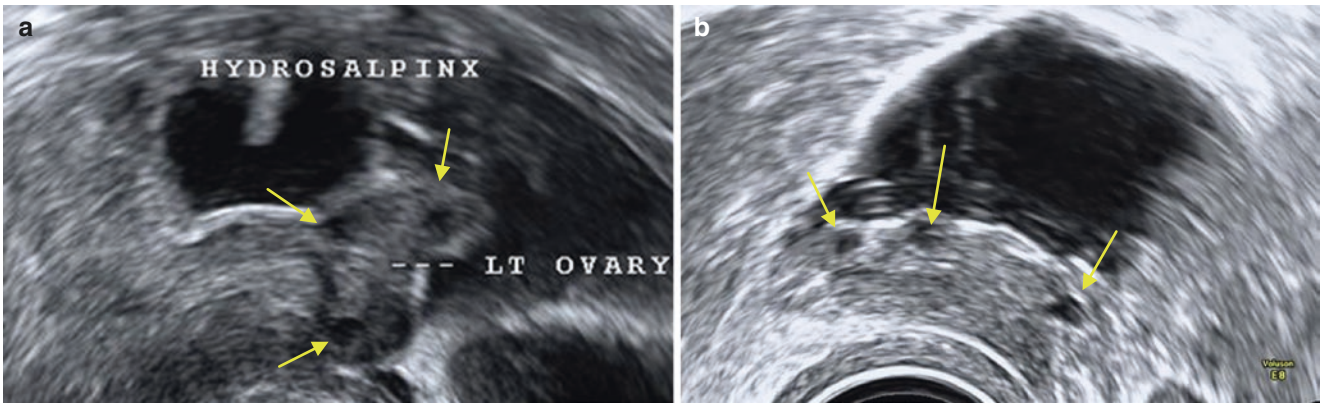

Fig. 2.45 Visualising the margins of the ovary by the presence of antral follicles (*arrows*) along its margins in two different patients. (**a**) Ovary adherent to a malignant tubal mass. (**b**) Ovary lying along one side of a pseudoperitoneal cyst

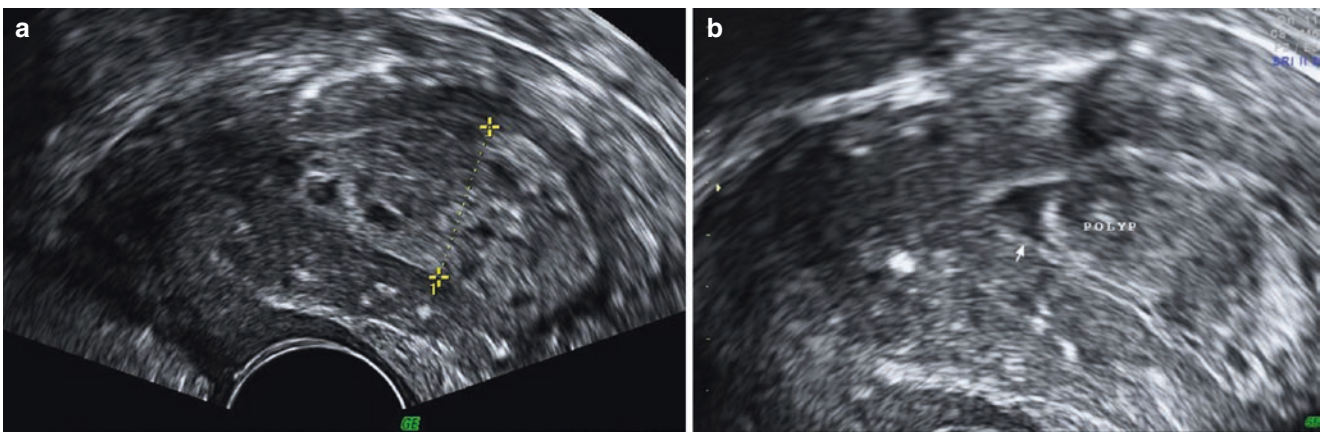

Fig. 2.46 Endometrial polyp presenting as a case with thickened endometrium. (**a**) Thick endometrium with tiny cystic spaces. (**b**) Lower end of the endometrial cavity showing minimal fluid and the lower margins of an endometrial polyp, which helped in diagnosing the condition

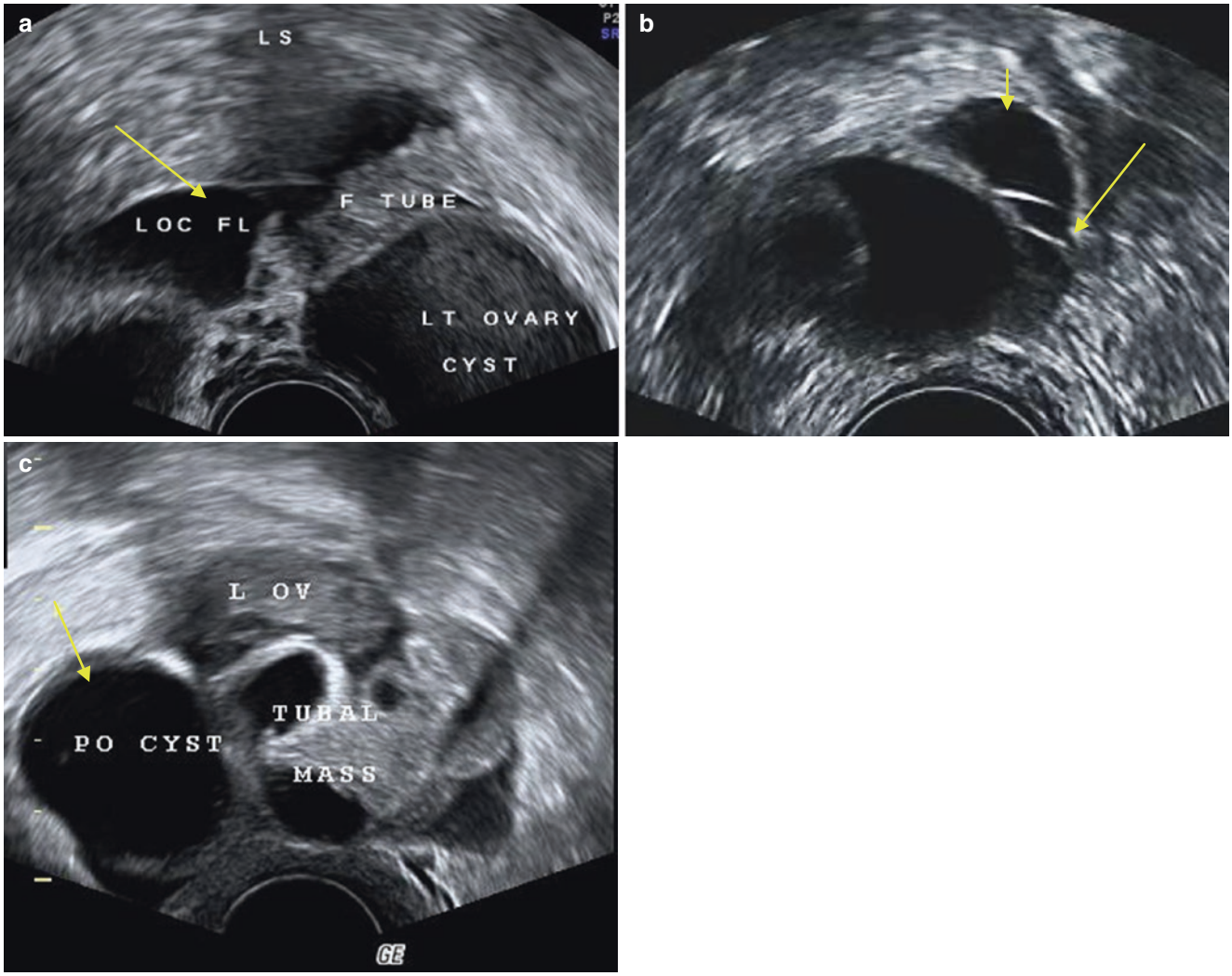

Fig. 2.47 Assessing origin of adnexal cystic areas in three different cases. (**a**) Loculated fluid (*arrow*) showing irregular margins. (**b**) Loculated periovarian fluid (*short arrow*) showing narrow extension (*long arrow*) of fluid between tissue planes. (**c**) Paraovarian cyst (*arrow*) showing circumscribed regular margins

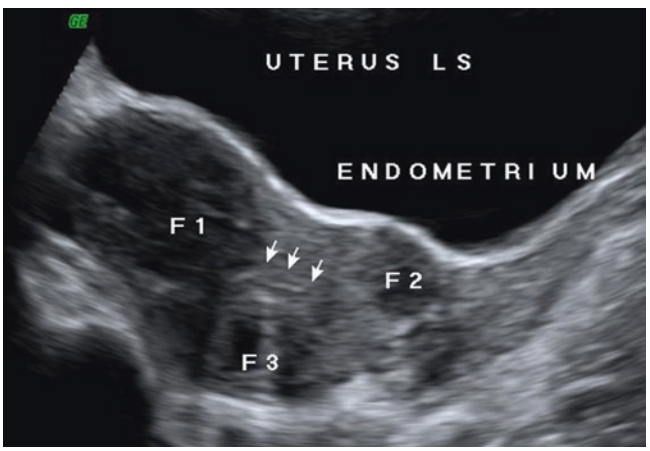

Fig. 2.48 TAS of uterus showing multiple fibroids. *Arrows* showing endometrium. Locating the endometrium is essential for fibroid mapping

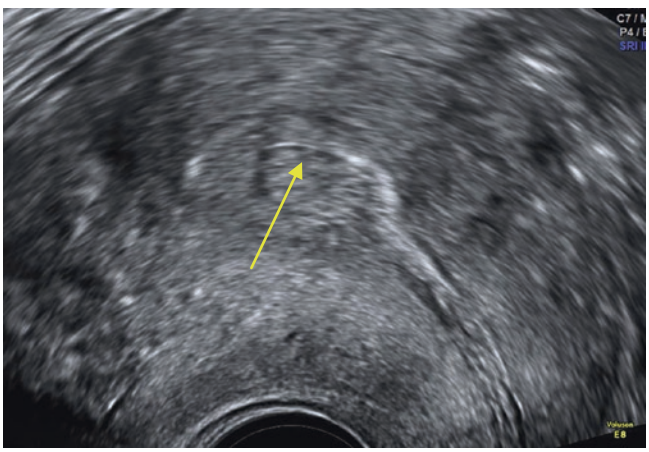

Fig. 2.49 Hyperechoic line (*arrow*) along the interface between the smooth walls of the polyp and the endometrium

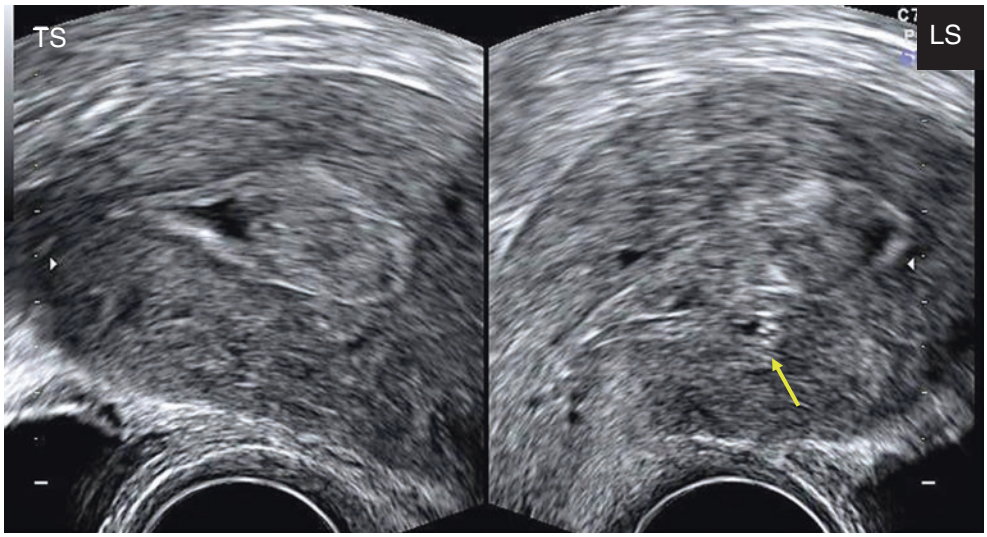

Fig. 2.50 Reproducibility of pathology in different planes. TS and LS of uterus showing RPOC. Endometrial outlines on LS are not well visualised because of the submucosal adenomyoma (*arrow*). TS views of the endometrial cavity help in confirming the presence of RPOC

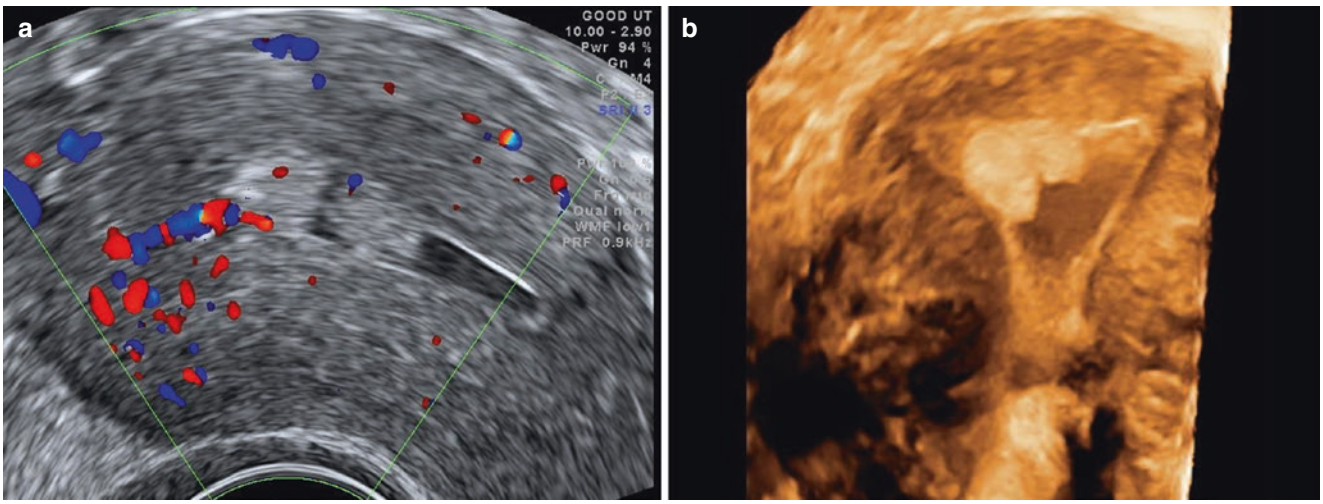

Fig. 2.51 Confirming the presence of lesion with multiple modalities. Polyps seen on greyscale confirmed by (**a**) Doppler by the presence of a feeder vessel (the feeder vessel of one of the two polyps is seen in this image) and (**b**) by 3D rendering

2.6 Sonohysterography (SHG)

Sonohysterography (Figs. 2.52, 2.53, and 2.54) is an enhanced technique of doing a transvaginal scan. This can be done with either gel or saline infusion into the endometrial cavity. Saline infusion sonohysterogram (SIS) is more popular and involves instillation of saline into the endometrial cavity with a simultaneous transvaginal scan. The advantage of instilling saline is that it distends the endometrial cavity, outlining any intracavitary lesions distinctly. SIS is more accurate than TVS for endometrial pathology and less invasive than hysteroscopy.

Indications

- Abnormal uterine bleeding.
- Thickened endometrium particularly in postmenopausal women.
- Submucous fibroids to assess its grade and the possibility of a hysteroscopic resection.
- The presence of intracavitary lesions which are difficult to delineate.
- Other indications include infertility and recurrent miscarriage.
- It can also be used to assess tubal patency.

It is contraindicated in the presence of or the suspicion of pregnancy or PID.

Technique

It should be done between Day 6 and Day 10 of the menstrual cycle when the endometrium is the thinnest and the patient is not likely to be pregnant. In postmenopausal women it can be done at any time.

Prophylactic antibiotic may be administered. In some centres the use of prophylactic antibiotic is a routine, while in other centres it is used only in those patients with known tubal occlusion or peritubal adhesions. Pain may be prevented or minimised by administering a non-steroidal anti-inflammatory drug (NSAID), half an hour to one hour prior to the procedure.

A routine transvaginal scan should be done prior to SIS. After taking the patient's written consent, the parts are cleaned with Betadine. With the help of a speculum, the cervix is visualised and may be held with the help of a tenaculum or a vulsellum, if required. A size 7 F catheter (sonohysterography catheter), flushed with saline (to ensure there are no air bubbles), is inserted into the cervical canal. In cases with cervical stenosis, a cervical dilator may be carefully used. Once the catheter is inside, the catheter balloon is inflated, and then saline, preferably warm, is instilled with the help of a syringe into the endometrial cavity. Initially about 10 ml is instilled, but if required, further instillation may be done (up to 40 ml). If the balloon of the catheter is obscuring visualisation, it may be deflated. It has been noticed that Doppler flows in tissues may be minimised during SIS due to the pressure effect of the instilled fluid.

The presence of air bubbles and suboptimal distension of the endometrial cavity may result in poor evaluation of endometrial pathology. SIS may be technically unsuccessful if the cervix is stenosed and the catheter cannot be passed through the cervical canal or if the endometrial cavity cannot be distended.

This procedure can also be done using a size 7 infant feeding tube which is stiffer and easier to insert into the endometrial cavity. The disadvantage, however, is that very often the instilled saline may drain out quickly, resulting in suboptimal distension of the endometrial cavity.

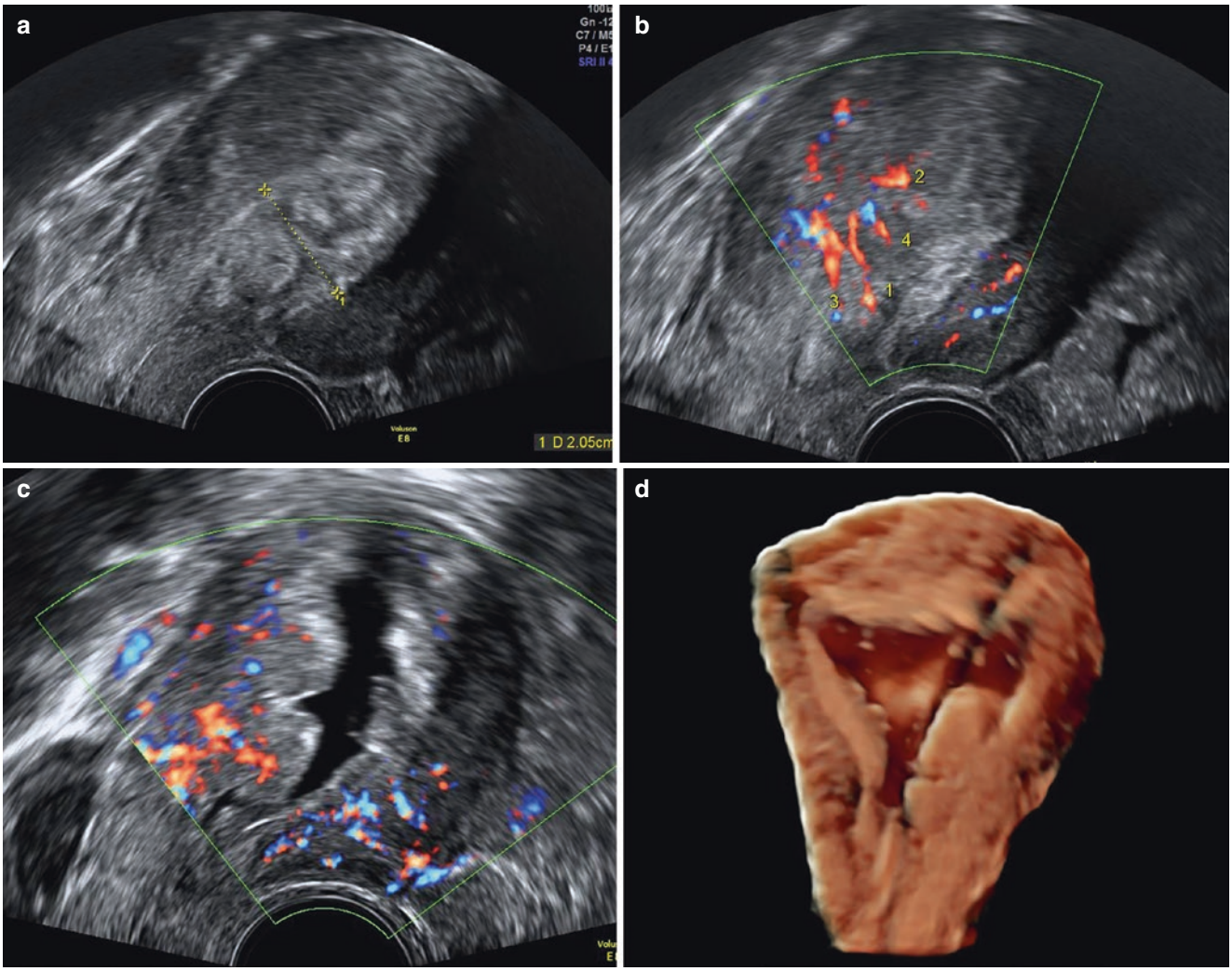

Fig. 2.52 A case of cystic hyperplasia with polypoid endometrium. (**a**) Regular TVS – greyscale image of uterus showing thickened complex endometrium. (**b**) Doppler showing multiple vessels crossing the EMJ on regular TVS. (**c**) SHG showing fluid in the endometrial cavity and a posterior polypoidal endometrium with vascular flow. (**d**) SHG with 3D rendered image of the uterus showing the polypoidal endometrium along its lateral walls

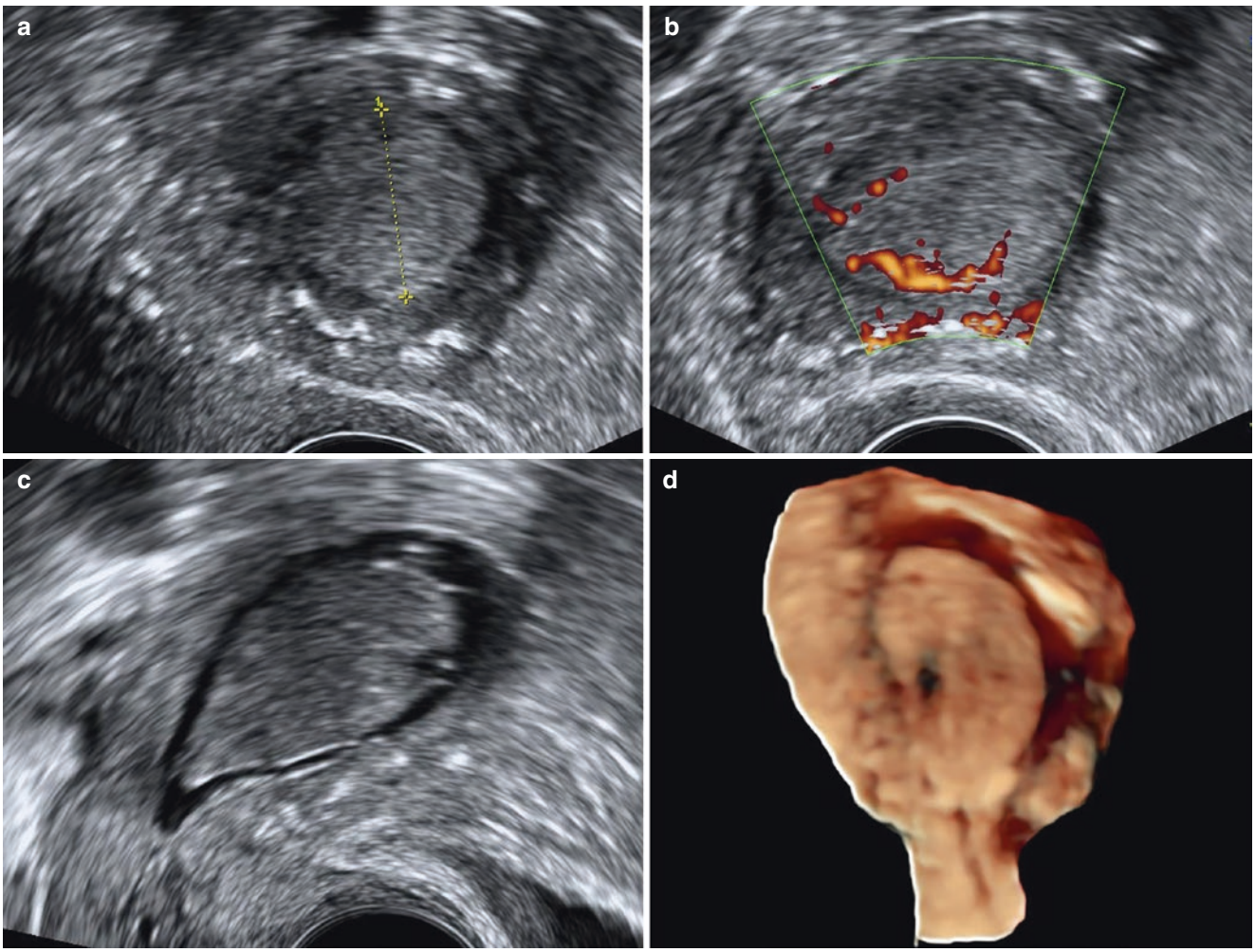

Fig. 2.53 Endometrial polyp in a postmenopausal patient. (**a**) Regular TVS showing a thick hyperechoic endometrium of 19 mm. (**b**) Regular TVS showing vessels in the endometrium on Doppler. No single prominent feeder vessel was, however, noted. (**c**) SHG showing an unanticipated teardrop-shaped large endometrial polyp conforming to the shape of the endometrial cavity. (**d**) 3D rendered image showing the endometrial polyp attached to the posterolateral wall of the uterus

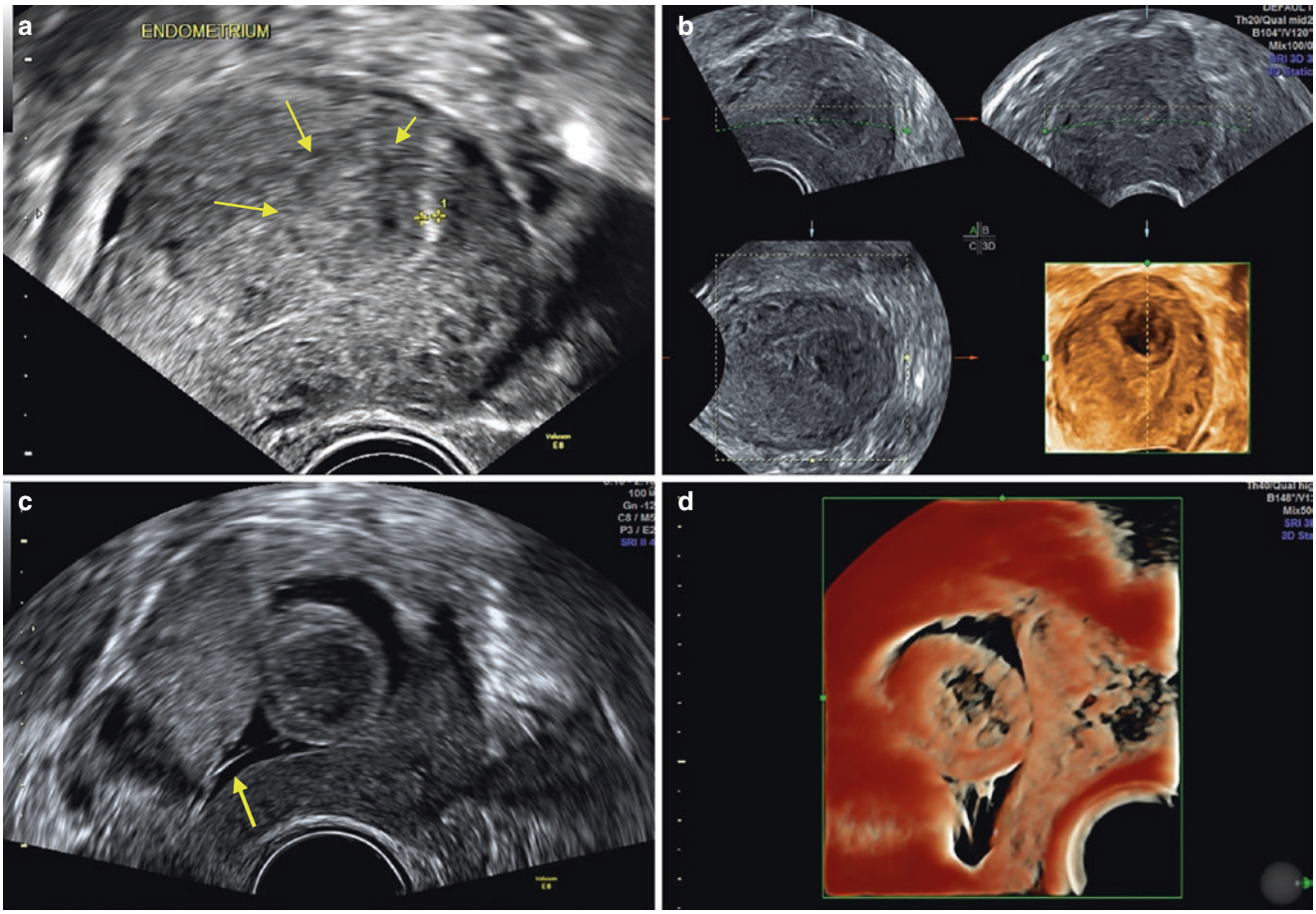

Fig. 2.54 Submucous fibroid. (**a**) Regular TVS showing a poorly defined fibroid in the endometrial cavity with the anterior endometrium measured. (**b**) Regular TVS with 3D rendering. The fibroid seen in multiplanar view. (**c**) SHG on greyscale showing a completely intracavitary submucous fibroid arising from the posterior wall. Catheter seen in situ (*arrow*). (**d**) SHG with 3D rendering showing completely intracavitary submucous fibroid

2.7 Gel Sonovaginography (GSV)

Gel sonovaginography is an enhanced technique of doing a transvaginal scan, wherein about 20 ml of ultrasound gel is instilled into the vagina, followed by ultrasound evaluation by a transvaginal probe.

Visualisation of the cervix and vagina is known to be suboptimal on regular transvaginal scan. This is primarily because of close proximity of these structures to the transvaginal probe and the collapsed vaginal lumen. The advantages of instilling intravaginal gel are:

- It creates a stand-off between the probe and the structures that have been evaluated resulting in better resolution.
- The intravaginal gel partially distends the vagina, so spatial orientation, relationship between various structures and inner vaginal contours are better assessed.
- It surrounds the various structures (cervix, vagina and any lesion) and fills narrow gaps between tissue planes, thereby enhancing delineation.

GSV is therefore useful in assessing a variety of known or suspected local pathologies of the cervix and vagina (and surrounding structures), where regular TVS is known to have its limitations. Its utility also lies in its capability to rule out pathology in suspected cases.

Indications

Cases are selected predominantly during the process of regular TVS, when a lesion is either seen or suspected (which include a mass, an area of increased vascularity, a feeder vessel in the cervical canal, thickened vaginal walls and uterine anomalies). Other cases are those, where the referring clinician has seen or has a strong suspicion of some local pathology on bimanual or per speculum. *GSV is not done on pregnant women and on women with active bleeding*.

GSV can be used in cases with:

- Uterine anomalies: to assess the cervix and vagina for any septum.
- Cervical polyps (Fig. 2.56): to assess the number, size, location, origin and vascularity of the polyps.
- Cervical and vaginal cancers (Fig. 2.57): to assess the presence of the lesion, its vascularity, location and extent.
- Deep infiltrating endometriosis: to assess the involvement and extent of lesions in the cervix, vagina and anterior rectal wall.

Technique (Fig. 2.55)

Following a regular TVS, consent should be taken after informing the patient of the procedure. A 20 ml syringe is filled with ultrasound gel in such a manner that there are minimal air bubbles within. To fill in such a manner, a fresh new bottle of gel (company packed) is held with its mouth facing downwards, preferably by an assistant. The syringe is introduced into the lower part of the inverted bottle. Then, instead of pulling the plunger out to fill the syringe, as is the usual practice, the plunger is held steady in position, and the barrel (outer sleeve) is slowly pushed further up into the inverted bottle of gel so as to fill the 20 ml syringe with minimal air bubbles within. Next, the syringe is gently introduced into the vagina directed by the fingers of the right hand in the vagina. The fingers of the right hand are then removed and the syringe gently pushed further inside the vagina to introduce the gel into the upper vagina (mainly in the posterior fornix).

It is important to assess the lower vagina initially before assessing the upper vagina and the cervix. The initial few minutes are the best time to make the assessment, as with the passage of time, air bubbles begin to collect along the surface of the cervix and upper vagina.

After completing the examination, the patient is asked to empty her bladder once more and strain after doing so, so that most of the gel passes out.

If too many air bubbles are introduced accidentally, preventing proper evaluation, repeating the procedure in the same sitting is not helpful in dismissing the air bubbles. In such cases, gel sonovaginography can be redone the following day with good results.

GSV is an effective technique for assessment of a variety of known or suspected local cervical and vaginal pathologies, where regular TVS is known to have its limitations. It is well tolerated in an outpatient setting, requires a single operator and can be performed at a single visit as an extension of regular TVS.

Cases where GSV has been resorted to have been referenced throughout the book in various chapters depending upon the pathology studied.

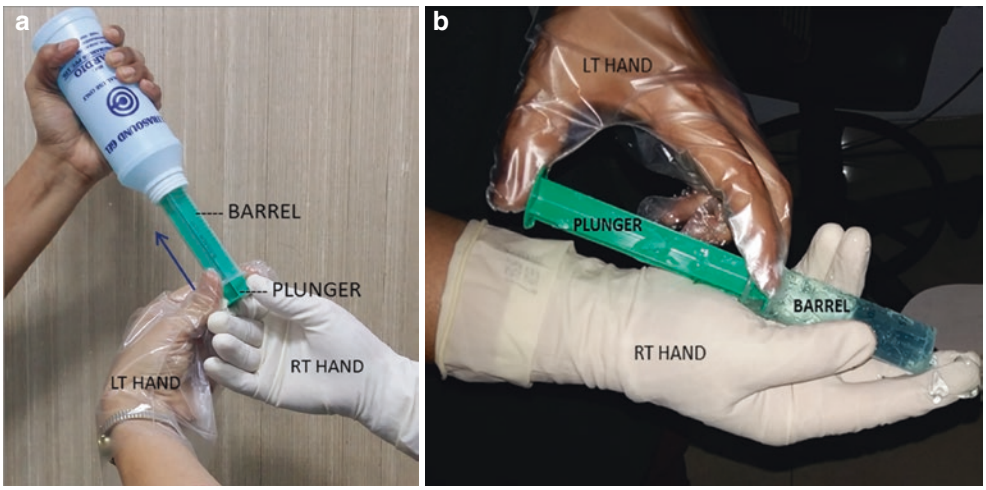

Fig. 2.55 Technique of GSV. (**a**) Technique of filling the 20 ml syringe. A bottle container of ultrasound gel is held with its mouth facing downwards, and the syringe is introduced into the lower part of the inverted bottle. The plunger is held steady in position and the outer barrel is slowly pushed further up into the inverted bottle of gel so as to fill the syringe. (**b**) Technique of instilling gel into the vagina. The syringe is held in such a manner that its tip (hub end) lies in the groove between the index and the middle finger. It is then gently introduced into the vagina, directed by the fingers of the right hand in the vagina. The fingers of the right hand are then removed and the syringe gently advanced into the vagina. The plunger of the syringe is pushed, thus introducing the gel into the vagina

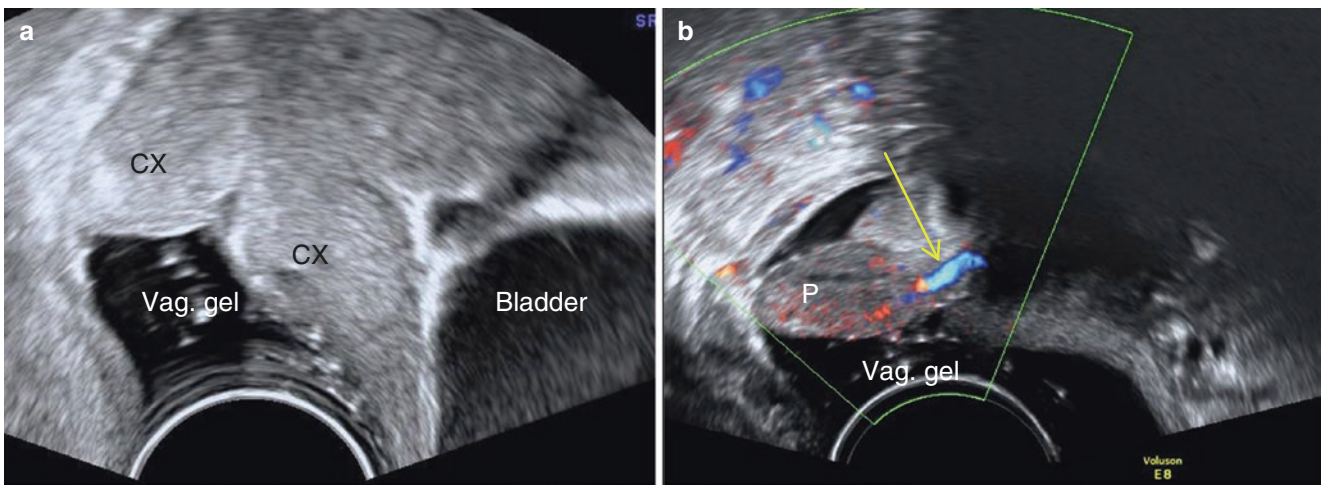

Fig. 2.56 GSV. (**a**) LS of the normal cervix and vagina. (**b**) LS of the cervix and vagina showing a cervical polyp (P) with a feeder vessel (*arrow*)

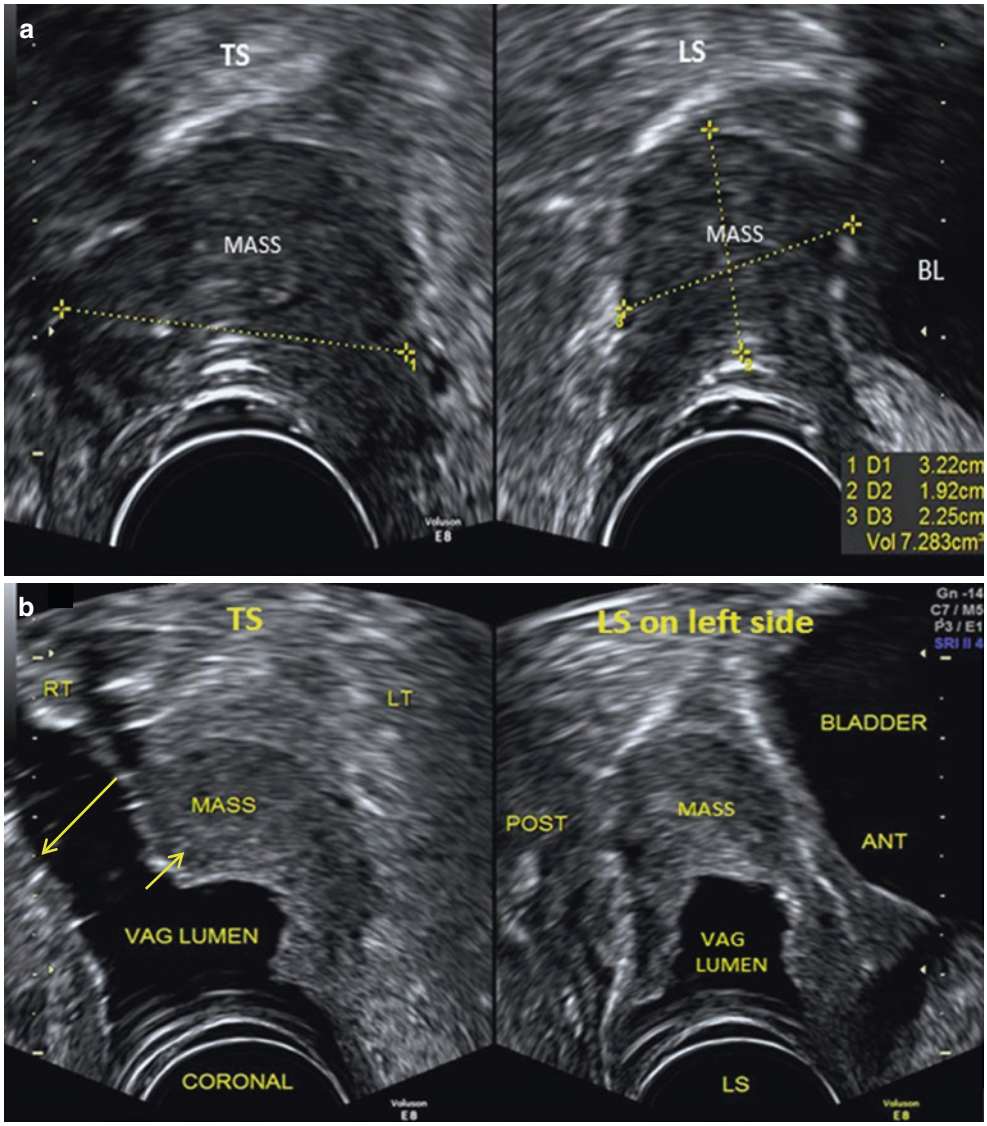

Fig. 2.57 Vaginal cancer in a post-hysterectomy patient. (**a**) Mass seen at vaginal vault on regular TVS is measured – vaginal walls not delineated. (**b**) GSV – vaginal walls (*long arrow*) and tumour mass (*short arrow*) well visualised. Image (**b**) with gel corresponds to image (**a**) without gel

Suggested Reading

Allison SJ et al (2011) Saline-infused Sonohysterography: Tips for Achieving Greater Success. Radiographics 31(7):1991–2004

Ando H et al (2004) Which infertile women should be indicated for sonohysterography? Ultrasound Obstet Gynecol 24:566–571. doi:10.1002/uog.172

Jurkovic D (2002) Three-dimensional ultrasound in gynecology: a critical evaluation. Ultrasound Obstet Gynecol 19:109–117. doi:10.1046/j.0960-7692.2001.00654

Schwärzler P et al (1998) An evaluation of sonohysterography and diagnostic hysteroscopy for the assessment of intrauterine pathology. Ultrasound Obstet Gynecol 11:337–342. doi:10.1046/j.1469-0705.1998.11050337

Sibal M (2016) Gel Sonovaginography: A New Way of Evaluating a Variety of Local Vaginal and Cervical Disorders. J Ultrasound Med 35(12):2699–2715

Sladkevicius P et al (2007) Contribution of morphological assessment of the vessel tree by three-dimensional ultrasound to a correct diagnosis of malignancy in ovarian masses. Ultrasound Obstet Gynecol 30:874–882. doi:10.1002/uog.5150

Testa AC et al (2009) Dynamic and interactive gynecological ultrasound examination. Ultrasound Obstet Gynecol 34:225–229. doi:10.1002/uog.7309

Ultrasound Evaluation of Myometrium

3

The myometrium is the muscular tissue of the uterus and the cervix, which encloses the uterine cavity and its lining, the endometrium. The myometrium is generally isoechoic (similar to the liver) and homogeneous. The myometrial echogenicity, thickness, contour and presence of any mass or cysts are noted during ultrasound examination. The two commonly encountered pathologies of the myometrium are fibroids and adenomyosis.

3.1 Evaluation of Myometrium

The myometrium can be evaluated both on transabdominal and transvaginal scan. Ideally, like in all other conditions, both TAS and TVS should be done, as they complement each other. In myometrial pathologies like fibroids and adenomyosis, the uterus is sometimes of large size extending beyond the pelvis, and a TAS becomes essential to evaluate the uterus. In addition, TVS may be suboptimal if there is a large mass (like a fibroid) in the cervix or lower corpus that causes shadowing and prevents assessment of the structures above it. When the uterus is of a large size, one may not require a very full bladder because the large uterus itself often pushes the bowels away into the upper abdomen.

The evaluation of the uterus should be systematic, and reporting should be standardised. The MUSA (Morphological Uterus Sonographic Assessment) statement is a consensus statement by a panel of experts (MUSA consensus group) for terms, definitions and measurements for describing and reporting the myometrium and its pathologies. The terms and definitions laid down by the MUSA will be relied on for the most part in this chapter.

The uterus is first evaluated in the sagittal and transverse sections on 2D. 3D is used to get a coronal section of the uterus, which provides good information of the external uterine contour, cavity shape, endomyometrial junction and relation of myometrial pathology to the endometrial mucosa and serosa. Dopplers are used as and when relevant, typically when pathology is noted.

Measurements (Figs. 3.1, 3.2 and 3.3)

- *Uterine size*: With myometrial pathologies, the uterus is often enlarged. It could be asymmetrically enlarged or globally enlarged. The uterus is measured in three dimensions:
  - The total length of the uterus is the length from the upper margin of the uterine fundus to the external os in the sagittal section of the uterus.
  - The anteroposterior diameter of the uterus is the maximum AP measurement in the sagittal section of the uterus.
  - The transverse diameter of the uterus is the maximum transverse measurement taken in the transverse section of the uterus.
- The thickness of the anterior and posterior myometrial walls is measured from the external uterine serosa to the endometrial margins and should include the JZ. The measurement is done in the sagittal plane, perpendicular to the endometrium, in a single image where the endometrium is thickest. The myometrial walls are not measured routinely, unless there is some pathology or asymmetry noted.
- Any mass, like a fibroid, seen within the myometrium is measured in three orthogonal dimensions (three measurements perpendicular to each other), in two images whose plane is perpendicular to each other (as explained in Chap. 2).

Qualitative Assessment of the Myometrium (Fig. 3.4)

- The outer serosal contour of the uterus is noted to see if it is regular or not.
- The uterine myometrial echogenicity is assessed as uniform (homogeneous) or non-uniform (heterogeneous).
- The normal myometrium is used as a standard to evaluate echogenicity of other structures in the myometrium, i.e., structures that are as echogenic as the normal myometrium are considered to be isoechoic. Lesions that are less echogenic are termed hypoechoic, whereas those which are more echogenic are termed hyperechoic.

M. Sibal, *Ultrasound in Gynecology*, DOI 10.1007/978-981-10-2714-7_3

- The symmetry of the myometrial walls is then assessed. Asymmetrical thickening of the myometrium is often due to pathology. If the walls are of symmetric thickness, then one does not need to measure them.
- The myometrium is also assessed for the presence of any mass or cyst. These are further assessed for their echogenicity, blood flows, acoustic shadowing and relation to the endometrial mucosa and outer serosa.
- In order to assess the location of the pathology in the myometrium, it is important to delineate the endometrial cavity which could be a challenge when there are existing myometrial pathologies like fibroids. One useful tip that may help to trace the endometrium is to find the cervical canal and trace it upwards.

Assessing the 'Junctional Zone' (JZ) (Fig. 3.5)
The junctional zone is basically the inner myometrium composed of longitudinal and circular closely packed smooth muscle fibres. The JZ is visualised as a hypoechoic (dark), halo (layer) just beside the endometrium. It is clearly visualised on 3D rendered images and VCI (discussed in Chap. 2).

- The JZ may be well defined or poorly defined.
- It may be regular, irregular or interrupted.
- It may not be possible to assess the junctional zone in a mid-positioned uterus or shadowing by fibroids.
- In adenomyosis (discussed later in a separate section), the JZ shows tiny cystic spaces, hyperechogenic dots, hyperechoic buds or echogenic lines. It may also be thickened in cases of adenomyosis.

Doppler Assessment (Figs. 3.6 and 3.7)
The arcuate vessels can be seen in the outer part of the myometrium running parallel to the serosa. Perpendicular to the arcuate vessels are the radial arteries and veins. Flow can be seen in these arcuate and radial vessels of the myometrium. Power Doppler is preferred to colour Doppler in assessing flows in the myometrium because power Doppler is more sensitive to detect flows in small vessels and low-velocity flows.

Whenever a lesion is visualised, its vascularity should be reported using subjective colour scoring from 1 to 4 (discussed in detail in Chap. 2 under the section on Doppler). One can also do a spectral flow analysis to assess resistance to flow (RI or PI) and flow velocity (PSV) in a vessel.

Lesions of the myometrium may show circumferential flow running along the periphery of the lesion or intralesional flow running through the mass.

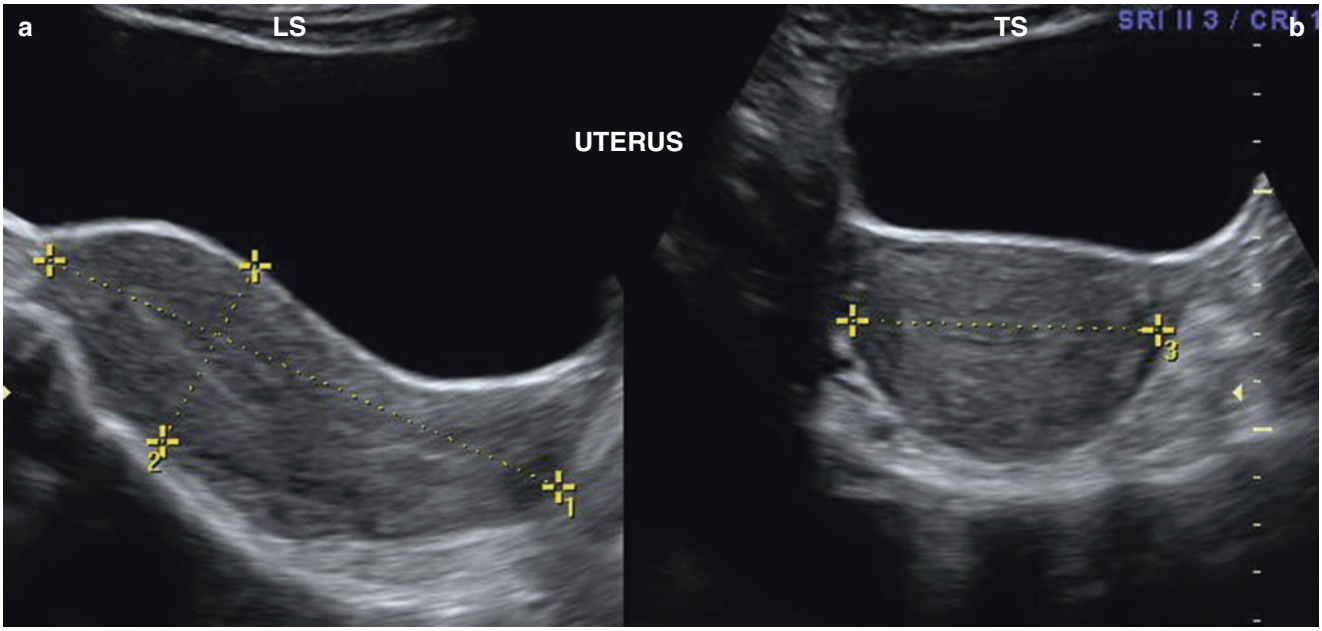

Fig. 3.1 Uterus measured on TAS. (**a**) LS and (**b**) TS views

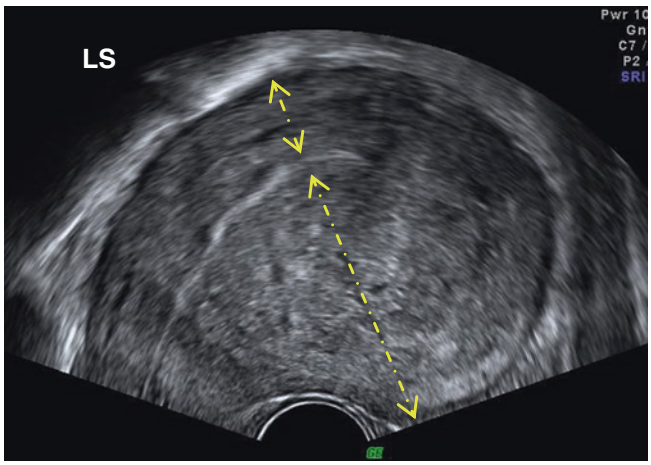

Fig. 3.2 Thickness of asymmetrical myometrial walls measured in a midsagittal section, perpendicular to the endometrium. The anterior wall is much thicker than the posterior wall

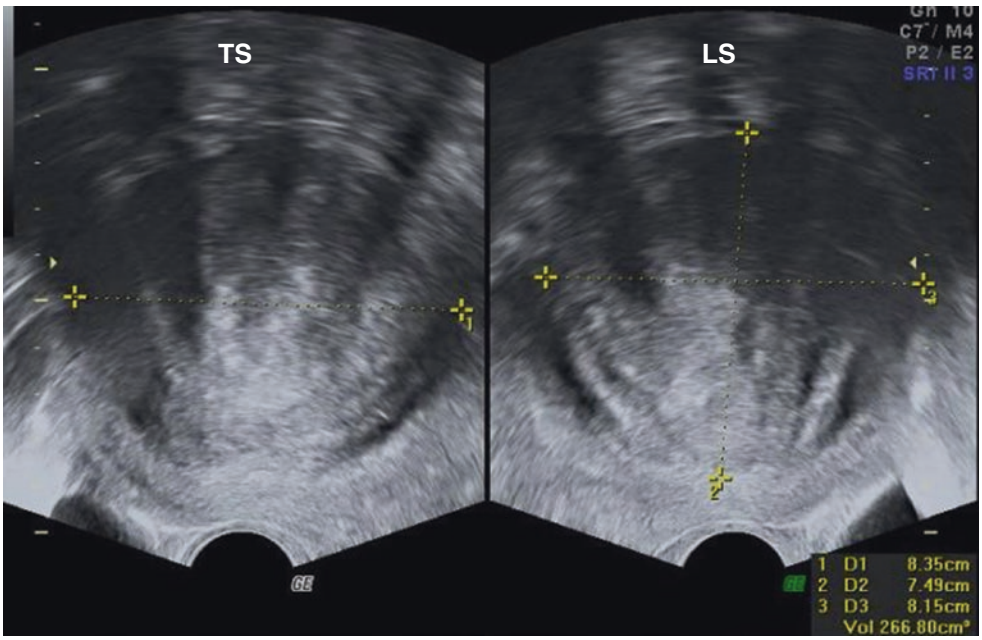

Fig. 3.3 Myometrial fibroid measured in three dimensions in two perpendicular planes

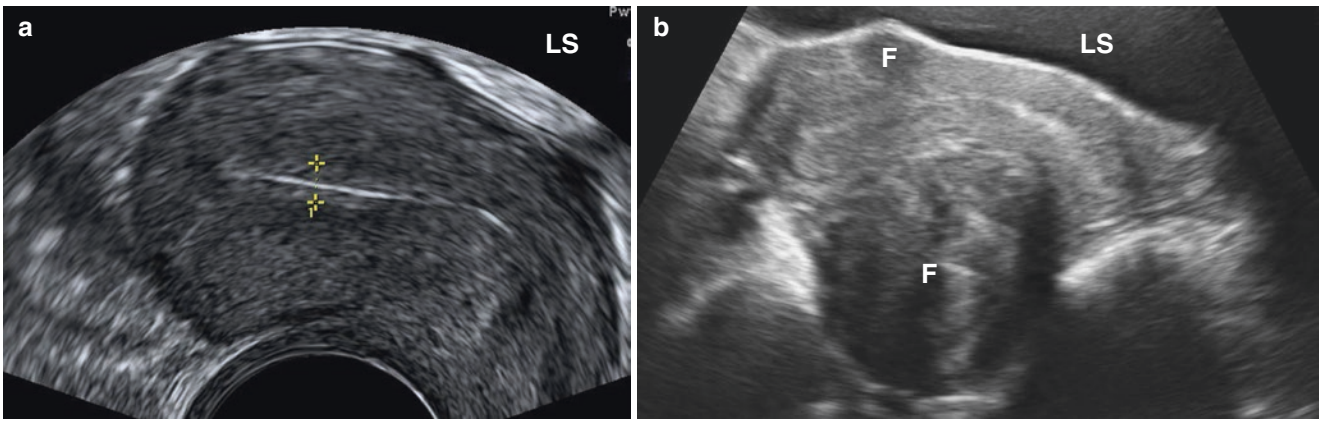

Fig. 3.4 Contour of uterus in two different cases. (**a**) Regular, in a normal uterus. (**b**) Irregular in a uterus with multiple fibroids (F), which are seen as circumscribed hypoechoic masses with shadowing

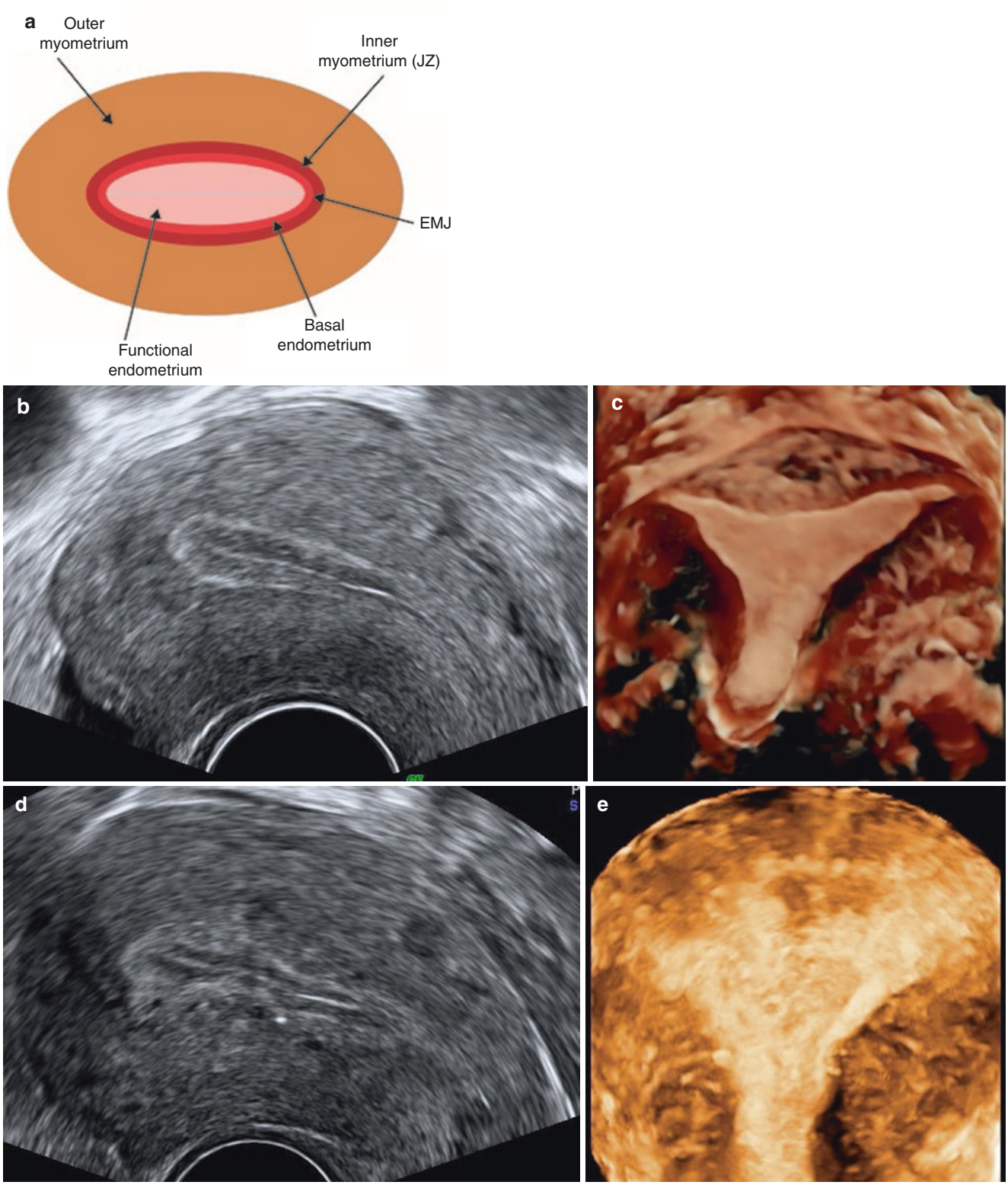

Fig. 3.5 Endomyometrial junction (EMJ). (**a**) Diagrammatic representation. (**b**, **c**) Regular EMJ on 2D and 3D. (**d**, **e**) Irregular EMJ on 2D and 3D in a patient with adenomyosis

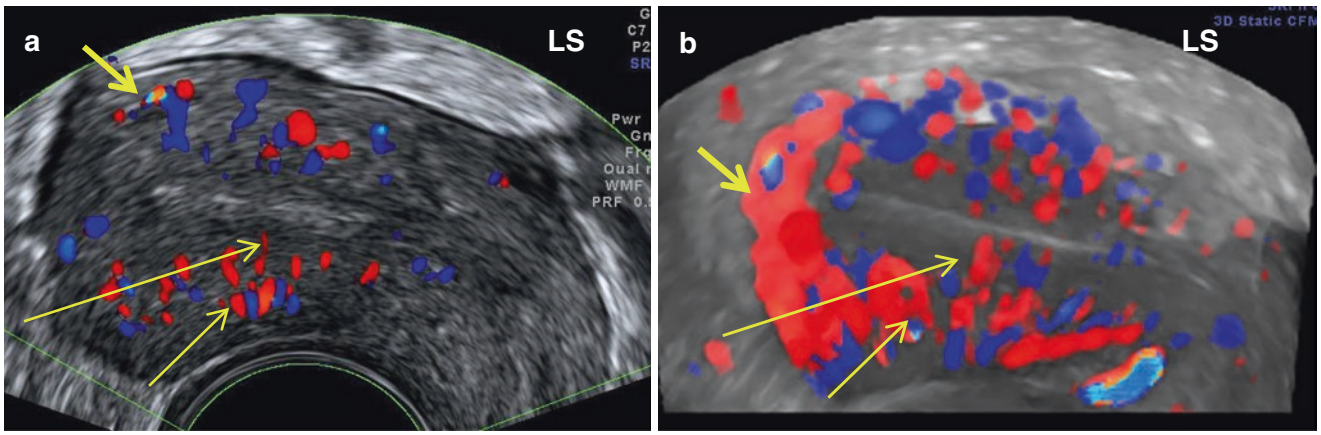

Fig. 3.6 Normal vasculature of myometrium on (**a**) colour Doppler and (**b**) on 3D glass body display. *Short thick arrows* showing arcuate vessels, *medium-sized arrows* showing radial vessels and *long arrows* showing spiral vessels

Fig. 3.7 Peripheral flow seen on Doppler around a fibroid

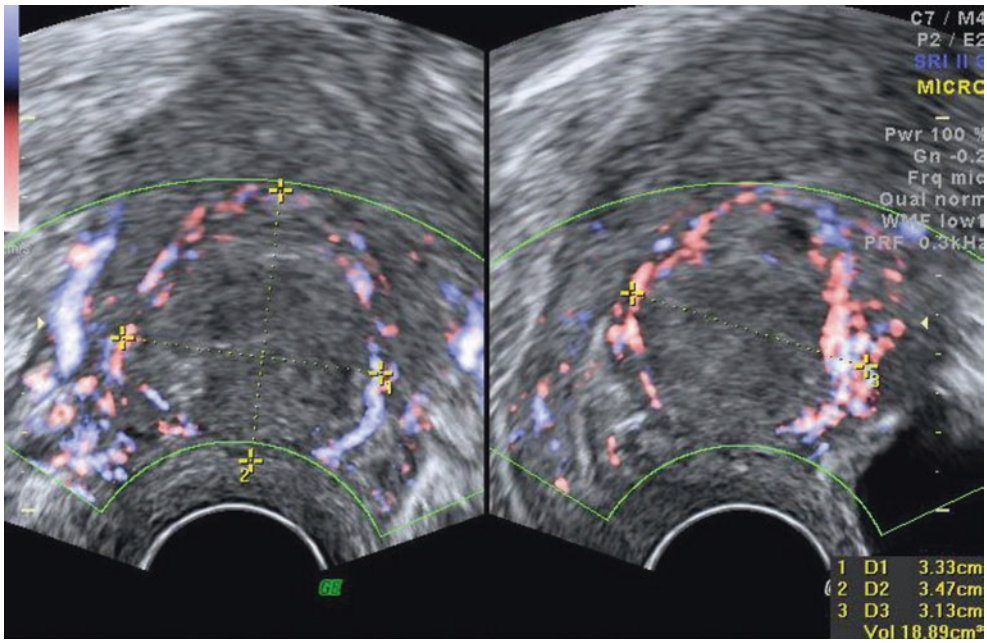

3.2 Normal Myometrium (Figs. 3.8, 3.9 and 3.10)

Uterine size, myometrial thickness and the proportion of the uterine body to the cervix change with the age of an individual and occurrence of pregnancy.

Neonatal uterus: The uterus is relatively prominent because of exposure to maternal hormones with an average uterine length of 3.5 cm and thickness of 1.4 cm.

Paediatric uterus (Fig. 3.8): The uterus in the paediatric age group is usually less than 3 cm and becomes 3–4.5 cm in the prepubertal age group. At puberty the uterus is usually 5–8 cm long. The cervix in the paediatric age group is prominent and equal in proportion to the uterine body. At puberty, the uterine body becomes thicker and pear shaped with a uterine body to cervix ratio of about 1.5: 1.

Uterus in the reproductive age group (Fig. 3.9): The size of the normal uterus varies with parity. Dimensions of a normal uterus are about 8 cm in length, 4 cm in AP diameter and 5 cm in width, with the multiparous uterus being about a centimetre larger in each dimension. The uterine body is approximately twice the size of the cervix. After delivery, the uterus undergoes physiological evolution during the 6–8 weeks of puerperium to return to its normal size. Immediately after delivery, the uterus is about 20 cm in length, and after 3 weeks, it is about 11 cm in length.

Postmenopausal uterus (Fig. 3.10): The uterus is smaller in size, usually less than 7.5 cm. This of course depends on the time since menopause, parity of the patient and the presence of pre-existing myometrial pathology. The uterine body to cervix ratio approaches 1:1. In elderly postmenopausal women (particularly those with vascular disease, diabetes or hypertension), calcified arcuate vessels are noted. These are seen in the outer myometrium as peripheral bright scattered foci with some shadowing which are arranged circumferentially around the uterus.

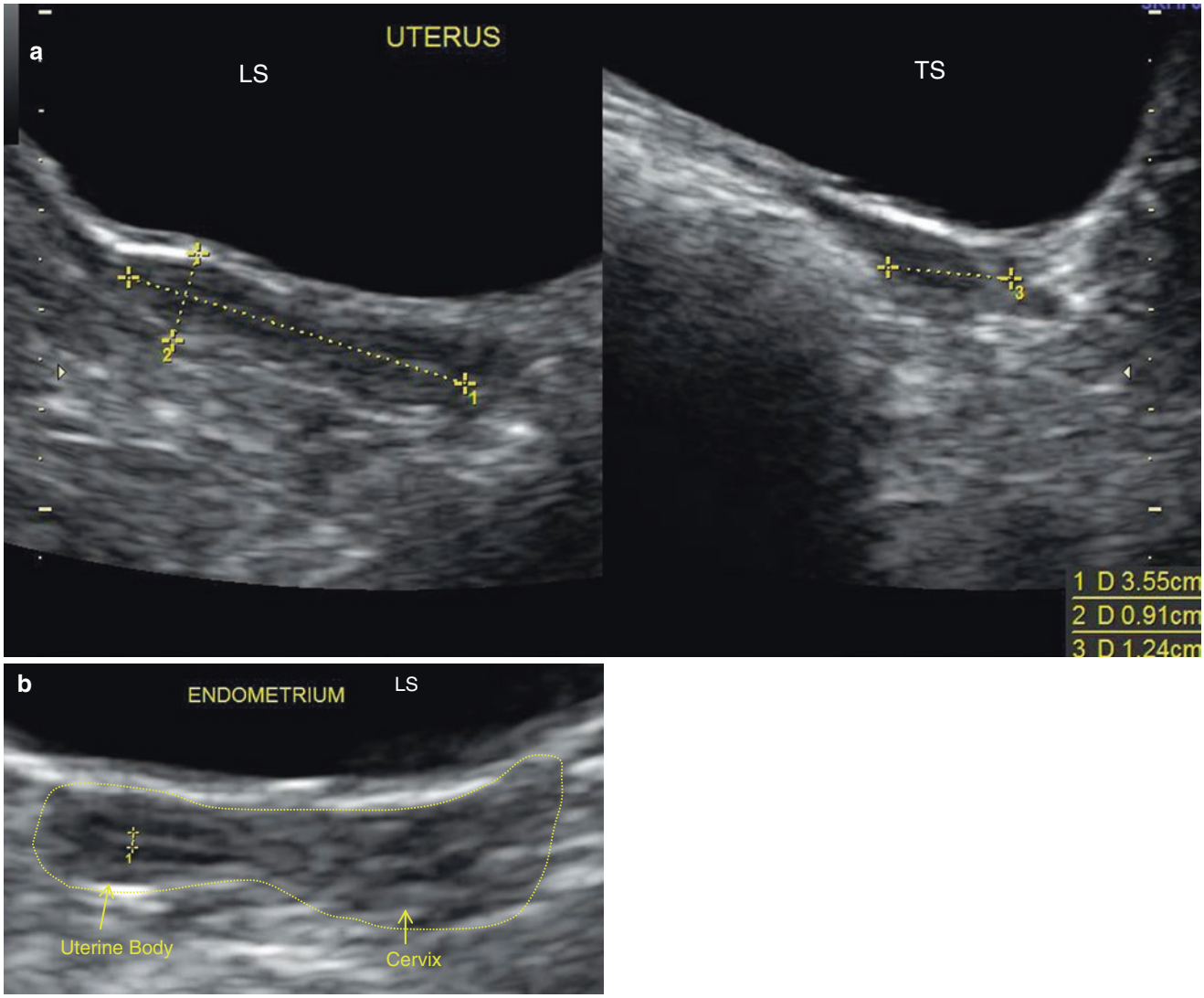

Fig. 3.8 Prepubertal uterus (**a**) measuring 3.5 × 0.9 × 1.2 cm. (**b**) Cervix appears relatively bulkier than the uterus

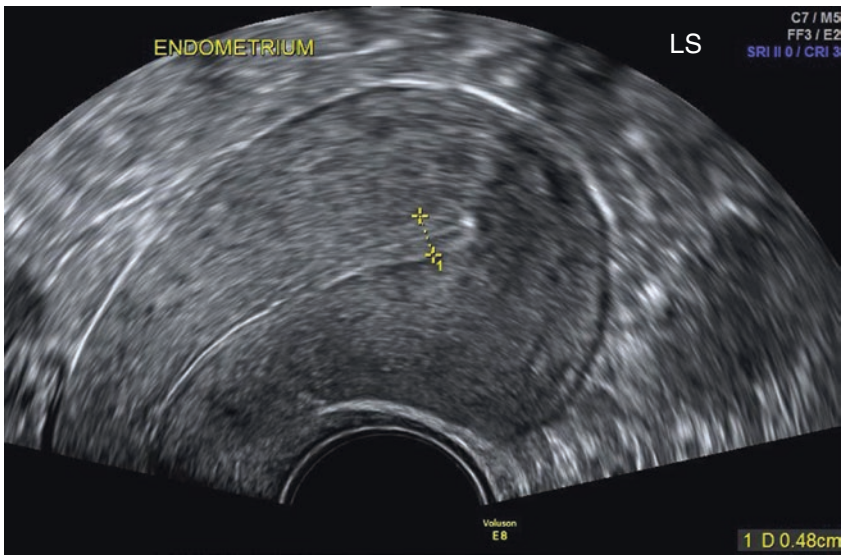

Fig. 3.9 Uterus in a patient of the reproductive age group showing normal homogeneous myometrium

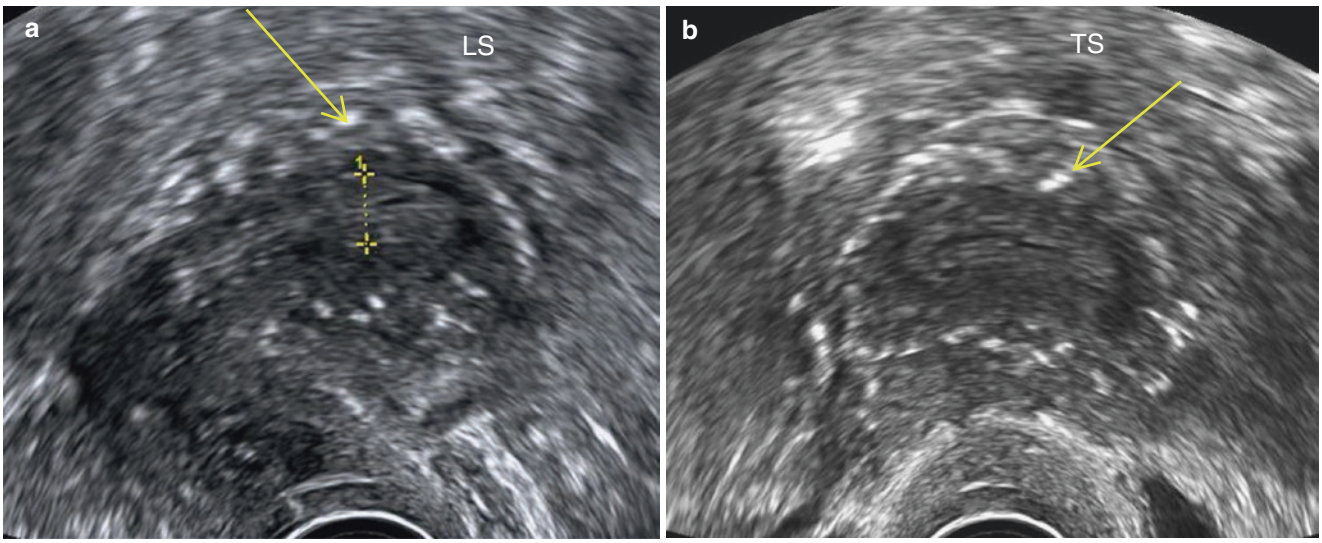

Fig. 3.10 Postmenopausal uterus with calcified arcuate vessels seen as hyperechoic scattered foci close to the uterine periphery (*arrows*), on (**a**) LS and (**b**) TS of the uterus

3.3 Fibroids (Leiomyoma or Myoma)

Fibroids, also known as leiomyomas, are benign tumours of the myometrium. They are composed of smooth muscle cells and connective tissue in densely packed whorls. They are common, and about 40 % of women by the age of 40 years have fibroids. Very often they are multiple.

Many of the women with fibroids are asymptomatic, while others may have symptoms like menorrhagia, polymenorrhagia, intermenstrual bleeding, dysmenorrhoea and subfertility. With submucous fibroids and fibroid polyps, intermenstrual bleeding (metrorrhagia) could be a presenting complaint.

Ultrasound Features of Fibroids (Figs. 3.11, 3.12, 3.13, 3.14, 3.15, 3.16 and 3.17)

- Fibroids typically appear as round, well-defined, oval or lobulated solid masses seen in the uterus or arising from it.
- Fibroids show variable echogenicity depending upon the proportion of muscle cells and fibrous stroma and the presence of any degenerative changes. They can appear from hypoechoic to hyperechoic.
- Fibroids generally show linear stripy fan-shaped internal acoustic shadowing and also shadowing from its edges (reported as 'edge shadows').
- They may show calcification and cavitation.
- On Doppler, fibroids typically show pericapsular flow (i.e. circumferential flow around its margins). Some amount of intralesional flow is also commonly seen within the fibroid. Some fibroids may, however, show high vascularity (increased vascularity seems to be related to increased cellularity in fibroids).

Despite the variable appearance of fibroids, diagnosing them on ultrasound is not challenging because any mass in the uterus (once an adenomyoma is excluded) or arising from it is almost always a fibroid.

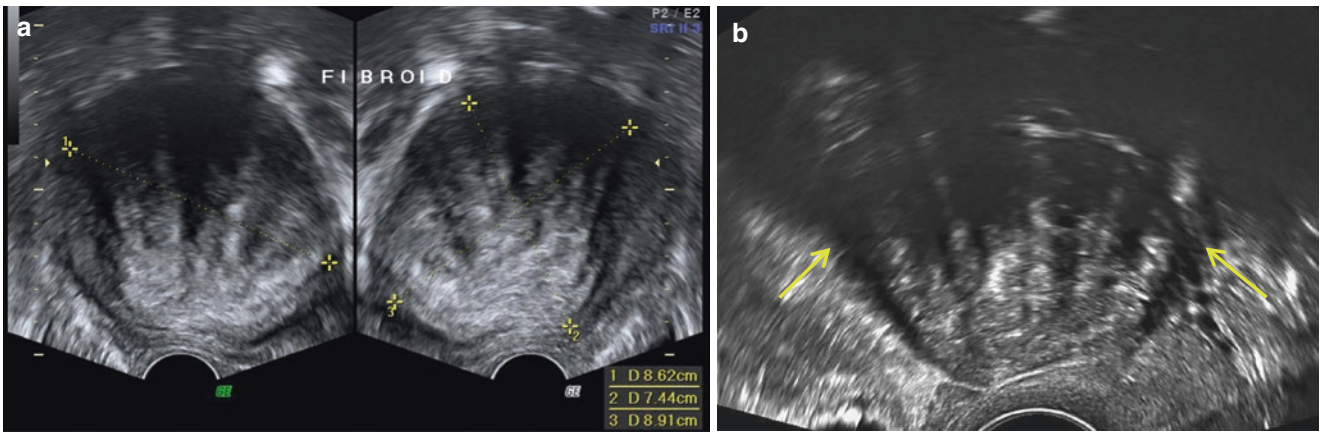

Fig. 3.11 Typical fibroids (**a, b**) are seen on ultrasound as well-demarcated, solid masses with stripy, linear, fan-shaped, internal shadowing and shadowing from their edges (*arrows*)

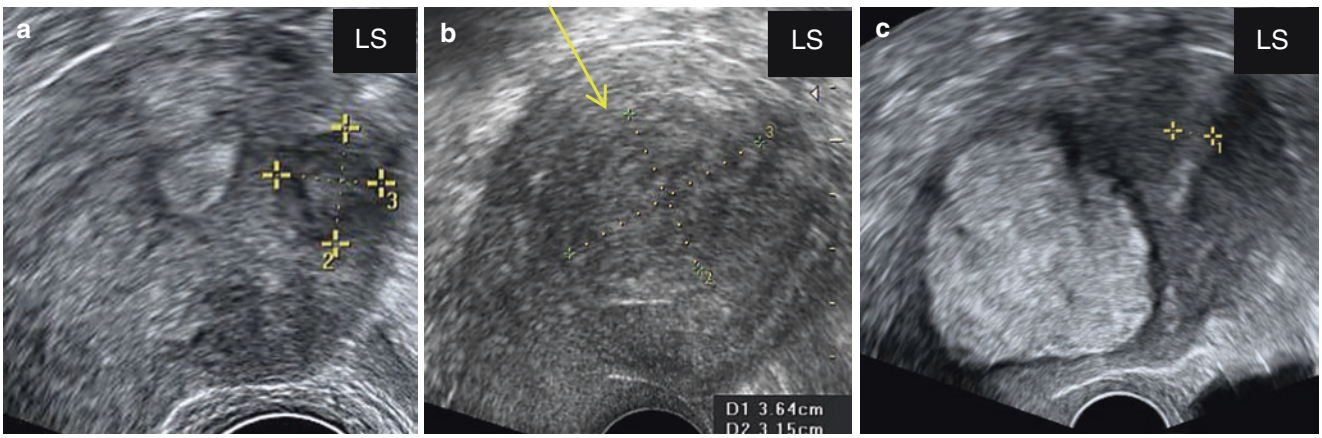

Fig. 3.12 Fibroids showing varying echogenicity. (**a**) Hypoechoic, (**b**) isoechoic (*arrow*) and (**c**) hyperechoic

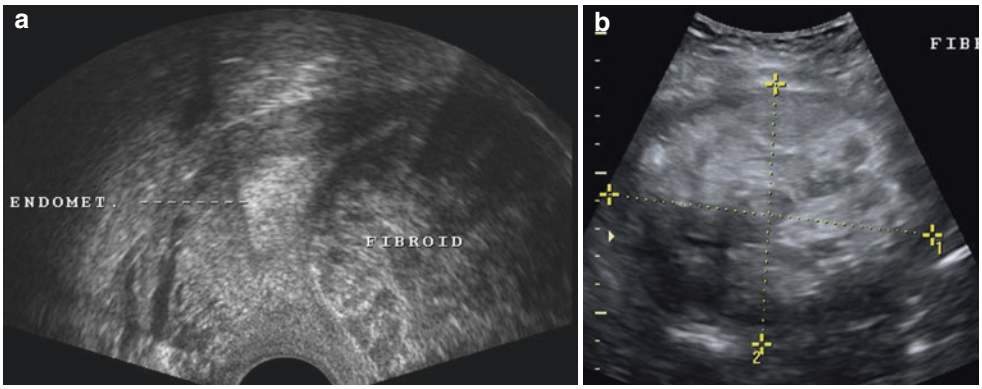

Fig. 3.13 Fibroids (**a, b**) showing complex internal echoes

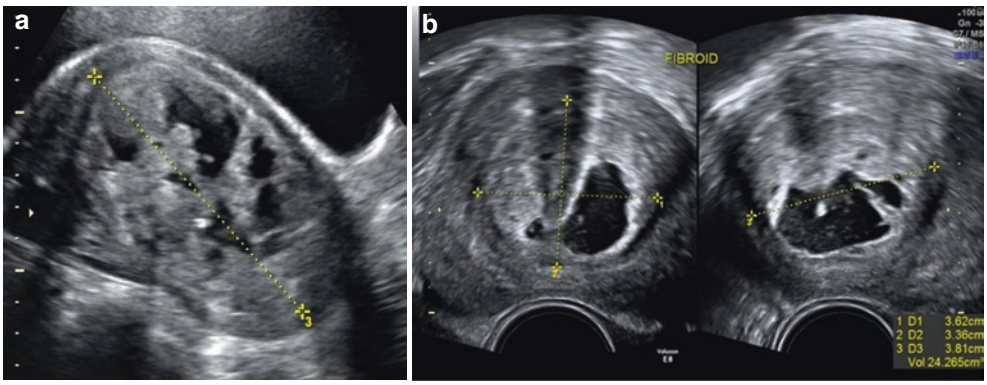

Fig. 3.14 Fibroids (**a, b**) showing cavitation (seen as irregular, anechoic or hypoechoic, cystic areas within the fibroid)

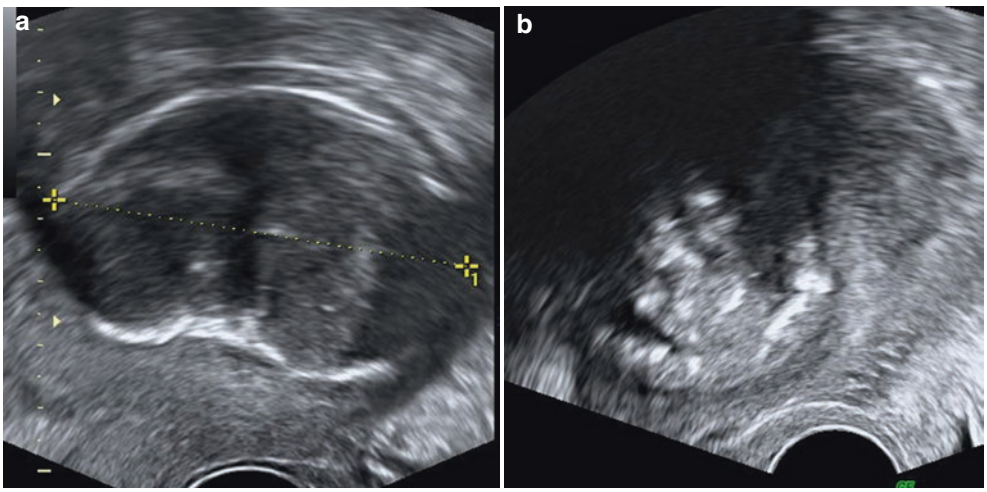

Fig. 3.15 Fibroids showing calcification. (**a**) Peripheral calcification, appearing like a shell around the fibroid. (**b**) Internal calcification causing acoustic shadowing

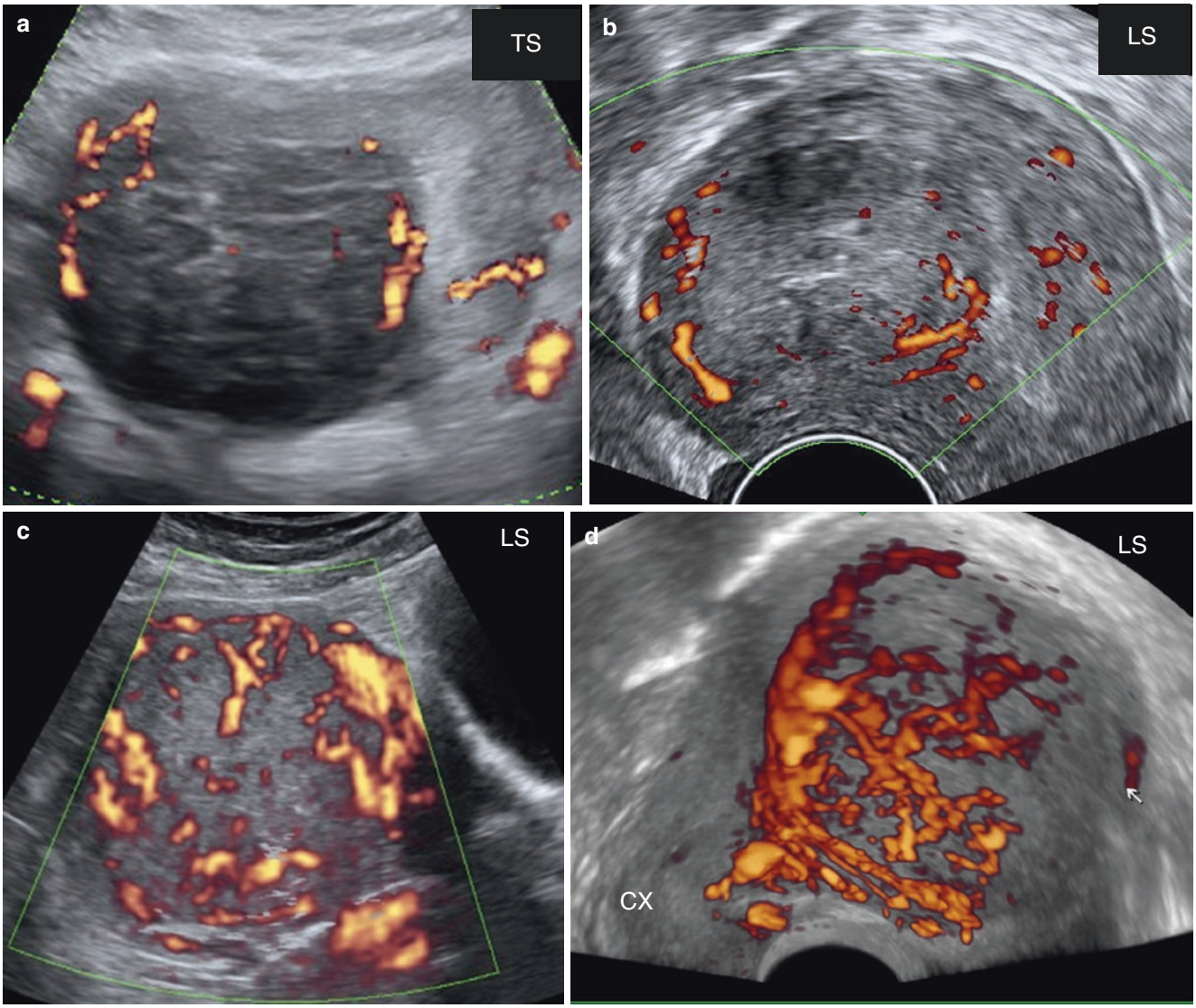

Fig. 3.16 Vascularity of fibroids. (**a**, **b**) Fibroids showing typical peripheral vascularity. (**c**) Atypical fibroid with significant internal vascularity. (**d**) 3D power Doppler with glass body display showing the vascular morphology in fibroids with high vascularity

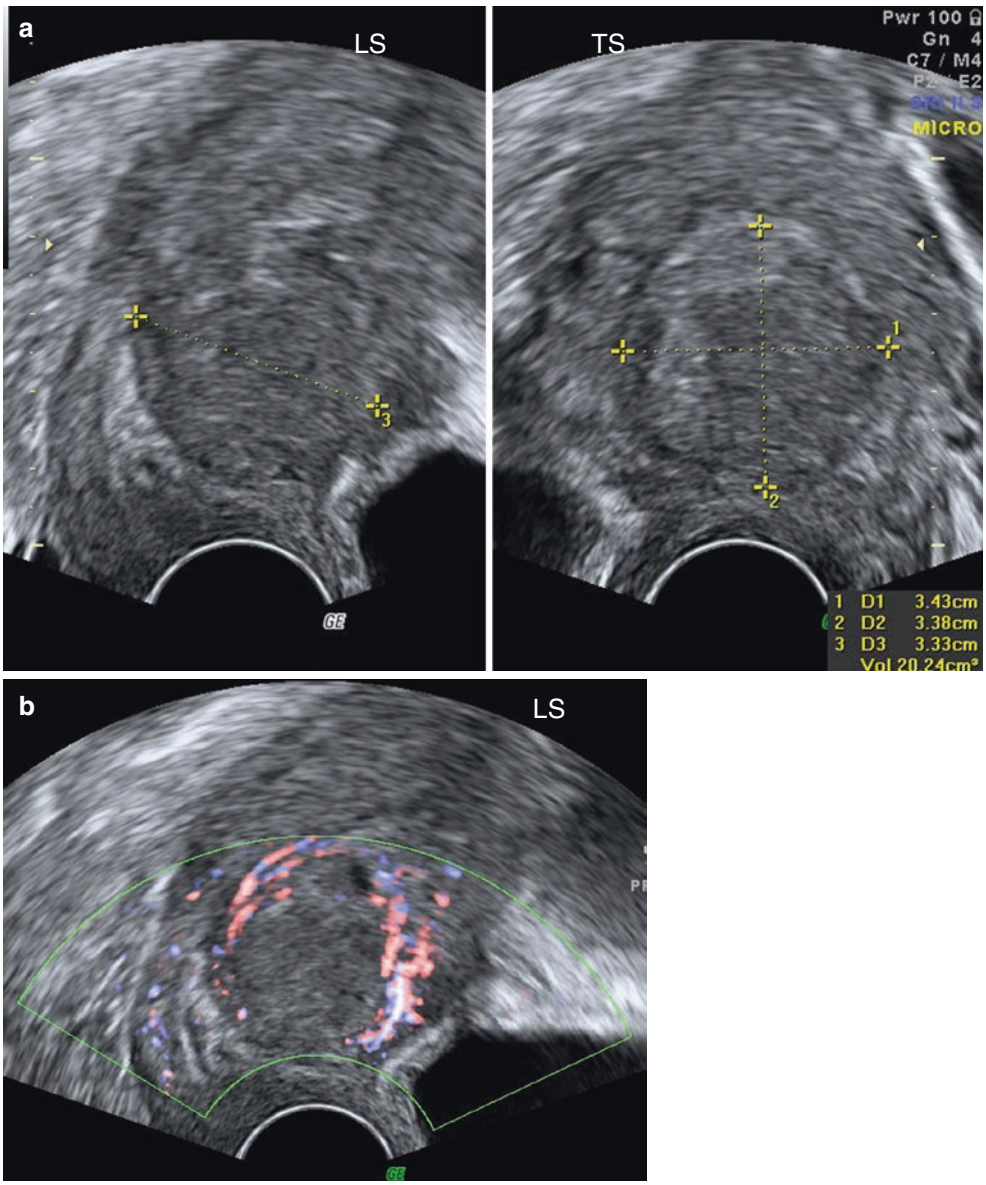

Fig. 3.17 Fibroid. (**a**) Isoechoic fibroid seen in the anterior wall of uterus with its margins not clearly defined. (**b**) Peripheral vascularity helped define the margins of the fibroid and confirm the diagnosis

3.3.1 Fibroid Mapping

3.3.1.1 Basics of Fibroid Mapping (Figs. 3.18, 3.19 and 3.20)

To map or describe the location of any mass like a fibroid, in the uterus, one must know four parameters:

1. How superior or inferior the mass is. For this, the uterus can be divided into fundus, upper corpus, midcorpus, lower corpus and cervix.
2. How anterior or posterior the mass is. The mass could be in the anterior wall or the posterior wall.
3. How much to the left or right the mass is. The mass could be right sided, left sided or in the midline.
4. How close is the mass to the inner endometrial mucosa or the outer serosa? The mass could be subserous, intramural or submucous. A fibroid or mass reaching both the serosa and the mucosa is termed transmural. In some cases, noting the exact distance of a fibroid from the mucosa or serosa provides useful information to the surgeon in planning surgical management. This is particularly so in cases of submucous fibroids which are being considered for hysteroscopic resection, where the thickness of the remaining overlying myometrium becomes important.

At times, the uterine architecture is significantly distorted by multiple fibroids making their location within the uterine body difficult to ascertain. To locate them, finding the endometrial stripe is important. If this becomes difficult due to shadowing by multiple fibroids, tracing it up from the cervical canal is usually helpful.

Fibroids can be located and mapped with the help of a 2D live scan, by gently moving the probe from the left to the right in a longitudinal section and from up to down in a transverse section. Visualisation of the fibroid in a coronal section is better on 3D, particularly in assessing the relation of the fibroid to the endometrial cavity.

Locating the fibroid or 'fibroid mapping' is very important because:

- It gives us information about whether the fibroid is the cause for the patient's symptoms. For example, fibroids that are submucous are more likely to cause menorrhagia; fibroid polyps are more likely to cause metrorrhagia and dysmenorrhoea.
- It also helps to decide if surgery is required and, if so, the type of surgery that is appropriate – a hysterectomy, myomectomy or a hysteroscopic resection.
- A good mapping also helps the surgeon during surgery to know the exact site of the various fibroids for a proper surgical approach and to ensure that all the fibroids are managed optimally.

Submucous fibroids have again been graded into:

G0 – completely intracavitary
G1 – more than 50 % intracavitary
G2 – less than 50 % intracavitary

Presently it is suggested in the MUSA consensus statement that the site of any well-defined myometrial lesion like a fibroid should be reported based on FIGO classification of fibroids:

- 0 = pedunculated, intracavitary (completely within the endometrial cavity)
- 1 = submucosal, less than 50 % intramural
- 2 = submucosal, more than or equal to 50 % intramural
- 3 = 100 % intramural but in contact with endometrium
- 4 = intramural
- 5 = subserosal, more than or equal to 50 % intramural
- 6 = subserosal, less than 50 % intramural
- 7 = subserosal pedunculated
- 8 = other (cervical, parasitic)

The locations of transmural fibroids in this FIGO classification are described as '2–5'.

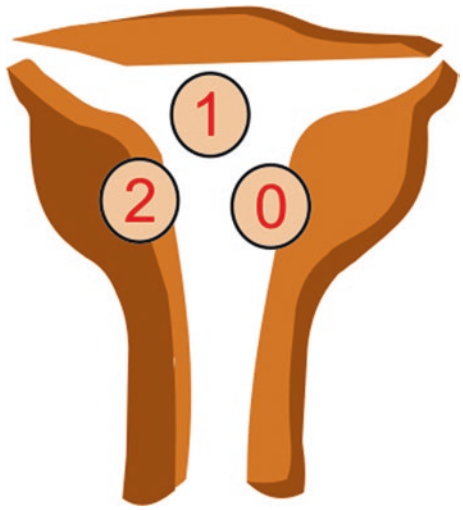

Fig. 3.18 Diagrammatic representation of submucous fibroids. *G0* is completely intracavitary, *G1* is less than 50% intracavitary and *G2* is more than 50% intracavitary

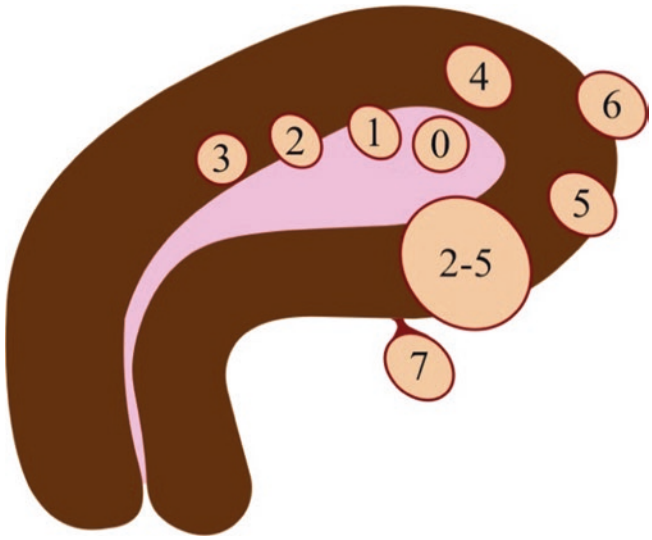

Fig. 3.19 FIGO classification of fibroids

Fig. 3.20 Endometrium identified in this case with multiple fibroids. This is crucial for fibroid mapping

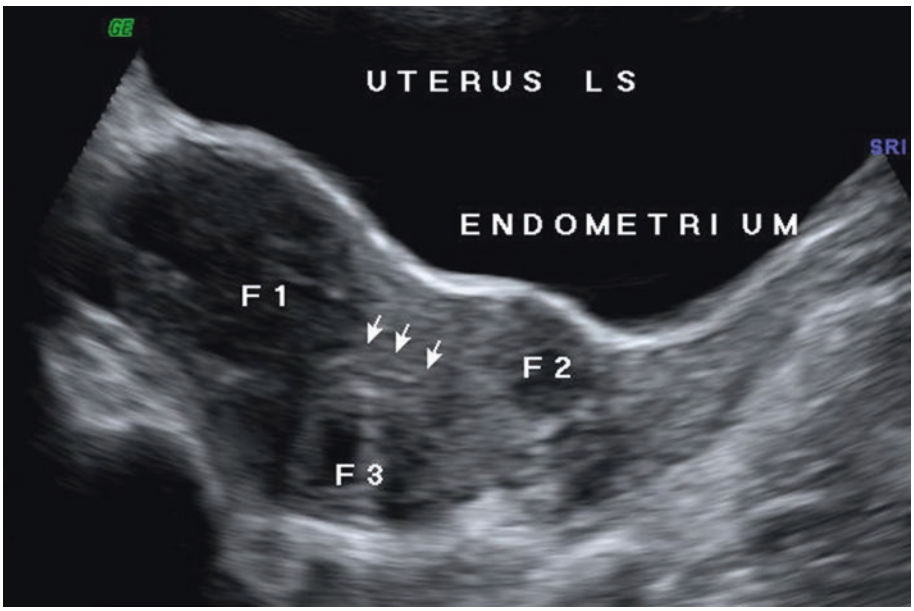

3.3.1.2 Site of Origin of a Fibroid (Figs. 3.21, 3.22 and 3.23)

The site of origin of a fibroid can be deciphered by noting Doppler flows to the fibroid. A fibroid that is attached to the uterine body through a vascular pedicle is called a subserous pedunculated fibroid (if attached to the outside of the uterine surface) and a submucosal fibroid polyp (if attached to the inside of the uterine cavity).

A fibroid may appear as an adnexal solid mass, but a careful search of its vascular pedicle, connecting it to the uterine body, will help in clinching the diagnosis of a subserous pedunculated fibroid (except perhaps in the case of a true broad ligament fibroid). Also, identifying the ovaries separate from such an adnexal mass will help in differentiating it from a solid or solid-cystic ovarian mass.

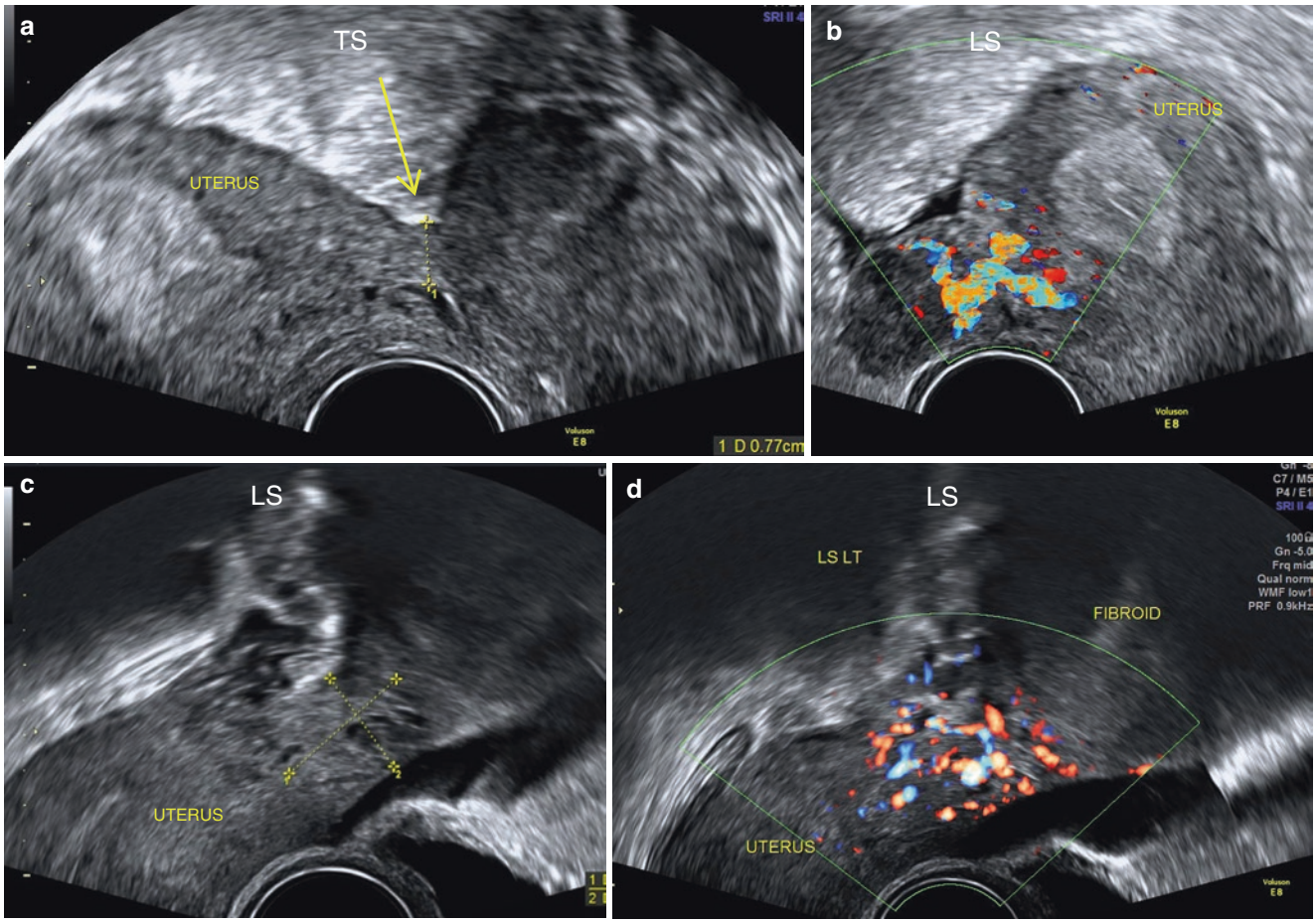

Fig. 3.21 Subserous pedunculated fibroids. (**a**) A large fibroid seen attached to the uterus through an isoechoic, 7.7 mm broad pedicle (*arrow*). (**b**) A subserous fibroid with flow approaching it from its origin in the posterior wall of the uterus. (**c**, **d**) A large, subserous fibroid arising from the anterior fundal wall of the uterine fundus. A broad pedicle is seen on greyscale and with Doppler

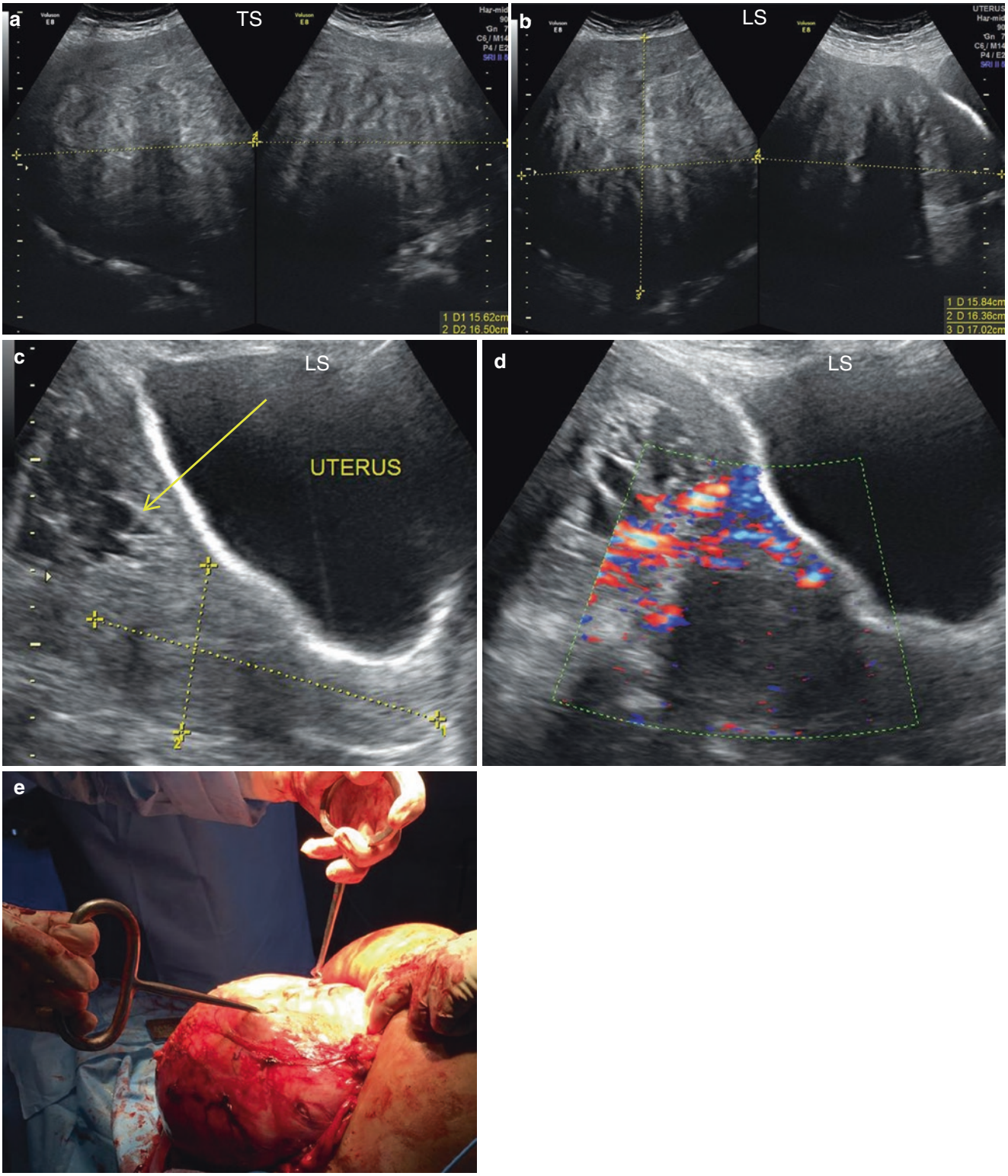

Fig. 3.22 Large fibroid of volume 9.27 L presenting as a huge, firm abdominal mass extending from the pelvis to the xiphisternum. (**a**) Transverse dimension of fibroid measured by the help of dual images with measurements from each end to a common reference point. (**b**) AP diameter of the fibroid is seen as a single vertical line in the first half of the image. Length of the fibroid measured in a similar manner with dual images, as the transverse dimension. (**c**) LS of the uterus on TAS with a broad attachment of this large fibroid to the anterior wall of the uterus at the upper corpus (*arrow*). (**d**) Vascular flow from the uterus onto the fibroid at its attachment. (**e**) Specimen of fibroid at surgery. The fibroid is being pulled out of the abdomen with the help of two myomectomy screws

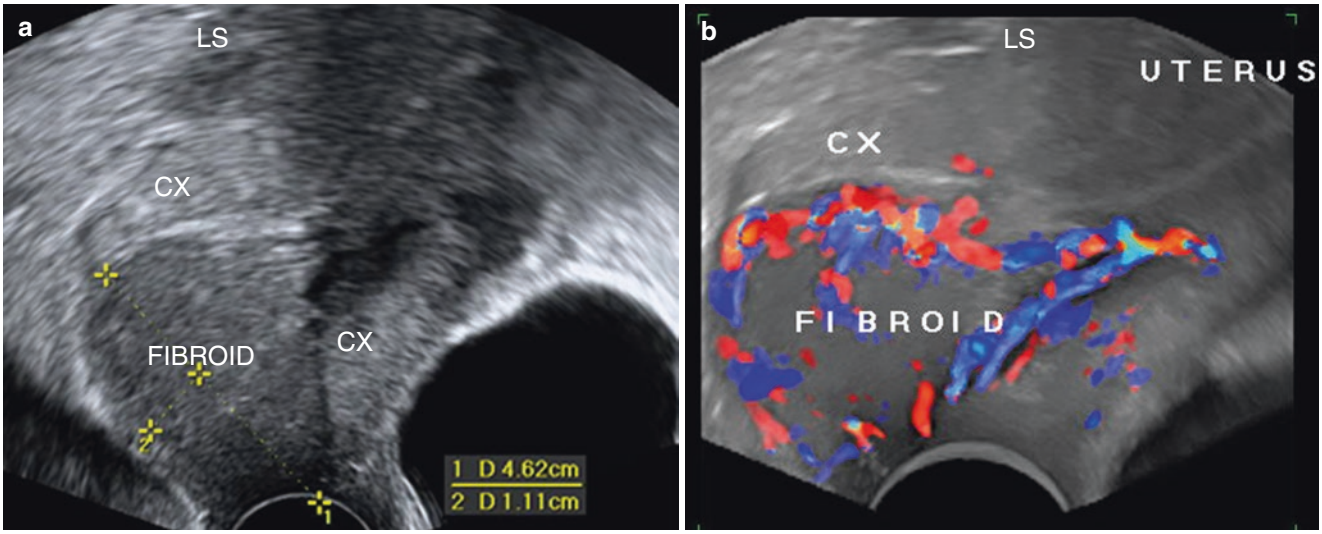

Fig. 3.23 Fibroid polyp. (**a**) Fibroid protruding out through the cervical os. (**b**) Its site of origin from the anterior wall of the lower corpus of the uterus is seen on 3D Doppler with glass body display

3.3.1.3 Role of 3D in Fibroid Mapping (Figs. 3.24, 3.25 and 3.26)

Fibroids can be located and mapped with 2D imaging on longitudinal and transverse sections of the uterus. But visualisation of the coronal section requires 3D. 3D is particularly helpful in assesing the relation of a fibroid to the endometrial cavity. 3D assessment for preoperative grading of submucous fibroids has been described to be more accurate with a sonohysterogram (Leone UOG 2007). MRI may be considered for fibroid mapping when there are more than five fibroids or if the uterus is very large (more than 375 cc).

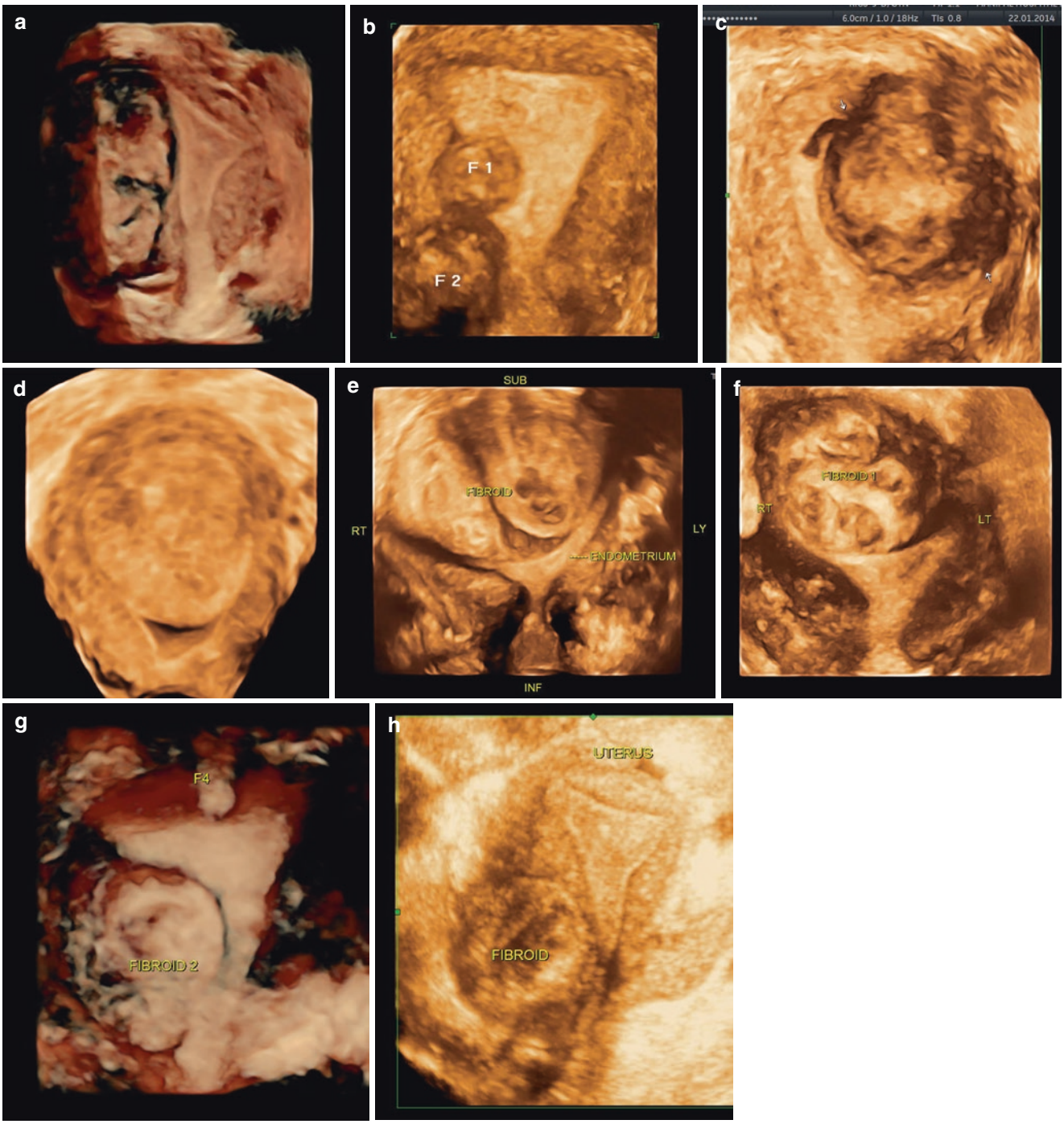

Fig. 3.24 3D rendered coronal images of a uterus showing fibroids' relationship to the endometrial cavity. All the fibroids (**a**–**g**) except for the fibroid in (**h**) are submucous and are seen distorting the shape of the endometrial cavity

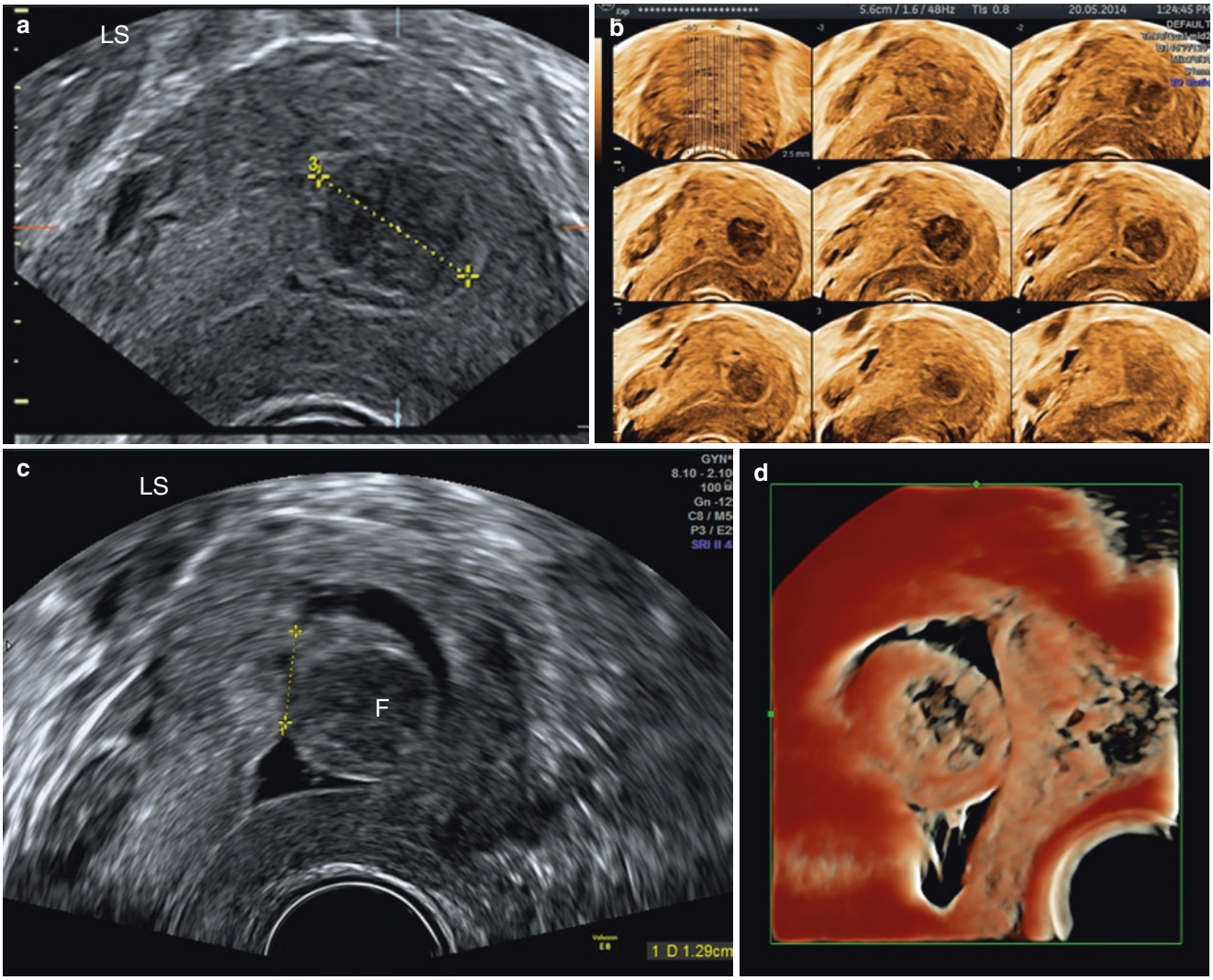

Fig. 3.25 Submucous fibroid seen on (**a**) regular TVS, (**b**) TUI, (**c**) SHG – showing fluid surrounding a completely intracavitary fibroid (F). Its attachment to the posterior wall of the uterus is measured in the image. (**d**) 3D rendered image of the same

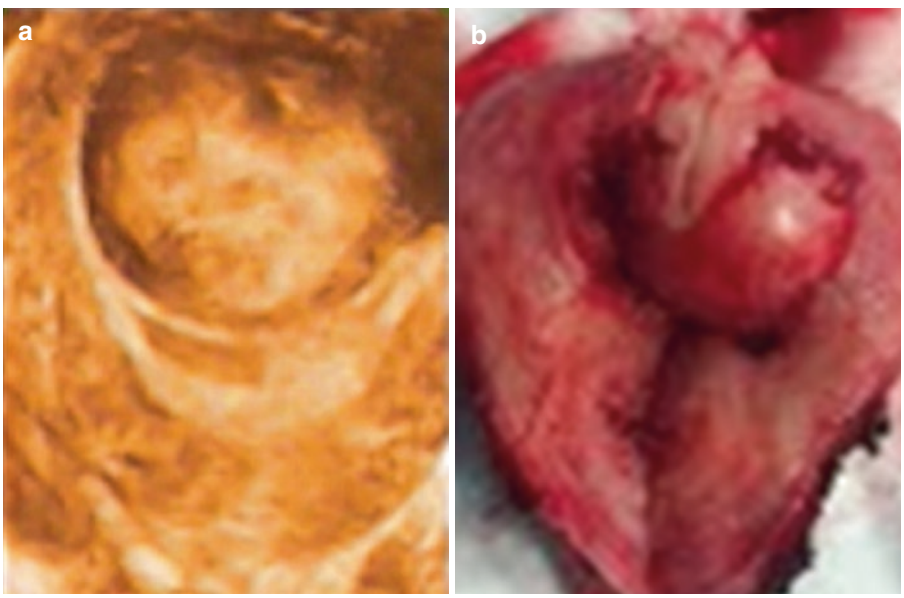

Fig. 3.26 Submucous fibroid. (**a**) 3D rendered image where the inferior margins are well made out due to the presence of minimal intracavitary fluid. (**b**) Post-operative specimen of the same, correlating well with the 3D rendered image in (**a**)

3.3.1.4 Reporting of Fibroids/Fibroid Mapping (Figs. 3.27 and 3.28)

The ultrasound report of fibroid mapping should include the location of the fibroid using the four parameters described in Sect. 3.3.1.1 above. If considered relevant, the measurement of their distance from the mucosa and serosa should be reported. Relevant 2D and 3D images should also be attached to the report. A diagrammatic representation of the fibroid sketched in one or more planes is very useful to the referring clinicians for a better understanding of the location of the fibroids.

Fibroid mapping is essential particularly in symptomatic women, for management. It may not be essential in asymptomatic women who are either postmenopausal or have no further desire for fertility. In such cases, their location in four parameters (mentioned above) may be reported, but fine details and diagrams are not essential. If a uterus is riddled with fibroids, it is appropriate to mention, measure and map a few relevant ones (especially the submucous and the large ones). Also, one should mention that there are many smaller ones that have not been measured or mapped.

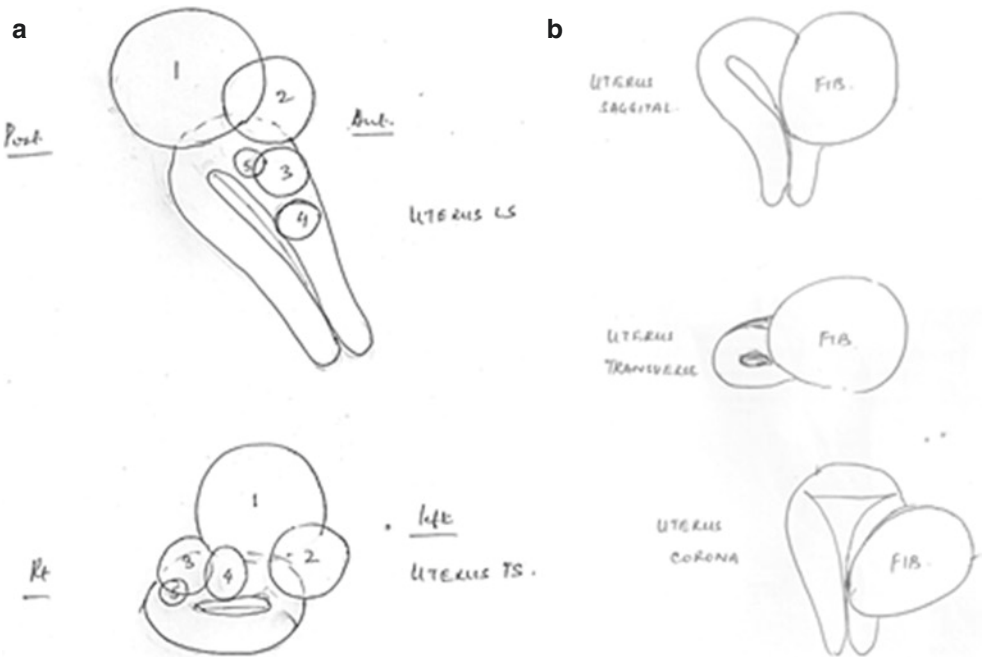

Fig. 3.27 Reporting of fibroid mapping with diagrams. (**a**) LS and TS views of uterus showing five fibroids. (**b**) LS, TS and coronal images showing a single fibroid

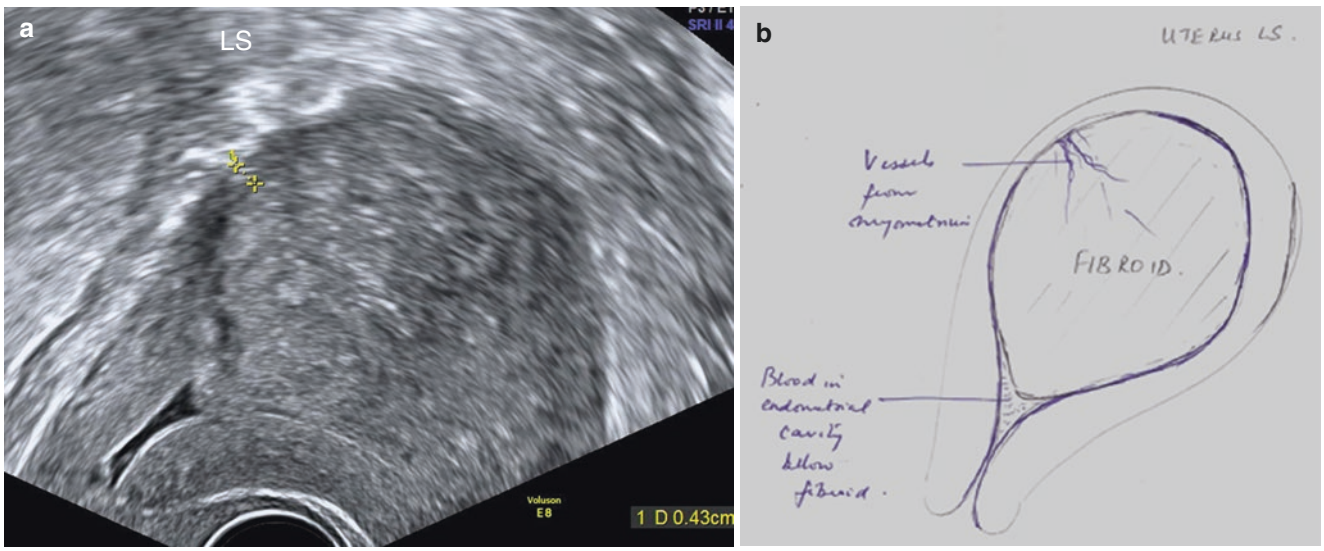

Fig. 3.28 (**a**) Intracavitary fibroid arising from the posterior wall with a very thin overlying myometrium of 4 mm. (**b**) Diagrammatic representation of the same

3.3.2 Red Degeneration (Fig. 3.29)

Most pregnant women with fibroids are asymptomatic. Some, however, may experience complications like pain, bleeding or miscarriage. When a fibroid causes pain in pregnancy, the most common cause is red degeneration, which is believed to occur when a fibroid outstrips its blood supply. This is a rare condition and even more rare in non-pregnant women. Patients complain of acute abdominal pain which may be associated with nausea, vomiting and low-grade fever. On examination there is a tender palpable mass. Ultrasound can detect the fibroid, but it is not sensitive in diagnosing red degeneration. Ultrasound examination shows a tender fibroid with absence of vascularity or poor vascularity. The fibroid usually shows a rapid increase in size, which can be assessed if previous reports are available. If infarction and necrosis have set in, it may show a mixed echogenic appearance. This may not be noted in early cases. On MRI, these fibroids typically show an increased T1 signal intensity. Most often, red degeneration is self-limiting and managed conservatively.

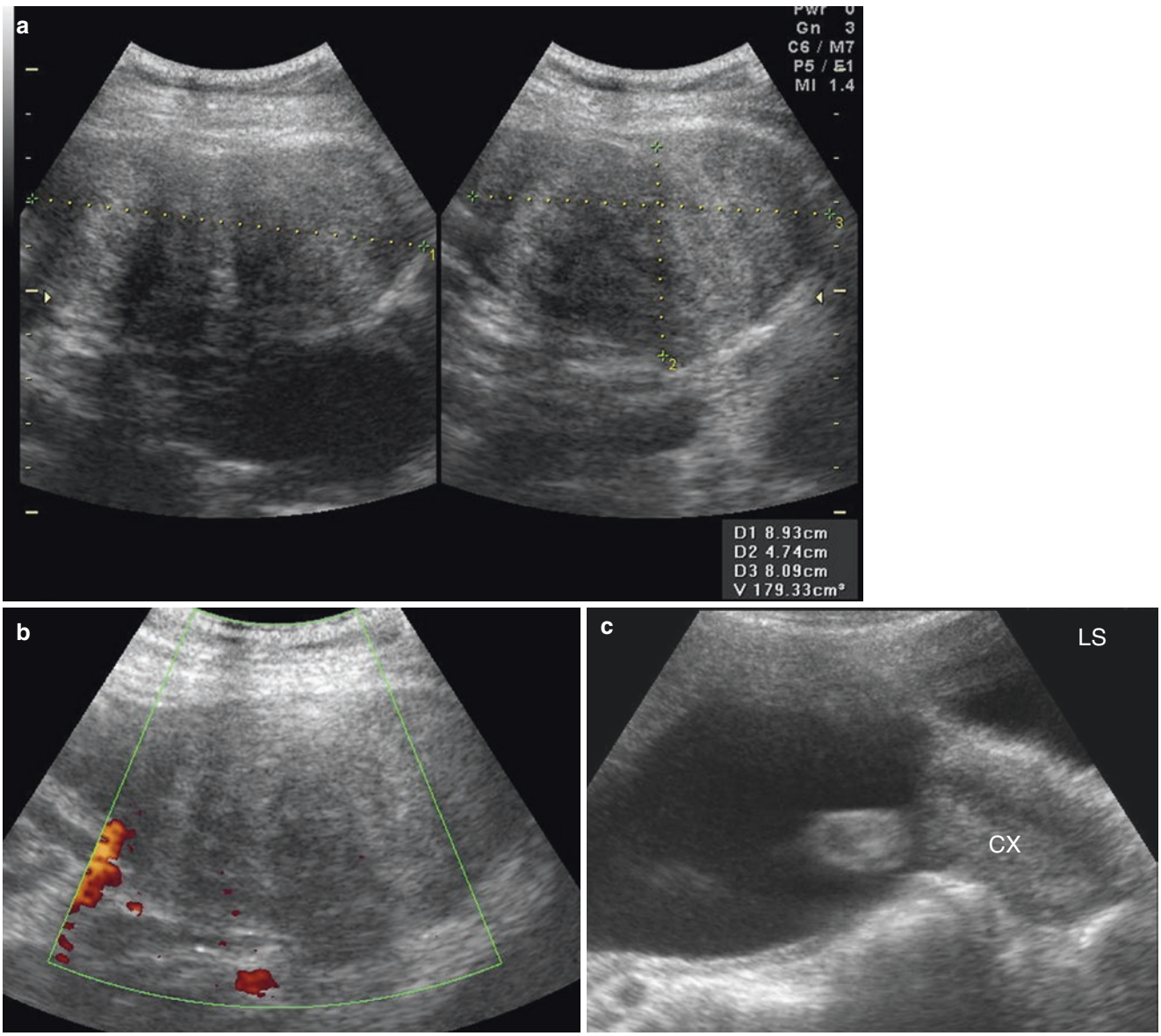

Fig. 3.29 Suspected case of red degeneration of a fibroid. A 23-week-pregnant lady, known to have a fibroid, presented with acute abdominal pain. On ultrasound examination, the fibroid was very tender. (**a**) Fibroid on measurement was found to have increased in size suddenly. (**b**) No flow was seen on power Doppler in the fibroid. (**c**) Cervix was found to be of normal length, and there was no evidence of placental abruption

3.3.3 Fibroid Embolization (Figs. 3.30 and 3.31)

Uterine fibroid embolisation is an alternative to hysterectomy. Post-embolisation complications are pain, nausea, vomiting and low-grade fever that peak at 24 hours and usually subside in a week. Air may be seen in the fibroid after embolisation – a feature thought to be the result of gas filling potential spaces.

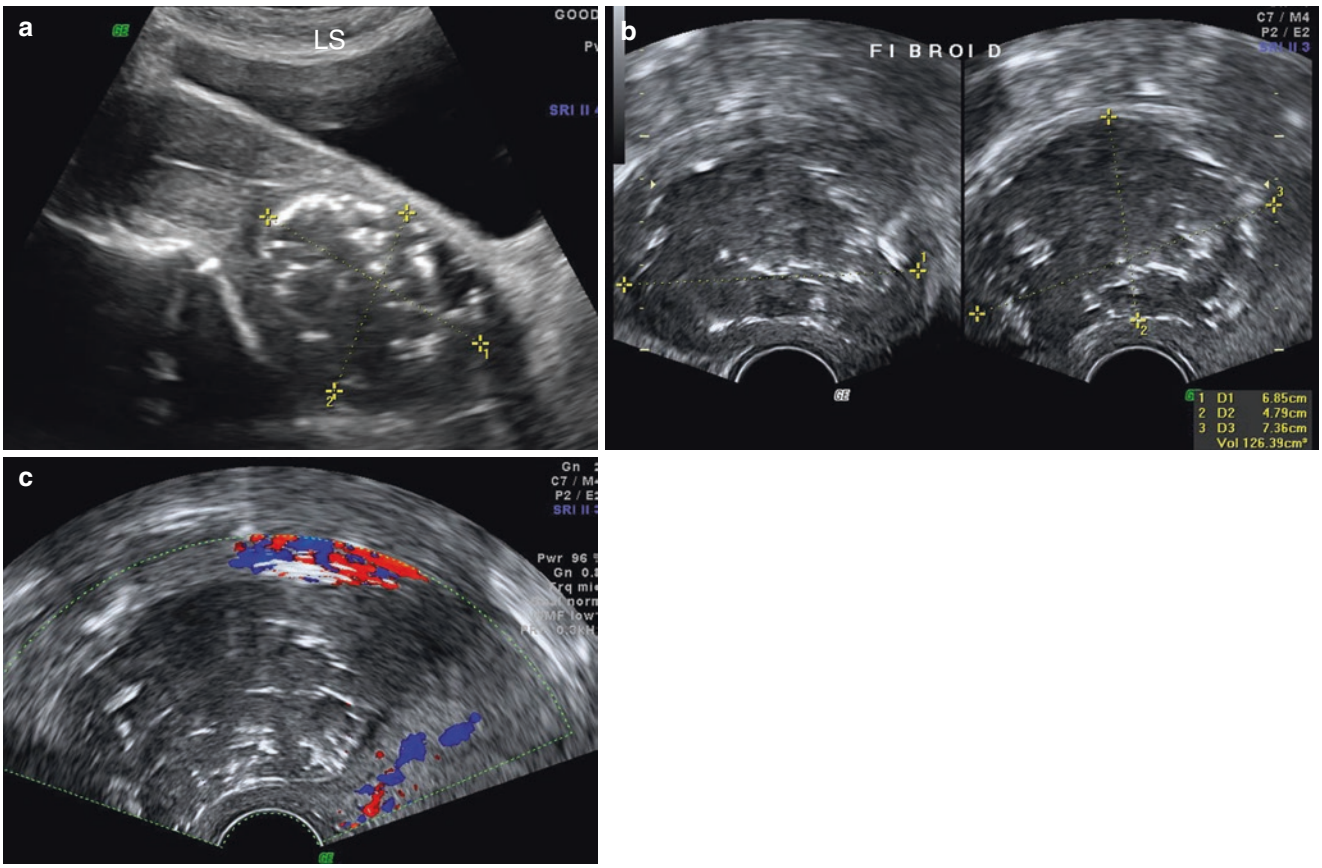

Fig. 3.30 Fibroid seen on the third day after embolisation. The patient presented with acute abdominal pain. On ultrasound, the fibroid was found to be tender. (**a**) LS of a uterus showing a posterior wall, lower corpus and upper cervical fibroid. (**b**) Fibroid is measured. It showed a 10 % increase in size from the previous scan done a month earlier. Scattered bright linear echoes suggestive of air are seen within the fibroid which were not seen in the earlier scan done a month ago. This is a known feature following embolisation. (**c**) No flow was seen on Doppler in the fibroid, which is expected following embolisation

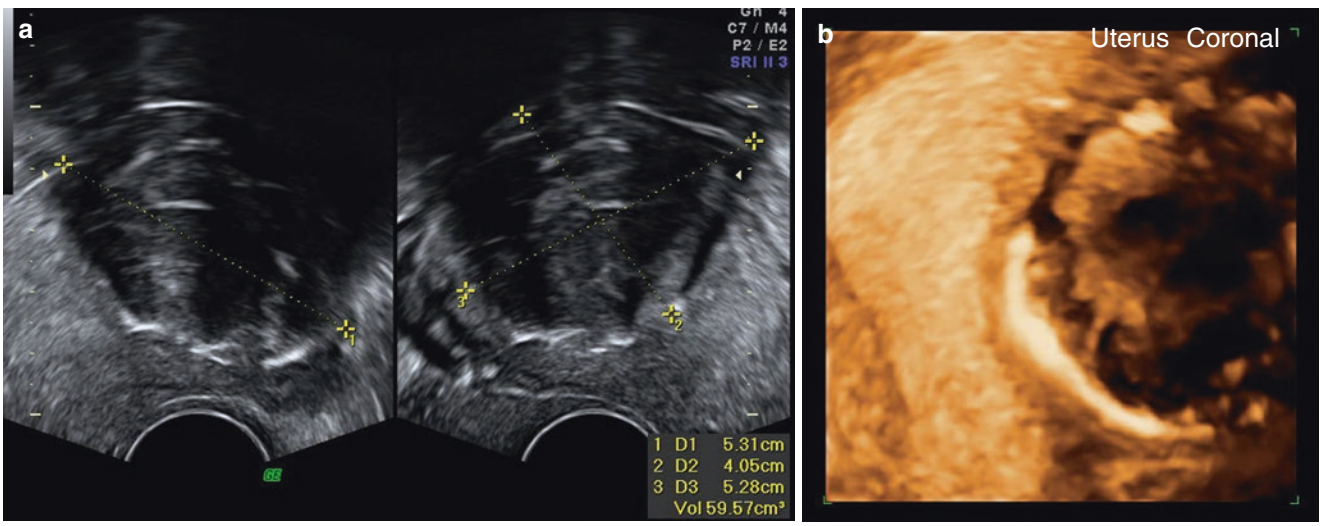

Fig. 3.31 Fibroid embolised 8 years earlier, showing dense peripheral calcification. This is a known finding post embolisation that is seen on (**a**) 2D greyscale and (**b**) 3D rendering

3.3.4 Diffuse Uterine Leiomyomatosis (Figs. 3.32 and 3.33)

This is a benign and extremely rare condition, where the uterus is symmetrically enlarged as a result of almost complete replacement of the myometrium by innumerable poorly defined confluent leiomyomatous nodules.

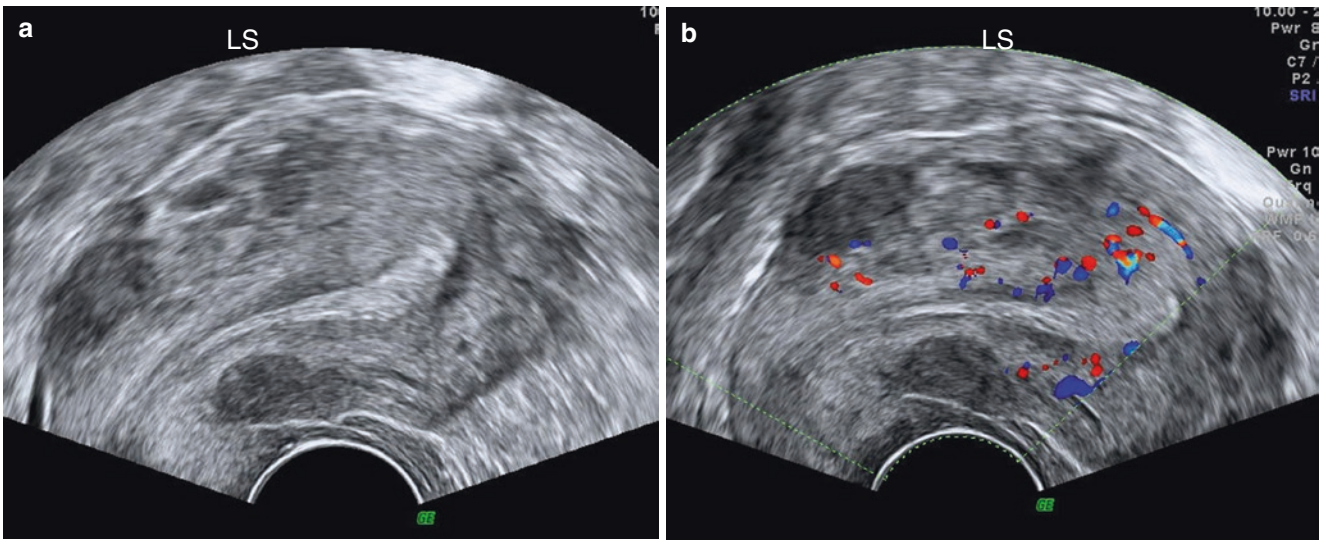

Fig. 3.32 Diffuse uterine leiomyomatosis. LS of uterus on (**a**) greyscale and (**b**) Doppler, showing multiple hypoechoic, poorly defined, irregular areas, giving the uterus a heterogeneous appearance. The margins of most of the fibroids are difficult to delineate

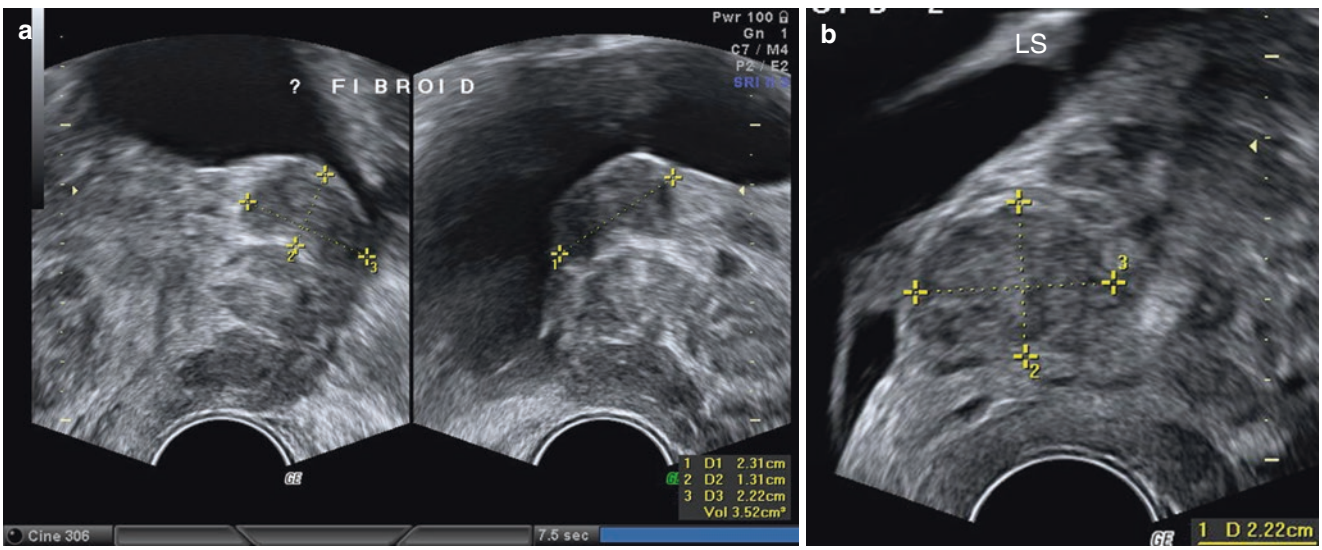

Fig. 3.33 Diffuse uterine leiomyomatosis in a patient who had undergone myomectomy. (**a**) Loculated fluid is seen adjoining the uterus, probably secondary to surgery. Uterus shows multiple hypoechoic areas, many of which have poorly defined margins, giving the uterus a heterogeneous appearance. One of the larger fibroids is measured in the image. (**b**) LS of uterus showing a well-defined fibroid along with multiple poorly defined hypoechoic areas

3.3.5 Disseminated Peritoneal Leiomyomatosis (DPL) (Fig. 3.34)

This is an exceedingly rare condition characterised by discreet smooth muscle nodules, scattered throughout the peritoneum of the abdomen and pelvis. This condition can occur spontaneously or iatrogenically after surgical seeding. The aetiology of DPL remains controversial, but it is suspected that the disease originates from metaplasia of subperitoneal mesenchymal cells. It is common in women of the reproductive age group. It is usually associated with elevated levels of exogenous or endogenous oestrogen. This is an established, yet rare complication associated with laparoscopic morcellation of fibroids.

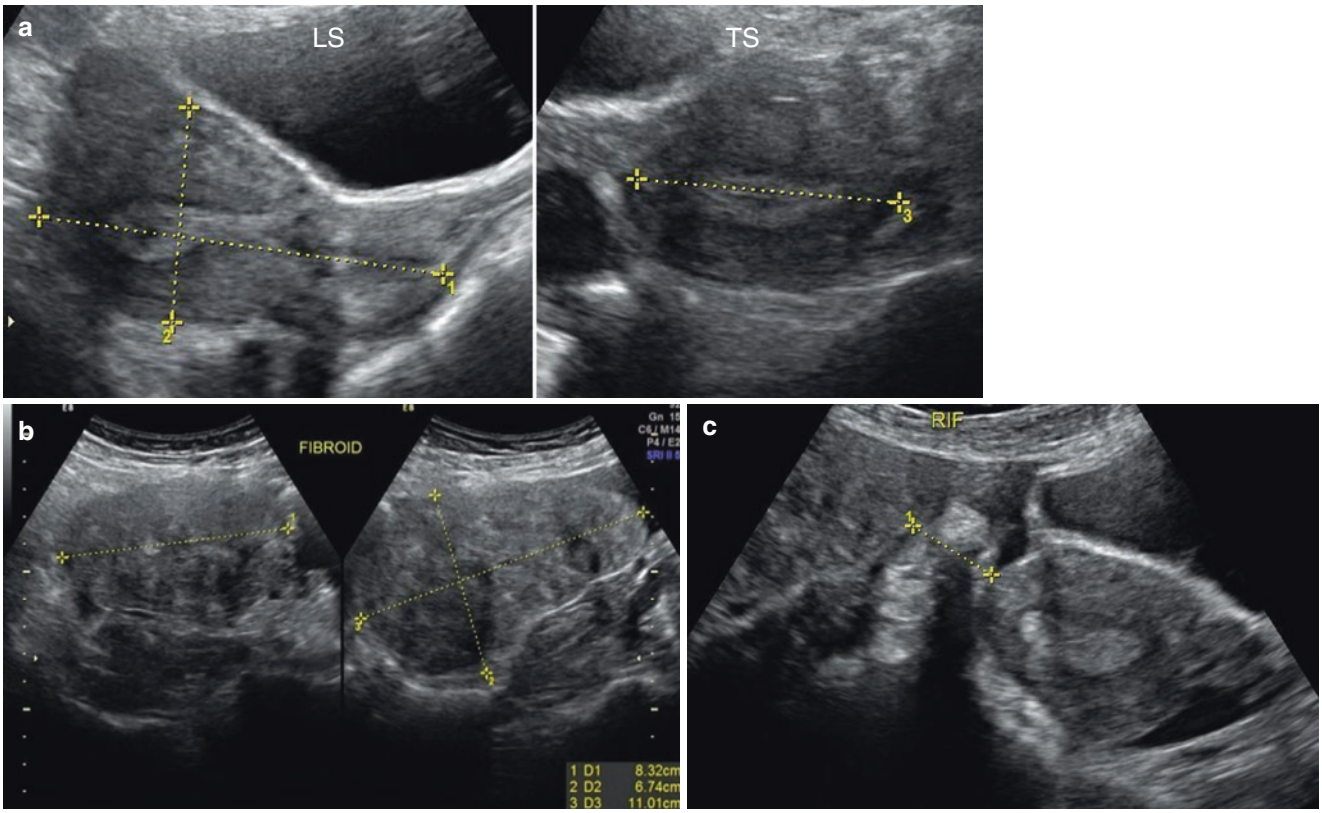

Fig. 3.34 Case of disseminated peritoneal leiomyomatosis with multiple fibroids in the peritoneal cavity. Turbid fluid and adhesions were noted in the pelvis. The patient had undergone a laparoscopic myomectomy (with morcellation) for a large fibroid, 6 years prior to this scan. She now presented with abdominal pain. (**a**) Uterus measured on LS and TS, which appears essentially normal. (**b**) Large fibroid (8 × 6 x 11 cm) seen in the RIF. (**c**) This fibroid, seen in image (**b**), was seen distinctly separate and 2.2 cm away from the uterus. It was attached to the peritoneal wall. (**d**) Fibroid (5 × 3 × 5 cm) seen attached to the peritoneum in the LIF. It was also a significant distance away from the uterus. Minimal flow seen along the periphery of this fibroid. (**e**) Another fibroid (5 × 2 × 4 cm) seen in the right lower abdomen. (**f**) TVS showing a small fibroid (1.4 × 1.2 × 1.3 cm) close to the posterior wall of the uterus but attached to the peritoneal surface and not the uterus. (**g**) Another fibroid seen attached to the pelvic wall lateral to the right ovary

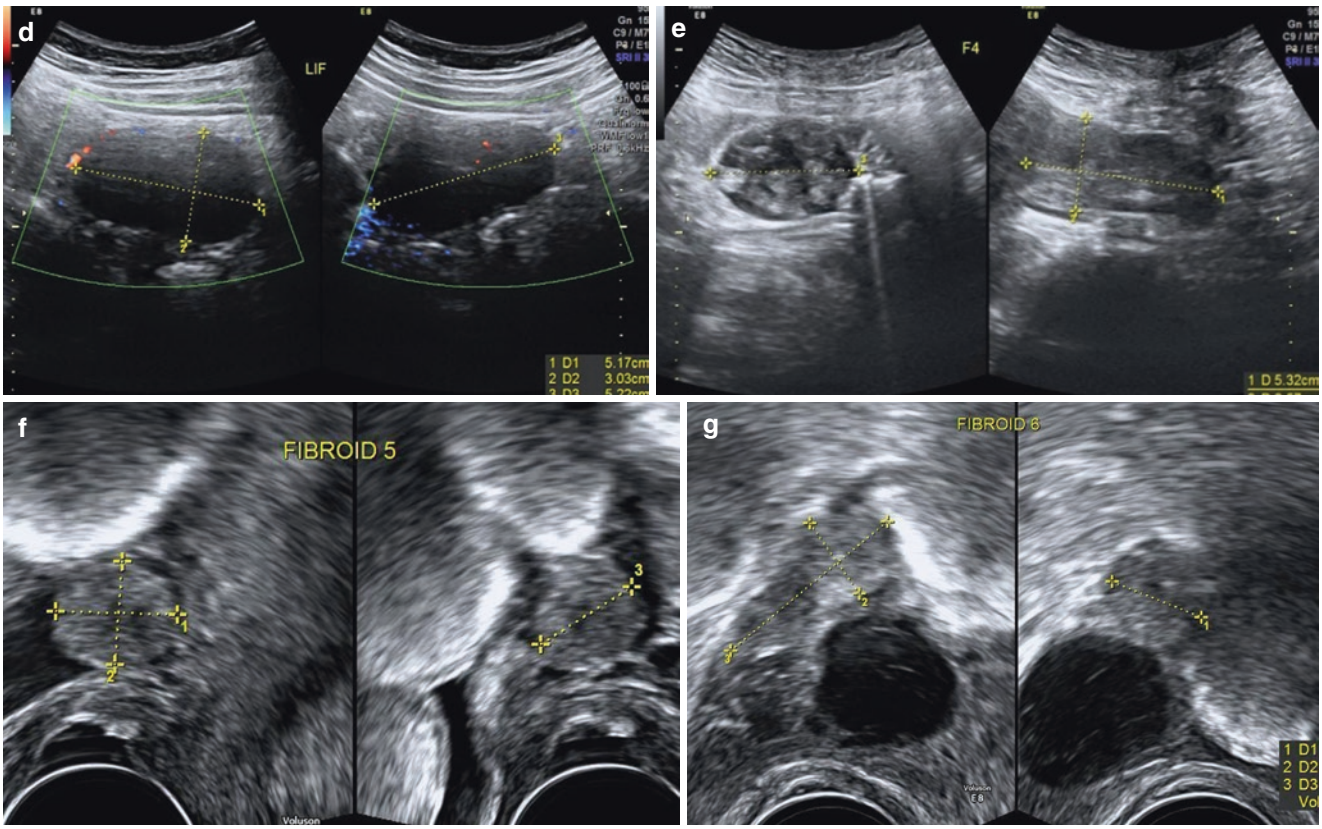

Fig. 3.34 (continued)

Summary: Fibroid

- Fibroids are a commonly seen pathology, with women being either asymptomatic or complaining of excessive bleeding, dysmenorrhoea, etc.
- On ultrasound, they appear as solid masses in the uterus or arising from it. They have variable echogenicity and well-defined margins. They show both linear coarse stripy shadowing and shadowing from their edges. Typically, pericapsular flow is seen. Some may show calcification or cavitation.
- Atypical, large and vascular fibroids are to be evaluated carefully and rescanned in a short period, as there is very small chance of these being malignant sarcomas.
- Fibroid mapping and relationship of the fibroids to the endometrial mucosa are particularly important for appropriate management. If possible, a sketched diagram should be provided with the report.

3.4 Adenomyosis and Adenomyomas

Adenomyosis is another common gynecological disorder where there is proliferation of endometrial glands and stroma within the myometrium along with hypertrophy and hyperplasia of surrounding adjacent myometrium. Adenomyosis is seen in about 20% of women. In most women, there are no known causes for the adenomyosis. However, in some women it is seen associated with deep infiltrating endometriosis or obstruction to antegrade menstrual flow (as is seen in the uterine wall of a non-communicating uterine horn). Women with adenomyosis may be asymptomatic but could suffer from menorrhagia, polymenorrhagia, dysmenorrhoea and infertility.

Ultrasound Features of Adenomyosis and Adenomyoma (Figs. 3.35, 3.36, 3.37, 3.38, 3.39, 3.40, 3.41, 3.42, 3.43, 3.44, 3.45 and 3.46)

- The uterus is generally enlarged and globular (with the uterine contour being maintained). It is symmetrically enlarged when adenomyosis involves the entire uterine body or asymmetrical if it is limited to only some areas of the uterus. The myometrial walls may be asymmetrically thickened. An adenomyoma is a focal area of adenomyosis with poorly circumscribed margins.
- The shape of the endometrial cavity is maintained because of the diffuse myometrial involvement (unlike what might be seen with fibroids). This helps in distinguishing it from a large fibroid where the endometrial lining may be pushed by the fibroid to one side. In adenomyosis, the endometrium is seen passing through the globular mass (enlarged adenomyotic uterus).
- Myometrium shows coarse echotexture with linear acoustic shadowing (described as 'fan-shaped' shadowing or 'rain in the forest' appearance). Edge shadows are not seen because the lesion does not have well-defined margins.
- Small myometrial cysts are seen. Some may be large and measurable, but generally they are not measurable individually and are seen as tiny hypoechoic or anechoic microcysts dispersed within the myometrium. The cystic contents may be anechoic, but generally the cysts are hypoechoic with turbid contents within. The cystic spaces may be surrounded by a hyperechoic rim.
- Hyperechoic islands of endometrial tissue may be seen within the myometrium. They may be regular, irregular or ill-defined and are typically seen in the submucosal area.
- The junctional zone is a very important site for diagnosis of adenomyosis. It can be assessed better on 3D imaging (multiplanar, rendered or VCI):
  - The JZ may be ill-defined as a result of which endometrial margins may be difficult to delineate.
  - The JZ may be thickened and this is better visualized with 3D imaging. There are studies focusing on the thickness of the JZ in the diagnosis of adenomyosis (Exacoustos UOG 2011).
  - Hyperechogenic subendometrial buds and lines (almost perpendicular to the endometrial cavity and arising from it) can also be seen in the JZ.
  - The JZ may show hyperechogenic spots.
  - Tiny cystic spaces may be seen in the junctional zone, along the endomyometrial junction, and their presence in an otherwise grossly appearing normal uterus is considered to be a feature of early adenomyosis.
  - The JZ as a result of these hyperechogenic buds, lines and cystic spaces appears irregular.
- On Doppler, the affected myometrium may show increased vascularity (which is intralesional and not circumferential like in fibroids).
- The uterus may be tender during TVS examination.
- In classic adenomyosis, the myometrial invasion by the endometrium is directly from the endometrium lining the cavity, and, therefore, features are well noticed in the JZ. However, in women with endometriosis, the invasion is from the endometrial implants on the serosal surface of the uterus (from endometriomas or DIE nodules) (Kishi Y., AMJ Ob Gyn 2012). In women with adenomyosis associated with deep infiltrating endometriosis of the posterior compartment, the uterus is retroflexed at the mid-corpus due to the fixity of its posterior wall and fundus posteriorly. This gives the uterus an 'ear shape' or a 'question mark shape' (called the 'question mark sign').

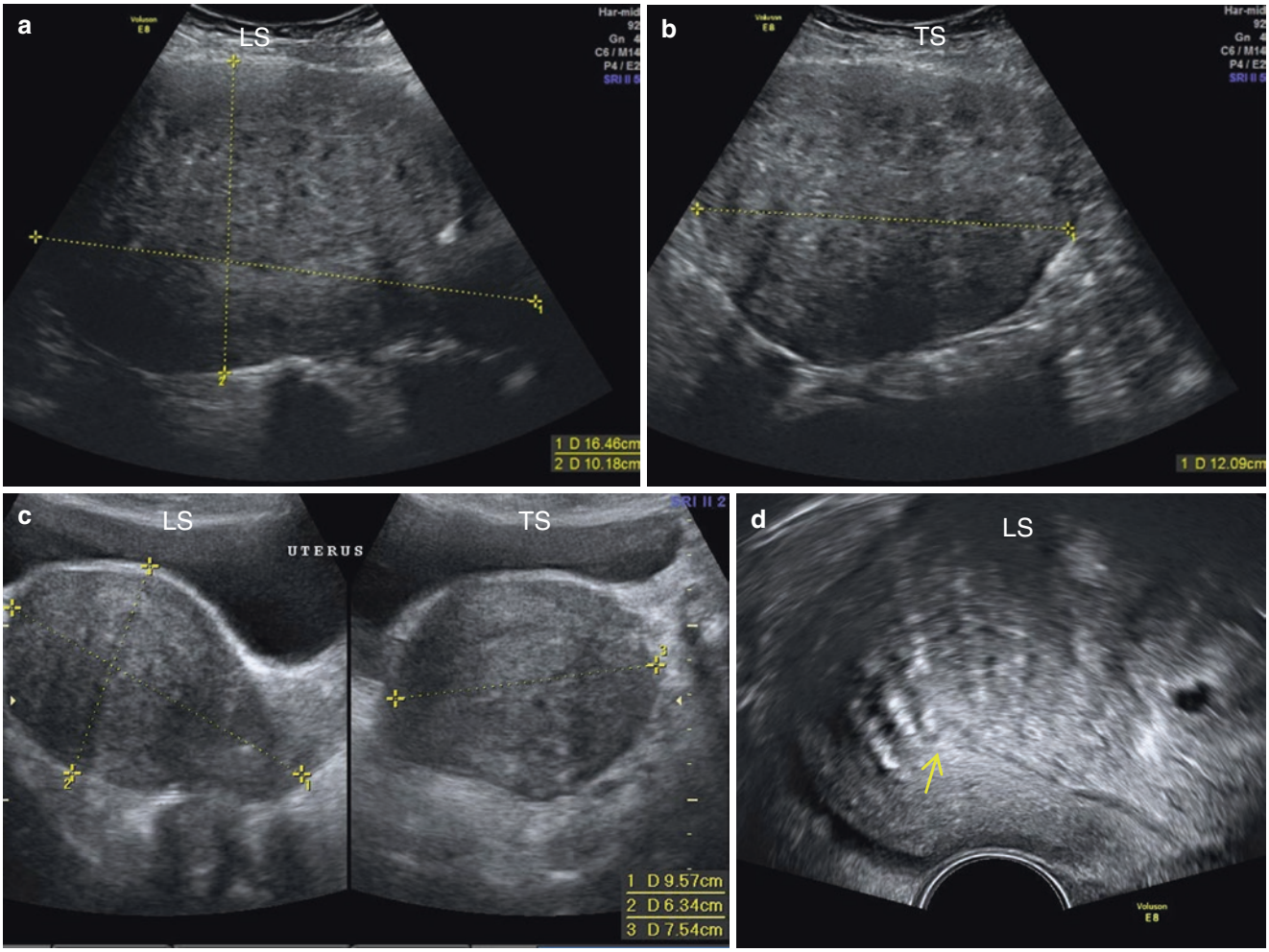

Fig. 3.35 Enlarged globular uterus secondary to diffuse adenomyosis. Myometrium in these cases shows coarse echotexture with linear shadowing. No edge shadows are noted. (**a**, **b**) Case 1, LS and TS of the uterus. (**c**) Case 2, LS and TS of the uterus. (**d**) Case 3, LS showing the endometrium (*arrows*) passing through the middle of the globular mass formed by the adenomyotic uterine body

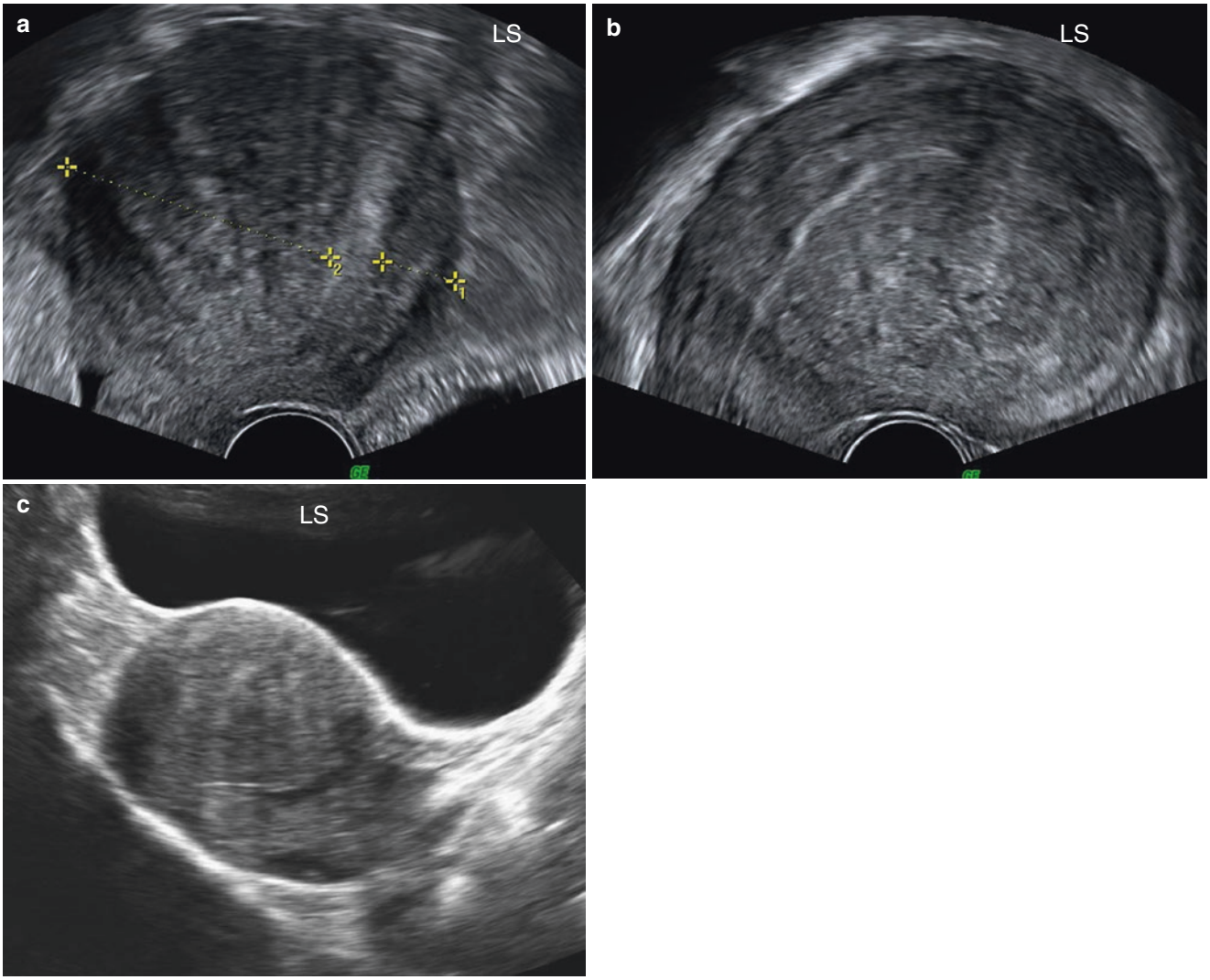

Fig. 3.36 Cases with asymmetrical adenomyosis involving (**a**) mainly the posterior wall, (**b**) mainly the anterior wall, (**c**) anterior wall (on TAS). In (**a**) and (**c**), typical fan-shaped linear shadowing is noted

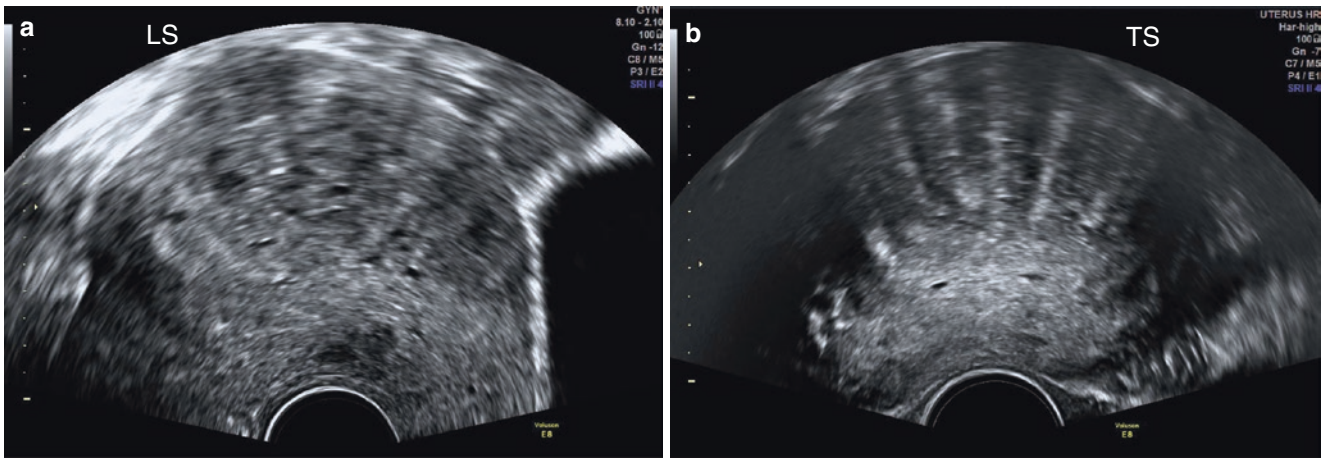

Fig. 3.37 Adenomyosis (**a**) LS and (**b**) TS of the uterus. Tiny myometrial cysts are seen dispersed within the myometrium, giving it a coarse echotexture with linear shadowing

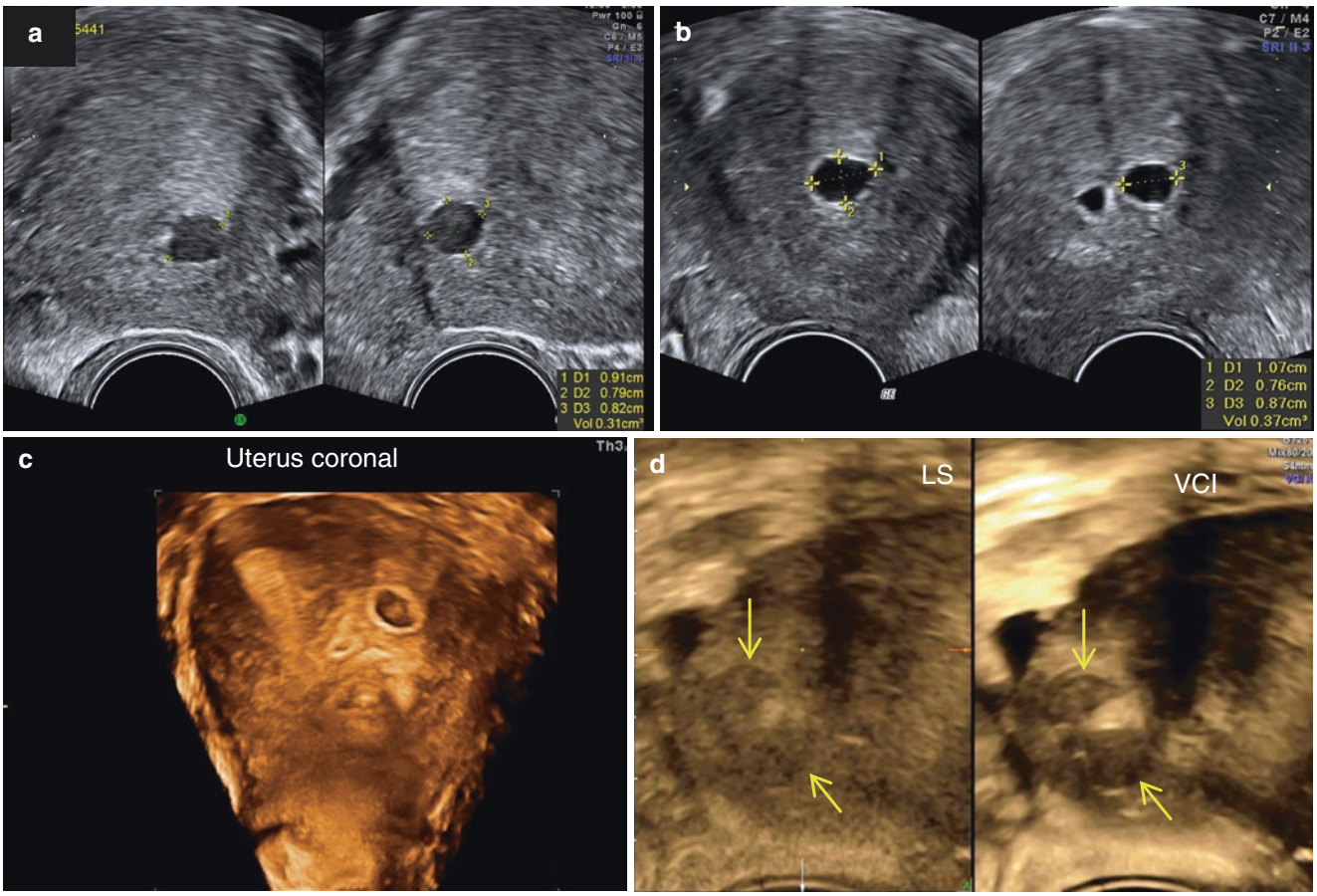

Fig. 3.38 Myometrial cysts in adenomyosis. (**a**) Tiny myometrial cysts seen showing turbid contents. (**b**) Myometrial cysts show hyperechoic margins. (**c**) 3D rendered image showing myometrial cysts with hyperechoic margins. (**d**) Large myometrial cysts (*arrows*) seen showing turbid contents in the posterior wall of the uterine fundus in a patient who had undergone a cystectomy for an endometrioma but found no relief from pain. The margins of the cysts were not distinct, and therefore VCI was utilised (in the image on the right half) for better delineation of the myometrial cysts

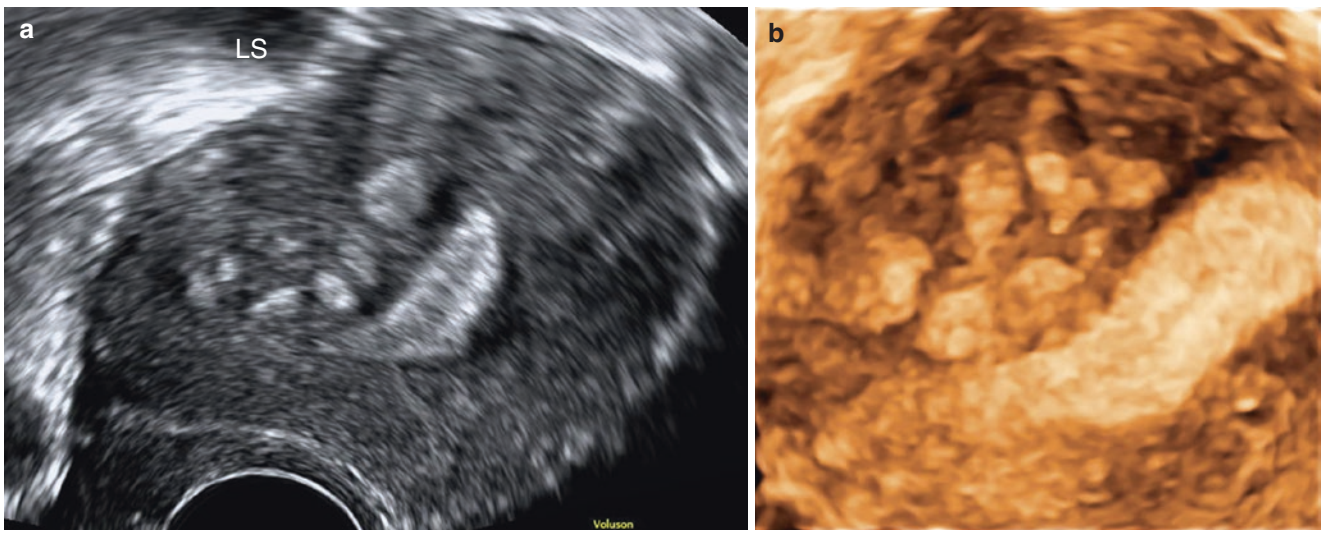

Fig. 3.39 Hyperechoic islands of endometrial tissue are seen within the myometrium of the posterior wall mainly in the submucous area, on (**a**) 2D greyscale and (**b**) 3D rendering

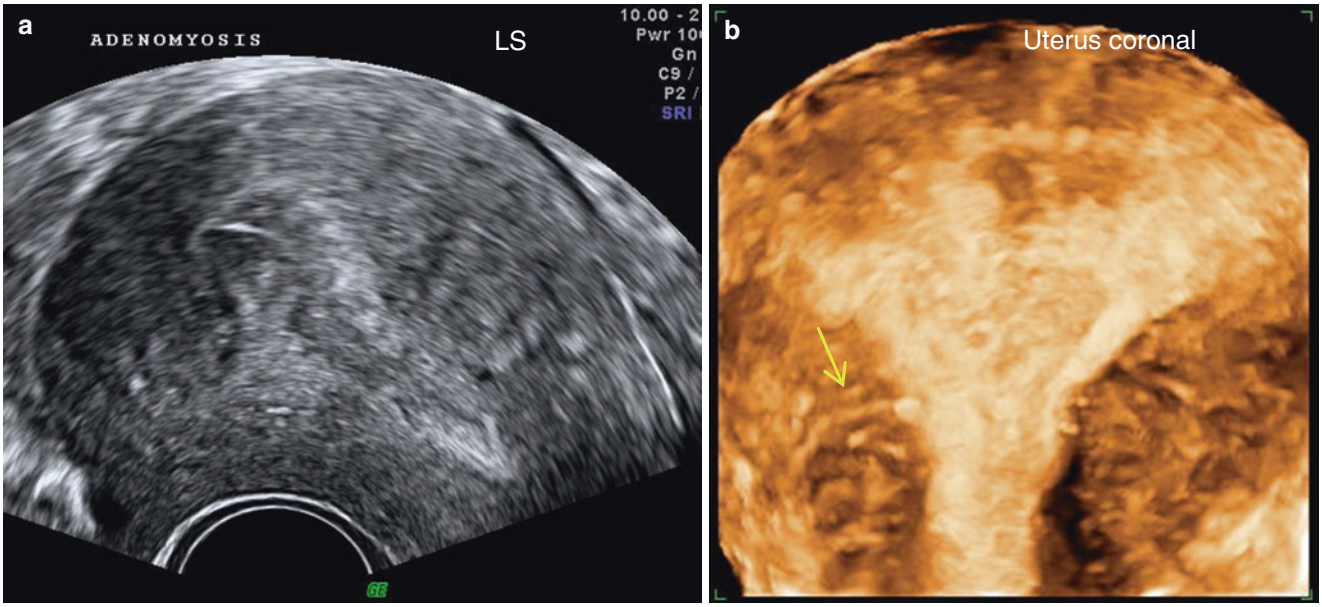

Fig. 3.40 Case of diffuse adenomyosis. (**a**) Ill-defined EMJ on 2D greyscale. (**b**) 3D rendered image showing irregular/poorly defined EMJ (particularly superiorly). Small hyperechoic lines (*arrow*) are seen arising from the EMJ – a known feature of adenomyosis

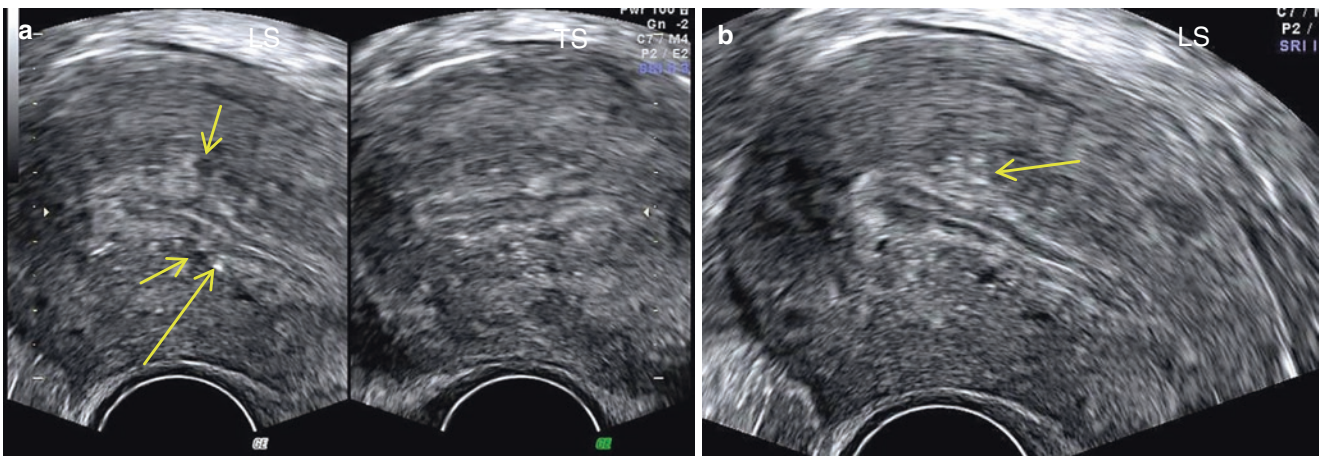

Fig. 3.41 JZ in a case of adenomyosis. (**a**) Irregular EMJ showing tiny cystic spaces (*short arrows*) and hyperechogenic foci (*long arrow*) in the JZ. (**b**) Irregular EMJ showing hyperechogenic, subendometrial buds/lines in the JZ (*arrow*)

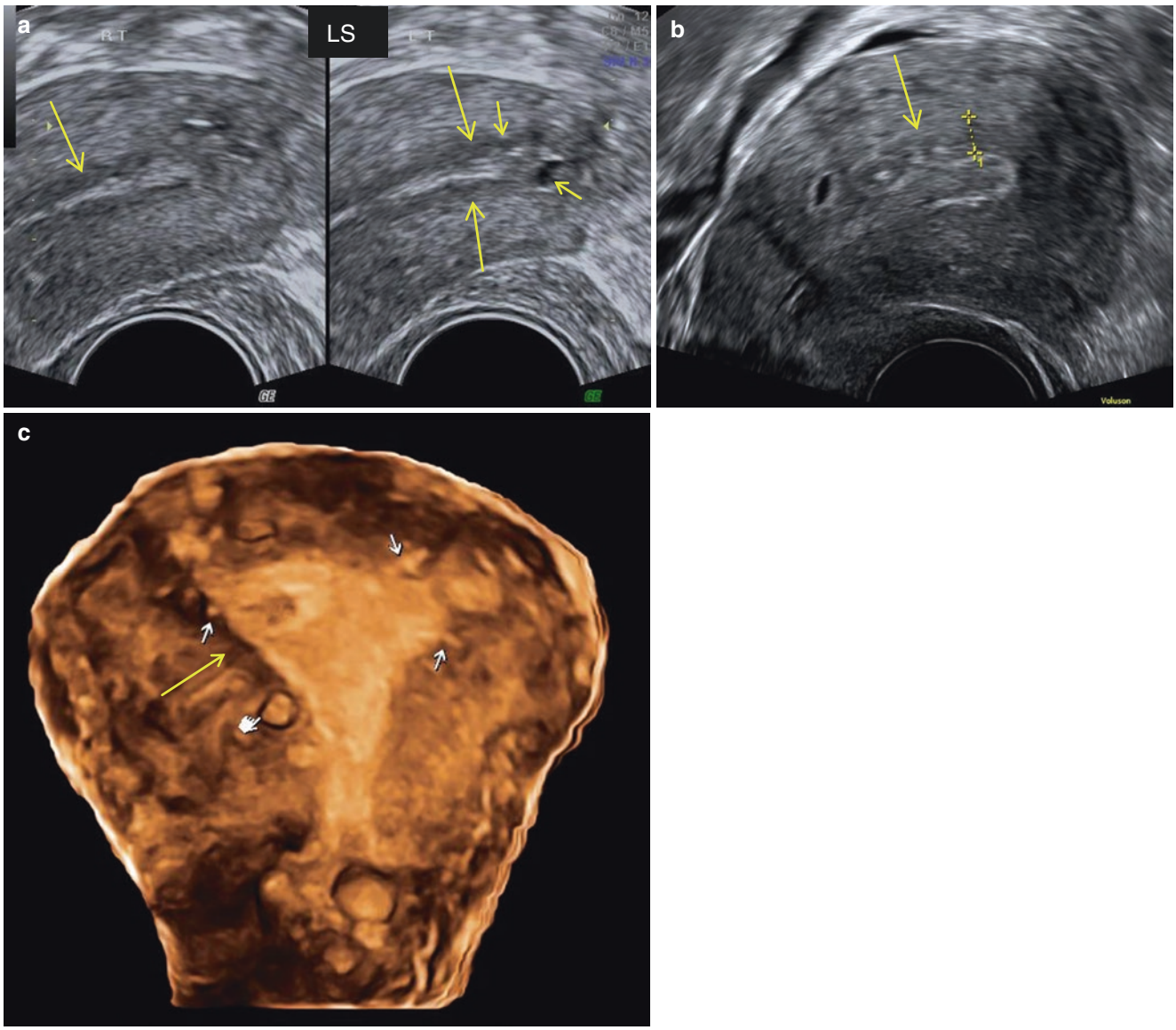

Fig. 3.42 Cases of adenomyosis showing thickened JZ (*long arrows*). (**a**) Case 1, showing, in addition, a few cystic spaces (*short arrows*). (**b**) Case 2, seen on greyscale. (**c**) Case 3, a 3D rendered coronal image with the JZ showing, in addition, hyperechoic endometrial buds (*short arrows*), cystic space (*pointer*) and an irregular endomyometrial junction

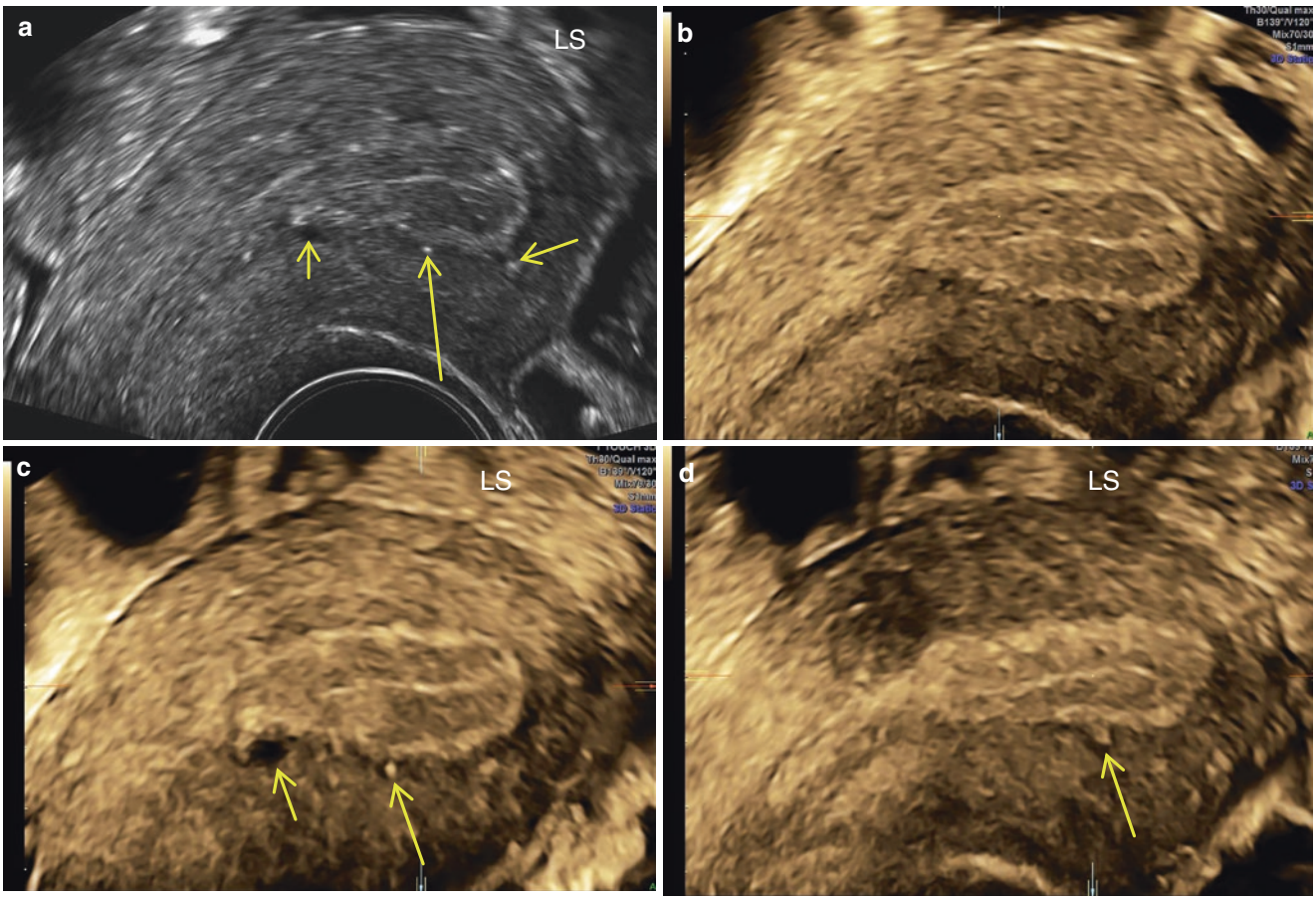

Fig. 3.43 JZ in a case of adenomyosis (**a**) on 2D greyscale showing cystic space (*short arrow*), hyperechogenic foci (*long arrow*) and hyperechoic endometrial buds (*medium length arrow*). (**b**–**d**) On 3D multiplanar imaging with VCI, the JZ is more distinct. (**c**) Cystic space (*short arrow*), hyperechogenic foci (*long arrow*) and (**d**) hyperechoic endometrial bud (*arrow*)

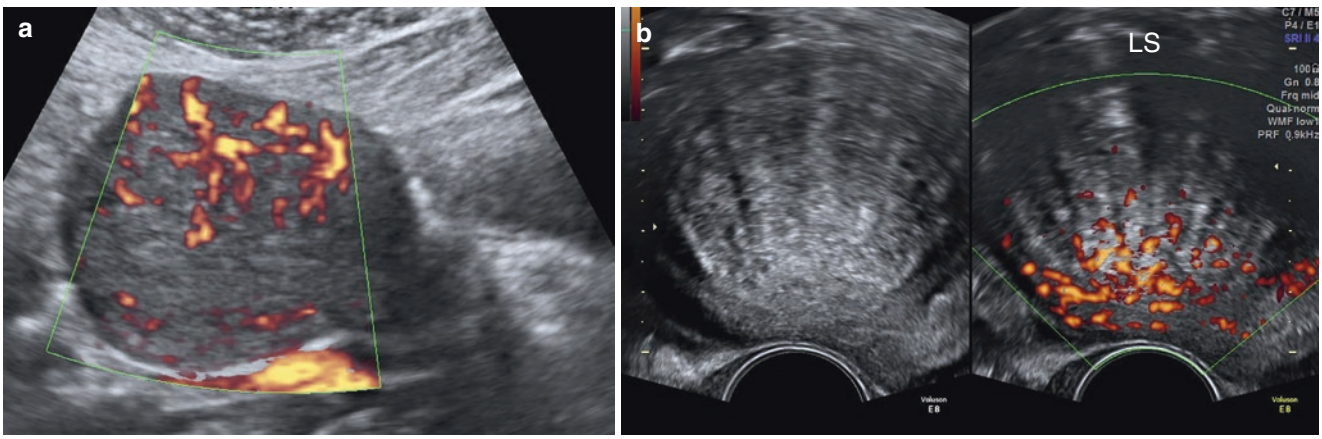

Fig. 3.44 Vascularity may be increased in adenomyosis. (**a**) Increased in the anterior myometrium (on TAS) in a case of anterior wall adenomyosis. (**b**) The globular adenomyotic myometrium shows flow within, i.e. intralesional flow (unlike a fibroid which typically shows peripheral flow)

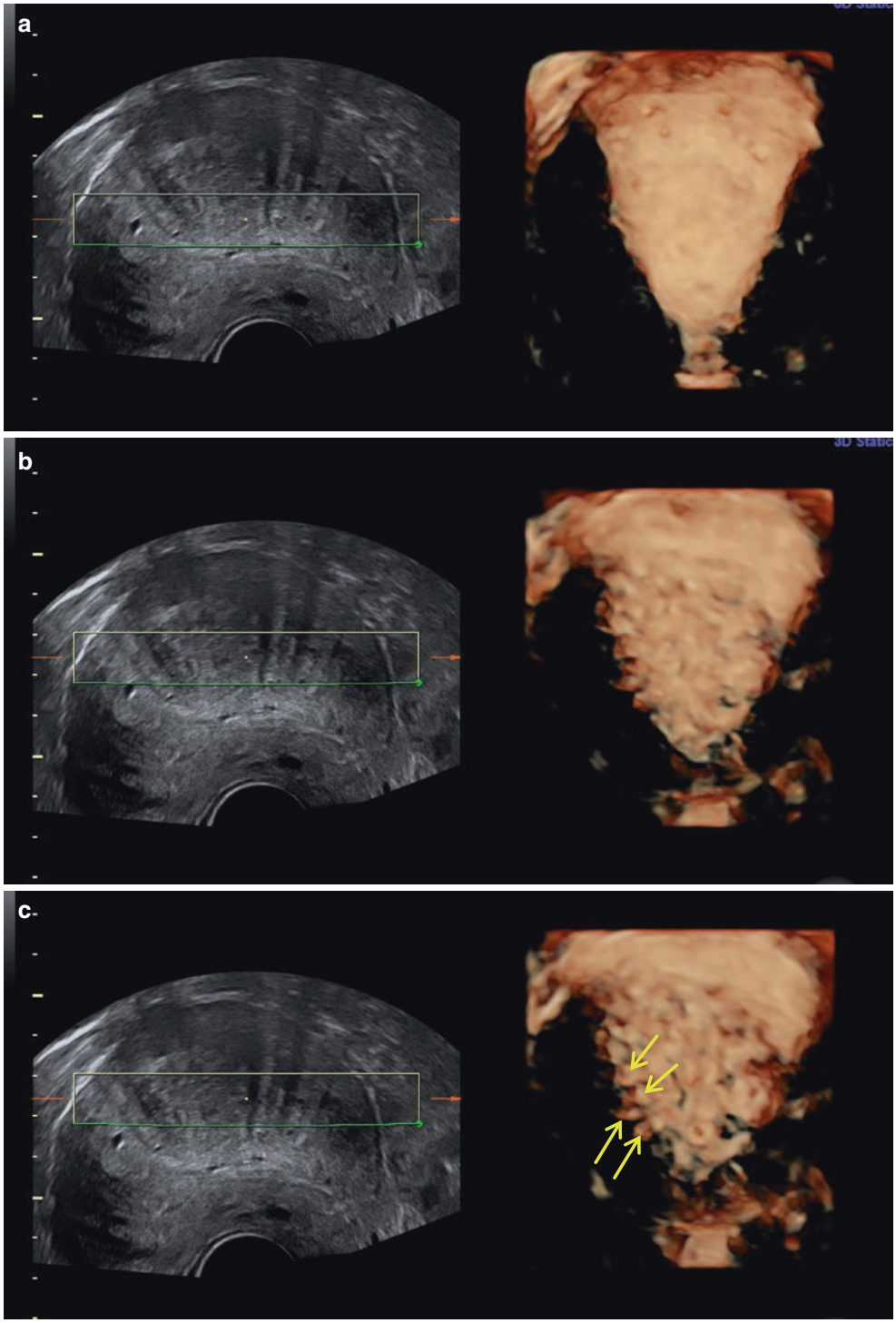

Fig. 3.45 3D rendered coronal views in a case of adenomyosis of the JZ with the plane of rendering, (**a**) through the endometrium primarily showing irregularity along its lateral margins, (**b**) closer to EMJ, showing significant irregularity in the anterior wall and the lateral margins, (**c**) in the JZ, just anterior to the endometrium, showing multiple endometrial buds (*arrows*) giving it an irregular appearance

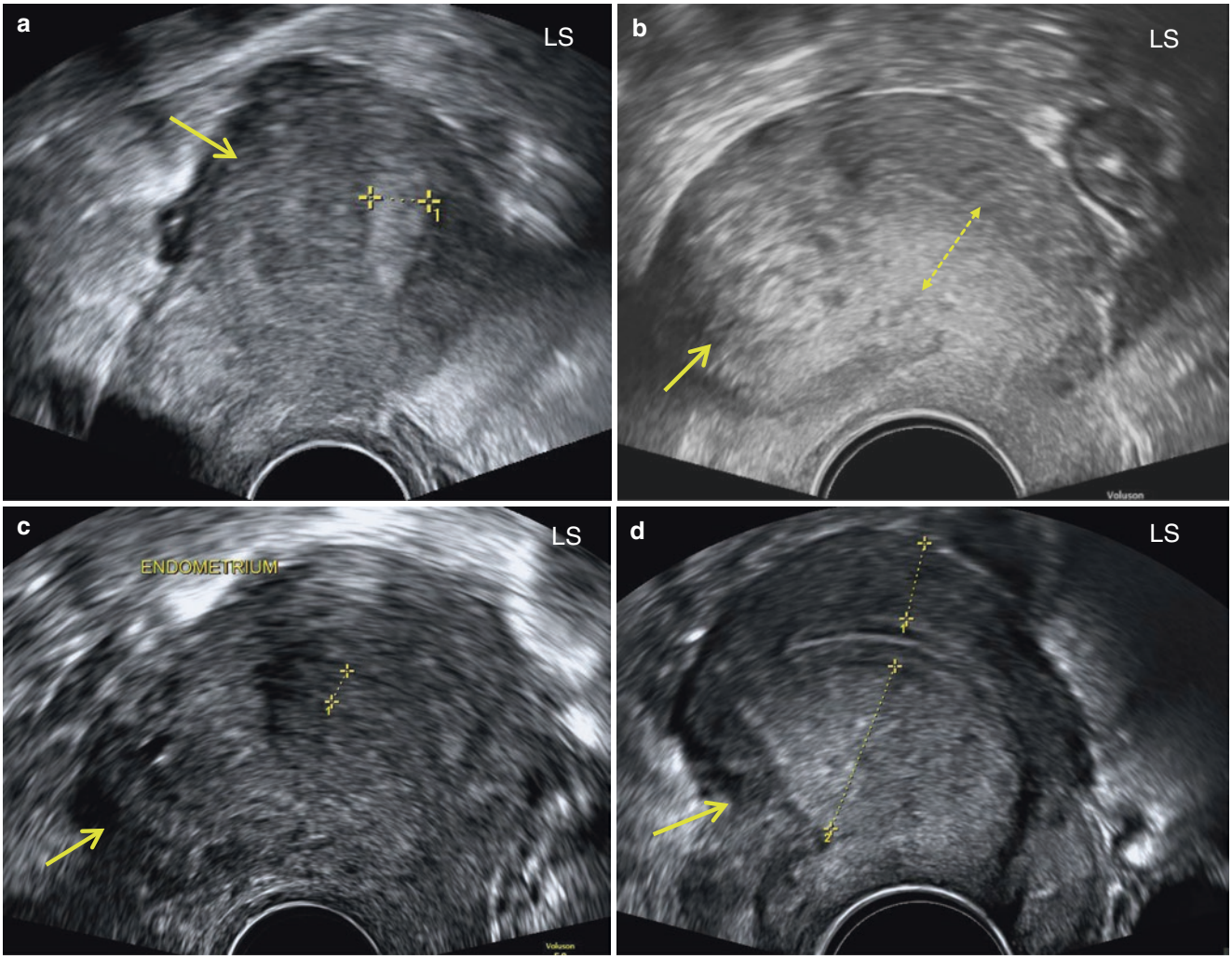

Fig. 3.46 (**a**–**d**) Four cases of posterior compartment DIE showing thick and coarse posterior walls (*arrows*) suggestive of adenomyosis

3.4.1 **Adenomyoma** (Figs. 3.47 and 3.48)

An adenomyoma is a focal area of adenomyosis and, therefore, shows the same features described on ultrasound as adenomyosis. The lesion, though focal, is not well defined. It shows 'fan-shaped' shadowing, heterogeneous echoes with cystic spaces, hyperechogenic islands of endometrial tissue, etc. They are typically seen in the submucosal area because of direct myometrial invasion from the endometrium. At times, adenomyomas may protrude into the endometrial cavity. On Doppler, flow in the adenomyoma is intralesional, i.e. central (which is important sometimes in confirming diagnosis and differentiating it from a fibroid).

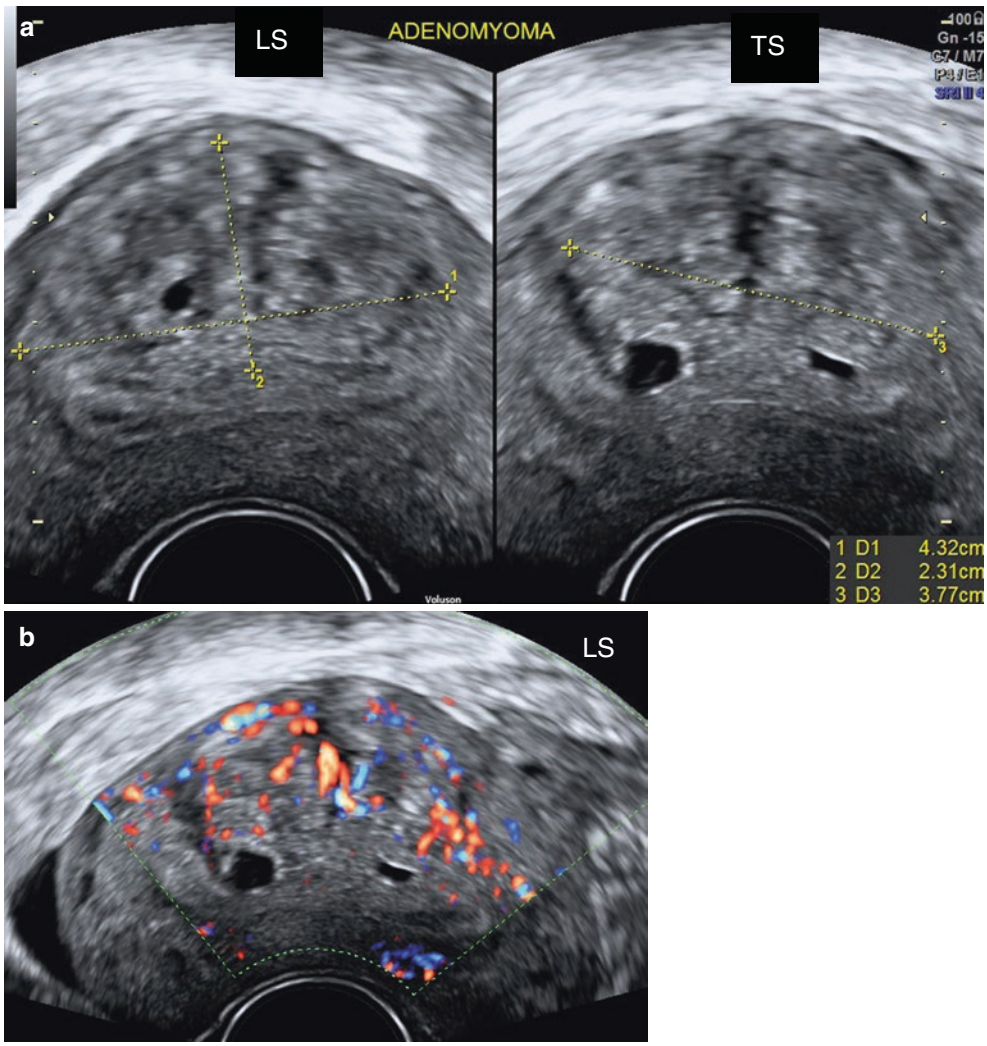

Fig. 3.47 Adenomyoma. (**a**) LS and TS of a large anterior wall adenomyoma showing coarse echoes, linear acoustic shadowing and tiny cystic spaces, some of which show hyperechoic margins. It is seen bulging into the anterior endometrium and is extending from the mucosa, almost up to the serosa. (**b**) Increased vascularity of the adenomyoma on Doppler

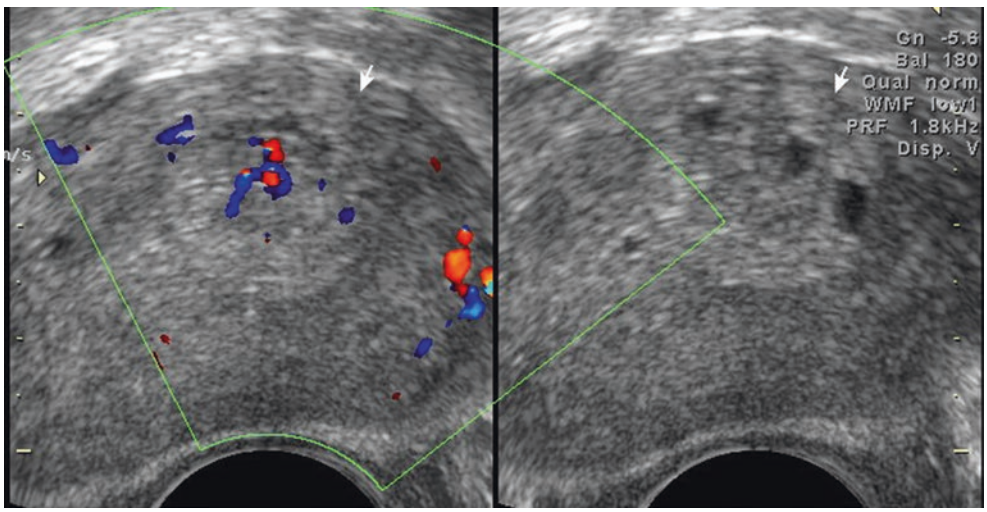

Fig. 3.48 Poorly circumscribed area showing coarse echoes, cystic spaces and central vascularity, suggestive of an adenomyoma seen on (**a**) Doppler and (**b**) greyscale

Summary: Adenomyosis/Adenomyoma

- Adenomyosis is a common gynecological disorder in women of reproductive age with typical complaints being menorrhagia and dysmenorrhoea.
- Typical ultrasound features include a globular enlargement of uterus, often with asymmetrically thickened walls. Myometrium shows coarse echotexture with tiny myometrial cysts and linear shadowing. Endometrial margins are poorly defined and JZ may show tiny cystic spaces, hyperechogenic dots, buds and echogenic lines.
- A focal area of adenomyosis is termed an adenomyoma.
- In women with endometriosis, particularly deep infiltrating endometriosis of the posterior compartment, the posterior wall of the uterus may show features of adenomyosis.
- It is important to differentiate adenomyosis and adenomyoma from fibroids as their management differs considerably.

Differentiation between a fibroid and an adenomyoma or adenomyosis

This can sometimes be challenging. The differentiation is, however, important in the management of these patients. The most significant point in management being that fibroids can be enucleated surgically unlike adenomyoma.

Features that help differentiate the two are tabulated below (Fig. 3.49).

Feature	Typical fibroid	Adenomyoma/ adenomyosis
Uterine contour	Regular or lobulated	Regular
Margins	Well defined and smooth	Poorly defined and irregular
Shape	Round/oval/lobulated	Ill-defined
Shadowing	Internal linear shadowing and edge shadows	Internal linear with no edge shadows
Vascularity	Mainly circumferential	Intralesional (central)
Junctional zone	Typical adenomyotic JZ abnormalities not seen. The JZ is usually well defined but may be stretched around the fibroid	JZ shows the typical adenomyotic features (ill-defined, irregular, thickened, tiny cystic spaces and echogenic buds/lines)

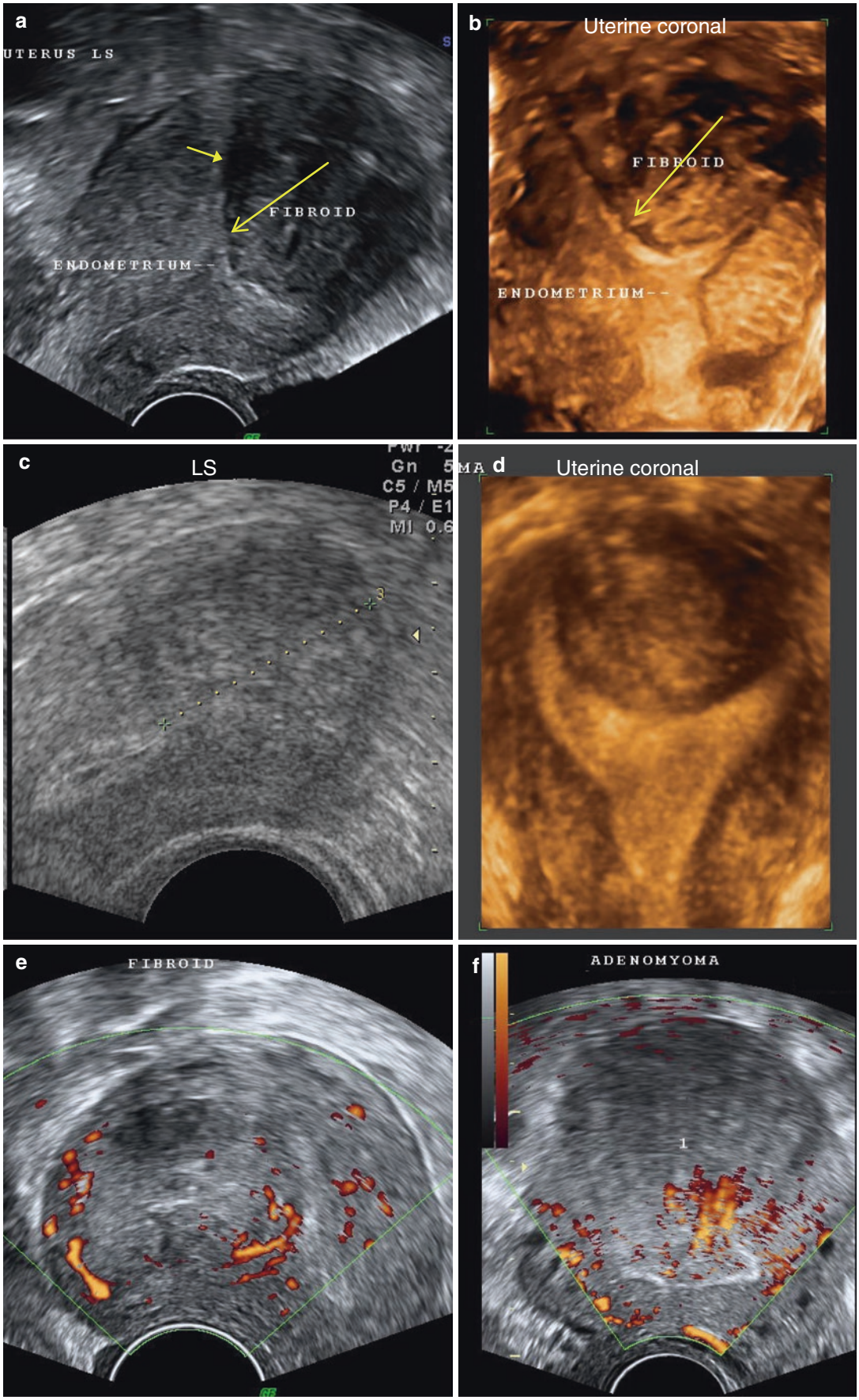

Fig. 3.49 Differentiating between a fibroid and adenomyoma/adenomyosis. (**a**, **b**) Fundal fibroid showing well-defined margins on 2D and 3D (*arrow*). Edge shadows are seen (*short arrow*). The endometrial deformity is not uniform. (**c**, **d**) Adenomyosis, particularly of the uterine fundus. (**c**) On greyscale, showing poorly defined margins and no edge shadowing. (**d**) 3D showing regular, uniform, concave deformity of the upper margin of the endometrium. (**e**) Fibroid showing peripheral vascularity. (**f**) Adenomyoma showing central vascularity

3.5 Sarcoma

Uterine sarcomas are malignant myometrial lesions. They are very rare, and their ultrasound features may be indistinct from that of ordinary fibroids. In addition, their symptoms are similar to that of fibroids which include dysmenorrhoea, menorrhagia and pelvic pain. They are, therefore, most often diagnosed only at surgery.

They tend to be seen in slightly older women (perimenopausal women).

Ultrasound Features of Sarcoma (Fig. 3.50)

- They are typically single and large tumours appearing similar to fibroids, particularly the ones that appear atypical.
- They are either hypoechoic or isoechoic.
- They usually do not show the typical stripy shadows of a fibroid.
- They may appear heterogeneous and may show irregular anechoic/hypoechoic cystic areas due to necrosis.
- Their margins may be regular or irregular (due to invasion into the surrounding myometrium).
- On Doppler, they tend to be more vascularised than fibroids. Flow may be central and chaotic with irregular and randomly dispersed vessels (as is seen with malignant masses). Typically the flow is of low resistance (RI less than 0.42) and high velocity (more than 42 cm/sec). It is suggested that Doppler flows should be assessed in all large and atypical fibroids from multiple sites.
- Rapid growth of the mass and the uterus is often seen in sarcomas.

The prediction of uterine sarcoma by ultrasound is based primarily on small retrospective case series, and, therefore, there are no established guidelines. It is, however, suggested that all large fibroids, particularly atypical or heterogeneous ones, should be assessed with Doppler and be followed up closely. A rescan of these masses in a case of sarcoma would typically show a rapid increase in size, unlike a benign fibroid.

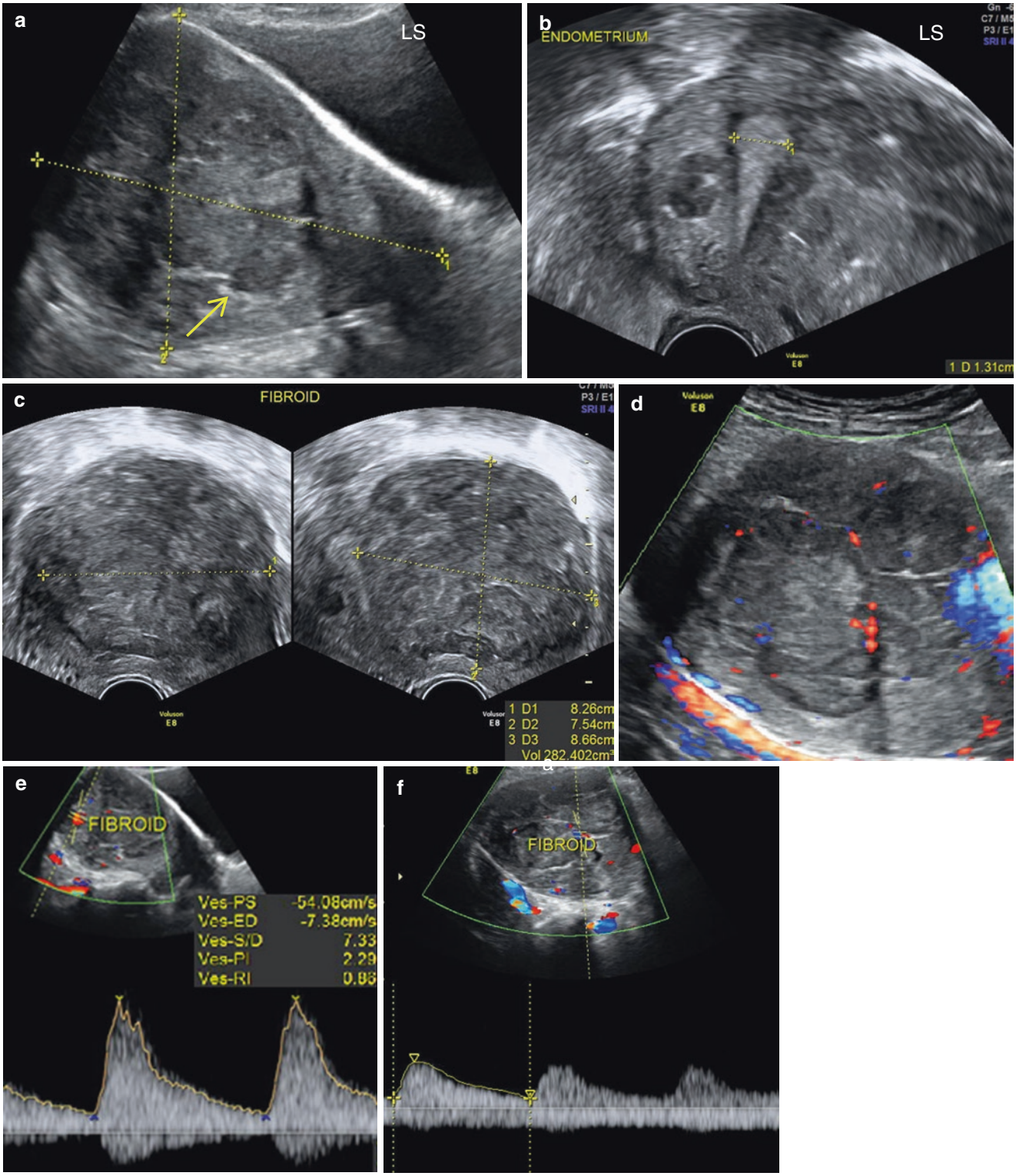

Fig. 3.50 Case of leiomyosarcoma. (**a**) Enlarged uterus showing a mass with slightly irregular outline (*arrow*) – in retrospect, suggestive of myometrial invasion. (**b**) TVS-LS of uterus with a small posterior wall fibroid and a large heterogeneous mass in its anterior wall appearing like an atypical fibroid. (**c**) Large, circumscribed, heterogeneous mass which was thought to be an atypical fibroid (measuring 8.2 × 7.5 × 8.6 cm). It did not show typical stripy shadows of a fibroid. (**d**) The mass was lobulated and showed flow within its septae, another atypical finding for a fibroid. (**e**, **f**) Flow in the mass showed variable flow indices, when assessed from different sites. A high PSV of 54.0 cm/sec in (**e**)

Suggested Reading

Bosch VD et al (2015) Terms, definitions and measurements to describe sonographic features of myometrium and uterine masses: a consensus opinion from the Morphological Uterus Sonographic Assessment (MUSA) group. Ultrasound Obstet Gynecol 46(3):284–298

Covarrubias DA et al (2009) Multimodality imaging findings of leiomyomatosis peritonealis disseminata. Ultrasound Obstet Gynecol 33:247–249. doi:10.1002/uog.6293

Exacoustos C et al (2011) Adenomyosis: three-dimensional sonographic findings of the junctional zone and correlation with histology. Ultrasound Obstet Gynecol 37:471–479. doi:10.1002/uog.8900

Garel L et al (2001) US of the pediatric female pelvis: a clinical perspective. Radiographics 21(6):1393–1407

Giunchi S (2010) OC27.05: uterine sarcomas: clinical and sonographic characteristics. Ultrasound Obstet Gynecol 36:50. doi:10.1002/uog.7920

Kepkep K et al (2007) Transvaginal sonography in the diagnosis of adenomyosis: which findings are most accurate? Ultrasound Obstet Gynecol 30:341–345. doi:10.1002/uog.3985

Kishi Y et al (2012) Four subtypes of adenomyosis assessed by magnetic resonance imaging and their specification. Am J Obstet Gynecol 207(2):114–117

Kurjak A, Žalud I (1991) The characterization of uterine tumors by transvaginal color Doppler. Ultrasound Obstet Gynecol 1:50–52. doi:10.1046/j.1469-0705.1991.01010050

Leone FPG et al (2007) Sonohysterography in the preoperative grading of submucous myomas: considerations on three-dimensional methodology. Ultrasound Obstet Gynecol 29:717–718. doi:10.1002/uog.4043

Murase E et al (1999) Uterine leiomyomas: histopathologic features, MR imaging findings, differential diagnosis, and treatment. Radiographics 5:1179–1197

Reinhold C (1999) Uterine adenomyosis: endovaginal US and MR imaging features with histopathologic correlation. Radiographics: 19: suppl 1, S147–S160

Ultrasound Evaluation of Endometrium

4

Endometrium is the mucous membrane that lines the inside of the uterus. It has a cell-rich connective tissue that surrounds the endometrial glands. It is composed of two layers: the superficial functional layer and the deeper basal layer. In each menstrual cycle, the superficial functional layer of the endometrium is shed and reconstituted from the underlying basal layer. Its thickness, morphology and vascularity change throughout the menstrual cycle in women of reproductive age.

4.1 Evaluation of Endometrium

The evaluation of the endometrium should be systematic, and reporting should be standardised. The IETA (International Endometrial Tumor Analysis group) statement is a consensus statement that has been published by a panel of experts (IETA consensus group) for terms, definitions and measurements for describing and reporting the endometrium and its pathologies.

The evaluation of the endometrium and uterine cavity can be done both by TAS and TVS. The TVS route is considered ideal for evaluating the endometrium. However, TAS may help, particularly in the presence of fibroids, an enlarged uterus or a mid-positioned (axially placed) uterus. Transrectal ultrasound scan should be considered if TVS is not possible due to any condition like vaginismus. It is best to do both a TAS and a TVS scan, because very often they complement each other.

The uterus is scanned (on 2D) in the sagittal plane from one cornu to the other and in the transverse plane from the cervix to the fundus. This gives us a good overall view of the uterus in the sagittal and transverse sections. 3D is useful for visualisation of the coronal section of the uterus which provides better information of the uterine cavity and EMJ (endomyometrial junction). Once the overview is done on ultrasound, the magnification should be increased focusing on the area of interest, i.e. the endometrium.

Generally the endometrium is easy to visualise. However, it may be difficult to study the endometrium in a mid-positioned uterus, because structures that lie perpendicular to the ultrasound beam are clearly visible but structures lying parallel to it are not. In such cases, one can place the probe in the anterior or posterior fornix and push on the cervix to retrovert or antevert the uterus further, to try and make the endometrium more perpendicular to the beam. TAS in such cases may provide better resolution. If visualisation is suboptimal, then that must be mentioned in the report. Saline or gel instillation (sonohysterogram) may help in better evaluation of the endometrium in cases where assessment is difficult or in those with an intracavitary pathology.

Measurements (Figs. 4.1, 4.2, 4.3, 4.4 and 4.5)

- The endometrium is measured in a sagittal plane. The measurement is taken perpendicular to the endometrial midline, where the endometrium is thickest, excluding the hypoechoic adjoining myometrium. Two-layer thickness is measured and reported in millimetres (rounded off to 1 decimal point). If there is intracavitary fluid, then a single-layer thickness is measured where it is thickest, and it should be mentioned in the report that it is a single-layer thickness, or one can add the thickness of the endometrium of the opposite wall and report a two-layer thickness. When the endometrium cannot be visualised clearly, as is sometimes the case with a mid-positioned uterus, it should be reported as nonmeasurable.
- When an intracavitary pathology is present, the total endometrial thickness including the lesion should be recorded. If an intracavitary myoma is clearly identified, then it should not be included in the measurement of endometrial thickness. Intracavitary lesions should be measured in millimetres in three perpendicular dimensions (as explained in Chap. 2). This helps calculate the volume of the lesion.
- The amount of intracavitary fluid can be measured in three perpendicular dimensions to assess the volume. The IETA recommendation is that intracavitary fluid should be defined by its largest measurement in the sagittal plane.

M. Sibal, *Ultrasound in Gynecology*, DOI 10.1007/978-981-10-2714-7_4

Qualitative Assessment of the Endometrium (Figs. 4.6, 4.7 and 4.8)

This includes the assessment of the endometrial echogenicity, the endometrial midline and the endomyometrial junction (EMJ).

- The echogenicity of the endometrium is compared with that of the myometrium. It could be hyperechoic, isoechoic or hypoechoic.
- The endometrial echogenicity is considered uniform, if the endometrium is homogeneous with symmetrical anterior and posterior walls. The echogenicity is termed non-uniform, if the endometrium appears heterogeneous, asymmetrical or cystic.
- The endometrial midline is the interface between the opposing surfaces of the two endometrial walls. It is defined as 'linear' if it is straight and hyperechogenic; 'non-linear' if it is waved and hyperechogenic; and 'irregular' or 'not defined' in the absence of any distinct midline echoes.
- The EMJ is basically the outer margin of the endometrium. It could be described as regular, irregular, interrupted or not defined.
- When an intracavitary lesion is present, a bright line is generally seen at the interface between the lesion and the endometrial walls, particularly if the lesion is smooth walled. If any lesion is seen within the cavity, its morphology should be described, i.e. its margins, echogenicity and vascularity.
- Intracavitary lesions are better visualised in the presence of fluid in the endometrial cavity (including sonohysterogram). The lesion is defined as 'extended' if the endometrial abnormality involves 25 % or more of the endometrial surface, and as localised if less than 25 % of the endometrial surface is involved. Localised lesions are defined as 'pedunculated', if their maximum transverse diameter is less than the diameter of its base, and 'sessile' if their maximum transverse diameter is more than the diameter of its base.
- In the presence of fluid in the endometrial cavity (including sonohysterogram), the endometrial outline (i.e. the endometrial surface facing the uterine cavity) is defined as 'smooth' if it appears regular; as having endometrial folds if there are multiple thickened 'undulating' areas with a regular profile; as 'polypoid' if there are deep indentations; or as 'irregular' if the surface is cauliflower-like or sharply toothed ('spiky').

Doppler (Fig. 4.9)

For Doppler evaluation of the endometrium, the colour/power Doppler box should include the endometrium with the surrounding myometrium. Magnification is important and the Doppler setting should be optimised to ensure maximal sensitivity for blood flow (details in the section on Doppler in Chap. 2).

- Vascularity is assessed subjectively by the use of colour score from 1 to 4, 1 being no colour and 4 being maximal colour (details in the section on Doppler in Chap. 2). Spectral wave forms can also be used to measure RI and PI of lesions in some cases.
- The vascular pattern in the endometrium is reported with respect to the presence or absence of 'dominant' vessels. A 'dominant' vessel is defined as a distinct vessel crossing the EMJ. This may show branching within the endometrium. 'Dominant' vessels could be a single vessel (feeder vessel or pedicle artery sign) or could be multiple having either a 'focal origin' at the EMJ or a 'multifocal origin'. Other vascular patterns include scattered vessels in the endometrium, without origin at EMJ and circular flow (e.g., submucous fibroid).

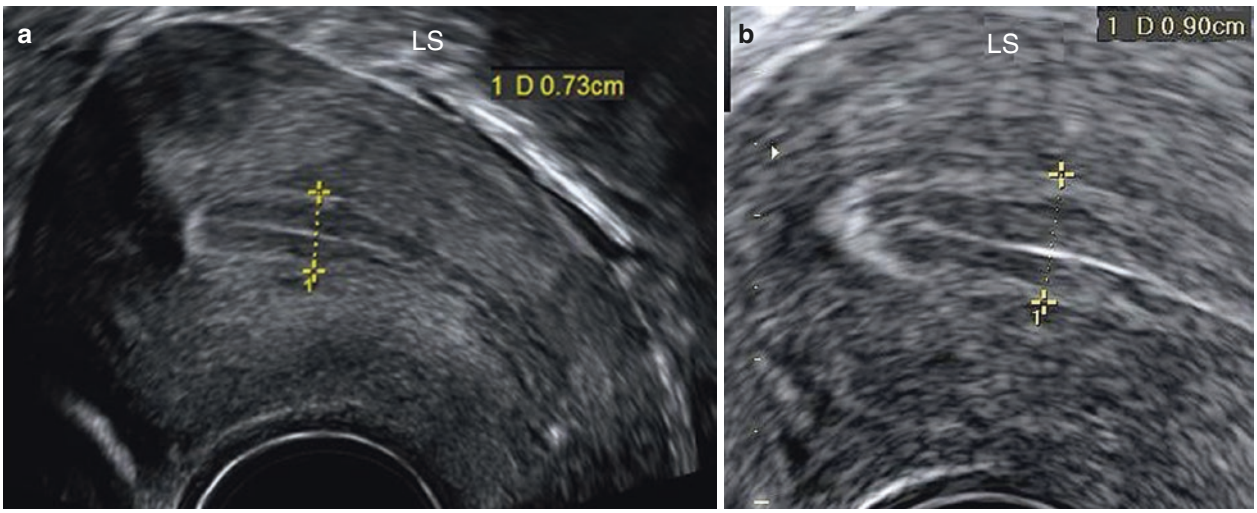

Fig. 4.1 (**a**, **b**) Endometrium is measured in the midsagittal section of the uterus perpendicular to the endometrial midline, excluding the hypoechoic adjoining myometrium. The measurement is most accurate when the ultrasound beam is perpendicular to the endometrial stripe

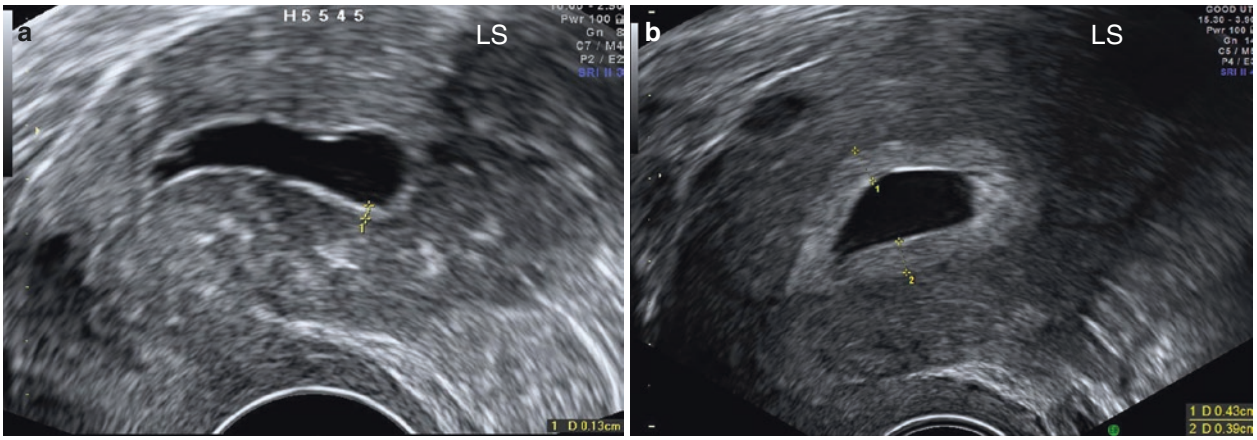

Fig. 4.2 Measuring the endometrium in the presence of intracavitary fluid. (**a**) A single-layer thickness is measured and reported as such, or (**b**) one may measure the endometrial thickness of the opposite walls and add the two for reporting

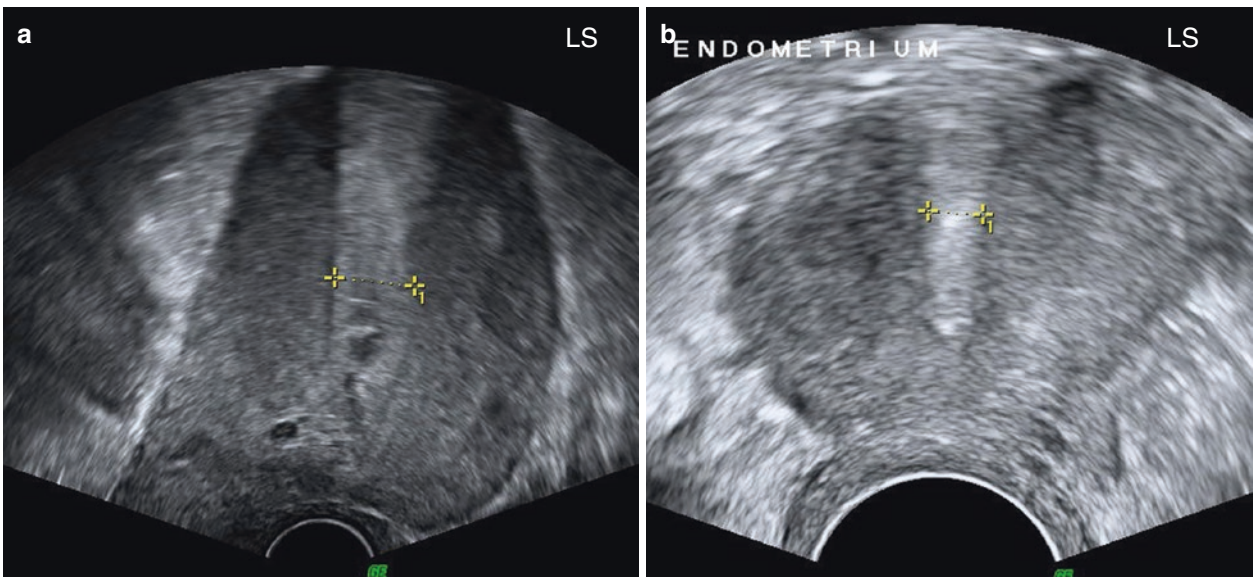

Fig. 4.3 (**a**, **b**) In a mid-positioned uterus, the endometrium is difficult to measure and assess, as the ultrasound beam lies parallel to the endometrial stripe

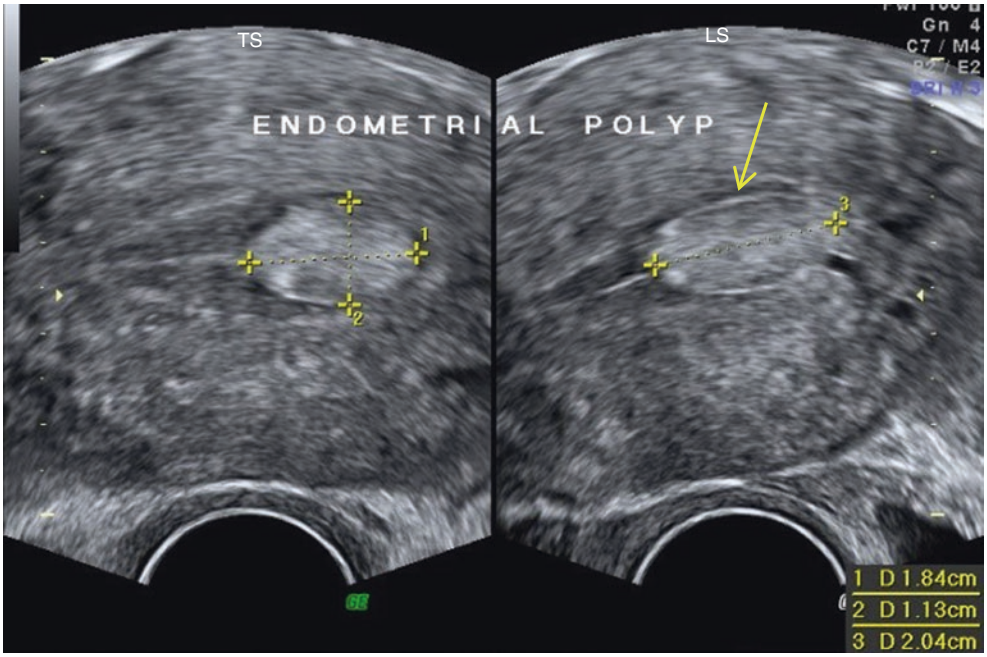

Fig. 4.4 Intracavitary pathologies like polyps should be measured in three perpendicular dimensions so that their volume can be calculated. *Arrow* shows a hyperechoic line between the polyp and the endometrium

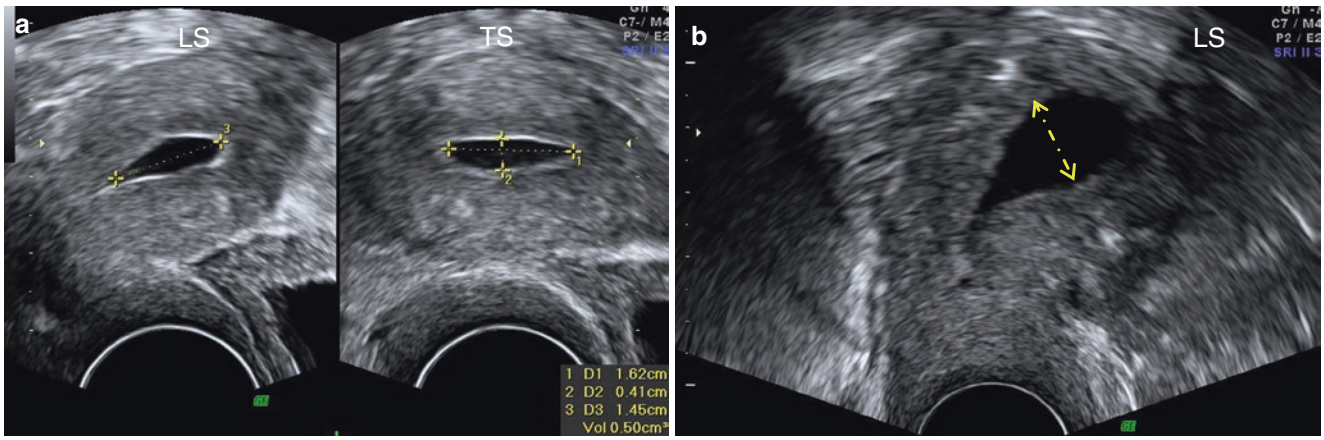

Fig. 4.5 Intracavitary fluid measured (**a**) in three perpendicular dimensions to obtain volume or (**b**) as the largest measurement in the sagittal plane (IETA recommendation)

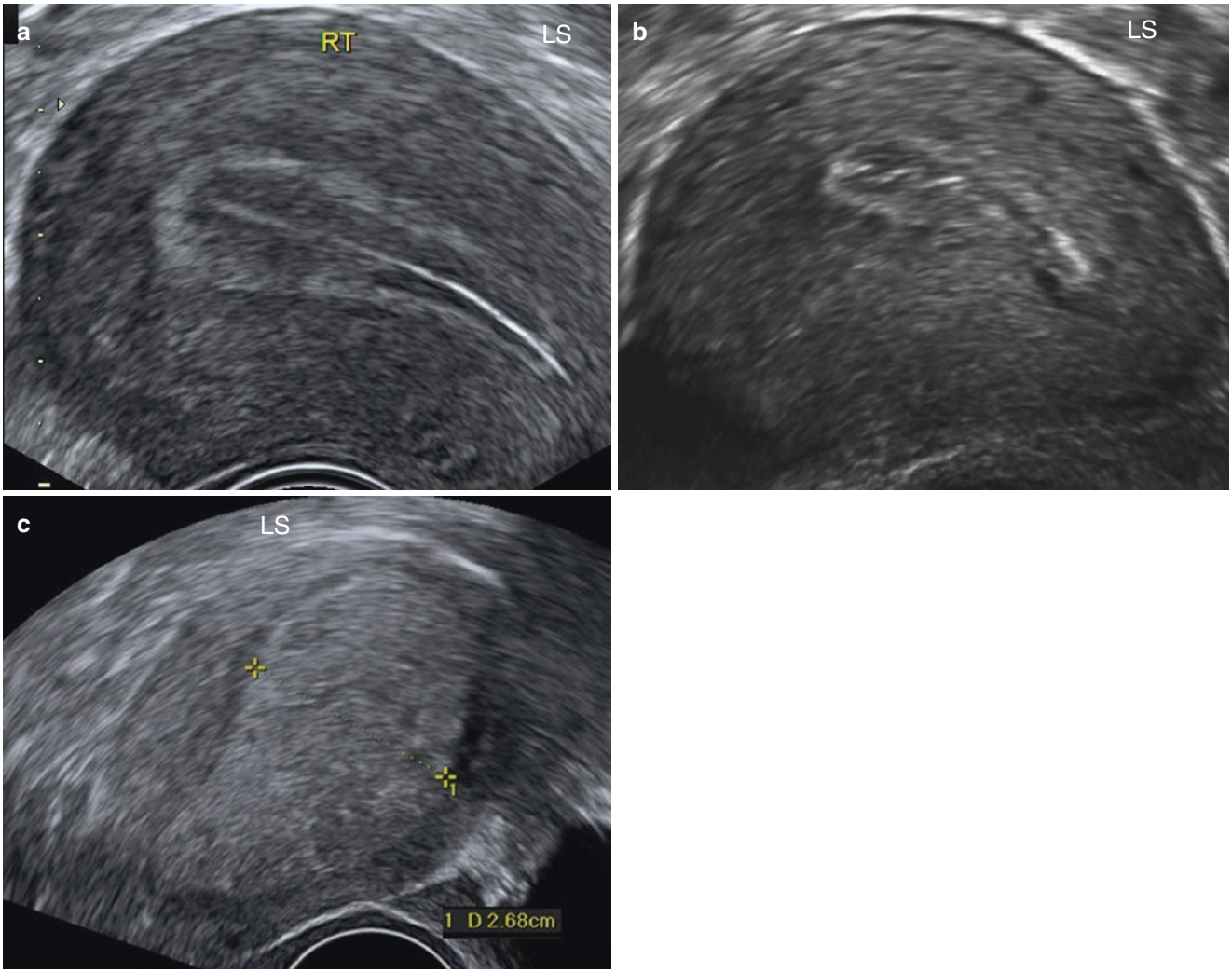

Fig. 4.6 The endometrial midline: (**a**) linear, (**b**) non-linear, (**c**) not defined. The endometrium in (**c**) is hyperechoic and thick

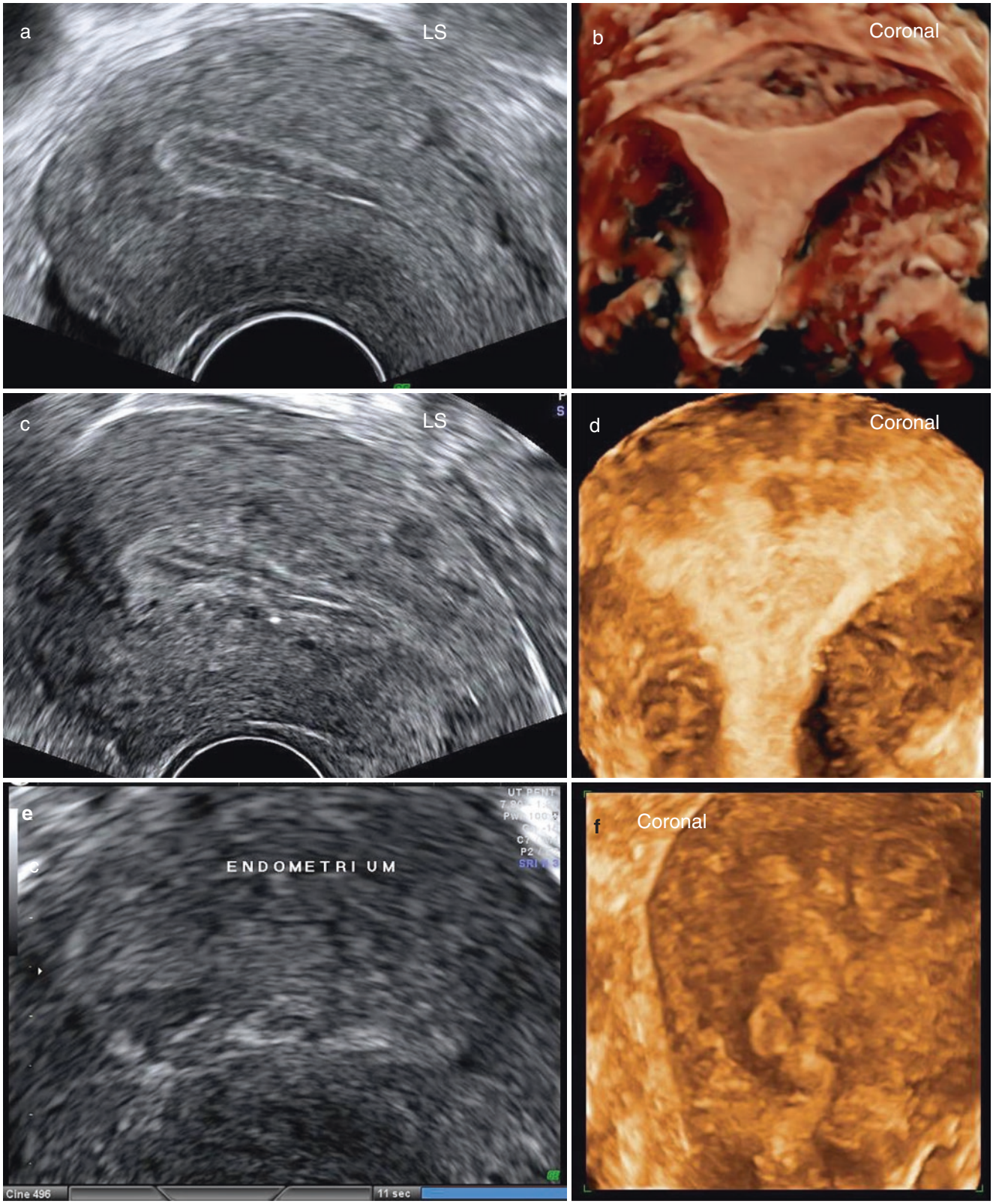

Fig. 4.7 Endomyometrial junction 2D and 3D coronal view: (**a**) and (**b**) regular, (**c**) and (**d**) irregular, (**e**) and (**f**) not defined

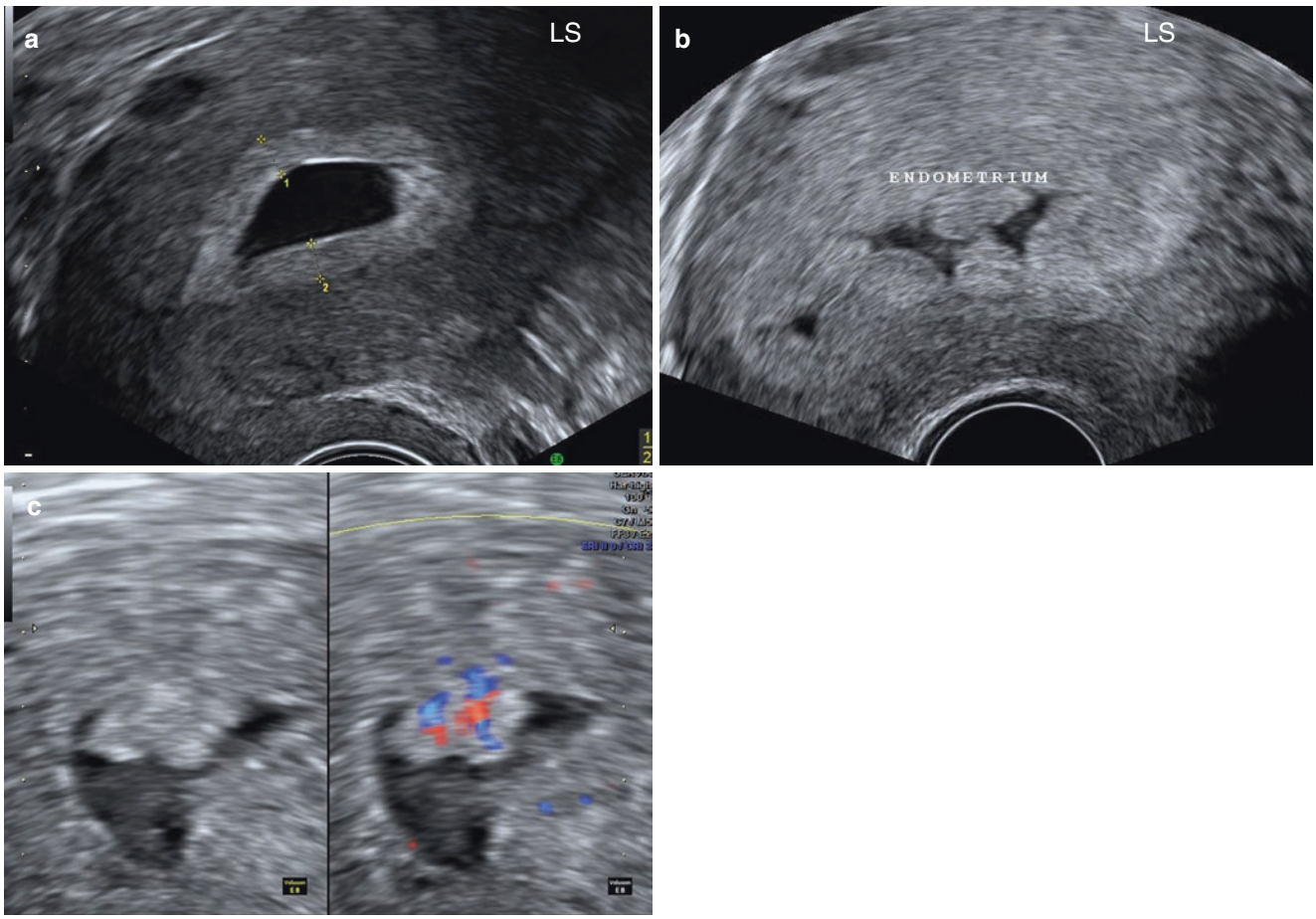

Fig. 4.8 Endometrial outline: (**a**) regular, (**b**) polypoidal, (**c**) irregular

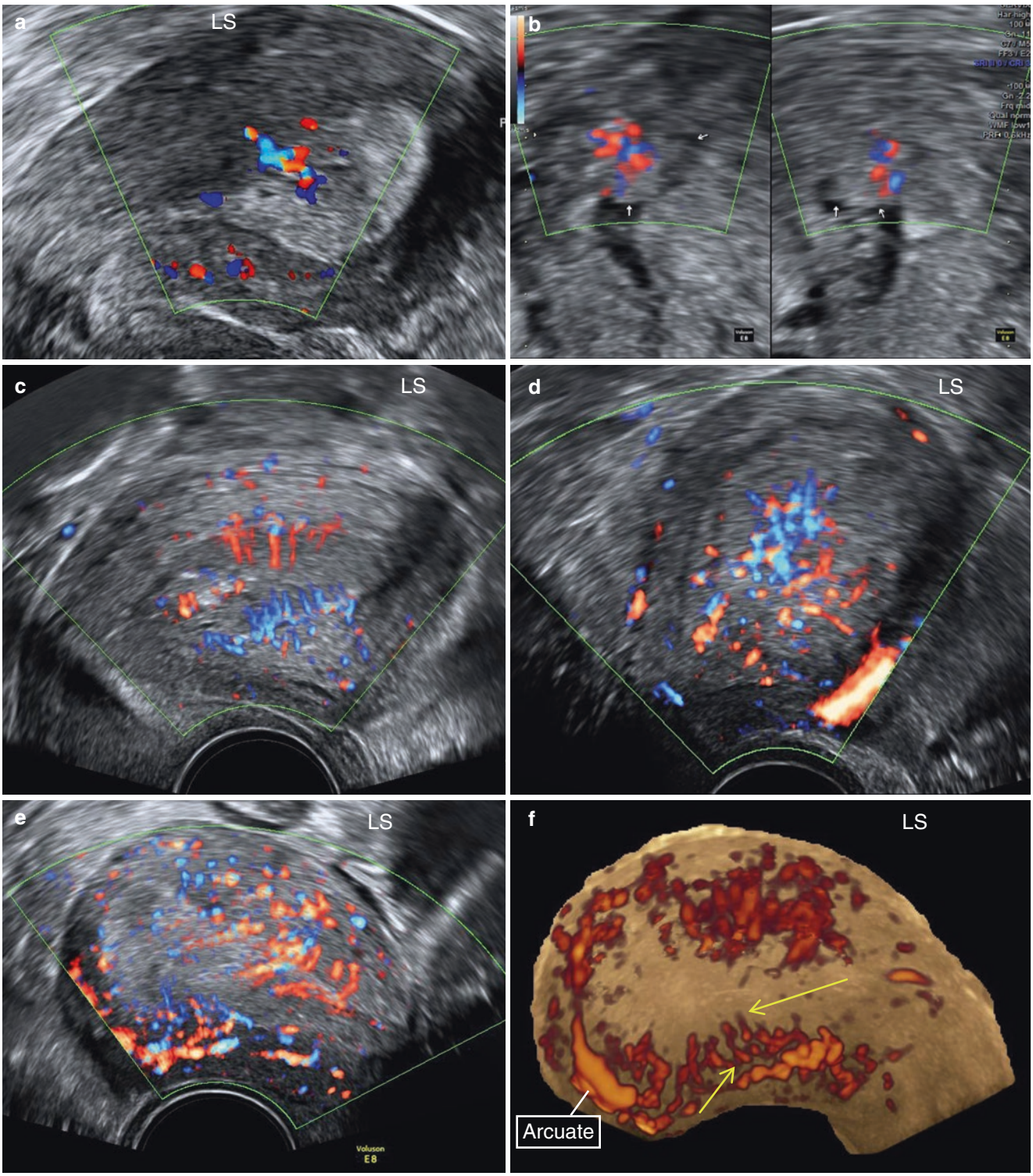

Fig. 4.9 Vascular pattern in endometrium. (**a**) Dominant single vessel with origin at EMJ – endometrial polyp. (**b**) Multiple vessels with focal origin at EMJ – focal endometrial carcinoma. (**c**) Multifocal origin at EMJ – endometrial hyperplasia. (**d**) Scattered vessels without origin at EMJ – invasive endometrial carcinoma. (**e**) Multifocal origin at EMJ – normal secretory endometrium (note the similarity in pattern with endometrial hyperplasia in (**c**)). (**f**) Same case as (**e**) flow with 3D glass body display, showing arcuate vessels, radial vessels (*short arrow*) and spiral arteries (*long arrow*) in a normal secretory endometrium

4.2 Normal Endometrium

Endometrial thickness, morphology and vascularity change throughout the menstrual cycle in women in the reproductive age group. In addition, the endometrium appears different in women prior to menarche and after menopause.

Most often the endometrial types seen and reported on ultrasound are menstruating, proliferative, early secretory, secretory and hyperechoic.

4.2.1 Endometrium in Paediatric Age Group (Fig. 4.10)

The endometrium appears as a thin echogenic line, and a small percentage of neonates have minimal fluid collection within the endometrial cavity. At the onset of puberty, the endometrium gradually increases in thickness and becomes like that of an adult.

4.2.2 Endometrium in Reproductive Age Group (Figs. 4.11 and 4.12)

Endometrial changes during the menstrual cycle, parallel cyclical ovarian changes.

- *Menstrual phase* (*Day 1–6 of menstrual cycle**):
  During menstruation, the endometrium appears hyperechoic and complex. By the end of menstruation, the endometrium is thin, about 1–4 mm in thickness. Baseline scans in women on the treatment for infertility are done on Day 2 or 3 of the menstrual cycle. No subendometrial flow is seen at this time.
- *Proliferative phase or follicular phase* (*Day 6–14 of menstrual cycle**):
  The endometrium gradually increases in thickness from 5 mm to about 10–12 mm. At the time of administrating the hCG injection in women undergoing follicular imaging for infertility, the endometrial thickness should be at least 6 mm, and the results are best when the thickness is 8 mm. The proliferative phase endometrium is typically seen as a three-layer endometrium with an echogenic basal layer, a hypoechoic inner functional layer and an echogenic midline at the interphase of the two layers. Minimal intracavitary fluid may be seen in the preovulatory phase. The vascularity of the endometrium gradually increases to a maximum, just prior to ovulation.
- *Secretory phase or luteal phase* (*Day 14–28 of menstrual cycle**):
  The endometrial thickness may decrease minimally at ovulation, but after that it increases gradually in thickness (7–15 mm). The endometrium also becomes hyperechoic starting from the periphery towards the centre. This increased echogenicity is believed to be due to stromal oedema and the presence of mucus and glycogen in the glands. This stromal oedema is also responsible for the increased echogenicity of the myometrium beyond it due to acoustic enhancement.

Endometrium in the Post-partum Period

The endometrium following delivery is less than 2 cm. Some amount of fluid, blood products and echogenic debris, including a small amount of gas, are normal in the first week after delivery and may be seen up to 3 weeks post-partum.

4.2.3 Endometrium in Postmenopausal Women (Fig. 4.13)

The normal postmenopausal endometrium is thin, homogeneous and echogenic. In postmenopausal women, simple measurement of the endometrial thickness is useful in assessing the risk for endometrial cancer (unlike in premenopausal women). An endometrial thickness of 4 mm or less decreases the likelihood for endometrial cancer by a factor of 10, in a postmenopausal woman.

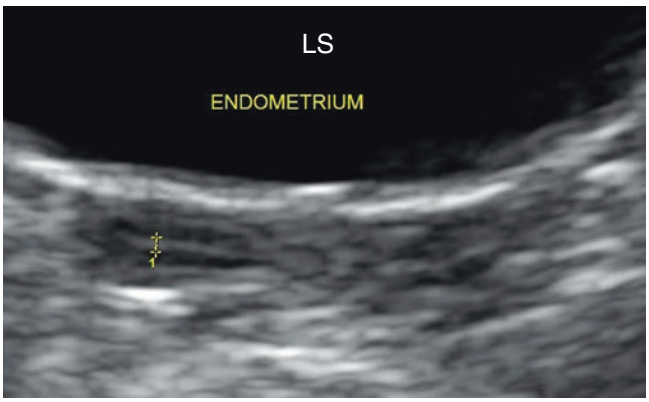

Fig. 4.10 Thin echogenic endometrium measuring 1 mm, in a premenarchal girl

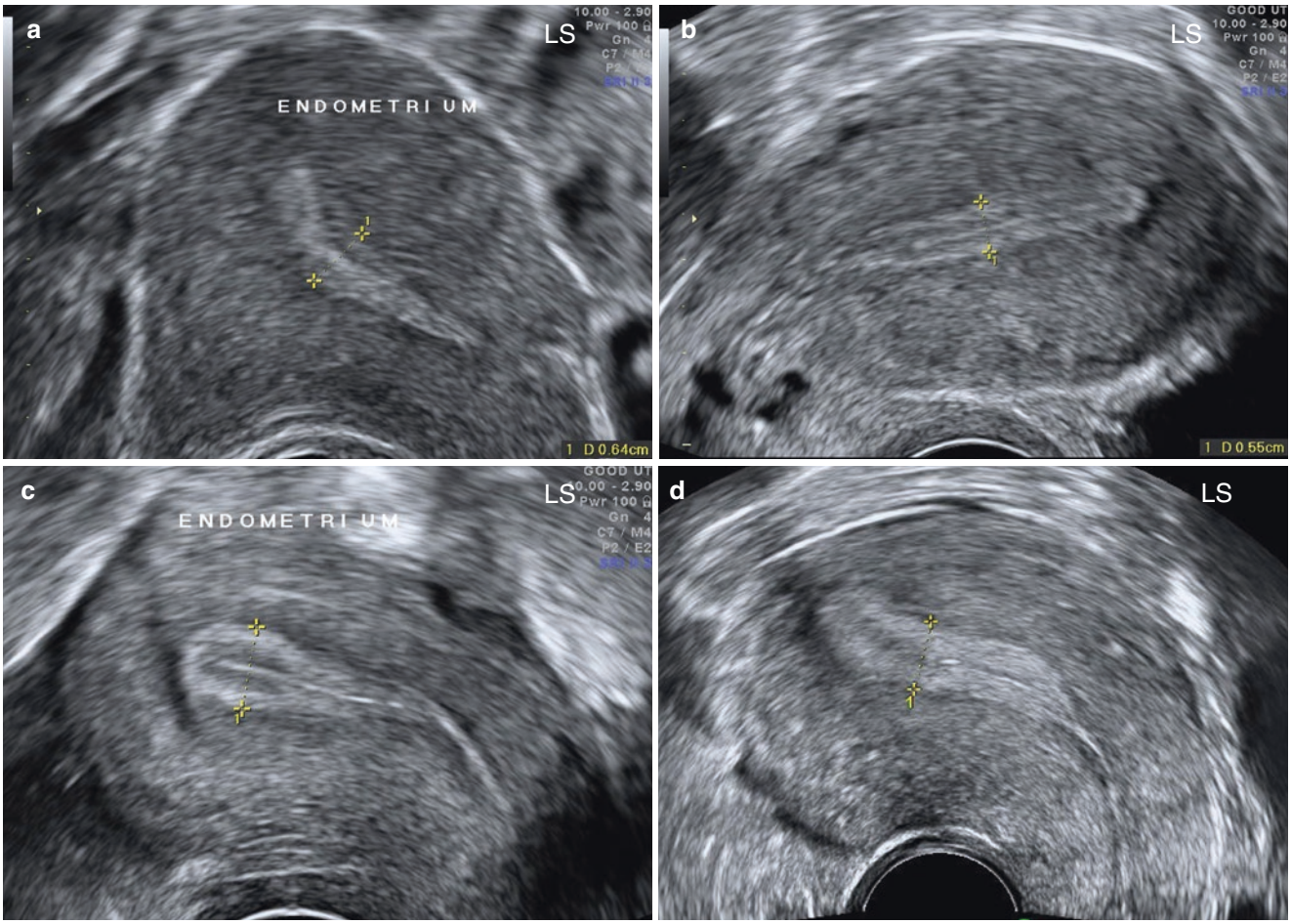

Fig. 4.11 Endometrium in different phases of menstrual cycle. (**a**) Menstruating endometrium, (**b**) proliferative endometrium, (**c**) early secretory endometrium, (**d**) secretory endometrium

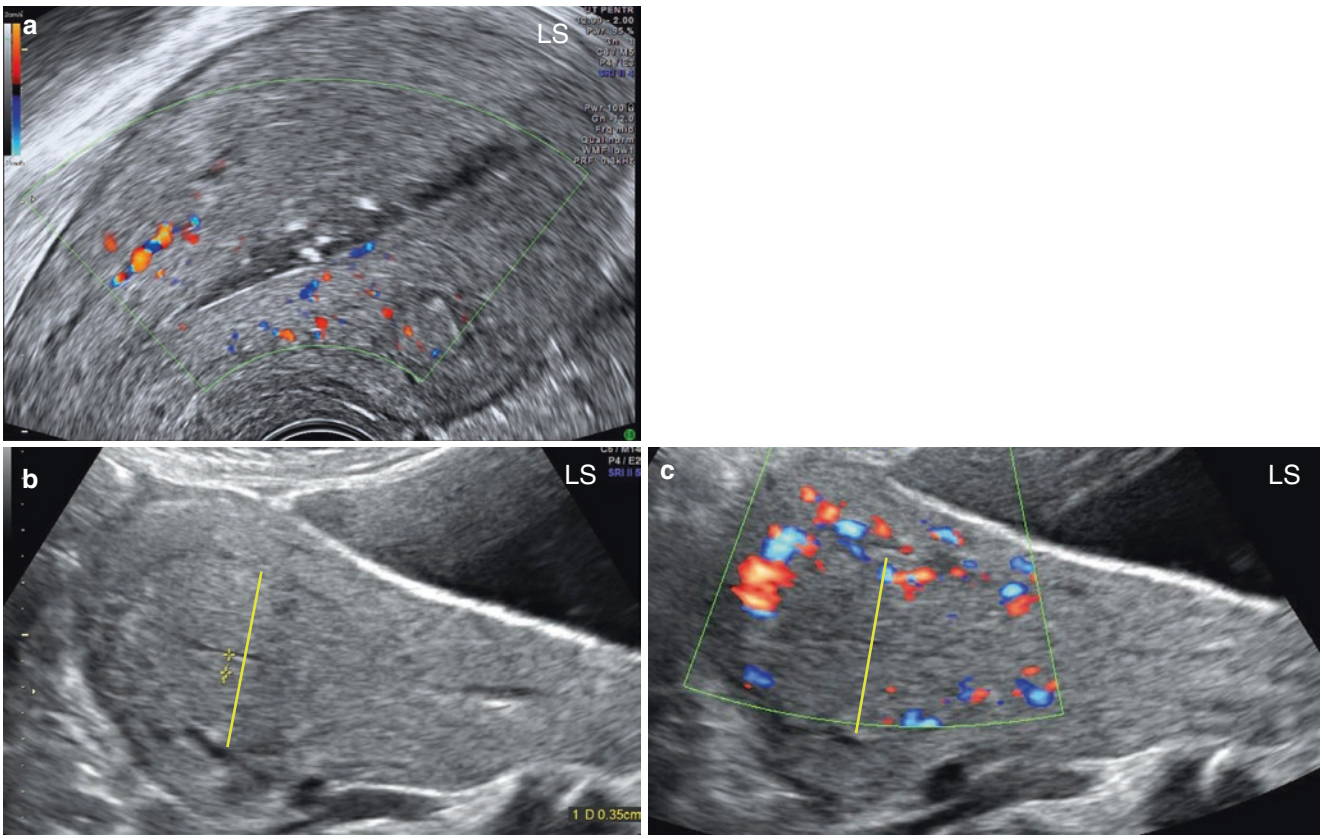

Fig. 4.12 Normal post-partum endometrium. (**a**) Post-partum second week – fluid, debris and minimal gas shadows seen in the endometrial cavity. Single-layer thickness of the endometrium was 4.4 mm. (**b**, **c**) Uterus – on post-partum Day 18 with (**b**) single-layer endometrial thickness of 3.5 mm. This can be wrongly interpreted as being much thicker (*marked in the image*) because of isoechoic endometrium and prominent arcuate vessels wrongly interpreted as the EMJ. (**c**) Arcuate vessels seen on Doppler

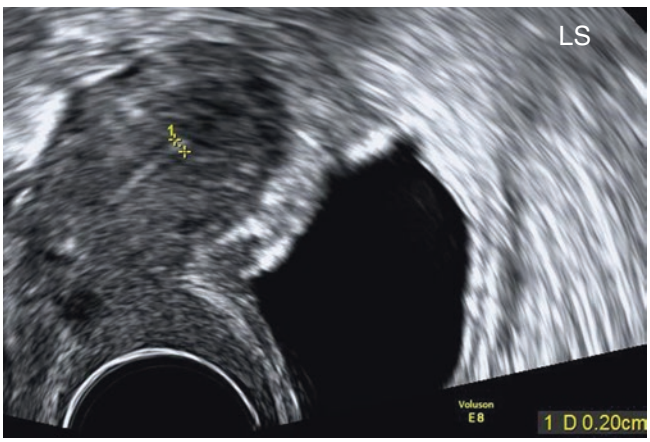

Fig. 4.13 Thin echogenic endometrium measuring 2 mm, in a postmenopausal lady

4.3 Endometrial Polyps

Endometrial polyps are frequently diagnosed in both symptomatic and asymptomatic women. They are growths arising from the endometrial lining of the uterus and may be associated with hyperplasia. Though most are benign, some may show malignancy within.

Polyps could cause intermenstrual spotting and infertility/subfertility. Polyps that cause abnormal uterine bleeding are more likely to be polyps with atypical hyperplasia.

Ultrasound Features of Endometrial Polyps (Figs. 4.14, 4.15, 4.16, 4.17, 4.18, 4.19, 4.20, 4.21, 4.22, 4.23, 4.24, 4.25, 4.26, 4.27, 4.28, 4.29, 4.30 and 4.31)

- A polyp typically appears as a circumscribed hyperechoic area within the endometrial cavity and, therefore, is better seen in a proliferative endometrium. The polyp is measured in three perpendicular dimensions.
- Very often, a fine hyperechoic line is seen around the polyp along the interphase between the polyp and the surrounding endometrium (similar to the central line in a proliferative endometrium). This hyperechoic line is seen to be discontinuous at the site of entry of the feeder vessel into the polyp. The presence of this hyperechoic line often helps in delineating a polyp on 2D, in a hyperechoic or secretory endometrium.
- Sometimes these polyps show tiny cystic spaces within. The cystic spaces relate to dilated endometrial glands within the polyp. In postmenopausal women with a thick endometrium, a focal area with small cystic areas within should raise the possibility of an endometrial polyp. Polyps in patients on tamoxifen also show cystic spaces.
- At times they are fleshy and large, and these could be adenomyomatous polyps.
- On Doppler, a dominant vessel ('feeder vessel'/'pedicle artery sign') is seen approaching the polyp from the adjoining myometrium across the EMJ. This vessel may show branching within the polyp. This feeder vessel is very helpful in making a diagnosis of polyps and also in identifying the site of origin of the polyp within the endometrial cavity. The average RI for feeder vessels of polyps is about 0.6.
- One may not see the feeder vessel of a polyp. This could happen if the Doppler settings are not proper or the direction of flow in the vessel is perpendicular to the ultrasound beam. In the latter case, angulating the probe could help. Sometimes the vessel is better seen on TAS than TVS because the direction of flow on TVS may be perpendicular, but on TAS it may be parallel, enabling visualisation of the vessel.
- These polyps are often visualised well on 3D rendered coronal images of the uterine cavity.
- Polyps could be multiple, each with its individual feeder vessel.
- Some of these polyps may have a long pedicle, and though they may originate higher up, they may be seen much lower down, often in the cervical canal.
- When there is fluid in the endometrial cavity, either blood or at sonohysterogram, polyps are well visualised. They are seen as echogenic, smooth-surfaced, intracavitary masses. Their site of origin is also well seen. The polyp may be broad based or sessile.
- Sometimes, one is able to see the rounded, blunt lower margins of a polyp in the endometrial cavity, especially if there is some minimal fluid below it, which helps in differentiating it from a thickened endometrium.
- Some polyps show hyperplastic endometrium, and in rare cases they could be malignant. One must consider the possibility of malignancy in a polyp especially if they are fleshy and heterogeneous, and a Doppler study of the feeder vessel shows a low RI of 0.42 or below.
- Sometimes clots within the endometrial cavity can mimic a polyp. However, neither feeder vessel nor flow will be seen in these clots. One must be aware of the artefact caused by menstrual flow of blood in the endometrial cavity. This could even produce a tracing like that of a venous flow on pulse wave Doppler. However, no arterial flow will ever be seen in the case of a clot. In addition, menstrual flow is seen along the periphery of clots, unlike polyps where vascular flow is seen within the tissue of the polyp. Also, if one applies pressure with the probe, in cases with menstrual flow artefacts, a reversal of flow direction may be noticed (blue to red or vice versa).

In cases with clots appearing like polyps, the clots may be dislodged or missing either when a repeat scan is done after the patient has been asked to strain or if the scan is repeated after a day or two.

As mentioned earlier, the best time to evaluate the endometrium for polyps is the proliferative phase (Day 9–12 of menstrual cycle). The polyp stands out clearly in the triple line pattern of the proliferative endometrium. In all other types of endometrium, a polyp may not be clearly seen since it is isoechoic with the rest of the endometrium. In such

cases, the hyperechoic line around the polyp and the feeder vessel may help in diagnosis.

A thick endometrium diagnosed on greyscale ultrasound sometimes turns out to be a polyp on Doppler (on visualisation of the feeder vessel) or at surgery

A mid-positioned uterus often results in suboptimal evaluation of the endometrium on TVS, and therefore a polyp can be missed. In some of these cases, it may be better visualised on TAS instead.

Polyps, particularly small ones, can be left unattended unless they are symptomatic. Hysteroscopy is the method of choice for management. It is important to note that often a polyp presenting as a thickened endometrium is missed on regular D&C, and there is scanty endometrium on curettage. This is because the curette has missed the polyp and gone around it curetting the surrounding thin endometrium. The referring gynecologist is surprised that the ultrasound report mentioned a thick endometrium and there were hardly any curettings!

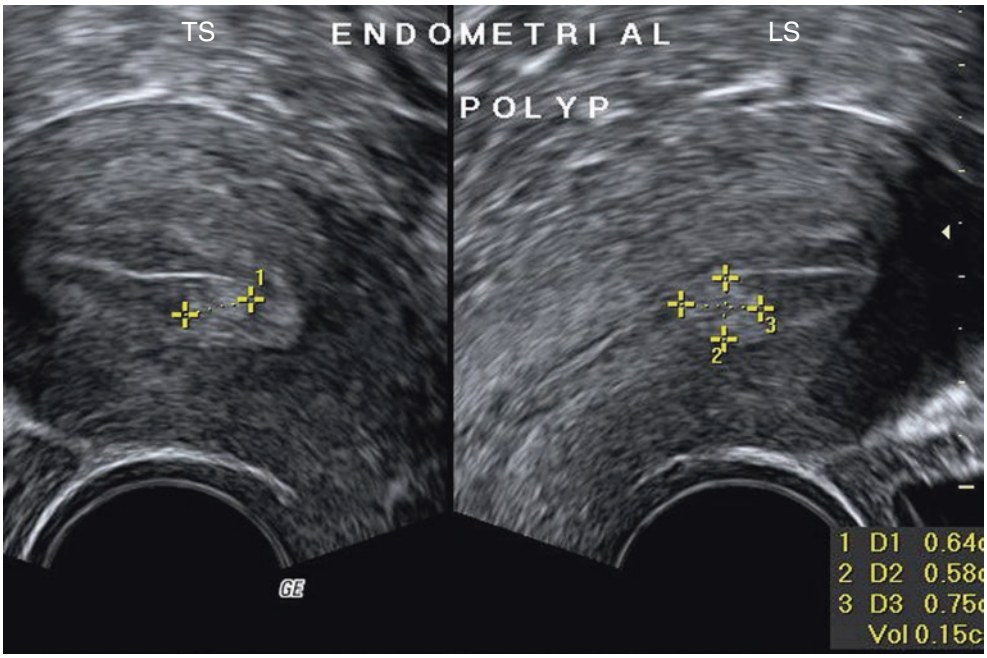

Fig. 4.14 Hyperechoic small polyp in a proliferative endometrium

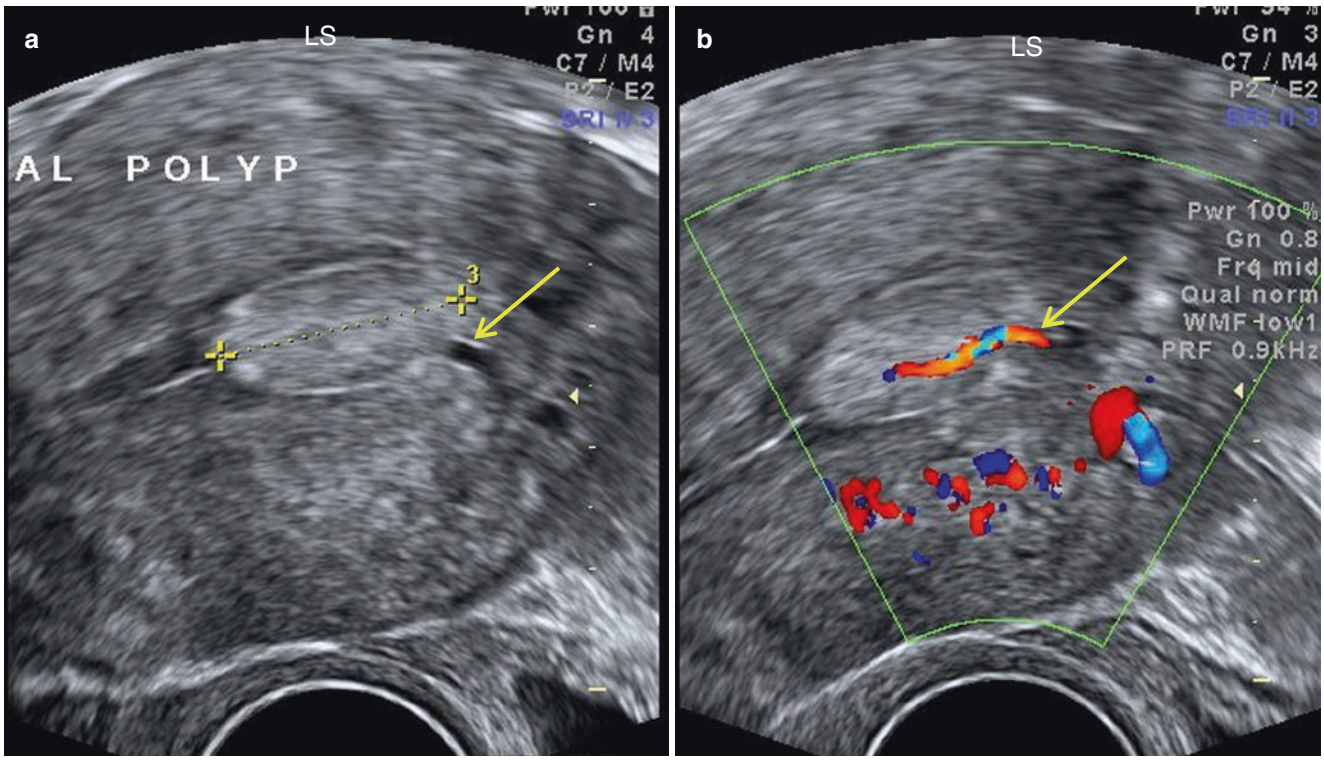

Fig. 4.15 Hyperechoic polyp clearly visualised in a proliferative endometrium. The hyperechoic line surrounding the polyp is discontinuous at the site of entry of the feeder vessel (*arrow*) which is seen on (**a**) greyscale and (**b**) Doppler

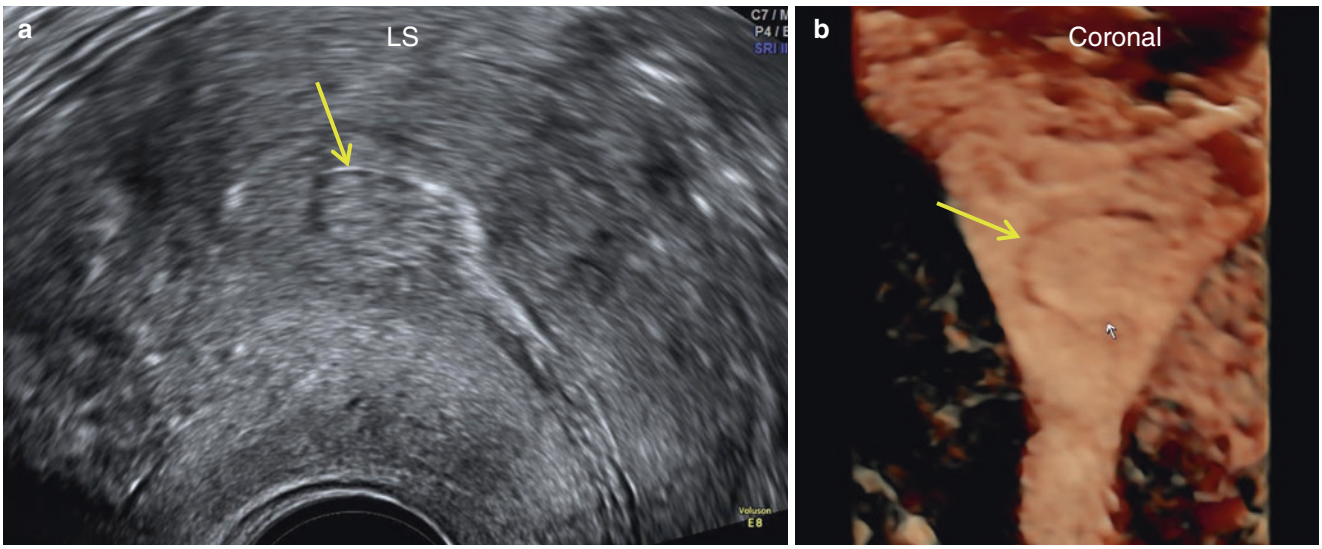

Fig. 4.16 Polyp in a secretory endometrium. Hyperechoic line (*arrows*) between polyp and endometrium helps delineate and diagnose the polyp (**a**) on 2D greyscale and (**b**) on 3D

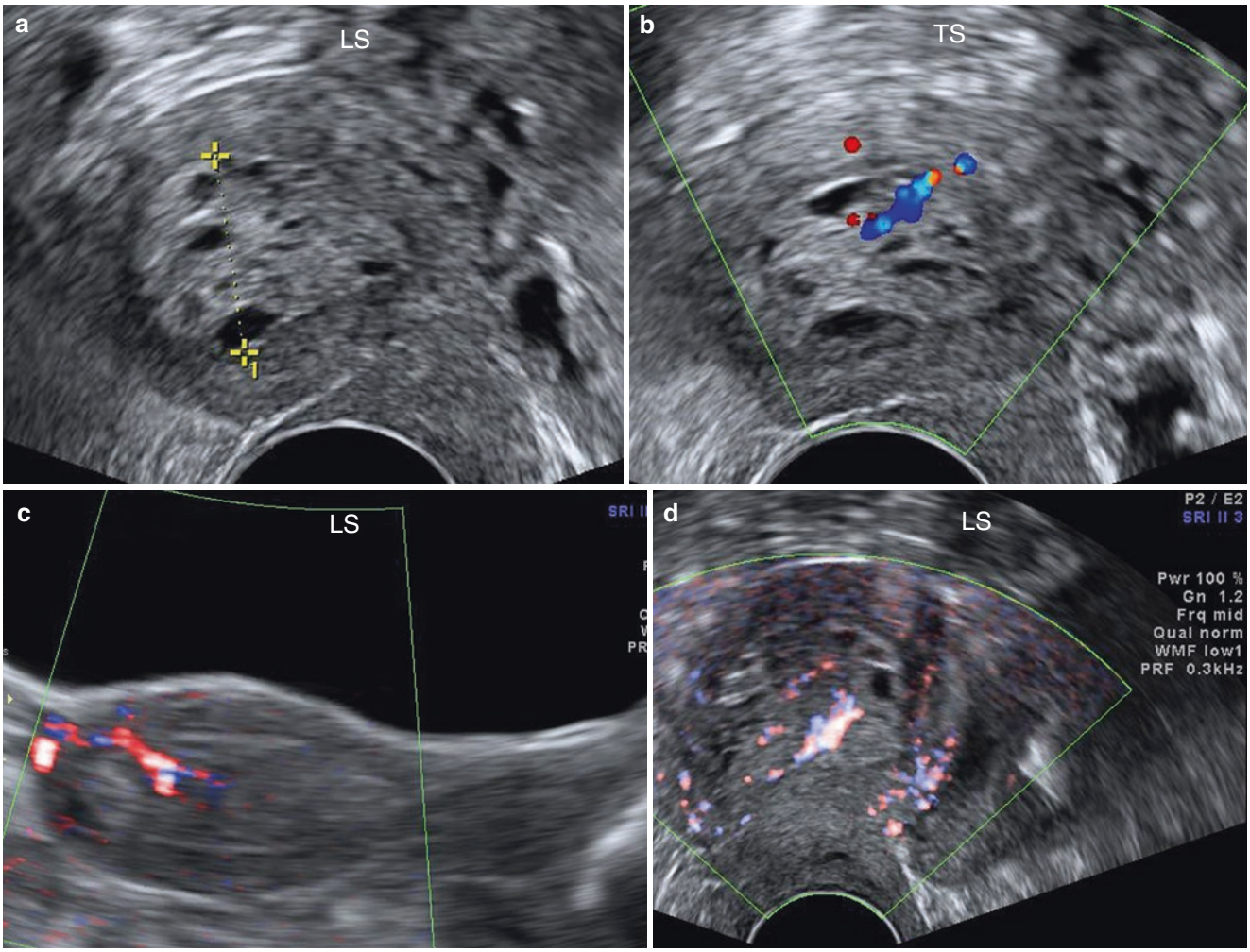

Fig. 4.17 (**a**, **b**) 67-year-old postmenopausal lady with an endometrial thickness of 17.8 mm. (**a**) Polyp with tiny cystic spaces. (**b**) Feeder vessels supplying the polyp, (**c**, **d**) 70-year-old postmenopausal lady with ET of 26 mm. (**c**) TAS – a, single prominent feeder vessel crossing the EMJ and branching within the thickened endometrium raises a high possibility of an endometrial polyp; (**d**) TVS – flow seen in the endometrium in more than one vessel (PRF 0.3), but despite repeated attempts, the origin of flow across the EMJ is not seen. With TVS alone, it was not possible to see the feeder vessel from the EMJ probably because it is perpendicular to the ultrasound beam at its origin. To improve accuracy of diagnosis, doing both TAS and TVS routinely is therefore ideal

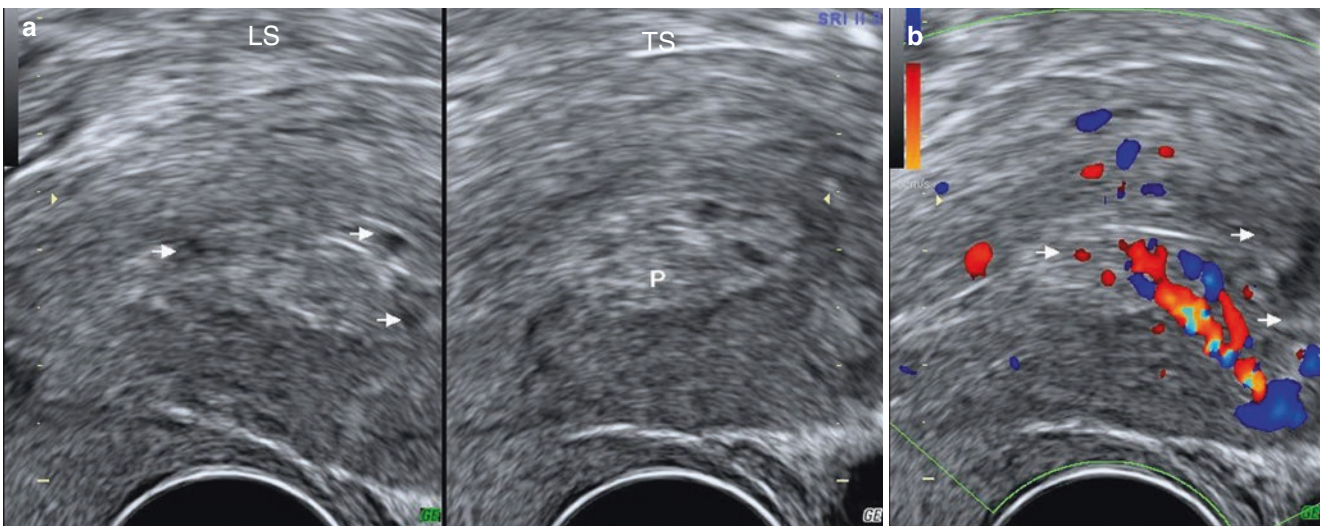

Fig. 4.18 Patient on tamoxifen for carcinoma breast. (**a**) Shows a polyp and cystic spaces (*small white arrows*) in the endometrium. (**b**) Shows the feeder vessel of the polyp

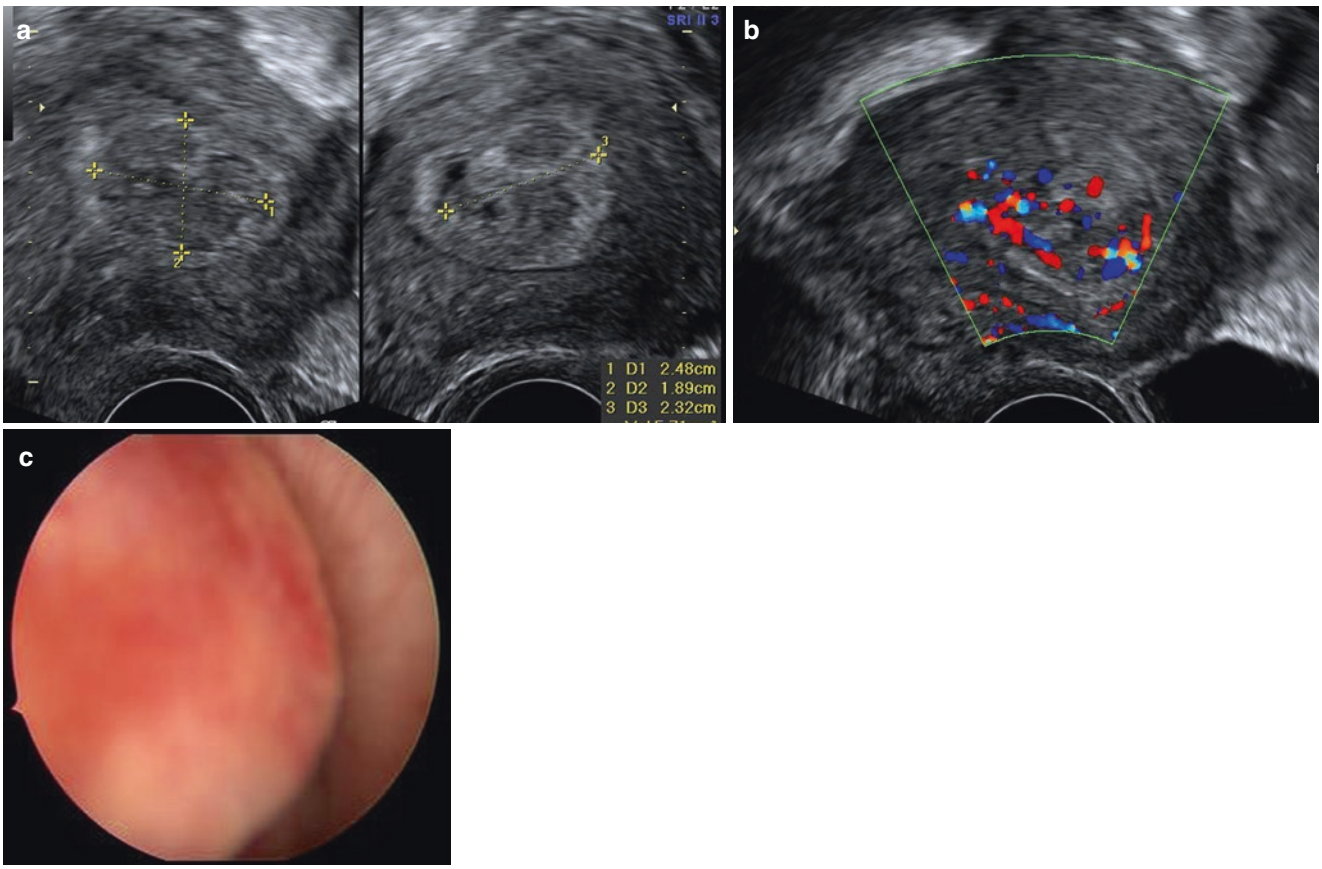

Fig. 4.19 Adenomyomatous polyp. (**a**) Seen on greyscale. (**b**) Showing Doppler flow. (**c**) Seen at hysteroscopy

Fig. 4.20 Pedicle artery sign: A dominant feeder vessel is seen approaching the polyp across the EMJ

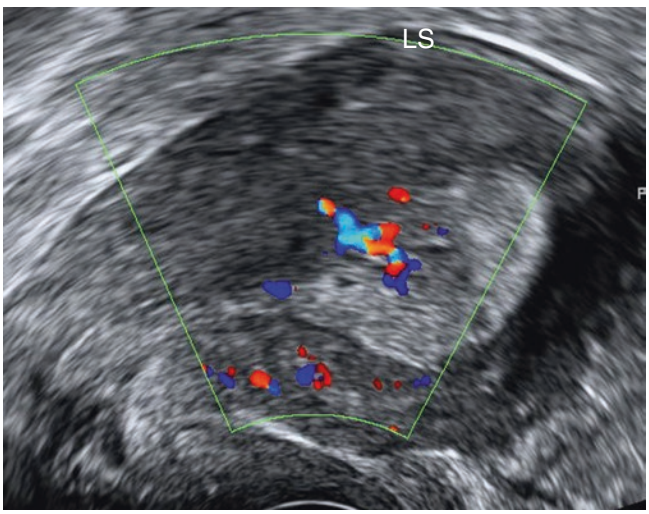

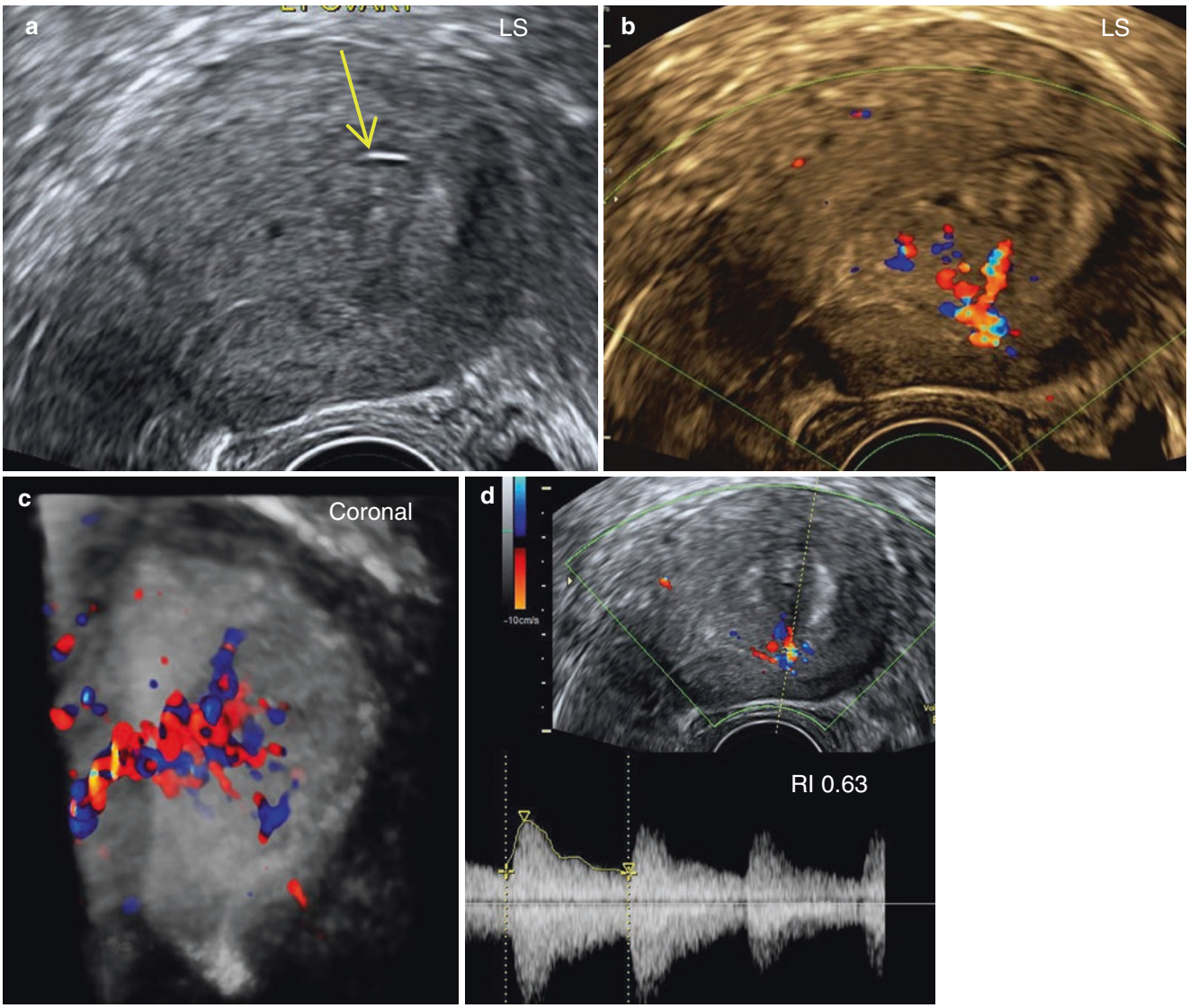

Fig. 4.21 (**a**) Thickened isoechoic endometrium with a hyperechoic line (*arrow*) raising a suspicion of a polyp. (**b**) A single feeder vessel with branching, suggestive of an endometrial polyp. (**c**) Glass body rendering of the polyp with feeder vessel. Branching of the feeder vessel within the polyp is well seen. (**d**) Spectral Doppler flow of feeder vessel. *HPE:* polyp with complex hyperplasia without atypia

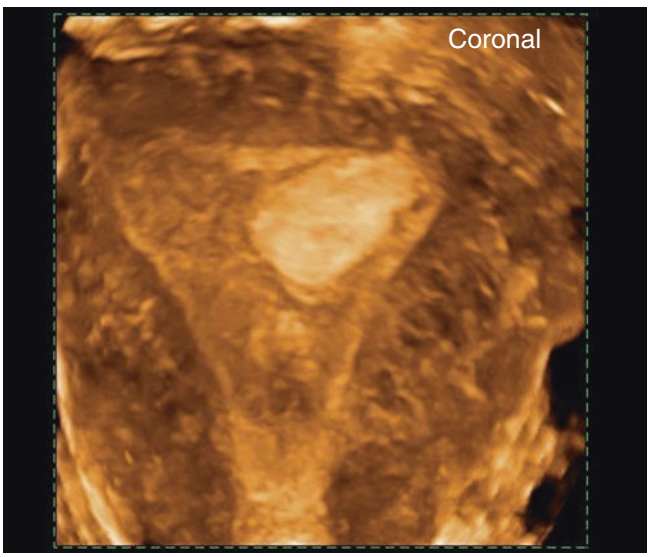

Fig. 4.22 Endometrial polyp well seen on 3D rendered coronal image view of the endometrial cavity. In this case, there was minimal fluid in the endometrial cavity, and therefore the polyp is well delineated

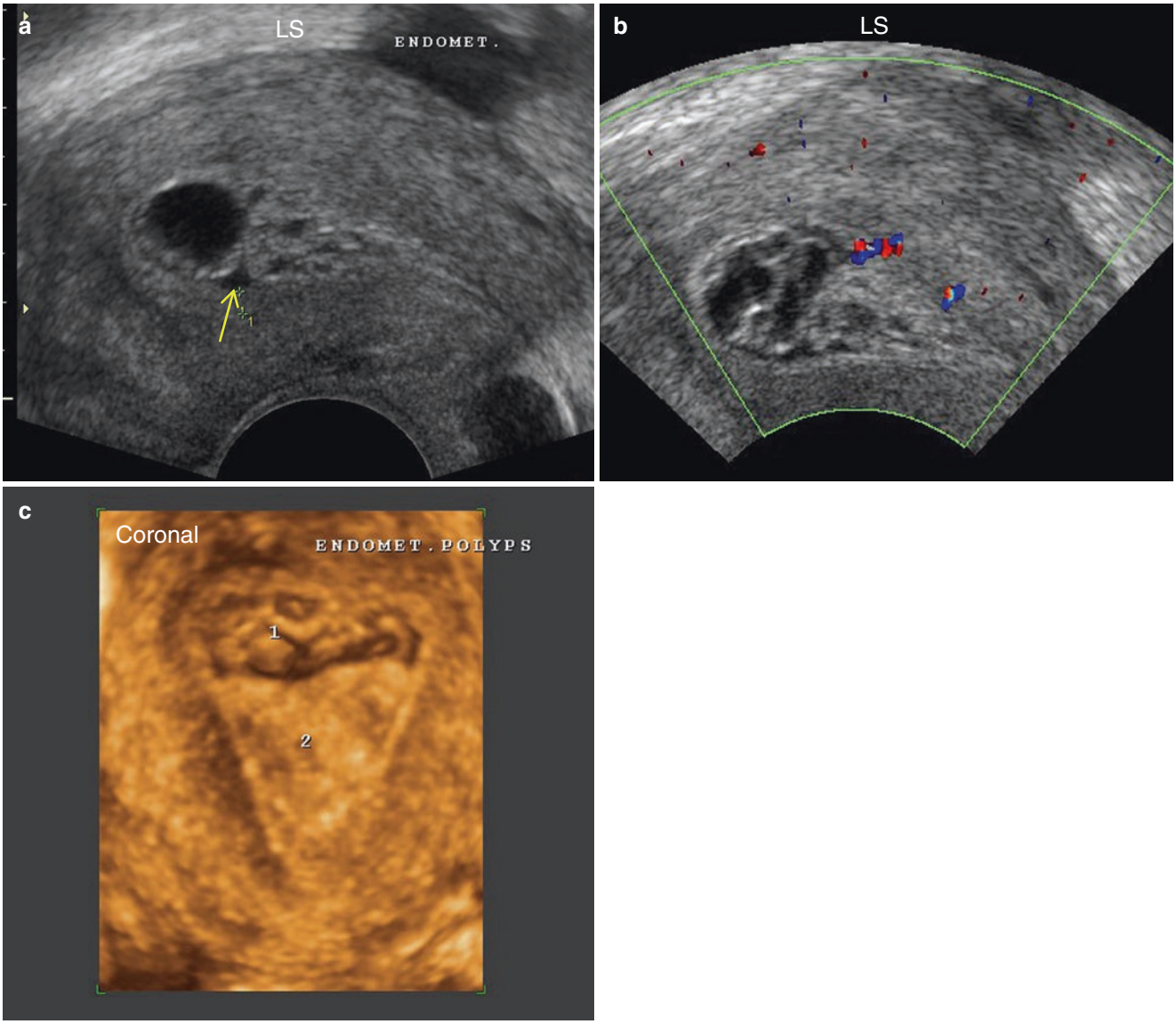

Fig. 4.23 Two endometrial polyps showing cystic spaces seen distinctly. (**a**) A narrow anechoic wedge seen between the two (*arrow*) on greyscale. (**b**) Each polyp has its own feeder vessel arising from the anterior uterine wall. (**c**) 3D rendered image showing the two polyps

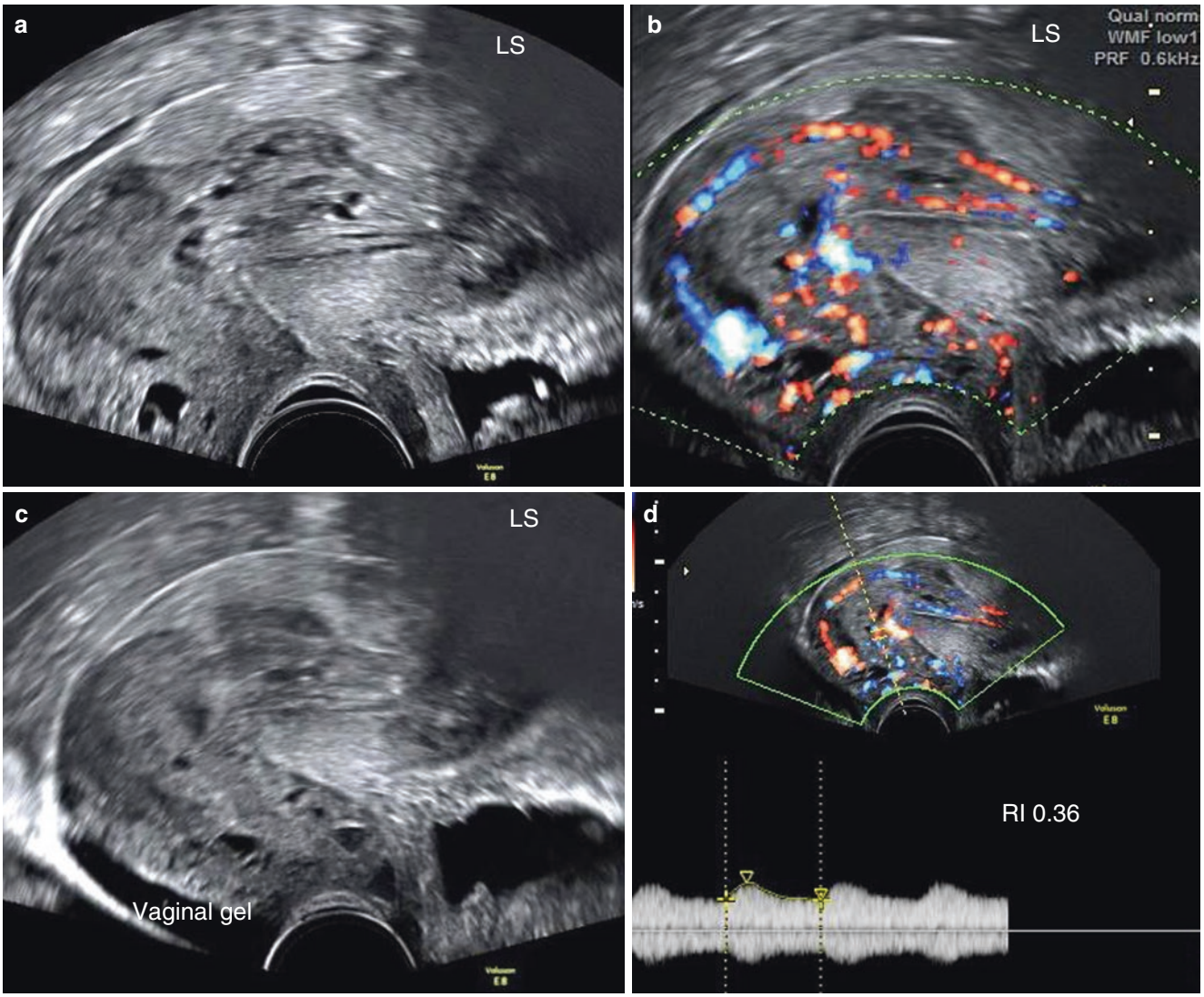

Fig. 4.24 Endometrial polyp seen arising from the upper corpus of the uterus and presenting as a fleshy, large (42.7 cm^3) polyp with multiple cystic spaces protruding out of the cervix . The external os diameter was 1.8 cm. Polyp seen (**a**) on greyscale and (**b**) on Doppler. (**c**) Lower margins of the polyp are well seen on GSV. (**d**) The polyp shows high vascularity with low resistance flows. One of the causes for such flows (high colour score and low RI) can be superadded infection. *HPE:* endometrial polyp with cystic hyperplasia

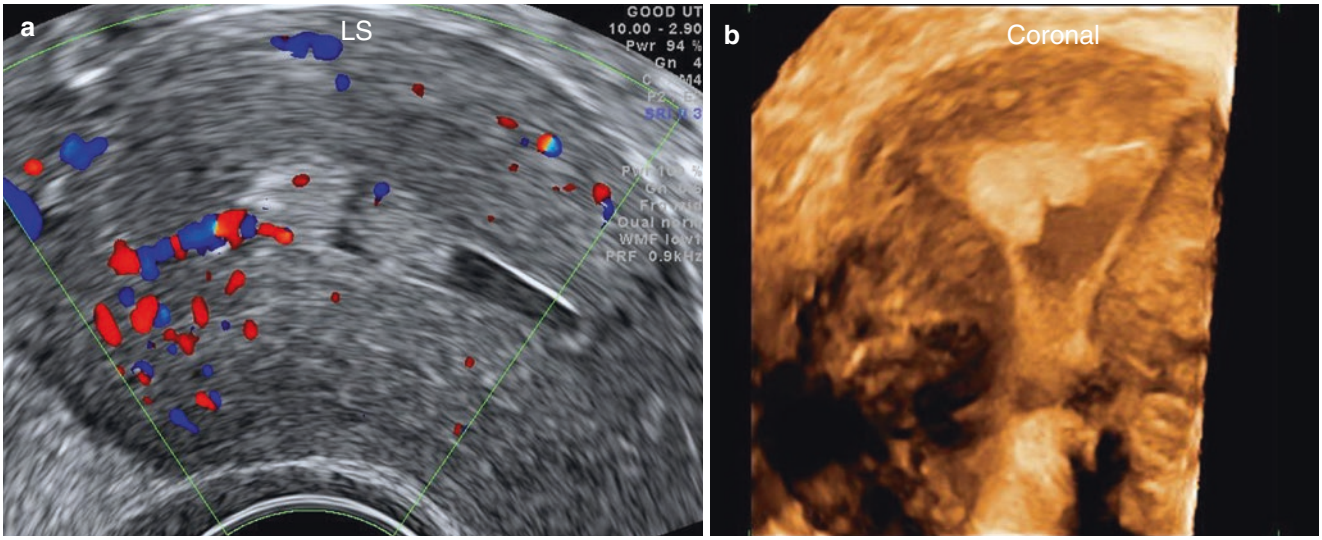

Fig. 4.25 Blood in the endometrial cavity enhancing delineation of two endometrial polyps (**a**) on 2D with Doppler and (**b**) on 3D

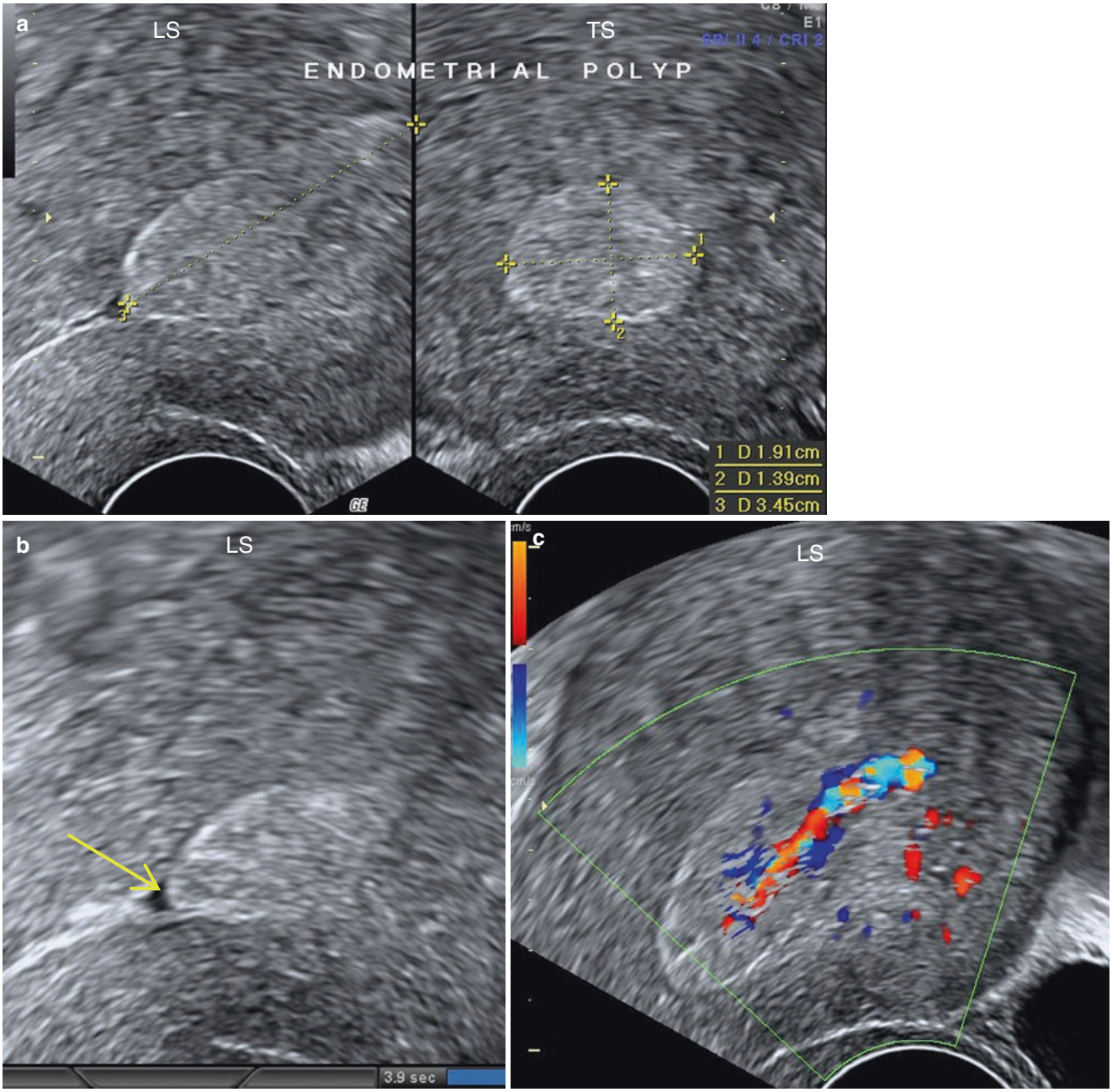

Fig. 4.26 (**a**) Hyperechoic, 4.4 cm long polyp seen filling the endometrial cavity. (**b**) Lower rounded end of polyp (*arrow*) is visualised which helps in differentiating it from other causes of thickened endometrium. (**c**) The feeder vessel of the polyp is seen approaching it from the anterior wall of the uterus. *HPE:* simple hyperplasia

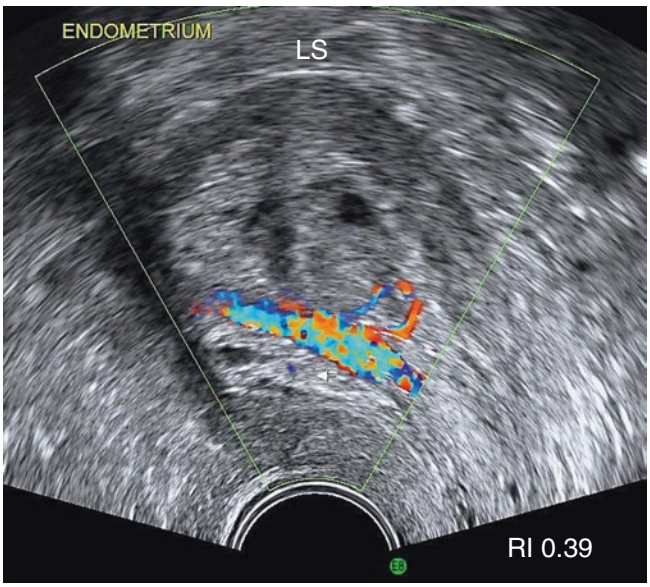

Fig. 4.27 Large, fleshy polyp with a thick feeder vessel showing low RI. *HPE:* endometrioid adenocarcinoma arising in an adenomyomatous polyp

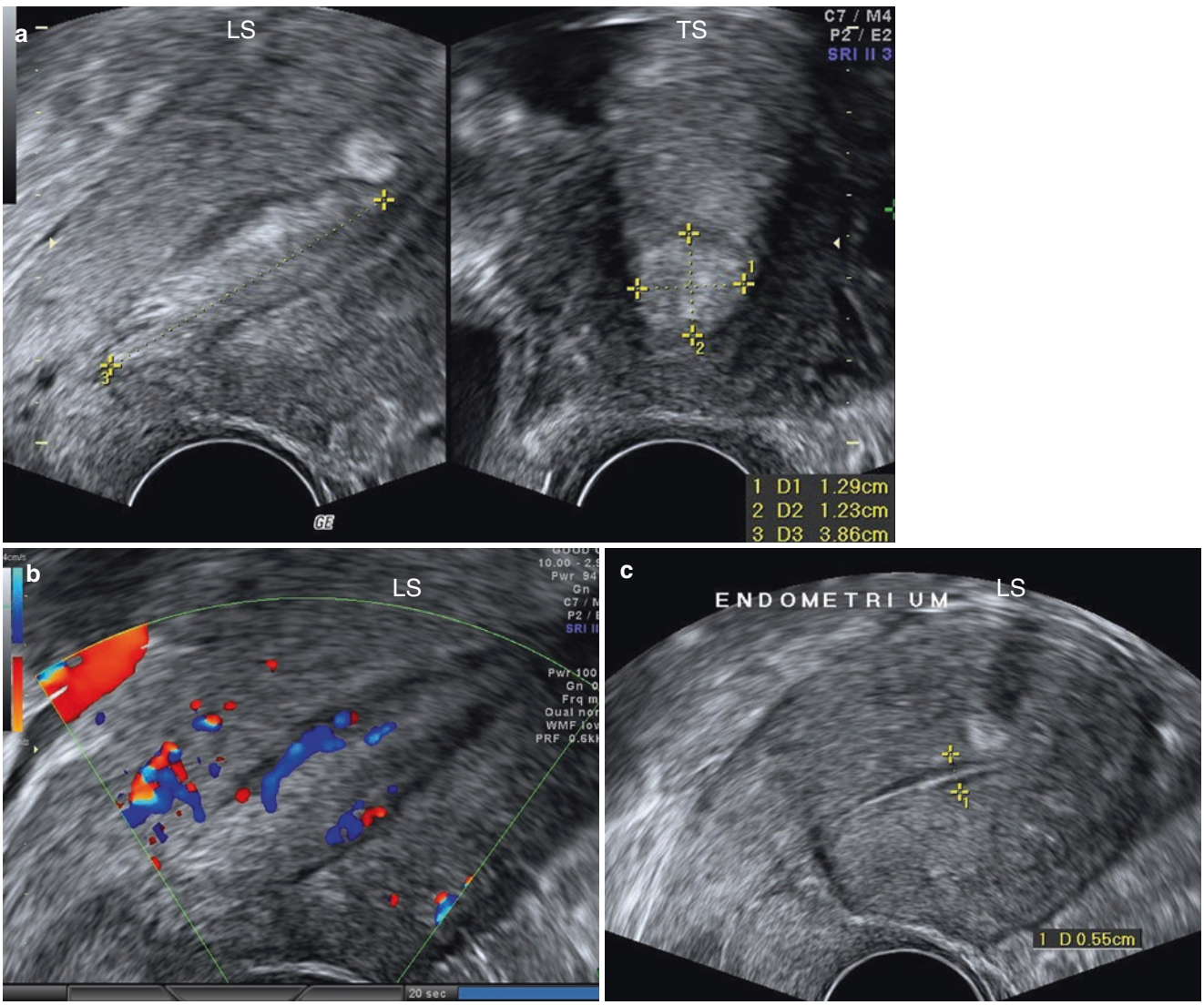

Fig. 4.28 (**a**) Hyperechoic clot filling the endometrial cavity in a menstruating patient complaining of menorrhagia, which can raise a suspicion of a fleshy endometrial polyp. (**b**) Flow seen on colour Doppler is the menstrual flow. This raises a false suspicion of flow within an endometrial polyp. (**c**) Empty uterine cavity noted the next day, confirming the diagnosis of a clot in the endometrial cavity the previous day

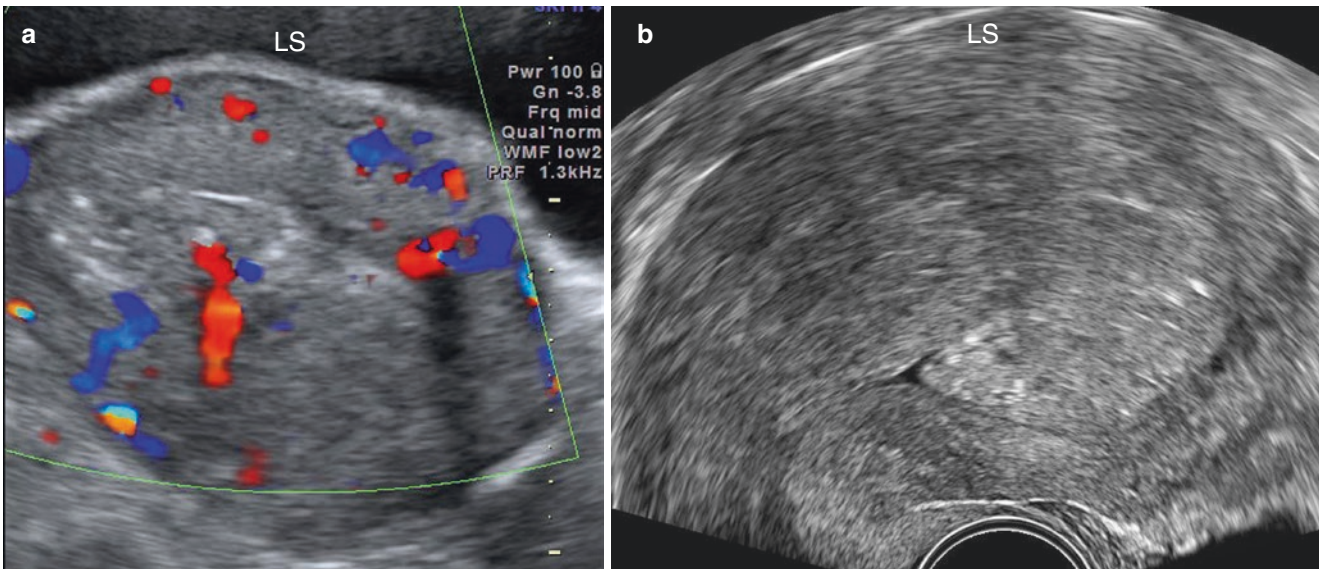

Fig. 4.29 Thickened endometrium with hyperechoic scattered foci within. (**a**) TAS – shows feeder vessel. (**b**) TVS – shows the rounded lower end of polyp. *HPE:* adenomyomatous polyp

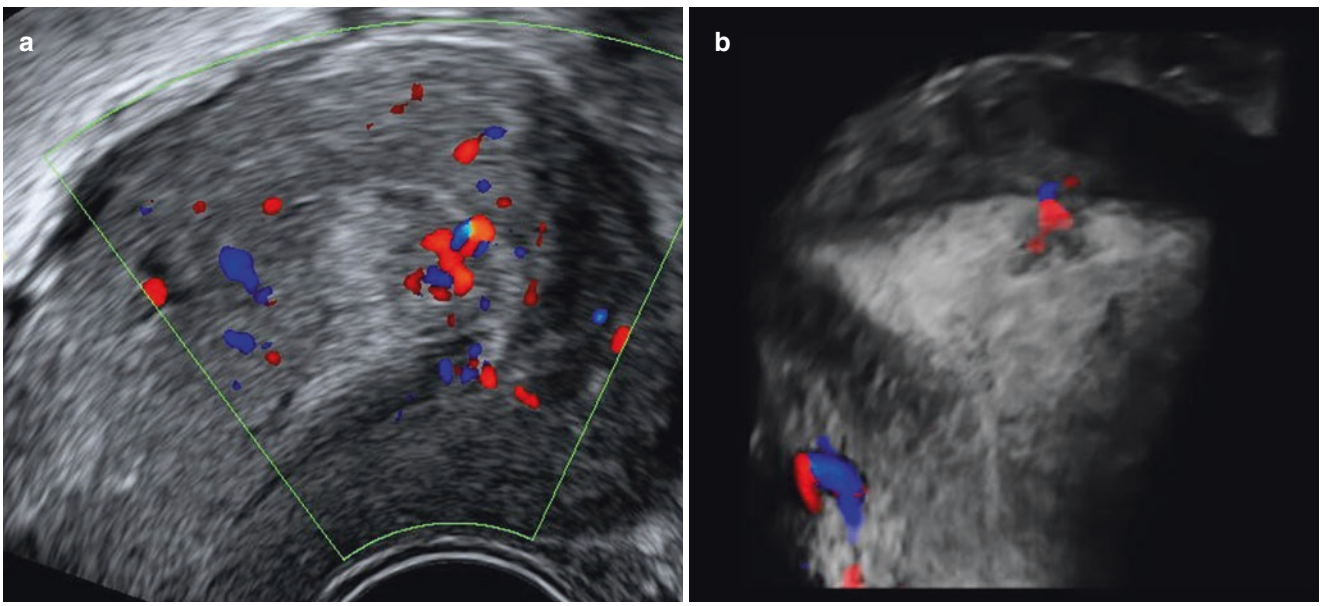

Fig. 4.30 Hypoechoic polyp with a feeder vessel approaching it from the uterine fundus on (**a**) Doppler and (**b**) 3D with glass body rendering

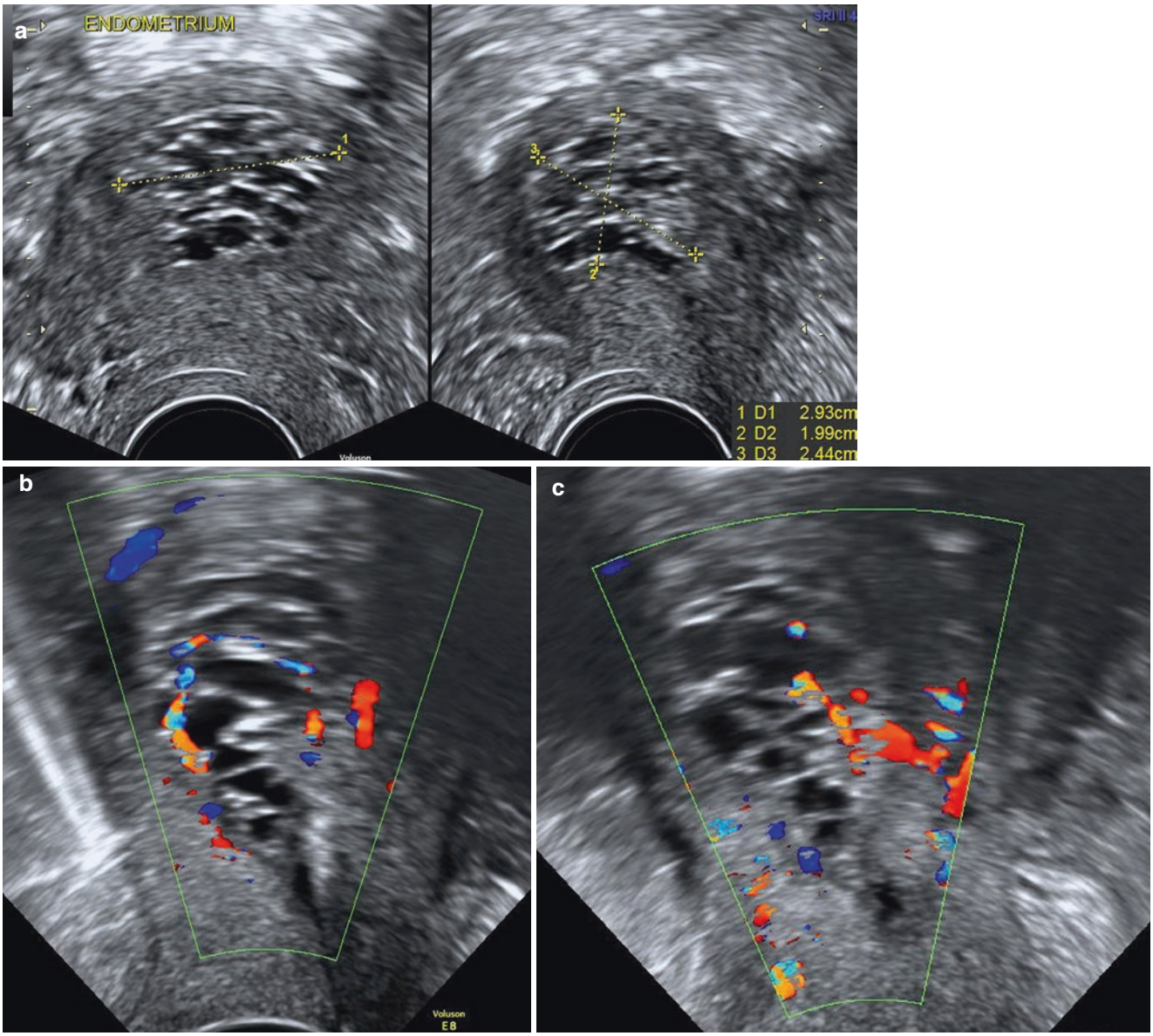

Fig. 4.31 (**a**) Polyp with cystic hyperplasia. (**b**, **c**) Feeder vessel is difficult to trace. This happens in polyps that are primarily cystic with minimal stroma

Summary: Endometrial Polyps

- Endometrial polyps are commonly seen in both symptomatic and asymptomatic women. They may present with intermenstrual spotting or subfertility.
- On ultrasound, they appear as hyperechoic circumscribed areas and are best seen in the proliferative phase. The presence of hyperechoic bright margins between the polyp and endometrium and a single feeder vessel are useful in clinching diagnosis. Polyps may show cystic spaces and may be single or multiple.
- Some polyps may be large and fleshy (e.g. adenomyomatous polyps). On rare occasions, polyps may show malignant tissue within.

4.4 Endometrial Hyperplasia

Endometrial hyperplasia is a condition where there is a proliferation of the endometrial glands that may progress to, or coexist with, endometrial carcinoma. About one-third of endometrial carcinomas are believed to be preceded by hyperplasia. In hyperplasia, there is an increase in the endometrial gland to stroma ratio. Based on glandular features, endometrial hyperplasia is classified into:

- Simple hyperplasia: The glands are mildly crowded and frequently cystically dilated (commonly termed 'cystic hyperplasia').
- Complex hyperplasia: The glands are crowded (with more than 50 % gland to stroma ratio) and disorganised.

Nuclear atypia can be seen in both types but is infrequent in simple hyperplasia and more common in complex hyperplasia.

Risk factors for endometrial hyperplasia are similar to those of endometrial carcinoma. Most of these risk factors are related to excessive or chronic exposure to unopposed oestrogen, as is noted in women with anovulatory cycles, polycystic ovaries and obesity. Women with endometrial hyperplasia most often belong to the perimenopausal age group and present with menorrhagia (prolonged and heavy flow), with or without preceding amenorrhoea.

Ultrasound Features of Endometrial Hyperplasia
(Figs. 4.32, 4.33, 4.34, 4.35, 4.36, 4.37, 4.38, 4.39, 4.40, 4.41, 4.42 and 4.43)
Endometrial hyperplasia is difficult to diagnose on ultrasound, as ultrasound findings can overlap with both that of a normal endometrium and an endometrial malignancy. Since endometrial hyperplasia is a histologic diagnosis, a definitive diagnosis would require endometrial biopsy.

Ultrasound is the primary imaging modality in women presenting with excessive uterine bleeding, which includes cases with endometrial hyperplasia.

- Thickened endometrium – endometrial thickness is usually increased. Normal acceptable thickness of the endometrium, in a postmenopausal woman, is 4 mm or less. Therefore, a thickness of 5 mm or more would be considered a thickened endometrium and raise the possibility of a polyp, endometrial hyperplasia or malignancy. In premenopausal women, it is difficult to assign a cut-off. In them, a thickness of 5 mm or less on D4 to D6 (of the menstrual cycle) is considered normal. So, values above that or, as some suggest, a measurement of more than 15 mm at any time in the menstrual cycle could be considered a thickened endometrium with likelihood of a pathology. Endometrial hyperplasia is most often diffuse but could less commonly be focal.
- The endometrium may appear three layered, echogenic or heterogeneous. Tiny cystic spaces may be seen in the endometrium of a patient with cystic hyperplasia, giving it a 'Swiss cheese appearance'.
- The endometrium may be polypoid, which may appear as a non-linear endometrial midline, or as multiple polypoid protrusions in patients with fluid or blood in the endometrial cavity (including at sonohysterogram).
- Vascularity of the endometrium generally increases with multifocal single-scattered peripheral vessels seen crossing the EMJ. These vessels typically show a linear or gently curved path and are more uniformly scattered as compared to those in cases with endometrial cancer.
- In women who are bleeding during the time of evaluation, the endometrium could appear heterogeneous, with blood and clots within the endometrial cavity.
- Since hyperplasia is associated with hyperestrogenia, one must search for causes of high oestrogen levels. On ultrasound, therefore, the ovaries must be assessed for a polycystic appearance or an oestrogen-producing tumour. Very often, however, the ovaries are normal.
- The endometrium of patients on progesterone therapy for endometrial hyperplasia with atypia or carcinoma endometrium in situ, appears thick and very vascular and shows focal cystic changes. This raises concerns, and in the author's experience in such cases when the endometrial biopsy was repeated, histopathologically, there was significant improvement in these cases, in comparison to their pre-progesterone tissue biopsy.

4.4.1 Tamoxifen-Associated Endometrial Changes (Fig. 4.44)

Tamoxifen is a drug used in the treatment of breast cancer. It has a pro-estrogenic effect on the endometrium, increasing the prevalence of endometrial hyperplasia, polyps and carcinoma. In these women, the endometrium may appear thickened and cystic on ultrasound. The degree of endometrial thickening is believed to be related to the duration of tamoxifen therapy.

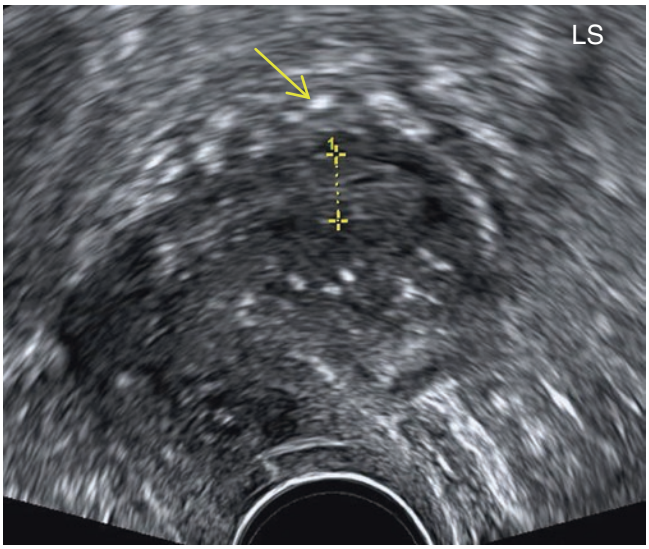

Fig. 4.32 An 85-year-old postmenopausal lady with a thick endometrium of 8.1 mm. Calcification of arcuate vessels seen (*arrow*)

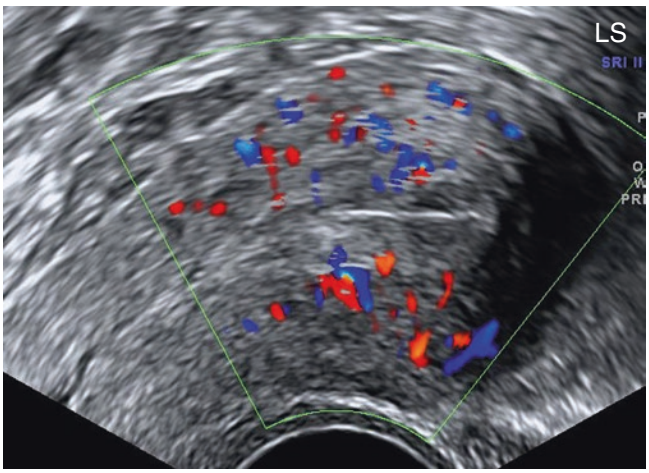

Fig. 4.33 Endometrial hyperplasia with a three-layer endometrium

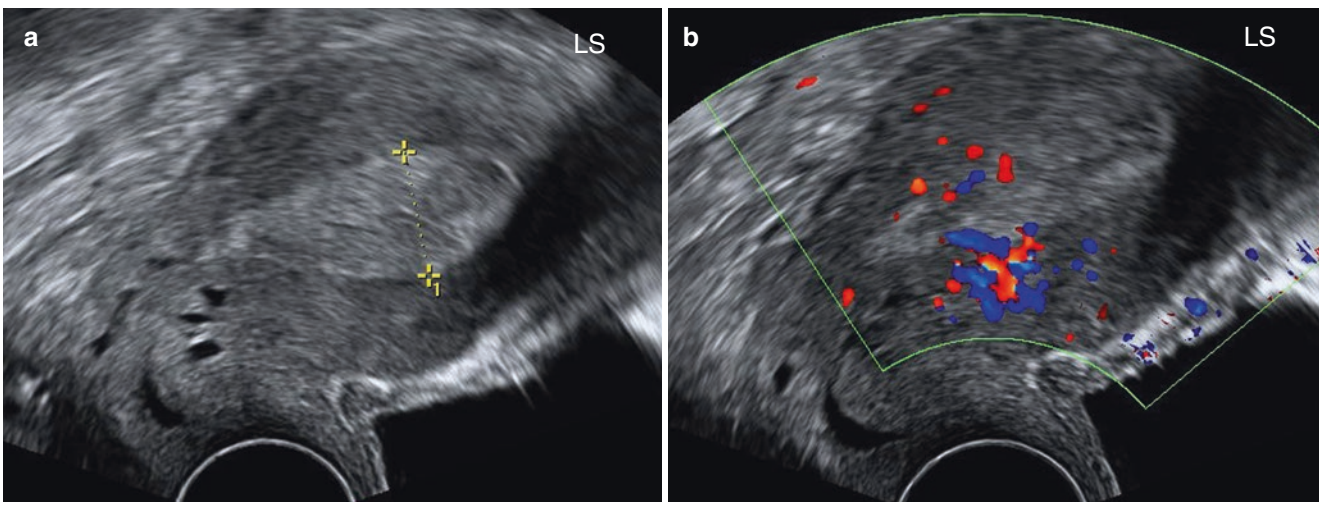

Fig. 4.34 Endometrial hyperplasia. (**a**) Echogenic endometrium. (**b**) Vessels seen crossing the EMJ. *HPE:* complex hyperplasia with atypia

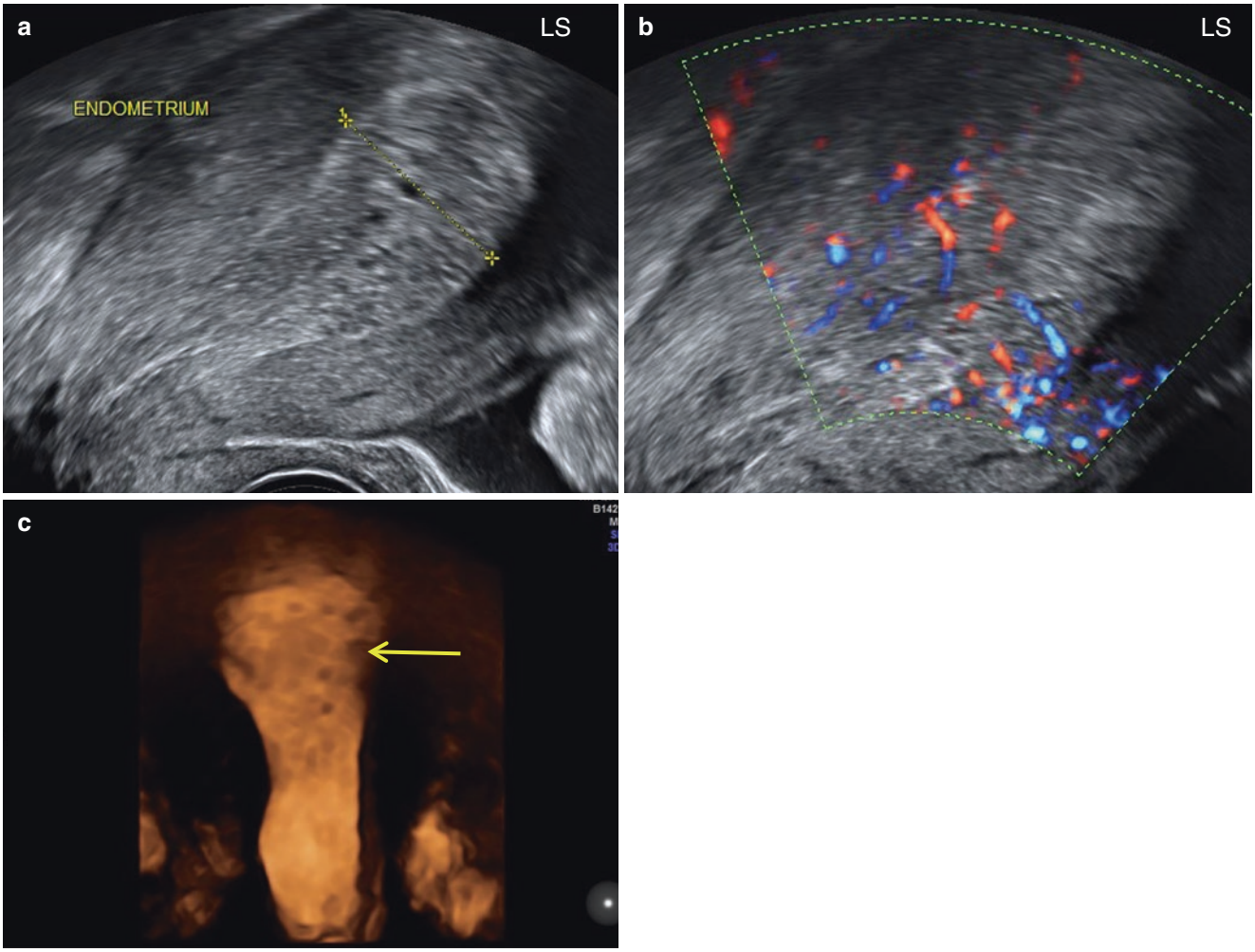

Fig. 4.35 Endometrial hyperplasia. (**a**) Echogenic endometrium of 25 mm with tiny cystic spaces. (**b**) Multifocal linear single vessels crossing the EMJ. (**c**) 3D rendered image of an endometrium showing tiny cysts (*arrow*). *HPE:* simple cystic hyperplasia

Fig. 4.36 A 22-year-old, known case of polycystic ovaries with history of infrequent cycles and menorrhagia. 17 mm thick cystic endometrium with multiple vessels crossing the EMJ, likely to be a case of simple cystic hyperplasia

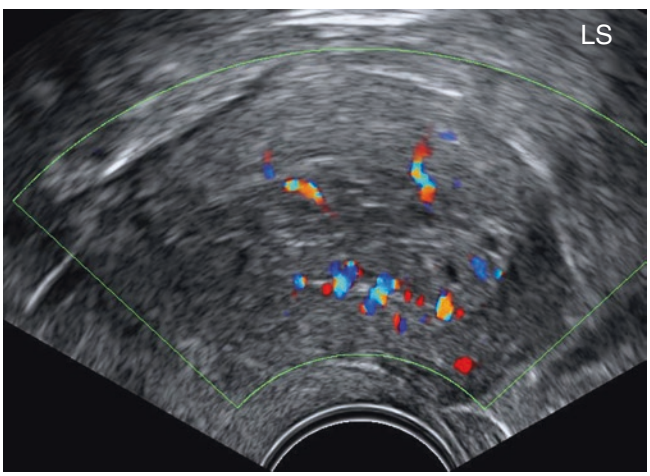

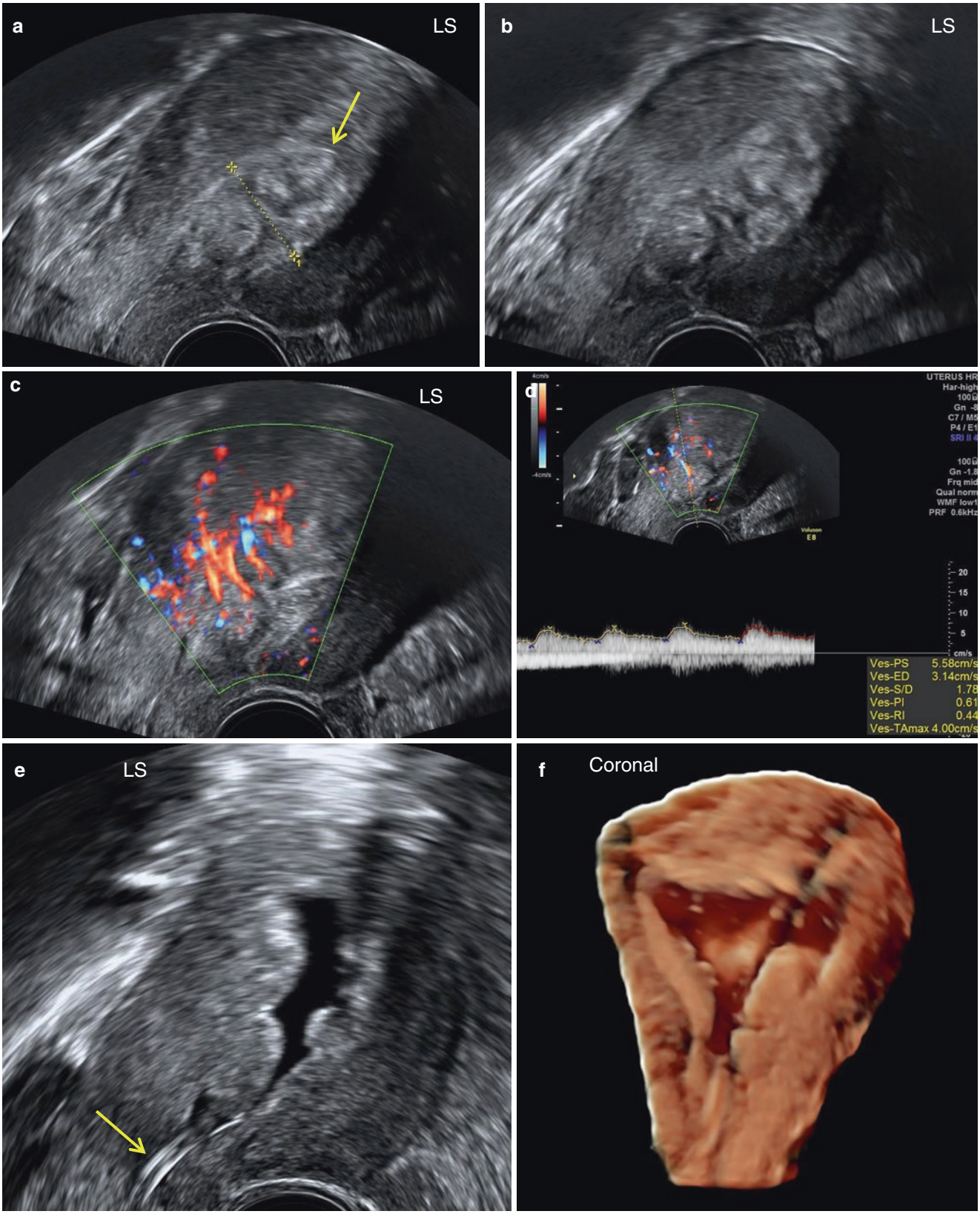

Fig. 4.37 Endometrial hyperplasia in a 37-year-old lady with intermenstrual spotting. (**a**, **b**) Endometrium appears thick and polypoid. White hyperechoic line (*arrow*) seen which is typical of polyps. (**c**) Multiple linear vessels seen crossing the EMJ. (**d**) Spectral flow showing RI of 0.44. (**e**) Polypoid endometrium seen on saline sonohysterography. Infusion catheter seen in the image (*arrow*). (**f**) 3D rendered imaging of endometrial cavity showing polypoid endometrium on SHG. *HPE:* simple hyperplasia

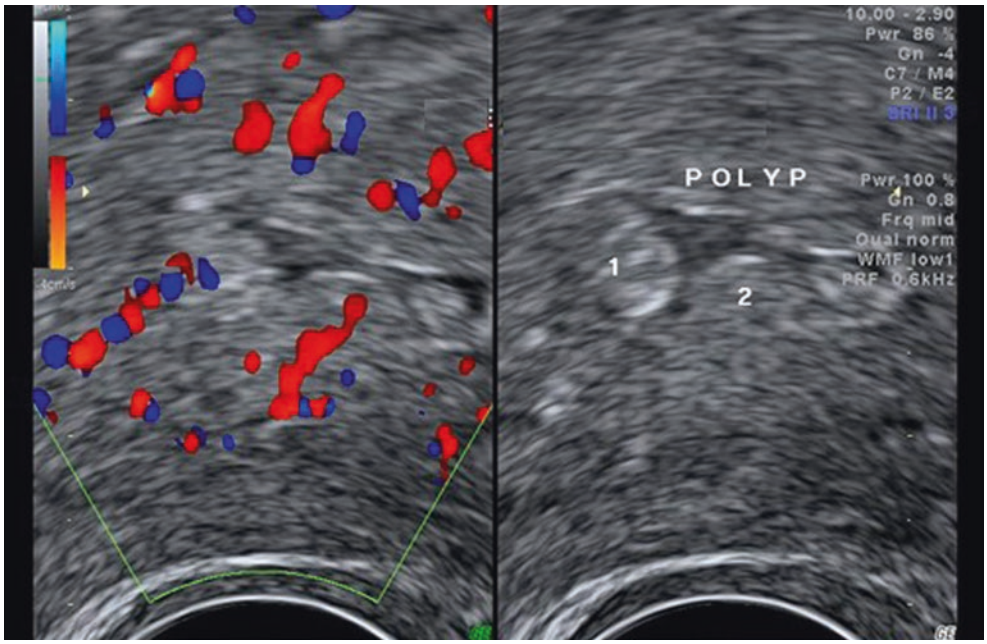

Fig. 4.38 Polypoid endometrium with multiple vessels crossing the EMJ

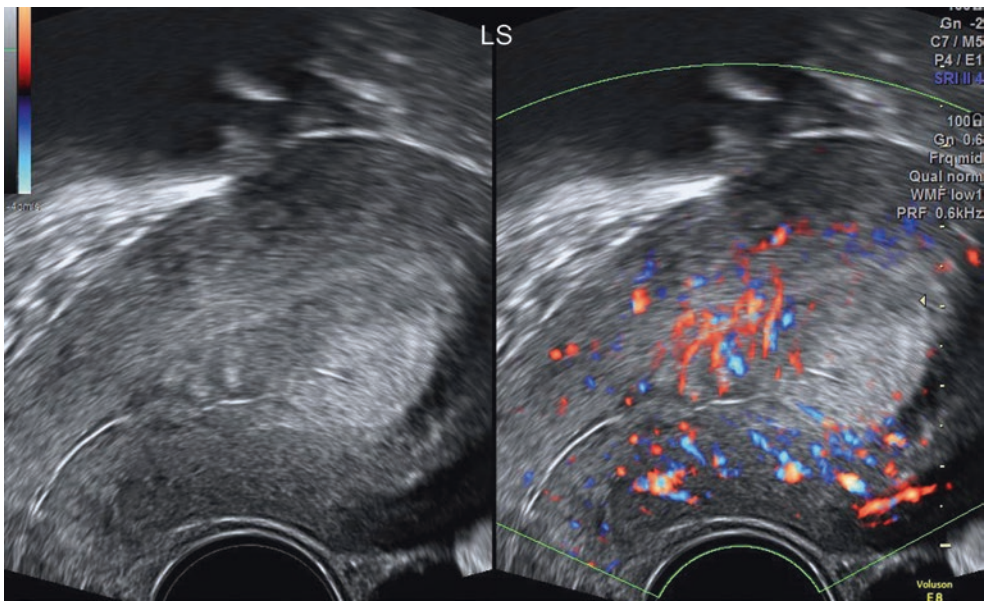

Fig. 4.39 H/o menorrhagia since 4 months – thickened echogenic endometrium of 20 mm with multifocal single-scattered peripheral linear vessels crossing the EMJ. *HPE:* simple hyperplasia

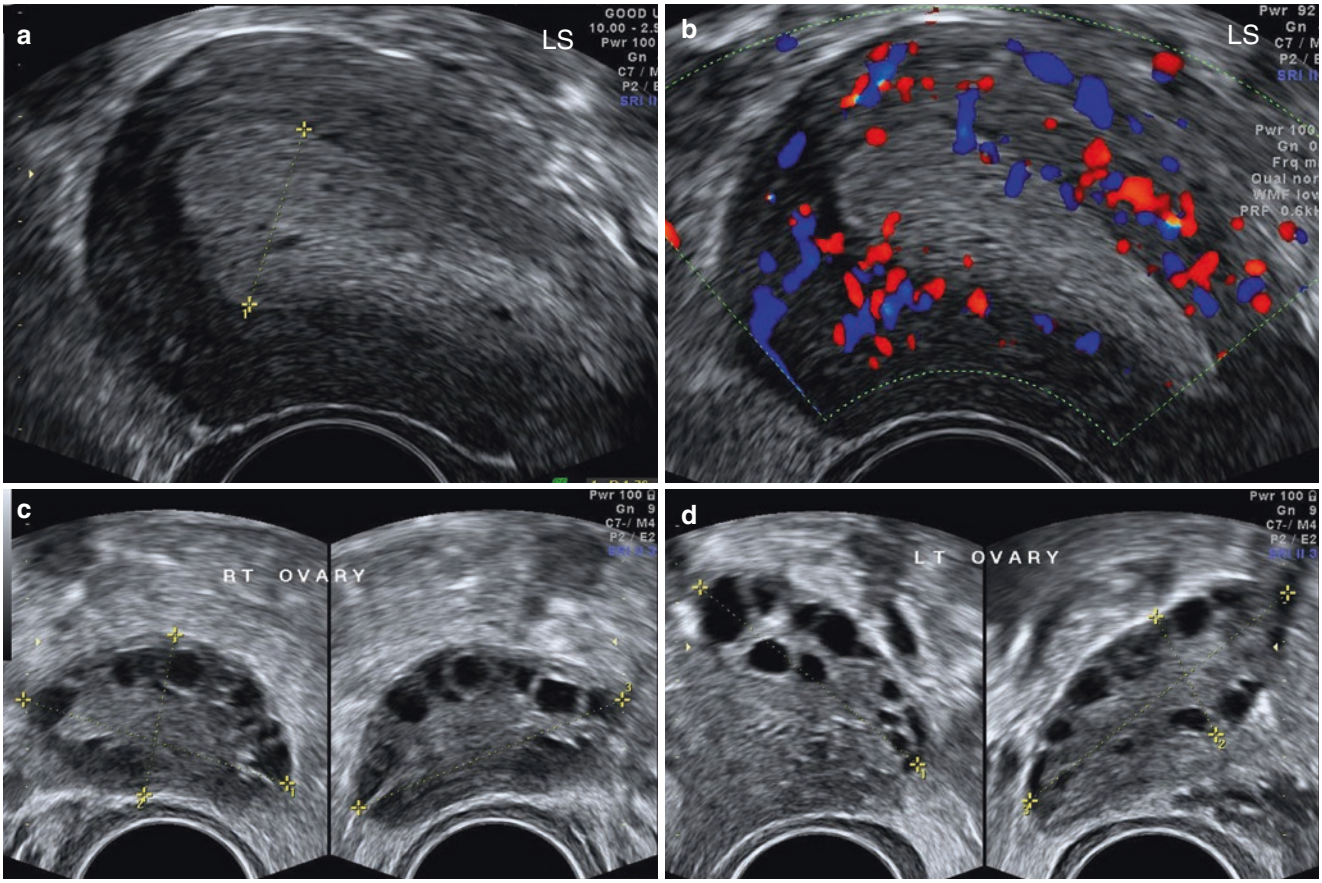

Fig. 4.40 Endometrial hyperplasia. (**a**) Thickened endometrium with tiny cystic spaces. (**b**) Multiple vessels crossing the EMJ. (**c**, **d**) Bilateral polycystic ovaries. *HPE:* simple cystic hyperplasia

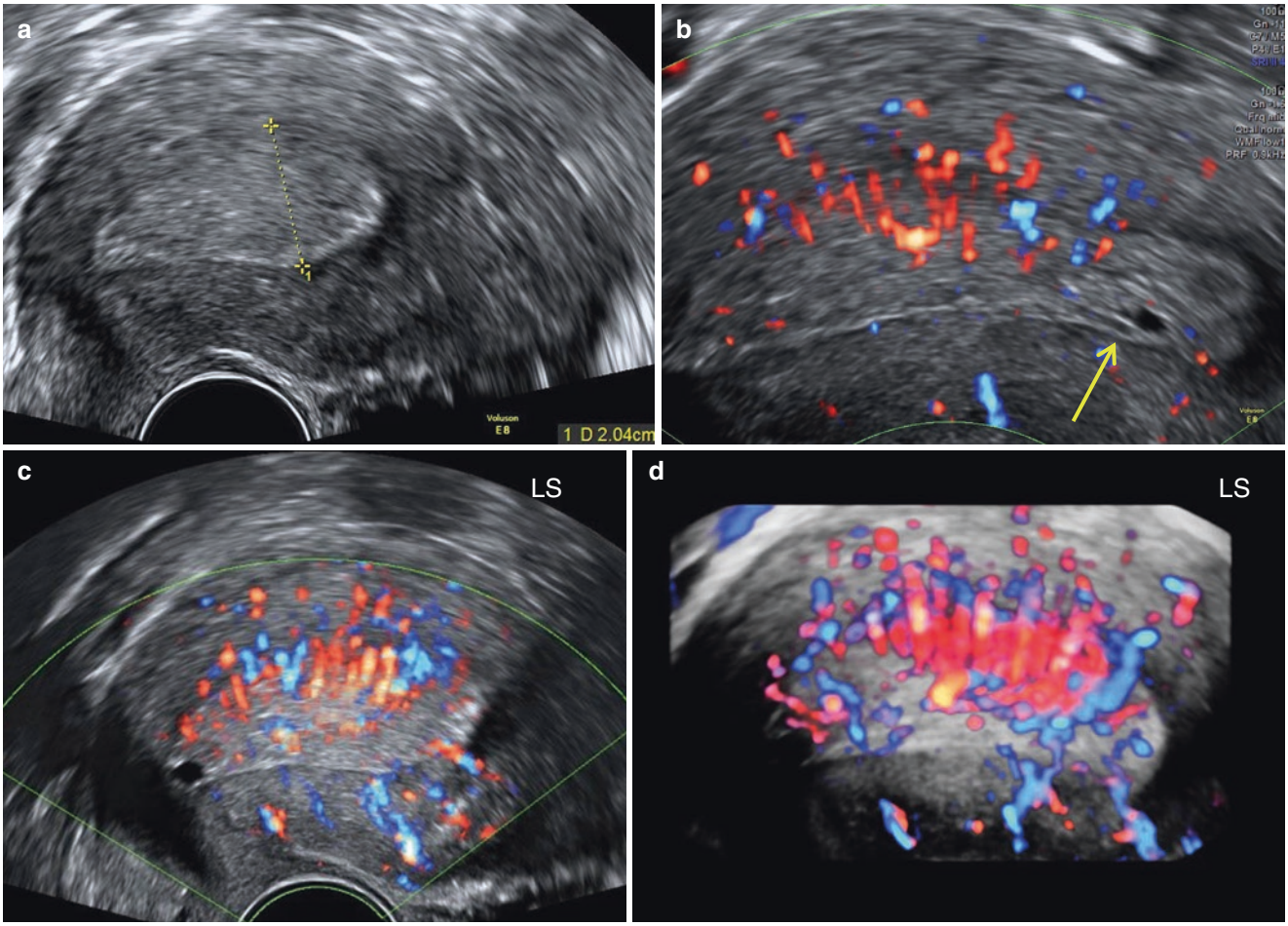

Fig. 4.41 A 31-year-old, known case of endometrioid carcinoma Grade 1 and PCO, on progesterone therapy. (**a**) 20 mm thick hyperechoic endometrium. (**b**) Focal area of cystic changes in the endometrium (*arrow*). Multifocal linear single vessels seen crossing the EMJ. (**c**) On colour Doppler and (**d**) on 3D Doppler with glass body display

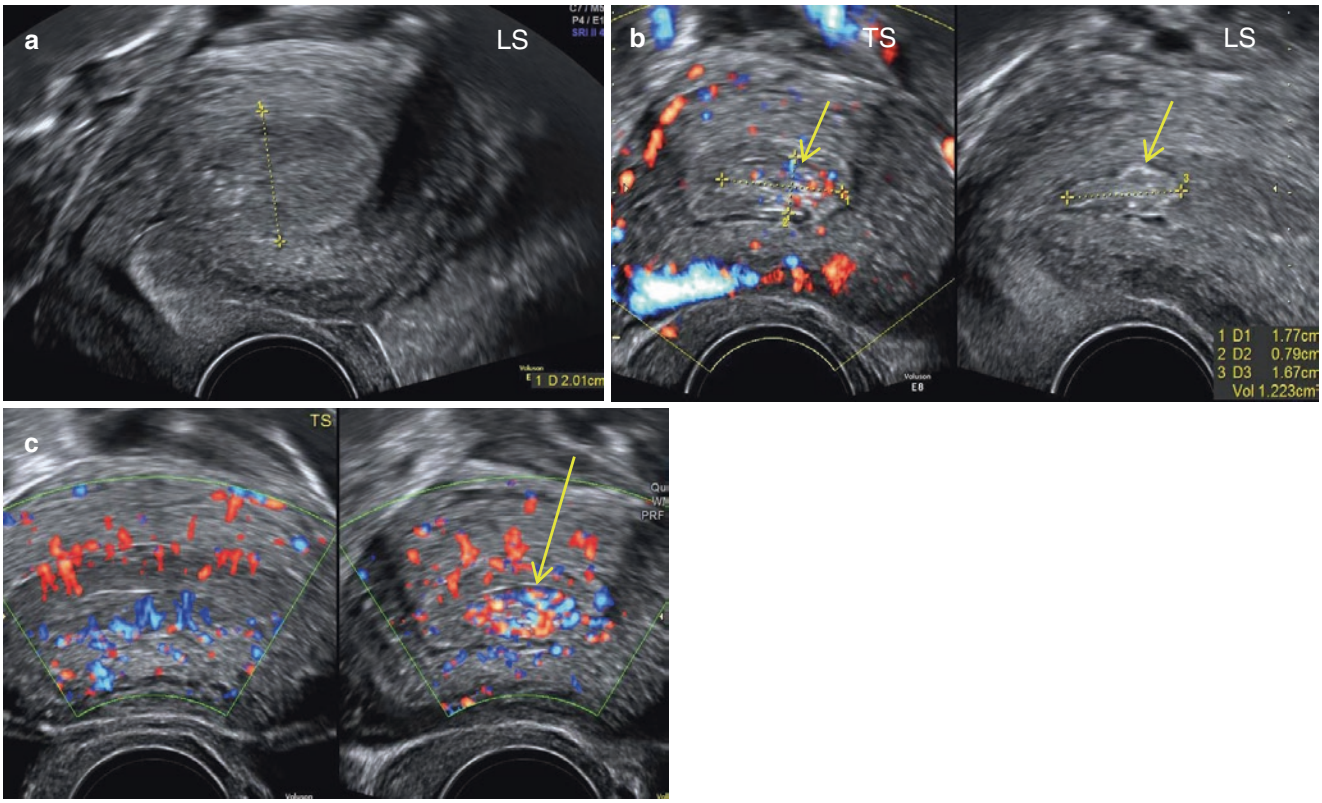

Fig. 4.42 A 29-year-old patient, diagnosed to have PCO 3 years prior to the scan. Curettage for intermenstrual spotting showed carcinoma endometrium in situ, for which the patient was on progesterone. (**a**) Thick endometrium of 20 mm. (**b**) A small hyperechoic polypoid area (*arrow*) is seen in the lower corpus. (**c**) Multifocal linear single vessels seen crossing the EMJ. The polypoid area (*arrow*) shows high vascularity in the image on the right. Hysteroscopy and biopsy were repeated in view of high vascularity particularly in the polyp. *Repeat HPE showed a great improvement in tissue cytology with no atypia and progestational effect on the endometrium*

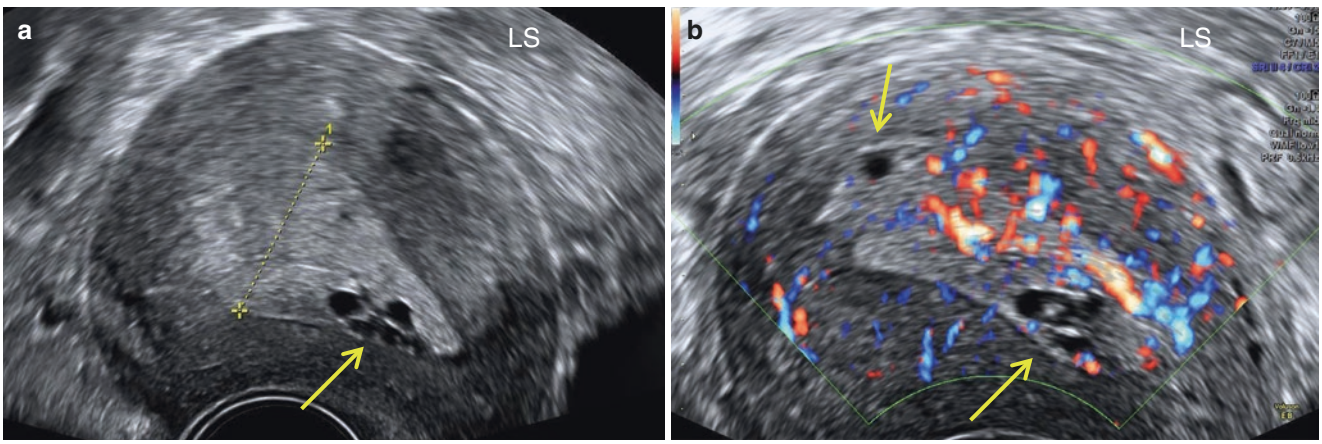

Fig. 4.43 Known case of complex hyperplasia with atypia, on progesterone therapy. (**a, b**) Thickened endometrium is seen with two focal areas of cystic changes in the endometrium (*arrows*). (**b**) Endometrium shows increased vascularity with multifocal scattered linear vessels

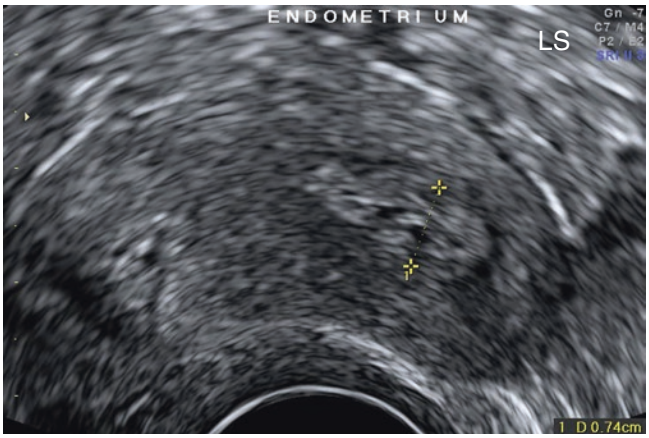

Fig. 4.44 A 40-year-old patient on treatment for carcinoma breast. She was on GnRH analogues for ovarian suppression and tamoxifen. 7.4 mm thick endometrium with cystic changes is seen which is typical of patients on tamoxifen therapy

Summary: Endometrial Hyperplasia

- This condition is usually secondary to long-standing unopposed oestrogen effect on the endometrium. Most women complain of menorrhagia.
- On ultrasound, endometrium is thick and shows multifocal single-scattered peripheral linear vessels crossing the EMJ. The endometrium may appear three layered, echogenic or heterogeneous. Tiny cystic spaces may be seen.
- Differentiation from endometrial carcinoma is difficult in most cases, and a diagnosis is made only on biopsy.

4.5 Endometrial Malignancy

Endometrial carcinoma is the most common gynecological malignancy. Fortunately, however, about 95 % of these patients are symptomatic, because of which early diagnosis and management is usually possible. The commonest type of endometrial carcinoma is endometrial adenocarcinoma (about 90 % of cases). Ten percent of the cases comprise of rare cell types like papillary serous, clear cell or mucinous.

The common symptoms of women with endometrial carcinoma are postmenopausal bleeding, menorrhagia (heavy flow and flow lasting for a long period), metrorrhagia and sometimes excessive vaginal discharge, which may be blood stained or foul smelling.

Ultrasound Features of Endometrial Malignancy
(Figs. 4.45, 4.46, 4.47, 4.48, 4.49, 4.50, 4.51, 4.52, 4.53, 4.54 and 4.55)

- Thickened endometrium – endometrial thickness is usually increased. In postmenopausal women, a thickness of 5 mm or more is considered a thickened endometrium and raises the possibility of pathology including malignancy. In premenopausal women, it is difficult to assign a cut-off. Values above 15 mm at any time in the cycle could be considered a thickened endometrium with a likelihood of pathology.
- The endometrial volume generally increases. More than 13 ml increases the possibility of malignancy.
- Heterogeneous endometrial tissue.
- The lesion may be diffuse or focal. At times, the lesion is seen extending into the cervix. This is important to look for, as cervical extension of the tumour may alter management protocols.
- Intracavitary fluid may be seen due to necrosis and presence of blood in the endometrial cavity. Minimal intracavitary fluid in the absence of other pathology is, however, often found to be related to benign conditions like cervical stenosis, submucous fibroids, etc.
- The EMJ may be disrupted due to myometrial invasion by the tumour which may be seen on 2D, on 3D or with the help of Doppler. The best evaluation of myometrial invasion is with 3D VCI. One can walk through the volume showing the VCI image to check the entire EMJ for invasion. Areas of thick normal-looking myometrium with regular EMJ (i.e. areas showing no invasion) act as a good control for assessing myometrial invasion.
- On Doppler, there is increased vascularity in the endometrium. Randomly dispersed vessels may be seen in the endometrium. The vessels may or may not be seen originating from the EMJ on 2D Doppler. The vascular morphology is best studied on 3D power Doppler with glass body display (described in detail in the section on Doppler in Chap. 2). The vessels are tortuous and show increased or abnormal branching. The size of the vessels may be irregular, and looping and bridging may be seen. The vascular pattern is difficult to assess unless the endometrium is sufficiently thick. Doppler may, at times, assist in picking up myometrial invasion across the EMJ by recognising increased flow in that area. Doppler can help determine the site of tumour invasion due to its high vascularity, ensuring that the biopsy is done in that region.
- It has been suggested that spectral Doppler may show low resistance flows in endometrial carcinoma. However, a significant overlap in Doppler indices decreases its utility in differentiating benign from malignant lesions.
- Occasionally, an endometrial polyp may show malignant features. Such polyps are more likely to be large and heterogeneous with feeder vessels showing a low RI.
- If there is sufficient fluid or blood in the endometrial cavity (including sonohysterogram), findings may be more discreet. Heterogenicity and irregular surface of the endometrium are more common in malignant than in benign endometrium. An irregular endometrial outline was shown to have a positive LR of 10. Doppler evaluation with saline infusion showed a decrease in blood flow as compared to the prior TVS in 25 % of patients in a study (Epstein UOG 2006). It is, therefore, recommended that Doppler examinations should be done before saline infusion.

Concerns have been raised that saline infusion could lead to intraperitoneal dissemination of malignant cells in women with endometrial malignancy. Five-year survival has been reported to be the same in women with early endometrial cancer who have undergone hysteroscopy before laparotomy, as compared to those that did not have preoperative hysteroscopy. Saline infusion sonohysterography is therefore considered a safe procedure, even in women with endometrial cancer.

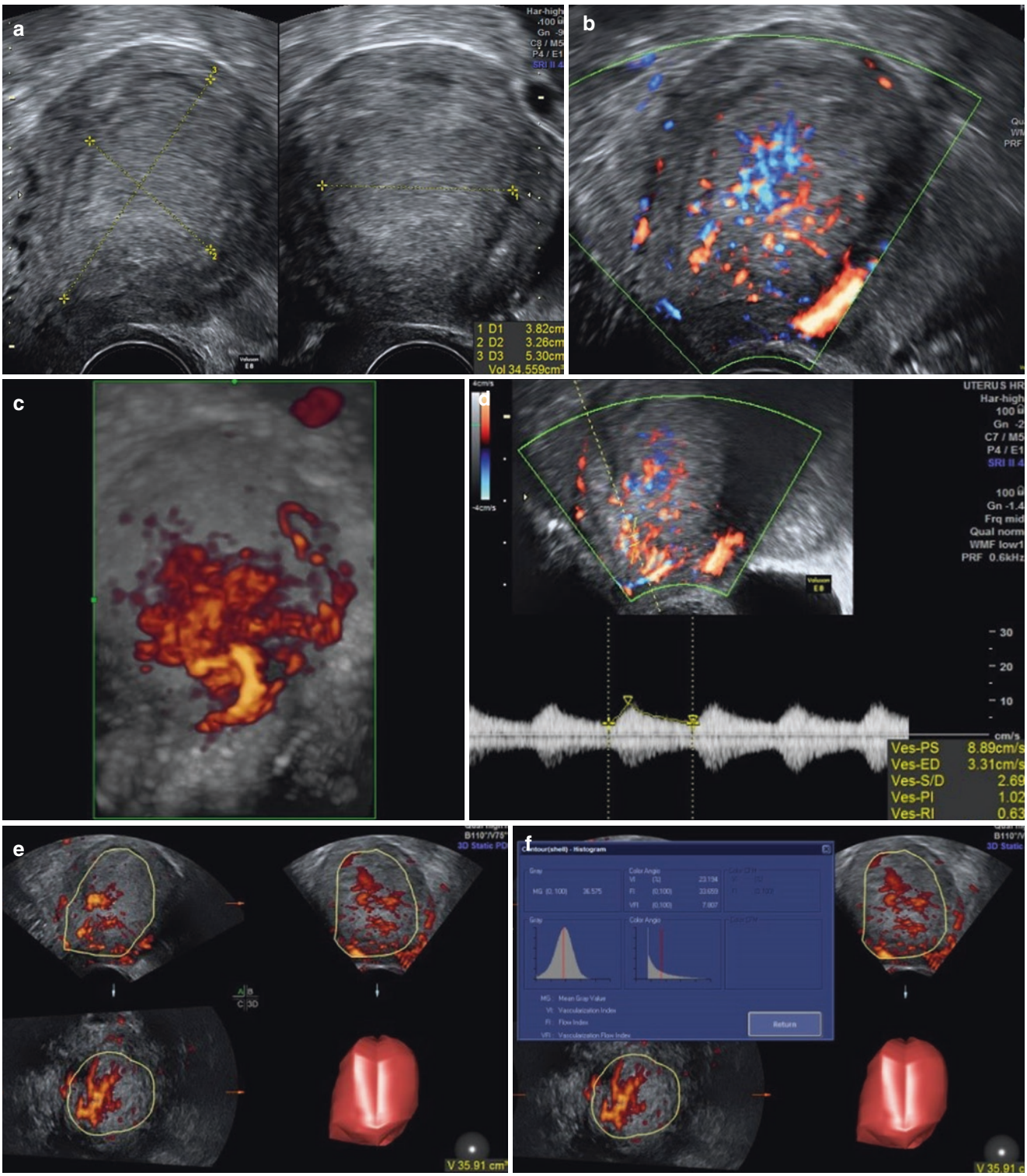

Fig. 4.45 Endometrial carcinoma in a 70-year-old patient with postmenopausal bleeding. (**a**) Thickened (32 mm) hyperechoic slightly heterogeneous endometrium with increased endometrial volume (34.5 cc). (**b**) Increased vascularity (*colour score 4*) noted in the endometrium with non-linear vessels that show up either as colour signals or short segments of vessels, most often not originating from the EMJ on 2D Doppler. (**c**) Power Doppler with 3D glass body image is best in depicting abnormal vascular morphology, as is seen here with irregular size of vessels and abnormal branching. (**d**) Flow in endometrial tissue showing RI of 0.63. (**e**) Endometrial volume (35.9 c) measured using 3D VOCAL software. (**f**) 3D power Doppler with volume histogram to assess vascular flow quantitatively. (**g**) 3D study with VCI showing irregular outline due to myometrial invasion in the posterosuperior wall of the uterus (*arrows*). (**h**) 3D power Doppler with VCI showing an irregular EMJ (*arrows*) and flow in the endometrial tissue. (**i**) Postoperative specimen showing a cut section of the uterus. Bulky endometrial tissue is noted. *HPE:* endometrioid adenocarcinoma with more than 50% myometrial invasion. Cervix was free of tumour

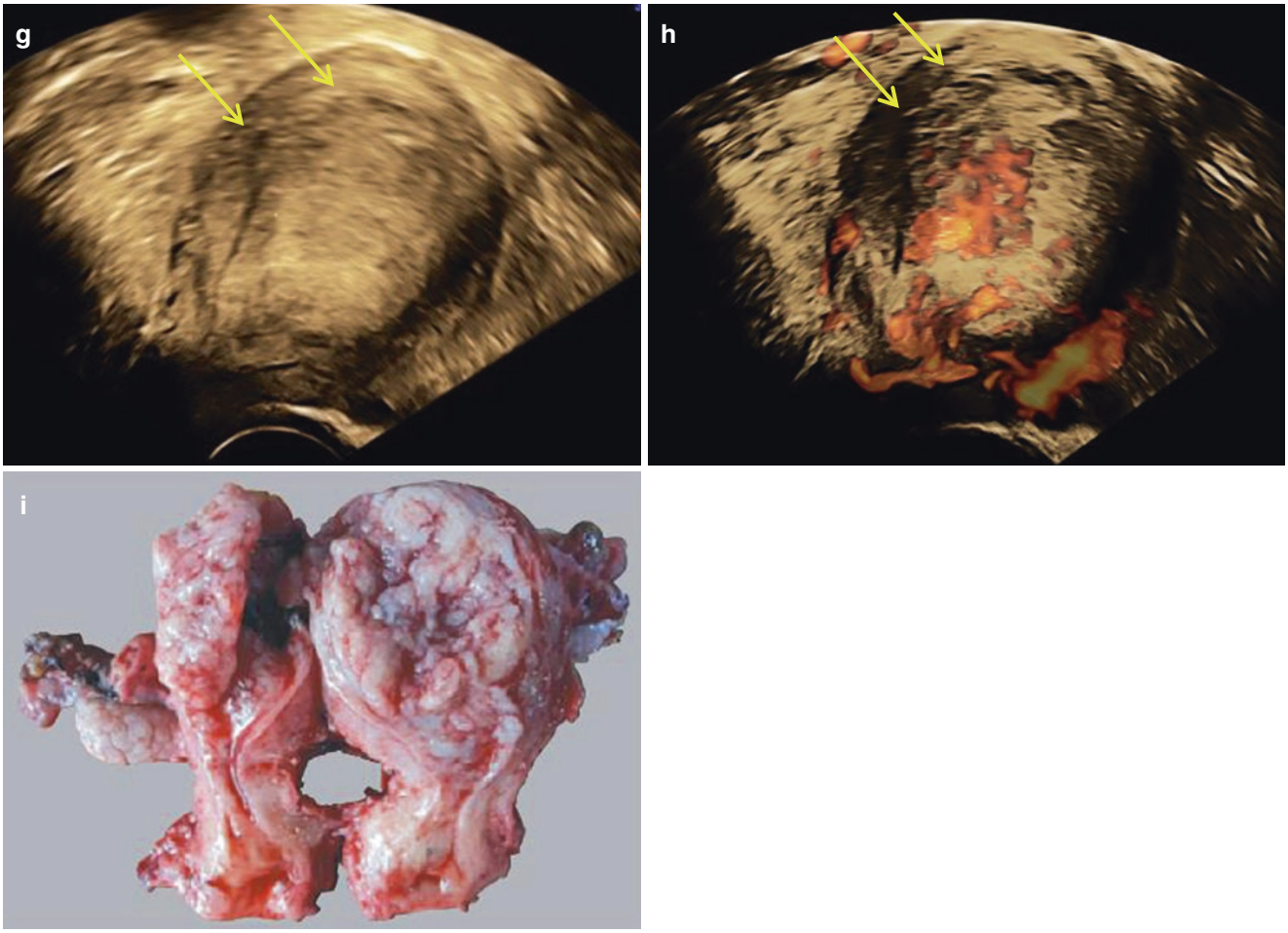

Fig. 4.45 (continued)

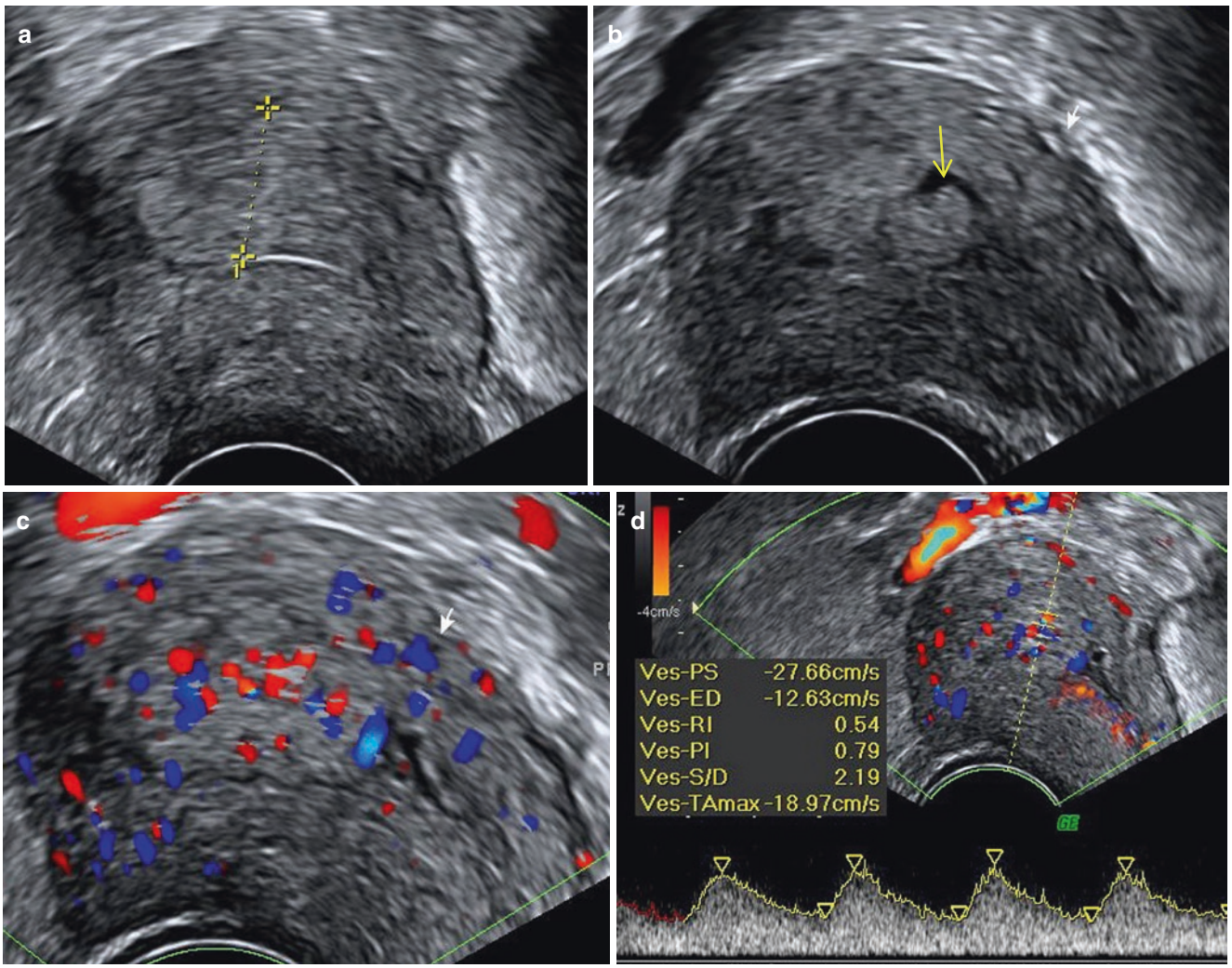

Fig. 4.46 Endometrial carcinoma. (**a**) Thickened (14.2 mm) heterogeneous endometrium. (**b**) Intracavitary fluid seen delineating the irregular outline (*arrow*) of the endometrial malignant tissue. (**c**) Increased vascularity of the endometrial tissue is seen with randomly dispersed vessels, which are not seen emerging directly from the EMJ. (**d**) Flow in the endometrium with RI of 0.54 and PSV of 27.6 cm/sec

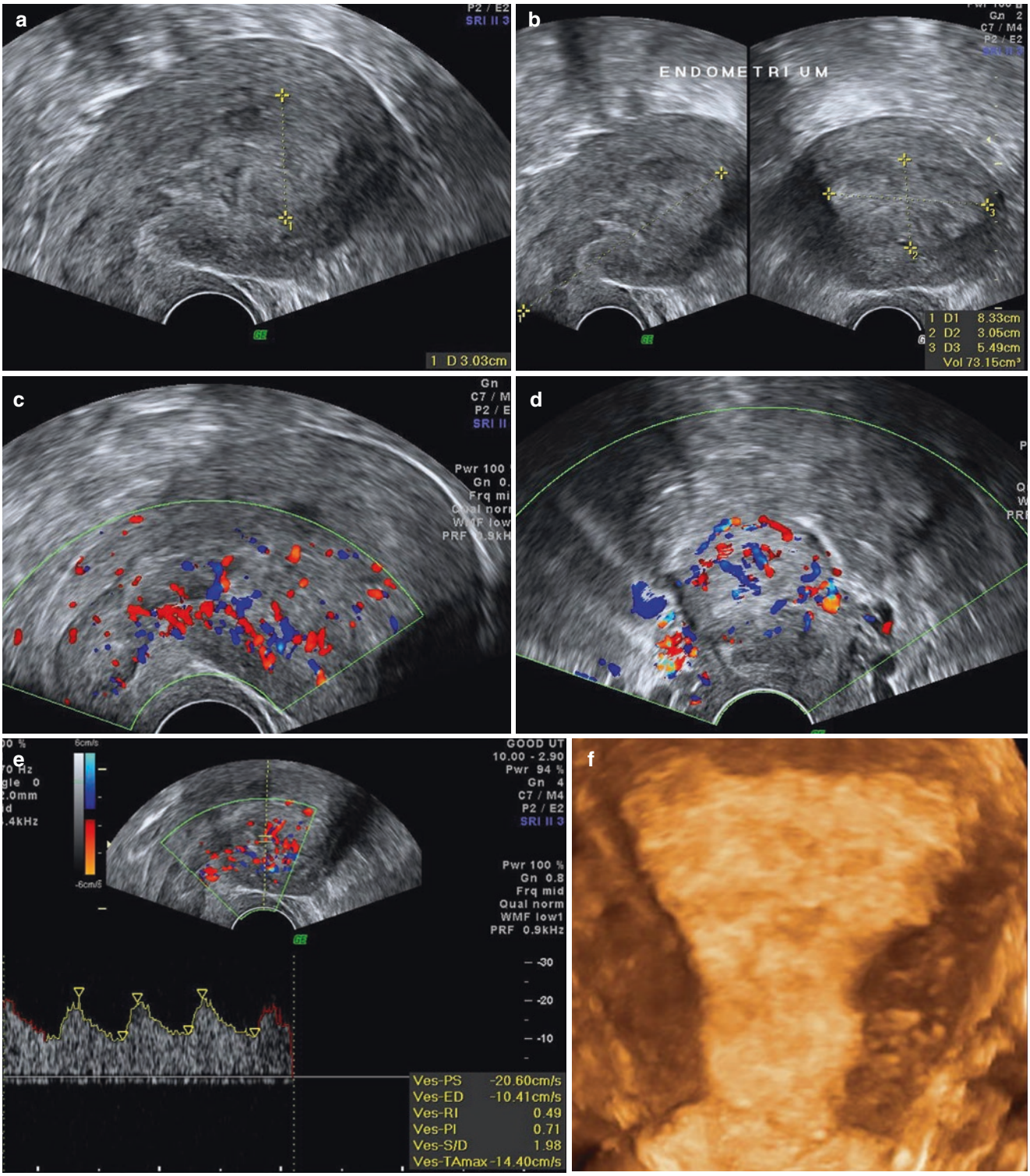

Fig. 4.47 Endometrial carcinoma in a 62-year-old patient. (**a**) Thickened endometrium of 30.3 mm with the thickened tissue seen extending into the cervical canal. (**b**) Increased endometrial volume of 73 cc. (**c**) Endometrial tissue showing increased vascularity with randomly dispersed vessels. Flow is also seen in the tissue extending into the cervical canal. (**d**) Transverse section of cervical canal showing flow from the cervical walls into the tissue. (**e**) Endometrial flow shows a RI of 0.49. (**f**) 3D rendered image showing irregular endometrial margins. *HPE:* endometrioid carcinoma with less than 50 % myometrial invasion

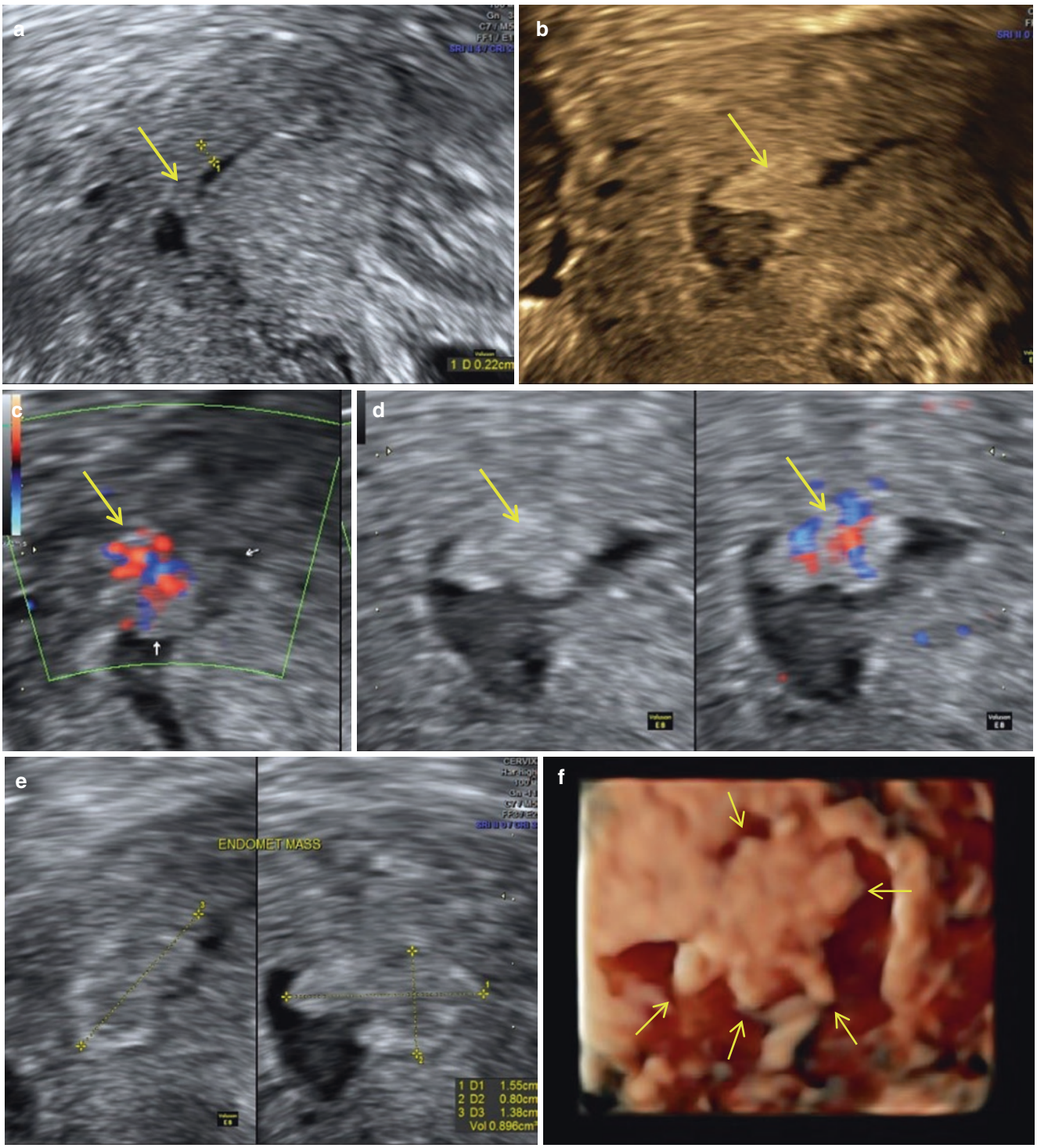

Fig. 4.48 Endometrial carcinoma in a 65-year-old patient with 1-month history of postmenopausal bleeding. (**a**) Minimal fluid seen in the endometrial cavity with a single-layer endometrial thickness of 2.2 mm. A small focal irregularity (*arrow*) noted in the posterior endometrial wall of the lower corpus. (**b**) The same seen in sepia mode (*arrow*). (**c**, **d**) This focal solid tissue (*arrows*) showed irregular margins and flow approaching it from the posterior wall through a few small vessels crossing the EMJ. (**e**) Focal solid irregular area measured 15 × 8 × 13 mm (Vol: 0.9 ml). (**f**) 3D rendered image of the same showing spiky irregular margins (*arrows*). These were well seen because of the surrounding fluid in the endometrial cavity. *HPE:* endometrioid adenocarcinoma of less than 1 cm with less than 50% myometrial invasion

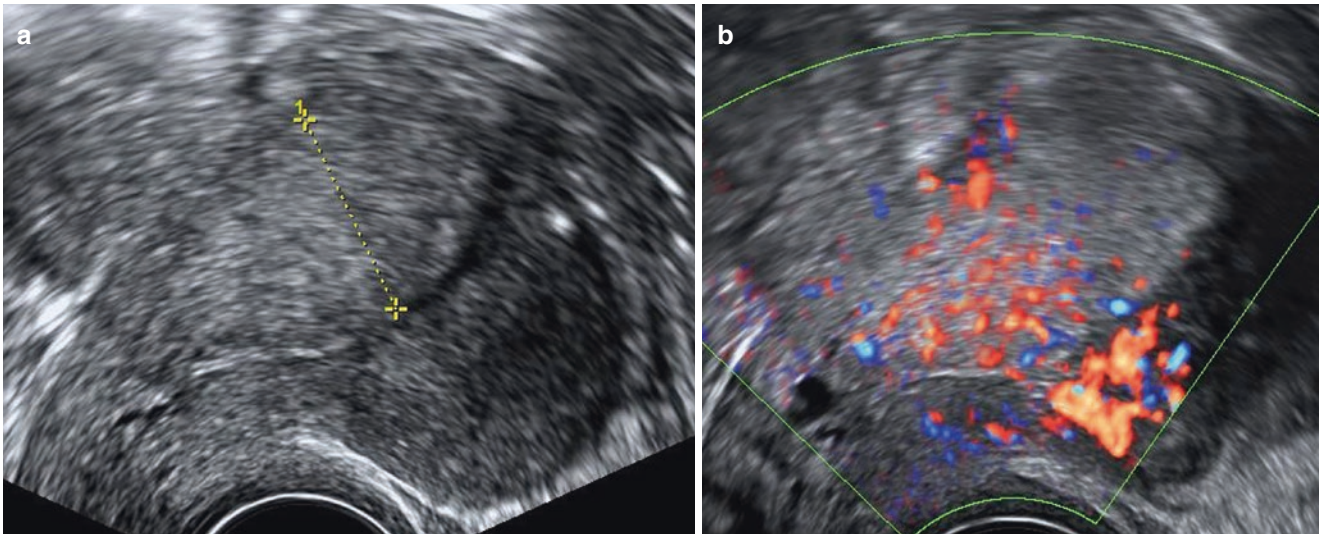

Fig. 4.49 Endometrial carcinoma in a 78-year-old patient. (**a**) Hyperechoic thick endometrium. (**b**) Increased endometrial vascularity. The vessels are not linear and are not seen originating from the EMJ on 2D Doppler. *HPE:* endometrioid carcinoma

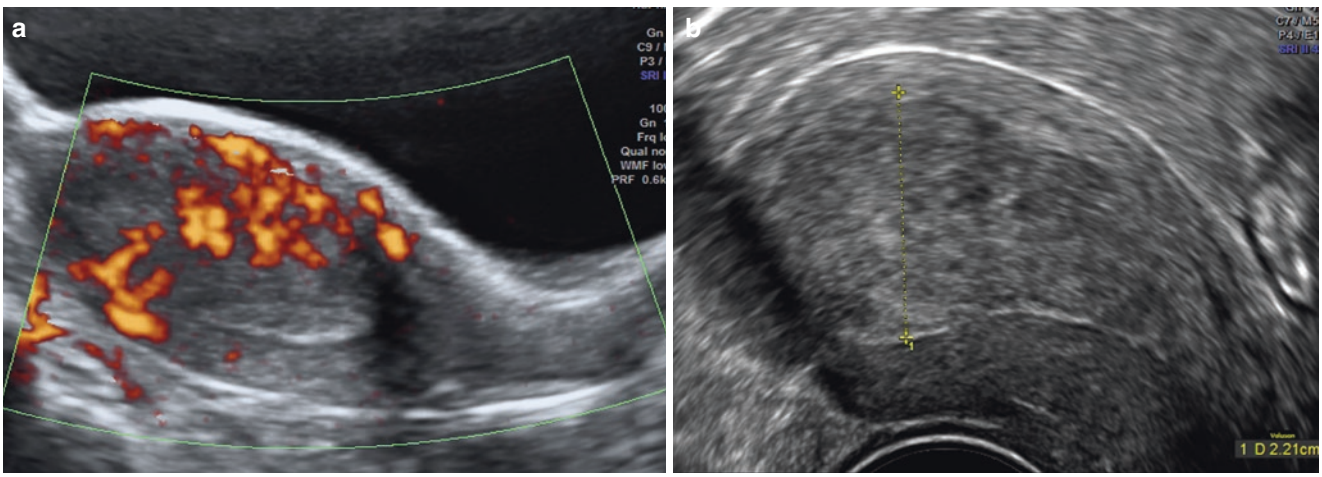

Fig. 4.50 Endometrial carcinoma in a 57-year-old patient. LS views of the uterus. (**a**) TAS – thickened endometrium with increased endometrial vascularity is seen with a few vessels crossing the EMJ, anteriorly and posteriorly. (**b**) TVS – thickened heterogeneous endometrium with increased endometrium volume of 13.5 cc. (**c**) Increased endometrial vascularity on 2D power Doppler showing short segments of vessels with only some crossing the EMJ. (**d**) 3D power Doppler with glass body image showing the entire abnormal vascular morphology. (**e**) 3D with VCI showing normal EMJ and a myometrial thickness of 5 mm to the right of the midline. (**f**) 3D with VCI showing an irregular disrupted EMJ (*arrows*) secondary to myometrial invasion to the left of the midline. The overlying myometrium is just 1.3 mm (*long arrow*), suggesting that there is more than 50 % myometrial invasion. (**g**) Regular 2D imaging of the uterus showing the EMJ, looking normal though not well defined to the right of the midline (*long arrow*) and poorly defined (*short arrows*) to the left of the midline. Here myometrial invasion is not well made out. (This is the area corresponding to the area of myometrial invasion in image (**e**) using 3D VCI.) *HPE:* endometrioid carcinoma with more than 50 % myometrial invasion

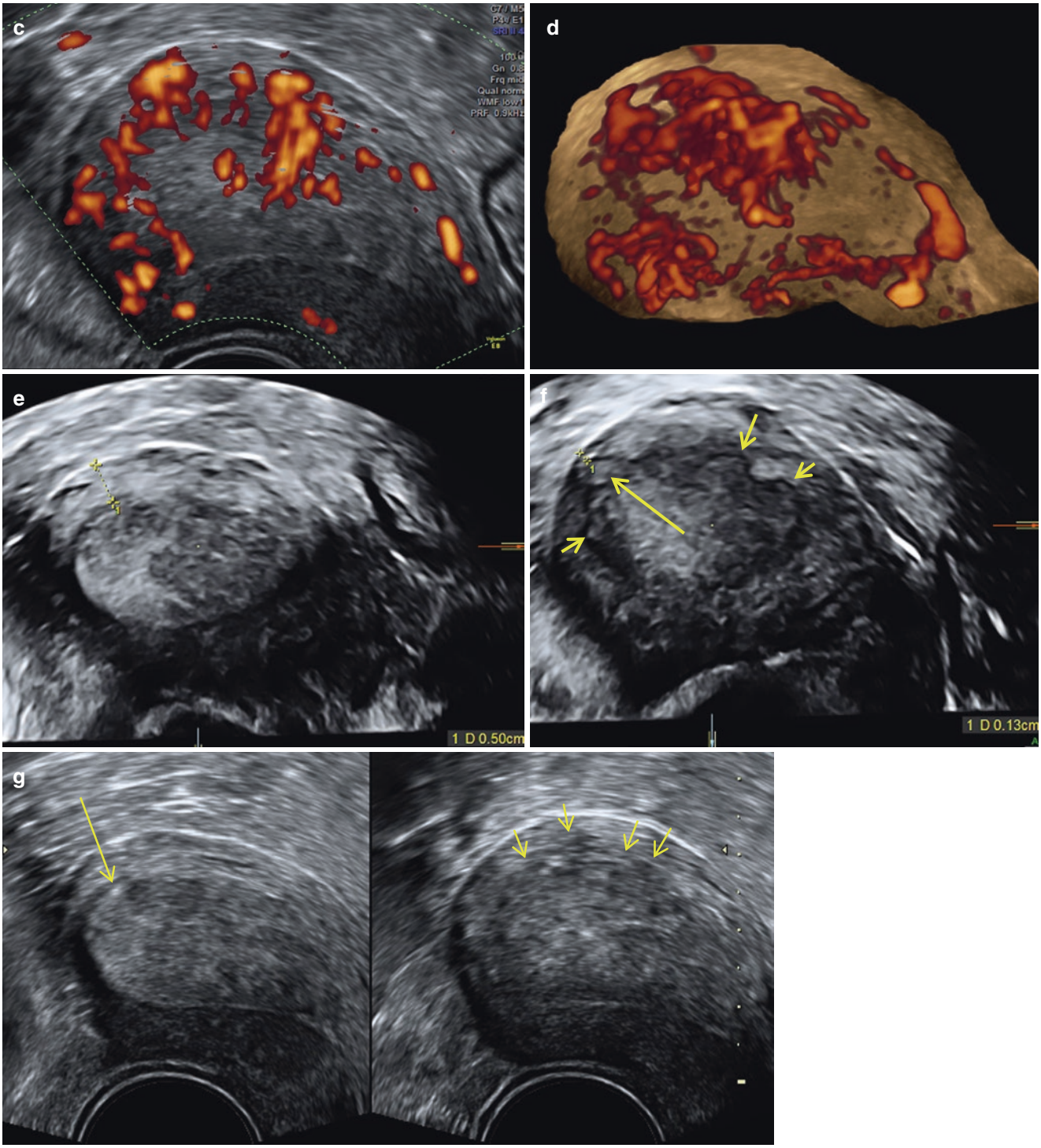

Fig. 4.50 (continued)

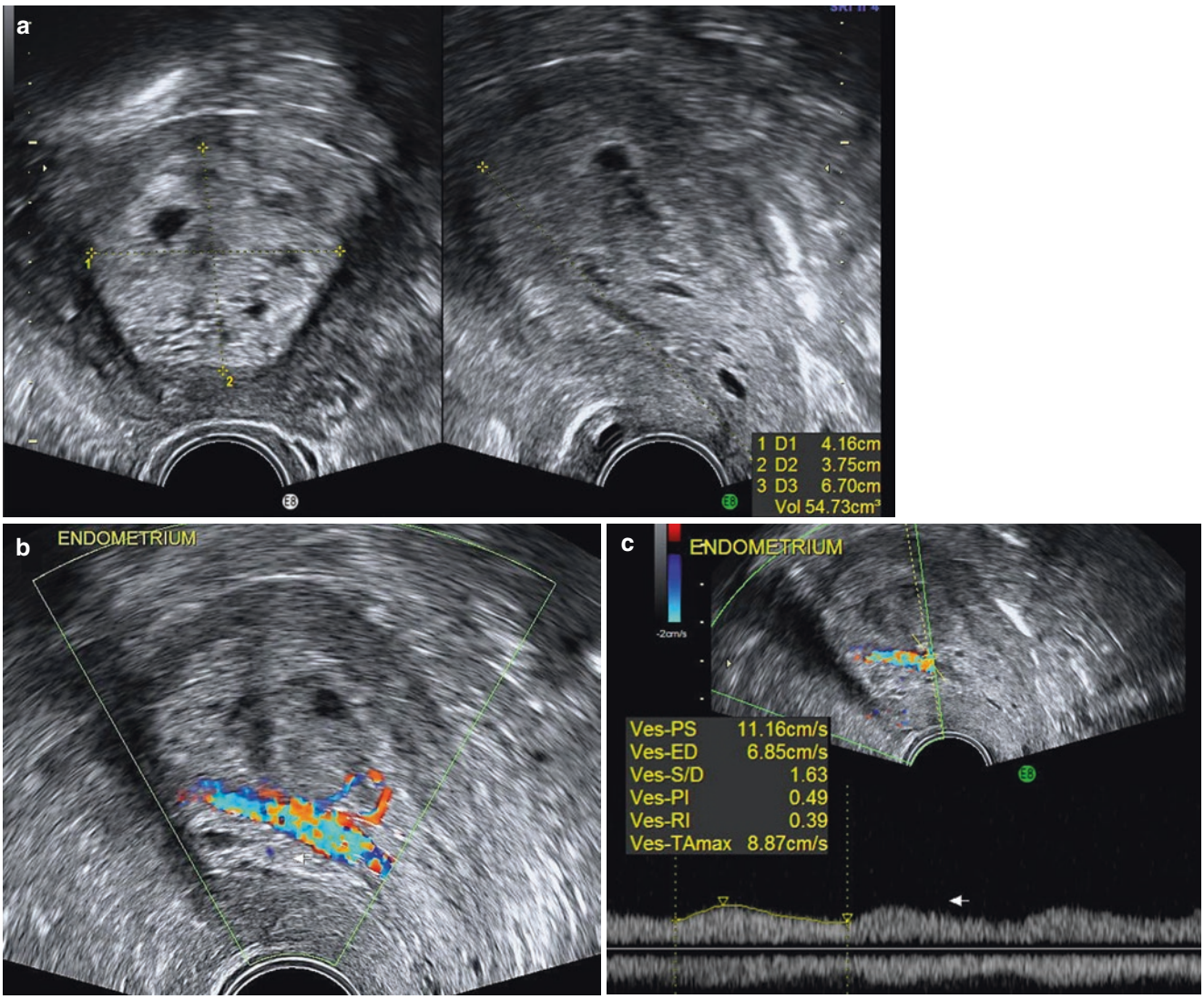

Fig. 4.51 Carcinoma in an endometrial polyp seen in a 61-year-old patient with a history of blood-stained white discharge of one-and-a-half-month duration. (**a**) Thickened hyperechoic endometrium with cystic spaces and a volume of 54 cc. (**b**) A single large feeder vessel noted arising from the posterior uterine wall. (**c**) The feeder vessel shows a low RI of 0.39. *HPE:* endometrioid adenocarcinoma in an adenomyomatous polyp

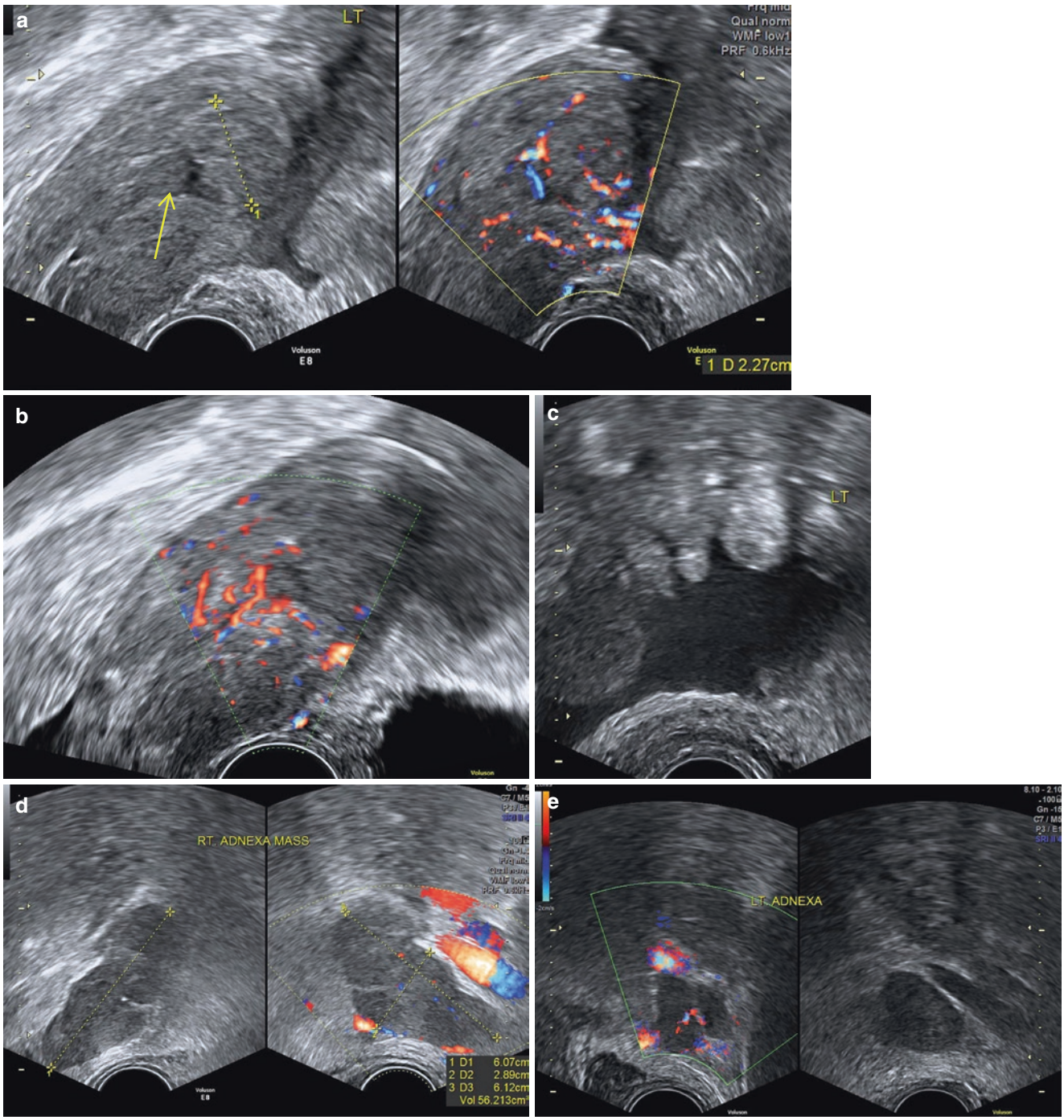

Fig. 4.52 Endometrial carcinoma in a 68-year-old patient with a 4-month history of postmenopausal bleeding. (**a**) Thickened heterogeneous endometrium of 22.7 mm showing minimal intracavitary fluid (*arrow*). Flow is seen within the endometrial tissue, which is seen as a solid circumscribed tissue at the upper corpus. (**b**) Flow is also seen in the endometrium of the mid corpus and lower corpus with RI 0.53. (**c**) Ascitic fluid is seen in the right lower abdomen. (**d**, **e**) Right and left adnexal masses seen along the external iliac vessels. The masses are heterogeneous and show vascularity, suggestive of metastatic lymph nodes. *HPE:* endometrioid adenocarcinoma. PET scan showed spread to iliac, aortic and supraclavicular lymph nodes

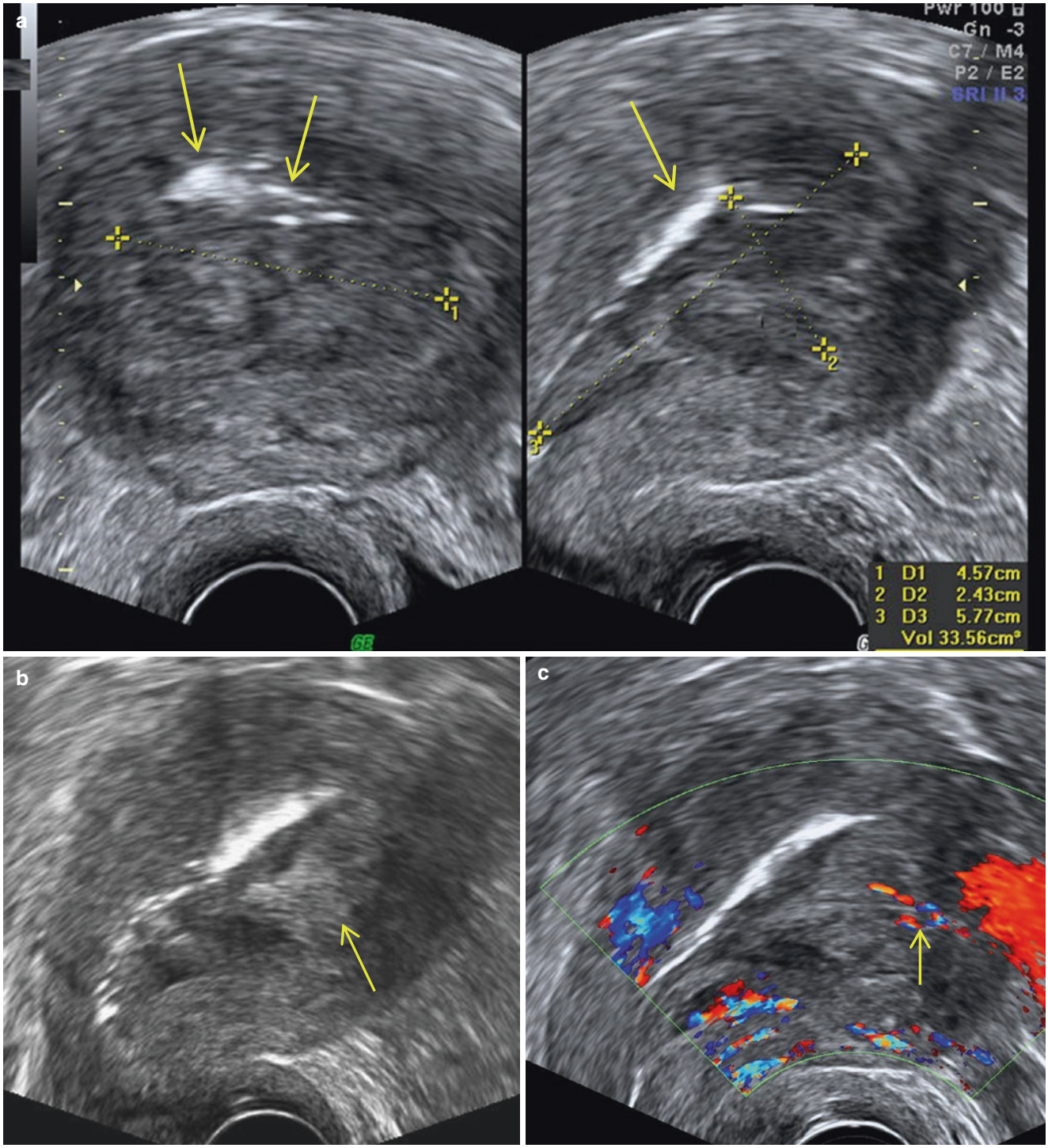

Fig. 4.53 Endometrial carcinoma with pyometra in a postmenopausal lady who presented with bleeding. (**a**) Endometrial cavity showing complex echoes and a volume of 34.5 cc. Scattered echogenic areas seen along the posterior wall of the anteflexed uterus suggestive of air in the endometrial cavity (*arrows*) caused by anaerobic infection. (**b**) Solid tissue is seen in the upper corpus (*arrow*). The rest of the endometrial cavity appears filled with turbid complex fluid (blood and pus). (**c**) Solid tissue (*arrow*) showing Doppler flow from the anterior wall. (**d**) 3D rendered image showing complex echoes in the endometrial cavity and air echoes (*arrows*) which appear bright. (**e**) Postoperative specimen of the endometrial curettings. *HPE:* endometrioid carcinoma with high-grade malignancy and extensive necrosis

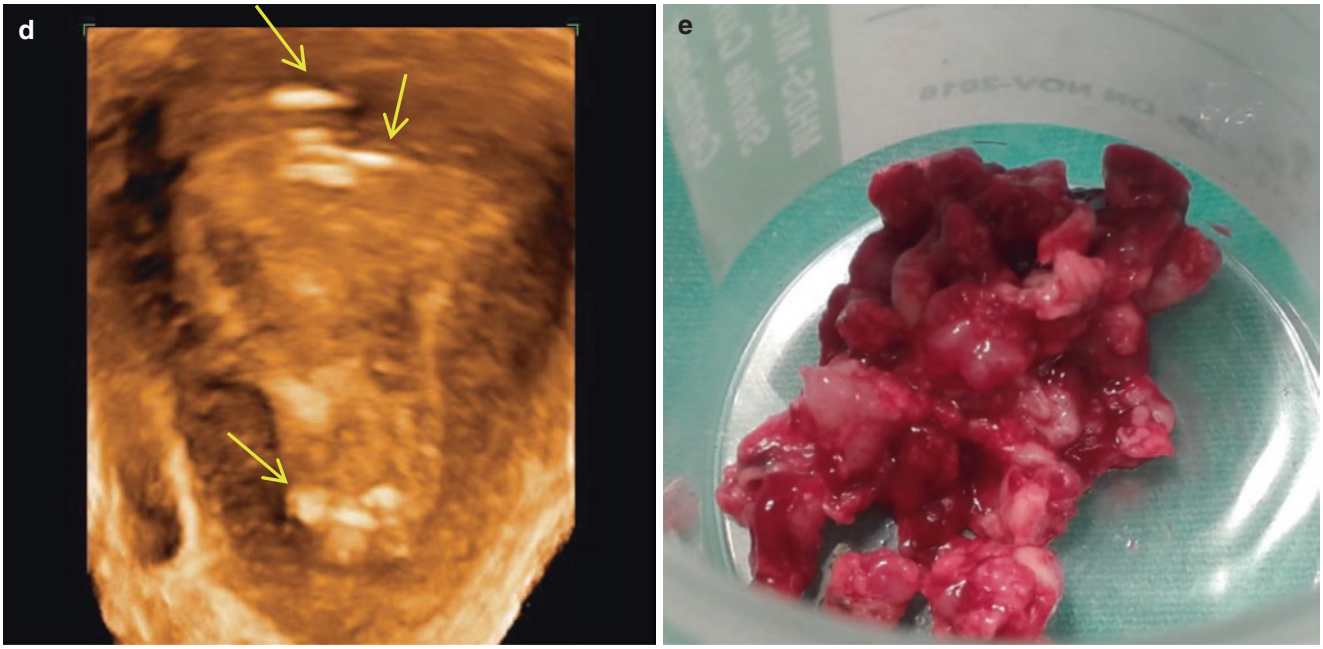

Fig. 4.53 (continued)

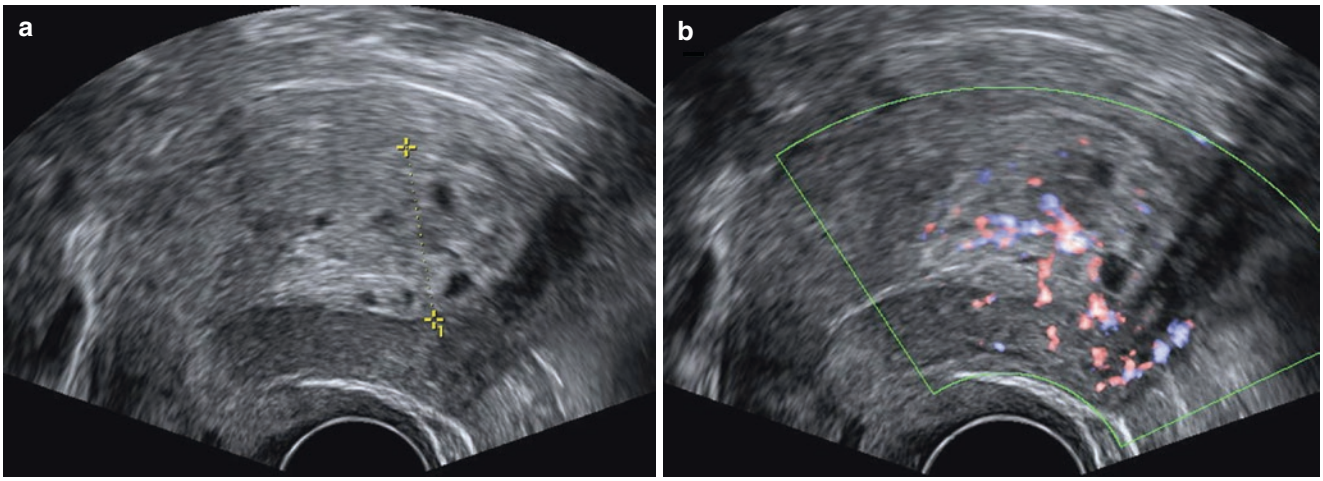

Fig. 4.54 Endometrial cancer in a 64-year-old patient who presented with postmenopausal bleeding of 4 years' duration. (**a**) Hyperechoic thickened endometrium of 27.3 mm seen. Small cystic spaces are seen in the endometrial tissue. (**b**) Endometrium showing increased vascularity. *HPE:* mucinous carcinoma of the endometrium

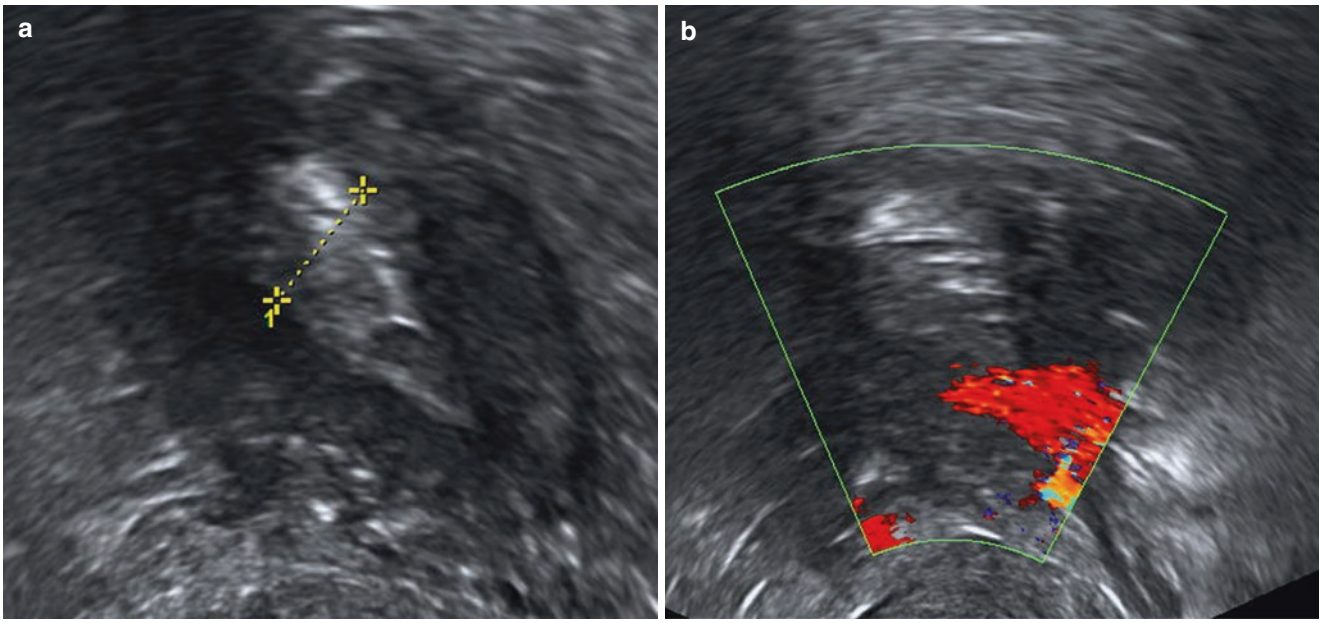

Fig. 4.55 A 73-year-old patient with obesity and the first episode of postmenopausal bleeding. (**a**, **b**) Visualisation is suboptimal both on greyscale and Doppler. Endometrial thickness was 1.5 cm. On ultrasound, the only finding in a postmenopausal patient with endometrial carcinoma may be a thickened endometrium as in this case. *HPE:* endometrioid adenocarcinoma

Summary: Endometrial Malignancy

- Endometrial carcinoma is commonly seen in postmenopausal women, who most often present with postmenopausal bleeding.
- On ultrasound, the endometrium is usually thickened and differentiation from endometrial hyperplasia may be difficult. The endometrial tissue is typically heterogeneous, and the endometrial margins lining the cavity are irregular (this can be seen in the presence of sufficient intracavitary fluid or on sonohysterogram). On Doppler vascularity is increased with multifocal vessels or multiple vessels from one focal area. Not all vessels show origin from the EMJ. The vessel morphology is abnormal with irregular size and excessive branching.
- The EMJ may be disrupted or poorly defined suggesting myometrial invasion.
- Diagnosis of malignancy can only be made on biopsy of the endometrial lesion.

4.6 Differential Diagnosis of Thickened Endometrium (Fig. 4.56)

The three likely pathologies in women with thickened endometrium are endometrial polyp, hyperplastic endometrium and endometrial carcinoma (after having ruled out an intracavitary fibroid).

In premenopausal and perimenopausal women, about 1 % of those that undergo curettage have malignancy, whereas in postmenopausal women, the percentage increases to 10 %.

Prior to differentiation between these three conditions, it is important to know what measurement defines a 'thickened' endometrium. Normal acceptable thickness of the endometrium, in a postmenopausal woman, is 4 mm or less. Therefore, a thickness of 5 mm or more would be considered a thickened endometrium and raise the possibility of a polyp, endometrial hyperplasia or malignancy. In premenopausal women, it is difficult to assign a cut-off. In them, a thickness of 5 mm or less on D4 to D6 (of the menstrual cycle) is considered normal. So values above that or, as some suggest, a measurement of more than 15 mm at any time in the cycle could be considered a thickened endometrium with likelihood of pathology.

Ultrasound (TVS) is the primary modality of investigation in women with abnormal uterine bleeding or thickened endometrium. In some cases, a diagnosis may be made (e.g. submucous fibroid or endometrial polyp), while in others, its utility is in helping select those patients that require biopsy, which provides the final definitive diagnosis.

Factors that help to differentiate between these three conditions are (Fig. 4.56):

- Polyps are usually hyperechoic and well defined. If they fill the entire endometrial cavity, then their smooth, well-defined margins can be seen on SHG.
- Heterogeneous endometrial tissue and presence of intracavitary fluid – more likely to be carcinoma.
- Endometrial volume: Average is 2.6 ml for polyp, 7.8 ml for hyperplasia and 37 ml for carcinoma. Cut-off suggested for malignancy is 13 ml.
- EMJ is usually uniform in a polyp and hyperplasia but may be disrupted in cases of a carcinoma with myometrial invasion. VCI helps delineate the EMJ better.
- Vascular pattern on 2D Doppler: (**a**) A single feeder vessel likely to be a polyp; (**b**) multifocal scattered linear vessels crossing the EMJ, likely to be endometrial hyperplasia; (**c**) randomly dispersed vessels that are not seen originating from EMJ, likely to be endometrial carcinoma.
- Vascular morphology on 3D power Doppler: Same as seen on 2D Doppler (mentioned above) in a polyp and cases of endometrial hyperplasia. In carcinoma, however, abnormal vascular tree with tortuous vessels, variable calibre, looping, bridging and excessive branching may be seen.

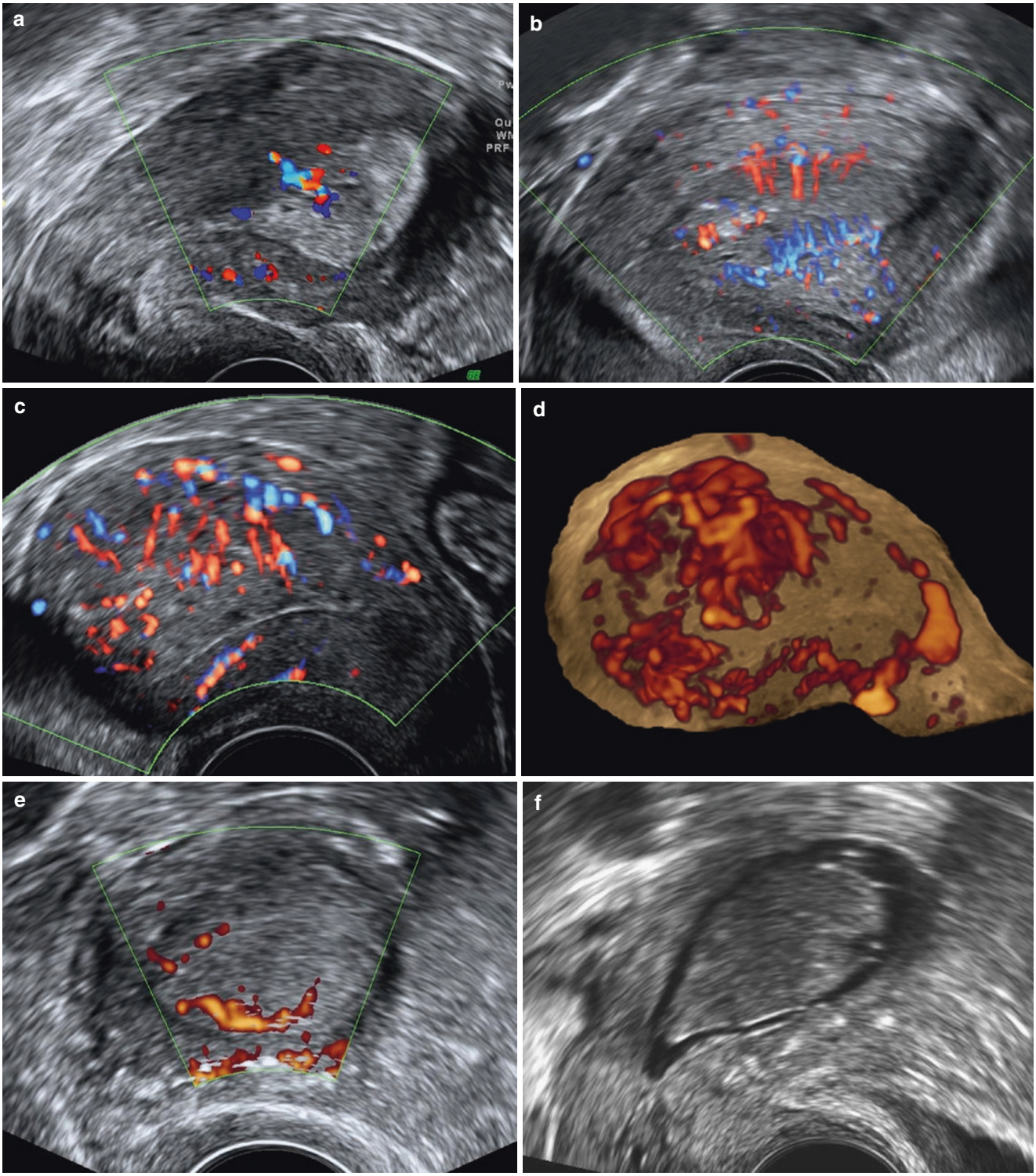

Fig. 4.56 Differential diagnosis of a thickened endometrium. (**a**) Single feeder vessel – polyp. (**b**) Multifocal scattered linear vessels crossing the EMJ – endometrial hyperplasia. (**c**) Randomly dispersed vessels that may not originate from EMJ – endometrial carcinoma. (**d**) 3D power Doppler of the case in (**c**) with a glass body display showing abnormal morphology (explained in the section on Doppler in Chap. 2 and in the legend of image 2.26 (**c**)). (**e**) Thickened endometrium in a postmenopausal patient measuring 19 mm. In view of the vascular pattern, this raised the suspicion of carcinoma endometrium or hyperplasia. (**f**) However, on SHG in the above patient, to our surprise, it turned out to be a large endometrial polyp. This case illustrates that diagnosis of a thickened endometrium is challenging. It often requires further study with SHG and is very often only diagnosed on hysteroscopy or biopsy and histopathology

4.7 Asherman's Syndrome or Intrauterine Adhesions

Intrauterine adhesions or endometrial scarring is usually post-traumatic or postsurgical, following curettage or manual removal of placenta in a gravid uterus. It can also occur because of trauma to a non-gravid uterus during resection of a submucous fibroid or septum. It may also be seen following endometrial ablation and uterine artery embolisation. It can be seen with infections like genital tuberculosis. This is the result of the normal wound-healing process of the endometrium which gets replaced by fibrous tissue, which in turn causes the opposing endometrial surfaces to bond with each other. This results in the formation of intrauterine adhesions with deficient endometrium in that area. There may however be pockets of functional endometrium in the non-scarred area. In the scarred area, the distinction between the functional and basal layers of the endometrium is lost. Intrauterine adhesions can involve both the myometrial and the endometrial layers.

Depending on the extent of scarring, patients with Asherman's syndrome may be asymptomatic or can have scanty or absent periods. Some patients may complain of cyclical pain due to obstruction to the outflow of menstrual blood (from the functional endometrium not affected by scarring). It can also result in infertility and recurrent miscarriage.

Ultrasound Features of Asherman's Syndrome or Intrauterine Adhesions (Figs. 4.57, 4.58, 4.59, 4.60 and 4.61)

- Endometrial scars are seen as hypoechoic breaks in the endometrial continuity.
- Endometrial margins may be irregular.
- There may be endometrial pockets seen with loculated fluid within.
- 3D evaluation of the endometrial cavity is useful in assessing the extent of scarring.
- The scarred area may extend onto the adjoining myometrium.
- In cases with coexistent subendometrial fibrosis, the fibrotic scar tissue may appear echogenic and show acoustic shadowing.
- On sonohysterography, the synechiae appear as avascular echogenic bands bridging the uterine cavity. In some cases, there may be difficulty in distending the cavity, if the scarring is significant.

Ultrasound evaluation of the endometrium for intrauterine synechiae is best done when the endometrium is thick, as is seen in the late proliferative phase or the secretory phase.

Hysteroscopy is not only useful in diagnosis but can also help with simultaneous management of these cases by hysteroscopic adhesiolysis.

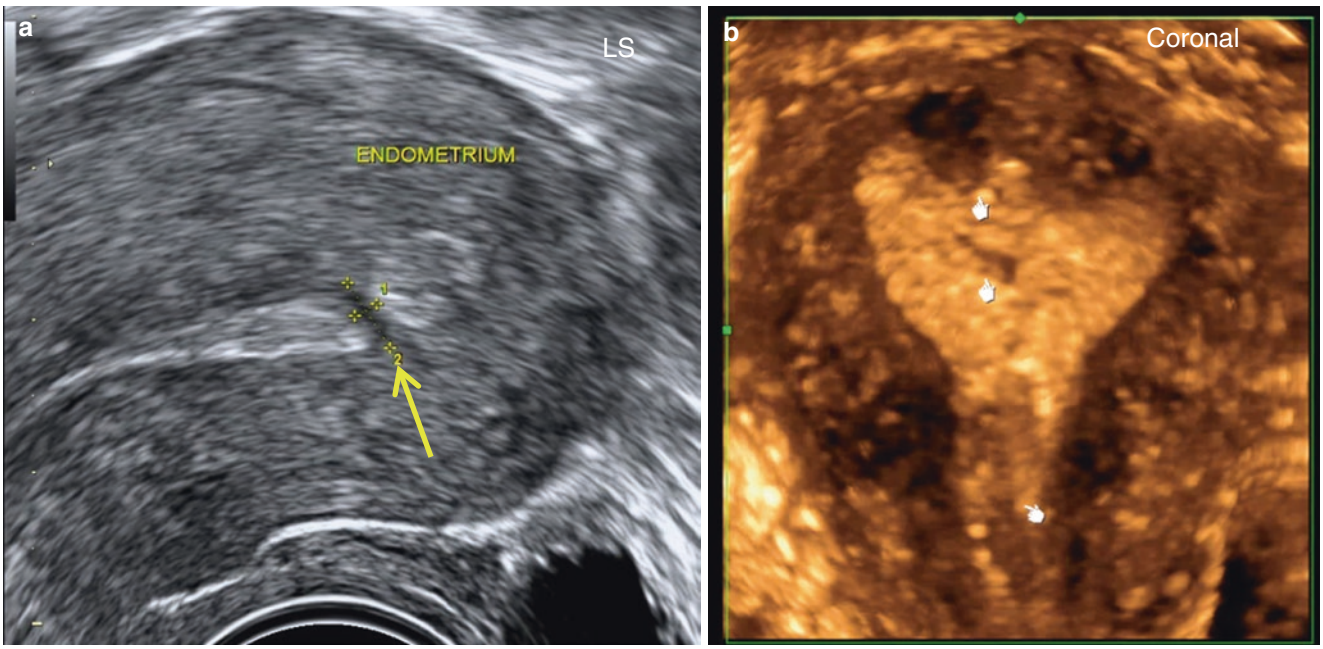

Fig. 4.57 Asherman's syndrome. (**a**) Greyscale showing a break in the hyperechoic endometrium which is seen as a hypoechoic linear disruption in the endometrial continuity at the upper corpus (*arrow*). (**b**) 3D rendered image of the same case showing multiple areas of scar tissue (*pointers*) and irregular endomyometrial junction, particularly along the upper margins

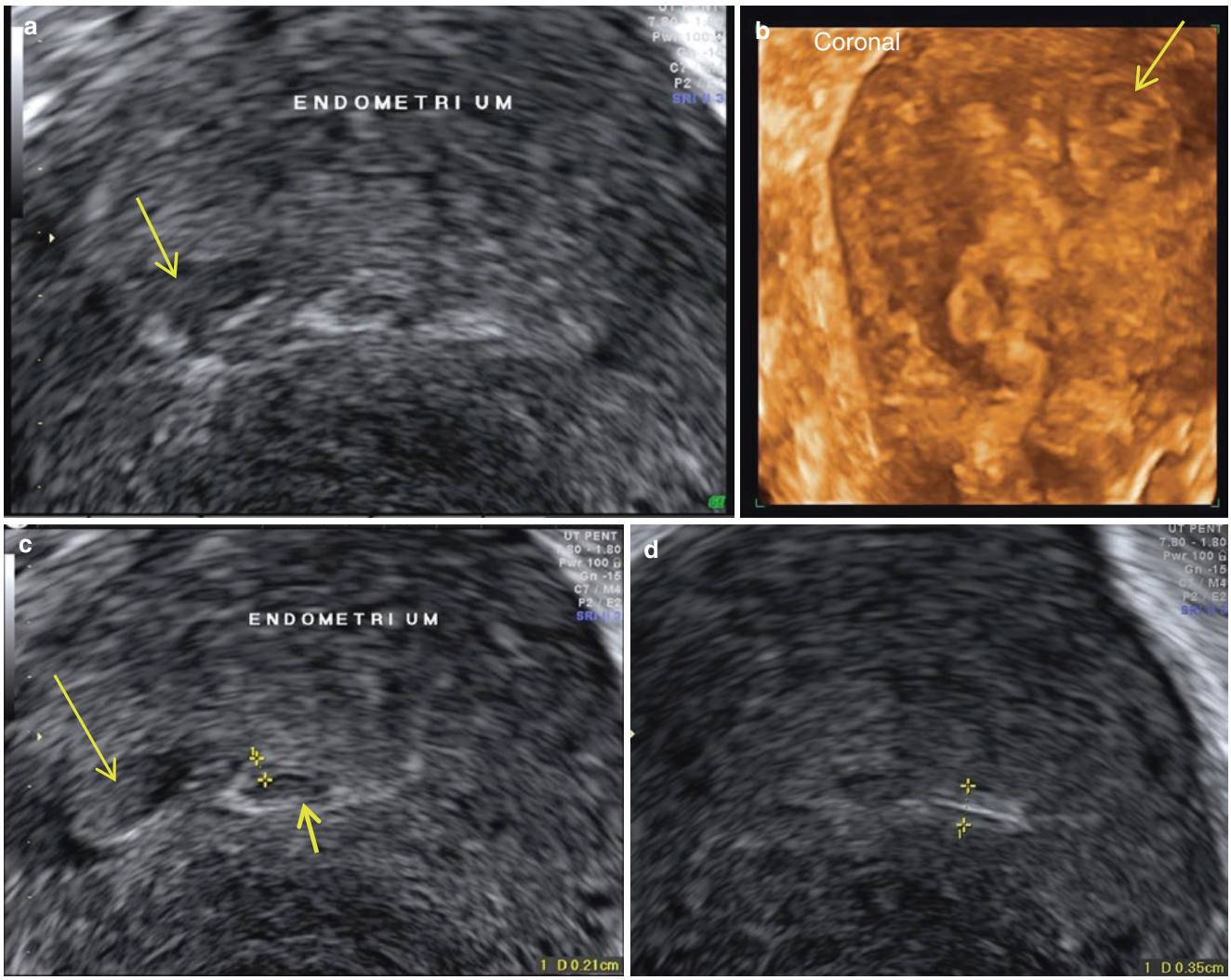

Fig. 4.58 Case of Asherman's syndrome. (**a**) Endometrial outline cannot be delineated. Endometrial tissue is seen as scattered, irregular, hyperechoic and poorly defined areas. Focal area of turbid collection is noted (*arrow*). (**b**) 3D rendered image of the same showing a completely distorted endometrial outline and a small pocket of a localised turbid collection (*arrow*). (**c**) Minimal fluid is seen in a short segment of the endometrial cavity (*short arrow*) with single-layer thickness of endometrium marked. Just beside this is a focal area of the turbid collection (*long arrow*). (**d**) A small segment of endometrium seen appearing thin and proliferative

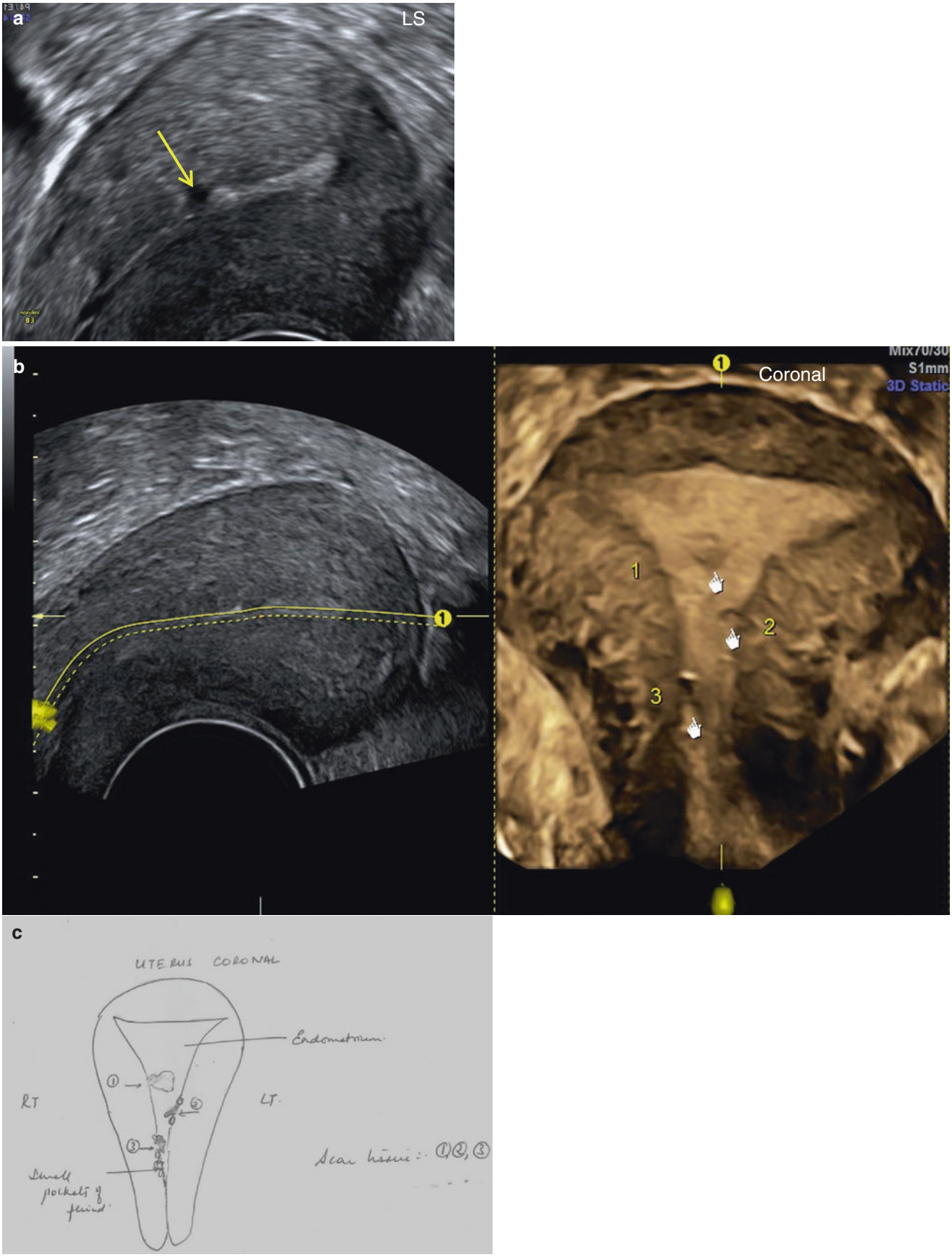

Fig. 4.59 Case of Asherman's syndrome. (**a**) Hypoechoic area seen at the midcorpus along the posterior EMJ, extending into the endometrial cavity. It is seen as a break in the hyperechoic endometrium. (**b**) 3D image with polyline showing three small areas of scar tissue (*marked with pointers*). (**c**) Diagrammatic representation of the same which is handed over to the patient along with the report

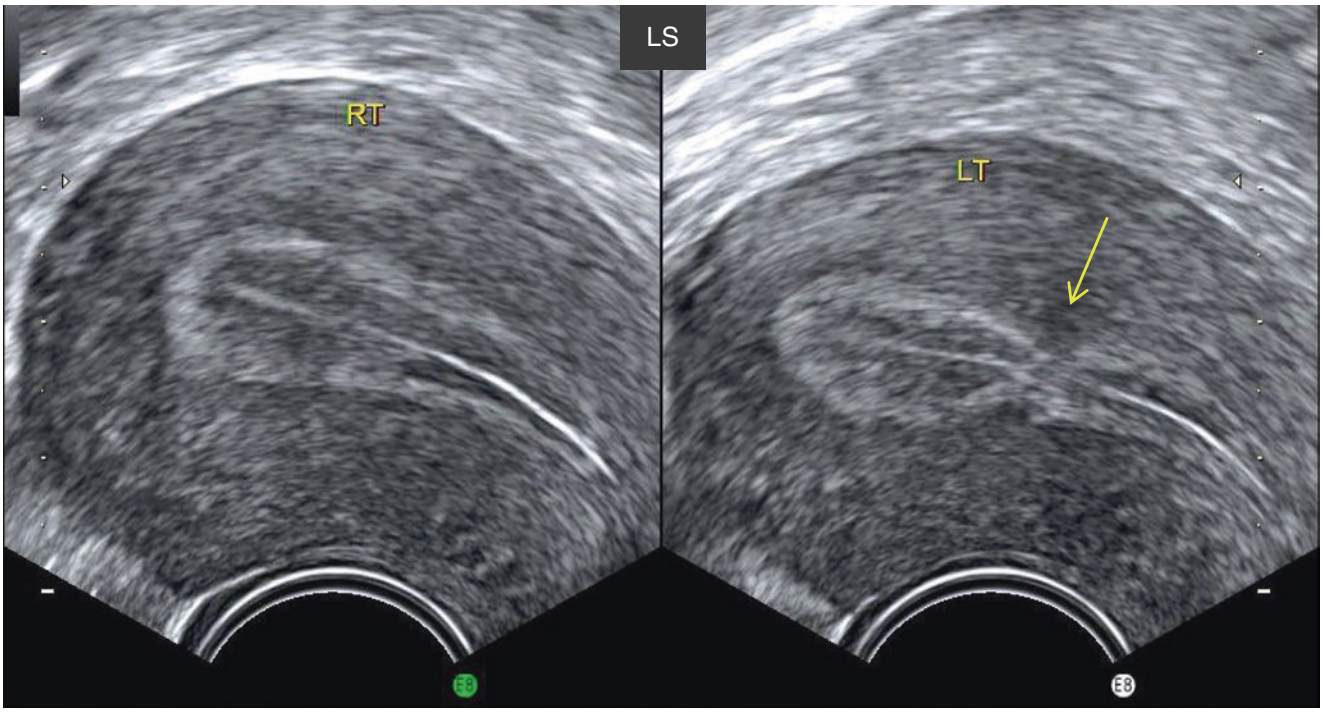

Fig. 4.60 Case of Asherman's syndrome. Endometrial scarring is best seen when the endometrium is thick, as is seen in the image above. The scar tissue on the left side (*arrow*) of the endometrium can be compared with the normal-appearing endometrium on the right side

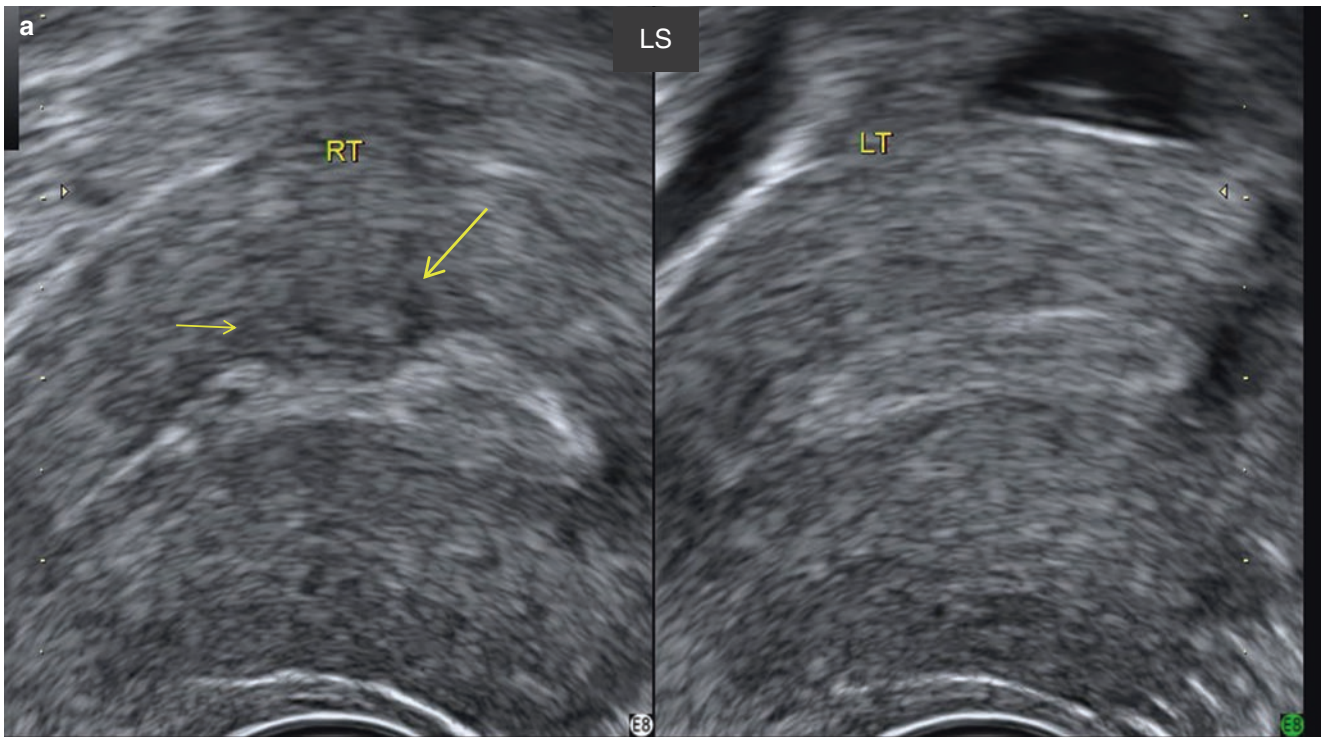

Fig. 4.61 Case of Asherman's syndrome. (**a**) Scar tissue on the right side (*areas within arrows*) seen as a hypoechoic irregular area along the EMJ, producing an irregular endometrial outline. The scar tissue is seen extending onto the adjoining myometrium, but in the myometrium, the margins are diffuse. (**b**) 3D rendered image of the same case showing two areas of scarring

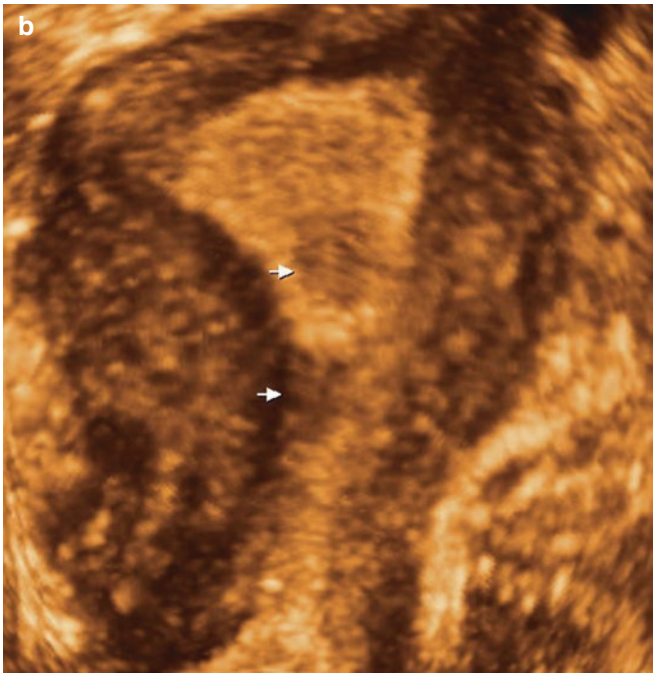

Fig. 4.61 (continued)

Summary: Asherman's Syndrome

- Asherman's syndrome is secondary to endometrial scarring usually following trauma caused by surgical procedures, like curettage or manual removal of placenta. It may also be caused by chronic infections like tuberculosis. Patients typically present with amenorrhoea or scanty periods and infertility.
- On ultrasound, they are seen as hypoechoic breaks in the endometrial continuity which can be assessed well on 3D rendered imaging. Endometrial margins may be irregular, and there may be pockets of loculated menstrual fluid.
- Hysterosonography and hysteroscopy may demonstrate synechiae. Occasionally, however, if there are significant adhesions, there may be difficulty in distending the uterine cavity.

4.8 Subendometrial Fibrosis (Figs. 4.62 and 4.63)

In subendometrial fibrosis, the fibrosis occurs in the deeper basal endometrial layer with no loss of the functional endometrium. It should not be confused with intrauterine adhesions (Asherman's syndrome). Subendometrial fibrosis can occur following invasive intrauterine procedures, particularly manual removal of placenta. On ultrasound, it is seen as echogenic foci in the basal endometrium close to the EMJ. The condition is not usually associated with menstrual or fertility issues, and women are asymptomatic. At times, however, both intrauterine adhesions and subendometrial fibrosis may coexist because they are both caused by trauma.

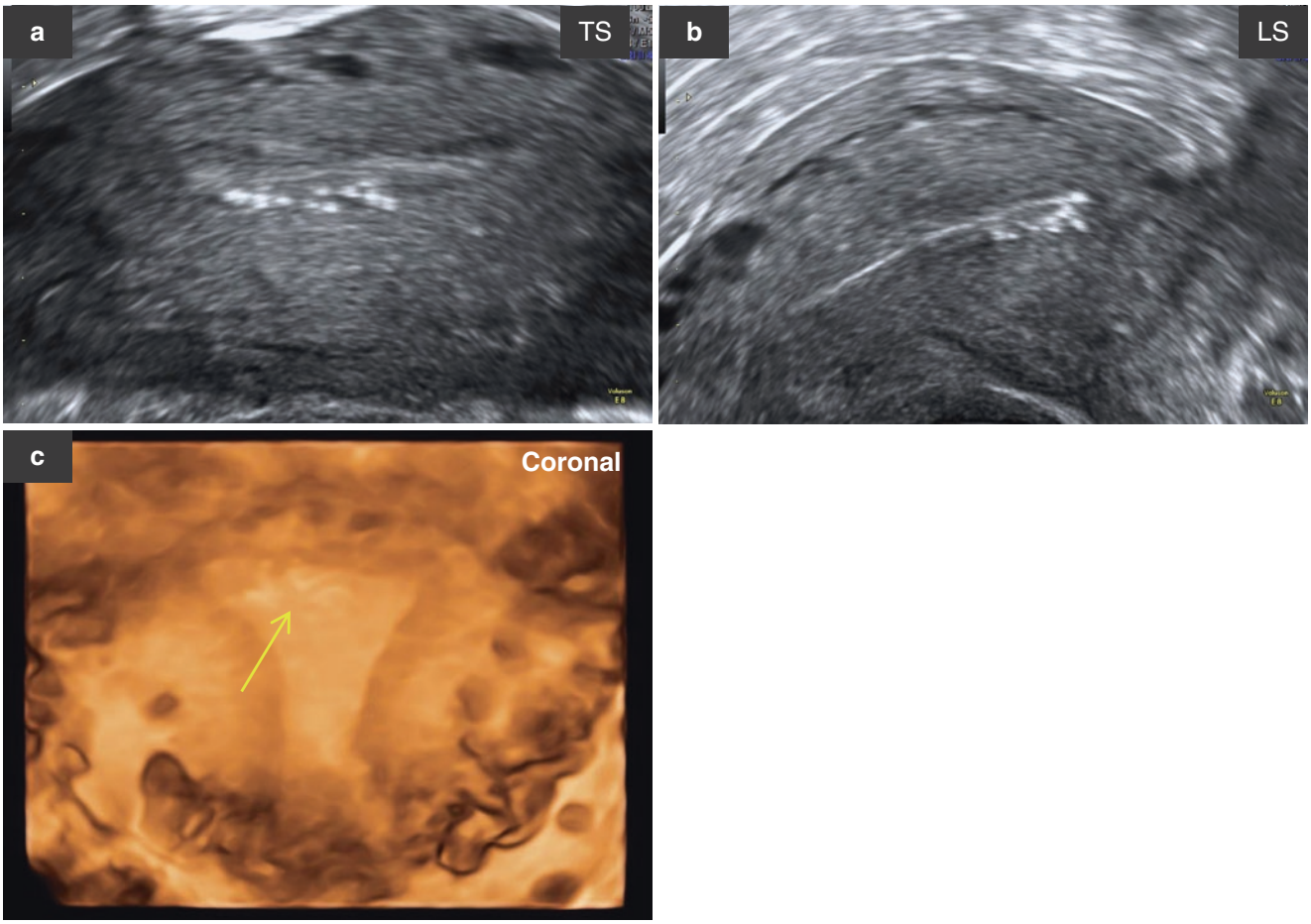

Fig. 4.62 Subendometrial fibrosis in a patient with a history of manual removal of placenta during the last child birth (1 ½ years ago). (**a**, **b**) Echogenic scattered foci seen close to the EMJ with superficial endometrium appearing normal on TS and LS. (**c**) 3D rendered coronal image of an endometrium showing intact endometrial margins with a faint impression of the underlying fibrosis (*arrow*)

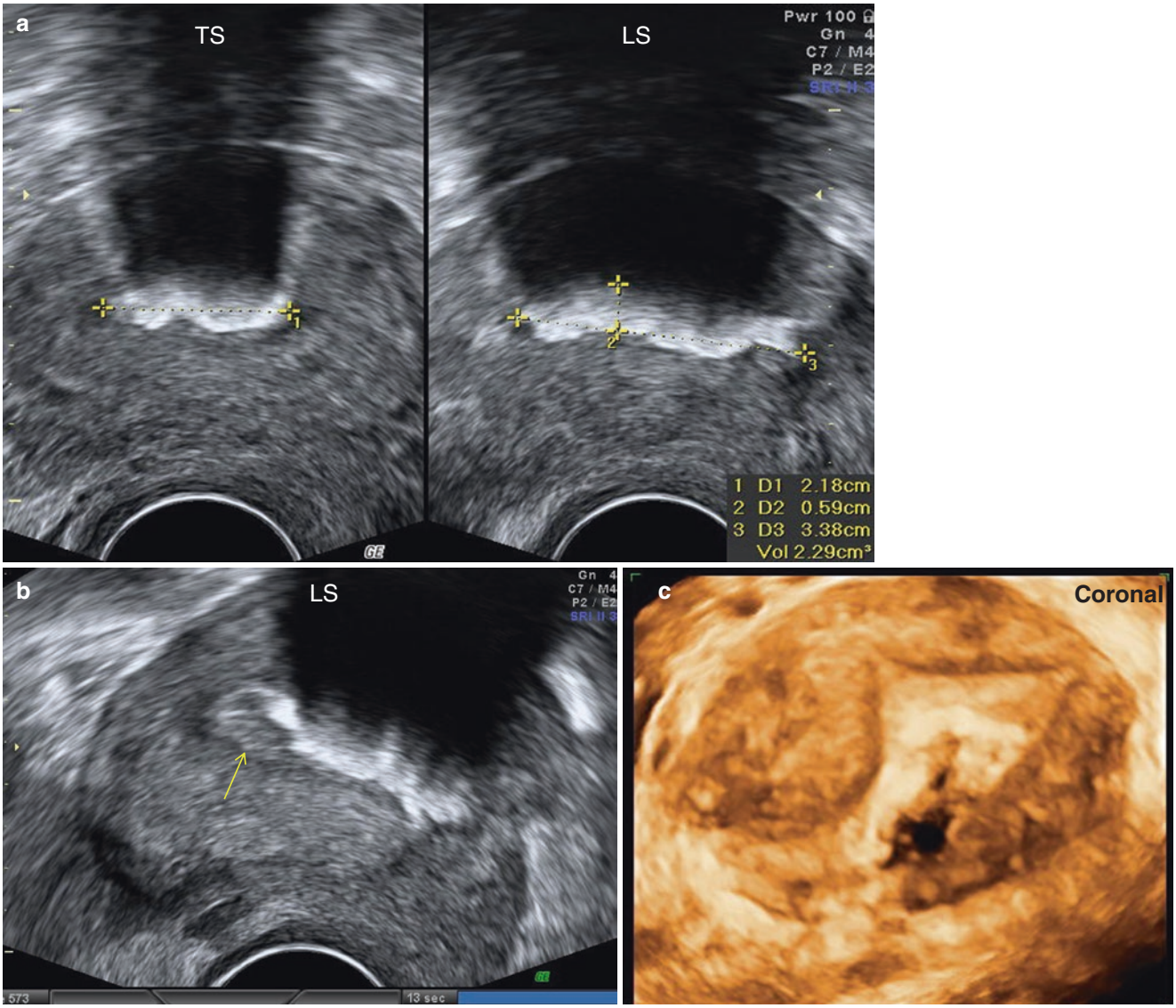

Fig. 4.63 Subendometrial fibrosis, seen in an asymptomatic patient with a history of manual removal of adherent placenta. (**a**) A hyperechoic irregular band of tissue is seen in the endometrium with significant acoustic shadowing, suggestive of dense fibrotic and calcified tissue. (**b**) The upper end of the endometrium appears normal (*arrow*). (**c**) 3D rendered image of the same showing fibrotic tissue which appears as a hyperechoic irregular area in the endometrium of the mid corpus and lower corpus. The scar tissue is seen as dark in some parts, mainly in the lower endometrium and adjoining myometrium. This area appears dark because of acoustic shadowing by the scar tissue. In this image, therefore, the plane of rendering has passed partly proximal to the scar tissue and partly distal to it (in the area of acoustic shadowing). Normal upper endometrium (*arrow*) with two cornua is seen

4.9 Endometritis

Endometritis refers to the inflammation of the endometrium. Endometritis can be divided into pregnancy-related endometritis and pregnancy-unrelated endometritis. When it is unrelated to pregnancy, endometritis is considered a part of the spectrum of PID. In PID, the endometrium is less susceptible to infection than the fallopian tube. This is so, particularly in women of the reproductive age group, because the endometrium is shed cyclically during menstruation. Occasionally however, the endometrium may be the sole focus of infection. Endometritis could be acute or chronic.

Acute endometritis in non-obstetric population is commonly associated with PID and invasive gynecologic procedures. In obstetric cases, post-partum infection is the most common cause of acute endometritis. Acute endometritis seen as a part of PID usually presents with symptoms that are like that of PID – which is fever and lower abdominal pain. Acute endometritis in post-partum women is more florid, and the patient may present with fever, pain, bleeding (secondary haemorrhage) and foul-smelling lochia. In severe cases of puerperal infection, the patient may present with generalised septicaemia.

Chronic endometritis in obstetrics, is seen in patients with RPOC. In a non-obstetric population, it may be associated with chronic infections like tuberculosis, intrauterine contraceptive devices and neoplastic masses (like endometrial carcinoma and a submucous fibroid). It can also be seen in patients who have undergone radiation therapy. In a large majority, however, no cause is identifiable. Patients with chronic endometritis may be symptomatic or asymptomatic. These women may present with abnormal uterine bleeding, excessive intermenstrual bleeding or with amenorrhoea. Patients may also complain of vague crampy lower abdominal pain or vaginal discharge that may be foul smelling. In chronic infections like tuberculosis, the patient is often asymptomatic with no clinical findings. Tuberculosis is often diagnosed in women with infertility when the endometrial curetting is subjected to testing.

Ultrasound Features of Endometritis (Figs. 4.64, 4.65, 4.66, 4.67 and 4.68)

- Ultrasound appearance of the uterus and endometrium may be normal, as in cases of chronic infection like tuberculosis.
- Intracavitary fluid may be seen, which may be minimal. It is usually turbid (blood and/or pus). This fluid may show some hyperechoic debris within.
- The endometrium may appear thickened, irregular and heterogeneous.
- Increased vascularity in the endometrium and adjoining myometrium may be noted.
- There may be some retained products of conception, or occasionally, a piece of gauze, etc. may be accidentally left behind (gossypiboma) within the uterine cavity.
- The uterus may be sub-involuted in cases with puerperal endometritis.
- In some cases, a neoplastic growth may be seen in the endometrial cavity.
- In tuberculosis endometritis, few adhesions may be noted within the endometrial cavity. In long-standing cases, with fibrosis setting in, hyperechoic foci may be seen along the endomyometrial junction. There may be scarring of the endometrium (Asherman's syndrome – discussed in the section above) and an irregular endometrial outline.
- In infection with anaerobic organisms, there may be air within the endometrial cavity which is seen as bright scattered echoes with dirty acoustic shadowing. Most often, air in the uterine cavity is seen in the nondependent parts of the cavity above the turbid fluid. It is important to note that the presence of air in the uterine cavity (pneumatometra) may be a normal finding, particularly in the first 3 weeks of puerperium. However, when seen in a patient with clinical features of PID, it is suggestive of anaerobic endometritis.
- The adnexa may show evidence of PID in the form of tubo-ovarian masses, pyosalpinx, etc.
- In cases with severe widespread infection, there may be evidence of pus elsewhere in the pelvic cavity which may extend into the abdominal cavity.
- The uterus may be tender during transvaginal scan (TVS).

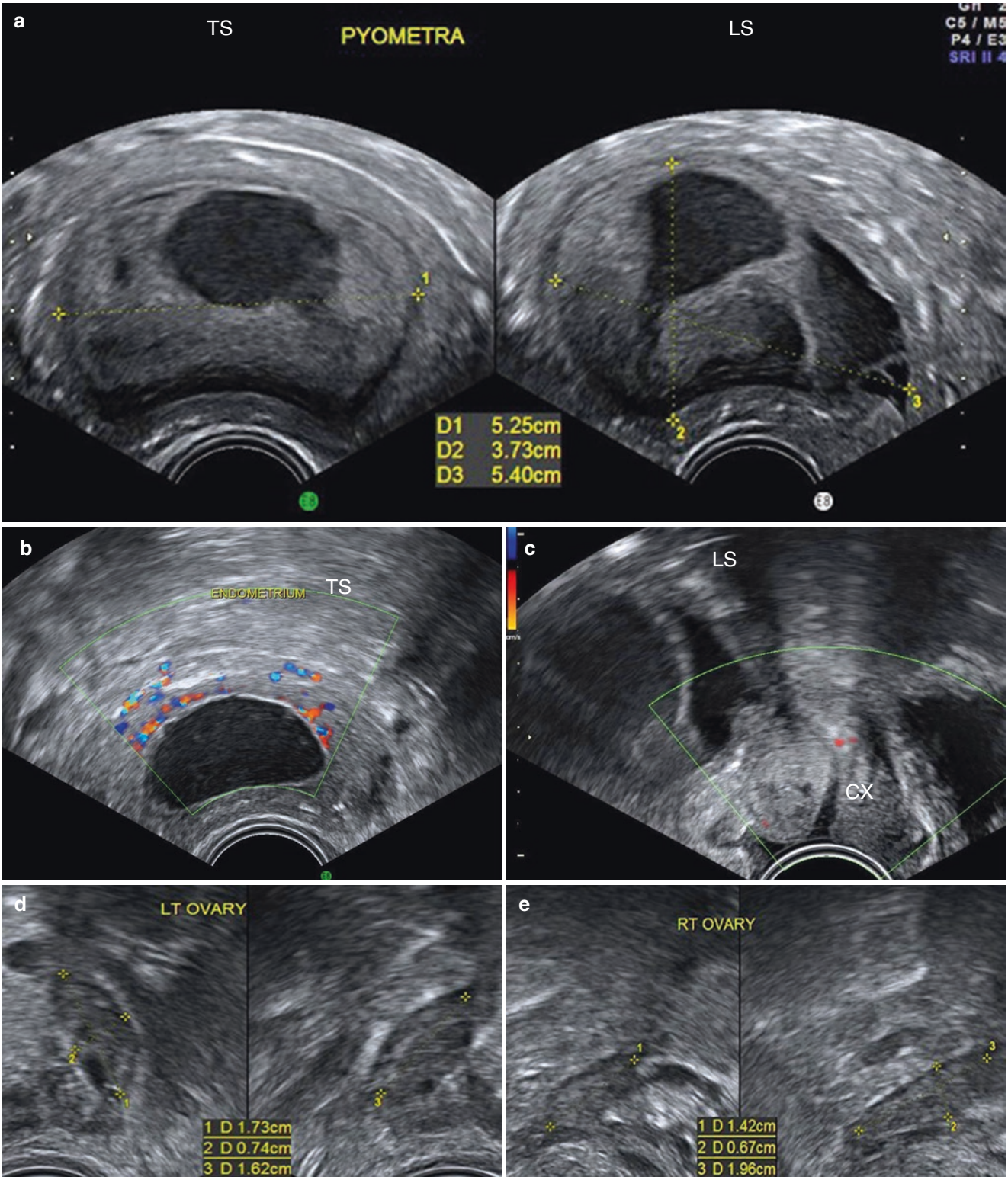

Fig. 4.64 A 65-year-old patient who presented with a 10-day history of foul-smelling discharge. (**a**) Endometrial cavity is seen filled with turbid contents showing mixed echoes, suggestive of pus (Vol, 55 cc). (**b**) On Doppler, the subendometrial area shows moderate vascularity (which is not a normal finding in postmenopausal women). (**c**) The cervix in this patient was examined to rule out any local cause for the pyometra, like a cervical malignancy. In this patient, no abnormality was noted. (**d**, **e**) Both the adnexa appeared normal with bilateral atrophic ovaries. *HPE:* scanty endometrium with no malignancy noted in the endometrial and the endocervical curettings

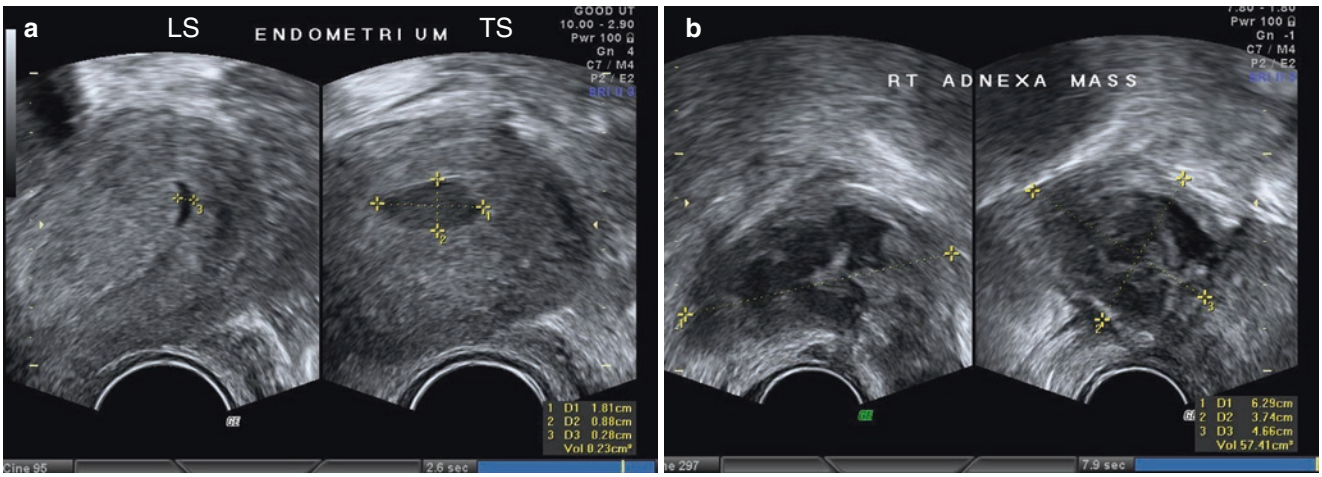

Fig. 4.65 (**a**) Minimal turbid fluid collection seen in the endometrial cavity of a patient with PID. (**b**) Right adnexa showing a complex TO mass with pyosalpinx in the same patient

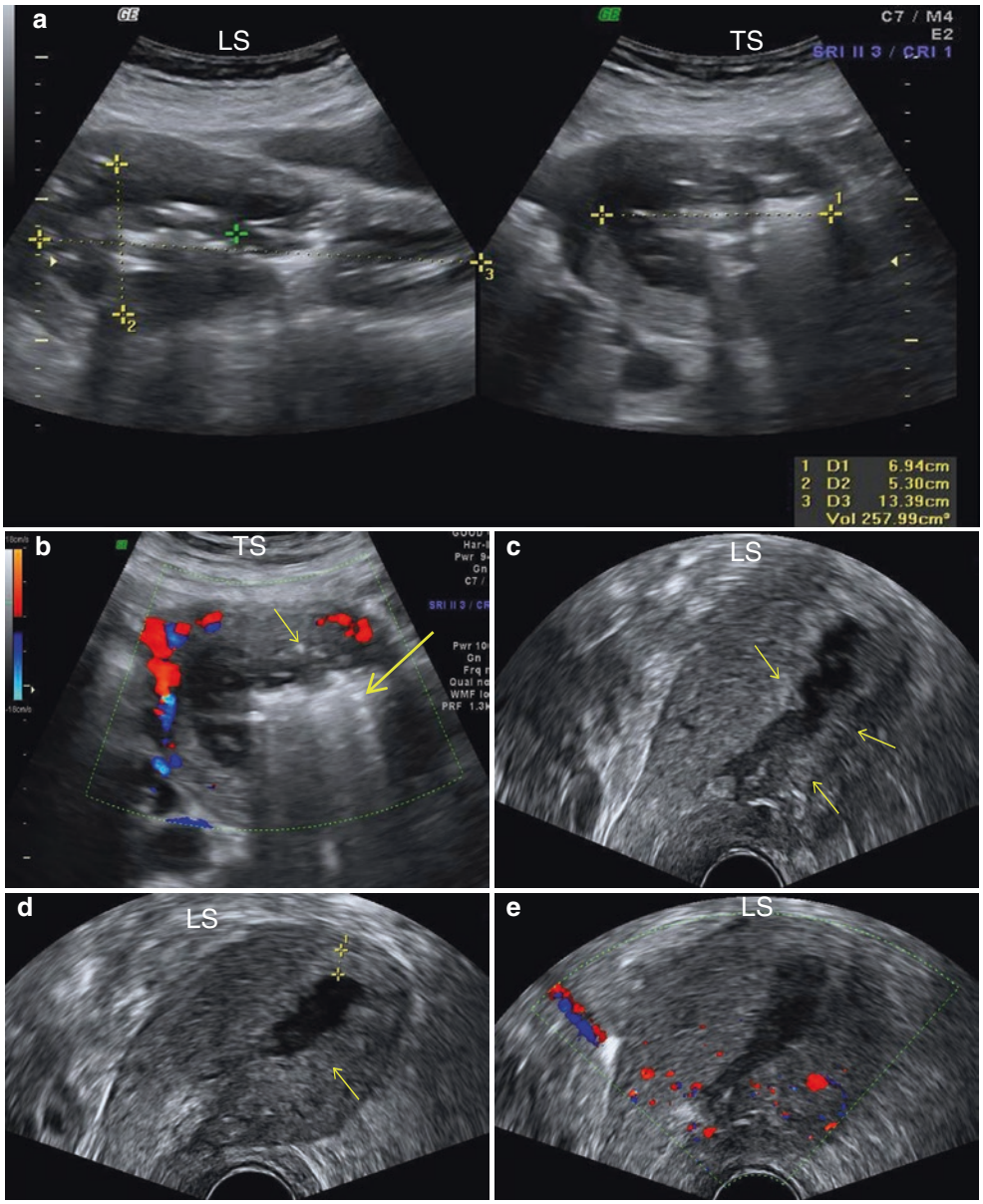

Fig. 4.66 Patient had a twin delivery with atonic PPH 25 days earlier. She complained of bleeding PV since delivery and spasmodic lower abdominal pain since 3 days. Scan done elsewhere reported a suspicion of an intrauterine foreign body. (**a**) Uterine cavity is seen filled with fluid showing scattered hyperechoic areas with dirty acoustic shadowing suggestive of air secondary to anaerobic infection (volume of the contents in the cavity was 258 cc). No evidence of retained tissue was noted, which may be because of the large uterine size and air shadows. (**b**) Transverse section of uterus showing fluid with some debris (*short arrow*) and a hyperechoic area with acoustic shadowing, more to the left of the uterine cavity (*long arrow*). Moderate vascularity was noted in the subendometrial area. (**c–e**) Two days post dilatation and curettage with removal of retained products. A thick endometrium with irregular endometrial margins (*arrows*) and intracavitary fluid with debris is seen. No significant flow is seen in the endometrium or adjoining myometrium, probably because the patient was already on antibiotics

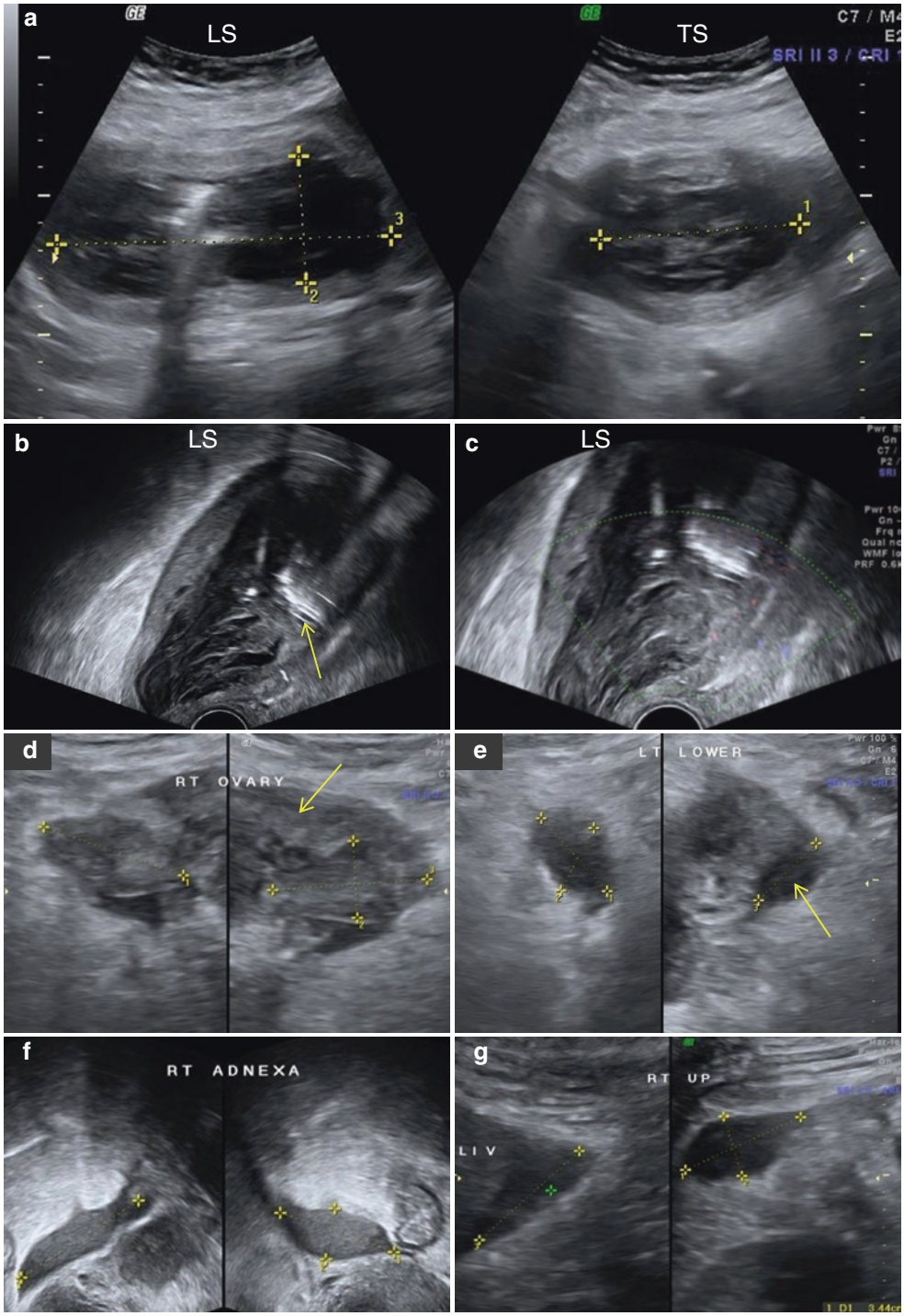

Fig. 4.67 Patient presented 23 days after LSCS done for abruptio placentae, with abdominal pain and heavy bleeding. (**a**) TAS – uterine cavity was filled with turbid fluid showing hyperechoic gas echoes with shadowing. No obvious retained tissue was noted. (**b**) TVS – turbid contents (206 cc) with complex echoes and stretchy hyperechoic linear bands suggestive of pus are seen filling the entire uterine cavity almost up to the external os. Hyperechoic gas echoes (*arrow*) with shadowing seen along the anterior uterine wall. (**c**) No significant flow seen on Doppler in the endometrium, which is often the case with endometritis. (**d**, **e**) Turbid collection is seen surrounding the ovaries, bilaterally (*arrows*). (**f**) Turbid fluid suggestive of pus is seen in the right lower abdomen and (**g**) in the right subdiaphragmatic area. At surgery, the abdominal cavity was found to have multiple pockets of pus which were drained, and peritoneal lavage was given

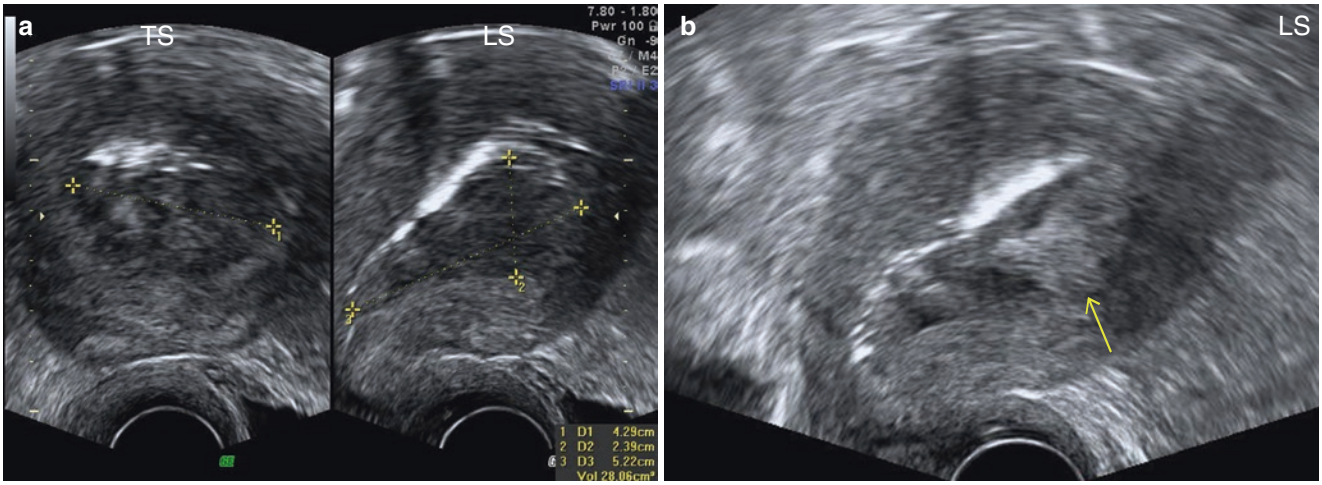

Fig. 4.68 Pyometra in a patient with endometrial carcinoma. (**a**) Turbid complex fluid with air echoes is seen in the endometrial cavity, suggestive of pyometra with anaerobic infection. (**b**) Solid tissue (*arrow*) seen in the upper uterine cavity which showed flow on Doppler, suggestive of a neoplastic growth

Summary: Endometritis

- Signs and symptoms are often non-specific and depend upon whether it is acute or chronic and whether it is seen in patients with PID or in women in the puerperal period.
- Diagnosis of endometritis is challenging because sonographic findings may vary from normal to minimal intracavitary fluid to frank pus in the uterine cavity.
- Tuberculosis endometritis is often diagnosed in women with infertility, many of them being asymptomatic. Adhesions and fibrosis may, however, be noted in the endometrium.
- Acute puerperal infection tends to be more florid.
- Depending upon the aetiology, one may see RPOC or a neoplastic mass within the endometrial cavity.

4.10 Intracavitary Fluid in the Uterus (Figs. 4.69, 4.70, 4.71, 4.72, 4.73 and 4.74)

Fluid in the uterine cavity may be clear (anechoic) or turbid. Clear fluid could be serum or mucin. Turbid fluid could either be blood (hematometra) or pus (pyometra). Pyometra is discussed in the previous section (Figs. 4.64, 4.65, 4.67 and 4.68).

A tiny amount of clear fluid seen in the endometrial cavity may be normal in postmenopausal women. However, any significant amount of fluid collection or turbid collection requires careful evaluation as they may be associated with endometrial cancers and cervical cancers. Another cause for fluid collection in postmenopausal women could be cervical stenosis.

In premenopausal women, most often, the intrauterine collection is blood associated with menstruation or pregnancy. It could also be retained menstrual blood in a patient with hematometrocolpos, acutely retroflexed uterus and cervical stenosis.

In the presence of endometritis, turbid fluid suggestive of pus may be seen in the endometrial cavity.

Minimal fluid may also be seen in the presence of polyps and submucosal fibroids. A small amount of clear fluid in the endometrial cavity may be a finding in patients with carcinoma of the fallopian tube.

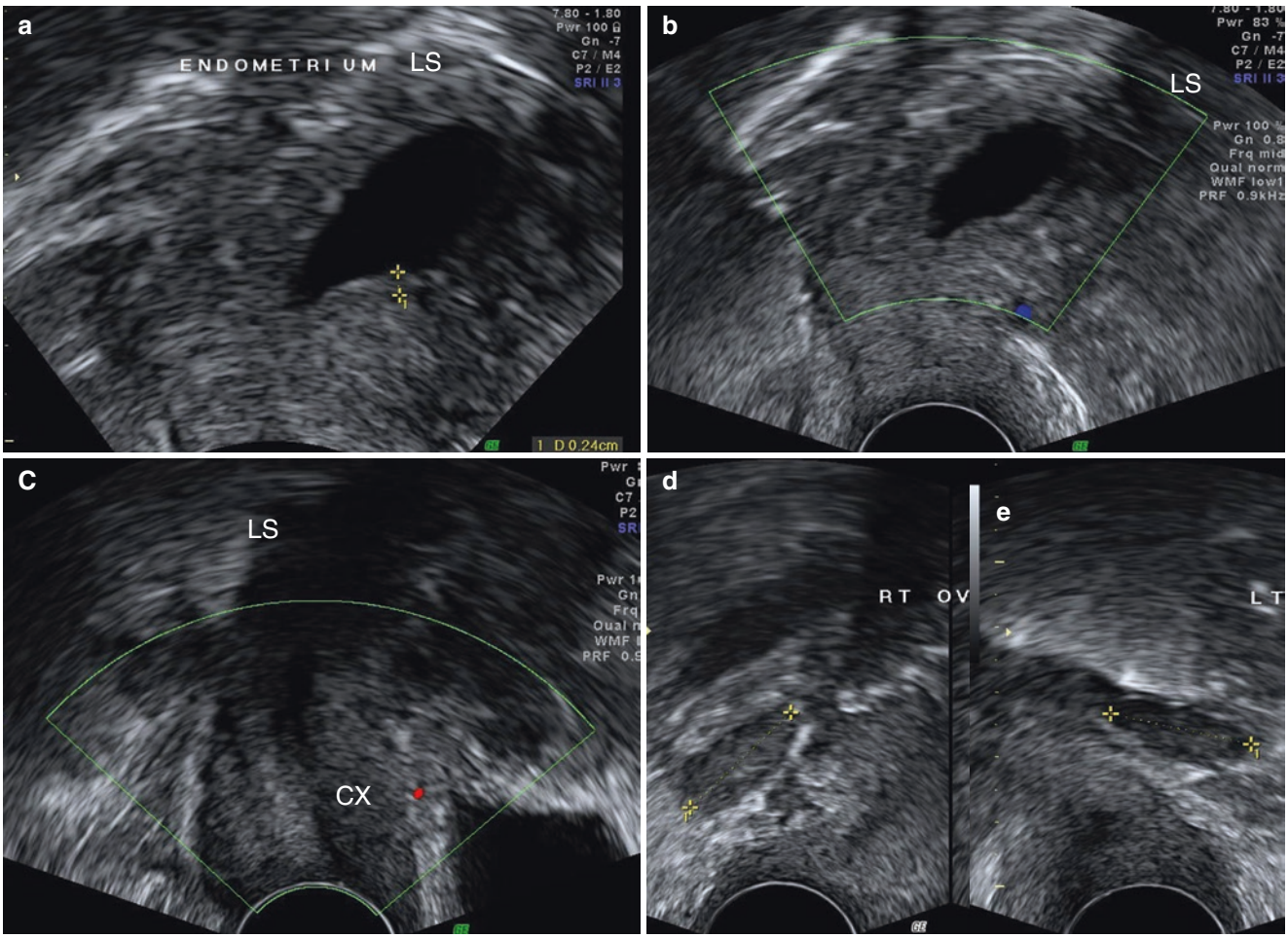

Fig. 4.69 (**a**) Anechoic fluid collection in a postmenopausal lady with a thin endometrium. (**b**) No abnormal flow seen on Doppler. (**c**) The cervix in this case appeared normal with no evidence of local pathology as a cause for the collection. (**d**, **e**) Normal atrophic ovaries are seen

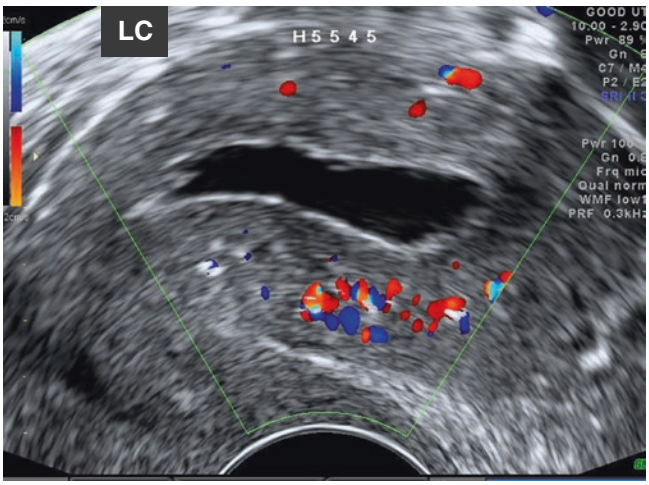

Fig. 4.70 Postmenopausal lady with a thin endometrium and anechoic fluid collection

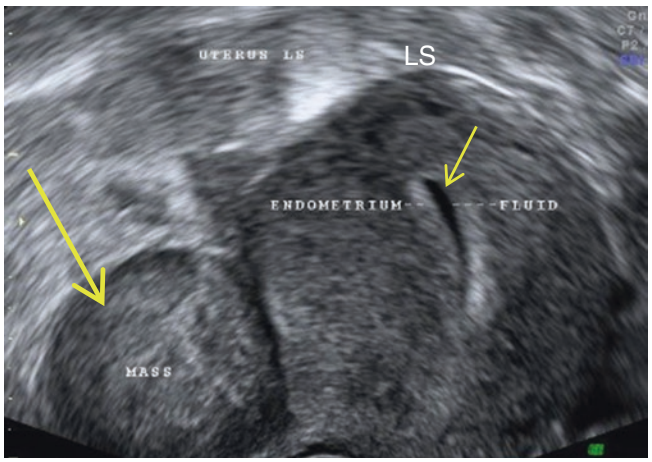

Fig. 4.71 Minimal clear intracavitary fluid (*short arrow*) in a lady with fallopian tube carcinoma. The malignant mass is seen just behind the uterus (*long arrow*)

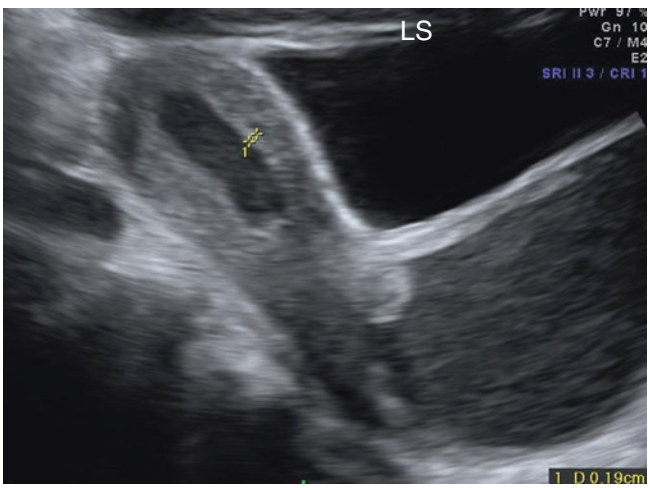

Fig. 4.72 A case of imperforate hymen with hematometrocolpos

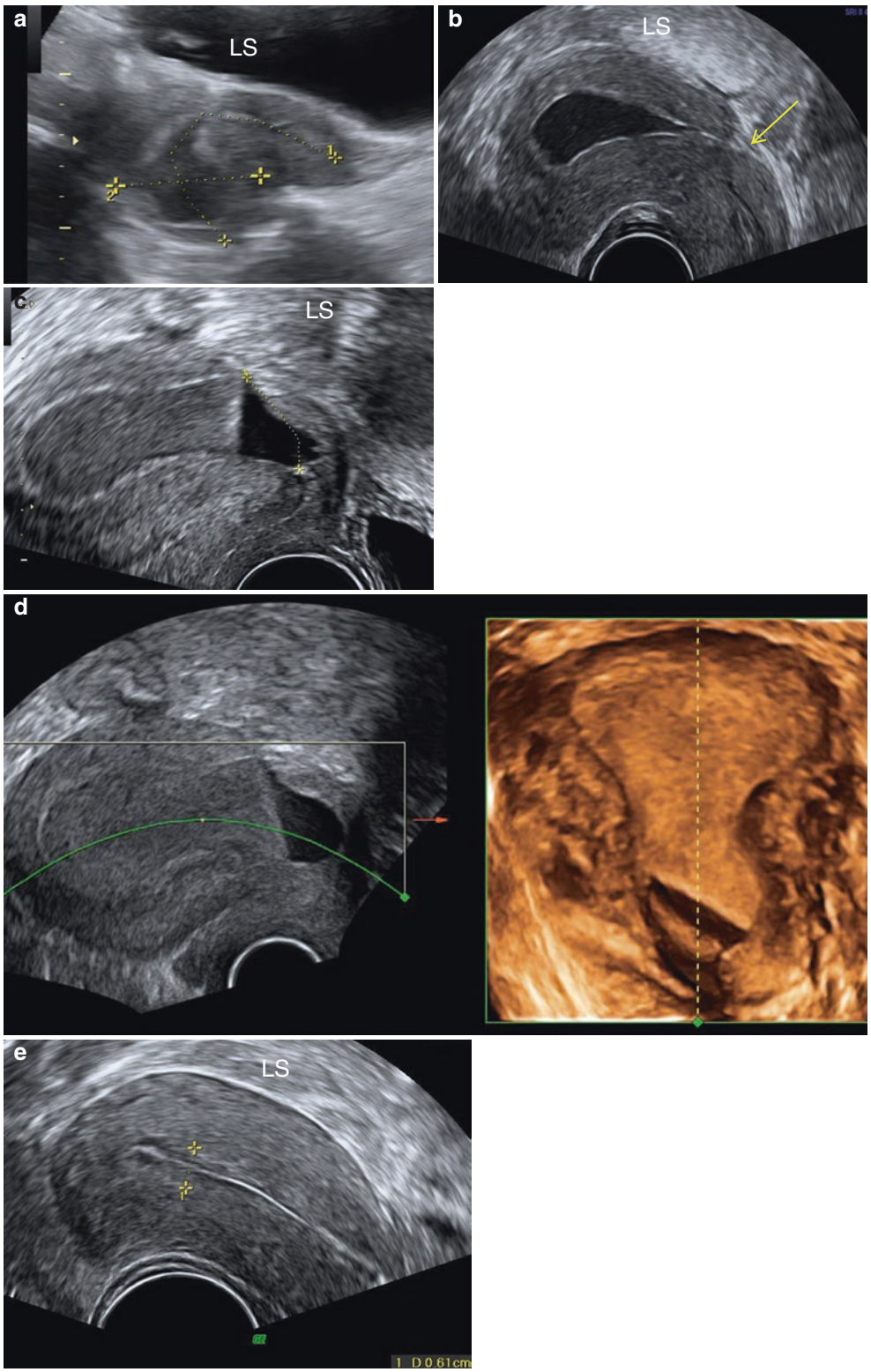

Fig. 4.73 Hematometra seen in a patient with an acutely retroflexed uterus. This could be caused by acute retroflexion, with probable contribution by scarring at the site of previous LSCS. Patient had undergone surgical termination of a subsequent pregnancy, 3 months prior. Following the termination, she gave history of amenorrhoea. (**a**) TAS – image showing an acutely retroflexed uterus with turbid contents. (**b**) TVS – showing the same and the LSCS scar (*arrow*). (**c**) Patient returned 12 days later with severe abdominal pain associated with vomiting following the intake of Cytotec medication (which was prescribed by her clinician to assist in uterine emptying). Turbid collection suggestive of blood is seen in the endometrial cavity. Volume had increased in 12 days from 6.7 cc. to 44.5 cc. The intrauterine fluid collection shows a fluid–fluid level with denser contents in the dependent upper cavity of the retroflexed uterus. (**d**) 3D rendering of the same showing the linear fluid–fluid level. (**e**) Patient had bleeding for 5 days commencing on the day of previous scan (corresponding to image (**c**, **d**)). Scan done a few days later showed a normal endometrial cavity with no hematometra

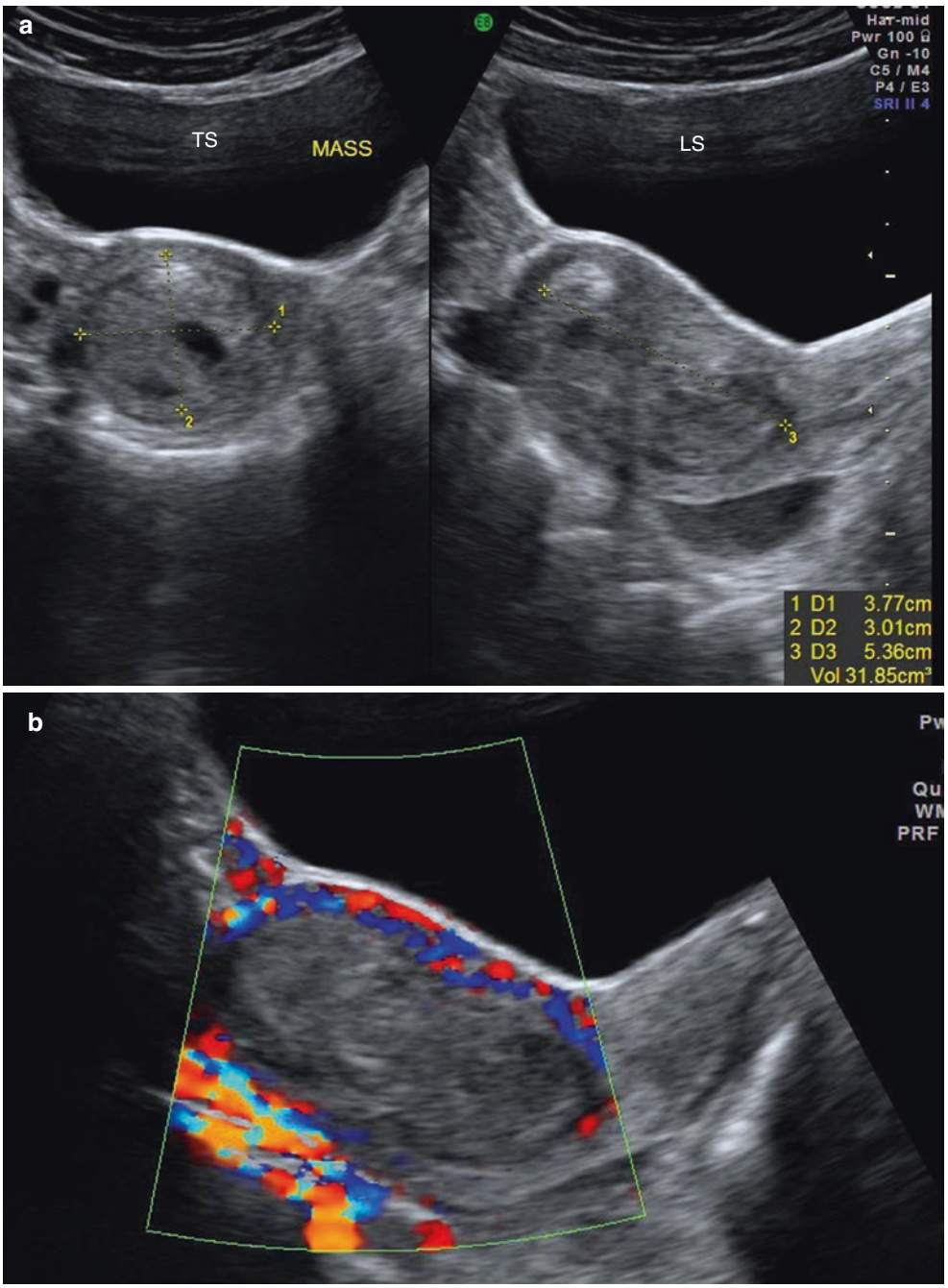

Fig. 4.74 Hematometra in a 22-year-old patient, who presented with menorrhagia since menarche. (**a**) Intrauterine clot appears complex resembling an intrauterine mass or polyp. (**b**) On Doppler, no flow was seen in the intracavitary clot. Blood and clots may be seen in the uterine cavity in a menstruating patient

Suggested Reading

Amin TN et al (2015) Ultrasound and intrauterine adhesions: a novel structured approach to diagnosis and management. Ultrasound Obstet Gynecol 46(2):131–139. doi:10.1002/uog.14927

Bosch VD et al (2011) Effect of gel-instillation sonography on Doppler ultrasound findings in endometrial polyps. Ultrasound Obstet Gynecol 38(3):355–359

Breijer MC et al (2012) Capacity of endometrial thickness measurement to diagnose endometrial carcinoma in asymptomatic postmenopausal women: a systematic review and meta-analysis. Ultrasound Obstet Gynecol 40(6):621–629

Dueholm M et al (2015) Two- and three-dimensional transvaginal ultrasound with power Doppler angiography and gel infusion sonography for diagnosis of endometrial malignancy. Ultrasound Obstet Gynecol 45(6):734–743

Epstein E, Valentin L (2006) Gray-scale ultrasound morphology in the presence or absence of intrauterine fluid and vascularity as assessed by color Doppler for discrimination between benign and malignant endometrium in women with postmenopausal bleeding. Ultrasound Obstet Gynecol 28(1):89–95

Epstein E et al (2011) Gray-scale and color Doppler ultrasound characteristics of endometrial cancer in relation to stage, grade and tumor size. Ultrasound Obstet Gynecol 38:586–593

Fischerova D (2011) Ultrasound scanning of the pelvis and abdomen for staging of gynecological tumors: a review. Ultrasound Obstet Gynecol 38:246–266. doi:10.1002/uog.10054

Kwon TH et al (2003) P128: ultrasonographic findings of endometrial polyp. Ultrasound Obstet Gynecol 22:105–106. doi:10.1002/uog.593

Langer JE et al (2012) Radiographics: imaging of the female pelvis through the life cycle. Radiographics 32(6):1575–1597

Leone FPG et al (2009) Terms, definitions and measurements to describe the sonographic features of the endometrium and intrauterine lesions: a consensus opinion from the International Endometrial Tumor Analysis (IETA) group. Ultrasound Obstet Gynecol 35:103–112

Mascilini F et al (2013) Evaluating myometrial and cervical invasion in women with endometrial cancer: comparing subjective assessment with objective measurement techniques. Ultrasound Obstet Gynecol 42(3):353–358

Nalaboff KM et al (2001) Imaging the endometrium: disease and normal variants – RSNA. Radiographics 21:1409–1424

Opolskiene G et al (2010) Three-dimensional ultrasound imaging for discrimination between benign and malignant endometrium in women with postmenopausal bleeding and sonographic endometrial thickness of at least 4.5 mm. Ultrasound Obstet Gynecol 35(1):94–102

Pal A et al (2000) Diagnosis of Asherman's syndrome with three-dimensional ultrasound. Ultrasound Obstet Gynecol 15(4):341–343

Parsons AK, Sanders RC (2007) OP17.07: menometrorrhagia due to impaired uterine drainage. Ultrasound Obstet Gynecol 30:514. doi:10.1002/uog.4585

Savelli L et al (2003) Transvaginal sonographic appearance of anaerobic endometritis. Ultrasound Obstet Gynecol 21:624–625. doi:10.1002/uog.107

Schwärzler P et al (1998) An evaluation of sonohysterography and diagnostic hysteroscopy for the assessment of intrauterine pathology. Ultrasound Obstet Gynecol 11(5):337–342

Steinkeler JA et al (2009) Female infertility: a systematic approach to radiologic imaging and diagnosis. Radiographics 29:1353–1370

Valentin L (2014) Ultrasound deserves to play a prominent role in the diagnosis and management of endometrial cancer. Ultrasound Obstet Gynecol 43:483–487

Ultrasound Evaluation of the Cervix

5

The cervix is the muscular lower end of the uterus. Its inner cervical canal is continuous with the endometrial cavity above at the internal os, and its muscular myometrium is continuous with the myometrium of the uterine body. The cervix is fusiform in shape and has a central cervical canal which extends from the internal os to the external os with its narrowest portion at the internal os. The portion of the cervix above the attachment of the vaginal vault is called the supravaginal cervix, and the lower cervix below the attachment of the vaginal vault that protrudes into the vagina is called the 'portio vaginalis'. Cervical pathologies include nabothian cysts, polyps, fibroids, uterine anomalies, ectopic pregnancy, endometriosis and carcinoma. Fibroids, congenital anomalies and cervical ectopic are dealt with in their respective chapters. Congenital cervical anomalies are discussed in the chapter on uterine anomalies. Cervical fibroids are briefly discussed in this chapter.

5.1 Evaluation of the Cervix and Its Normal Appearance

Measurements

The length of the cervix, on an average, is 3–4 cm and the diameter is about 2–3 cm. The cervix is about half the size of the uterine body in the reproductive age group. In prepubertal girls, the cervix is prominent and almost similar in size to that of the uterus.

Appearance (Fig. 5.1)

- The cervix is homogeneous in echotexture with echogenicity similar (i.e. isoechoic) to that of the myometrium of the uterine body.
- The central canal is lined by cervical mucosa that usually appears hypoechoic and contains the endocervical glands. This cervical mucus makes it easy to identify the cervix and differentiate it from the uterine body above it.
- The internal os can be identified by the fact that:
  - It is the narrowest part of the uterine cavity where the endometrial cavity is continuous with the cervical canal.
  - The cervical mucosa can be seen to taper off and end at the internal os.
  - The uterine arteries enter the uterus at the level of the internal os.

  This feature is especially helpful when the normal cervical architecture is distorted by pathological lesions.
- The external os is small and round in a nulliparous woman but appears as a larger transverse slit in a woman who has had a normal vaginal delivery. The os can be seen on the transverse section of the cervix but is better seen on a 3D rendering of the external os, especially with GSV.
- The cervical canal just prior to ovulation shows anechoic cervical mucus which improves visualisation of the cervical canal on ultrasound. This helps in the diagnosis of cases with cervical polyps and congenital anomalies of the cervix.

Doppler

- The uterine arteries can be identified on both sides of the cervix at the level of the internal os.
- The presence of an abnormal vessel in the cervical canal should raise a high suspicion of a feeder vessel of a polyp at the cervix, which may be originating either from the cervix or the endometrium above.
- Cervical carcinoma is difficult to detect on 2D especially when it is small and isoechoic. On Doppler, these lesions are easier to pick up because most of them are highly vascular.

Tips to Improve Ultrasound Diagnosis of Cervical Lesions (Fig. 5.2)

- The assessment of the cervix should be a part of all routine gynecological ultrasound examinations. Lesions of the cervix are often missed on ultrasound because most of

M. Sibal, *Ultrasound in Gynecology*, DOI 10.1007/978-981-10-2714-7_5

the sonologists proceed directly to the uterine body and adnexa in search of gynecological pathology, leaving out the assessment of the cervix.

- Since visualisation of the cervix on ultrasound is suboptimal at times, because of its proximity to the TVS probe, withdrawing the probe a little helps to evaluate the cervix. One may push on the cervix with the probe placed in one of the fornices to further antevert or retrovert the uterus so that the cervix lies more perpendicular to the ultrasound beam and is seen better. When cervical pathology is seen or suspected, gel sonovaginography (GSV) may be resorted to (dealt with in Chap. 2) for better visualisation of the pathology.
- Doppler evaluation of the cervix should be done routinely in all patients to help detect cervical lesions like polyps and carcinomas, which may otherwise be missed on 2D greyscale (as the assessment of the cervix is relatively suboptimal on TVS).

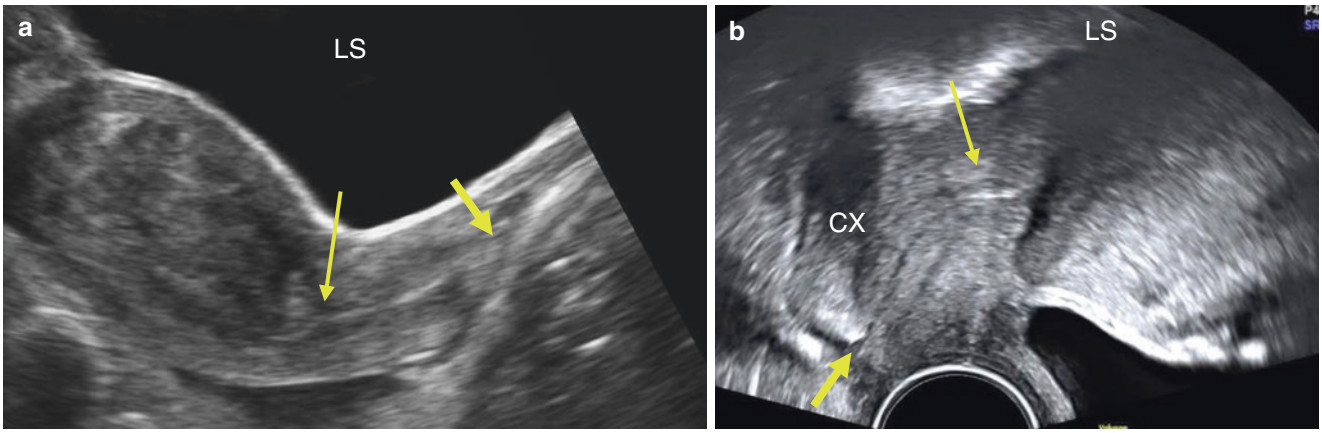

Fig. 5.1 Uterus with cervix on TAS (**a**) and TVS (**b**). *Long arrows* show the internal os; *short arrows* show the external os

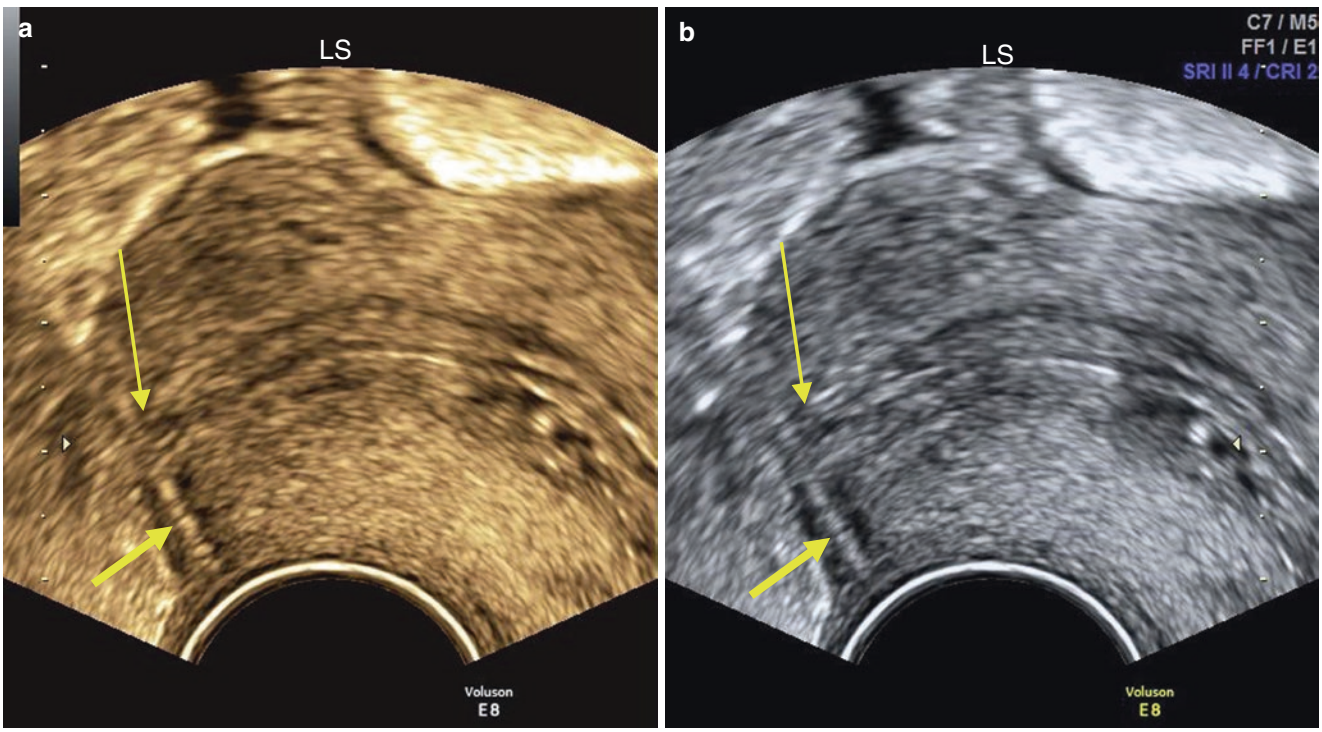

Fig. 5.2 When the USG beam is perpendicular to the cervical canal, the entire cervical mucosa and the posterior wall of the upper vagina (*short arrows*) abutting the external os of the cervix (*long arrows*) is well visualised. (**a**) The cervix in sepia mode, which is supposed to enhance perception by the human eye. (**b**) Greyscale image of the cervix corresponding to (**a**)

5.2 Nabothian Cysts

Nabothian cysts, also known as nabothian follicles, are common retention cysts seen in the cervix. They are formed as a result of the retention of mucoid secretions in the endocervical glands. They are a sequel to the healing process of chronic cervicitis, minor trauma of cervix or vaginal delivery. Being asymptomatic, they are generally picked up on ultrasound done for other pathologies. Their main significance lies in distinguishing them from other cervical lesions like DIE, which may also show cystic lesions in the cervix.

Ultrasound Features of Nabothian Cysts (Figs. 5.3, 5.4 and 5.5)

- These are seen as discreet round or oval cystic spaces in the walls of the cervix, most often close to the mucosa.
- They are usually multiple.
- They are generally anechoic but may show turbid contents.
- No increase in vascularity is noted around the cysts, on Doppler.

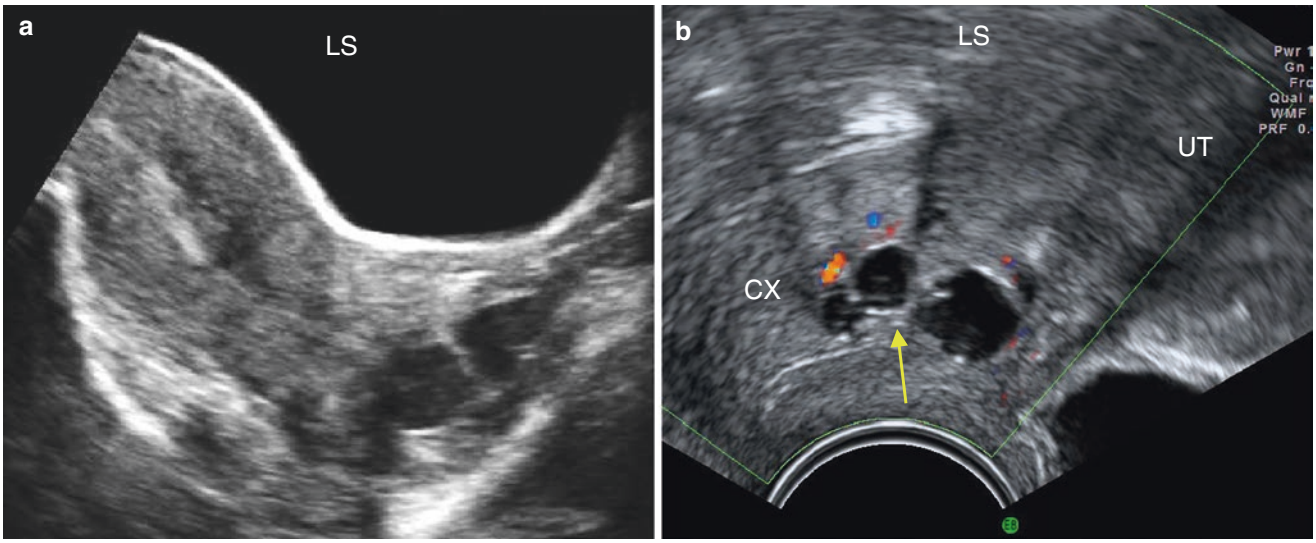

Fig. 5.3 Nabothian follicles seen in the cervix on (**a**) TAS and (**b**) TVS. These are seen as anechoic cystic areas in the cervix on either side of the cervical canal (*arrow*)

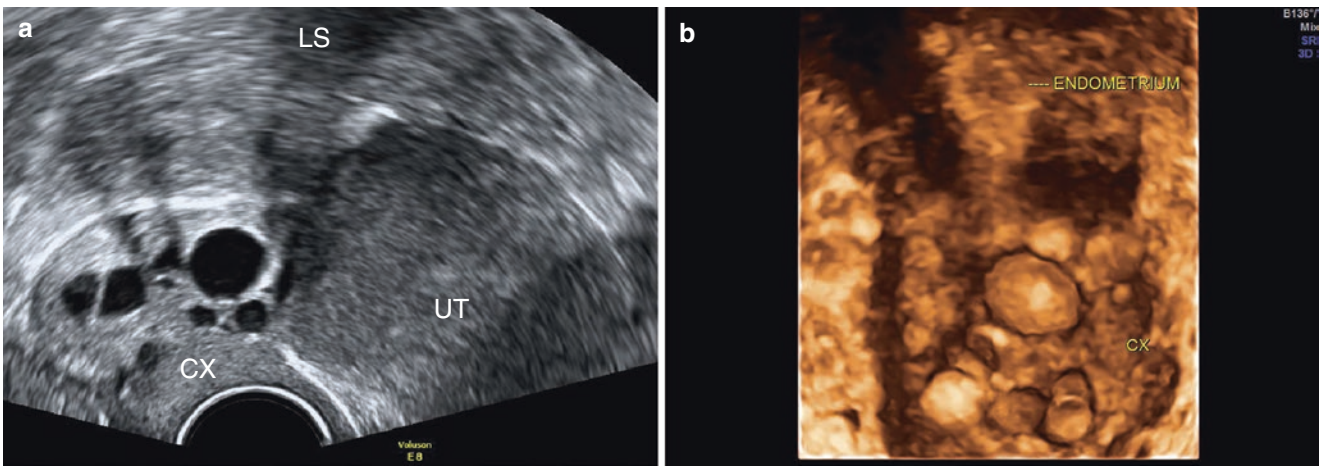

Fig. 5.4 Occasionally, nabothian follicles are many in number, giving the cervix a multicystic appearance: (**a**) on 2D and (**b**) on 3D

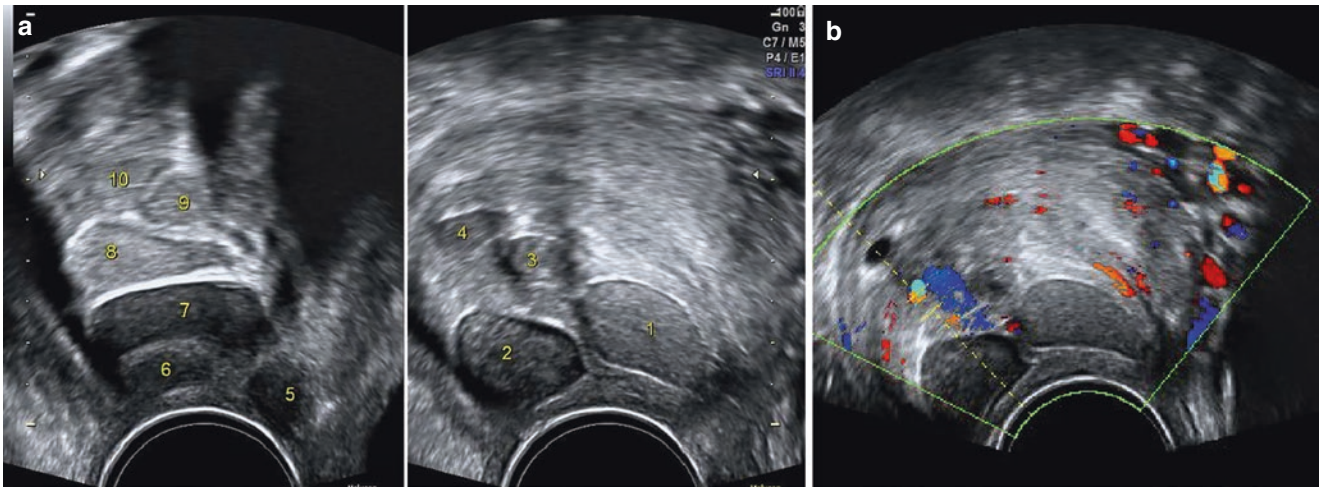

Fig. 5.5 Cervix with multiple (more than 10) nabothian cysts. (**a**) Nabothian cysts showing turbid contents. (**b**) Doppler evaluation done to help with differential diagnosis. *HPE:* chronic cervicitis

5.3 Cervical Polyps

Cervical polyps are solid circumscribed lesions seen at the cervix. They have a vascular connective tissue stroma and are covered with epithelium. Polyps in the cervix may be seen in the cervical canal or protruding out of the external os into the vagina. They may be sessile but most are pedunculated with a slender pedicle. These polyps may arise from the cervix or from the uterine cavity above. Malignancy is rarely found in polyps arising from the cervix, yet, if excised, they must be subjected to histological evaluation.

Cervical polyps are common in women in the reproductive age group, usually in their 40s. Most of these patients are asymptomatic. Symptomatic cases may present with intermenstrual bleeding, post-coital bleeding and vaginal discharge.

Ultrasound Features of Cervical Polyps (Figs. 5.6, 5.7, 5.8, 5.9, 5.10, 5.11, 5.12, 5.13 and 5.14)

- They are typically solid hyperechoic or isoechoic masses seen either in the cervical canal or protruding out through the external os. Rarely, they may show cystic areas within.
- They are usually circumscribed, oval- or 'tear drop'-shaped masses but may be irregular or frond-like in appearance.
- Their margins are usually smooth, and very often these can be identified in the cervix because of the bright line formed at the interphase of the cervical mucosa with the smooth walls of the polyp.
- They may be multiple.
- They can often be identified as separate pedunculated masses by pushing with the TVS probe with consequential movement of the polyp within the cervical canal or vagina.
- On Doppler, flow is seen within these polyps. By tracing the feeder vessel upwards (which may require some angulation of the probe), the site of origin of the polyp can be ascertained. Sometimes polyps in the cervical canal or protruding out of the cervical os may be originating from high up in the endometrial cavity. Very often, a polyp may be detected because of the suspicion raised by a feeder vessel in the cervical canal.
- Larger fleshy polyps may show high vascularity because of the nature of the tissue or secondary infection. Very often, these fleshy polyps are adenomyomatous polyps (showing muscle and glandular tissue) arising from the endometrium.
- Visualisation of cervical polyps is difficult due to the proximity of the cervix to the probe. At mid-cycle, when cervical mucus in the canal is present, these may be better visualised. In other cases, GSV may be used to evaluate these polyps. On GSV, these polyps (especially if they are soft and supple), due to slight pressure from instilled gel, are seen to abut the external os, obliterating it.
- 3D rendering of the cervix and external os, particularly with GSV, may also help to delineate the polyp.

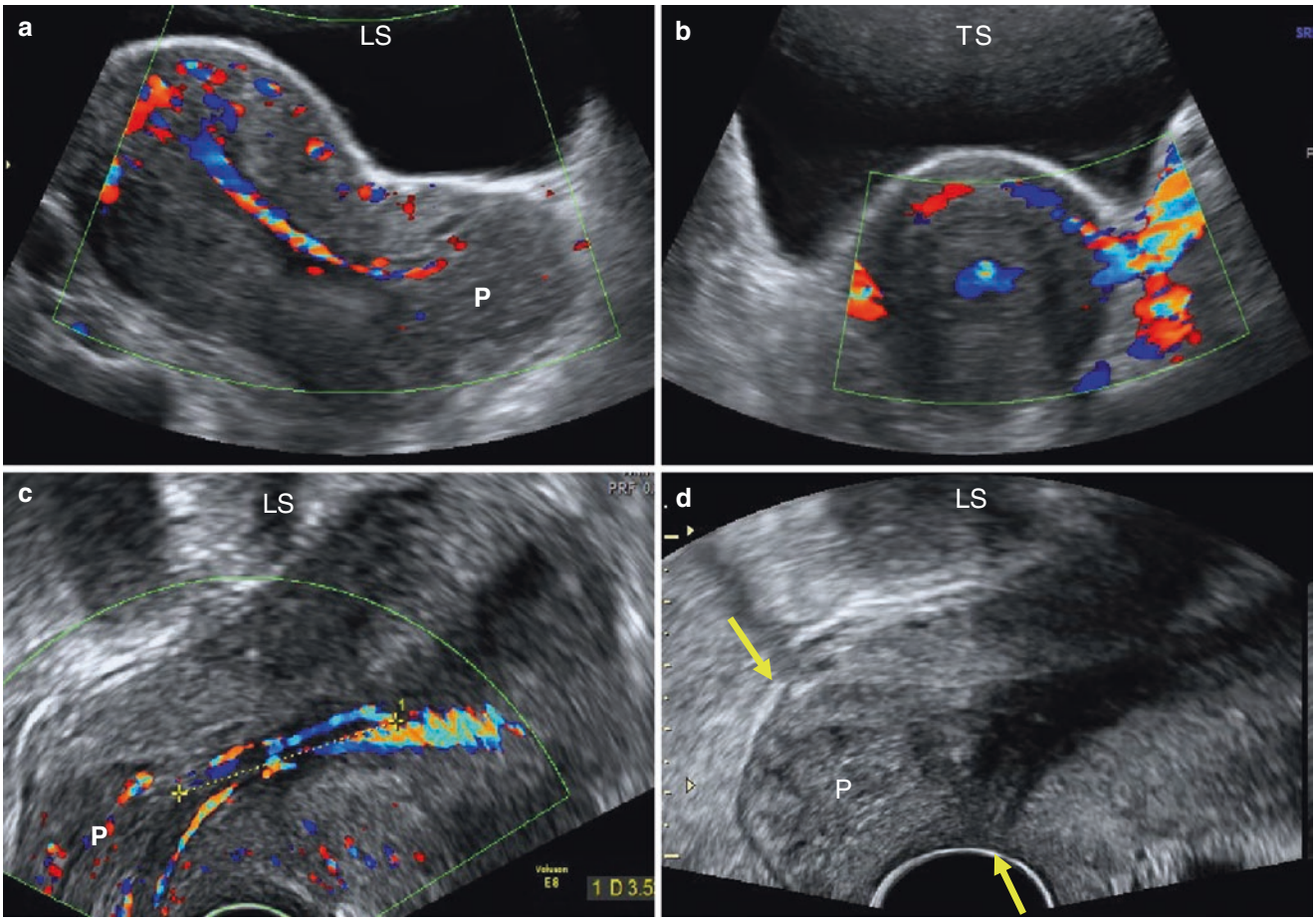

Fig. 5.6 Cervical polyp arising from the anterior wall of the upper corpus of the uterus. (**a**) A feeder vessel is seen on TAS extending from upper corpus to the upper end of the polyp (*P*). (**b**) Transverse section of feeder vessel at the internal os (determined by the uterine arteries entering the uterus at this level). (**c**) Feeder vessel of the polyp on TVS (RI-0.34). (**d**) Polyp protruding out of external os. *Arrows* showing the splayed cervical lips. *HPE:* adenomyomatous polyp

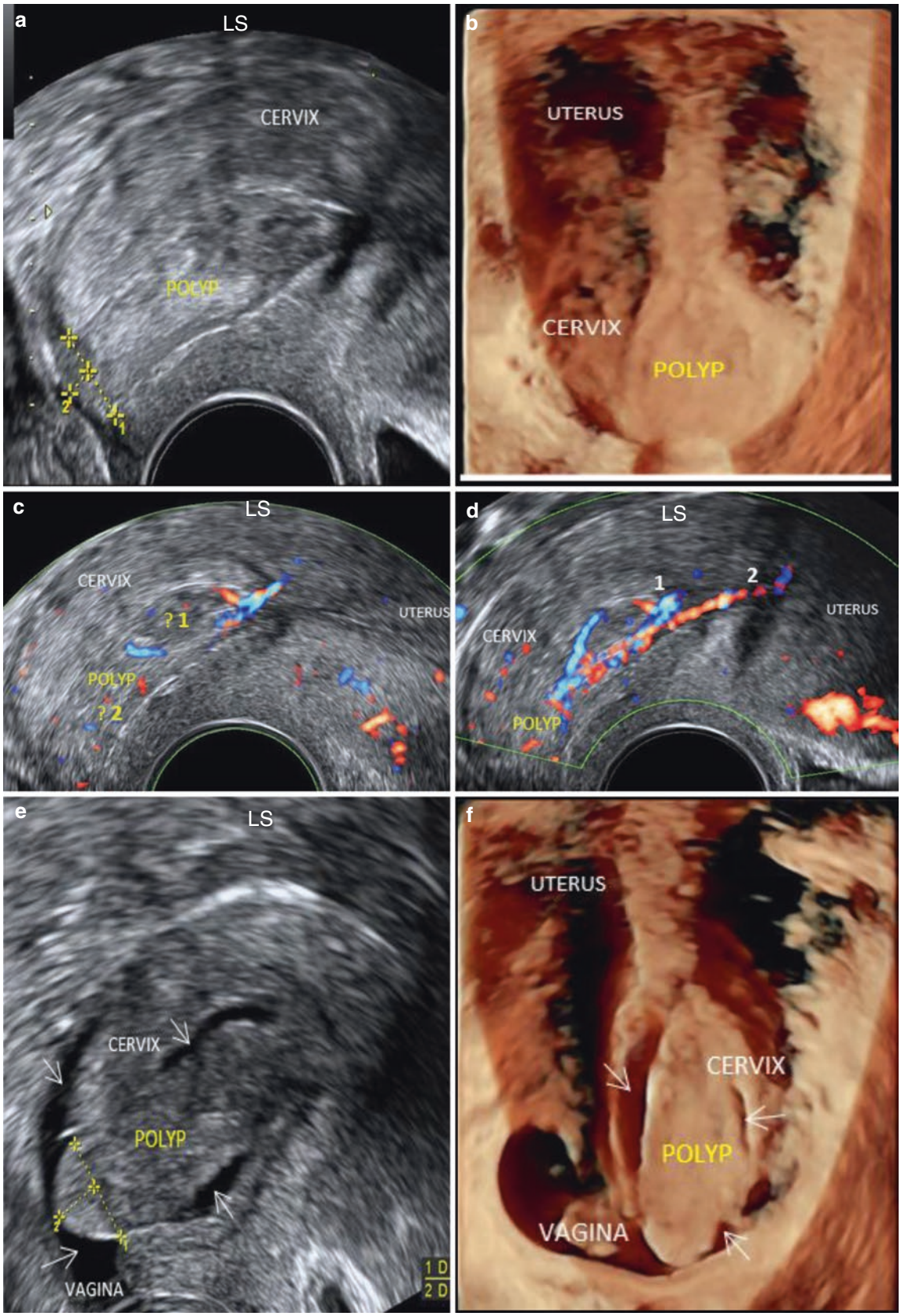

Fig. 5.7 Polyp in the cervical canal which is protruding out from the cervical os. (**a**–**d**) Are images on regular TVS. The polyp is seen in the cervical canal (**a**) on 2D and (**b**) 3D. The lower margin of the polyp is seen protruding out of the external os. (**c**, **d**) On Doppler, there was a suspicion of two polyps (labelled as 1 and 2) because of the vascular pattern of flow with two vessels approaching the polyp (one venous and one arterial) from two different locations above the polyp. (**e**, **f**) Images on GSV. Single polyp is better seen and delineated on 2D and 3D with GSV

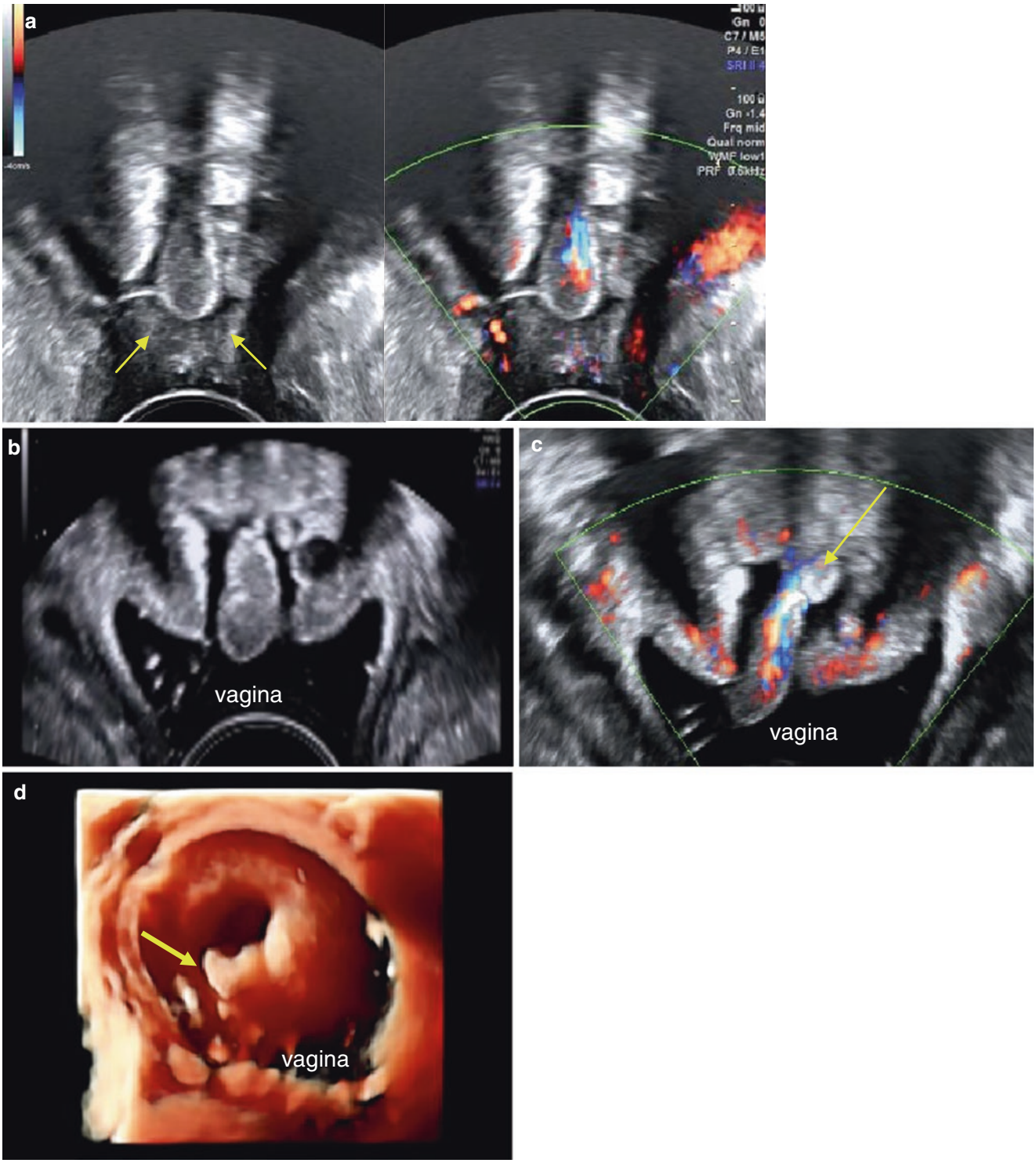

Fig. 5.8 (**a**) Tear-shaped polyp seen in cervical canal on regular TVS – on greyscale and on colour Doppler. The vaginal walls (*arrows*) are seen just below the polyp opposing each other in the midline. (**b–d**) GSV – because of the intravaginal gel, the vaginal walls are seen apart and the lateral fornices are clearly visible. Gel is also seen surrounding the polyp. (**b**) Polyp on greyscale. (**c**) Polyp with feeder vessel approaching it from the cervical walls above. A smaller polyp (*arrow*) is seen close to its base. (**d**) 3D rendered image of the cervical os with the polyp (*arrow*) protruding out

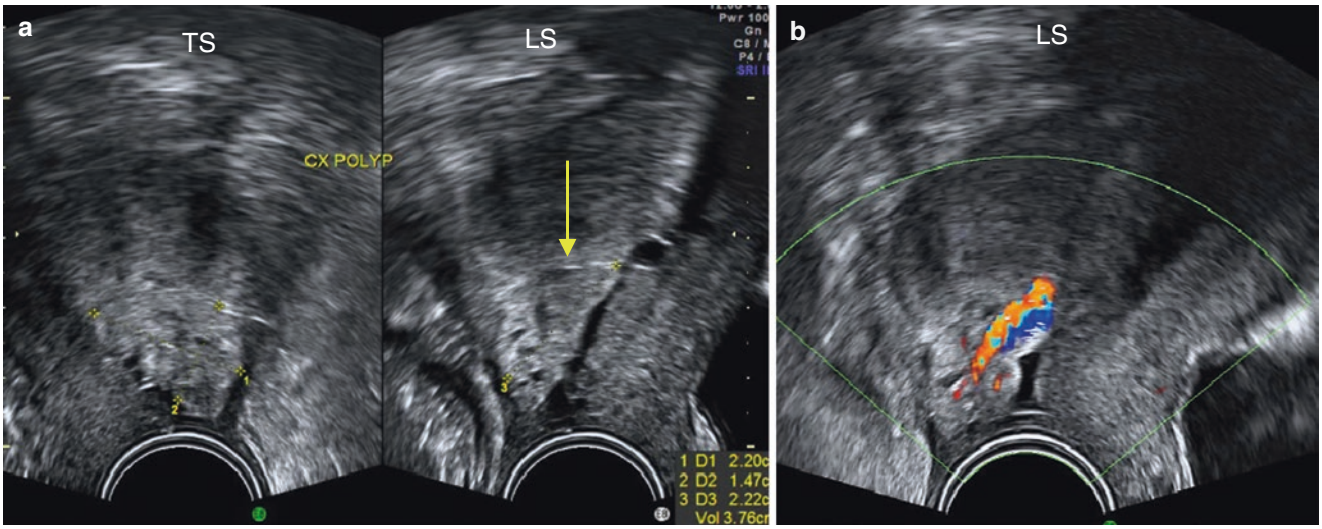

Fig. 5.9 (**a**) Irregular polyp seen in cervical canal. *Arrow* showing hyperechoic line between the polyp and wall of the cervical canal. (**b**) Feeder vessel of the polyp seen

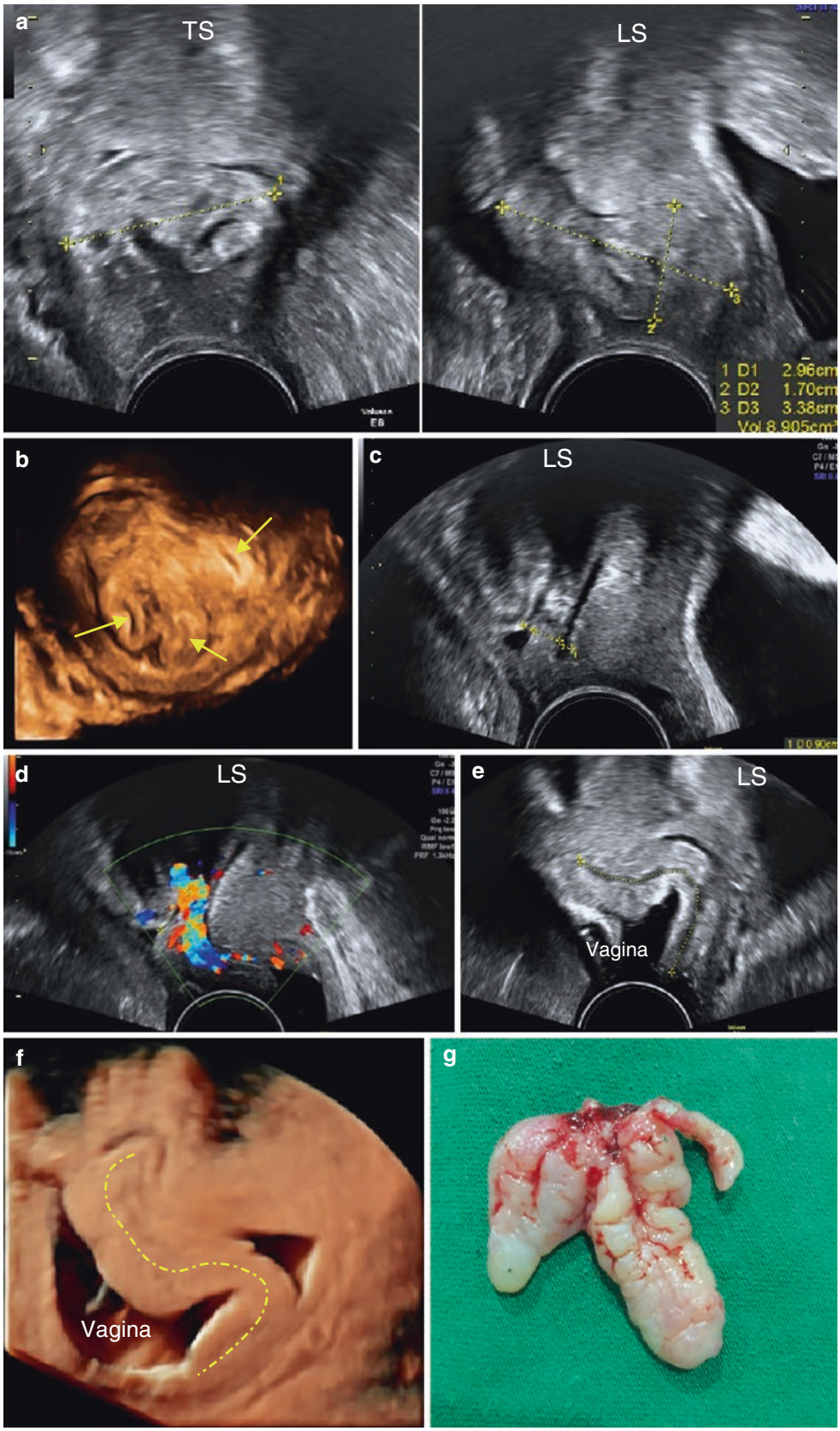

Fig. 5.10 (**a**) Irregular polypoid mass seen in the vagina just below the cervix on regular TVS. (**b**) 3D rendering of the same, showing three frond-like projections with central hypoechoic linear areas suggestive of vascular core (*arrows*) of the fronds. (**c**) Pedicle of the polyp at the external os. (**d**) Doppler flow in pedicle. (**e**) Fronds of polyp seen on GSV. (**f**) 3D rendering of the longest frond seen on GSV is traced in the image. (**g**) Gross morphology of the excised specimen correlating with USG in (**b**) *HPE:* benign cervical polyp

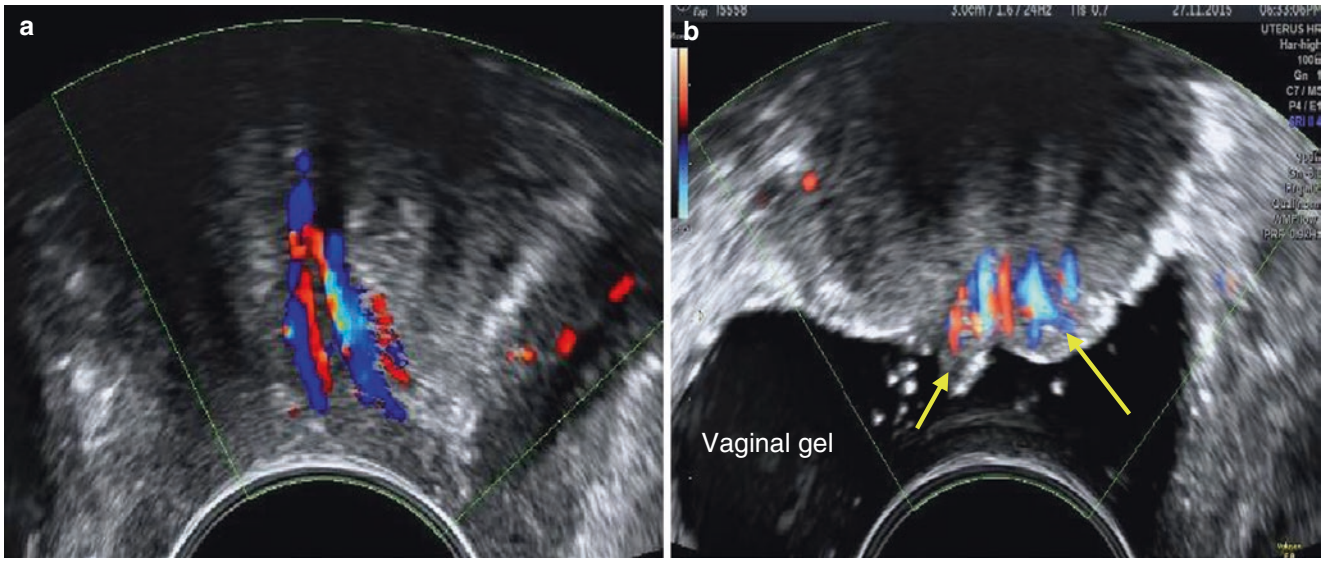

Fig. 5.11 Polyp was seen per speculum clinically. (**a**) Regular TVS – vessels were seen in the cervical canal but polyp was difficult to delineate. (**b**) GSV – two polyps (*arrows*) seen at the cervical os which were obliterating the external cervical os

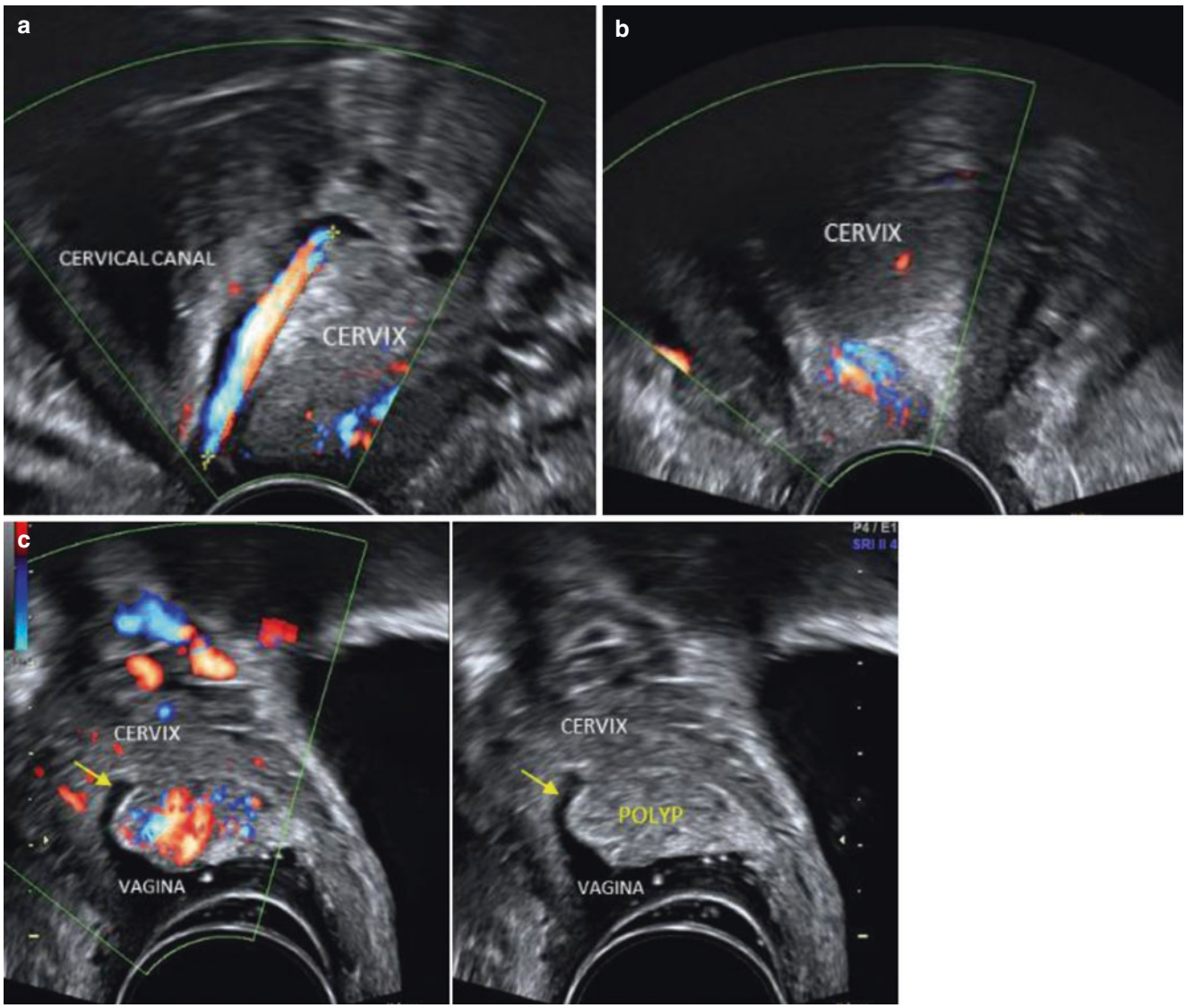

Fig. 5.12 (**a**) Vessel in the cervical canal raises a high suspicion that it could be a feeder vessel of a polyp lying below it. (**b**) Regular TVS – polyp is difficult to delineate. (**c**, **d**) GSV – polyp is clearly seen because of the gel surrounding the polyp and filling narrow gaps (*arrows*) between tissue planes

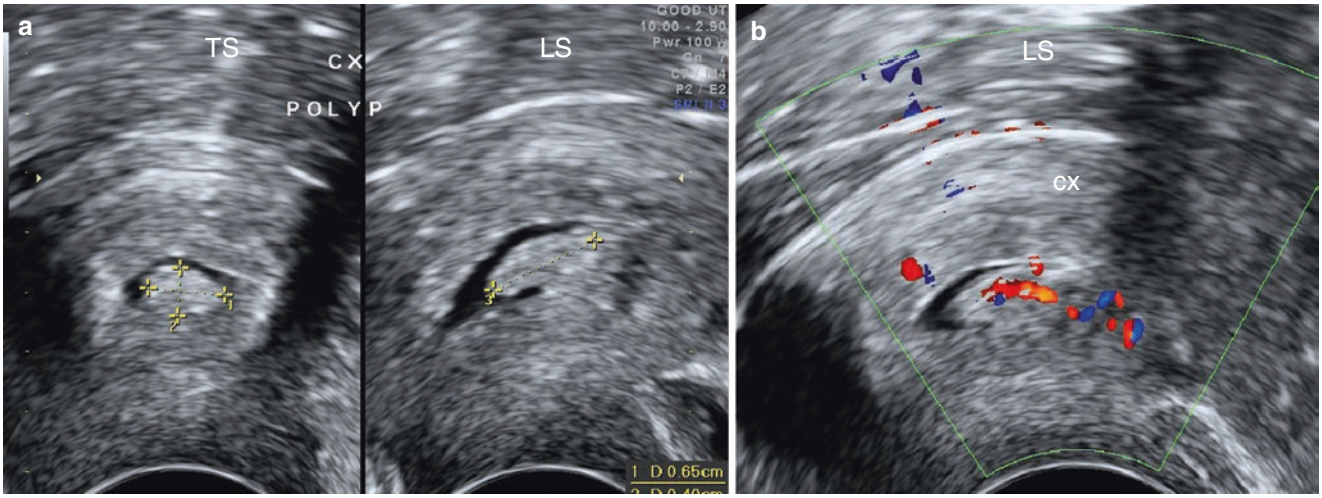

Fig. 5.13 (**a**) Small cervical polyp which is seen because of mucous in the cervical canal. (**b**) Feeder vessel is seen approaching it from the anterior cervical wall

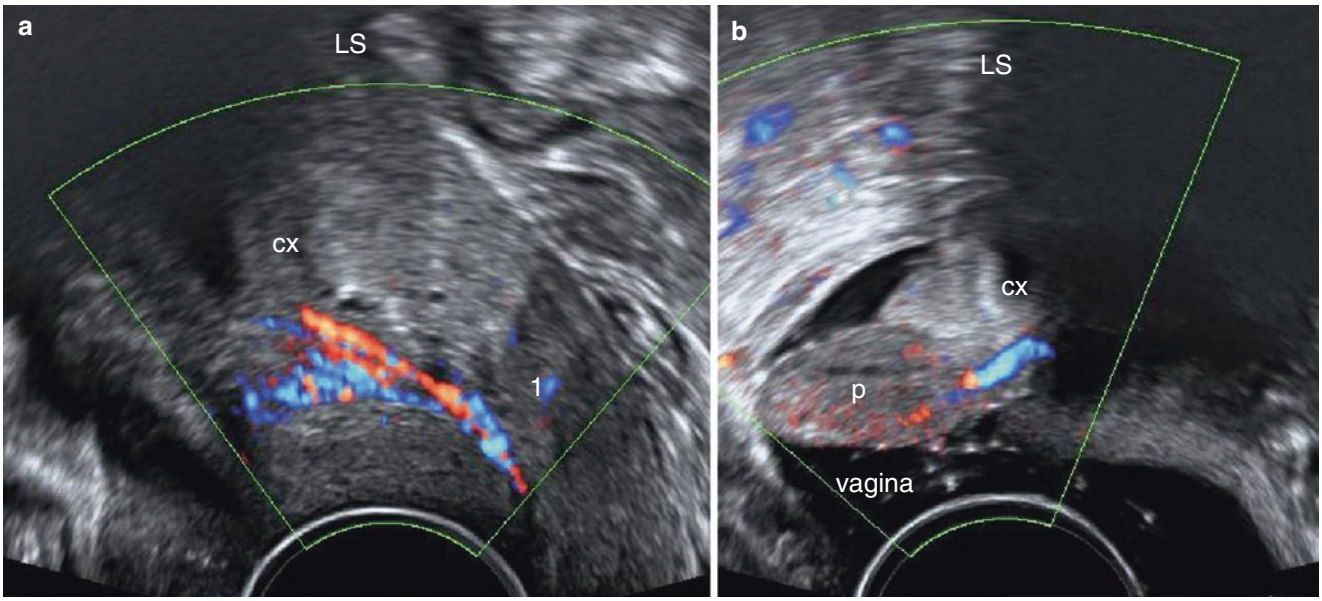

Fig. 5.14 (**a**) Feeder vessel seen in the cervical canal on a regular TVS, but the polyp was difficult to delineate. (**b**) On GSV, polyp seen clearly outlined with its feeder vessel and protruding out of the cervical os

Summary: Cervical Polyp

- These are commonly seen in benign lesions. Most cases are asymptomatic or complain of intermenstrual or post-coital bleeding.
- On ultrasound, they typically appear as oval- or 'tear drop'-shaped solid masses either in the cervical canal or protruding out of the external os. A feeder vessel is seen which helps locate the site of origin of polyp and often helps raise suspicion of a possible cervical polyp.
- GSV is useful in evaluating suspected or known cervical polyps.

5.4 **Cervical Fibroids** (Figs. 5.15, 5.16 and 5.17)

Cervical fibroids are less common, as compared to uterine fibroids. Clinically, they may cause symptoms due to pressure on the bladder or bowel. Cervical fibroids can obstruct normal deliveries because they are located along the birth canal. They may arise from the cervical myometrium and grow pushing the surrounding structures, or they are seen replacing the cervical wall, or they may be seen as pedunculated submucosal masses with significant dysmenorrhoea, menorrhagia, intermenstrual bleeding and vaginal discharge. Surgical management of cervical fibroids is more challenging than those of the uterine body.

The ultrasound features of cervical fibroids are similar to fibroids elsewhere in the uterine body and are dealt with in Chap. 3, in the section on fibroids. On TVS, these fibroids may hamper the view of structures beyond them due to shadowing. Their mapping and origin (deciphered from the site of vascular supply) is often better assessed on TAS than TVS. The uterine body above the cervical fibroid also most often requires evaluation on TAS.

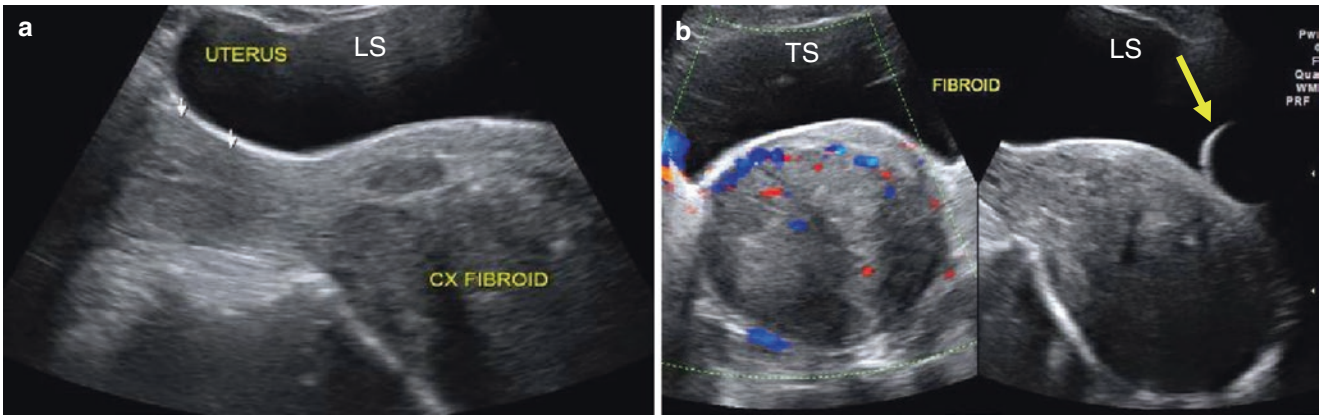

Fig. 5.15 Cervical fibroid causing bladder neck obstruction. Patient presented with difficulty in passing urine since 3 days. (**a**) Small uterine body seen above the posterior wall cervical fibroid. (**b**) Fibroid on transverse and long section. Catheter is seen in situ (*arrow*)

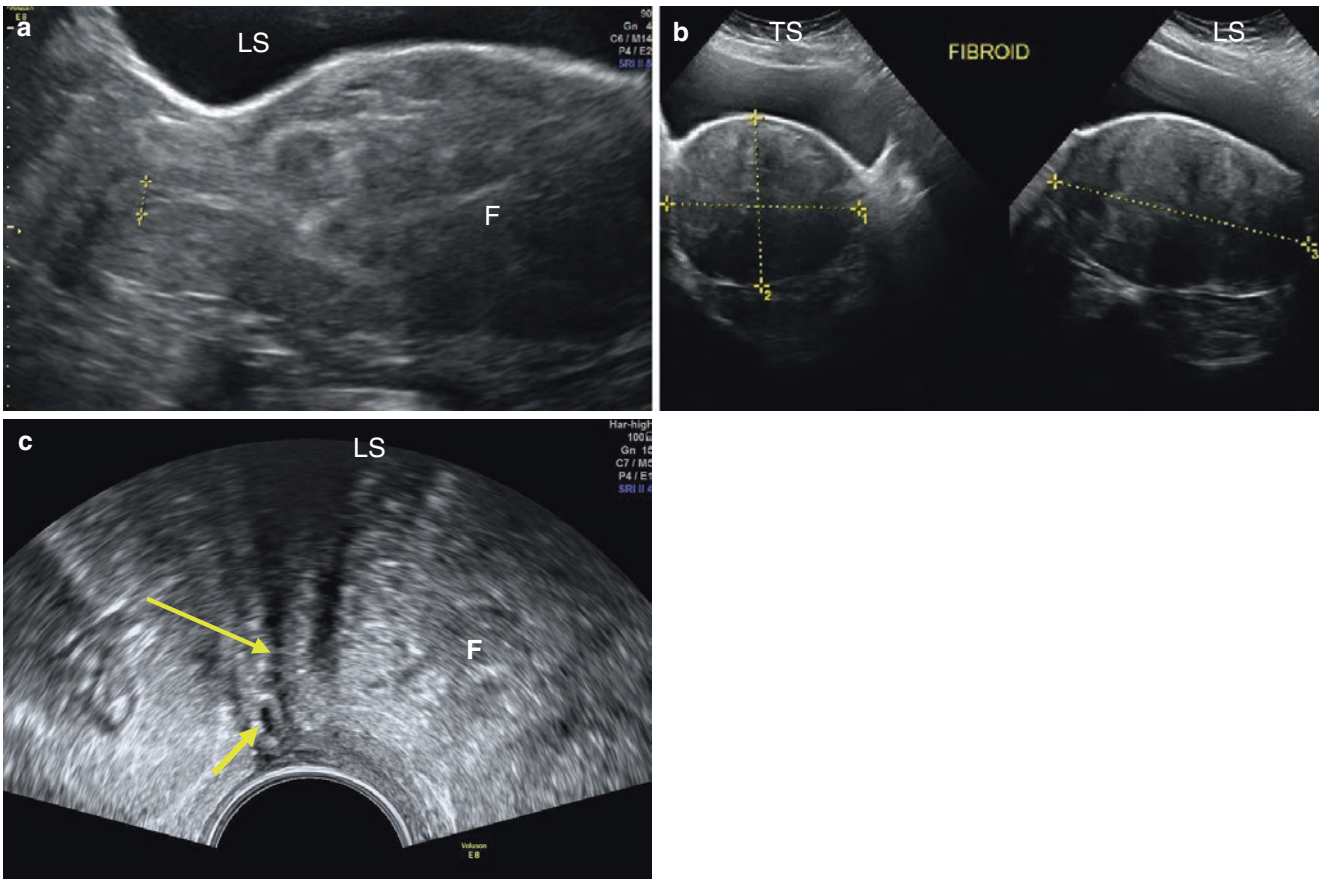

Fig. 5.16 (**a**, **b**) TAS – a large anterior cervical fibroid measuring 10×9×14 cm (volume – 725 cc). (**c**) TVS – the anterior lip of the cervix is replaced by the fibroid (*F*). Post lip with small nabothian follicle (*small arrow*) and the cervical canal (*long arrow*) are also seen

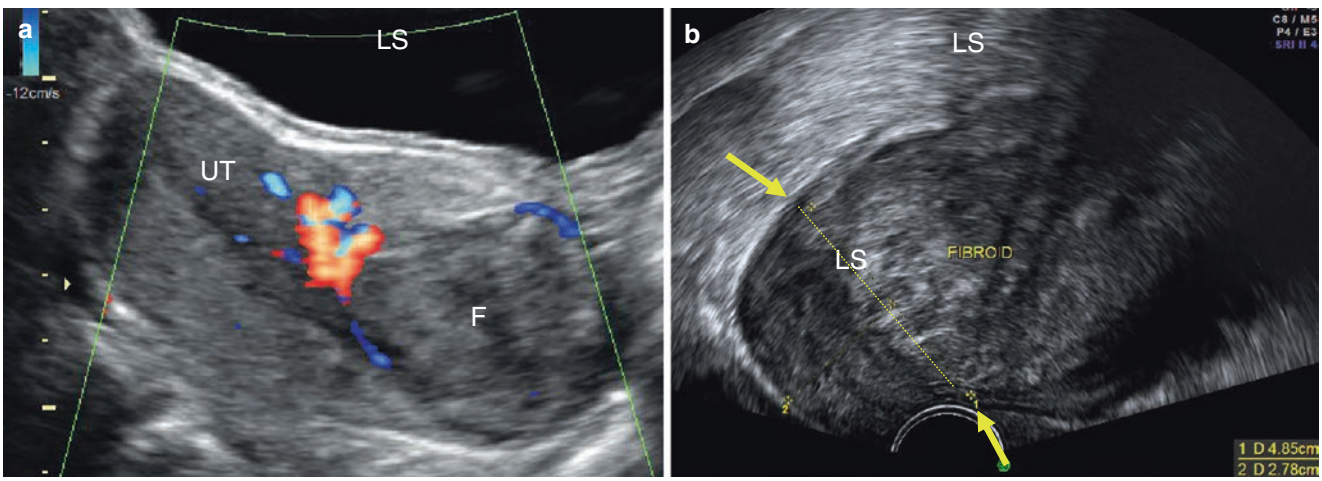

Fig. 5.17 (**a**) TAS – fibroid (*F*) seen in the cervical canal. Vascular flow to fibroid shows its origin from the anterior uterine wall of the lower corpus. (**b**) TVS – fibroid seen protruding out of the cervix. Cervical lips (*arrows*) are about 5.8 cm apart. Dilated or distended external os shown with a straight line

5.5 Cervical Carcinoma

Cervical carcinoma is a common malignancy, particularly in some countries like India, where it is more common than endometrial carcinoma, especially in women from low socioeconomic backgrounds. It is seen in relatively younger women that belong to the reproductive age group. Human papillomavirus (HPV) is believed to be primarily involved in the aetiology of cervical cancer.

The two major types of cervical cancer are squamous cell carcinoma and adenocarcinoma. Squamous cell carcinoma is more common, but their incidence is decreasing in many countries due to cytological screening (Pap smear).

In the early stages, women are asymptomatic. Early cases may be picked up following investigations for an abnormal Pap smear. Women who are symptomatic may present with post-coital bleeding, intermenstrual bleeding or vaginal discharge. In advanced cases that have spread to the parametrium, bowel or bladder, patients may complain of pain and bladder or bowel symptoms.

Ultrasound evaluation of carcinoma of the cervix is generally considered suboptimal. FIGO staging of cancer of the cervix is based on clinical examination of the patient, which today is considered inaccurate. Presently, in most cases, carcinoma of the cervix is evaluated by MRI. Of late there has been an increasing amount of literature with studies showing high accuracy of ultrasound in the detection and the evaluation of cervical cancer. Confirmation of diagnosis is by tissue biopsy. Ultrasound can help not only in the detection of small tumours but also in staging if done systematically. It is also helpful in the evaluation of a residual tumour following treatment. Both MRI and ultrasound, however, are not adequate for assessing lymph node metastasis.

Ultrasound Features of Cervical Carcinoma (Figs. 5.18, 5.19, 5.20, 5.21, 5.22, 5.23, 5.24, 5.25 and 5.26)
(Please refer to 'Tips to Improve Ultrasound Diagnosis of Cervical Lesions' given earlier in the chapter.)

- These lesions appear as solid masses in the cervix. Squamous cell carcinomas are more likely to appear hypoechoic, whereas adenocarcinomas are more often isoechoic. Larger lesions that have undergone some necrosis appear more heterogeneous.
- Their margins may be difficult to delineate on greyscale (particularly the isoechoic lesions). On pushing the cervix with a TVS probe to assess firmness/elasticity, the malignant tissue appears firm and noncompressible, which often helps in defining the margins of the lesion (Testa UOG 2009).
- Doppler also helps in detecting and defining the margins of the tumour, as most of the tumours show high vascularity. Subjective evaluation by colour score is found to be more useful than 2D or 3D flow indices. Abnormal vascular pattern with irregular calibre and abnormal branching may be noted in bulky masses, on 3D power Doppler with glass body display.
- The location of the tumour should also be mentioned, i.e. whether it is exophytic or endophytic. This can be done by identifying the cervical canal and the relation of the tumour to it.
- The lesion should be measured in three dimensions (as explained in Chap. 2). The maximum dimension should be also be measured which may be in any plane, as FIGO staging includes the size of the tumour and the treatment varies in various stages.
- In small lesions, it is important to measure the distance between the internal os and the upper margin of the tumour, particularly in women who would like a fertility sparing local surgical procedure like conisation.
- The stromal infiltration should be assessed by checking on the thickness of the tumour-free cervical stroma around the margins of the lesion.
- Infiltration into the uterovesical space or bladder wall and into the rectovaginal septum or rectum should be assessed by pushing these structures with the TVS probe and assessing the sliding of the bladder and rectum along the vaginal and cervical walls (bladder wall infiltration is better noted when the bladder is partially filled with urine).
- Parametrial infiltration is seen as irregular margins of the tumour mass with bud-like hypoechoic extensions (interrupting the hyperechoic external visceral fascia surrounding the cervix and vagina) into the surrounding parametrium. This can be assessed well on the transverse and coronal sections of the uterus. The distance of the parametrial infiltration from the external iliac vessels will give us an idea as to whether the mass is extending up to the lateral pelvic wall.
- Extension of the tumour onto the vaginal wall should also be assessed, as it alters the staging of the lesion.
- Some patients may show turbid collection in the endometrial cavity due to obstruction of the cervical canal by the tumour. In postmenopausal women with a turbid collection in the endometrial cavity (though often a common finding in women with no pathology), one must carefully evaluate the cervix for any subtle malignancy.

- Kidneys should be evaluated for any evidence of hydronephrosis, which could be a complication of cervical cancer.
- Lymph node assessment should be attempted by tracing the external iliac vessels from the inguinal area onto the pelvis up to the aortic bifurcation on a transabdominal scan.

Instead of a regular transvaginal scan, a transrectal scan can also be done which has the advantage of a lower probability of bleeding from the lesion on contact with the vaginal probe.

In the author's view, gel sonovaginography is an ideal technique which helps to delineate the exophytic lesion very well, and also the vaginal extensions of the tumour, by partially filling and distending the upper vagina. The assessment of the entire tumour (in the cervix, vagina, parametrium) on greyscale and Doppler is also much better on GSV because the gel creates a stand-off resulting in better resolution. GSV is not resorted to if the patient is bleeding actively.

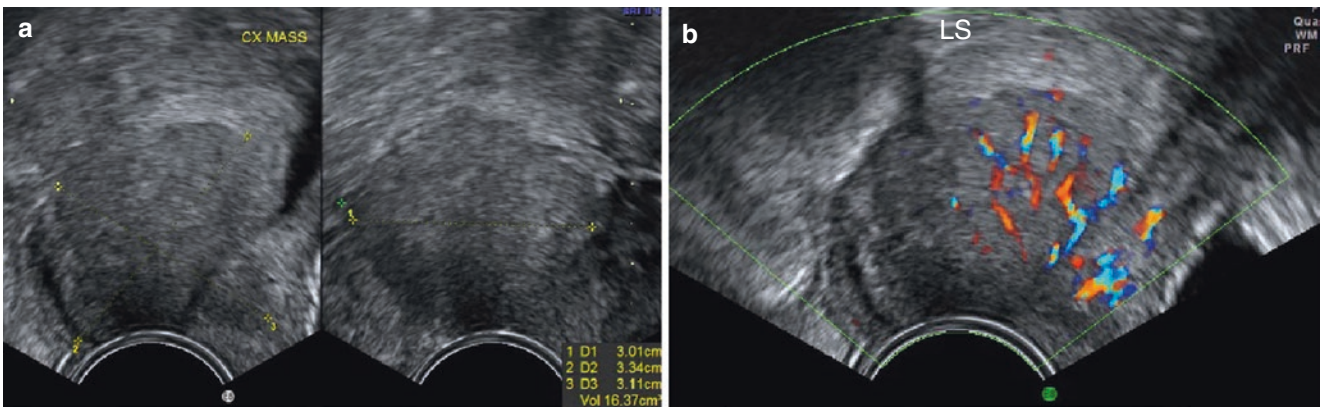

Fig. 5.18 Hypoechoic mass seen in the cervix and upper vagina. (**a**) Mass measured in all three dimensions. (**b**) Increased flow noted within the mass. *HPE:* squamous cell carcinoma

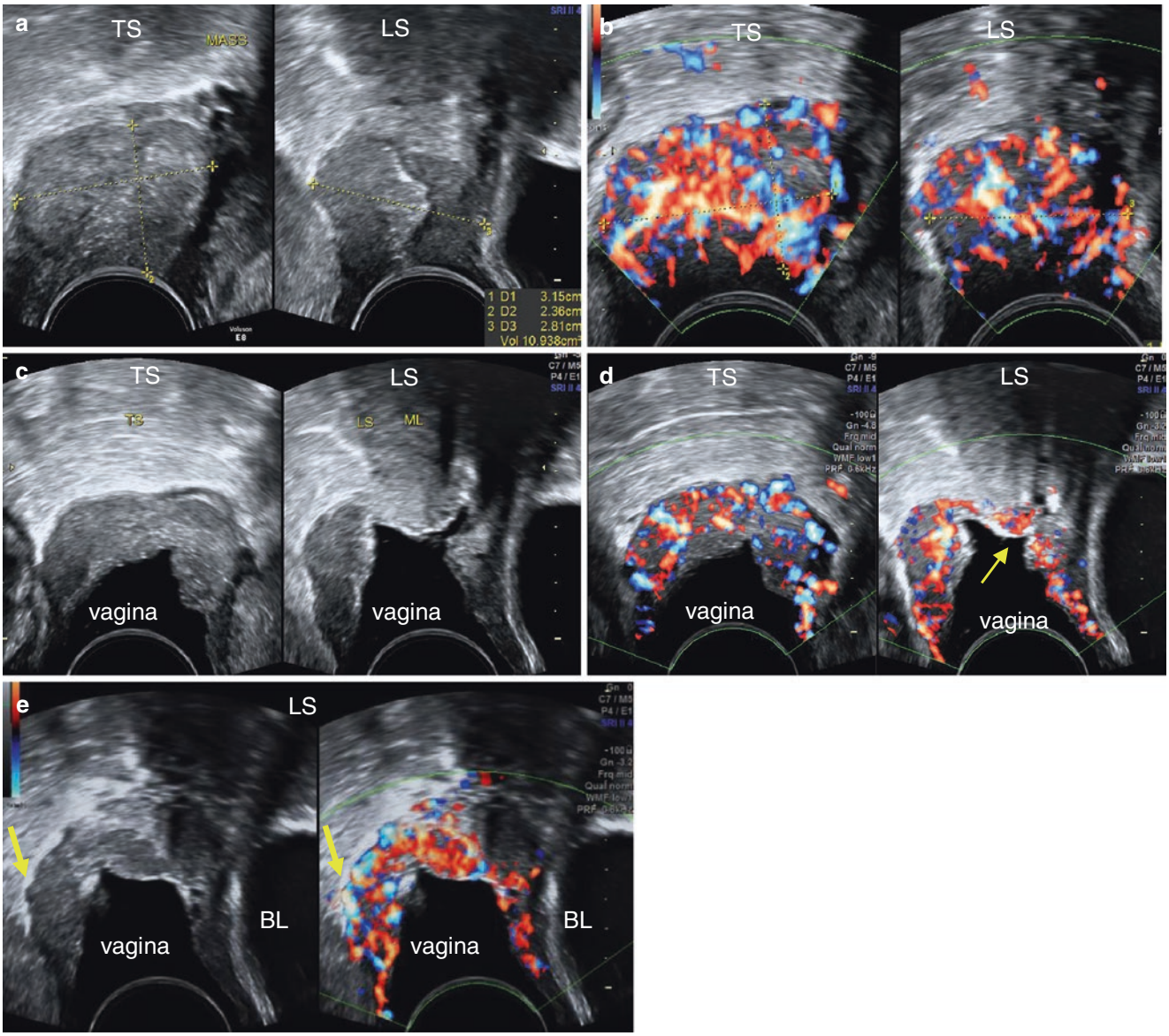

Fig. 5.19 58-year-old lady referred with a neoplastic mass in the vagina. (**a**) Hypoechoic slightly heterogeneous mass seen in upper vagina. (**b**) Increased vascularity noted in the mass. (**c–e**) On GSV, vaginal walls are seen apart with a clear delineation of the tumour margins, the lower cervix and the external os. In (**d**), the vascularity helps assess the extension of tumour into the cervical lips around the external os (*arrow*). This makes primarily a cervical cancer (and not vaginal). (**e**) On careful observation, the irregularity of the white external fascia of the posterior vaginal wall on greyscale and Doppler suggests early paravaginal extension (*arrows*). *HPE:* squamous cell carcinoma

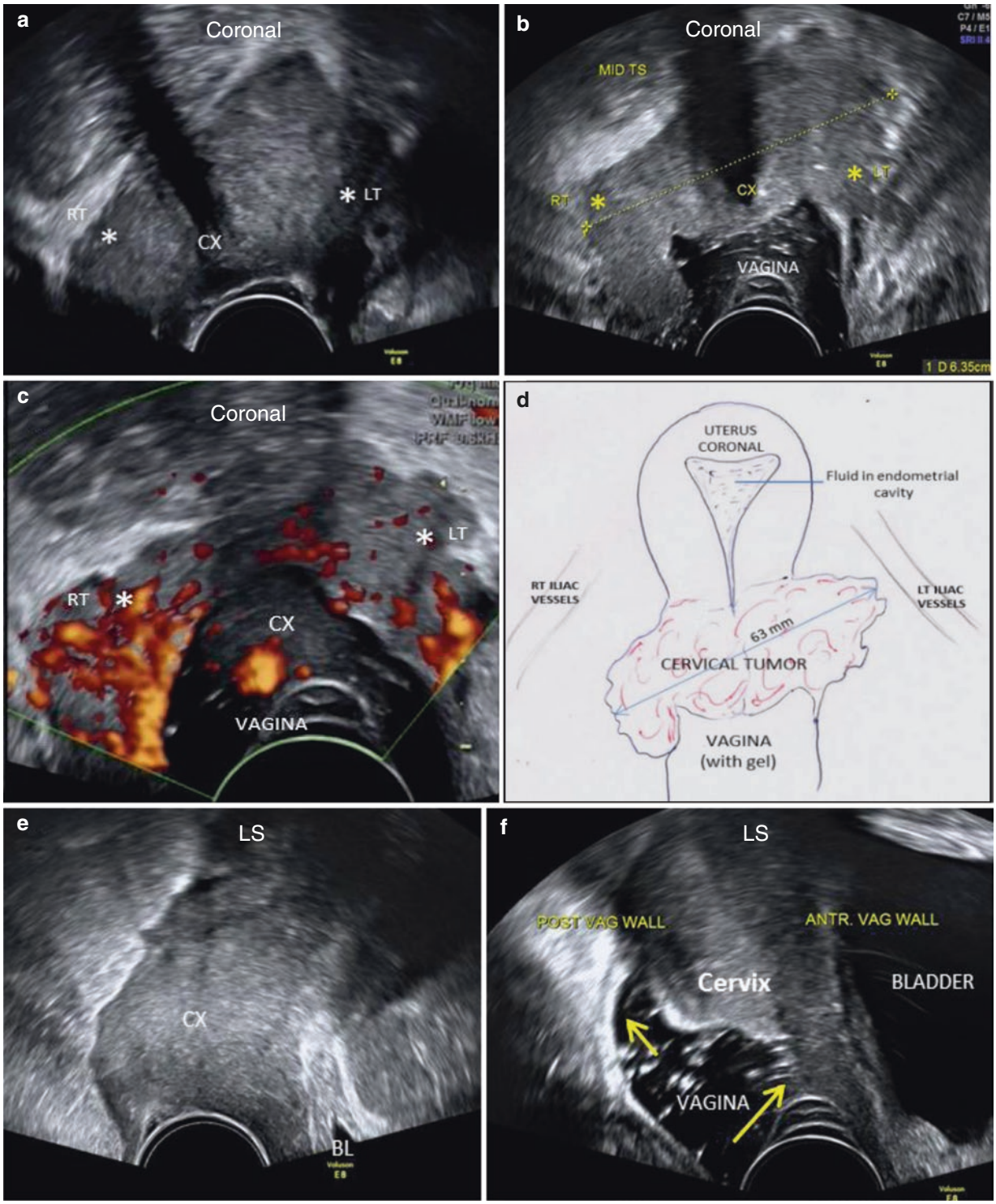

Fig. 5.20 A case of squamous cell carcinoma. (**a**) Coronal section of the cervix on regular TVS showing hypoechoic mass involving cervix and extending into the right and left parametrium (RT and LT). Vaginal walls are difficult to identify. (**b**, **c**) GSV – coronal section showing extension of tumour from the cervix onto the vagina and parametrium on greyscale and Doppler. Maximum dimension of tumour measured. (**d**) Diagrammatic representation of the tumour in the coronal section. The tumour was almost reaching the iliac vessels along the left pelvic wall. (**e**) Sagittal section of the vagina and cervix on regular TVS showing the cervical tumour. (**f**, **g**) GSV – sagittal section showing tumour spreading to the adjoining anterior vagina (*long arrows*) on greyscale and Doppler. The *short arrows* show a normal posterior vaginal wall. (**h**) Diagrammatic representation of the tumour in sagittal section. (**i**, **j**) Sagittal and coronal sections of the tumour showing irregularity of the white external fascia of the cervix due to bud-like extensions (*arrows*) of the tumour into the posterior and left parametrium. (**k**) Normal right kidney. Left kidney shows hydronephrosis suggestive of left ureteric involvement

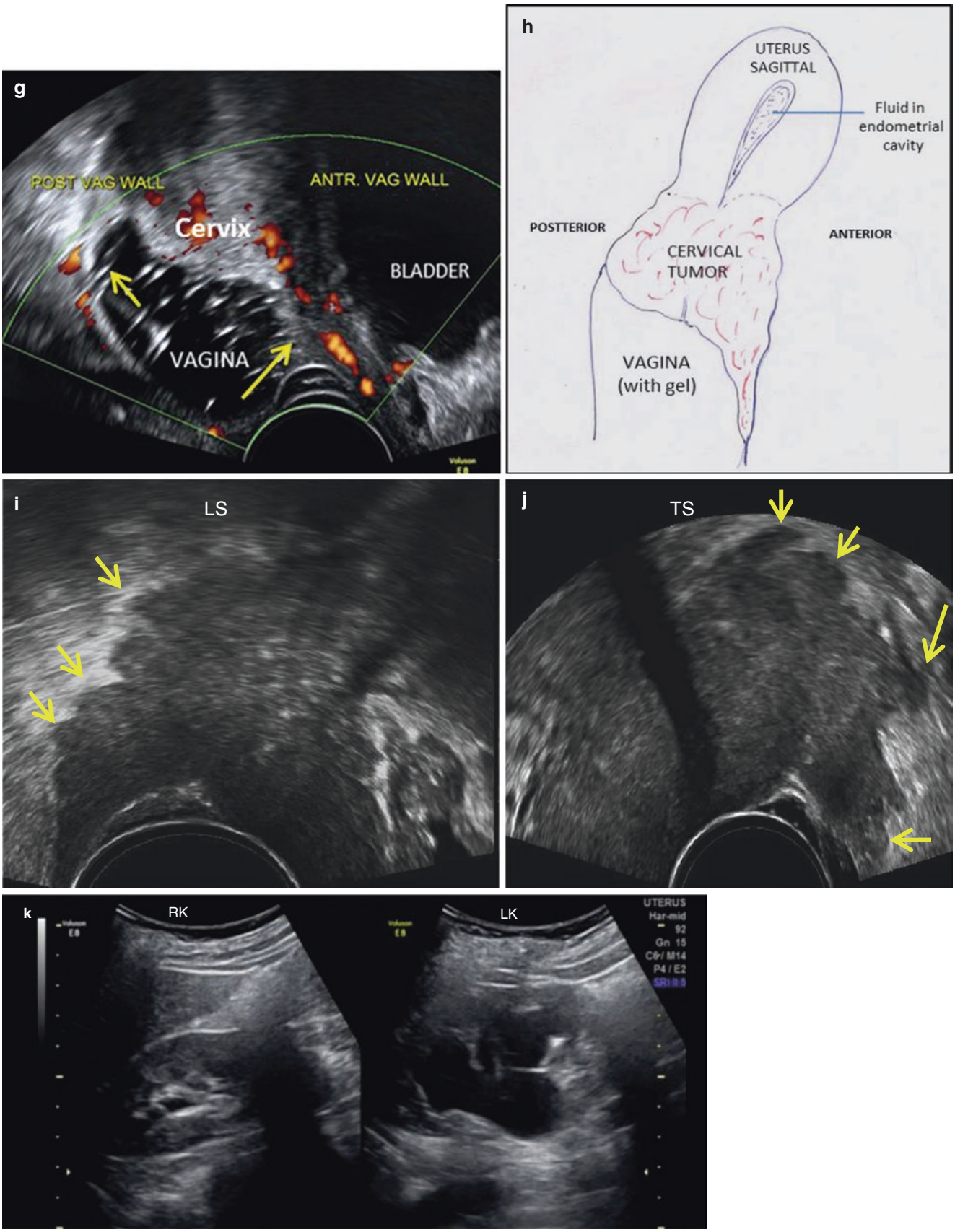

Fig. 5.20 (continued)

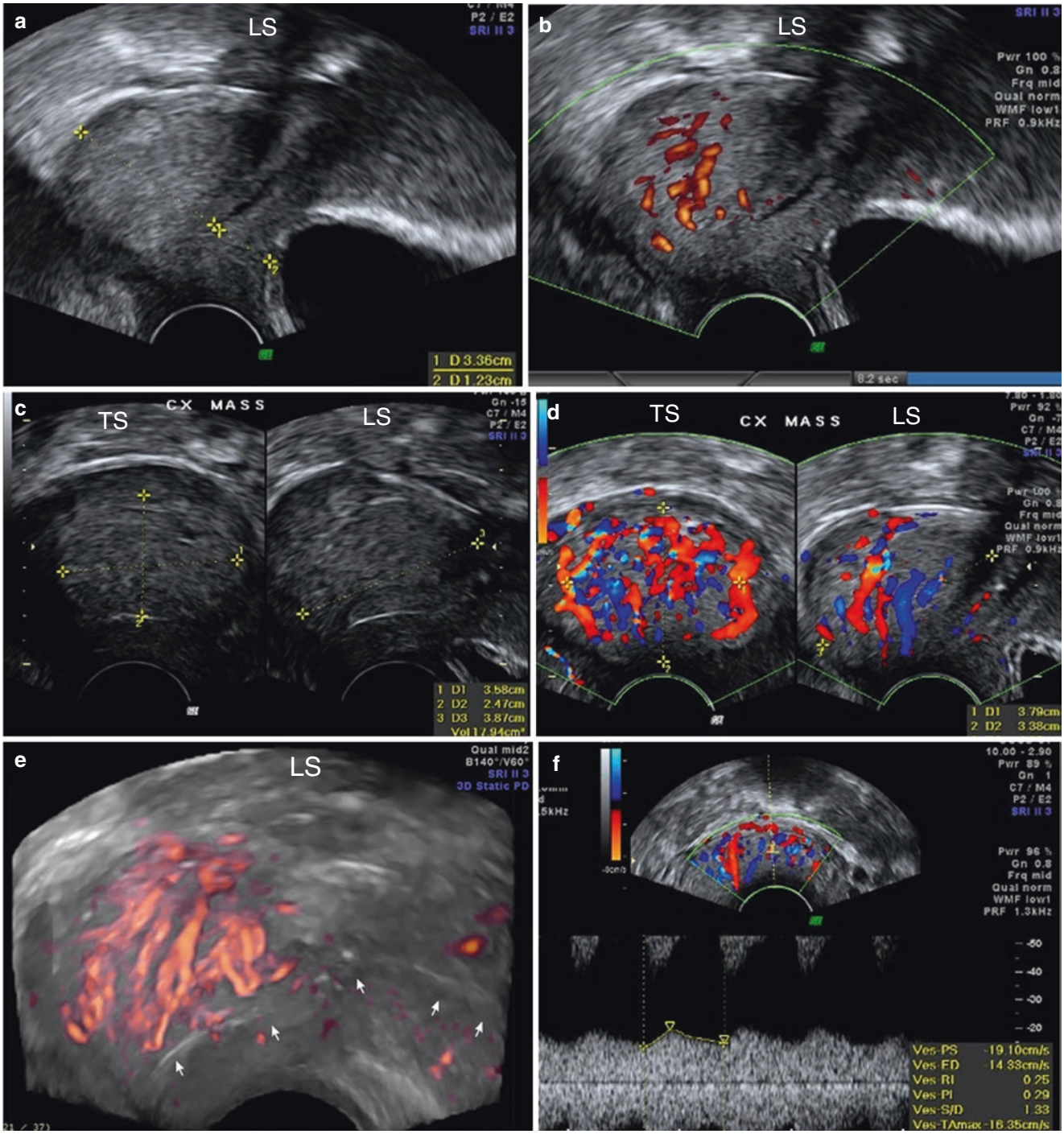

Fig. 5.21 42-year-old lady with a history of white discharge since 2 years and post-coital bleeding since 5 months. (**a**) On greyscale, the posterior wall of the cervix appeared thick and bulky. (**b**) Increased flow is seen in this bulky posterior wall on Doppler. (**c**) Isoechoic mass measured on 2D greyscale. (**d**) High vascularity (colour score of 4), seen in the mass, raises a high suspicion of malignancy. (**e**) 3D glass rendered image with power Doppler shows the abnormal vascular pattern (irregular calibre, looping and abnormal branching) which is seen in malignant masses. With rotation and cine loop, this is even better perceived. The cervical canal is seen (*small arrows*), and the tumour is seen to be endophytic. (**f**) Flow in the tumour shows a low RI of 0.29. In some other vessels of the same mass, the RI was higher (up to 0.67). (**g**, **h**) Iliac vessels should be traced in all cases of carcinoma of the cervix to look for metastatic iliac lymph nodes. Here, none were seen. *HPE:* endocervical adenocarcinoma

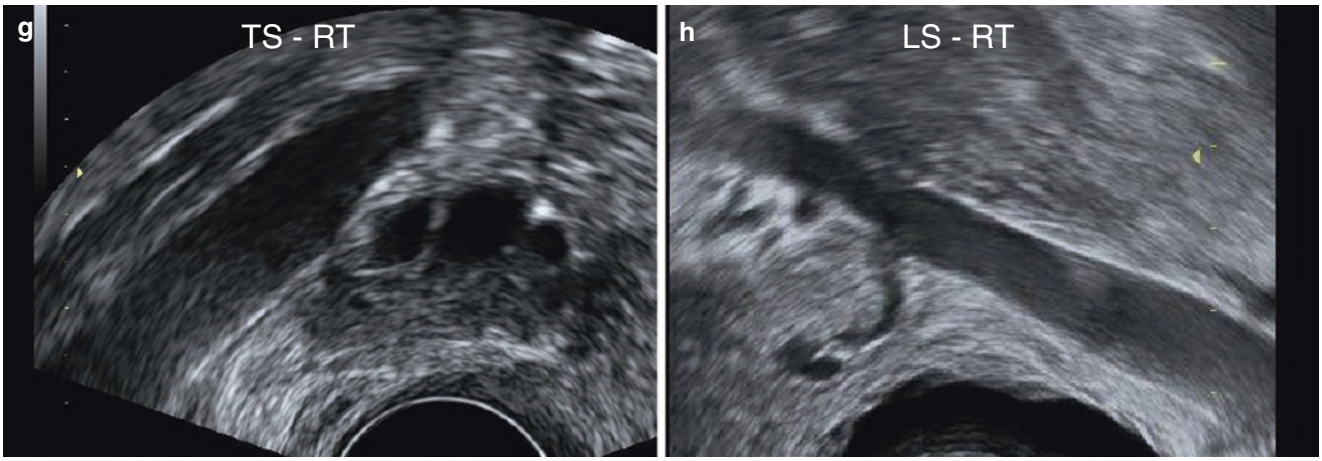

Fig. 5.21 (continued)

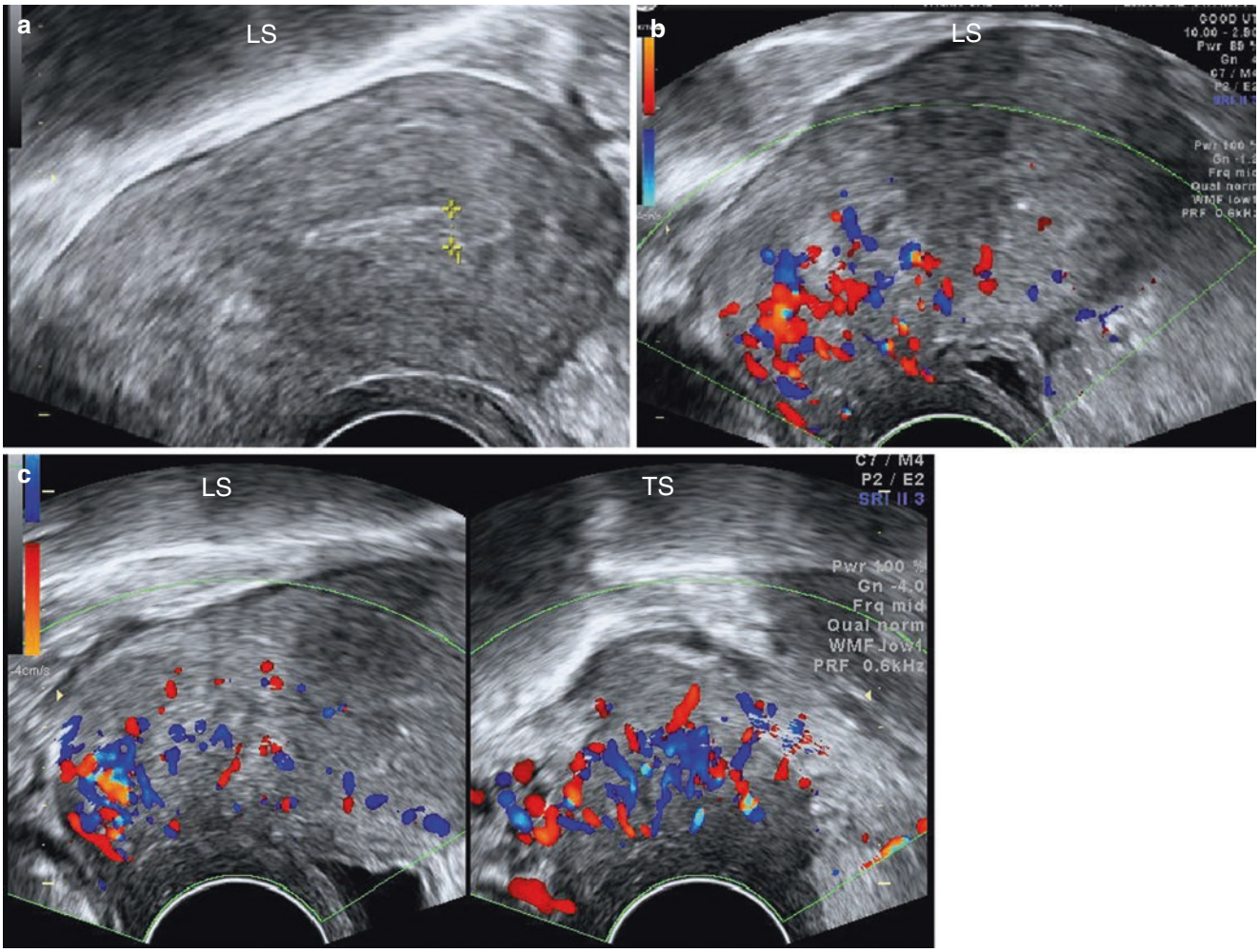

Fig. 5.22 Squamous cell carcinoma extending into the lower uterine corpus. (**a**) Greyscale image showing a bulky, heterogeneous cervix with the margins of the tumour difficult to delineate. (**b**) Suspicious area that was seen on greyscale shows increased flow on Doppler. (**c**) Heterogeneous cervix with the tumour margins and cervical canal not well delineated. Doppler helped identify the neoplastic tissue

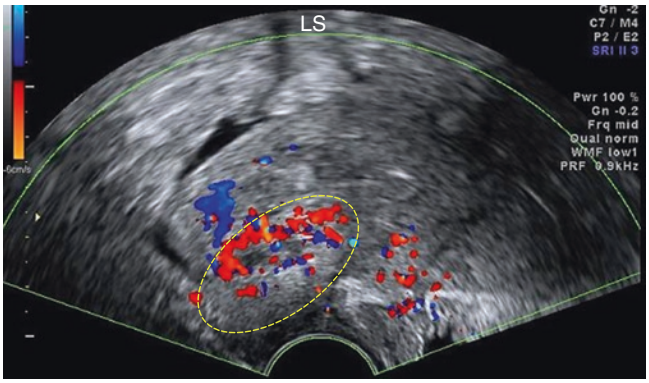

Fig. 5.23 Early squamous cell carcinoma of the cervix (oval outline). Anterior cervical wall is bulky with increased vascularity in a focal area

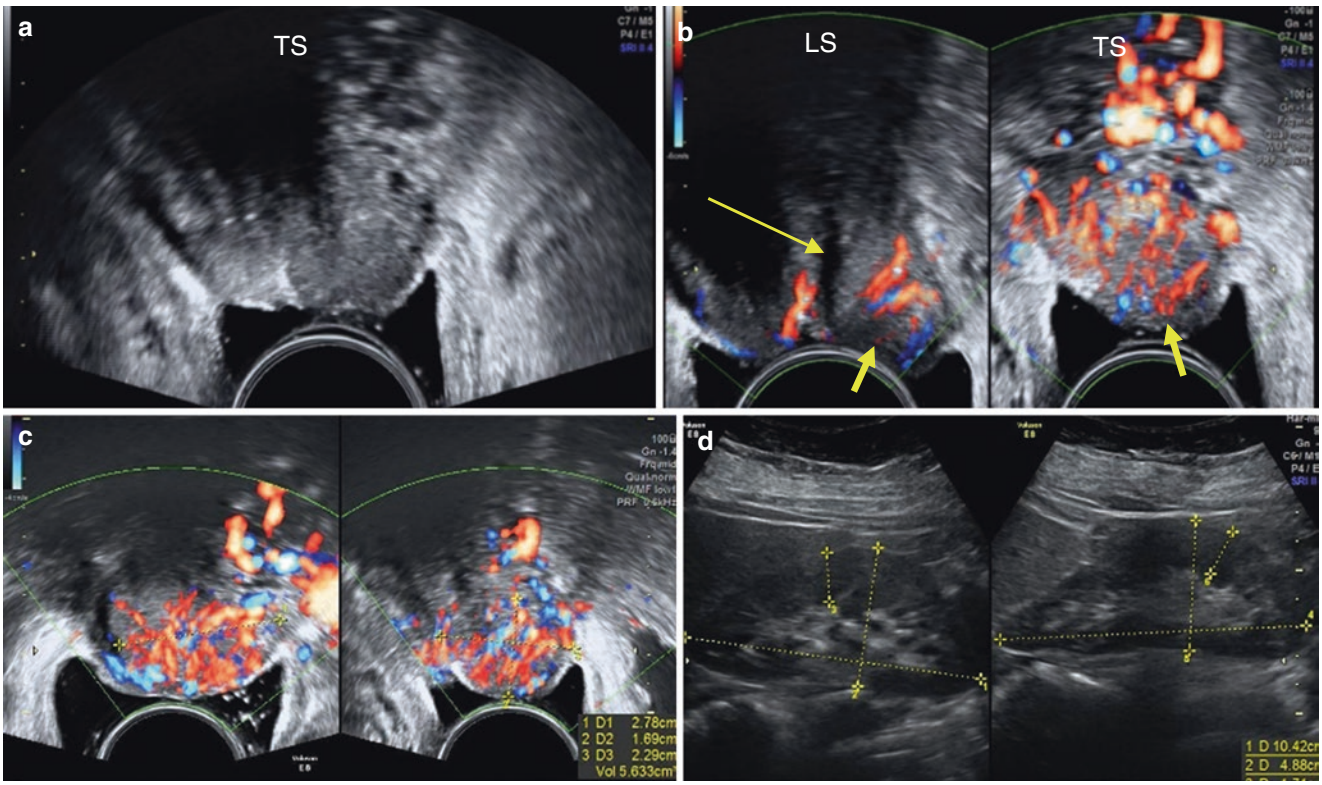

Fig. 5.24 Case of squamous cell carcinoma of cervix Stage III. Scan was done to assess tumour size after six doses of RT. (**a**) Small hypoechoic lesion is seen in the anterior lip of the cervix. (**b**) Cervical canal (*long arrow*) seen. Flow seen in tumour mass (*short arrows*). (**c**) Extent of the mass is seen better with Doppler. (**d**) Normal kidneys, with no evidence of hydronephrosis

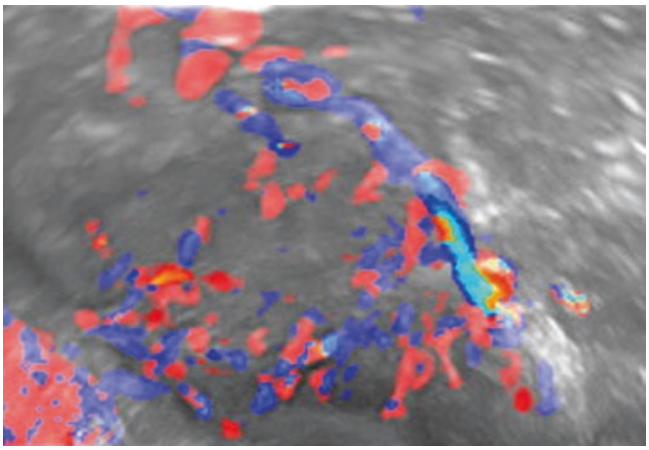

Fig. 5.25 3D HD Doppler with glass body display, showing abnormal morphology of tumour vessels in a case of carcinoma cervix

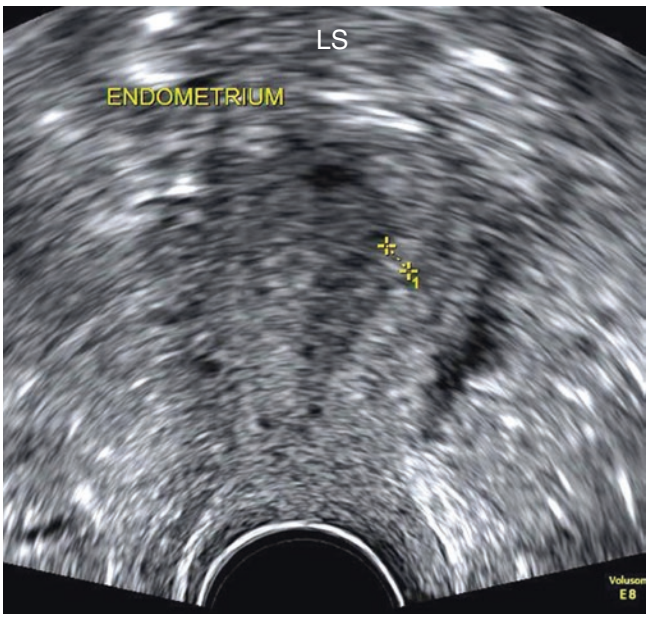

Fig. 5.26 Intrauterine turbid collection seen in a case of carcinoma cervix

Summary: Cervical Carcinoma

- This is a malignancy commonly seen in many developing countries. Typical symptoms are post-coital bleeding, intermenstrual bleeding and vaginal discharge.
- Ultrasound is useful in detecting the presence of tumour, assessing the spread and evaluating the residual tumour after treatment. Though FIGO staging is clinical and MRI is the most common modality used to assess spread, ultrasound, in many recent articles, has been found to be as effective as MRI in staging.
- On ultrasound, these appear as solid isoechoic or hypoechoic lesions that show high vascularity. Their size, distance from internal os and spread to adjoining structures, including the parametrium, can be assessed on regular TVS or transrectal ultrasound. GSV, in the author's opinion, is also a great technique to assess the tumour and its spread.

Suggested Reading

Belitsos P et al (2012) Three-dimensional power Doppler ultrasound for the study of cervical cancer and precancerous lesions. Ultrasound Obstet Gynecol 40:576–581. doi:10.1002/uog.11134

Chiappa V et al (2015) Agreement of two-dimensional and three-dimensional transvaginal ultrasound with magnetic resonance imaging in assessment of parametrial infiltration in cervical cancer. Ultrasound Obstet Gynecol 45:459–469. doi:10.1002/uog.14637

Epstein E et al (2010) Sonographic characteristics of squamous cell cancer and adenocarcinoma of the uterine cervix. Ultrasound Obstet Gynecol 36:512–516. doi:10.1002/uog.7638

Fischerova D (2011) Ultrasound scanning of the pelvis and abdomen for staging of gynecological tumors: a review. Ultrasound Obstet Gynecol 38:246–266. doi:10.1002/uog.10054

Gaurilcikas A et al (2011) Early-stage cervical cancer: agreement between ultrasound and histopathological findings with regard to tumor size and extent of local disease. Ultrasound Obstet Gynecol 38:707–715. doi:10.1002/uog.9037

Sibal M (2016) Gel Sonovaginography: A New Way of Evaluating a Variety of Local Vaginal and Cervical Disorders. J Ultrasound Med 35(12):2699–2715

Testa AC et al (2009) Dynamic and interactive gynecological ultrasound examination. Ultrasound Obstet Gynecol 34:225–229. doi:10.1002/uog.7309

Wildenberg JC et al (2016) US of the nongravid cervix with multimodality imaging correlation: normal appearance, pathologic conditions, and diagnostic pitfalls. RadioGraphics 36(2):596–617

Ultrasound Evaluation of the Vagina

6

The vagina is a structure that is generally overlooked during the ultrasound imaging of the female pelvis done for the detection of gynecological disease.

On a transabdominal ultrasound (TS) in the midsagittal plane, the normal vagina is seen below the uterus as a hypoechoic elongated structure with a central bright linear echo (which represents the collapsed vaginal lumen between opposing vaginal walls). On TAS, only the upper half of the vagina can be seen, as the lower part is obscured by shadowing from the pubic symphysis.

On a transvaginal scan, evaluating the vagina is possible, though often considered suboptimal because of the proximity of the vagina to the probe and the collapsed nature of the vaginal walls. MRI has therefore been commonly used in the diagnostic evaluation of the vagina. Transrectal examination may help when TVS is not possible or there is local bleeding. Gel sonovaginography (GSV) has been used by the author for evaluating suspected or known vaginal pathology as it provides better resolution and spatial orientation.

For ultrasound (TVS) evaluation, it is important that the probe, once introduced into the vagina, is gradually moved upwards, while simultaneously evaluating the anterior and posterior vaginal walls. The vagina is limited on its outer surface by the hyperechoic visceral facia. The posterior vaginal wall is in close proximity to the anterior muscularis of the anus and rectum, and the anterior vaginal wall is in close proximity to the urethra and the base of the bladder. The space between the hyperechoic outer margin of the vagina and the rectum is called the rectovaginal space, while that between the outer margin of the vagina and the bladder is called the vesicovaginal space. Both of these spaces are comprised of areolar tissue.

The common vaginal pathologies encountered are congenital vaginal anomalies, vaginal cysts, vaginal masses and deep infiltrating endometriosis.

6.1 Normal Vagina (Fig. 6.1)

The vagina is a collapsed fibromuscular tubular sheath extending from the vulva to the uterus with the cervix projecting into its upper end. The average length of the vagina is generally 7–9 cm, with the posterior wall being longer than the anterior wall. The vaginal fornices are the upper part of the vagina, and based on their relation to the cervix, they are arbitrarily divided into the anterior, the posterior and the two lateral fornices. The vaginal wall is made up of three layers – the inner mucosa (stratified squamous epithelium), the muscularis (connective tissue and smooth muscle fibres) and the adventitia (endopelvic visceral fascia surrounding the vagina). A small amount of urine within the vaginal lumen in girls of the paediatric age group could be a normal finding.

M. Sibal, *Ultrasound in Gynecology*, DOI 10.1007/978-981-10-2714-7_6

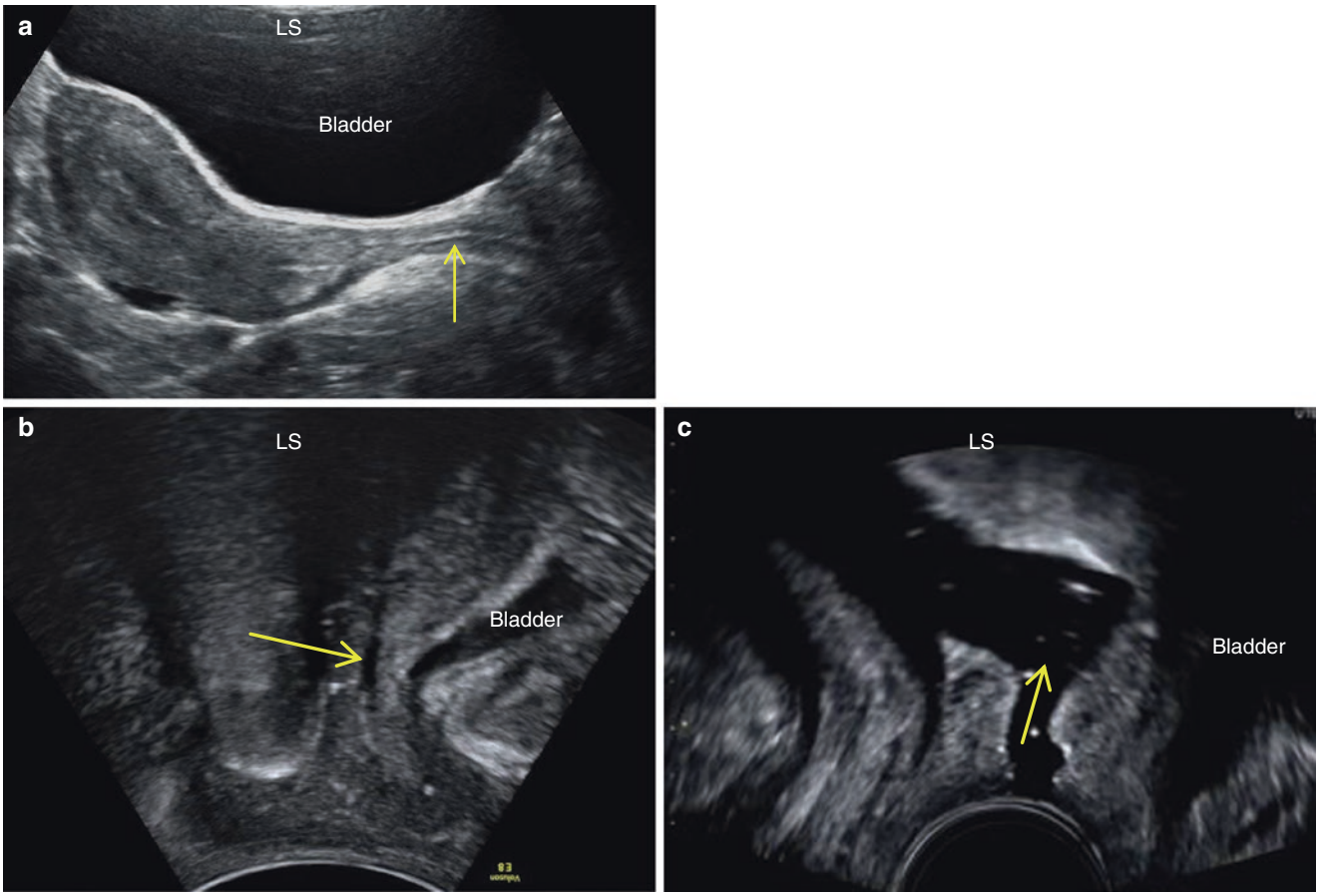

Fig. 6.1 Normal vagina (**a**) TAS – the lumen of the upper vagina is seen as a hyperechoic line (*arrow*) extending down from the lower end of the cervix. The lower vagina cannot be seen due to shadowing by the pubic bones. (**b**) TVS – the vagina is not clearly visualised because of its collapsed lumen (*arrow* showing the lumen of the distal vagina). (**c**) GSV – corresponding to the image in (**b**). Here the vaginal walls are seen apart because of the intervening gel (*arrow*), which facilitates optimal visualisation of the vaginal walls and its lumen

6.2 Congenital Vaginal Anomalies

The upper two-third of the vagina develops from paired Mullerian ducts (from which the uterus and cervix also develop), and the lower one-third develops from paired sinovaginal bulbs. The paired Mullerian and sinovaginal components are solid to begin with. Later, they get canalised. They fuse together with that of the contralateral side to form a common canal. In addition, the Mullerian and sinovaginal components also fuse together to form a single common vagina. A persistent transverse septum can result from incomplete canalisation at various levels of the vagina. If the lateral fusion or resorption of the paired Mullerian ducts is abnormal, a longitudinal septum will result (which is common in association with anomalies of the uterus and cervix like a septate uterus or a bicornuate uterus). *Longitudinal and transverse vaginal septa* are dealt with in the chapter on 'Uterine Anomalies'.

Imperforate hymen is a common congenital abnormality of the female genital tract with a prevalence of about 0.1 %. This has also been dealt with in the chapter on 'Uterine Anomalies' (Chapter 12).

6.3 Vaginal Cysts (Figs. 6.2, 6.3, 6.4, 6.5, 6.6, 6.7)

Vaginal cysts are most often incidental findings seen on ultrasound or MRI. Common vaginal cysts are Gartner duct cysts, Mullerian cysts and Bartholin gland cysts. Periurethral cysts (like Skene gland cysts) may also be seen adjoining the vaginal wall.

Other less common vaginal cysts are endometriotic cysts (in association with DIE), inclusion cysts (area of previous surgery), dermoid cysts, etc.

6.3.1 Gartner Duct Cysts and Mullerian Cysts

These cysts result from incomplete regression of the Wolffian (mesonephric) duct or Mullerian (paramesonephric) duct, respectively. It is not possible to differentiate these on ultrasound, and clinically their distinction is of little importance. They are usually asymptomatic unless they are infected, at which time they could cause pain and discomfort.

Ultrasound Features of Gartner Duct Cysts and Mullerian Cysts (Figs. 6.2 and 6.3)

- These cysts are typically seen along the anterolateral wall of the upper vagina, but they may be present anywhere along the lateral aspect of the vagina. The location of the cyst can be found out by observing their relationship to the TVS probe. As the probe is gradually moved upwards, the cyst slides to one side of the probe which lets us know on which side of the vaginal wall the cyst is located.
- They are seen as unilocular well-defined cysts, varying in size from 1 to 7 cm, with an average of about 2 cm.
- Their contents may be anechoic but may appear hypoechoic when they have turbid contents.
- They are non-tender.
- If infected, they may show turbid contents with thick and vascular walls.

6.3.2 Bartholin Gland Cysts

Bartholin glands are mucin-secreting glands that could develop into retention cysts because of the obstruction of their duct, by trauma or infection. These are usually asymptomatic but may get infected and undergo abscess formation, at which time they may be very painful and tender. The patient may complain of a mass at the introitus. The treatment of Bartholin gland cysts appears simple but recurrence is known. These cysts can rarely be malignant.

Ultrasound Features of Bartholin Gland Cysts (Figs. 6.4 and 6.5)

- These cysts are seen located posterolateral to the vaginal introitus (medial to labia minora).
- They are seen as unilocular well-defined cysts, usually 1–4 cm in size.
- Their contents often show internal echoes because of the mucin content or due to infection.
- They are non-tender, unless infected.
- Infected cysts may show thick vascular walls with turbid contents.
- The presence of solid tissue and septa raises the possibility of malignancy.

6.3.3 Skene Gland Cysts

Skene glands are paired glands that lie close to the external urethral meatus with their ducts draining into the urethra. Cysts of the Skene gland may develop due to obstruction of their ducts by infection. They are usually asymptomatic but if they get infected, can cause pain, dysuria, dyspareunia or discharge. These paraurethral cysts can be differentiated from urethral diverticulae (that are seen higher up) by their position low

down, close to the urethral meatus and by the fact that on compressing the Skene's cyst, there is no extravasation of fluid.

Ultrasound Features of Skene Gland Cysts (Fig. 6.6)

- These cysts are seen just anterior to the lower vagina, on either side of the external urethral meatus.
- They are seen as unilocular cysts with smooth margins.
- Their contents are usually anechoic but may show internal echoes, if infected.
- They are non-tender, unless infected.
- They are thick walled and vascular, if infected.

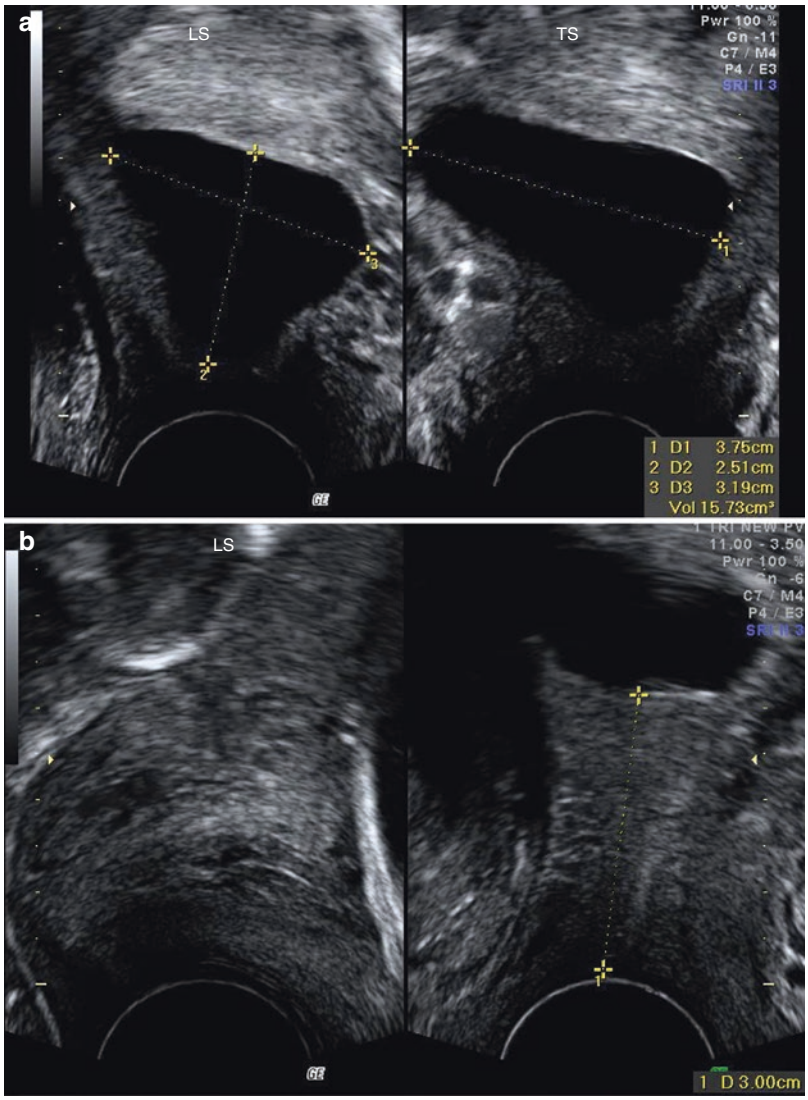

Fig. 6.2 Vaginal cyst. (**a**) A large anechoic cyst is seen in the anterolateral vaginal wall. (**b**) Normal cervix and vagina is seen below the cyst. The lower end of the cyst was some distance away from the introitus. This could either be a Gartner duct cyst or a Mullerian cyst

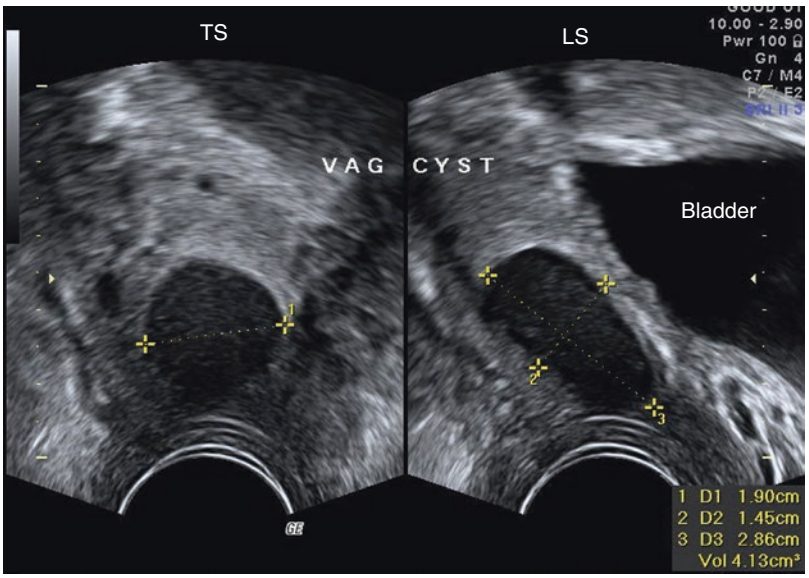

Fig. 6.3 Vaginal cyst. Unilocular turbid cyst in the anterolateral wall of the upper vagina. This could either be a Gartner duct cyst or a Mullerian cyst

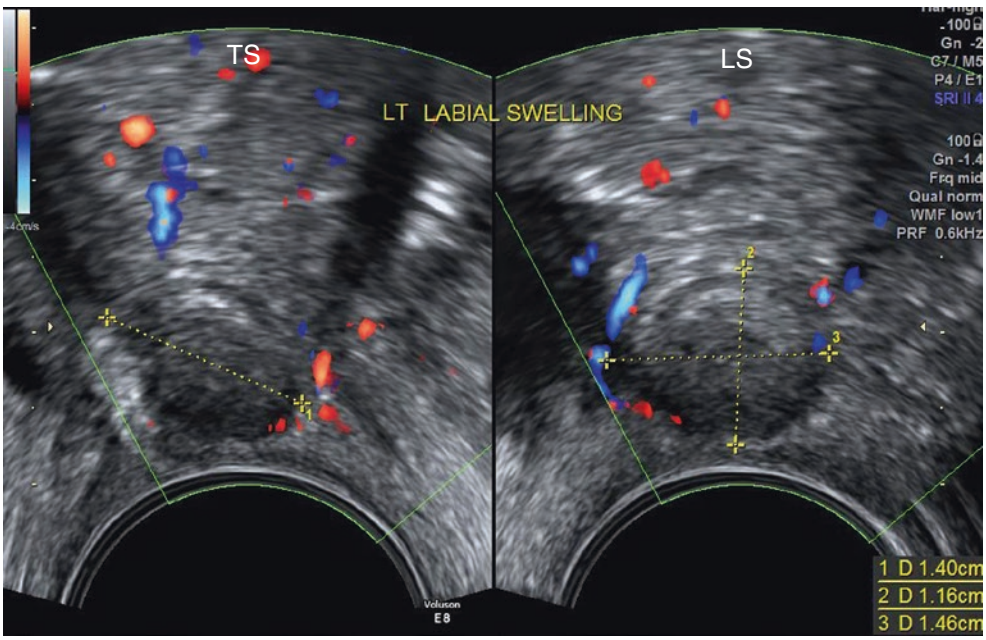

Fig. 6.4 Bartholin gland cyst. A well-defined circumscribed mass seen just above and posterolateral to the vaginal introitus with turbid contents. It did not show any significant flow on Doppler and was not tender

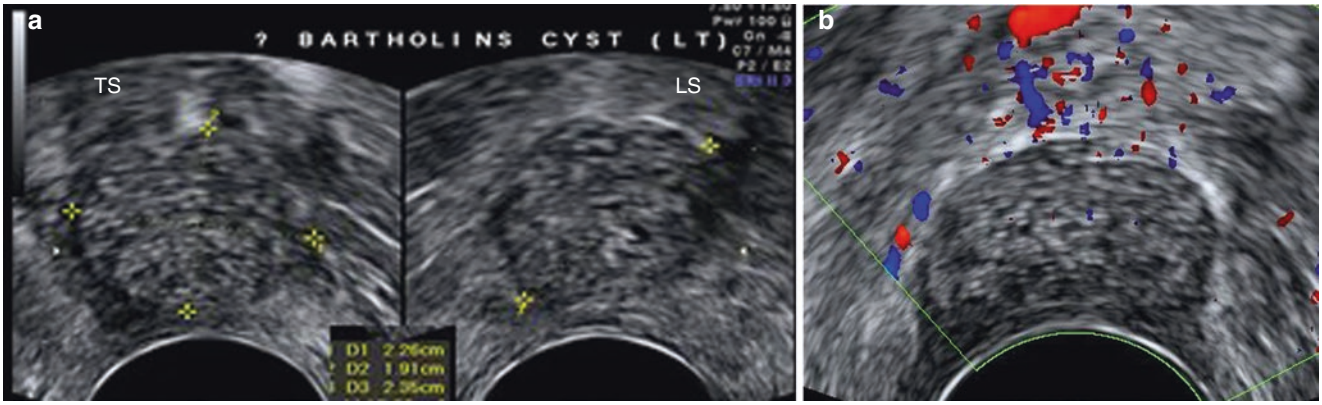

Fig. 6.5 Bartholin gland cyst. (**a**) Hyperechoic scattered foci within. (**b**) No significant flow is seen on Doppler in the cyst walls

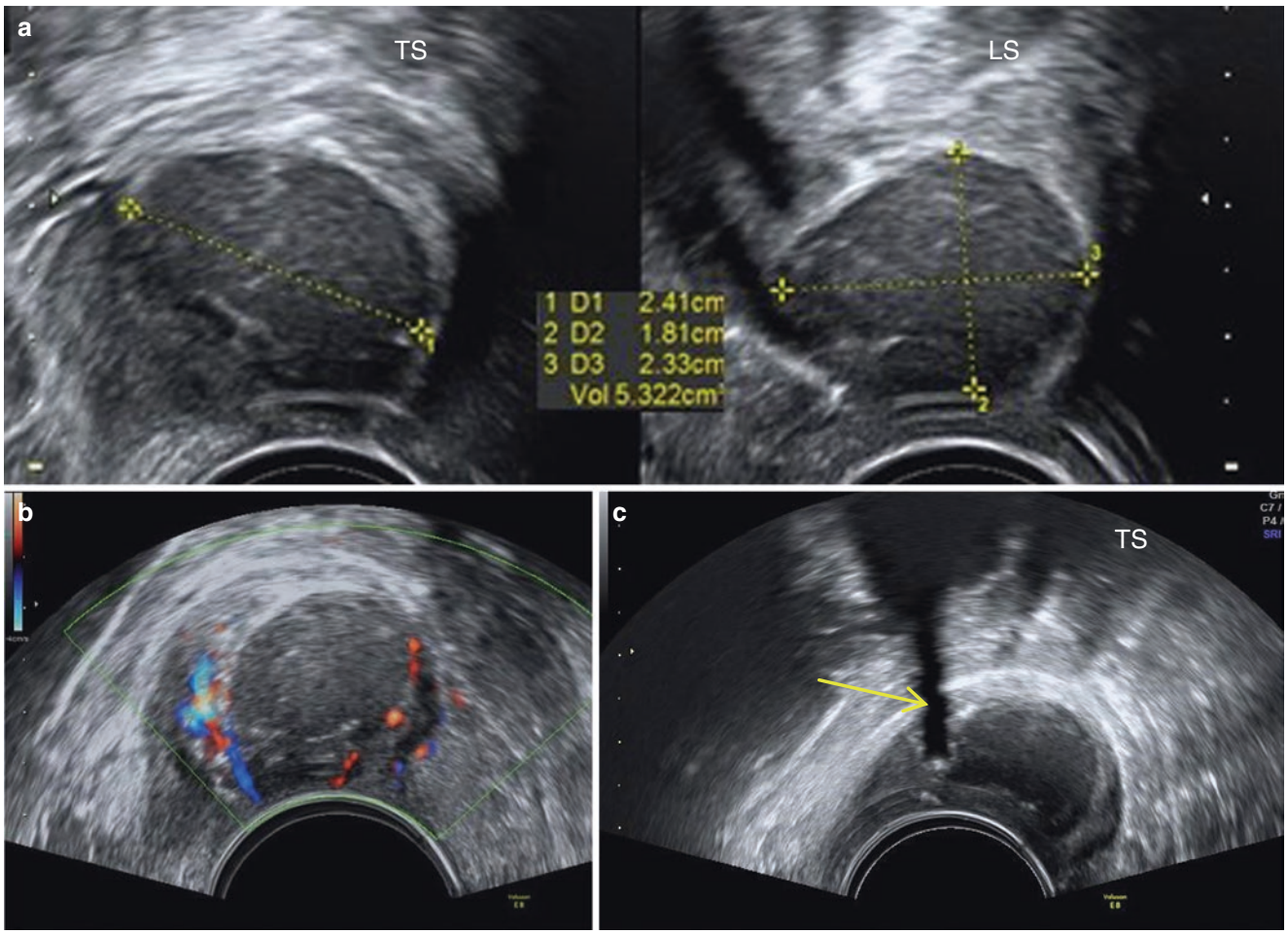

Fig. 6.6 Infected Skene gland cyst. Patient presented with burning micturition and was found to have a small anterior vaginal wall cyst. (**a**) Cyst shows turbid contents. (**b**) Minimal vascularity noted in the cyst walls. (**c**) It was a left-sided paraurethral cyst. In this image, shadowing (*arrow*) from a urethral catheter in situ is noted. There was no intervening tissue between the urethra and the cyst. The cyst was not communicating with the urethra

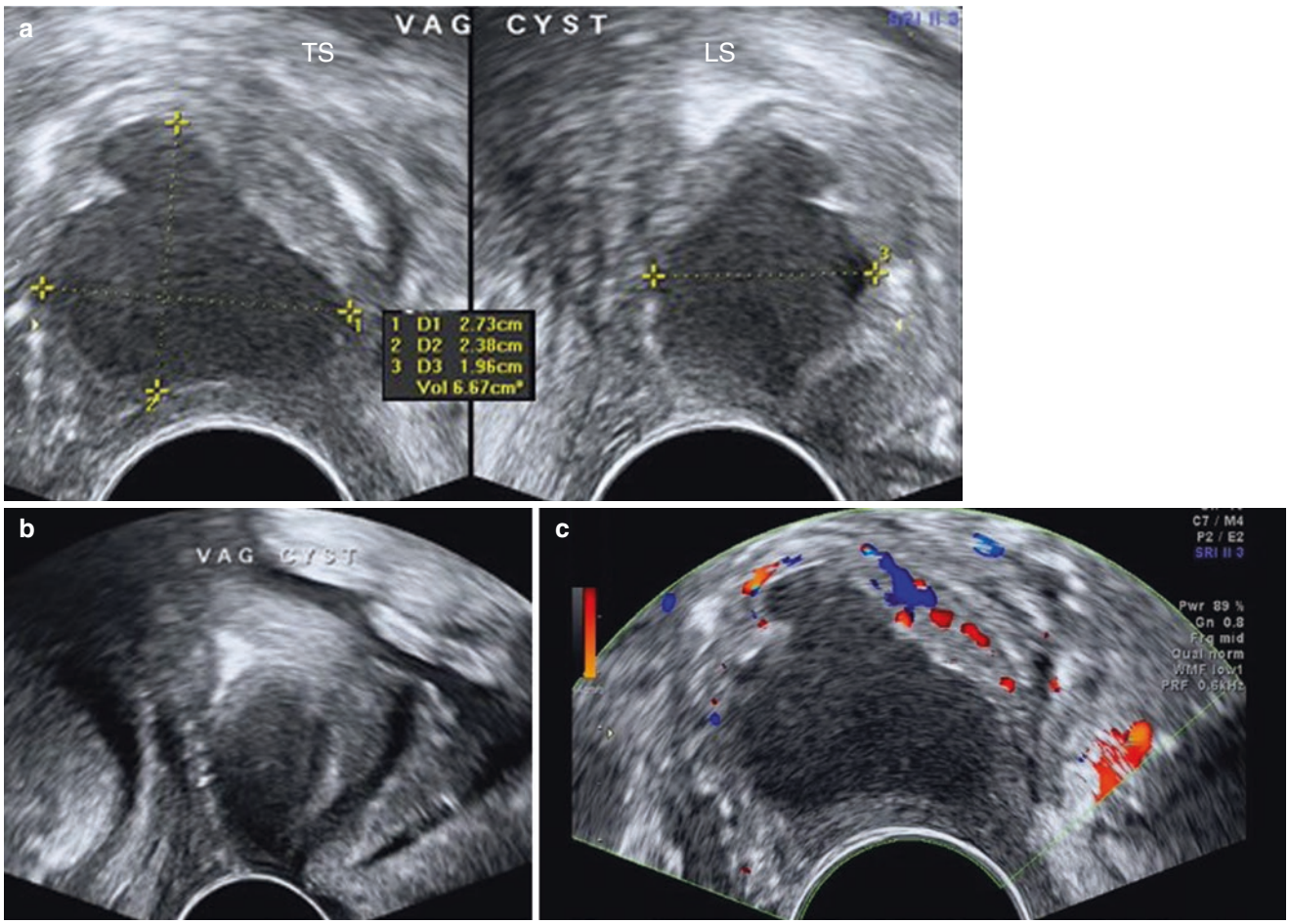

Fig. 6.7 Endometriotic cyst of the vaginal wall. Patient presented with a vaginal mass, intermittent pain and a few episodes of spontaneous discharge from the cyst. During gynecological examination, thick chocolate-coloured fluid was seen draining out the cyst suggestive of endometriotic fluid. (**a**) Cyst showing turbid contents and thick walls. (**b**) Cyst is seen in the anterior wall, just behind the bladder and more to the right. (**c**) Cyst walls showing moderate vascularity (RI 0.76)

Summary of Vaginal Cysts

- Vaginal cysts can be of varied aetiology. They are most often asymptomatic except if secondarily infected. Very rarely are they malignant.
- Gartner duct cysts (remnants of mesonephric ducts) and Mullerian cysts (remnants of paramesonephric ducts) are common cysts seen along the anterolateral part of the upper vagina but may be seen anywhere along the lateral wall of the vagina.
- Bartholin gland cysts are seen in the posterolateral wall of the vagina, close to the vaginal introitus.
- Skene gland cysts are paraurethral cysts seen along the anterior wall of the lower vagina.
- On ultrasound, these cysts appear as well-defined unilocular cysts with anechoic or hypoechoic contents. If infected, they show thick vascular walls with turbid contents.

6.4 Vaginal Masses and Vaginal Cancer

Vaginal masses are not commonly encountered, especially in isolation. Fibroids (leiomyomas) of the vagina are rare. It is more common to find a fibroid in the vaginal lumen which is protruding out of the cervical canal (fibroid polyp – Fig. 6.8) or arising from the cervix and distending the vagina. Occasionally, a benign vaginal polypoid mass may be seen (Fig. 6.9).

Malignant masses of the vagina can be both primary and metastatic. Metastatic carcinomas are much more common (constituting about 80 % of vaginal malignancies) than primary. Spread may occur from contiguous cancers like that of the cervix, vulva or from distant sites through the lymphatic system or the bloodstream or haematogenous spread.

Primary Vaginal Carcinoma

Primary vaginal carcinomas are rare (1–2 % of all gynecological cancers) and are most often squamous cell carcinomas. Other carcinomas are clear cell carcinoma (seen in very young women, often in their teens, associated with intrauterine exposure to DES), melanoma, sarcoma botryoides (in children of the paediatric age group) and leiomyosarcoma.

Vaginal carcinoma (squamous cell) is mostly seen in postmenopausal women, but many have also been reported in very young women. Painless vaginal bleeding, often intermenstrual or post-coital, is the commonest symptom. Vaginal discharge and pelvic pain are also common symptoms. If the tumour has spread to the surrounding bladder or bowel, the patient may complain of dysuria, haematuria, urgency, painful defecation and constipation.

Most cases are picked up on clinical per-speculum examination or colposcopy following a positive PAP smear test. Diagnosis is made on biopsy of the lesion, and staging is done with CT or MRI, though not a FIGO recommendation. Today one can do a good assessment on ultrasound which, though not an established recommendation, is a simple initial assessment modality. It may also be accidentally picked up on an ultrasound done for abnormal bleeding, especially if the lesion is small and was hidden by the blades of the speculum on a prior clinical examination.

Ultrasound Features of Vaginal Carcinoma (Figs. 6.10, 6.11, 6.12)

Evaluation can be done with regular TVS, transrectal scan (especially if there is bleeding or vaginal stenosis) or GSV:

- They are more common in the upper one-third of the vagina and least in the middle one-third. It is important to examine the cervix because the tumour may be an extension from a primary cervical tumour and may not be a primary vaginal carcinoma.
- They are typically hypoechoic, solid tumour masses. Larger ones may appear heterogeneous if there is necrosis within.
- They show increased vascularity (colour score 3 or 4) with vessels most often appearing to arise perpendicularly from the vaginal walls. In large masses, the vascular morphology is abnormal (as in other malignancies), which is best assessed with 3D power Doppler and glass body display.
- Their extension into the paravaginal tissue, bladder or rectum can be assessed on ultrasound and should be done in the sagittal and transverse planes. The tumour is seen as a hypoechoic irregular vascular extension penetrating the external vaginal hyperechoic visceral fascia. The sliding sign of the bladder and rectum along the outer walls of the cervix and vagina, on pressure with the TVS probe, may be absent if there is involvement of the adjoining bladder or bowel wall.
- On regular TVS, their outline and area of spread are difficult to assess as the vagina is a collapsed structure. On GSV, however, the extent of spread along the walls, the extravaginal extension and the vascular pattern can be better assessed.
- A vaginal cancer lesion that involves the cervix (considered so, if the lesion extends up to the external os) or vulva is considered to be a primary cervical or vulval cancer.

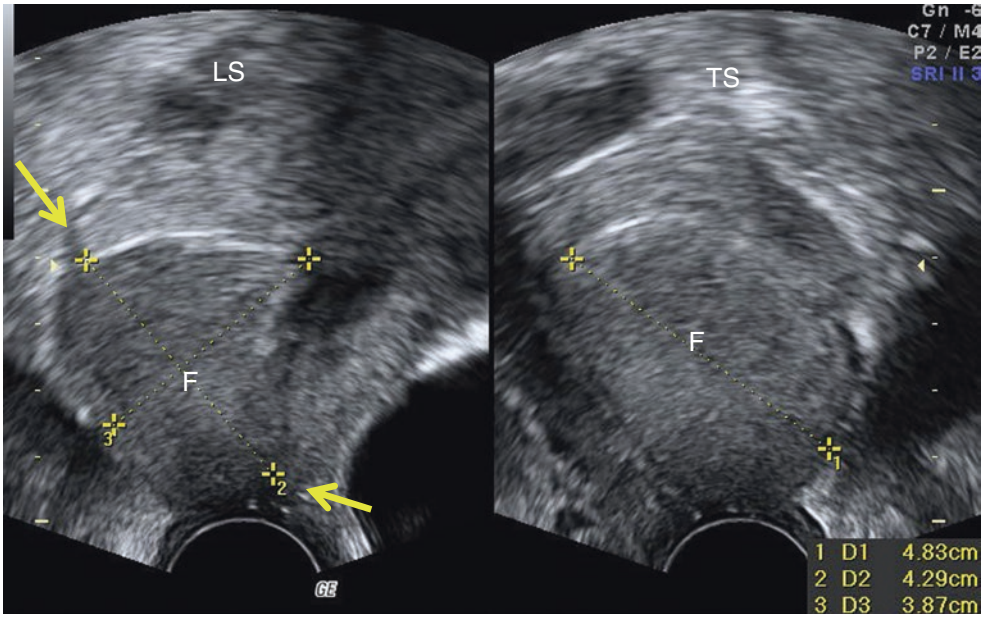

Fig. 6.8 Fibroid polyp (*F*) seen in the upper vagina protruding out of cervical os (cervical lips marked with *arrows*)

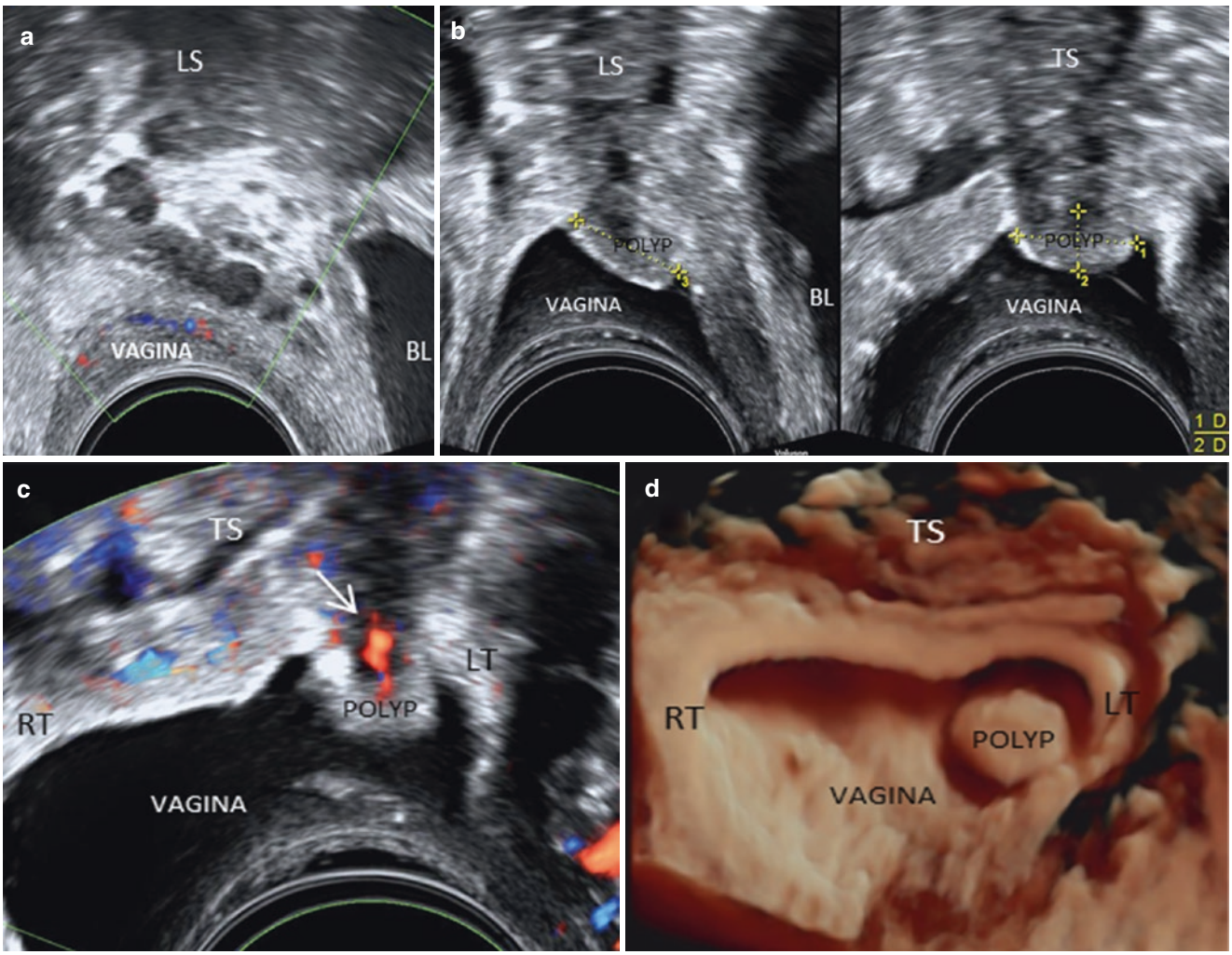

Fig. 6.9 Benign polypoidal mass in the vagina. Patient had undergone a vaginal hysterectomy for cervical dysplasia some years ago. On a routine check, the patient was found to have a polyp on the left side of the vaginal vault. (**a**) Polyp is not visualised on regular TVS. (**b**) On GSV a small vaginal polyp is seen, which is measured in the image. The polyp shows acoustic shadowing. (**c**) A small feeder vessel is seen extending from the vaginal vault into the polyp. No supravaginal extension of the lesion is noted. (**d**) 3D rendered image showing a small circumscribed smooth-walled polyp. Features suggested a benign lesion and the patient was managed conservatively with follow-up

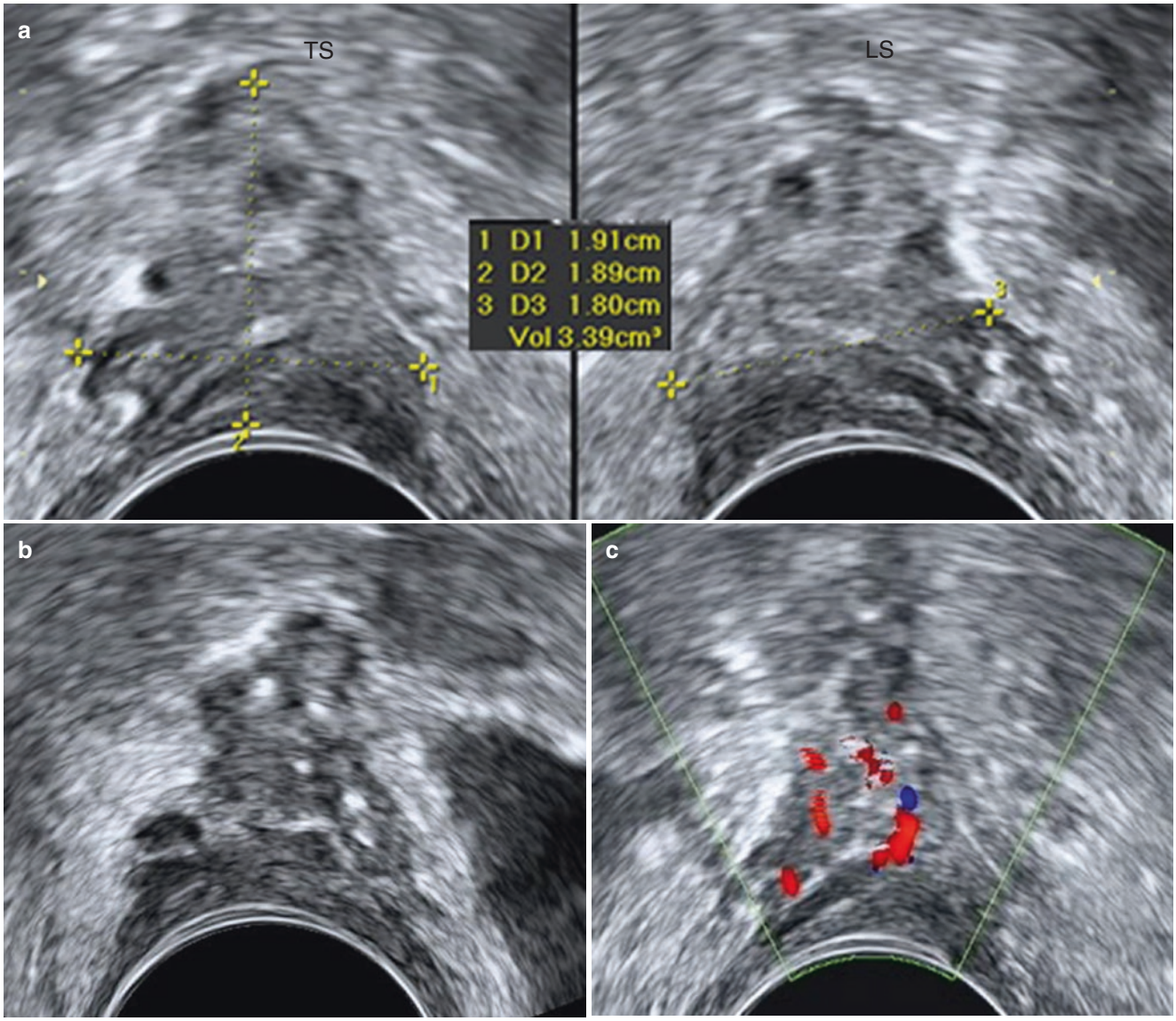

Fig. 6.10 Vaginal vault metastasis. Patient had undergone panhysterectomy for an endometrial carcinoma the previous year. Clinical examination showed a polypoid growth in the vagina. (**a**) A solid heterogeneous mass was seen at the vaginal vault. (**b**) Irregular margins of the mass are seen. (**c**) The mass showed flow within on Doppler. *HPE:* metastatic endometrioid adenocarcinoma

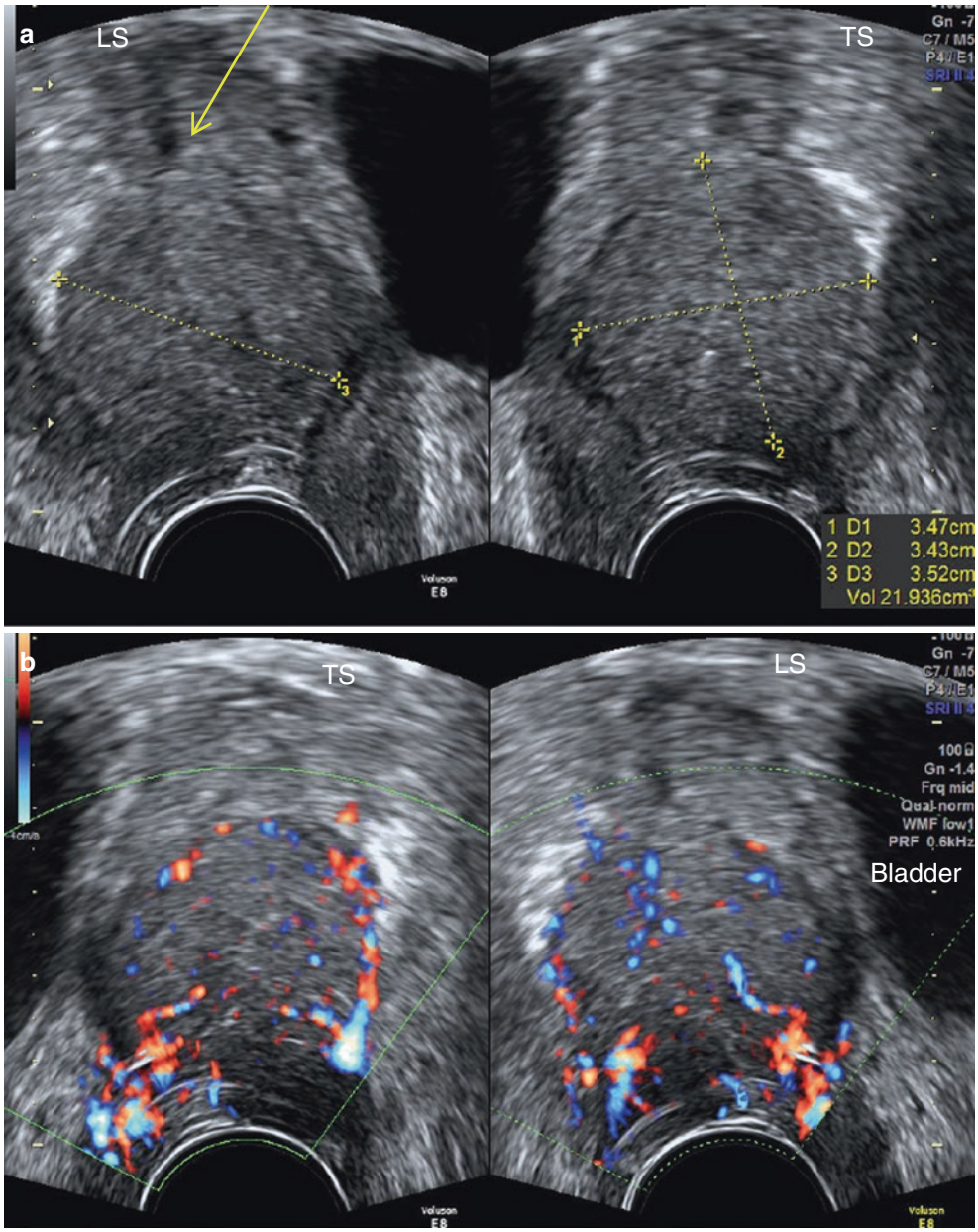

Fig. 6.11 Malignant mass involving the cervix and upper vagina. (**a**) A hypoechoic, solid, heterogeneous mass is seen in the upper vagina. The mass was extending into the cervix, up to the external os (*arrow*), because of which this mass is not considered to be a vaginal cancer but a case of cancer of the cervix. (**b**) Mass showing moderate vascularity

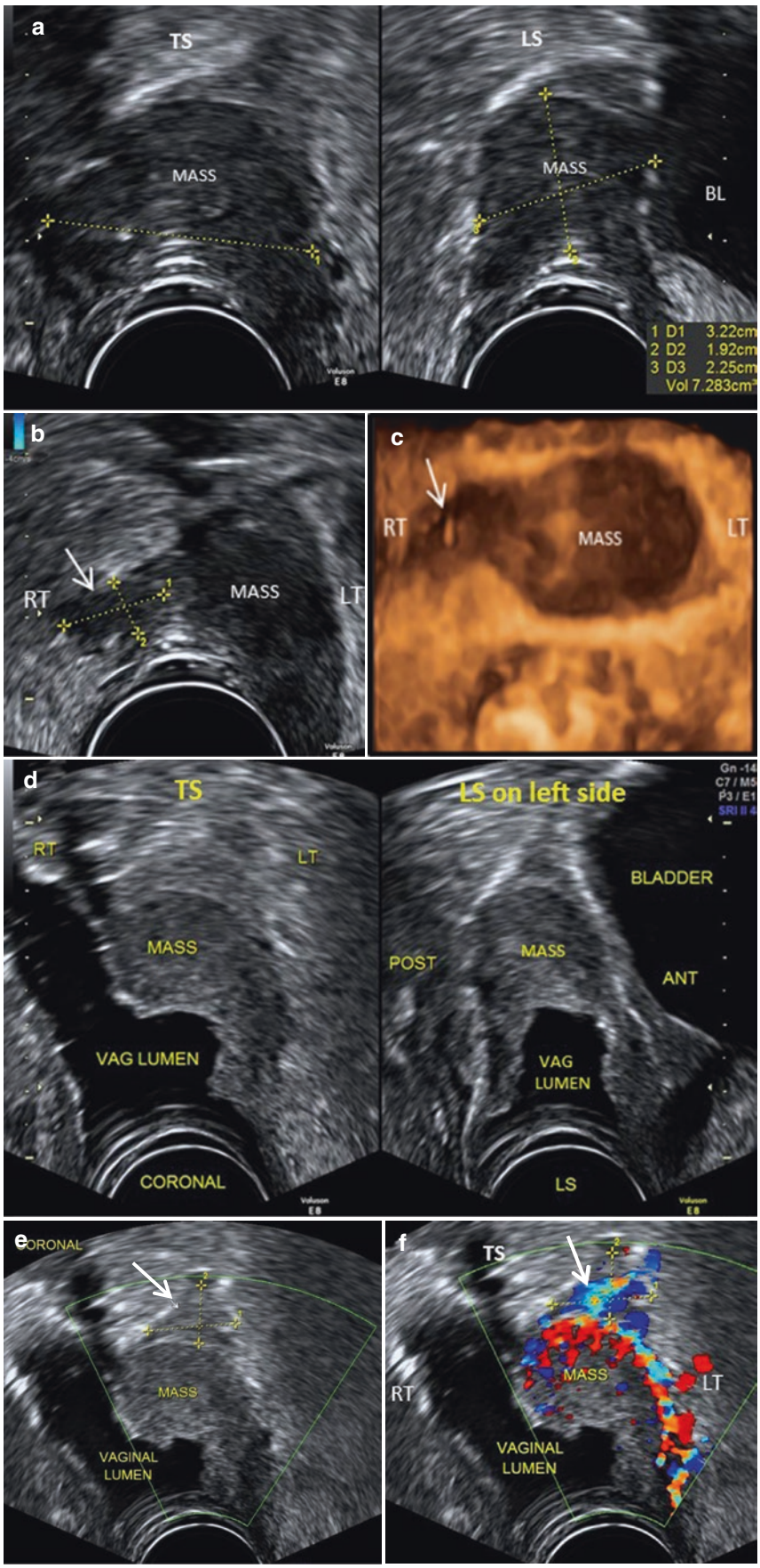

Fig. 6.12 Primary vaginal carcinoma. Hysterectomy was done 18 years ago for menorrhagia. Patient presented with bleeding. (**a**–**c**) Regular TVS. (**a**) Showing hypoechoic mass in the upper vagina, (**b**, **c**) 2D and 3D images showing a hypoechoic narrow extension (*arrows*) onto the right side, raising a suspicion of right paravaginal infiltration. (**d**–**f**) GSV – mass seen involving the left side of the vagina. The right extension seen earlier on regular TVS was found to be the normal collapsed vagina on the right side, which, on being filled up with vaginal gel, displayed the normal vaginal walls. Supravaginal extension of the mass is seen on greyscale and on Doppler (*arrows*) in (**e**) and (**f**)

Summary: Vaginal Carcinoma

- Vaginal carcinoma is rare. Most vaginal carcinomas are metastatic spreads from the adjoining cervix or vulva or from distant sites through the bloodstream or the lymphatic channels.
- On ultrasound, they are typically seen as hypoechoic, solid, vascular masses which appear heterogeneous if there is necrosis within. Extension into neighbouring bladder, rectum or paravaginal tissue should be assessed.
- A vaginal cancer that involves the cervix (once the external os is involved) is considered to be a primary cervical cancer, and one which involves the vulva is considered to be a primary vulval cancer.
- GSV provides better evaluation of the mass. A transrectal scan may be preferred to a TVS in masses that bleed on touch.

6.5 Other Vaginal Pathologies

6.5.1 Vaginal DIE

This is usually seen in association with endometriosis elsewhere in the pelvis. Vaginal DIE is most often continuous with rectal DIE when it is termed rectovaginal DIE. Associated cervical and uterosacral DIE may also be seen. This is discussed in detail in the chapter on endometriosis (Chapter 8).

6.5.2 Foreign Body in the Vagina (Fig. 6.13)

These could be retained tampons, pessaries, surgical gauze, etc. Most often, foreign bodies in the vagina can be visualised on a per-speculum examination without the need for an ultrasound. However, in cases where a speculum examination is not feasible, as in young girls or women who have had recent surgery, ultrasound may be helpful in diagnosis. Occasionally, it could be an incidental finding (e.g. a forgotten pessary).

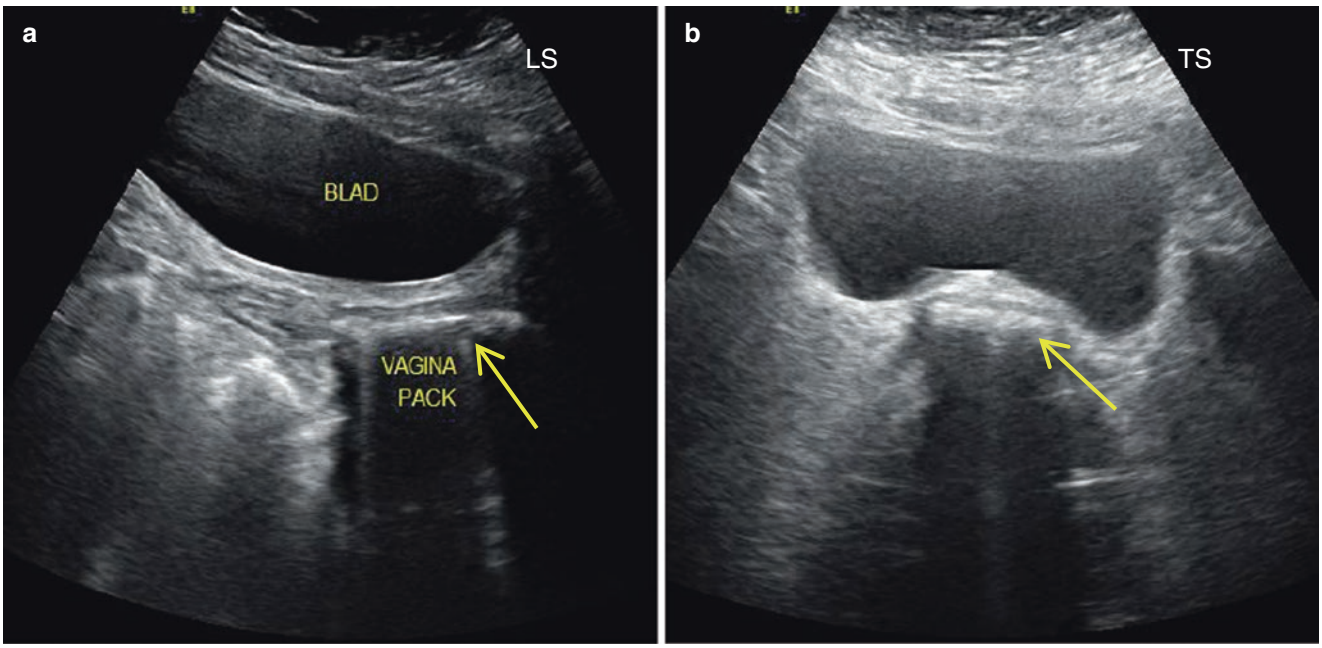

Fig. 6.13 Vaginal pack that was placed in the vaginal vault for bleeding, two and a half weeks after hysterectomy. Scan was done to rule out any intra-abdominal bleed. On scan, no evidence of intra-abdominal bleed was noted. The vaginal pack (*arrows*) is seen on (**a**) LS and (**b**) TS as a hyperechoic linear area with significant acoustic shadowing

6.6 Vulval Carcinoma (Fig. 6.14)

Vulvar cancer is cancer that occurs on the outer surface area of the female genitalia. The vulva is the area of the skin that surrounds the urethra and the vagina. Vulvar cancer commonly forms as a lump or a sore on the vulva that often causes itching. Though it can occur at any age, vulvar cancer is most commonly seen in older women. Patients may present with a lump, local itching, discolouration of skin or a growth at the vulva.

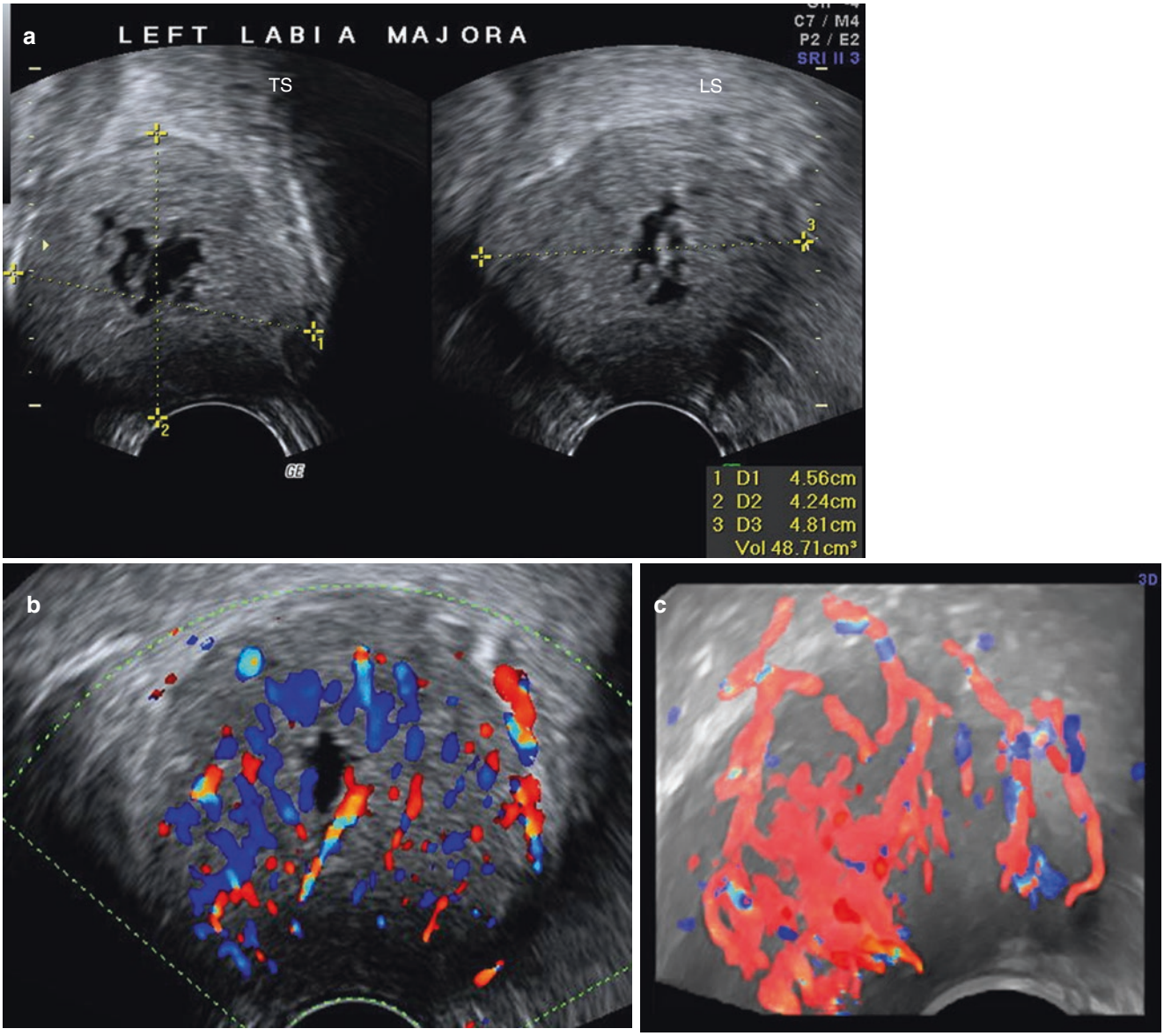

Fig. 6.14 Vulval carcinoma. (**a**) A circumscribed, solid, heterogeneous mass is seen. It shows an irregular, central, cystic area suggestive of necrosis. (**b**) The mass shows high vascularity (colour score of 4). (**c**) 3D Doppler with glass body display shows abnormal vascular morphology of the mass

Suggested Reading

Fischerova D (2011) Ultrasound scanning of the pelvis and abdomen for staging of gynecological tumors: a review. Ultrasound Obstet Gynecol 38:246–266. doi:10.1002/uog.10054

Sibal M (2016) Gel Sonovaginography: A New Way of Evaluating a Variety of Local Vaginal and Cervical Disorders. J Ultrasound Med 35(12):2699–2715

Walker DK et al (2011) Overlooked diseases of the vagina: a directed anatomic-pathologic approach for imaging assessment. Radiographics 31:1583–1598

Wang X et al (2014) Transvaginal sonographic features of perineal masses in the female lower urogenital tract: a retrospective study of 71 patients. Ultrasound Obstet Gynecol 43:702–710. doi:10.1002/uog.13251

Ultrasound Evaluation of Ovaries

7

Ovaries are bilateral ovoid masses on either side of the uterus that have a dual function of producing hormones and ova. Each ovary is anchored in the pelvis by the mesovarium to the posterior surface of the broad ligament, by the utero-ovarian ligament to the uterus and by the suspensory ligament to the lateral pelvic wall. These ligamentous structures are lax and not rigid, and consequently the position of the ovaries varies in different patients and in the same patient at different times.

7.1 Evaluation of Ovaries and Persistent Adnexal Masses

7.1.1 Morphology, Measurement and Doppler Evaluation of the Ovary and Ovarian Masses (Including Persistent Adnexal Masses)

- The ovaries (Fig. 7.1) are identified in the reproductive age group by the presence of follicles. They are typically located just medial to the external iliac vessels and anterior to the internal iliac vessels. Therefore, on a transverse section, the external iliac vessels lie lateral to it, and on a longitudinal section, the internal iliac vessels lie posterior to it. Most often, the ovaries are easy to locate on either side of the uterus, but at times this can be challenging. This is more likely in postmenopausal women with atrophic (small in size and without follicles) ovaries. The ovaries can usually be located on ultrasound by angulating the probe from a TS view of the uterus along the hypoechoic utero-ovarian ligament from one cornu to the lateral pelvic wall. Another method to locate the ovary is to trace along the external iliac vessels in a transverse section of the pelvis. The normal ovary in a woman of reproductive age group shows a few antral follicles. Antral follicles are seen as small anechoic cysts in the ovary, 2–9 mm in diameter. A developing follicle or corpus luteum (CL) may also be seen, depending on the phase of the menstrual cycle. Details of assessing developing follicles and corpus luteum are given in the section on follicular tracking in Chap. 13. The ovaries are measured in all cases. Their mobility is also assessed by applying pressure with the TVS probe. Normally the ovaries are mobile structures and slide along or can be made to move away from the uterus and lateral pelvic wall. However, they could be adherent to the uterus or the lateral pelvic wall in the presence of pathological conditions like endometriosis.
- If there is an ovarian mass, then the ovary is evaluated further in detail as given below, primarily based on IOTA recommendations.

Morphological Description (Figs. 7.2, 7.3, 7.4, 7.5, 7.6, 7.7, 7.8 and 7.9)

- *Crescent sign* (Fig. 7.2): An ovarian mass may show ovarian tissue adjoining and stretched around it, called the 'crescent sign', which helps in determining its ovarian origin. In large masses, the ovarian tissue may be completely compressed, such that no ovarian tissue is identifiable around it.
- *Solid component* (Fig. 7.3): The presence of a solid tissue increases the likelihood of malignancy. Doppler flow helps to confirm the presence of solid tissue. The solid tissue may be present along the margins of the mass or may be present within the mass. Some ovarian masses may be completely solid. The presence of a papillary projection (as described later) is also considered a solid component of a cyst. The absence of solid tissue in a mass (i.e. a completely cystic mass) increases the likelihood of it being benign.
- *Papilla* (Fig. 7.4): Any solid projection into the cavity from the cyst wall, with a height of at least 3 mm (from the inner margin of the cyst), is considered a papilla. The presence of a papilla increases the likelihood of malignancy.
  Any solid projection of less than 3 mm is considered an irregularity in the cyst wall. If the maximum diameter of the largest solid component or papilla is less than 7 mm, then there is a high probability that the mass is a benign cystadenofibroma.

M. Sibal, *Ultrasound in Gynecology*, DOI 10.1007/978-981-10-2714-7_7

- *Septum and a number of locules* (Figs. 7.5 and 7.6): A septum is a strand of tissue originating from one wall of the cyst to the other. The correct way to measure the septum is when it is perpendicular to the ultrasound beam. Septae of less than 3 mm are more commonly seen in benign cysts, whereas septae which are more than 3 mm and irregular are more commonly associated with malignant masses.
  In the absence of septum, a cyst is considered unilocular. A cyst with one or more septae is considered multilocular. The locules may vary from 2 to as many as 100. An incomplete septum as seen in a hydrosalpinx is not considered a true septum, and the cystic mass is still considered unilocular.
  Unilocular cysts are more likely to be benign.
- *Walls of the mass* (Fig. 7.7): The more irregular the inner walls of a cystic mass or the external walls of a solid mass, the more likely it is to be malignant.
- *Contents of a cyst* (Fig. 7.8): The contents of a cyst are not useful in assessing the likelihood of malignancy. However, it is often useful in the characterisation of the mass into various histopathologies. The cyst may be anechoic, show low-grade internal echoes, be hypoechoic with a ground glass appearance or show mixed echoes with hypoechoic and hyperechoic contents. The cystic contents may show fluid–fluid level.
- *Acoustic shadowing* (Fig. 7.9): Loss of echoes beyond a sound-absorbing structure is called acoustic shadowing. It is seen typically in dermoids, fibromas and behind the papillae of a cystadenofibroma. The presence of acoustic shadowing increases the likelihood of the mass being benign significantly.

Measurements (Figs. 7.10 and 7.11)

- Lesions and ovaries – The size of both the ovaries and any lesion should be measured in three perpendicular dimensions (x, y and z) in two perpendicular planes and given in millimetres (as explained in Chap. 2). From this, the volume of the mass can be calculated by the formula '$x \times y \times z \times 0.523$'.
  At times, the cyst is very large and its entire margins cannot be visualised in a single screen. One can increase the sector angle and depth. However, with very large masses, even this may not suffice. In such cases, in order to approximately measure these masses (particularly the length of the mass per abdomen which may be difficult), one can resort to a dual image on screen, so that one margin of the mass to beyond the centre of the mass is captured in the image on one half of the screen and the opposite margin to beyond the centre of the mass is captured in the image on the other half of the screen. The length of the mass is measured in two parts. One measurement is taken from one margin to some common reference point closer to the centre in one image and the second, from the same reference point in the second image to the other opposite margin of the mass. The final length is the sum of these two measurements. A large cyst can also be measured using the panoramic imaging mode, available in some ultrasound machines.
  - Septum (Fig. 7.5) – The septum is measured where it appears to be the thickest (not close to its attachment to the internal cyst wall). It is preferable to measure a septum with the ultrasound beam perpendicular to it.
  - Papilla – The largest projection is measured in three dimensions, in two perpendicular planes (height, base and base). The number of separate papillary projections should also be noted. When in doubt about the number of papillae, particularly when they appear to merge with one another, it is recommended that the worst-case scenario should be applied. For example, if there is a doubt of 3–5 papillae, it is better to consider it as 5 papillae.
  - The number of locules in the tumour is also assessed (1 to 10 and more than 10).
  - The largest solid component should be measured in three orthogonal diameters in two perpendicular planes. This applies to papillary projections also, if it is the largest solid component.
  - Fluid in POD – It is measured in a sagittal section of the uterus, and the largest AP measurement is noted in millimetres.

Doppler Study (Figs. 7.12 and 7.13)

- *Doppler study of the ovarian mass*: The entire tumour should be examined by Doppler imaging. Flow may be seen in the walls, septae, solid areas and papillae. Flow within solid areas and papillae is, however, more often associated with malignancy. For Doppler flow assessment, settings must be optimised. Generally, the PRF should be set at 0.3 for colour Doppler and 0.6 for power Doppler (in some machines, this is equivalent to velocity scale of 3–6 cm/sec). Thereafter, the Doppler gain should be increased until artefacts appear, following which gain should be gradually reduced to when the artefacts just disappear. Ultrasound frequency should be at least 5.0 MHz and wall filter should be between 30–50 Hz. It is useful to have preadjusted Doppler settings for gynecological scans to save time and for appropriate evaluation.
  - *Colour index* (Fig. 7.12): The most accepted method of assessing Doppler flows is colour scoring, a subjective semi-quantitative evaluation where scores are given from 1 to 4:
    1 – no flow
    2 – minimal flow (few colour spots)
    3 – moderate flow
    4 – abundant flow
    The absence of flow (colour score 1) increases the likelihood of the mass being benign. Colour score of

3–4 increases the likelihood for malignancy but may also be seen in benign adnexal masses, infections, corpus luteum and trophoblastic tissue.

Flow indices (Fig. 7.13): When several samples are taken, the set of results with the highest peak systolic velocity (PSV) and the corresponding values of PI and RI are selected. Malignant masses generally show flow with low resistance, i.e. an RI of less than 0.4 and PI of less than 1.0. However, a significant overlap is seen between benign and malignant masses with low RI seen in only 25 % of malignant lesions. This is, therefore, less helpful in diagnosis.

– *Colour distribution*: The location of flow may also help in assessing the possibility of malignancy. Malignant masses are more likely to have central flow, while in benign ones, flow is more likely to be peripheral. However, there is a significant overlap noted.

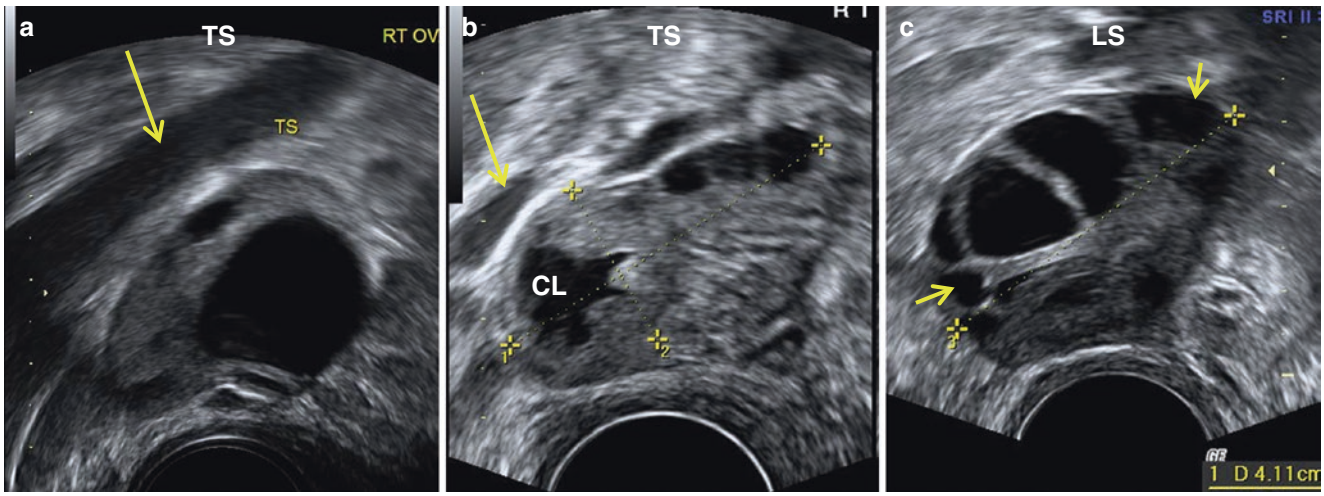

Fig. 7.1 Normal ovaries. (**a**) Ovary with a developing follicle. External iliac vessels (*arrow*) are seen just lateral to the ovary. (**b**) The ovary shows a corpus luteum. External iliac vessels (*arrow*) are seen lateral to the ovary. (**c**) The ovary shows antral follicles (*arrows*)

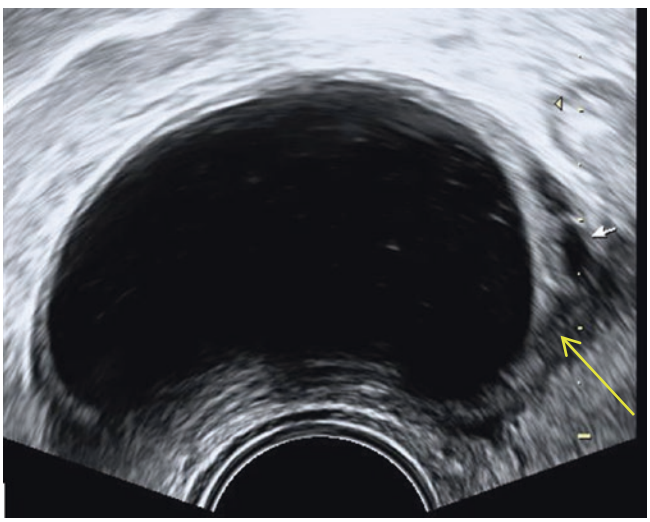

Fig. 7.2 Crescent sign – crescent-shaped ovarian tissue seen adjacent to the ovarian cyst (*arrow*), which is stretched around the cyst as if it were hugging the cyst

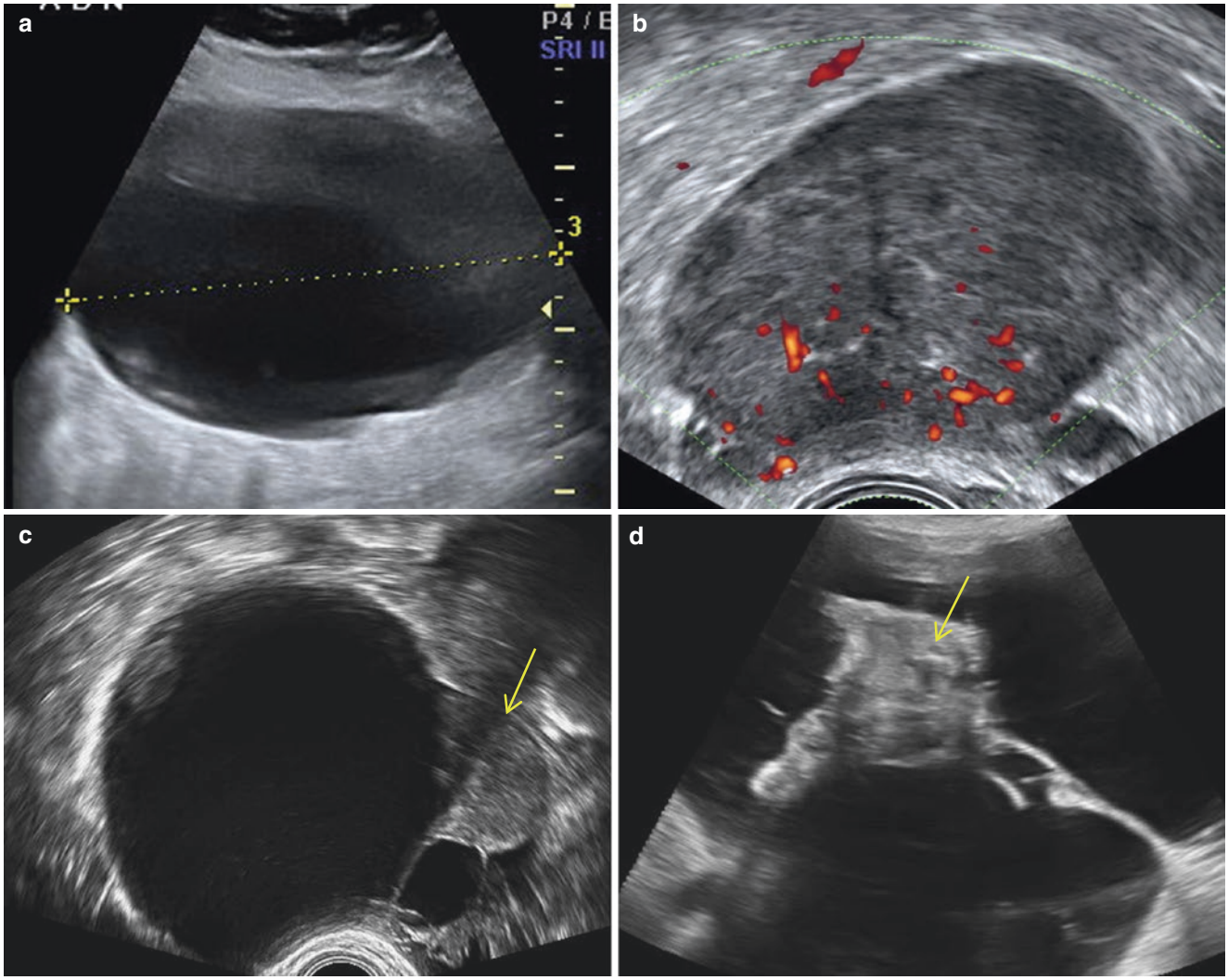

Fig. 7.3 (**a**) No solid component. (**b**) Completely solid mass. (**c**) Solid area (*arrow*) along the outer margins of the mass. (**d**) Solid area (*arrow*) within a predominantly cystic mass

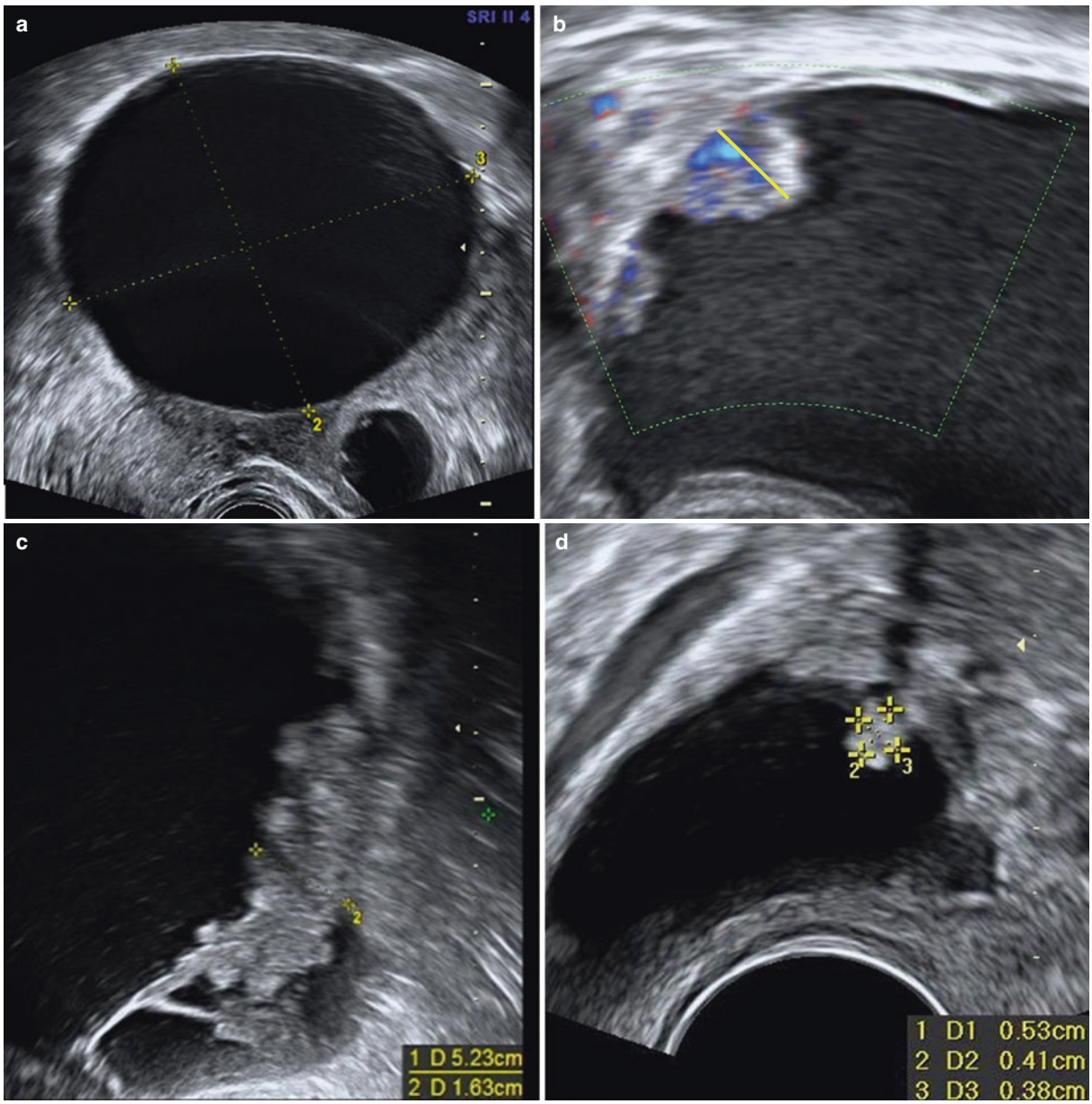

Fig. 7.4 (**a**) No papilla seen. (**b**) Single papilla seen with height of papilla measured in the image. (**c**) Multiple irregular papillae seen along the septae. (**d**) Maximum diameter of papilla is less than 7 mm in this case of a cystadenofibroma

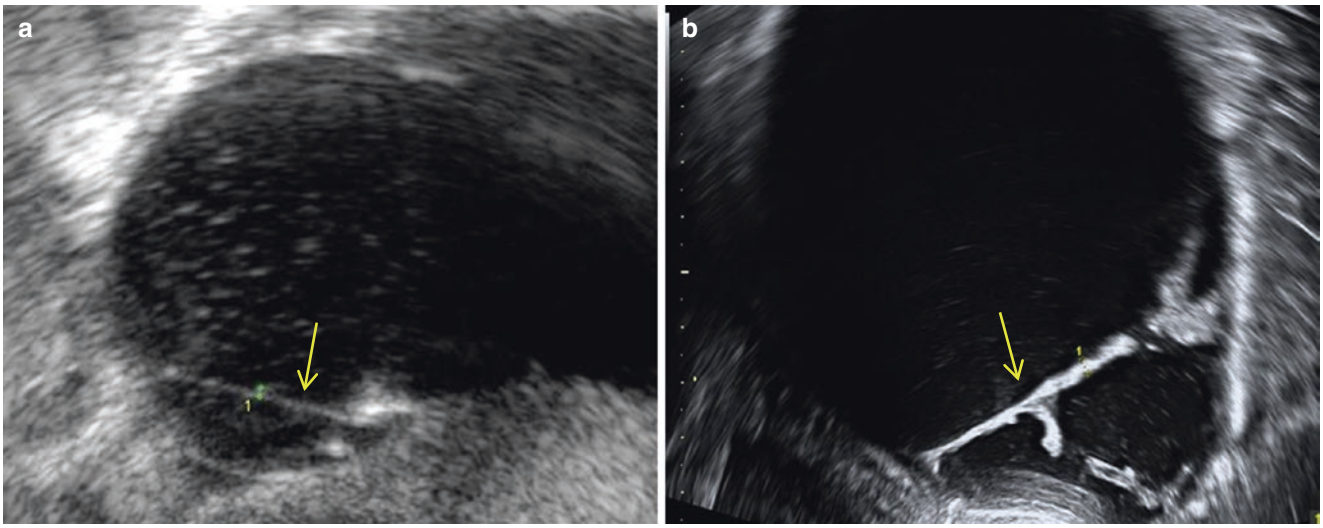

Fig. 7.5 (**a**) Thin septum (*arrow*). (**b**) Thick slightly irregular septum (*arrow*)

Fig. 7.6 (**a**) Unilocular cyst. (**b**) Multilocular cyst

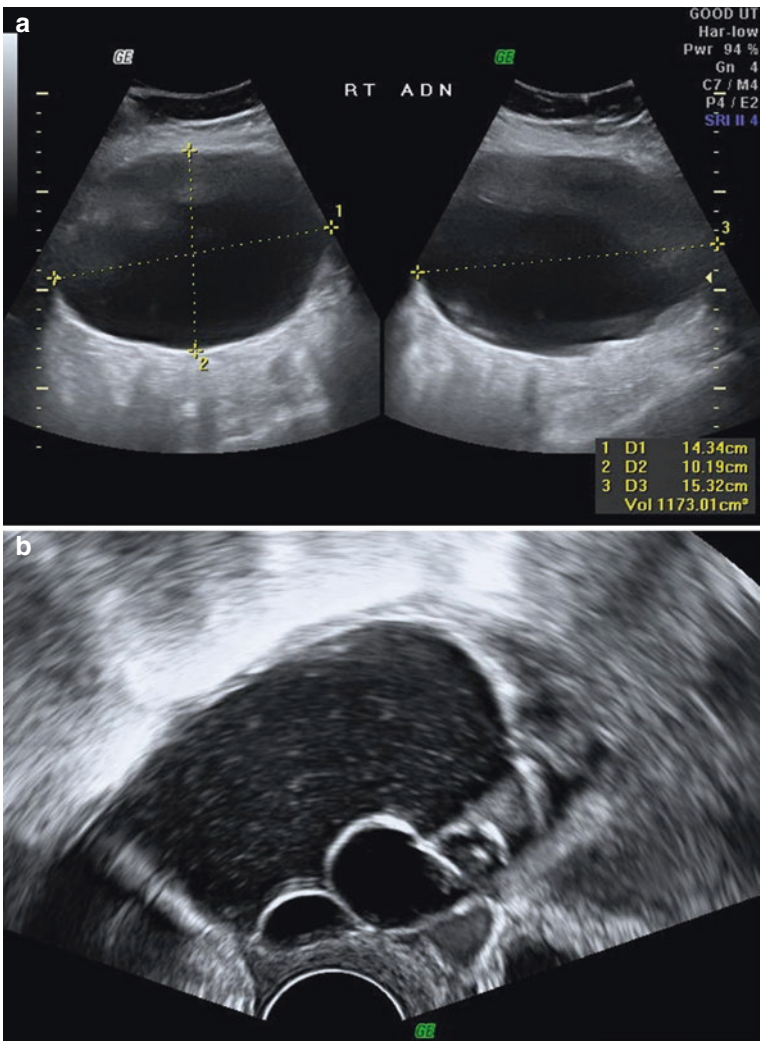

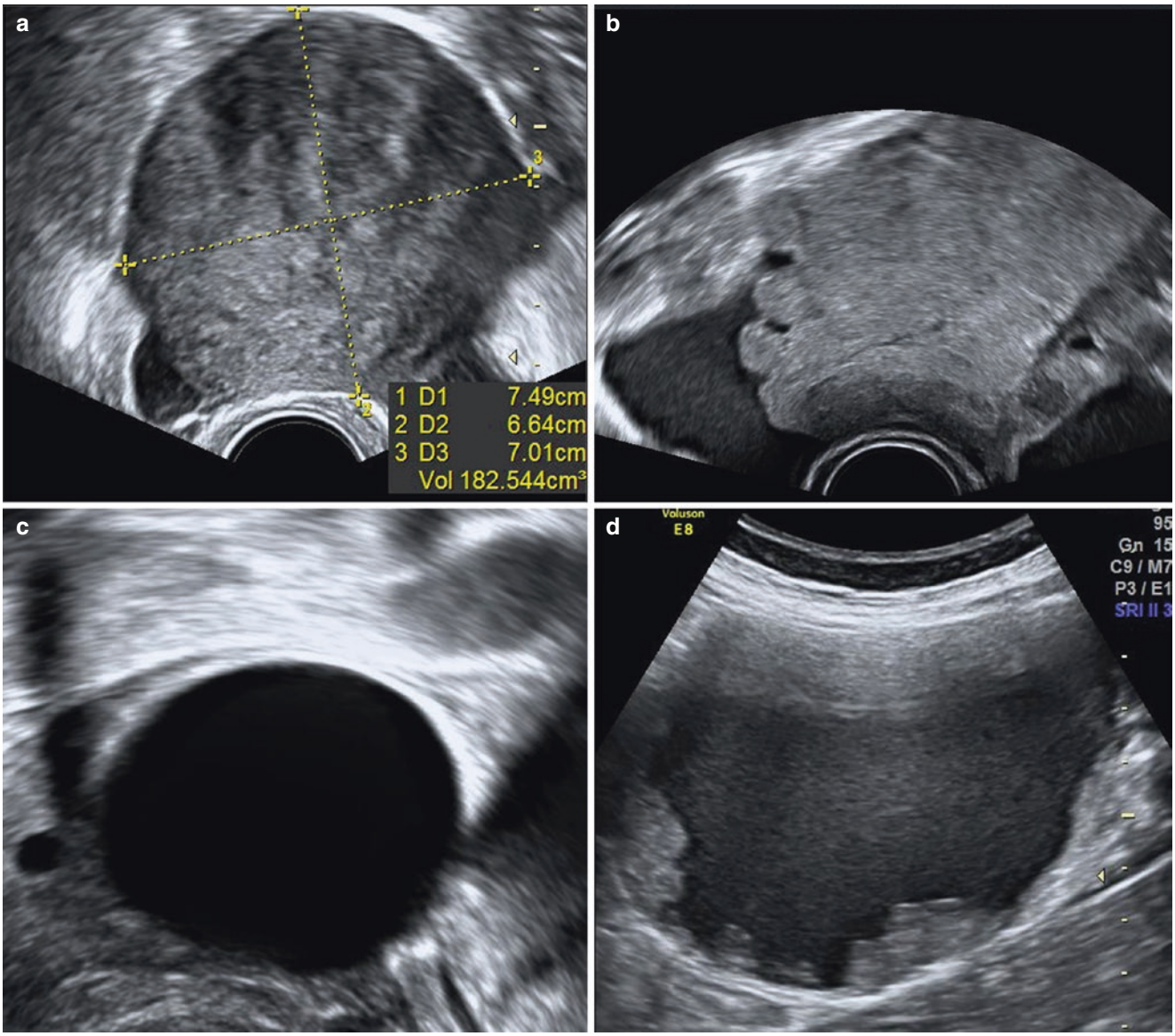

Fig. 7.7 (**a**) Solid tumour with regular, smooth, outer margins. (**b**) Solid tumour with irregular, lobulated, outer margins. (**c**) Smooth inner walls of a cystic mass. (**d**) Irregular inner walls of cystic mass with multiple papillae

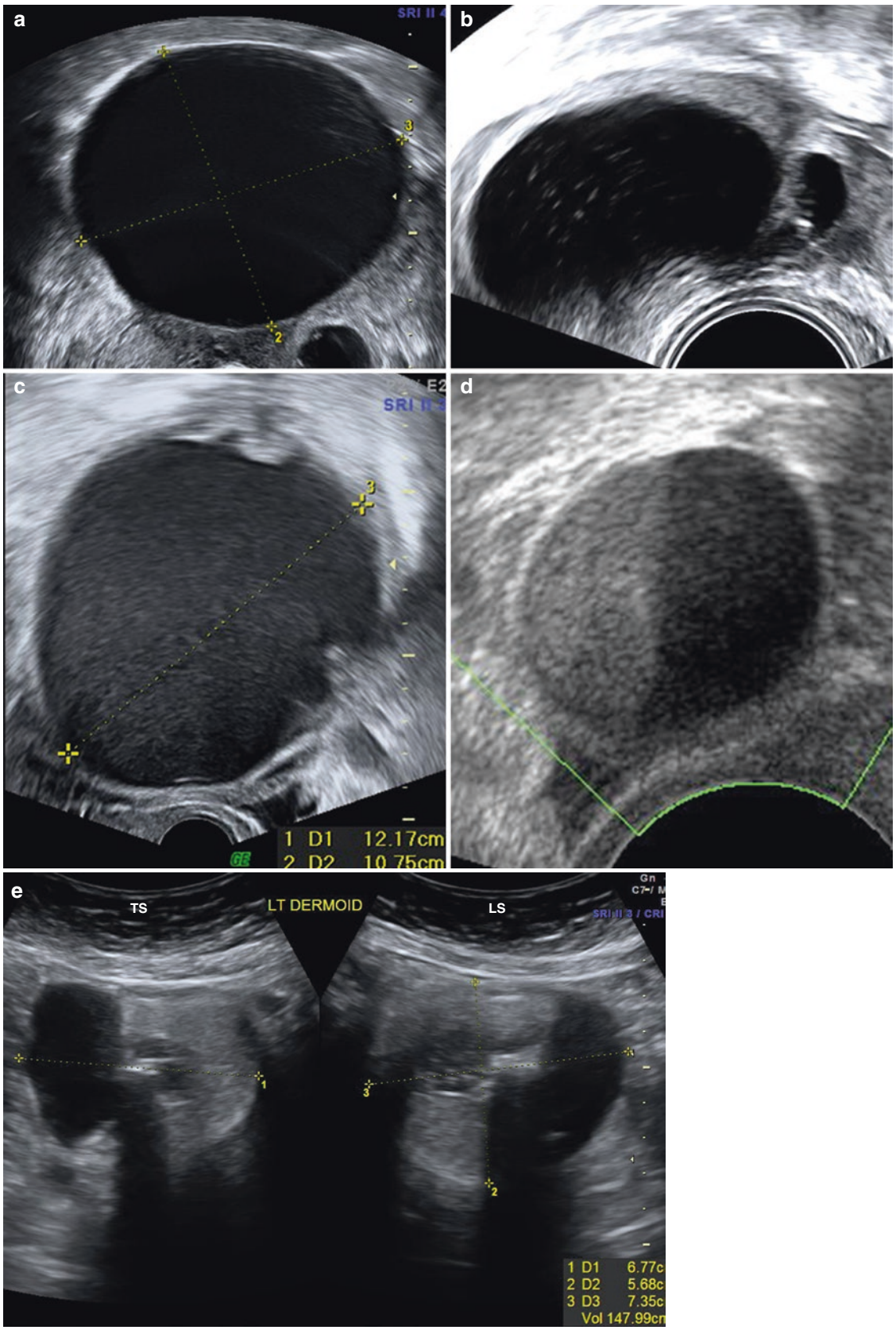

Fig. 7.8 Contents of a cyst: (**a**) anechoic, (**b**) with low-grade internal echoes, (**c**) hypoechoic, (**d**) with fluid–fluid level, (**e**) with mixed echoes

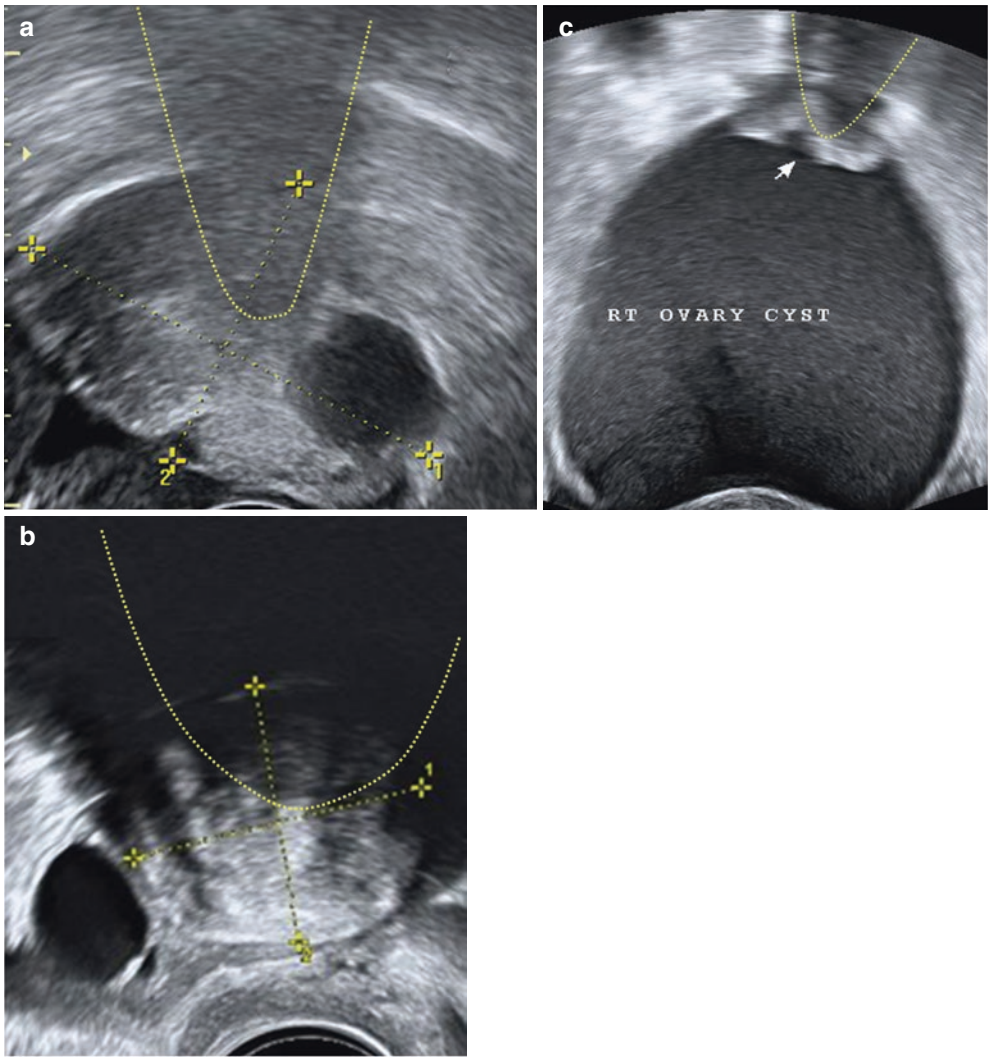

Fig. 7.9 Acoustic shadowing in (**a**) dermoid, (**b**) fibroma, (**c**) papilla of a serous cystadenoma fibroma. Shadows are outlined in the images

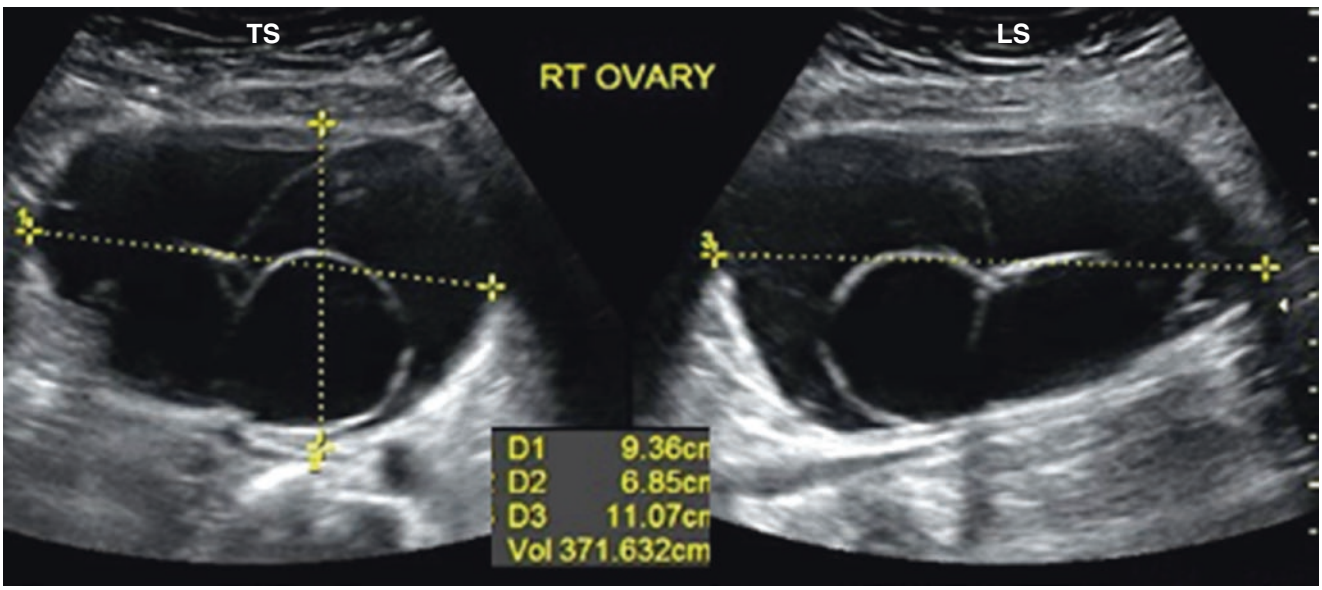

Fig. 7.10 Cyst measured in the three largest dimensions in two perpendicular planes. When ovarian tissue is not seen around the cyst, the measurement of both the cyst and the ovary is the same

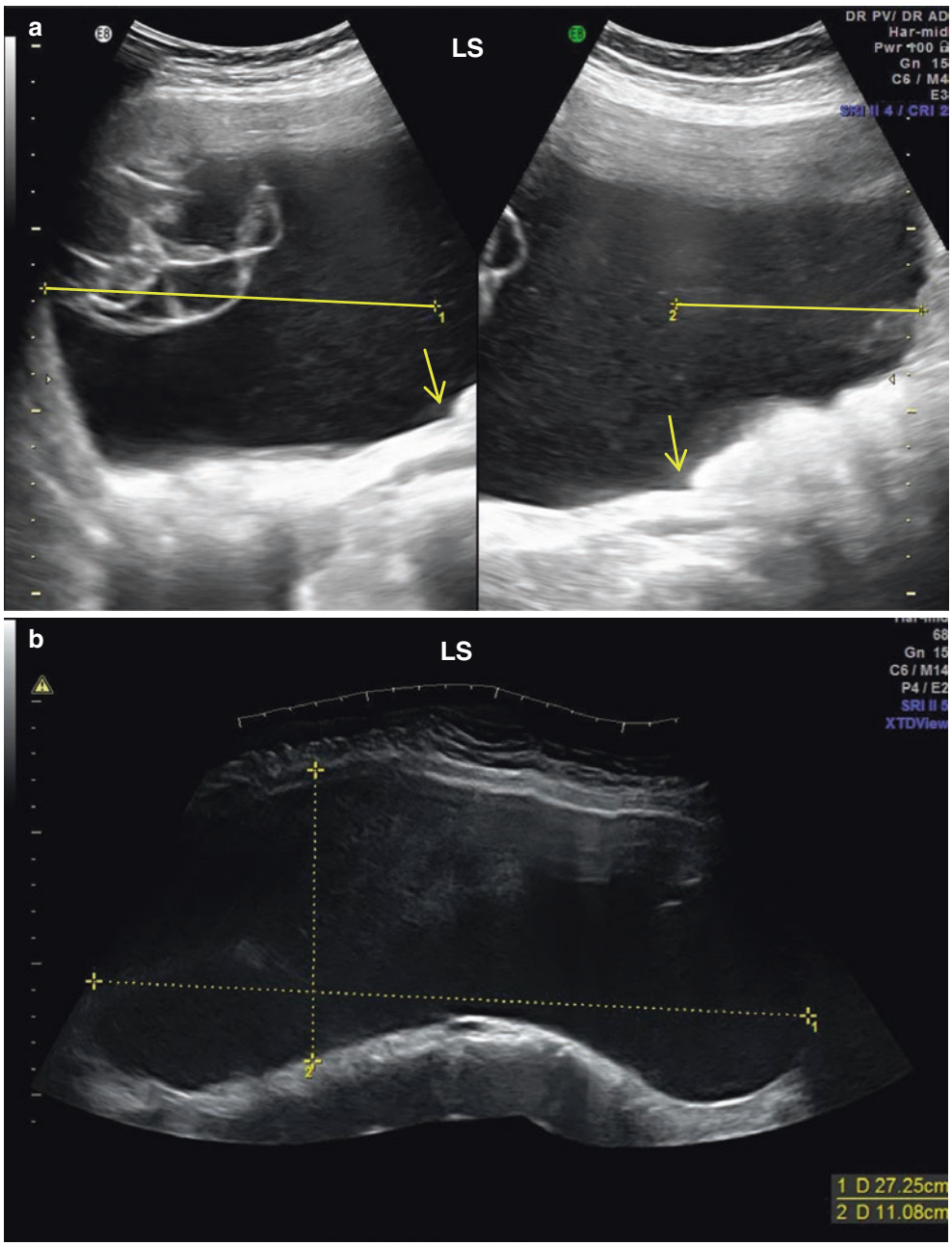

Fig. 7.11 Measuring the length of a large cyst. (**a**) Here the mass is imaged on a split screen as it is too large to fit in a single screen. The length of the mass is measured using a common reference point (*arrows*). (**b**) A large cyst can also be measured using the panoramic imaging mode, available in some ultrasound machines

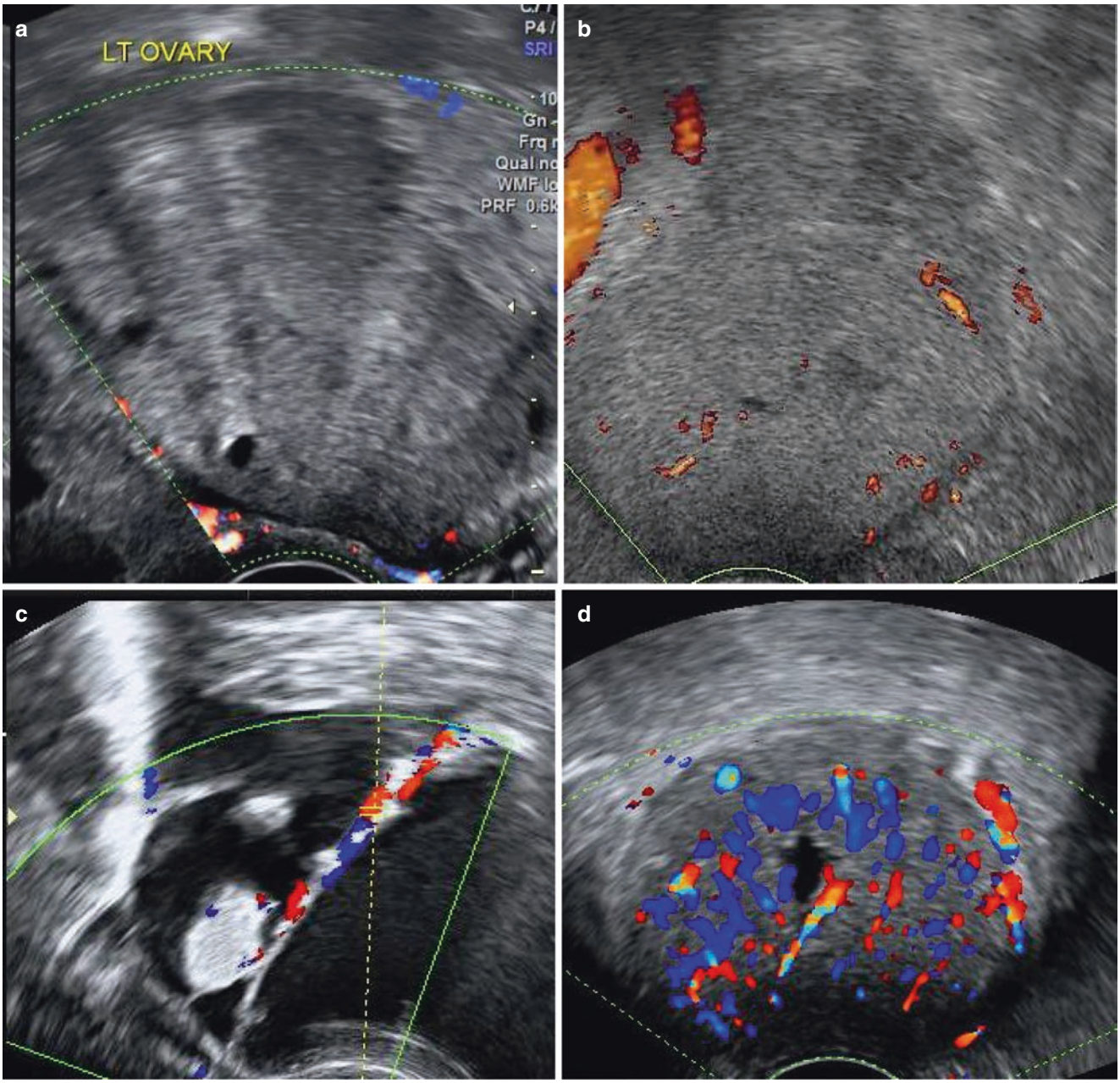

Fig. 7.12 Colour score: (**a**) Score 1 – no flow. (**b**) Score 2 – minimal flow. (**c**) Score 3 – moderate flow. (**d**) Score 4 – abundant flow

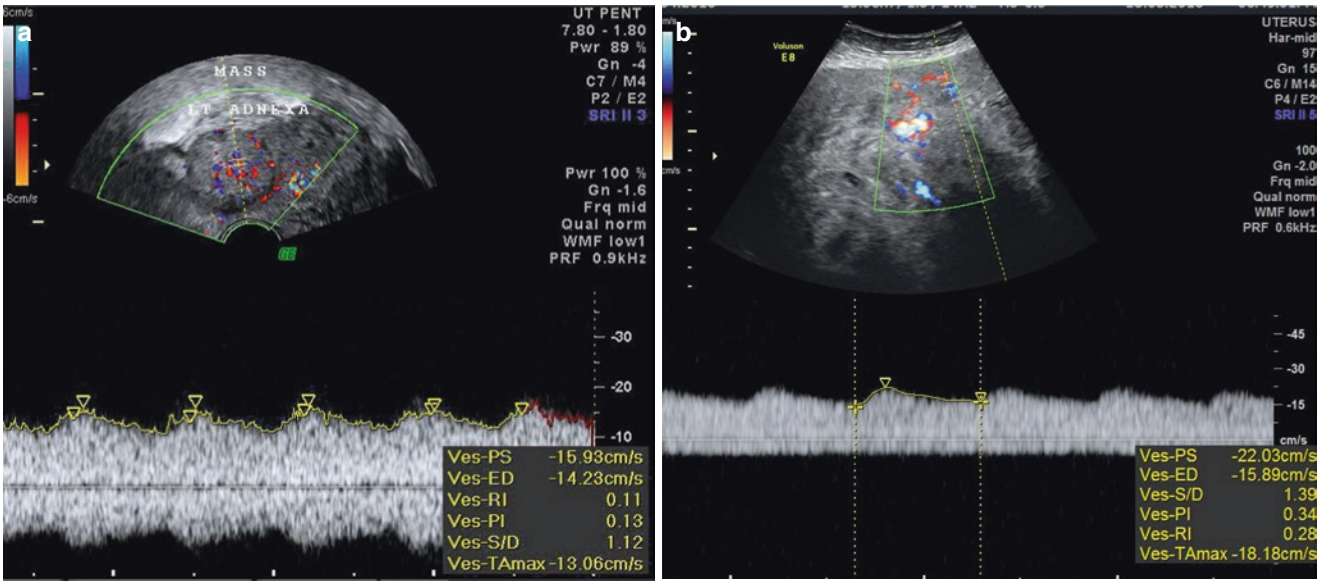

Fig. 7.13 Low-resistance flow in (**a**) malignant mass (fallopian tube carcinoma), (**b**) benign mass (fibroid)

7.1.2 Morphological Classification of Ovarian/Adnexal Masses (Fig. 7.14)

As per IOTA recommendations, all adnexal masses are classified into one of the five types mentioned below, based on greyscale imaging. The likelihood of malignancy for each of these types is also mentioned in the table below.

The presence of a solid tissue, as seen in this table, increases the likelihood of malignancy significantly. The more heterogeneous and irregular the solid area, the higher is the likelihood of malignancy. Also, central flow in a solid area or a papilla increases the likelihood of malignancy.

Timmerman et al. UOG (2008)

Type	Malignant (%)
Unilocular (no solid areas or papillae)	1.3
Multilocular (no solid areas or papillae)	10
Unilocular solid[a]	37
Multilocular solid[a]	43
Solid[b] (80 % or more of the tumour appears solid)	65

[a]'Solid' includes the presence of papillae
[b]Based on subjective evaluation on 2D greyscale

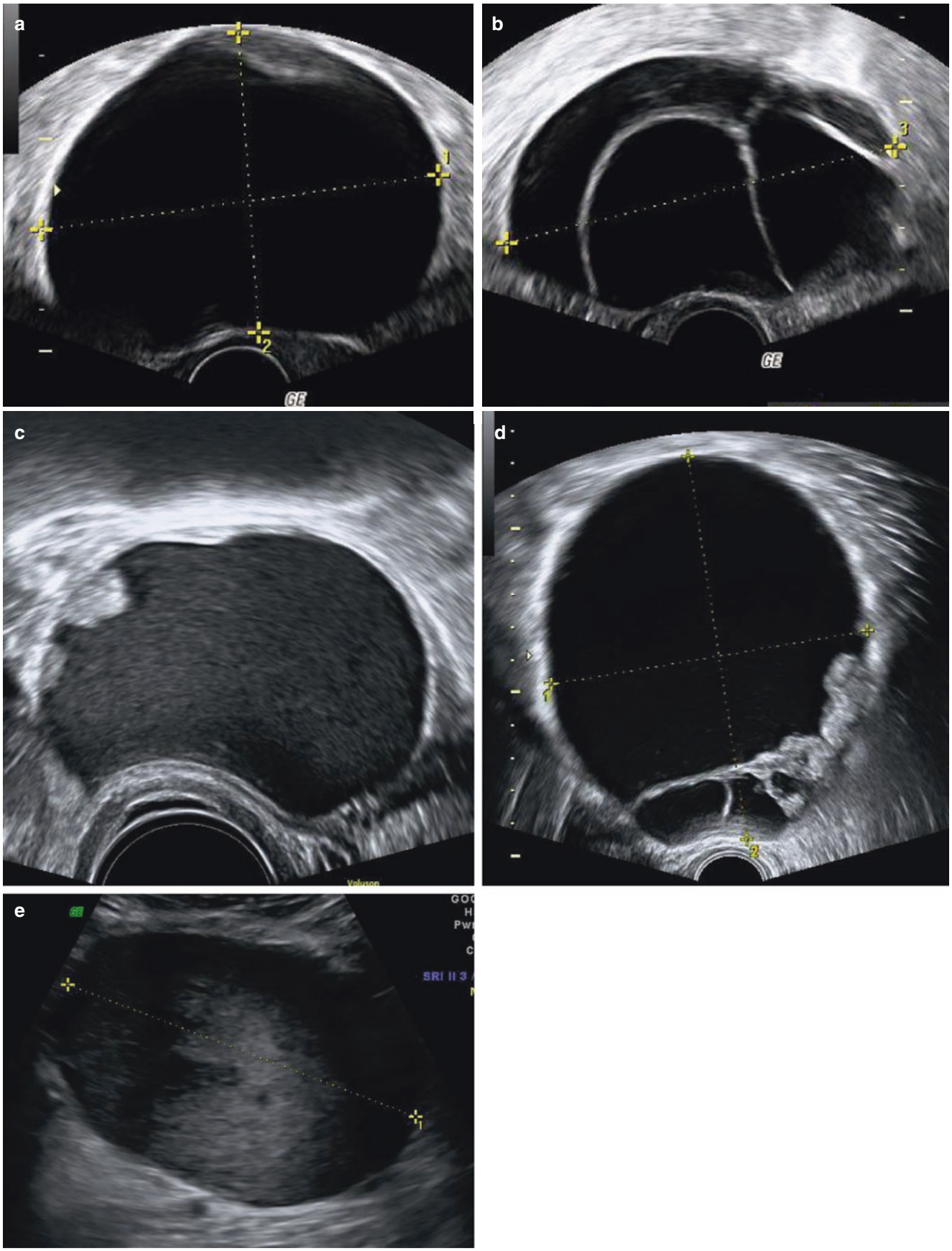

Fig. 7.14 Morphological classification of ovarian neoplasms: (**a**) unilocular, (**b**) multilocular, (**c**) unilocular solid, (**d**) multilocular solid, (**e**) solid

7.2 Normal Ovaries

Ovaries vary in size and appearance not only based on the age of the individual but also through the menstrual cycle due to hormonal influences.

Neonatal Ovaries (Fig. 7.15) The ovaries are located above the true pelvis and, therefore, easily seen on TAS. They move deeper into the pelvis as the child grows. At birth, the typical volume of the ovary is about 1 cc but may reach up to 3.5 cc due to the abrupt rise in FSH following a decrease in oestrogen and progesterone that reaches the fetus in intrauterine life from maternal circulation. Ovarian follicles have been noted as early as 28 weeks of gestation, and follicles of less than 9 mm may be seen in neonatal ovaries. Occasionally, the development of larger physiological cyst (more than 1 cm) may be seen in both fetal and neonatal ovaries and most resolve spontaneously. About 20% of neonates have ovarian cysts of more than 1 cm.

Paediatric Ovaries (Fig. 7.16) The ovarian volume up to the age of about 7 years is about 0.5–1.5 cc increasing to 4 cc just before puberty. Larger physiological cyst (more than 1 cm) may be seen in prepubertal ovary. Ovarian volume of more than 4 cc and the presence of six or more follicles in girls younger than 7 years should raise the suspicion of precocious puberty.

Reproductive Ovaries (Fig. 7.17) The ovarian volume may vary from 4 to 20 cc with an average of about 5–6.5 cc. Developing and immature (antral follicles 2–9 mm) can be seen throughout the entire cycle and appear as unilocular, anechoic well-defined cysts. In the first half of the menstrual cycle, one or more dominant follicles grow to about 20–25 mm and then rupture spontaneously at ovulation. After ovulation, it becomes the corpus luteum (CL) and undergoes cellular hypertrophy and increased vascularity. A corpus luteum is seen on ultrasound as a thick-walled cyst often with irregular margins and low-resistance flow around it on Doppler. The irregular inner margins of a corpus luteum often give it a classic 'crenated appearance'. The contents of the corpus luteum usually show turbid fluid with internal echoes. A CL is usually less than 3 cm but may occasionally be larger and may appear complex showing clots within.

Postmenopausal Ovaries (Fig. 7.18) Normal postmenopausal ovaries are smaller in size (1.2–5.8 cc), less echoic and show fewer follicles than in premenopausal women. Because of their small size and the absence of follicles, they are often difficult to locate, both on TAS and TVS. Small punctate echogenic foci are often seen in postmenopausal ovaries, which helps in identifying the ovaries in postmenopausal women. The ovarian size correlates with the duration of menopause. A volume of more than 8 cc or an ovary that is twice as large as the contralateral ovary is considered abnormal. Simple ovarian cysts may be seen in postmenopausal women, particularly in early menopause. In late menopause also, a smaller cyst (less than 1 cm) may be seen and should be reported if noted.

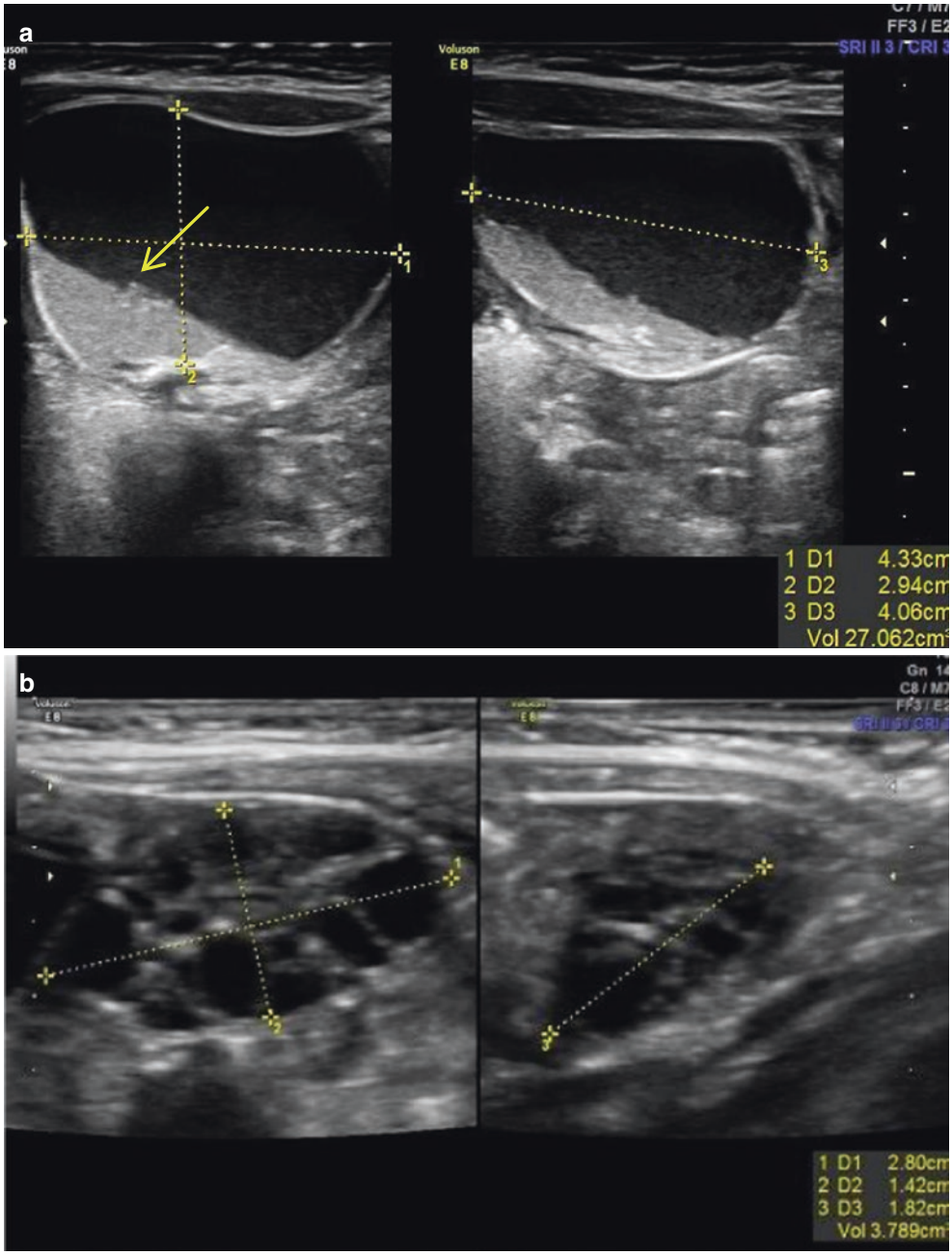

Fig. 7.15 Neonatal ovaries in a 32-day-old baby who was on follow-up for a right ovarian cyst detected antenatally. (**a**) Haemorrhagic right ovarian cyst of 27 cc showing debris in its posterior dependent part (*arrow*). (**b**) Multicystic left ovary measuring 2.8 × 1.4 × 1.8 cm (volume 3.8 cc). This (multicystic ovary) is seen in some infants, secondary to rise in FSH due to a sudden fall in oestrogen and progesterone levels that were present at higher levels in neonatal life from maternal circulation. Uterus measured 3.0 × 1.1 × 1.3 cm

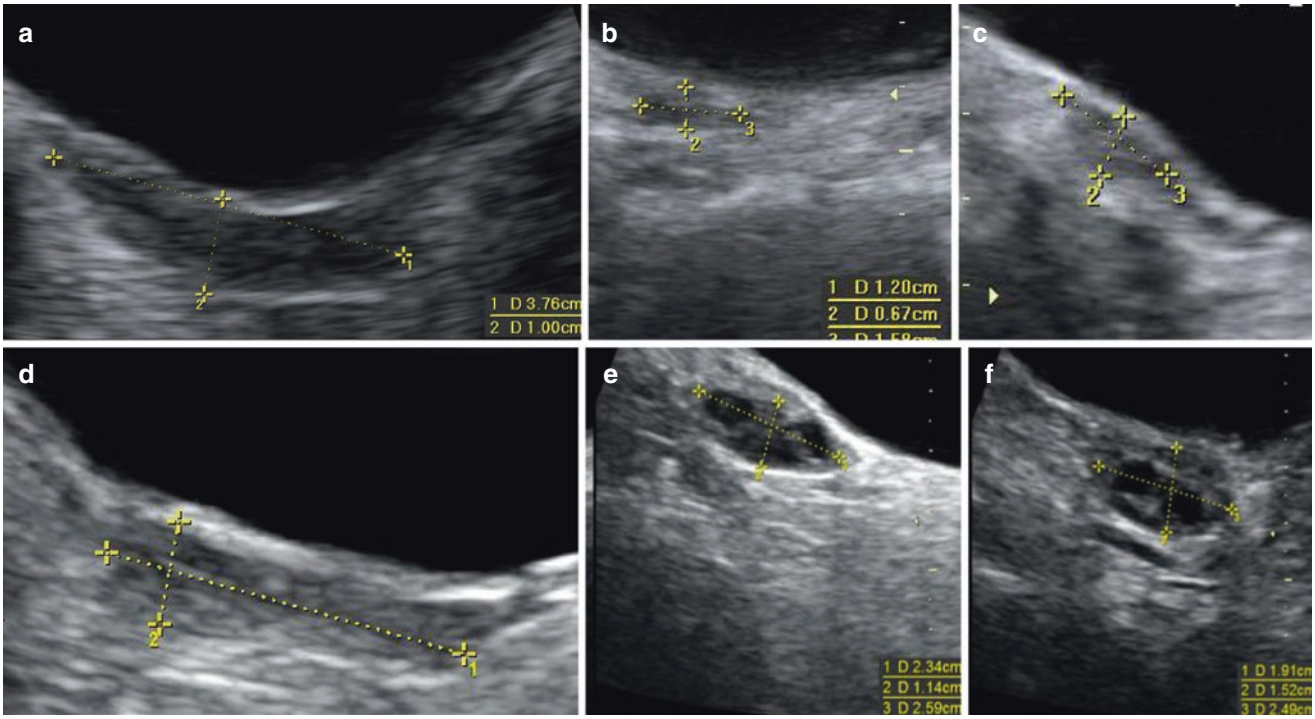

Fig. 7.16 (**a–c**) Case 1 – Paediatric ovaries in a 6-year-old girl. (**a**) The uterus measures 3.7×1.0×1.6 cm. (**b**) Right ovary 1.2×0.6×1.5 cm. (**c**) Left ovary 1.3×0.7×1.5 cm. No follicles are seen in either ovary. (**d–f**) Case 2 – Prepubertal ovaries in an 11-year-old. (**d**) The uterus measures 3.5×1×1.2 cm. (**e**) Right ovary 2.3×1.1×2.6 cm. (**f**) Left ovary 1.3×0.7×1.5 cm. Follicles are seen in both ovaries

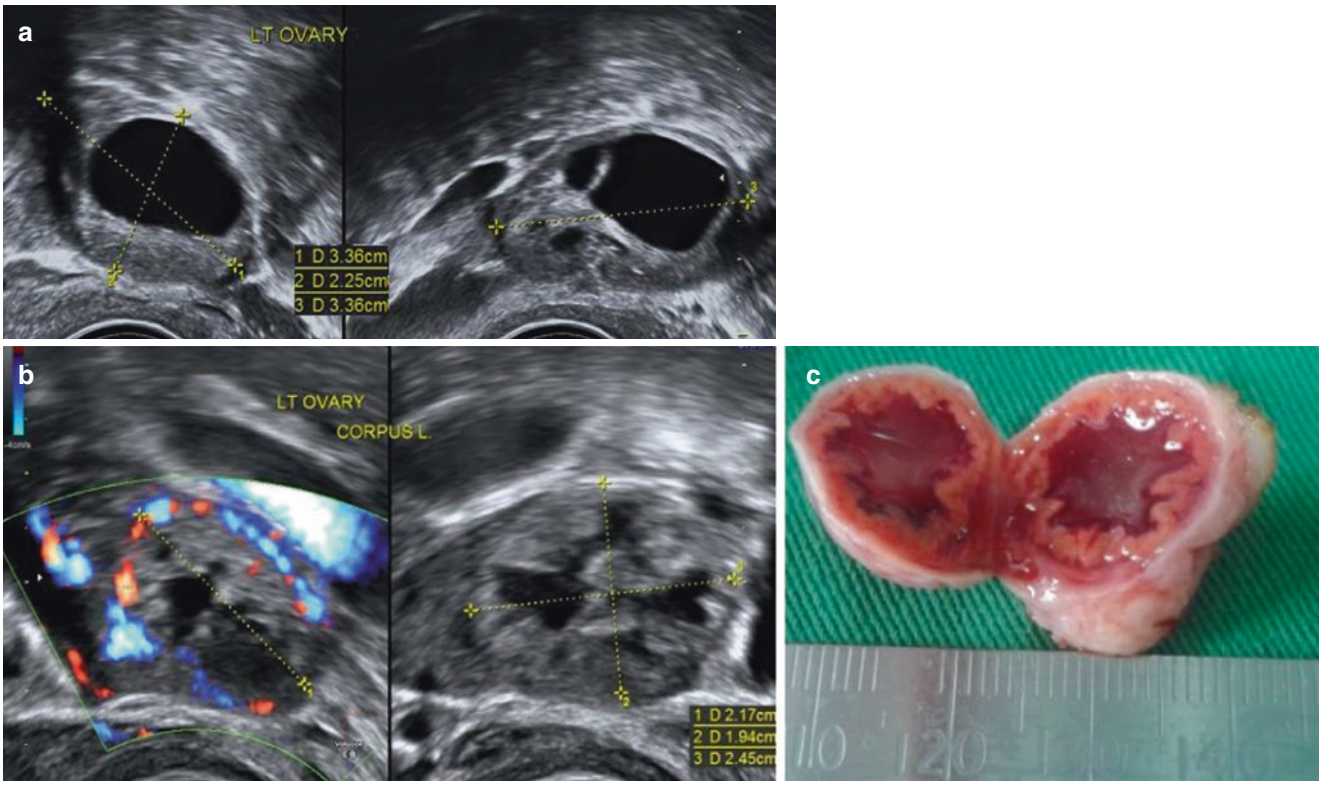

Fig. 7.17 Ovaries of women in the reproductive age group. (**a**) The ovary shows a developing follicle (in the proliferative phase of the menstrual cycle). (**b**) The ovary shows a corpus luteum (in the secretory phase of the menstrual cycle). (**c**) Specimen of a corpus luteum from an excised ovary

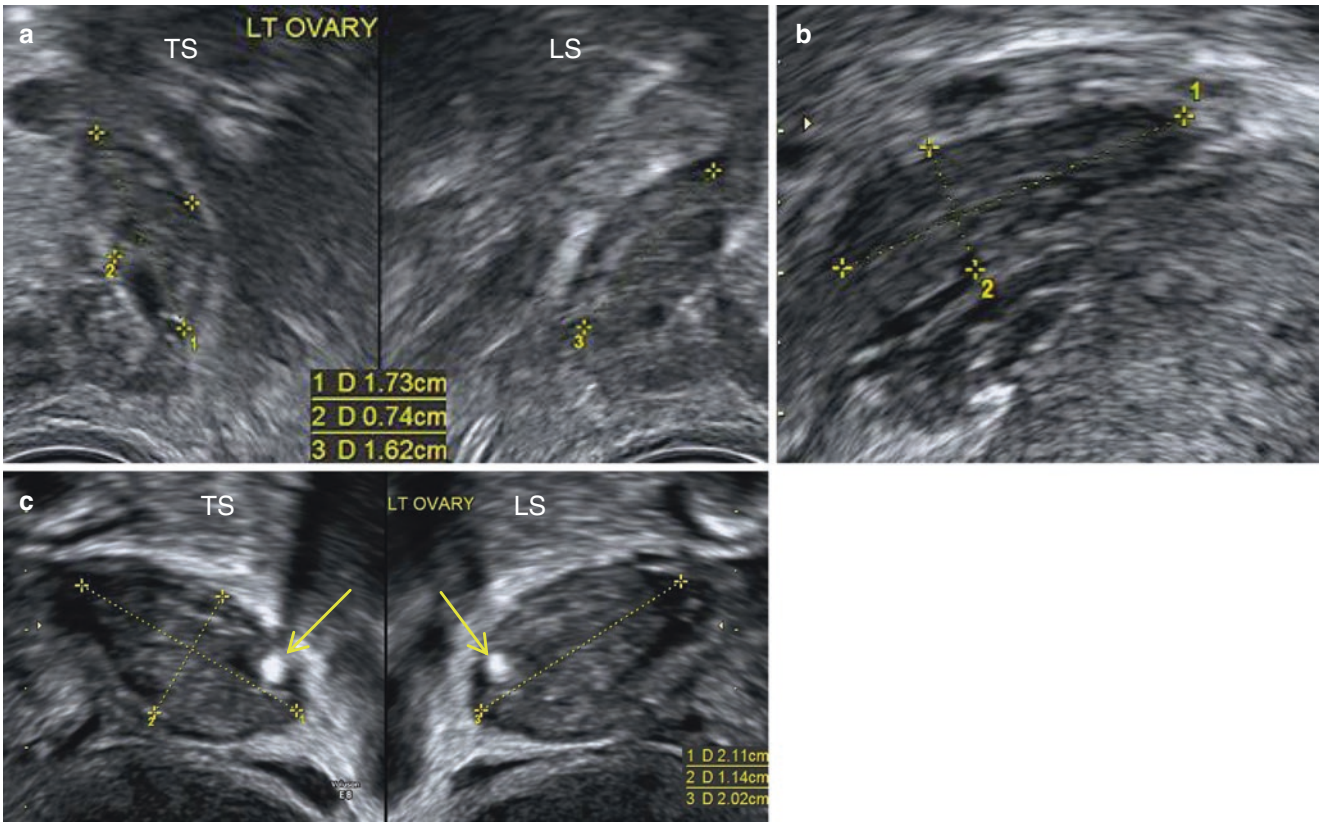

Fig. 7.18 Postmenopausal ovary. (**a**) Shows small ovarian size. (**b**) Ovaries show no follicle. (**c**) Small punctate echogenic focus (*arrows*) seen in the ovary, which if present is often very useful while searching for the ovaries during TVS, in postmenopausal women

7.3 Polycystic Ovaries (PCO)

Polycystic ovarian syndrome (PCOS) is the commonest endocrinal abnormality seen in about 6.6% in women in the reproductive age group. This syndrome carries significant health risk, including diabetes, cardiovascular disease, endometrial hyperplasia and infertility. Most of these women present with infertility, amenorrhoea or oligomenorrhoea, menorrhagia, obesity and hirsutism. Endometrial hyperplasia and, occasionally, endometrial carcinoma may be seen in these women, secondary to long-term exposure to unopposed oestrogen.

There is no universal consensus on diagnostic criteria. In 1935, Stein and Leventhal first described a condition consisting of amenorrhoea, obesity and masculinising features, now known as polycystic ovarian syndrome. The Rotterdam PCOS consensus group brought out criteria in 2003 for the definition of PCOS. The *Rotterdam criteria* require at least two of the three conditions given below to be present for the *diagnosis of PCOS*:

1. Anovulation or oligoovulation.
2. Clinical or biochemical signs of hyperandrogenism.
3. Polycystic ovaries on ultrasound – The Rotterdam criteria for polycystic ovaries on ultrasound are more than 12 or more follicles measuring 2–9 mm and/or an ovarian volume more than 10 cc in one or both ovaries. Later it was believed that instead of the criterion of more than 12 follicles, a criterion of more than 19 follicles was more appropriate. The new PCO criterion proposed (HR 2013), however, is an antral follicle count of 25 or more. Here, it is assumed that the evaluation is done by a transvaginal scan that can provide good resolution. Rotterdam criteria, however, remain at more than 12 follicles, probably because TVS is not routinely used the world over.

Ultrasound Features of Polycystic Ovary (PCO)
(Figs. 7.19 and 7.20**)**
Evaluation of the ovaries for the diagnosis of polycystic ovary should ideally be done between day 2 and day 4 of the menstrual cycle by a transvaginal scan (if possible). Patient should not be or recently have been on hormonal medication.

- Antral follicle count (AFC) is increased: The presence of antral follicles (2–9 mm) in one or both ovaries. The number of antral follicles for diagnosis will vary depending on what criteria are used in each institution. Rotterdam criteria are an AFC of more than 12. However, most centres now consider an AFC of 25 or more for diagnosing PCO.
- Ovarian volume is increased: An ovarian volume of more than 10 cc is used for the diagnosis of PCO (in the absence of a dominant follicle or a corpus luteum).
- Peripherally arranged antral follicles ('pearl necklace appearance') are seen in classic polycystic ovaries. However, it is not a requisite for the diagnosis of PCO based on Rotterdam criteria.
- Abundant stroma is a feature of classical polycystic ovaries which is seen centrally. It is generally more hyperechoic than usual. This stroma generally shows increased vascularity.
- 3D ultrasound with volume analysis is being increasingly used for the diagnosis of PCO and for the evaluation of PCO in patients undergoing ovulation induction. This helps to enhance the accuracy, speed and ease of measuring AFC. Ovarian volume can also be calculated with 3D volume studies.
- The endometrium in patients with polycystic ovaries may be thickened, heterogeneous, with tiny cysts and show increased vascularity. This could be secondary to endometrial hyperplasia or, rarely, endometrial carcinoma.

7.3.1 PCO in the Absence of PCOS

The presence of polycystic ovaries (PCO) is seen in about 23% of women of reproductive age group; however, only some of these have PCOS (i.e. associated anovulation and hirsutism). The significance of PCO in the absence of the syndrome primarily lies in the fact that these women are more likely to hyperstimulate with gonadotrophins during ovulation induction. Since a large number of women with polycystic ovaries on ultrasound do not have polycystic ovarian syndrome (which is a disease associated with a lot of other medical issues), it may be prudent to communicate this in the ultrasound report, stating that though the ovaries appear polycystic, it does not imply diagnosis of polycystic ovarian syndrome, which requires other features of hyperandrogenism and/or ovulatory dysfunction.

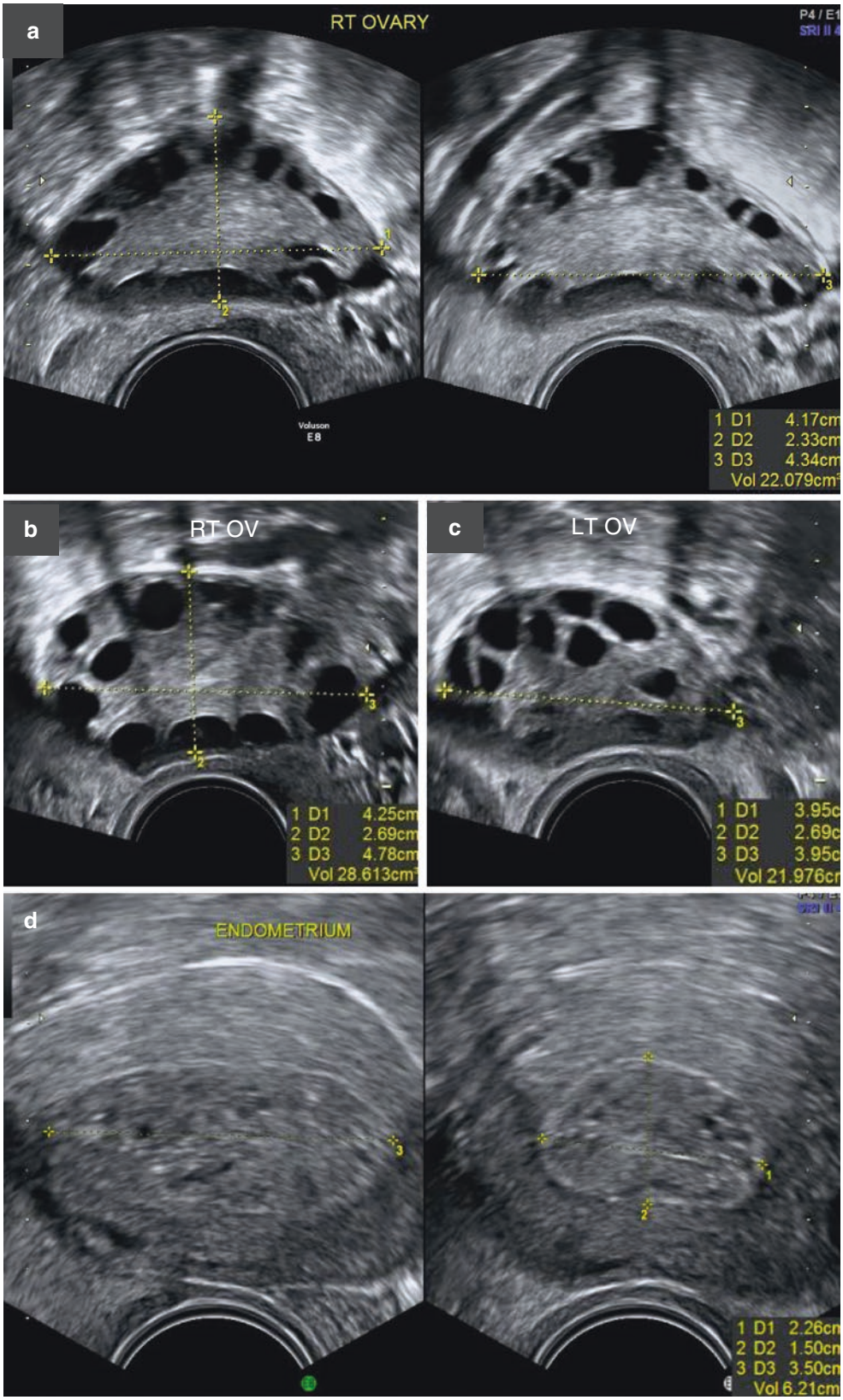

Fig. 7.19 (**a**) Case 1 – A classic case of polycystic ovaries with peripherally arranged antral follicles ('pearl necklace appearance'), central hyperechoic, bulky stroma and increased ovarian volume. (**b**, **c**) Case 2 – Polycystic ovaries showing increased antral follicle count. Ovarian volume is also increased. (**d**) Thickened endometrium showing small cystic spaces suggestive of cystic hyperplasia in Case 2

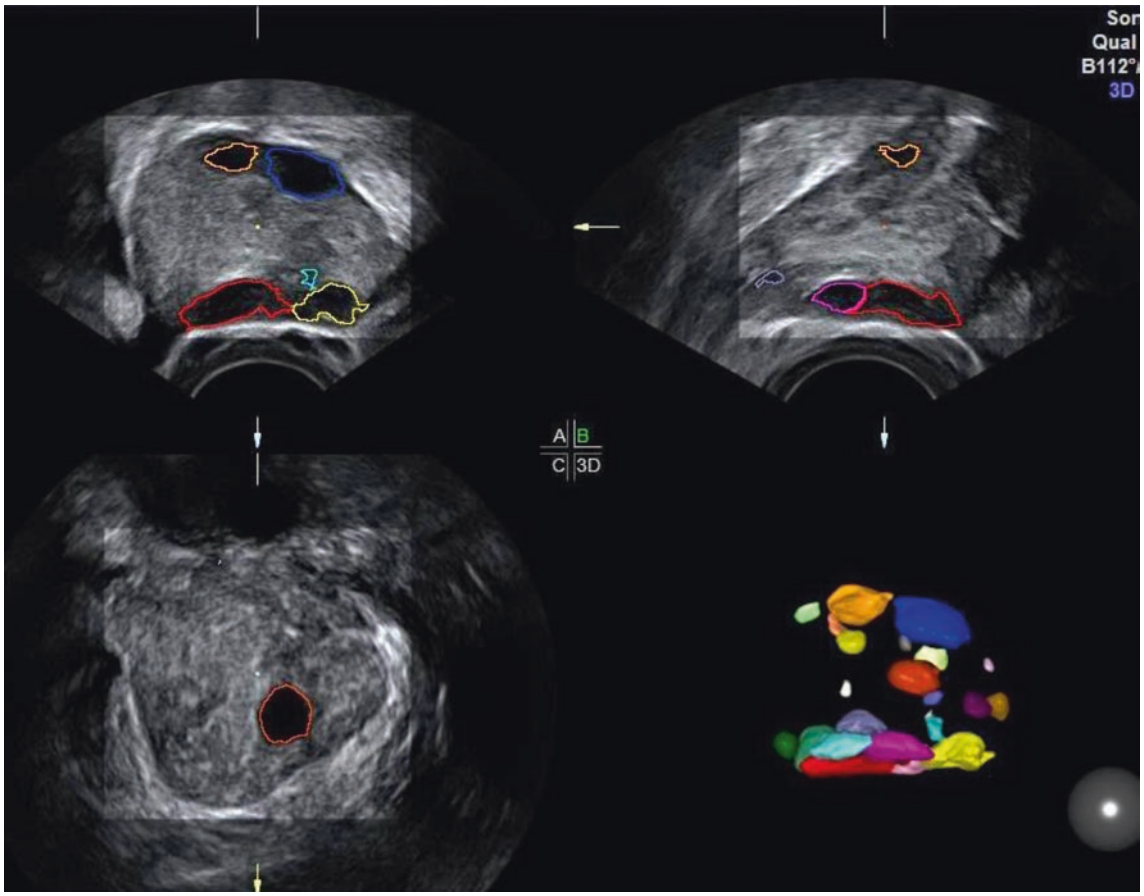

Fig. 7.20 SonoAVC software is useful in obtaining an antral follicle count. This is particularly useful in the treatment of women with infertility. It provides an accurate and quick way of counting antral follicles

7.4 Ovarian Masses

Ovarian masses can be broadly classified into functional cysts, endometriomas and neoplastic masses.

Other causes of ovarian enlargement are masses of inflammatory origin (discussed in Chap. 9 in the section on PID), hyperstimulation (discussed in Chap. 13), ovarian torsion (discussed in Chap. 11) and ovarian ectopic (discussed in Chap. 10 in the section on ectopic pregnancies).

The differential diagnosis for ovarian masses is dealt with in Chap. 14 in the section on adnexal masses.

7.4.1 Functional or Physiological Cysts (Figs. 7.21, 7.22 and 7.23)

All functional cysts of the ovary are unilocular and are generally less than 8 cm. They are usually unilateral (unless the patient is undergoing ovulation induction). Any fluid containing mass in the ovary is a cyst; therefore, all follicles are cysts. One must, however, avoid the term cyst for a regular ovarian follicle because for most patients, the term cyst has a pathological connotation. Follicles that have a diameter of more than 3 cm can be called a *follicular cyst*. Follicular cysts are generally asymptomatic.

A *corpus luteal cyst* is usually thick walled and seen in the secretory phase of the menstrual cycle. Corpus luteal cysts may be symptomatic and occasionally may cause acute pain and haemoperitoneum due to haemorrhage from a corpus luteal cyst. In pregnancy, corpus luteal cysts may be larger and persist for a longer period. Their size reaches a maximum at about 10 weeks, and they generally regress by about 16 weeks of pregnancy. Corpus luteal cysts are generally haemorrhagic cysts but could be simple clear cysts.

A *haemorrhagic cyst* is most often a corpus luteal cyst, but it could also be a follicular cyst with haemorrhage. An endometrioma with recent haemorrhage can also show features of a haemorrhagic cyst.

Ultrasound Features of a Haemorrhagic Cyst (Fig. 7.23)

- Unilocular
- Generally thick walled
- It shows internal echoes which may be hyperechoic (when haemorrhage is recent) or reticular, giving it a 'cobweb' appearance, or it may show diffuse low-grade internal echoes (especially when it is regressing).
- A clot within a haemorrhagic cyst may retract away from the cyst wall and the demarcation is often clearly seen. Clots usually have concave margins facing the lumen of the cyst. The entire margin of the clot facing the cyst wall may not be adherent to the cyst wall, and part of it may be seen some distance away from the cyst wall. The clot, in addition, may show jelly-like movements on intermittent pressure by the TVS probe. Most importantly, a clot will not show any flow within it on Doppler because it is avascular. This is a very important feature to help differentiate it from solid tissue within a cyst, which is generally of great concern.
- The appearance of a haemorrhagic cyst varies with time as the haemorrhage within gradually resolves.

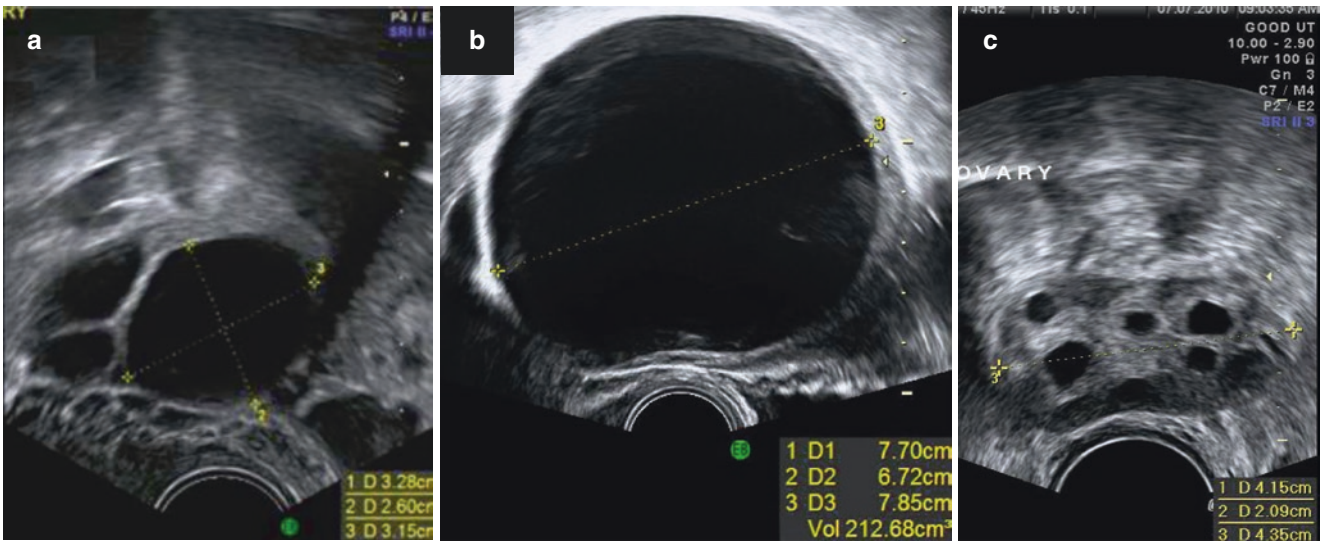

Fig. 7.21 Physiological cyst. (**a**) Follicular cyst. (**b**) Corpus luteal cyst (212 ml) in a pregnant lady. (**c**) CL cyst in '**b**' has regressed completely following pregnancy

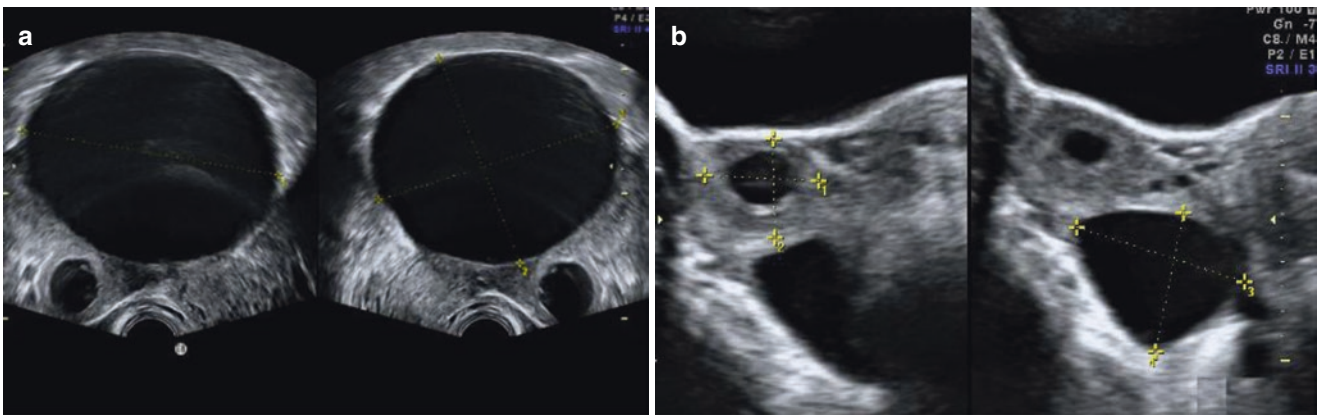

Fig. 7.22 Corpus luteal cyst. (**a**) At early pregnancy scan, the cyst was large. (**b**) At NT scan, the cyst had regressed

Fig. 7.23 Haemorrhagic cysts vary in appearance. (**a**) Hyperechoic areas within. (**b**) Hypoechoic with few internal echoes. (**c**) Reticular appearance of the clot within the cyst. Clot retracting away from the cyst wall (*arrow*). (**d**, **e**) Clot within the cyst shows concave margins (characteristic feature). (**f**, **g**) Haemorrhagic cyst does not show flow within on Doppler, which helps differentiate it from masses with solid tissue within

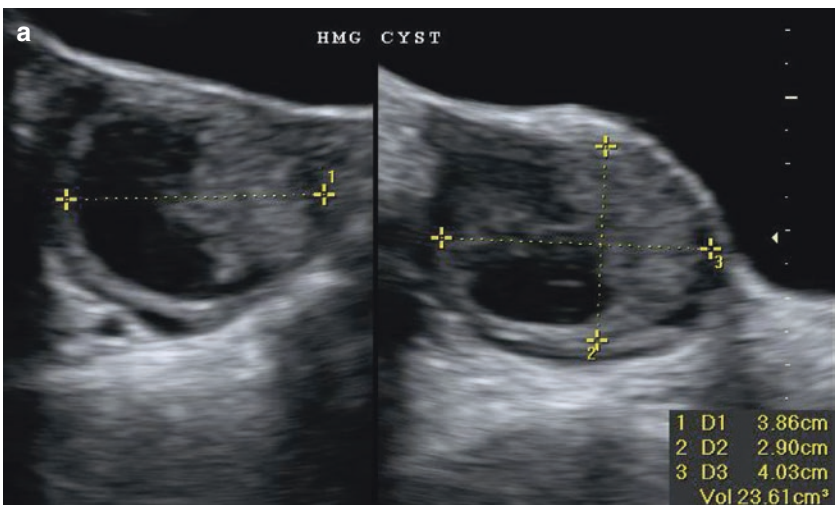

Fig. 7.23 (continued)

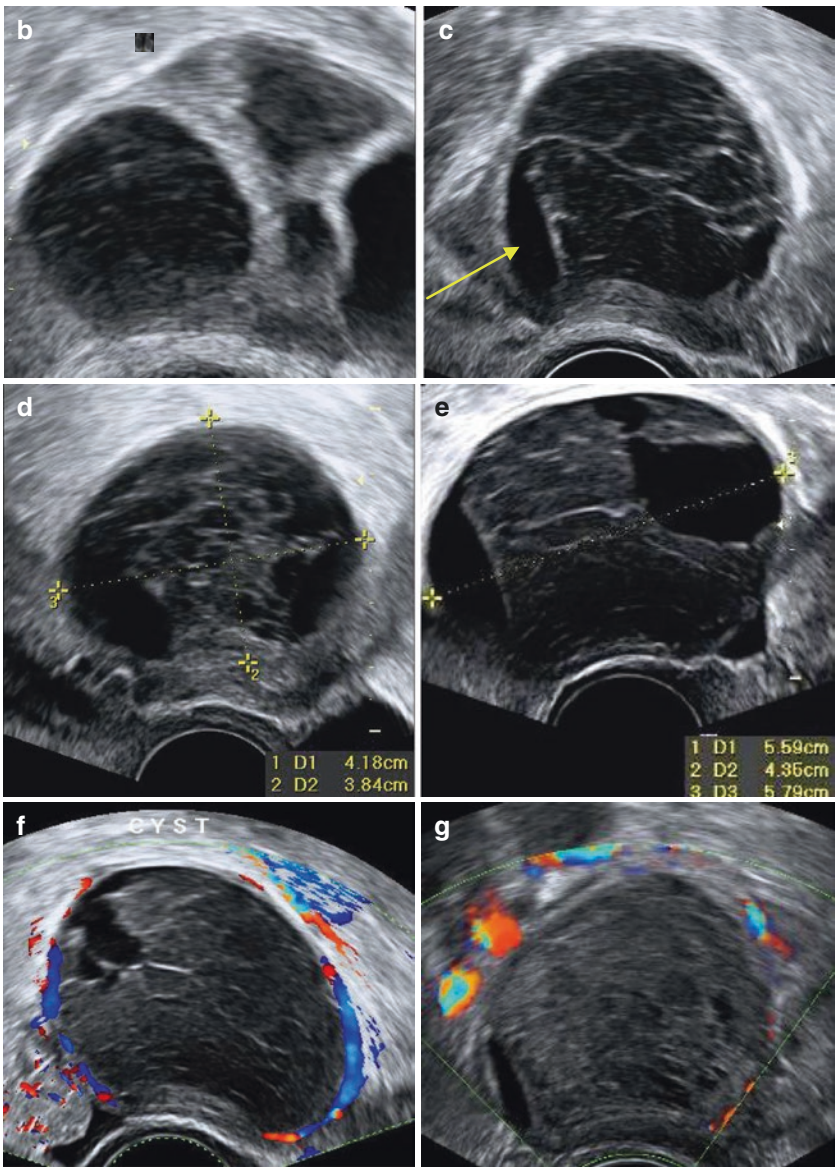

Summary: Functional Cysts

- History and Symptoms
  - Women are of the reproductive age group.
  - It is important to correlate the findings with the phase of the menstrual cycle and pregnancy status.
  - Previous reports and images are also useful for correlation.
- On ultrasound, these cysts are unilocular, clear or haemorrhagic (complex echoes) and generally less than 8 cm.
- Follow-up is useful when in doubt. On rescan after 2–3 months, the cyst will either show complete regression or would have changed in size and appearance.

7.4.2 Endometriotic Cysts (Endometriomas)

Endometrial tissue is seen within the ovary in cases with endometriomas. Endometriotic cysts are also called 'chocolate' cysts because of the thick chocolate-coloured fluid within these cysts. Further information on endometriosis is available in Chap. 8.

Ultrasound Features of Ovarian Endometriomas
(Figs. 7.24, 7.25, 7.26, 7.27, 7.28, 7.29, 7.30 and 7.31)

- Typically they appear as well-defined hypoechoic cysts with uniform low-grade internal echoes, which gives them a 'ground glass' appearance.
  Not all 'ground glass' cysts are, however, endometriotic. In premenopausal women, the majority are endometriotic, a few are malignant and the rest are benign. However, in postmenopausal women, the majority are malignant and the rest are endometriotic or benign.

GROUND GLASS CYSTS	ENDOMETRIOTIC	MALIGNANT
PRE MENOPAUSAL	83%	3.8%
POST MENOPAUSAL	15.6%	44%

Holsbeke et al. UOG 2010

  Cysts with thick turbid fluid can sometimes give the appearance of being solid masses. They can be differentiated from each other (as elucidated in Chap. 1).
- Endometriotic cysts are often multiple and bilateral.
  The multiple cysts are often closely packed, giving them a multilocular appearance and making it difficult to outline them at times. In such cases, the number of cysts can be identified as follows:
  1. The walls of the cysts can be visualised as bright lines or darker linear shadows.
  2. Doppler flow is often seen in the cyst walls/ovarian tissue intervening between the cysts.
  3. Density of echoes may differ in each cyst.

  Sometimes, the cysts within an ovary are seen communicating with each other due to disruption of the intervening tissue. This is more often seen following conservative surgery for endometriosis.
- Cyst walls
  - Typically the cyst walls are thick and regular.
  - At times, wall nodularity may be noticed because of hyperechoic, irregular areas along the inner cyst walls which are nothing but clot and debris secondary to the haemorrhage within.
  - Small hyperechoic foci are often seen in the cyst walls of these endometriotic cysts. They are believed to be cholesterol deposits in the cyst walls and are seen in about 35% of endometriomas. As an isolated marker for endometriomas, they have the highest LR of 6.2. The LR increases to 32 if these hyperechoic foci are seen in a 'ground glass' cyst. An association between hyperechoic foci in the cyst walls and endometriomas is well established. Hyperechoic foci in sonographically normal ovaries are not, however, predictive of endometriosis.
  - On Doppler, the cyst walls show minimal high-resistance flow with colour score of 2–3. Increased flow may be seen in pregnancy or with secondary infection.
- In some cysts, fluid–fluid level may be seen with the denser fluid in the dependent part (usually the inferior and posterior part) of the cyst.
- Clots within these cysts, secondary to haemorrhage, appear as irregular hyperechoic areas within a hypoechoic 'ground glass' background.
  These clots often show jelly-like movements on release of pressure. In addition, generally these clots have concave margins facing the cavity. Also, they are not attached to the cyst wall along their entire length (i.e. parts of the clots are usually some distance away from the cyst wall). Clots are avascular, and this feature is very important in distinguishing these areas of haemorrhage from solid tissue within a cyst that could have a similar appearance. For this, however, Doppler settings must be optimised (discussed in the section on Doppler in Chap. 1). The importance of this is highlighted in the case illustrated in Fig. 7.29.
- The presence of adhesions is another common finding in patients with endometriotic cysts. One may see periovarian adhesions with loculated fluid.
  The ovaries may be adherent to the uterine wall (i.e. 'sliding sign' is absent). Any attempts to move the ovaries by applying pressure will cause pain. The ovaries often lie in the pouch of Douglas adherent to the posterior wall of the uterus, very close to each other and at times even adherent to each other, termed the 'kissing ovaries'.

Endometriotic cysts with hyperechoic areas of haemorrhage within could appear like haemorrhagic physiological cysts, and at times it may be difficult to distinguish at a single scan. In a repeat scan, after 2 months, a physiological cyst would have disappeared or at least regressed, unlike an endometriotic cyst which may in fact have increased in size marginally.

Associated malignancy is seen in about 0.5–1.0% of endometriomas. It can also occur in endometriotic tissues elsewhere including foci of deep infiltrating endometriosis. As a result, the lifetime risk for ovarian cancer is believed to be higher in women with endometriosis. The common malignancies in endometriomas are clear cell carcinoma and endometrioid carcinoma.

Features that suggest possible malignant transformation/association are:

- Vascularised solid component in an endometriotic cyst.
- Rapidly enlarging mass or abundant blood flow in any endometriotic focus.
- High levels or rapid rise in CA 125 levels. (A baseline CA 125 may therefore be ideal in women with endometriosis.)

Malignancy is more common in women with large cysts (more than 9 cm), cases with severe and long-standing endometriosis, women over 45 years and those with a history of infertility.

Keeping in mind the possibility of associated malignancy and potential for malignant transformation, it is important to follow up cases diagnosed with endometriosis. It is also important to report any suspicion of malignancy on ultrasound for proper surgical decision and so that the pathologist evaluates these suspected areas carefully.

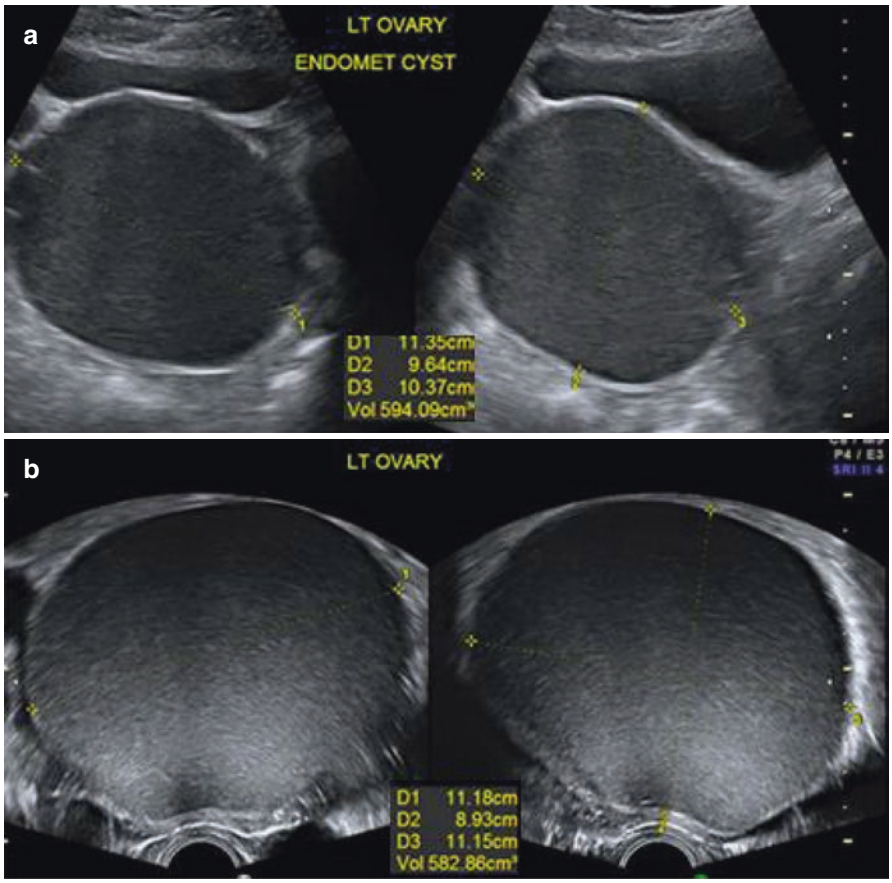

Fig. 7.24 Characteristic 'ground glass' appearance of endometriotic cysts. (**a**) On TAS, (**b**) on TVS

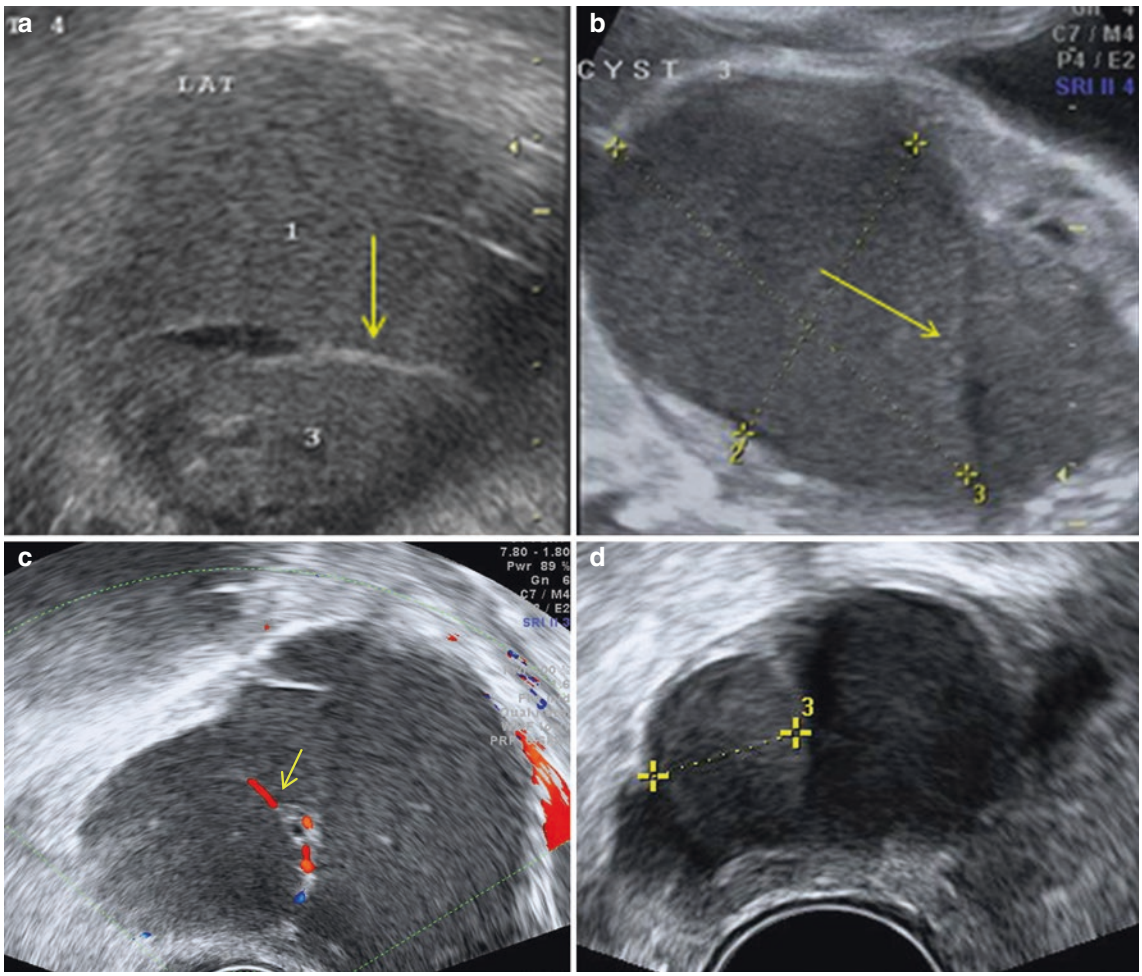

Fig. 7.25 Multiple endometriotic cysts giving the ovary a multilocular appearance. Features that help delineate and count these cysts are (**a**) hyperechoic linear compressed ovarian tissue between cysts (*arrow*), (**b**) dark linear shadow between two cysts (*arrow*), (**c**) flow in the compressed ovarian tissue between cysts (*arrow*), (**d**) varying echodensities of the cysts

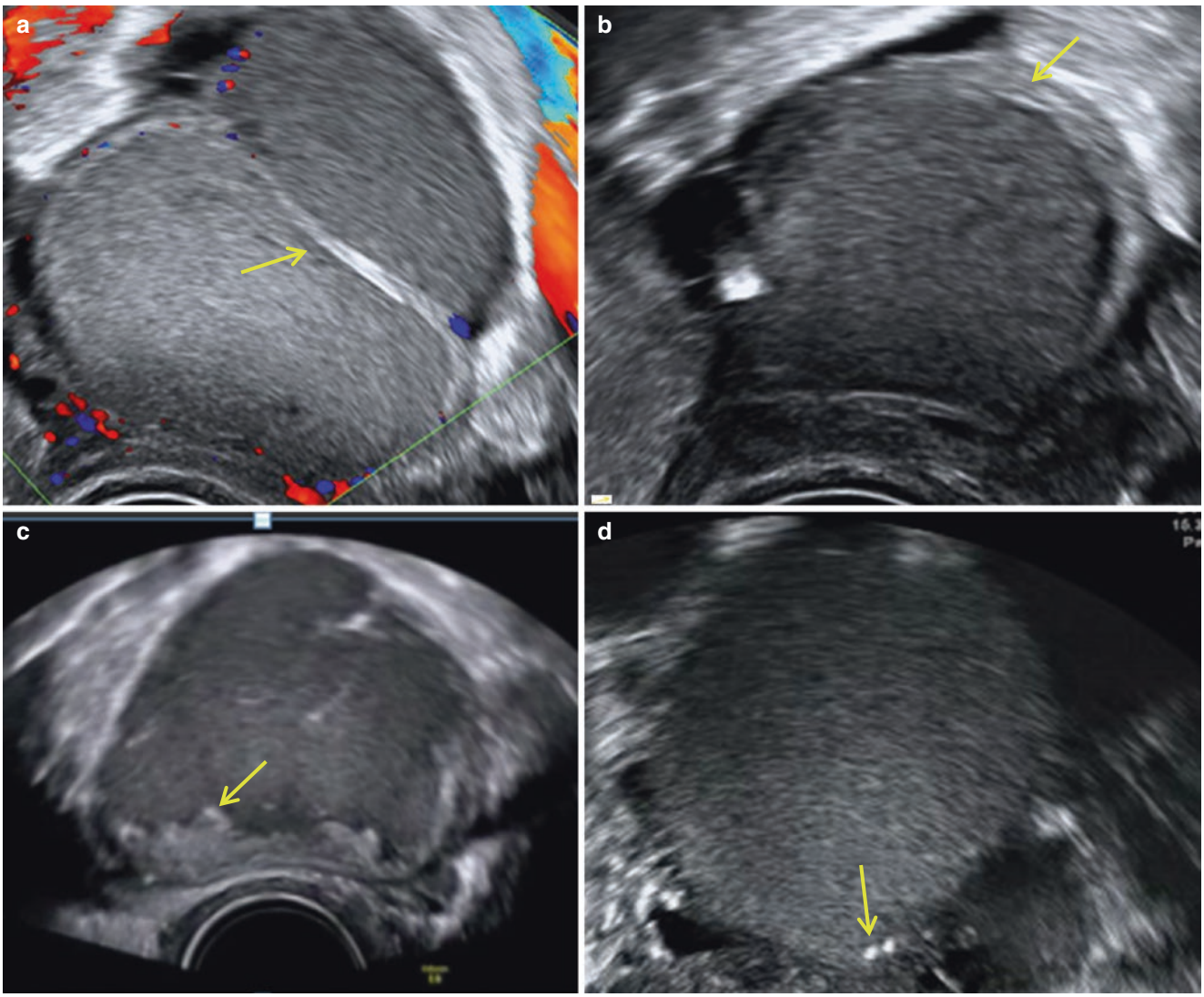

Fig. 7.26 Cyst walls are (**a**) uniform and regular (*arrow*), (**b**) thick (*arrow*), (**c**) irregular due to clot and debris along the cyst walls (*arrow*). (**d**) Hyperechoic foci are seen in the cyst wall (*arrow*)

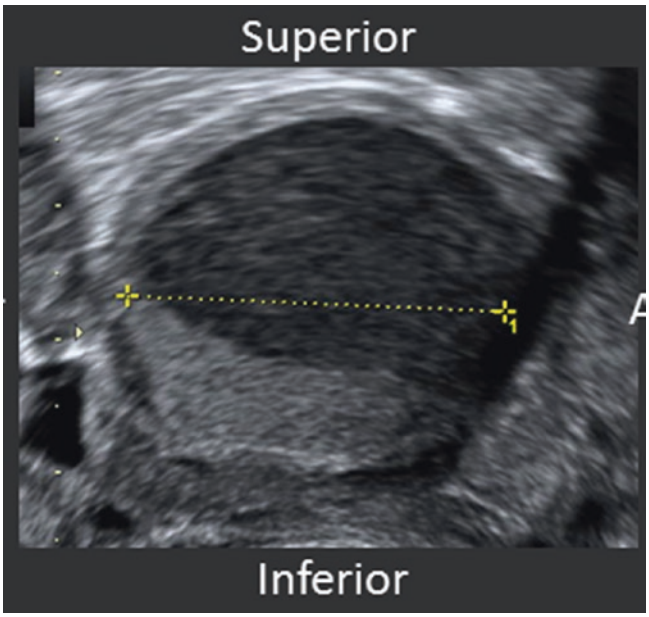

Fig. 7.27 Endometriotic cyst showing fluid–fluid level with denser fluid in the inferior dependent part

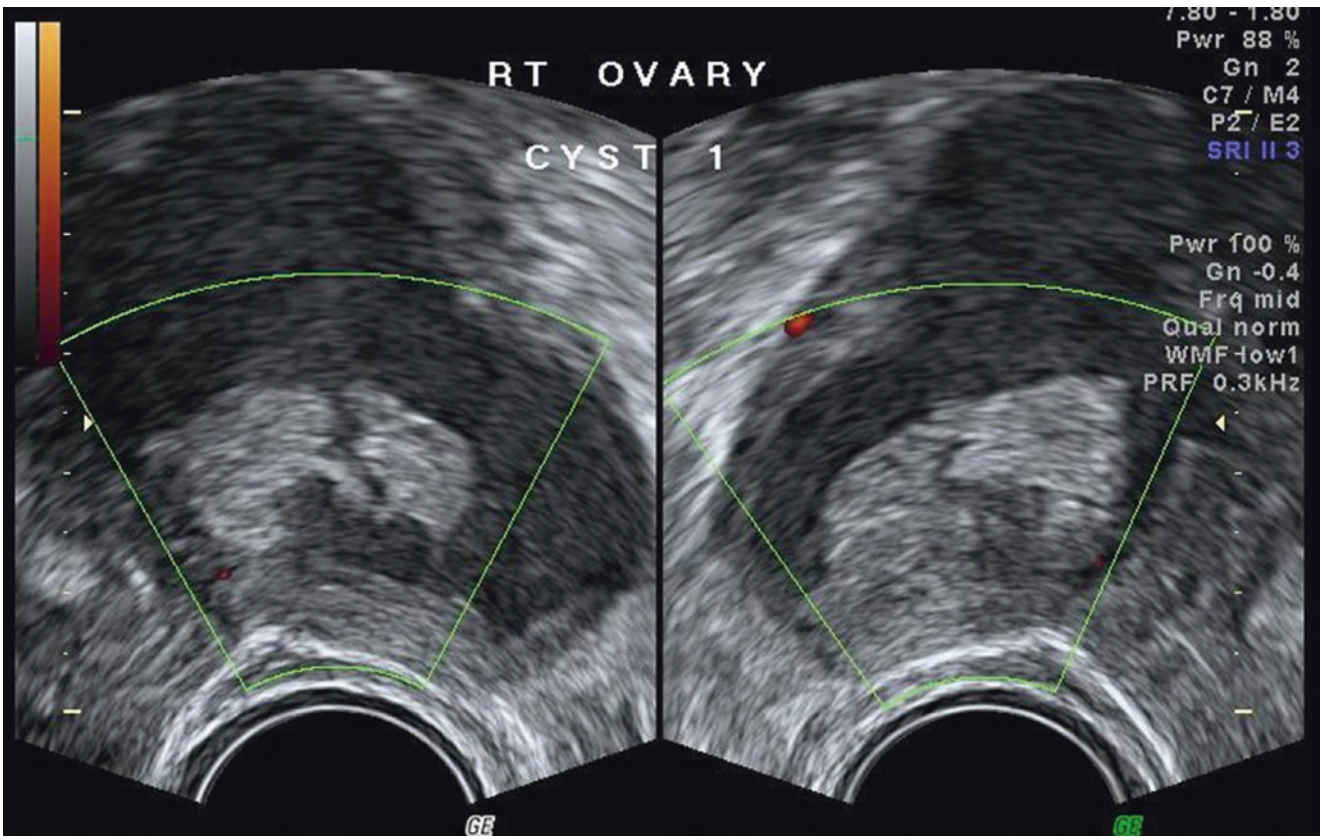

Fig. 7.28 Endometriotic cyst with recent haemorrhage, showing a hyperechoic and irregular clot within

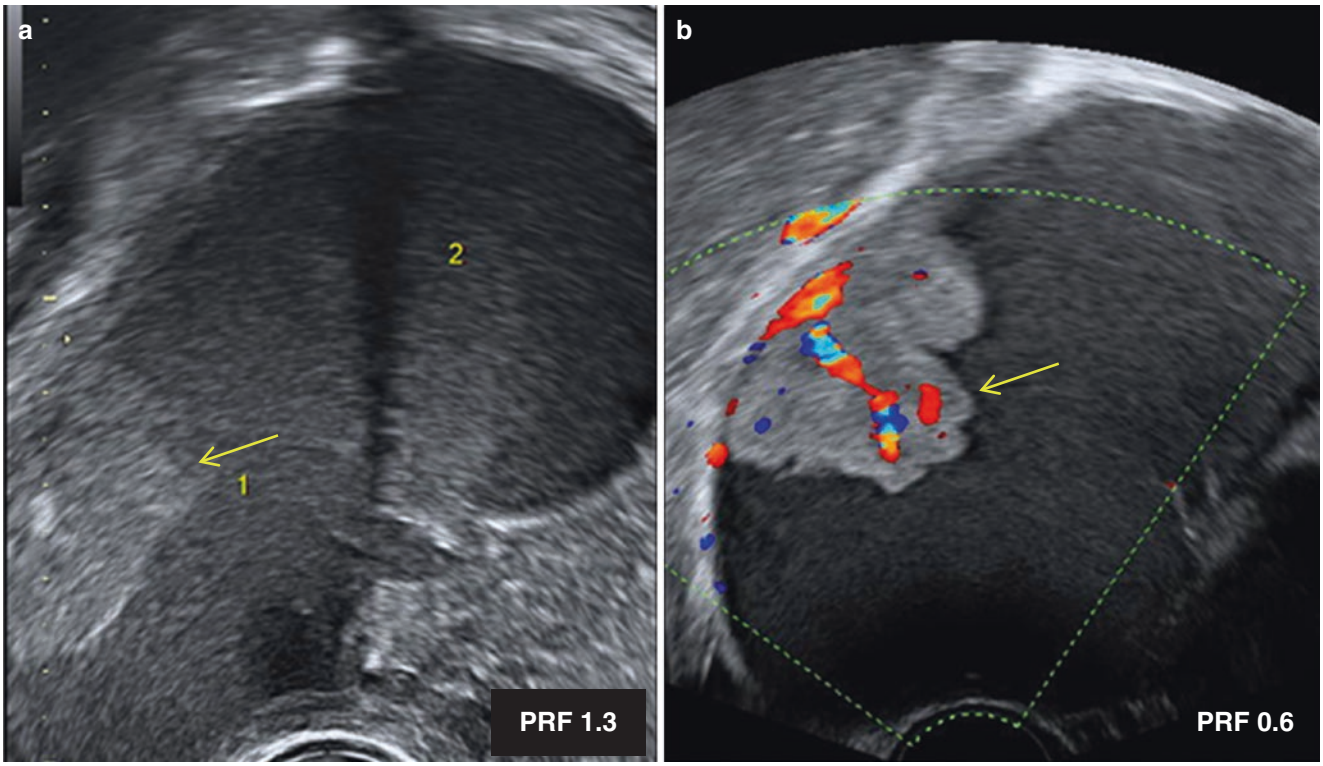

Fig. 7.29 (**a**) 8 cm right ovarian endometriotic cyst in a 34-year-old lady on treatment for infertility. Laparoscopic partial cystectomy was done to retain ovarian tissue in view of infertility. *HPE*: endometrioma. (**b**) Scan done 3 months following surgery showed a solid area with vascularity (*arrow*) suggestive of malignancy. A similar area (*arrow*) was seen in the image (**a**) at the earlier scan done 3 months prior to the surgery. This was, however, mistaken for a clot as the PRF was high and therefore flow in that area was not picked up. Patient underwent a second surgery. *HPE:* endometrioid carcinoma (Grade 2) arising in the background of endometriosis

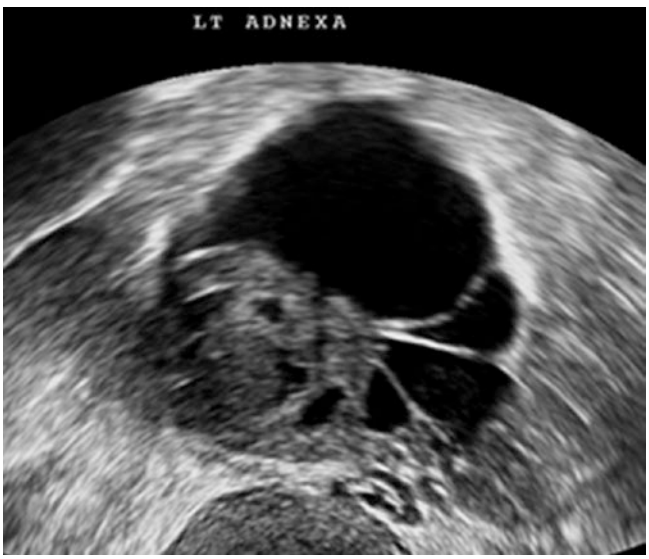

Fig. 7.30 Periovarian adhesions with loculated fluid commonly seen in patients with endometriosis

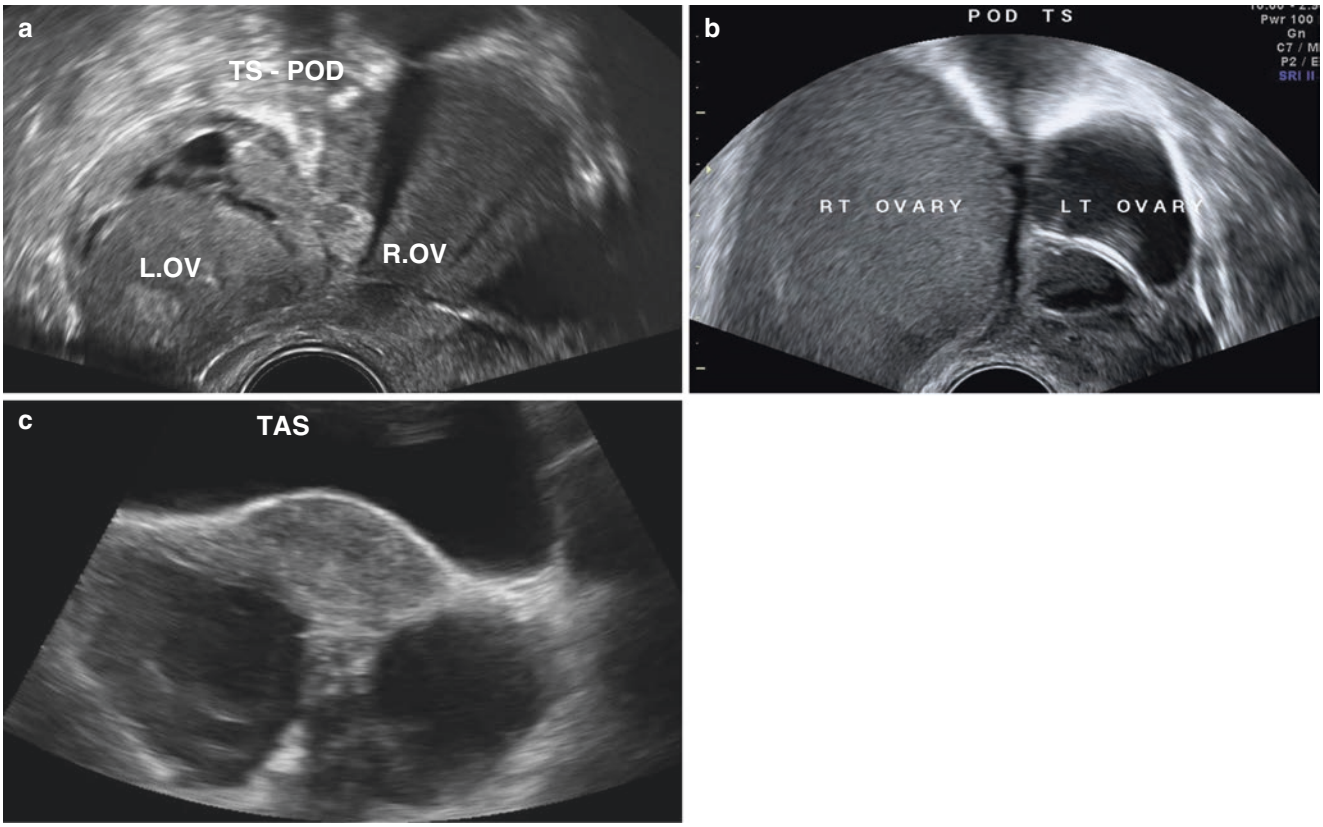

Fig. 7.31 'Kissing ovaries' refer to ovaries with endometriotic cysts, placed beside each other. They are adherent to each other and to the posterior wall of the uterus, in the pouch of Douglas. (**a**, **b**) TVS (**c**) TAS

7.4.2.1 Decidualised Endometriotic Cysts (Figs. 7.32 and 7.33)

During pregnancy, endometriotic cysts often show papillary solid projections and increased vascularity because of decidual changes in the endometrial tissue lining these cysts. These cysts are called decidualised endometriotic cysts. Very often, especially when the patient is not a known case of endometriosis and is examined for the first time, these cysts with solid vascular tissue raise a high suspicion of malignancy. Typical ultrasound features of decidualised endometriotic cysts are rounded papillary projections with smooth contour, in a 'ground glass' background. Other features of endometriosis like multiple cysts, adhesions and hyperechoic foci in the cyst walls also help to reassure that these are endometriotic cysts and are not malignant in nature. These cysts generally subside in the third trimester and completely regress following pregnancy but may reappear in a subsequent pregnancy.

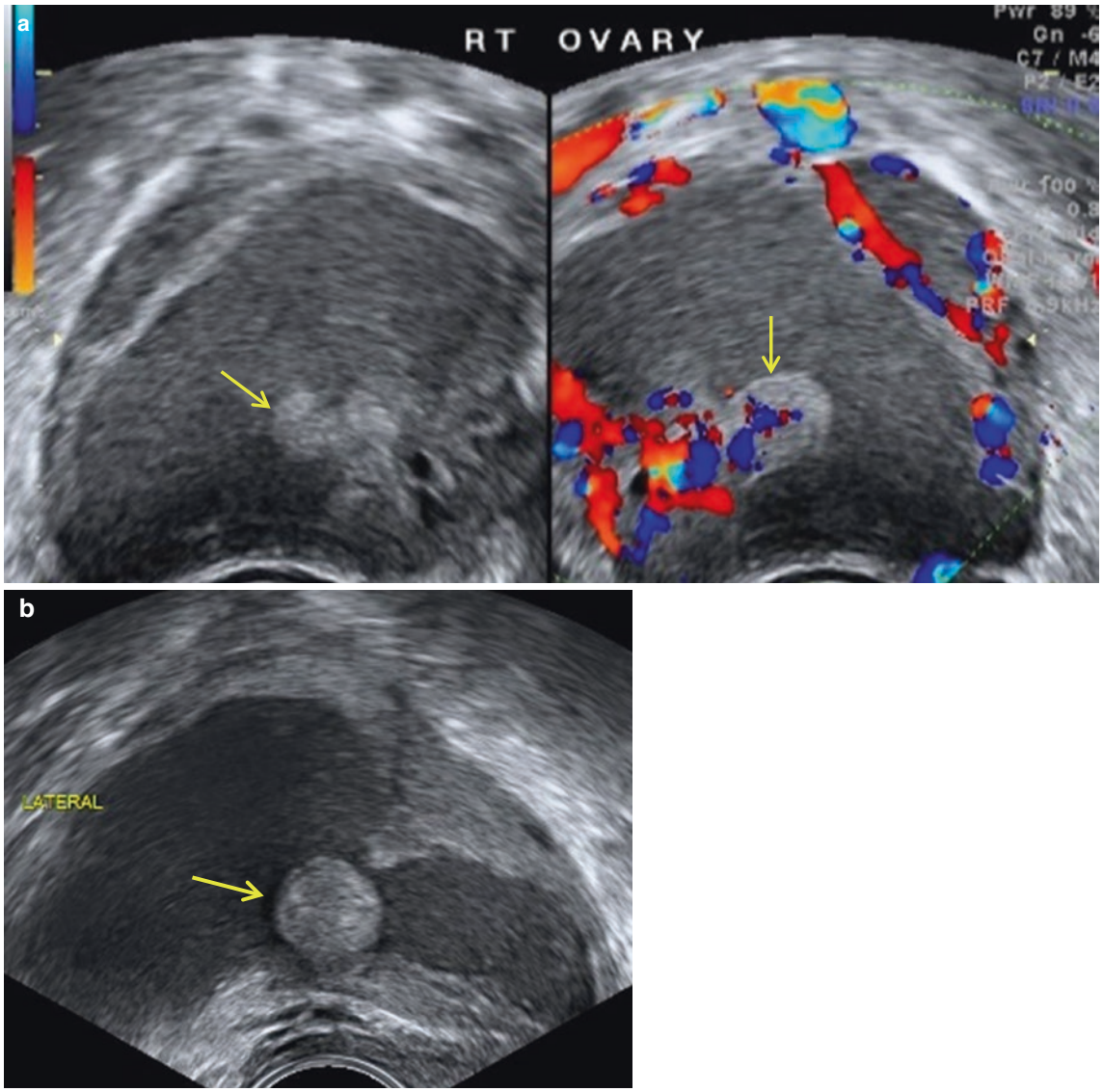

Fig. 7.32 (**a**) Right ovary showing two hypoechoic cysts with a solid vascular area in the larger cyst (*arrows*) in a pregnant lady at NT scan. (**b**) Characteristic rounded papillary projection with a smooth contour is noted in the decidualised endometriotic cyst (*arrow*)

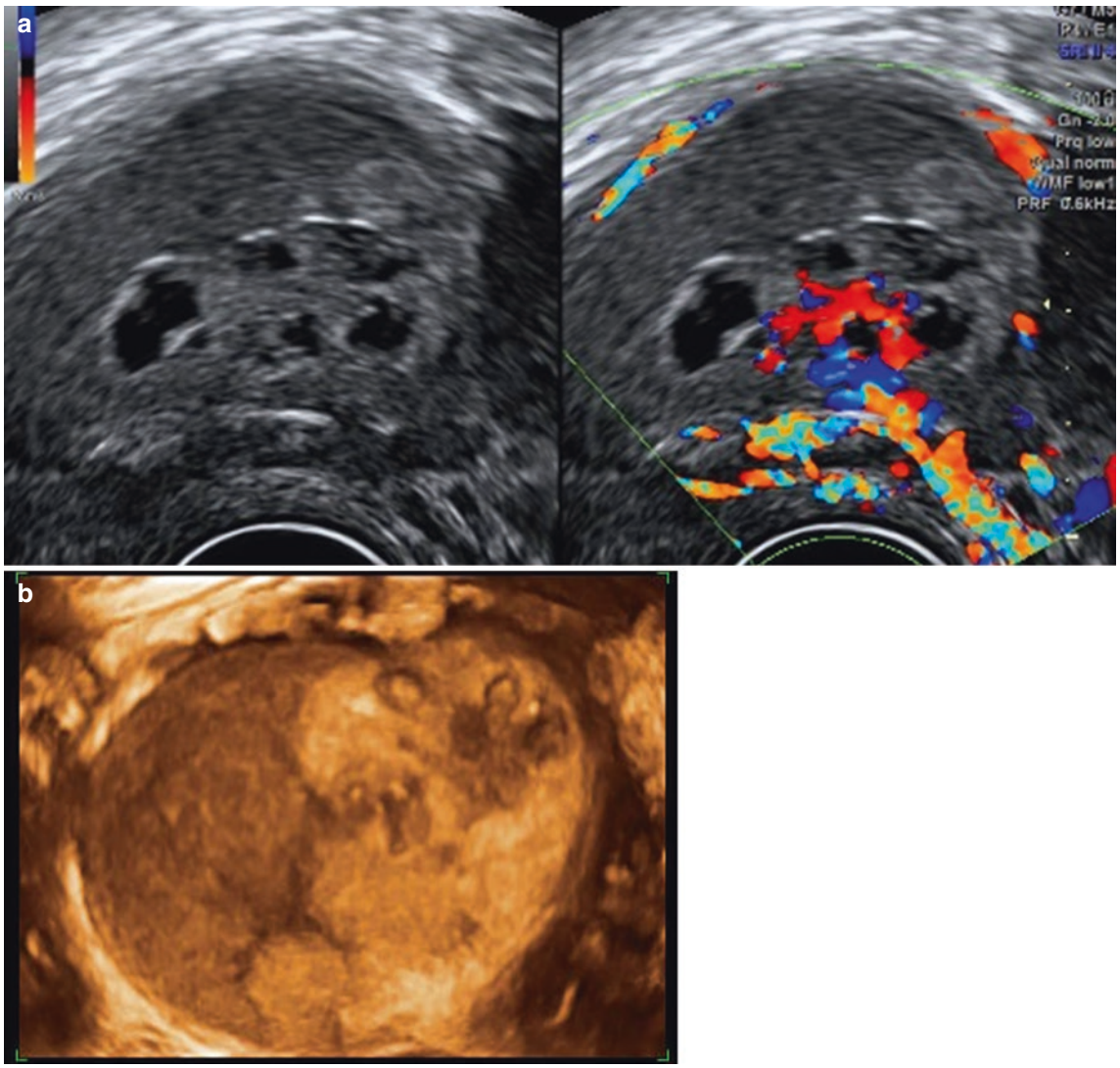

Fig. 7.33 (**a**) Decidualised endometriotic cyst where the solid tissue in the cyst shows cystic spaces within and high vascularity. The contour of the solid projections into the cyst wall is not clearly seen on 2D grey scale due to the thick turbid fluid within the cyst. (**b**) 3D rendered image was obtained, which shows the rounded contour of the papillary projections

Summary: Endometrioma

- These are seen in women of the reproductive age group with symptoms of dysmenorrhoea, chronic pelvic pain and infertility.
- Previous report and images are important for correlation.
- On ultrasound, they appear as unilocular hypoechoic cysts with uniform, low-grade internal echoes ('ground glass' appearance) and hyperechoic foci in the cyst walls (seen in about 30 % of cases). Lesions are often multiple and bilateral. Ovaries are often adherent to the uterine wall and bowel adhesions may also be noted (the absence of sliding sign).
- When in doubt about the nature of a cyst, a follow-up scan may help in confirming the diagnosis.
- In women with endometriosis, nodules of deep infiltrating endometriosis may be present and therefore a search for them is warranted when an endometriotic cyst is seen.

7.4.3 Ovarian Neoplasms

Ovarian cancer is the most lethal of gynecological malignancies primarily because patients are asymptomatic in the initial stages, and the diagnosis is therefore made when the disease is advanced.

Ovarian neoplasms can be broadly classified into epithelial tumours, germ cell tumours, sex cord–stromal tumours and metastatic tumours. Ultrasound should always describe the morphology of the mass. It is very important to ascertain the likelihood of malignancy for proper management of these masses, which is best done subjectively but can also be done based on IOTA guidelines and models. Optimal management (which includes whether to operate or not, and what type of surgery, if the decision to operate is made), however, does not only demand the distinction between benign and malignant pathology (dealt with in Chap. 14) but also ideally requires diagnosis of the specific pathology. This may be easy in some cases, like dermoid cysts, because of classical sonographic features. In others, it may be more difficult. Of late, efforts have been made to try and differentiate between these masses based on sonographic features of the mass.

Classification of Ovarian Neoplasms

Ovarian neoplasms can broadly be divided into epithelial tumours, germ cell tumours, sex cord–stromal tumours and metastatic tumours.

- *Epithelial tumours* arise from the surface epithelium of the ovary. They are the commonest ovarian tumours. They may be benign, borderline malignant or malignant. Malignant is more common in postmenopausal women. Serous and mucinous cysts are most common. They may show septae and papillae.
  - Serous
  - Mucinous
  - Endometrioid
  - Clear cell
  - Brenner's
  - Undifferentiated
- *Germ cell tumours* arise from the primordial germ cells (that also give rise to the ovum). They are seen in younger women. Dermoid cysts (or mature teratoma) are frequent and benign and typically show acoustic shadowing. Others are rare, malignant and usually solid (but may show cystic areas).
  - Teratomas
    Mature teratomas (dermoid cysts)
    Immature teratomas
  - Dysgerminoma
  - Yolk sac tumour
  - Choriocarcinoma
- *Sex cord–stromal tumours* arise from the ovarian stromal cells (theca and granulosa cells) and are rare. Many of these are hormone producing. Many are solid but may show cystic areas.
  - Granulosa cell tumours
  - Sertoli–Leydig cell tumours
  - Fibroma/fibrothecoma
- *Metastatic tumours* are secondary tumours in the ovary, with primaries mainly in the breast and gastrointestinal tract. Most are solid and often bilateral. Depending on the primary, their appearance can vary.

7.4.3.1 Epithelial Tumours

Epithelial ovarian neoplasms constitute the bulk of ovarian neoplasms. About 85 % of ovarian neoplasms are epithelial. They originate from the ovarian surface epithelium (mesothelium) which may invaginate into the underlying stroma. These could be serous, mucinous, endometrioid, clear cell, Brenner or undifferentiated. All epithelial neoplasms can be benign, borderline (i.e. having low malignant potential – the absence of stromal invasion) or malignant (carcinomas) based on their histological findings. In benign tumours, serous and mucinous are common. Benign endometrioid and clear cell tumours are rare.

Borderline tumours are more often seen in younger women and are commonly serous or mucinous in nature. They have a better prognosis than the malignant ones.

Malignant epithelial tumours are more common in older women. Solid vascular tissue is more common in malignant varieties. CA 125 levels are often elevated in women with epithelial malignant tumours.

Most women with epithelial tumours are asymptomatic. With large masses, the patient may present with abdominal distension or mass per abdomen.

Patients with malignant tumours may be asymptomatic initially, as a result of which ovarian malignancies are often discovered in late stages with poor 5-year survival rates. Once the tumour spreads, patients may present with typical features of malignancy like abdominal discomfort, weight loss, dyspepsia, ascites and a pelvic mass.

The commonest epithelial tumours are serous and mucinous, which are discussed below. Endometrioid carcinomas

are associated with cancer of the endometrium in 30 % of cases. Both endometrioid and clear cell carcinomas are associated with pelvic endometriosis. Brenner tumours are rare, most often benign and commonly appear solid with no or minimal flow on Doppler. More than half show acoustic shadowing. Calcification is often seen in a Brenner tumour.

Serous
- 30 % of ovarian neoplasms.
- 50–70 % are benign.
- Papillae are more common in serous cysts.

Mucinous
- 25–30 % of ovarian neoplasms.
- 80–85 % are benign.
- Septae are more common in mucinous cysts (multiloculated).

Serous Epithelial Tumours

These could be benign (Figs. 7.34, 7.35, 7.36 and 7.37), borderline (Fig. 7.38) or malignant (Figs. 7.39 and 7.40) tumours.

Ultrasound Features of Serous Epithelial Tumour

(Figs. 7.34, 7.35, 7.36, 7.37, 7.38, 7.39 and 7.40)

- These may be unilocular or multilocular. Benign cysts tend to be unilocular or to have fewer locules.
- Serous cysts may be bilateral (both in benign and malignant tumours), more so the malignant ones.
- The septae are usually few in number. In the benign tumours, they tend to be smooth and thin, whereas in malignant ones, they tend to be thick and irregular.
- Papillae may be seen in serous cysts, including benign ones. The borderline tumours tend to have a higher number of papillae, while in the malignant ones, the number is even higher (which may fuse to form large masses of solid tissue within the cyst).
- Solid tissue (other than papillae) is a feature of malignant serous adenocarcinomas. Solid tissue may be seen either between the locules or on one side of the mass, or the mass may be predominantly solid.
- Some tumors on ultrasound may show scattered, punctate, bright foci suggestive of microcalcifications, due to the presence of psammoma bodies. Psammoma bodies are concentric, lamellated, calcified structures that are typically less dense than most calcifying masses. Therefore, they usually do not show acoustic shadowing. Though not commonly seen, when present, the tumour is likely to be a borderline or low grade malignant serous tumor. Brenners tumors, thecomas and gonadoblastomas may show other forms of dystrophic calcification that mimic psammomatous calcifications.
- The fluid in a benign cyst is typically anechoic but may show fine low-grade internal echoes. Borderline and malignant cysts are more likely to show fluid with internal echoes.
- On Doppler, benign tumours show minimal flow in both the septae and the cyst wall. The malignant ones, however, show increased flow, particularly in the papillae and solid areas.
- Ascites may be seen in cases with a malignant serous cyst.

Serous Cystadenoma

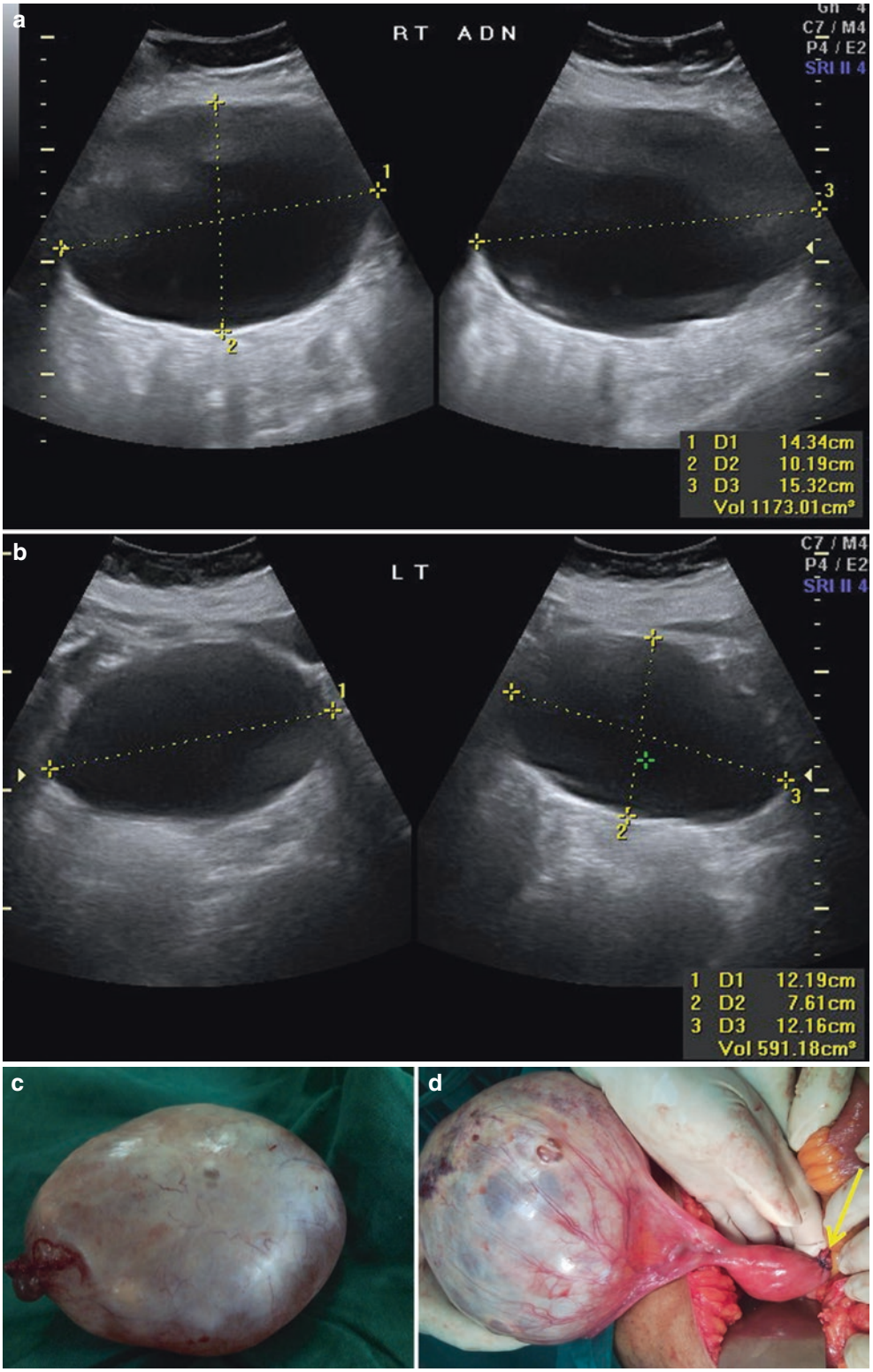

Fig. 7.34 Bilateral large unilocular serous cystadenomas in a 75-year-old patient. (**a**) Right cyst. (**b**) Left cyst. (**c**) Specimen of the excised left ovarian serous cyst. (**d**) At surgery, the uterus with site of excision of the left ovary (*arrow*) and the right ovarian cyst which was yet to be excised

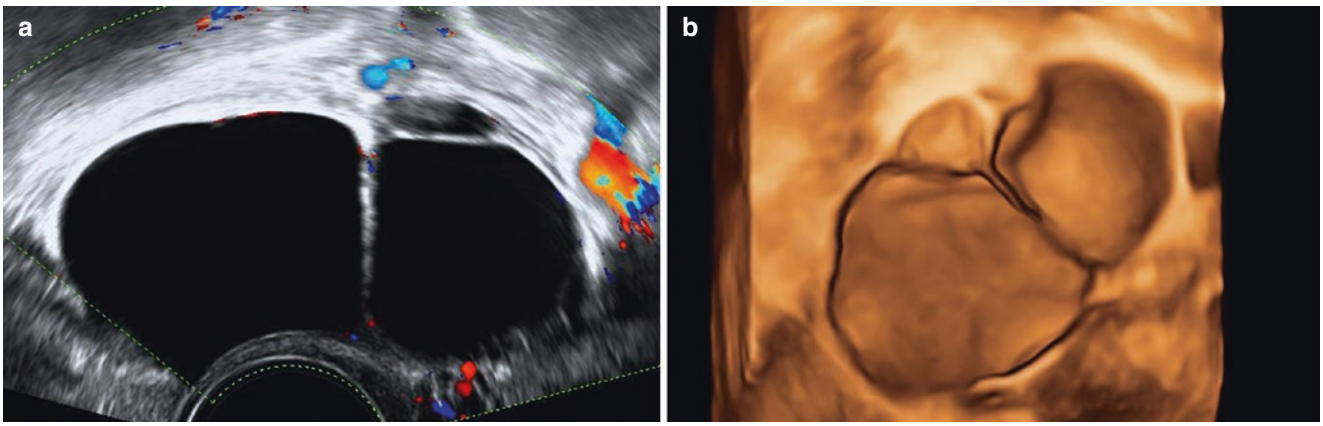

Fig. 7.35 Multiloculated serous cystadenoma showing septae. (**a**) Greyscale, (**b**) 3D rendered image

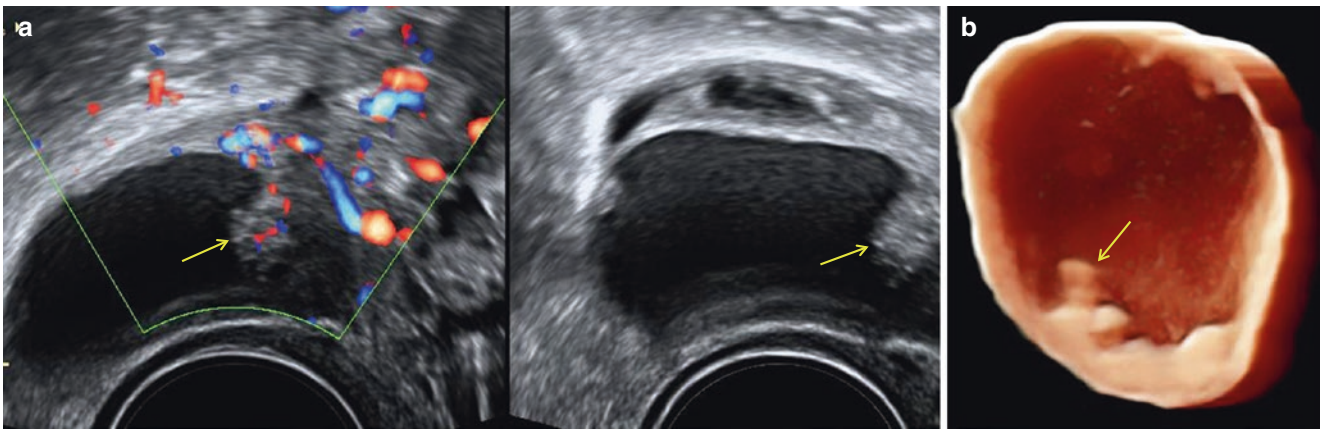

Fig. 7.36 Benign serous cyst adenoma with papillae (*arrows*). (**a**) 2D, (**b**) 3D rendered image

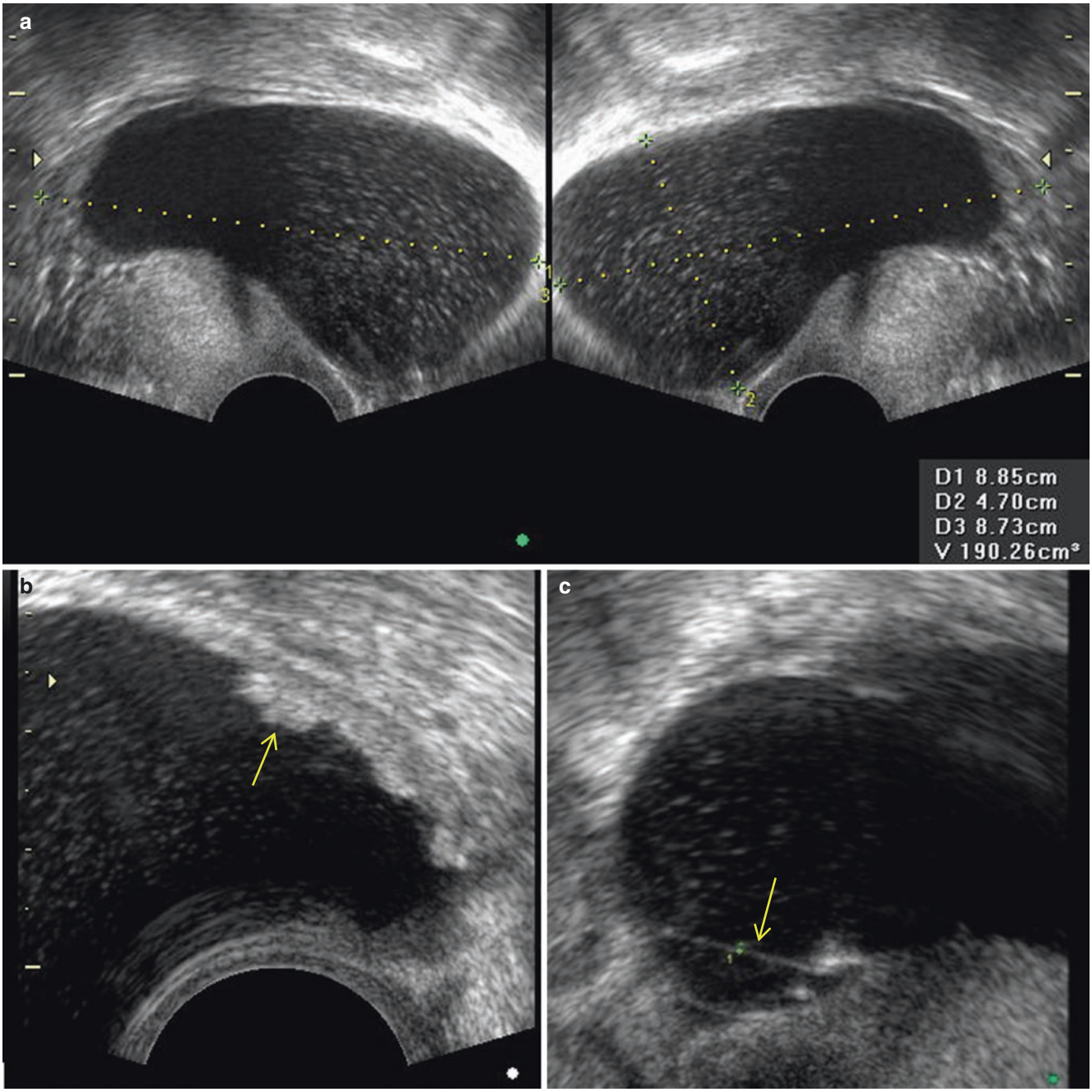

Fig. 7.37 Benign serous cyst adenoma. (**a**) Cyst shows low-grade internal echoes. (**b**) Few blunt papillae (*arrow*) are seen. (**c**) A thin septum is also seen (*arrow*)

Borderline Serous Tumours

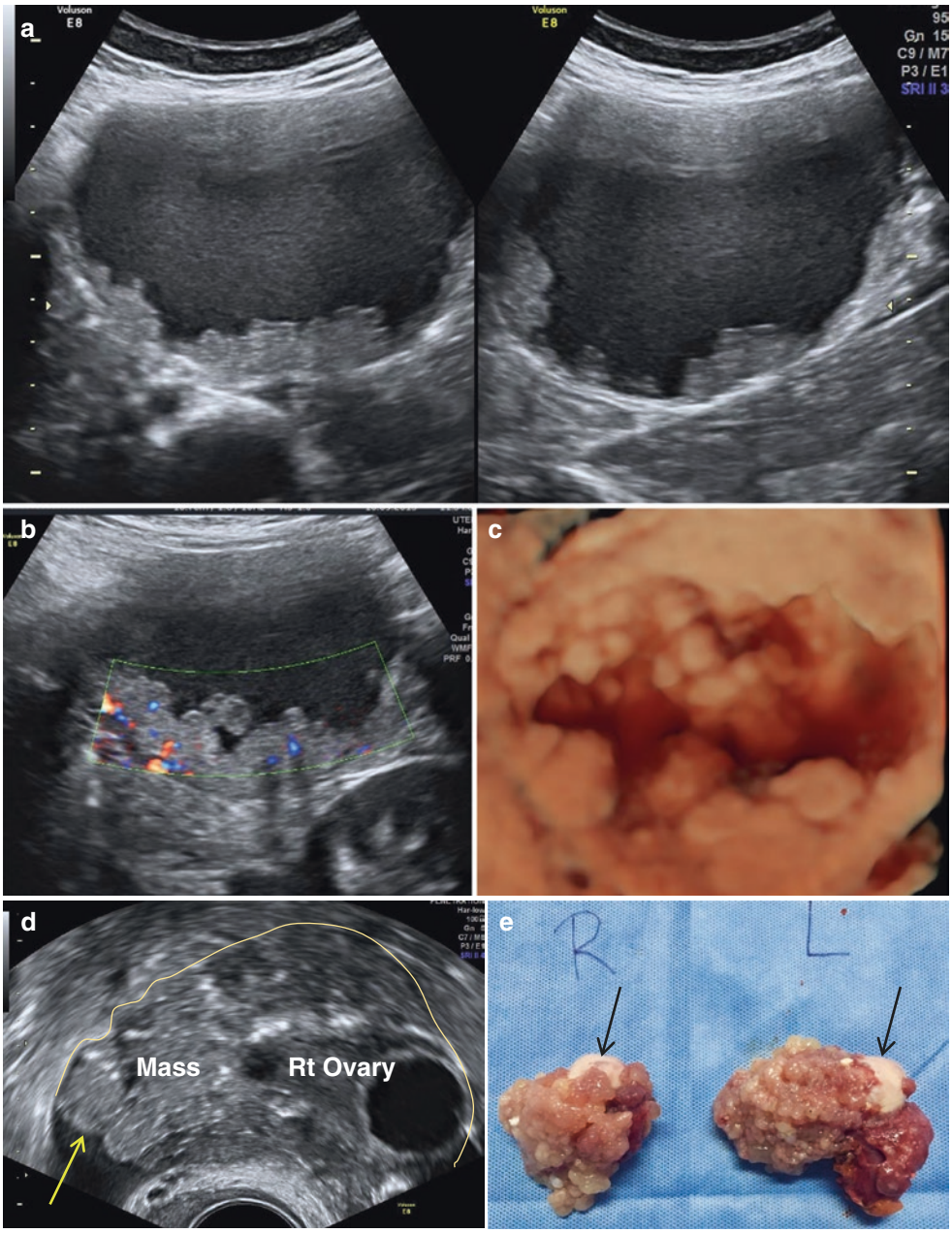

Fig. 7.38 Borderline serous tumour in two different cases. Case 1-(**a**) Multiple papillae are seen along the cyst walls. (**b**) Flow is seen within the papillae on Doppler. (**c**) 3D rendered image of the cyst showing papillae. Case 2-Case of bilateral psammomatous borderline serous tumor (**d**) 'V' shaped solid mass seen along the superior, posterior and inferior margins of the right ovary. The mass shows multiple hyperechoic foci and irregular outer margins (*arrow*). Its upper margin is outlined, as it is difficult to delineate from surrounding tissues. The mass was vascular with a colour score of 3. (**e**) Post-operative specimen of right ovary (R) and left ovary (L) showing the papillary outer surface of the mass surrounding the ovaries (*arrows*)

Serous Cystadenocarcinoma

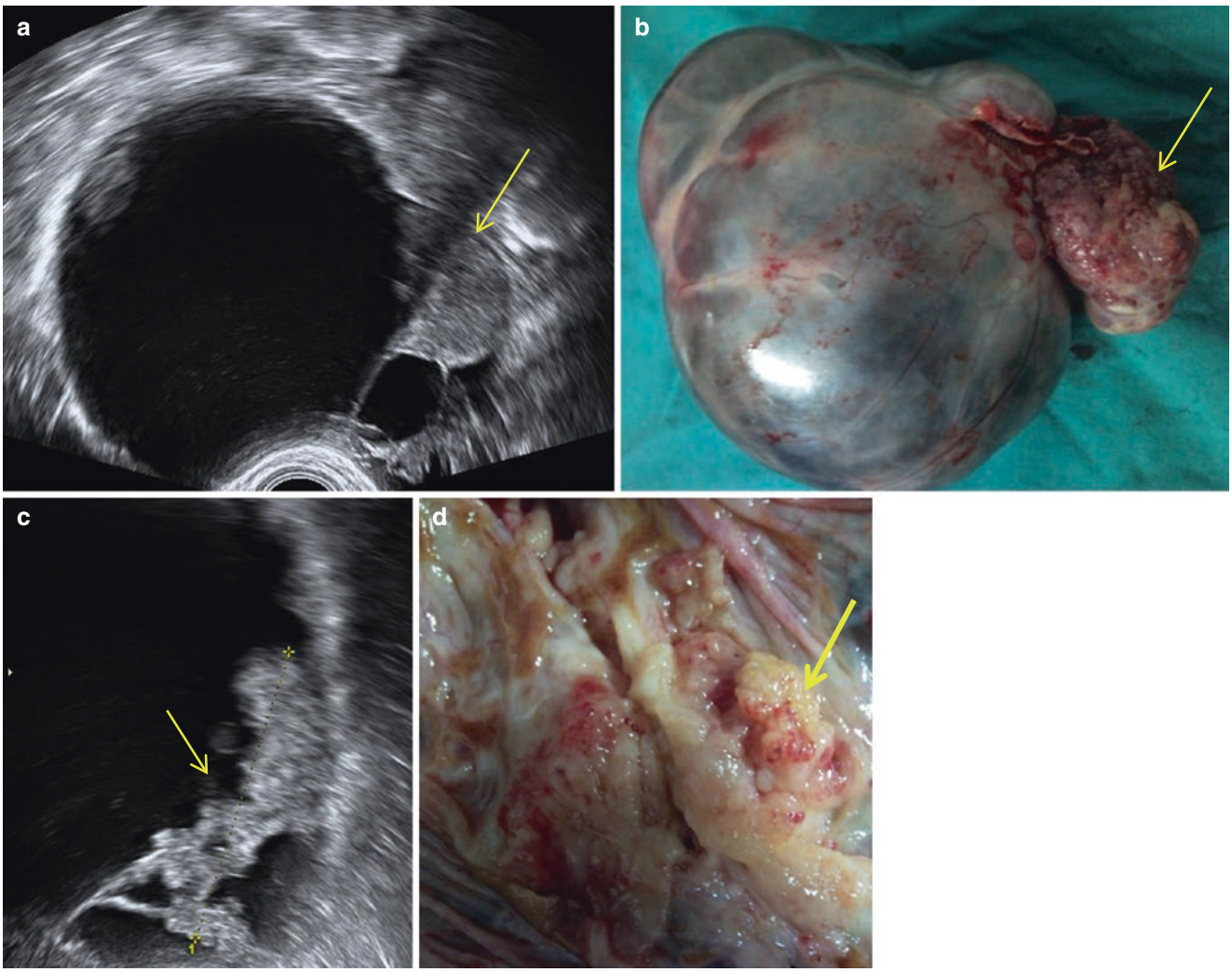

Fig. 7.39 Papillary serous cyst adenocarcinoma. (**a**) Solid area is seen along the outer aspect of the mass (*arrow*). (**b**) Corresponding post-operative specimen showing the solid area (*arrow*). (**c**) Irregular septae with papillae seen within the cyst walls (*arrow*). (**d**) Corresponding post-operative specimen showing multiple papillae (*arrow*)

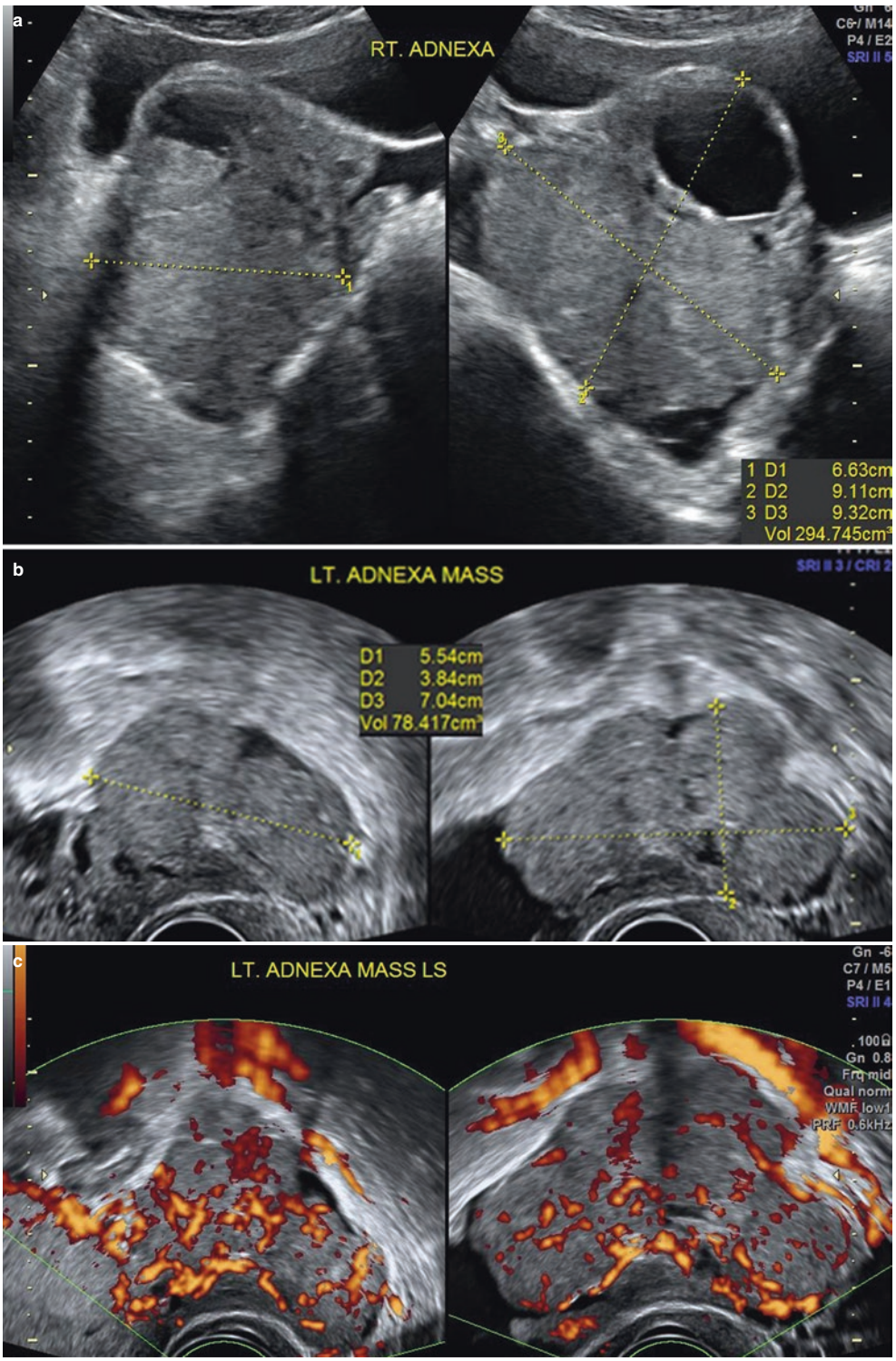

Fig. 7.40 Bilateral high-grade serous cystadenocarcinoma. A 42-year-old woman presented with a complaint of a bloating sensation of the abdomen. CA 125 value was more than 1000 IU/mL. (**a**) Enlarged right ovary with solid and cystic areas. (**b**) Left ovary replaced by a solid lobulated mass. (**c**) Left neoplastic ovary showing high vascularity (colour score 4). (**d**) The mass showing low-resistance flow (RI 0.24). (**e**) 3D power Doppler with glass body display showing high and abnormal vascular morphology of the neoplastic mass. (**f**) Power Doppler showing high vascularity in both ovarian masses. (**g**) Right ovarian mass showing irregular lobulated external margins (*arrow*) which are well seen because of the surrounding ascitic fluid

Fig. 7.40 (continued)

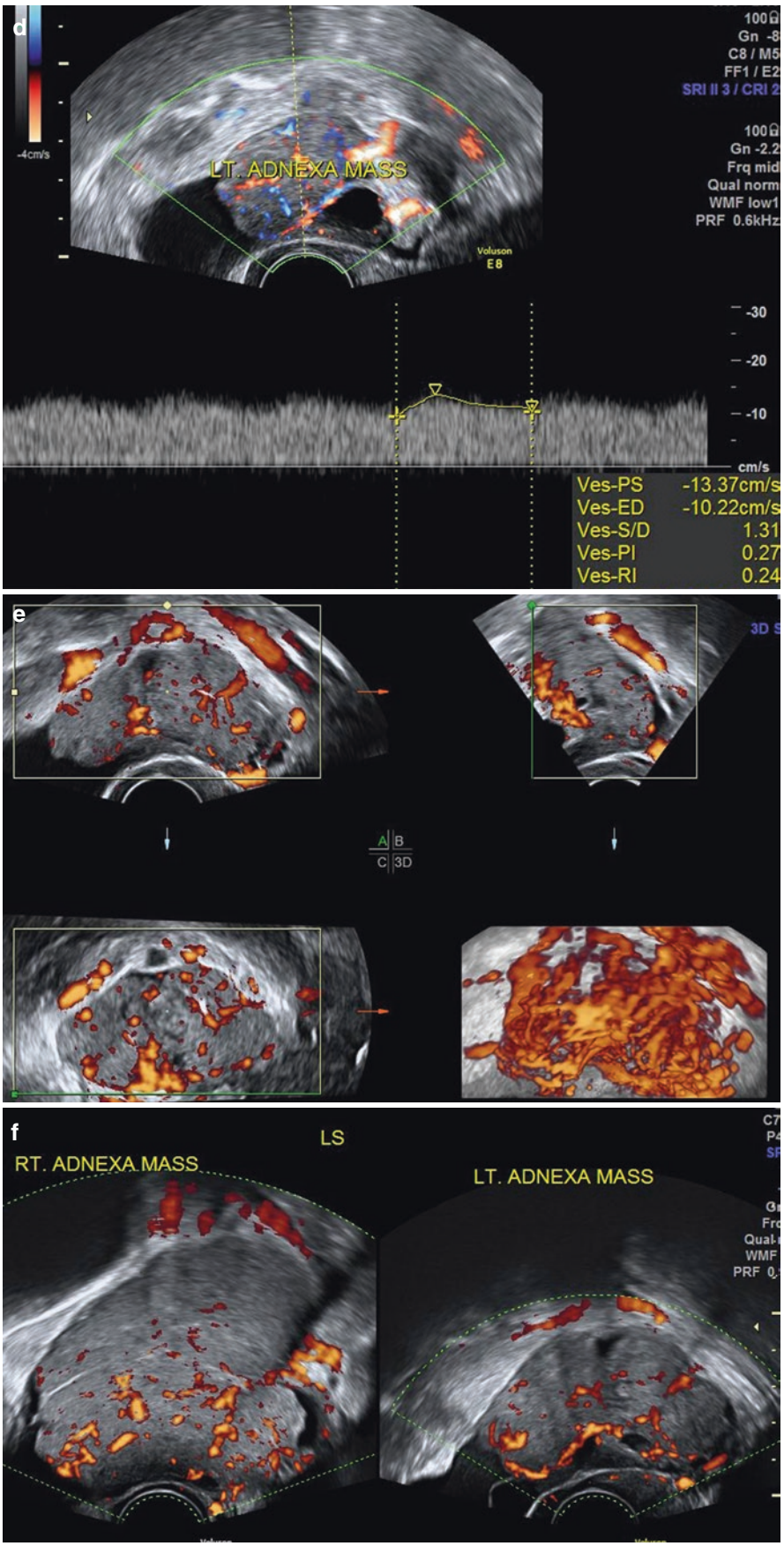

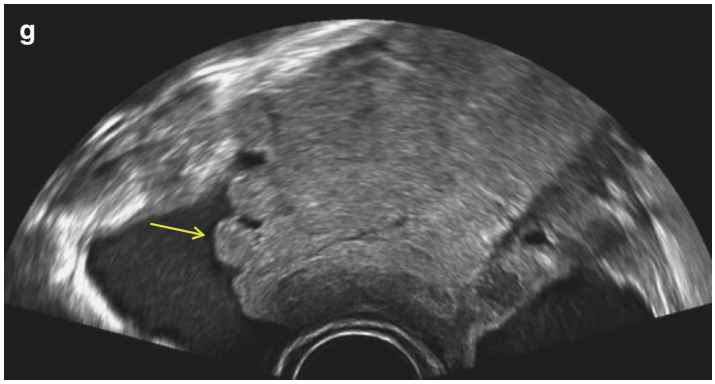

Fig. 7.40 (continued)

Serous Cystadenofibroma (Figs. 7.41 and 7.42)
Serous cystadenofibromas are ovarian cysts that contain both epithelial and fibrous stromal elements. They are almost always benign and only very rarely malignant. They may have solid components which are typically only short stubby papillae. These show acoustic shadowing and minimal flow on Doppler.

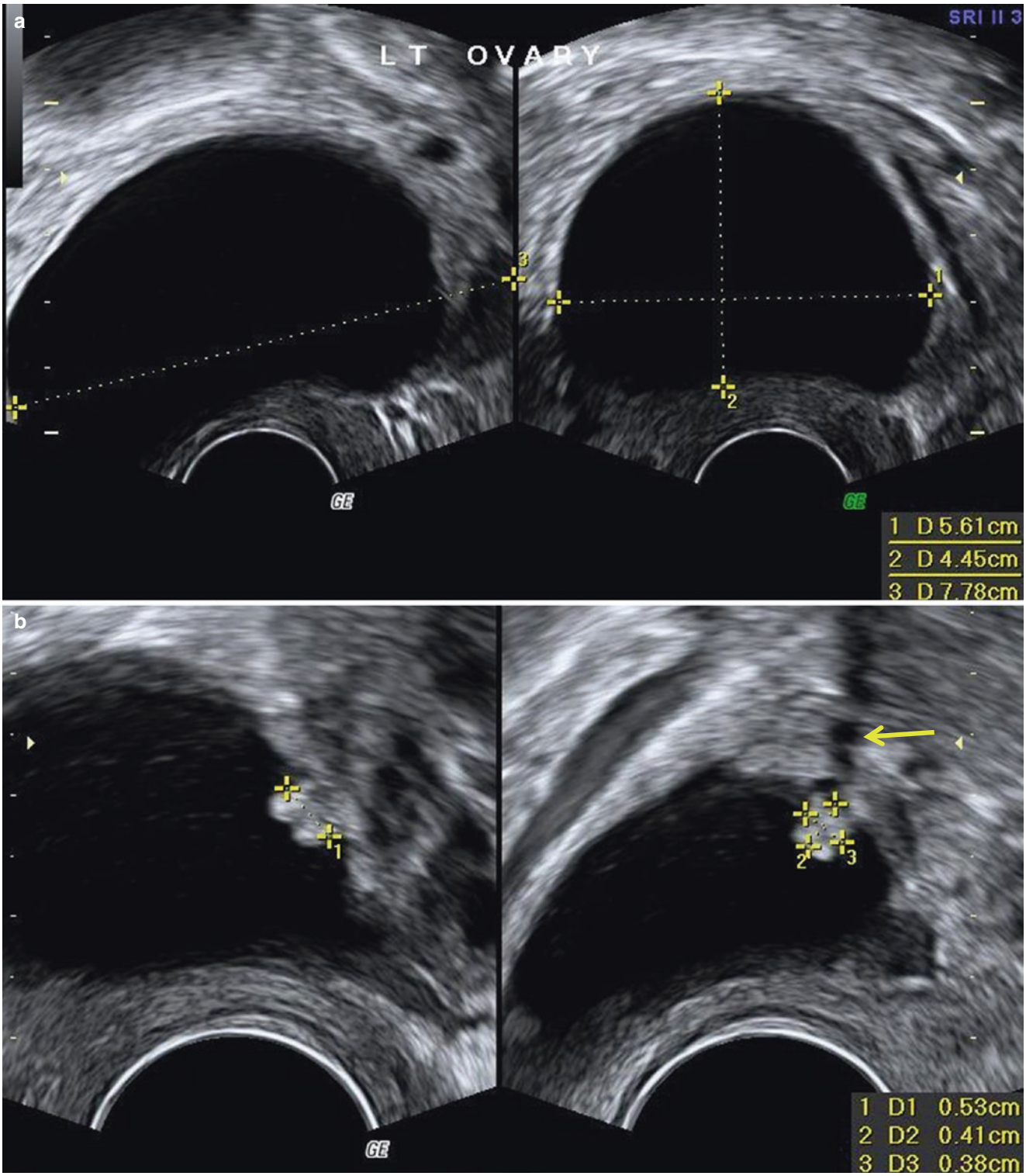

Fig. 7.41 Serous cystadenofibroma. (**a**) Cyst with anechoic contents. (**b**) Short stubby papilla showing acoustic shadowing (*arrow*)

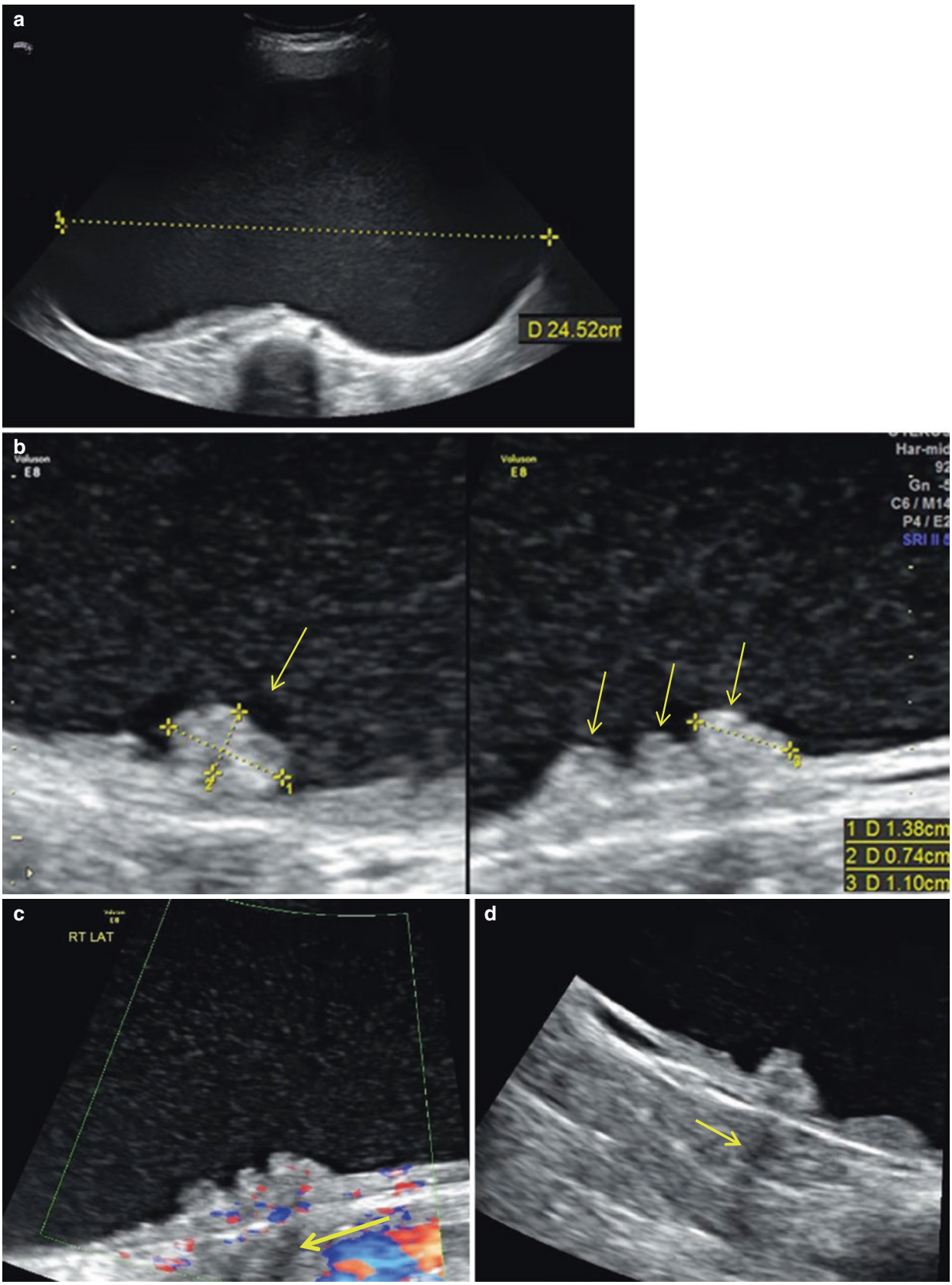

Fig. 7.42 Serous cystadenofibroma. (**a**) Cyst with large dimensions (5.4 L). (**b**) Papillae seen along the inner cyst wall (*arrows*) localised to a small part of cyst wall. (**c**, **d**) Papillae showing acoustic shadowing (*arrows*). (**e**) 3D rendered image of cyst wall showing papillae (*arrow*). (**f**) Post-operative cut section of the specimen showing the inner cyst wall in the area with the papillae (*arrow*). The rest of the cyst wall was smooth as was seen on ultrasound. (**g**) Post-operative gross specimen

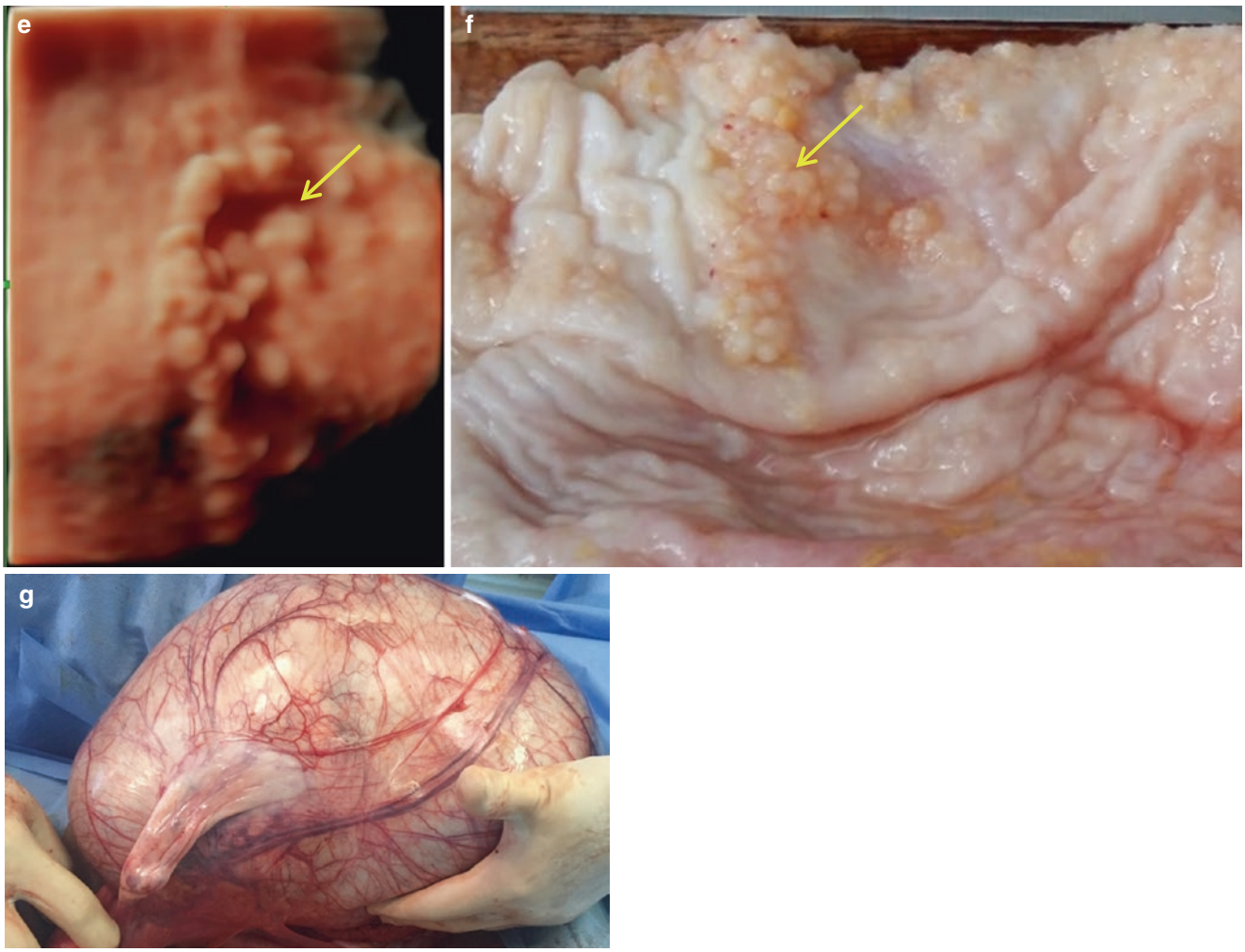

Fig. 7.42 (continued)

Mucinous Cysts

These could be benign (Figs. 7.43, 7.44, 7.45, 7.46, 7.47 and 7.48), borderline (Figs. 7.49, 7.50, 7.51 and 7.52) or malignant (Fig. 7.53) tumours.

Ultrasound Features of Mucinous Cysts (Figs. 7.43, 7.44, 7.45, 7.46, 7.47, 7.48, 7.49, 7.50, 7.51, 7.52 and 7.53)

- Mucinous cysts are typically multilocular but may be unilocular.
- They are often large in size.
- Mucinous cysts are only very occasionally bilateral.
- Their septae typically appear rigid and bright.
- The contents of the locules may vary in echogenicity. The locules may be anechoic or show varying amount of internal echoes.
- Borderline mucinous cysts typically show a cluster of tiny locules (often localised to an area). At times, because the locules are small and closely packed, it could give the appearance of an almost solid tissue filled with tiny locules.
- Malignant mucinous tumours often show solid tissue.
- On Doppler, flow may be seen in the septae and the cyst walls. In borderline tumours, the area with the closely packed cysts, in particular, shows vascularity. Malignant tumours are likely to show high vascularity, particularly in any solid tissue within.

Ascites may be seen. With malignant mucinous cysts, ascitic fluid often shows increased turbidity.

Mucinous Cystadenoma

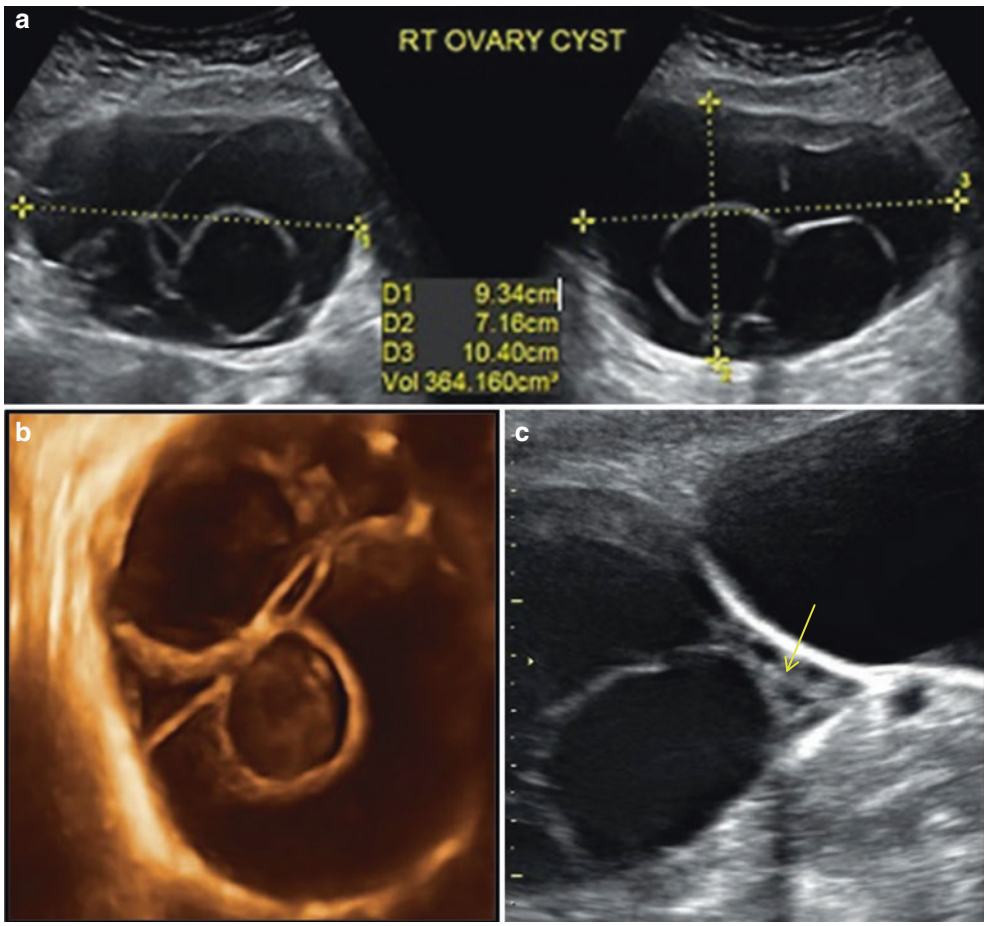

Fig. 7.43 Mucinous cystadenoma in a 19-year-old patient. (**a**) Multiloculated cyst. (**b**) 3D rendered image. (**c**) Ovarian crescent sign (*arrow*)

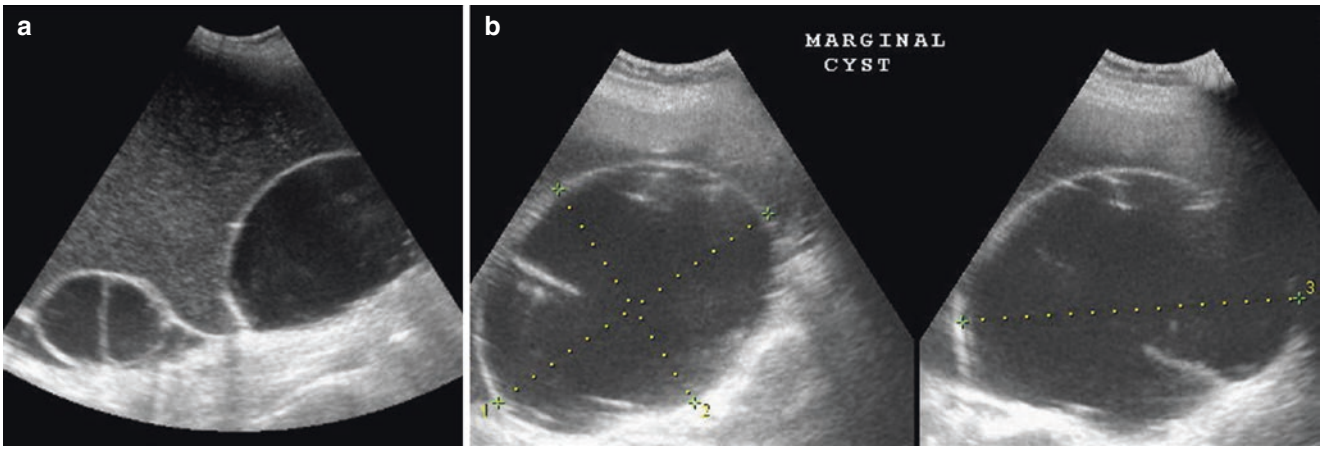

Fig. 7.44 A 10 L large mucinous cystadenoma. (**a**) Bright, rigid septae with locules showing varying echodensity. (**b**) Largest locule was found to be of 1000 cc

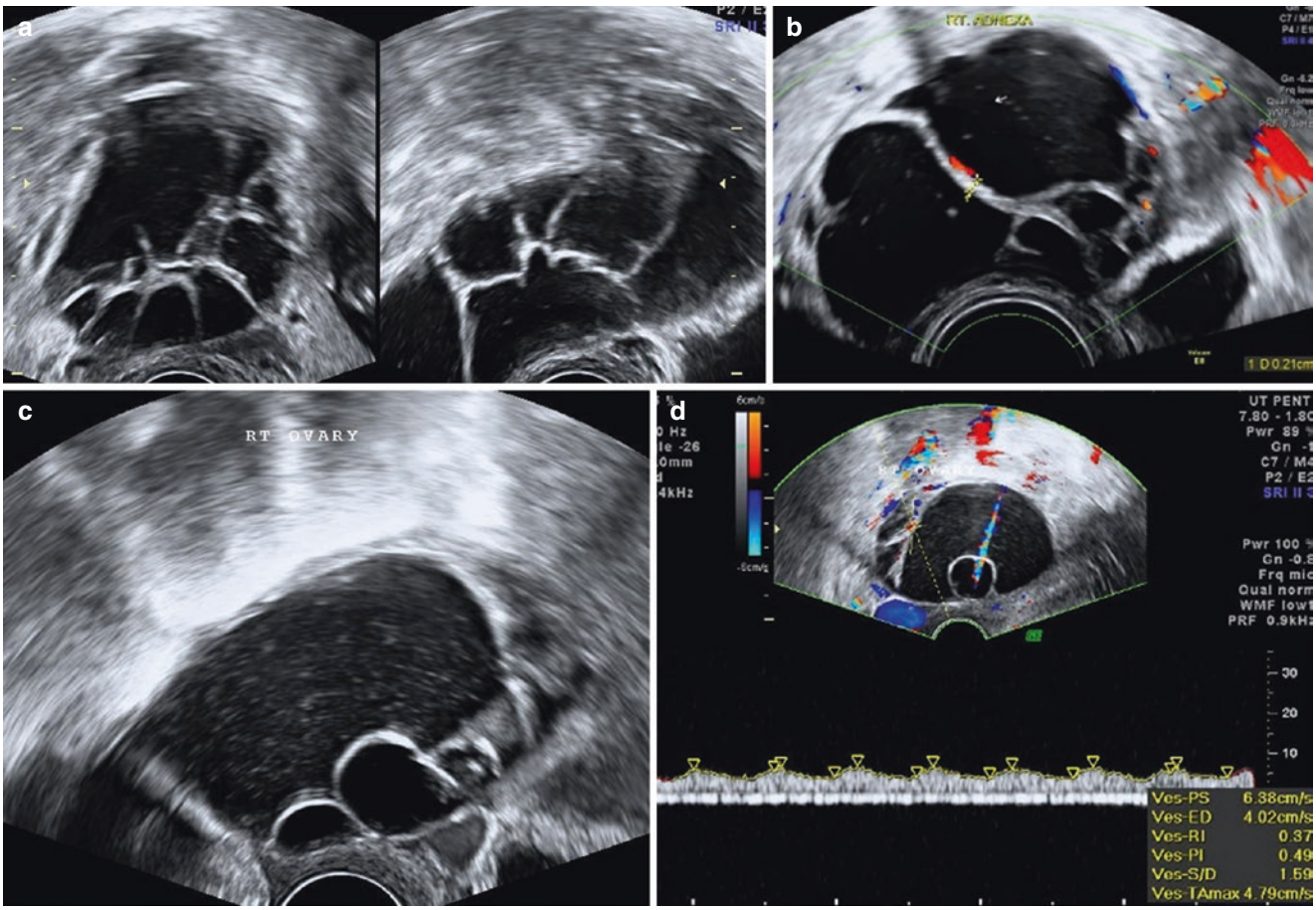

Fig. 7.45 Multilocular mucinous cystadenomas. (**a**) Multiple septae. (**b**) Low vascularity. (**c**) Locules show varying echodensity. (**d**) Cyst wall showing low-resistance flow with RI of 0.37

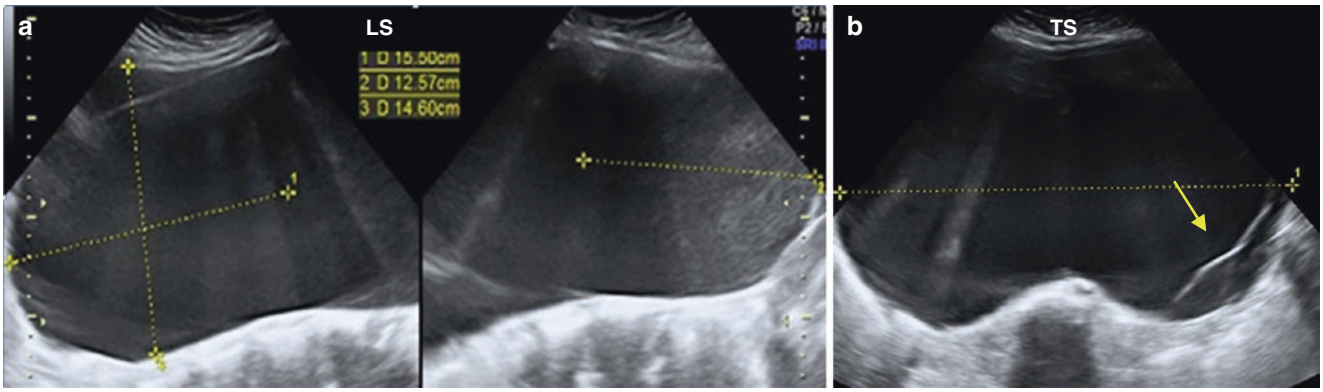

Fig. 7.46 A 6.9 L large mucinous cystadenoma. (**a**, **b**) A single small septum is seen (*arrow*)

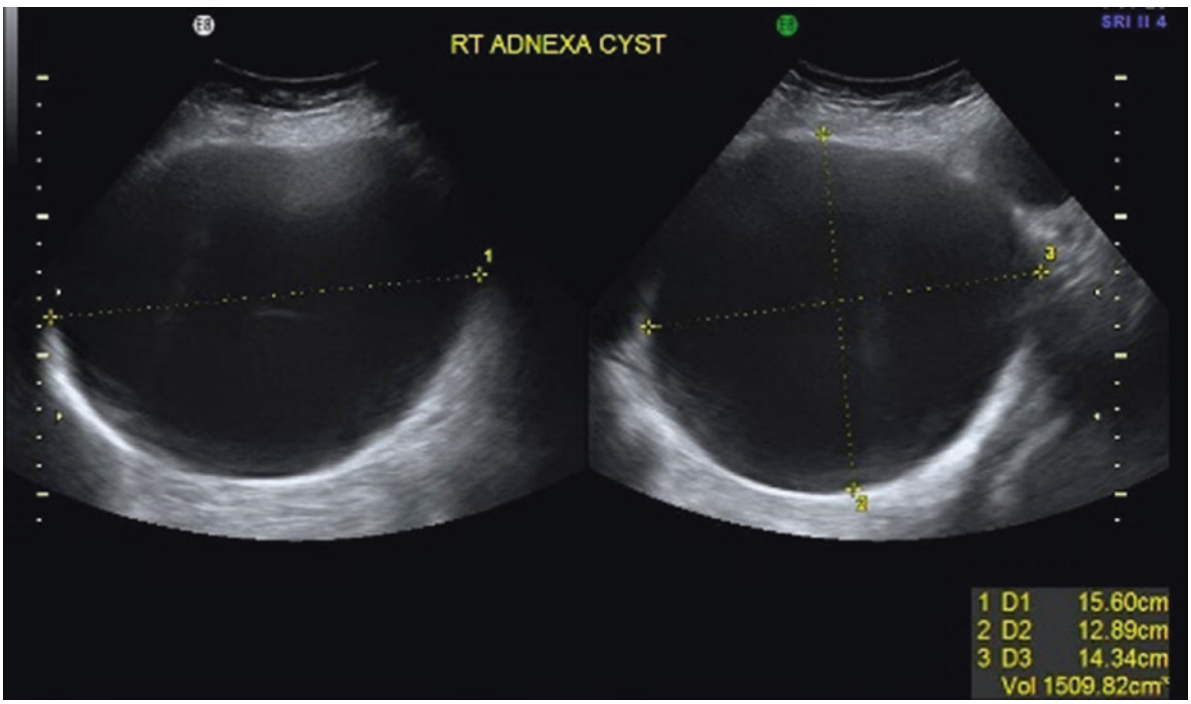

Fig. 7.47 Unilocular mucinous cystadenoma (volume 1.5 L)

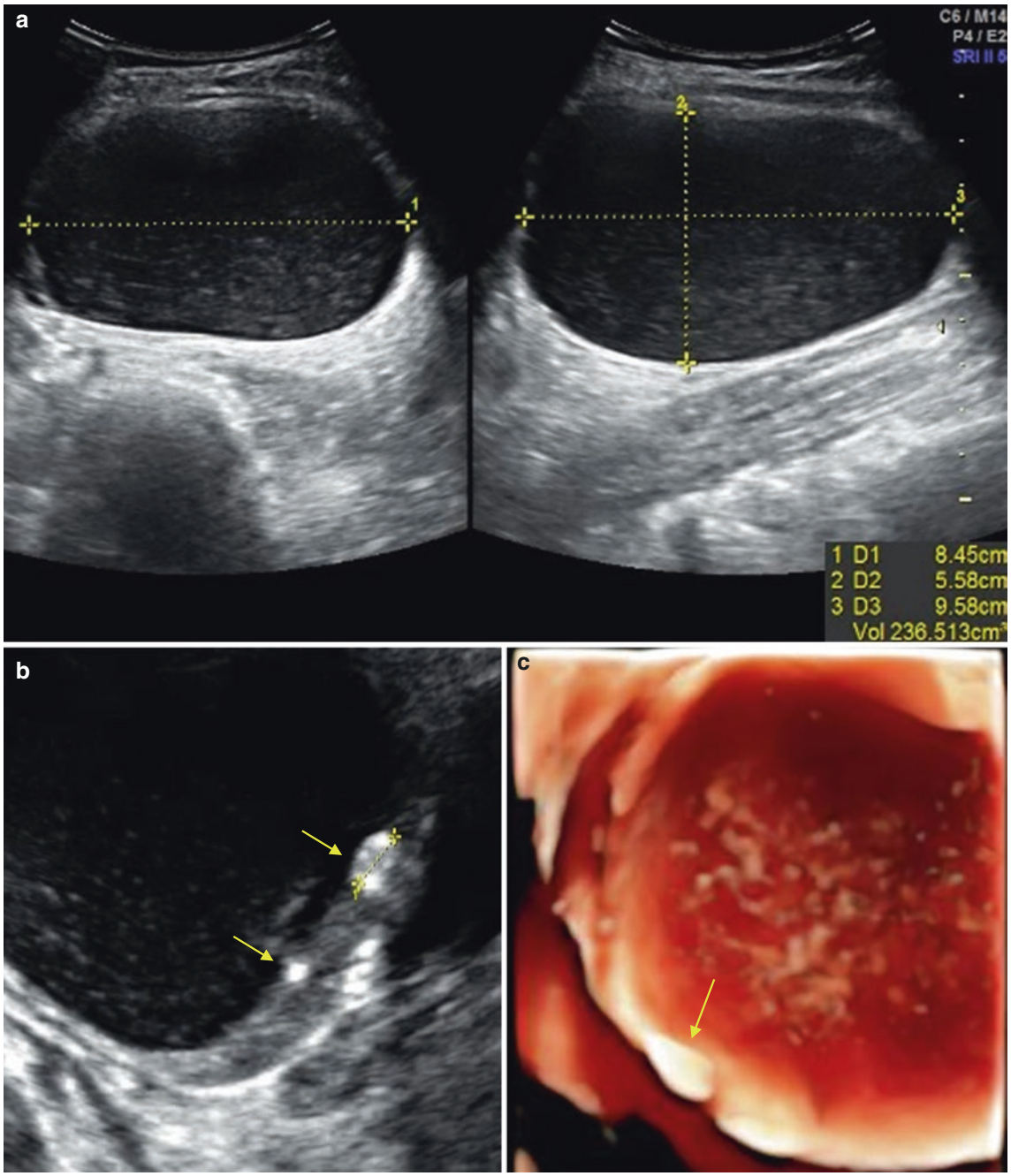

Fig. 7.48 Unilocular mucinous cystadenoma in a 17-year-old patient who presented with torsion. (**a**) Cyst shows low-grade internal echoes which could be because of the associated torsion. (**b**) Two foci of calcification (*arrows*) seen in the cyst wall. (**c**) 3D rendered image of the cyst showing internal echoes and a bright focus of calcification in the cyst wall (*arrow*)

Borderline Mucinous Cysts

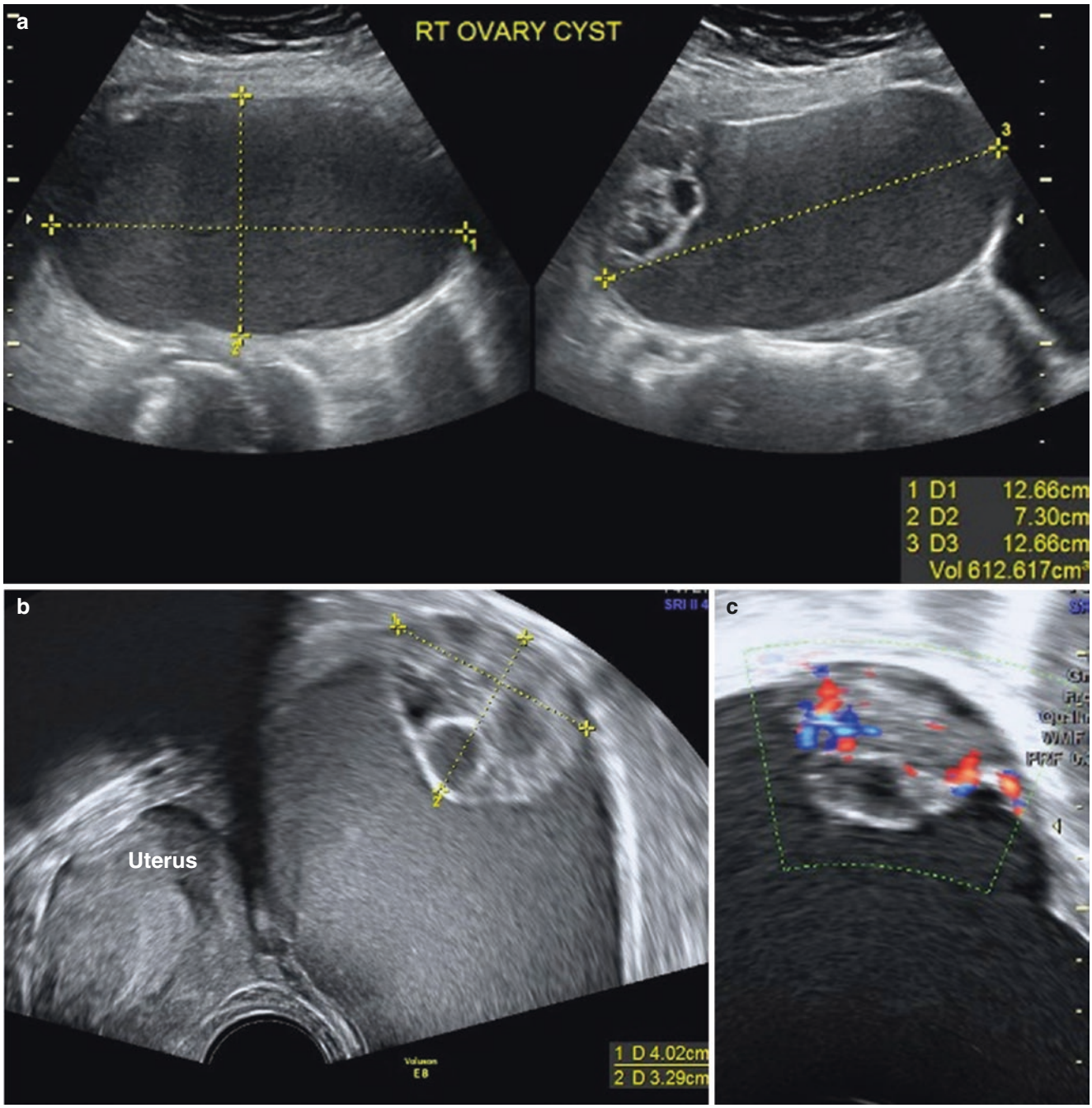

Fig. 7.49 Borderline mucinous cyst with torsion. (**a**) Cyst showing focal area of multiple locules. (**b**) Cyst is seen anterior to the uterus on TVS. It shows turbid contents and a circumscribed focal multilocular area. (**c**) Flow is seen in this area with a colour score of 3. (**d**) Enlarged image of the focal multicystic area showing multiple tiny locules that are very close, giving it a solid appearance in some parts, (**e**) pedicle of torsed ovary showing the whirlpool sign on greyscale and Doppler (*arrows*)

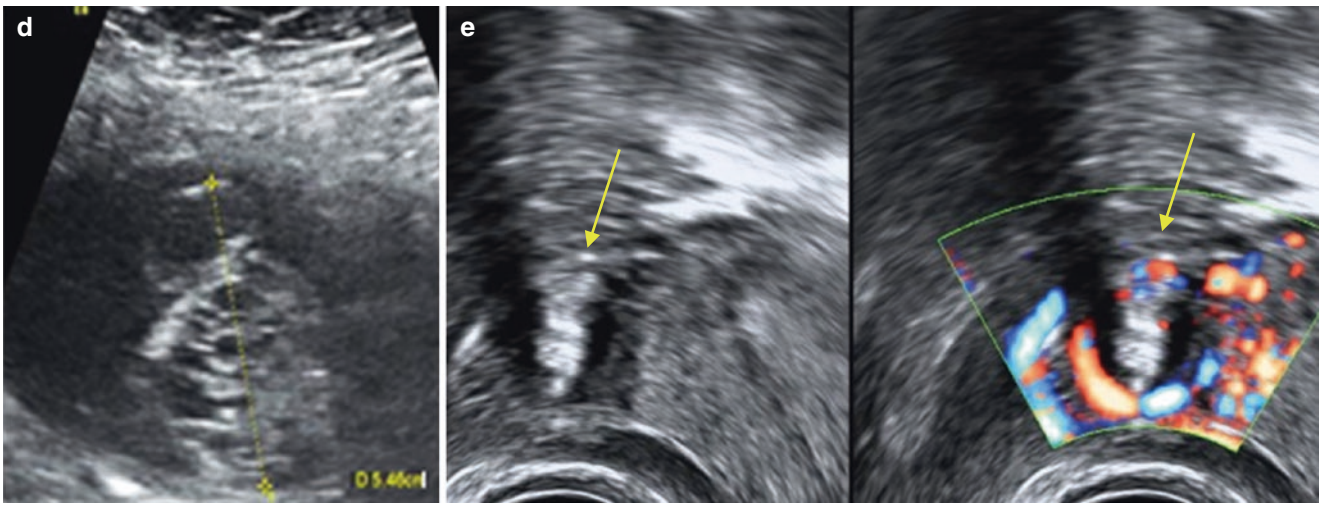

Fig. 7.49 (continued)

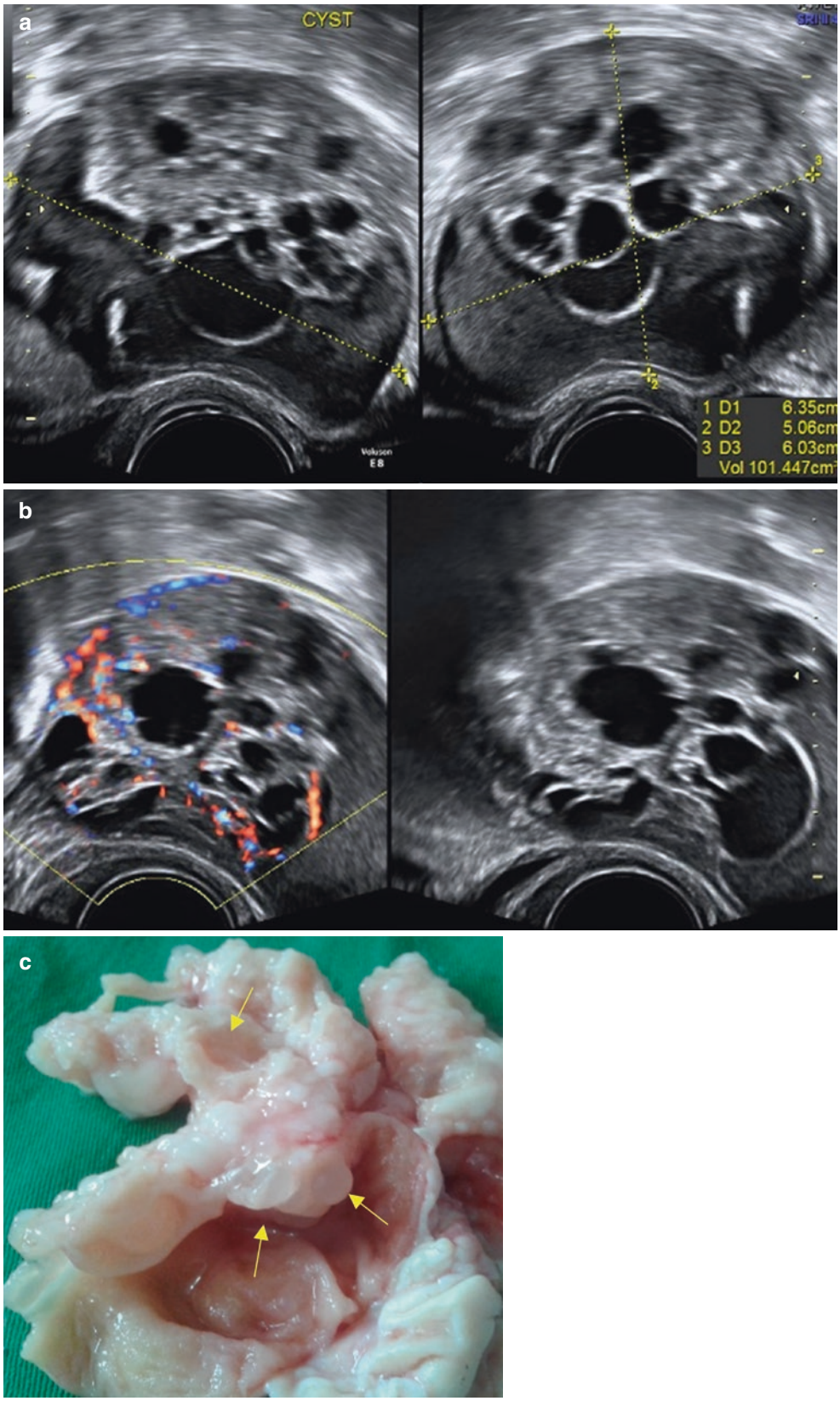

Fig. 7.50 Borderline mucinous cyst in a 24-year-old patient. (**a**) Volume of about 100 cc. The contents are turbid and the small multiple locules are so close that it gives the appearance of being solid. (**b**) Cyst shows moderate vascularity with colour score of 3. (**c**) Cut section of the post-operative specimen showing multiple small fluid-filled locules (*arrows*)

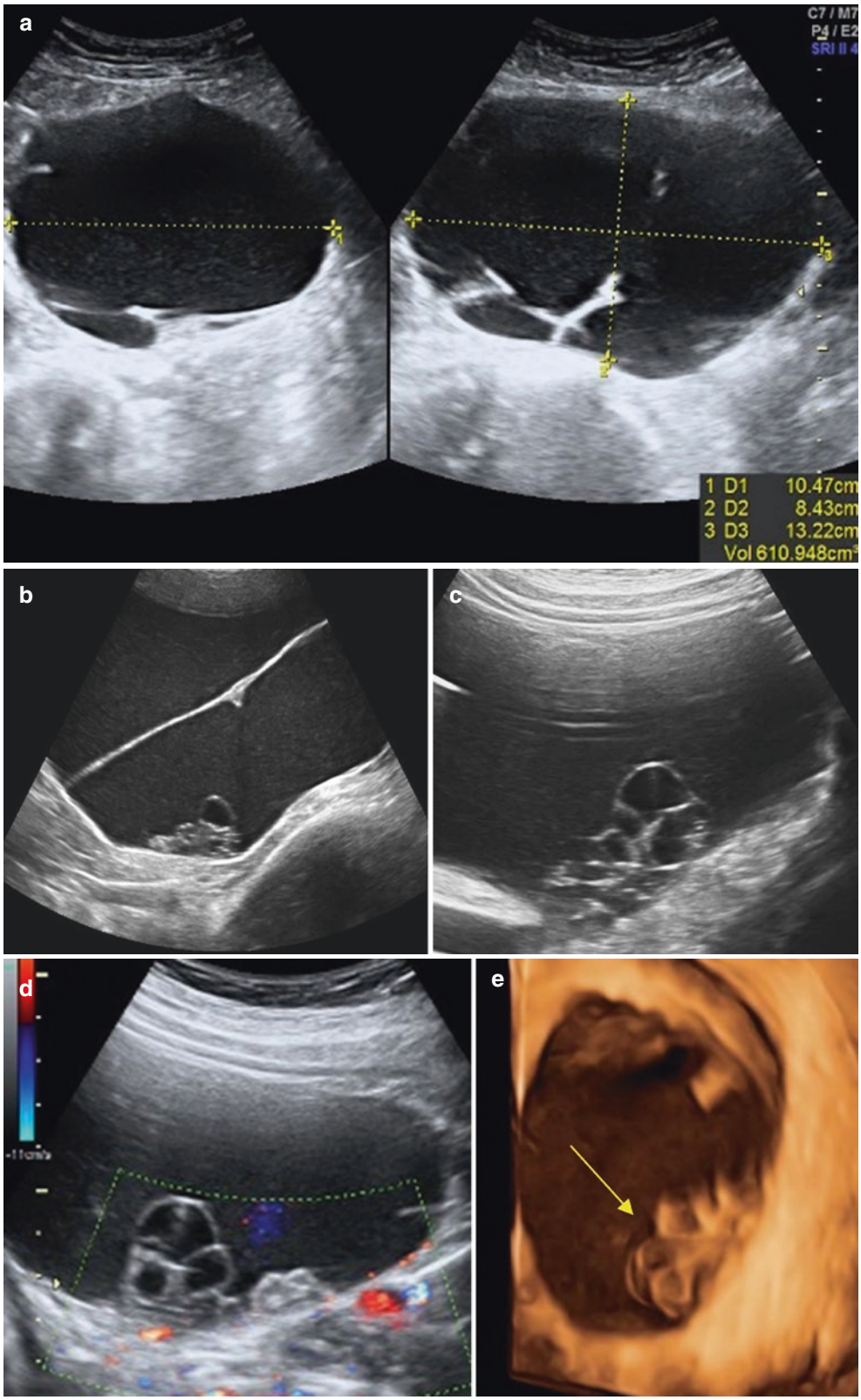

Fig. 7.51 Borderline mucinous cyst in a pregnant woman. (**a**) At an early pregnancy scan – cyst shows septae and a volume of 610 cc. (**b**) At 36 weeks of pregnancy – the cyst volume increased to 1931 cc. Cyst shows septae and turbid contents. (**c**) Focal area of small crowded locules seen. (**d**) This area shows low vascularity, probably because of the increased distance from the probe. (**e**) 3D rendered image of cyst showing focal area of small multilocular cyst (*arrow*)

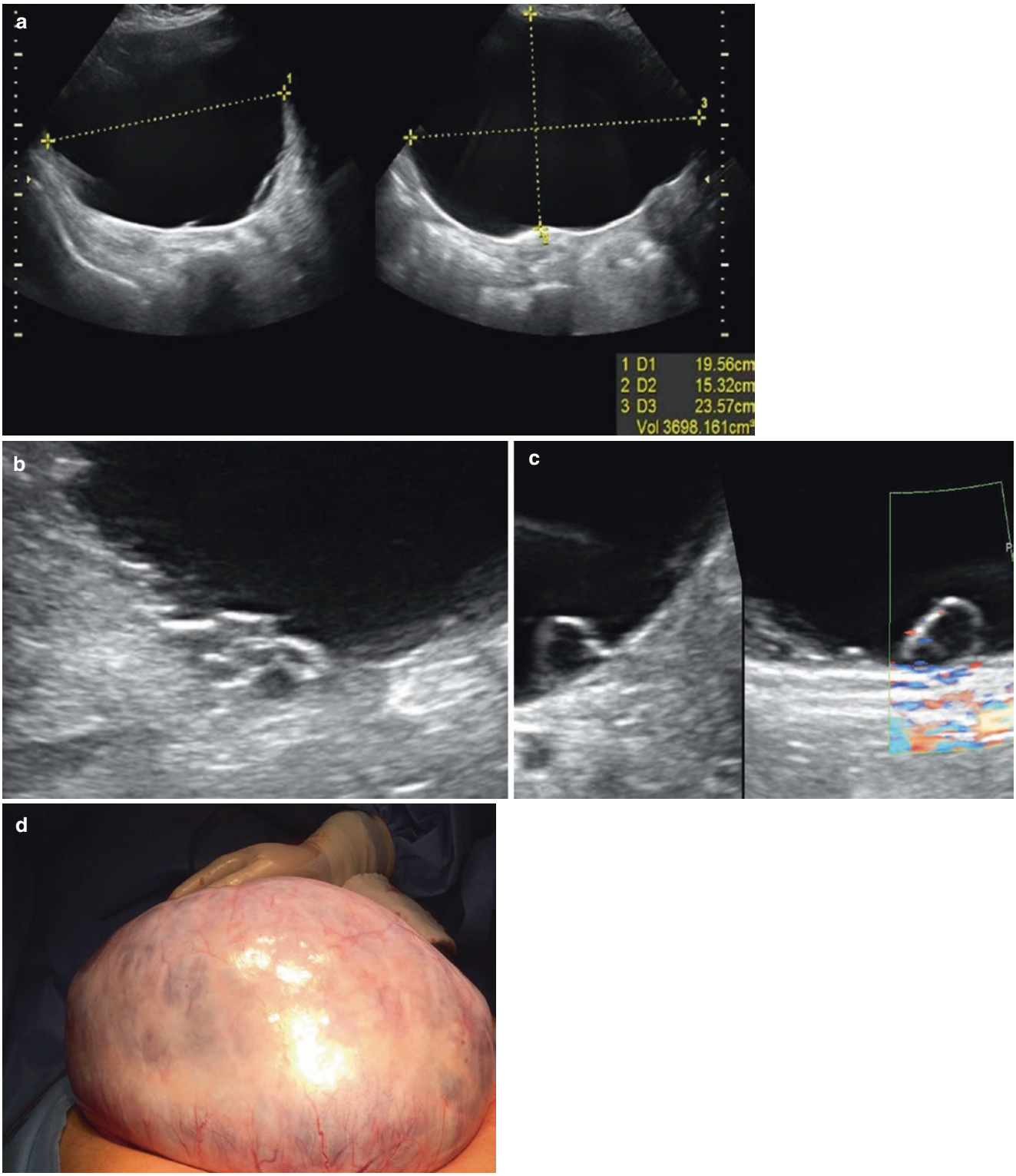

Fig. 7.52 Borderline mucinous cyst in a 56-year-old postmenopausal lady. (**a**) Large dimensions of cyst (3.698 L). (**b**) Focal small area showing multiple locules. (**c**) Minimal vascularity noted in the walls of the locule. (**d**) Specimen of the cyst at surgery

Mucinous Cystadenocarcinoma

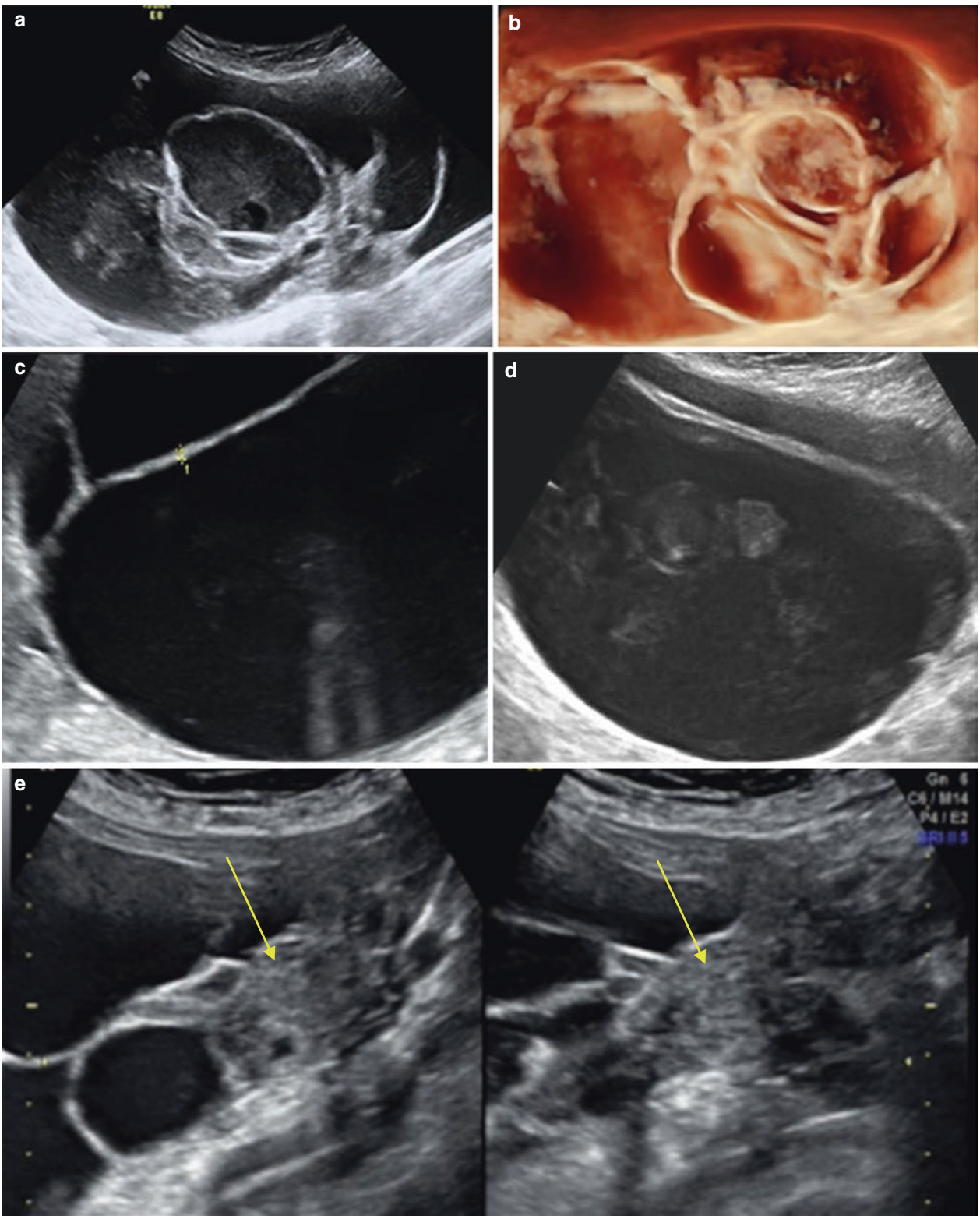

Fig. 7.53 Unilateral mucinous cystadenocarcinoma in a 59-year-old postmenopausal lady. (**a**) Large left ovarian cyst (volume 1.69 L) showing multiple locules that show turbid contents with varying echodensity. (**b**) 3D rendered image of the same. (**c**) Cyst showing septum. (**d**) Locules showing turbid contents with mixed echoes. (**e**) Inferior part of the cyst showing small locules and solid tissue (*arrows*). (**f**, **g**) Flow is seen in this focal area of small locules and solid tissue, with a colour score of 3. (**h**) Flow showed a low RI of 0.41. (**i**) Atrophic right ovary. (**j**) Turbid fluid with complex echoes and debris seen in the POD. (**k**) Ascitic fluid seen in the abdominal cavity. (**l**) Post-operative specimen. (**m**) Mucinous fluid with different colour tones is seen oozing out of the locules of the cyst on incision. (**n**) Cut section of the cyst showing solid area in one part of the cyst. (*CA 125 – 250.7 IU/mL*)

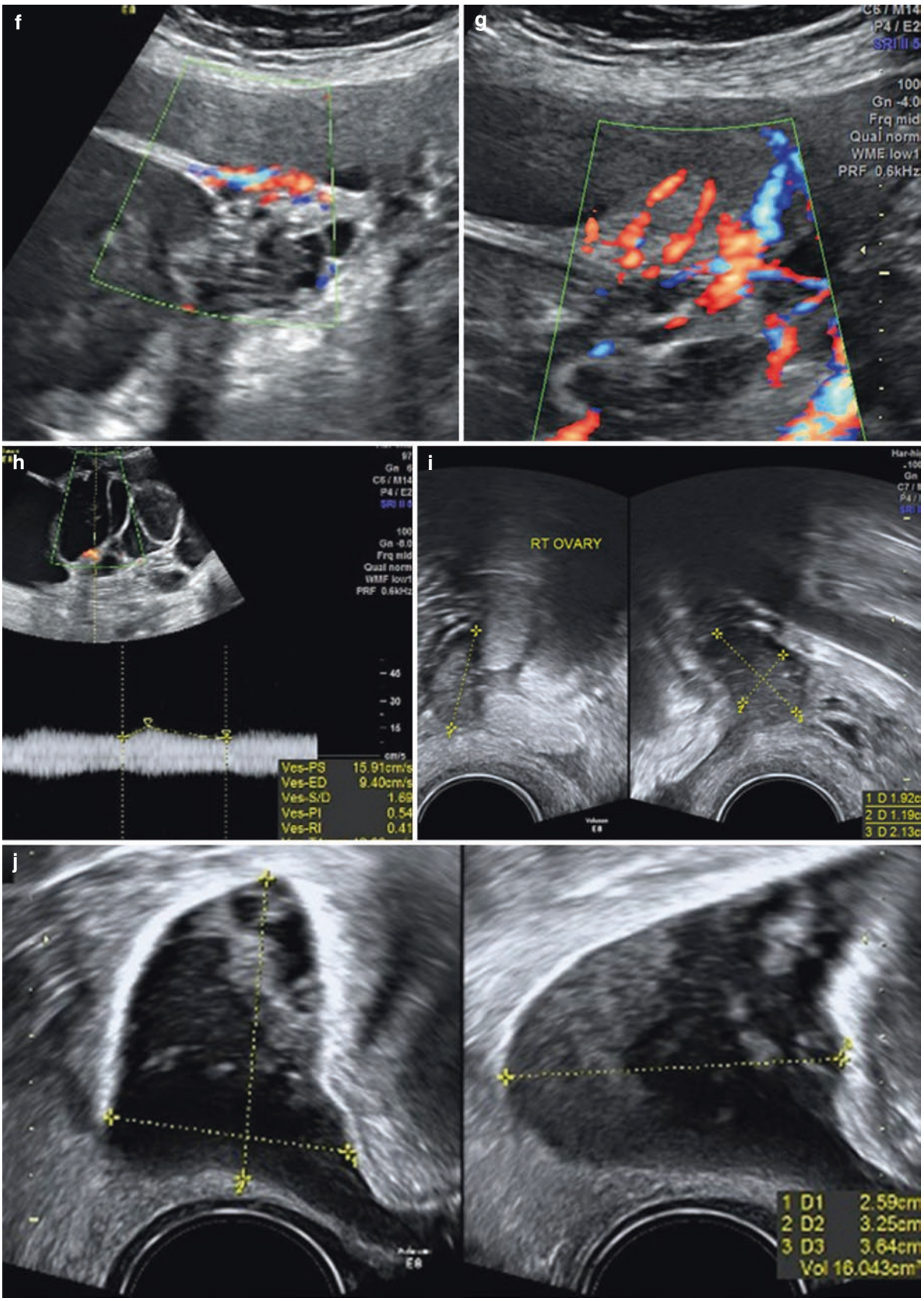

Fig. 7.53 (continued)

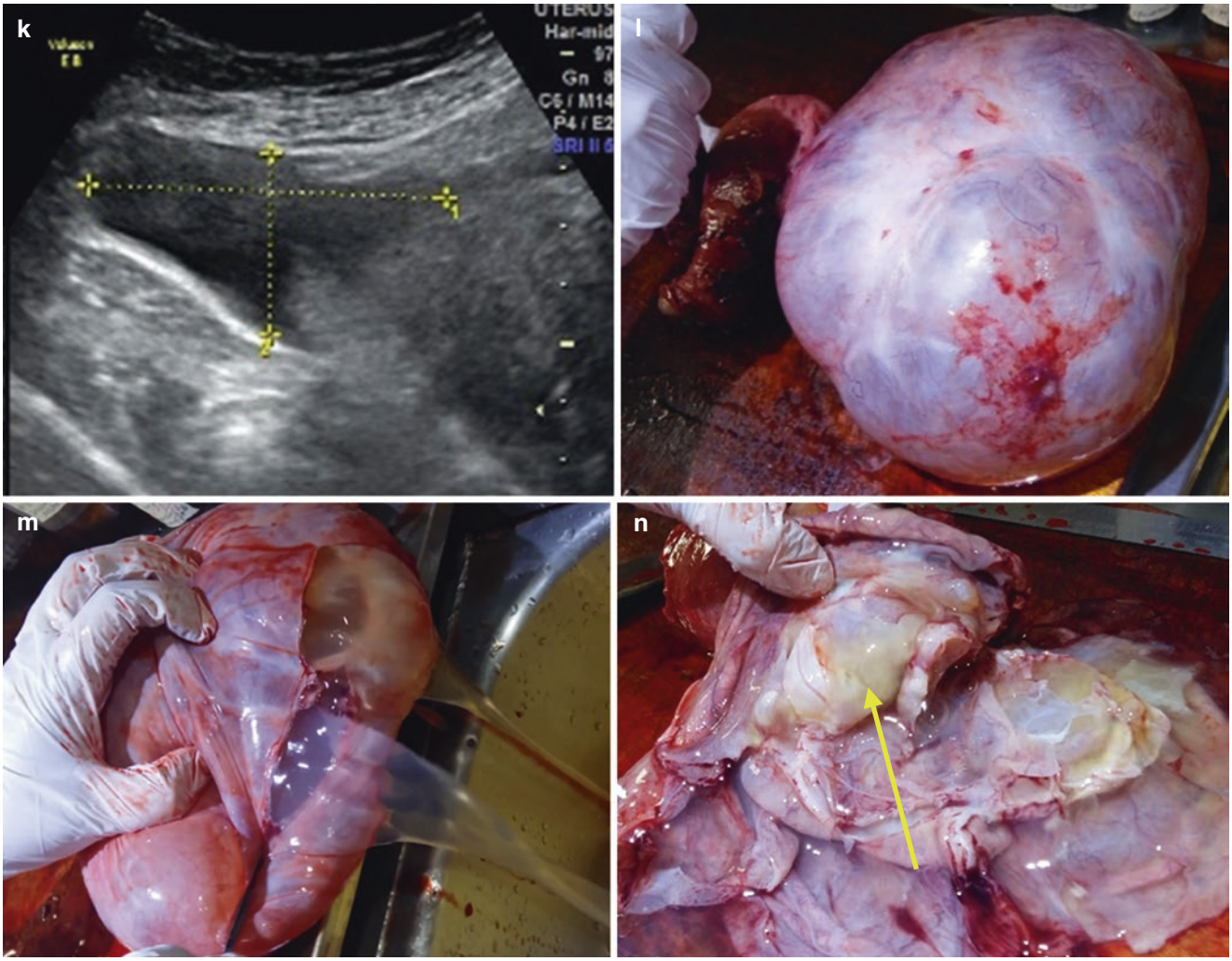

Fig. 7.53 (continued)

7.4.3.2 Germ Cell Tumours

They arise from primordial germ cells. They are more commonly seen in adolescents and young adults. The commonest germ cell tumour encountered is a dermoid (also known as a mature cystic teratoma).

Other tumours are malignant and include immature teratomas, dysgerminoma, yolk sac tumours (also known as endodermal sinus tumours), embryonal carcinoma and choriocarcinoma.

Dermoids (Mature Cystic Teratoma)

They constitute about 20 % of all ovarian tumours. They are common in young women of the childbearing age group. They are usually asymptomatic and therefore often first picked up on an ultrasound done in pregnancy. They can, however, present with pain because of torsion or may first present as a clinically palpable mass. They may be multiple and are bilateral in 10–15 % of cases.

Ultrasound Features of Dermoids (Figs. 7.54, 7.55, 7.56, 7.57, 7.58, 7.59, 7.60, 7.61, 7.62, 7.63, 7.64, 7.65, 7.66, 7.67 and 7.68)

Dermoids have a wide range of sonographic appearance, yet the positive predictive value when diagnosed on ultrasound is about 98 % (Patel et al., AJR, 1998).

- Dermoids are typically complex cysts with hypoechoic and echogenic components. The echogenic components, because of their fat content, tend to be seen in the non-dependent portions of the cyst (unlike cysts with debris where the hyperechoic contents are seen in the dependent part of the cyst).
- These typically show acoustic shadowing from their hyperechoic contents. This is very useful in making a confident diagnosis of a dermoid.
- Because of the acoustic shadowing, the entire cyst margins may not be seen. Often, just the proximal echogenic margins are noted on ultrasound, with acoustic shadowing distal to it, resembling the bowel. This is referred to as the 'tip of the iceberg' sign.
- Bright scattered linear echoes may be seen within the cyst (caused by the presence of hair in the cyst), which are often helpful in diagnosis.
- Sometimes, one may see a dermoid mesh formed by hair within the cyst. Typically, these radiate out from a protuberance of solid tissue within the cyst, called the 'Rokitansky nodule'.
- Multiple echogenic, circumscribed, tiny foci may be seen within the cyst, formed by a combination of hair with sebaceous secretions.
- A very small dermoid may appear as a small circumscribed echogenic mass within the ovary.
- Minimal flow may be seen on Doppler in the cyst walls.
- Dermoids are bilateral in 10–15 % of the cases and, rarely, may be multiple in an ovary.
- The margins of a dermoid may be difficult to delineate because of acoustic shadowing and resemblance with the bowel. One method to delineate is to push the mass with the probe. The entire part that moves en masse is the dermoid, and thus its margins can be deciphered.
- At times, a TAS scan is the only way to delineate and assess a large dermoid.

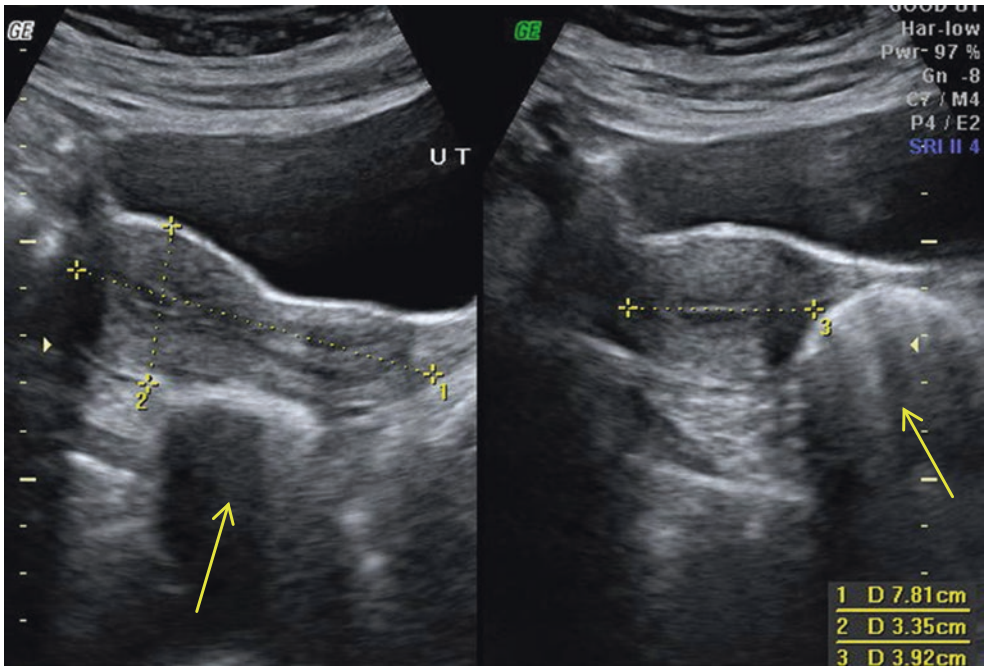

Fig. 7.54 Dermoid (*arrows*) on TAS resembling the bowel. Echogenic proximal margins with distal acoustic shadowing – 'tip of the iceberg' sign

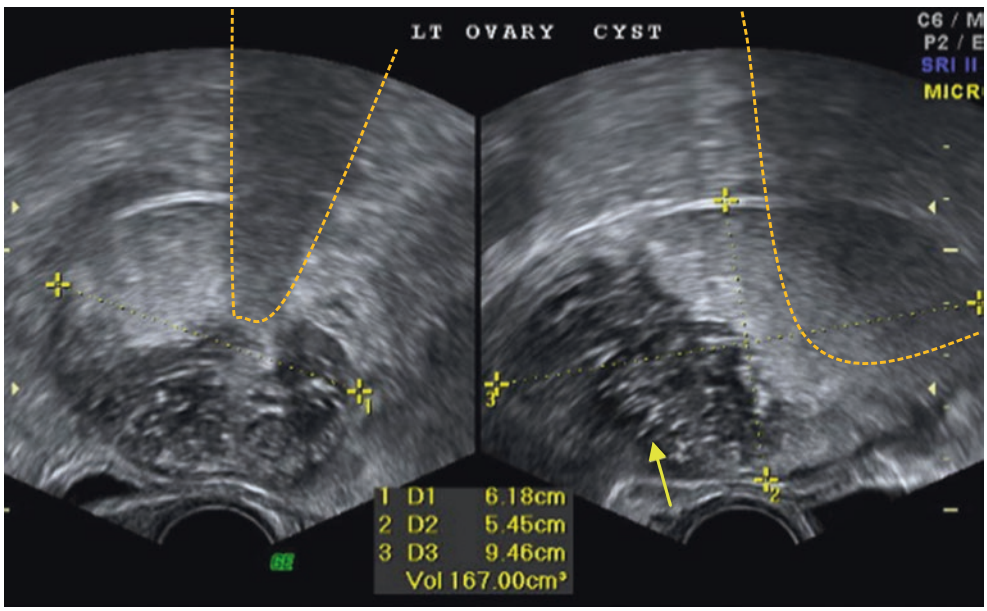

Fig. 7.55 Typical ultrasound findings in a dermoid cyst showing complex echoes, acoustic shadowing (outlined) and fine linear scattered echoes (*arrow*), suggestive of hair

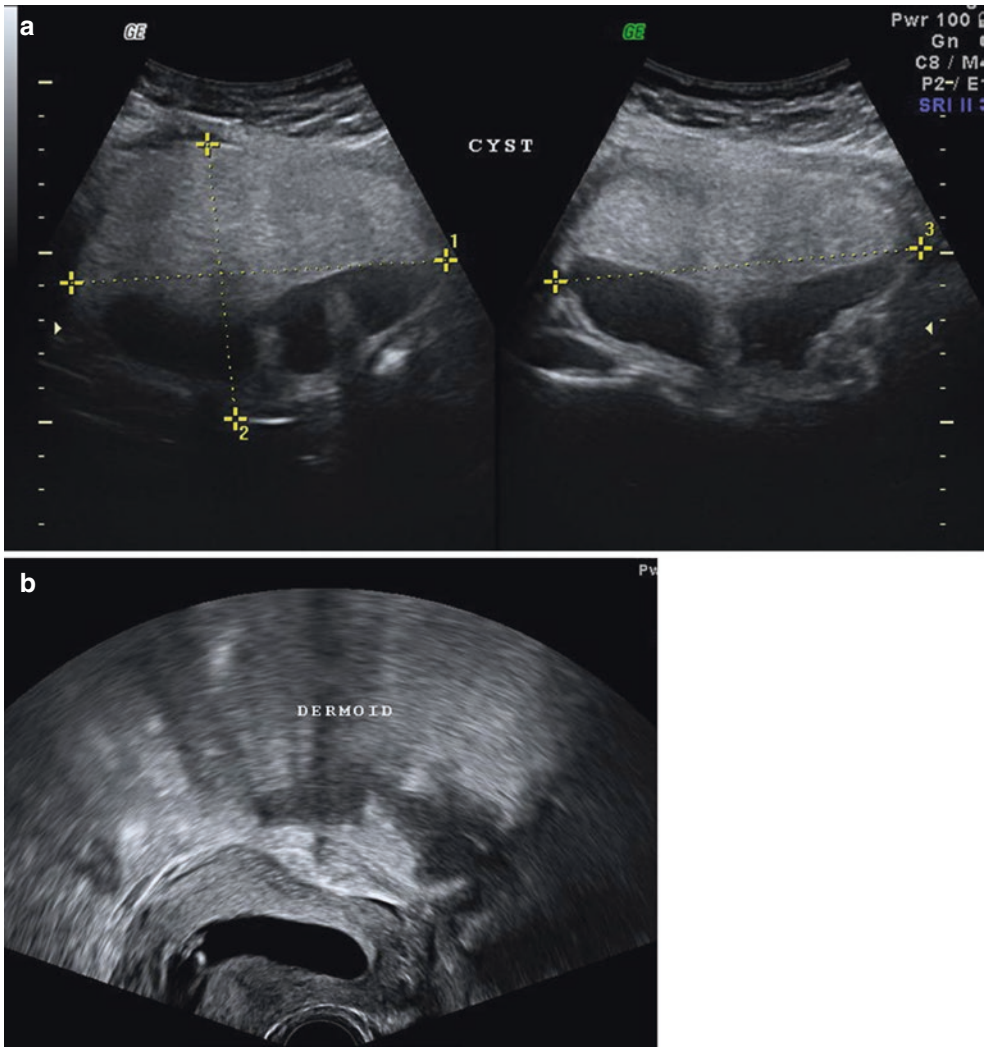

Fig. 7.56 Dermoid. (**a**) 500 cc dermoid better visualised and measured on TAS. (**b**) TVS showing gravid uterus with only the lower part of dermoid cyst visualised

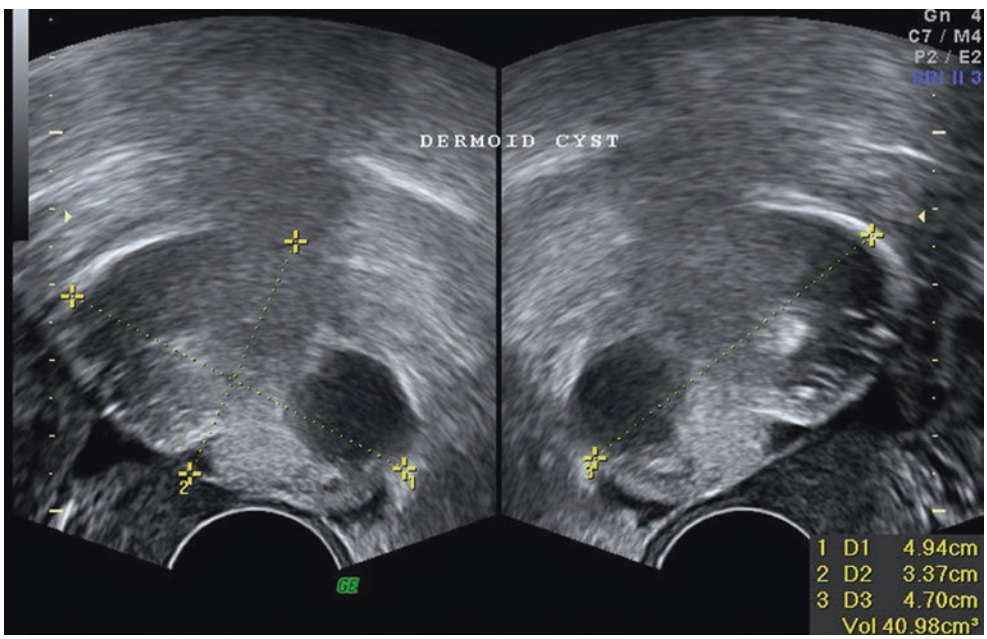

Fig. 7.57 A complex dermoid cyst with echogenic components showing acoustic shadowing. There is a small, circumscribed anechoic cystic area within

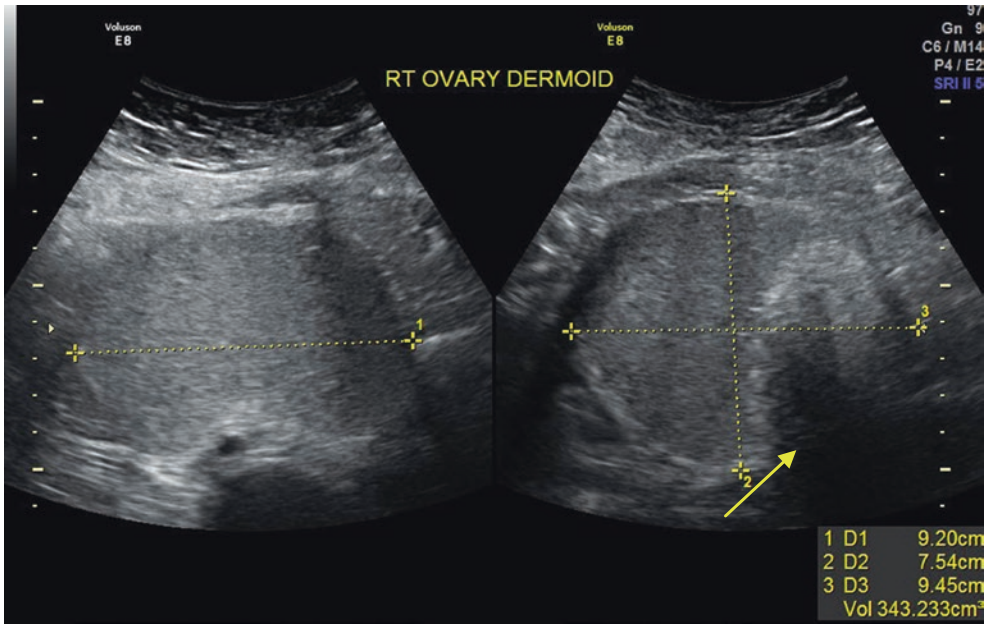

Fig. 7.58 Dermoid cyst showing turbid hypoechoic contents with a ground glass appearance. The presence of acoustic shadowing (*arrow*) helped clinch the diagnosis

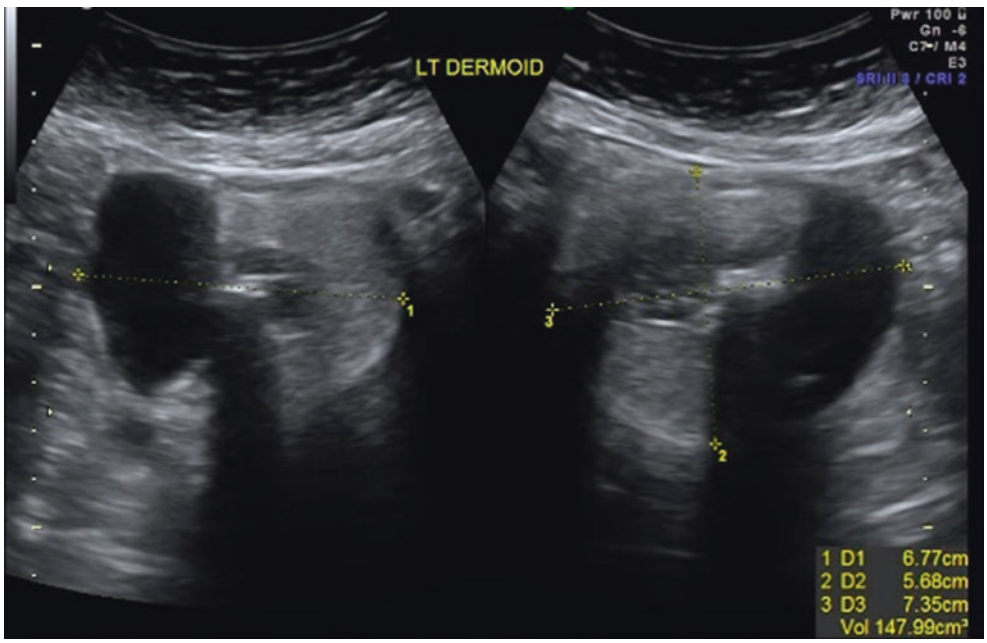

Fig. 7.59 Complex dermoid cyst showing fluid–fluid levels and acoustic shadowing

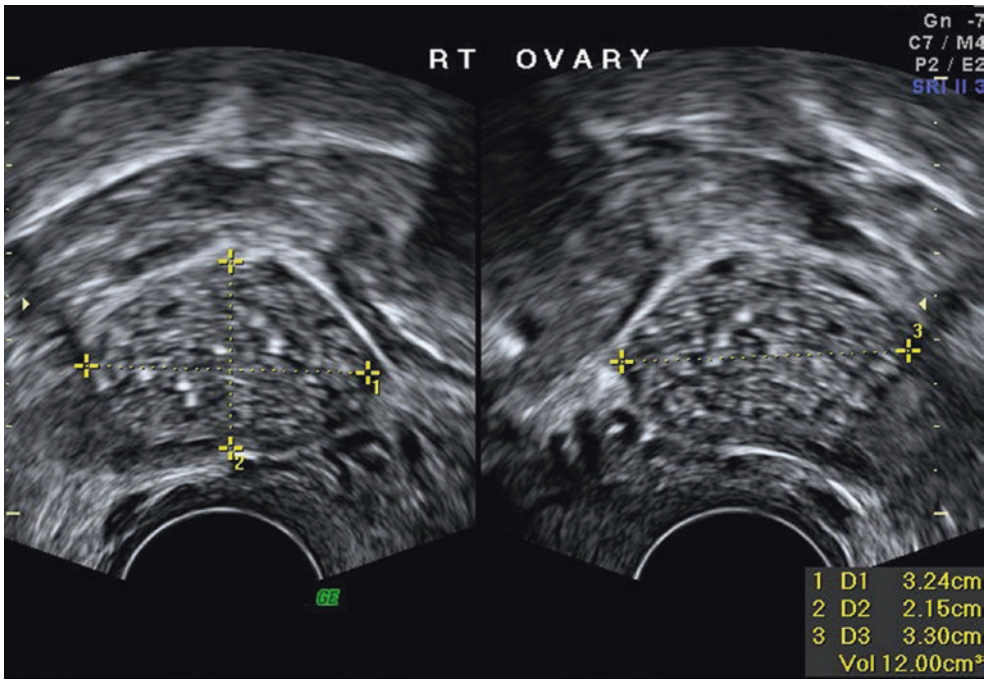

Fig. 7.60 Dermoid cyst showing multiple echogenic spherical structures within

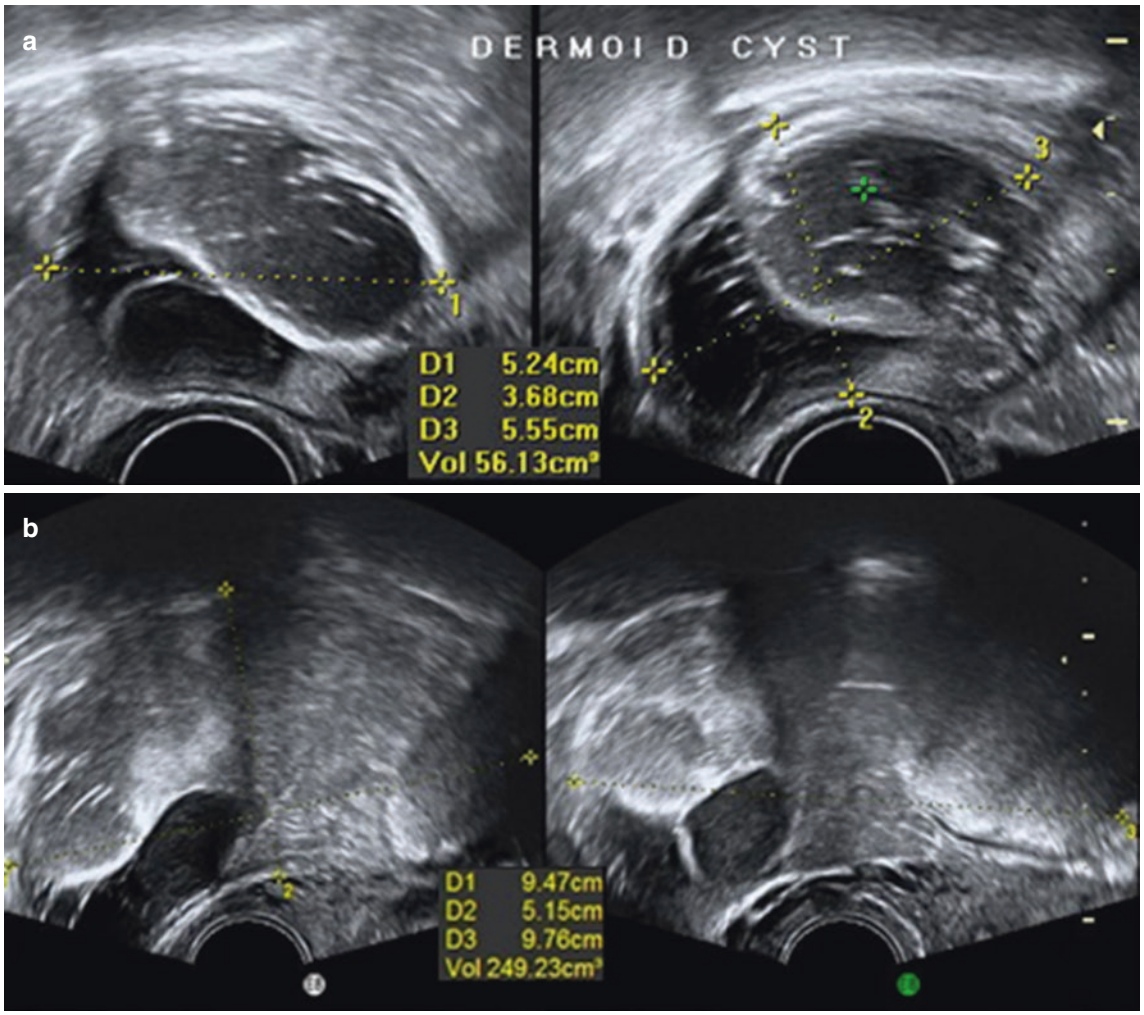

Fig. 7.61 Dermoid cyst. (**a**) Initial measurement showed a dermoid cyst of 56 cc. (**b**) The cyst, however, was found to be much larger (249 cc). This is because the margins of a large dermoid are generally difficult to delineate

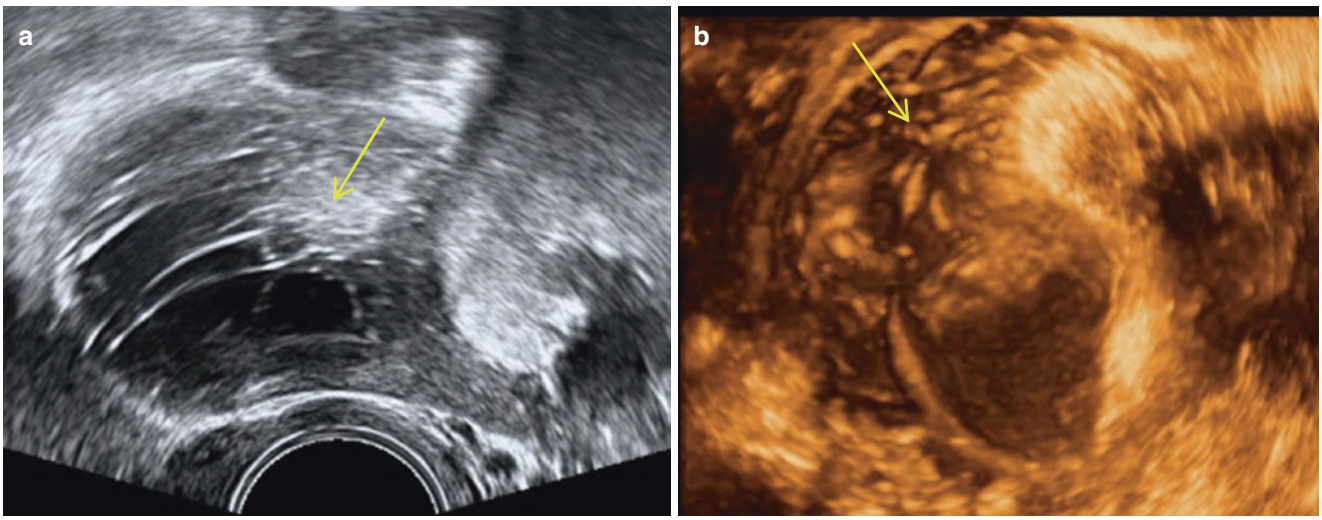

Fig. 7.62 Dermoid showing Rokitansky nodule (*arrows*) (**a**) on 2D, (**b**) on 3D. Multiple linear echoes suggestive of hair are seen radiating out from this nodule, forming a dermoid mesh

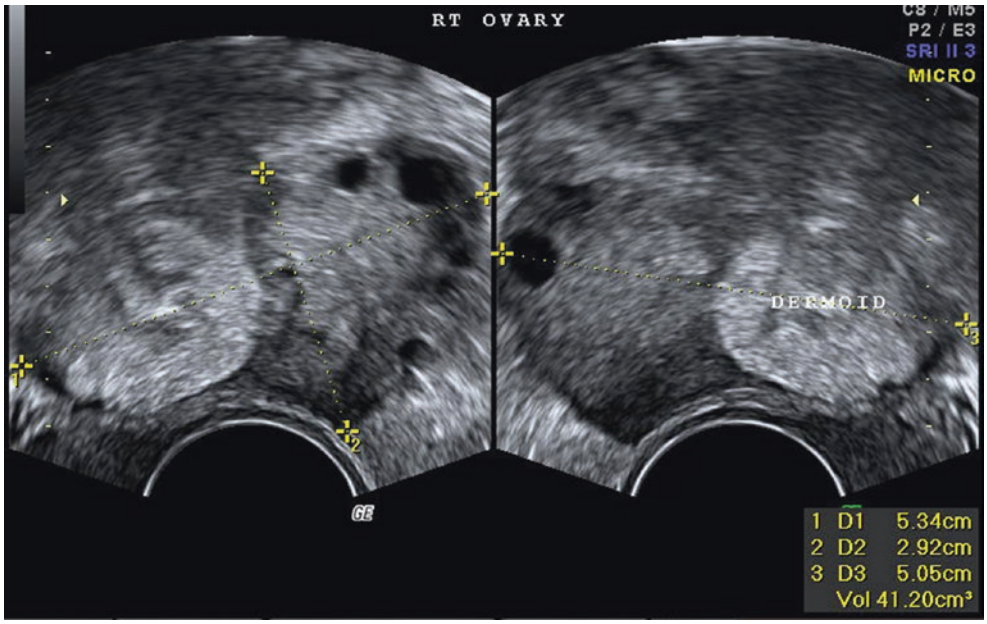

Fig. 7.63 Dermoid seen as a hyperechoic circumscribed mass within an ovary

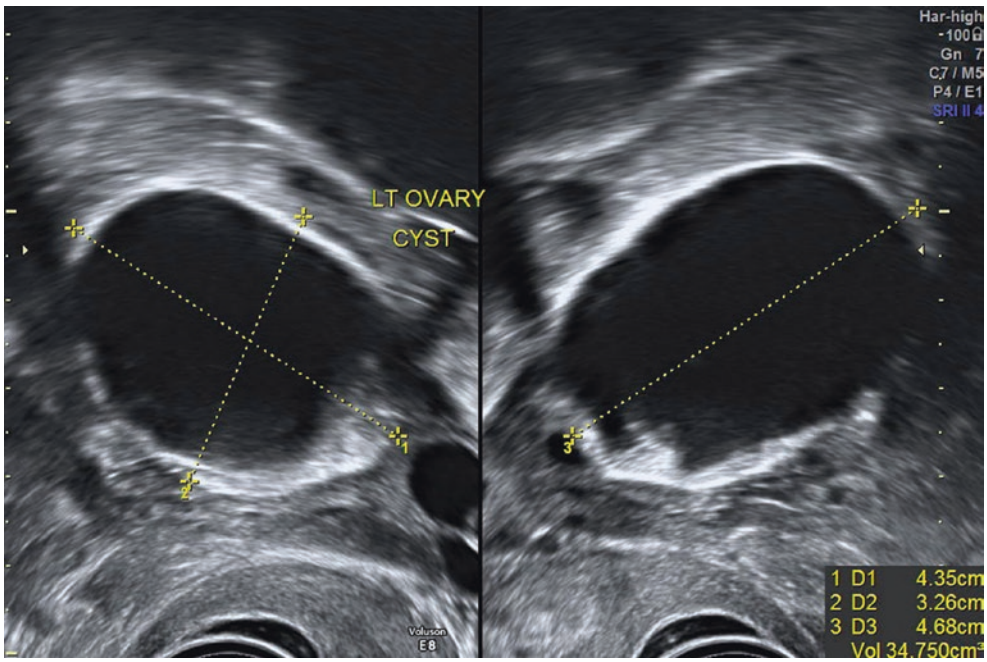

Fig. 7.64 Dermoid seen as a predominantly anechoic cyst. The irregular hyperechoic wall thickening with minimal shadowing raised the possibility of a dermoid, and this was confirmed on histopathology

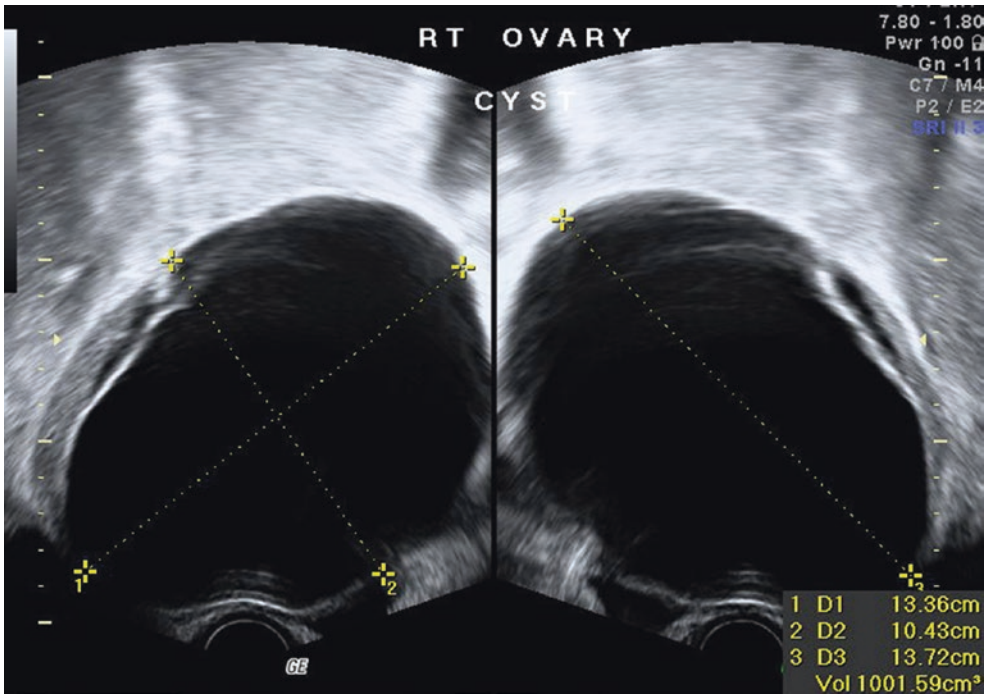

Fig. 7.65 Atypical dermoid cyst showing anechoic contents and a septum. Here again, the hyperechoic superior walls with loss of resolution beyond raised the suspicion of a dermoid. *HPE:* dermoid cyst

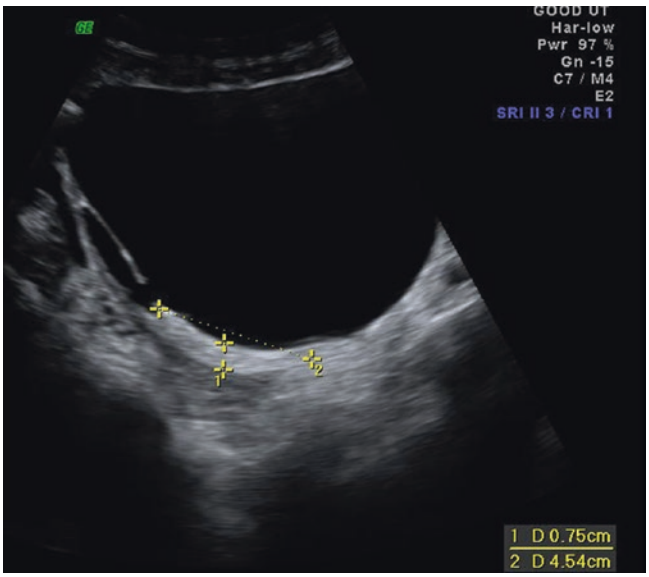

Fig. 7.66 Dermoid. TAS showing a large atypical dermoid with anechoic contents, a septum and a crescent-shaped hyperechoic thickening along one part of the cyst wall. This hyperechoic, irregular thickening in the cyst wall is sometimes the only feature that raises the suspicion of the cyst being a dermoid. *HPE:* dermoid cyst

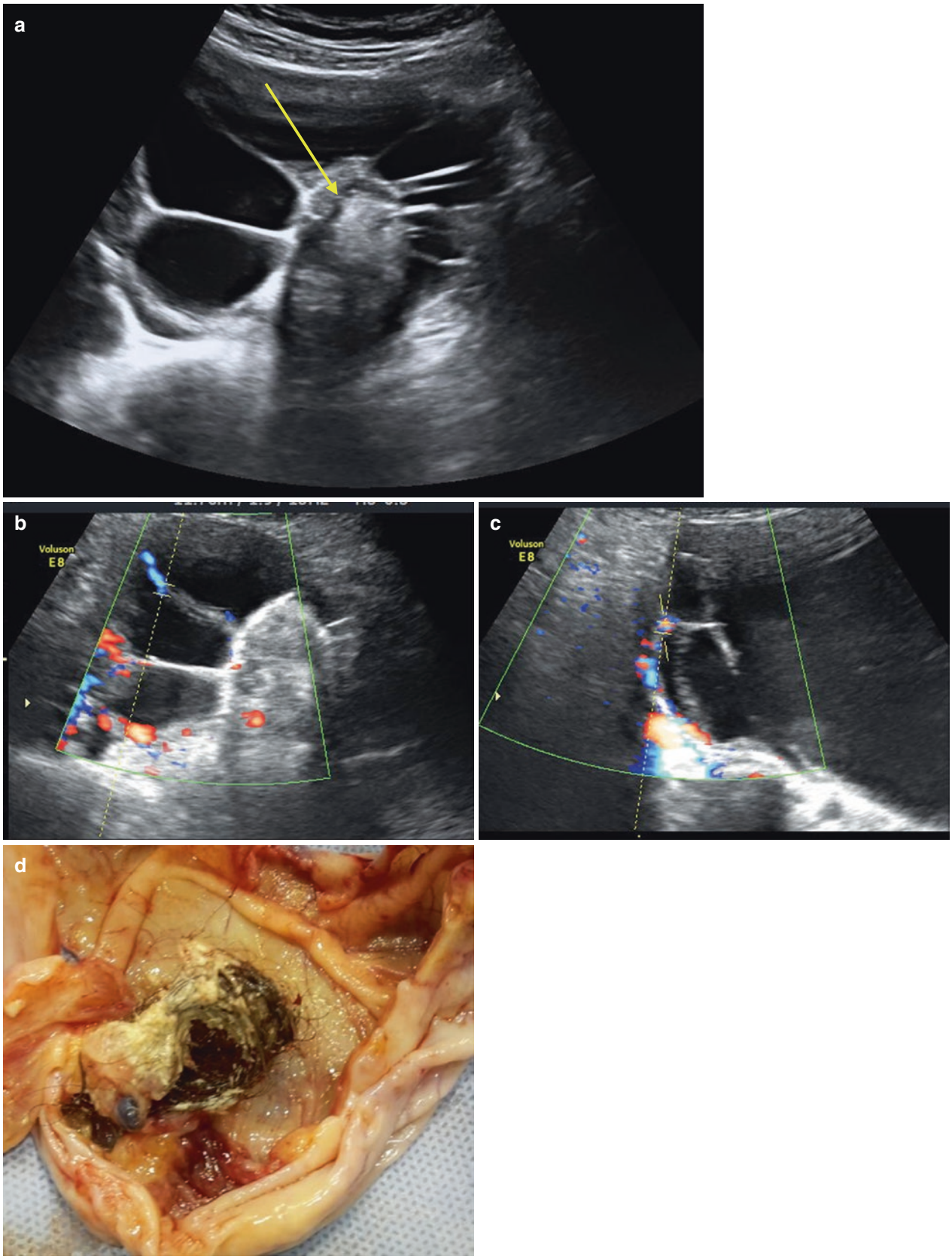

Fig. 7.67 Atypical dermoid with septae. (**a**) Multiple septae are seen radiating out of a solid-appearing mass showing acoustic shadowing suggestive of a Rokitansky nodule (*arrow*). (**b**) Flow seen on Doppler in the septae. (**c**) Doppler flow seen in the cyst walls. (**d**) Post-operative cut section of a cyst showing hair and sebaceous material

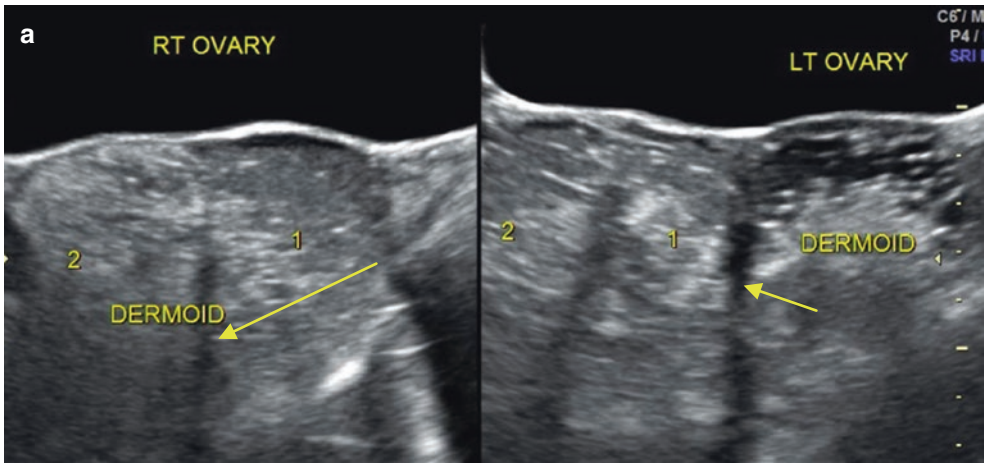

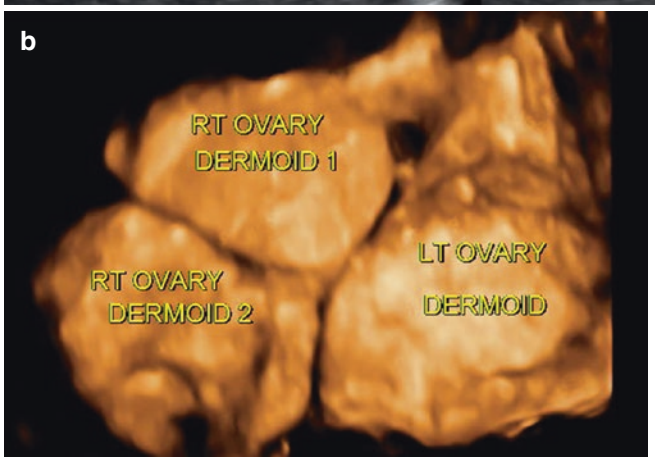

Fig. 7.68 Multiple dermoids. (**a**) On TAS, the entire pelvis showed complex areas with acoustic shadowing and linear echoes highly suggestive of the contents of a dermoid. The uterus was identified with difficulty, lying between and behind the dermoid cysts on either side. There was a suspicion of there being two dermoids in the right ovary because of a linear hypoechoic shadow running anteroposteriorly on the right side (*long arrow*) in addition to a similar linear shadowing between the right and left ovary (*short arrow*). (**b**) 3D rendering of the pelvis was done which also showed the presence of two right ovarian dermoids and one left ovarian dermoid. Findings were confirmed later, at surgery

Malignant Germ Cell Tumour

These include immature teratomas, dysgerminoma, endodermal sinus tumours (also known as yolk sac tumours), embryonal carcinoma and choriocarcinoma.

Malignant germ cell tumours are often of mixed variety with 2–3 cell types coexisting. They are associated with increased tumour markers like AFP (yolk sac tumour) and HCG. The commonest are yolk sac tumours and immature teratomas.

Ultrasound Features of Malignant Germ Cell Tumour

(Figs. 7.69, 7.70, 7.71 and 7.72)

- They are usually unilateral.
- They are predominantly solid masses with intervening septae giving them a lobulated appearance.
- The solid tissue generally shows heterogeneous internal echogenicity.
- Some may show solid and cystic areas.
- On Doppler, flow may be seen in the solid areas or in the septae with moderate or high vascularity.

Dysgerminoma (Figs. 7.73 and 7.74)

These are rare malignant germ cell tumours seen in young women (median age 20 years). Dysgerminoma is the most common malignant ovarian germ cell tumour diagnosed in pregnancy. It may also be seen in patients with primary amenorrhoea, where it may be associated with gonadal dysgenesis and gonadoblastoma. Dysgerminomas are usually pure dysgerminomas and are not mixed with other germ cell tumours. These tumours are generally well-defined, purely solid masses. They have a smooth or sometimes lobulated outer contour. The solid mass is divided into different lobules and shows nonhomogeneous internal echogenicity. The mass usually shows moderate to high vascularity.

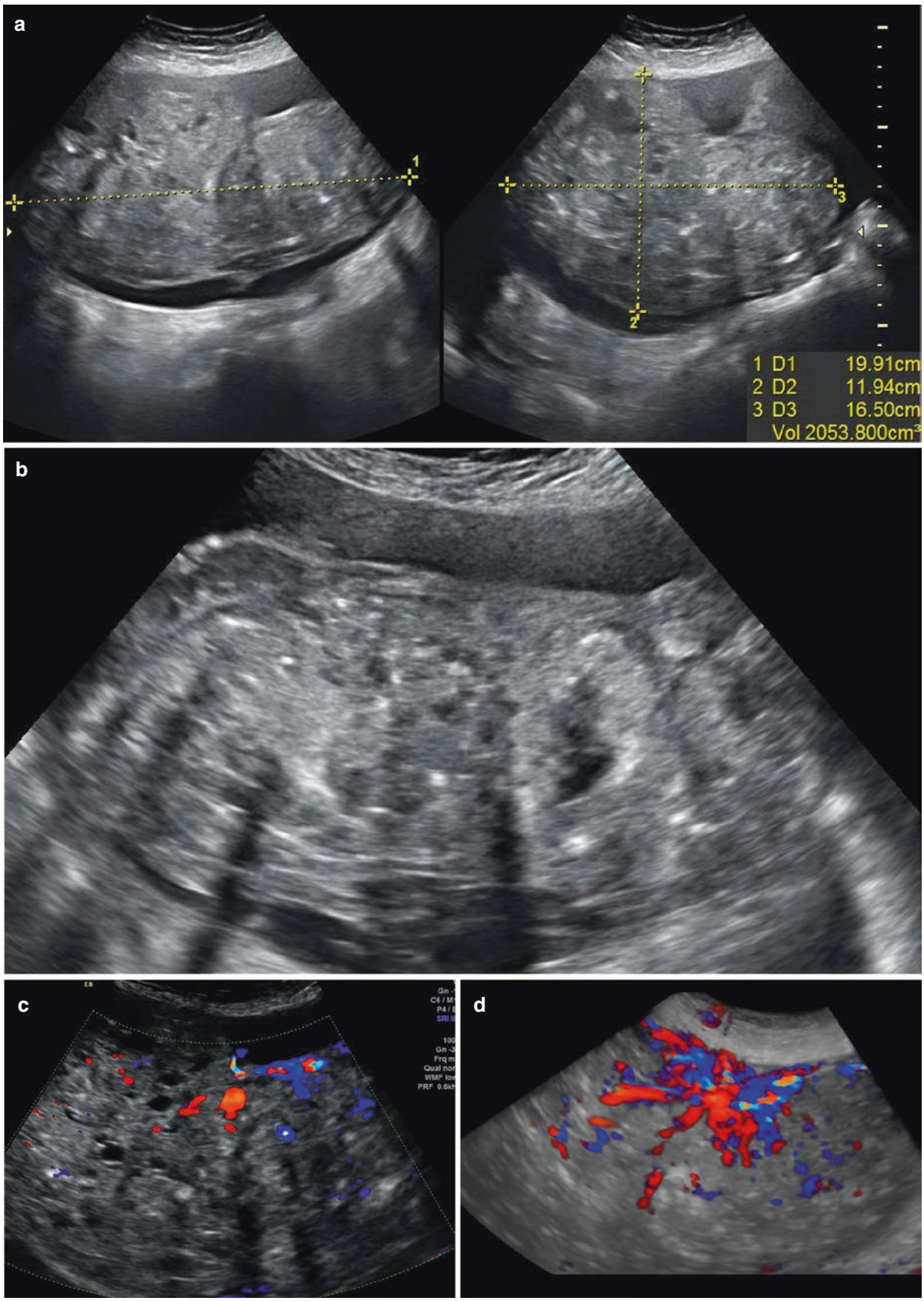

Fig. 7.69 Immature teratoma Grade 3 – in a 24-year-old patient with 1 month history of abdominal pain, loss of weight and fever. (**a**) Greyscale shows a solid, heterogeneous mass (2053cc) with a lobulated external contour and ascitic fluid surrounding it. 1300cc of ascitic fluid was seen in the abdomen. (**b**) The mass is heterogeneous, shows few cystic spaces, some acoustic shadowing and scattered echogenic foci of calcification. Immature teratomas are known to be large with prominent, solid, heterogeneous components, that often show calcification. (**c**) Flow is seen in the mass (RI of 0.42). (**d**) 3D colour Doppler shows abundant flow within the mass. AFP was 2000 ng/ml (elevated). At surgery significant ascites and abdominal metastasis were noted

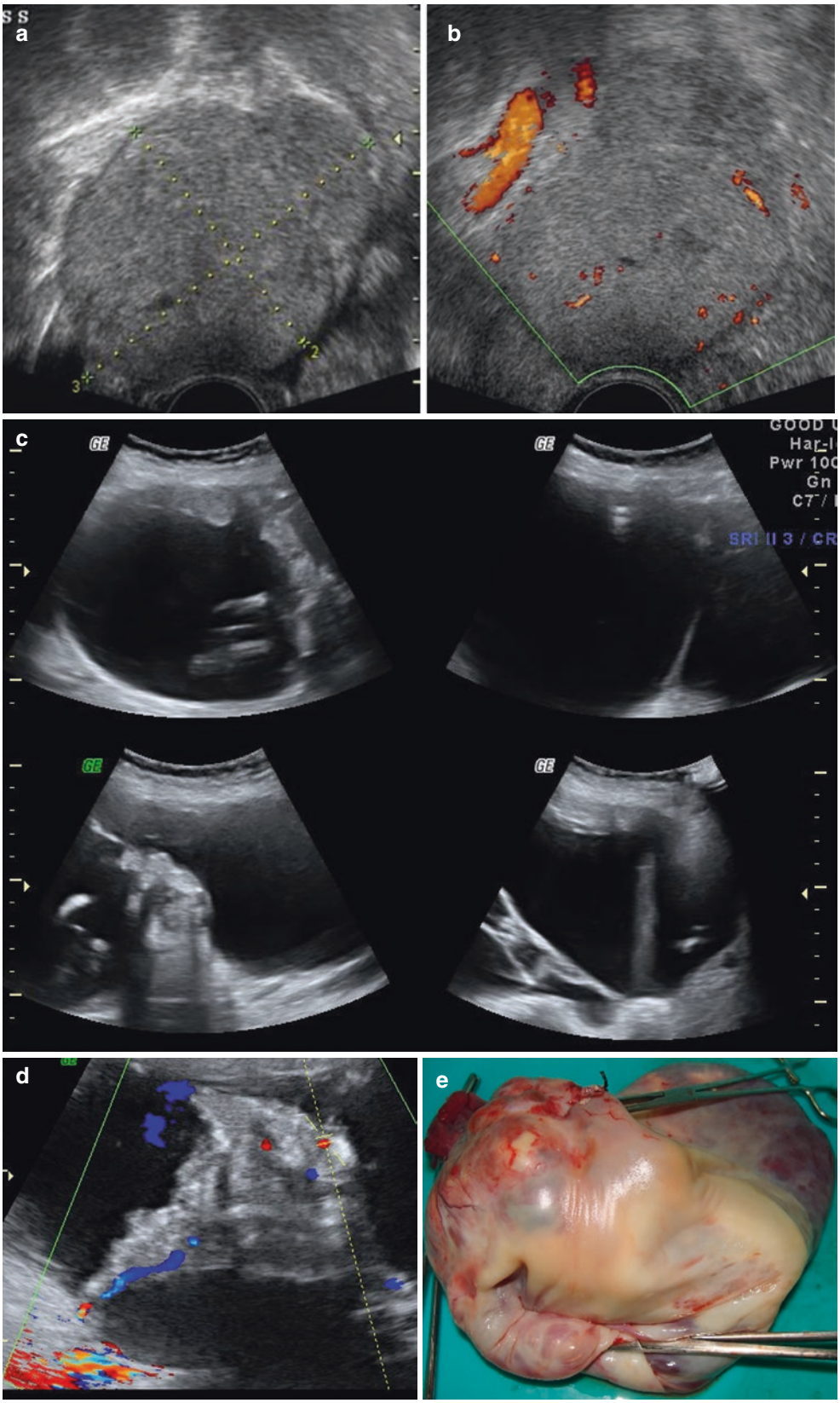

Fig. 7.70 Mixed germ cell tumour in 2 cases (a, b) Case 1 - Left ovarian (yolk sac and embryonal) – in a 30-year-old patient. (**a**) Greyscale shows a solid heterogeneous mass with a lobulated external contour. (**b**) Minimal flow seen in the mass – predominantly in the septae. AFP was 818 ng/ml (elevated) and HCG levels were normal. (c, d, e) Case 2 - Right ovarian - in a 26-year-old patient. (**c**) Images of a large (5803cc), multilocular solid tumour seen in all the four quadrants of the abdomen. It shows cystic areas, solid areas and septae. (**d**) Large (589 cc), irregular, heterogeneous, solid area seen within the cyst. showing flow on Doppler. (**e**) Post-operative specimen

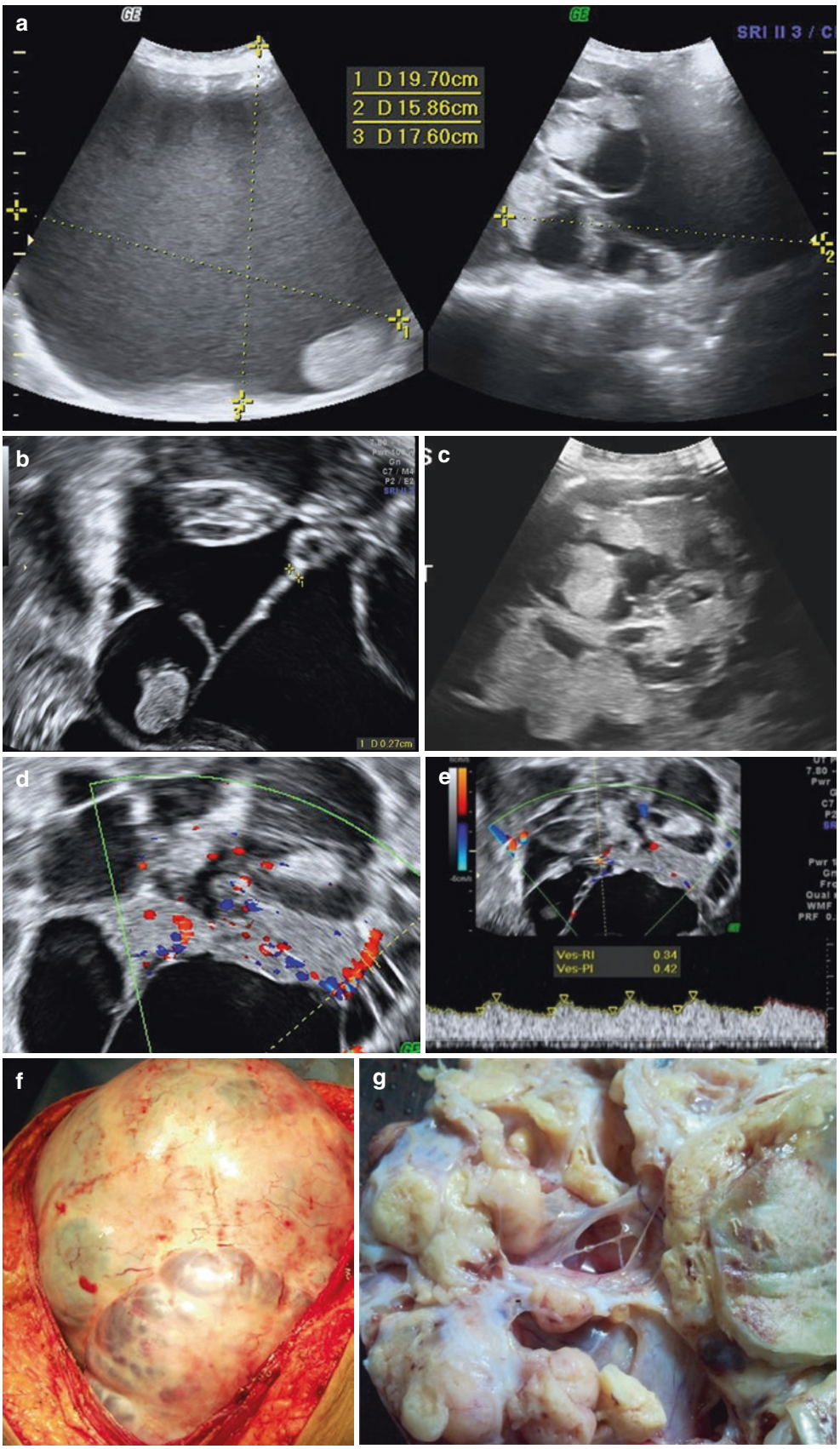

Fig. 7.71 Yolk sac tumour (endometrioid type) in a 31-year-old patient. (**a**) Image showing a large, multilocular solid mass (9148 cc). (**b**) Irregular thick septae. (**c**) Multiple circumscribed solid masses seen within. (**d**) Flow seen in the solid tissue and septae. (**e**) Flow showed a low RI of 0.34. (**f**) Post-operative specimen that weighed 5.9 kg. (**g**) Cut section showing septae and solid areas

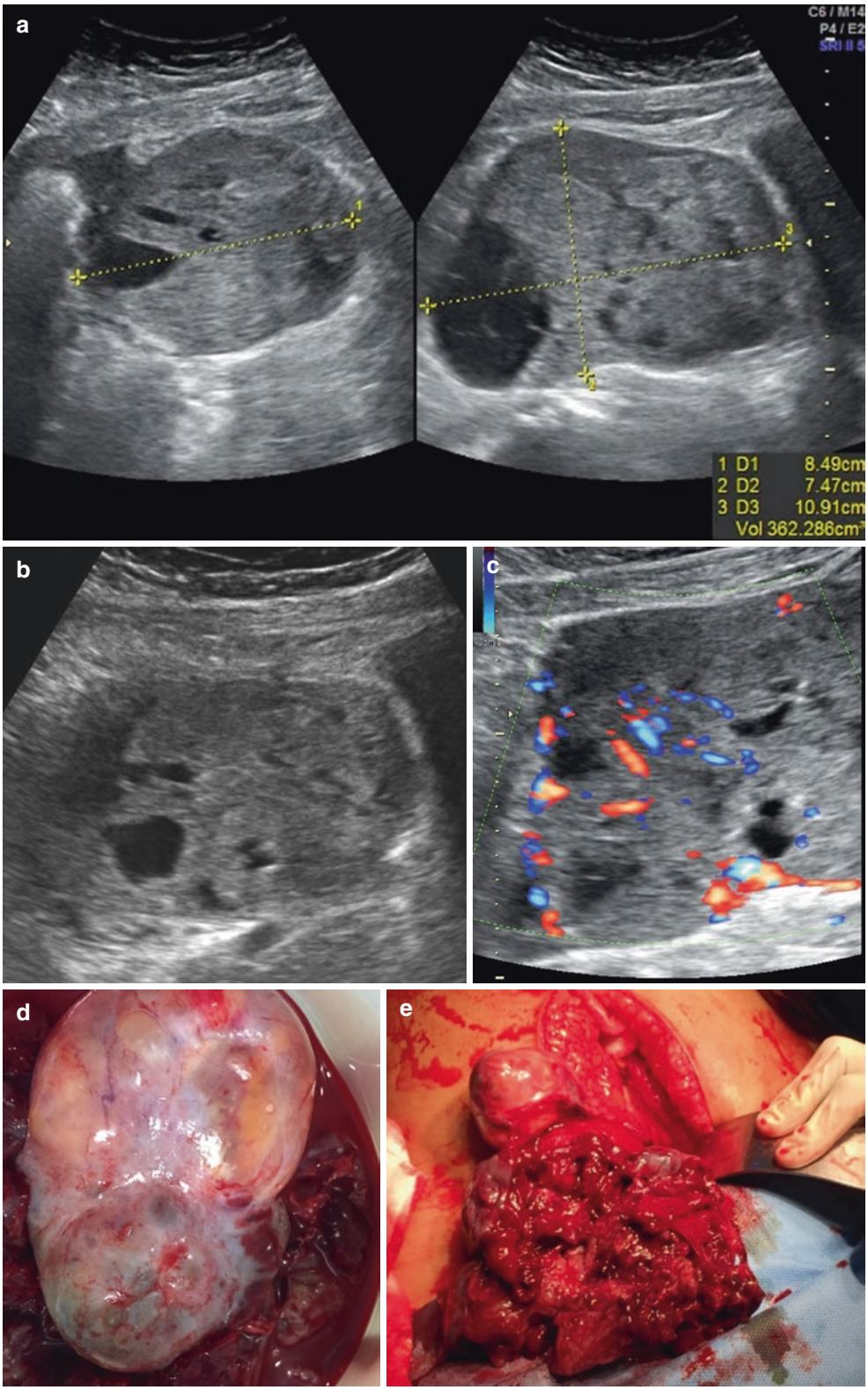

Fig. 7.72 Ruptured yolk sac tumour – in a 22-year-old patient with a history of abdominal pain of 1 week duration. (**a**) Heterogeneous, predominantly solid mass (362 cc). (**b**) Solid tissue showing poorly defined margins at its superior end. (**c**) Flow seen on Doppler within the mass, with a low RI of 0.4. (**d**) Post-operative specimen of the tumour showing external intact surface. (**e**) The macroscopic appearance of the contents of the ruptured cyst

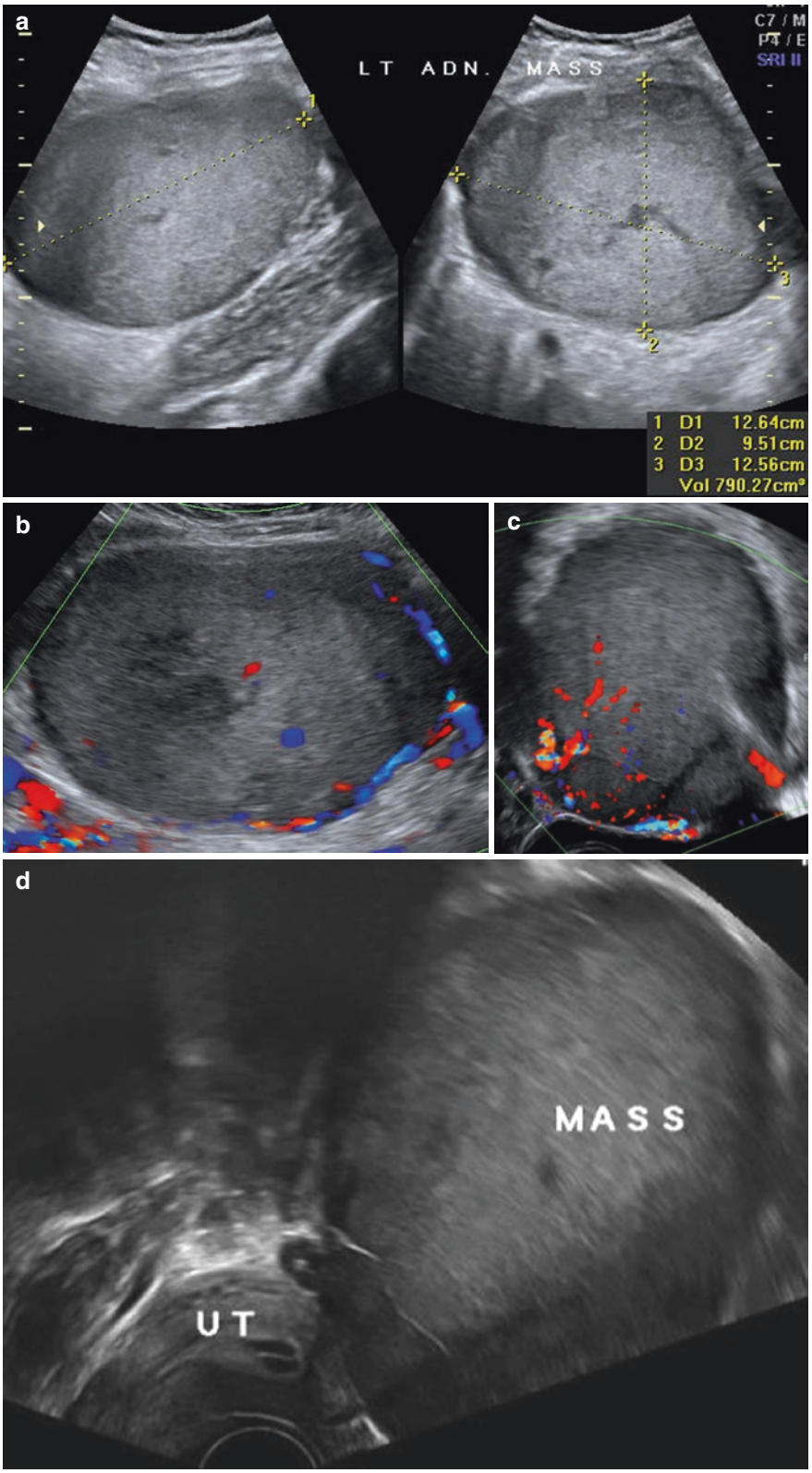

Fig. 7.73 Dysgerminoma in a 27-year-old patient. (**a**) Image of a circumscribed, completely solid mass (790 cc) with a fairly regular outline of its outer surface. (**b**) Mass showing hypoechoic, irregular, central, heterogeneous area. (**c**) Doppler flow noted in the mass. The RI was 0.44. (**d**) TVS – shows a large mass, anterosuperior to the uterine fundus. (**e**) Section of the dysgerminoma showing a septum (*arrow*) that divided the tumour into lobules. (**f**) Post-operative specimen

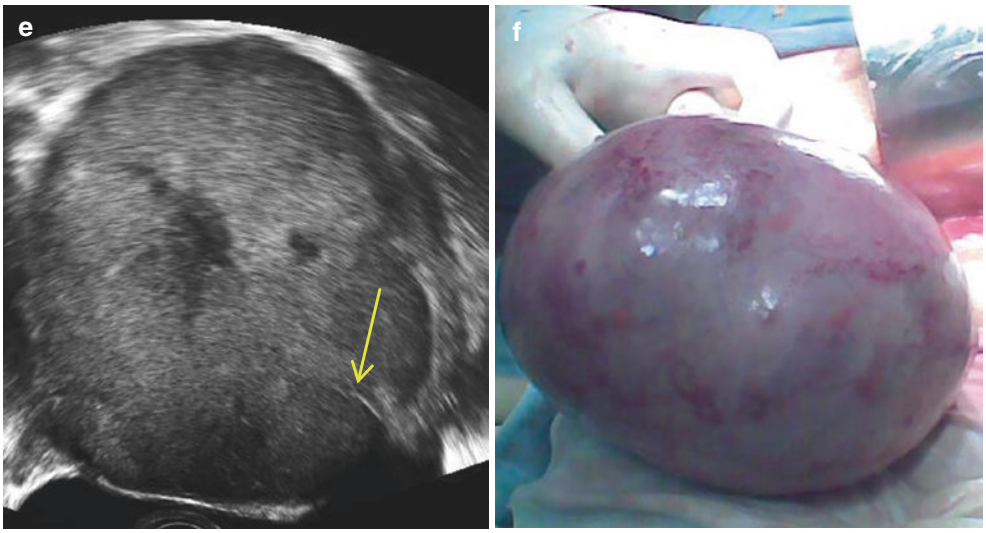

Fig. 7.73 (continued)

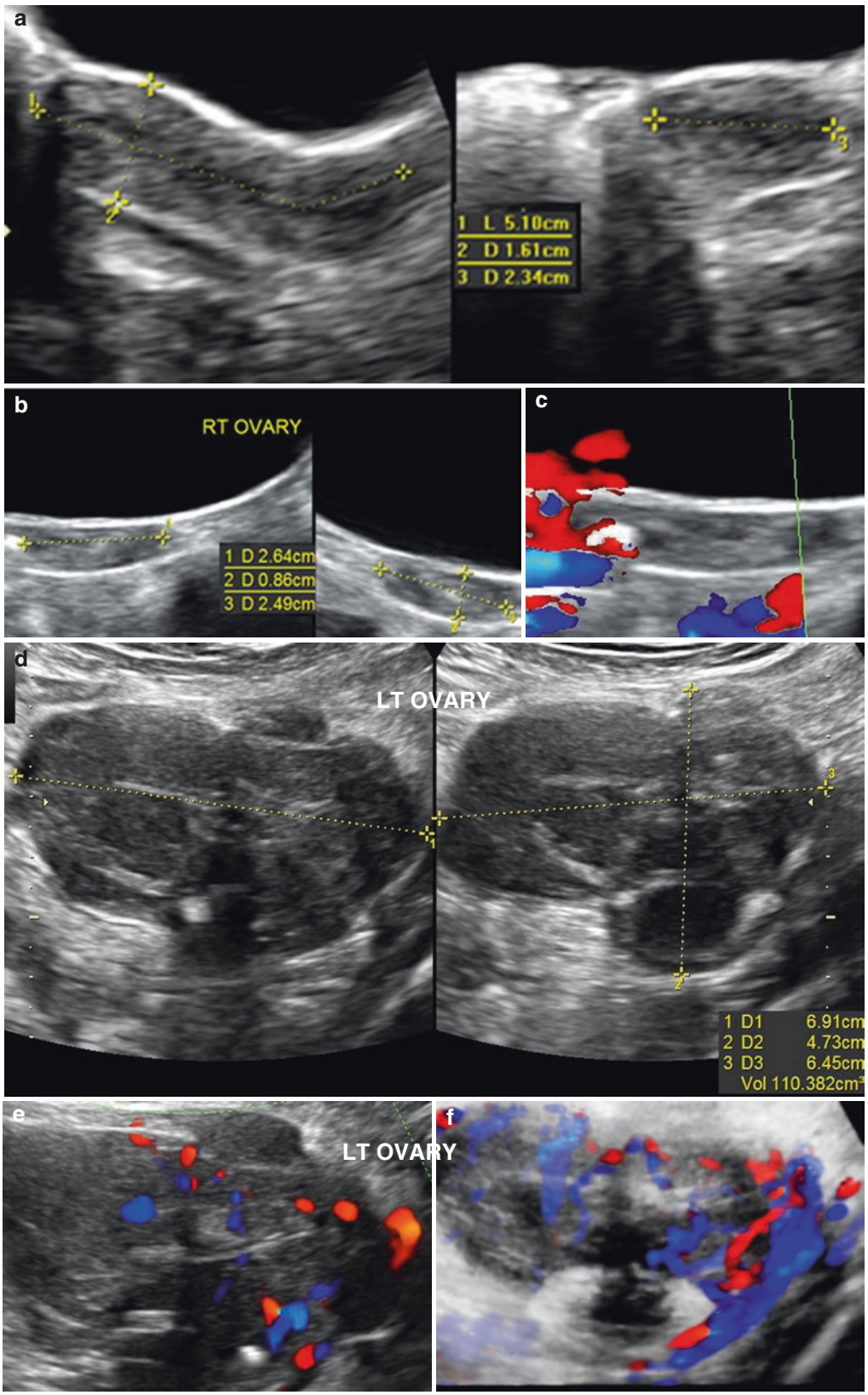

Fig. 7.74 Dysgerminoma and gonadoblastoma in a 20-year-old patient with dysgenetic gonads. Patient gave a history of primary amenorrhoea with periods only on withdrawal of hormonal medication. Transabdominal ultrasound alone was done. (**a**) Hypoplastic uterus measuring 5.1 × 1.6 × 2.3 cm. (**b**) Right ovary appears small. (**c**) No flows seen on Doppler in the right ovary. (**d**) Left ovary replaced by a nonhomogeneous, hypoechoic, solid mass. The mass shows septae dividing the solid tissue into lobules. It has irregular lobulated outer margins. (**e**, **f**) Flow seen in left ovary on 2D Doppler and 3D glass angio mode. *HPE:* left ovary showed dysgerminoma probably overgrown on a background of gonadoblastoma. Right ovary showed features suggestive of gonadoblastoma with a small focus of dysgerminoma

Sex Cord–Stromal Tumours

This includes granulosa cell tumours, Sertoli/Leydig cell tumours, thecomas and fibromas. These are typically solid tumours.

Granulosa Cell Tumour

Granulosa cell tumours are rare ovarian neoplasms. Fifty percent occur in postmenopausal women and 5 % in prepubertal girls. They are the commonest of the sex cord–stromal tumours and are the most common hormone-producing ovarian tumours (oestrogen-producing tumours). Patients often present with a history of menstrual irregularities, which facilitates early diagnosis. Endometrial hyperplasia and occasionally endometrial carcinoma may be seen in these hyperestrogenic women. Prepubertal girls may present with precocious puberty. Serum estradiol levels are raised and are useful in diagnosis both in premenopausal and postmenopausal women. These are regarded as malignant tumours with varying malignant potential, but most are slow growing (low malignant potential).

Ultrasound Features of Granulosa Cell Tumour (Fig. 7.75)

- They are usually large tumours (average 10 cm).
- Most often they are solid masses with circumscribed 'moth-eaten' cystic areas, giving it a 'Swiss cheese' appearance. In the multilocular type, the locules tend to be multiple.
- They may be purely solid in 40 % of the cases.
- The solid component usually shows heterogeneous echogenicity.
- They usually show moderate to high vascularity.

Sertoli and Sertoli–Leydig Cell Tumours

They are rare tumours that show a varying amount of Sertoli cells, Leydig cells and fibroblasts. They are sometimes known as androblastomas. These tumours have varying malignant potential and are common in young women. Sertoli–Leydig cell tumours may have androgenic, estrogenic or progestogenic manifestations (like menstrual disturbance, hirsutism or balding). However, many have no endocrine manifestations.

Ultrasound Features of Sertoli and Sertoli–Leydig Cell Tumours

- These could be solid or multilocular solid tumours.
- They vary in size from small to moderate.
- They show moderate to high vascularity in their solid component.

Leydig Cell Tumours

These rare tumours are more common in postmenopausal women and are almost always benign. They produce androgens resulting in hyperandrogenic features in most cases (like hair loss and menstrual irregularities), which are often mild.

Ultrasound features of Leydig Cell Tumours

- These are solid tumours.
- They are typically small (mean diameter of 2.4 cm). Since they are small, they are often missed.
- They show high vascularity.

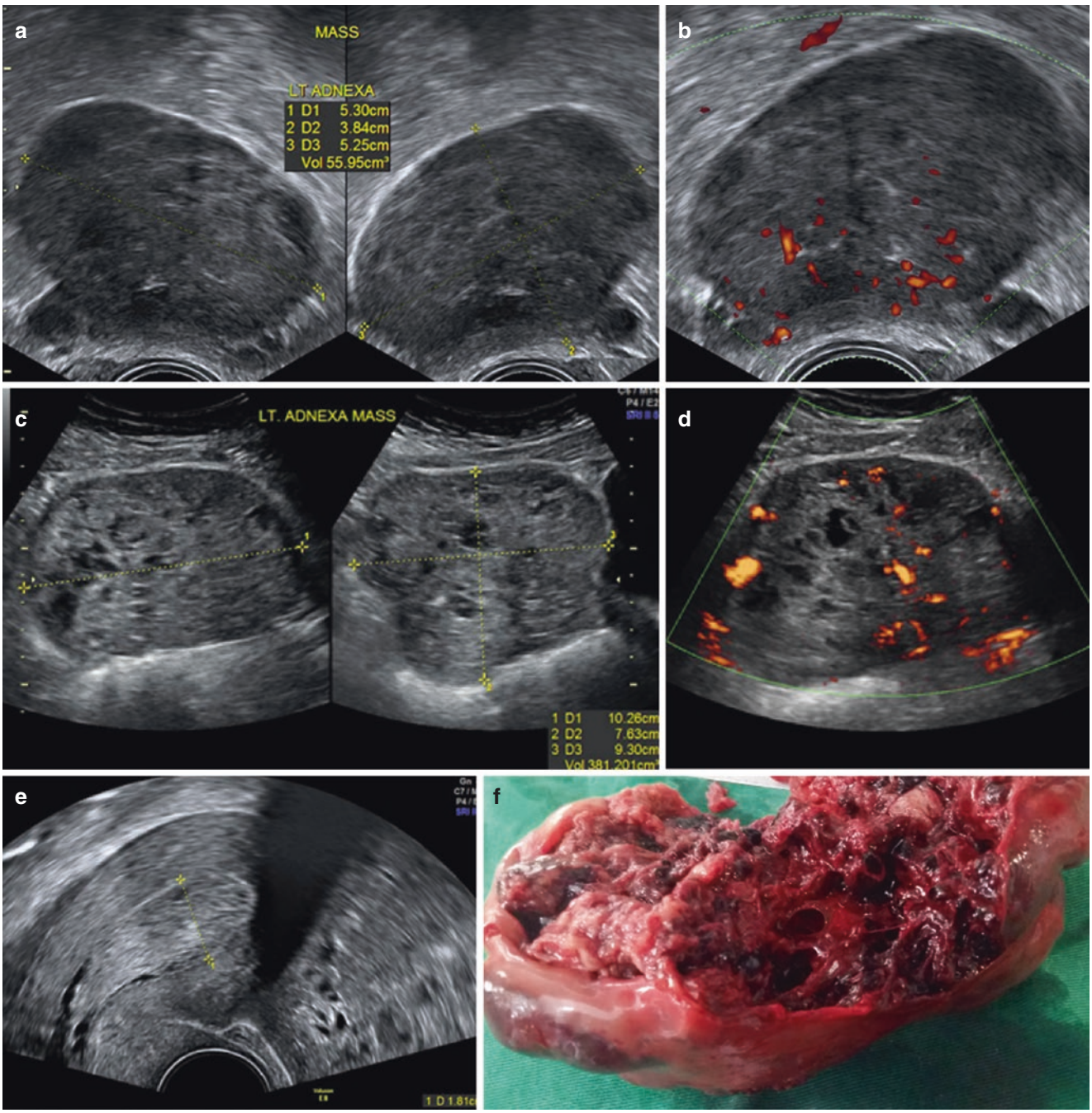

Fig. 7.75 Granulosa cell tumour in two different cases. (**a**, **b**) Case 1: 50-year-old patient who presented with menorrhagia. (**a**) Completely solid, heterogeneous mass seen with relatively smooth outer margins, (**b**) Low vascularity noted in the mass on power Doppler with PRF of 0.3, (**c, d, e, f**) Case 2: 38-year-old known case of polycystic ovaries, presented with history of menorrhagia since 2 years and continuous bleeding PV since 2 1/2 months. (**c**) Mass with bosselated outer margins and 'swiss cheese' appearance. (**d**) Vascularity noted in the mass (2) Thickened endometrium measuring 18 mm. (**e**) Cut section of post operative specimen showing classic 'swiss cheese' appearance and bosselated outer surface. Inhibin levels were elevated in the patient (preoperative-118 pg/ml)

Fibromas and Fibrothecoma

Fibromas constitute about 6% of all primary ovarian neoplasms and two-third of sex cord–stromal tumours. These are benign tumours arising from the stromal component of the ovaries. Fibroma cells are spindle cells that produce collagen and thecoma cells are stromal cells that resemble perifollicular thecal cells. The tumours are either fibromas or fibrothecomas, with fibromas being more common (78% in a study – Paladini UOG 2009). Majority of women are postmenopausal, and most of them are asymptomatic. However, they may present with mass abdomen, features of associated ascites or hydrothorax or, rarely, torsion.

Ultrasound Features of Fibromas and Fibrothecoma
(Figs. 7.76, 7.77, 7.78 and 7.79)

- They are usually unilateral.
- They appear as well-circumscribed, round, oval or slightly lobulated masses.
- They are typically solid but may show some cystic spaces. The atypical ones show large cystic spaces when their differentiation from malignant masses may be challenging.
- Most of them (about two-third) show stripy acoustic shadows like that of a fibroid.
- These fibromas show minimal or moderate flow on Doppler (colour score 2–3). Flow in the centre of fibromas is usually poor.
- Fibrothecomas, because of their thecal component, generally have higher cellularity. These are more vascular, are more likely to be lobulated and show lesser acoustic shadowing.
- Free fluid is seen in about 50% of patients, in POD. In a few patients ascites may be noted. The presence of hydrothorax (classically right sided), along with ascites in cases with solid benign ovarian tumours like these, is known as Meigs syndrome.

Gorlin syndrome (Fig. 7.80) (also known as nevoid basal cell carcinoma syndrome) is a rare autosomal dominant disorder where, in 75% of the cases, women have bilateral fibromas. These fibromas may be hyalinised or calcified. These women have characteristic facial features with frontal bossing, hypertelorism and mandibular prognathia.

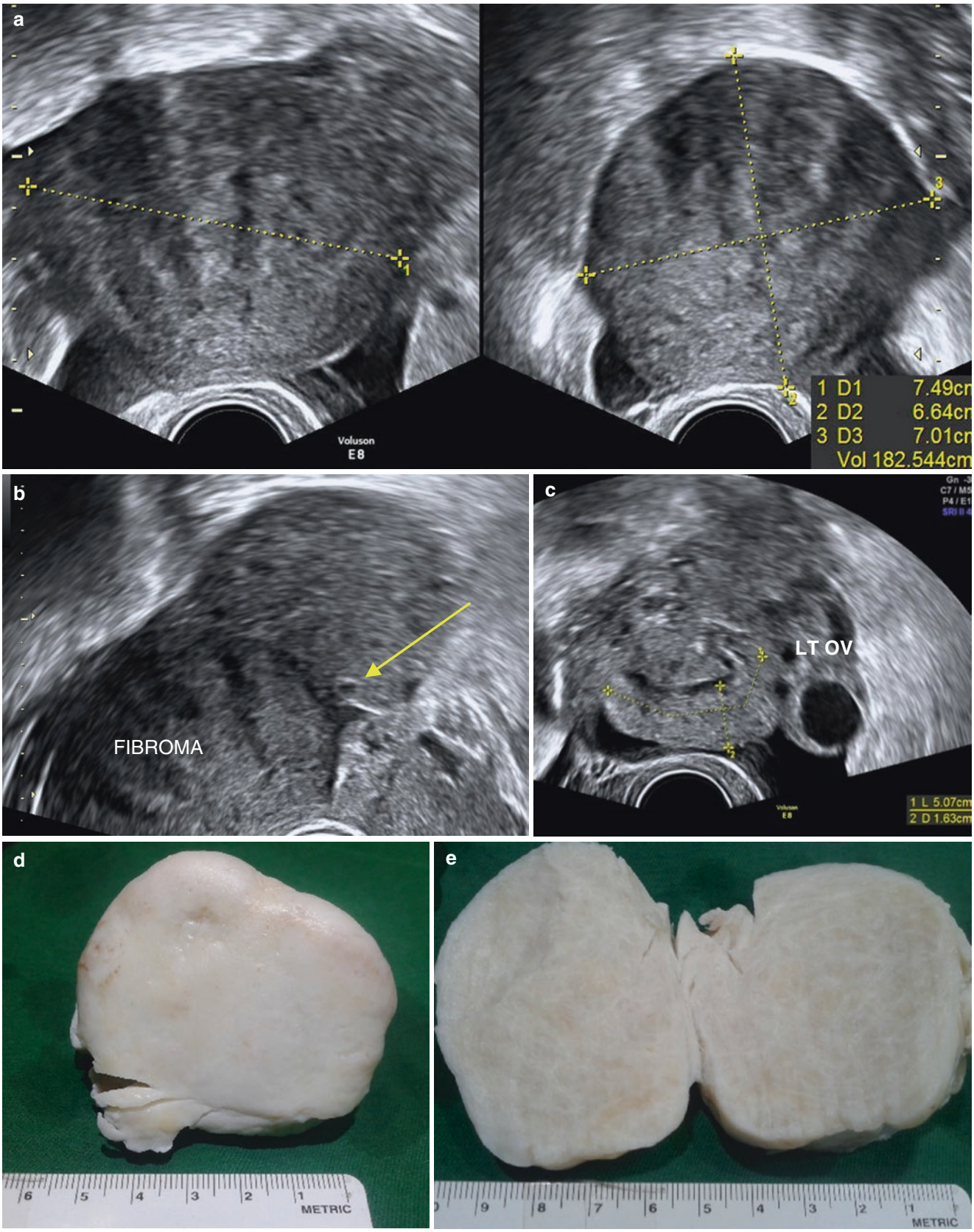

Fig. 7.76 Fibroma with associated torsion in a 33-year-old. Patient presented with abdominal pain. (**a**) Right ovarian circumscribed solid mass (about 7 cm) with a smooth outer contour and stripy acoustic shadowing, suggestive of a fibroma. (**b**) An enlarged right ovary with oedematous ovarian tissue in its superior part and a circumscribed solid mass (the fibroma) in its inferior part. Antral follicle with hyperechoic thick margins seen in the ovarian tissue suggestive of follicular ring sign (*arrow*). (**c**) Oedematous segment of the right fallopian tube (which had also undergone torsion) is measured in the image. The normal left ovary is seen beside it. (**d**) Post-operative specimen showing the outer surface of the excised fibroma. (**e**) Cut section of the fibroma

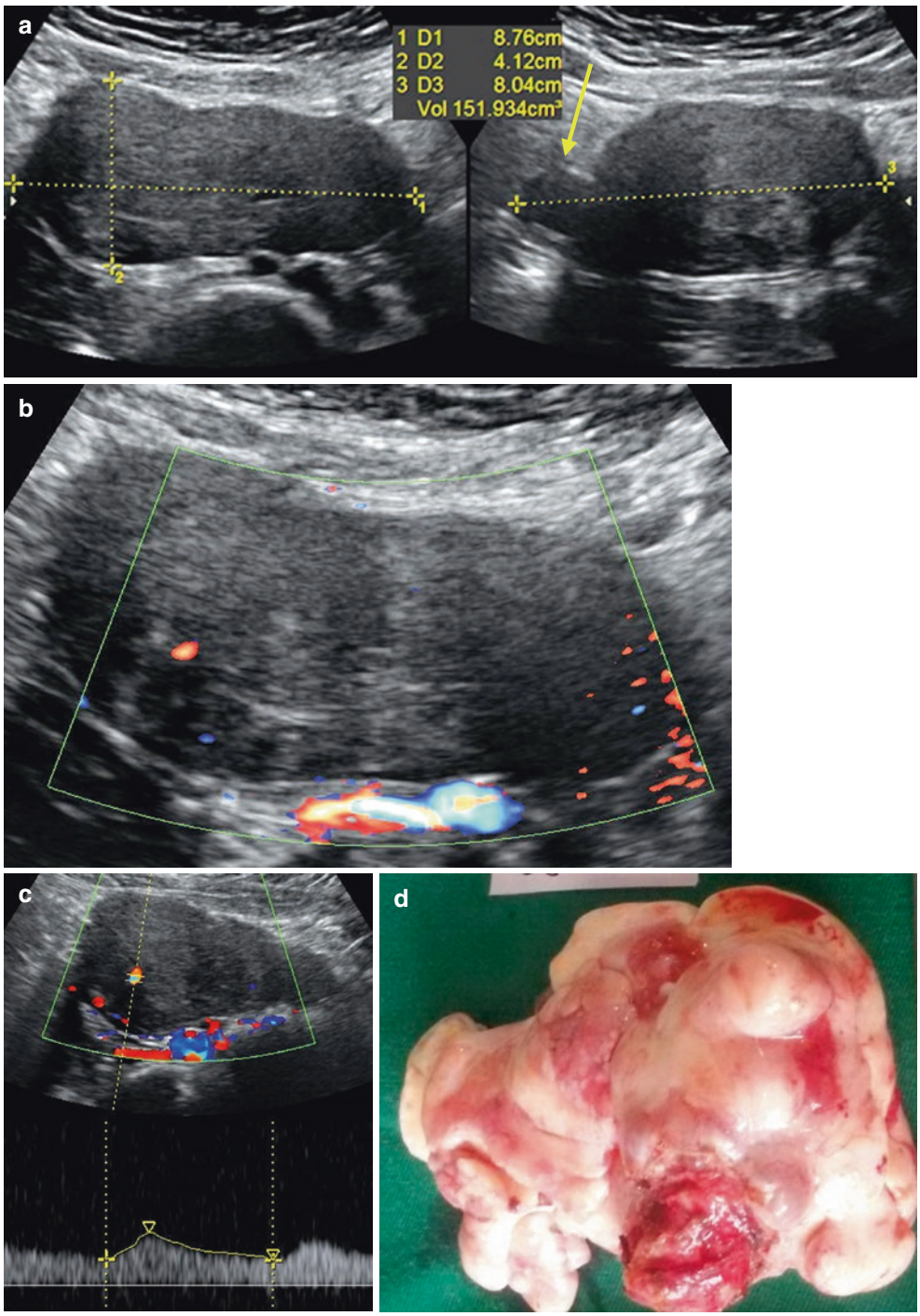

Fig. 7.77 Ovarian fibroma in a pregnant patient. (**a**) A hypoechoic solid mass with lobulated outer margins (*arrow*) and some amount of acoustic shadowing. (**b**) Minimal flow seen on Doppler (with PRF of 0.3). (**c**) Flow showed RI of 0.53. (**d**) Post-operative specimen of the ovarian fibroma

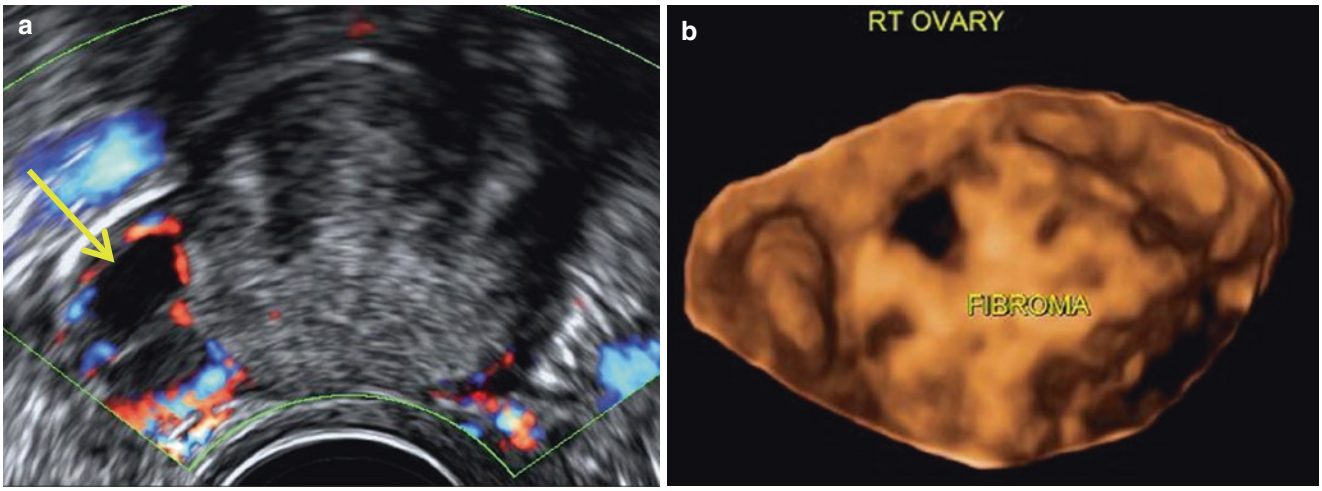

Fig. 7.78 Fibroma. Right ovary seen with a circumscribed solid mass. (**a**) Mass shows stripy shadows. Ovarian tissue with follicles is seen along its lateral margins – ovarian 'crescent sign' (*arrow*). (**b**) 3D rendered image showing the fibroma within the right ovary

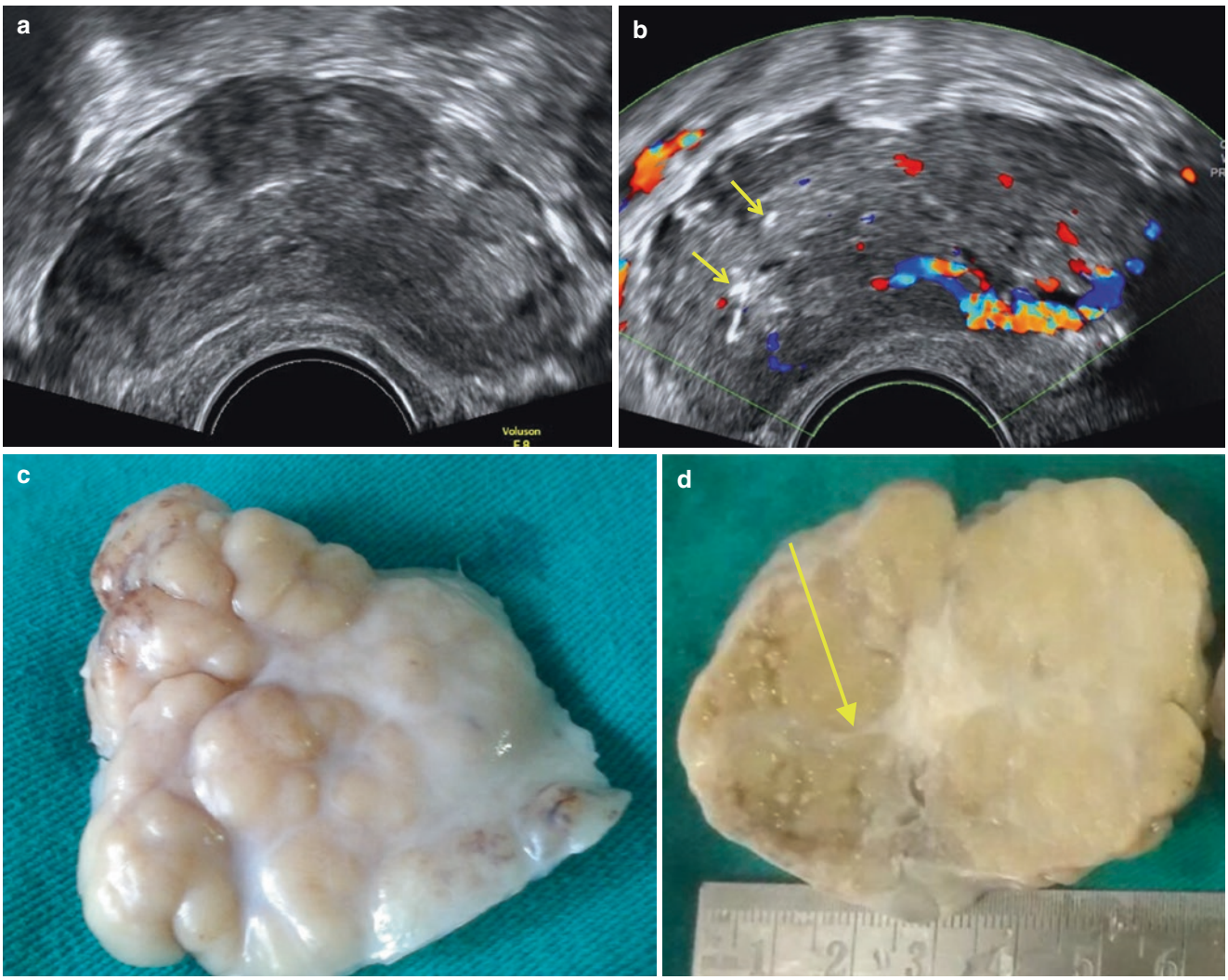

Fig. 7.79 Fibrothecoma in a 26-year-old patient. (**a**) Completely solid, hypoechoic, heterogeneous mass with lobulated margins. The mass showed some amount of shadowing. (**b**) Flow is seen in the mass with a prominent vessel approaching it from its lateral margin. The rest of the mass did not show abundant flow within. Few small foci of calcification (*arrows*) are present (this is seen occasionally in thecomas). (**c**) Post-operative specimen showing the outer lobulated surface. (**d**) Cut section of the tumour showing septae (*arrow*) dividing the solid tissue into lobules

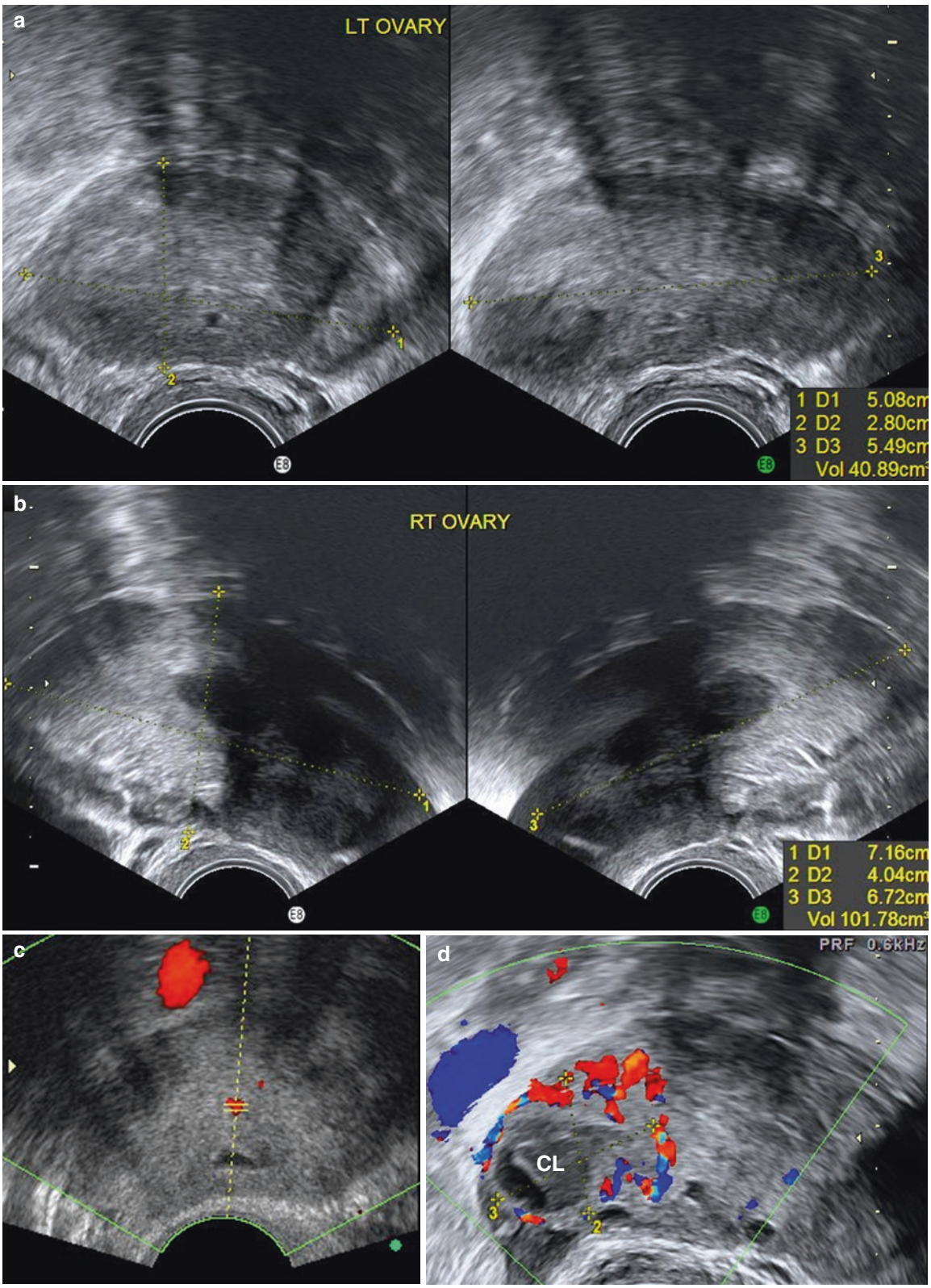

Fig. 7.80 Gorlin syndrome in a 29-year-old patient who came for an early pregnancy scan. Patient gave a history of ovarian biopsy elsewhere which she reported orally to have revealed fibrotic tissue. A very small intrauterine sac was seen. (**a**) The left ovary was bulky and showed stripy shadows with a few follicles within. (**b**) Solid, complex, enlarged right ovary showing significant acoustic shadowing. Though both the ovaries appeared fibrotic, with acoustic shadowing, no well-defined fibroma could be delineated within. A few small, scattered follicles were seen. (**c**) Minimal flow is seen in the ovary on Doppler. (**d**) A corpus luteum (CL) was seen in the left ovary

7.4.3.3 Metastatic Ovarian Masses

The ovary is a common site of metastasis from malignant tumours, most commonly arising from the breast, stomach and large bowel. These tumours are usually bilateral. Krukenberg tumours are traditionally described as mucin-filled 'signet ring' cells (on cytology) with the primary site being the stomach, breast, large bowel or appendix. Ovarian metastasis may be detected during the follow-up of patients with other malignancies, but the majority (about 57 %) are detected before the primary lesion. Most women are postmenopausal with high CA 125 levels. About half the patients are asymptomatic, and the symptomatic ones may present with a pelvic mass, ascites, dyspepsia, etc. The prognosis is poor in most cases.

Ultrasound Features of Metastatic Ovarian Masses
(Figs. 7.81, 7.82 and 7.83)
Ultrasound features of these metastatic tumours have been broadly divided into two major categories, depending on the origin of their primary tumour (Testa UOG 2007).

Category A: Tumours that metastasize from the breast, stomach, uterus and lymphoma are typically solid (about 93 % – Testa UOG 2007).

Category B: Those from the colon, rectum, appendix and biliary tract are either multilocular solid or multilocular with just about 18 % being solid. These also tend to be larger.

Other studies have shown similar overall findings, with the majority being solid. Those metastasizing from the breast are solid, smaller and more vascular. Those metastasizing from the stomach, tend to be solid, but in one-third of these cases cystic components, may be seen. The metastatic tumors from colorectal primaries, are usually multilocular.

The ultrasound findings of metastatic ovarian tumours are:

- They are frequently bilateral. Those from the stomach are bilateral in more than 50 % of the cases.
- Many of them are solid tumours (93 % of category A and 18 % of category B).
- The solid tumours are typically homogeneously solid, but if there is necrosis, they show heterogeneous echoes.
- Most of the tumours of category B and very few of category A are multilocular or multilocular solid. These usually have a large number of locules, and the septae may be so close that it may be difficult to decide on ultrasound whether there is a solid part in that area. Intracystic septae may be fragmented, probably due to necrosis. Colorectal carcinomas are typically multilocular. Multilocular morphology is more common in metastatic compared to primary ovarian carcinomas.
- The margins of the solid tumours are more often well defined, while those of category B tumours (multiloculated or multiloculated solid) are very often irregular and without a recognisable outer capsule.
- The contents within the loculated lesions could be anechoic or show low-grade echoes.
- Papillary projections are not frequently seen (only in about 12 %) in metastatic tumours compared to primary ovarian carcinomas.
- On Doppler, flow often shows moderate to high vascularity (colour core 3–4).
- Metastatic tumours show lower PI and RI and significantly higher PSV, as compared to primary ovarian carcinomas.
- 'Lead vessel' has been described to be the main or major vessel penetrating from the periphery of the mass to the centre, with a tree-shaped branching morphology. This is very typical of metastatic solid tumours (seen in 52 % – Testa UOG 2008). It was not seen in multilocular or multilocular solid metastatic tumours and was seen in only 0.01 % of primary ovarian cancers.
- Krukenberg tumours are typically solid tumours of moderate size, with bosselated outer surfaces and a lead vessel providing flow to the mass.

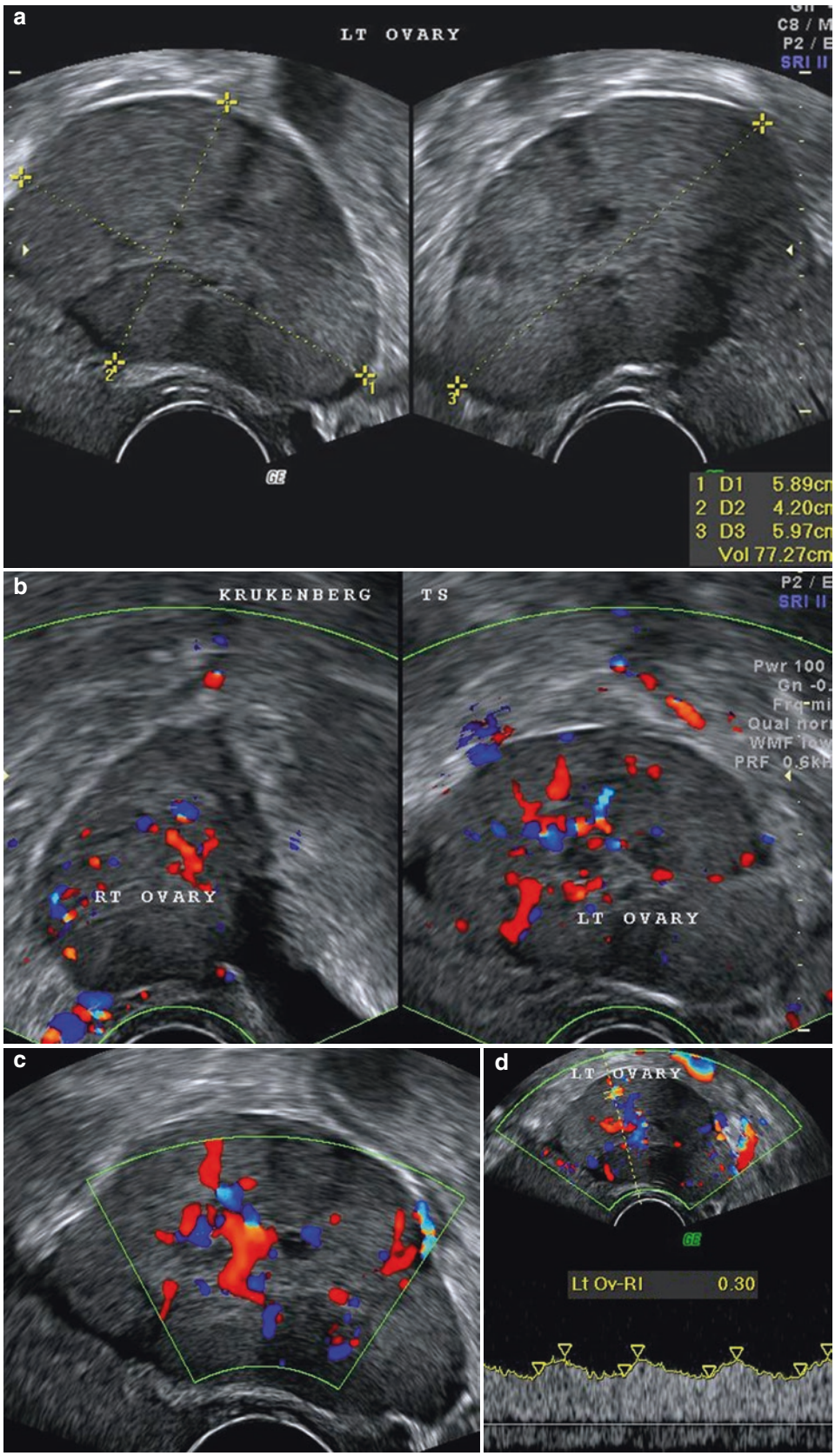

Fig. 7.81 Krukenberg tumour in a 32-year-old lady. Patient had undergone surgery and chemotherapy for breast cancer. (**a**) Left ovary replaced by a completely solid, hypoechoic, heterogeneous, well-defined mass. (**b**) High vascularity noted in both the ovaries. (**c**, **d**) Prominent vessel is seen within the mass, which might have been the 'lead vessel' described in literature. However, its entry into the ovarian mass is not visualised in this image. Flow showed a low RI of 0.3

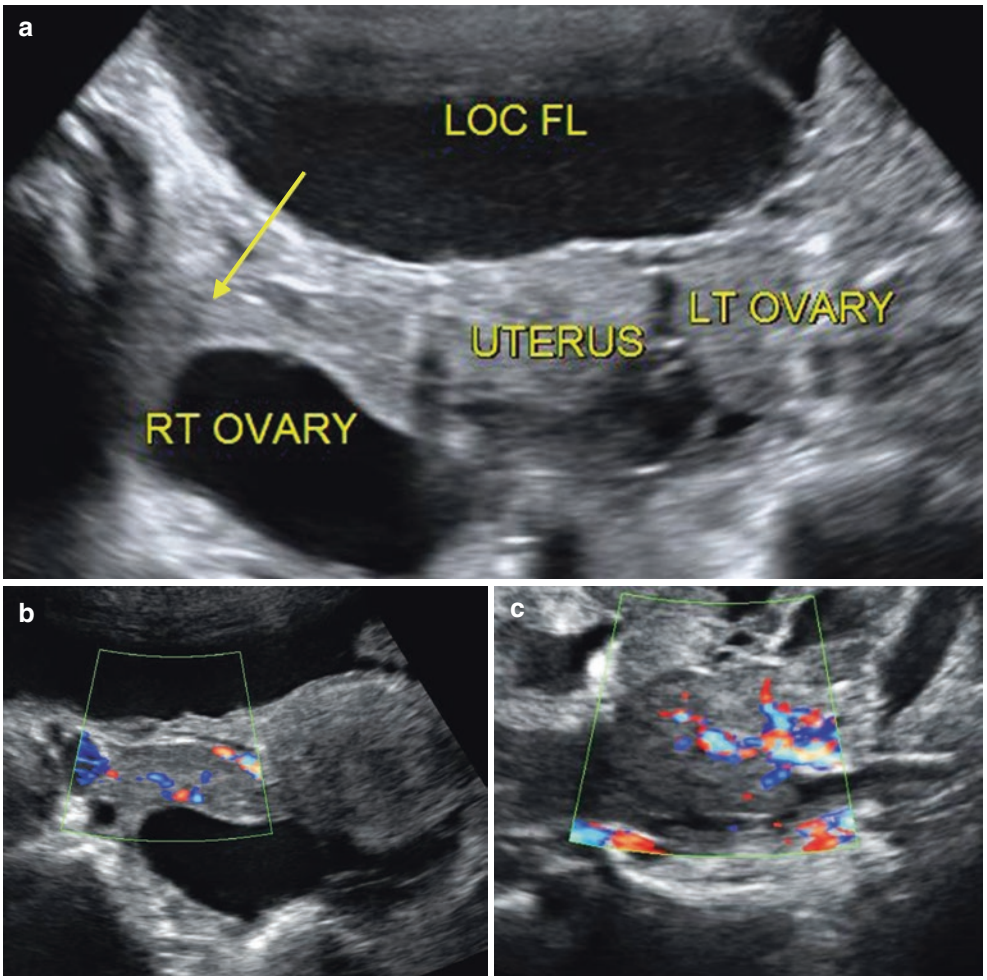

Fig. 7.82 Krukenberg tumour in a 49-year-old patient with a gastric adenocarcinoma and perforation of the gastric tumour. Bilateral ovarian metastasis. (**a**) TS of the pelvis showing the uterus with the ovaries on both sides. The right ovary showed an anechoic cystic area with solid tissue anteriorly (*arrow*). The left ovary appeared completely solid. Loculated ascitic fluid seen anterior to the uterus and the ovaries. (**b**) The right ovary shows flow in its solid tissue. (**c**) The solid left ovary shows a lead vessel entering the mass from its lateral margin

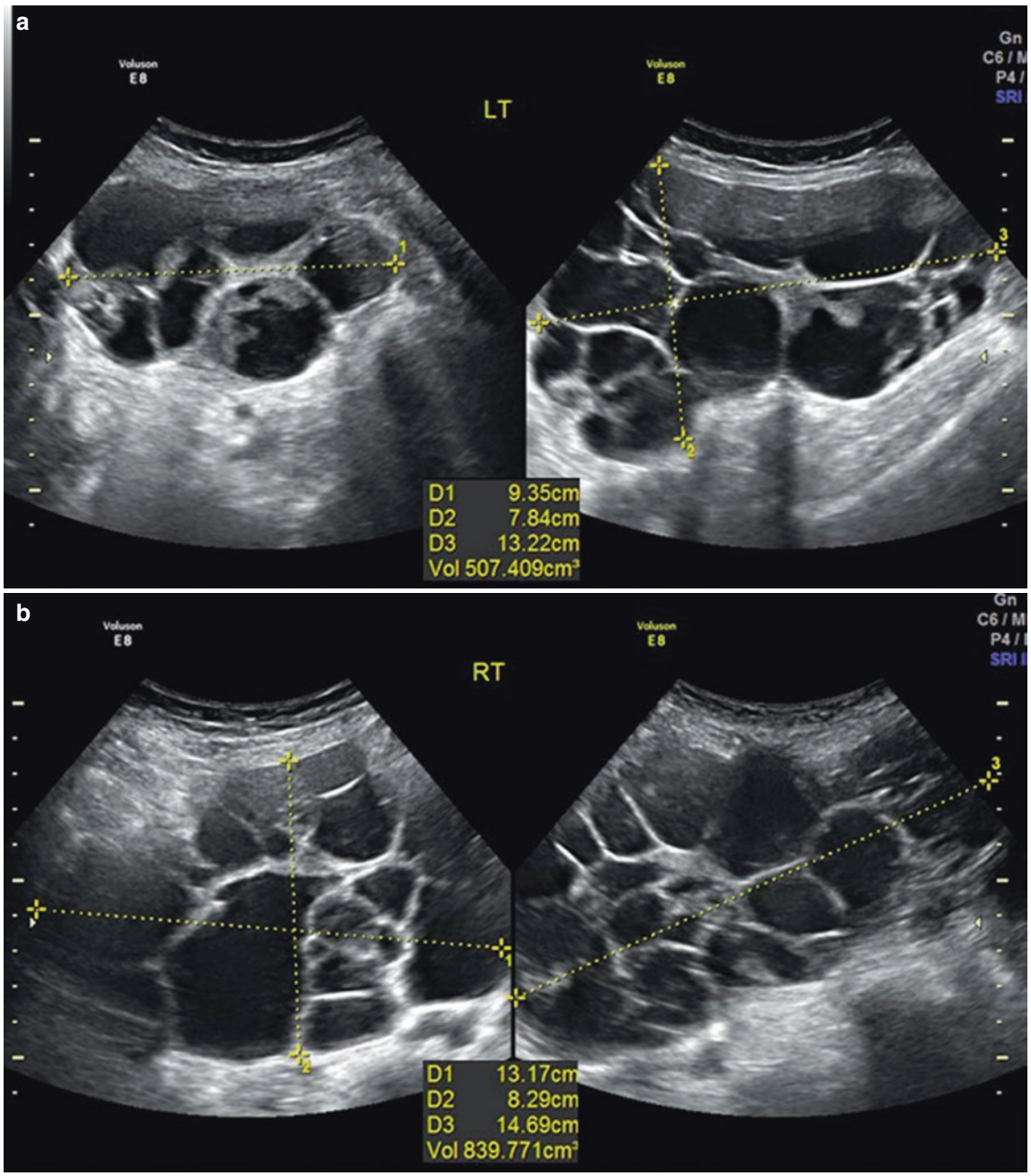

Fig. 7.83 Bilateral ovarian metastasis from an anorectal carcinoma in a 36-year-old patient. (**a**, **b**) Large, multiloculated cystic ovaries seen bilaterally. Volume of the left ovary was 507 cc, and volume of the right ovary was 840 cc. Very minimal stroma is seen between the locules. (**c**) The locules showed turbid fluid with variable echogenicity. (**d**) Flow with moderate vascularity was seen in the septae of the loculated ovary. (**e**) The uterus seen positioned over an enlarged, complex bowel mass on TAS. (**f**) The anorectal mass shows vascularity on TVS. (**g**) Anorectal mass measured on TVS

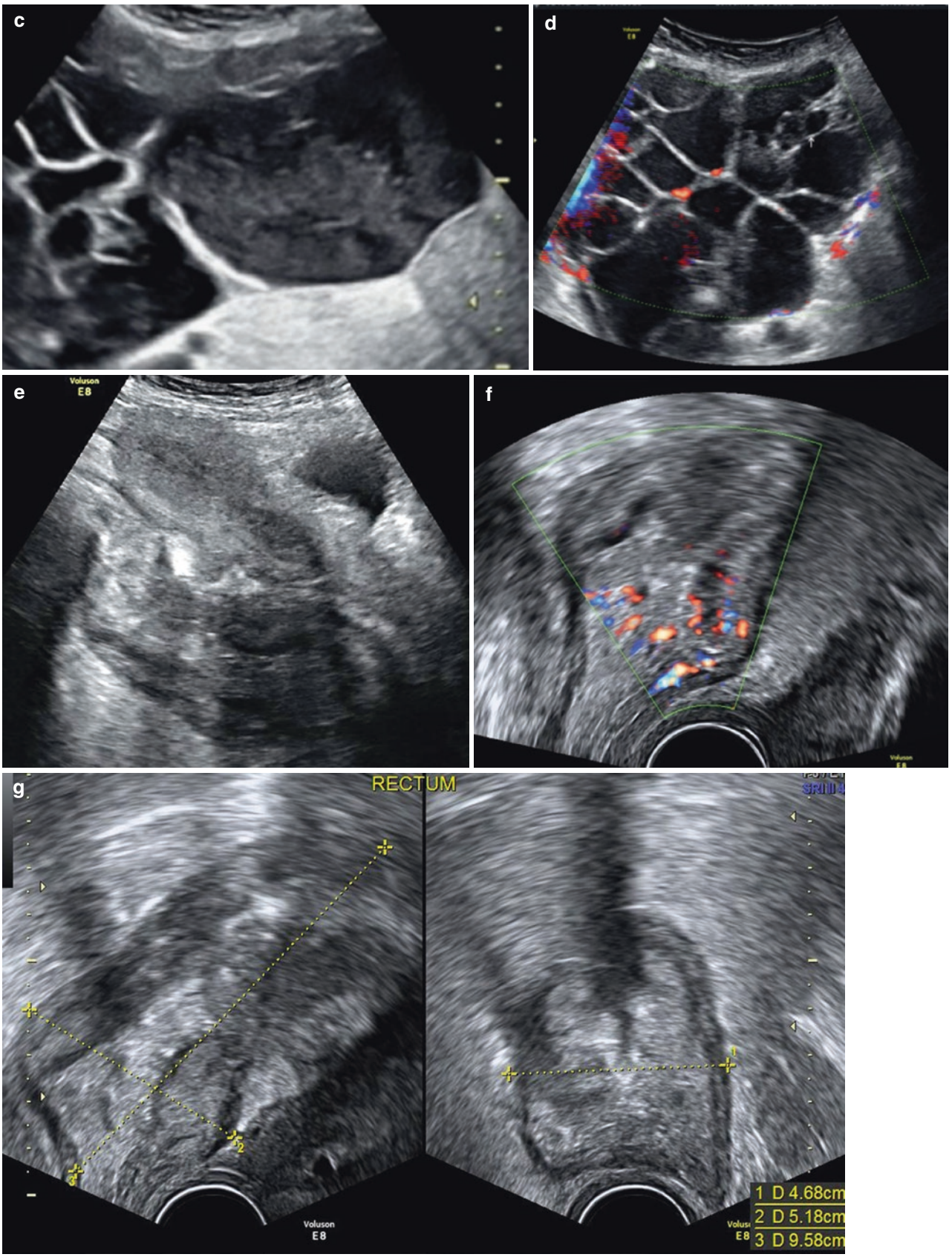

Fig. 7.83 (continued)

Summary: Ovarian Neoplasms

- Age of patients and symptomatology vary depending upon the type of neoplasm. Many patients are asymptomatic. Others may present with abdominal distension, pelvic mass or rare complications like torsion and rupture. Malignant ones may be associated with weight loss and dyspepsia.
- Past history and reports are important for correlation.
- Findings vary depending upon the type of neoplasm.
  - *Epithelial tumours* are the commonest with most tumours being serous and mucinous. These are commonly benign but could be borderline malignant or malignant. They may show septae and papillae.
  - *Germ cell tumours* – Dermoids are benign commonly seen tumours. Typical ultrasound feature is a complex cyst with acoustic shadowing.
    Other germ cell tumours are malignant and seen in young adults. They are predominantly solid and usually unilateral.
  - *Sex cord–stromal tumours* include fibromas and hormone-producing tumours like granulosa cell tumour. Fibromas typically appear as solid masses with stripy shadowing, and granulosa cell tumour may either be solid or cystic ('Swiss cheese' appearance).
  - *Metastatic tumours* – Common primaries are from the breast and GIT. Those from the breast, stomach, lymphoma and uterus are typically solid, while those from the colon, rectum, appendix and biliary tract are most often multilocular or multilocular solid.
- Ultrasound report should describe the morphology (using IOTA terminology). In some cases, diagnosis of the histological nature of the mass is possible. In others, the impression of the nature of the mass, i.e. benign or malignant, should be provided.

Suggested Reading

Campbell S (2012) Ovarian cancer: role of ultrasound in preoperative diagnosis and population screening. Ultrasound Obstet Gynecol 40:245–254. doi:10.1002/uog.12281

Catteau-Jonard S et al (2012) Polycystic ovaries at ultrasound: normal variant or silent polycystic ovary syndrome? Ultrasound Obstet Gynecol 40:223–229

Demidov VN, Lipatenkova J, Vikhareva O, Van Holsbeke C, Timmerman D, Valentin L (2008) Imaging of gynecological disease (2): clinical and ultrasound characteristics of Sertoli cell tumors, Sertoli–Leydig cell tumors and Leydig cell tumors. Ultrasound Obstet Gynecol 31:85–91. doi:10.1002/uog.5227

Exacoustos C et al (2005) Preoperative sonographic features of borderline ovarian tumors. Ultrasound Obstet Gynecol 25:50–59. doi:10.1002/uog.1823

Fischerova D (2011) Ultrasound scanning of the pelvis and abdomen for staging of gynecological tumors: a review. Ultrasound Obstet Gynecol 38:246–266. doi:10.1002/uog.10054

Guerriero S et al (2012) Preoperative diagnosis of metastatic ovarian cancer is related to origin of primary tumor. Ultrasound Obstet Gynecol 39:581–586. doi:10.1002/uog.10120

Guerriero S et al (2011) Imaging of gynecological disease (6): clinical and ultrasound characteristics of ovarian dysgerminoma. Ultrasound Obstet Gynecol 37:596–602. doi:10.1002/uog.8958

Kaijser J et al (2013) Improving strategies for diagnosing ovarian cancer: a summary of the International Ovarian Tumor Analysis (IOTA) studies. Ultrasound Obstet Gynecol 41:9–20. doi:10.1002/uog.12323

Laing FC, Allison SJ (2012) US of the ovary and adnexa: to worry or not to worry? Radiographics 32:1621–1639

Lam PM et al (2009) Polycystic ovarian syndrome: a misnomer for an enigmatic disease. Ultrasound Obstet Gynecol 33(6):621–627

Langer JE et al (2012) Imaging of the female pelvis through the life cycle. Radiographics 32:1575–1597

Mascilini F et al (2014) Imaging in gynecological disease (10): clinical and ultrasound characteristics of decidualized endometriomas surgically removed during pregnancy. Ultrasound Obstet Gynecol 44:354–360. doi:10.1002/uog.13323

Paladini D et al (2009) Imaging in gynecological disease (5): clinical and ultrasound characteristics in fibroma and fibrothecoma of the ovary. Ultrasound Obstet Gynecol 34:188–195. doi:10.1002/uog.6394

Patel MD et al (1998) Cystic teratomas of the ovary; diagnostic value of sonography. Am J Roentgenol 171:1061–1065

Saksouk FA, Johnson Samuel C (2004) Recognition of the ovaries and ovarian origin of pelvic masses with CT. Radiographics 24(1):S133–S146

Sayasneh A et al (2015) Accuracy of ultrasonography performed by examiners with varied training and experience in predicting specific pathology of adnexal masses. Ultrasound Obstet Gynecol 45:605–612. doi:10.1002/uog.14675

Sokalska A et al (2009) Diagnostic accuracy of transvaginal ultrasound examination for assigning a specific diagnosis to adnexal masses. Ultrasound Obstet Gynecol 34:462–470. doi:10.1002/uog.6444

Testa AC (2007) Imaging in gynecological disease (1): ultrasound features of metastases in the ovaries differ depending on the origin of the primary tumor. Ultrasound Obstet Gynecol 29:505–511. doi:10.1002/uog.4020

Testa AC et al (2008) The 'lead vessel': a vascular ultrasound feature of metastasis in the ovaries. Ultrasound Obstet Gynecol 31:218–221. doi:10.1002/uog.5251

Testa AC et al (2011) Ovarian cancer arising in endometrioid cysts: ultrasound findings. Ultrasound Obstet Gynecol 38:99–106. doi:10.1002/uog.8970

Timmerman D et al (2000) Terms, definitions and measurements to describe the sonographic features of adnexal tumors: a consensus opinion from the International Ovarian Tumor Analysis (IOTA) Group. Ultrasound Obstet Gynecol 16:500–505

Valentin L (1999) Pattern recognition of pelvic masses by gray-scale ultrasound imaging: the contribution of Doppler ultrasound. Ultrasound Obstet Gynecol 14:338–347. doi:10.1046/j.1469-0705.1999.14050338

Valentin L et al (2013) Unilocular adnexal cysts with papillary projections but no other solid components: is there a diagnostic method that can classify them reliably as benign or malignant before surgery? Ultrasound Obstet Gynecol 41:570–581. doi:10.1002/uog.12294

Van Holsbeke C et al (2010) Endometriomas: their ultrasound characteristics. Ultrasound Obstet Gynecol 35:730–740. doi:10.1002/uog.7668

Holsbeke V et al (2008) Imaging of gynecological disease (3): clinical and ultrasound characteristics of granulosa cell tumors of the ovary. Ultrasound Obstet Gynecol 31:450–456. doi:10.1002/uog.5279

Yazbek J et al (2007) Accuracy of ultrasound subjective 'pattern recognition' for the diagnosis of borderline ovarian tumors. Ultrasound Obstet Gynecol 29:489–495. doi:10.1002/uog.4002

Endometriosis

8

Endometriosis is the presence of ectopic endometrial glands and stroma (basically endometrial tissue) seen outside of the uterus.

This is commonly seen in women belonging to the reproductive age group, who present with symptoms such as dysmenorrhoea, chronic pelvic pain and subfertility/infertility. Women, however, may be asymptomatic, and endometriosis may be incidentally diagnosed on an ultrasound or during laparoscopy.

Endometriosis is seen in about 4–13 % of women of the reproductive age and in 25–50 % of women with infertility.

Endometriotic lesions could be superficial or deep (more than 5 mm from the peritoneal surface). Based on their location, they can be grouped into three categories:

1. Ovaries and pelvic peritoneum: This is the most common site. It is important to note that tiny superficial endometriotic lesions of the pelvic peritoneum or on the ovarian surface (i.e., the gunshot or powder-burn lesions seen on laparoscopy), cannot be picked up on ultrasound.
2. Deep infiltrating endometriosis of the pelvis: This is seen in 15–30 % of women with endometriosis. Lesions (endometrial tissue) penetrate into the retroperitoneal space or the walls of the pelvic organs, to a depth of at least 5 mm. Common locations are the uterosacral, rectosigmoid, vagina, bladder and ureter.
3. Extra-pelvic endometriosis: This is endometriosis seen outside the pelvis, involving the abdominal wall, lungs, etc.

Please note: Endometriomas of the ovary have been discussed in detail in the chapter on ovarian masses (Chap. 7).

8.1 Deep Infiltrating Endometriosis (DIE)

Here, the lesions (endometrial tissue) penetrate into the retroperitoneal space and/or the walls of the pelvic organs to a depth of at least 5 mm. Common locations are the uterosacral, rectosigmoid, vagina, bladder, ureter, etc. This is seen in 15–30 % of women with endometriosis.

Significance of DIE

- DIE causes pain which can be very distressing. The pain could be in the form of dysmenorrhoea, dyspareunia, chronic pelvic pain or bladder and bowel symptoms like dysuria and painful defecation.
- DIE is often not diagnosed on ultrasound as visualizing and detecting these lesions requires high suspicion and knowledge of the spectrum of DIE.
- DIE can affect the pelvic organs by either by primary involvement or by secondary involvement, caused by anatomic distortion of a structure due to fibrotic retraction of an adjoining DIE nodule. This can lead to complications such as hydronephrosis.
- DIE nodules have the potential to undergo malignant transformation.
- In pregnancy, they can increase in size and vascularity and may become painful or affect pelvic organs for the first time, in pregnancy.
- Diagnosing DIE is very important for optimal planning of surgery. If DIE is anticipated, appropriate consent can be taken from the patient, and the primary surgeon may decide to involve a colorectal surgeon or urologist.

Ultrasound Features of DIE Nodules (In General)
(Figs. 8.1 and 8.2)

Transvaginal scan is the diagnostic modality of choice.

- DIE lesions are usually fusiform or nodular in shape.
- The lesions appear hypoechoic.
- They have diffuse borders.
- They are firm and may show some amount of acoustic shadowing.
- They are typically solid but could be solid and cystic, or only cystic.

M. Sibal, *Ultrasound in Gynecology*, DOI 10.1007/978-981-10-2714-7_8

- They are most often poorly vascularised.
- They are generally tender and therefore a pain/tenderness-guided approach during TVS is useful in locating them.
- They are multiple in about 20 % of causes.

In some cases, where the ovaries appear normal on scan, these DIE nodules are not suspected and therefore more likely to be missed.

For the diagnosis of DIE, other diagnostic modalities like MRI, CT and barium studies can also be resorted to. However, transvaginal scan is the modality of choice because it is the least expensive, least invasive and has a sensitivity of 81.1 % and a specificity of 94.2 % (Vimercati et al. 2012). This high specificity and sensitivity is because transvaginal scan is dynamic and interactive, allowing evaluation of tenderness and adhesions, in addition to having a high resolution.

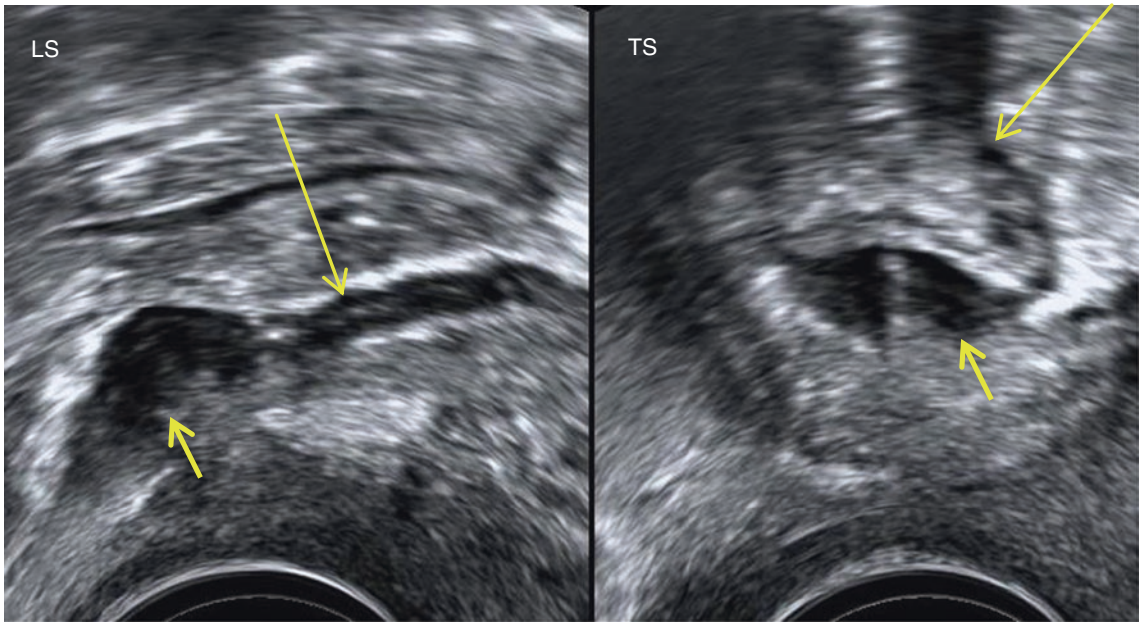

Fig. 8.1 Bowel DIE. Longitudinal section and transverse section of a DIE nodule (*short arrows*) involving the anterior rectal wall. The nodule is hypoechoic with diffuse borders. On *LS*, the normal anterior rectal muscularis above the lesion shows a fine hyperechoic line within, which separates the outer longitudinal from the inner circular muscular layer (*long arrow*). On *TS*, the nodule shows acoustic shadowing suggestive of fibrotic elements within the DIE nodule. *TS* of the bowel gives a 'signet-ring' appearance because of the nodule in one part of the bowel wall with normal muscularis (*long arrow*) seen all around the bowel wall

Fig. 8.2 DIE lesion (*arrow*) showing poor vascularity on Doppler

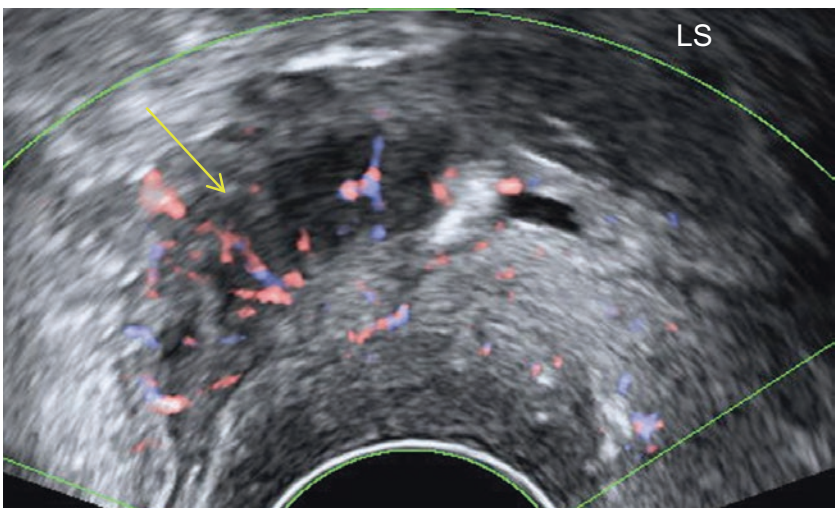

8.1.1 DIE of Large Bowel (Rectosigmoid)

This primarily involves the anterior muscularis of the rectosigmoid. The anterior muscularis of the rectum can be traced just behind the vagina and along the posterior wall of the uterus. There is a fine white line which is seen within it that divides the anterior muscularis into an inner layer of circular muscle fibres and an outer layer of longitudinal muscle fibres. Just within the muscularis lies the hyperechoic submucosa. Within the submucosa is the dark central linear area, which is the lumen of the large bowel. Patients with endometriosis of the bowel may be asymptomatic or may complain of dysmenorrhoea, painful defecation or mucoid/bloody rectal discharge during periods.

Ultrasound Features of DIE of Large Bowel (Rectosigmoid) (Figs. 8.1, 8.2, 8.3, 8.4 and 8.5)

- Fusiform-shaped lesions along the anterior muscularis of the large bowel. The typical appearance (thin hyperechoic line) of the bowel muscularis in that area is lost but can be seen above and below it.
- The affected anterior muscularis of the bowel loop with DIE is much thicker than the corresponding posterior muscularis.
- On a longitudinal section, they appear as thickened areas of the anterior muscularis, and on cross section, the bowel gives a 'signet ring' appearance.
- At times, one may see hyperechoic linear echoes radiating out of a DIE nodule, giving it a 'Red Indian hairdo' appearance from which it derives the term 'Red Indian hair dress' sign. This appearance is because of the involvement of the bowel submucosa due to fibrotic retraction by the DIE nodule. This typical feature is prominent on ultrasound and is therefore helpful in picking up DIE lesions.
- Lesions that are seen beyond the uterine fundus are generally considered to be involving the sigmoid, while those below the uterine fundus are considered to be rectal, though it is not possible to have a clear-cut delineation of the rectosigmoid junction on ultrasound.
- One should measure the distance between the lower end of the nodule and the anal verge, because lesions that are less than 7 cm from the anal verge are more difficult to manage surgically than those which are higher up.
- The DIE nodules are most often adherent to the posterior wall of the uterus, because of which there is an absence of the sliding sign (bowels sliding along the posterior wall of the uterus and vaginal fornix). This absent sliding sign has a high LR of 23.6 for rectal DIE (Hudelist et al. 2013).

Transvaginal scan has a very high pickup for rectosigmoid endometriosis (sensitivity of 91 % and specificity of 98 %). For lesions that are high up in the sigmoid (beyond the reach of a transvaginal scan), a double contrast barium enema may be useful.

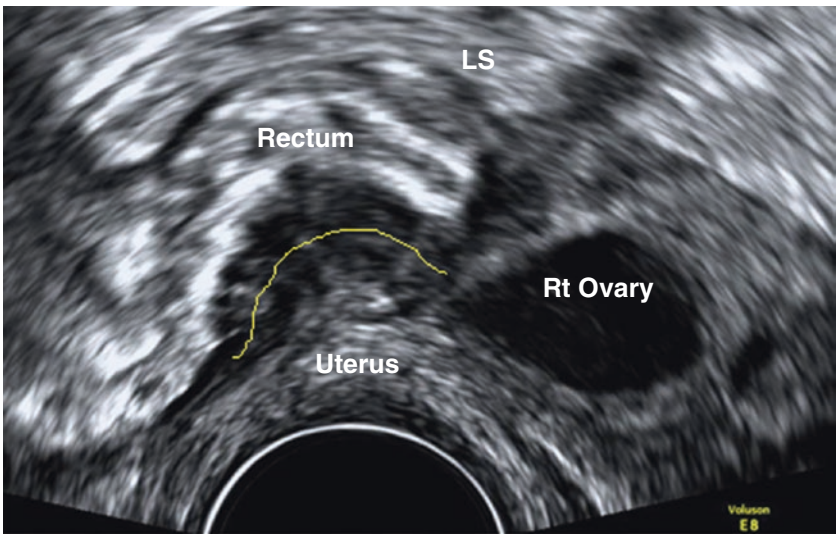

Fig. 8.3 DIE nodule (traced) is seen involving the anterior rectal wall. The nodule was seen in the POD, adherent to the posterior wall of the uterus and the right ovary

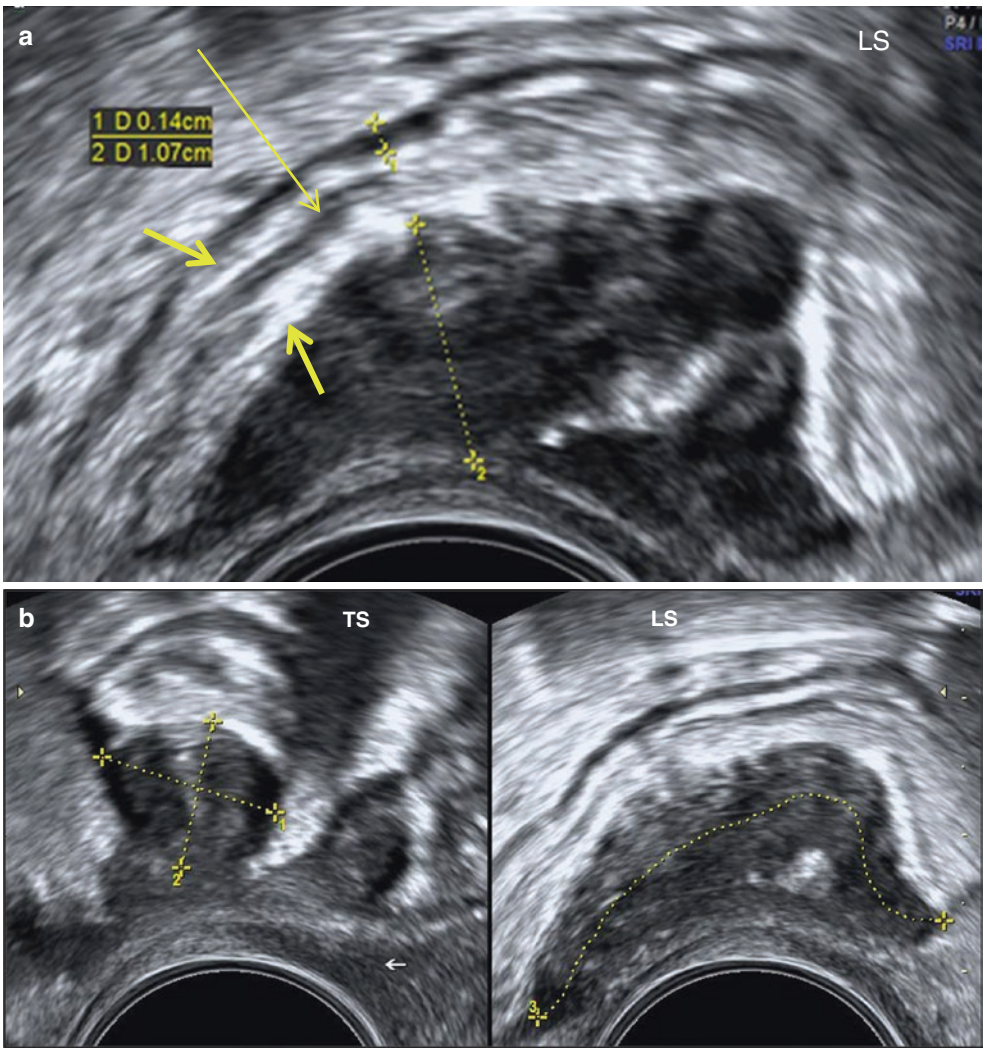

Fig. 8.4 Rectosigmoid DIE in a 32-year-old lady who complained of severe pain in the rectal region with mucoid discharge per rectum during periods. Colonoscopy and ultrasound scans done elsewhere were reported as normal. **(a)** The anterior muscularis of the bowel loop is much thicker than the posterior muscularis in the area of the DIE nodule. Just within the muscularis, the hyperechoic submucosa (*short arrows*) is seen, and within that is a dark linear area, which is the central lumen of the bowel (*long arrow*). (**b**) *TS* and *LS* view of the DIE nodule. Typical 'signet ring' appearance is noted on *TS*, (**c**) DIE nodule showing moderate to high vascularity. (**d**, **e**) Both ovaries appeared normal

Fig. 8.4 (continued)

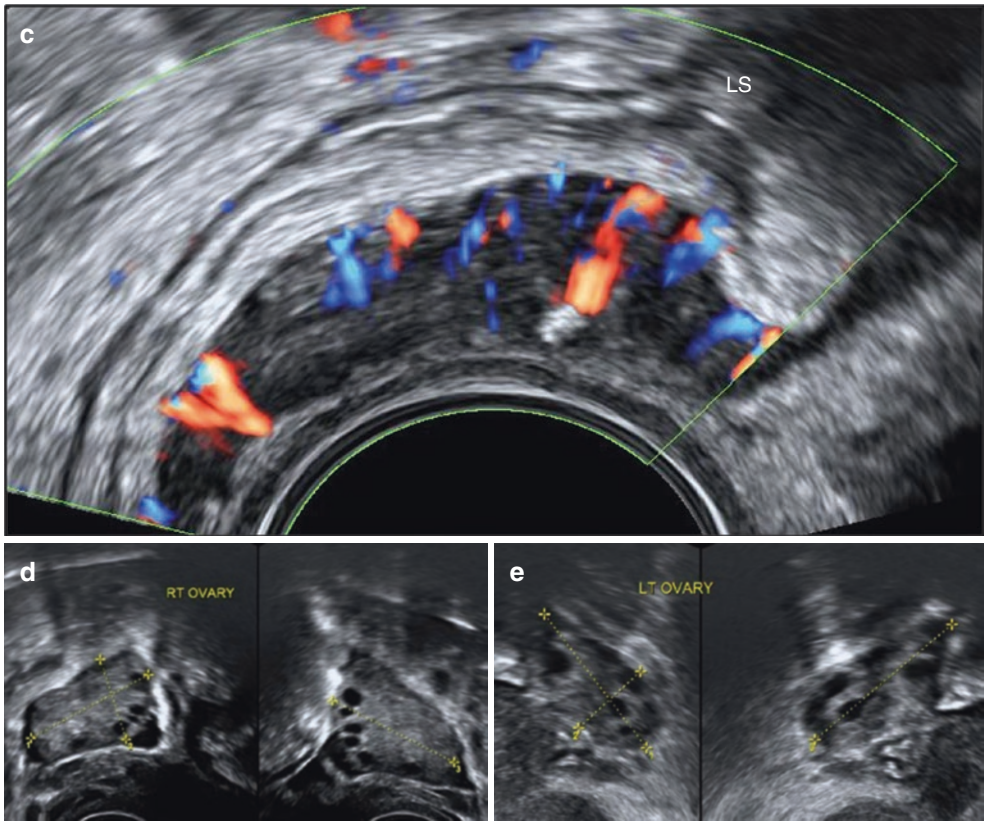

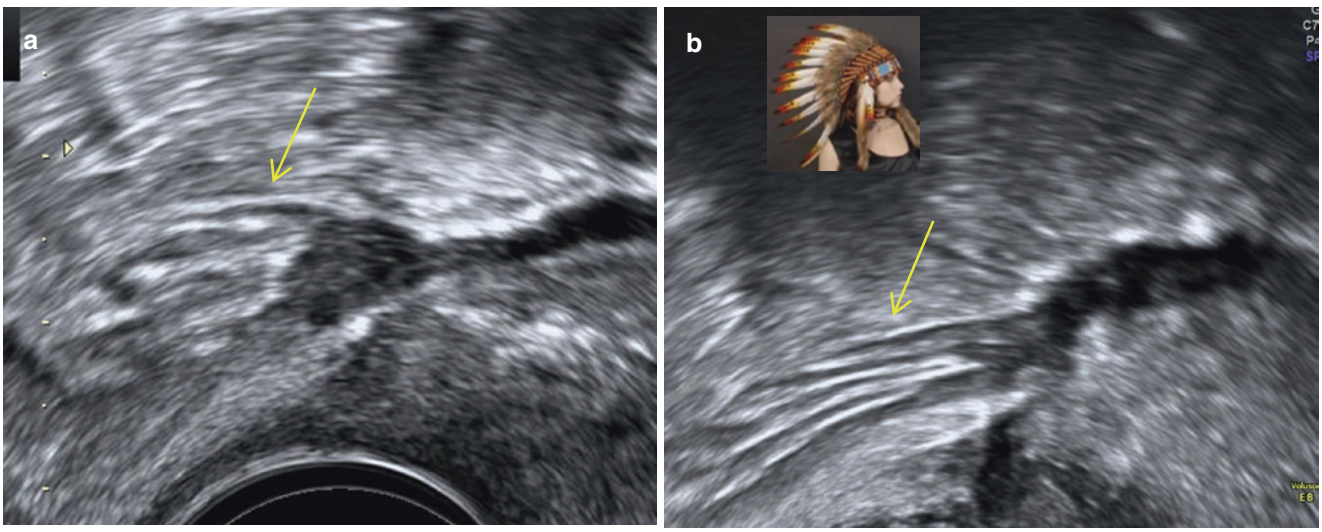

Fig. 8.5 (**a**, **b**) 'Red Indian hair dress' sign seen in two different cases of bowel DIE. The images show hyperechoic linear echoes (*arrows*) radiating out from the DIE nodule resembling a 'Red Indian hairdo'. This typical feature is prominent on ultrasound and is therefore helpful in picking up DIE lesions

8.1.2 DIE of the Vaginal Wall

DIE can also involve the walls of the vagina, commonly the posterior wall and very often in continuity with rectal DIE, forming a rectovaginal DIE lesion. Patients can be asymptomatic or complain of dysmenorrhoea or dyspareunia. If the adjoining bowel is involved, then the patient may present with rectal symptoms.

Ultrasound Features of Vaginal DIE (Figs. 8.6, 8.7 and 8.8)

- The affected vaginal wall appears thickened and hypoechoic with diffuse borders. It shows poor vascularity. Comparison with the vaginal wall elsewhere provides a convenient control.
- In cases with rectovaginal DIE, there is a breach in the rectovaginal septum (the normal rectovaginal septum appears like a hyperechoic line separating the rectum and the vagina), where the rectal DIE is continuous with the vaginal DIE.
- Vaginal and rectovaginal DIEs are more difficult to diagnose because of the proximity of these structures to the TVS probe. Therefore, gel sonovaginography (GSV) is usually resorted to at our centre, wherein, 20 ml of gel is instilled into the vagina for better resolution of the lesion.

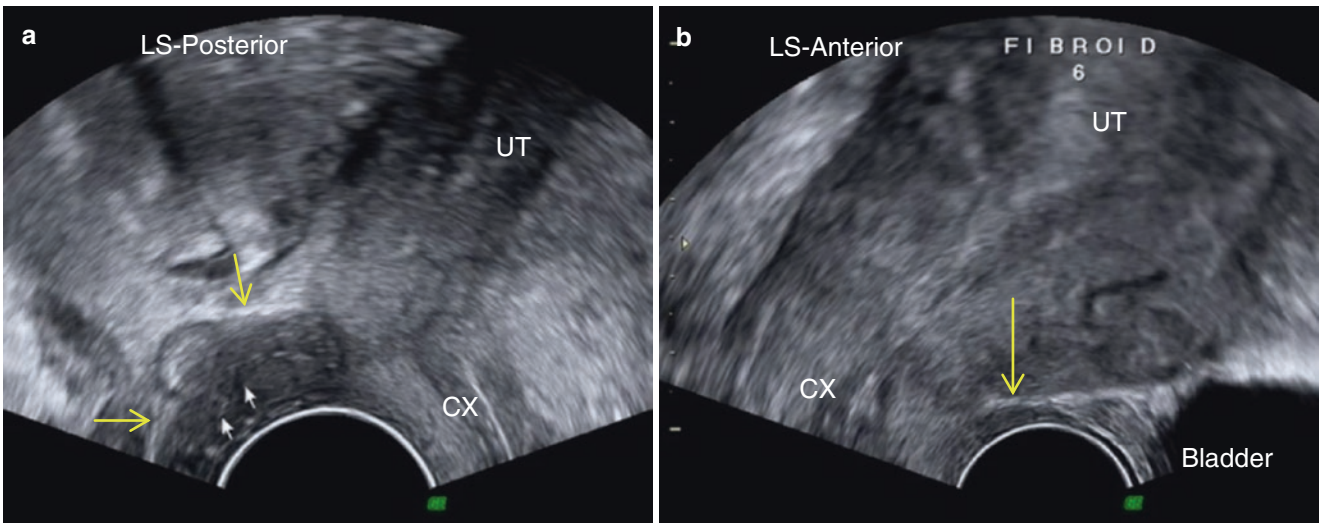

Fig. 8.6 Vaginal DIE: (**a**) Longitudinal section of the posterior fornix. The probe in this image is in the posterior fornix with the cervix (CX) lying anteriorly and the posterior vaginal wall with the hypoechoic DIE nodule posteriorly (*small arrows*). (**b**) Longitudinal section of the anterior fornix (in this image the probe is in the anterior fornix), showing normal anterior vaginal walls (*long arrow*)

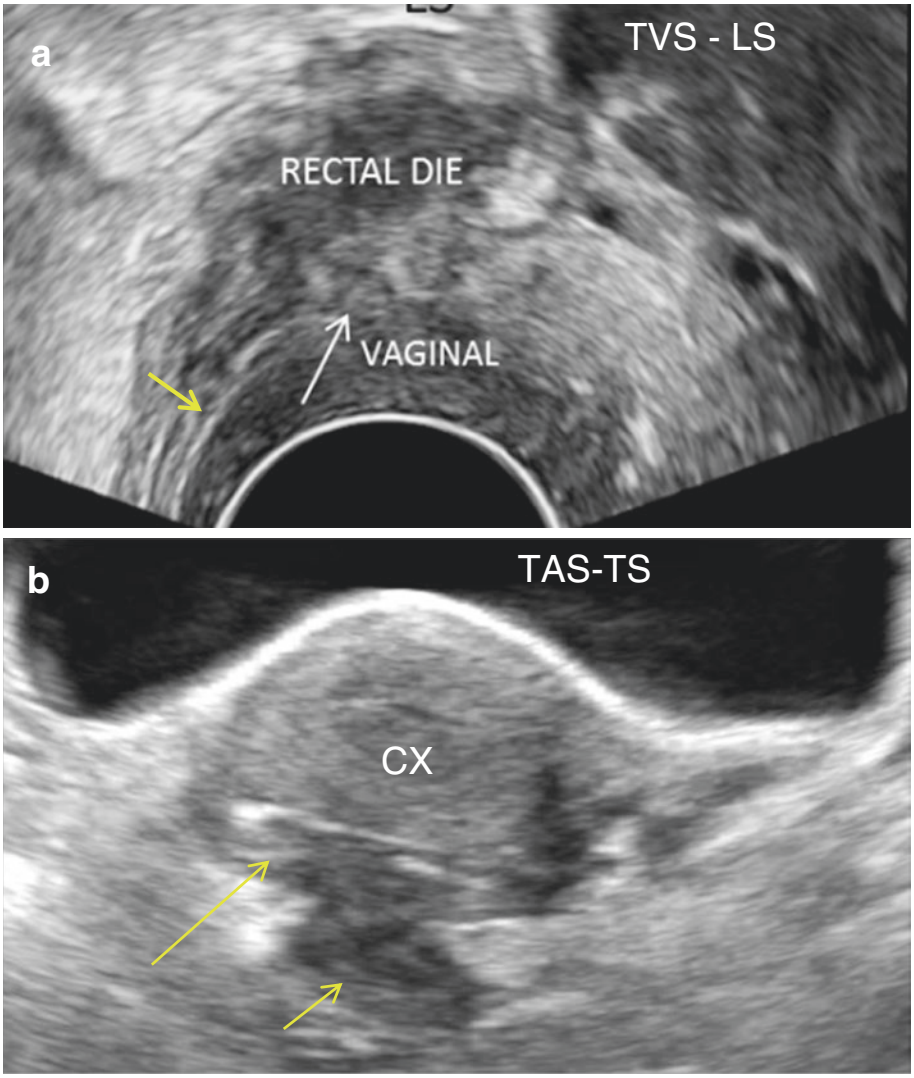

Fig. 8.7 Rectovaginal DIE: (**a**) Longitudinal section of posterior fornix showing a hypoechoic, thickened DIE lesion of the vagina and rectum. The normal rectovaginal septum between the normal rectum and vagina is seen as a hyperechoic line (*short arrow*). There is a breach in the upper part of the RV septum (*long arrow*) where the rectal DIE and the vaginal DIEs are continuous. (**b**) The rectovaginal DIE was also seen on TAS. The image shows a TS of the cervix (*CX*), thickened vaginal wall with the DIE lesion (*long arrow*) and the rectal DIE (*short arrow*). The two DIE lesions with their communication form an 'hourglass' lesion

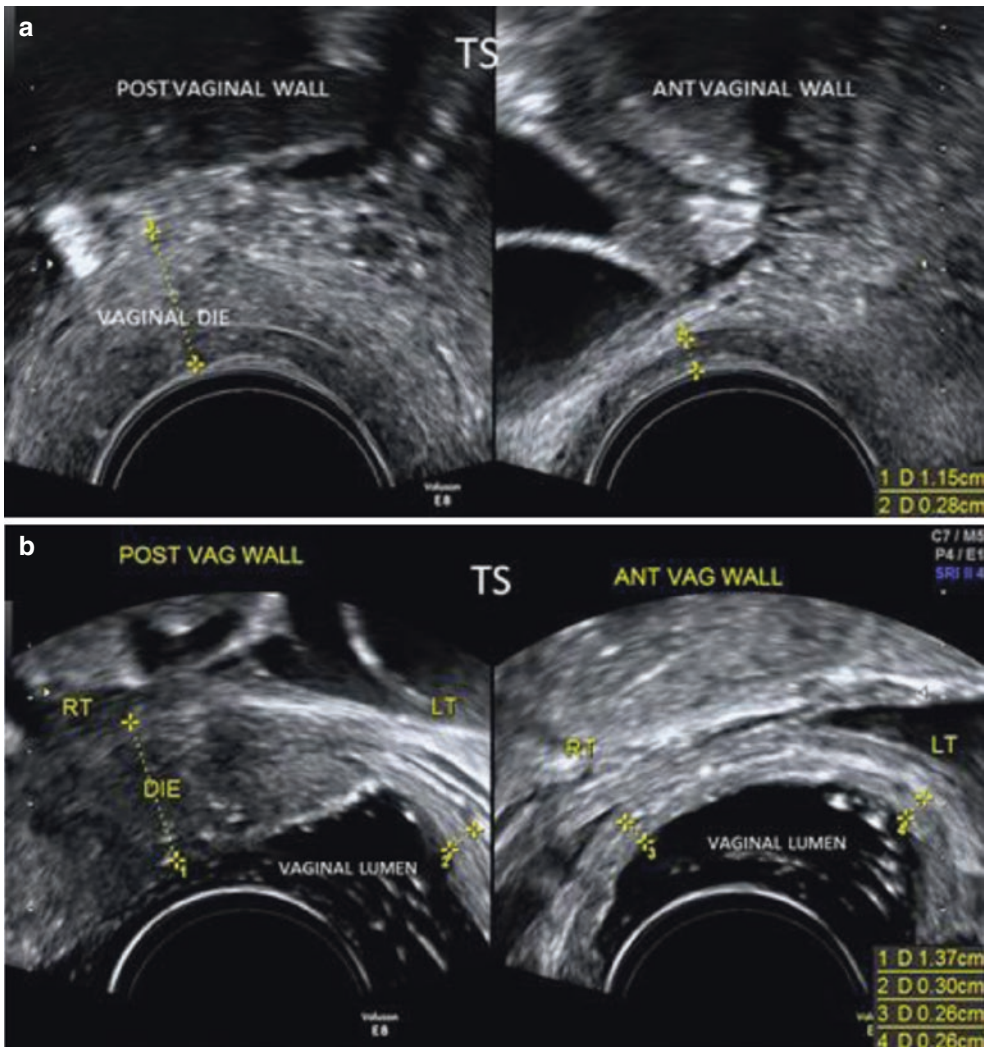

Fig. 8.8 Vaginal DIE. (**a**) Regular TVS showing the transverse section of the posterior and the anterior vaginal walls. Posterior vaginal wall is thickened on the right side. (**b**) GSV showing the same area as above. However, because of the separation of the vaginal walls by vaginal gel, the lesion is better delineated and the normal vagina anteriorly and on the left side posteriorly is well seen

8.1.3 Cervical DIE

This is a rare condition that is most often associated with DIE of the adjacent vagina, rectovagina or uterosacral ligament. Women with cervical DIE may be asymptomatic or give a history of dysmenorrhoea and dyspareunia. These women are sometimes referred to the sonologist for evaluation of a firm nodular cervical or forniceal mass felt at a bimanual clinical examination.

Ultrasound Features of Cervical DIE (Fig. 8.9)

- Cervical wall in that area is thick and firm.
- It may show cystic spaces.
- Margins are ill defined.
- Acoustic shadowing may be noted
- Mass is usually tender to touch.
- It shows poor vascularity.

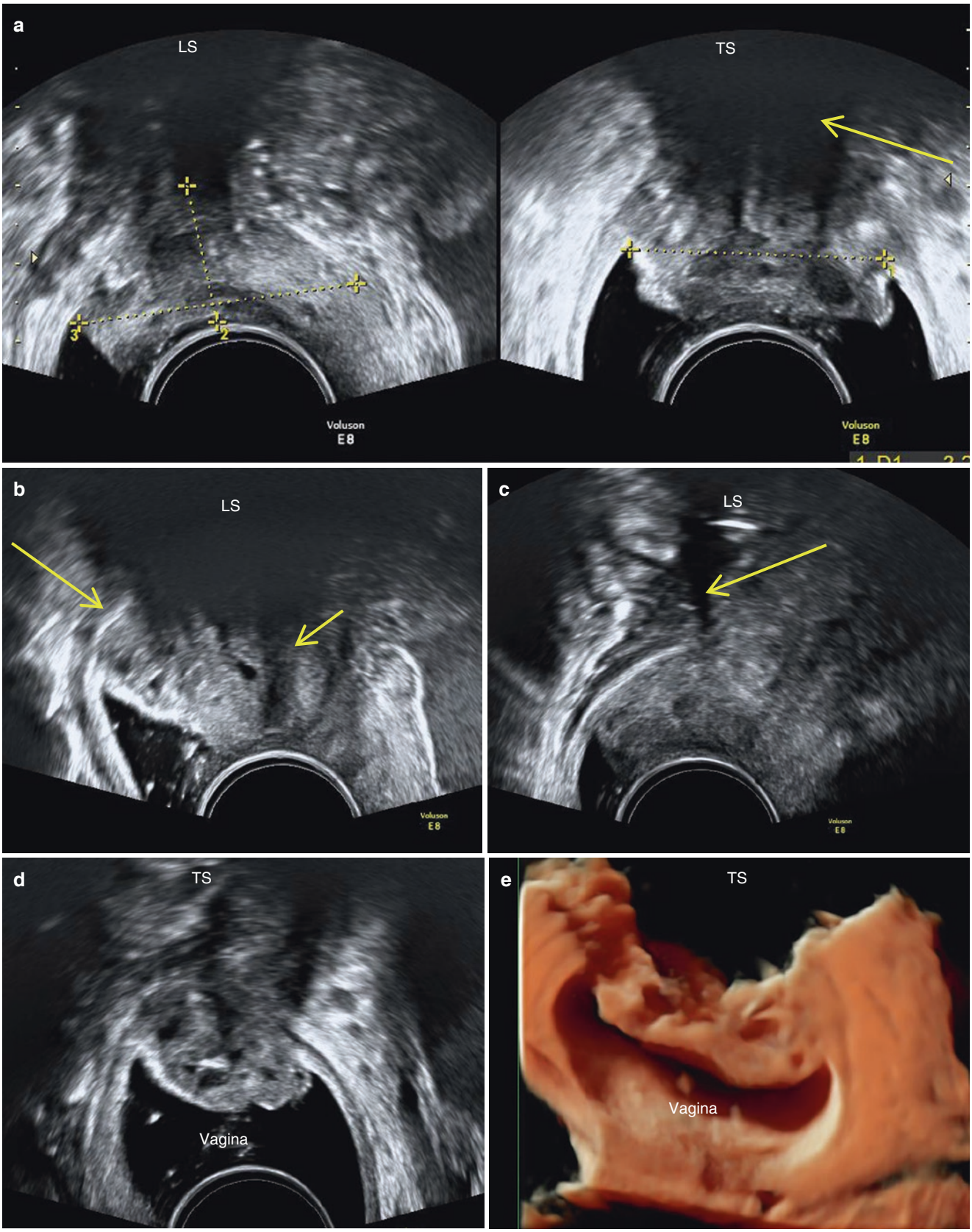

Fig. 8.9 Cervical DIE. (**a**) A thickened, complex lesion of the cervix is seen, which is measured on *LS* and *TS*. The lesion shows irregular margins, heterogeneous echotexture with a few cystic spaces, and acoustic shadowing (*arrow*). (**b**) Longitudinal section of the *upper vagina* and cervix showing the cervical canal (*short arrow*) and thickened heterogeneous posterior wall of the cervix, continuous with a similarly thickened vagina due to vaginal DIE (*long arrow*). (**c**) *LS* of the posterior compartment showing rectal DIE (*arrow*) which was continuous with the cervical and vaginal DIE forming a contiguous DIE nodule involving the cervix, vagina and rectum. (**d**) Transverse section of the distal, posterior lip of the cervix affected by DIE showing cystic spaces and irregular margins. (**e**) 3D rendered image of the same – corresponding to image (**d**)

8.1.4 Uterosacral DIE (Figs. 8.10 and 8.11)

The uterosacral ligaments may also be involved with deep infiltrating endometriosis. Uterosacral DIE is difficult to diagnose, because the uterosacrals are not anatomic structures that we generally can identify on a routine ultrasound, In addition, uterosacral DIE in isolation is usually small. They are seen posterolateral to the cervix, and a comparison with the opposite side provides a convenient control.

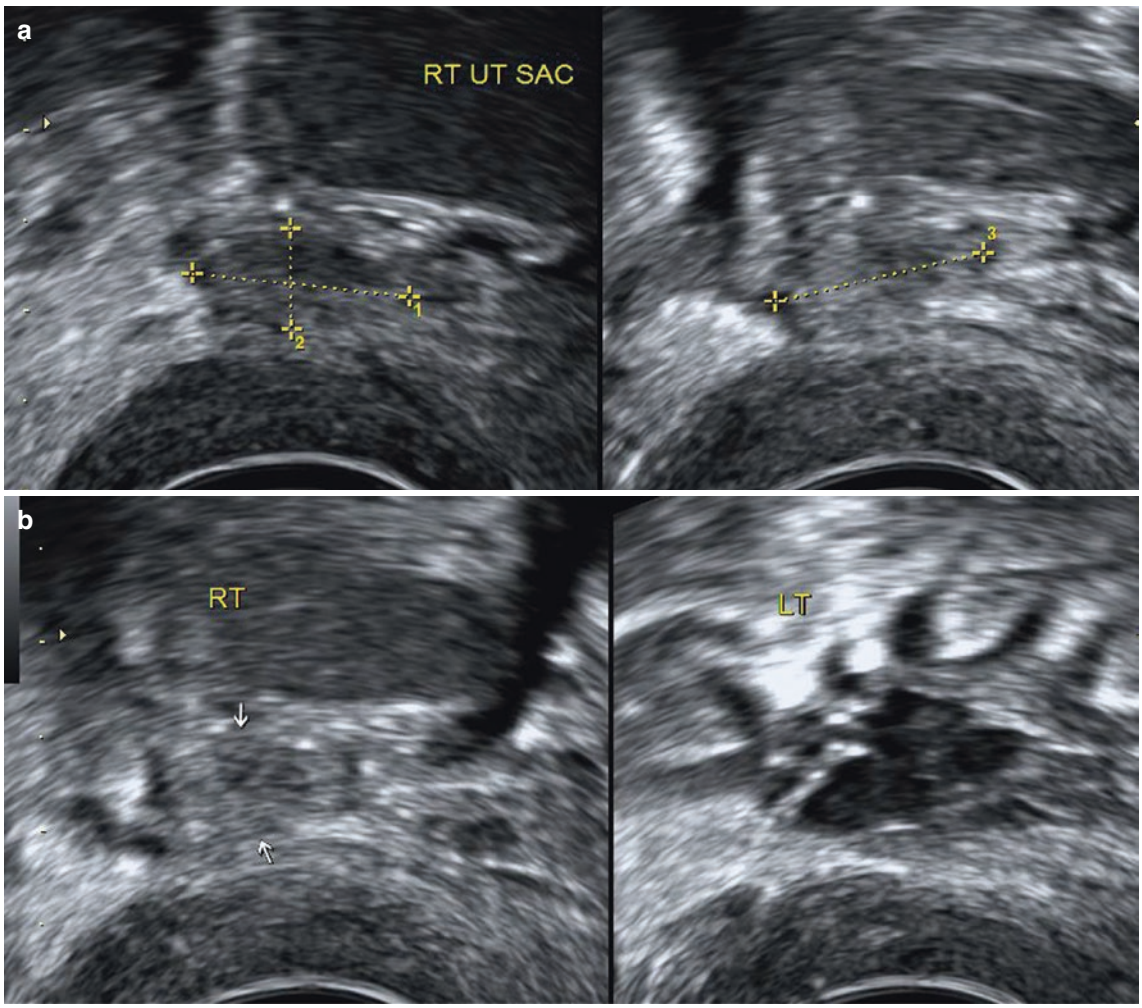

Fig. 8.10 Uterosacral DIE in a patient with right-sided rectovaginal DIE. (**a**) The lesion is seen as an oval, hypoechoic, diffuse, small mass (measured in the image). (**b**) Comparison with the contralateral side helps in making a diagnosis

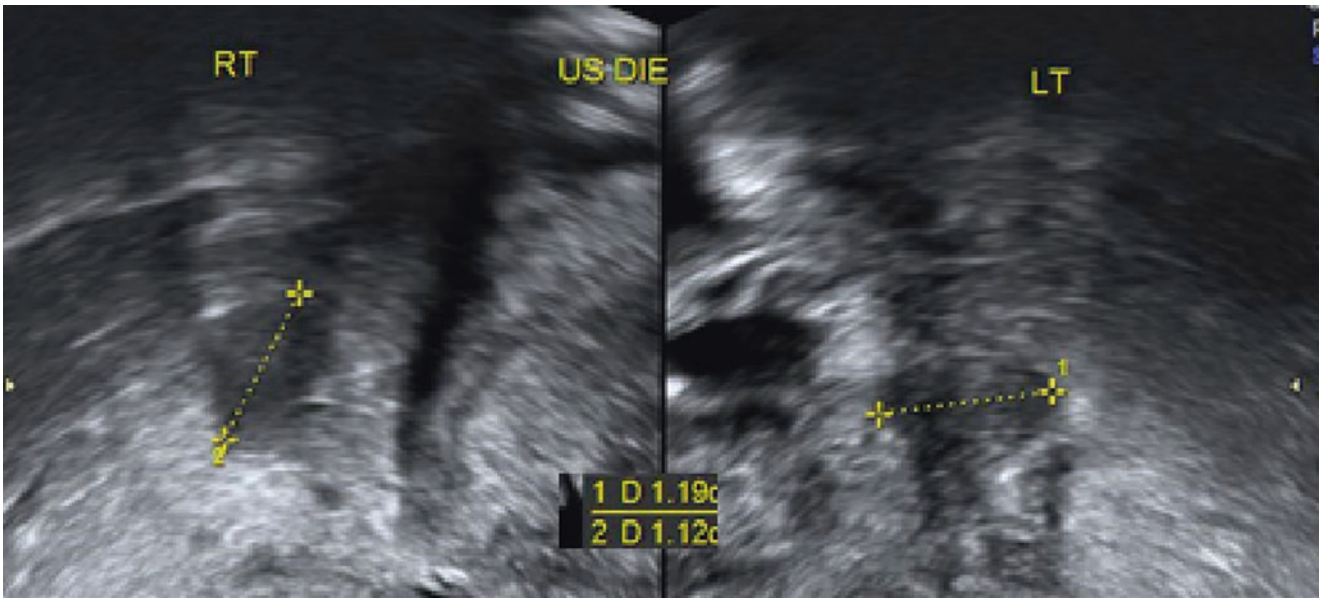

Fig. 8.11 Bilateral uterosacral DIE seen as small oval hypoechoic diffuse masses

8.1.5 Bladder DIE

The bladder wall (generally the dome or the base of the bladder) can also get affected by DIE. Bladder DIE is probably underdiagnosed because symptoms are usually non-specific, mimicking recurrent cystitis. They include dysuria, urgency, frequency, suprapubic pain, vesical tenesmus, incontinence and haematuria. Bladder DIE lesions seem to originate from adenomyosis of the anterior abdominal wall and may be continuous with it. In a study by Eisenberg et al. (2015), all 11 cases of bladder DIE showed uterine adenomyosis with the lesion extending directly from the anterior uterine wall in 9 out of the 11 cases.

Ultrasound Features of Bladder DIE (Fig. 8.12)
For ultrasound diagnosis of bladder DIE, it is very important that the bladder is partially filled so as to visualise the bladder wall and mucosa. The lesion can be missed if TVS alone is done with an empty bladder.

- The bladder wall at the site of the lesion is thickened.
- The lesions are diffuse, round or comma-shaped. They are hypoechoic and show low vascularity.
- The lesion may be seen protruding into the lumen of the bladder both on 2D and 3D.
- Most often, the lesions are continuous with the adenomyotic anterior uterine wall, giving it an 'hourglass' appearance.
- The distance of the lesion from the trigone should be assessed because lesions near the trigone are challenging to resect.

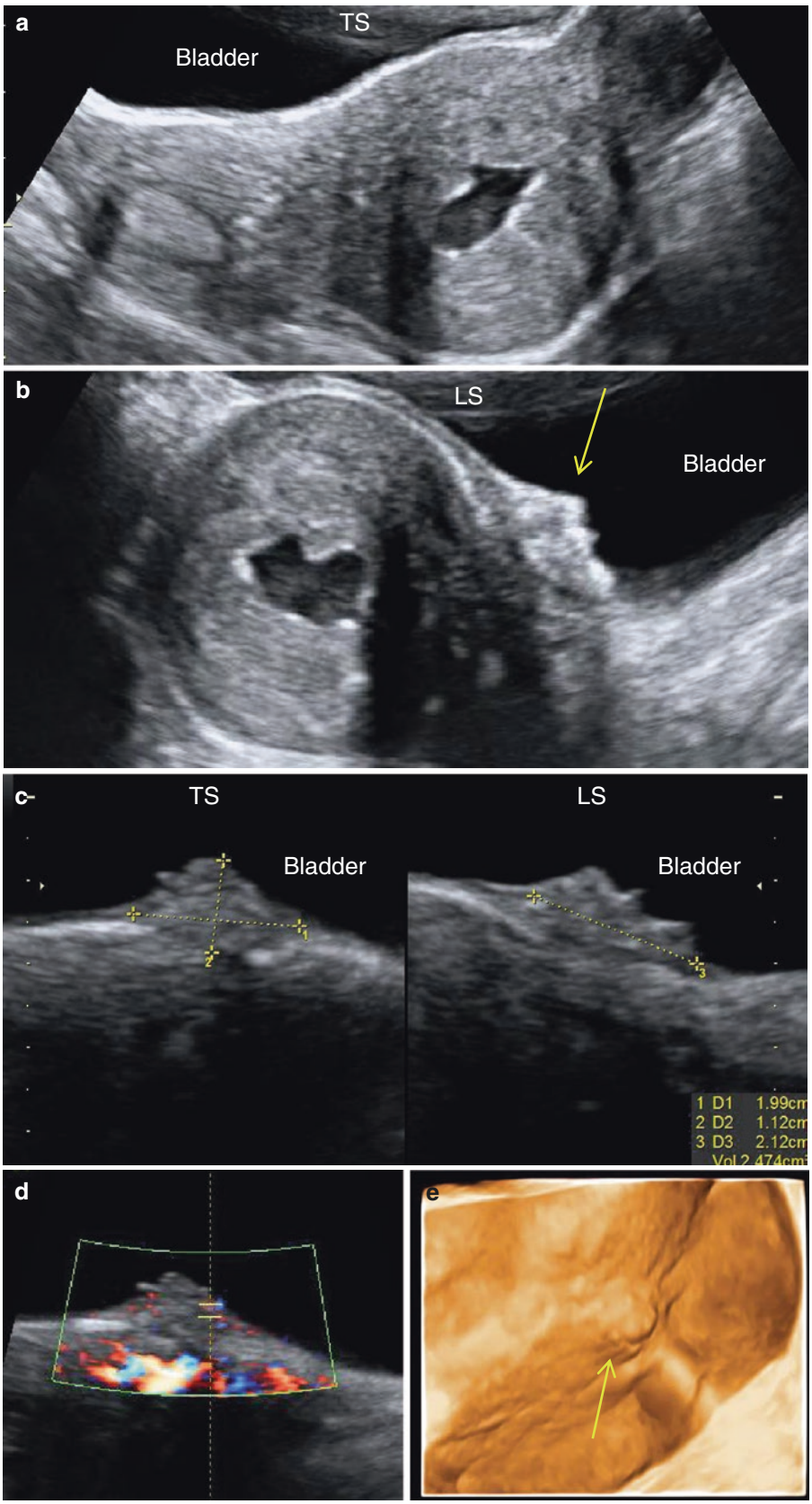

Fig. 8.12 Bladder DIE. (**a**) A unicornuate right-sided uterus with a non-communicating left horn that shows adenomyotic changes and minimal turbid blood in the endometrial cavity. (**b**) LS of the rudimentary horn showing an irregular hyperechoic area (*arrow*) protruding into the bladder. (**c**) TS and LS view showing bladder DIE which is seen as an irregular, hypoechoic mass protruding into the bladder. The bladder DIE lesion is continuous with the adenomyotic anterior wall of the non-communicating horn. (**d**) DIE nodule showing poor vascularity. (**e**) 3D rendered image of the inner wall of the bladder, showing a small irregular protrusion of the DIE nodule (*arrow*) into the bladder

8.1.6 DIE Involving the Ureters (Figs. 8.13 and 8.14)

The ureters may be primarily involved by DIE or be secondarily affected due to fibrotic retraction by an adjoining DIE nodule. The resulting hydroureteronephrosis is often managed by stenting, which is not always a permanent solution.

The ureters can generally be visualised close to the bladder base unilaterally in all and bilaterally in 92.7 % of cases (Pateman et al. 2013). From the long section view of the bladder base and urethra, the probe is angled to one side to visualise the distal ureter and then rotated to a small extent to visualise a better length of the ureter. The ureters are seen as oblique hypoechoic structures entering the bladder base. Another technique is to first locate the entry point of the ureter in the bladder and then to angulate and trace the ureter upwards. The ureter shows peristalsis, and pressure from the TVS probe usually induces peristalsis. The median diameter of the ureter at peristalsis is reported to be 2.9 mm (Pateman et al. 2013). In cases with obstruction, the portion of the ureter above the obstruction will be seen to dilate significantly, and reverse peristalsis may be seen, particularly if the obstruction is significant.

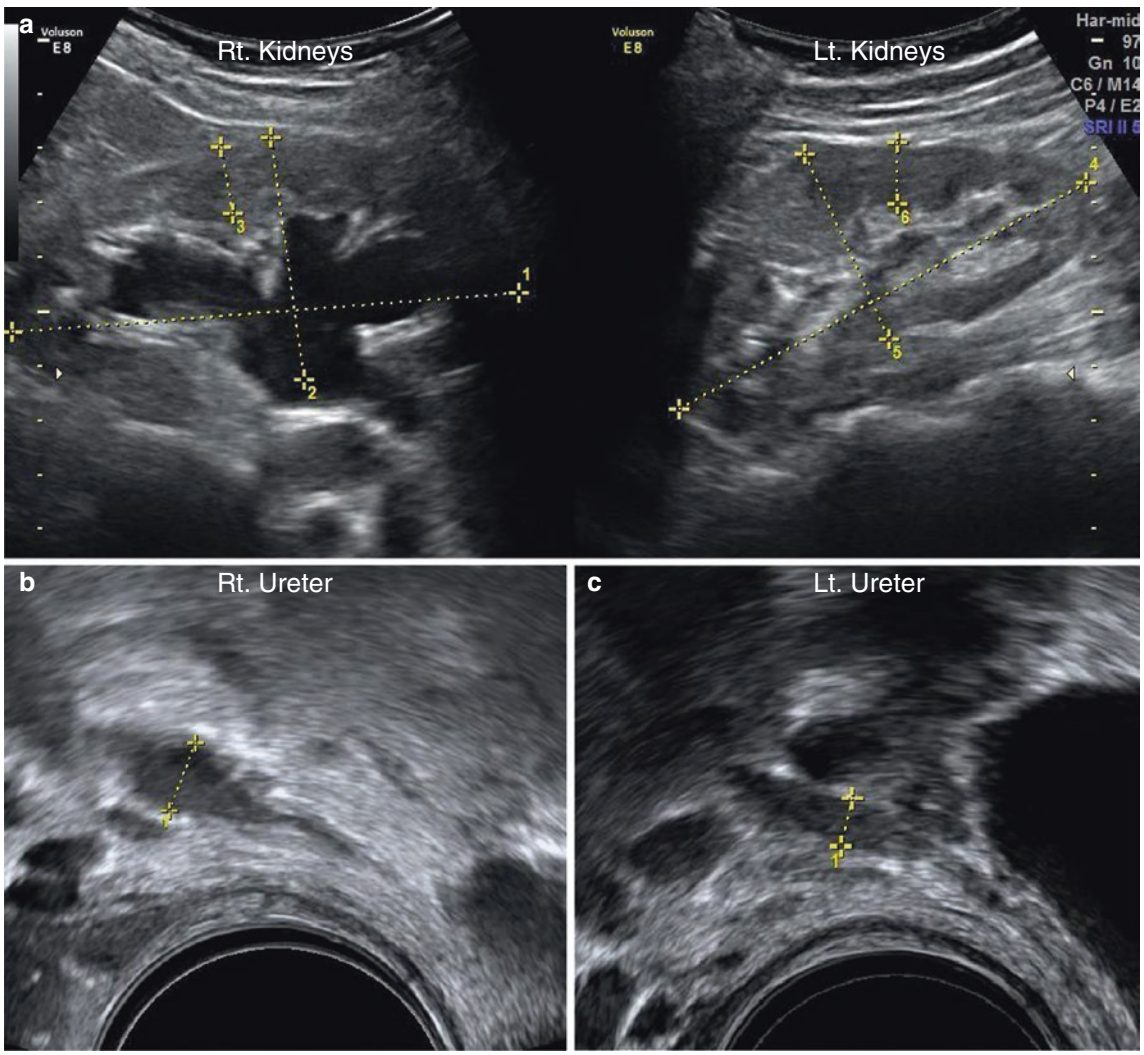

Fig. 8.13 The kidney and ureter in a patient with rectovaginal DIE. (**a**) Shows a right-sided hydronephrosis with a normal left kidney. (**b**, **c**) Right and left ureter showing minimal dilatation on the right side

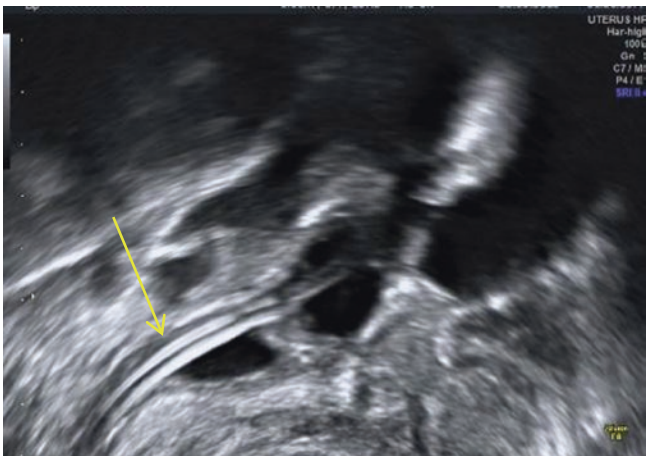

Fig. 8.14 Ureter with a stent (*arrow*) seen in a patient with right-sided hydroureteronephrosis, secondary to DIE

8.1.7 Uterus in Cases with DIE (Figs. 8.15 and 8.16)

In patients with DIE involving the posterior compartment, the uterus is typically retroflexed at the mid corpus with the fundus directed posteriorly, giving the uterus an '*ear*' shaped (also known as '*comma*' shaped or '*question mark*' shaped) appearance. Generally retroflexion of the uterus occurs at the isthmus, but in these cases, with posterior compartment DIE, it occurs higher up at the mid corpus.

Another common feature of the uterus in cases with DIE is *adenomyosis* which usually involves the posterior wall of the uterus, because of the more common posterior compartment endometriosis.

Therefore, if the uterus is 'ear shaped' or there is posterior wall adenomyosis, one must suspect pelvic endometriosis and DIE.

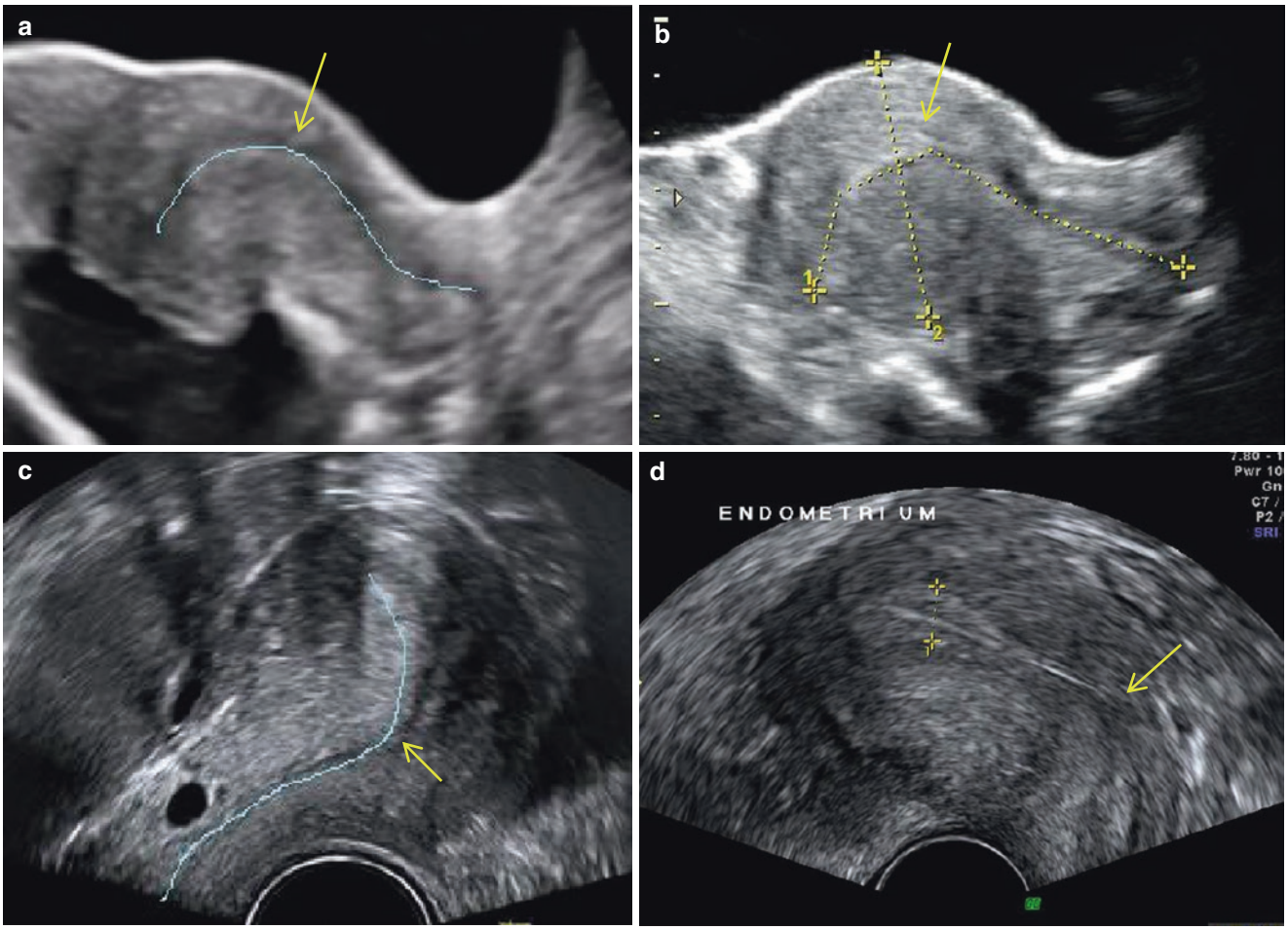

Fig. 8.15 (**a**–**c**) '*Ear' shaped* or '*question mark*' shaped uterus with retroflexion at the midcorpus (*arrows*) on (**a**, **b**) TAS and (**c**) TVS. (**d**) Normal uterus in comparison, where the retroflexion occurs lower down (*arrow*) – at the isthmus (i.e., the junction of the cervix with the uterine body)

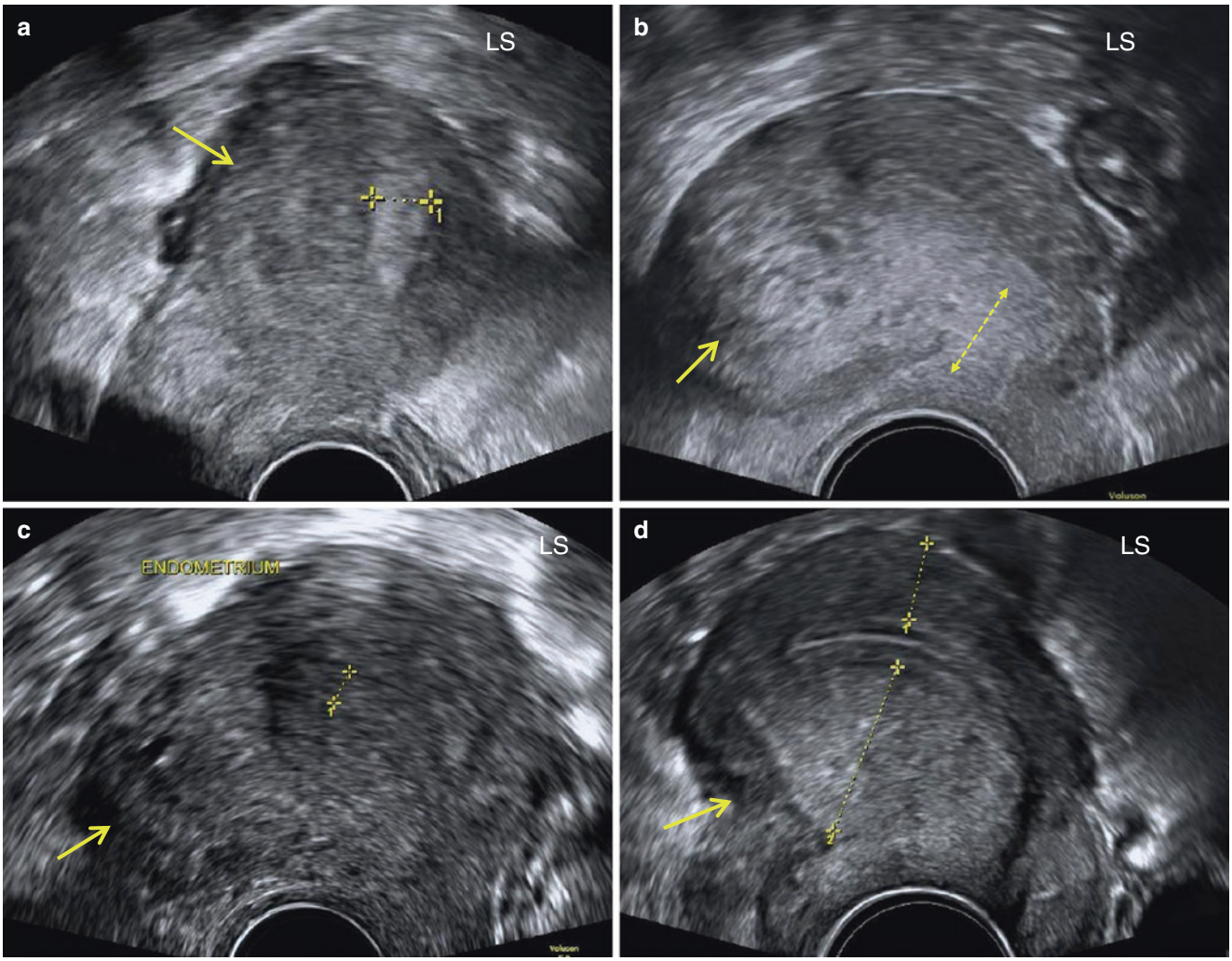

Fig. 8.16 (**a**, **b**, **c**, **d**) Four cases of posterior compartment DIE showing thick and coarse posterior walls (*arrows*) suggestive of adenomyosis

Summary: DIE

- DIE lesions appear as fusiform/nodular, firm, tender, lesions with diffuse borders and poor vascularity. Common sites are the rectosigmoid, uterosacrals, vaginal wall and bladder.
- The lesions are often not diagnosed due to lack of the knowledge of the spectrum of DIE.
- Think DIE in women with chronic pelvic pain, endometriomas, absent sliding sign (bowel adhesions), an ear-shaped uterine body and adenomyosis.
- TVS is the modality of choice and the approach should be pain guided.
- Proper pre-operative evaluation in patients with endometriosis is important (particularly for DIE) for optimal planning of surgery.

8.2 Extra-Pelvic Endometriosis

Though extra-pelvic endometriosis is rare, several cases of endometriosis of the abdominal wall, the lung, the pleura, the diaphragm, the pericardium and the gastrointestinal tract have been reported in literature. Symptoms vary depending on the site of endometrial tissue implantation. The diagnosis of this entity is not easy. Diagnosis is by the presence of endometrial tissue from the site, which is often difficult to locate. The catamenial (related to periods), periodic, cyclical symptoms (or worsening of symptoms) help raise a clinical suspicion of extra-pelvic endometriosis in these patients. Fluid tapped (pleural or ascitic) from such patients will appear haemorrhagic and is negative for malignancy and tuberculosis. Obtaining endometrial glandular tissue in the fluid is unlikely, and, most often, all that is noted on cytology is the presence of haemosiderophages (haemosiderin-laden macrophages). Managing these cases is also more challenging and varies from simple observation to medical or surgical treatment or a combination of these.

8.2.1 Abdominal Wall Endometriosis

Abdominal wall endometriosis is the most common type of the extra-pelvic endometriosis. It is often a consequence of LSCS or laparotomy wherein the uterine cavity was opened. It can, however, be found in the absence of a history of such surgery, and even in the absence of any pelvic endometriosis. Patients may complain of recurrent cyclical pain in the involved area during periods. They may also complain of tenderness or a palpable mass, usually at the site of their abdominal scar. Most often, however, pain is atypical, making diagnosis difficult.

Ultrasound Features of Abdominal Wall Endometriosis (Figs. 8.17, 8.18 and 8.19)

- The lesions are seen in the anterior abdominal wall (often close to the site of the abdominal scar).
- They are typically hypoechoic and heterogeneous with fuzzy borders.
- They show poor vascularity.
- They may show some amount of acoustic shadowing.
- The lesion may involve only the subcutaneous tissue or both the subcutaneous and the underline muscle that is extending on to both sides of the rectus sheath.
- The lesion may occasionally be seen extending directly from the anterior wall of the uterus.
- Lesions are firm, and the overlying skin may be discoloured if the lesion is superficial.
- They are usually tender to touch.
- The lesions are better seen with high-frequency linear probes rather than standard curvilinear probes because of the close proximity of these lesions to the abdominal probe.
- Comparison with normal abdominal wall elsewhere, provides a convenient control.

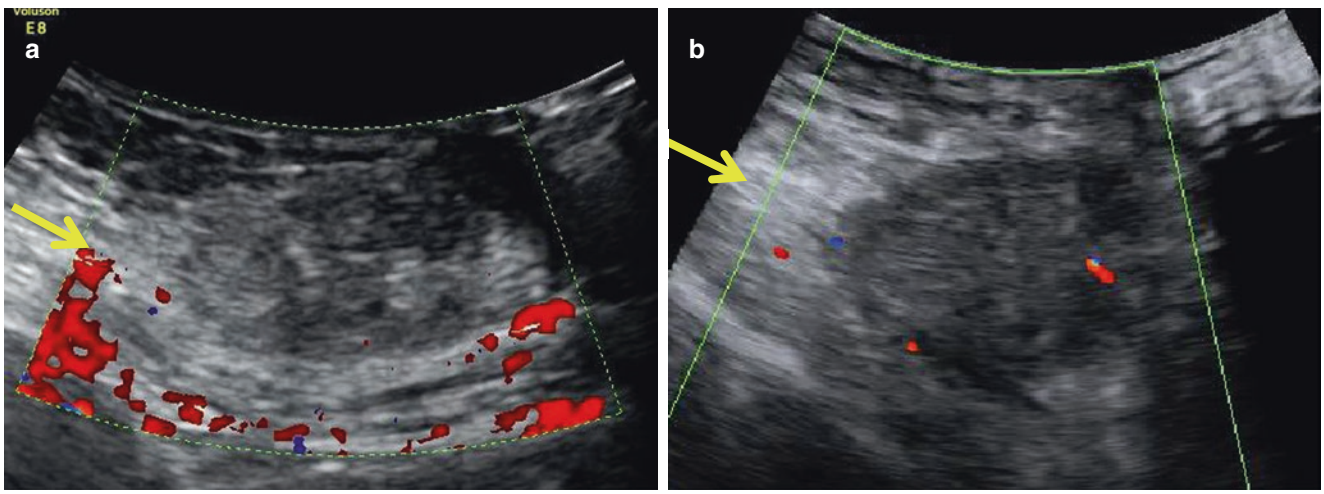

Fig. 8.17 Abdominal wall endometriosis in two different patients showing vaguely circumscribed hypoechoic complex areas with poor vascularity and minimal acoustic shadowing. (**a**) Superficial – in the subcutaneous tissue and (**b**) Deep – extending deeper beyond the rectus sheath (*arrows*)

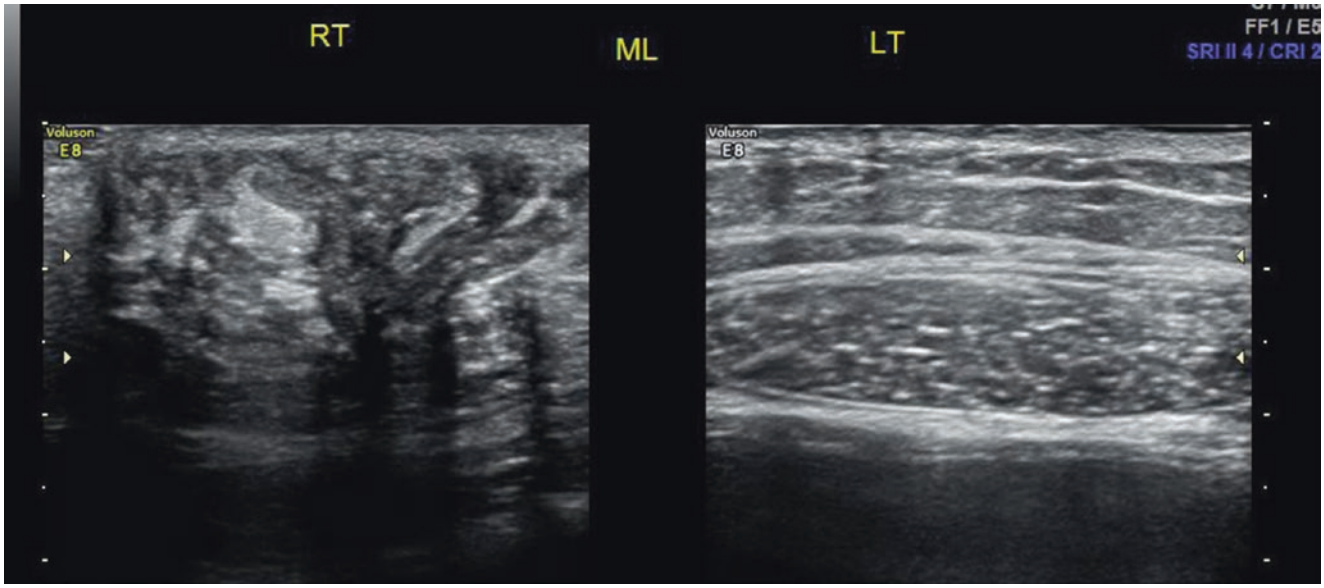

Fig. 8.18 Abdominal wall endometriosis on the right side of the abdomen imaged with a high-frequency linear probe. It is seen as a poorly defined, heterogeneous mass with some acoustic shadowing. Normal abdominal wall tissue is seen on the left side of the same patient, serving as a convenient control

Fig. 8.19 Abdominal wall endometriosis (*arrow*), extending directly from the anterior wall of the uterus

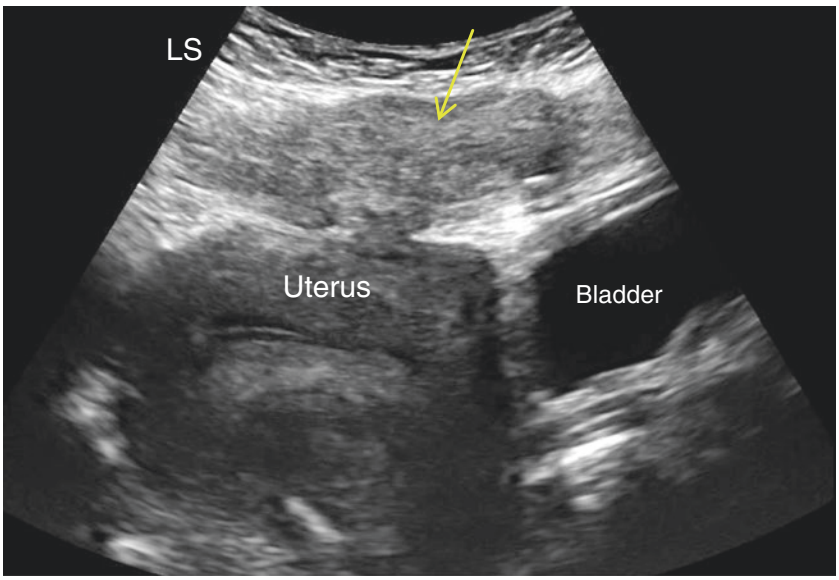

8.2.2 Abdominal and Thoracic Endometriosis (Fig. 8.20)

Thoracic endometriosis usually involves the pleura, the pericardium and rarely the diaphragm. Most often, the patient presents with catamenial (related to periods) pneumothorax, haemothorax, haemoptysis and chest pain. On ultrasound, turbid fluid and adhesions may be noted in the thoracic cavity.

Extra-pelvic endometriosis may also involve the intestines (the most common site being distal ileum and caecum) with patients complaining of nausea, vomiting, loss of appetite, diarrhoea, cramping, abdominal bloating, etc., all getting worse during periods.

Endometriosis can rarely involve the liver, gall bladder and kidney.

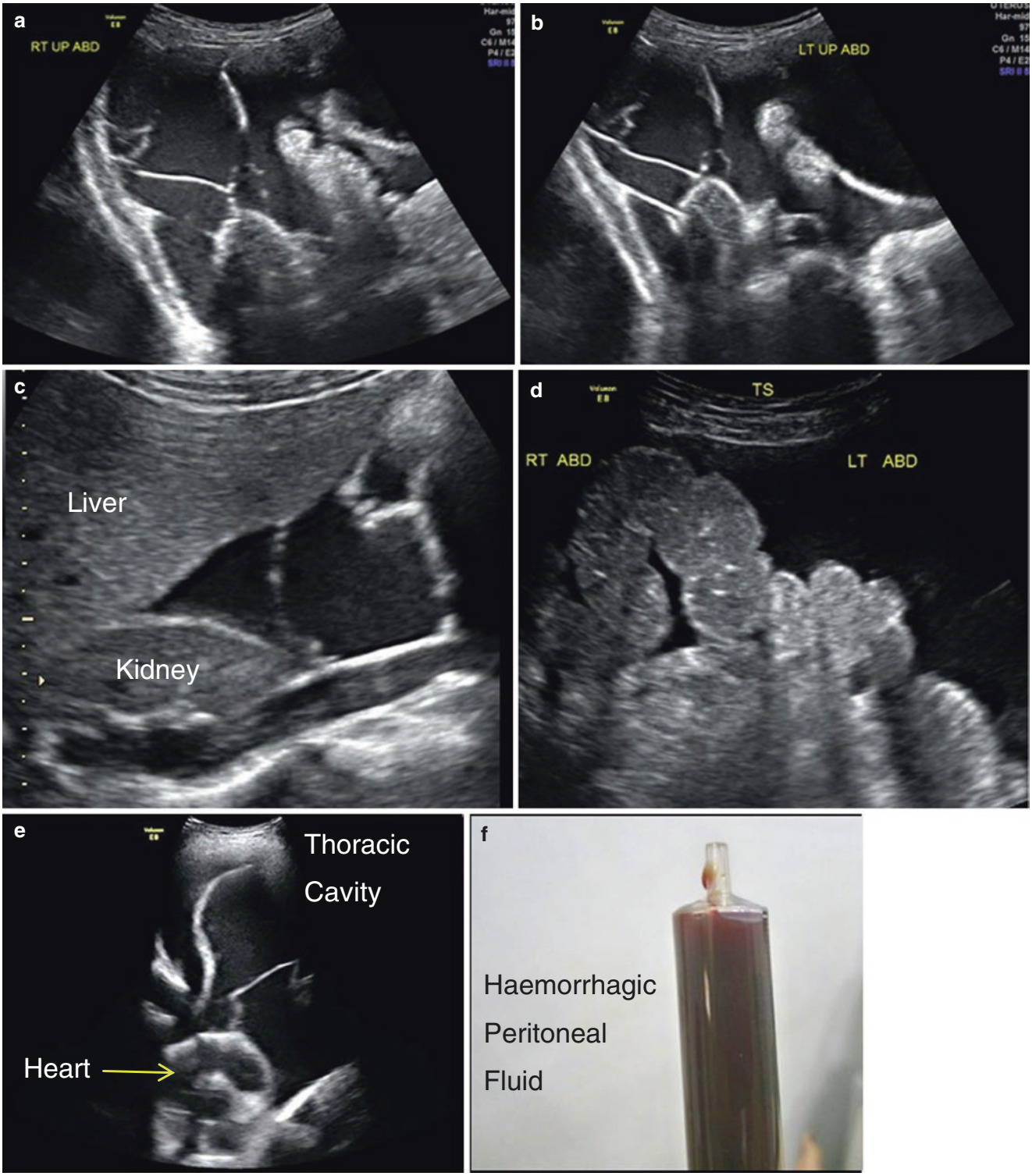

Fig. 8.20 Abdominal and thoracic endometriosis in a 27-year-old lady. She complained of dysmenorrhoea, breathlessness and vomiting during periods. She gave a history of pleural effusion, which had been tapped elsewhere and reported as 'haemorrhagic fluid negative for malignant cells and negative for tuberculosis'. She was referred for a scan because the clinician felt a nodule in the posterior fornix. On scan, it was found she had pelvic endometriosis and DIE. Turbid fluid and adhesions were seen in the general peritoneal cavity. (**a**, **b**) Images showing turbid fluid with multiple adhesions in the right and left upper abdomen. (**c**) Turbid fluid and adhesions seen between the liver and right kidney. (**d**) *TS* of the mid abdomen showing a significant amount of turbid fluid surrounding the bowel loops. (**e**) Thoracic cavity with *arrow* pointing at the heart (which was seen pumping in real time) lying within turbid fluid, with adhesions all around. In the image, one can see only fluid between the rib cage and the heart. (**f**) Sample of the peritoneal fluid that was tapped at our centre, showing haemorrhagic fluid. The fluid was negative for malignant cells and tuberculosis, but haemosiderophages were present

Suggested Reading

Chamié LP et al (2011) Findings of pelvic endometriosis at transvaginal US, MR imaging, and laparoscopy. Radiographics 31(4):E77–E100

Donato D et al (2015) Question mark form of uterus: a simple sonographic sign associated with the presence of adenomyosis. Ultrasound Obstet Gynecol 46:126–127. doi:10.1002/uog.14750

Eisenberg VH et al (2015) OP15.06 Bladder detrusor endometriosis: where does it come from? Ultrasound Obstet Gynecol 46:98. doi:10.1002/uog.15242

Guerriero S et al (2011) Ultrasonography in deep endometriosis: a consensus opinion from the International Deep Endometriosis Analysis (IDEA) group. A preliminary statement. Ultrasound Obstet Gynecol 38:265

Guerriero G et al (2016) Systematic approach to sonographic evaluation of the pelvis in women with suspected endometriosis, including terms, definitions and measurements: a consensus opinion from the International Deep Endometriosis Analysis (IDEA) group. Ultrasound Obstet Gynecol. doi:10.1002/uog.15955

Hudelist G et al (2009) Combination of transvaginal sonography and clinical examination for preoperative diagnosis of pelvic endometriosis. Hum Reprod 24(5):1018–1024

Hudelist G et al (2011) Transvaginal sonography vs. clinical examination in the preoperative diagnosis of deep infiltrating endometriosis. Ultrasound Obstet Gynecol 37(4):480–487

Hudelist G et al (2013) Uterine sliding sign: a simple sonographic predictor for presence of deep infiltrating endometriosis of the rectum. Ultrasound Obstet Gynecol 41:692–695

Pateman K et al (2013) Visualization of ureters on standard gynecological transvaginal scan: a feasibility study. Ultrasound Obstet Gynecol 41:696–701

Piketty M et al (2009) Preoperative work-up for patients with deeply infiltrating endometriosis: transvaginal ultrasonography must definitely be the first-line imaging examination. Hum Reprod 24(3):602–607

Reid S et al (2011) Sonovaginography: redefining the concept of a "normal pelvis" on transvaginal ultrasound pre-laparoscopic intervention for suspected endometriosis. AJUM 14(2):21–24

Reid S et al (2014) Office gel sonovaginography for the prediction of posterior deep infiltrating endometriosis: a multicenter prospective observational study. Ultrasound Obstet Gynecol 44:710–718

Savelli L et al (2009) Diagnostic accuracy and potential limitations of transvaginal sonography for bladder endometriosis. Ultrasound Obstet Gynecol 34:595–600. doi:10.1002/uog.7356

Vimercati A et al (2012) Accuracy of transvaginal sonography and contrast-enhanced magnetic resonance-colonography for the presurgical staging of deep infiltrating endometriosis. Ultrasound Obstet Gynecol 40(5):592–603. doi:10.1002/uog.11179

Ultrasound Evaluation of Adnexal Pathology

9

9.1 Fallopian Tube

The fallopian tube is anatomically divided into four segments: the proximal interstitial part (which lies within the uterine myometrium), the isthmus (which has thicker walls), the ampulla (which is thin walled) and the infundibulum (which is the distal end of the fallopian tube), ending in the fimbriae. The fallopian tube is lined with ciliated epithelium.

The normal fallopian tube is difficult to visualise on ultrasound unless it is surrounded by fluid, as is often seen following ovulation. The normal fallopian tube appears as an elongated, undulating, isoechoic structure about 8–10 mm wide. Doppler flows can be seen in the normal fallopian tube and pulse Doppler tracing shows a protodiastolic notch (which is not seen in ovarian tissue), which may help in identifying the tube. The tube is generally located lateral to the ovary, between the ovary and the lateral pelvic wall. During ovulation, when free fluid is seen in the POD, fimbriae may be seen floating within the fluid in the POD. The lumen of the fallopian tube is not seen unless it is distended with fluid, and depending on the type of fluid within, possibilities include:

- Hydrosalpinx – with clear (anechoic) fluid in its lumen, which may be the result of chronic infections, tubal ligation or tubal malignancy.
- Pyosalpinx – with pus (turbid fluid) in its lumen seen in acute PID.
- Hematosalpinx – with blood (turbid fluid) in its lumen. This may be seen in cases with tubal ectopic pregnancy, endometriosis, torsion of a hydrosalpinx or associated with hematometra.

A tubal mass when distended with fluid appears sausage shaped and shows incomplete septae, which is because of infolding of its walls, as the tube bends over itself. The incomplete septum, if seen, is specific of a cystic mass of tubal origin.

Tubal pathology includes infection, torsion, ectopic and neoplasia. Infection and neoplasia will be dealt with in this chapter. Ectopic pregnancy and torsion are dealt with in Chaps. 10 and 11, respectively. A tube may be twisted along with the ovary in about 60 % of cases of ovarian torsion. A diseased tube like one with a hydrosalpinx or a tubal ectopic can also undergo torsion independent of the ovary.

9.2 Pelvic Inflammatory Disease (PID)

Pelvic inflammatory disease is the infection and inflammation of the upper female genital tract. It is seen in women belonging to the reproductive age group and is more common in women with multiple sexual partners, women who use intrauterine contraceptive devices, post-abortal or puerperal women and in those who have undergone intrauterine procedures.

Pelvic infection primarily involves the fallopian tubes. However, the ovaries and the endometrium can also be involved. In PID, generally the involvement is bilateral. Infection of the endometrium is dealt with in Chap. 4.

Acute PID Typical symptoms of acute PID are pelvic pain, fever, dyspareunia and vaginal discharge. Clinical examination may reveal tenderness or a pelvic mass.

In PID generally the adnexal involvement is bilateral. Acute PID may resolve or proceed to chronic PID.

The *ultrasound findings* in PID vary based on the severity and the organs involved. They include:

1. *Essentially normal* – with just mild tenderness of adnexa and hazy margins of the ovary (Fig. 9.1).

2. *Tubal or a tubo-ovarian mass* – when the tube is inflamed (*salpingitis*).

Ultrasound Features of a Tubal or Tubo-ovarian Mass (Figs. 9.2, 9.3 and 9.4)

- The tube appears thickened (more than 10 mm in diameter).
- It shows increased vascularity. In acute infection, typically there are several, small vessels that run perpendicular to

M. Sibal, *Ultrasound in Gynecology*, DOI 10.1007/978-981-10-2714-7_9

the long axis of the tube. The flow in these vessels is generally of low RI (>0.45).
- Very often, the tubes and ovaries are adherent to each other forming a tubo-ovarian mass.
- The mass is tender to touch.

3. *Pyosalpinx* – this is nothing but an infected fallopian tube with pus in its lumen, typical of acute PID.

Ultrasound Features of a Pyosalpinx (Figs. 9.5, 9.6, 9.7, 9.8, 9.9, 9.10 and 9.11**)**

- A pyosalpinx appears as a fluid-filled tubular, somewhat folded or undulated mass. At times, the pyosalpinx may appear like a typical tubal mass showing an incomplete septum.
- It shows thick echogenic walls. A wall thickness of 5 mm or more implies acute PID.
- The walls show increased vascularity. Flow indices typically show low resistance (RI >0.45), but very often it is not so. In addition, variable values may be obtained in a given case.
- The lumen of the tube contains fluid showing low-grade internal echoes suggestive of turbid fluid (pus).
- On cross section, the pyosalpinx shows a relatively anechoic or hypoechoic central lumen with thick walls and mucosal folds – the so-called 'cogwheel sign' (because of its resemblance with a cogwheel). The cogwheel sign is pathognomonic of acute infection of the fallopian tube.
- In acute PID, the pyosalpinx is typically tender to touch.

4. *Tubo-ovarian abscess* – in some cases, pus is seen both in the tube and the ovary, forming a tubo-ovarian abscess.

Ultrasound Features of a Tubo-ovarian Abscess (Figs. 9.12, 9.13, 9.14, 9.15, 9.16, 9.17 and 9.18)

- This could appear as a unilocular or multilocular thick-walled structure.
- High vascularity is noted in its walls. Flow indices typically show low resistance (RI >0.45), but often it is not so.
- The fluid within the cystic spaces is turbid (shows low-grade internal echoes). The relatively hyperechoic areas, seen at times within the hypoechoic purulent contents, usually appear as wavy/linear, stretchy (i.e., lengthen on pressure) bands.
- It may be difficult to distinguish between the tubal and the ovarian components. Generally, the tubal component (pyosalpinx) has cystic spaces communicating with each other, whereas the ovarian component (abscess) has circumscribed collections which occasionally may communicate with the pyosalpinx. At times when there are multiple ovarian purulent collections, the intervening wall may undergo necrosis, and the cystic areas may communicate with each other through the breach in the intervening septum.
- Very often, however, the tube cannot be differentiated from the ovary in a tubo-ovarian abscess.
- The masses are usually very tender.
- These masses are usually adherent to the uterine walls.
- There may be pus seen in the POD and around the masses.

5. *Pus in the POD* (Figs. 9.19 and 9.20) – in acute PID, one may see turbid fluid in the POD suggestive of pus. Since it is not encapsulated, the margins of the collection are irregular and angulated, filling the gaps between the tissue planes. This pus may be drained transvaginally primarily for culture and sensitivity. Draining out large quantities of pus may bring symptomatic relief to the patient.

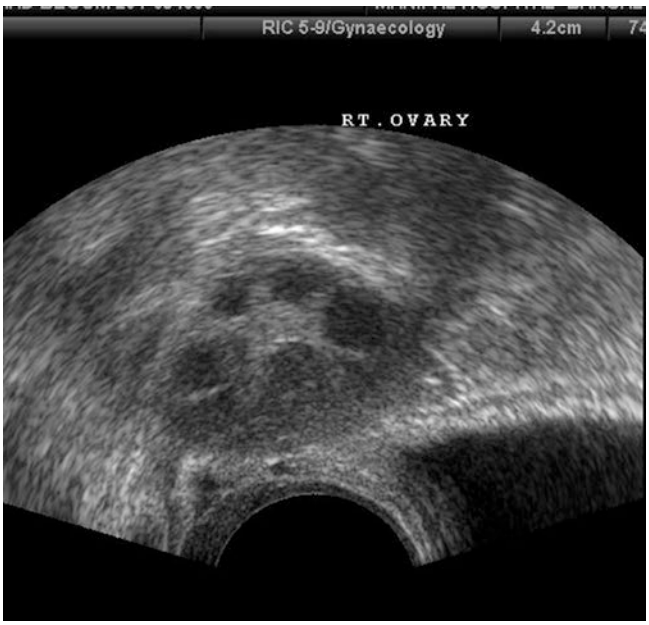

Fig. 9.1 Ovaries showing slightly hazy margins in a patient with PID

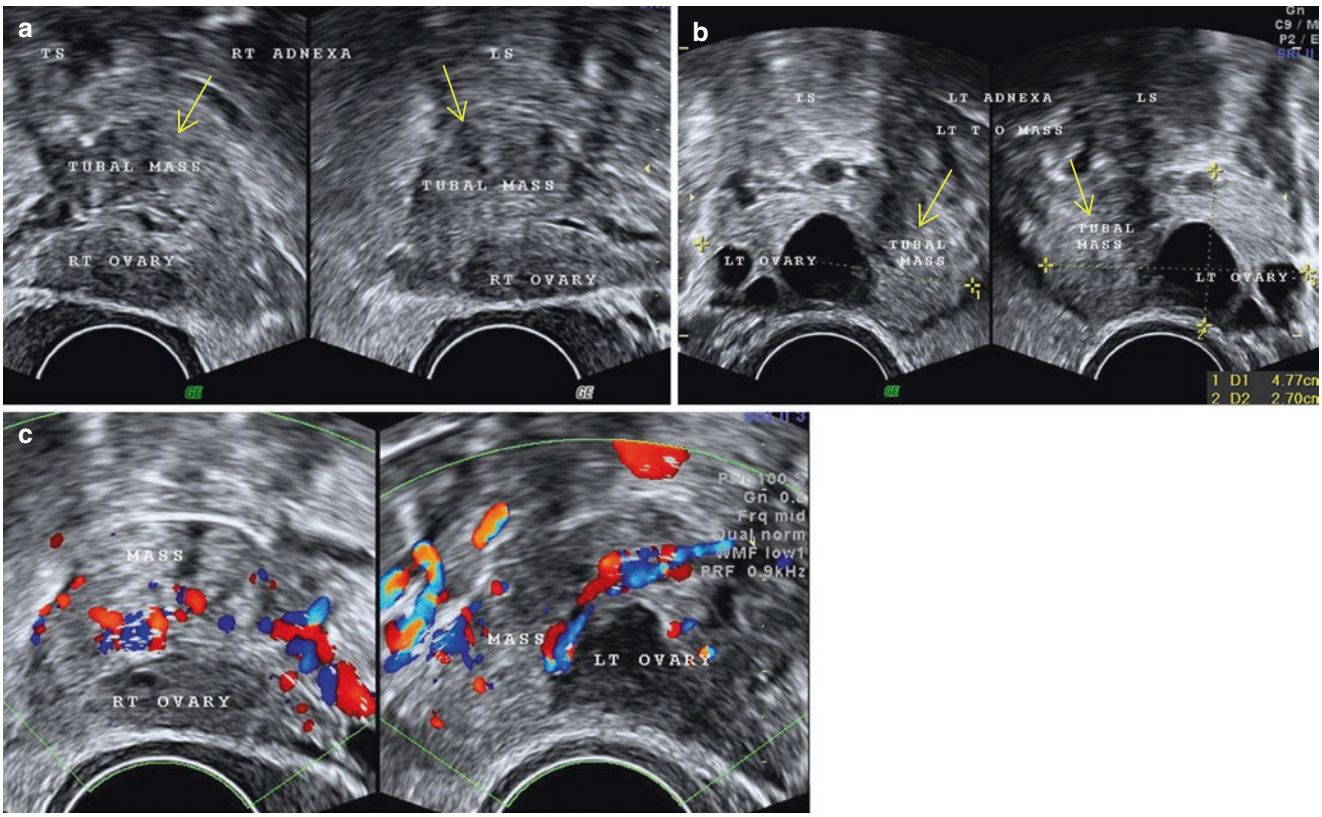

Fig. 9.2 Tubo-ovarian mass. (**a**) Right adnexa shows the right ovary inferiorly and a complex elongated tubal mass (*arrow*) superiorly. (**b**) Left adnexal mass showing the left ovary with follicles and a solid tubal mass (*arrow*) posterolateral to the left ovary. (**c**) Left and right TO masses showing increased vascularity of the tubal components

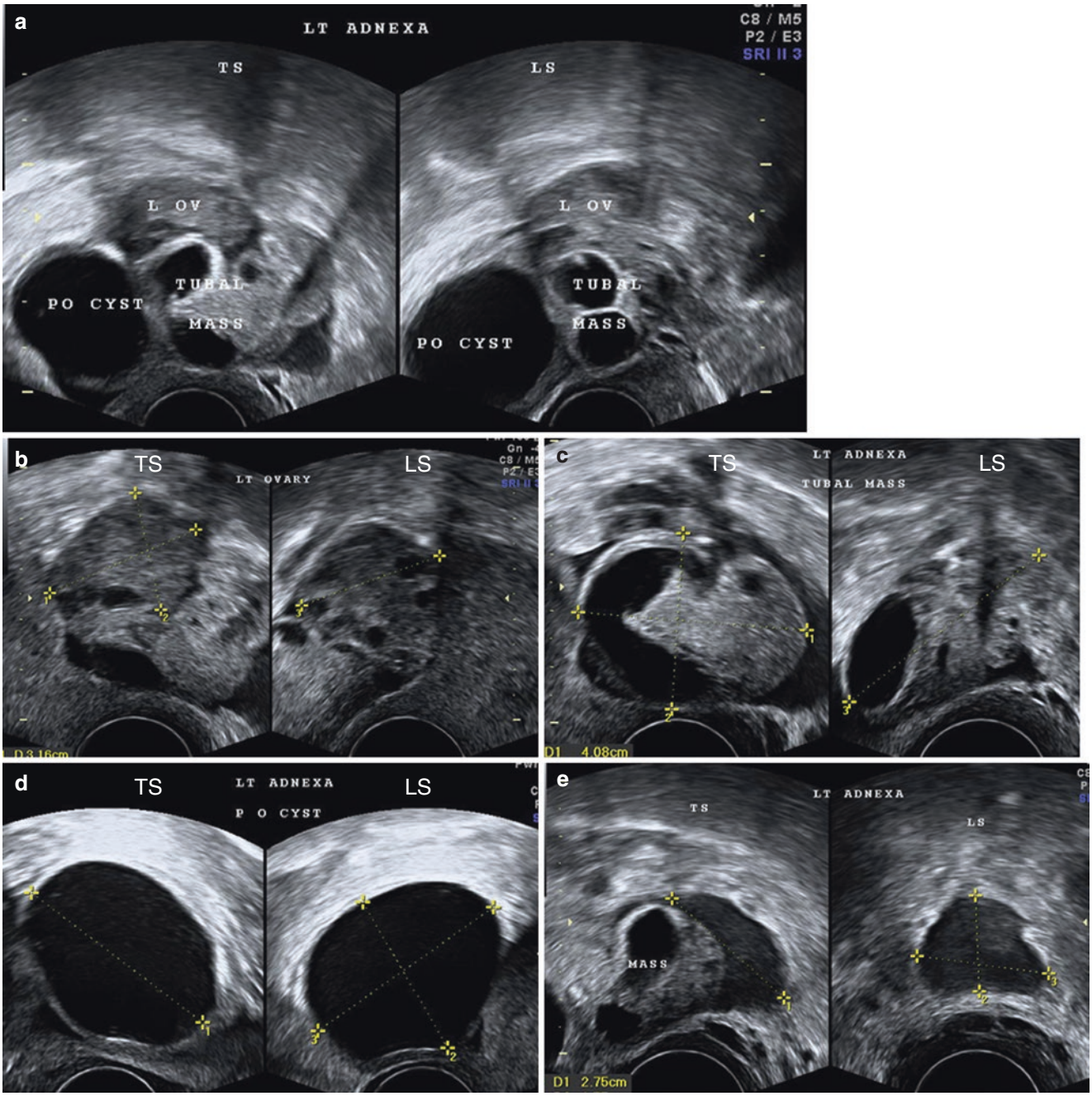

Fig. 9.3 Left adnexal TO mass. (**a**) A complex TO mass with solid and cystic areas. It was composed of different adnexal components. (**b**) Left ovary that formed a part of the mass. (**c**) Left tubal mass with hydrosalpinx formed the second component. (**d**) PO cyst with turbid contents was another component of the TO mass. (**e**) Turbid fluid suggestive of pus surrounding the TO mass. (**f**) Scan following treatment with antibiotics shows a resolution of pathology. The left ovary shows hazy margins and the PO cyst shows fluid–fluid level, with the denser debris in its posterior dependent part. No obvious tubal mass was noted

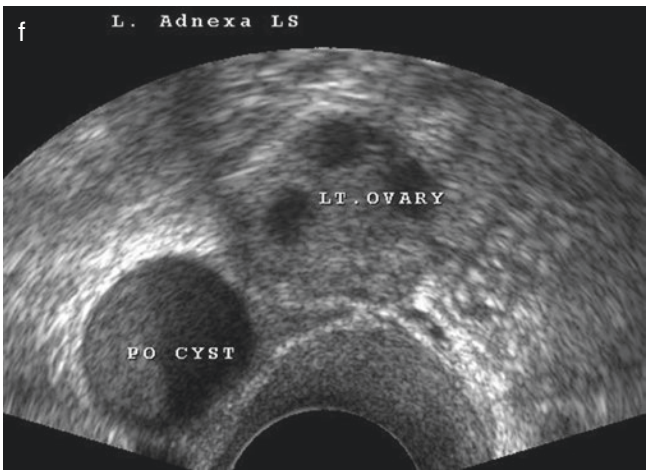

Fig. 9.3 (continued)

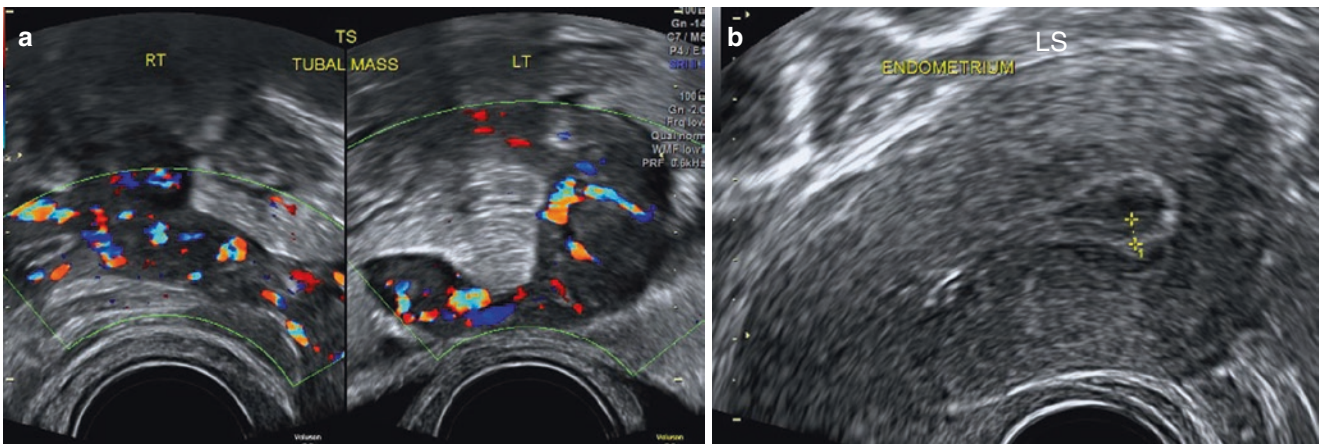

Fig. 9.4 Salpingitis in a patient on treatment for tuberculosis. (**a**) Bilateral hypoechoic elongated masses showing high vascularity suggestive of bilateral inflamed tubal masses. (**b**) Minimal turbid fluid seen in the endometrial cavity suggestive of associated endometritis

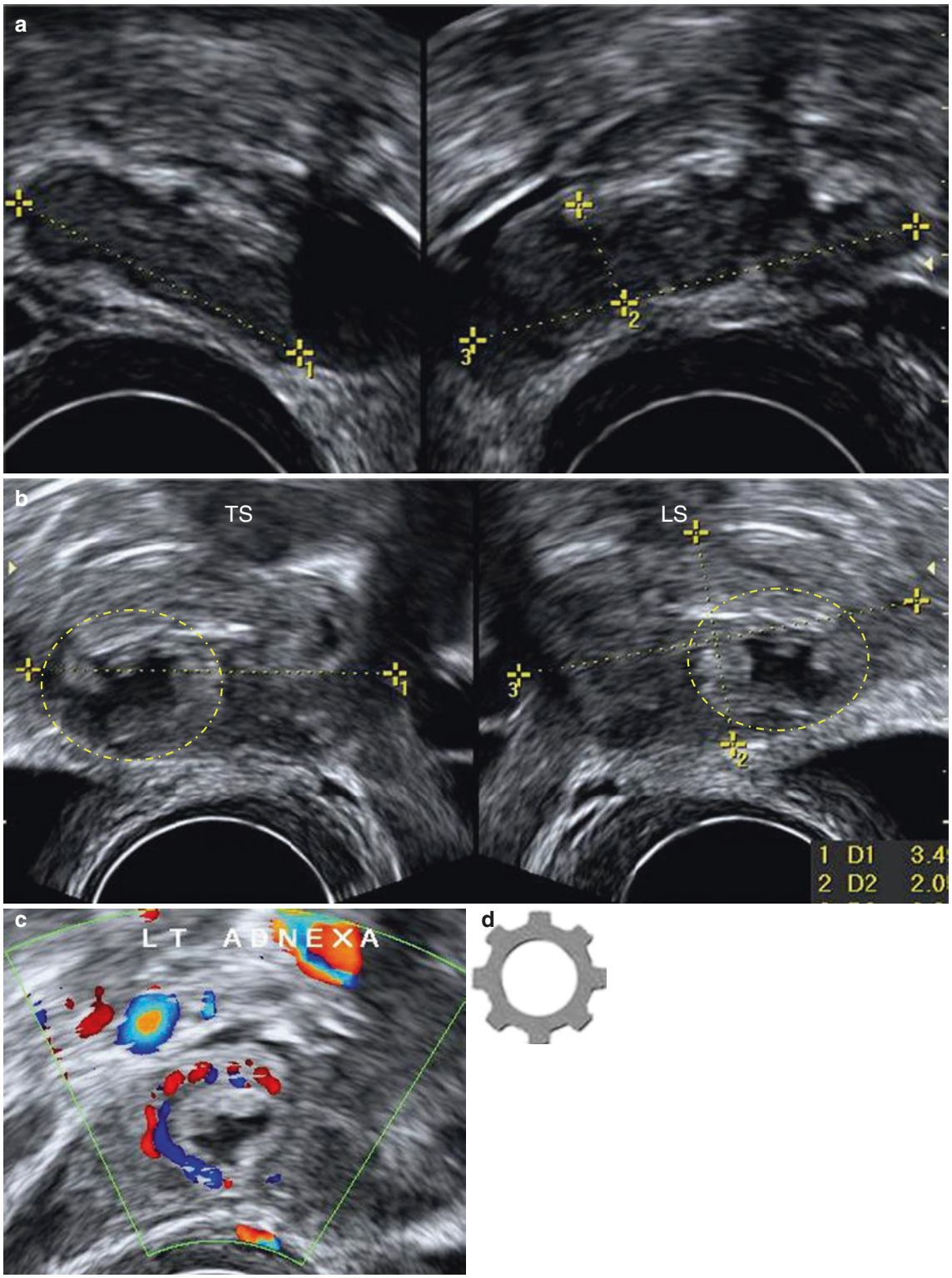

Fig. 9.5 Bilateral pyosalpinx. (**a**) Right fallopian tube with thick turbid contents. (**b**) Complex left adnexal tubal mass showing a cross section of the fallopian tube which shows thick, hyperechoic walls with prominent mucosal folds (cogwheel sign – outlined in image). (**c**) Cross section of the pyosalpinx showing increased flow in its walls. (**d**) Diagrammatic representation of a cogwheel

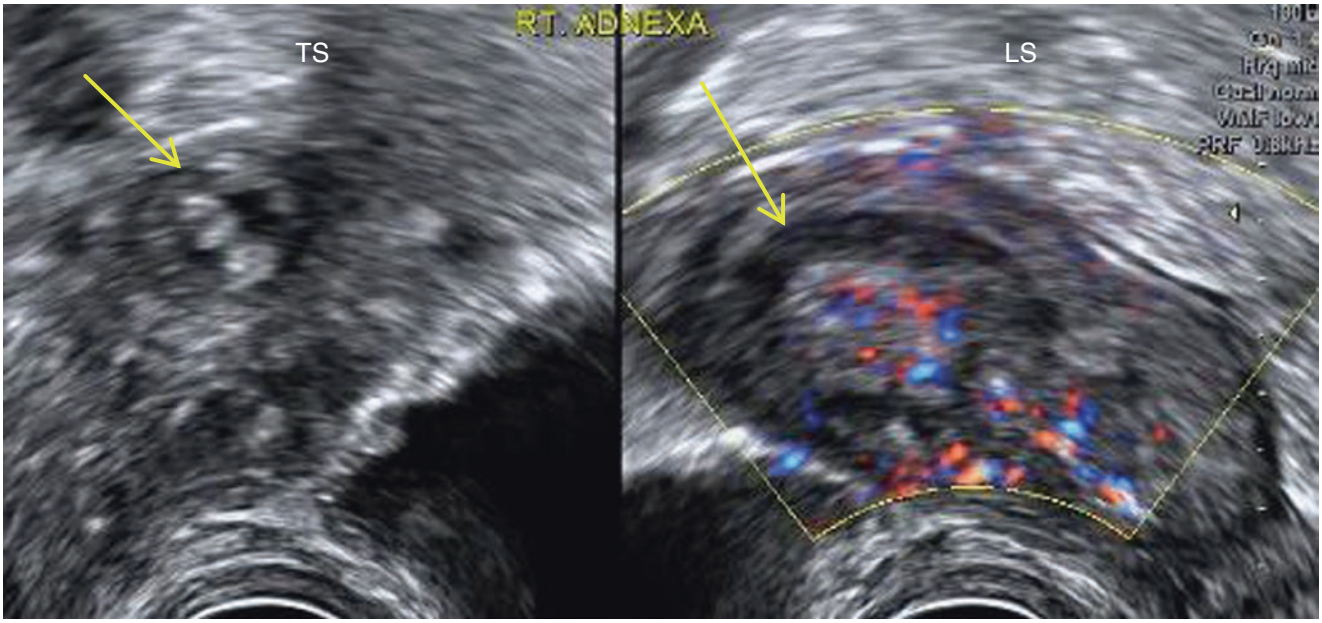

Fig. 9.6 Pyosalpinx – TS of the right adnexa showing a cross section of a pyosalpinx (*arrow*) with hyperechoic, swollen tubal walls and mucosa (cogwheel sign). LS showing thickened tubal walls with turbid fluid in its lumen (*arrow*). Increased vascularity is seen in the tubal walls

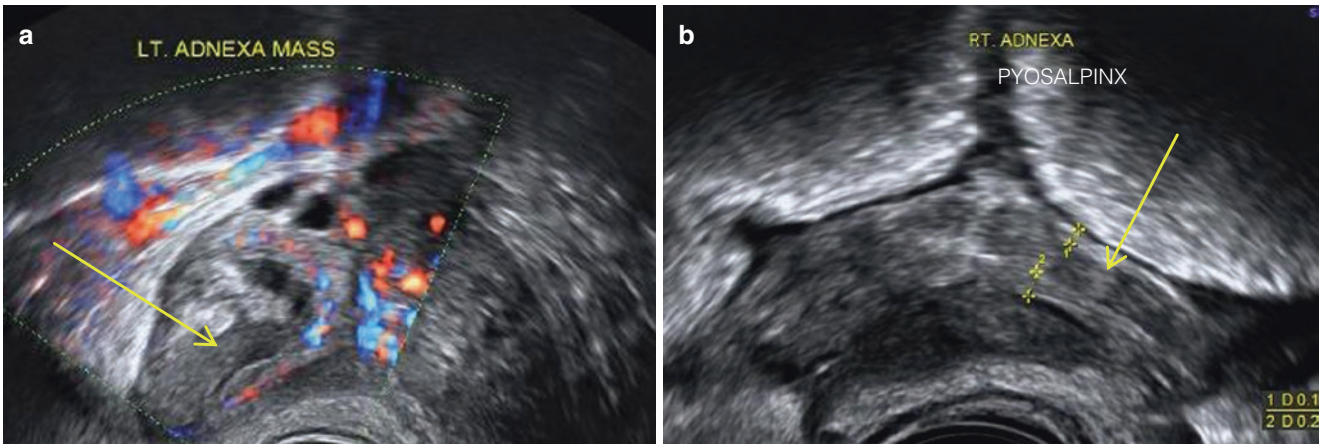

Fig. 9.7 Bilateral pyosalpinx. (**a**) Left pyosalpinx seen as a complex mass with an irregular elongated lumen showing turbid contents (pus) within (*arrow*). The walls of the lumen are thick and show increased vascularity. (**b**) Right pyosalpinx seen as an elongated mass with turbid contents (pus) in its lumen (*arrow*) and thick tubal walls surrounding the lumen

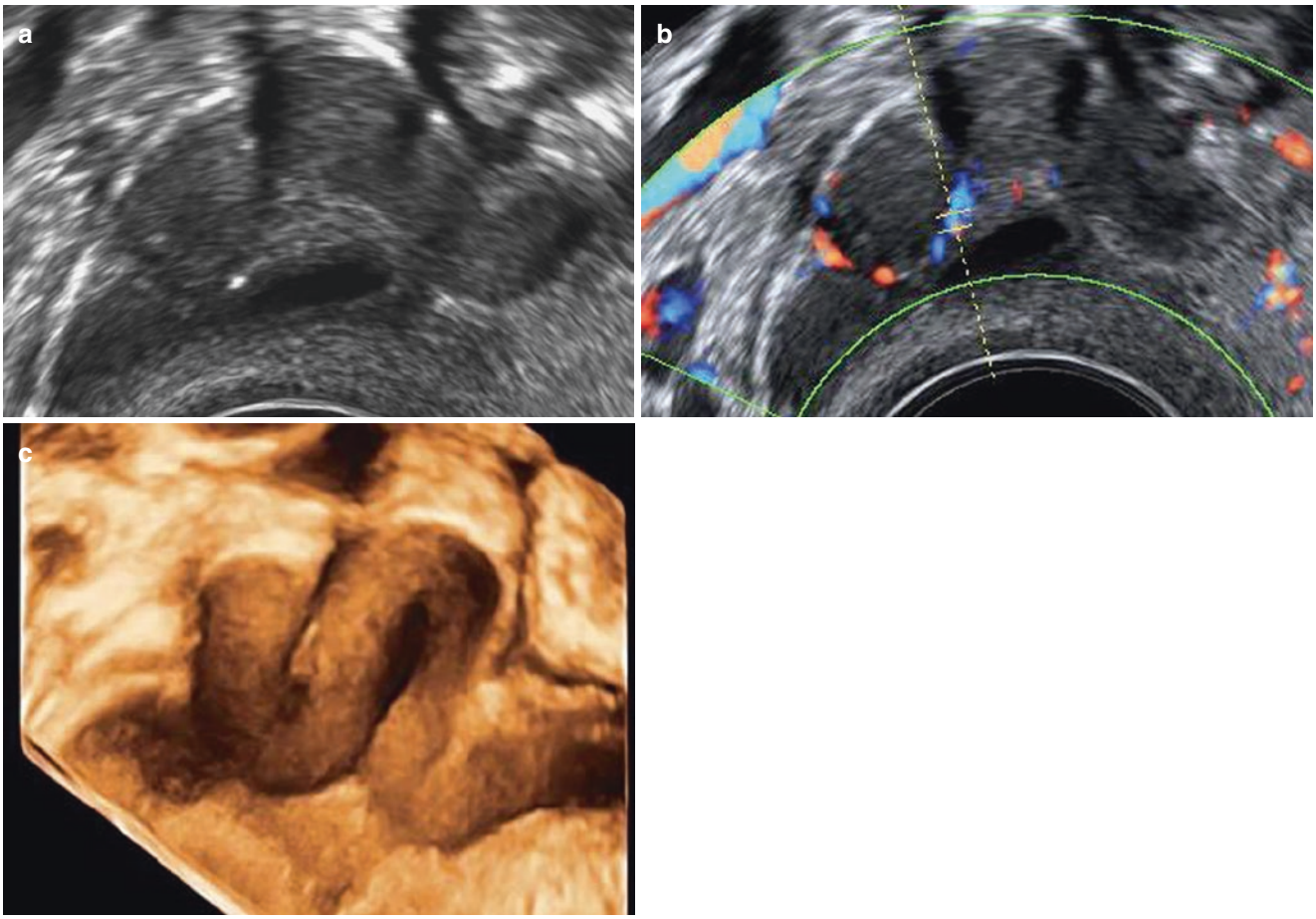

Fig. 9.8 Pyosalpinx. (**a**) Greyscale image showing a tubular undulating mass with dilated tubal lumen, which shows hypoechoic turbid contents suggestive of pus. (**b**) Increased flow in the walls of the pyosalpinx. (**c**) 3D rendered image showing the folded tubal mass with turbid contents within

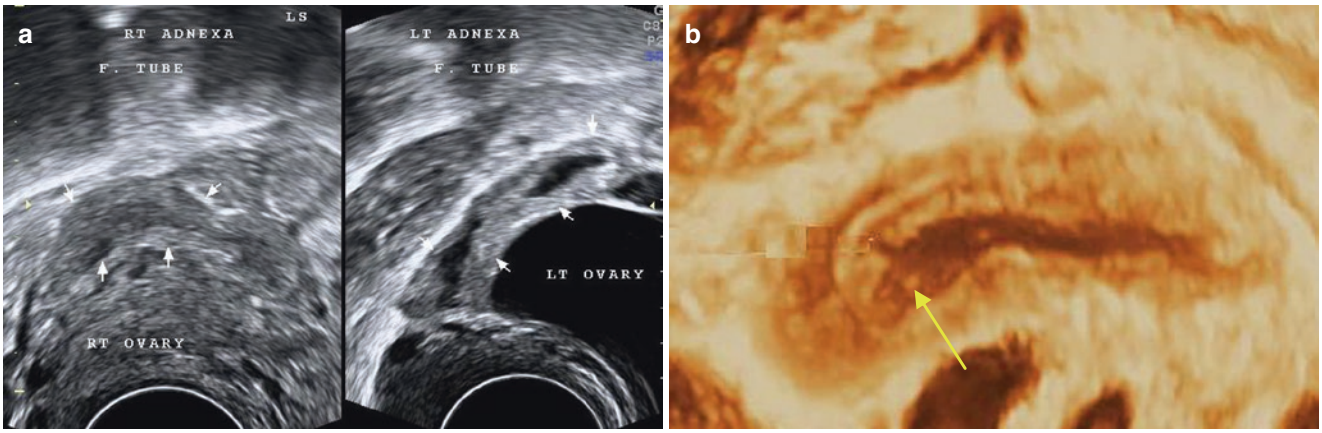

Fig. 9.9 Bilateral pyosalpinx. (**a**) Greyscale image with right tube showing thick walls with pus within. Left adnexal tubal mass showing fluid only in some segments of the tube. (**b**) 3D rendered image showing swollen tubal mucosa and turbid contents, with few scattered debris within its lumen (*arrow*)

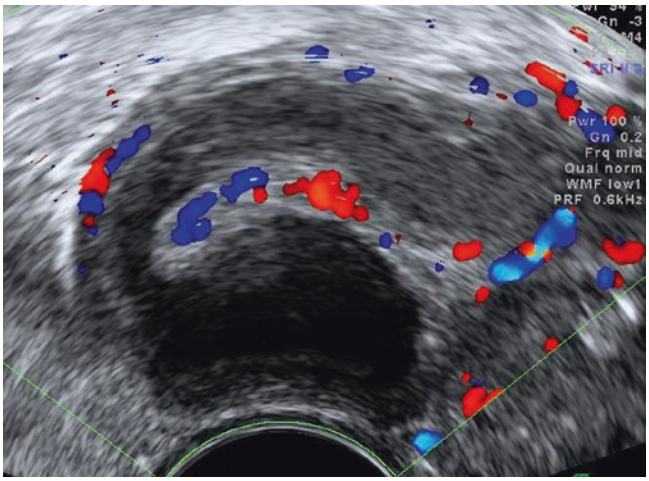

Fig. 9.10 Pyosalpinx – folded tube showing turbid contents suggestive of pus. The walls of the tube are thick and vascular. A thick incomplete septum is seen because of the folding of the tube on itself

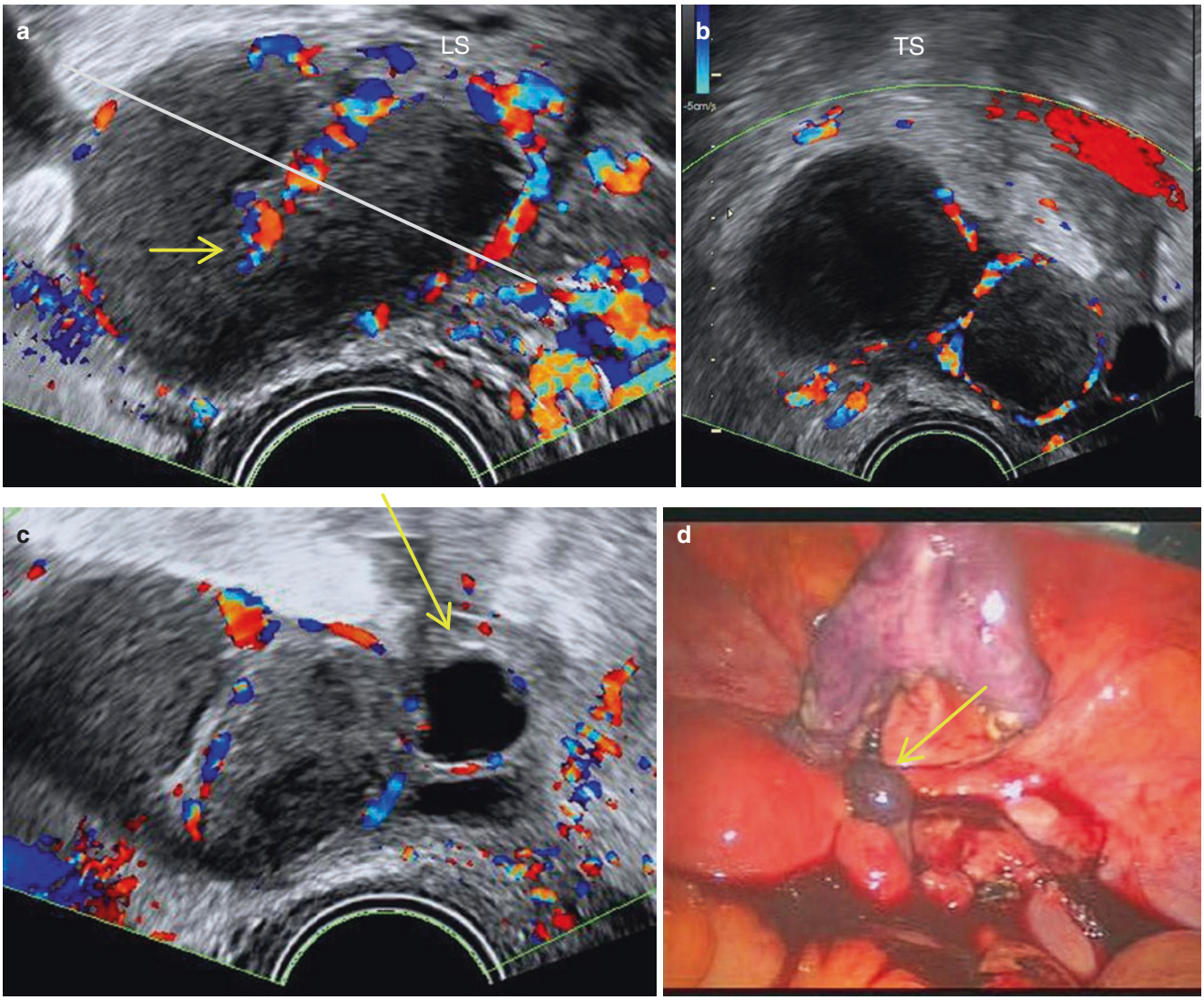

Fig. 9.11 Unilateral pyosalpinx. (**a**) Showing incomplete septum (*arrow*), thick walls with high vascularity and turbid contents. (**b**) Section across the plane (*long white line*) shown in (**a**) resulting in two cross sections of the single pyosalpinx. (**c**) A small fimbrial cyst (*arrow*) is seen beside the pyosalpinx showing thick vascular walls. (**d**) Inflamed fimbrial cyst (*arrow*) attached to the pyosalpinx seen at laparoscopy

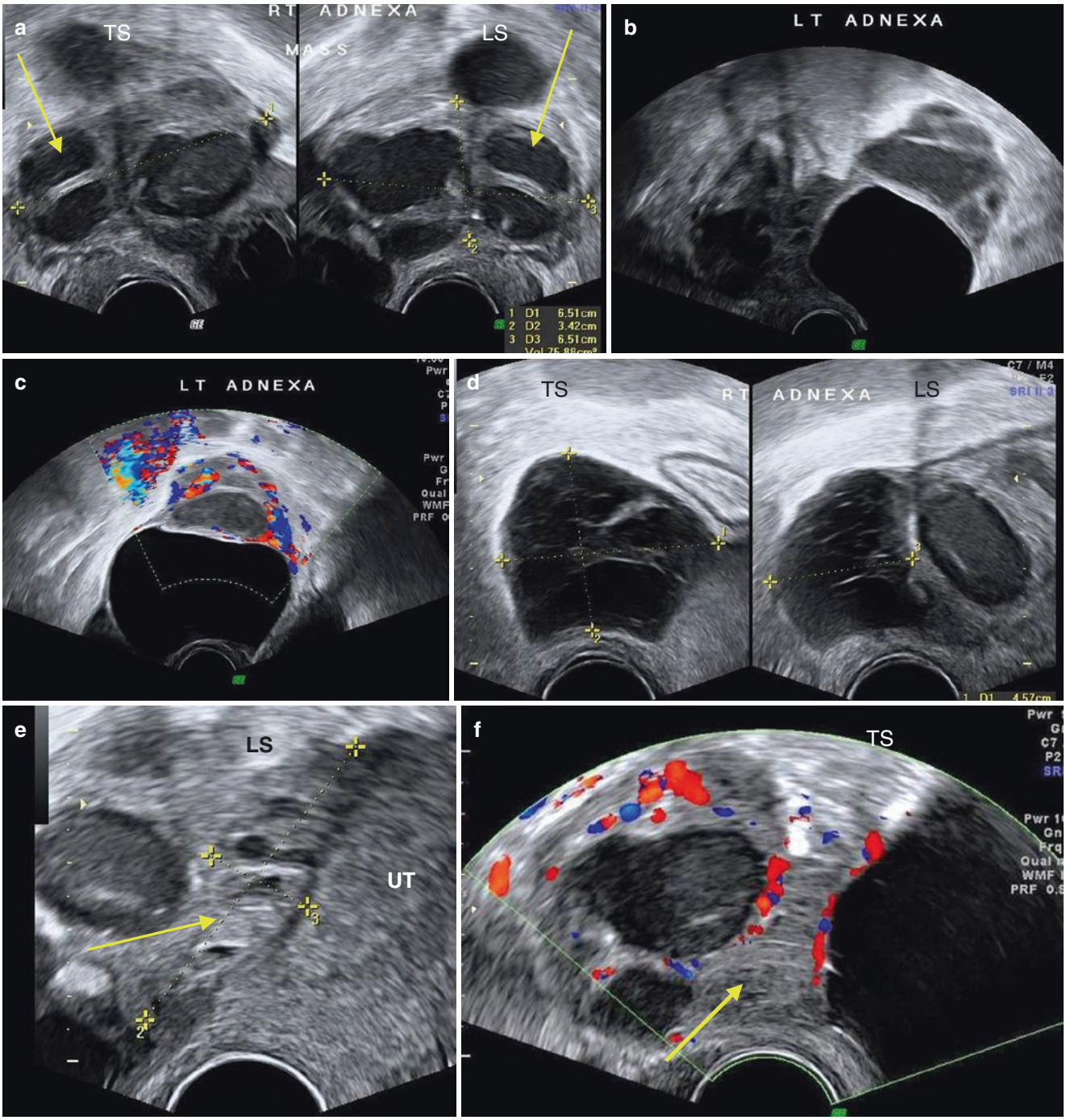

Fig. 9.12 Bilateral tubo-ovarian abscesses seen as multilocular, thick-walled masses. (**a**) Right adnexa (TO abscess) – showing a cystic area in right ovary with turbid contents (probably pus). Tubal component is seen with turbid contents in its lumen (*arrows*). (**b**) Transverse section showing left paraovarian cyst with a multilocular cystic mass (TO abscess) superior to it. (**c**) Moderate vascularity noted in the left adnexal mass. (**d**) Pus in the POD is seen as a hypoechoic area with linear hyperechoic strands within. (**e**,**f**) Thick hyperechoic bands suggestive of organised strands of pus seen between the posterior wall of the uterus and the right adnexal mass (*arrow*) and also between the two adnexal masses (*arrow*) in the POD

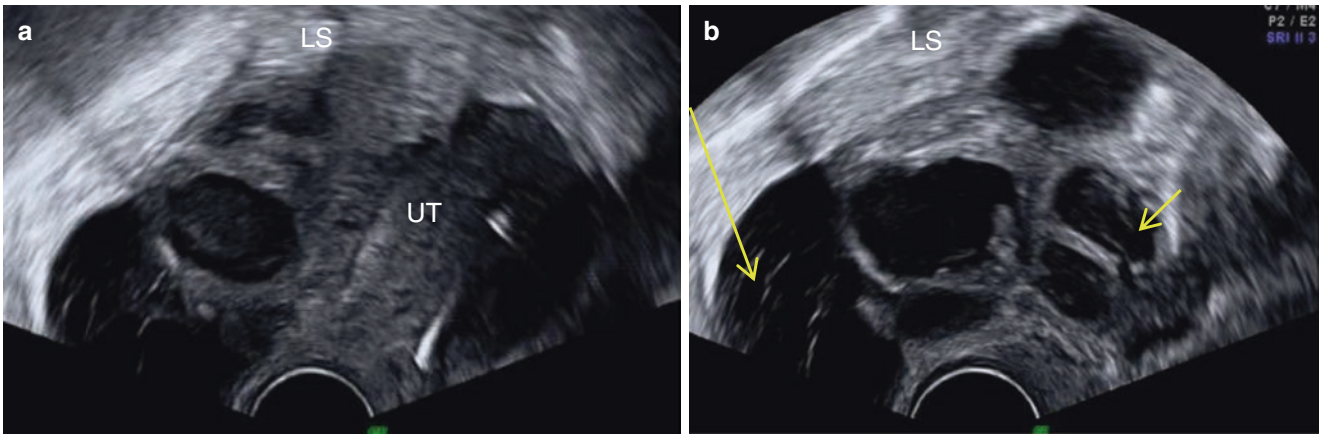

Fig. 9.13 TO abscess. (**a**) IUCD is seen in the endometrial cavity with a complex mass (the TO abscess) posterior to the uterus, in the POD. (**b**) Long section of the TO abscess showing a pyosalpinx anteriorly (*short arrow*) and pus collection posteriorly (*long arrow*)

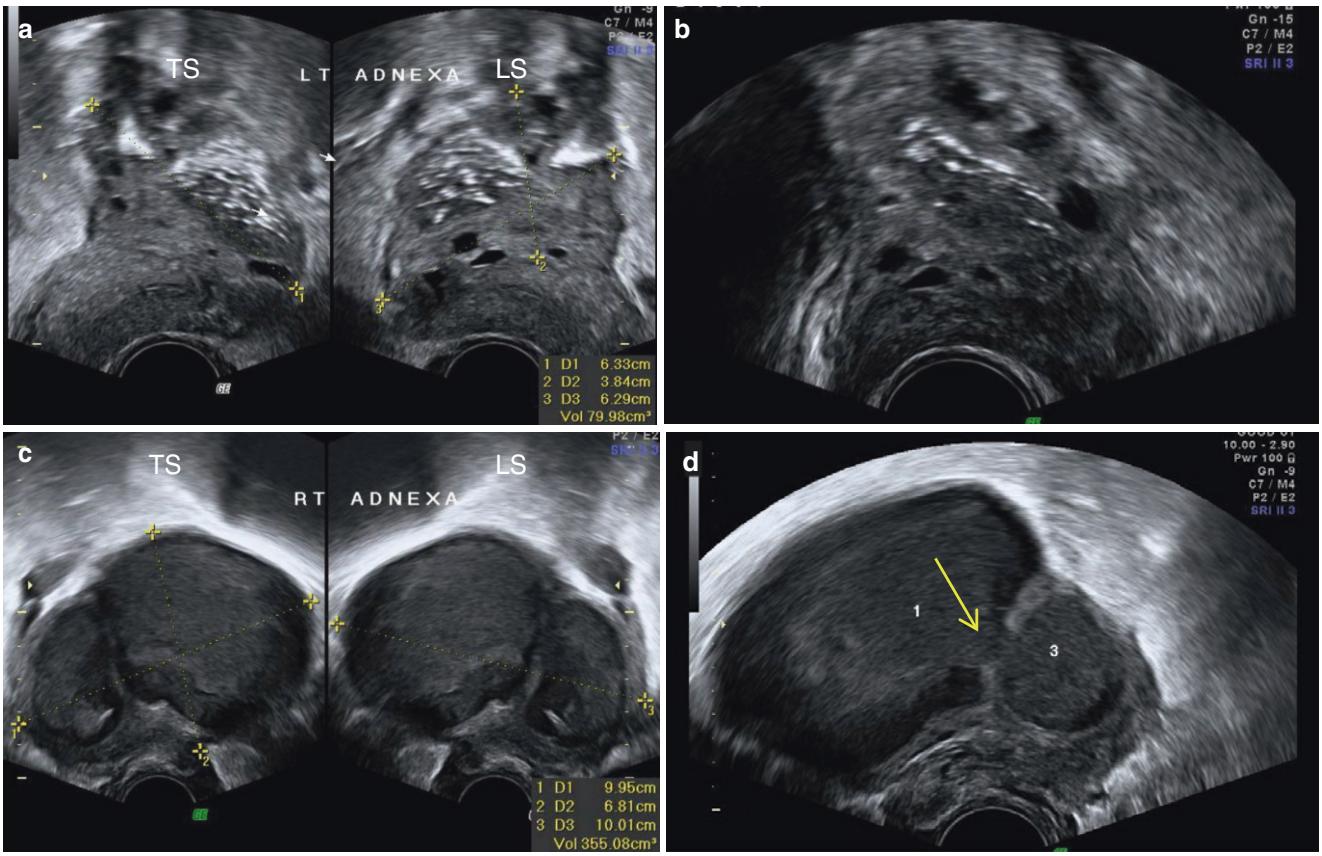

Fig. 9.14 Bilateral TO abscess. (**a**) Left adnexa: complex left adnexal mass seen with some ovarian tissue in its inferior part. Hyperechoic scattered echoes seen within the mass. (**b**) Tubal component of the TO mass is seen with a linear arrangement of scattered hyperechoic foci suggestive of air within its lumen, secondary to infection by gas-producing organisms. (**c**) Multilocular right adnexal mass showing thick turbid contents suggestive of pus. (**d**) Locules are seen communicating with each other (*arrow*). 300 ml of pus was drained from the right TO mass

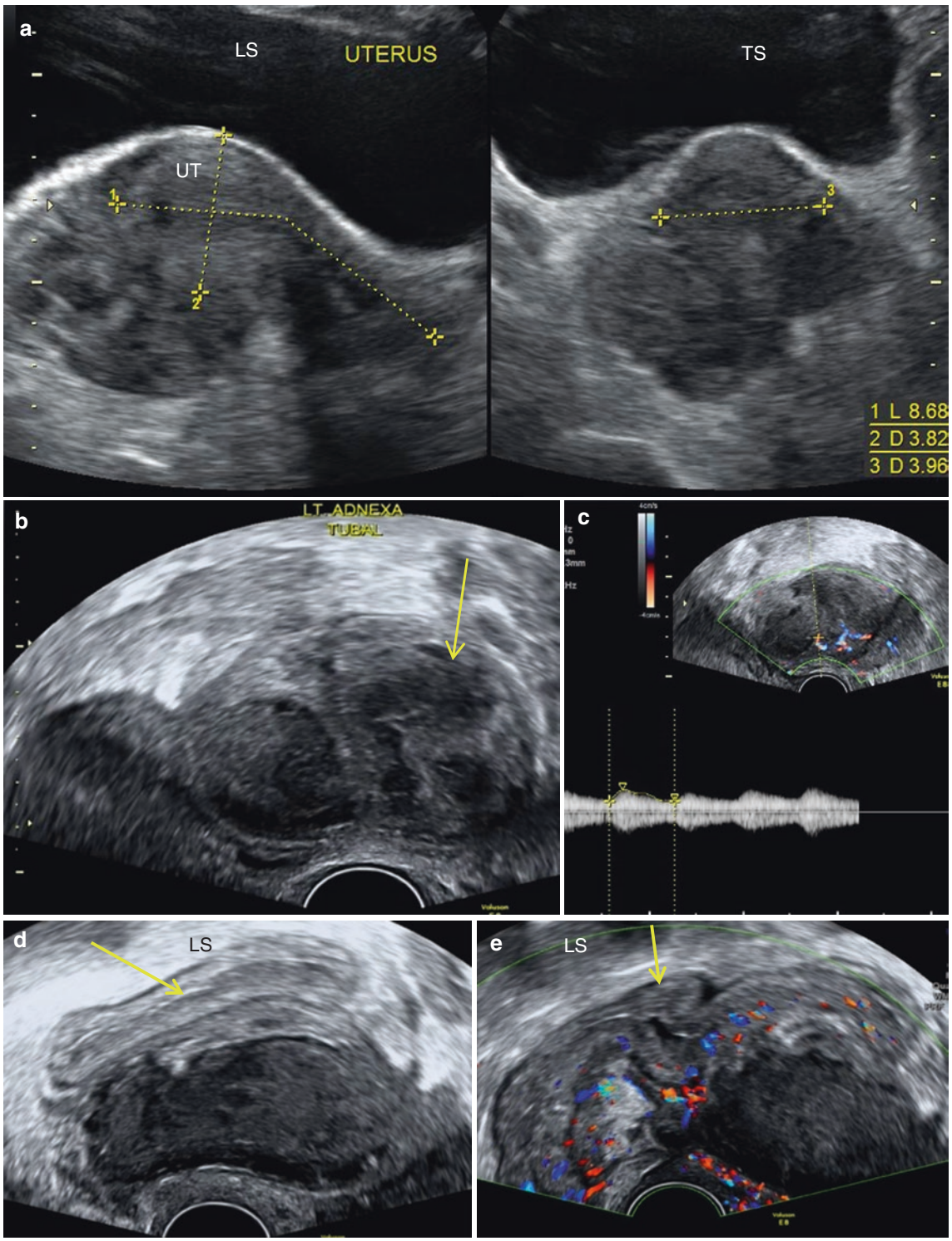

Fig. 9.15 Bilateral TO abscesses. (**a**) TAS – uterus seen anteriorly. Complex hypoechoic masses are seen behind the uterus bilaterally. On TAS, details cannot be assessed. (**b**) TVS – left-sided TO abscess seen. The tubal component (*arrow*) shows cystic irregular spaces with turbid fluid, communicating with each other. (**c**) Flow in the mass shows an RI of 0.5. (**d**) TVS – right adnexal mass showing a pyosalpinx (*arrow*), seen as a hyperechoic, thick, elongated mass with turbid contents within, which was placed over a large area with purulent (turbid) contents, probably an ovarian abscess. (**e**) The right pyosalpinx (*arrow*) shows thick vascular walls

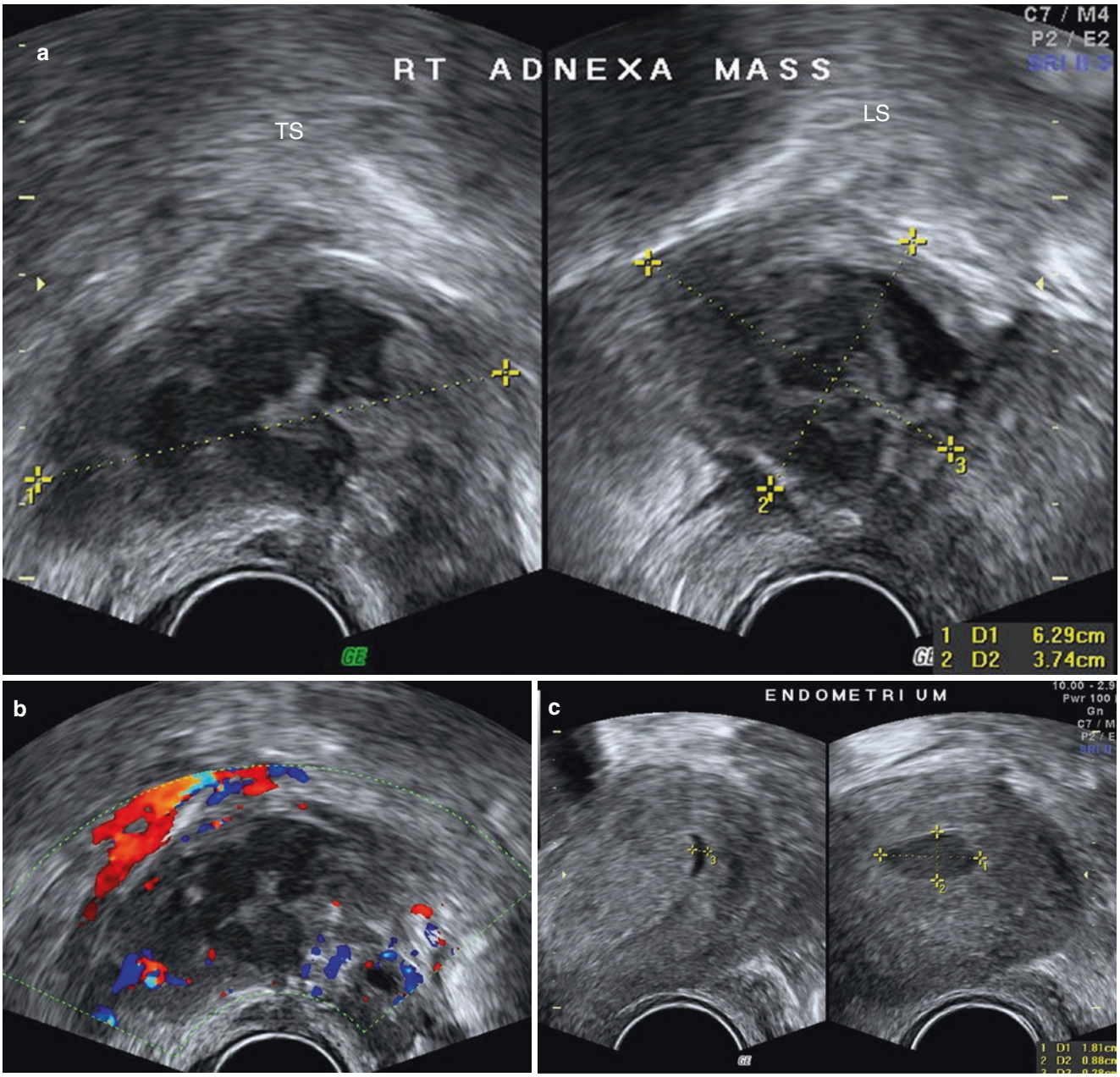

Fig. 9.16 Acute superimposed on chronic PID. Patient who gave a past history of PID, presented with lower abdominal pain and fever. (**a**) Complex right adnexal mass showing cystic spaces with turbid contents communicating with each other, suggestive of a TO abscess. (**b**) Mass showed mild to moderate vascularity. (**c**) Minimal turbid collection seen in the endometrial cavity suggestive of associated endometritis

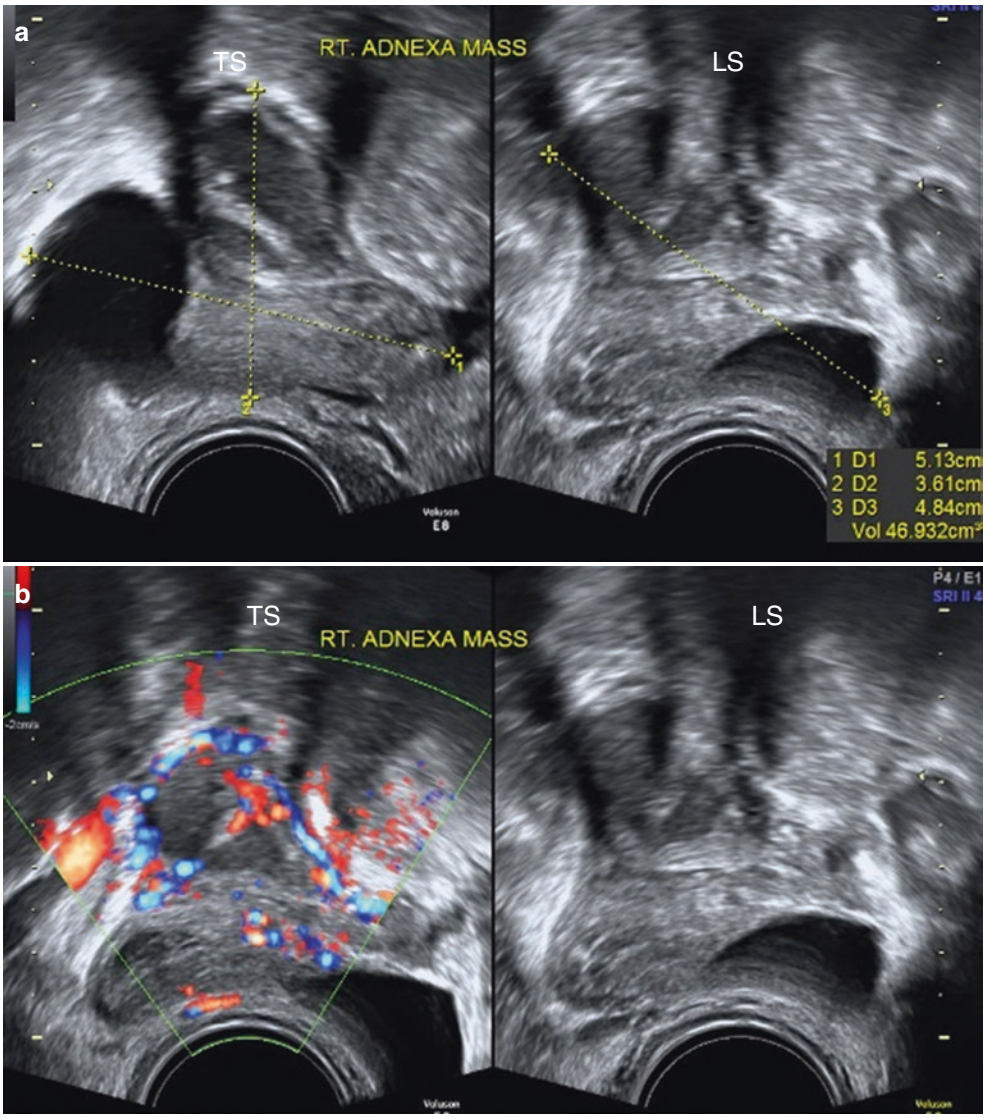

Fig. 9.17 TO mass with pyosalpinx. (**a**) Complex mass seen with solid and cystic areas. Tubal component identified by the presence of turbid fluid (*arrows*) within thick-walled structures that were communicating with each other on angulating the probe. (**b**) Increased vascularity noted in the tubal walls

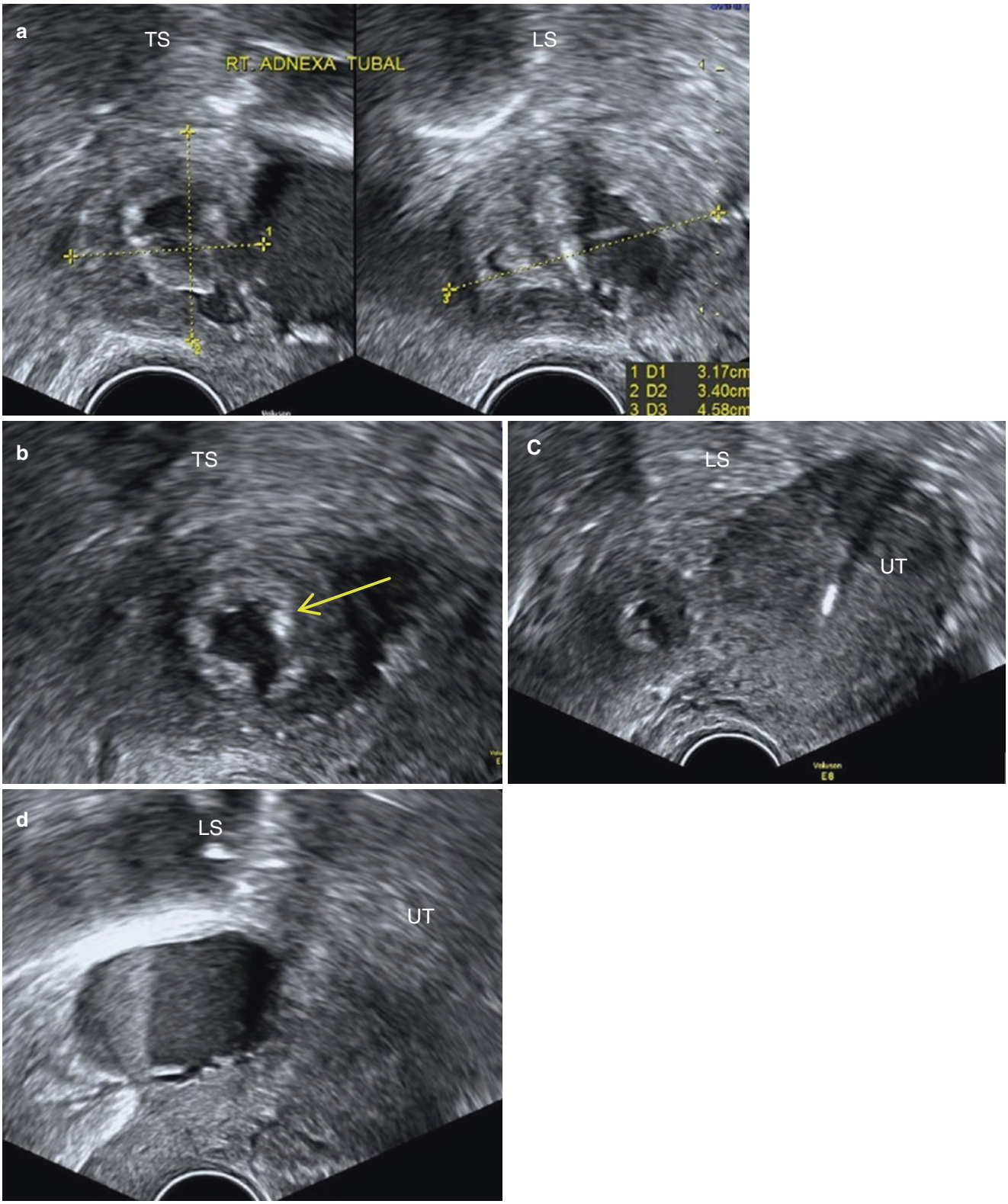

Fig. 9.18 PID with right-sided tubo-ovarian mass. (**a**) Complex mass seen with no ovarian tissue identified. (**b**) In one section, the cogwheel pattern suggestive of a cross section of a pyosalpinx is seen (*arrow*). (**c**) IUCD is seen in the endometrial cavity. The right tubal mass was adherent to the posterior walls of the uterus. (**d**) Loculated area of pus collection is seen in the POD, showing fluid–fluid level

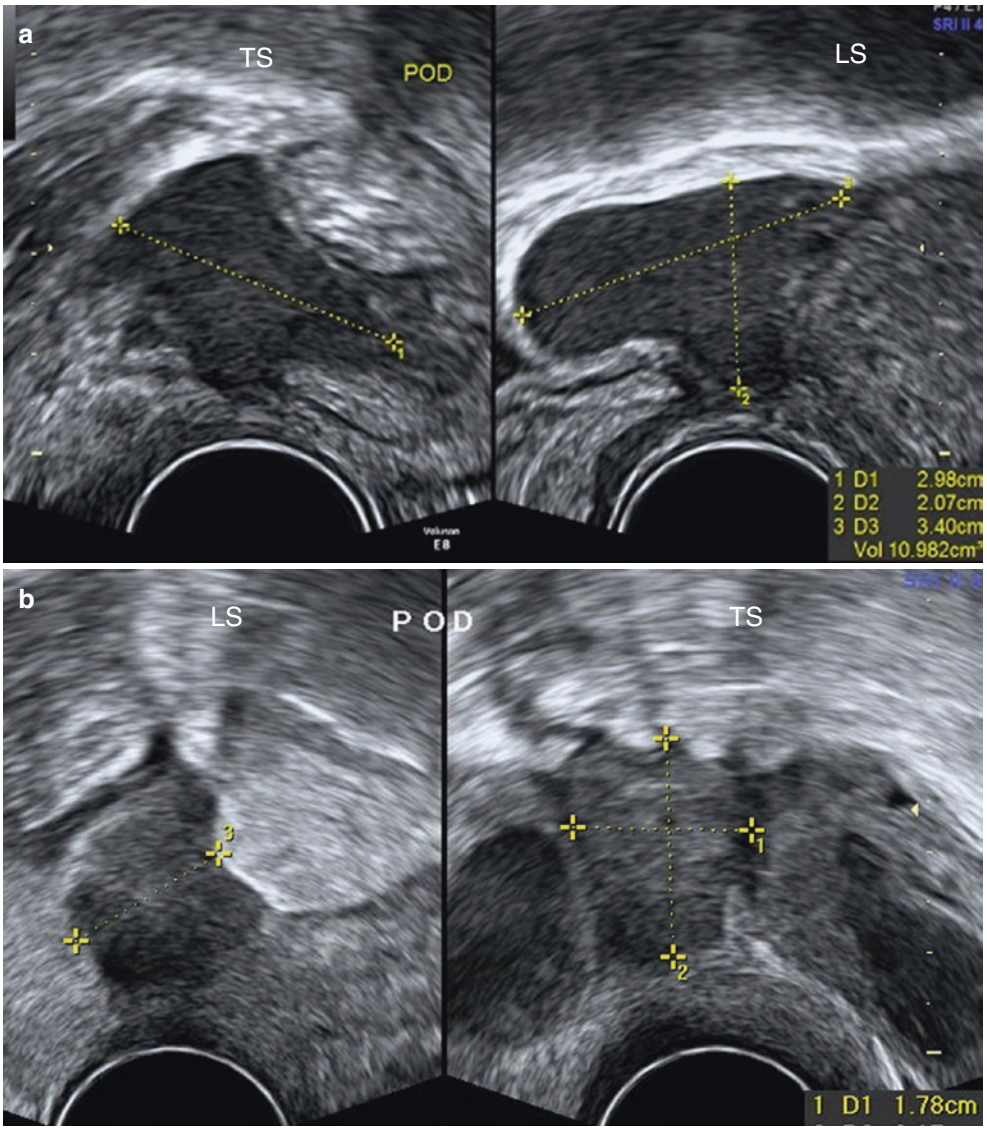

Fig. 9.19 Pus in two different cases, seen as a hypoechoic area with uniform low-grade internal echoes. (**a**) Pus in the POD. (**b**) Pus seen lying between bilateral TO abscesses in the POD

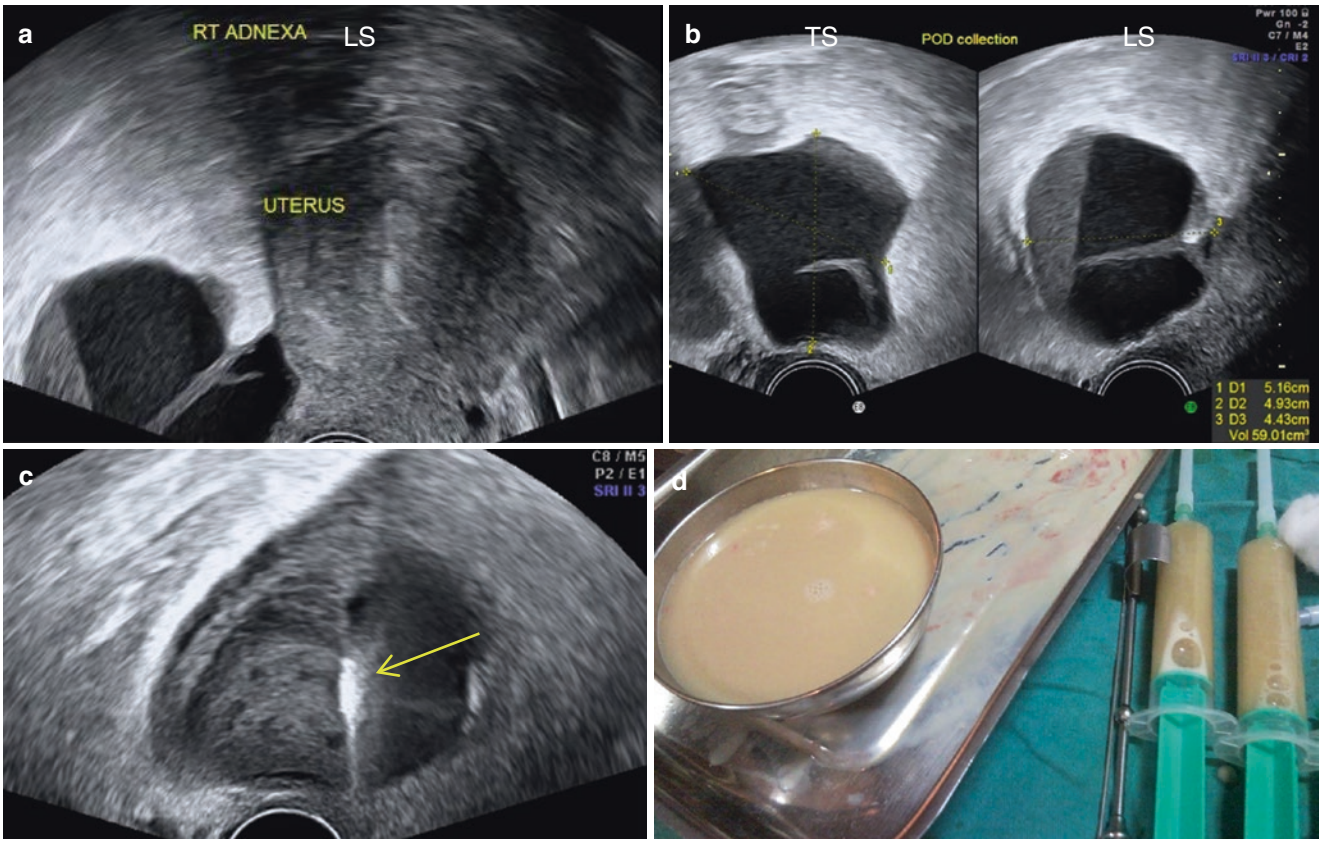

Fig. 9.20 (**a**) Long section of the uterus showing pus in the POD. (**b**) Collection in the POD showing a fluid–fluid level. (**c**) Drainage of pus in POD with a needle (*arrow*) seen in situ. (**d**) 220 ml of pus which was drained from the POD

Summary: Acute PID

- It is common in women belonging to the reproductive age group, and the infection is often secondary to instrumentation or is sexually transmitted.
- Associated features include fever and pain in the abdomen.
- It is typically bilateral, and ultrasound findings depend upon severity of disease from mild tenderness with hazy borders and increased vascularity of adnexa to a solid TO mass, pyosalpinx or a tubo-ovarian abscess.
- A pyosalpinx shows thick vascular tubal walls with turbid (hypoechoic) fluid within, and its cross section gives a 'cogwheel' appearance.

9.3 Chronic PID

A typical example of chronic PID is tuberculosis.

Ultrasound Features of Chronic PID (Fig. 9.21)

- The presence of a *hydrosalpinx*.
- Solid, thick (10 mm or more) *tubal masses* with hyperechoic walls, showing mild to moderate vascularity.
- The structures are usually *not tender*, unless there is a superadded acute infection, in which case findings may overlap with that of acute PID.
- *Pelvic adhesions with loculated fluid* (*peritoneal inclusion cysts*) are often a significant finding in tuberculosis, and the uterus and ovaries may appear enmeshed in the adhesions. The ovaries and bowels may also appear adherent to the uterus. Other causes for pelvic adhesions are endometriosis and previous surgery.
- *Ovarian abscess*, which is seen as a persistent cystic mass with turbid contents in the ovary, could be an occasional finding.
- *Hyperechoic foci along the surface of the ovary* is another reported finding associated with chronic infections, particularly tuberculosis.

In abdominopelvic tuberculosis, the most common findings are ascites, peritoneal inclusion cysts, matted bowel loops, complex tubal masses and, in a small percentage, general peritoneal thickening seen over the pelvic organs. Ovaries are usually normal. Ultrasound cannot diagnose but raises a suspicion of tuberculosis and is useful in monitoring the response to therapy.

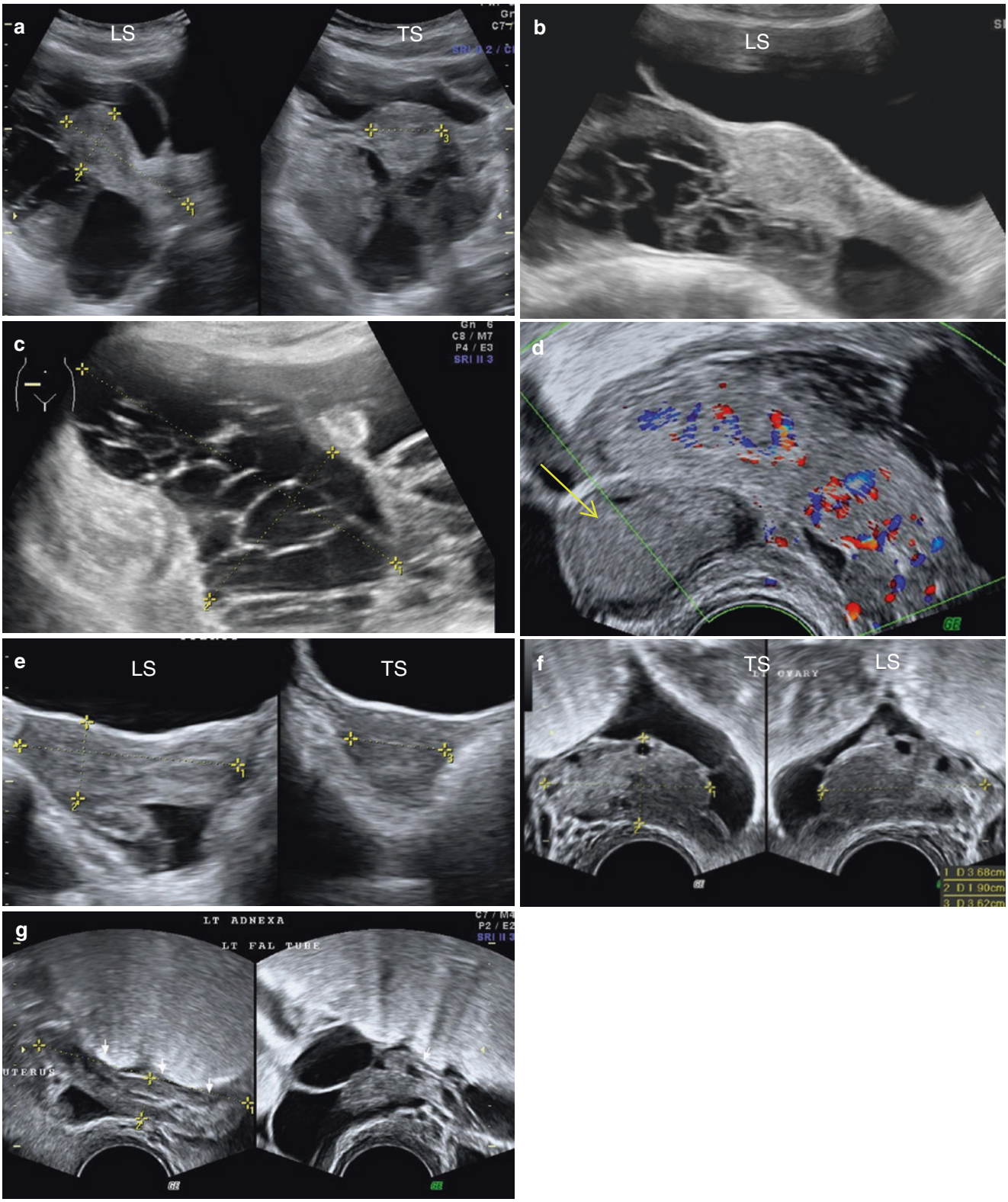

Fig. 9.21 Case of pelvic tuberculosis. (**a**) TAS – showing the uterus surrounded by loculated fluid and adhesions. (**b**) Multiple adhesion seen in the POD and above the uterine fundus. (**c**) Transverse section of the right lower abdomen showing multiple dense adhesions. (**d**) Solid, thick, hyperechoic tubal mass showing moderate vascularity suggestive of salpingitis. Ovary shows an isoechoic cystic area, probably an ovarian abscess (*arrow*), (**e**, **f**, **g**) Scan following 3 weeks of treatment with antituberculosis medication. (**e**) Uterus seen with minimal adhesions and loculated fluid posterior to it (compare with image (**a**)). (**f**) Ovarian cystic collection reduced in size and appearing more hypoechoic (compare with image (**d**)). (**g**) Left adnexa showing an elongated tubal mass with minimal fluid in its lumen (compare with image (**d**)). The image on the right side shows minimal periovarian adhesions

Summary: Chronic PID

- This is either a sequel of acute PID or secondary to chronic infections like tuberculosis.
- This tends to be bilateral and hydrosalpinx is a known feature of chronic PID. Other features include TO masses with ovaries and hydrosalpinx adherent to each other and pelvic adhesions with pelvic organs adherent to each other. Loculated fluid is often seen between the adhesions.

9.4 Hydrosalpinx

As mentioned earlier, a hydrosalpinx is a tubal mass with clear fluid in its lumen. It is usually the end result of a chronic or past infection, which may have been subclinical. It can also be seen following tubectomy. Most patients are asymptomatic, and hydrosalpinges are usually found incidentally on ultrasound done for other reasons. Occasionally, they may undergo torsion. Clinically they are of significance because they may be mistaken for a cystic ovarian mass, particularly in postmenopausal women where the atrophic small ovaries may not be visualised. They are usually bilateral.

Ultrasound Features of Hydrosalpinx (Figs. 9.22, 9.23, 9.24, 9.25, 9.26 and 9.27)

- A cystic mass with anechoic fluid.
- Elongated mass which is often retort shaped or sausage shaped.
- Presence of incomplete septae, formed as a result of tubal infolding. If present, they are very specific of a tubal mass.
- The walls of the hydrosalpinx are thin and show minimal vascularity.
- 'Beads-on-string' appearance – on cross section, the walls of the hydrosalpinx show hyperechoic mural nodules (>3 mm in height), which are nothing but compressed endosalpingeal (tubal mucosal) folds giving it a 'beads-on-string' appearance. Interestingly most often there are three prominent nodules in a cross section of the hydrosalpinx (like a 'therefore' abbreviation).
- On cross section, they may appear like multiple circumscribed cystic spaces beside each other, but on angulating the probe, they appear as elongated cystic areas communicating with one another.
- On 3D ultrasound, their morphology is often well seen because of a better depth perception. The compressed tubal mucosal folds may also be seen as linear folds on a 3D rendered image. 3D ultrasound is, however, not essential for diagnosis.
- The differential diagnosis for a hydrosalpinx is any elongated cystic mass in the pelvis like a blood vessel or a fluid-filled intestine. Blood vessels will show colour filling on Doppler, while intestines show peristalsis, unlike a hydrosalpinx.

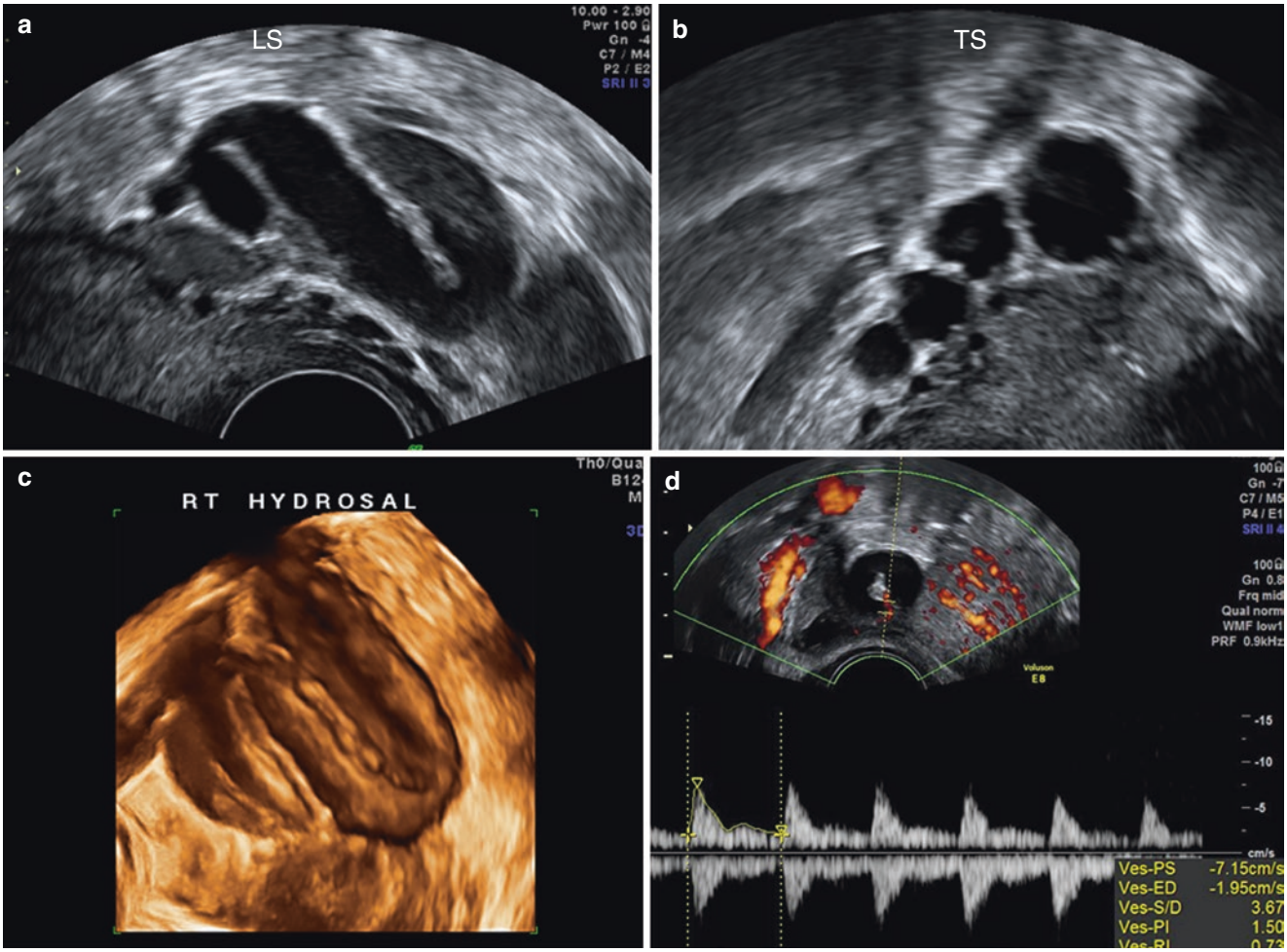

Fig. 9.22 (**a**) Long section of a hydrosalpinx showing incomplete septae and anechoic cystic contents. (**b**) Transverse section of the hydrosalpinx perpendicular to the section in image (**a**), showing multiple, circumscribed, cystic areas with anechoic contents and beaded thin walls. (**c**) 3D rendered image of the hydrosalpinx. (**d**) Minimal flow with spectral Doppler showing protodiastolic notch (which is typical of tubal tissue flows)

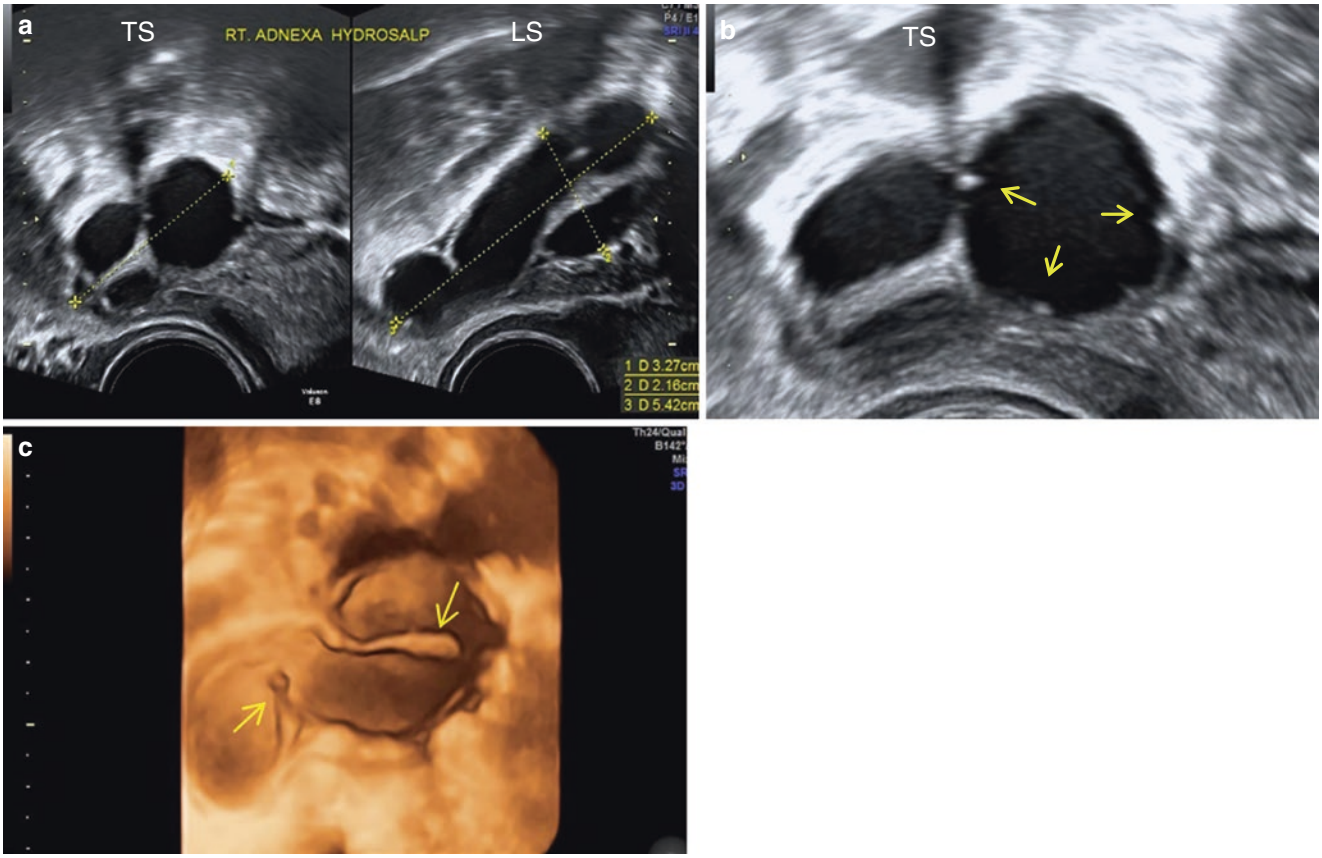

Fig. 9.23 Three different cases of hydrosalpinx. (**a**) Sausage-shaped elongated hydrosalpinx. (**b**) Cross section of hydrosalpinx showing tiny hyperechoic bead-like nodularity along its walls (compressed tubal mucosal folds) (*short arrows*). (**c**) 3D rendered image showing incomplete septae (*arrows*)

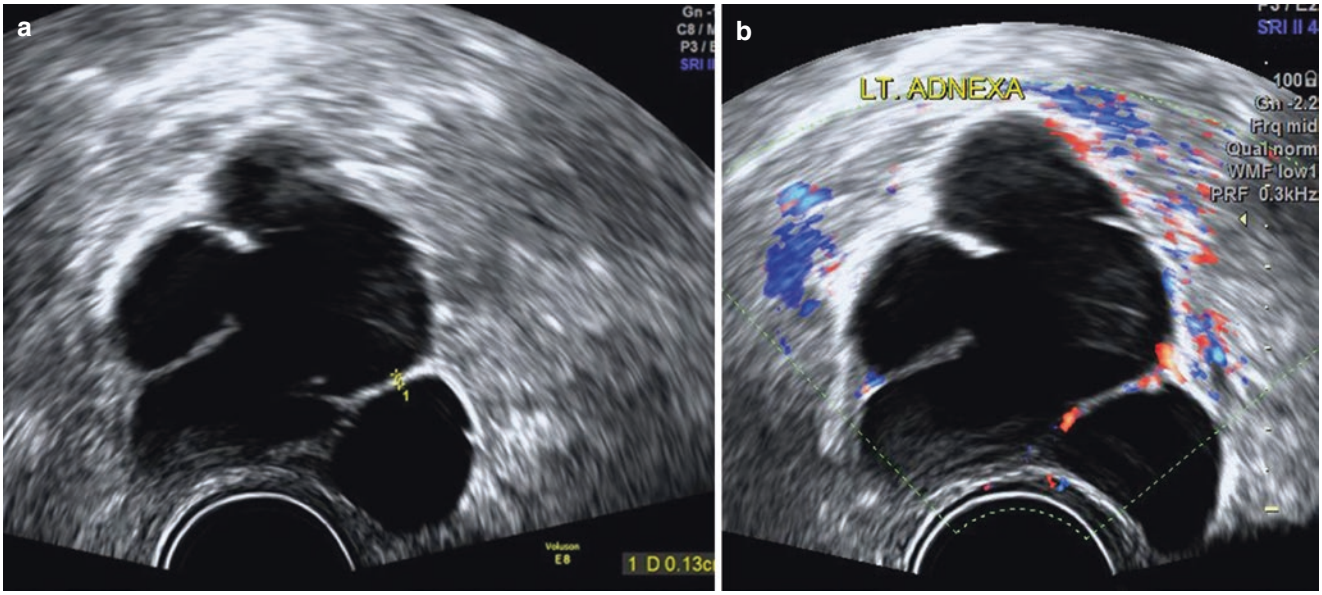

Fig. 9.24 (**a**) Hydrosalpinx seen as globular cystic mass with thin incomplete septae. (**b**) Minimal flow seen in the walls of the hydrosalpinx

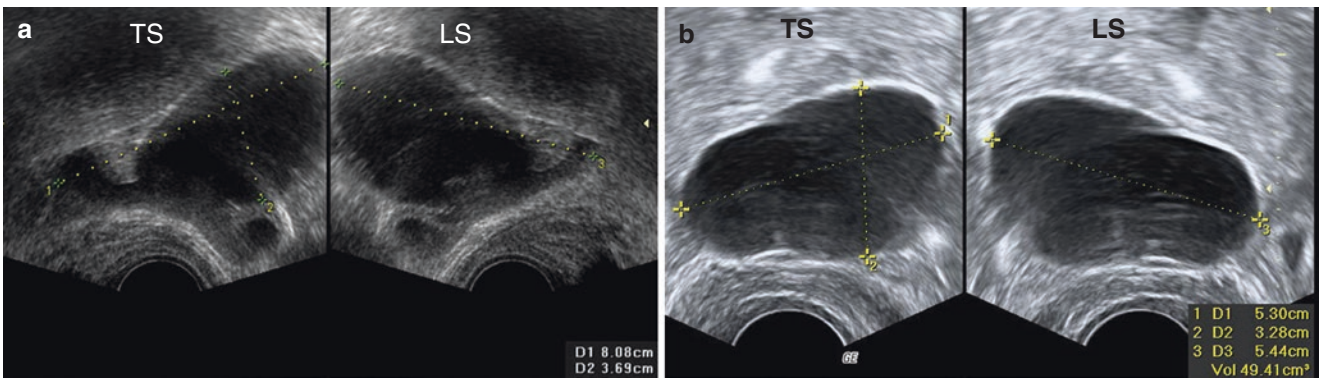

Fig. 9.25 Hydrosalpinx. (**a**) Retort shaped. (**b**) Oval shaped

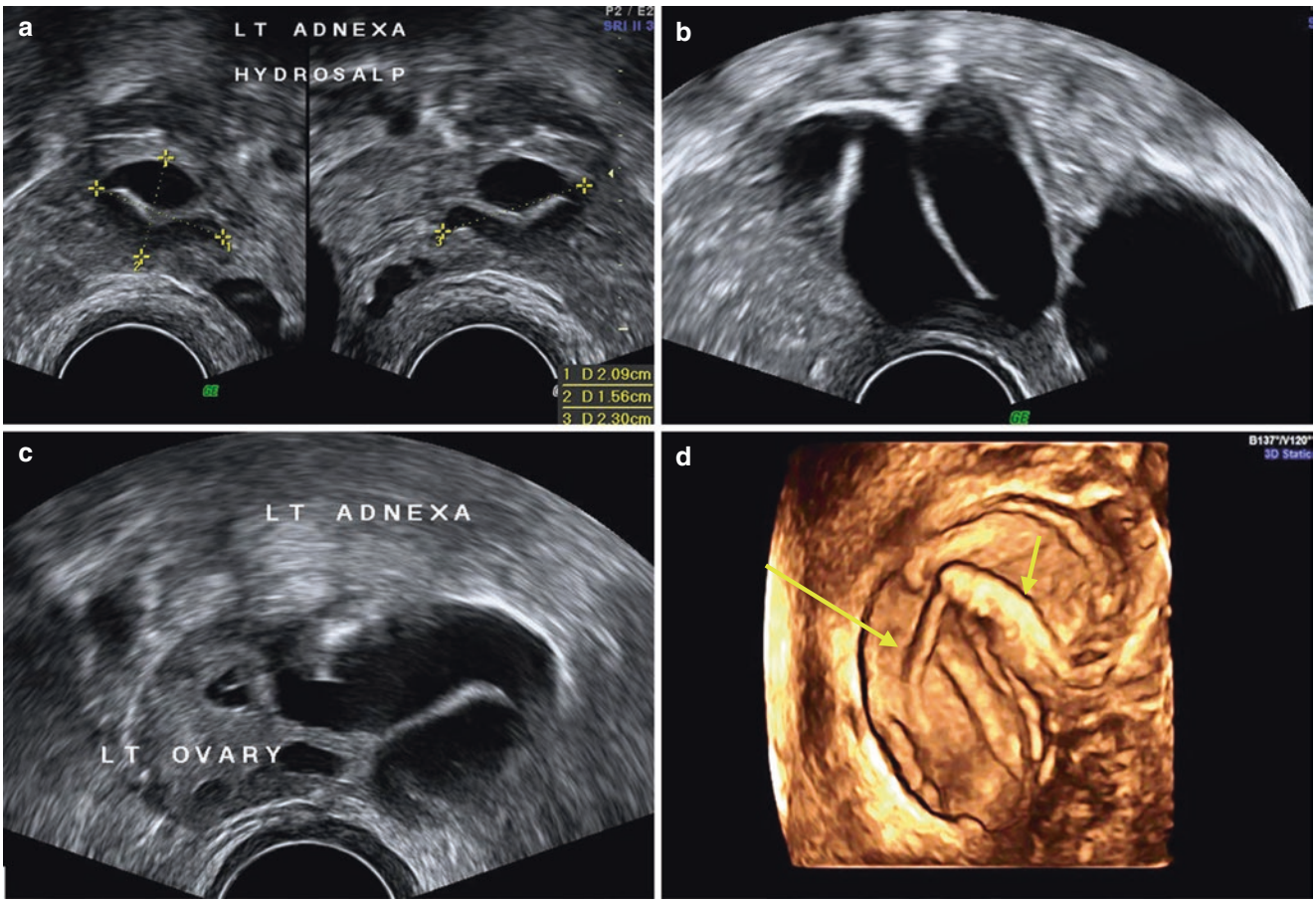

Fig. 9.26 Hydrosalpinx showing thin incomplete septae in different cases. (**a**–**c**) Hydrosalpinges seen on greyscale. (**d**) 3D rendered image of a hydrosalpinx showing the incomplete septum (*short arrow*) and compressed mucosal folds (*long arrow*)

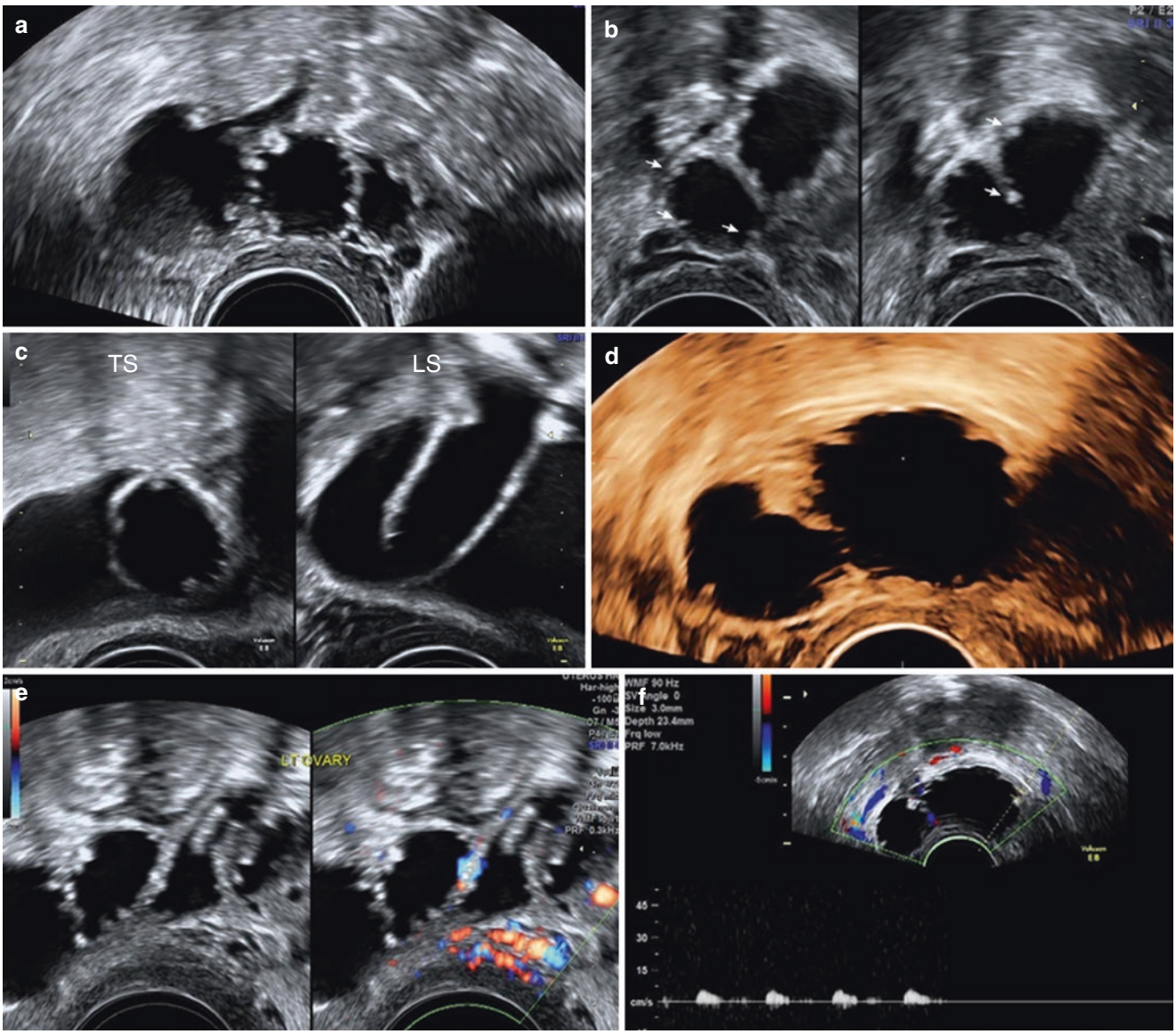

Fig. 9.27 (**a**–**e**) Hydrosalpinges showing 'beads-on-string' appearance (in cross-sectional views). (**e**, **f**) Walls of a hydrosalpinx showing poor vascularity

Features differentiating a hydrosalpinx from a pyosalpinx:

Features	Pyosalpinx	Hydrosalpinx
Pathology	Acute PID	Chronic PID
Shape	Elongated/undulating	Sausage/retort
Incomplete septum	Occasionally seen	Commonly seen
Walls	Thick >5 mm	Thin
Vascularity	High	Low
Mucosal folds	Swollen	Compressed
Transverse section	'Cogwheel' appearance	'Beads-on-string' appearance
Contents	Turbid fluid – hypoechoic	Clear fluid – anechoic

At times, tubal morphology on ultrasound may appear between a pyosalpinx and a hydrosalpinx. This may be seen with subacute infections, or during the transition from acute to chronic PID, or in cases with acute on chronic infection.

9.5 Tubal Malignancy

Malignancy of the fallopian tube is very rare, comprising about 0.18–1.6 % of all gynecological malignancies. Its incidence is probably underestimated because very often, particularly in advanced cases, it may be attributed to ovarian carcinoma. The most common fallopian tube carcinoma is serous adenocarcinoma (in about 80 %). Others include endometrioid, clear cell, mucinous or undifferentiated carcinomas. Serous tubal intraepithelial carcinoma (STIC) is believed to be a precursor of carcinoma of the fallopian tube and probably also the ovary. It is more common in nulliparous women, those with a history of infertility and chronic infection. The women in these cases are usually postmenopausal. Most often, the distal two-third of the tube is involved.

The women with tubal carcinoma may be asymptomatic or present with vaginal bleeding, abdominal pain, excessive watery discharge or a pelvic mass. The 'Latzko triad' includes intermittent colicky pelvic pain, pelvic mass and bloody–watery discharge. These classical symptoms of tubal carcinoma are only seen in about 10 % of patients. Watery discharge (hydrops tubae profluens) is a very classic feature of women with fallopian tube carcinoma but is seen in only 20 % of women. The diagnosis of tubal carcinoma is by histopathology. The treatment and prognosis are similar to that of ovarian carcinoma.

Ultrasound Features of Tubal Malignancy (Figs. 9.28 and 9.29)

- It typically presents as a solid mass but may show a few cystic spaces within the solid tissue.
- The solid mass appears ovoid or may be a sausage-shaped structure.
- The solid tissue shows moderate to high vascularity (in most cases it is highly vascularised). The flow into the mass is typically seen from, and perpendicular to the outer walls of the mass.
- Very often, fluid is seen within the tubal lumen forming a hydrosalpinx. The contents are generally anechoic. This has been termed 'hydrops tubae profluens'.
- Solid vascular tissue protruding into a hydrosalpinx is highly suggestive of fallopian tube carcinoma. This solid tissue could either fill the entire tubal lumen and adjoin or protrude into the hydrosalpinx from one side, or it may be seen as solid tissue projecting into the lumen of the hydrosalpinx from one wall like a large papilla. Most often, in tubal carcinoma the number of such papillae is one or a few at the most.
- Normal ovary or ovarian tissue may be seen alongside the solid mass. The probability of a tubal neoplasia is particularly high if the entire ovarian margins can be delineated.
- Clear watery fluid may also be seen in the endometrial cavity.
- Free fluid is commonly seen in the pelvis.

Differential diagnosis is ovarian neoplasia or a subserous fibroid and in some cases may be a true diagnostic challenge.

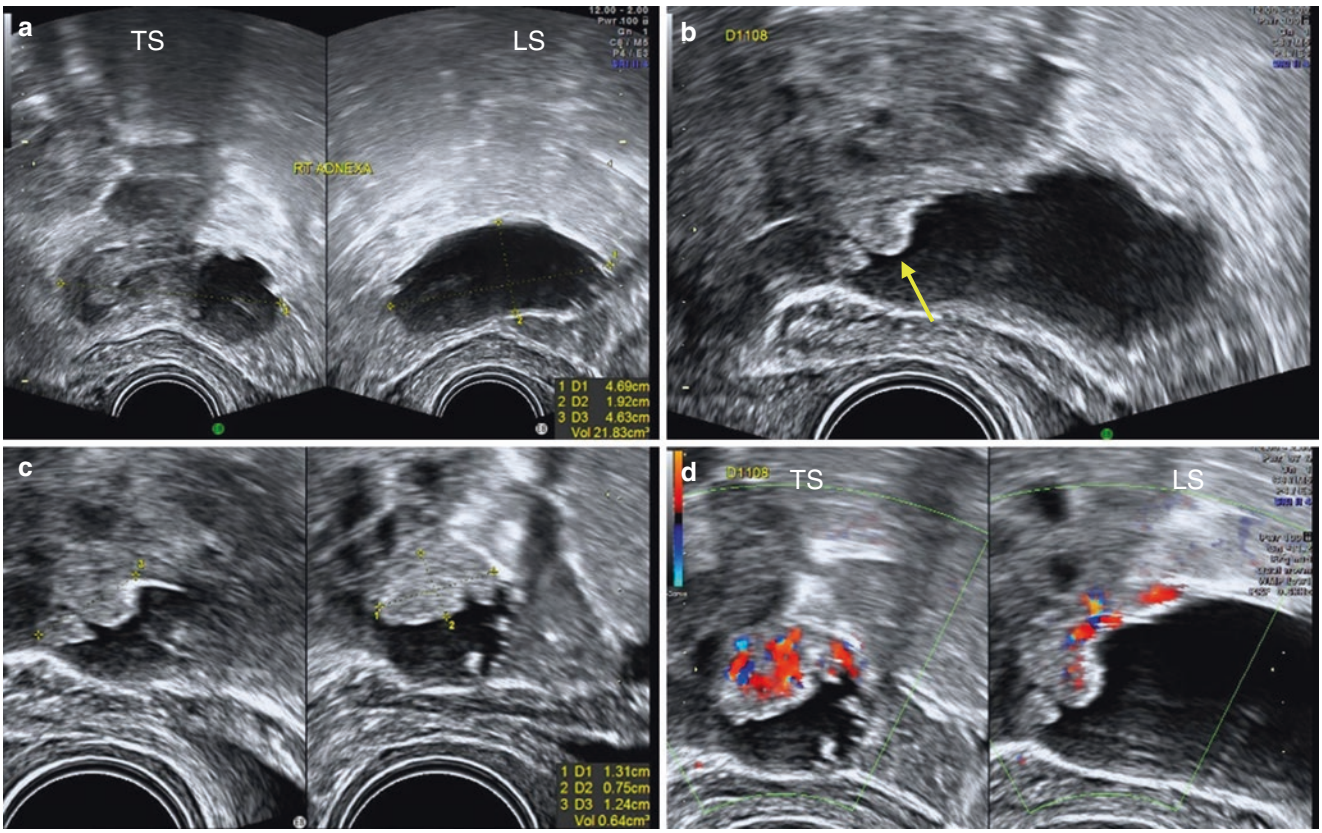

Fig. 9.28 Case in which fallopian tube carcinoma was suspected. (**a**) Hydrosalpinx on *TS* and *LS*. *TS* image shows compressed mucosal folds as beads along its inner walls. (**b**) *LS* view of a hydrosalpinx shows a small, irregular, hyperechoic protrusion (*arrow*) into its lumen, from its superior wall. (**c**) The solid protruding mass measured about 13 mm × 7 mm × 12 mm. (**d**) Mass protruding into the hydrosalpinx showing high vascularity raising a very high suspicion of a malignant neoplastic mass

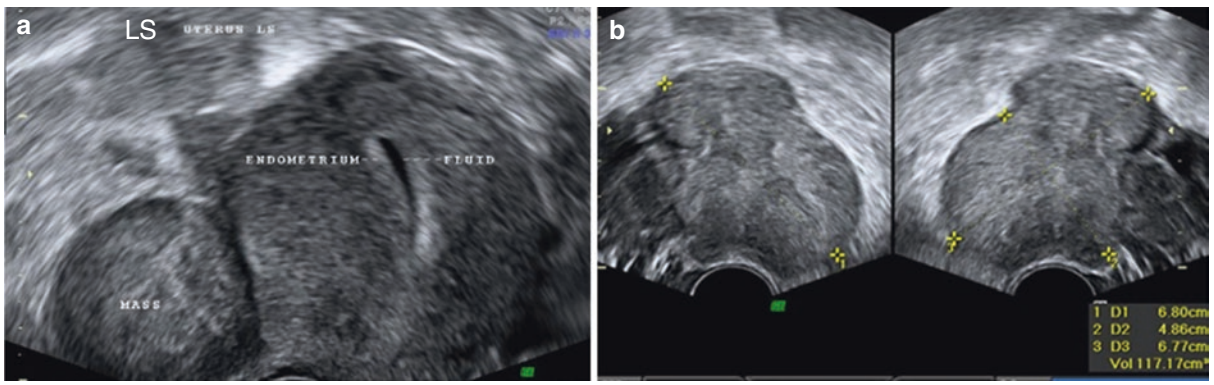

Fig. 9.29 Case of fallopian tube carcinoma. (**a**) Longitudinal section of the uterus showing minimal anechoic fluid in the endometrial cavity. The neoplastic solid mass is seen behind the uterus in the POD. (**b**) A solid heterogeneous mass is seen in the left adnexa. (**c**) Increased vascularity is seen in the mass with vessels seen arising perpendicularly from the outer walls. (**d**) One end of the mass shows a small cystic area with an incomplete septum (*short arrow*) suggestive of a hydrosalpinx. Just inferior to this, the entire left ovary is seen. (**e**) A solid mass (*arrow*) is seen protruding into the hydrosalpinx, highly suggestive of a neoplastic mass of the fallopian tube. (**f**) Flow in the mass showed a low RI of 0.13. (**g**) Operative specimen showing the neoplastic fallopian tubal mass (*arrow*)

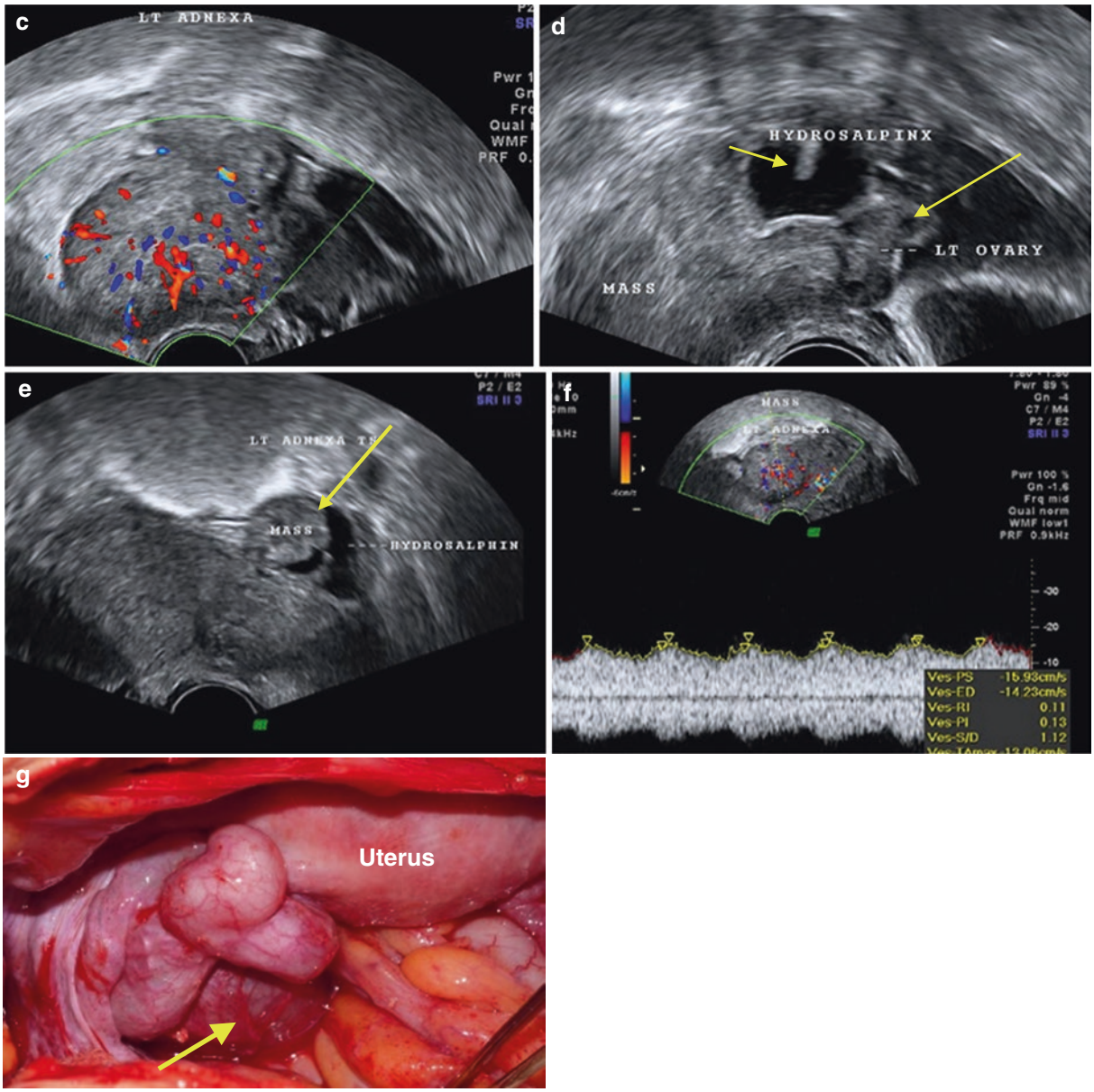

Fig. 9.29 continued

Summary: Tubal Malignancy

- Rare malignancy seen commonly in postmenopausal women.
- Clinical presentation: abdominal pain, bloody–watery discharge and pelvic mass.
- On ultrasound, it typically appears as a solid adnexal mass or a solid mass with a hydrosalpinx or a solid papillary projection into a hydrosalpinx, with the solid tissue showing high vascularity.
- Differential diagnosis is an ovarian neoplasm or a subserous fibroid. Presence of a normal ovary, separate from the mass, helps differentiate it from ovarian masses.

9.6 Paraovarian and Paratubal Cysts

Paraovarian cysts account for 10–20 % of adnexal masses. These are epithelium-lined, fluid-filled cysts seen in the adnexa adjacent to the ovary and the fallopian tube. Paraovarian cysts are remnants of mesonephric (Wolffian) ducts. Paratubal cysts include mesosalpingeal cysts, hydatid cysts of Morgagni (also known as fimbrial cysts) and those arising from Mullerian (paramesonephric) duct remnants. Paratubal cysts are usually a little away from the ovary, while paraovarian cysts are seen adjacent to the ovary.

They are commonly found in women belonging to the reproductive age group. Most of them are benign and asymptomatic, and their significance is mainly because of their resemblance with other cystic masses in the adnexa, more so in postmenopausal women. Occasionally, however, they may be neoplastic or may undergo torsion.

Fimbrial cysts (hydatid cysts of Morgagni) are a type of paratubal cysts seen as small, anechoic, unilocular and smooth-walled cysts. They are frequently multiple and appear as pedunculated cysts connected to the *fimbriae* of the fallopian tubes. Occasionally, when there is fluid in the pelvic cavity, one may see these cysts moving in the pelvic fluid along with the fimbriae to which they are attached, when a specific diagnosis can be made. Most often, however, they are reported as paraovarian cysts.

Ultrasound Features of Paraovarian and Paratubal Cysts (Figs. 9.30, 9.31, 9.32, 9.33, 9.34, 9.35 and 9.36)

- These cysts are seen separate from the ovaries or, if adjacent to the ovaries, can be pushed away from them (sliding or splitting sign). A few may be adherent to the ovary, which makes it difficult to differentiate them from exophytic ovarian cysts.
- They are usually unilocular, thin-walled, round or oval cysts. However, neoplastic ones may appear septate.
- They are typically anechoic, unless they have undergone torsion (when there may be blood within the lumen giving the fluid a turbid appearance), are neoplastic (contents may show internal echoes) or are affected by PID (may show turbid fluid or debris within). Most often they are small but may be moderate in size. Only rarely are they large, when they may be neoplastic.
- Their walls are thin and smooth and show minimal vascularity. Exceptions are infections (when the walls may be thick and vascular) or torsion (when the walls may be thick and avascular).
- Presence of solid tissue within a paraovarian cyst may suggest a benign or malignant neoplasm, which is very rare.

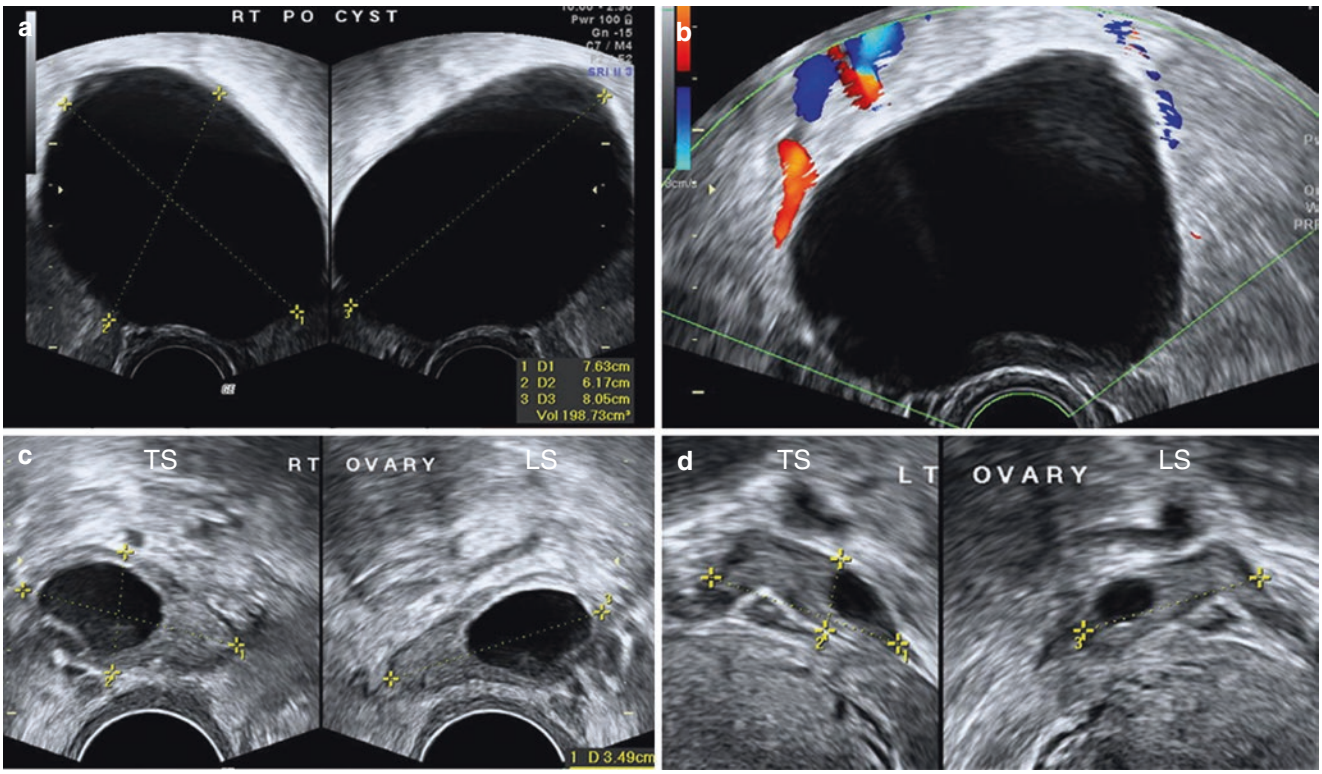

Fig. 9.30 Case of PO cyst with typical ultrasound findings. (**a**) Anechoic, unilocular, thin-walled cyst (198 cc). (**b**) Cyst wall shows low vascularity. (**c**, **d**) Normal right and left ovaries are seen separate from the cyst

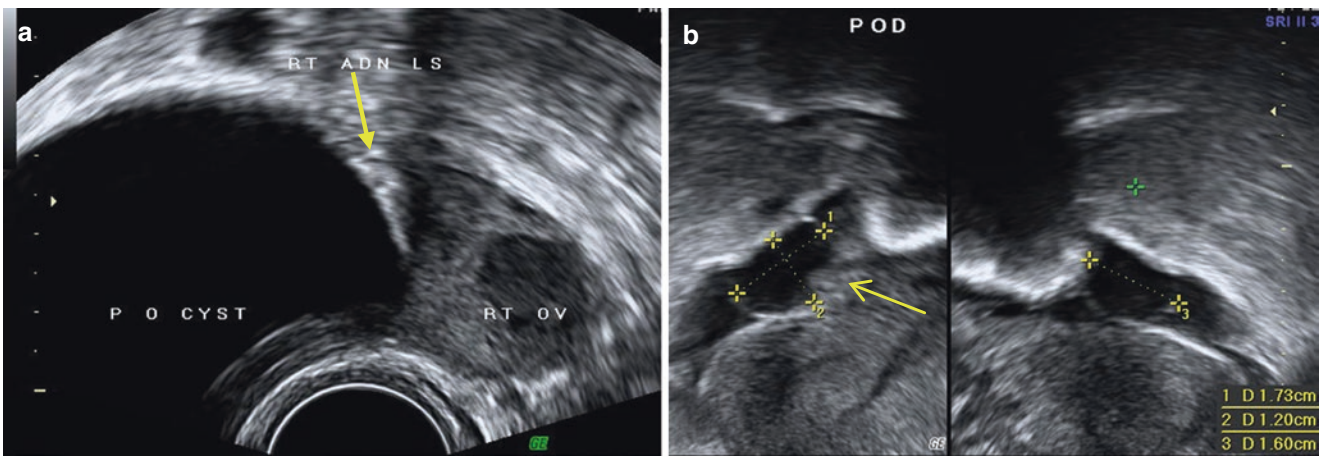

Fig. 9.31 (**a**) Case 1 – wedge of tissue (*arrow*) is seen intervening between the PO cyst and the right ovary suggesting that they are likely to be of different origin. (**b**) Case 2 – thin-walled fimbrial cyst seen with minimal fluid surrounding it. *Arrow* pointing at the minimal fimbrial tissue

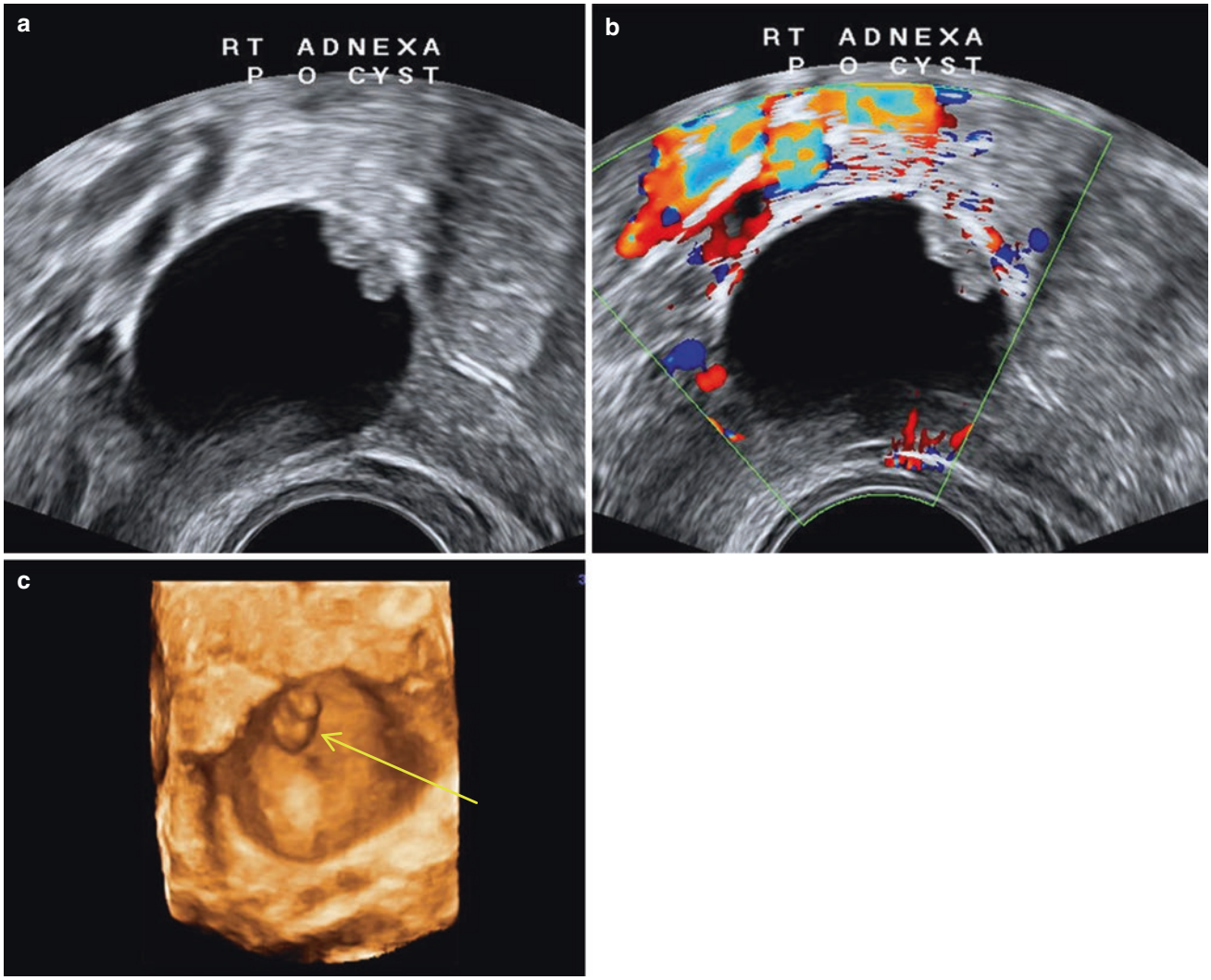

Fig. 9.32 (**a**) PO cyst showing two small papillary projections from the cyst wall. (**b**) Papillae showing poor vascularity. (**c**) 3D rendered image showing the two papillae within the cyst (*arrow*). *HPE:* papillary serous cystadenoma (of a PO cyst)

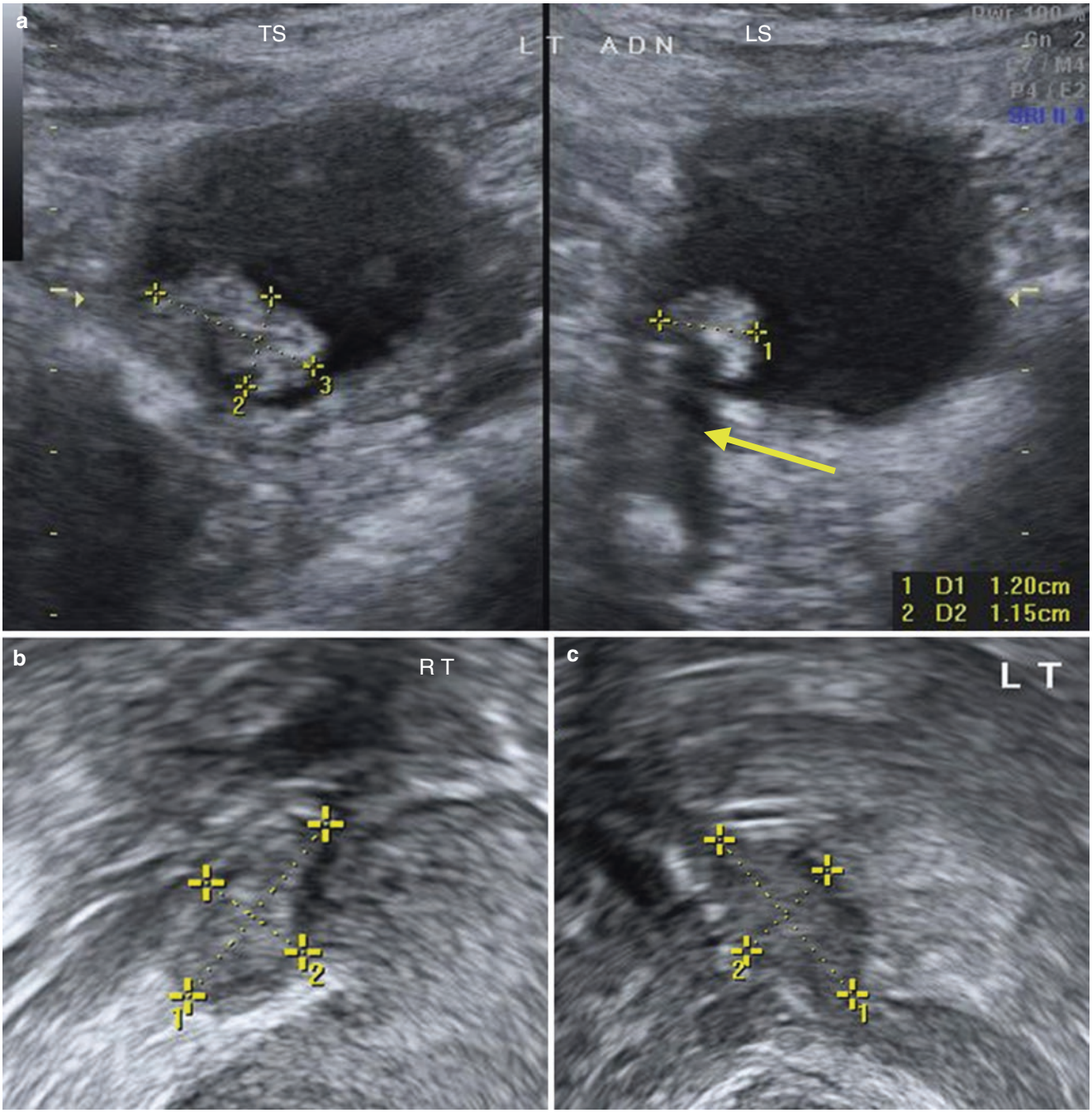

Fig. 9.33 (**a**) PO cyst showing a papilla protruding into it. The papilla showed acoustic shadowing (*arrow*), which is typical of a serous cystadenofibroma. (**b**,**c**) Atrophic right and left ovary, consistent with the patient's postmenopausal status. *HPE:* papillary serous cystadenofibroma of a PO cyst

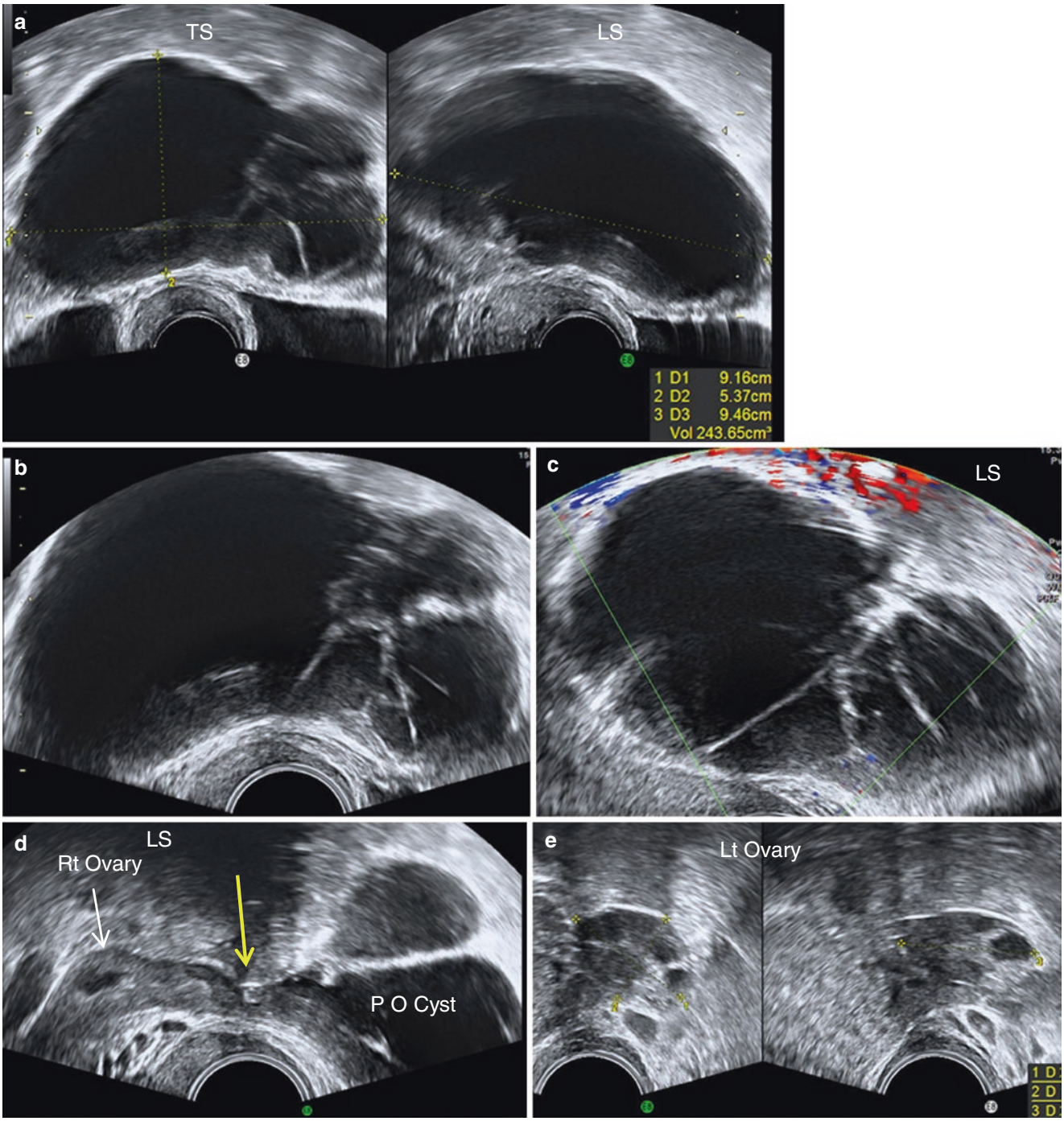

Fig. 9.34 PO cyst with septae. (**a**) Cyst measuring 240 cc. (**b**) Cyst showing dense fibrous septae that cause minimal acoustic shadowing. (**c**) No vascularity is seen in the cyst wall or septae. (**d**) Normal right ovary is seen adherent to one end of the PO cyst (*arrows*). The ovary could not be separated from the cyst on pressure with the TVS probe. (**e**) Left ovary appearing normal. *HPE:* serous cystadenoma of a PO cyst

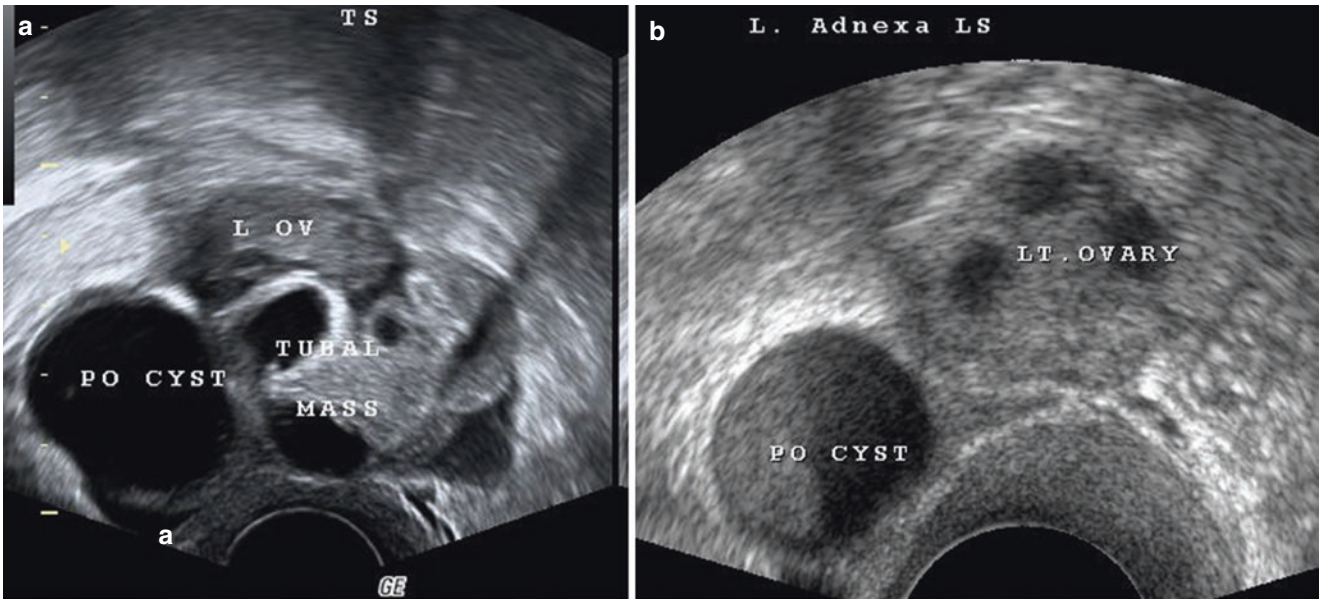

Fig. 9.35 Infected PO cyst. (**a**) Showing thick walls and forming a part of a TO mass in a patient with PID. (**b**) Scan image of the same patient following treatment with antibiotics. The cyst shows turbid contents with fluid–fluid level

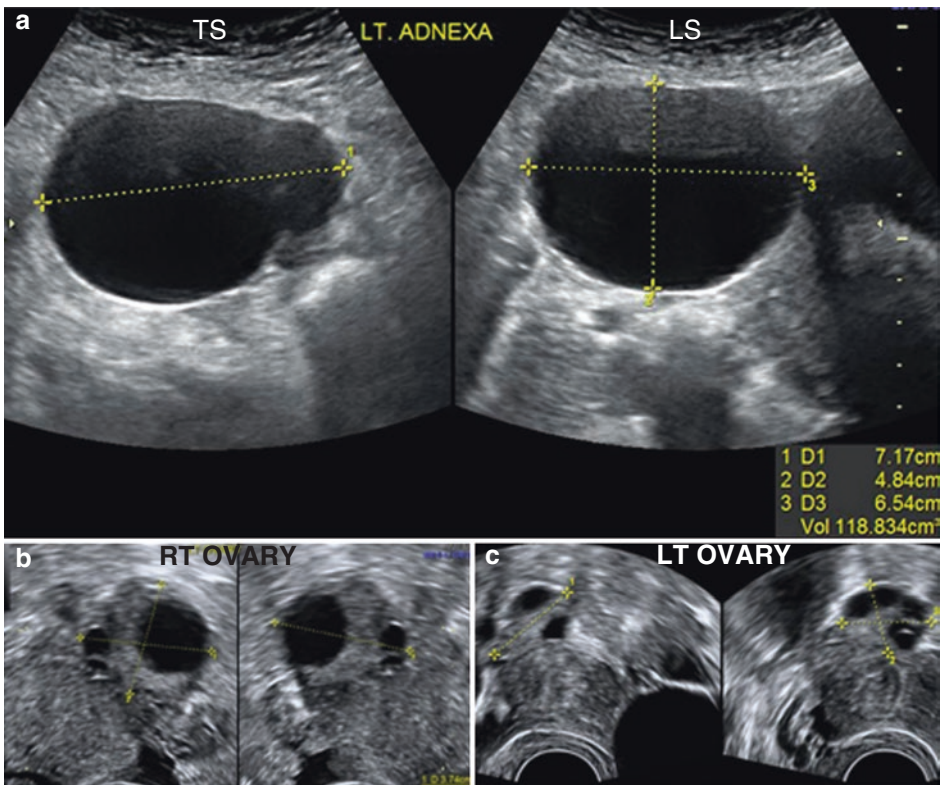

Fig. 9.36 PO cyst with torsion. Patient presented with acute abdominal pain. Scan done elsewhere had shown a left ovarian septate cyst. (**a**) TAS shows a 118 cc anechoic cyst. (**b**,**c**) Normal right and left ovary seen separate from the cyst. (**d**) TVS shows an anechoic cyst with septae. (**e**) Cyst walls showing flow with an RI of 0.65. (**f**) Twisted pedicle of the torsed PO cyst is seen showing a whirlpool sign on greyscale and Doppler (*arrows*)

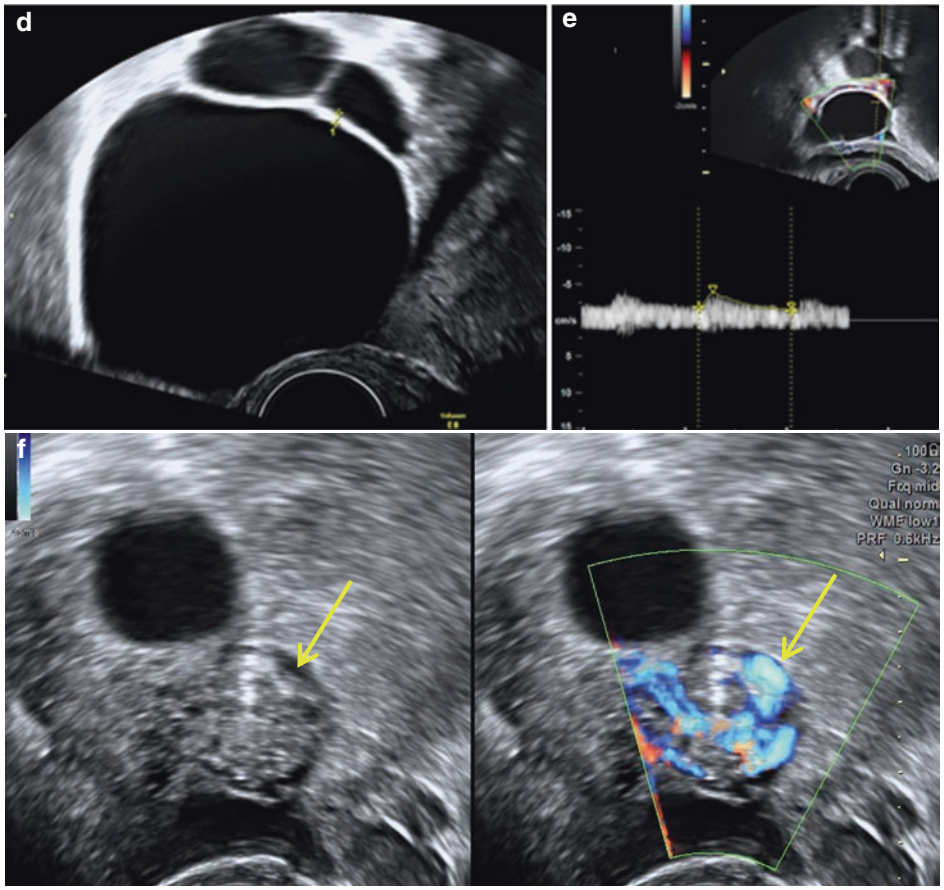

Fig. 9.36 continued

Summary: Paraovarian and Paratubal Cysts

- They are commonly found adnexal cysts that are usually benign and asymptomatic.
- They are seen separate from the ovary or can be pushed away from the ovary, and this helps in differentiating them from ovarian cysts.
- They are typically anechoic, unilocular, smooth-walled, simple cysts.
- They may occasionally be neoplastic or undergo torsion.

9.7 Peritoneal Inclusion Cysts

Peritoneal inclusion cysts are basically areas of loculated fluid trapped between adhesions. They are generally a result of peritoneal insult secondary to endometriosis, pelvic inflammatory disease or previous pelvic surgery, which results in fluid collection within adhesions. Most of these patients are asymptomatic unless there is an underlying pathology like endometriosis or PID. Peritoneal inclusion cysts are incidental findings on ultrasound. Their importance lies in the fact that they may be mistaken for other pathological adnexal cystic masses. This is particularly so if they are seen in a patient who has undergone surgery for an ovarian cyst, where they may be mistaken to be a recurrence of the ovarian pathology, or if they are seen in postmenopausal women where they are mistaken to be an ovarian neoplastic pathology (because small atrophic ovaries in postmenopausal women may not be visualized).

Ultrasound Features of Peritoneal Inclusion Cysts
(Figs. 9.37, 9.38, 9.39, 9.40 and 9.41)

- They are typically multilocular cystic masses that conform to the shape of an area in the pelvis between pelvic organs, giving them a bizarre shape.
- The contents are usually uniformly anechoic, but in some low level internal echoes may be seen.
- The septae are generally thin but may occasionally be thick in some parts
- These adhesions that appear like septae, unlike the septae of a neoplastic cyst, are under less pressure from the liquid content and therefore usually undulate and oscillate a little on pressure from the probe, the so-called 'flapping-sail' sign.
- Incomplete septae may also be seen because of infolding of these lax adhesions/septae but, unlike hydrosalpinges, they do not show the typical 'beads-on-string' appearance (the compressed tubal mucosal folds of hydrosalpinges).
- Small hyperechoic papillary projections or irregularities may occasionally be seen along the walls/septae of these cysts.
- On Doppler, in about half the cases, some minimal high resistance flow may be seen in the septae.
- Since these are loculated fluid collections within adhesions, the surrounding pelvic organs will show restricted mobility or may be fixed.
- The ovary may be seen lying within or beside the cystic mass. This could be misinterpreted to be a solid component of a neoplastic cyst, or the cyst may be assumed to be of ovarian origin because of the adjoining ovarian tissue. The ovaries can be made out to be separate from the cystic mass since most often they show antral follicles along the periphery, just within the outer margins (including the surface adjoining the peritoneal inclusion cyst).

Features that help distinguish peritoneal inclusion cysts from other adnexal cysts are:

- They are not well circumscribed like ovarian and paraovarian cysts.
- They are irregular in shape and are seen filling the spaces between other pelvic organs.
- Pointed beak-like or narrow extensions may be seen along their outer margins, as the fluid fills narrow gaps between tissue planes.
- The septae tend to be lax and show the 'flapping-sail' sign.

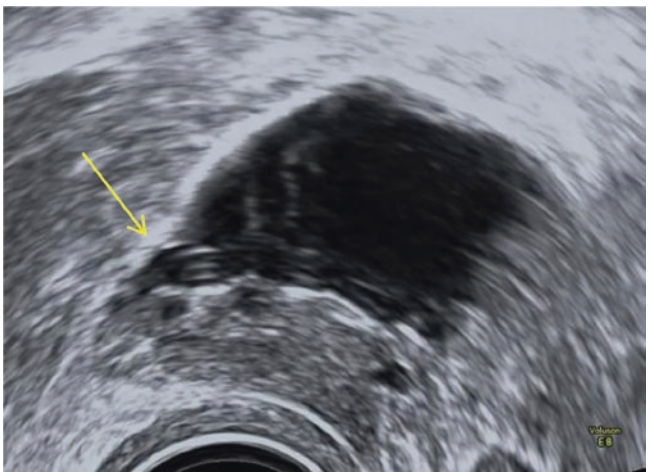

Fig. 9.37 Small area of loculated fluid seen just above the ovary showing a few flimsy adhesions. A narrow beak-like extension is seen (*arrow*)

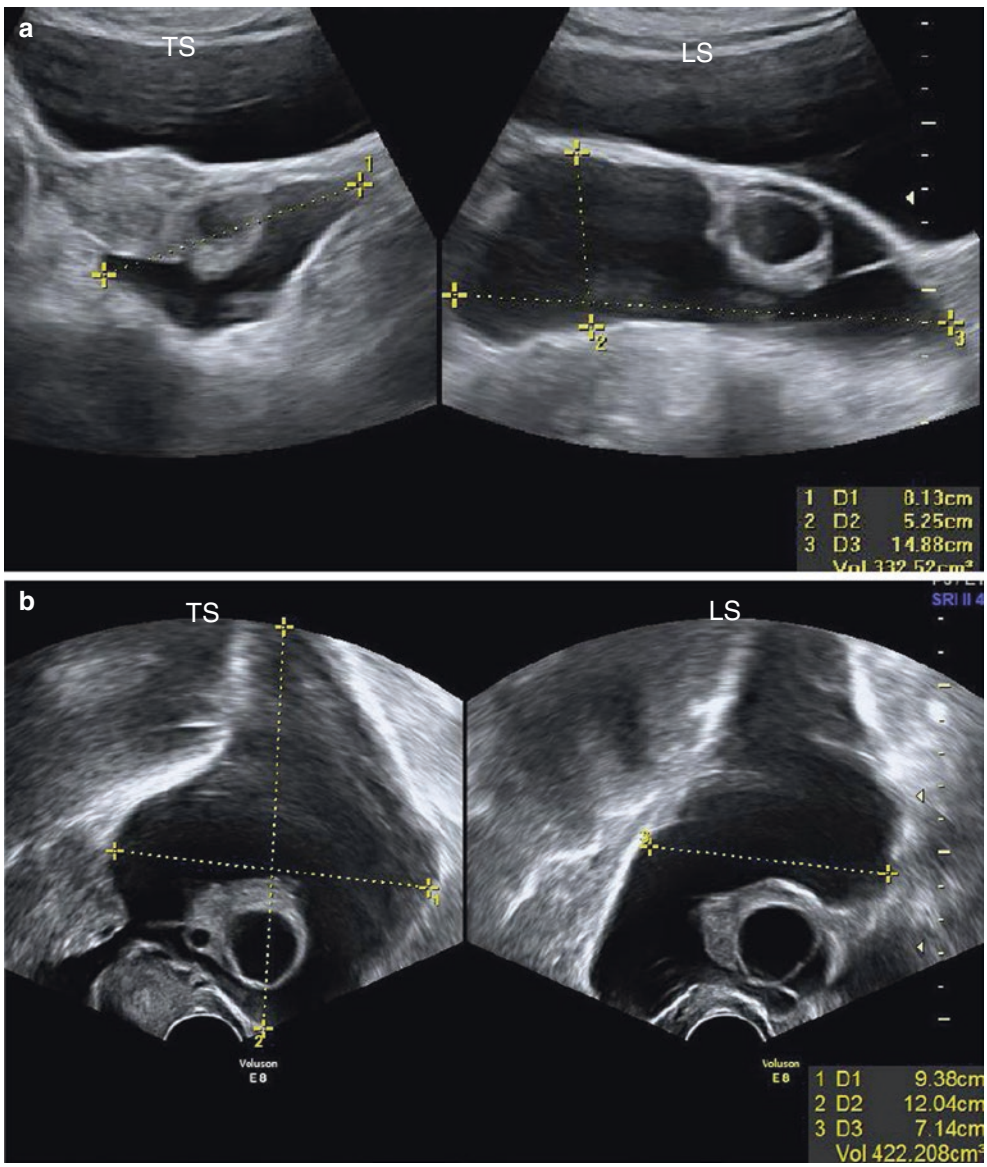

Fig. 9.38 Peritoneal inclusion cyst in a patient with previous surgery: (**a**) TAS, (**b**) TVS. The image shows that the cyst takes the shape of the peritoneal cavity in that area, filling the gaps and extending into the narrow crevices between the pelvic organs. The ovary is seen protruding into the peritoneal cyst

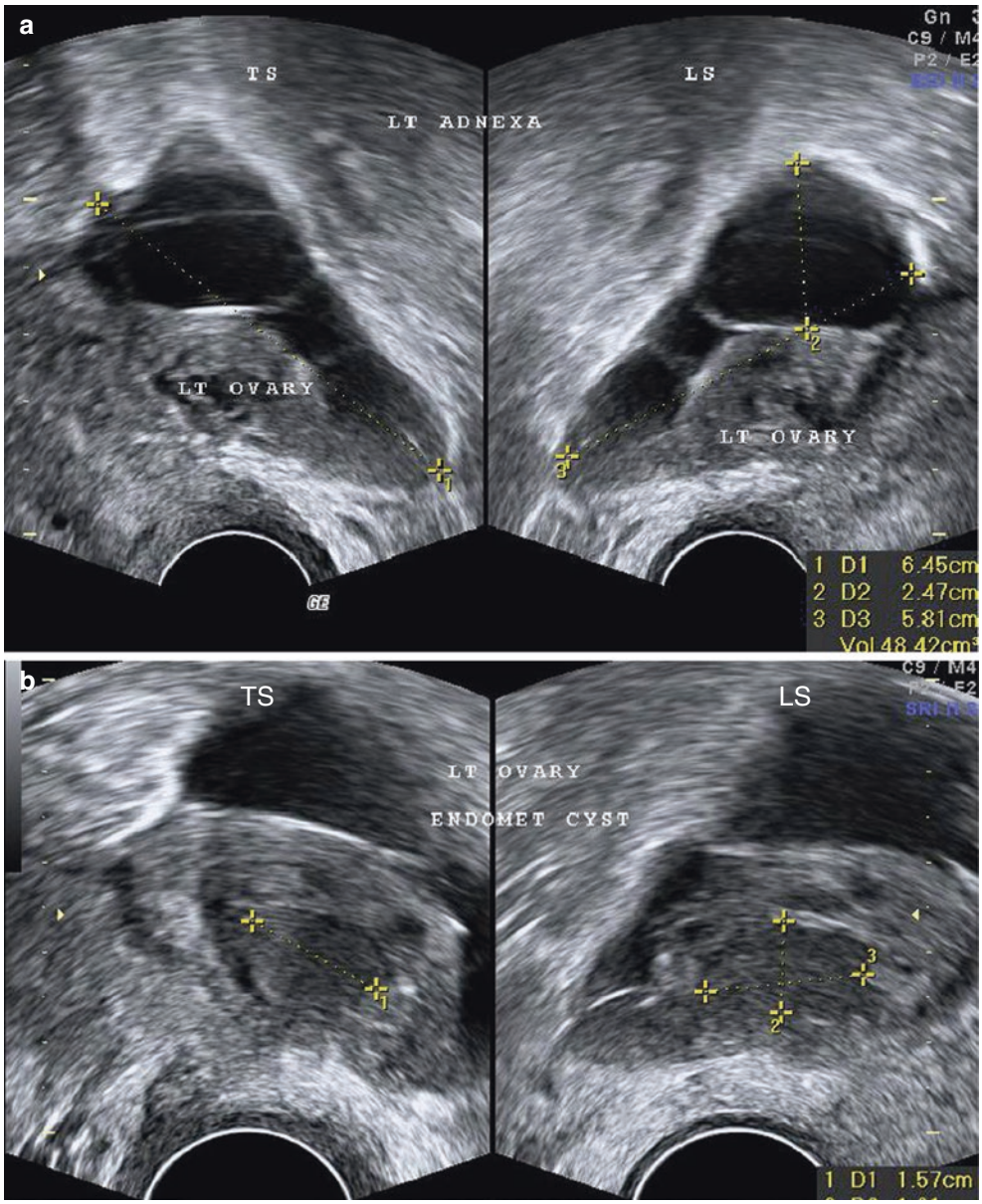

Fig. 9.39 Peritoneal inclusion cyst in a patient with endometriosis. (**a**) Ovary seen protruding into the cyst and multiple periovarian adhesions are noted. (**b**) The ovary shows a small endometriotic cyst

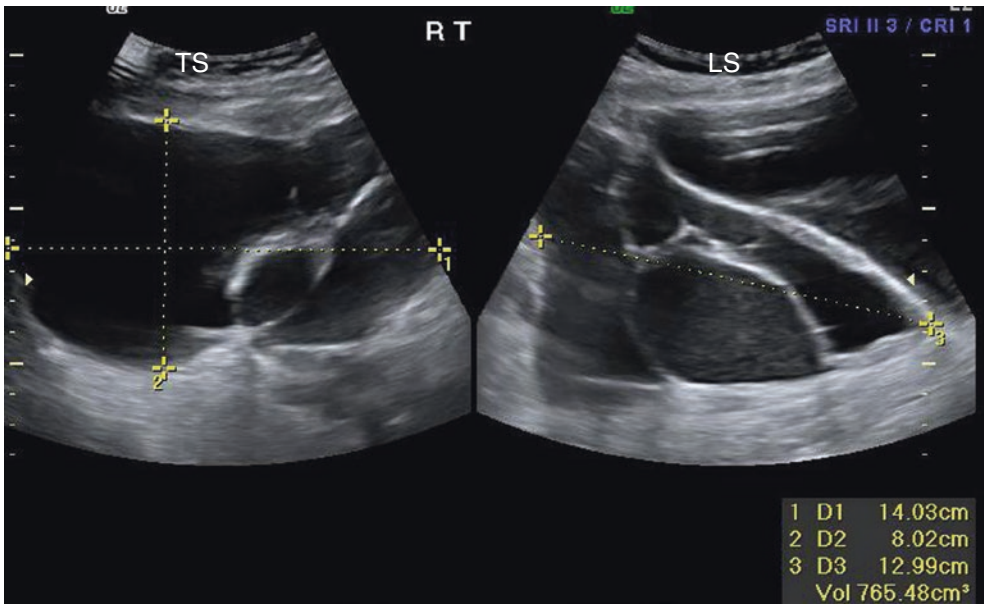

Fig. 9.40 Large peritoneal inclusion cyst (765 cc) in a patient treated for pelvic tuberculosis. Adhesions in this case appear thick and bright, and the loculated fluid within shows fine low-grade internal echoes

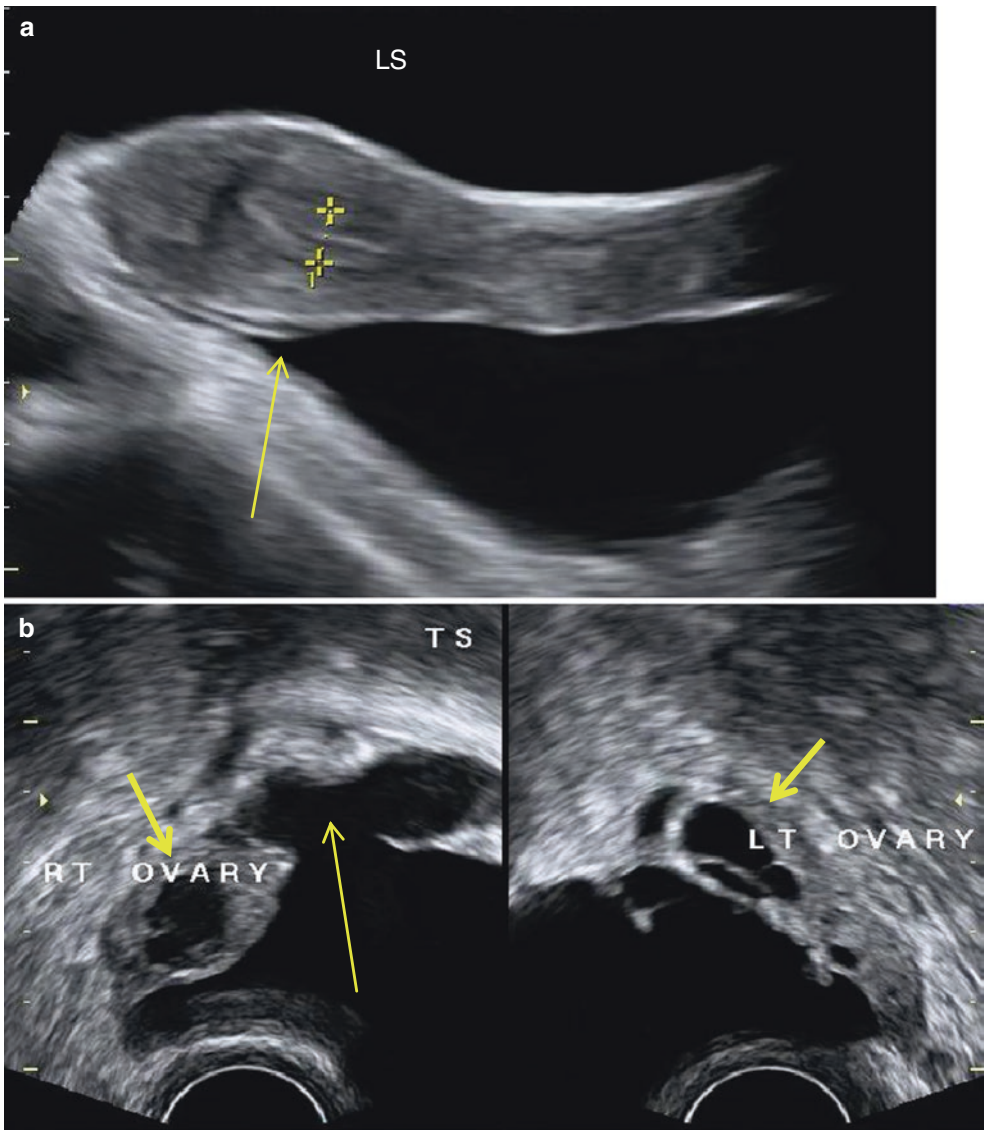

Fig. 9.41 Peritoneal inclusion cyst in a patient operated a few years ago for a left endometriotic cyst. (**a**) TAS – shows a uterus lying over a large peritoneal inclusion cyst. Narrow extension of fluid is seen at its upper margin behind the uterus (*arrow*), (**b**) TVS showing the right and left ovaries *(short arrows)* lying beside the cystic mass and adherent to the lateral pelvic walls. The irregular outline and shape of the cystic mass are seen well *(long arrow)*. (**c**) Locules showing contents with varying echogenicity (anechoic and hypoechoic). An incomplete septum (*long arrow*) and a small hyperechoic projection is seen in the cyst wall (*short arrow*), which is a feature known to be seen at times in these cysts

Fig. 9.41 continued

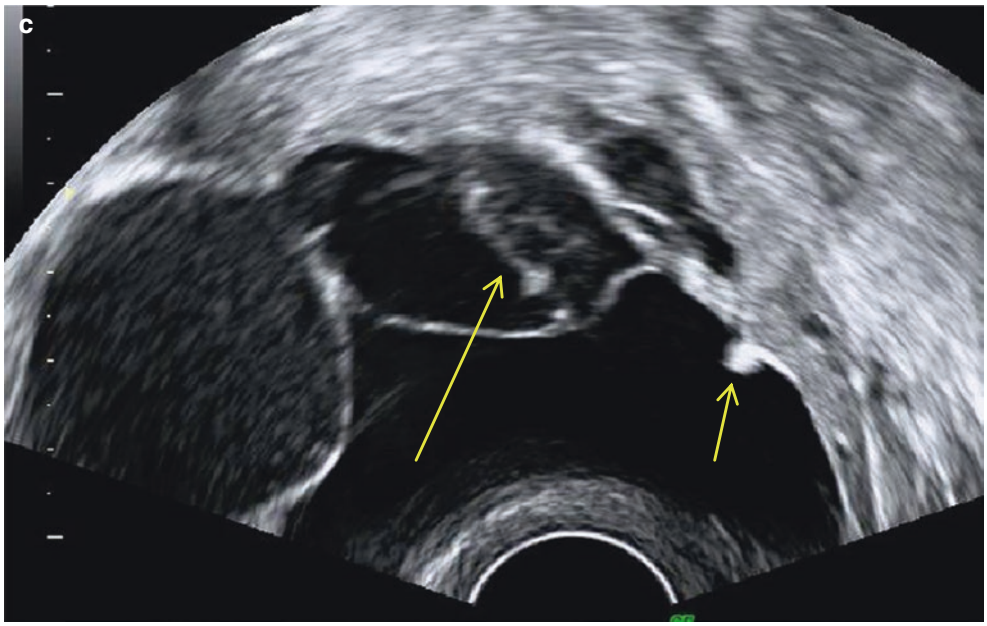

Summary: Peritoneal Inclusion Cysts

- These are seen in women with previous a history of surgery, history of chronic infections like tuberculosis or endometriosis.
- Most often these are easily diagnosed as areas of loculated fluid within adhesions.
- At times, diagnosis may be challenging and points in favour of peritoneal inclusion cyst are their non-circumscribed irregular outlines with beak-like narrow extensions between tissue planes.

Suggested Reading

Borgfeldt C, Andolf E (1999) Transvaginal sonographic ovarian findings in a random sample of women 25–40 years old. Ultrasound Obstet Gynecol 13:345–350. doi:10.1046/j.1469-0705.1999.13050345

Fischerova D (2011) Ultrasound scanning of the pelvis and abdomen for staging of gynecological tumors: a review. Ultrasound Obstet Gynecol 38:246–266. doi:10.1002/uog.10054

Gjelland K, Granberg S (2003) OC194: the diagnosis and ultrasound based management of tubo-ovarian abscess. Ultrasound Obstet Gynecol 22:52. doi:10.1002/uog.396

Ludovisi M et al (2014) Imaging in gynecological disease (9): clinical and ultrasound characteristics of tubal cancer. Ultrasound Obstet Gynecol 43:328–335. doi:10.1002/uog.12570

Molander P et al (2001) Transvaginal power Doppler findings in laparoscopically proven acute pelvic inflammatory disease. Ultrasound Obstet Gynecol 17:233–238. doi:10.1046/j.1469-0705.2001.00353

Panlilio-Vitriolo RR (2007) P43.14: ultrasonography in the diagnosis and follow-up of patients with abdominopelvic tuberculosis. Ultrasound Obstet Gynecol 30:617–618. doi:10.1002/uog.4951

Potter AW, Chandrasekhar CA (2008) US and CT evaluation of acute pelvic pain of gynaecologic origin in nonpregnant premenopausal patients. Radiographics 28:1645–1659

Rezvani M, Shaaban AM (2011) Fallopian tube disease in the nonpregnant patient. Radiographics 31(2):527–548

Savelli L et al (2004) Transvaginal sonographic appearance of peritoneal pseudocysts. Ultrasound Obstet Gynecol 23:284–288. doi:10.1002/uog.986

Timor-Tritsch IE et al (1998) Transvaginal sonographic markers of tubal inflammatory disease. Ultrasound Obstet Gynecol 12:56–66. doi:10.1046/j.1469-0705.1998.12010056

Valentin L, Akrawi D (2002) The natural history of adnexal cysts incidentally detected at transvaginal ultrasound examination in postmenopausal women. Ultrasound Obstet Gynecol 20:174–180. doi:10.1046/j.1469-0705.2002.00709

Ultrasound Evaluation of Pregnancy-Related Conditions

10

10.1 Ectopic Pregnancy

An ectopic pregnancy is a pregnancy located outside the normal endometrial cavity. A variety of ectopic pregnancies are possible based on the location. These include tubal (most common – about 95 % of all ectopic pregnancies), interstitial, cornual, cervical, ovarian, scar, intra-abdominal, intramyometrial and heterotopic pregnancies.

Ectopic pregnancy is more often seen in patients with a history of infertility, PID and a previous ectopic pregnancy. The incidence of ectopic pregnancy is on the rise on account of increasing in-vitro fertilisation (IVF) conceptions. Clinical features include amenorrhoea, a positive pregnancy test (or high serum beta hCG), spotting, abdominal pain and even hypovolemic shock.

Ultrasound is considered the modality of choice for diagnosis of ectopic pregnancy.

Ultrasound Features of an Ectopic Pregnancy (Fig. 10.1)

- The absence of an intrauterine gestational sac in the endometrial cavity (especially with a serum beta hCG value of more than 1000 mIU/mL), increases the likelihood of an ectopic pregnancy.
- The tissue of an ectopic pregnancy on ultrasound appears as a central cystic area (the gestational sac) surrounded by thick hyperechoic trophoblastic tissue, showing peripheral flow on Doppler. This is pathognomonic for an ectopic pregnancy but often cannot be demonstrated on ultrasound.
- The gestational sac may or may not show a yolk sac and fetal pole.
- On enlarging the image, on 2D greyscale, low-velocity flows within the trophoblastic tissue are often seen and often useful in confirming the diagnosis.
- In cases with ectopic pregnancies, the endometrium may show fluid collection, giving it the appearance of a gestational sac termed 'pseudo-gestational sac'. The differences between a true gestational sac and a 'pseudo-gestational sac' are discussed in Chap. 14.
- The endometrium undergoes decidualisation, and in a patient with an ectopic pregnancy. It can appear thick and may show multiple tiny cystic spaces (closer to the endomyometrial junction), which should not be mistaken for a tiny gestational sac.

Other than 'pseudo-gestational sac' and cysts in a decidualised endometrium, the differential diagnosis for an ectopic pregnancy includes a complete abortion and corpus luteal haemorrhage (discussed in Chap. 14).

Transabdominal scan is very useful in picking up an ectopic pregnancy because it pushes all the extra-pelvic structures (that could mimic or shadow a small ectopic pregnancy mass) out of the pelvis. This helps locate the site of any mass, even a small adnexal mass, and one is less likely to miss an ectopic pregnancy mass. Also, it helps to know exactly where to look for the ectopic pregnancy mass at the transvaginal scan that follows the transabdominal scan.

Diagnosis of an ectopic pregnancy is very important because they may present with acute pain and there is potential for rupture and intraperitoneal haemorrhage. The management of ectopic pregnancies other than tubal ectopic pregnancies is difficult, with intramuscular or local methotrexate and local potassium chloride being resorted to in some cases, depending upon the location of the ectopic pregnancy and its viability. Local administration of these agents is done under ultrasound guidance. The management of ruptured non-tubal ectopic pregnancies is even more challenging.

M. Sibal, *Ultrasound in Gynecology*, DOI 10.1007/978-981-10-2714-7_10

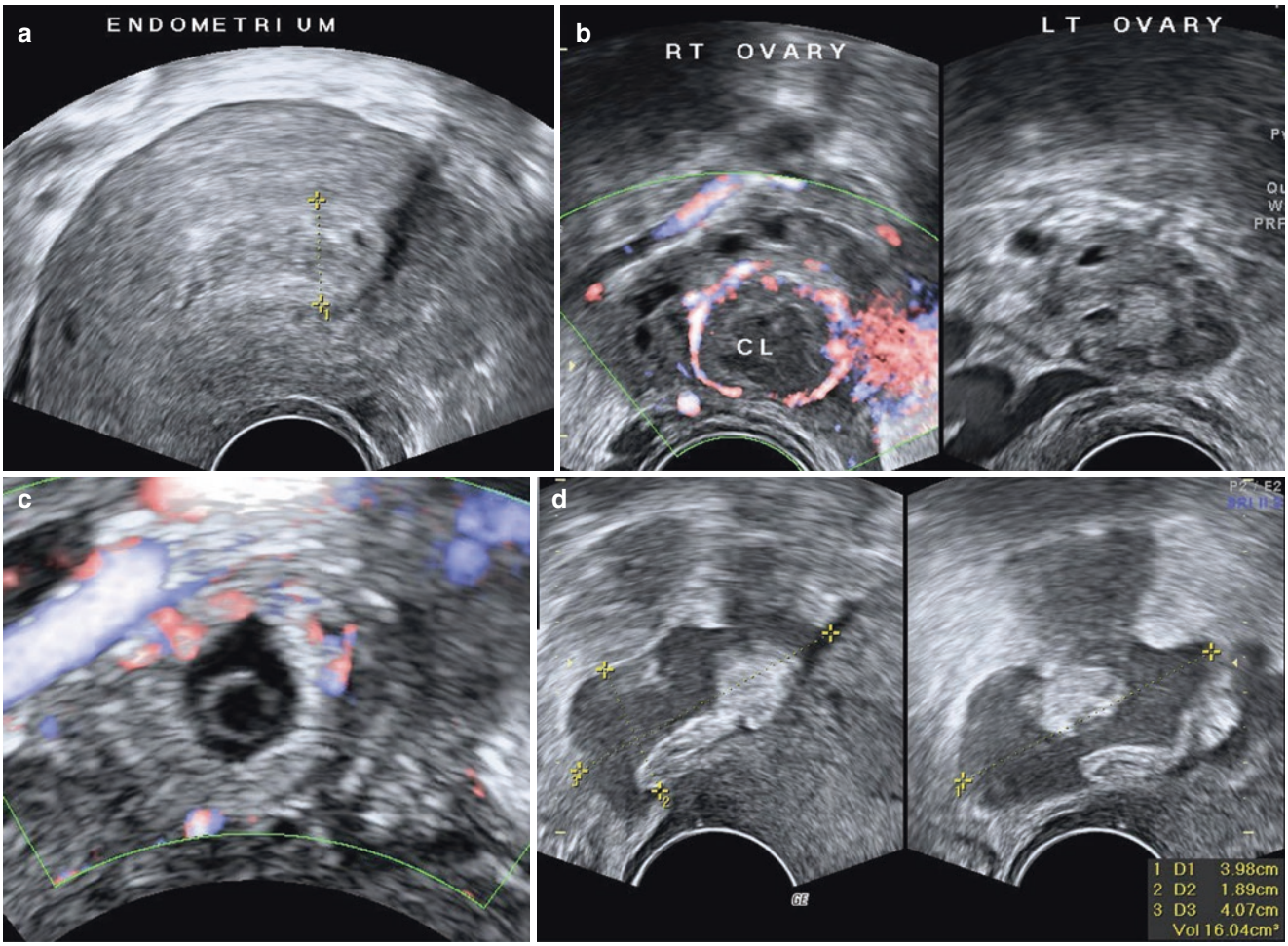

Fig. 10.1 Findings in a case of an ectopic pregnancy. (**a**) Echogenic endometrium with a few tiny cystic spaces suggestive of decidualised endometrium. Endometrial cavity showing no evidence of intrauterine pregnancy. (**b**) Ovaries showing a corpus luteum in the right ovary. (**c**) Ectopic pregnancy mass showing a central cystic area (i.e., the gestational sac) surrounded by a thick hyperechoic trophoblastic tissue, showing peripheral flow on Doppler. Yolk sac is seen within the gestational sac. This is pathognomonic of an ectopic pregnancy, but is not always seen. (**d**) Turbid-free fluid suggestive of blood is seen in the peritoneal cavity

10.1.1 Tubal Ectopic Pregnancy

This is the commonest type of ectopic pregnancy. The appearance on ultrasound varies depending upon how advanced the gestation is, and whether there is any associated bleeding from the lesion.

Ultrasound Features of Tubal Ectopic Pregnancy
(Figs. 10.2, 10.3, 10.4, 10.5, 10.6, 10.7, 10.8 and 10.9)

- The absence of an intrauterine pregnancy.
- The tubal ectopic pregnancy mass is seen as an extra-ovarian adnexal mass. It may be seen just adjacent to the ovary. The 'sliding sign' can be used to ascertain its extra-ovarian origin.
- Typically, it is a circumscribed mass, within which there is usually a gestational sac (seen as a central cystic space) showing thick hyperechoic trophoblastic tissue surrounding it.
- Within the gestational sac, one may or may not see a yolk sac and a fetal pole. The fetal pole will show pulsations if it is a live ectopic pregnancy. The presence of a yolk sac, a fetal pole or a fetal heart pulsation helps in making a confident diagnosis of an ectopic pregnancy.
- The trophoblastic tissue shows high peripheral vascularity (high-velocity, low-resistance flow), often termed 'ring-of-fire'.
- Ovaries appear normal with a corpus luteum. Most often, the corpus luteum is seen in the ipsilateral ovary but rarely, may be seen on the contralateral side. A corpus luteum can appear a little similar to an ectopic pregnancy, as it is circumscribed and may have a central cystic area.
- Doppler flows are of limited value in distinguishing an ectopic pregnancy from a corpus luteum. What helps in differentiating the two is the thick echogenic margins that surround the gestational sac of an ectopic pregnancy mass and its extra-ovarian location.
- Ectopic pregnancy masses are typically tender to touch.
- Sometimes the ectopic pregnancy mass may not be as well circumscribed or well defined as mentioned above, because of haemorrhage from the ectopic pregnancy resulting in a hematosalpinx. The hematosalpinx appears as an elongated tortuous heterogeneous mass seen in the adnexa often beside the ovary. At times, the ectopic gestational mass may be seen within the hematosalpinx.
- Haemorrhage from a ruptured tubal ectopic pregnancy or a tubal abortion could result in blood and clots surrounding the ectopic pregnancy mass forming a complex, heterogeneous (i.e., with hypoechoic and hyperechoic areas) avascular mass. If bleeding has been massive, the entire ovary, ectopic pregnancy mass, etc., might all be lying within a huge pelvic clot, and the tissue of the ectopic pregnancy may be difficult to identify on ultrasound, within the mass.
- In an ectopic pregnancy, the fluid in the pelvis is typically turbid (suggesting it is blood) due to tubal rupture. Sometimes the haemoperitoneum is massive, and blood and clots may be seen outside the pelvis, in the paracolic gutters and Morisson's pouch.
- An important differential diagnosis for a ruptured tubal ectopic pregnancy is a corpus luteal haemorrhage (discussed in Chap. 14). What helps distinguish the two is the absence of a well-defined extra-ovarian adnexal mass and a negative urine pregnancy test or normal levels of serum beta hCG, in the latter.

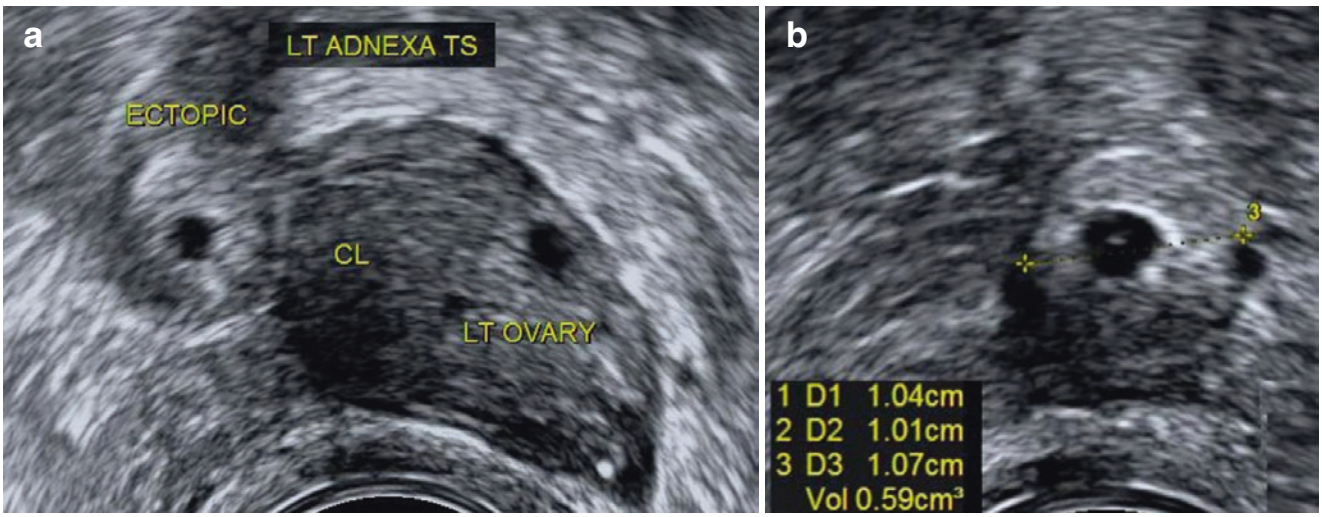

Fig. 10.2 Case of tubal ectopic pregnancy (**a**) Extra-ovarian adnexal mass is seen just adjacent to the ovary. (**b**) The ectopic pregnancy mass shows a central cystic area (the gestational sac) surrounded by thick hyperechoic trophoblastic tissue

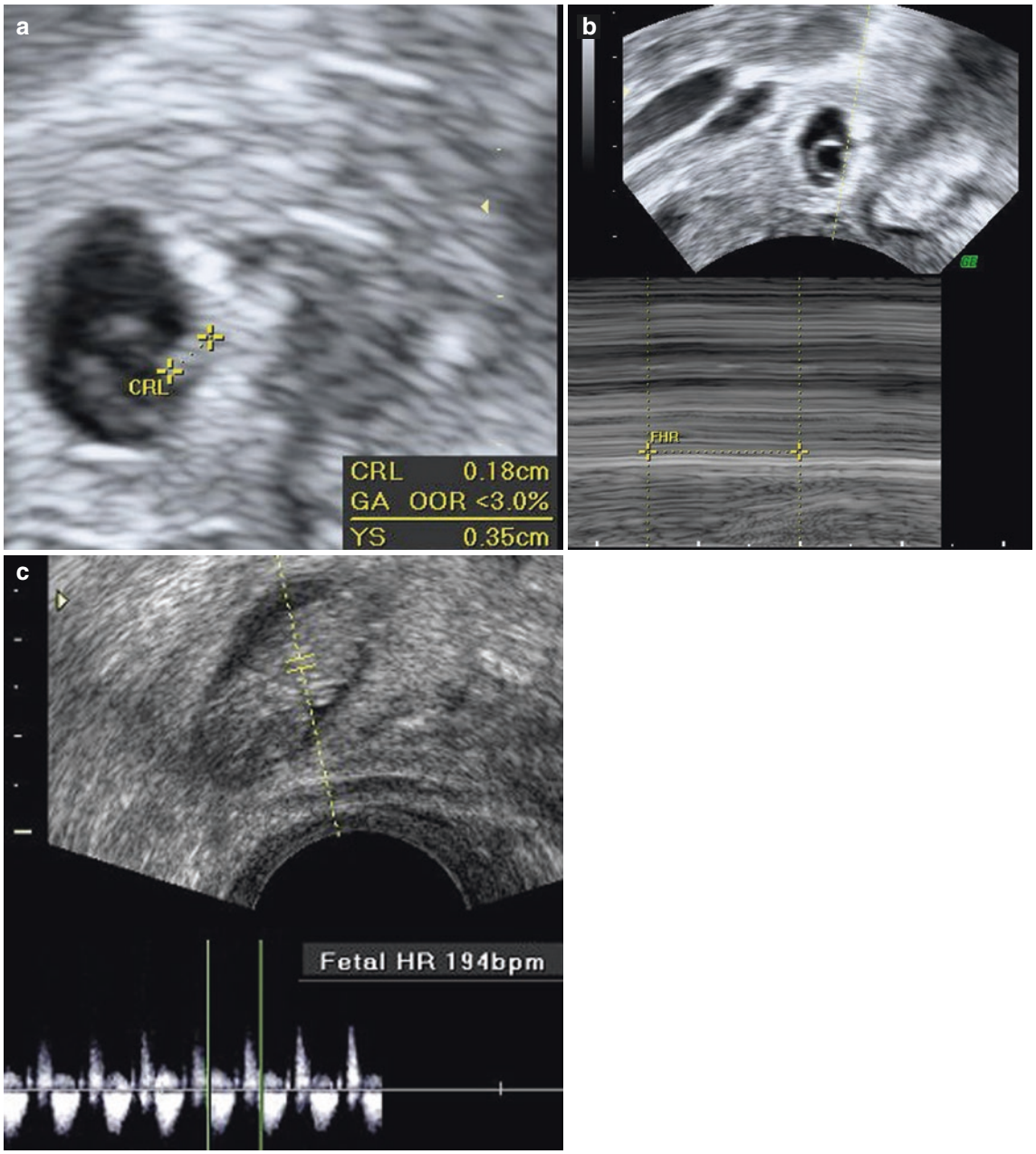

Fig. 10.3 Ectopic tubal pregnancies. (**a**) Case 1 - gestational sac showing yolk sac and a fetal pole. (**b**) Image showing tracing of fetal heart pulsation. (**c**) Case 2 - large fetal pole with fetal heart pulsation

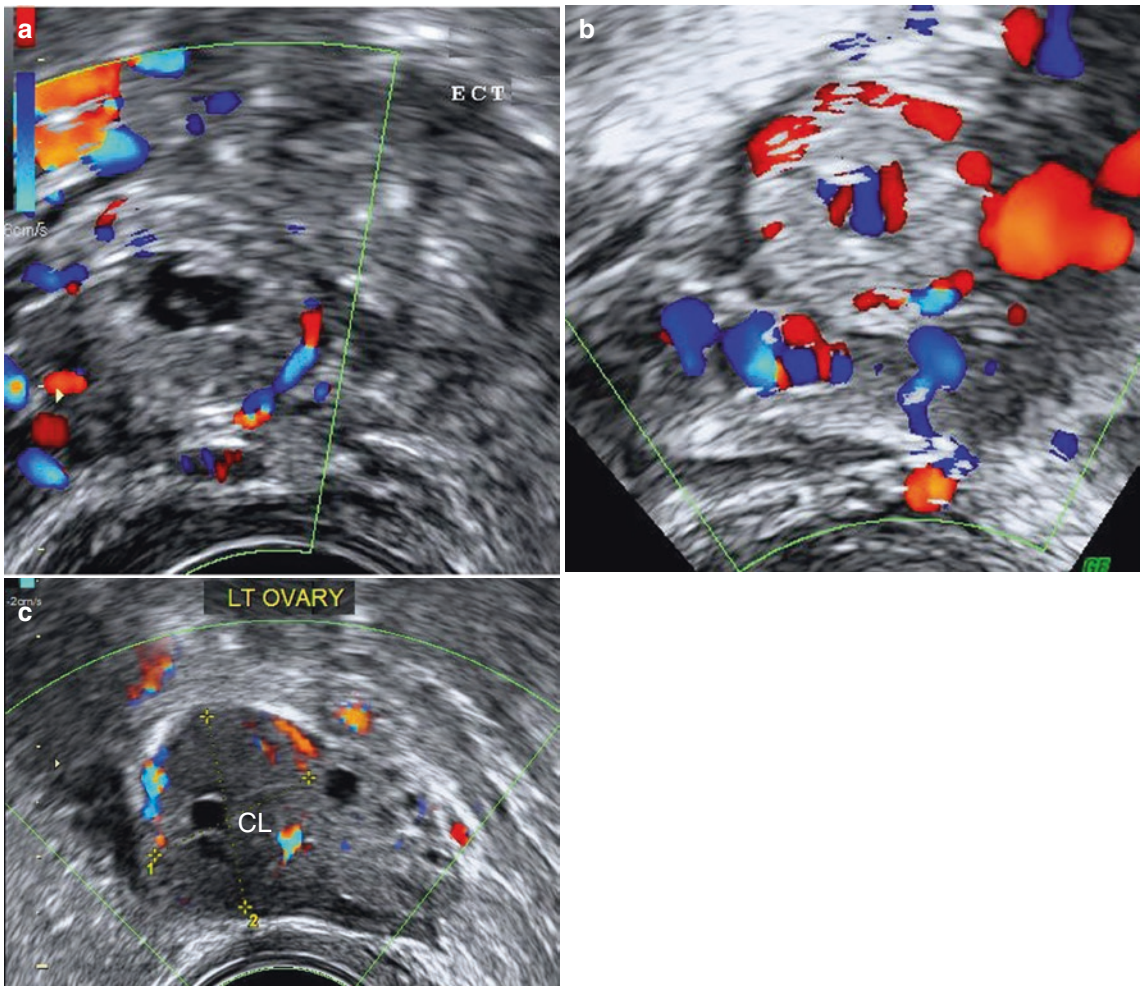

Fig. 10.4 Live tubal ectopic pregnancy. (**a**) Flow is seen surrounding the trophoblastic tissue. (**b**) In addition to peripheral vascularity, flow is seen in the centre of the ectopic pregnancy mass due to fetal heart pulsation. (**c**) The ovary shows a corpus luteum with a central cystic area and peripheral vascularity. The corpus luteum is, however, intra-ovarian, and does not show hyperechoic thick margins around the central cystic area

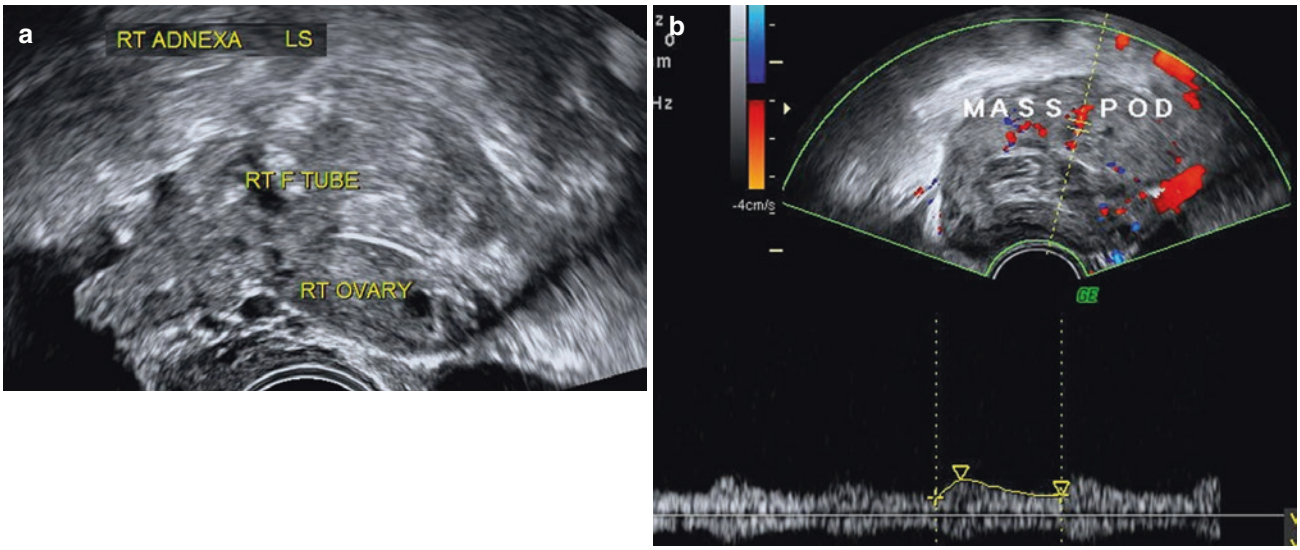

Fig. 10.5 Case of tubal ectopic pregnancy with hematosalpinx. (**a**) Hematosalpinx seen as an elongated tortuous heterogeneous mass just above the right ovary. Ectopic pregnancy tissue is not well visualised within the hematosalpinx. (**b**) The presence of ectopic pregnancy tissue was confirmed and located within the hematosalpinx, by the presence of flow around a suspicious hyperechoic area (the tissue of the ectopic pregnancy) which was seen on 2D grey scale in the hematosalpinx

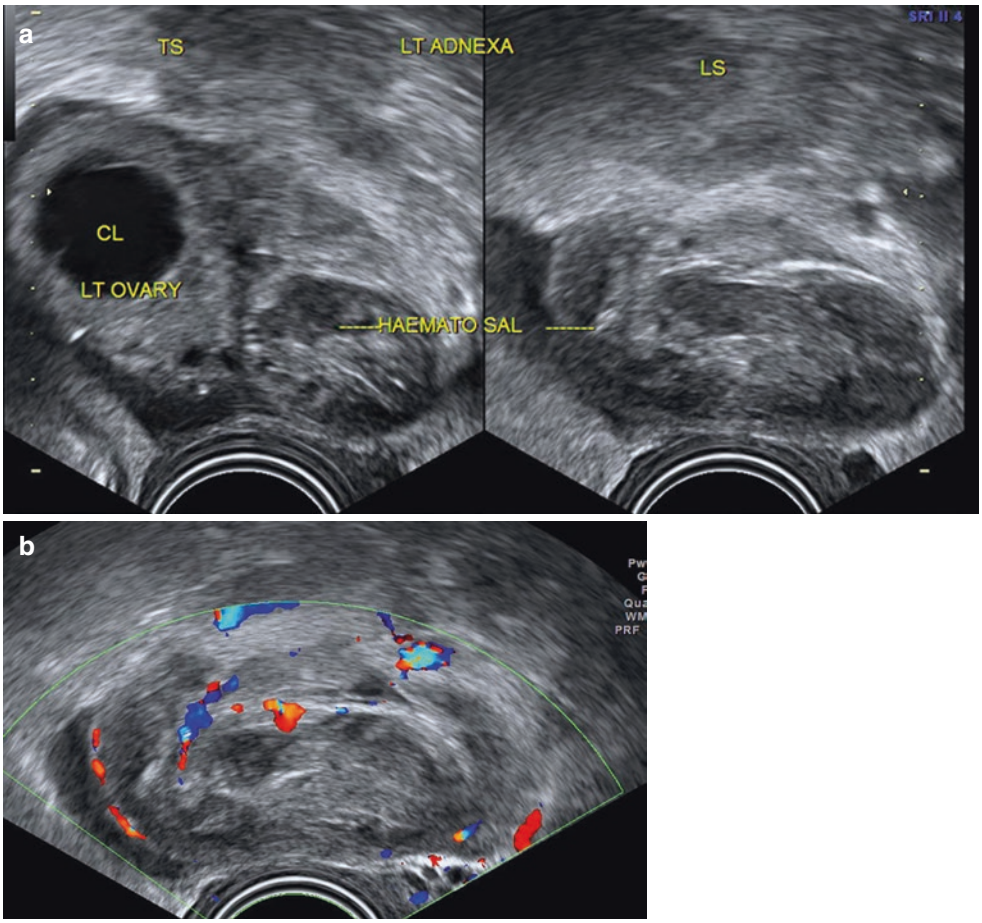

Fig. 10.6 Tubal ectopic pregnancy with hematosalpinx. (**a**) TS and LS view of the hematosalpinx. The hematosalpinx is seen just beside the left ovary. (**b**) Hematosalpinx seen as the complex mass which can resemble a clot. However, the presence of the flow in the walls of the tubal mass suggested that this is a hematosalpinx with a clot within, rather than an independent clot in the pelvis

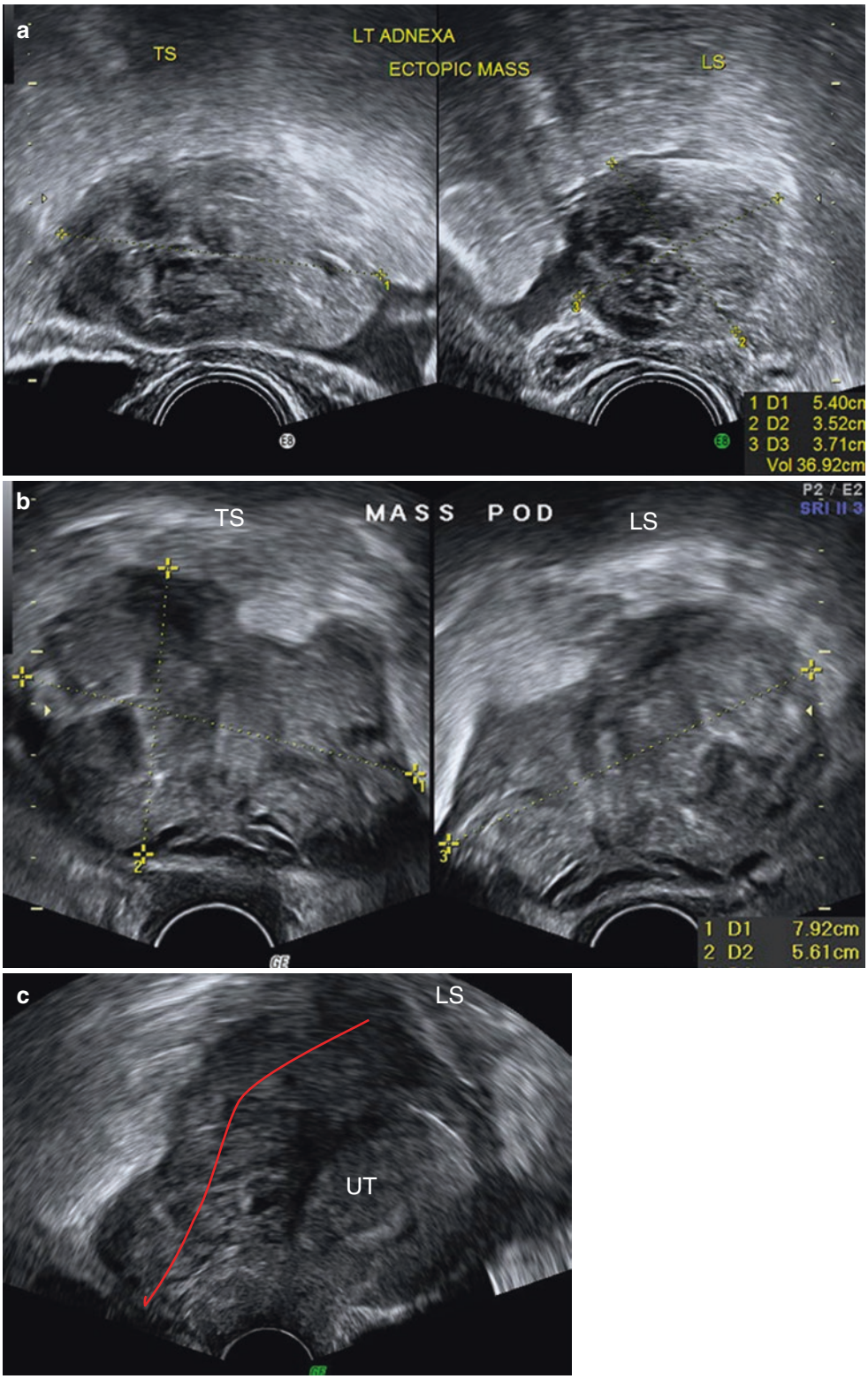

Fig. 10.7 Three different cases of ectopic pregnancy seen as a complex heterogeneous pelvic mass-suggestive of clots. (**a**, **b**) In all the images, the ectopic pregnancy tissue cannot be seen within the complex masses. (**c**) Massive clot (line traced across it) is seen in the POD, and in this case neither was the ectopic pregnancy mass, nor the ovary of that side, seen separately on scan

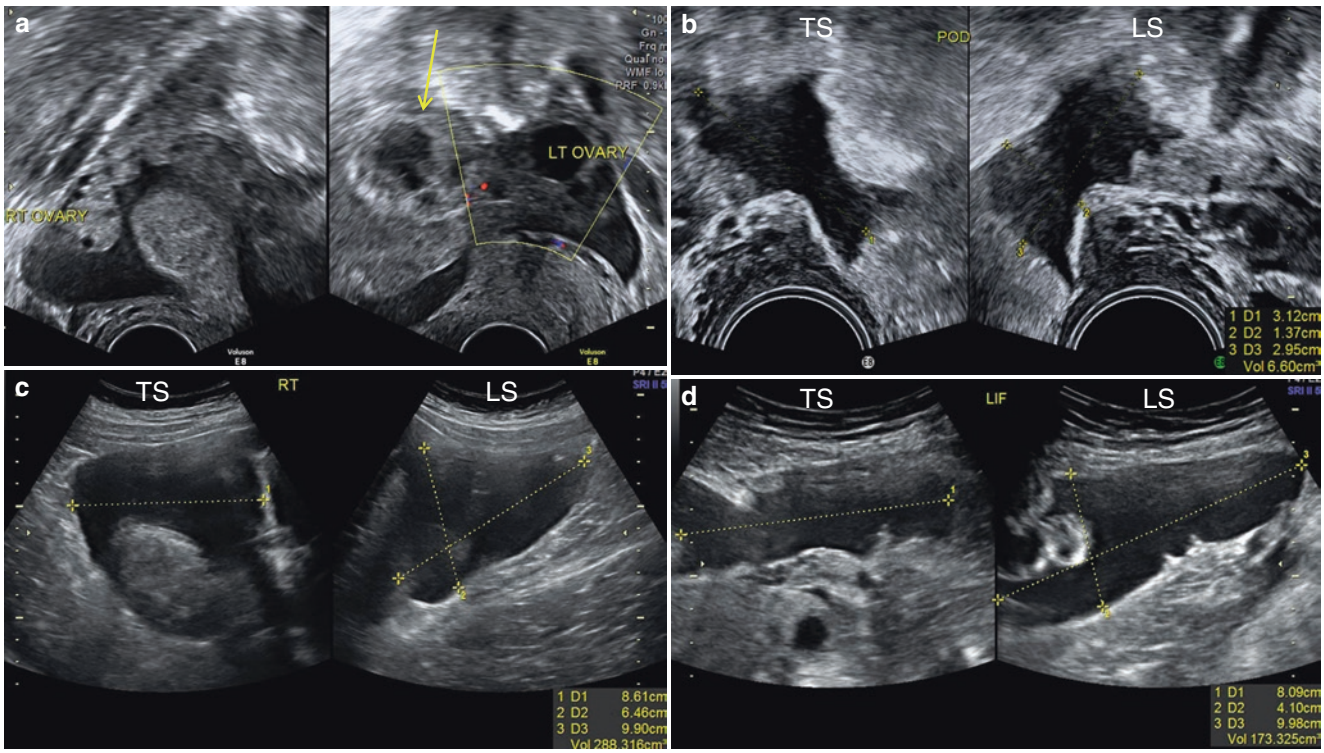

Fig. 10.8 Case of tubal ectopic pregnancy with significant haemoperitoneum. Turbid fluid suggestive of blood is seen in (**a**) the adnexa surrounding the ectopic pregnancy mass (*arrow*) and ovary, (**b**) the POD and (**c**, **d**) the general abdominal cavity

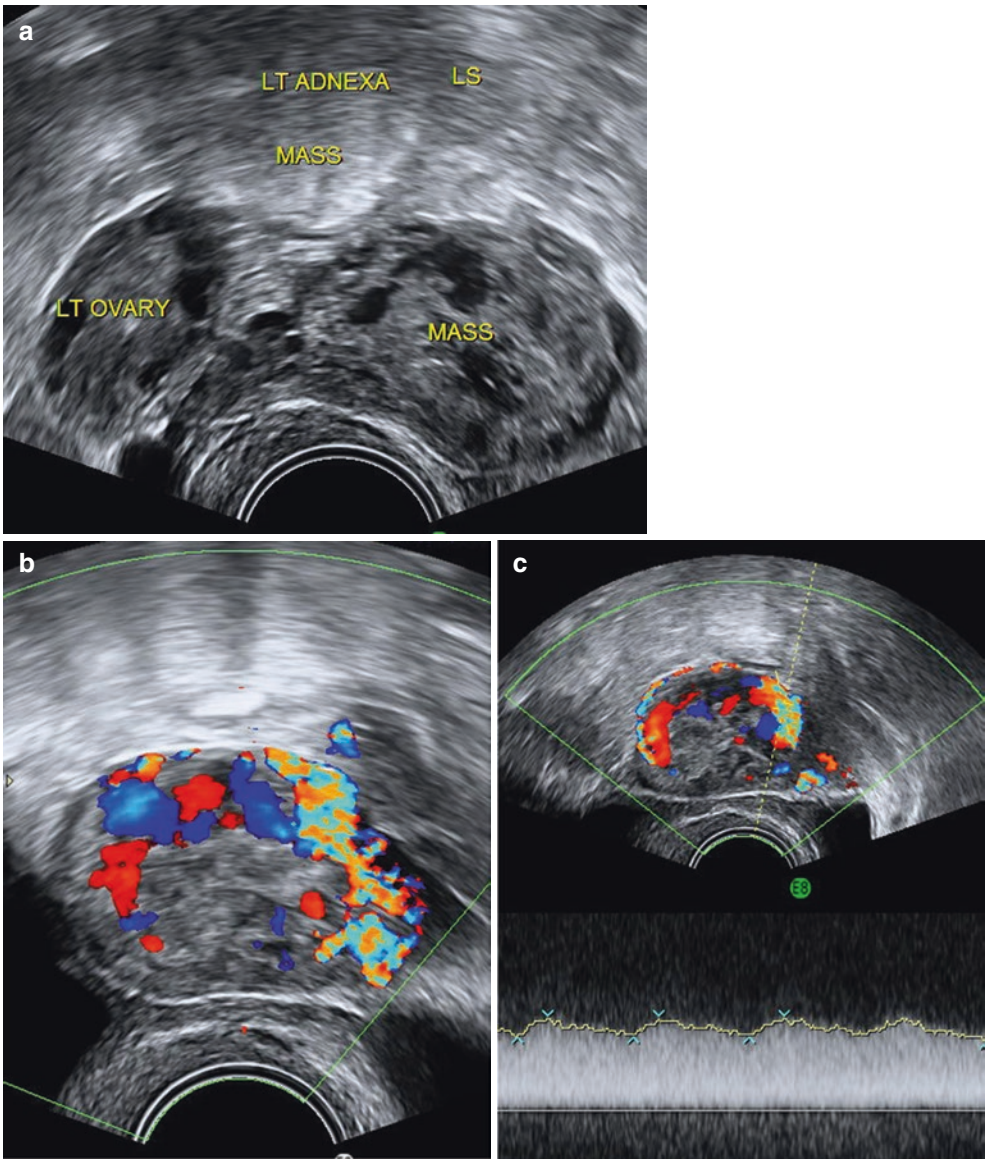

Fig. 10.9 Case of a failing tubal ectopic pregnancy with turbulent flow. (**a**) The ectopic pregnancy is seen just anterior to the left ovary and appears heterogenous because of prominent vessels within the trophoblastic tissue. (**b**) Turbulent flow with mosaic colour is seen within the trophoblastic tissue, similar to that of an AV malformation. (**c**) Flow in the trophoblastic tissue shows a low RI of 0.2 (also seen in AV malformations)

10.1.2 Interstitial Ectopic Pregnancy

This is a pregnancy located in the interstitial part of the fallopian tube. This is often wrongly termed as cornual ectopic pregnancy.

Ultrasound Features of Interstitial Ectopic Pregnancy (Figs. 10.10, 10.11, and 10.12)

- Here the tissue of the ectopic pregnancy (i.e., a circumscribed mass with a central cystic space suggestive of a gestational sac, surrounded by thick hyperechoic trophoblastic tissue that shows peripheral vascularity) is seen eccentrically located, just beyond the margins of the endometrial cavity. This is best seen on a 3D rendered coronal image of the uterine cavity.
- 'The interstitial line', a classic ultrasound feature of interstitial ectopic pregnancy, is a thin hyperechoic line seen extending from the superior and the lateral end of the endometrial cavity to the centre of the ectopic pregnancy mass.
- The ectopic pregnancy mass is seen surrounded by a thin myometrial rim.
- It appears as a mass bulging out at one cornual end of the uterus and moves en masse with the uterus.
- Like other ectopic pregnancies, the ectopic pregancy mass may be tender to touch.

At times, a normal intrauterine pregnancy close to the uterine cornua may be wrongly reported as an interstitial ectopic pregnancy, because of the uterine shape (Fig. 10.13). One must be aware of this possibility.

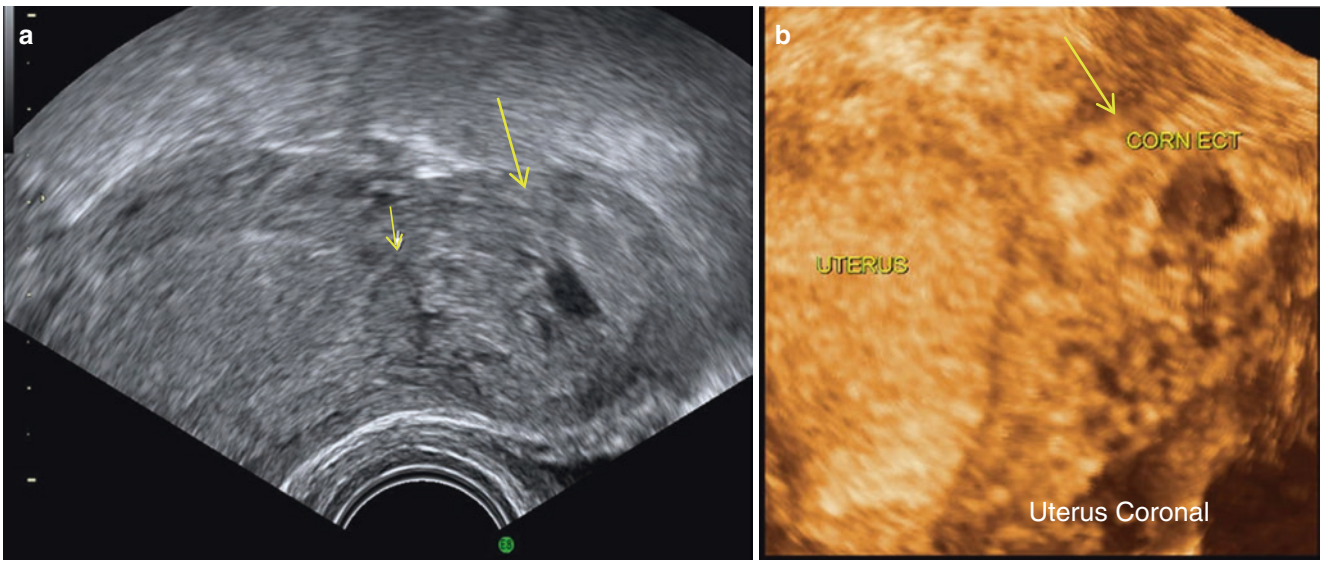

Fig. 10.10 Interstitial ectopic pregnancy. (**a**) Ectopic pregnancy tissue (*long arrow*) is visualised just beyond the endometrial margins on greyscale. The image shows the hyperechoic short interstitial line (*short arrow*) extending between endometrial margins and the ectopic pregnancy mass. The ectopic pregnancy mass is seen as a protrusion from the external surface of the uterus, protruding out at one cornua. (**b**) 3D pregnancy coronal image showing the ectopic pregnancy mass (*arrow*), beyond the endometrial margins

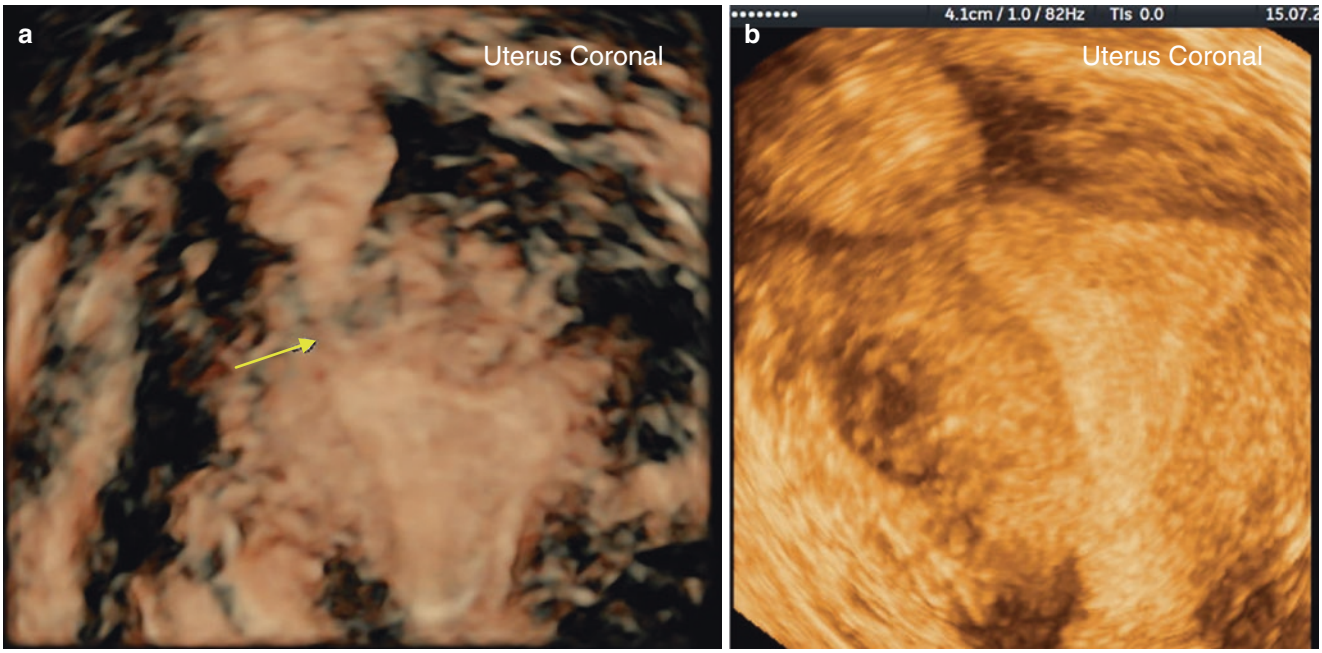

Fig. 10.11 Coronal image of two cases of interstitial ectopic pregnancy. (**a**) Interstitial line (*arrow*) is seen extending between the endometrial margins and the ectopic pregnancy mass. (**b**) 3D coronal image showing ectopic pregnancy tissue beyond the endometrial outline

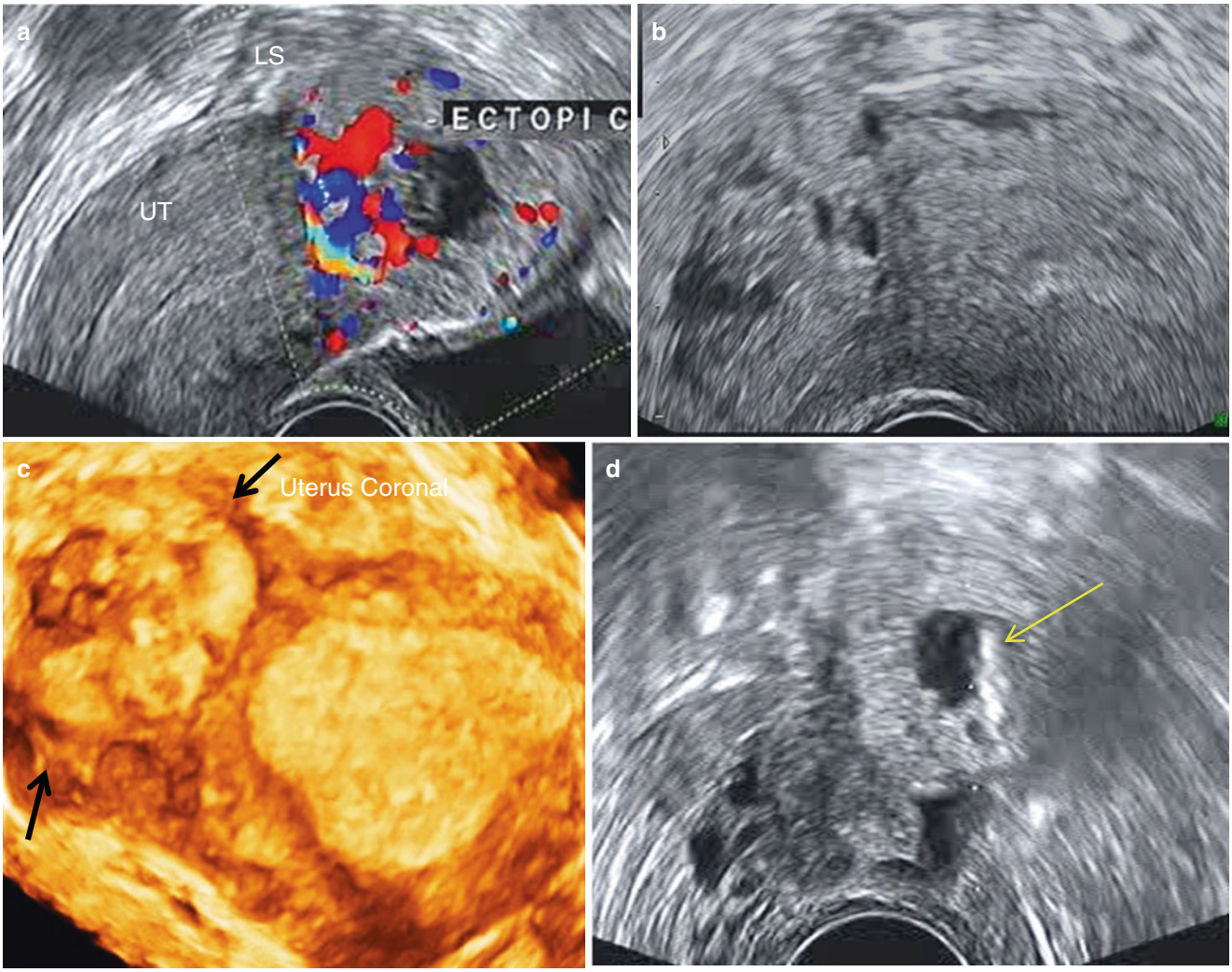

Fig. 10.12 Case of interstitial ectopic pregnancy. (**a**) Longitudinal section showing the ectopic pregnancy mass beyond the endometrial margins and bulging out of the uterine surface. The mass shows increased vascularity in the trophoblastic tissue. (**b**) Transverse section showing the ectopic pregnancy tissue and the uterine body. (**c**) Coronal image shows the ectopic pregnancy mass bulging out of the cornual end of the uterus. The ectopic mass is seen outside the endometrial margins. Thin myometrial tissue (*arrows*) is seen surrounding the ectopic pregnancy tissue. (**d**) Inj. methotrexate was administered locally for management. The needle is seen in situ (*arrow*) in the image

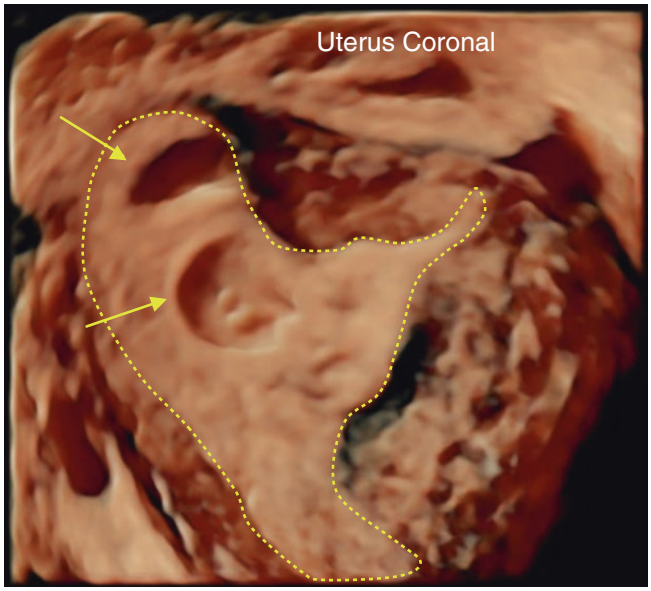

Fig. 10.13 Case of twin pregnancy (*arrows*) in a patient with an arcuate uterus. The upper sac was wrongly interpreted as a case of interstitial pregnancy. The gestational sac was, however, clearly seen within the endometrial margins (*outlined*) ruling out an interstitial pregnancy

10.1.3 Cornual Ectopic Pregnancy

This is pregnancy occurring in a non-communicating rudimentary horn of a uterus with a congenital anomaly. The pregnancy in these cases may extend for a longer duration, and is often picked up at rupture which causes severe pain and haemorrhage.

Ultrasound Features of Cornual Ectopic Pregnancy
(Figs. 10.14 and 10.15)

- Here, the pregnancy is seen in one horn of a bicornuate uterus, i.e. the non-communicating horn. It is important to demonstrate the lack of continuity between the endometrial cavity of the pregnant horn and the cervical canal below it.
- In cases of rupture (trophoblastic invasion of the entire wall), turbid fluid suggestive of blood may be seen in the pelvis.

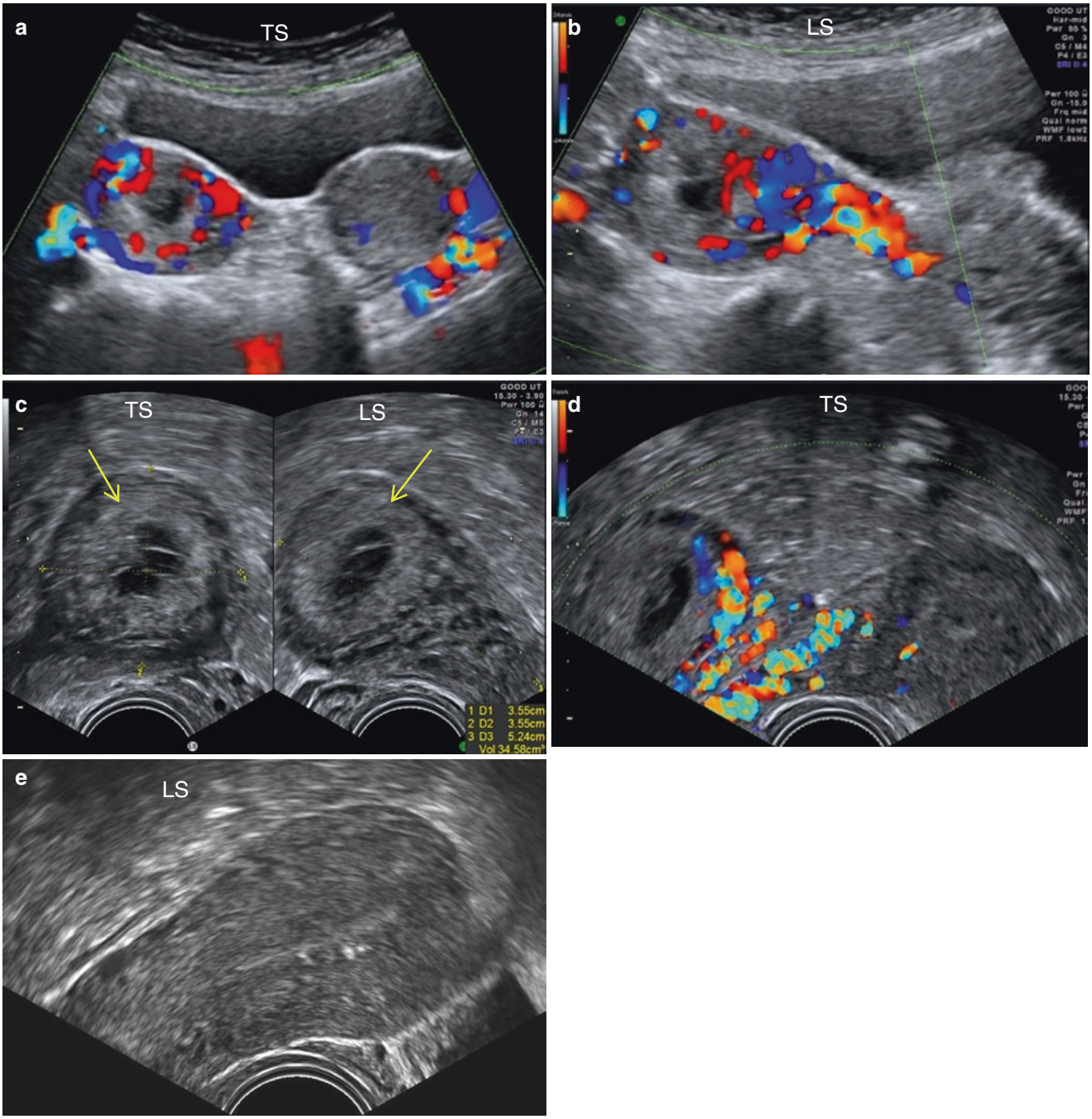

Fig. 10.14 Cornual ectopic pregnancy in a patient with a left-sided unicornuate uterus and a right-sided non-communicating rudimentary horn. (**a**) TS of the pelvis on TAS showing both horns of the uterus. The right gravid horn shows increased vascularity. (**b**) Longitudinal section showing the vascular pedicle of the non-communicating gravid horn connecting it to the main uterine body. (**c**) Ectopic pregnancy tissue is seen in the rudimentary horn which shows thick trophoblastic tissue (*arrows*). (**d**) Transverse section of the uterus on TVS showing the vascular pedicle connecting the rudimentary horn to the left unicornuate uterus. (**e**) Non-gravid, left-sided unicornuate uterus showing an empty endometrial cavity

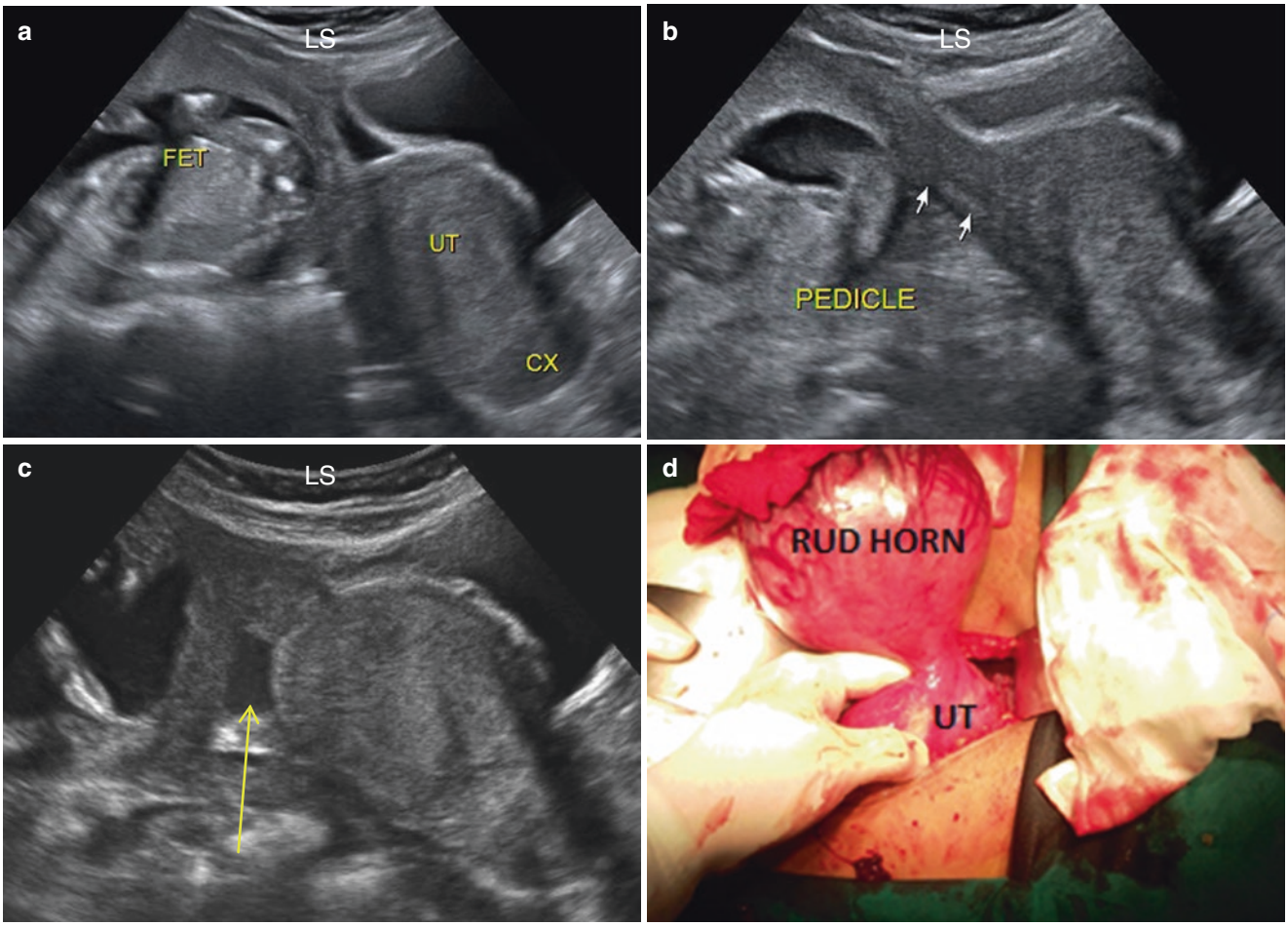

Fig. 10.15 Cornual ectopic pregnancy in a patient with 17 weeks of gestation who presented with acute abdominal pain. (**a**) Fetus (FET) in the non-communicating gravid horn above the uterus. (**b**) Non-canalised pedicle connecting the gravid horn to the main uterine body. This is important to demonstrate, in order to diagnose a cornual ectopic pregnancy wherein the cavity of the rudimentary horn does not communicate with the main uterine body posing a potential threat for rupture. This patient had been scanned earlier with a diagnosis of pregnancy in one horn of a bicornuate uterus and the 'non-communication' had been missed. (**c**) Turbid fluid seen below the pedicle suggestive of rupture of the gravid horn. (**d**) Rudimentary horn seen at surgery. 500 mL of blood was drained from the abdominal cavity and the rudimentary horn was excised

10.1.4 Ovarian Ectopic Pregnancy

Ovarian ectopic pregnancies are rare, constituting 0.5–1 % of all ectopic pregnancies.

Ultrasound Features of an Ovarian Ectopic Pregnancy (Figs. 10.16 and 10.17)

- The tissue of the ectopic pregnancy (i.e., the gestational sac ± yolk sac or fetal pole, surrounded by thick echogenic trophoblastic tissue showing Doppler flow around it) is seen surrounded by hypoechoic ovarian tissue.
- The corpus luteum may or may not be visualised in the same ovary.
- The trophoblastic tissue in most ovarian ectopic pregnancies is thicker and may not be well circumscribed. On enlarging the image on 2D greyscale, low-velocity flow within the trophoblastic tissue is seen and is useful in diagnosis. These flows are best picked up on power Doppler (or HD Doppler) and may be missed on regular colour Doppler, because of their low velocities.
- A tough differential diagnosis for an ovarian ectopic pregnancy is a corpus luteum. Conventionally, serum beta hCG values should be more than 1000 mIU/mL to confirm diagnosis.

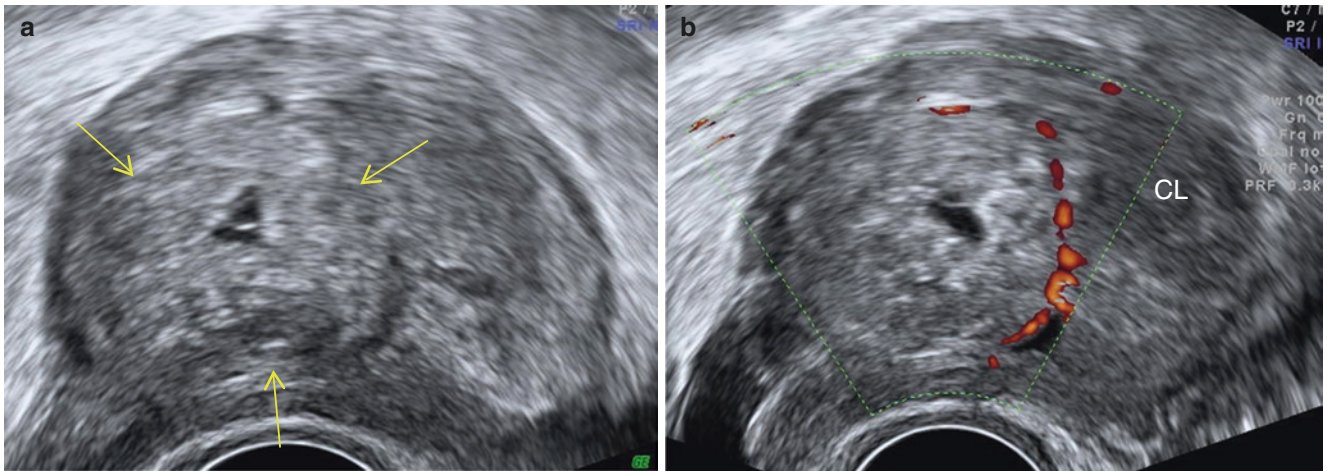

Fig. 10.16 A case of ovarian ectopic pregnancy. (**a**) The ovary is enlarged and shows a poorly defined circumscribed hyperechoic area suggestive of trophoblastic tissue (between *arrows*). Within this, a tiny cystic area suggestive of a gestational sac is seen. A small yolk sac is seen within. Ovarian tissue is seen around the ectopic pregnancy tissue. (**b**) Minimal peripheral flows seen on power Doppler around the trophoblastic tissue. A corpus luteum (*CL*) is seen just beside the ectopic pregnancy tissue in the same ovary. Beta hCG in this case was 2600 mIU/mL

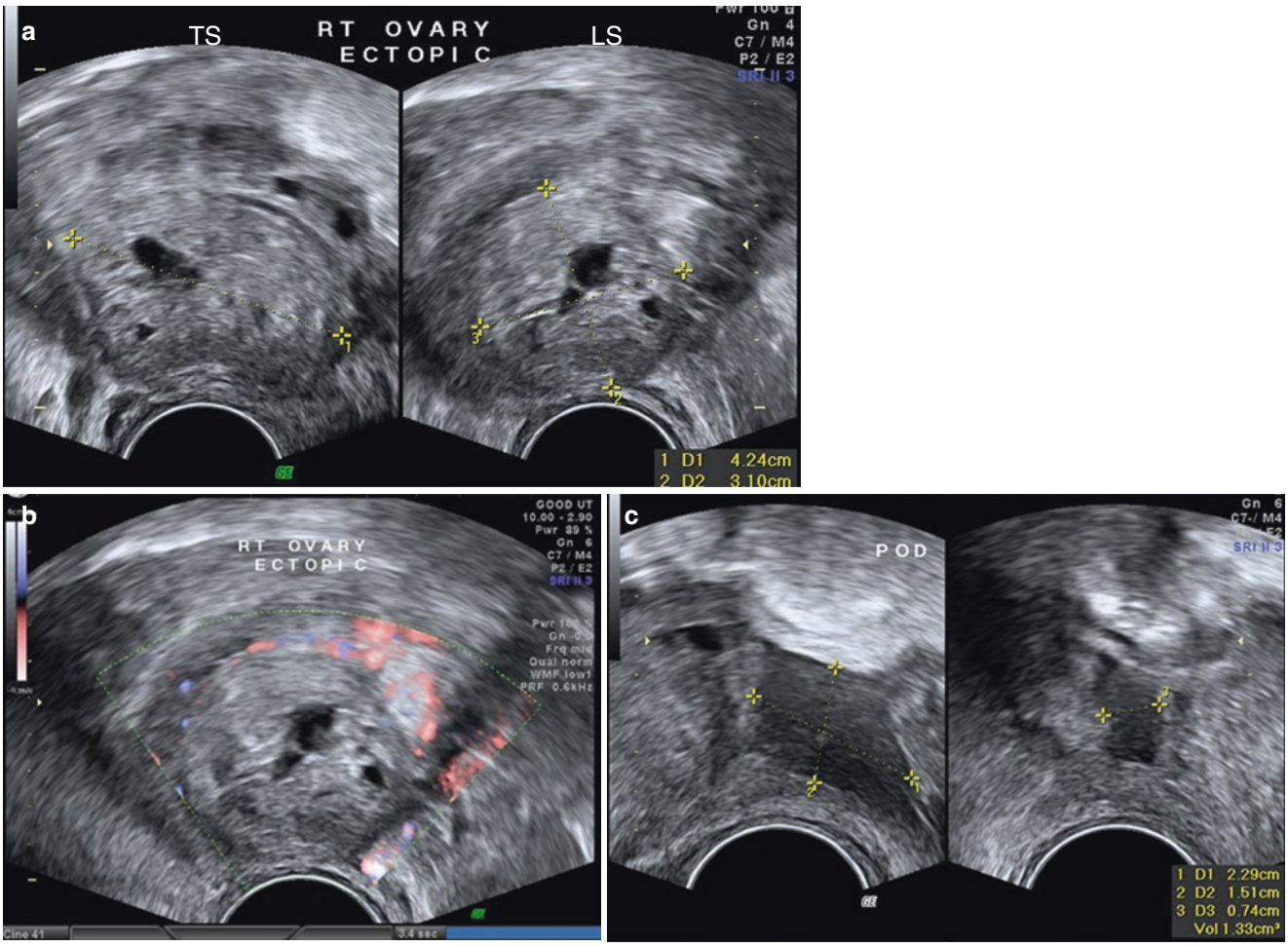

Fig. 10.17 A case of ovarian ectopic pregnancy. Patient had a laparoscopy done for a right tubal ectopic pregnancy. The tube was found to be normal and was apparently 'cleaned up'. In view of rising beta hCG and discomfort experienced by the patient, a scan was repeated, which revealed an ovarian ectopic pregnancy. (**a**) Thick trophoblastic tissue surrounding a central cystic space suggestive of a GS. (**b**) Flow was seen around the trophoblastic tissue on HD Doppler. (**c**) Turbid fluid suggestive of blood was seen in the POD, suggesting haemorrhage from the ectopic pregnancy. Beta hCG at the time of the scan was 4713 mIU/mL

10.1.5 Cervical Ectopic Pregnancy

This form of ectopic pregnancy is often missed because typically on ultrasound examination, one first examines the endometrial cavity followed by the adnexa, and the cervix is often forgotten.

Ultrasound Features of Cervical Ectopic Pregnancy
(Figs. 10.18 and 10.19)

- An empty endometrial cavity.
- 'Hourglass' shaped uterus with a barrel-shaped or ballooned-out cervix.
- The entire tissue of the ectopic pregnancy (i.e., the gestational sac ± yolk sac or fetal pole, surrounded by thick echogenic trophoblastic tissue showing Doppler flow around it) is seen in the cervix below the level of the internal os, that is, below the level at which the uterine arteries are seen entering the uterus (on TS).

An important differential diagnosis for a cervical ectopic pregnancy is incomplete or inevitable abortion (Figs. 10.20 and 10.21). The points that help differentiate the two are:

- The presence of peri-trophoblastic flow within the cervix and fetal heart pulsations, if present, help to confirm a cervical ectopic pregnancy.
- An open internal os, a dead embryo and a flattened GS are suggestive of an incomplete or inevitable abortion.
- Previous scan images showing an intrauterine gestation also help in diagnosing an incomplete or inevitable abortion.

Cases of cervical ectopic pregnancy that are managed with standard evacuation and curettage often present with massive bleeding that may be difficult to control.

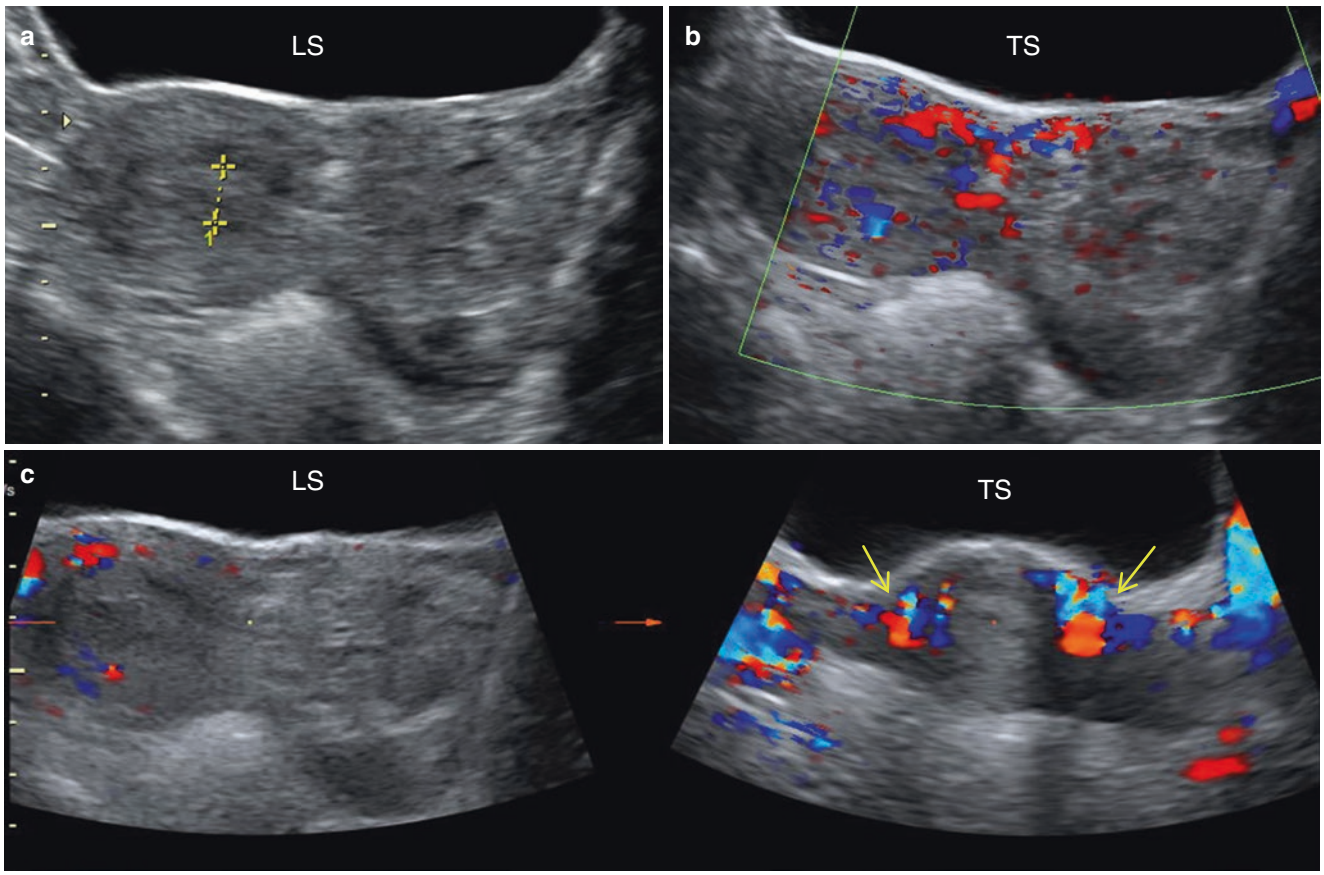

Fig. 10.18 Cervical ectopic pregnancy. Patient presented with spotting and a positive pregnancy test. (**a**) 'Hourglass'-shaped uterus noted, with a ballooned-out cervix. The cervix appeared heterogeneous and hyperechoic. Endometrial cavity was empty. (**b**) No significant flow seen on Doppler in the cervix. (**c**) On 3D Doppler, multiplanar sectional views revealed that the entire complex mass was below the level of the closed internal os (i.e. the level at which the uterine arteries (*arrows*) approach the uterus transversely, seen in the image on the right). The internal os was closed, which helped in making a diagnosis of a cervical ectopic pregnancy

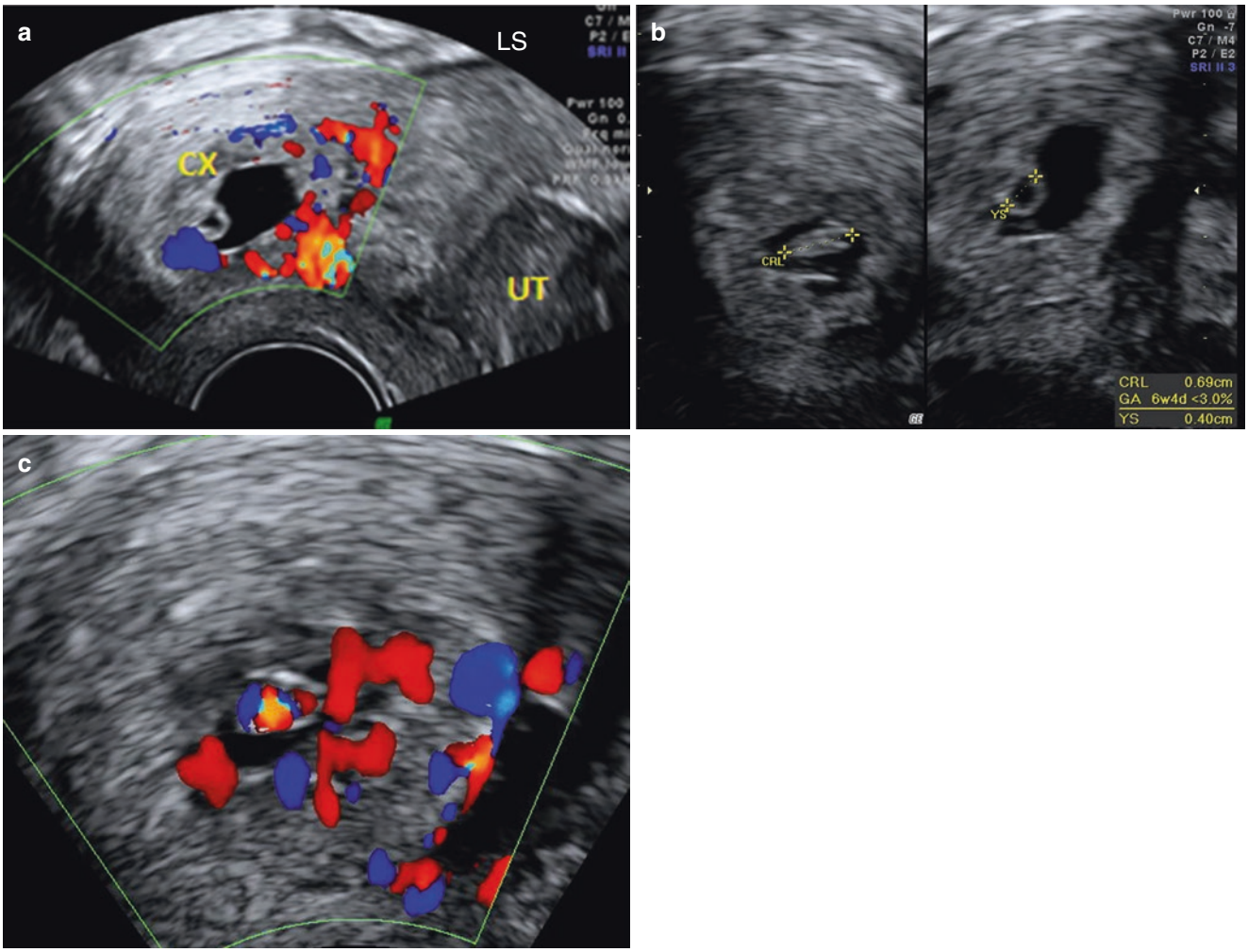

Fig. 10.19 Live cervical ectopic pregnancy. (**a**) Ballooned-out cervix with the ectopic pregnancy mass, within, that showed a central cystic area with vascular trophoblastic tissue surrounding it. (**b**) Fetal pole and yolk sac are seen within. (**c**) Fetal heart pulsations detected on Doppler

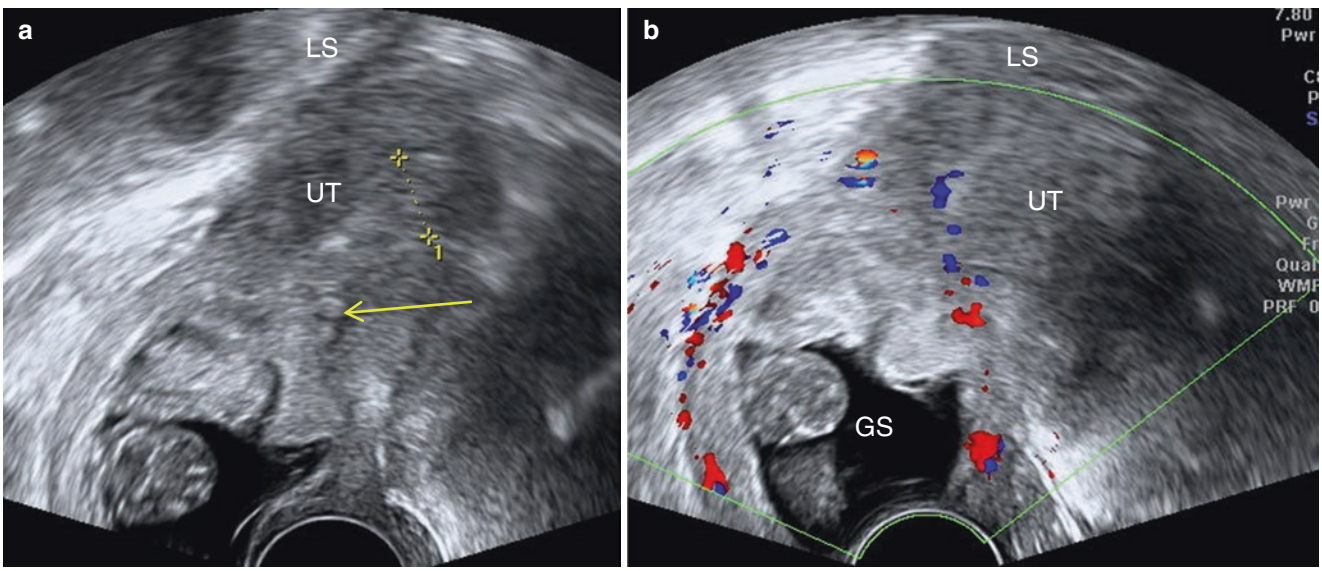

Fig. 10.20 (**a**) Inevitable abortion with pregnancy sac seen in the cervical canal and the internal os (*arrow*) was open. (**b**) In this case, no flow was seen in the trophoblastic tissue. The above findings suggested that this was a case of inevitable abortion

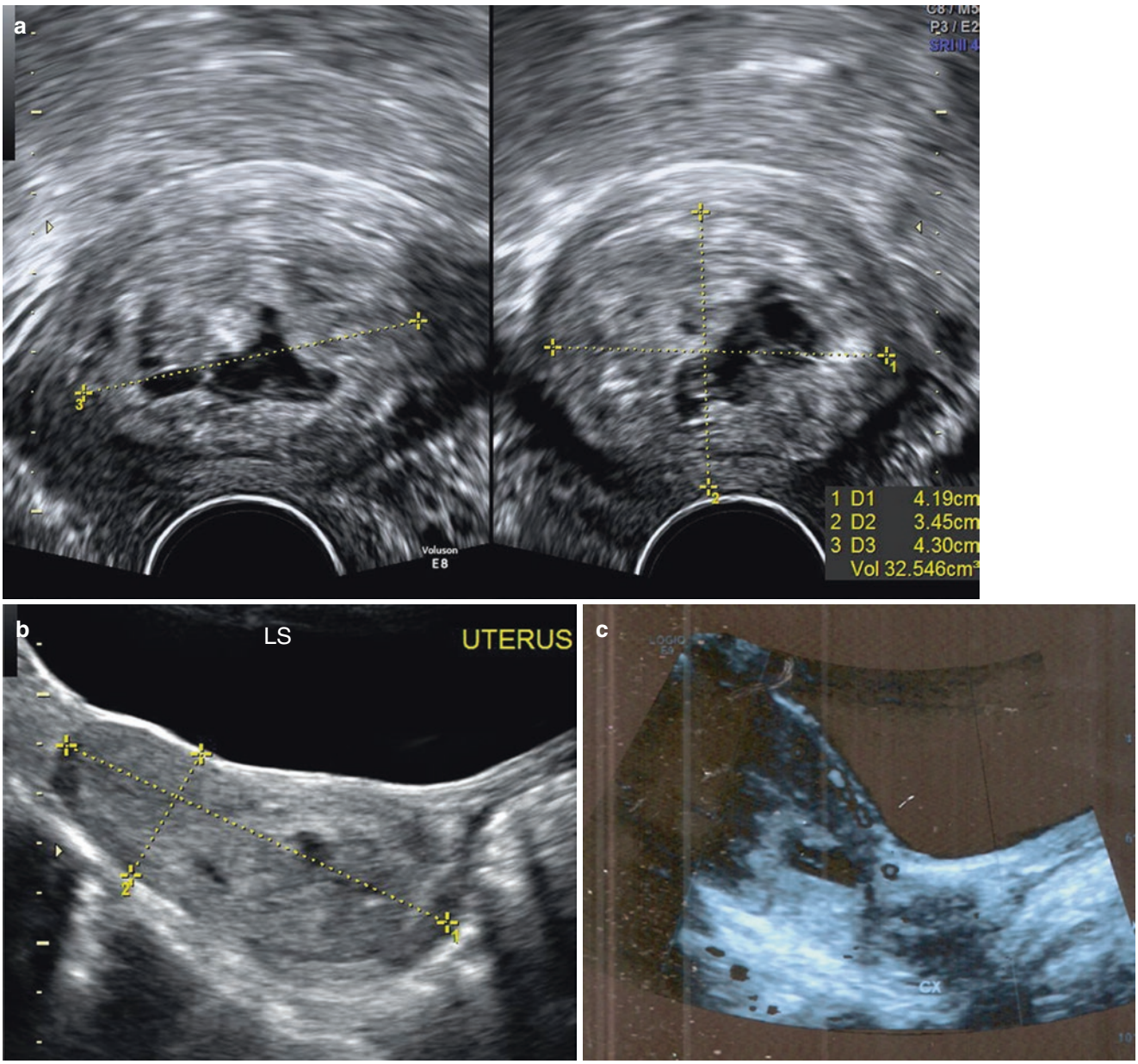

Fig. 10.21 Patient presented with heavy bleeding. (**a**) Ectopic pregnancy mass seen in the cervix with thick trophoblastic tissue and a central, irregular cystic space suggestive of a gestational sac. (**b**) TAS- the uterine body appeared normal and the cervix was ballooned out, showing trophoblastic tissue within. (**c**) Scanned image of the patient's previous report (done elsewhere a few days earlier) which shows a GS in the lower uterine cavity and a normal-appearing cervix. (**d**) On careful examination, it was seen that there was a thick vascular channel supplying the trophoblastic tissue from the posterior wall of the uterus at the midcorpus. From the image of the previous scan, it was easy to confirm that though this appeared like a cervical ectopic pregnancy, it was a case of inevitable abortion and was easily managed with surgical evacuation. (**e**) Vascular pedicle (*small arrows*) of the trophoblastic mass seen on greyscale and Doppler from the posterior myometrium, with the endometrium anterior to it (*long arrow*) appearing normal

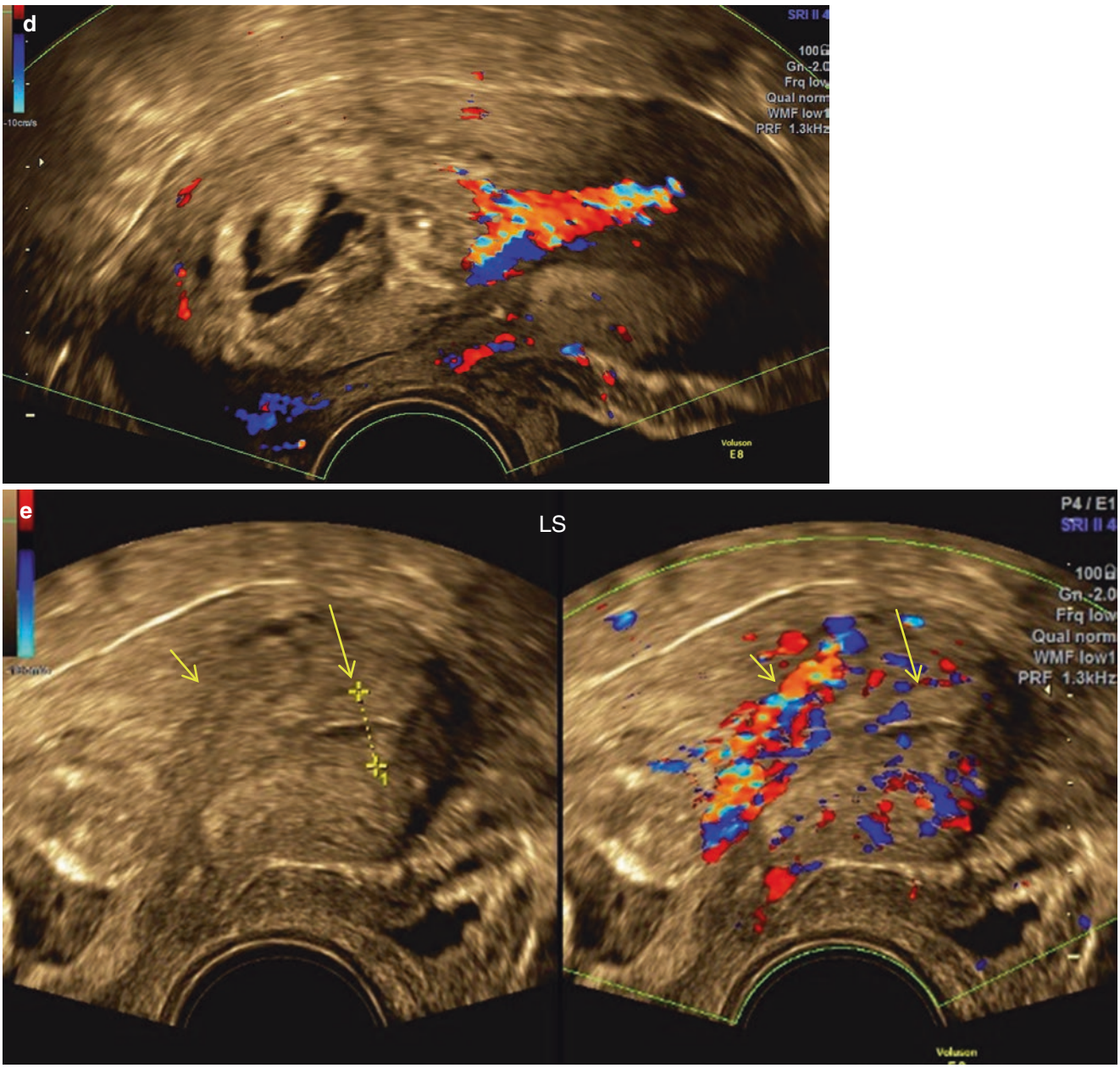

Fig. 10.21 (continued)

10.1.6 Scar Ectopic Pregnancy

Diagnosis of scar ectopic pregnancy requires a high index of suspicion in women with previous caesarean section. With increasing incidence of caesarean section, the incidence of scar ectopic pregnancy is also on the rise. A scar ectopic pregnancy, if left untreated, could result in uterine rupture or a morbidly adherent placental, which poses a problem at the time of delivery.

Ultrasound Features of Scar Ectopic Pregnancy
(Figs. 10.22 and 10.23)

- The tissues of the ectopic pregnancy (i.e., the gestational sac ± yolk sac or fetal pole, surrounded by thick echogenic trophoblastic tissue showing Doppler flow around it) is located in the enlarged LSCS scar.
- The anterior uterine wall bulges out anteriorly with no intervening myometrium between the ectopic pregnancy tissue and the overlying serosa.

Differential diagnosis for a scar ectopic pregnancy is a cervical ectopic pregnancy. The location of the uterine arteries that approach the uterus transversely at the level of the internal os, is useful in differentiating a cervical ectopic pregnancy (which lies below the uterine arteries) from a scar ectopic pregnancy (which lies above the uterine arteries). At times, 3D multiplanar sections are useful in assessing the same.

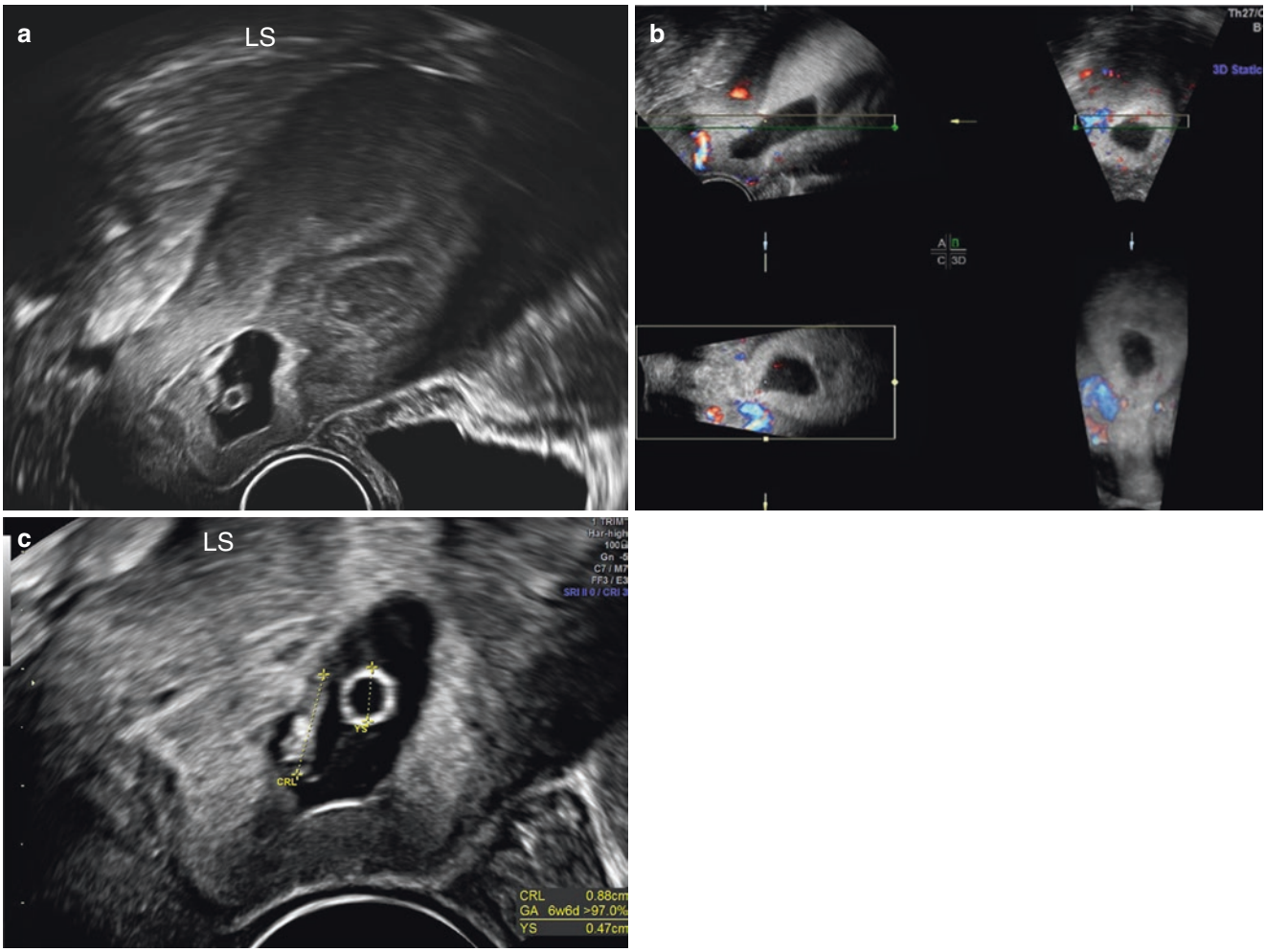

Fig. 10.22 Scar ectopic pregnancy. (**a**) GS with trophoblastic tissue is seen around the region of the LSCS scar. It was difficult to determine for sure whether the pregnancy was at the lower corpus and/or upper cervix. (**b**) 3D multiplanar sections were obtained, and by walking through the planes with the help of the intersecting dot, the diagnosis could be confirmed. The ectopic pregnancy tissue was seen above the level of the internal os (uterine arteries), confirming the diagnosis of a scar ectopic pregnancy. (**c**) Thick hyperechoic, trophoblastic tissue surrounds the GS. No intervening myometrium is seen between the trophoblastic tissue and the anterior serosa. Fetal pole and yolk sac are seen within the GS

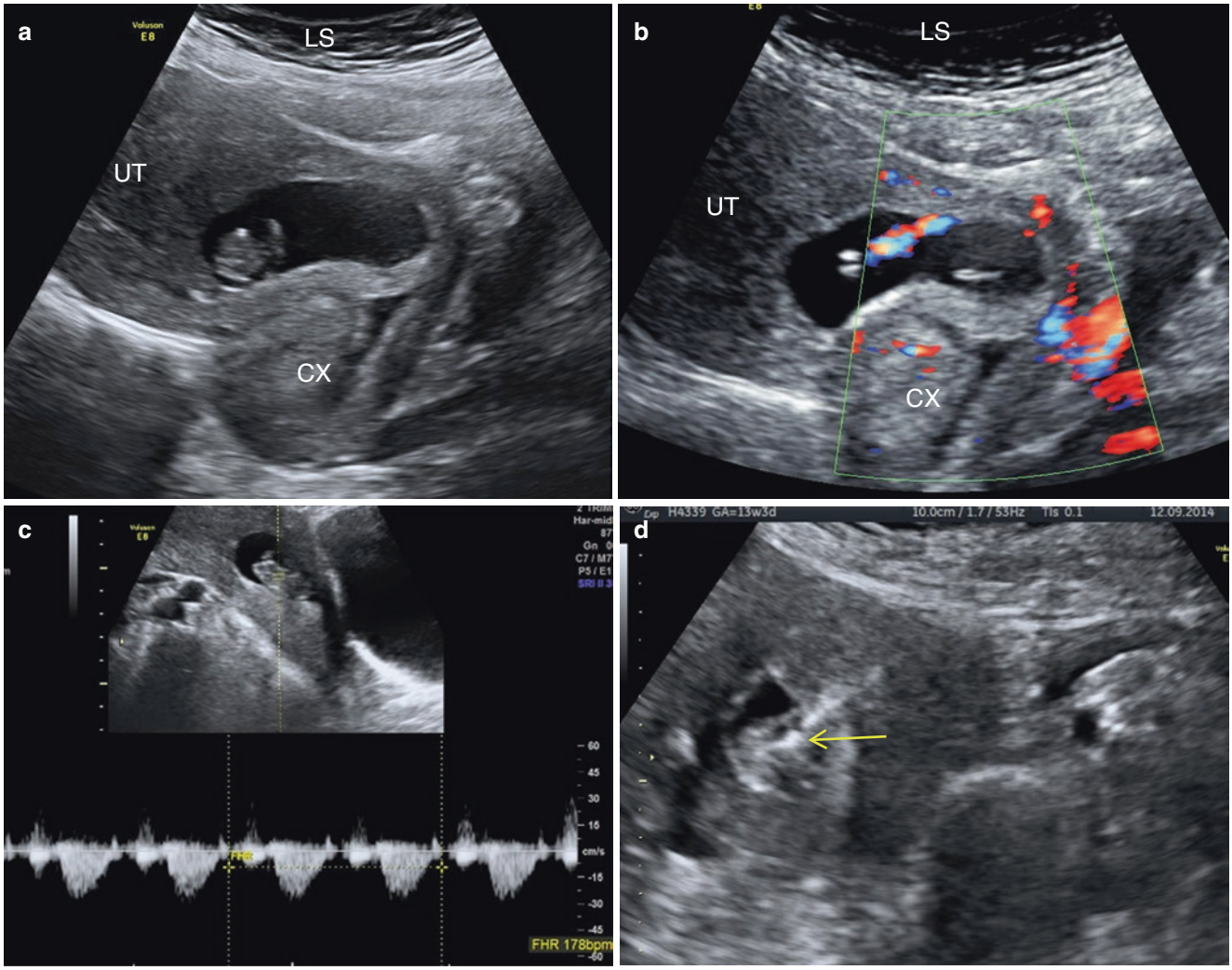

Fig. 10.23 Live scar ectopic pregnancy with a 10-week-old fetus. (**a**) The GS and trophoblastic tissue is seen bulging out of the anterior wall of the uterus at the site of the LSCS scar. (**b**) Flow is seen around the trophoblastic tissue and in the umbilical cord on Doppler. (**c**) Tracing of fetal heart pulsations. (**d**) Fetal reduction done with KCl. *Arrow* showing the needle

10.1.7 Intra-abdominal Pregnancy (Fig. 10.24)

A true intra-abdominal pregnancy is very rare. Here the pregnancy is implanted in the peritoneal cavity and the fetus grows within the abdominal cavity. Very often at diagnosis, the fetus is growth restricted or there is fetal demise.

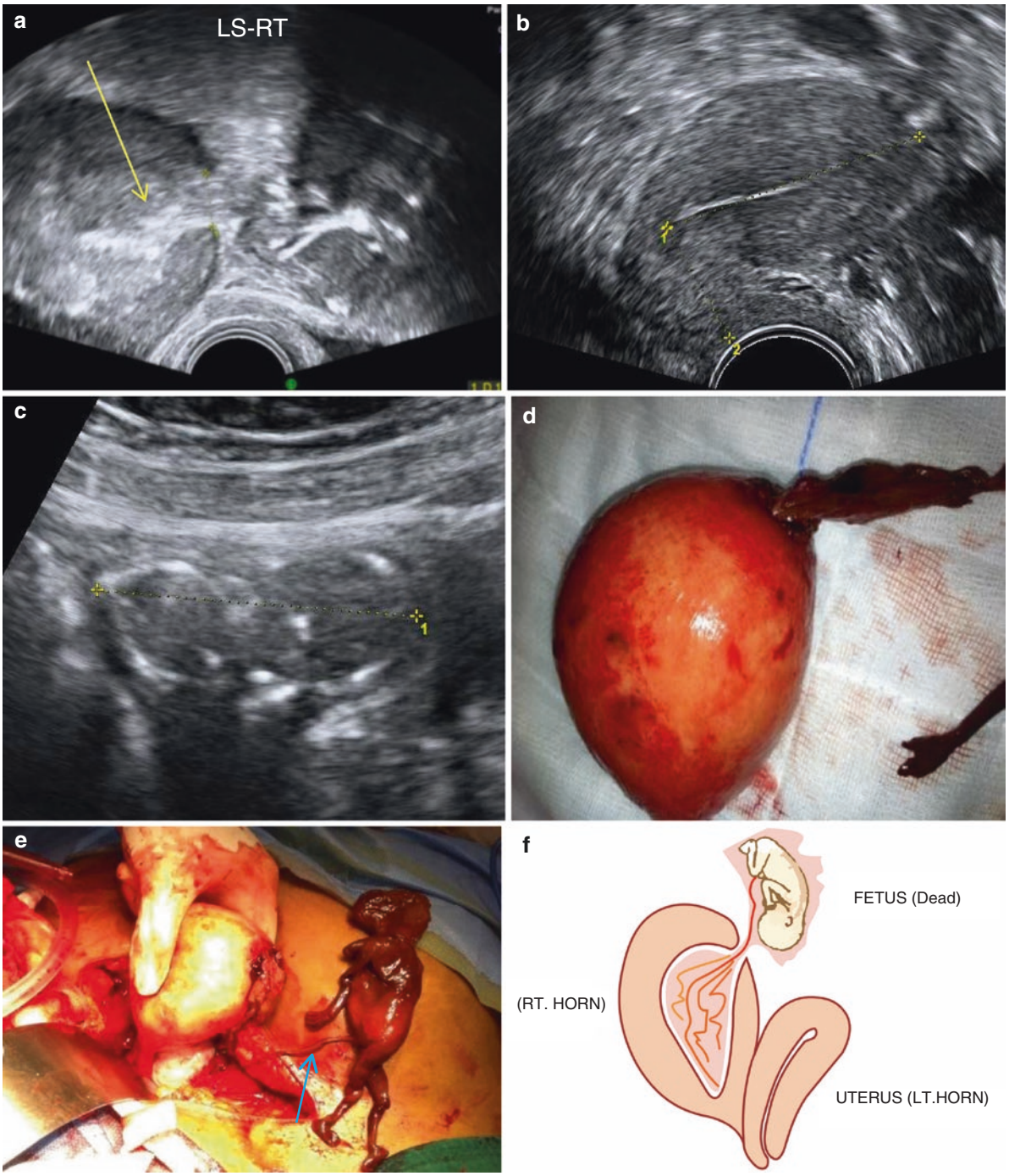

Fig. 10.24 Intra-abdominal dead fetus which perforated out from a non-communicating rudimentary horn. (**a**) Non-communicating uterine horn with a hyperechoic tract (*arrow*), from the endometrial cavity up to the serosa. (**b**) Normal left-sided uterine body. (**c**) Fetal bony tissue is seen as hyperechoic scattered echoes. (**d**) Post-operative specimen of the non-communicating right uterine horn with placental tissue and the umbilical cord protruding out of the perforation. (**e**) Dead fetus attached by the umbilical cord (*arrow*) to the placental tissue within the rudimentary horn. (**f**) Diagrammatic representation of scan findings in this case. The uterine perforation by trophoblastic tissue must have occurred early in pregnancy with the fetus escaping out of the rudimentary horn and continuing to grow intra-abdominally for a short period of time. This is, however, not a true abdominal pregnancy because the placenta was not implanted in the abdominal cavity

10.1.8 Heterotopic Pregnancy (Figs. 10.25 and 10.26)

Heterotopic pregnancy is a rare type of ectopic pregnancy, wherein along with an intrauterine pregnancy, an ectopic pregnancy co-exists. Most often, this is a tubal ectopic pregnancy. The incidence of heterotopic pregnancy is on the rise because of multiple conceptions with ovulation induction and IVF. This is often missed because the presence of an intrauterine pregnancy is generally considered reassuring in ruling out an ectopic pregnancy. Chances of diagnosing a heterotopic pregnancy is increased by awareness of the possibility, paying attention to the patient's complaint of pain, proper adnexal evaluation in all cases and a transabdominal scan prior to TVS.

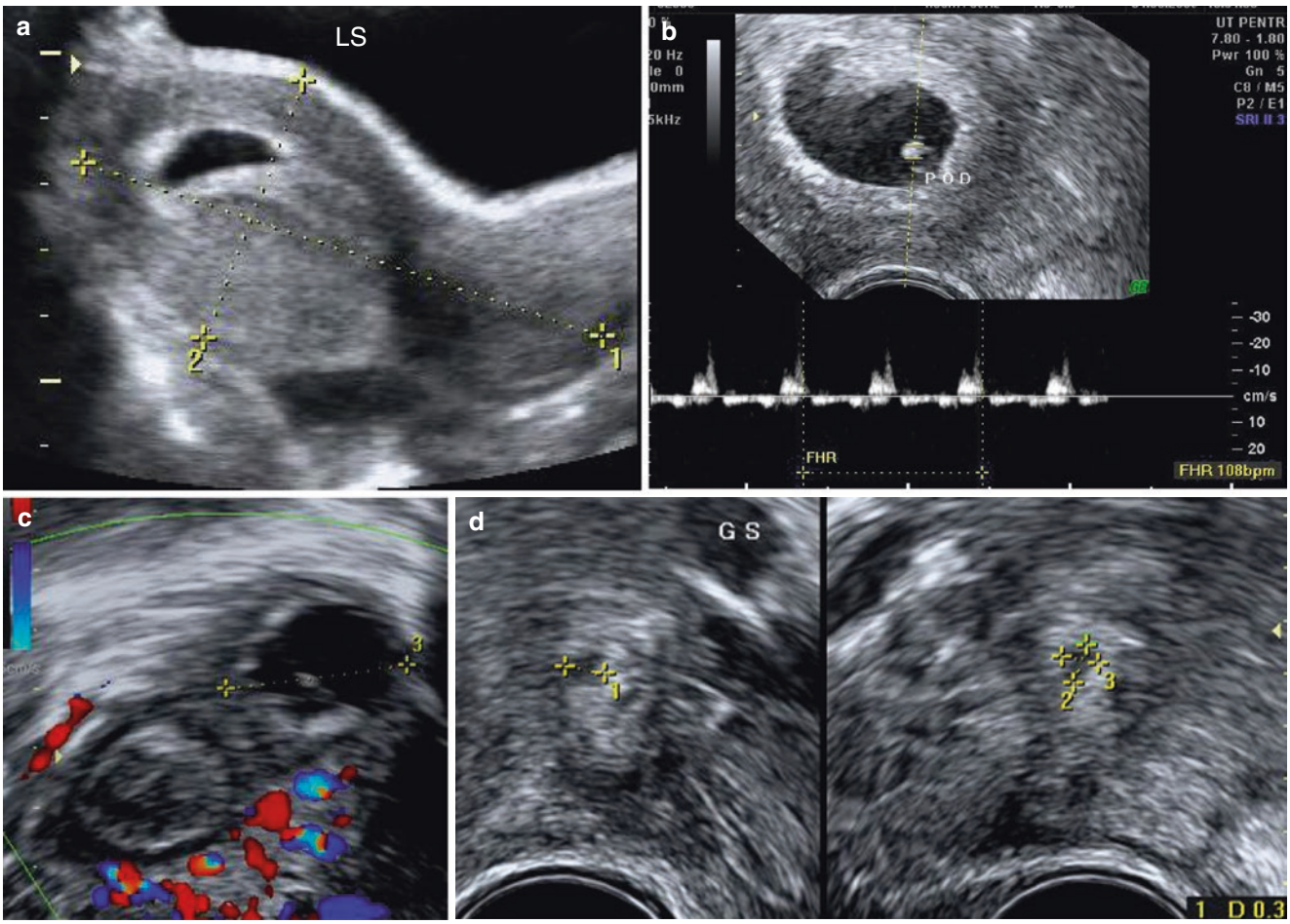

Fig. 10.25 Heterotopic pregnancy conceived with IVF. (**a**) Normal intrauterine pregnancy. (**b**) Fetal heart pulsations of intrauterine fetus noted. (**c**) Two corpora lutea seen in the left ovary. (**d**) Small, vaguely circumscribed hyperechoic area is seen in the adnexa with a tiny intrauterine sac, suggestive of a tubal ectopic pregnancy. This was tender to touch

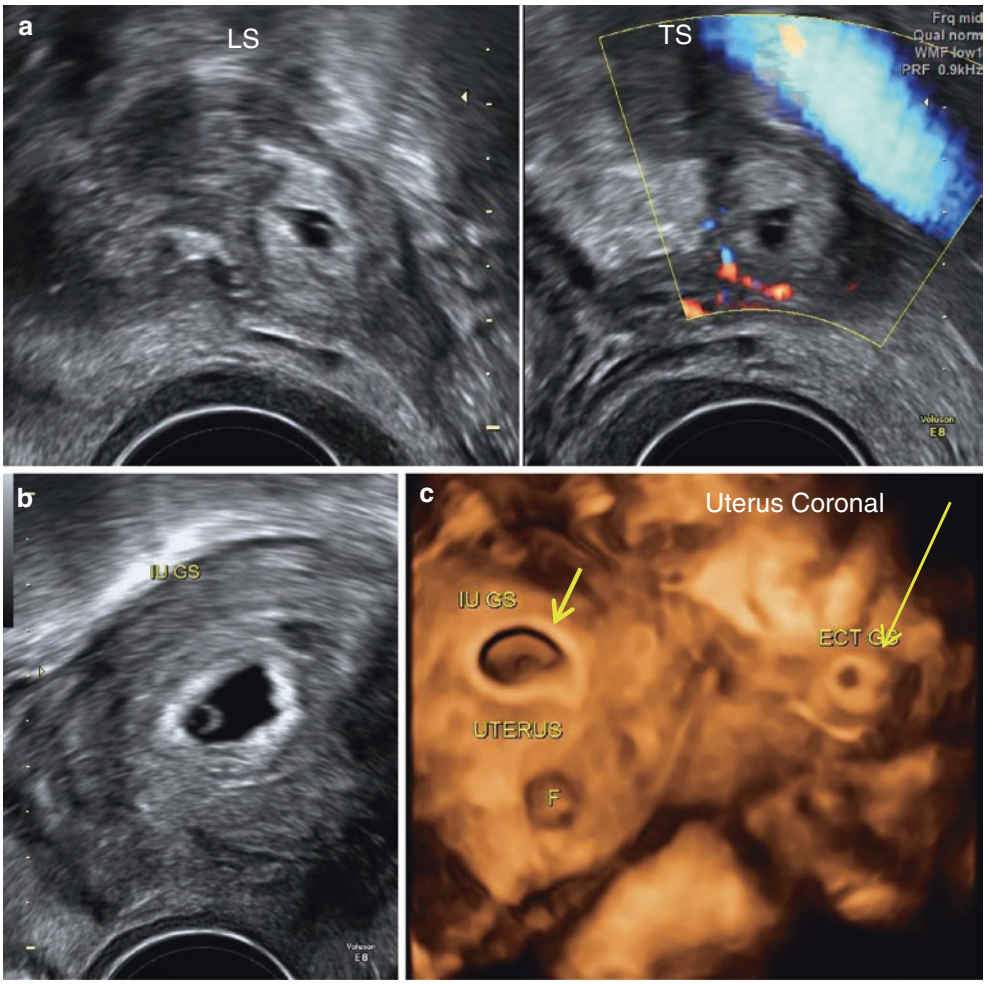

Fig. 10.26 Heterotopic pregnancy conceived with IVF. Patient who was diagnosed to have an intrauterine pregnancy, presented with abdominal pain and bleeding. (**a**) An elongated mass suggestive of a thickened tube, with a hyperechoic circumscribed area within, suggestive of an ectopic pregnancy mass is seen. Flow was seen around the trophoblastic tissue, and a small yolk sac was seen within the GS. (**b**) Intrauterine GS is seen. (**c**) 3D rendered image of the uterus and the adnexa showing both the intrauterine sac (*short arrow*) and the tubal ectopic pregnancy sac (*long arrow*)

10.1.9 Intra-myometrial Ectopic Pregnancy (Fig. 10.27)

This is a very rare form of ectopic pregnancy, where the ectopic pregnancy tissue is seen within the myometrium of the uterus, which surrounds it completely. The endometrial cavity is empty, but very often there is a thin vascular connection seen extending from the endometrial margins to the centre of this ectopic pregnancy tissue. This type of ectopic pregnancy has almost always been diagnosed intraoperatively and most often following rupture.

In all cases where a normal intrauterine pregnancy is not seen, the potential of an ectopic pregnancy exists. If there is no ectopic pregnancy noted, it is categorised as pregnancy of unknown location ('PUL') which is dealt with in Chap. 14.

If an ectopic pregnancy is diagnosed, its management depends upon clinical features and ultrasound findings. Those that are not managed surgically are followed up with serial serum beta hCG under close observation. A repeat scan is suggested in case the patient becomes symptomatic for any evidence of rupture, which can happen even with falling serum beta hCG levels and medical management with methotrexate. On follow-up scans, even with falling serum beta hCG, the ectopic pregnancy mass may seem to increase in size, which should not be interpreted as failure of medical management. The vascularity, however, generally diminishes. It is therefore suggested that the primary modality of follow-up in the case of ectopic pregnancies should be serial beta hCG and not ultrasound, with ultrasound being resorted to in patients who become symptomatic, and there is a suspicion of rupture.

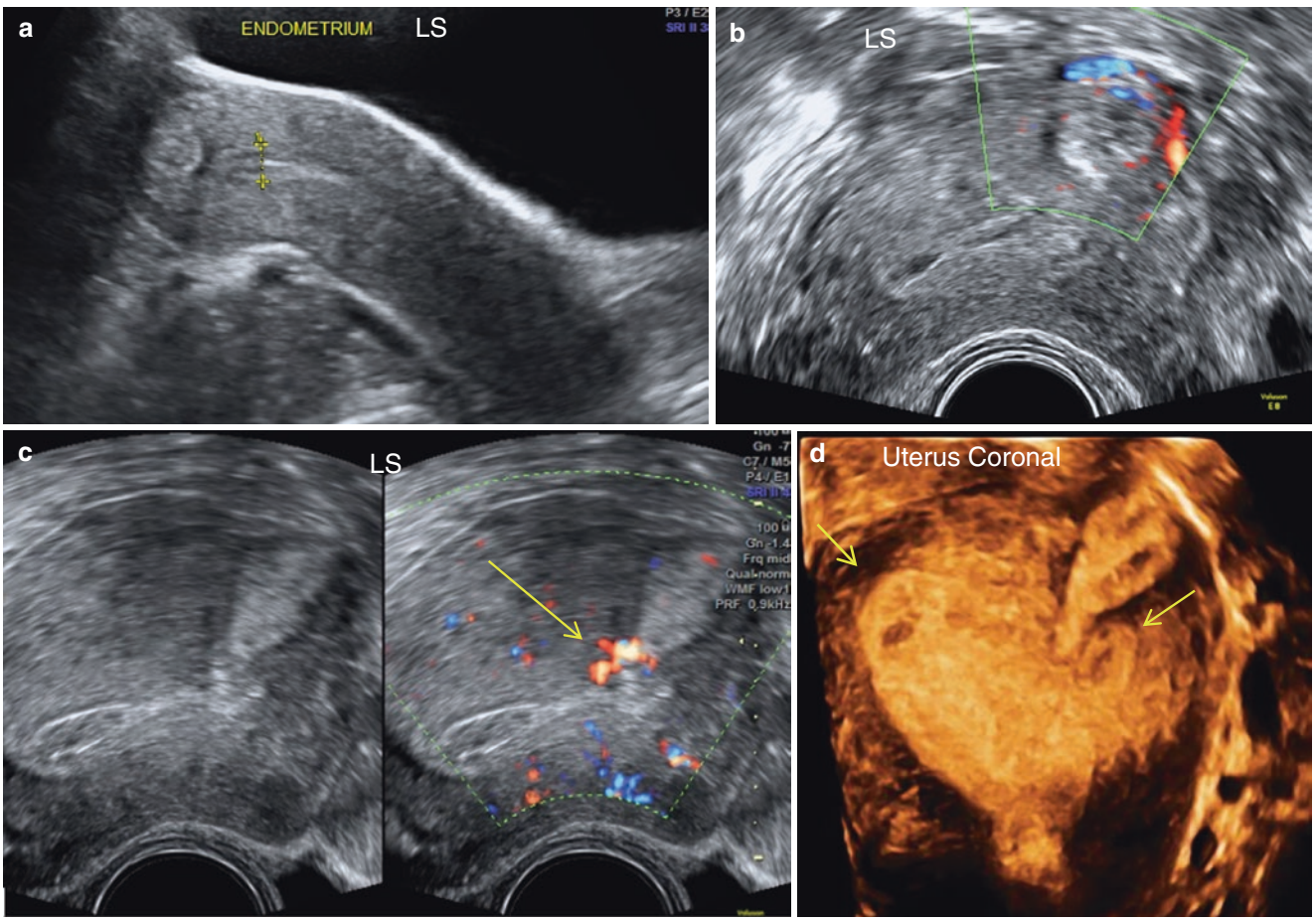

Fig. 10.27 Intra-myometrial ectopic pregnancy. Patient gave a history of elevated beta hCG and bleeding. Scan done elsewhere showed no evidence of intrauterine or extrauterine pregnancy, raising the suspicion of a spontaneous abortion. (**a**) TAS - Sagittal section of the uterus showing an empty endometrial cavity and a hyperechoic circumscribed complex mass in the myometrium, just above the upper end of the endometrium. (**b**) TVS - showing the same. Flow is seen around the hyperechoic circumscribed area. Images (**a**) and (**b**) raised the possibility of interstitial pregnancy. (**c**) Narrow hyperechoic vascular tract (*arrow*) is seen extending from the endometrium towards the ectopic pregnancy mass. (**d**) Coronal rendered image of the uterine cavity showing two cornual ends (*arrows*) of the endometrial cavity with the ectopic pregnancy mass arising from the left upper end of the endometrial cavity, just medial to the left cornua and lying completely within the myometrium. Patient was treated with injection methotrexate and the ectopic pregnancy mass regressed

Summary: Ectopic pregnancy

- Transvaginal scan is the modality of choice for the diagnosis of ectopic pregnancy. Clinical correlation with symptoms, history and serum beta hCG levels are important for diagnosis.
- Transabdominal scan prior to TVS improves the detection rate.
- During TVS, a careful search is to be made, and if there is no intrauterine pregnancy and there is no adnexal mass, one must not forget to look carefully at the two cornual ends and the cervix.
- Classic ultrasound features of an ectopic pregnancy are an empty uterine cavity and presence of an the ectopic gestational mass (typically seen as a cystic central gestational sac +/− yolk sac or fetal pole, surrounded by thick echogenic trophoblastic tissue showing Doppler flow around it).

10.2 Retained Products of Conception (RPOC)

Retained products of conception are placental and/or fetal tissue that remain in the uterine cavity after an abortion or pregnancy. Histopathological diagnosis of RPOC requires the presence of chorionic villi (persistent placental tissue). After pregnancy, the villi that remain undergo increasing fibrosis and exhibit variable vascularity which is probably why RPOC show variable vascularity on ultrasound.

Retained tissue is more often seen with spontaneous abortion or delivery than those that have undergone surgery. The incidence also varies with period of gestation being highest after mid-trimester abortions.

Typical clinical symptoms of RPOC are bleeding, either excessive in amount or persisting for an extended period of time (more than 2–3 weeks). Following an abortion or pregnancy, some amount of bleeding is normal for a week or two (being lesser with surgical evacuation).

Necrotic RPOC is prone to infection. Women with such infections may present with fever, pain, uterine tenderness or abnormal bleeding.

Evaluation for RPOC is not done in all cases routinely following delivery or abortion, unless there is a suspicion of some tissue being left behind (e.g. adherent placenta). This is because some amount of blood, clots, echogenic debris and fluid is normal in the immediate post-abortal or post-partum period. Beta hCG is usually not of help in the diagnosis as it normally persists for a few weeks after an uncomplicated pregnancy.

Ultrasound Features of RPOC (Figs. 10.28, 10.29, 10.30, 10.31, 10.32, 10.33, 10.34, 10.35, 10.36 and 10.37)

- RPOC typically appear as hyperechoic heterogeneous intracavitary masses. These intracavitary masses are at times much better visualised in a transverse section (after viewing on LS) of the entire endometrial cavity, scanned slowly from the cervix upwards to the upper end of the endometrial cavity.
- RPOC mass may appear to be extending into the adjoining myometrium with poor endomyometrial differentiation in that area.
- Retained placenta appears as thick hyperechoic tissue with increased vascularity approaching it from the underlying myometrium. If there is a focal single feeder vessel, it is often termed as a ‘placental polyp’. Sometimes, morbidly adherent placenta is consciously left behind, and these appear like hyperechoic thick placental cotyledons within the uterine cavity.
- The presence of Doppler flow in such a mass is useful in confirming a diagnosis, but the absence of flow does not rule out RPOC, as some RPOC may not be vascular. Most

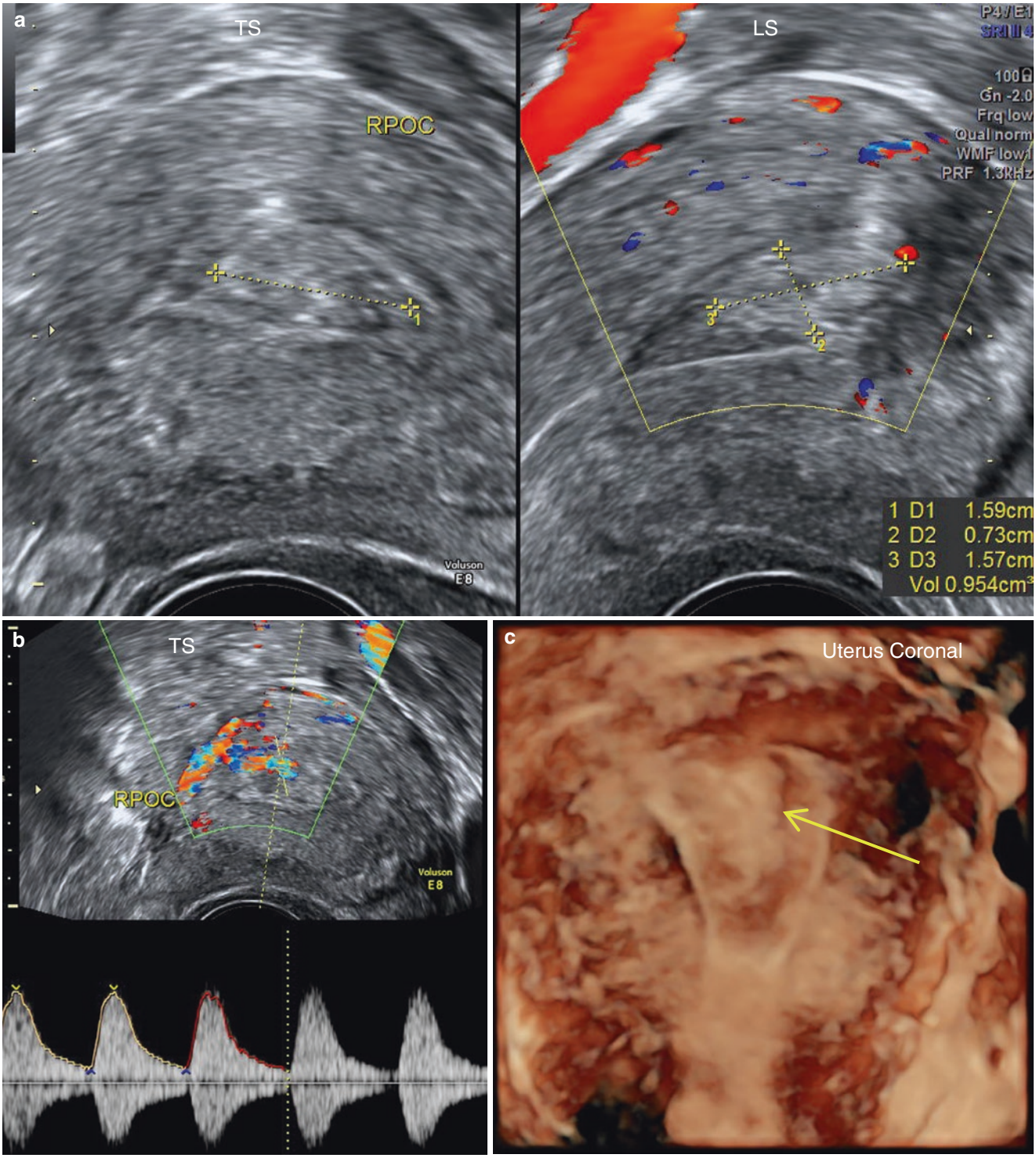

Fig. 10.28 RPOC following first trimester abortion. (**a**) Complex, hyperechoic intracavitary mass is seen in the upper endometrial cavity with turbid fluid suggestive of blood below it. (**b**) TS showing flow approaching the RPOC from the right uterine wall. (**c**) 3D rendered coronal image of the uterus showing an intracavitary mass - the RPOC

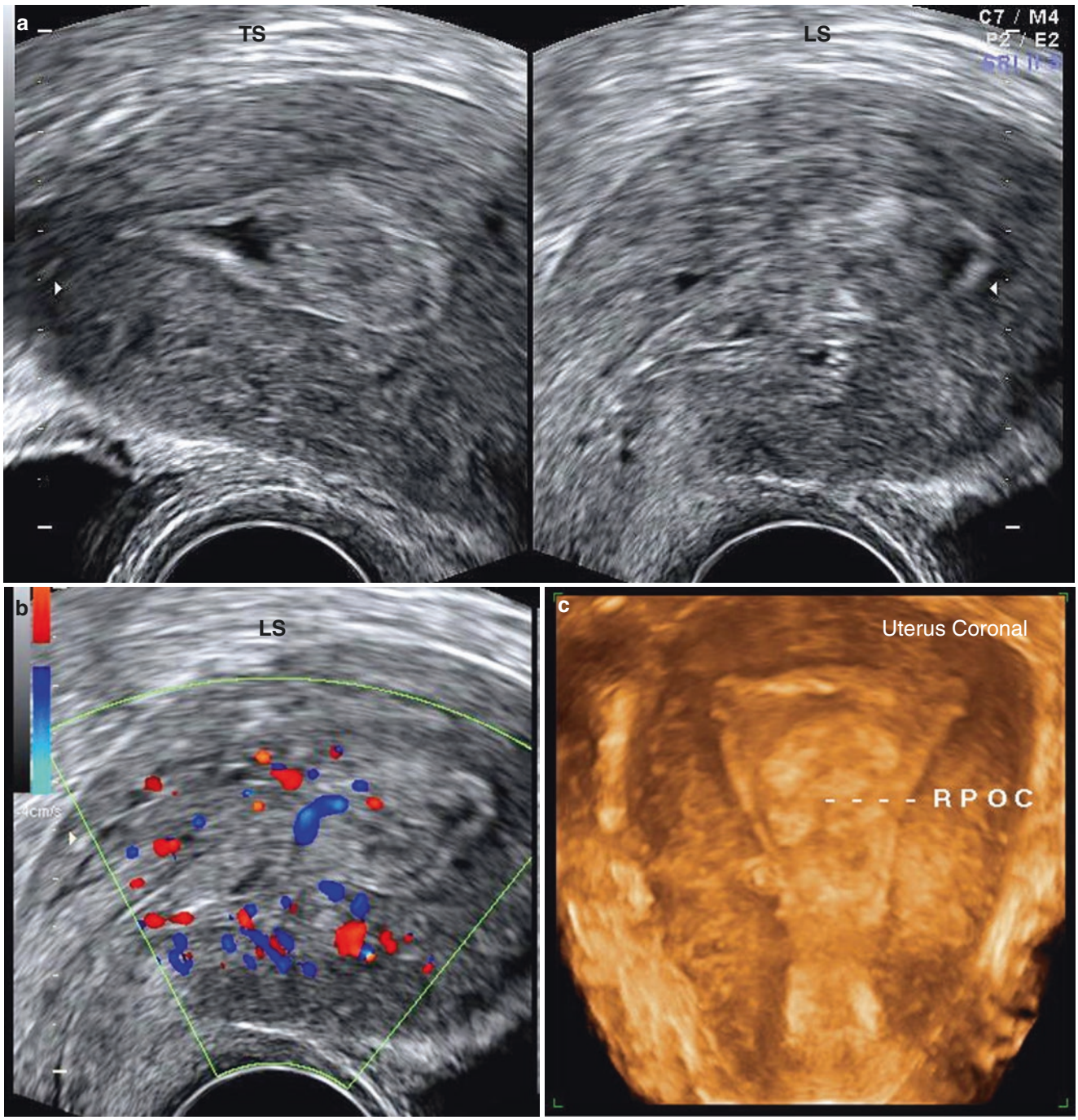

Fig. 10.29 RPOC following missed abortion with bleeding. (**a**) Hyperechoic, complex mass seen in the endometrial cavity. On TS, it appears completely within the cavity with minimal fluid on one side. On LS, the anterior margins were not well defined because of an anterior wall adenomyoma. (**b**) RPOC showing flow within, on Doppler, which helps to confirm diagnosis. (**c**) 3D rendered image showing the complex appearing RPOC within the endometrial cavity

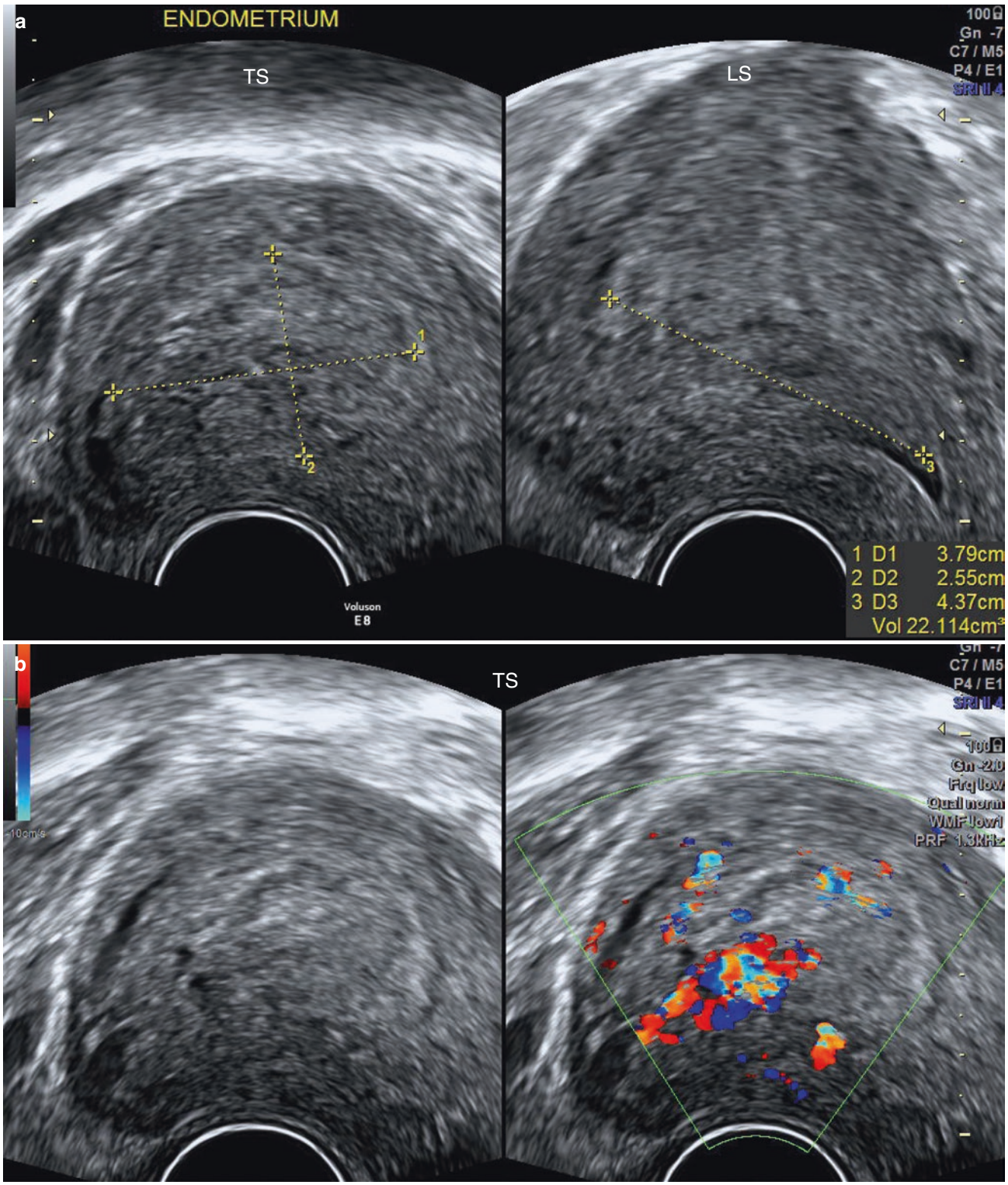

Fig. 10.30 RPOC following TOP at 17+ weeks of pregnancy. (**a**) Retained tissue which appears isoechoic with the surrounding myometrium is seen in the endometrial cavity - measured in this image. (**b**) Its presence was ascertained with the help of Doppler, which showed high vascularity within the mass

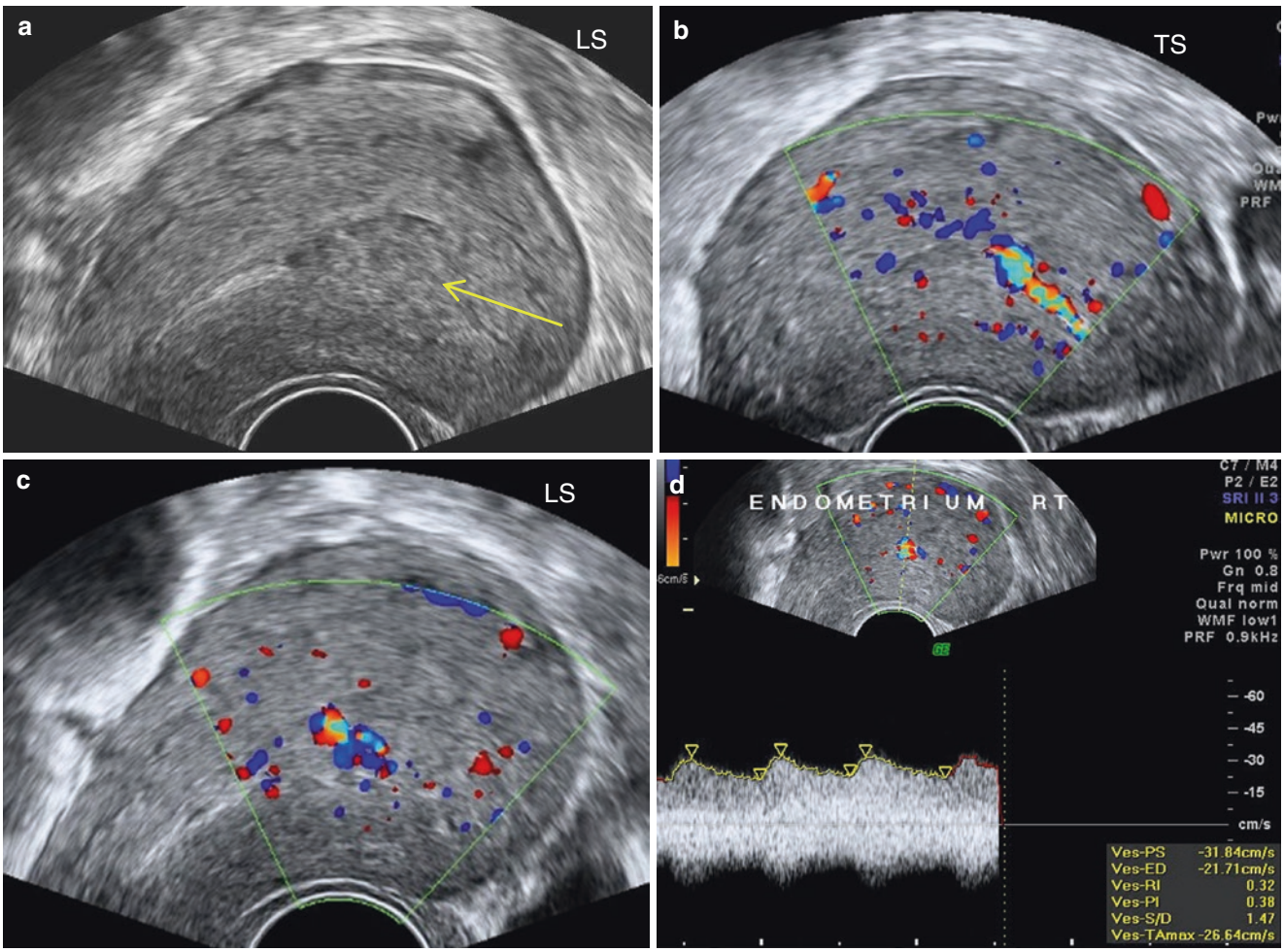

Fig. 10.31 RPOC following mid-trimester TOP. Patient was on conservative management for RPOC. Serum beta hCG a week prior was 19mIU/mL. Patient was given methotrexate following which she came for a scan. (**a**) An isoechoic mass is seen within the endometrial cavity at the upper corpus (*arrow*). The anterior EMJ in this area could not be delineated. (**b**) A vessel is seen approaching the RPOC from the anterior wall on the left side. (**c**) Flow is seen within the retained tissue. (**d**) Flow in the RPOC showed low RI of 0.32.

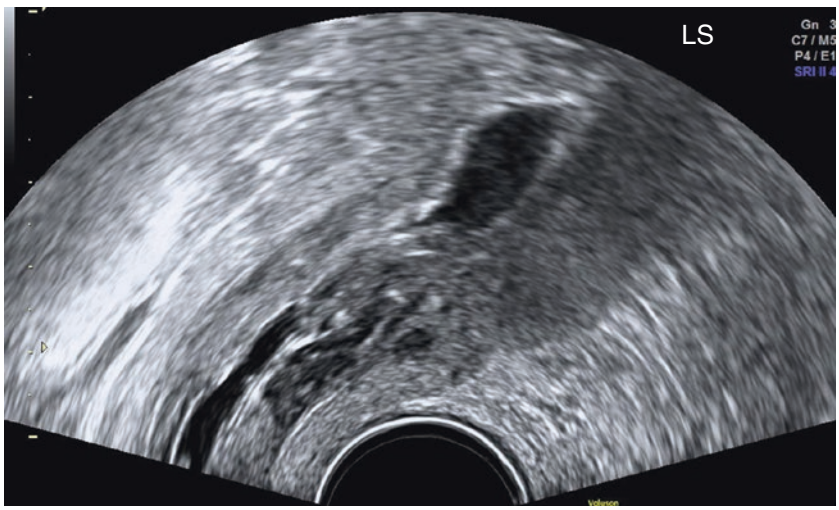

Fig. 10.32 TVS showing endometrial cavity with turbid fluid and a mass which shows. complex echoes. This showed low vascularity, and it was difficult to ascertain whether this was retained tissue or a clot within the endometrial cavity

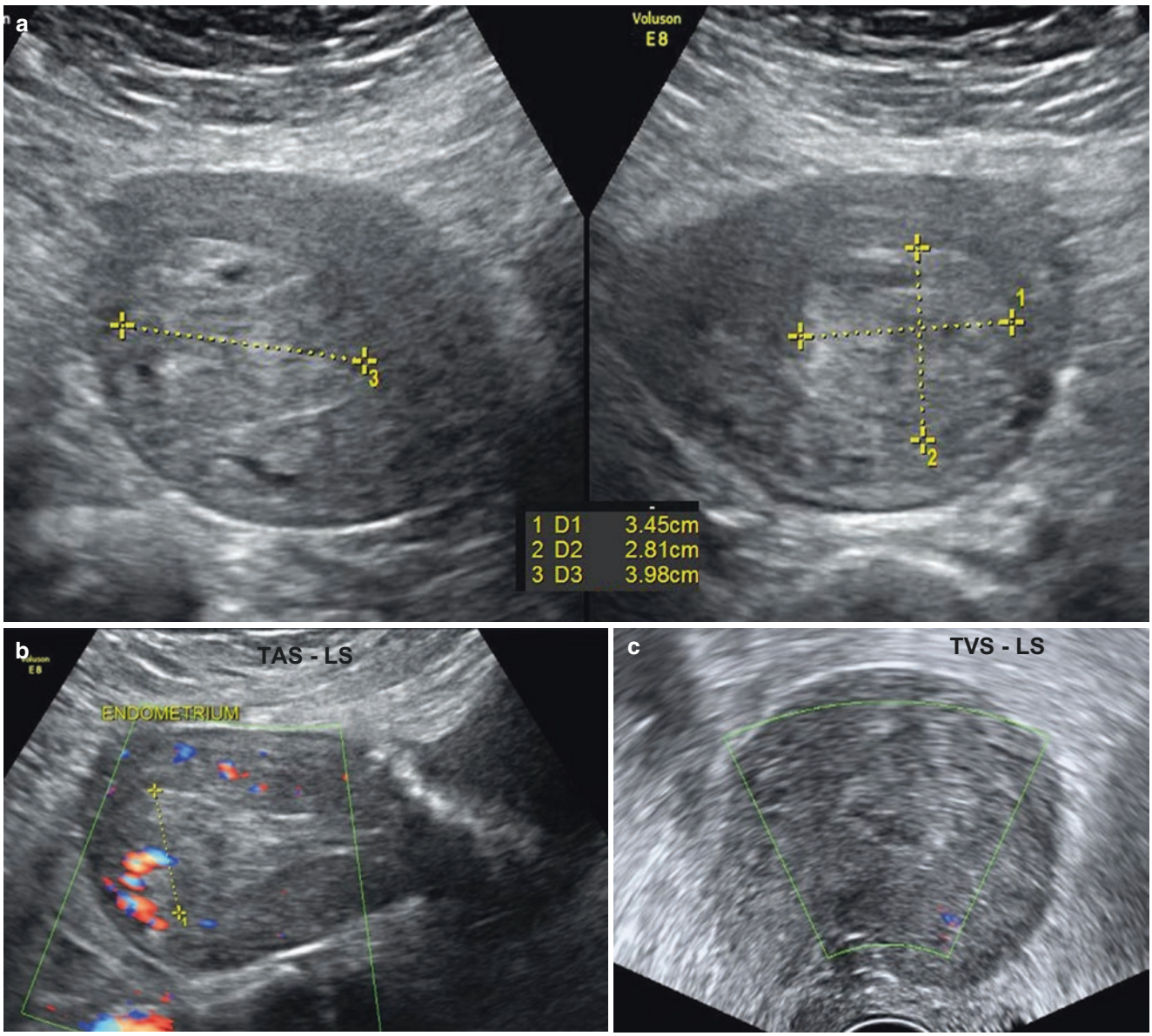

Fig. 10.33 Placental polyp. Patient presented with secondary PPH, following a full-term LSCS. (**a**) Circumscribed, hyperechoic, complex mass is seen in the upper uterine cavity, suggestive of retained placental tissue. (**b**) A single prominent vessel was seen approaching this area from the posterior wall of the uterus, confirming the diagnosis of retained placental tissue. (**c**) TVS showing the uterine body. Visualisation of RPOC and feeder vessel was, however, suboptimal because of the large uterine size and the mid-positioned uterus

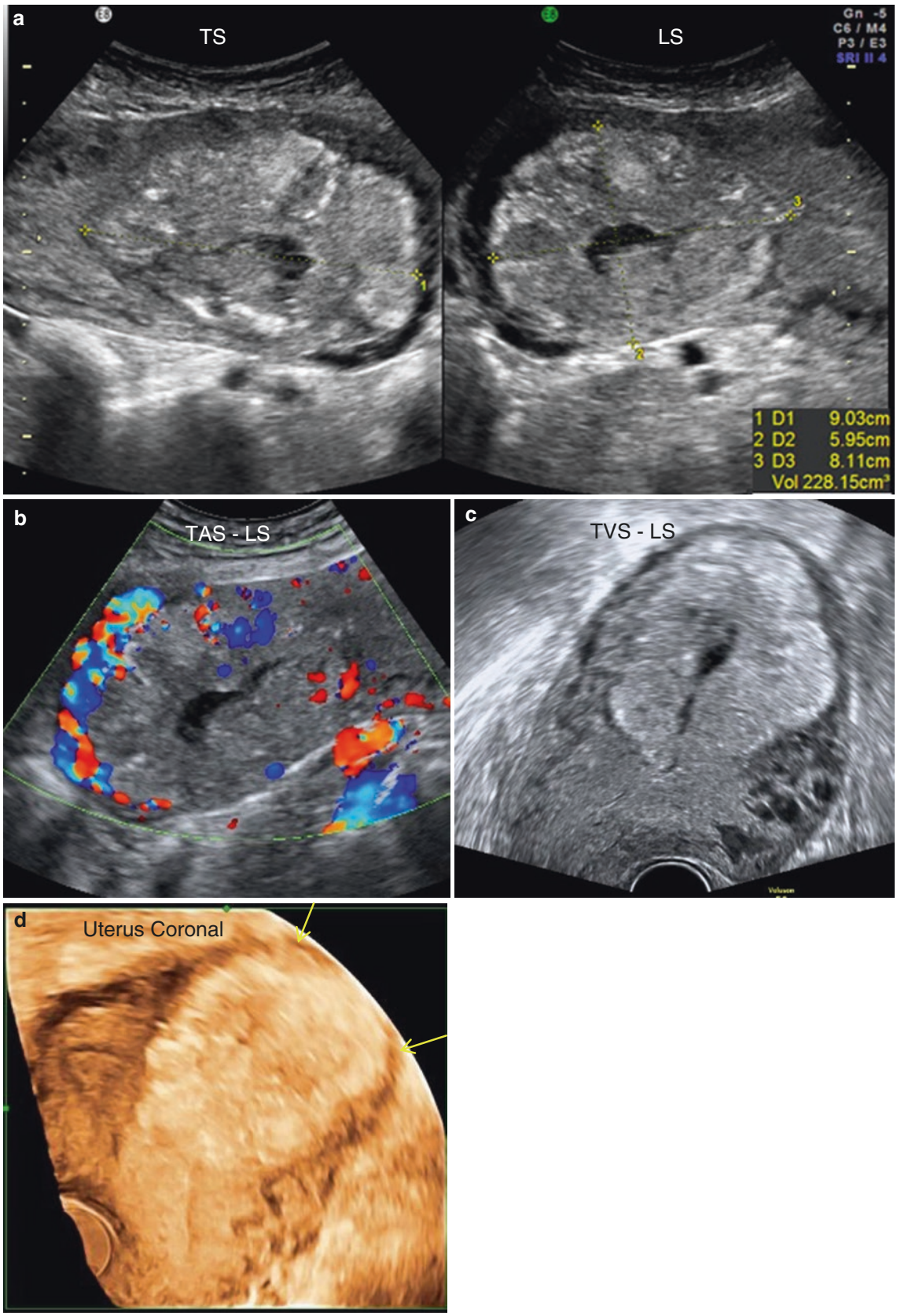

Fig. 10.34 Adherent retained placenta. Patient had a full-term normal delivery, a month prior to this scan. Manual removal of placenta was attempted following delivery, for retained placenta, but only a part of it could be separated and removed. (**a**) The uterus showing 228 mL of retained placental tissue, which is seen as a hyperechoic, complex, well-circumscribed mass. On TS, the surrounding myometrium appeared thin. (**b**) Flow is seen around the placental tissue. No significant amount of myometrium is seen between the vascular flow and the overlying serosa. (**c**) TVS - showing the retained placental tissue and a thinned out myometrium superiorly. (**d**) Coronal rendered image of the uterus showing the retained tissue in the left cornual region, with a thinned out overlying myometrium (*arrows*)

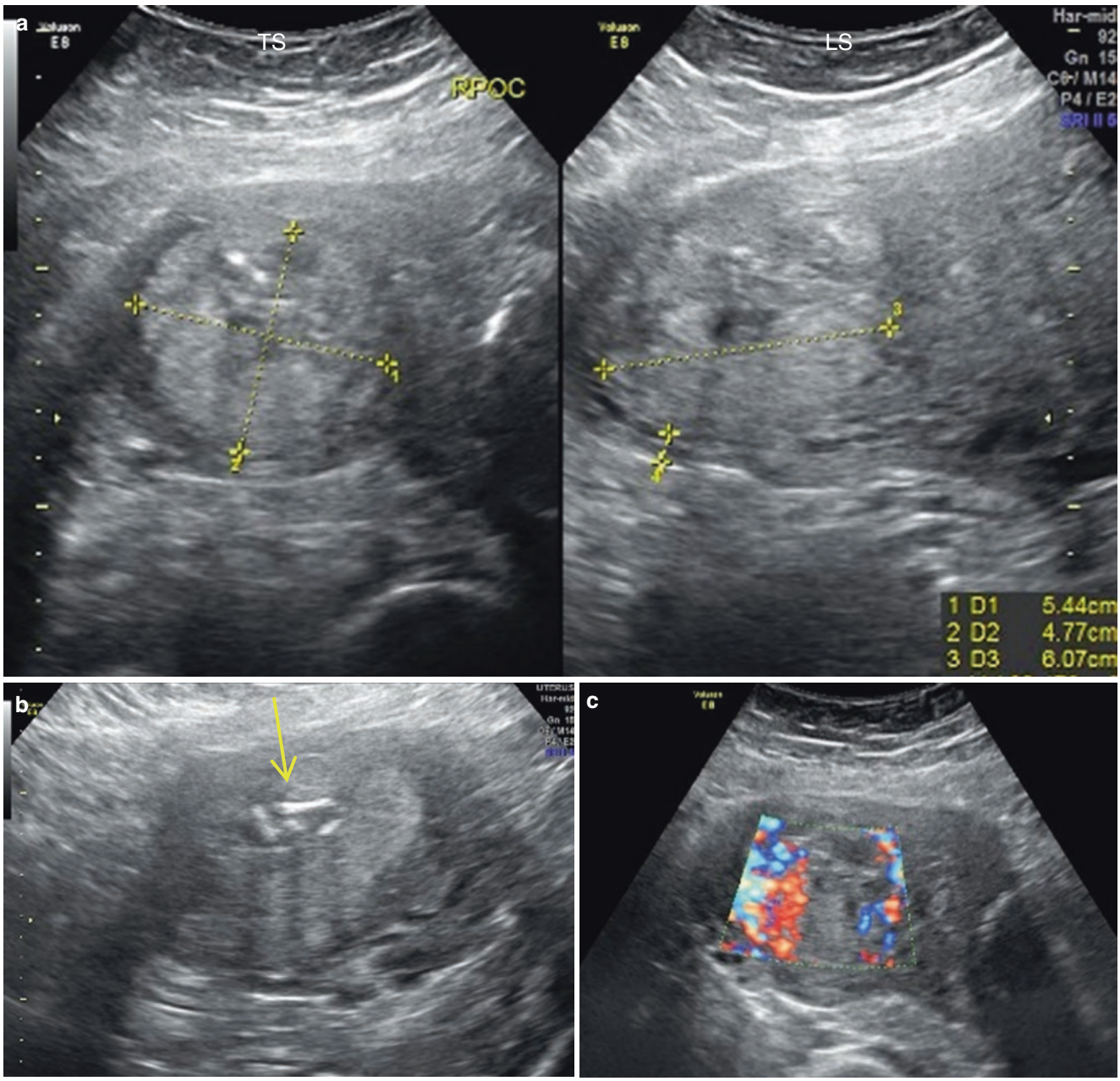

Fig. 10.35 Retained placenta and fetal tissue following missed abortion at 13 weeks. Patient had an adenomyotic uterus with multiple fibroids. USG-guided evacuation was done, but the procedure had to be abandoned as the fetal parts were high up and could not be reached. The patient presented with bleeding and a history of passing some fetal tissue. (**a**) Vaguely circumscribed hyperechoic mass is seen in the upper uterus with a few scattered hyperechoic areas within. (**b**) The hyperechoic bony retained fetal tissue (*arrow*) is seen causing acoustic shadowing. (**c**) Flow is seen in the RPOC on Doppler. The case was finally managed with hysterotomy

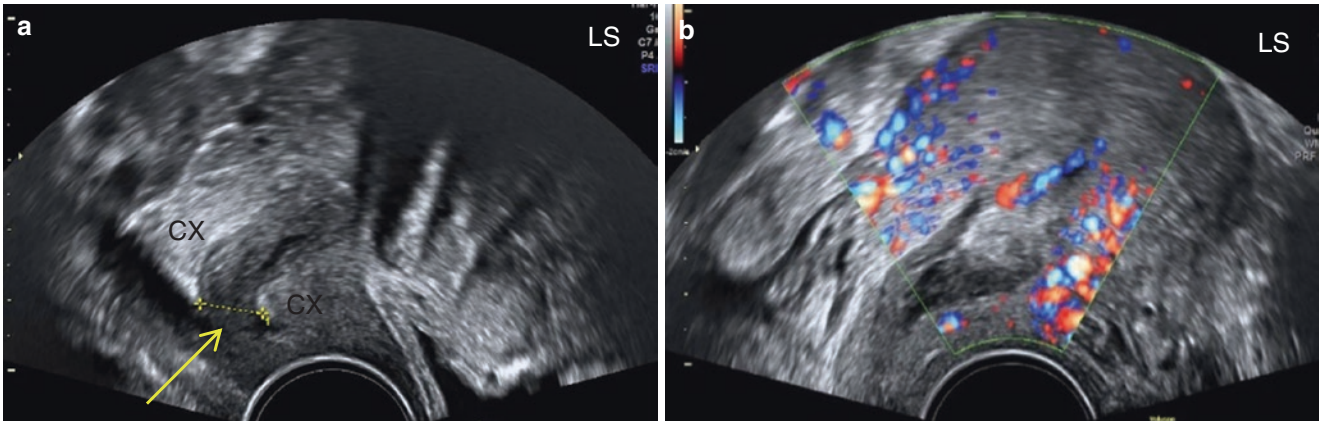

Fig. 10.36 RPOC with blood in the endometrial cavity in a patient who took medication for MTP. (**a**) Hypoechoic turbid fluid suggestive of blood is seen in the cervical canal. External os was dilated (*arrow*). (**b**) Hyperechoic complex RPOC with flow within is seen in the upper endometrial cavity

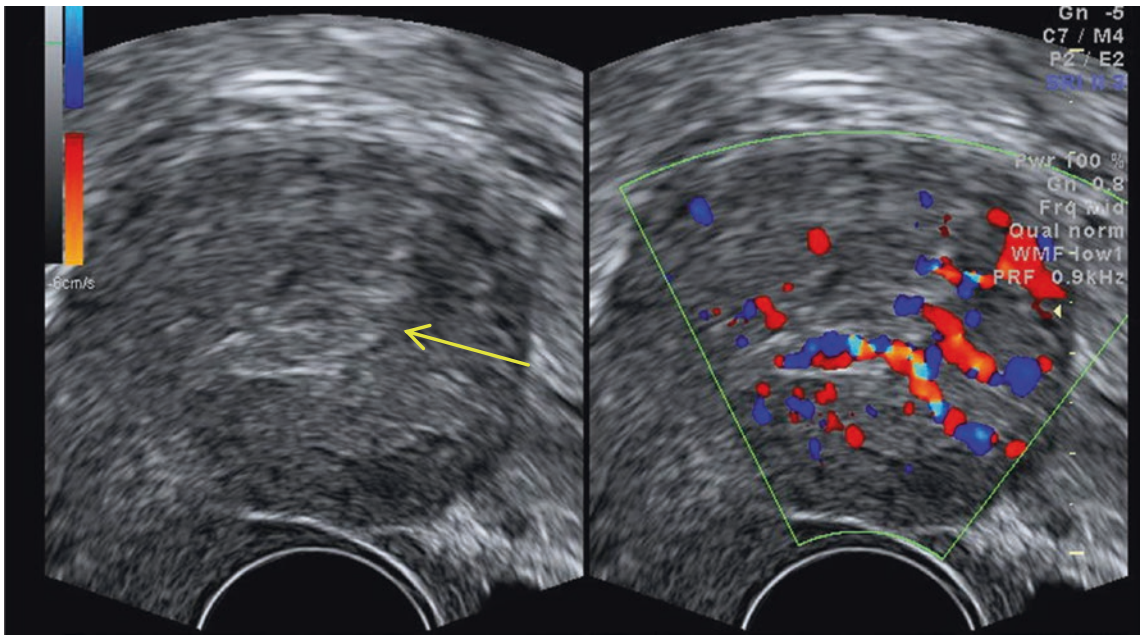

Fig. 10.37 RPOC. A poorly defined EMJ (*arrow*) showing flow from myometrium into the endometrium. Angulation of the probe may be required so as to see both the EMJ and the flow across it

often, avascular RPOC are not problematic and resolve spontaneously. Vascularity, if present, is always from the adjoining myometrium. The flow generally shows a low RI.

- Some RPOC may show turbulent flow like that of an AV malformation, with high velocity and low resistance.
- Turbid fluid suggestive of blood and clots may be seen along with RPOC in the endometrial cavity.
- Thickened endometrial echoes may indicate presence of RPOC. Various cut-offs have been used, though 10 mm appears to be most prevalent. This, however, has poor specificity, and RPOC may be present with thinner endometrium and may be absent with thicker endometrium.
- The appearance of RPOC varies with time. Initially, it may be less obvious, especially in a thick endometrium and with surrounding clots. With time, the RPOC gets more organised and becomes firm and hyperechoic. Clots around it have often passed out by then (unless the patient is bleeding actively) and if clots are present, they vary in echotexture from the RPOC. This helps in delineating the RPOC well. Sometimes the RPOC has partially passed out, which again changes its appearance in subsequent scans.

Differential Diagnosis

1. Blood clots and necrotic decidua may appear complex and hyperechoic but are avascular. They are seen within the endometrial cavity and may be very difficult to differentiate from avascular RPOC.
2. Increased vascularity of the myometrium of the placental bed following pregnancy (miscarriage or delivery) is common in the first few weeks following pregnancy. This could be focal or over a broad area and is of significance only if a placental remnant is seen.
3. AV malformations are known to show turbulent flow, but in these cases the lesion is mainly in the myometrium and comprised only of vascular channels. (Refer to section on AV malformations in – Chap. 13.)
4. Invasive moles may also show turbulent flow, but here the mass is primarily in the myometrium, often extending to more than the one-third the thickness of the myometrium, and beta hCG values are high.
5. Submucous fibroids, polyps or submucous adenomyomas may also appear similar to RPOCs (discussed in their respective chapters).

The presence of a complex hyperechoic vascular mass is very likely to be RPOC. False positives are high, especially when the RPOC is not vascular. The absence of an intracavitary mass, absence of complex intracavitary fluid and presence of a thin endometrium, however, helps to rule out RPOC.

Summary of RPOC

- Routine ultrasound is not recommended following delivery or abortion, unless there is a suspicion of some tissue left behind or the patient presents with bleeding (excessive or for a prolonged period) or with pain and fever.
- Typical RPOC appears as a hyperechoic heterogeneous intracavitary mass. It may or may not show vascularity. In the absence of vascularity, it may be difficult to distinguish it from clots or necrotic decidua in the endometrial cavity.
- The absence of an intracavitary mass, or complex intracavitary fluid and the presence of a thin endometrium, however, helps to rule out RPOC.

10.3 Gestational Trophoblastic Disease (GTD)

Gestational trophoblastic disease comprises a heterogeneous group of lesions resulting from an abnormal proliferation of the trophoblastic tissue of a placenta. These lesions include molar pregnancy, partial mole, invasive mole, choriocarcinoma, placental site trophoblastic tumour (PSTT) or epithelioid trophoblastic tumour (ETT).

Gestational trophoblastic neoplasia (GTN) includes invasive mole, choriocarcinoma, placental site trophoblastic tumour or epithelioid trophoblastic tumour that are either malignant or potentially malignant. In the absence of tissue diagnosis by histopathology, cases with persistently elevated beta hCG, following evacuation of molar pregnancy, are called persistent GTD.

Molar pregnancies (complete or partial) are managed by evacuation and GTNs primarily with chemotherapy. All GTDs require careful follow-up during and after treatment, primarily with beta hCG and often with imaging.

10.3.1 Molar Pregnancy

10.3.1.1 Molar Pregnancy: Complete Mole

This is the most common form of GTD representing 80 % of cases. A complete mole most commonly has a 46, XX karyotype with all chromosomes of paternal origin. Pathologically, the lesion shows hydropic villi and there are high circulating levels of beta hCG.

Women with molar pregnancy typically present with amenorrhoea, a positive pregnancy test, bleeding per vagina, pelvic discomfort and hyperemesis gravidarum. Serum Beta hCG levels, if done, shows unusually high values. In a case of complete mole extending beyond the first trimester, other clinical features may be seen, which include hyperthyroidism and early onset of pre-eclampsia.

Theca lutein cysts result from ovarian hyperstimulation due to high circulating levels of hCG. These cysts are bilateral, multiloculated and resolve a few weeks to months after treatment of the molar pregnancy. The presence of theca lutein cysts should raise a high suspicion of GTD. Theca lutein cysts may not be seen in the early cases in the first trimester of pregnancy. The possibility of development of GTN is significantly increased with complete mole (in about 20 %) most of which (75 %) are invasive mole, while about 25 % are choriocarcinoma, and other GTNs are rare. Follow-up with beta hCG following a molar evacuation is, therefore, essential. Ultrasound is the diagnostic modality of choice.

Ultrasound Features of Complete Mole (Figs. 10.38 and 10.39)

- The uterine cavity is filled with a heterogeneous mass showing small anechoic cystic spaces (vesicles). These cysts are hydropic chorionic villi and may vary in size from 1 to 30 mm. This has classically been described as a ‘snowstorm appearance’. The size of these cysts is seen to increase with increasing gestational age.

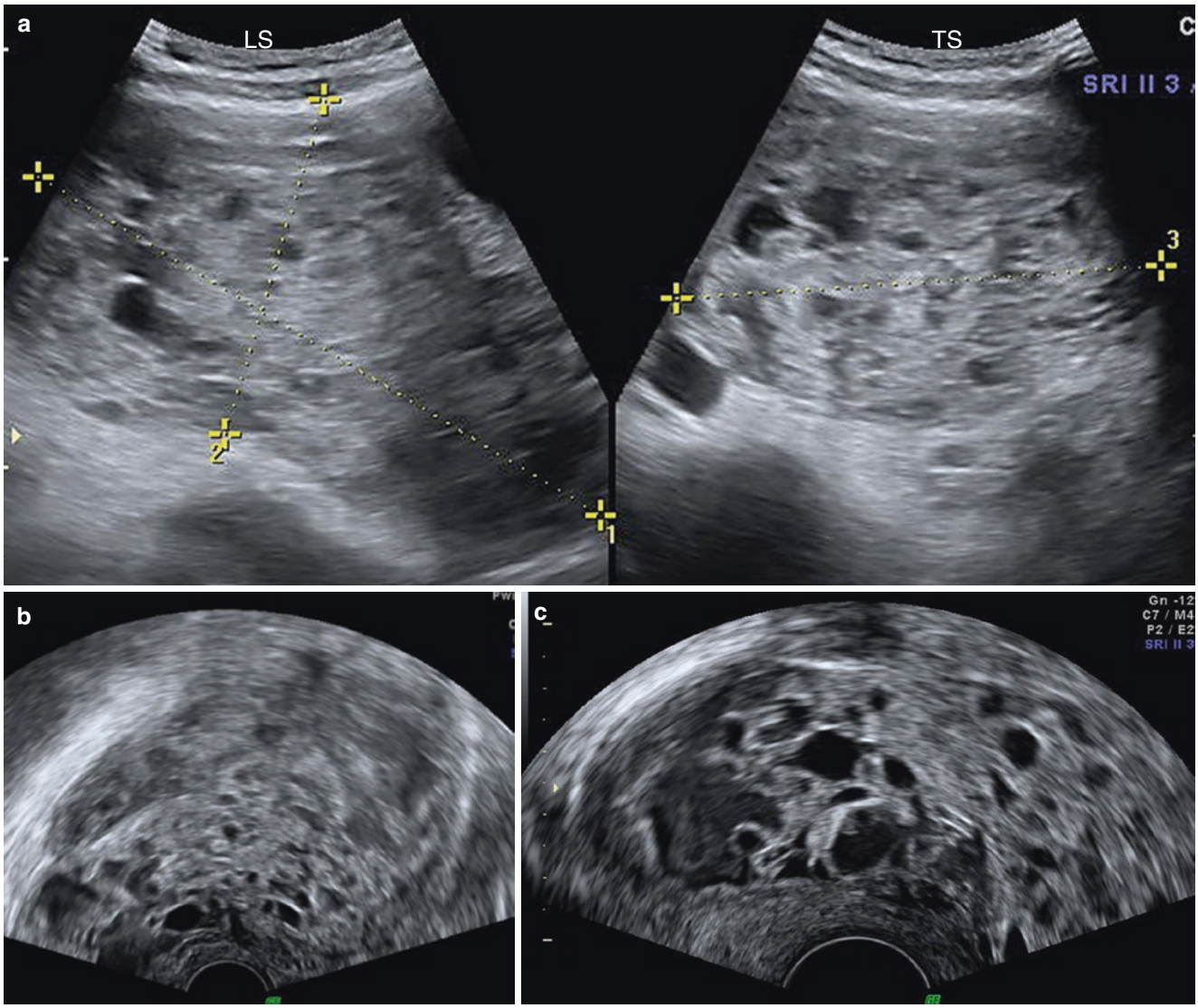

Fig. 10.38 Molar pregnancy (complete mole). The patient was diagnosed to have an incomplete abortion elsewhere, for which evacuation was done. The patient continued to bleed, and beta hCG was reported to be more than 3,00,000 mIU/mL. (**a**) Image shows the uterus with the entire uterine cavity (including most of the cervical canal), seen filled with a heterogeneous mass with tiny cysts, giving it a snowstorm appearance. (**b**–**d**) The mass shows multiple small anechoic cystic spaces within (the vesicles). (**e**, **f**) Doppler shows colour flow signals in various directions, filling the spaces between the vesicles. Flow is seen with a PSV of 17.84 cm/s and RI of 0.34 (low-velocity, low-resistance flows)

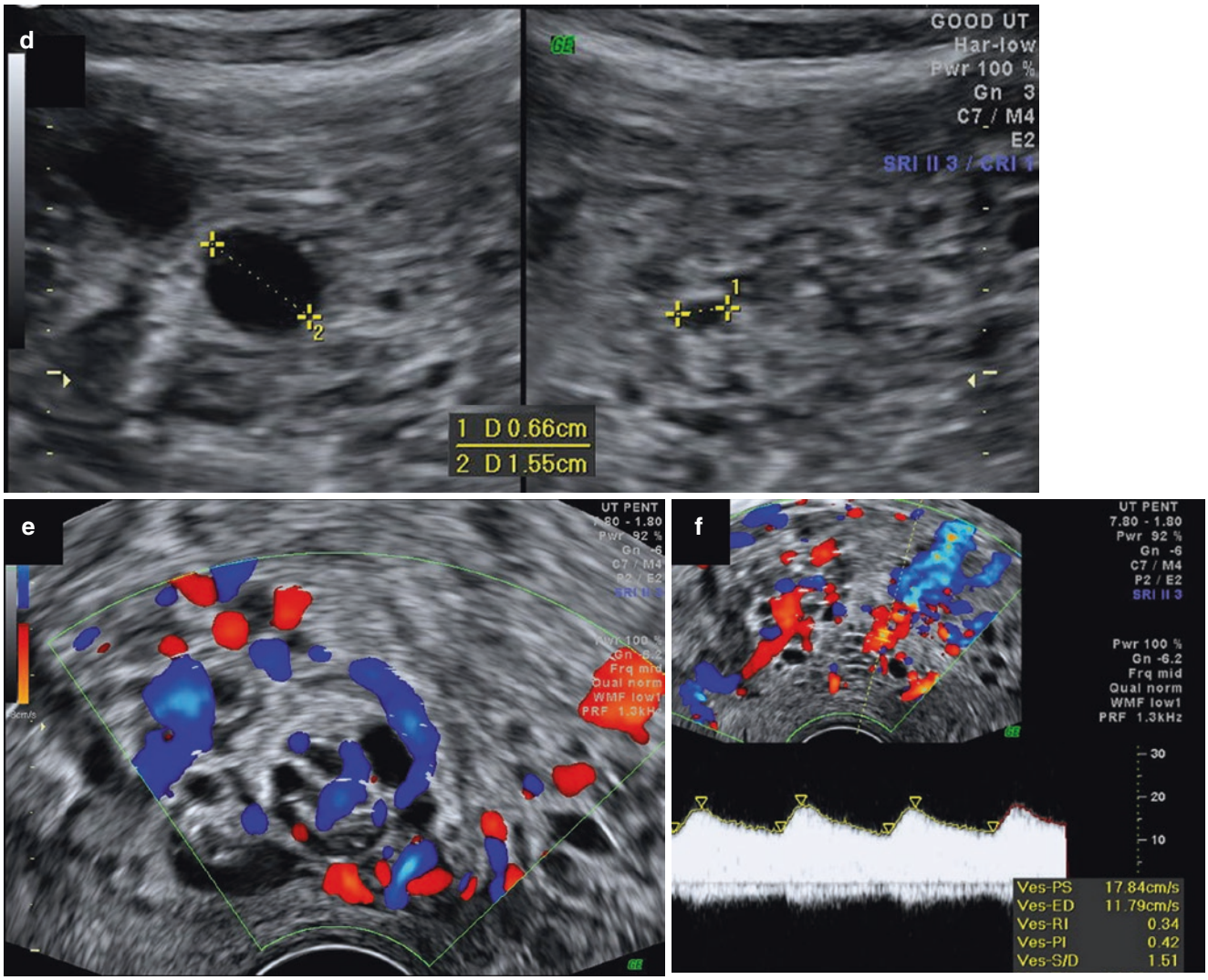

Fig. 10.38 (continued)

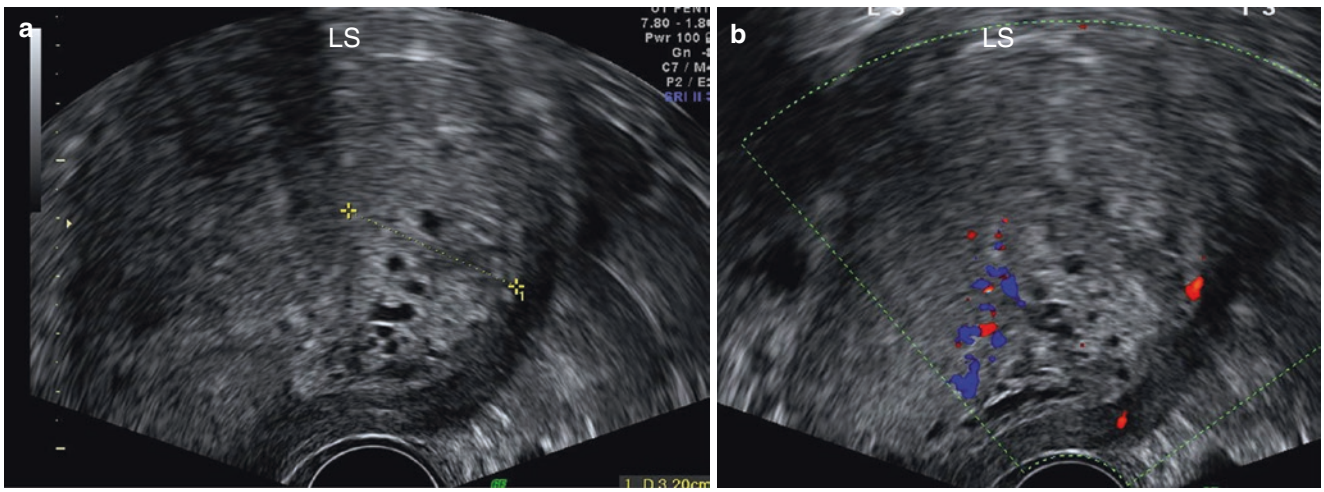

Fig. 10.39 Molar pregnancy (complete mole) at 8 weeks and 3 days. (**a**) The endometrium appeared thick (3.2 cm) and heterogeneous and showed tiny cystic spaces within, leading to the suspicion of a molar pregnancy. (**b**) No significant flow is seen on colour Doppler within this tissue, which may be because of the uterine position and low velocity of flows. Beta hCG in this patient was 1,51,236 mIU/mL

- In very early cases, these cysts may not be obvious, probably because the villi are too small to be visualised and on ultrasound there may be seen just as a central thickened mass of variable echogenicity within the endometrial cavity.
- The absence of a gestational sac and fetus.
- Sometimes, there is a large central fluid collection that mimics an anembryonic pregnancy, particularly in very early pregnancy.
- Doppler flow is seen within this heterogeneous mass, as colour flow signals in various directions, filling the space between the molar vesicles. This is because maternal blood streams into this area between the molar vesicles. On pulse wave, this inter-vesicle flow shows relatively low peak systolic velocity and low RI (average PSV 14 cm/s and average RI of 0.42). Low RI is also seen in the uterine, arcuate, radial and spiral arteries.
- Theca lutein cysts are seen bilaterally. They are multiple cysts of 2–3 cm with thin septae and clear fluid, often with some central stromal tissue, giving the ovary a 'spoke wheel' appearance. These may not be seen in association with early complete moles.
- In the first trimester, ultrasound features may not be classical, and differentiating cases of molar pregnancy from missed abortions that can also show hydropic changes in the placenta, is difficult. With an increasing use of ultrasound in early pregnancy, the majority of cases of molar pregnancy are diagnosed to be cases of missed miscarriages or anembryonic pregnancy on ultrasound. Therefore, it is suggested that histological examination of products of conception should be done in all cases of missed abortion undergoing surgical evacuation. Those with medical management should have serum beta hCG levels done, to help pick up molar pregnancy.

10.3.1.2 Molar Pregnancy: Partial Mole

Partial moles are usually triploid with two paternal sets of chromosome and one maternal set of chromosome. The beta hCG level of the partial mole is usually not very high, and therefore, they are less likely to be associated with theca lutein cysts. This is more commonly missed, as ultrasound features are not typical and because of the frequent presence of a gestational sac/fetus. The possibility of the development of GTN is only slightly increased with a partial mole. Follow-up with beta hCG should be done following evacuation.

Ultrasound Features of a Partial Mole (Fig. 10.40)

- A fetus may be identified which may not be viable, and if viable is growth restricted.
- Gestational sac is seen, but the amniotic fluid volume is reduced.
- The placenta is enlarged with cystic spaces seen in some parts.
- Theca lutein cysts are usually absent.
- This is even more likely than a complete mole to be misdiagnosed as a case of missed abortion. Most often, diagnosis is made on histopathology of evacuated products of conception.

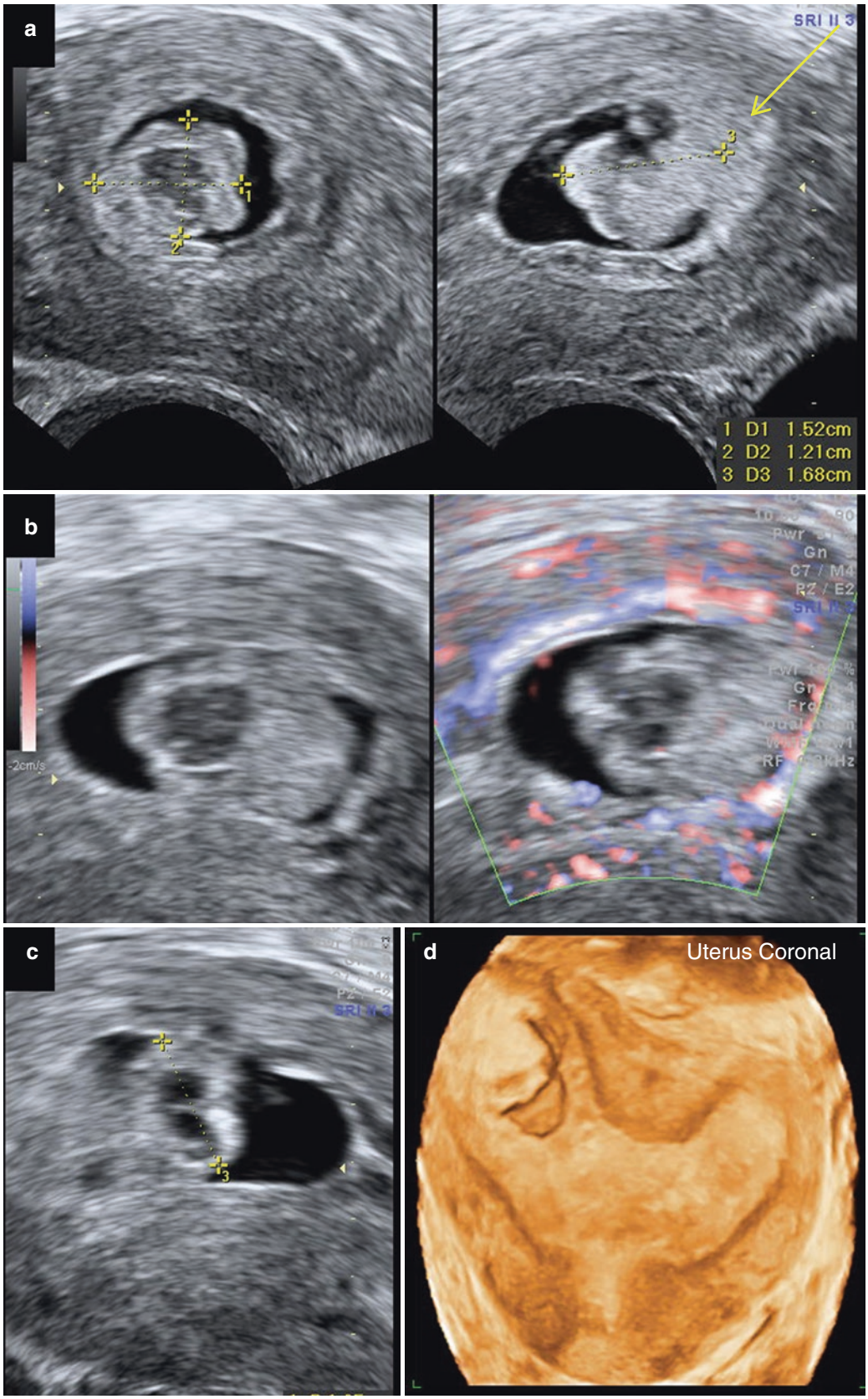

Fig. 10.40 Molar pregnancy (partial mole on HPE) in a patient with a subseptate uterus. A previous scan had shown an intrauterine GS and a subsequent scan had shown an intrauterine clot. Beta hCG was 45,847 mIU/mL. (**a**) GS is seen with a small hyperechoic protrusion from the placental tissue (*arrow*) into the GS. (**b**) A turbid cystic space seen within the placental protrusion and minimal flow is seen around the GS. No significant flow is seen within this protrusion. (**c**) In one section this protrusion showed two more smaller cystic spaces, raising the possibility of some molar features in the placenta. No fetal pole was seen. (**d**) 3D rendered coronal image of the uterus showing pregnancy in the right-sided cavity on the subseptate uterus

Summary of Molar Pregnancy

- It is the most common form of GTD, with patients presenting with amenorrhoea, irregular bleeding and high levels of beta hCG. Molar pregnancy includes both complete mole and partial mole.
- On ultrasound, typically the uterine cavity is filled with an echogenic mass showing small cystic areas and flow between the cystic areas, which is multidirectional. Theca lutein cysts may be seen. In a complete mole, no fetus is seen, whereas in a partial mole there may be an abnormal fetus or a gestational sac.
- Ultrasound findings are often not classical in the first trimester. Complete and particularly partial moles may have ultrasound findings similar to that of missed abortions. Therefore, if evacuation and histopathology are not planned in cases with missed abortion, estimation of serum beta hCG is ideal.
- All molar pregnancies require careful follow-up with serum hCG, following an evacuation.

10.3.2 Gestational Trophoblastic Neoplasia (GTN)

As mentioned above, GTN includes invasive mole, choriocarcinoma, placental site trophoblastic tumour (PSTT) or epithelioid trophoblastic tumour (ETT) that are either malignant or potentially malignant. Invasive mole and choriocarcinoma comprise most of these cases, as PSTT and ETT are rare. Most often GTN arises from a molar pregnancy, but it can also arise following miscarriages, normal pregnancies and ectopic pregnancies. Clinical presentation of GTN depends on whether the antecedent pregnancy was molar or non-molar. Features include elevated serum beta hCG, abnormal uterine bleeding, hyperthyroidism, ovarian theca lutein cysts, pelvic pain or symptoms due to metastasis. The vagina and lung are common metastatic sites and therefore evaluation is recommended.

To make a diagnosis, uterine curettage or other biopsy is not resorted to. GTN is most often a clinical diagnosis based on persistently elevated serum beta hCG after a molar pregnancy, or high beta hCG levels following a non-molar pregnancy (other causes of elevated hCG having been ruled out), supported by imaging findings that show pathology either locally in the uterus and ovaries or metastatic disease. Unlike other solid tumours, tissue diagnosis is not required prior to treatment.

10.3.2.1 Invasive Mole

Invasive mole is characterised by the presence of hydropic villi (molar tissue) invading into the myometrium. They only occasionally metastasize.

This is seen following a molar pregnancy and could be either following a complete or a partial mole. It is usually seen within 6 months of a molar pregnancy.

10.3.2.2 Choriocarcinoma

This is an anaplastic trophoblastic tissue (made up of both cytotrophoblasts and synctiotrophoblasts), without villi. It is invasive and highly vascular. This may be seen following a molar or a non-molar pregnancy. It is a highly malignant tumour with local myometrial invasion and metastasis being common. Beta hCG levels are usually extremely high.

10.3.2.3 Placental Site Trophoblastic Tumour (PSTT) and Epithelioid Trophoblastic Tumour (ETT)

These are rare types of GTN that commonly occur after a non-molar pregnancy, often several months or years following it. They originate from intermediate cells of extravillous trophoblast and secrete very low levels of hCG. Human placental lactogen (HPL) levels are however raised in PSTT, which can help with diagnosis. They are less vascular and metastasize less often as compared to choriocarcinomas. They are also more resistant to treatment with chemotherapy, and hysterectomy is the only proven cure.

Ultrasound Features of GTN (Figs. 10.41 and 10.42)
On ultrasound, these lesions (invasive mole, choriocarcinoma, PSTT and ETT) appear similar and are difficult to differentiate. Their ultrasound features are therefore being discussed together below:

- These appear as one or more poorly defined masses within the myometrium, that may extend up to the endometrium.
- It is important to measure these masses in three perpendicular dimensions (size is particularly important especially for follow-up of cases on treatment).
- They have a heterogeneous echotexture with solid and cystic areas within. These cystic areas could be fluid-filled cystic spaces (common in invasive mole), vascular channels or cystic areas secondary to haemorrhage and necrosis (common in choriocarcinoma). They are most often hyperechoic appearing.
- In cases of an invasive mole, the echotexture and vascularity are similar to that of a molar pregnancy, only seen

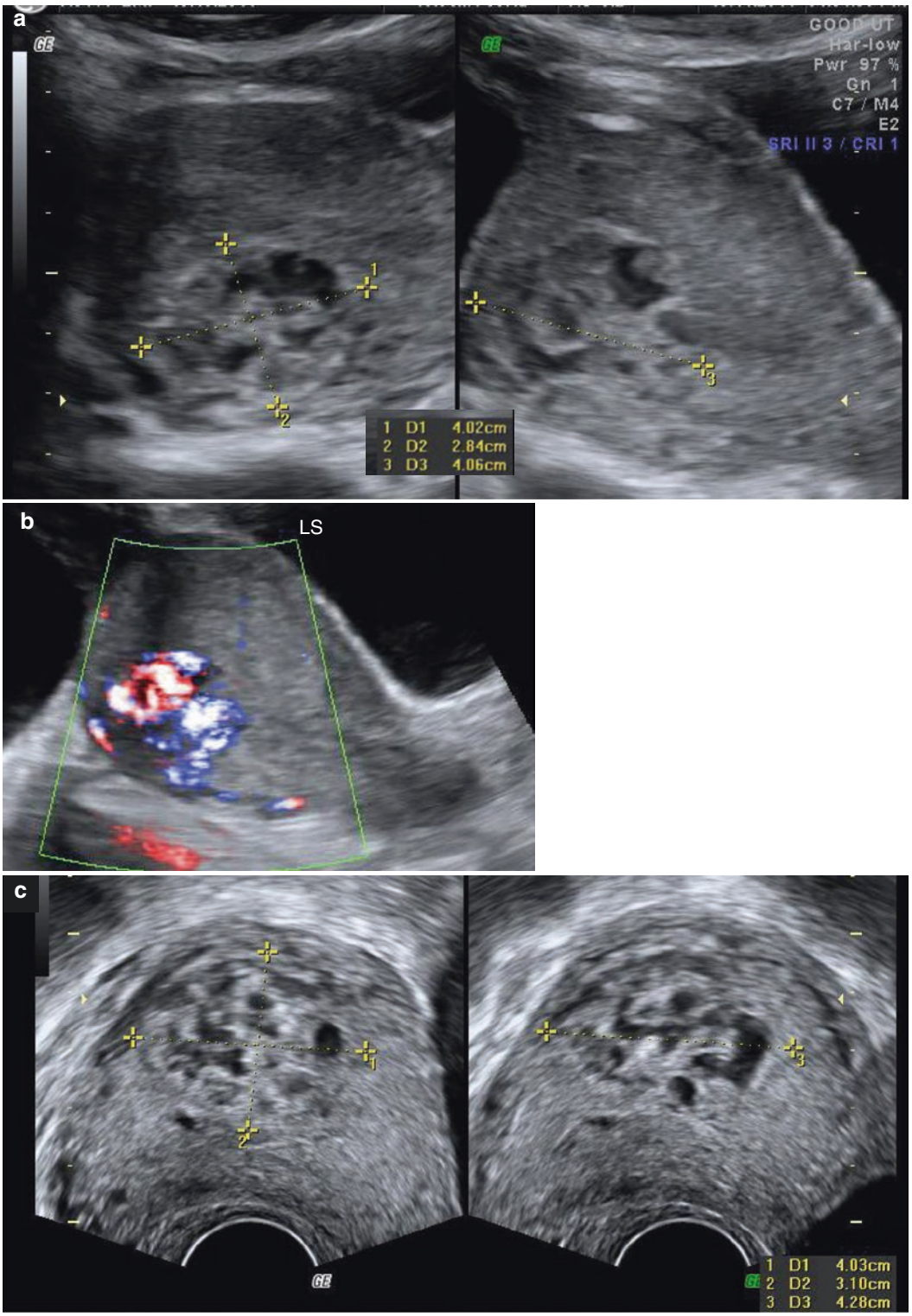

Fig. 10.41 Persistent GTD with a probable diagnosis of invasive mole. Patient had a molar pregnancy which was evacuated elsewhere (2 months prior to this scan). Following this, the patient had bloating sensation, abdominal pain and bleeding. Patient was later diagnosed to have persistent GTD with a beta hCG of 21,306 mIU/mL for which she had undergone five rounds of chemotherapy. She discontinued treatment a week prior to this scan since she found no relief of symptoms. Beta hCG 2 weeks prior to scan was 38,292 mIU/mL and on the day of the scan, had dropped to 6,117 mIU/mL. (**a**) Transabdominal scan showing a vaguely circumscribed hyperechoic cystic area in the posterior myometrium of the upper corpus. (**b**) Same, showing high vascularity on Doppler; (**c**) TVS - showing a poorly circumscribed hyperechoic mass filled with cystic spaces in the myometrium. It was reaching up to the endometrium. The EMJ in this area was not well defined. (**d**) Abundant flow and multidirectional flow seen in the mass on Doppler, as is seen in complete moles. (**e**) Flow showed PSV of 38 cm/s and RI of 0.35. (**f**) Glass body rendered image showing the vascular mass within the uterus. (**g**) Bilaterally enlarged ovaries showing multiple theca lutein cysts. The image (**g**) shows the typical a 'spoke wheel' appearance. (**h**) Minimal flow is seen in the thinned out ovarian tissue between the cysts. (**i**) 3D rendered image of the theca lutein cysts

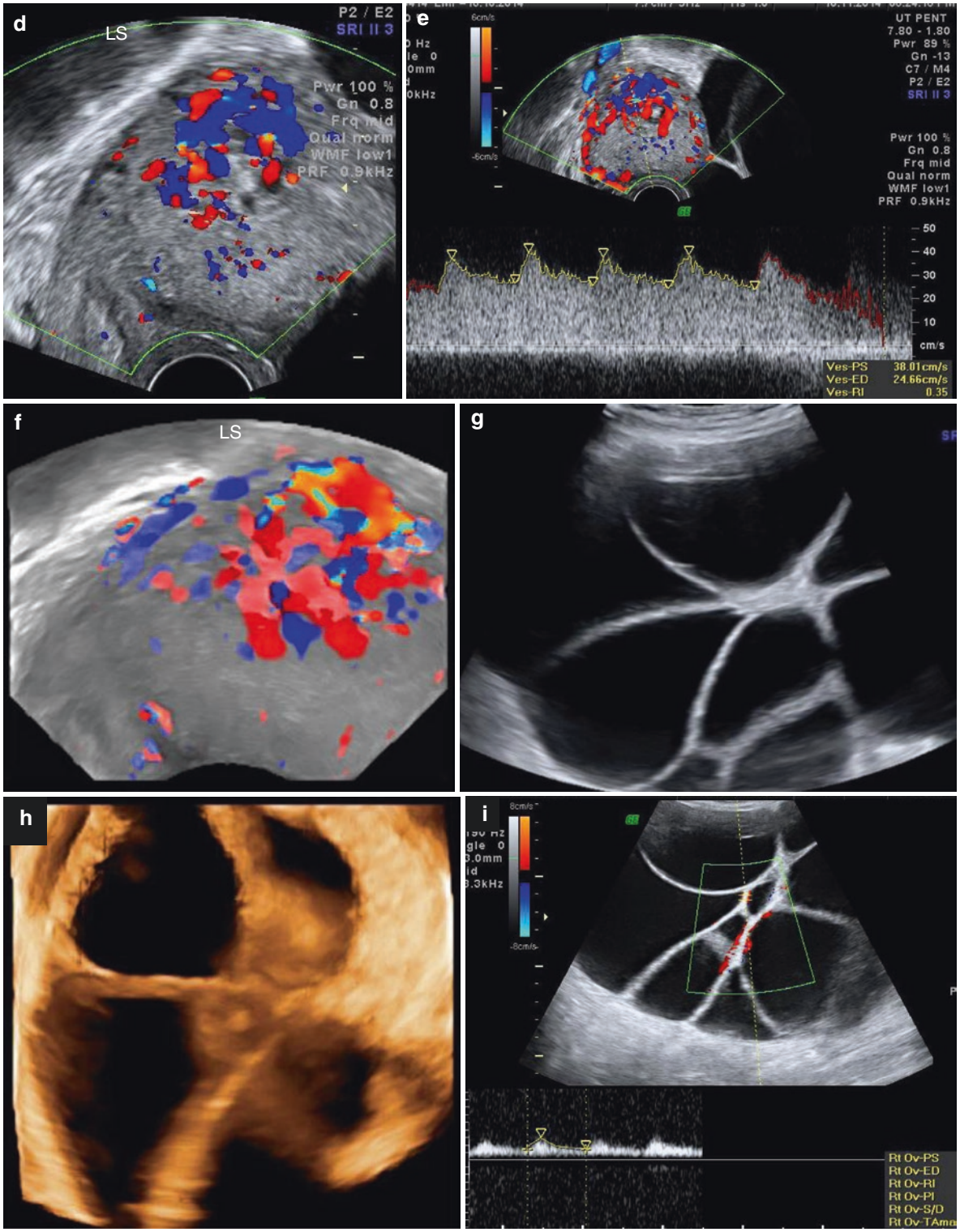

Fig. 10.41 (continued)

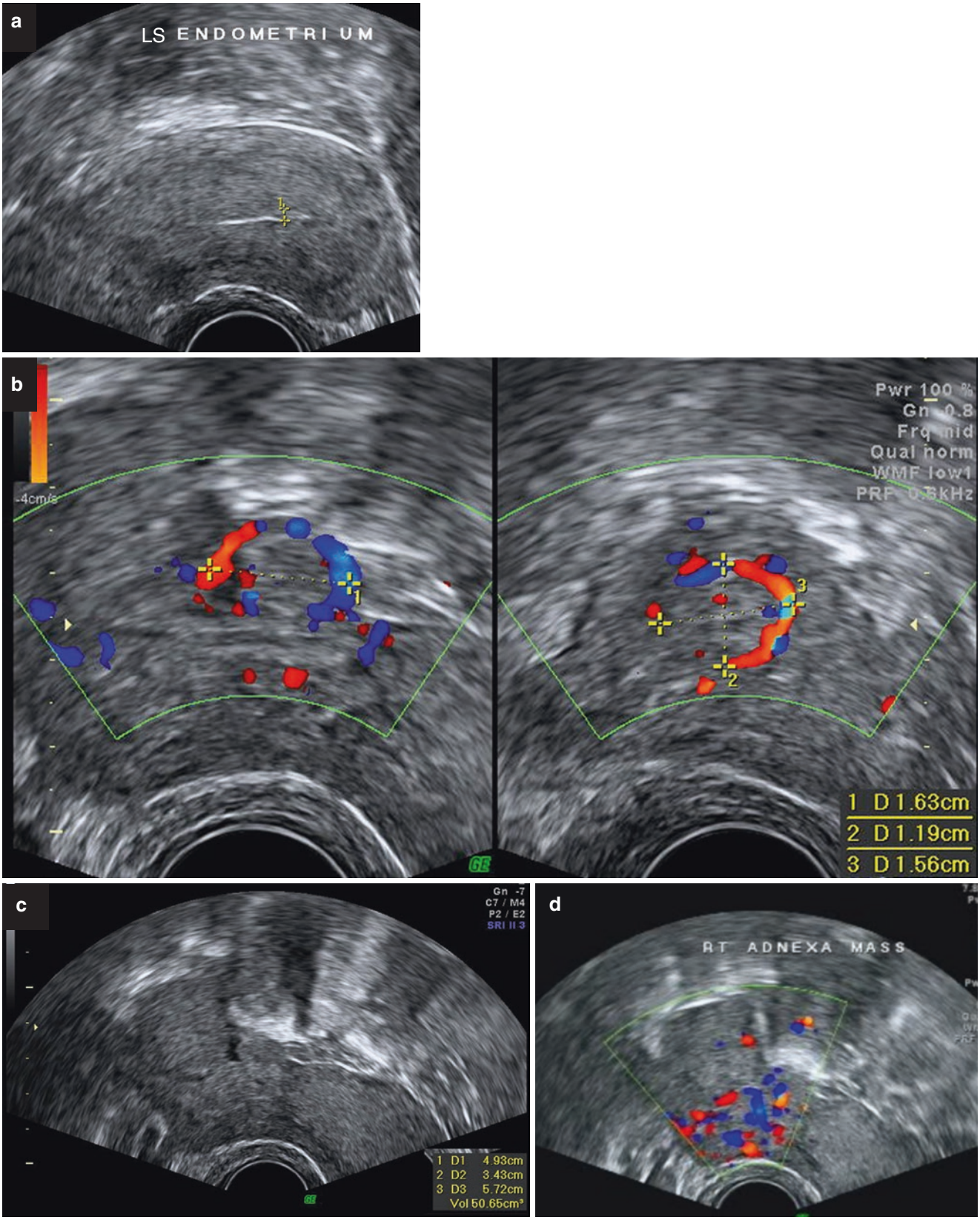

Fig. 10.42 GTN (probably choriocarcinoma) with thromboembolism of the right pulmonary artery. Patient had amenorrhoea for 6 months. UPT was positive and the patient took medication for a chemical TOP, following which there was no bleeding. UPT, however, remained positive, and the scan done elsewhere showed an empty uterine cavity. Patient presented with fever and respiratory symptoms of chest pain, cough and breathlessness. (**a**) Empty intrauterine cavity is seen. (**b**) A vaguely circumscribed slightly hyperechoic mass is seen close to the right uterine cornua with peripheral vascularity, resembling an interstitial ectopic pregnancy. (**c**) There was an irregular, isoechoic, heterogeneous, solid mass seen extending from the right upper end of the uterus into the surrounding areas. (**d**) This mass showed increased vascularity on Doppler. The findings were suggestive of a solid, neoplastic, malignant mass. Beta hCG was 8,03,419 mIU/mL after the scan. Findings suggested a GTN with a small, local mass in the uterus and local metastasis from the uterus into the surrounding structures along with thromboembolism of the pulmonary arteries

deep in the myometrium. The cystic spaces seen are hydropic villi.

- In choriocarcinoma, the tissue is more solid appearing and heterogeneous, with necrotic areas within appearing cystic.
- Increased vascularity with low-resistance flows is noted in and around the mass. Often there are dilated vessels in the surrounding myometrium.
- Arteriovenous shunts with turbulent flows, associated with neovascularisation with in the intra-myometrial mass, show up as chaotic vasculature with mosaic colours on Doppler and low-resistance (low RI) on spectral Doppler. This is common with invasive mole and choriocarcinoma.
- The RI in the uterine arteries is also often reduced.
- In cases of patients with a more extensive disease (usually cases of choriocarcinoma), the uterus may be heterogeneously enlarged, and the tumour may be seen extending into the parametrium and neighbouring pelvic organs.
- Theca lutein cysts are multiple due to high hCG levels causing bilaterally, enlarged, multicystic ovaries with a 'spoke wheel' appearance. These are uncommon in cases with PSTT because of lower levels of beta hCG.
- PSTT masses usually have indistinct margins and multiple cystic spaces, whereas ETT tends to have sharper borders.
- At follow-up scans (during treatment), these myometrial lesions are seen to become more hypoechoic and show a decrease in size and vascularity.

Summary of GTN

- This is a heterogeneous condition which can occur following a molar pregnancy, a normal pregnancy or an abortion.
- Invasive moles are locally invading GTN-which only occasionally metastasize and are seen following a complete or a partial mole.
- Choriocarcinoma is a highly malignant tumour associated with local invasion, distant metastasis and high hCG levels.
- Placental site trophoblastic tumor is rare and occurs usually after a non-molar pregnancy. They secrete lower levels of hCG and are more chemo-resistant.
- On ultrasound, these various GTN lesions in the uterus appear similar and it may be difficult to differentiate between them. They are seen as poorly defined heterogeneous myometrial lesions showing high vascularity. Invasive moles generally appear more cystic, whereas choriocarcinomas are more likely to be solid.

Suggested Reading

Abbasi S et al (2008) Role of clinical and ultrasound findings in the diagnosis of retained products of conception. Ultrasound Obstet Gynecol 32:704–707. doi:10.1002/uog.5391

Condous G et al (2007) Prediction of ectopic pregnancy in women with a pregnancy of unknown location. Ultrasound Obstet Gynecol 29:680–687. doi:10.1002/uog.4015

Green CL et al (1996) Gestational trophoblastic disease: a spectrum of radiologic diagnosis. Radiographics 16(6):1371–1384

Gun M, Mavrogiorgis M (2002) Cervical ectopic pregnancy: a case report and literature review. Ultrasound Obstet Gynecol 19:297–301. doi:10.1046/j.1469-0705.2002.00559

Jurkovic D, Mavrelos D (2007) Catch me if you scan: ultrasound diagnosis of ectopic pregnancy. Ultrasound Obstet Gynecol 30:1–7. doi:10.1002/uog.4077

Kirk E et al (2007) The accuracy of first trimester ultrasound in the diagnosis of hydatidiform mole. Ultrasound Obstet Gynecol 29:70–75. doi:10.1002/uog.3875

Levine D (2007) Ectopic Pregnancy. Radiology 245:385–397. doi:10.1148/radiol.2452061031

Mavrelos D et al (2007) Ultrasound diagnosis of ectopic pregnancy in the non-communicating horn of a unicornuate uterus (cornual pregnancy). Ultrasound Obstet Gynecol 30:765–770. doi:10.1002/uog.5131

Memtsa M et al (2013) Diagnosis and management of intramural ectopic pregnancy. Ultrasound Obstet Gynecol 42:359–362. doi:10.1002/uog.12437

Mulic-Lutvica A, Axelsson O (2006) Ultrasound finding of an echogenic mass in women with secondary postpartum hemorrhage is associated with retained placental tissue. Ultrasound Obstet Gynecol 28:312–319. doi:10.1002/uog.2849

Müngen E (2003) Vascular abnormalities of the uterus: have we recently over-diagnosed them? Ultrasound Obstet Gynecol 21:529–531. doi:10.1002/uog.163

Okumura M, Fushida K, Rezende WW, Schultz R, ZUGAIB M (2010) Sonographic appearance of gestational trophoblastic disease evolving into epithelioid trophoblastic tumor. Ultrasound Obstet Gynecol 36:249–251. doi:10.1002/uog.756

Richardson A et al (2016) Accuracy of first-trimester ultrasound in diagnosis of tubal ectopic pregnancy in the absence of an obvious extrauterine embryo: systematic review and meta-analysis. Ultrasound Obstet Gynecol 47:28–37. doi:10.1002/uog.14844

Sawyer E et al (2007) The value of measuring endometrial thickness and volume on transvaginal ultrasound scan for the diagnosis of incomplete miscarriage. Ultrasound Obstet Gynecol 29:205–209. doi:10.1002/uog.3914

Sebire NJ et al (2001) The diagnostic implications of routine ultrasound examination in histologically confirmed early molar pregnancies. Ultrasound Obstet Gynecol 18:662–665. doi:10.1046/j.0960-7692.2001.00589

Sellmyer MA et al (2013) Physiologic, histologic, and imaging features of retained products of conception. Radiographics 33(3):781–796

Seow K-M et al (2004) Cesarean scar pregnancy: issues in management. Ultrasound Obstet Gynecol 23:247–253. doi:10.1002/uog.974

Timor-Tritsch IE et al (2014) Cesarean scar pregnancy and early placenta accreta share common histology. Ultrasound Obstet Gynecol 43:383–395. doi:10.1002/uog.13282

Schoubroeck V et al (2004) Prospective evaluation of blood flow in the myometrium and uterine arteries in the puerperium. Ultrasound Obstet Gynecol 23:378–381. doi:10.1002/uog.963

Zhou Y et al (2013) Sonographic characteristics of placental site trophoblastic tumor. Ultrasound Obstet Gynecol 41:679–684. doi:10.1002/uog.12269

Zosmer N et al (2015) Natural history of early first-trimester pregnancies implanted in cesarean scars. Ultrasound Obstet Gynecol 46:367–375. doi:10.1002/uog.14775

Torsion

11

11.1 Ovarian Torsion

Torsion is one of the most common gynaecological emergencies. It is the result of the twisting of a structure or a mass, with resultant compromise in vascular flow. The ovary is the most common organ that undergoes torsion. In addition, torsion may also be seen in paraovarian cysts or tubal masses like a hydrosalpinx. Very often, the fallopian tube twists along with the ovary, a phenomenon referred to as adnexal torsion. Ovarian torsion can result in ischaemia and necrosis, which in turn could lead to loss of the ovary (Fig. 11.1).

Torsion is more common in ovaries that are enlarged with a mass and is less common in masses/ovaries that are fixed with adhesions, like in the cases of endometriosis and malignancies. Torsion in young girls is known to occur, at times, even in the absence of an ovarian mass. This has been explained by the possibility of long ligamentous supports of the ovary which increase the potential for ovarian torsion.

Right-sided torsion is more common than left, which is believed to be because of the presence of the sigmoid colon on the left, which reduces the likelihood of torsion due to limited space. Torsion is often triggered off by exercise or any other activity that causes a sudden change in intra-abdominal pressure. An early diagnosis of torsion is important for prompt management of these cases, so as to save the ovary. The present recommendation is laparoscopic detorsion of the ovary, with the ovary being left behind even if it looks gangrenous. This is because recovery of ovarian function is seen in more than 90% of ovaries on a follow-up scan done 6–8 weeks (up to 6 months) later. In the small remainder of cases, the ovaries become atrophic and no follicles are seen in follow-up scans (Oelsner et al. 2003). Surgical removal of the ovary is resorted to if there is a possibility of a malignant tumour or cyst, or in women who are postmenopausal or perimenopausal.

Diagnosis of torsion is by clinical suspicion, supported by ultrasound findings.

Clinical Features of Torsion

These are often non-specific and include:

- Pain which is usually of sudden onset, sharp and localised to the lower abdomen. It is generally moderate to severe in intensity with many patients, therefore presenting at the 'emergency' department of hospitals. Pain could be acute or intermittent. Very often there is a history of some activity, bowel movement or exercise, that triggered off the pain.
- History of nausea or vomiting is seen in about half the cases and a few may complain of pyrexia.
- Tenderness and/or a palpable mass is often noted on examination.

In most studies, the diagnostic accuracy of ultrasound for diagnosis of ovarian torsion was found to be about 50–75 %. Therefore, in most centres, laparoscopy is considered as the gold standard for diagnosis of torsion in patients with a clinical suspicion of torsion. However, in experienced hands, ultrasound accuracy can be improved significantly with proper and careful evaluation, to above 90%.

Ultrasound Features of Torsion

Ultrasound findings in torsion can be grouped into two broad categories – the first category includes ultrasound features that are commonly seen in torsion but are not very specific, and the second category includes three ultrasound features that are more specific and therefore more useful in diagnosis. The three features in the second category are the whirlpool sign of the pedicle, abnormal Doppler flows and the follicular ring sign.

A. Common ultrasound findings in torsion (non-specific) (Figs. 11.2, 11.3, 11.4, 11.5, 11.6, 11.7, 11.8, 11.9)
   - An *enlarged ovary* is a very common feature, but not specific to torsion. One of the reasons for an enlarged ovary in torsion is that torsion is known to occur in ovaries that are already enlarged (to 4–5 cm or more) due to functional cysts (like corpus luteal cysts), neoplastic masses (particularly dermoid cysts) and hyperstimu-

M. Sibal, *Ultrasound in Gynecology*, DOI 10.1007/978-981-10-2714-7_11

lated ovaries. Congestion and oedema of the ovary secondary to torsion also contribute to its increased size.

- *Cysts*, when present, are often *haemorrhagic and thick walled.*
- The *ovarian stroma appears oedematous* (enlarged/swollen, excessive stromal tissue with no/few follicles). The stroma may appear heterogeneous and a little hyperechoic, because of haemorrhage and oedema. The entire ovary may appear solid, particularly on a transabdominal scan. There may be complete loss of architecture in necrotic torsed ovaries.
- Torsed ovaries typically show *multiple, peripheral, cortical follicles*, because the oedematous stroma pushes the antral follicles to the periphery.
- The ovary may be placed in an *unusual location*, like anterior to the uterus or on the opposite side. It could also be impacted in the pouch of Douglas.
- The ovaries are generally *tender* to touch. If the patient has already been administered with some painkiller, then the tenderness may be significantly reduced.
- Some amount of *free fluid* is a very common feature of torsion, but again not specific. This is because minimal free fluid is seen in a large variety of cases that have nothing to do with torsion.
- The *pedicle* of the torsed ovary appears as an extra-ovarian mass. On long section, it appears as an elongated and heterogeneous mass. On transverse section, it is circumscribed and generally has a bright echogenic centre like a 'target sign' which is the central axis of the twisted pedicle. This 'target sign' is very useful in identifying the twisted pedicle in cases of torsion. The transverse section of the twisted pedicle can appear hyperechoic with multiple concentric hypoechoic stripes or may show hypoechoic beads within, which are nothing but engorged veins within the twisted pedicle.

  Though the pedicle is a more specific feature (i.e. it is not seen in other conditions), because its appearance can vary and resemble a large number of other pelvic structures (like the fallopian tube), identifying it can be difficult, limiting its diagnostic utility in torsion.
- Often the tube gets torsed along with the ovary. This is difficult to identify on ultrasound, because other than the fimbrial end, the tube does not have specific features to help identify it. Only occasionally (more often if there is fluid surrounding it), one may see a *thickened segment of the fallopian tube* close to the pedicle. This may or may not show flow, depending on the severity of torsion.

B. Specific ultrasound findings in torsion (which are useful in diagnosis) (Figs. 11.10, 11.11, 11.12, 11.13, 11.14, 11.15, 11.16, 11.17, 11.18 and 11.19)

- *Whirlpool sign of the pedicle* (Fig. 11.10): This refers to the spiral or whirlpool pattern seen in the transverse section of the pedicle on ultrasound, when the probe is gently moved along the long axis of the pedicle. Most often, in this transverse section of the pedicle, one can also see a central hyperechoic spot ('target sign' mentioned earlier). This 'target sign' helps not only in locating the twisted pedicle but also in obtaining the right section required to elicit the whirlpool sign.

  The whirlpool sign can be seen both on greyscale and Doppler. Addition of the whirlpool sign to other sonographic features has definitely increased the diagnostic accuracy of ultrasound. In addition, it is also very useful in the diagnosis of non-ovarian torsion (e.g. torsion of a hydrosalpinx or a para-ovarian cyst).

  The greatest limitation of this sign is that it requires some level of expertise/training, not only to locate the pedicle but also to get a transverse section of the pedicle and elicit the whirlpool sign. One trick in searching for the pedicle is to look between the uterus and the torsed ovary and between the torsed ovary and the lateral pelvic walls, as those are the most common sites where the pedicle is located.

  Another issue with the whirlpool sign that has been reported in studies is the presence of both false positives and false negatives.
- *Abnormal Doppler* flows (Figs. 11.11, 11.12 and 11.13): We know that following a twist, first venous and then arterial flow is lost (as the walls of the veins are thinner and more easily compressed than those of the arteries), and, finally, there is ischaemia and necrosis. Therefore, in a given case, one may see arterial and venous flow, or one may see only arterial flow (with no venous flow), or one may see no flow at all (i.e. no arterial and no venous flow).

  The greatest limitation of Doppler is that it is a late feature in torsion. Therefore, even if one sees normal flows, torsion cannot be ruled out.

  Another issue in some studies is a high false positive rate (in one such study, no flow was seen in 62.5% of cases that had no torsion). If settings are optimised, this is unlikely. (Doppler settings are discussed in Chap. 2.) For appropriate settings, the PRF should be brought down to 0.6 (or even to 0.3, if no flow is seen). Next the Doppler gain should be stepped up until artefacts are seen and then gradually turned down till the artefacts just disappear. Comparison with the contralateral normal ovary provides a good control for Doppler evaluation.
- *Follicular ring sign (FRS)* (Figs. 11.14, 11.15, 11.16, 11.17 and 11.18): 'Follicular rings' are prominent (1–2 mm thick) hyperechoic margins seen all around

the antral follicles of the torsed ovary. They can be seen on both transvaginal and transabdominal scans but are obviously better visualised on transvaginal scan. Again, comparison with the normal contralateral ovary provides a convenient control. This was initially an incidental observation, which was later published by the author. *The study showed that the 'follicular ring sign' is an early, easy, specific and frequently seen feature in torsion.*

The appearance of FRS is caused by oedema, swelling and haemorrhage that occurs around the walls of the antral follicles. We know that antral follicles have a good blood supply. Initially, when venous flow is obliterated but arterial flow continues, there is an increase in the hydrostatic pressure of the capillaries surrounding these follicles. This causes an ooze from the capillaries, with resultant oedema and haemorrhage. This was seen on both macroscopic and microscopic examination of the torsed ovaries in these cases (Fig. 11.17).

Follicular ring sign is an early feature in torsion, seen before there is a visible change in the ovarian tissues because of congestion and before blood flow to the ovary stops. In fact, it is very distinct in this early stage. As the condition progresses, however, the oedema and haemorrhage spread throughout the rest of the ovaries, and the 'follicular rings', though seen, are less distinct.

FRS is a feature that is easy to find, because one knows exactly where to look – the antral follicles of the torsed ovary. It does not, therefore, require much expertise and training.

Advantages of FRS

In small peripheral centres where Doppler machines may not be available, this sign is likely to help in diagnosis as it does not require any Doppler evaluation.

One limitation of FRS is that if antral follicles are not seen (like in a necrotic ovary or an ovary with a large cyst and minimal compressed ovarian tissue or one located far away from probe), then the FRS cannot be seen. Even in large cysts (including dermoids), if one carefully searches in the minimal ovarian tissue around the cyst, one is generally able to observe the antral follicles and the FRS.

Of the three specific features useful in diagnosis of ovarian torsion, the whirlpool sign is seen right from the beginning, the follicular ring sign is seen early in the course of torsion (when venous and lymphatic flow begins to get compromised) and the abnormal Doppler (absence of flow) is a much later feature.

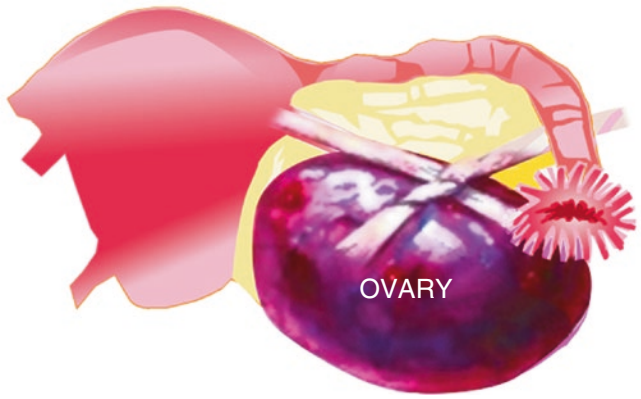

Fig. 11.1 Diagrammatic representation of ovarian torsion, with the ovary twisted on its ligamentary supports, causing ovarian ischaemia

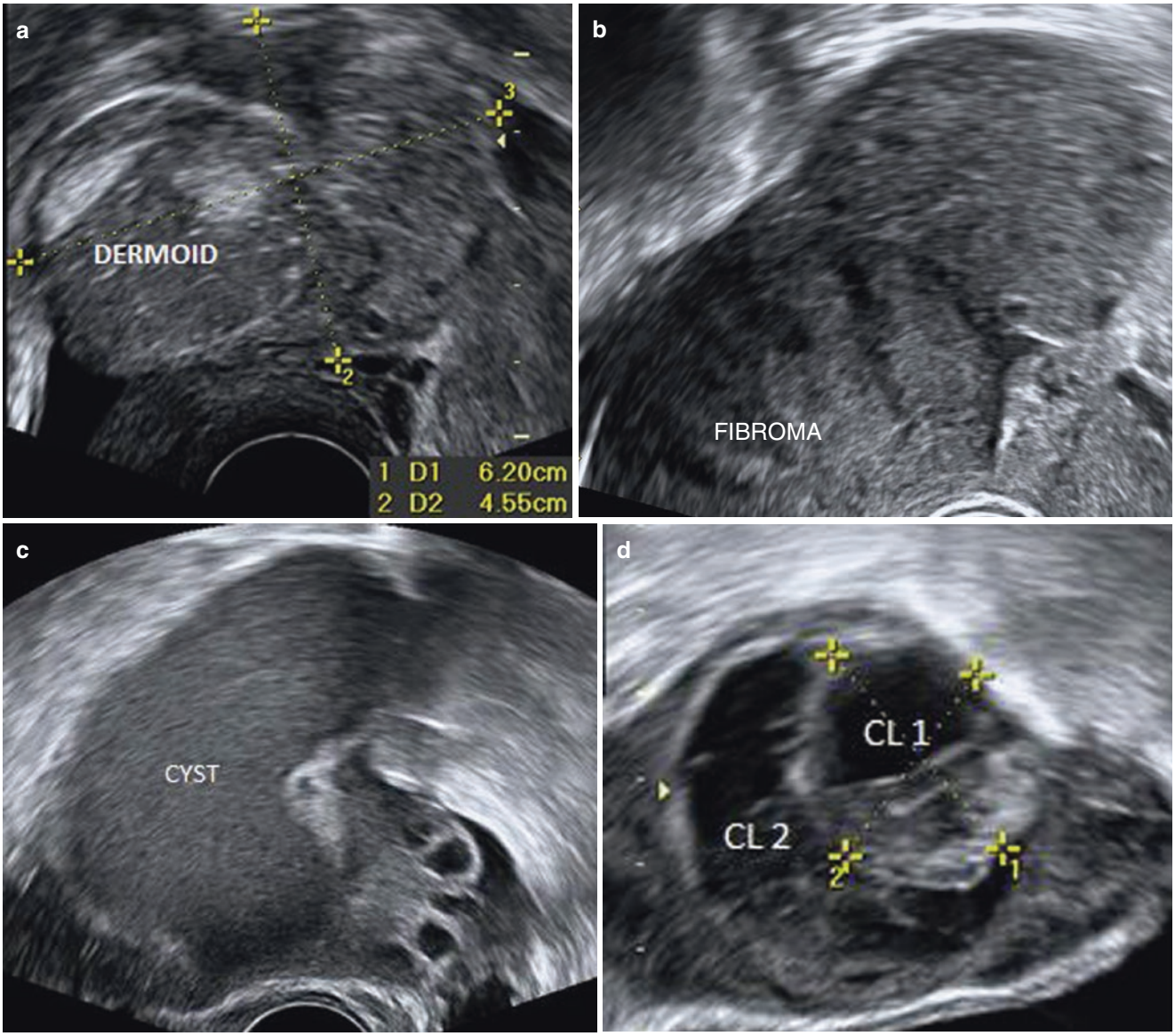

Fig. 11.2 Ovaries enlarged with cysts: (**a**) dermoid, (**b**) fibroma, (**c**) neoplastic serous cystadenoma, (**d**) corpus luteal cysts. (**c**, **d**) Cysts show turbid contents and thick walls

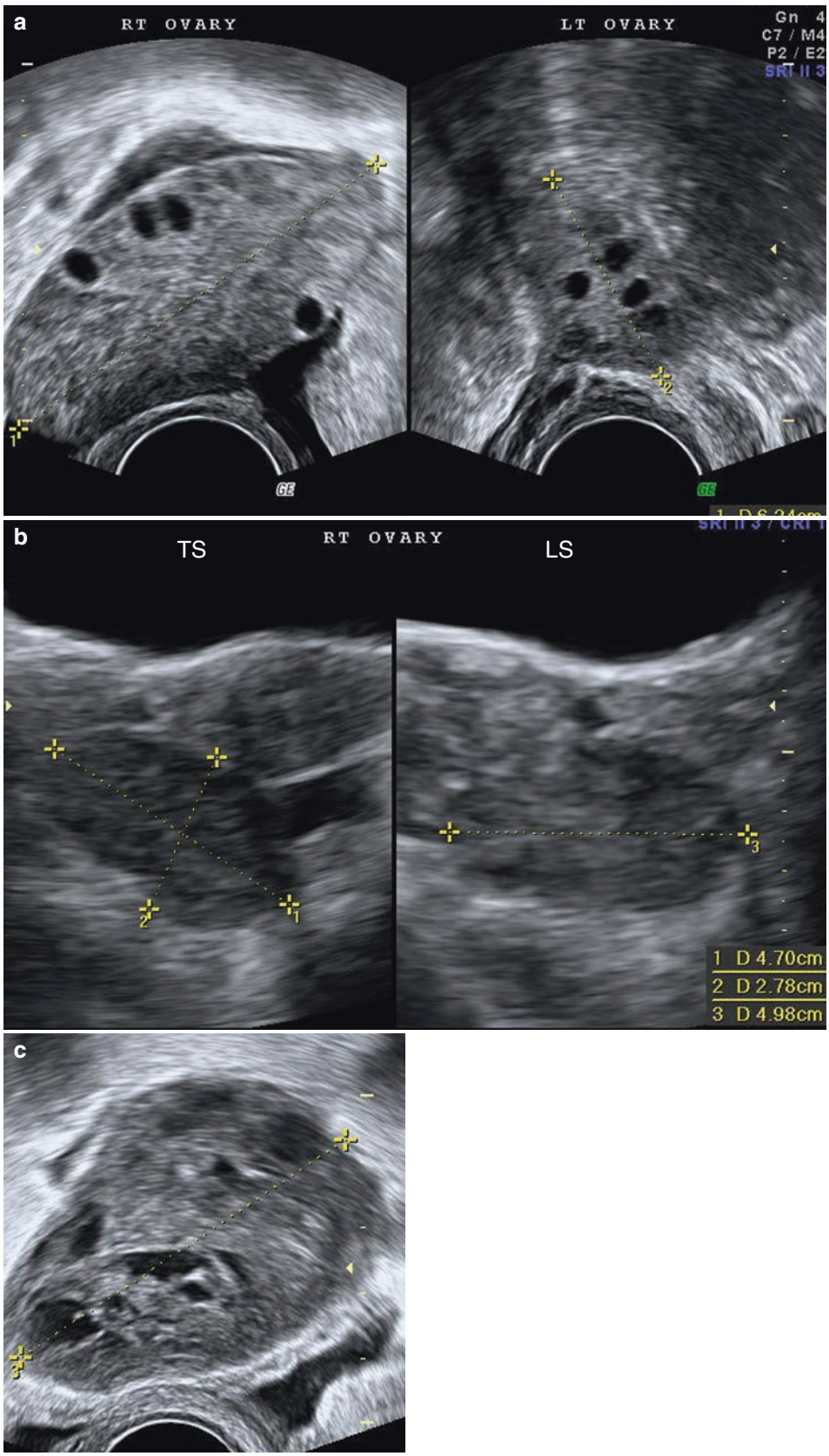

Fig. 11.3 Ovarian stroma in torsion. (**a**) Case of right ovarian torsion, with normal left ovary. The torsed right ovary shows peripheral, scattered antral follicles and thick hyperechoic, heterogeneous stroma, due to oedema and haemorrhage. (**b**) Solid-appearing torsed ovary on TAS. (**c**) Heterogeneous-appearing necrotic ovary with complete loss of architecture

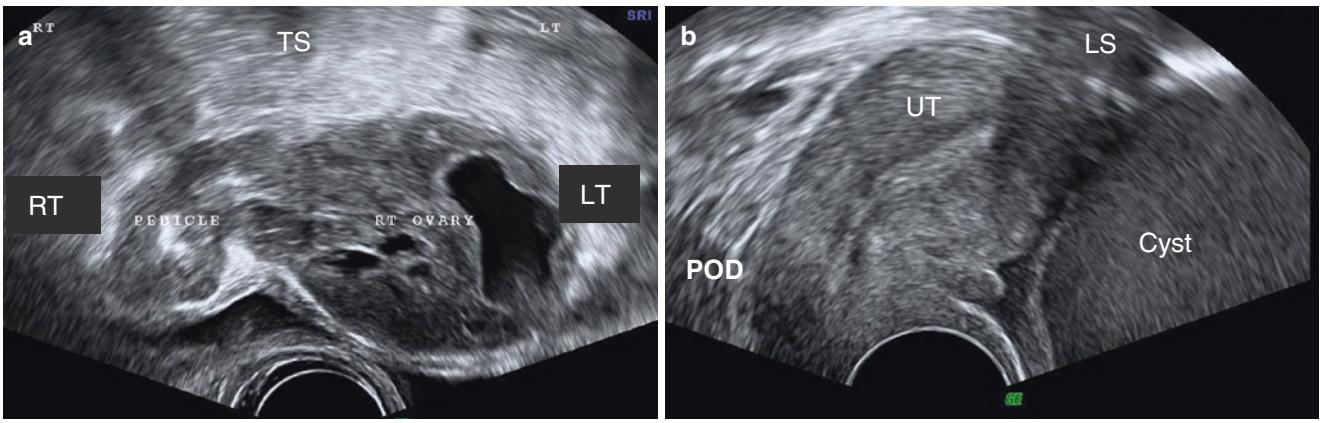

Fig. 11.4 Torsed ovaries in an unusual location. (**a**) Torsed right ovary seen on the left side of the abdomen. (**b**) Torsed ovary lying anterior to the uterus

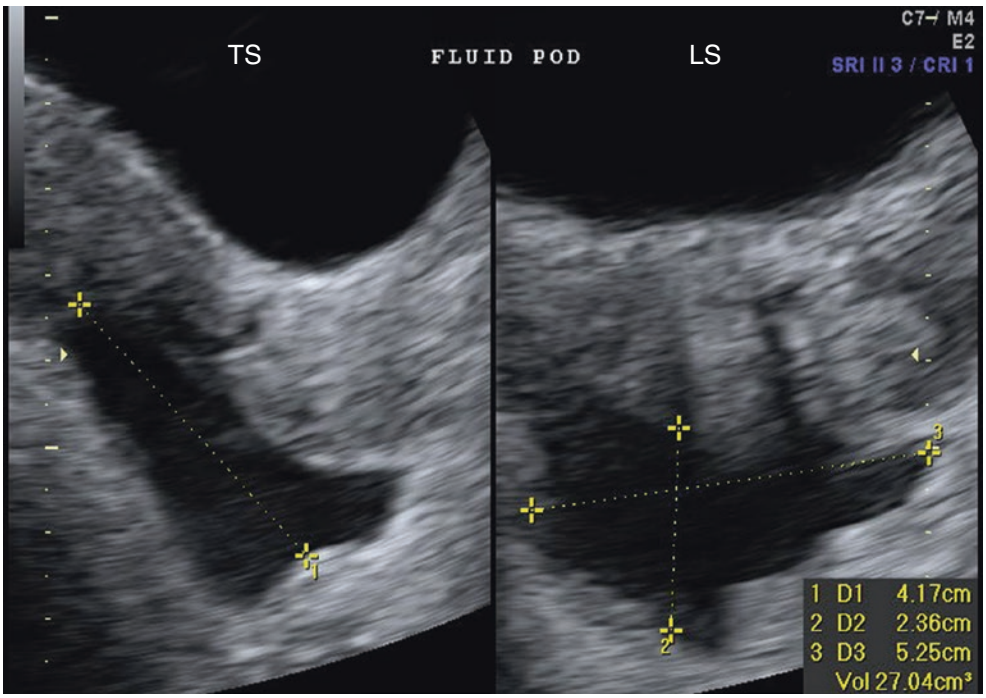

Fig. 11.5 Free fluid in the POD

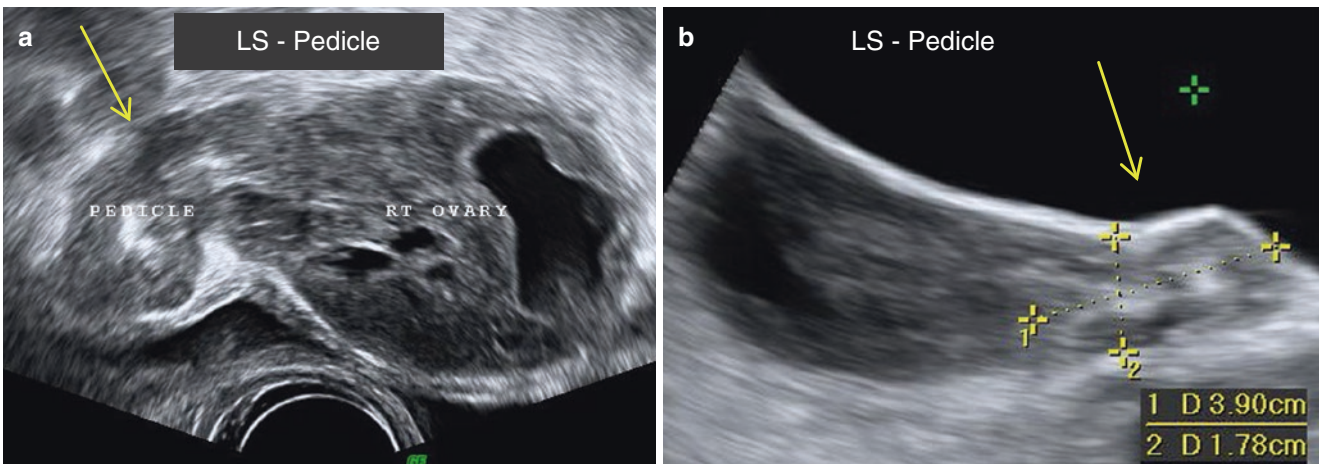

Fig. 11.6 (a, b) LS of the pedicles of torsed ovaries, appearing as an elongated, heterogeneous mass in two different cases (*arrows*)

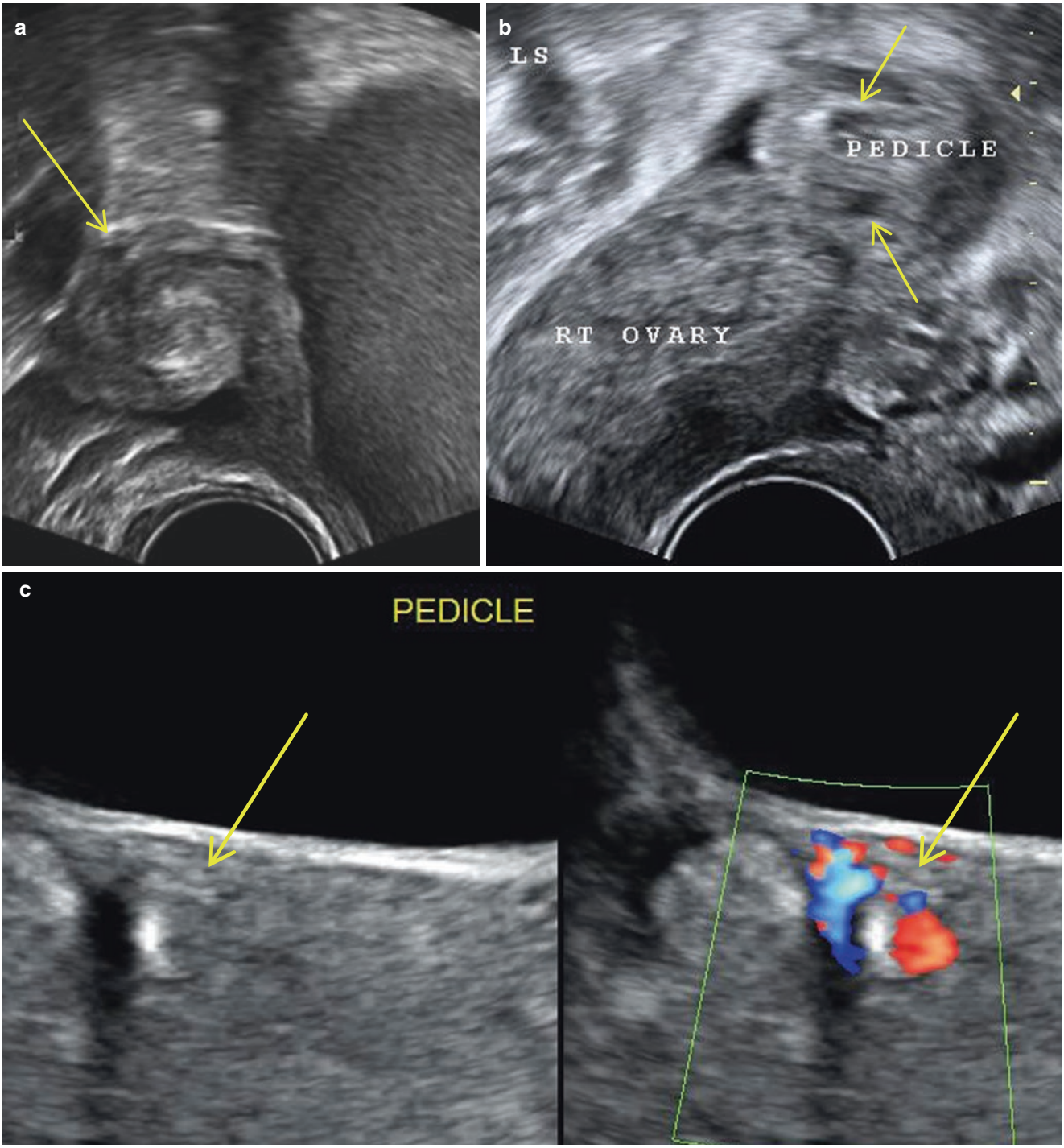

Fig. 11.7 TS of pedicles of torsed ovaries in three different patients. The pedicle appears as a circumscribed mass (**a**) that is hyperechoic with multiple concentric hypoechoic stripes (*arrow*), (**b**) has hypoechoic beads within (engorged veins) (*arrows*), (**c**) has a bright echogenic centre – 'target sign'

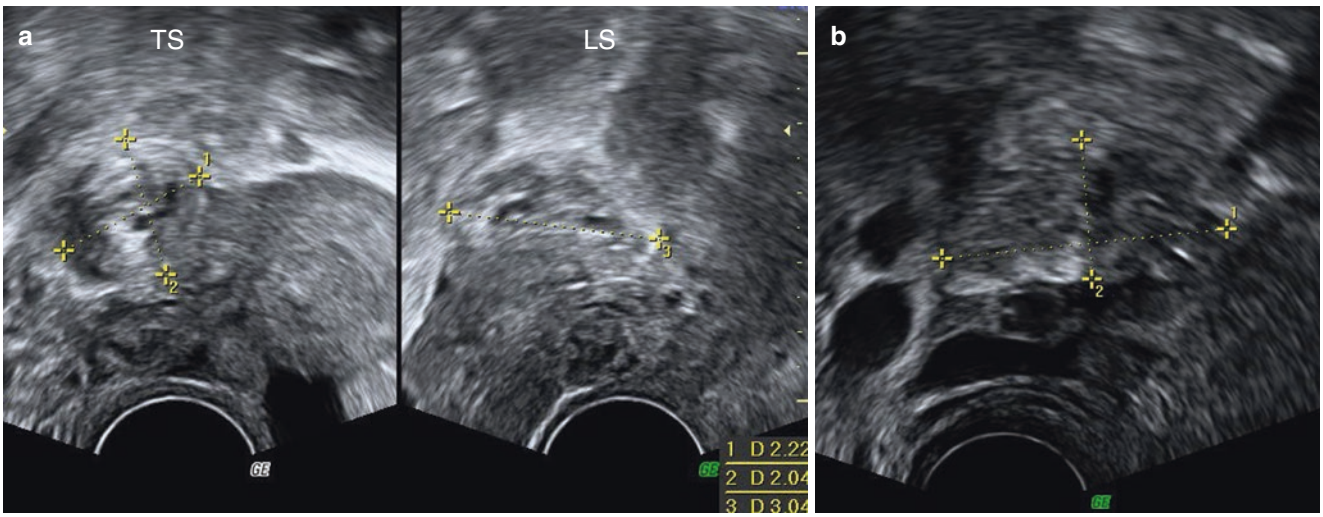

Fig. 11.8 Pedicles of torsed ovaries in two different cases (**a**, **b**) showing varied, atypical appearance, making them difficult to identify

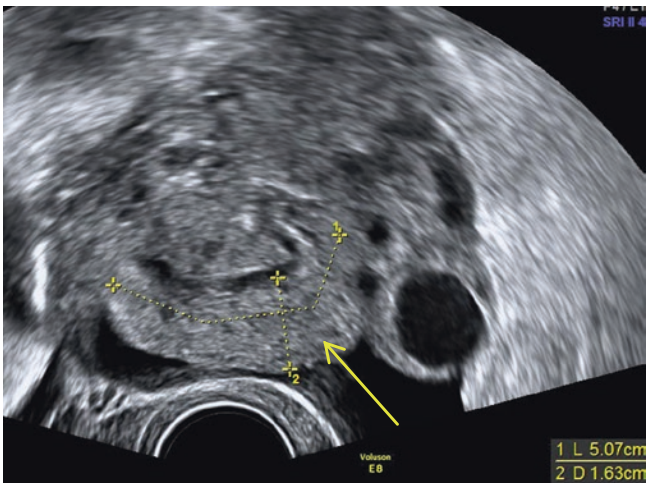

Fig. 11.9 A case of adnexal torsion, where the ovary had a fibroma. The image shows a thickened, hyperechoic segment of the fallopian tube (*arrow*), suggestive of associated tubal torsion

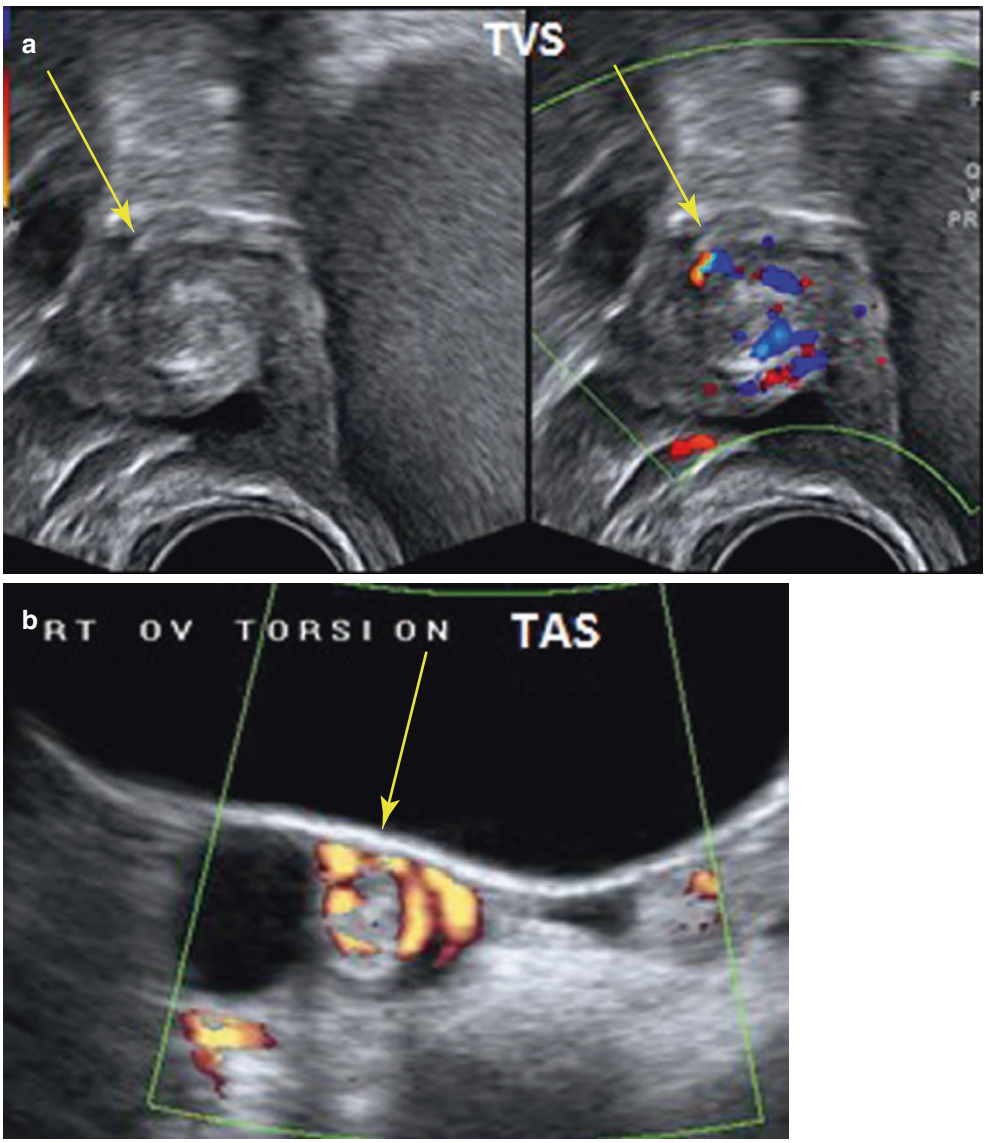

Fig. 11.10 Whirlpool sign (*arrows*). (**a**) TVS – on greyscale and colour Doppler and (**b**) TAS – with power Doppler. This is a real-time finding. On a frozen image, it is seen as a cross section of the pedicle with multiple concentric stripes of tissue on greyscale and as circularly placed vessels on Doppler

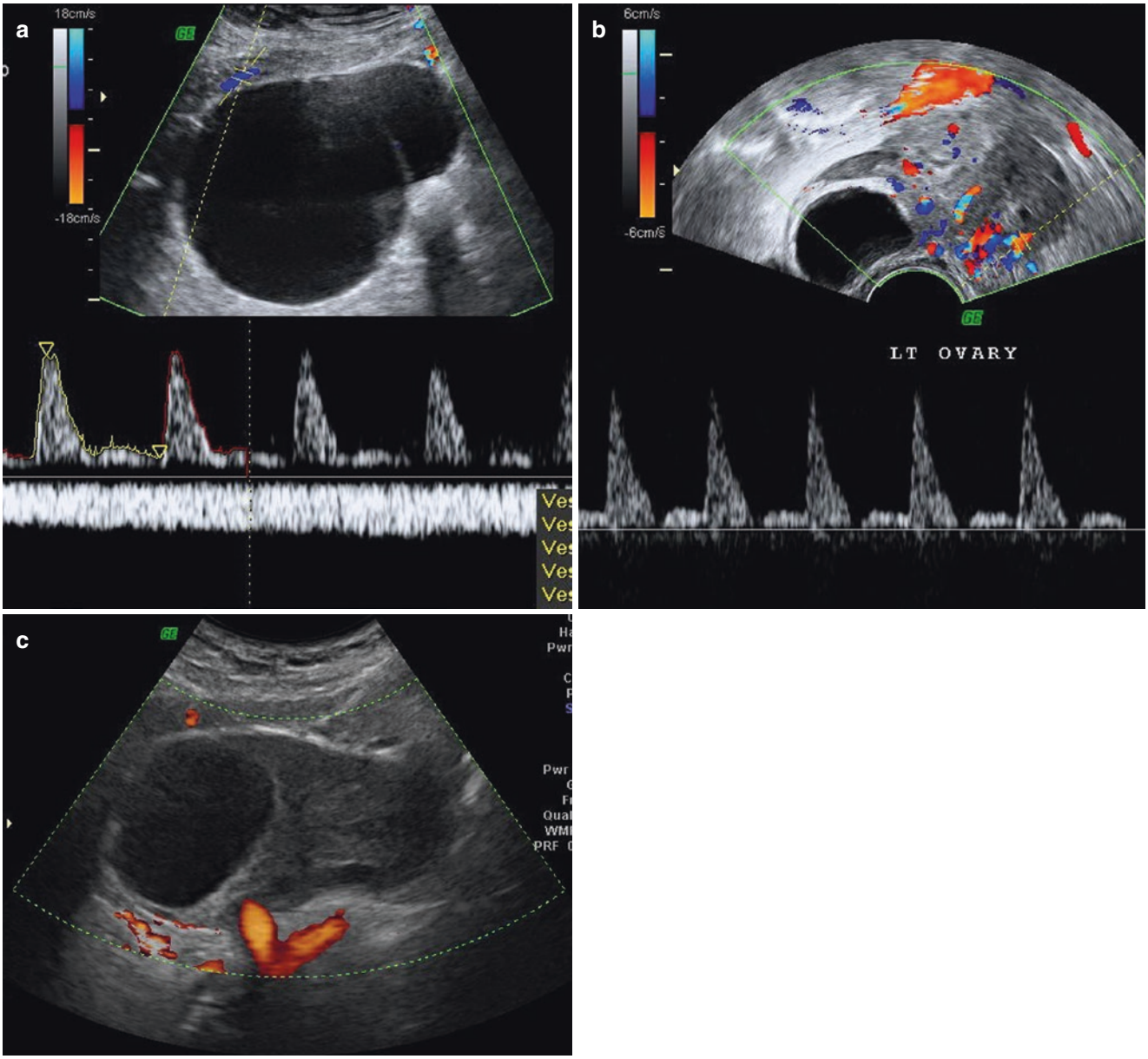

Fig. 11.11 Doppler in torsion. (**a**) Arterial and venous flow. (**b**) Only arterial flow. (**c**) No flow

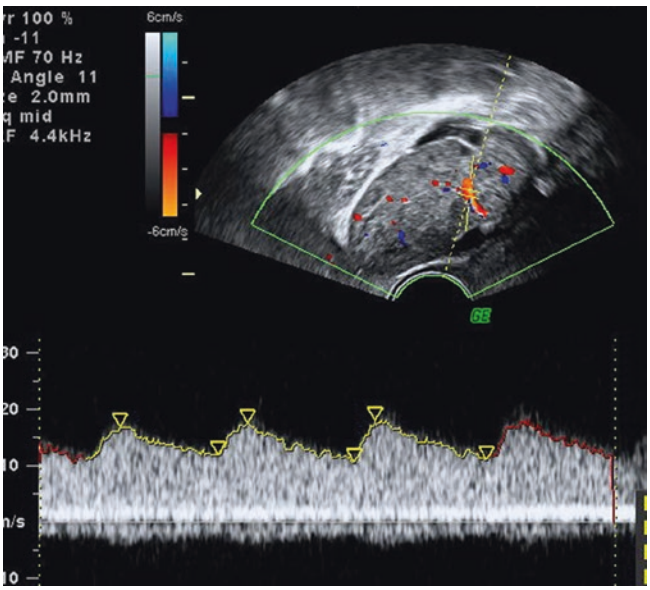

Fig. 11.12 High vascularity with low resistance flows, in a patient with early torsion. This may be seen in the early stages of torsion and can be misleading

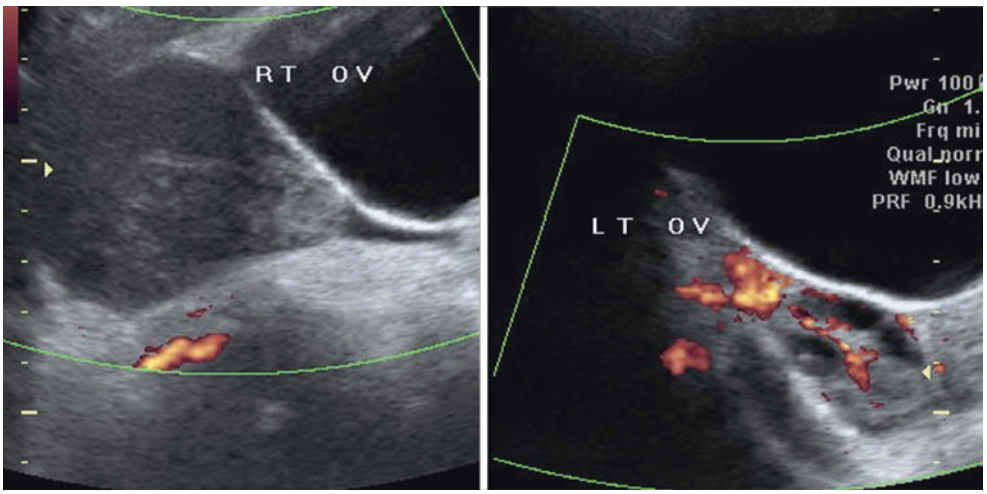

Fig. 11.13 Doppler assessment in a patient with right ovarian torsion, using the normal left ovary as a control. No flow is seen in the torsed right ovary, and good flow is seen in the normal contralateral ovary

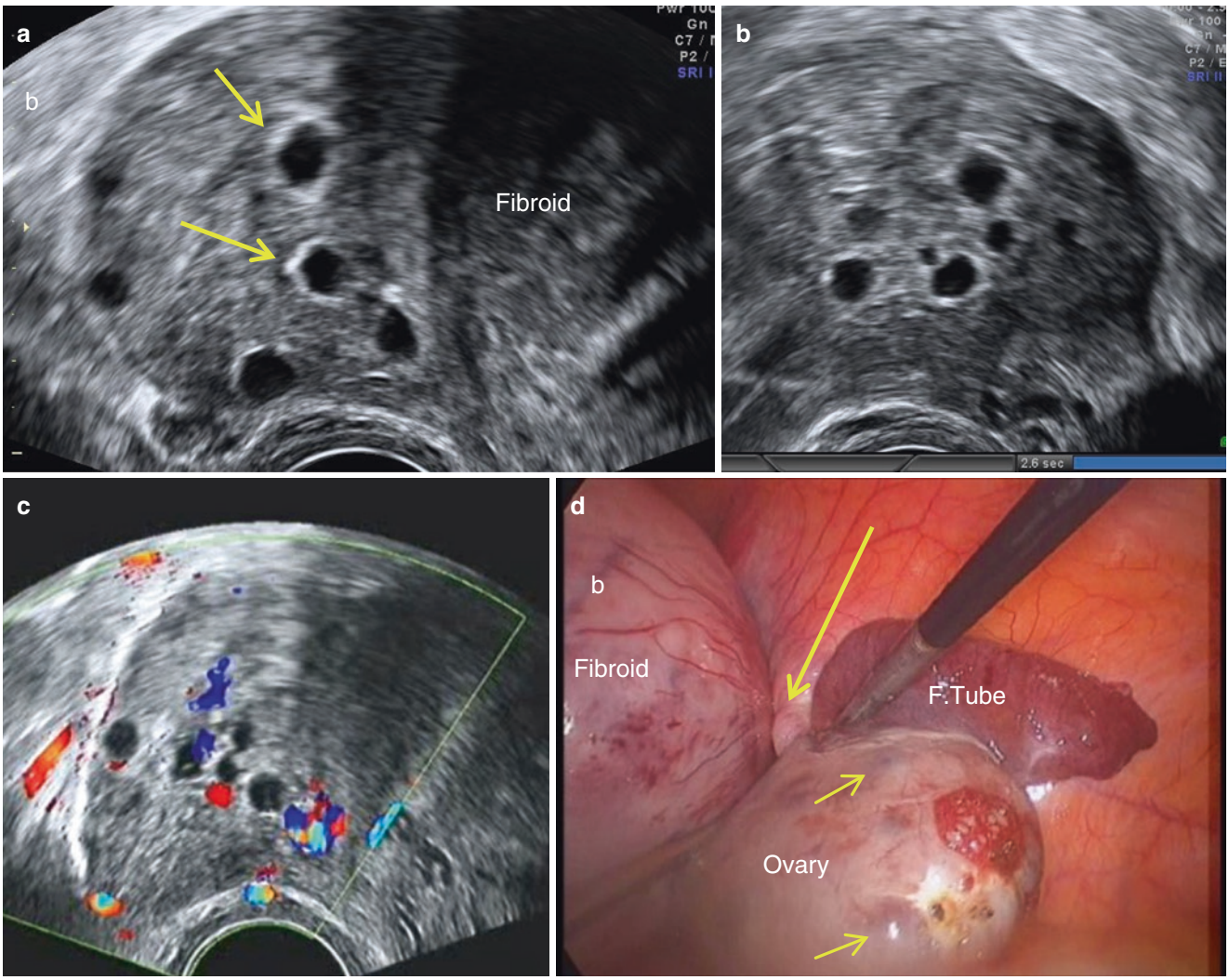

Fig. 11.14 Case of torsion in a patient known to have a large fibroid, who presented with acute abdominal pain, where the only specific finding was FRS. (**a**) Fibroid with ovarian tissue adjacent to it showing the follicular ring sign (hyperechoic thick margins around the antral follicles) (*arrows*). (**b**) Antral follicles were seen not only in the periphery but even in the centre of the ovarian stroma. (**c**) Good vascular flows seen in the ovary. (**d**) Laparoscopic image of ovary showing a normal-sized pinkish ovary, suggestive of very early torsion. Antral follicles are seen bulging out (*arrows*) of the ovarian surface. Site of twist (*long arrow*) on lateral pelvic wall concealed by the large fibroid. The oedematous torsed fallopian tube is also seen in the image

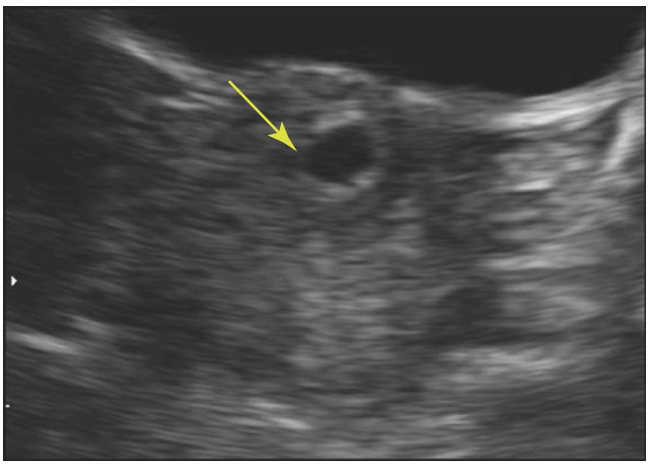

Fig. 11.15 FRS (*arrow*) seen on TAS

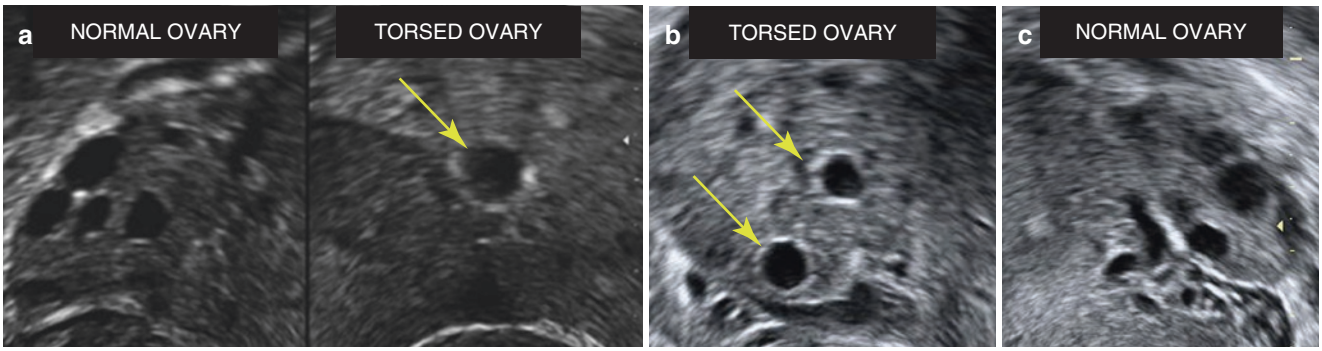

Fig. 11.16 Comparison with the contralateral normal ovary provides a convenient control for FRS. (**a**, **b**, **c**) Antral follicles with FRS in torsed ovary (*arrows*)

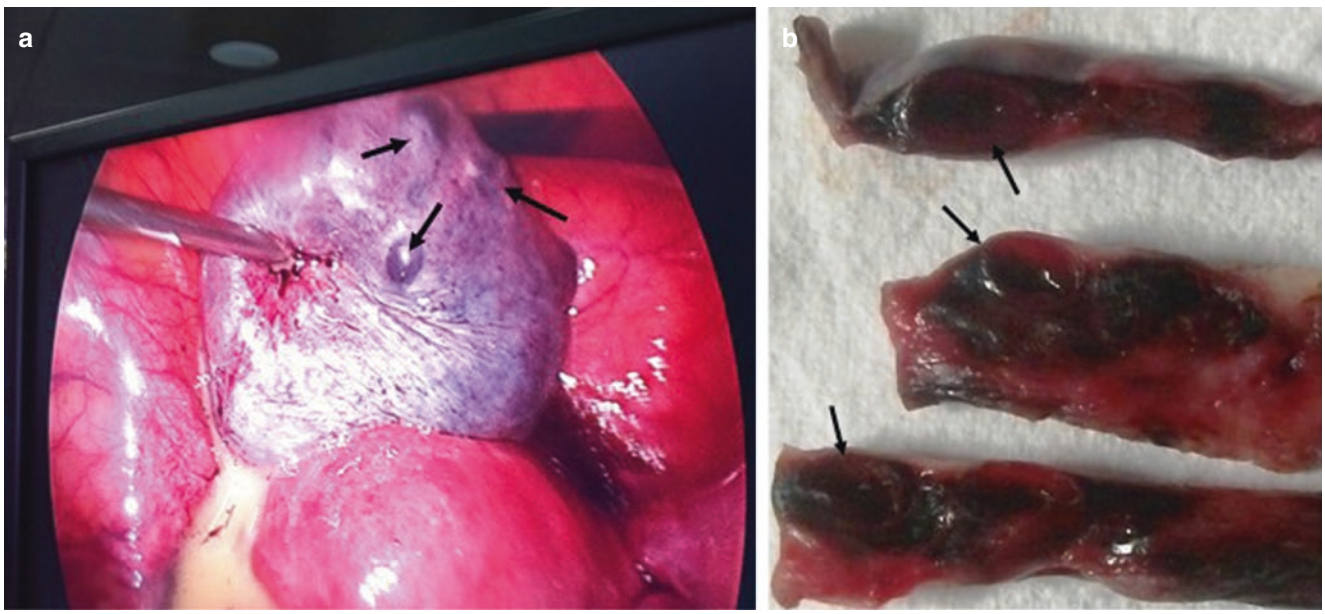

Fig. 11.17 Macroscopic evidence of FRS. (**a**) Laparoscopic image of a congested, purplish, torsed ovary, showing small, purple bulges on its surface. These are the surface antral follicles with oedematous walls. (**b**) Cut section of ovarian tissue showing swollen and haemorrhagic walls of the antral follicles

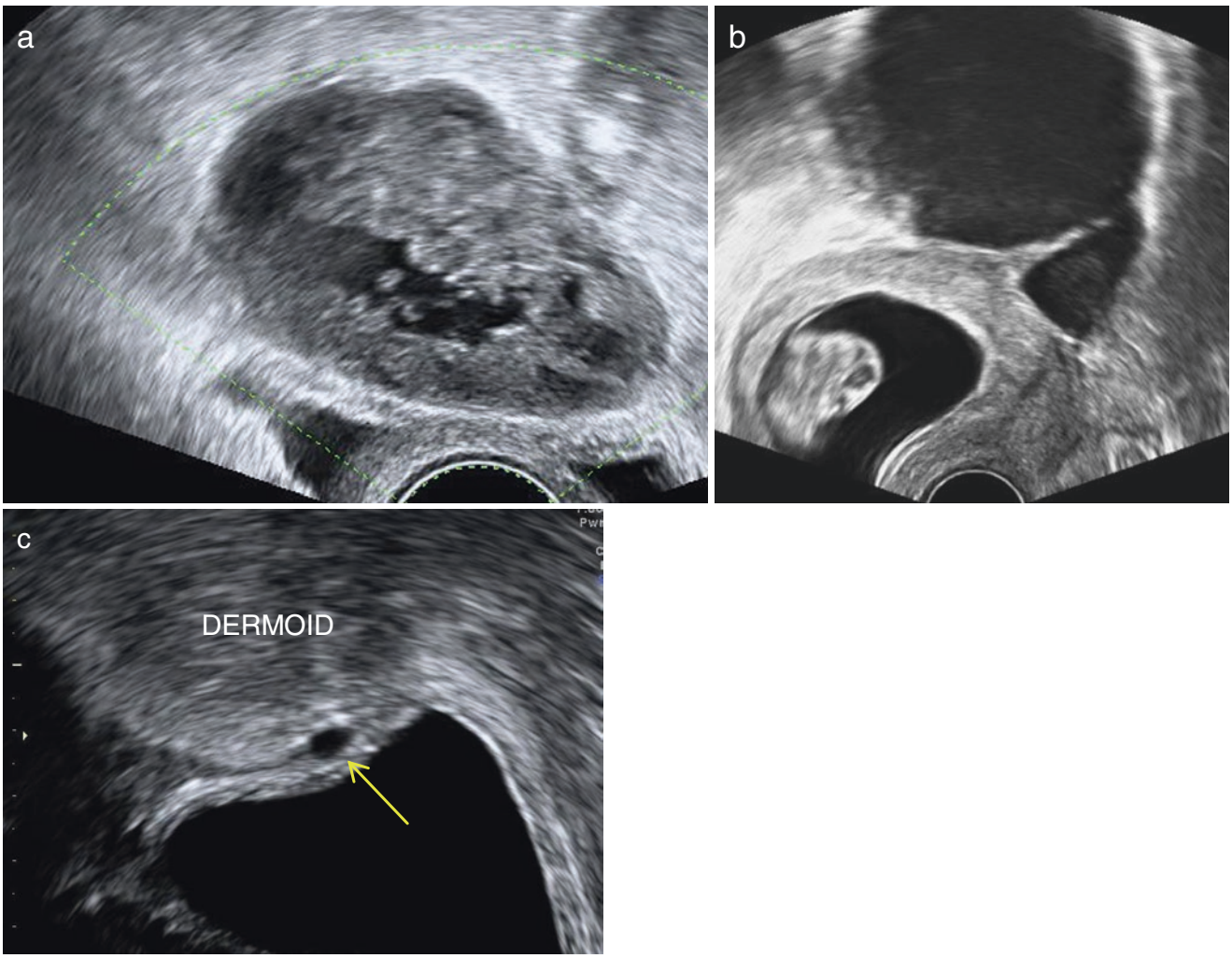

Fig. 11.18 FRS in three different cases with torsion. (**a**) FRS is not seen because the ovaries were necrotic and showed no antral follicles. (**b**) FRS is not seen because the cyst was far away from the probe and the ovarian tissue was compressed by the large cyst. Thus, the antral follicles could not be visualised. (**c**) Case of torsion with a dermoid, where minimal ovarian tissue was seen on TVS. The antral follicles with FRS (*arrow*) could be identified in the ovarian tissue

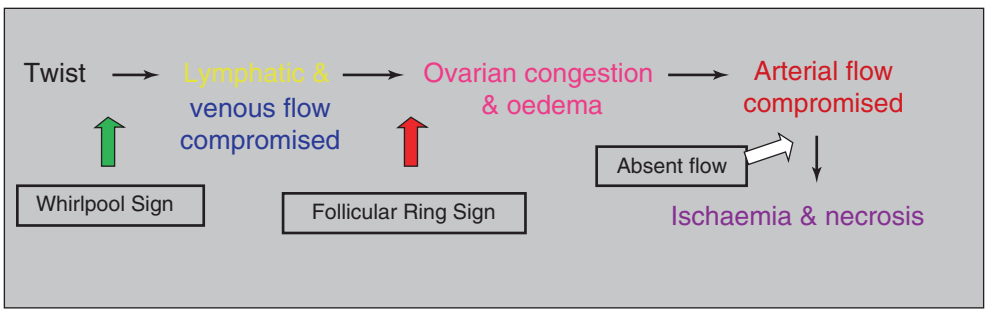

Fig. 11.19 Diagrammatic representation of the pathology of ovarian torsion in temporal succession, along with the three specific features that help in ultrasound diagnosis

Summary: Ovarian Torsion

- Diagnosis of torsion is based on clinical features supported by ultrasound findings. Clinical features raise suspicion but are not specific. Pain is the main presenting symptom.
- Ultrasound features
  A. *Common ultrasound features – but not very specific:*
     Large ovaries, abnormal position of ovary, oedema of ovarian stroma, peripheral follicles, free fluid and haemorrhagic cysts.
  B. *Ultrasound features with higher specificity:*
     1. Pedicle with the whirlpool sign – increases diagnostic accuracy significantly but *requires experience*
     2. Abnormal Doppler flows – a *late finding in torsion* (normal flow does not rule out torsion)
     3. Follicular ring sign – simple, early and frequently seen feature
- Management of these cases is by prompt surgical intervention, which involves laparoscopic detorsion of the ovary. The ovary should be left behind even if it looks gangrenous. A neoplastic cyst may be excised. The ovary may, however, be excised if there is a possibility of a malignant tumour or cyst, or if the patient is postmenopausal or perimenopausal.

11.2 Non-ovarian Torsion

Torsion of a hydrosalpinx or a paraovarian cyst also presents with acute pelvic pain. Here, all the ultrasound findings of ovarian torsion are not seen. The first part of the diagnosis is, of course, to diagnose a hydrosalpinx or a paraovarian cyst. This has been discussed in Chap. 9. A torsed hydrosalpinx could appear atypical – i.e. it could appear more globular than elongated, and the incomplete septum may not be seen.

Ultrasound Features of Non-ovarian Torsion
(Figs. 11.20, 11.21 and 11.22)

- The pedicle with the whirlpool sign is a specific feature of torsion similar to what is seen in ovarian torsion and is helpful in diagnosis.
- Absence of Doppler flows may also be a feature in an advanced case. This is more difficult to assess than in cases of ovarian torsion, because there isn't much solid tissue in the walls of these cases to look for flow.
- The follicular ring sign is, of course, not a feature because there are no antral follicles in the torsed mass.
- Other non-specific ultrasound features of torsion which may be seen are thicker walls (due to congestion and oedema), fluid within the mass showing internal echoes suggestive of haemorrhage, tenderness and free fluid in the pelvis.

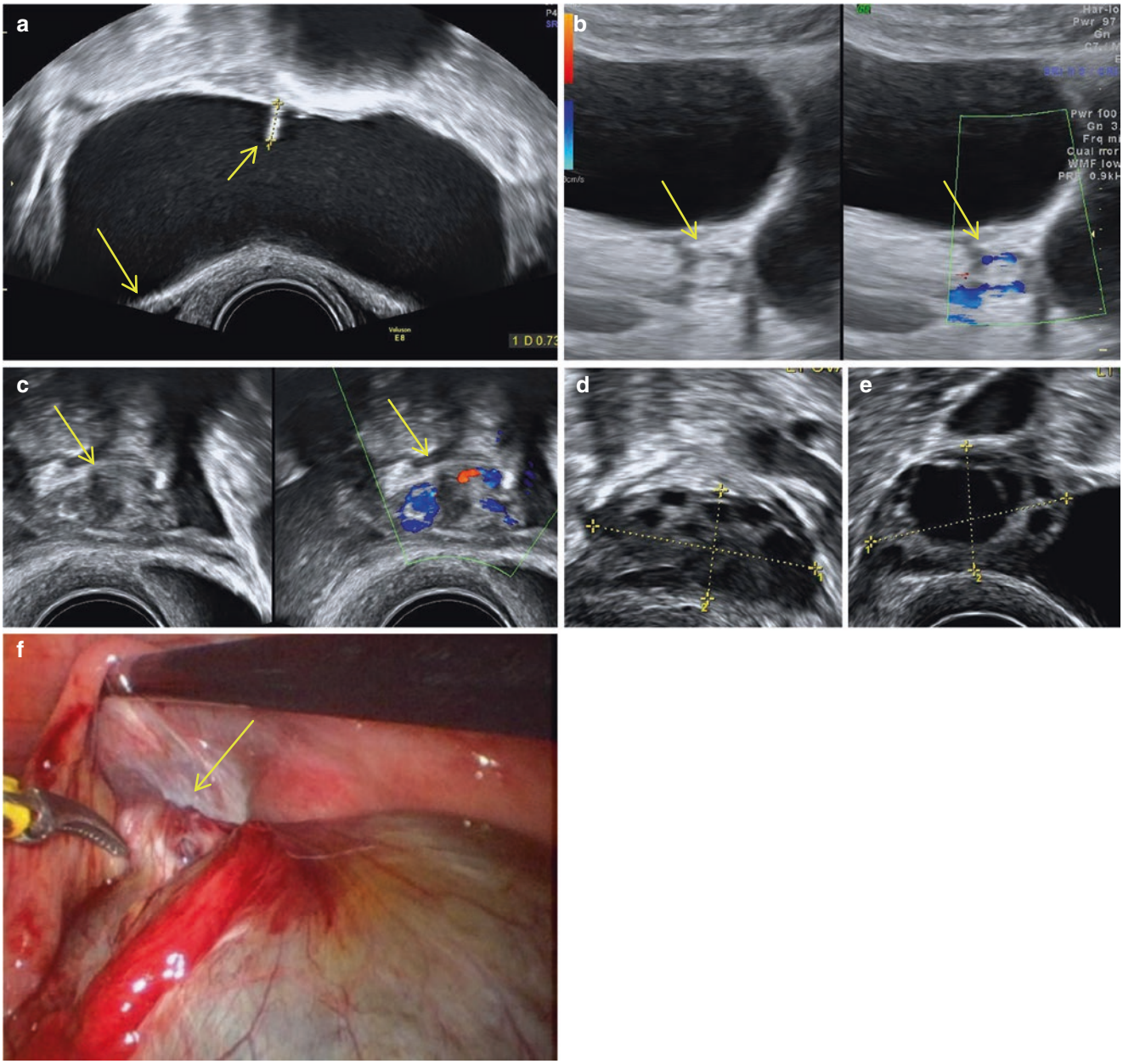

Fig. 11.20 Torsion of a left hydrosalpinx. (**a**) Elongated cystic mass with a short, incomplete septum (*short arrow*), turbid contents and thick walls (*long arrow*), suggestive of a torsed hydrosalpinx with haemorrhage within. (**b**) Whirlpool sign of pedicle seen on TAS in greyscale and Doppler (*arrows*). (**c**) Whirlpool sign on TVS in greyscale and Doppler (*arrows*). (**d**, **e**) Normal left and right ovaries of the patient. (**f**) Laparoscopic image of the torsed hydrosalpinx, showing the twist (*arrow*)

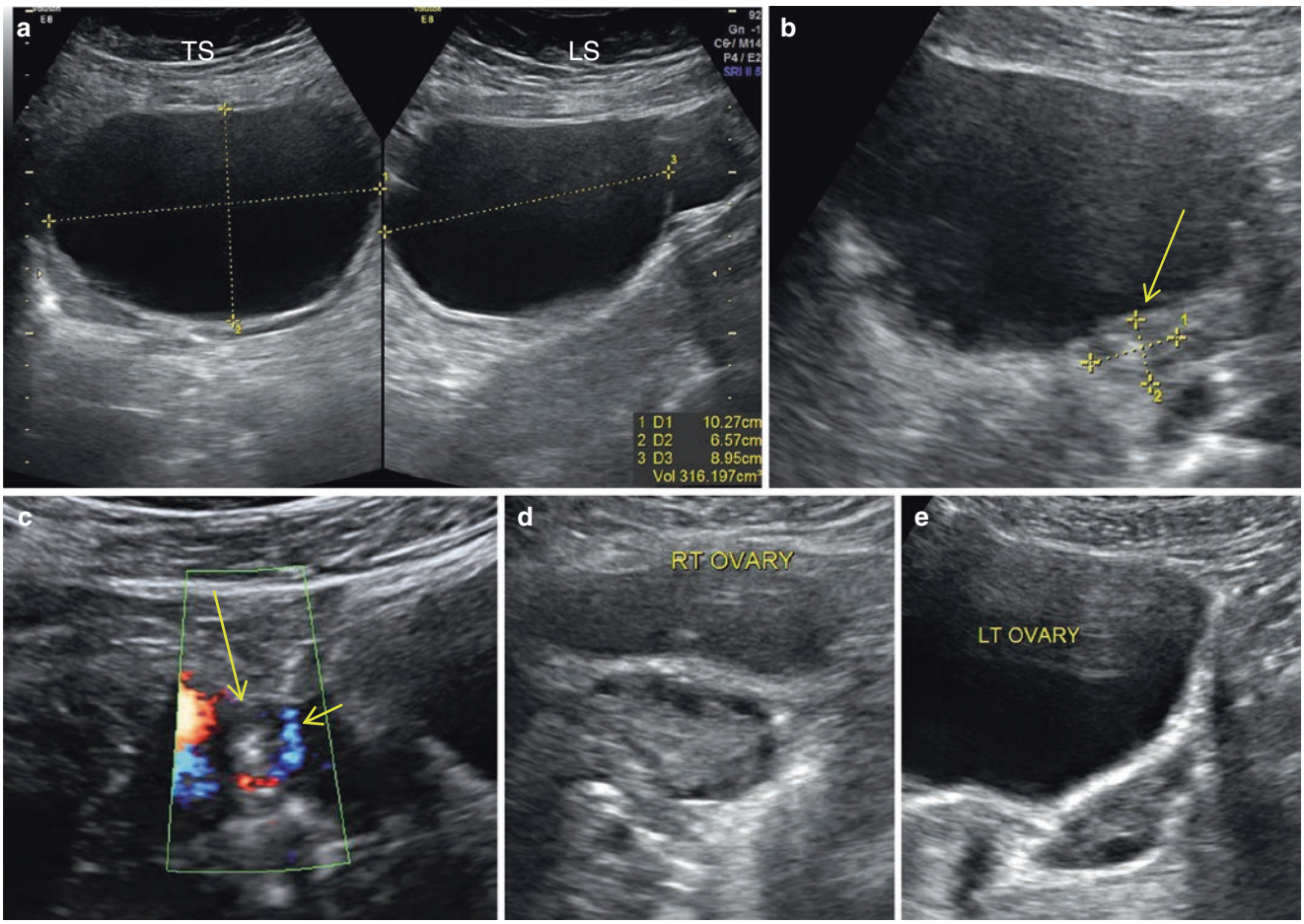

Fig. 11.21 Torsion of a paraovarian cyst. (**a**) PO cyst on TAS, with low-grade internal echoes. (**b**) Small cross section of pedicle (*arrow*) seen below the cyst on TAS. (**c**) Cross section of twisted pedicle showing the target sign (*long arrow*) and whirlpool sign (*short arrow*). (**d**, **e**) Normal right and left ovaries

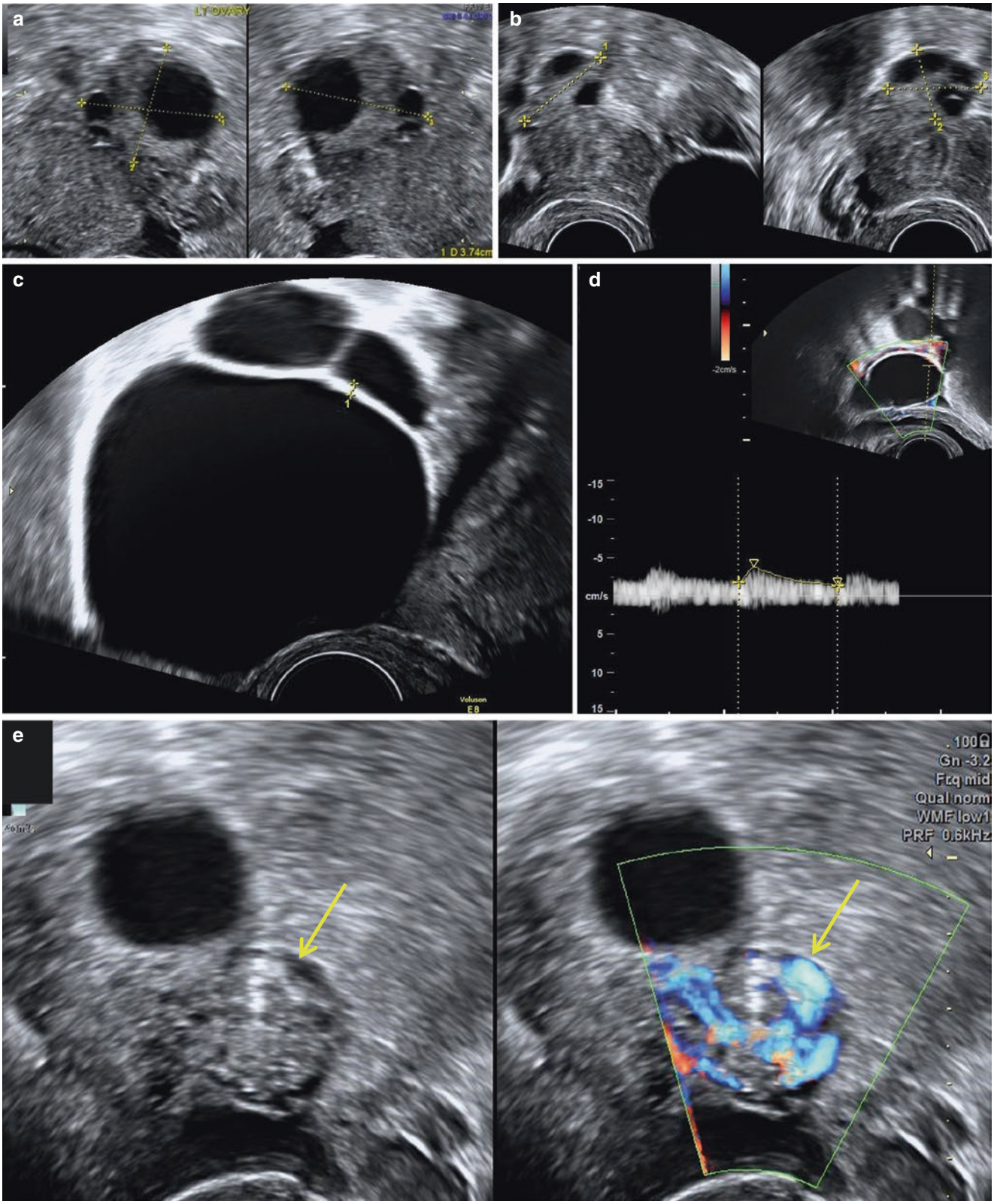

Fig. 11.22 Benign paraovarian cyst with early torsion. (**a**, **b**) Normal right and left ovary. (**c**) Septate PO cyst seen. (**d**) Cyst walls showing flow. (**e**) Twisted pedicle showing whirlpool sign on greyscale and Doppler (*arrows*)

Suggested Reading

Chang HC et al (2008) Pearls and pitfalls in diagnosis of ovarian torsion. Radiographics 28(5):1355–1368

Cohen SB et al (2001) Accuracy of the preoperative diagnosis in 100 emergency laparoscopies performed due to acute abdomen in nonpregnant women. J Am Assoc Gynecol Laparosc 8:92–94

Oelsner G et al (2003) Minimal surgery for the twisted ischaemic adnexa can preserve ovarian function. Hum Reprod 18(12):2599–2602. doi:10.1093/humrep/deg498

Potter AW, Chandrasekhar CA (2008) US and CT evaluation of acute pelvic pain of gynecologic origin in nonpregnant premenopausal patients. Radiographics 28(6):1645–1659

Mashiach R et al (2011) Sonographic diagnosis of ovarian torsion accuracy and predictive factors. J Ultrasound Med 30:1205–1210

Sibal M (2012) Follicular ring sign: a simple sonographic sign for early diagnosis of ovarian torsion. J Ultrasound Med 31(11):1803–1809

Valsky DV et al (2010) Added value of the grey-scale whirlpool sign in the diagnosis of adnexal torsion. Ultrasound Obstet Gynecol 36(5):630–634

Vijayaraghavan SB (2004) Sonographic whirlpool sign in ovarian torsion. J Ultrasound Med 23:1643–1649

Ultrasound Evaluation of Congenital Uterine Anomalies

12

Evaluation of uterine anomalies can be confusing because of the various diagnostic ultrasound criteria and available classifications. In this chapter, we have primarily followed the popular AFS classification. In order to better understand the types of anomalies, the chapter initially deals with embryopathogenesis. A brief account of the basic diagnostic criteria is initially discussed. Following this, the diagnosis of each type of anomaly, based on these criteria, is provided. The last part of this chapter deals with the evaluation of the cervix and vagina for congenital anomalies, which is not focused upon most often in literature, primarily because it is believed to be suboptimally assessed on regular TVS. Cervical and vaginal anomalies are generally associated with uterine anomalies. Here the fine points for ultrasound diagnosis of cervical and vaginal anomalies, including the useful novel use of GSV for accurate evaluation of these conditions, are provided.

The prevalence of uterine anomalies is believed to be between 4% and 7 % (Grimbizis and Campo 2012). The prevalence is higher in select populations, like recurrent aborters.

There is a higher incidence of associated renal abnormalities in women with uterine anomalies, because of related embryological development of these organs.

Many of these women with uterine anomalies are asymptomatic. Some may, however, present with the following clinical manifestations:

1. Reproductive health – particularly recurrent pregnancy losses. In subseptate uterus, there is an increased risk of first trimester loss. In arcuate uterus, there is an increased risk of second trimester loss and preterm labour. Abnormal fetal presentation is more common in women with uterine anomalies. Conceiving, however, is generally not an issue in patients with uterine anomalies.
2. Adolescent health issues like pain, as seen in haematocolpos and a non-communicating uterine horn.
3. Life-threatening emergencies like rupture of a cornual pregnancy.

12.1 Embryopathogenesis (Figs. 12.1, 12.2)

The uterus develops from two Mullerian (paramesonephric) ducts. Their lower ends fuse to form the upper two-third of the vagina, cervix and uterus. Their upper ends do not fuse, and they form the two fallopian tubes. The lower one-third of the vagina develops from the urogenital sinus. Fusion of the two Mullerian ducts occurs from below upwards. Following fusion, the intervening septum gets resorbed to form a common uterine cavity. The resorption also occurs from below, upwards. If there is any abnormality in the process of development, fusion or resorption, it results in a uterine anomaly.

The American Fertility Society (AFS) classification (Figs. 12.2 and 12.3), which is the most popular classification of uterine anomalies (and is followed in this chapter), is based on the stage of arrest of development, fusion or resorption in the above process.

M. Sibal, *Ultrasound in Gynecology*, DOI 10.1007/978-981-10-2714-7_12

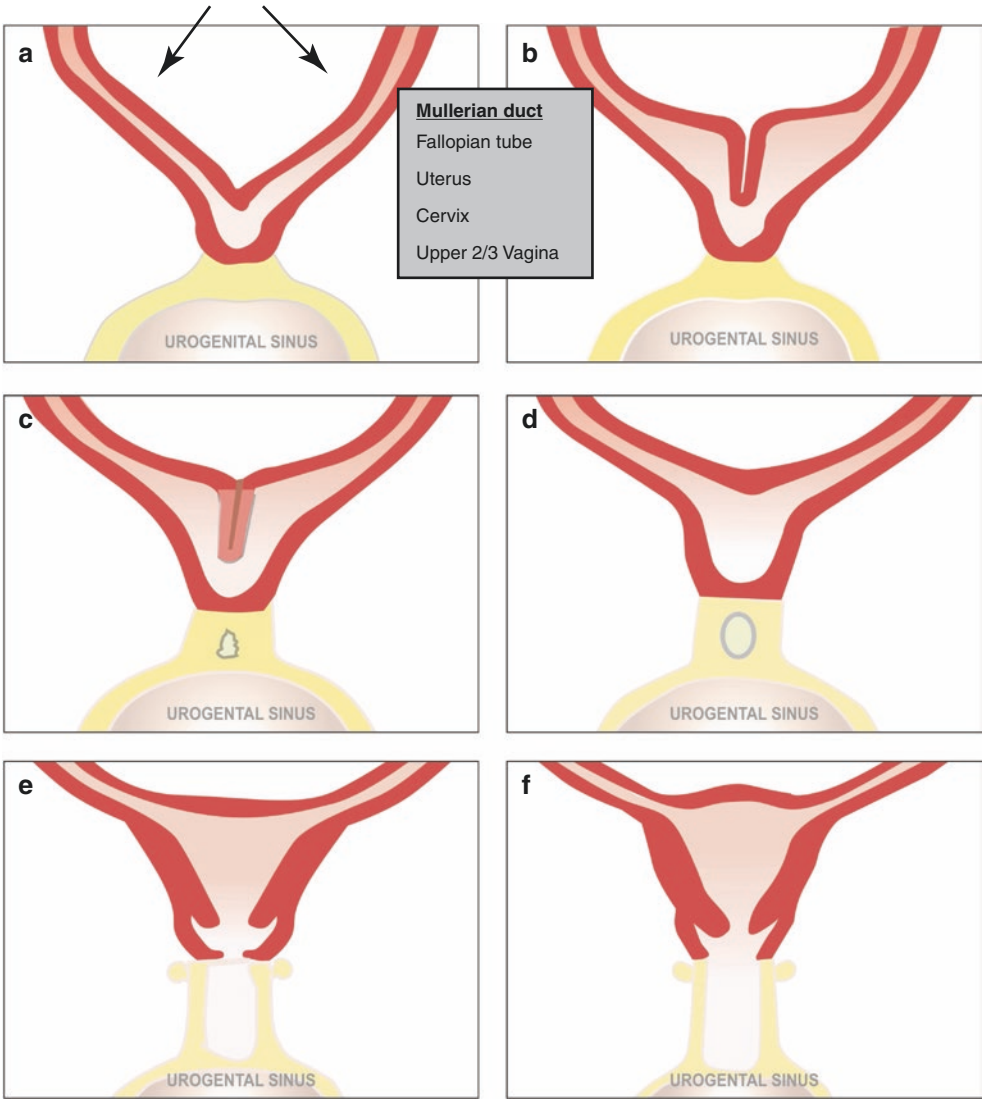

Fig. 12.1 Stages of embryological development of the female genital tract. (**a**) The uterus develops from the two Mullerian ducts (*arrows*). (**b**) The two ducts fuse together beginning from the lower end to form the uterus and the upper two-third of the vagina. The upper non-fused parts give rise to the fallopian tubes. (**c**) The intervening septum between the two fused ducts gradually gets resorbed starting from the lower end, moving upwards. (**d**) Single uterine cavity formed following resorption of the septum. (**e**) The upper two-third of the vagina arises from the Mullerian duct and the lower one-third from the urogenital sinus. (**f**) The transverse septum between the upper two-third and the lower one-third of the vagina gets resorbed forming a single vaginal cavity

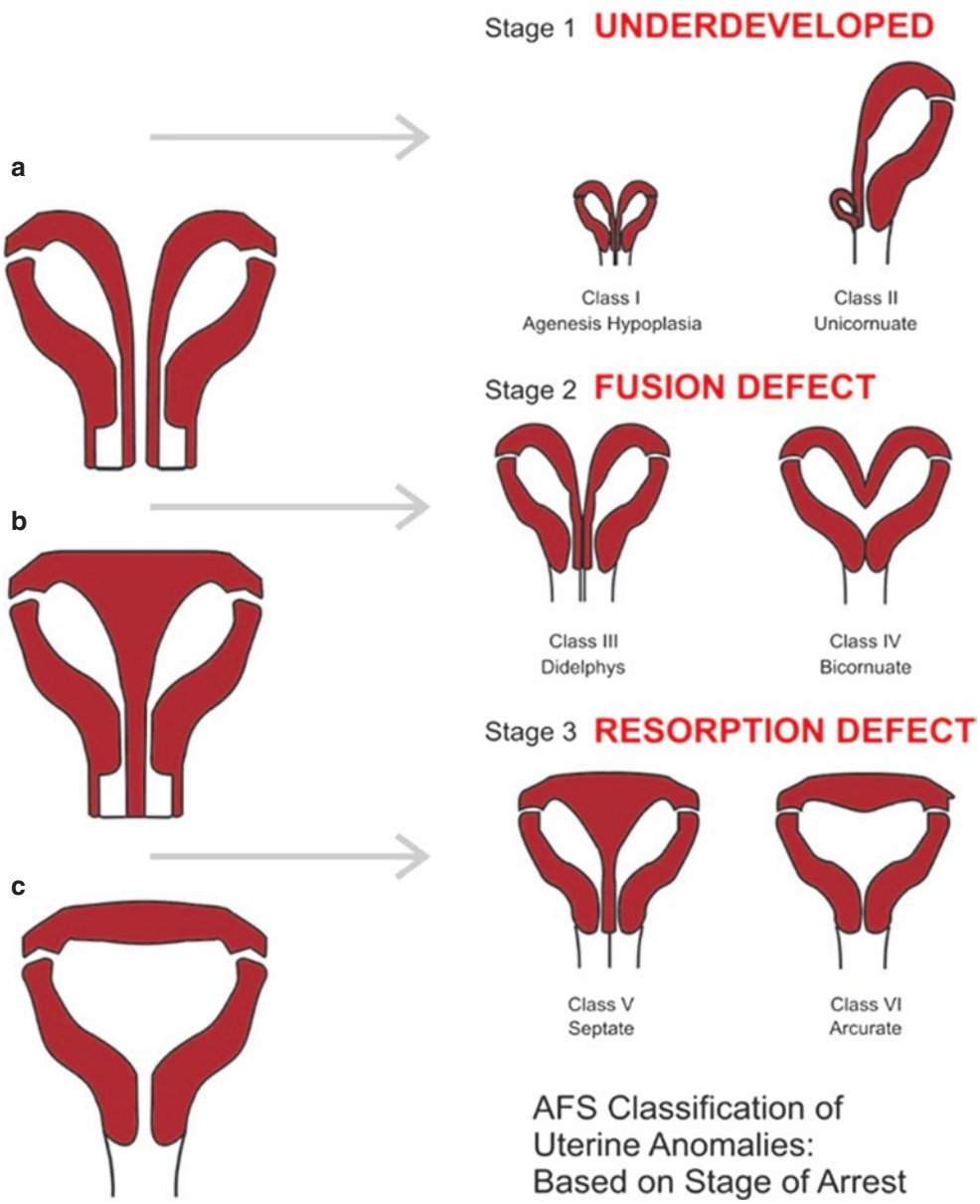

Fig 12.2 AFS classification of uterine anomalies: based on the stage of arrest. (**a**) If there is arrest prior to complete development of the two Mullerian ducts, it can result in agenesis or unicornuate uterus. (**b**) If there is arrest prior to complete fusion of the two Mullerian ducts, it can result in didelphys or bicornuate uterus. (**c**) If there is arrest prior to complete resorption of the intervening septum, it can result in septate or arcuate uterus

12.2 AFS Classification of Uterine Anomalies (Figs. 12.2 and 12.3)

Underdeveloped

Class I – *Mullerian agenesis or hypoplasia*; cases with agenesis or hypoplasia of part or whole of the Mullerian ducts

Class II – cases with underdevelopment of one of the Mullerian ducts resulting in a *unicornuate uterus*, which could again be of four types, as shown in Fig. 12.3

Fusion Defect

Class III – complete lack of fusion, resulting in a *didelphys uterus*

Class IV – partial defect in fusion, resulting in a *bicornuate uterus*

Resorption Defect

Class V – *septate uterus* (complete absence of resorption) and *subseptate uterus* (partial resorption defect).

Class VI – *arcuate uterus*; the fusion defect is minimal as a result of which there is a slight indentation of the uterine cavity.

Class VII – a *'T-shaped' uterus* which could be the result of intrauterine exposure to diethylstilbestrol.

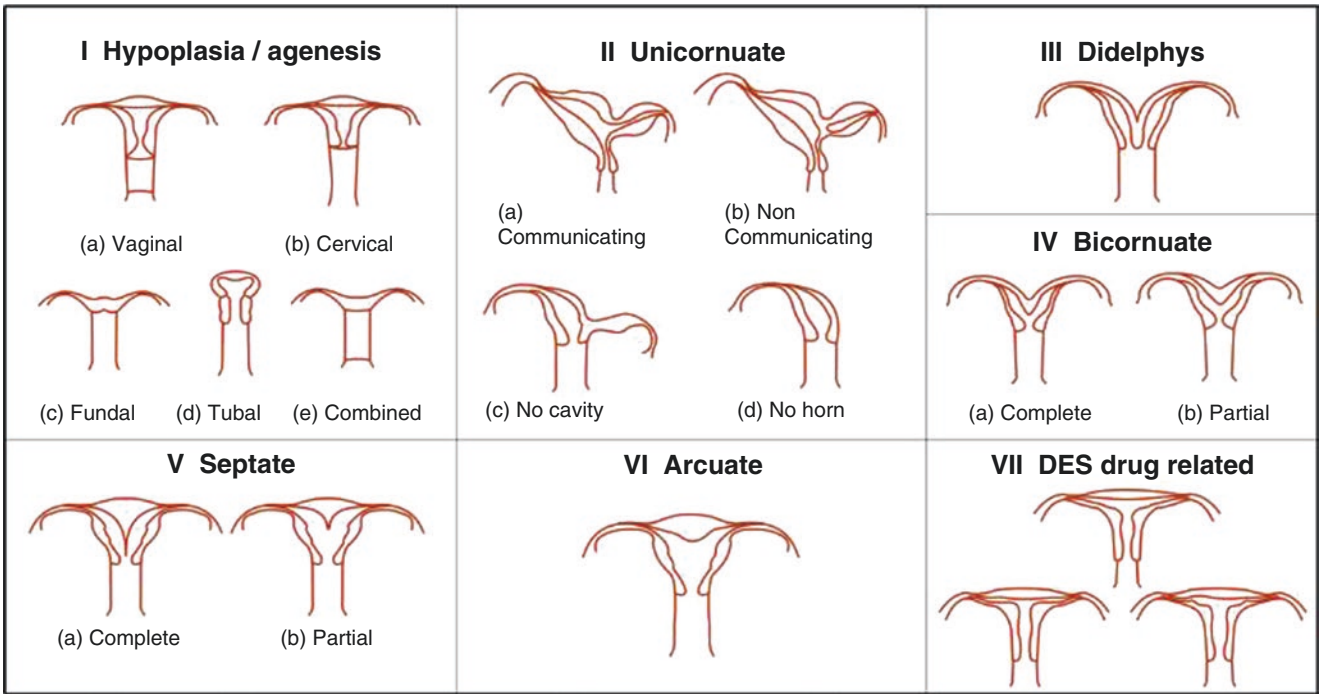

Fig. 12.3 AFS classification of uterine anomalies

12.3 Approach to Diagnosing a Uterine Anomaly

Diagnosis of uterine anomalies requires an assessment of the external fundal contour and an assessment of the shape of the inner uterine cavity.

The external fundal contour can be assessed at laparotomy and laparoscopy.

The inner uterine cavity can be assessed by hysteroscopy or hysterosalpingography (HSG).

However, the only modalities that can assess both the cavity and the external fundal contour are ultrasound and MRI.

Ultrasound is the primary diagnostic modality of choice because of its lower cost and easy availability.

Assessment in pregnancy is not likely to be accurate because of the altered shape and dimensions, which could be because of an eccentrically placed gestational sac. Patients should therefore be called about 2–3 months after abortion or delivery for identification and correct classification of any existent or suspected uterine anomaly.

Two-dimensional (2D) greyscale imaging helps raise the suspicion of a uterine anomaly and in some cases may even help to confirm the presence of a uterine anomaly. However, three-dimensional (3D) imaging is essential in confirming and diagnosing the type of uterine anomaly. The best time for evaluation is the secretory phase of the menstrual cycle, because the endometrium lining of the uterine cavity at that time is fluffy and oedematous and shows up well on 3D ultrasound.

Ultrasound Features That Raise Suspicion of Uterine Anomalies (Figs. 12.4 and 12.5)
On 2D ultrasound, findings in women with uterine anomalies are:

- Broad transverse diameter of the uterus.
- On transverse section, the endometrial cavity is seen splitting into two as one moves upwards from the cervix to the fundus.
- In some cases, two separate uterine bodies are seen (more obvious on transverse section at TAS).
- In a longitudinal section scan, on moving from one cornua to the other cornua, the endometrial length in the midline appears shorter, while on both cornual ends it appears longer.

3D ultrasound has been discussed in Chap. 2. Some points dealing with evaluation of uterine anomalies are being mentioned:

- The best time to evaluate the uterine anomaly is the secretory phase (when the endometrium is thick and oedematous), and the best time to evaluate the cervix is mid-cycle (around ovulation – when the cervix has abundant mucous).
- Typically, the best plane to take a 3D volume is the sagittal section of the uterus in the midline (the section where the endometrial length is minimal). The angle of sweep should be made as wide as possible.
- In cases with a broad fundus or two uterine horns placed far apart, the 3D sweep should be taken in a transverse section.
- Because the cervix and uterine body are often in different planes, they may have to be evaluated separately with rendering in two separate planes.
- Polyline is an effective new technique for simultaneous assessment of the cervical and uterine cavities in a single rendered image.
- Evaluation of the cervix and vagina is suboptimal on regular TVS because of the proximity of these structures to the probe and the collapsed vaginal walls. For evaluation of the cervix and vagina, the probe may have to be withdrawn a little for better visualisation. Gel sonovaginography (GSV) is a great technique to evaluate the cervix and the vagina (discussed in Chap. 2).
- It is sometimes easier to assess the uterine anomaly with 3D on a transabdominal scan with a full bladder, as compared to a transvaginal scan, because the uterus (its two horns and the cervix) gets more stretched and straightened out with a full bladder, making the rendered image much clearer.

On 3D ultrasound, the external fundal contour and the inner uterine cavity are both well visualised. A normal uterus has a convex external fundal contour, and the upper end of the uterine cavity is flat (Fig. 12.6).

A. The *external fundal contour* is considered abnormal if:

- The indentation of the myometrium in the midline is more than or equal to 10 mm.
- *The uterine fundus crosses below the line joining the upper end of the cavities on both sides or is less than or equal to 5 mm from it* (Troiano and McCarthy 2004). This is the method most accepted today and is followed in this chapter (Figs. 12.7 and 12.8).
- The indentation of the myometrium in the midline is more than 50% of the uterine wall thickness (the mean thickness of the anterior and posterior walls in the sagittal section). This is based on ESHRE classification.

B. *Shape of the uterine cavity* is considered abnormal if there is any indentation in its superior outline.

It is important to differentiate between arcuate and septate/subseptate uterus. The table below shows the various methods used, of which the angle at the centre is most commonly used for evaluation (Fig. 12.9).

ARCUATE

1. Angle at the centre is more than or equal to 90 degree
2. Indentation of less than 1.5 cm
3. Indentation of less than 50% uterine wall thickness

SEPTATE / SUBSEPTATE

1. Angle at the centre is less than 90 degree
2. Indentation of more than or equal to1.5 cm
3. Indentation of more than 50% uterine wall thickness

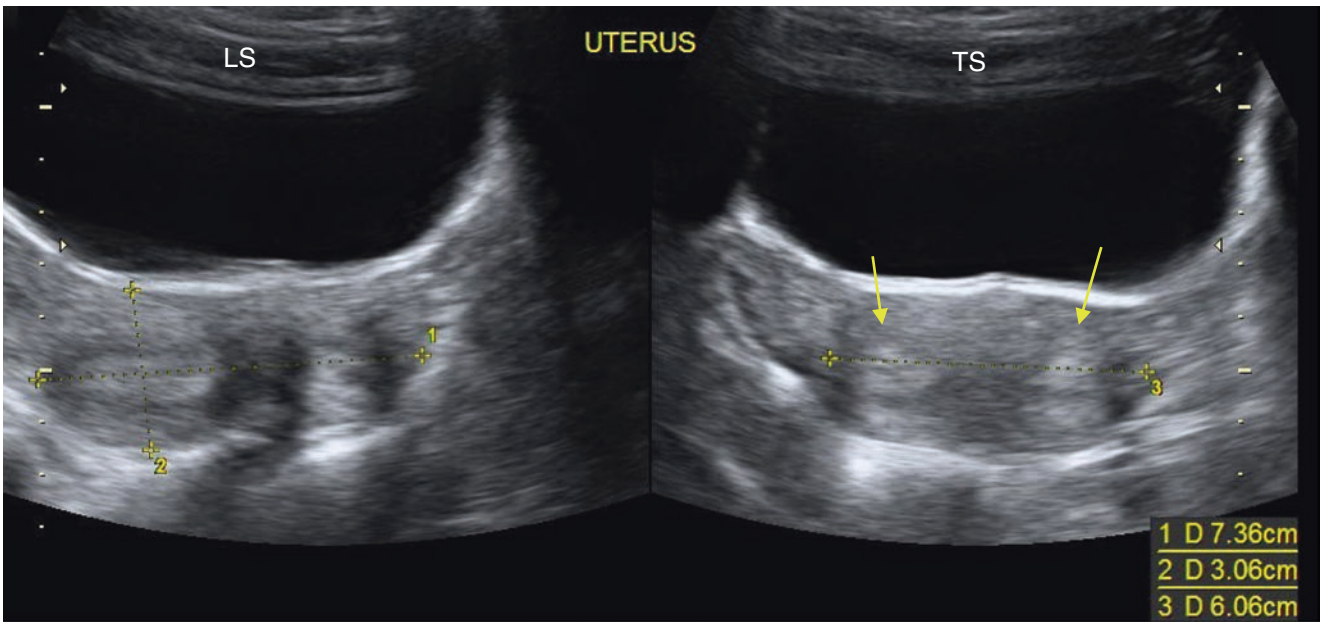

Fig. 12.4 Longitudinal and transverse section of the uterus showing increased transverse dimension of the uterus (6 cm) with two endometrial cavities

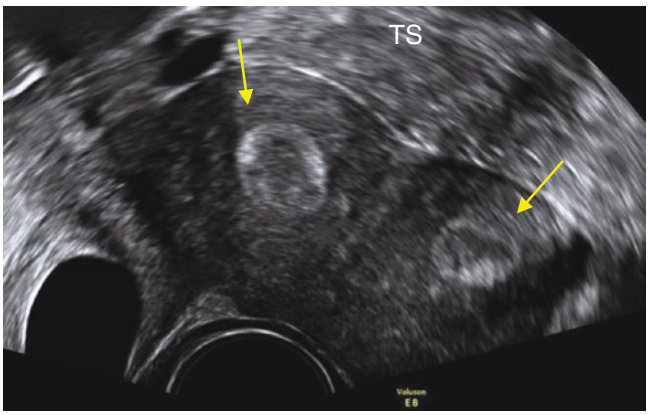

Fig. 12.5 TVS showing increased transverse diameter of the uterus with two endometrial cavities (*arrows*)

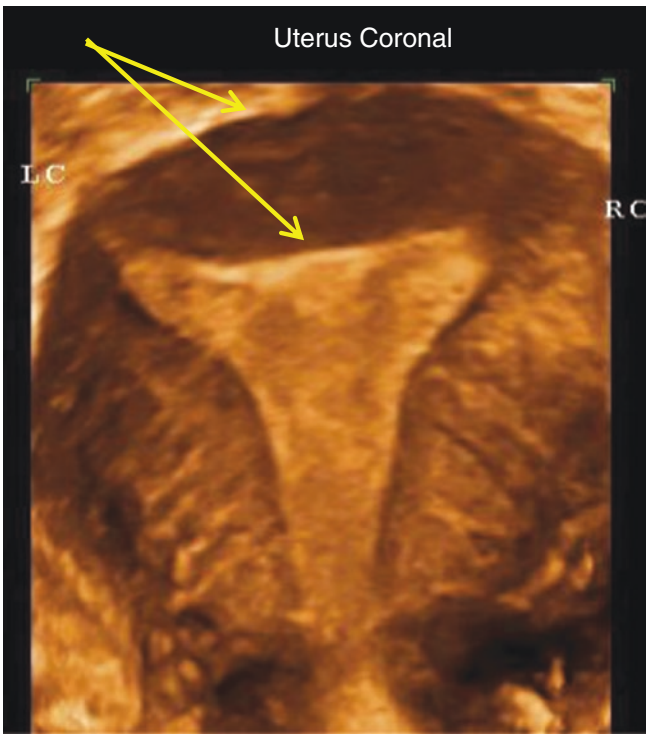

Fig. 12.6 3D rendered coronal image of a normal uterus showing a convex external fundal contour (*short arrow*) and the triangular shape of the inner uterine cavity of the uterus with the upper end of the uterine cavity being flat (*long arrow*)

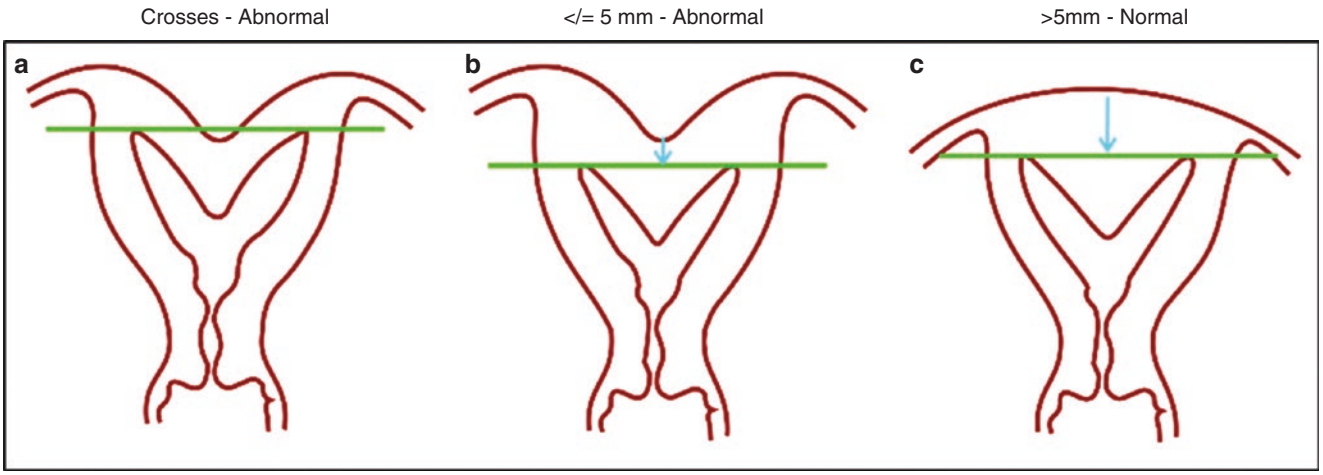

Fig. 12.7 Troiano and McCarthy's method of evaluating the external contour of the uterine fundus. The uterine fundus is considered abnormal (**a**) if it crosses below the line joining the upper end of the cavities on both sides and (**b**) if it is less than or equal to 5 mm from it. (**c**) If the uterine fundus is more than 5 mm from this line, the external contour of the fundus is considered normal

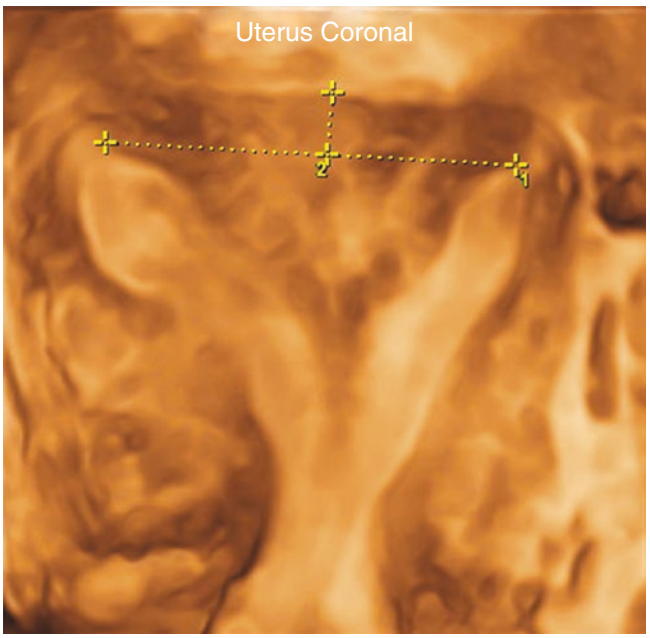

Fig. 12.8 Distance between the uterine fundus and the line joining the upper end of the cavities on both sides is measured to assess whether the external fundal contour is normal. If it is less than or equal to 5 mm, this would be considered as abnormal external fundal contour and the anomaly would be labelled as a bicornuate uterus. If it is more than 5 mm, the external fundal contour is considered normal and the anomaly would be labelled as a septate uterus

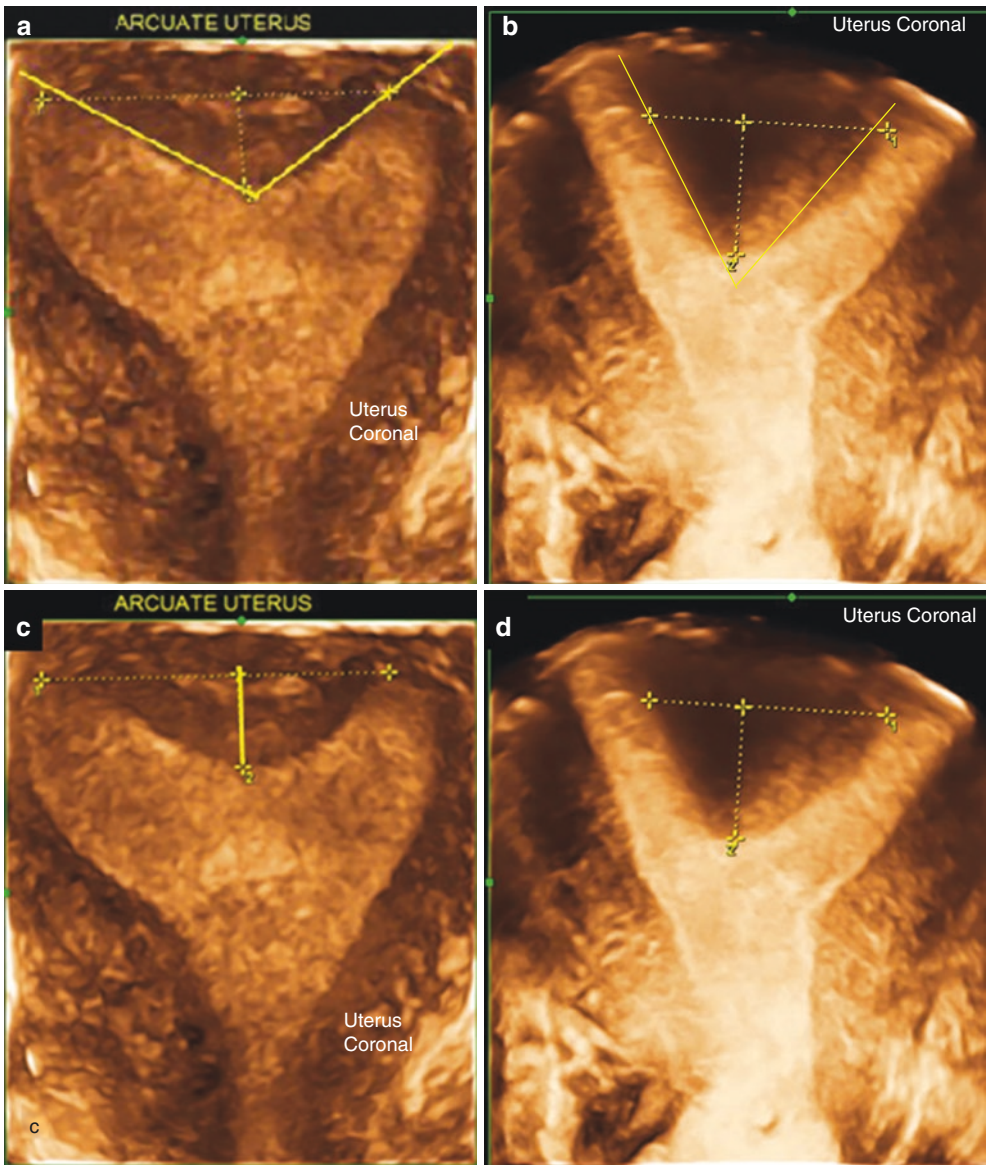

Fig. 12.9 Shape of the uterine cavity based on the angle at the centre: (**a**) arcuate (more than or equal to 90°) and (**b**) subseptate (less than 90°). Shape of the uterine cavity based on the depth of indentation of the cavity: (**c**) arcuate (less than 1.5 cm) and (**d**) subseptate (more than or equal to 1.5 cm)

12.4 Types of Uterine Anomalies

12.4.1 Arcuate Uterus (Fig. 12.10)

A. *External fundal contour:*

- Normal

B. *Shape of the uterine cavity:*

- Abnormal – indentation seen
- Angle at the centre between the two uterine cavities is obtuse (more than or equal to 90°)

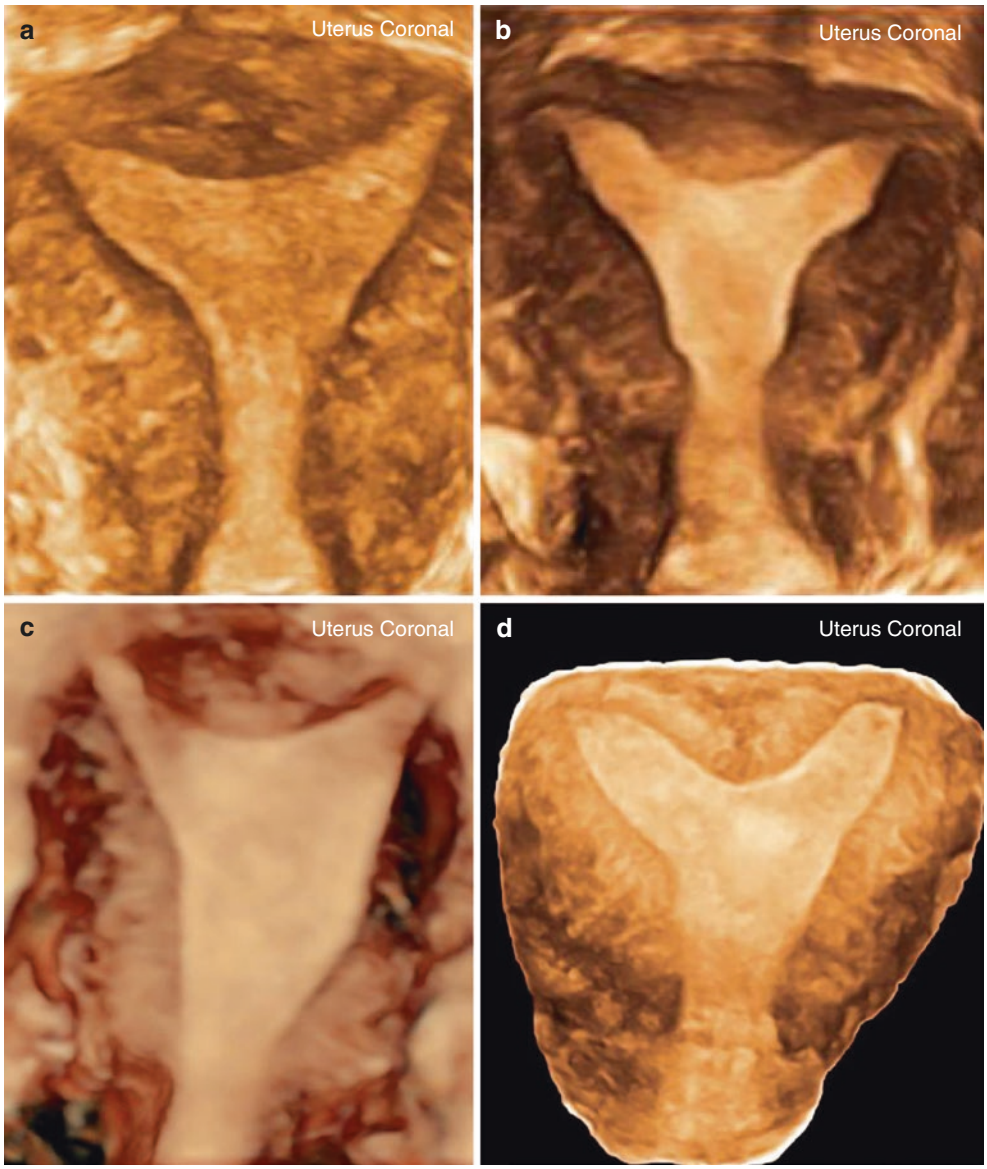

Fig. 12.10 Different cases of arcuate uterus with normal external fundal contour and indentation of the uterine cavity with angle more than or equal to 90°

The arcuate uterus is generally compatible with normal reproductive outcome. It is considered by some to be a normal anatomical variant. It is proposed that if the ratio of the height to the length is less than 10% (Fig. 12.11), it is not believed to be of clinical significance. It does not exist as a separate entity from a septate uterus in the new ESHRE classification.

At times, a normal intrauterine pregnancy close to the uterine cornua in a patient with an arcuate uterus may be wrongly reported as an interstitial ectopic pregnancy, because of the uterine shape. One must be aware about this possibility (Fig. 12.12).

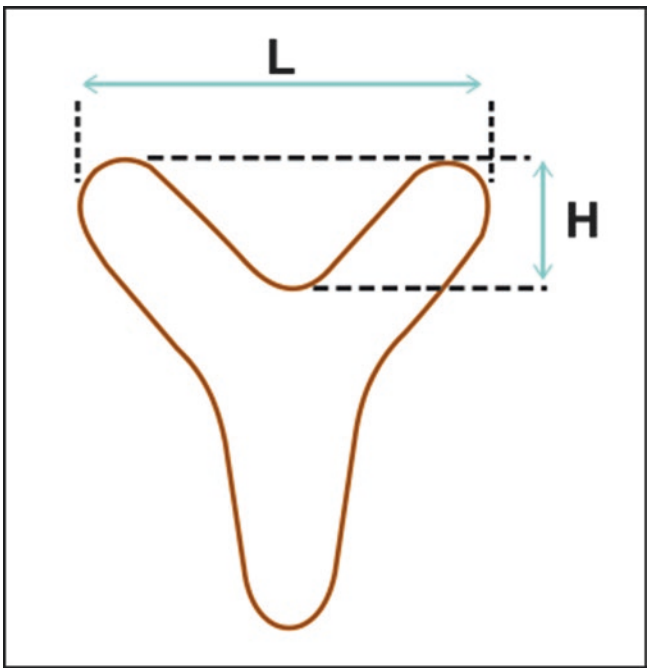

Fig. 12.11 In an arcuate uterus, if the ratio of height (*H*) to length (*L*) of the indentation is less than 10%, it is not believed to be of clinical significance

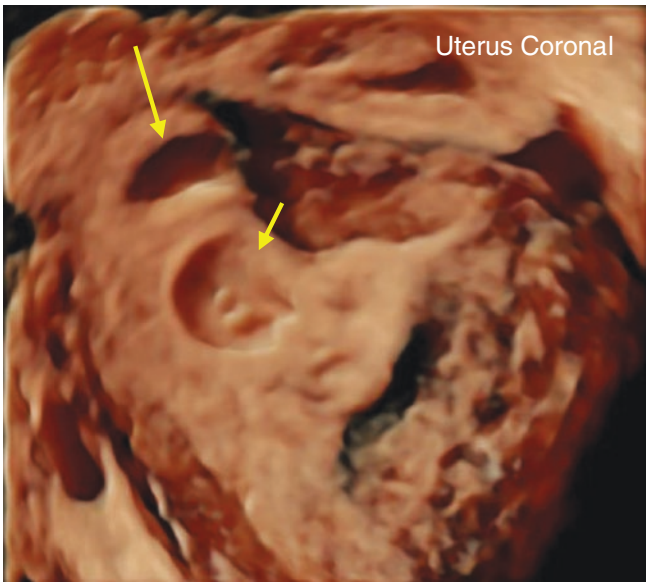

Fig. 12.12 Arcuate uterus with twin pregnancy sacs (*arrows*). The upper sac (*long arrow*) near the right cornua was wrongly interpreted to be an interstitial pregnancy but was in fact an intrauterine pregnancy well within the endometrial margins

12.4.2 Subseptate Uterus (Fig. 12.13)

A. *External fundal contour*:

- Normal

B. *Shape of the uterine cavity*:

- Abnormal – indentation seen
- Angle at the centre between the two uterine cavities is acute (less than 90°)
  - This indentation/septum does not reach up to the internal os.

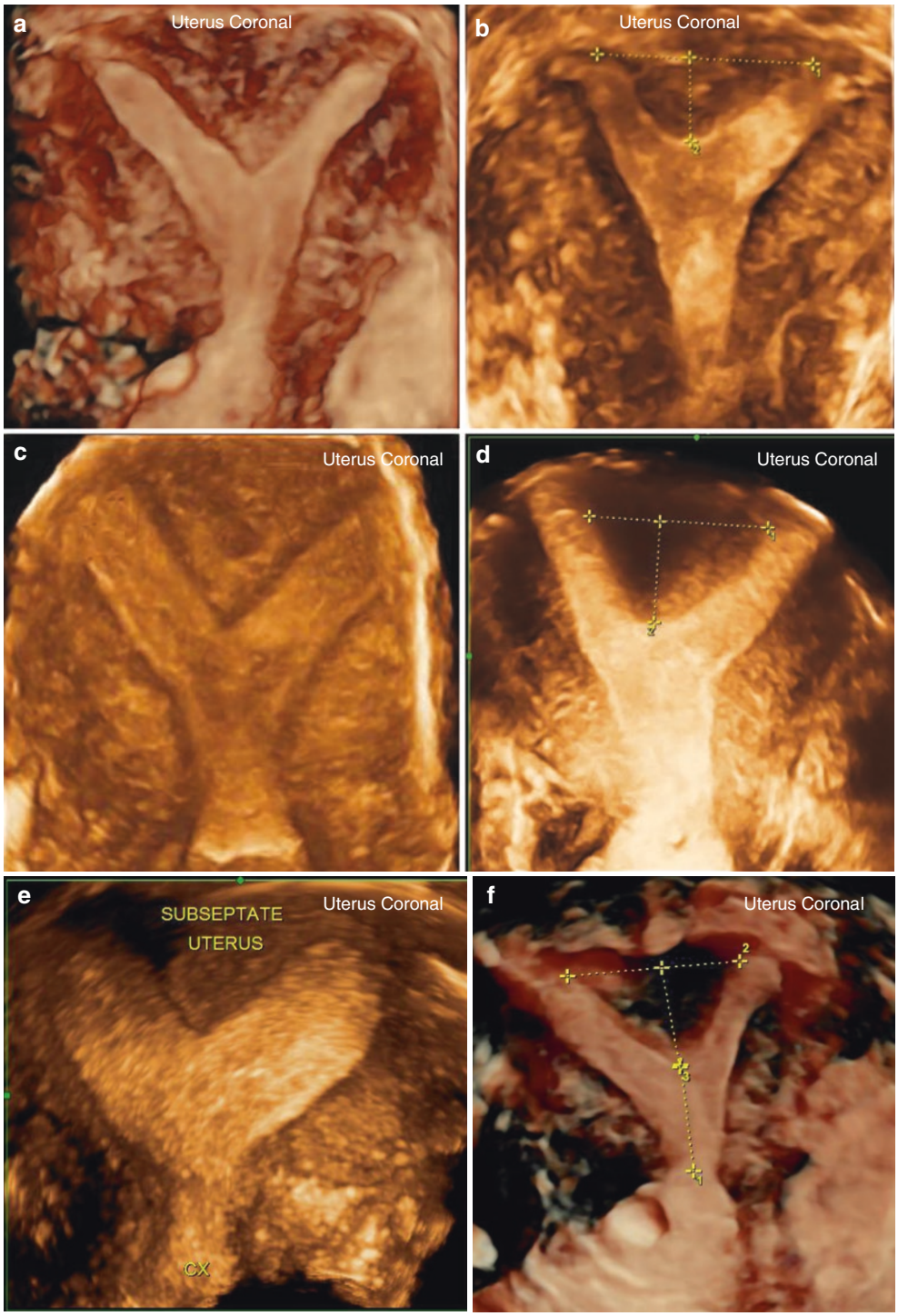

Fig. 12.13 Different cases of subseptate uterus with normal external fundal contour and indentation of the uterine cavity (less than 90°). The indentation/septum does not reach the internal os

12.4.3 Septate Uterus (Fig. 12.14)

A. *External fundal contour*:

- Normal

B. *Shape of the uterine cavity*:

- Abnormal – indentation seen
- Angle at the centre, between the two uterine cavities is acute (less than 90°)
  - This indentation/septum reaches up to the internal os or may extend beyond it.

Both septate and subseptate uterus are the most common anomalies seen, constituting about 55 % of all uterine anomalies. In 25 % of the cases, a vaginal septum is also seen.

Of the uterine anomalies, these have the poorest reproductive outcome with an increased incidence of spontaneous abortion and preterm delivery. Resection of the septum has been reported to decrease the risk of spontaneous abortion significantly.

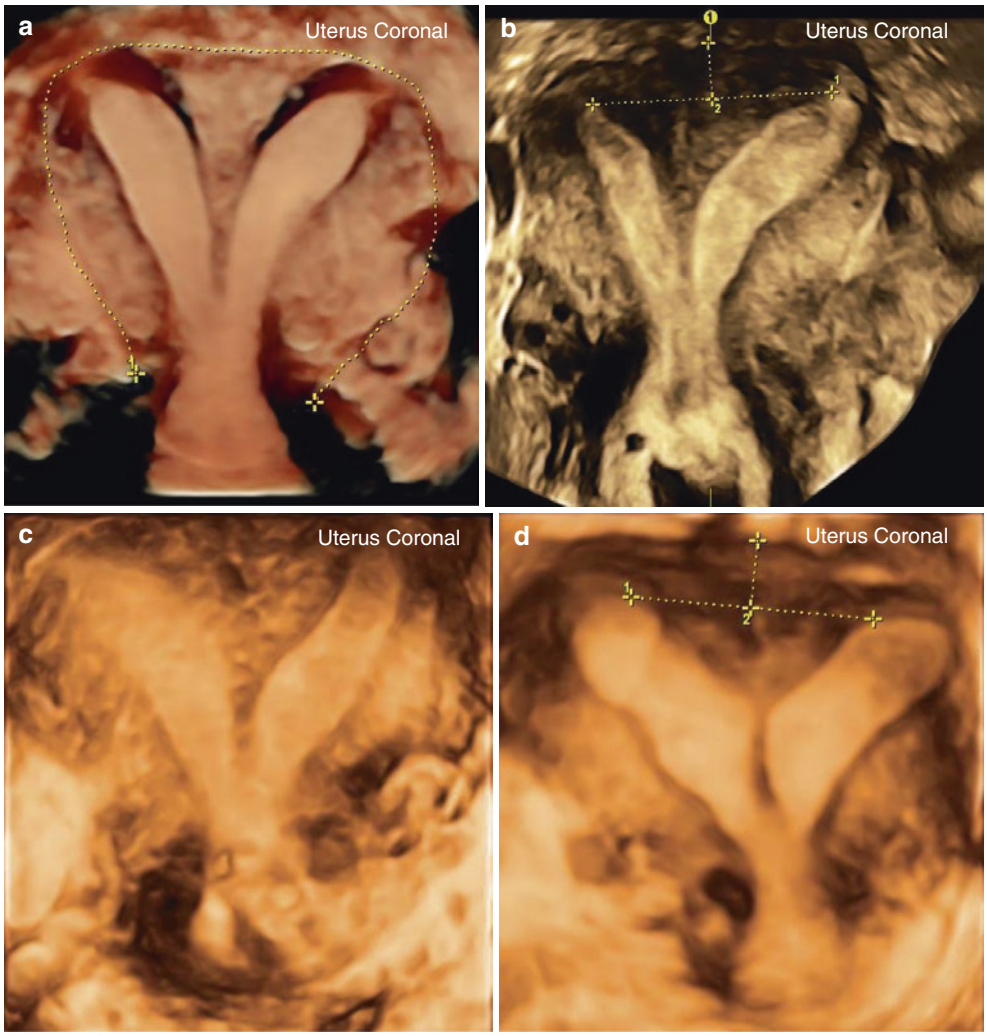

Fig. 12.14 Septate uterus with normal external fundal contour and indentation of the uterine cavity (less than 90°). The indentation/septum reaches up to the internal os and may extend beyond it

12.4.4 Bicornuate Uterus (Fig. 12.15)

A. *External fundal contour:*

- Abnormal with indentation (uterine fundus crosses below the line joining the upper end of the cavities on both sides or is less than or equal to 5 mm from it)

B. *Shape of the uterine cavity:*

- Abnormal – indentation seen
  - If the separation of the uterine cavity does not extend up to the internal os, it is termed as *partial bicornuate uterus.* The cervical canal may be single (unicollis) or double (bicollis).

This constitutes about 10 % of uterine anomalies; it can be complete (extending up to the internal os) or partial. It can be unicollis (single cervical canal) or bicollis (cervical septum with two cervical canals). Vaginal septum is seen in 25 % of these cases.

The reproductive outcome in these cases is better than in a septate uterus. The length of gestation increases with parity. This anomaly has the highest incidence of cervical incompetence. Surgical intervention is generally not indicated. In cases with recurrent pregnancy losses, metroplasty may be considered.

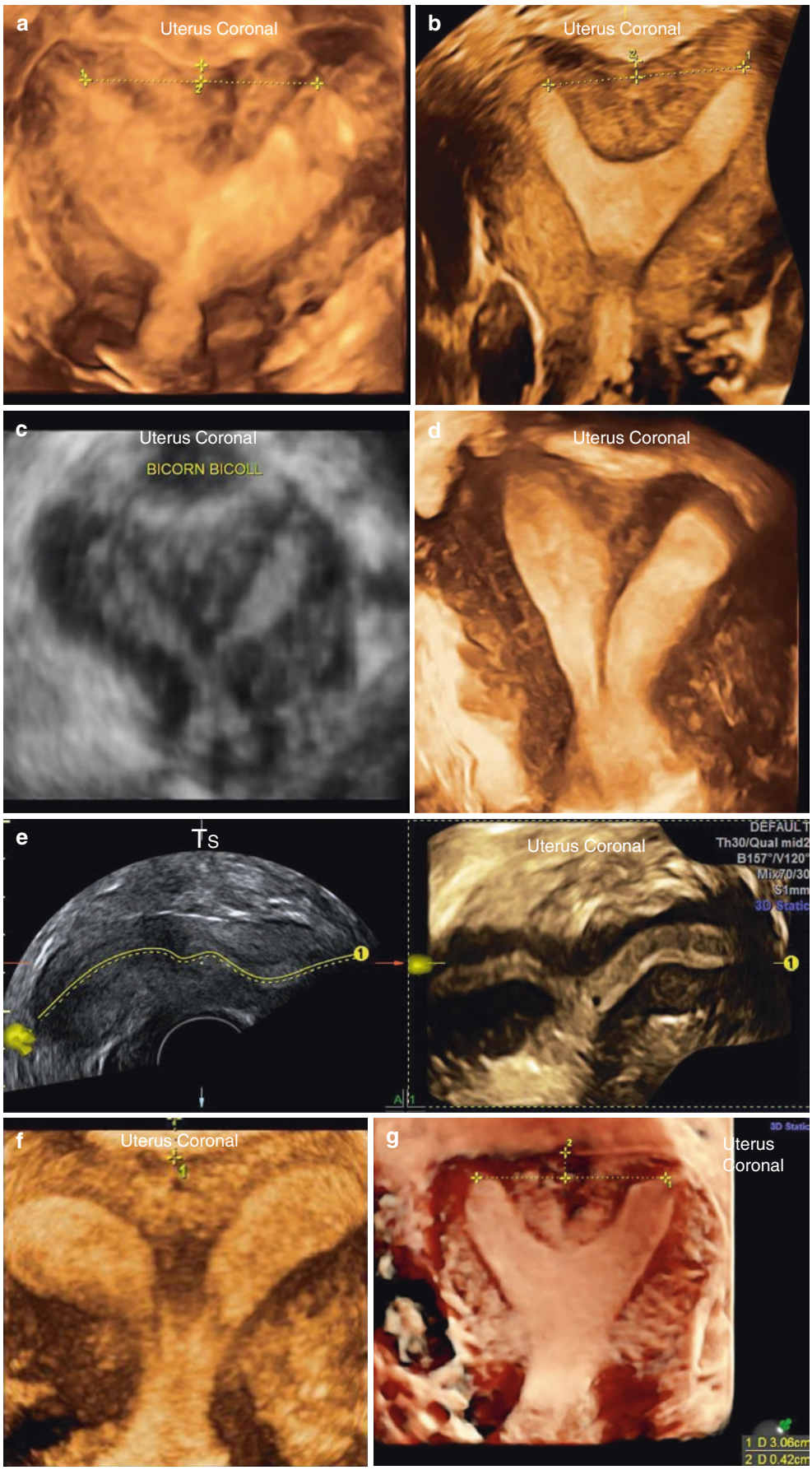

Fig. 12.15 Bicornuate uterus with abnormal external fundal contour with indentation (uterine fundus crosses below the line joining the upper end of the cavities on both sides or is less than or equal to 5 mm from it) along with indentation of the uterine cavity. (**a**, **b**) Partial bicornuate uterus. (**c**) Complete bicornuate bicollis uterus. (**d**) Complete bicornuate uterus. (**e**) Bicornuate unicollis uterus with splayed out uterine bodies. 3D rendering with polyline was useful in obtaining a coronal image of the uterus. (**f**) Bicornuate bicollis uterus. (**g**) As the distance between the upper end of the endometrial cavities and the fundal outline was less than 5 mm, and the septum was not reaching up to the internal os, this was labelled as a partial bicornuate uterus

12.4.5 Uterus Didelphys (Fig. 12.16)

A. *External fundal contour:*

- Abnormal with indentation (uterine fundus crosses below the line joining the upper end of the cavities on both sides or is less than or equal to 5 mm from it)

B. *Shape of the uterine cavity:*

- Abnormal – two separate uterine cavities

In these cases, two separate cervices are seen beside each other, as two separate cervical canals with a thick intervening myometrium.

3D evaluation is often difficult because the two uterine horns may be far apart, making it difficult to include them in a single sweep/image.

They constitute about 5 % of uterine anomalies. Vaginal septum is seen in 75 % of these cases. Spontaneous abortion and preterm delivery may be seen in these patients. If one side is obstructed, patients may suffer from dysmenorrhoea, adenomyosis and endometriosis. In women with recurrent losses of pregnancy, metroplasty may be considered.

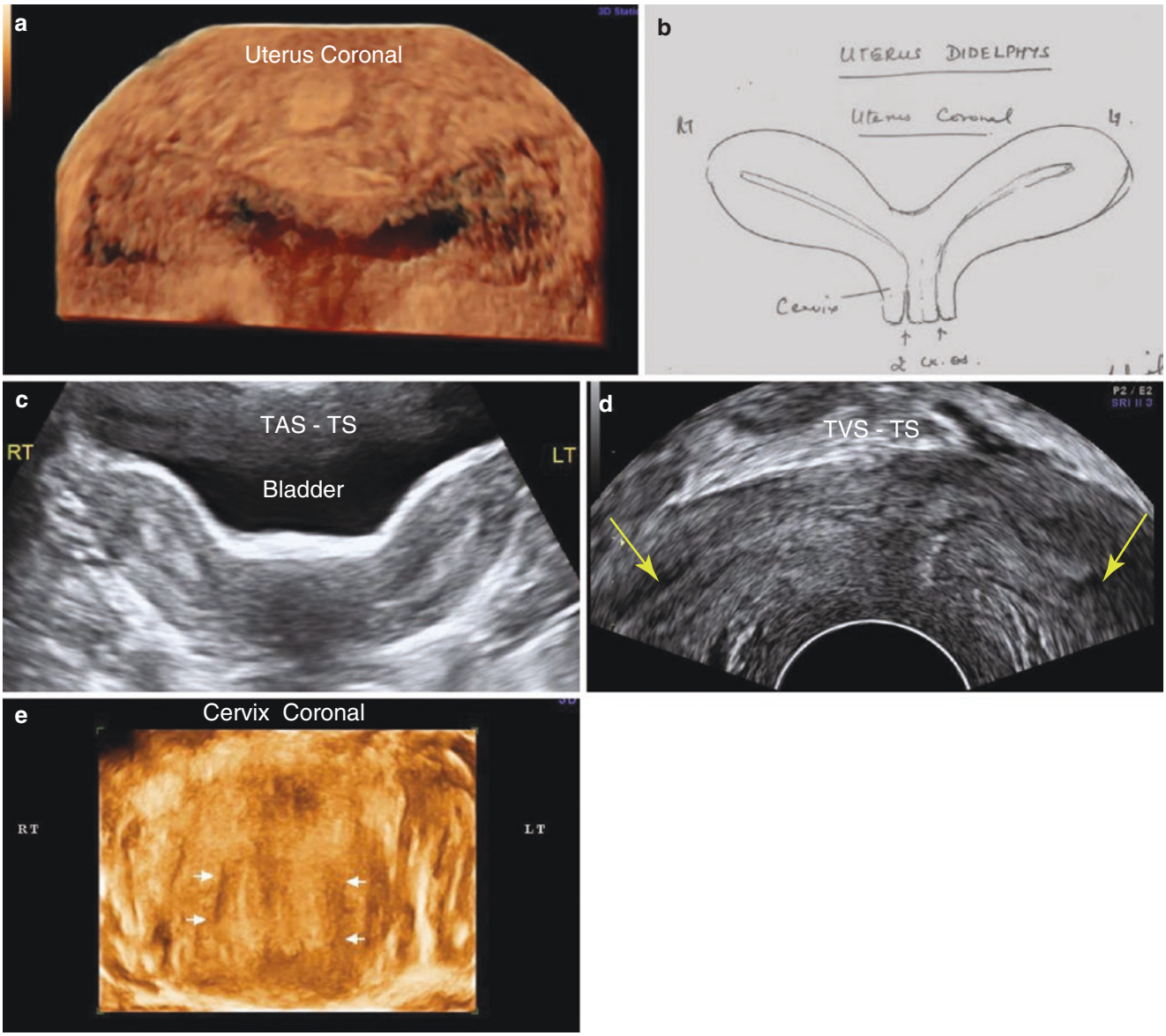

Fig. 12.16 Uterus didelphys with an abnormal external fundal contour (uterine fundus crosses below the line joining the upper end of the cavities on both sides or is less than or equal to 5 mm from it) and an abnormal uterine cavity (two separate uterine cavities). (**a**) Uterus didelphys in a postmenopausal lady. A single 3D rendered image showing both uterine horns was possible because of the small uterine size. (**b**) Diagrammatic representation of the same. (**c**) TAS image of a uterus didelphys showing an unconventional section of the uterine body. (**d**) Uterus didelphys on TVS with both the uterine cavities splayed apart (*arrows*). (**e**) 3D rendered image showing two separate cervices with thick intervening myometrium (cervical canal marked with *arrows*)

12.4.6 Unicornuate Uterus (Fig. 12.17)

A. *External fundal contour:*

- Normal

B. *Shape of the uterine cavity:*

- Abnormal – Banana shaped and deviated to one side, ending in a single cornua.

This is the most frequently missed anomaly because the external fundal contour appears normal, and, unless visualisation of both cornua is a routine, the presence of a single cornu may be missed.

It constitutes about 20 % of uterine anomalies. It may:

- Be isolated in 35 % of the cases.
- Have a rudimentary horn with no cavity in 33 % of the cases.
- Have a rudimentary horn with a cavity in 32 % of the cases. Of these, in 22 %, the cavity of the rudimentary horn is non-communicating (i.e., not communicating with the main uterine cavity), and in 10 % it communicates with the main uterine cavity.

Unicornuate uterus has the highest association with renal anomalies (40 %). An increased incidence of spontaneous abortions, preterm delivery, IUGR and abnormal fetal lie has been reported.

In cases with non-communicating rudimentary horn, there is an increase in incidence of cornual ectopic pregnancy, dysmenorrhoea, adenomyosis and endometriosis. Surgical resection of the rudimentary horn may be required in such cases.

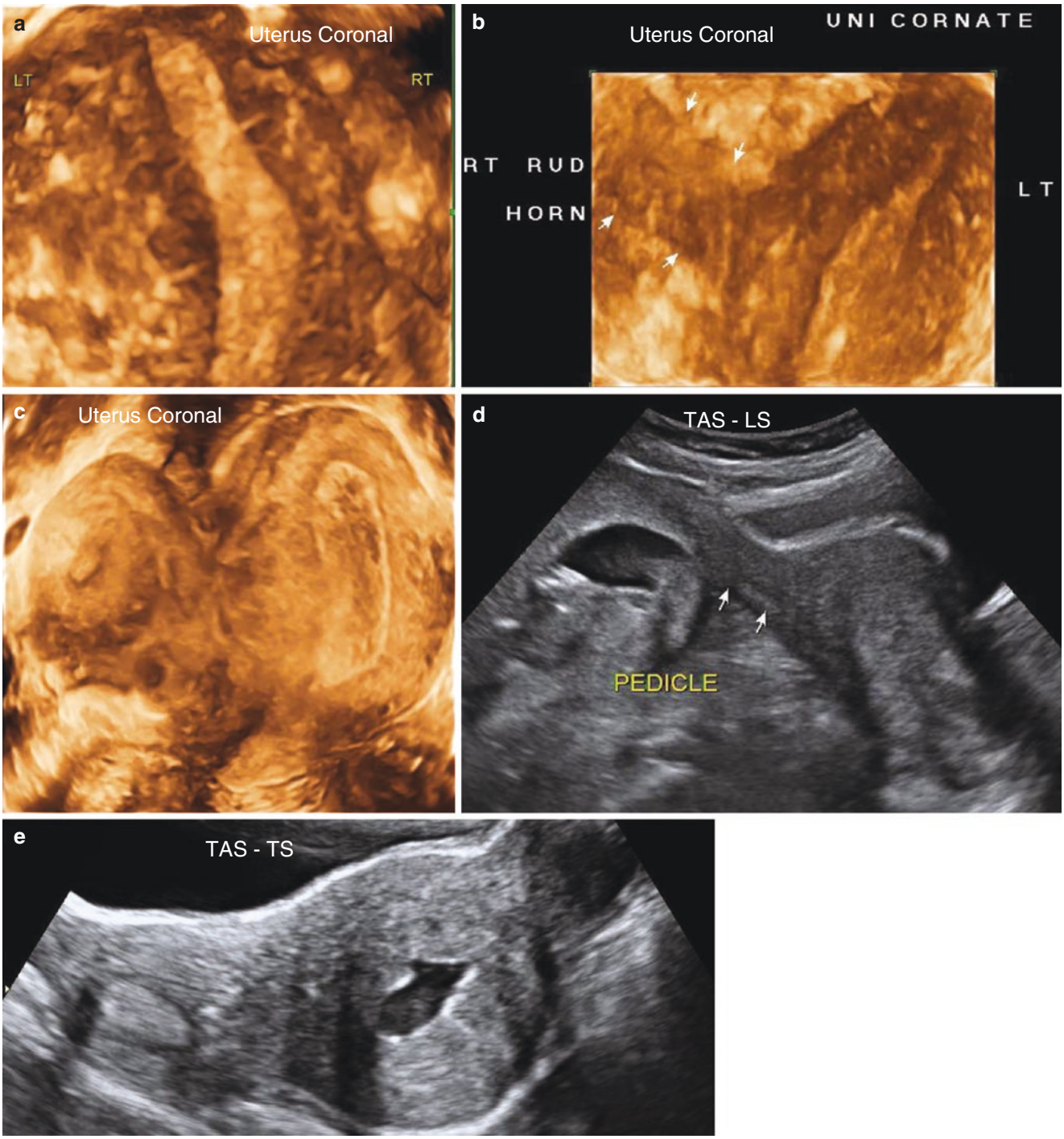

Fig. 12.17 Unicornuate uterus with normal external fundal contour and a banana-shaped uterine cavity, deviated to one side and ending in a single cornua. (**a**) True unicornuate uterus with no rudimentary horn. (**b**) Unicornuate uterus with a rudimentary horn with no endometrial cavity. (**c**) Unicornuate uterus with a rudimentary horn and a non-communicating endometrial cavity. (**d**) Unicornuate uterus with pregnancy in the non-communicating rudimentary horn – cornual ectopic pregnancy. (**e**) TAS – transverse section of a right unicornuate uterus with a left non-communicating rudimentary horn, showing hematometra and thick uterine walls secondary to adenomyosis

12.4.7 Absent/Hypoplastic Uterus (Figs. 12.18 and 12.19)

The uterus is either absent or is replaced by a very small rudimentary structure, just above the vagina. The ovaries are usually normal, and therefore these patients have normal secondary sexual characters. They most often present with primary amenorrhea.

This constitutes 5–10 % of uterine anomalies. The ovaries are visualised in true Mullerian agenesis (commonly known as 'Mayer–Rokitansky–Kuster–Hauser syndrome').

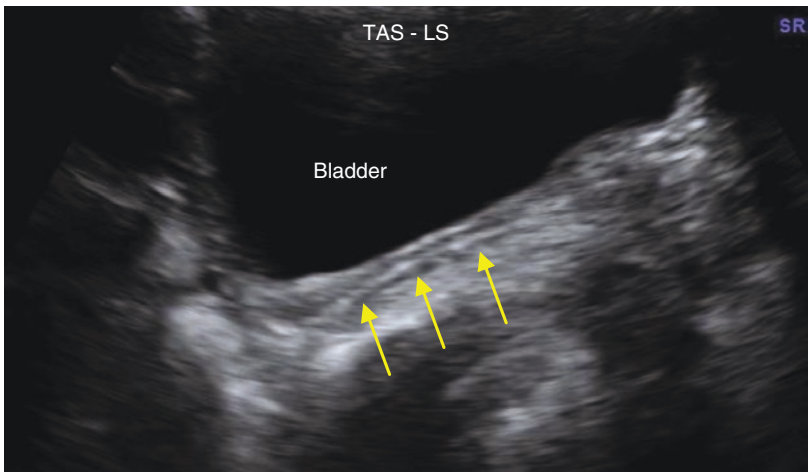

Fig. 12.18 Absent uterus. Vaginal lumen seen as a hyperechoic linear echo (*arrows*). Uterine body not seen above it

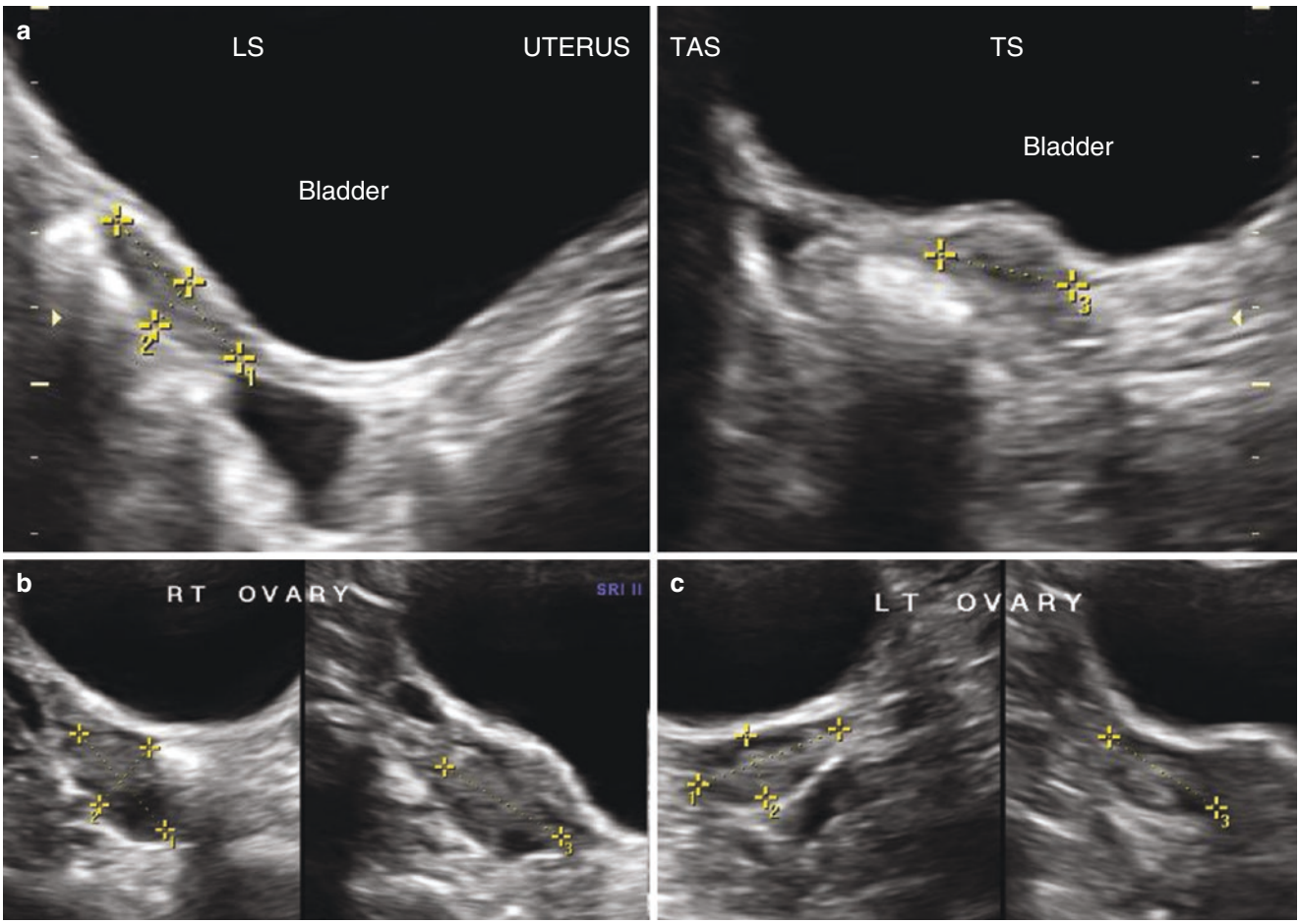

Fig. 12.19 Hypoplastic uterus in a patient with Mayer–Rokitansky–Kuster–Hauser syndrome. (**a**) Longitudinal section, (**b**) transverse section of the rudimentary uterus. (**c**, **d**) Normal right and left ovaries

12.4.8 'T-Shaped' Uterus (Fig. 12.20)

A. *External fundal contour:*

- Normal

B. *Shape of the uterine cavity:*

- Abnormal – 'T shaped'

'T-shaped' uterine cavity was a known complication of intrauterine exposure to diethylstilbestrol (DES), the use of which was discontinued in 1971. This abnormality may be seen even without a history of DES exposure.

Increased incidence of recurrent abortions and preterm delivery has been reported in these cases. In some cases, hysteroscopic metroplasty has shown improved reproductive outcome.

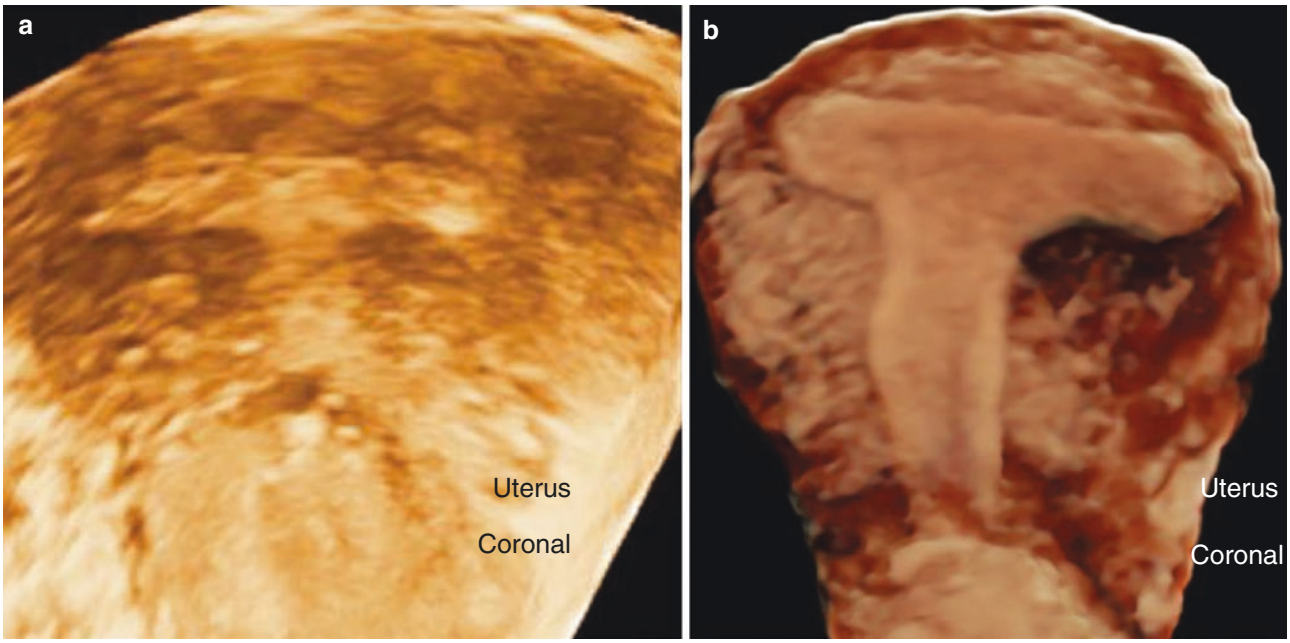

Fig. 12.20 T-shaped uterus with normal external contour and abnormal 'T-shaped' uterine cavity

12.5 Cervical and Vaginal Anomalies (Figs. 12.16e, 12.21, 12.22, 12.23, 12.24, 12.25, 12.26, 12.27, 12.28 and 12.29)

Very often, the embryological abnormal fusion and resorption may involve the cervix and the vagina. Evaluating these is more challenging because of the proximity of these structures to the vaginal probe. This can be overcome to some extent by partial withdrawal of the transvaginal probe, a little lower down into the vagina. In addition, the vagina is a collapsed structure making it difficult to evaluate the presence of a vaginal septum.

Cervix

The best time to evaluate the cervix for anomalies is during ovulation (mid-cycle – around Day 12 in a 28-day menstrual cycle). The cervical canal can be assessed on 2D, in a transverse plane. It is better seen on 3D, but evaluation on 3D may require a special technique, separate from standard rendered imaging of the uterine cavity. One could either take two separate volume sweeps, one for the uterine cavity and one for the cervix, or one may take a single sweep, but the rendering of the two has to be done separately. With newer machines, there is an additional facility called polyline, using which the plane of rendering can be traced in a curvilinear manner, along the uterocervical canal, thus facilitating simultaneous rendering of the entire uterocervical cavity. MRI is sometimes more informative than standard ultrasound in the evaluation of cervical anomalies.

Gel sonovaginography (GSV) may be resorted to for better assessment of the cervix, the cervical canal and the cervical os (whether there are 1 or 2).

Vagina

A *longitudinal vaginal septum* divides the vagina into two parallel cavities, and, unless one or both of the cavities are obstructed with resultant haematocolpos and hematometra, the longitudinal septum may go unrecognised both clinically and on ultrasound. If any one of the vaginal cavities is obstructed, the symptoms will be similar to that of a transverse vaginal septum. Septate vagina is often seen in women with uterine anomalies extending up to the cervix. On TVS scan, the probe tends to pass into one of the two vaginal cavities by default.

In most cases, the other collapsed vaginal cavity can be seen on careful observation, with the probe withdrawn lower into the vaginal canal, as a white echogenic line. This echogenic line is seen on ultrasound whenever two smooth surfaces approximate each other – in this case the two walls of other hemivagina.

Vaginal anomalies have been evaluated with MRI using various techniques. Their evaluation with GSV is very convenient and accurate. Gel can be instilled on both sides of the vaginal septum. One can evaluate the thickness, length and direction of the septum. Also the relation of the two cervical os to the septum can be assessed.

In some cases, a *transverse vaginal septum* may be seen. This is often due to defective resorption of the tissue between the upper two-third of the vagina developing from the Mullerian duct and the lower one-third developing from the urogenital sinus. This resorption should normally occur, resulting in a single vaginal canal. In these cases, the transvaginal probe does not reach up to the cervix. In some of these patients, there may be a small opening through which menstrual blood may flow out. However, in other cases, the transverse septum may be complete and intact, resulting in the patient presenting at menarche with primary amenorrhea and pain secondary to haematocolpos/hematometra.

A patient with *imperforate hymen* can also present with similar features as an intact transverse vaginal septum with primary amenorrhea, cyclical pain and haematocolpos/hematometra. It is a relatively common anomaly seen in about 0.1 % of women. During ultrasound, therefore, it is important to assess the thickness of the tissue below the haematocolpos so as to decide the surgical management of these cases. With imperforate hymen, a simple cruciate incision is the solution, whereas other transverse vaginal septum will require more complex surgeries.

In patients with Mullerian agenesis, the vagina may be very short and these patients may require vaginoplasty for normal coital function.

In patients with obstruction of menstrual flow due to a transverse vaginal septum or an imperforate hymen or a non-communicating hemivagina, the back pressure can result in pain. In long-standing cases, adenomyosis and endometriosis could also be a resultant complication.

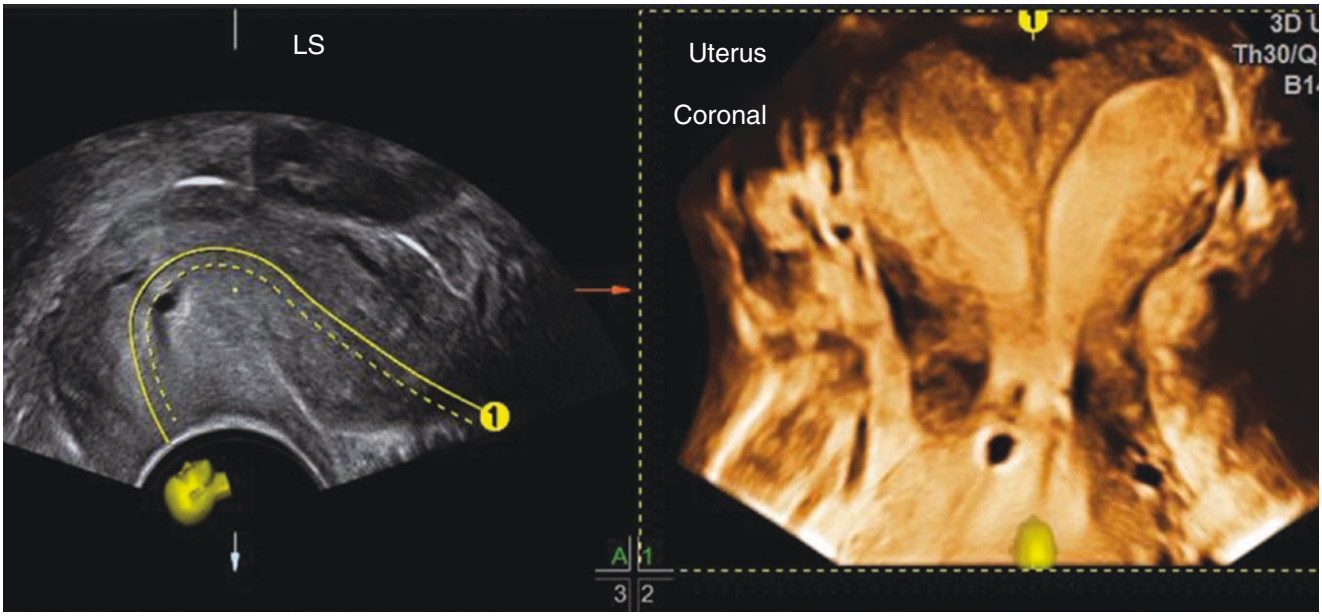

Fig. 12.21 Evaluation of the cervix can be challenging in case of uterine anomalies where there is significant retroflexion or anteflexion, because the coronal plane of the uterine body and the cervical canal is different. In this case of an anteflexed uterus, polyline was used so as to obtain a single image showing the coronal sections of both the uterus and the cervix

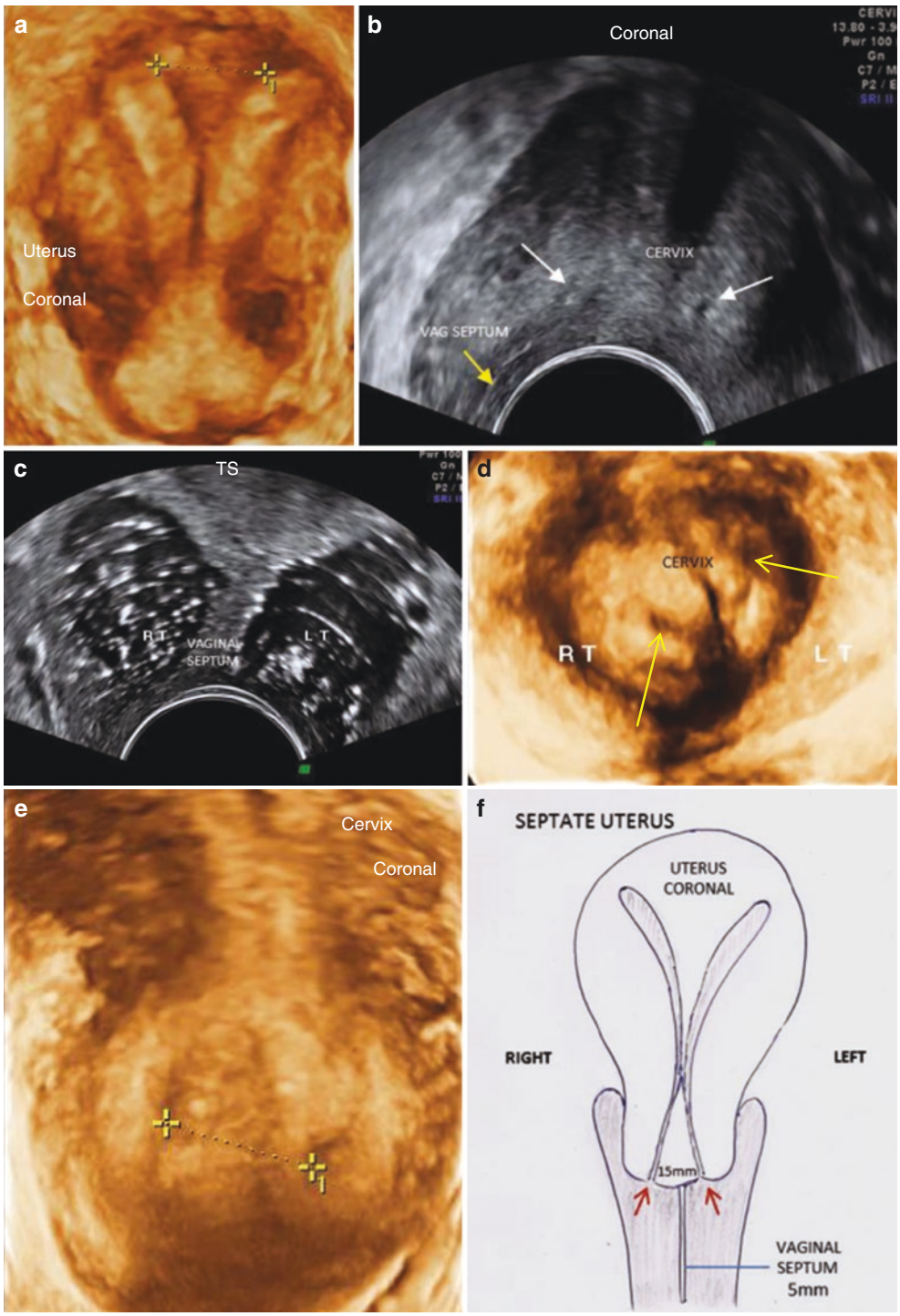

Fig. 12.22 Case of septate uterus with septate vagina. (**a**) 3D rendered coronal image of a septate uterus and cervix. (**b**) Probe is seen in one half of the vagina (partially withdrawn for better visualisation). The lower end of the two cervical canals (*arrows*) is seen and the lumen of the right-sided hemivagina is seen as a hyperechoic line (*short arrow*). (**c**) Transverse section of the septate vagina with gel within showing hyperechoic air bubbles. (**d**) 3D rendered image of the two cervical ostia (*arrows*) on either side of the septum, on GSV. (**e**) 3D rendered image of the two cervical canals on GSV. (**f**) Diagrammatic representation of the anomaly

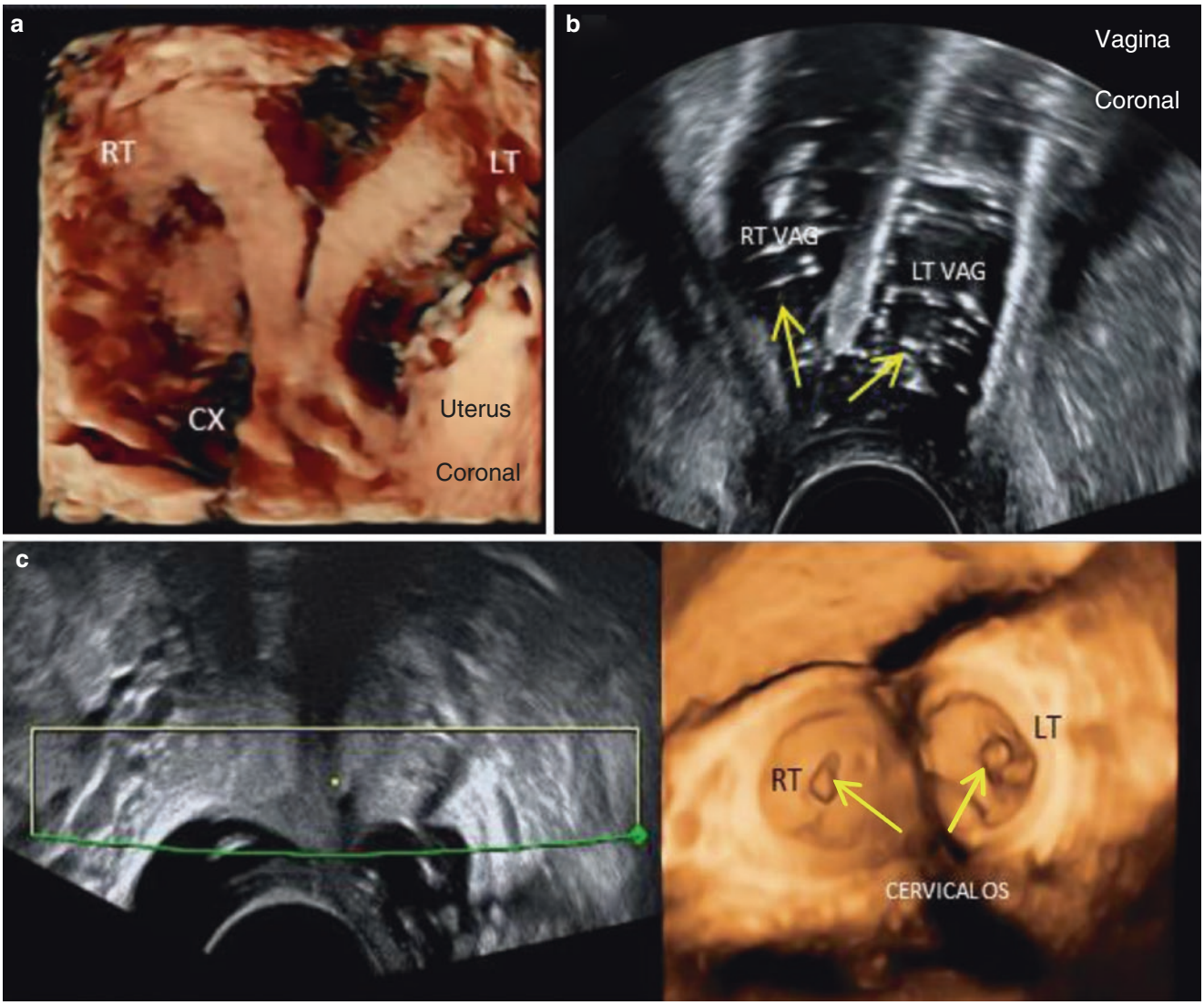

Fig. 12.23 Septate uterus, cervix and vagina (**a**) Coronal rendered image of the septate uterus. (**b**) Coronal section of the septate vagina with gel on either sides (*arrows*) of the vaginal septum. (**c**) GSV with 3D rendering, showing the two cervical os

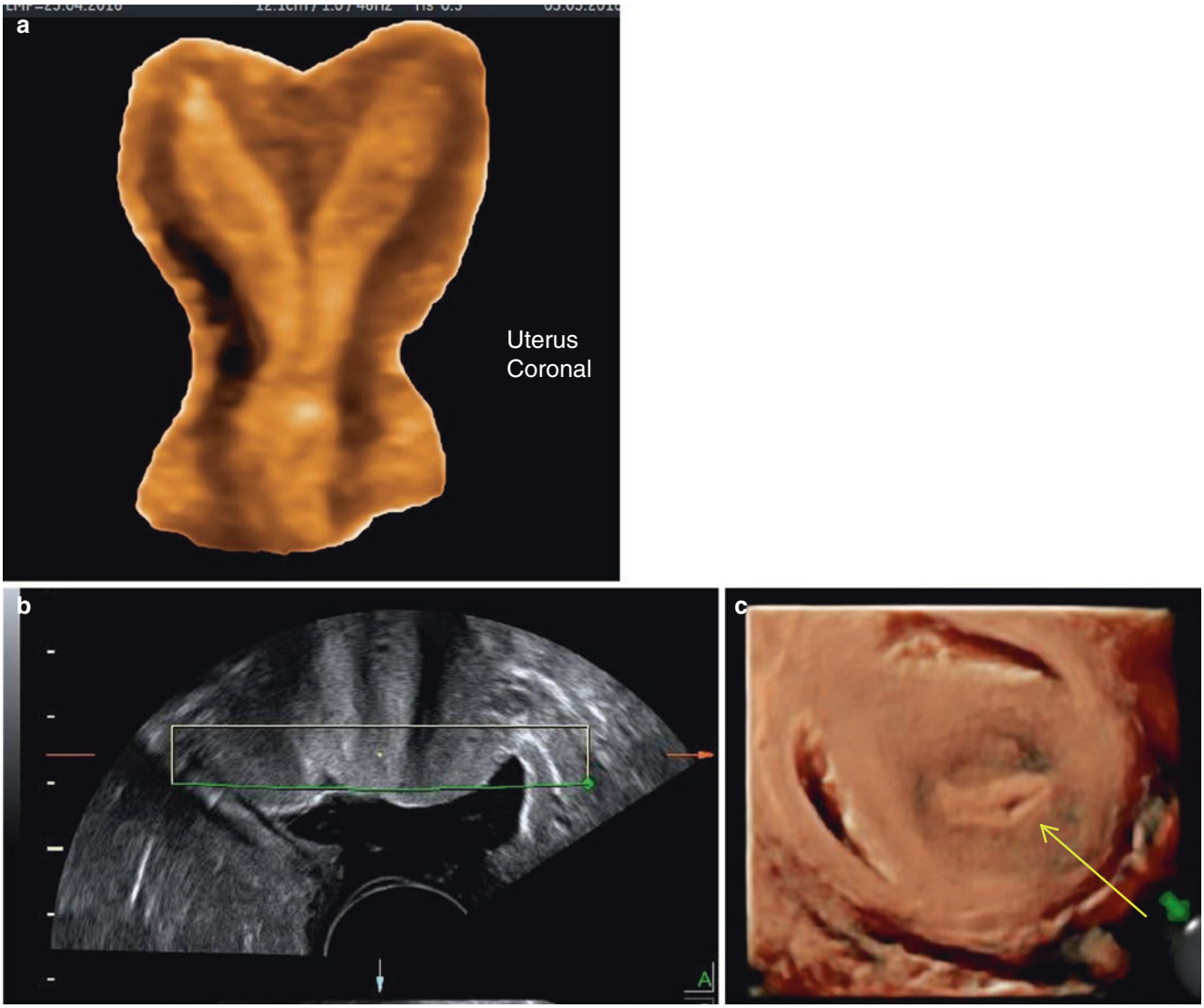

Fig. 12.24 Bicornuate uterus with a single cervix and a single vagina. (**a**) Shows a coronal rendered image of a complete bicornuate uterus. (**b**) GSV – image showing the plane of rendering used to evaluate the cervix and cervical os. (**c**) GSV with 3D rendering showing a single cervical os (*arrow*) seen as a transverse slit. In this case, there was a single flattened cervical canal narrow in the midline giving a false impression of a septum extending into the cervix as is seen in figure (**a**)

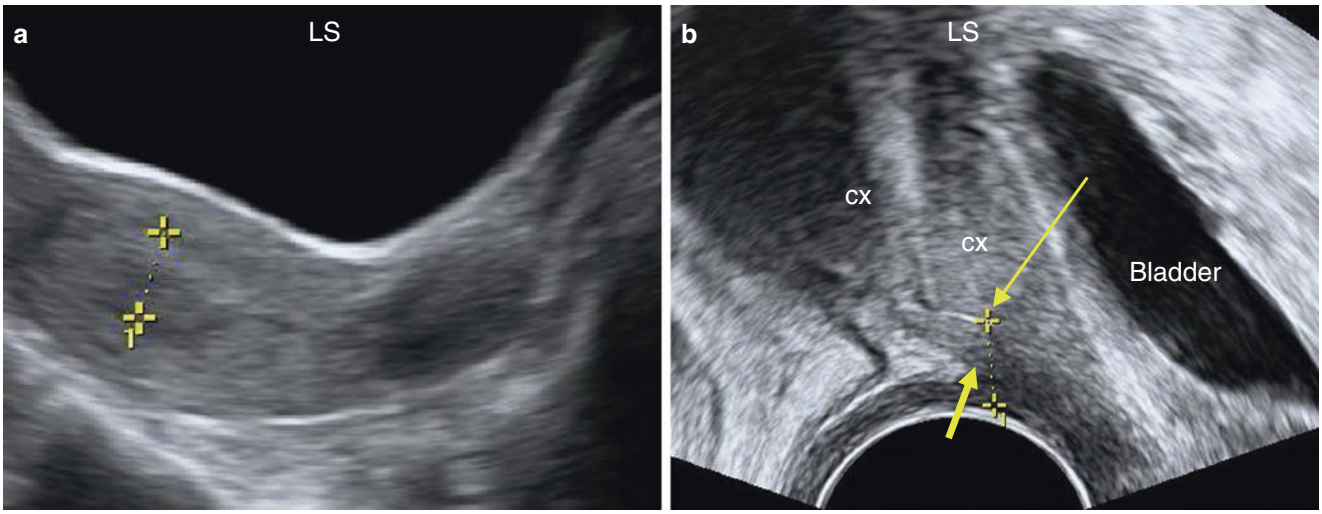

Fig. 12.25 Married woman with a transverse vaginal septum in the upper vagina. Patient presented with a history of abdominal pain and a positive pregnancy test. She gave no history of coital or menstrual problems. (**a**) TAS – no intrauterine pregnancy seen. (**b**) TVS – showing a transverse vaginal septum (*short arrow*) which is measured in the image, just below the cervix (*cx*). Hyperechoic line (*long arrow*) showing a smooth interface between the vaginal septum and the anterior lip of the cervix. A part of the bladder is seen in the image anteriorly

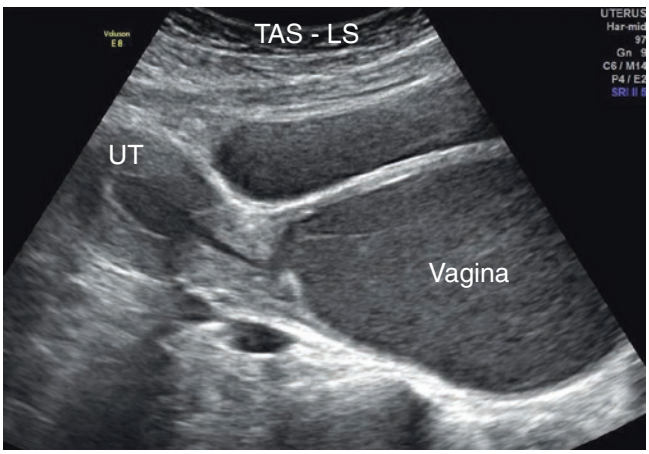

Fig. 12.26 Imperforate hymen with haematometrocolpos. The figure shows a grossly dilated vagina with turbid fluid suggestive of blood seen in the vagina (haematocolpos), cervical canal and uterine body due to backflow from the haematocolpos, resulting in a haematometrocolpos

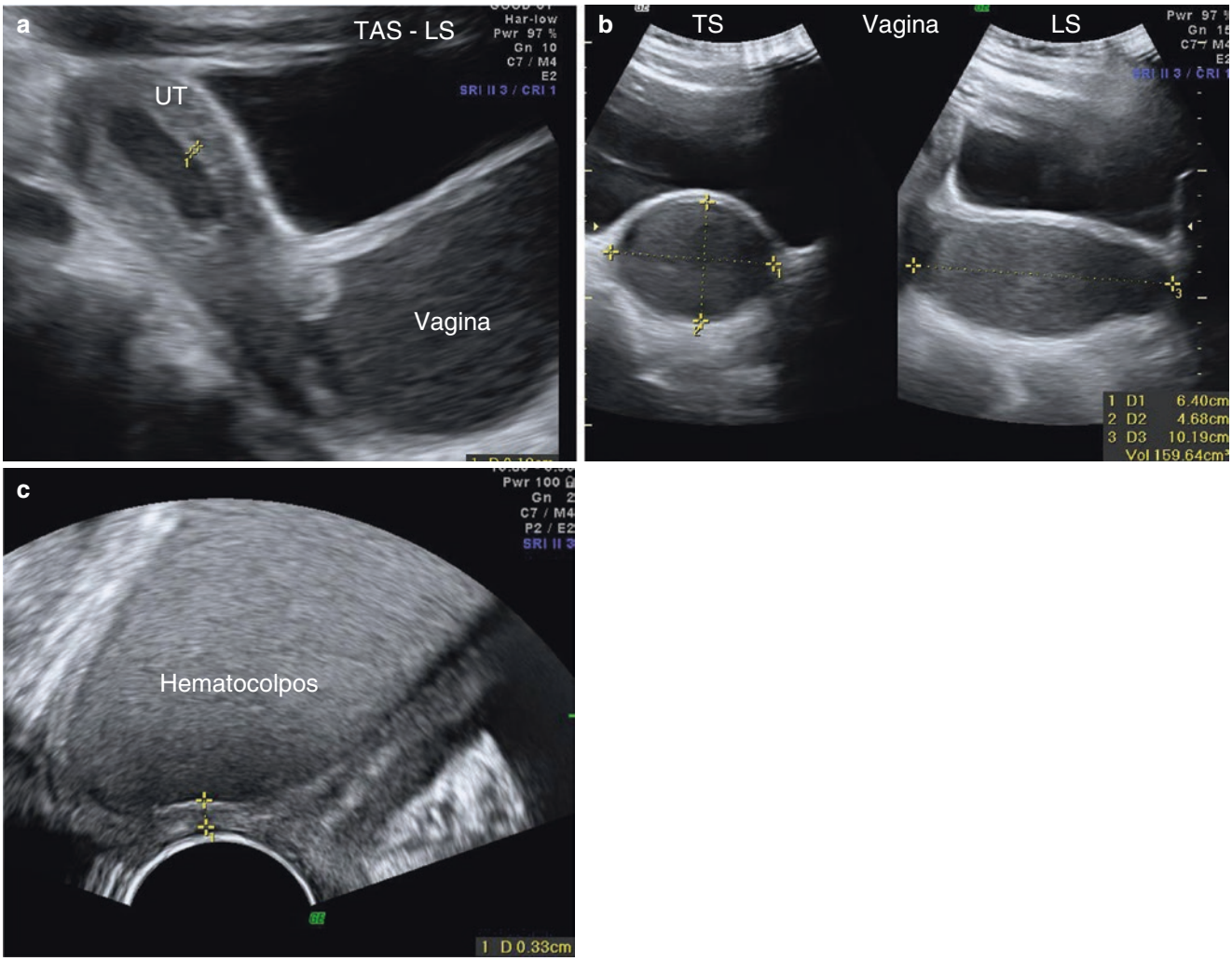

Fig. 12.27 Imperforate hymen with haematometrocolpos. Patient was a 14-year-old girl who presented with severe abdominal pain. (**a**) Sagittal section showing hematometra and haematocolpos. (**b**) Haematocolpos seen in the transverse and the sagittal section with a volume of 169cc. (**c**) Transperineal scan done to assess the thickness of the tissue below the haematocolpos. Here a thin imperforate hymen is seen. A simple cruciate incision was the solution

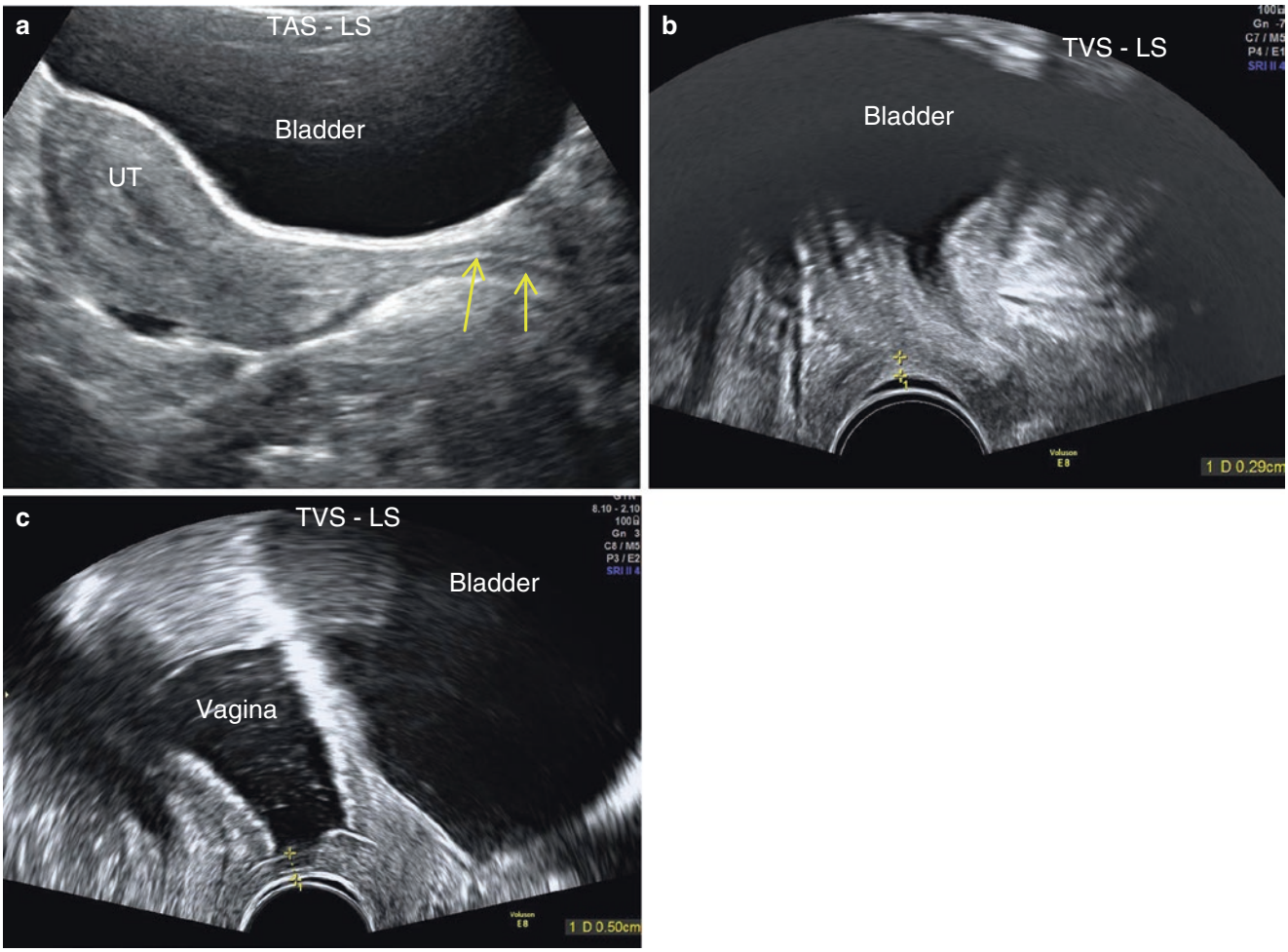

Fig. 12.28 Imperforate hymen with regular menses. A 24-year-old unmarried patient presented with a history of absent vaginal opening. (**a**) TAS showing the sagittal section of normal uterus and upper vagina (*arrow*). (**b**) Transperineal scan showed an obstruction suggestive of an imperforate hymen which is measured in the image. (**c**) In order to confirm the findings, a search was made for a possible opening in the hymen through which the patient had been menstruating. A small opening was found through which saline was infused into the vagina. This confirmed it to be a case of a simple imperforate hymen. Simple cruciate incision was sufficient to open out the vagina

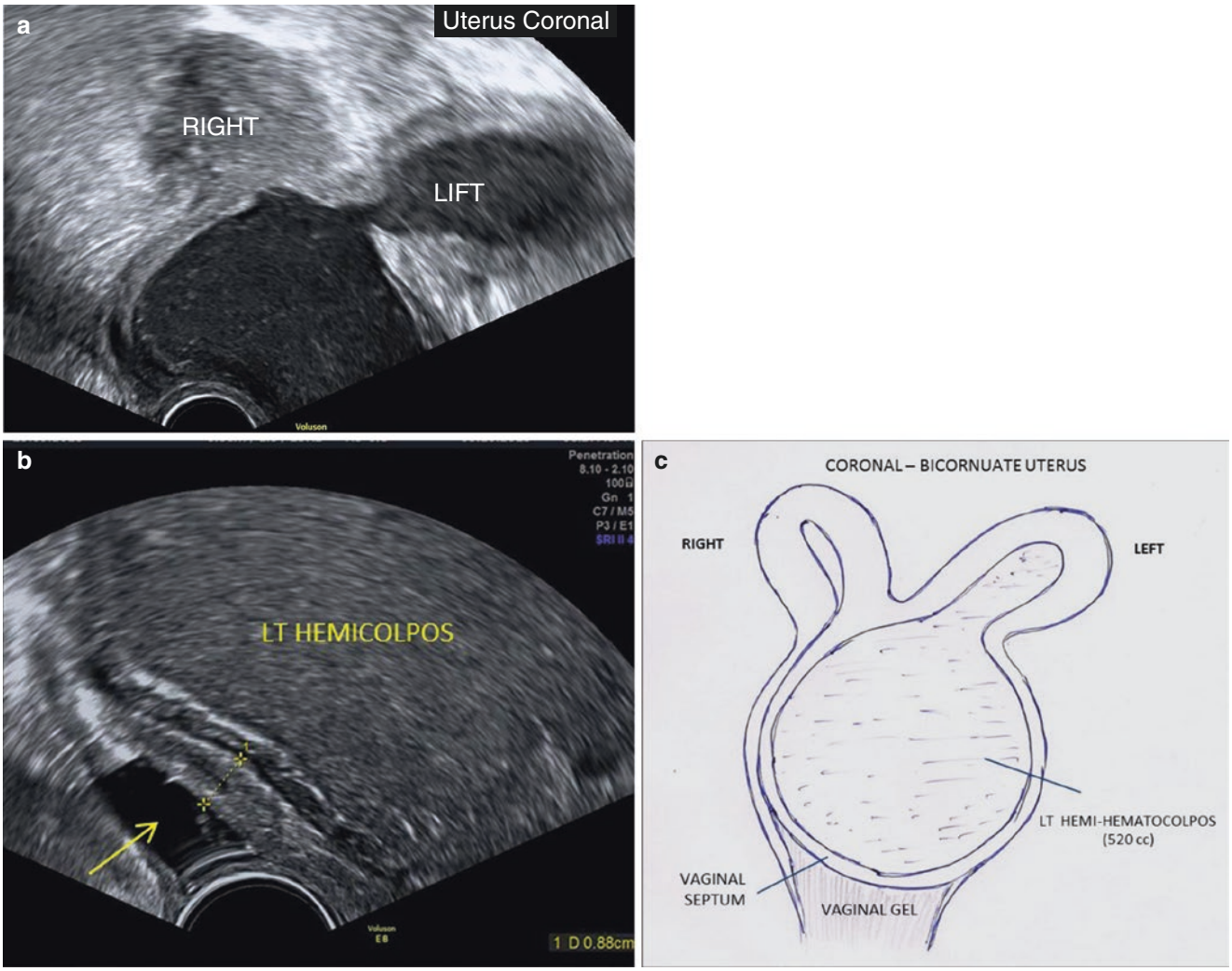

Fig. 12.29 Bicornuate uterus with hemi-haematometrocolpos. (**a**) TAS showing a coronal section of the bicornuate uterus with left-sided hemi-haematometrocolpos. (**b**) GSV done to assess the vaginal septum and locate the communicating left hemivagina (*arrow*). (**c**) Diagrammatic representation of the same. A simple cruciate incision was made over the septum to drain the left hemi-haematometrocolpos

12.6 ESHRE/ESGE Classification of Congenital Uterine Anomalies

The European Society of Human Reproduction and Embryology (ESHRE) and European Society for Gynaecological Endoscopy (ESGE) under the working name CONUTA (CONgenital UTerine Anomalies) have come up with a classification for congenital uterine anomalies (Fig. 12.30).

An important feature of this classification is that the cervix, vagina are to be assessed for coexistent anomalies. The presence, absence and if present, the type of cervical and vaginal anomaly should be reported.

As mentioned earlier, arcuate uterus is not classified as a separate entity, and a bicorporeal septate uterus is an added entity to characterise those uteri that have mixed features of septate and bicornuate uterus (i.e. a mixture of fusion and resorption defects).

Another important feature is that while reporting the uterine anomaly, a drawing of the same is to be included.

ESHRE/ESGE classification
Female genital tract anomalies

	Uterine anomaly		Cervical/vaginal anomaly	
	Main class	*Sub-class*	*Co-existent class*	
U0	Normal uterus		C0	*Normal cervix*
U1	Dysmorphic uterus	a. T-shaped b. Infantilis c. Others	C1	*Septate cervix*
U2	Septate uterus	a. Partial b. Complete	C2	*Double 'normal' cervix*
U3	Bicorporeal uterus	a. Partial b. Complete c. Bicorporeal septate	C3	*Unilateral cervical aplasia*
U4	Hemi-uterus	a. With rudimentary cavity (communicating or not horn) b. Without rudimentary cavity (horn without cavity/no horn)	C4	*Cervical aplasia*
U5	Aplastic	a. With rudimentary cavity (bi- or unilateral horn) b. Without rudimentary cavity (bi- or unilateral uterine remnants/aplasia)	V0	*Normal vagina*
U6	Unclassified malformations		V1	*Longitudinal non-obstructing vaginal septum*
			V2	*Longitudinal obstructing vaginal septum*
			V3	*Transverse vaginal septum and/or imperforate hymen*
			V4	*Vaginal aplasia*
U			*C*	*V*

Associated anomalies of non-Müllerian origin:

Drawing of the anomaly

Fig. 12.30 ESHRE/ESGE classification of uterine anomalies

12.7 Reporting Uterine Anomalies (Fig. 12.31)

Having evaluated the uterus, the cervix and the vagina in patients with uterine anomalies, reporting must be in sufficient detail so as to give the referring clinician clear information of the case, to enable proper counselling and management. One must therefore not only classify the anomaly but also include a description of the external fundal contour and the shape of the uterine cavity. Myometrial indentation or the septum must be measured (i.e. the distance between the two uterine cavities, also known as intercornual distance, and the depth of the intervening septum). One must mention if the septum is reaching up to the internal os, and, if not, the length of the common uterine cavity must be mentioned. The presence of any cervical and vaginal anomaly must also be reported. Most important of all, a diagrammatic representation of the uterine anomaly is to be provided with the report.

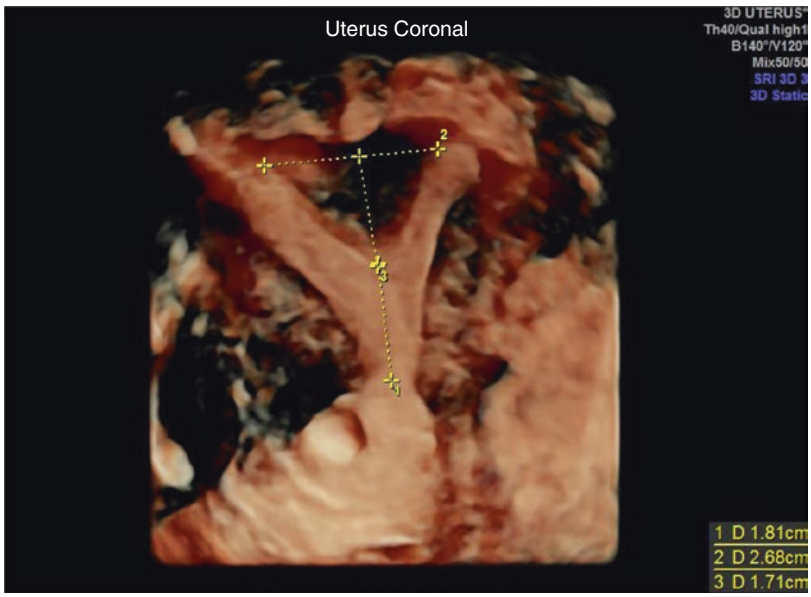

Fig. 12.31 3D coronal image of a subseptate uterus. The width of the septum at its upper end and its length are measured in the image. The residual length of the common uterine cavity below the septum up to the internal os is also measured and reported

Summary: Congenital Uterine Anomalies

- The most commonly used classification for uterine anomalies is the AFS classification, which is primarily based on the embryopathogenesis of anomalies.
- The presence of a uterine anomaly can be suspected on 2D ultrasound. However, for classification of the uterine anomaly evaluation by 3D ultrasound is essential.
- Diagnosing the type of uterine anomaly requires evaluation of both the external fundal contour and the shape of the uterine cavity.
- The cervix, vagina and kidney should be assessed for coexistent anomalies. Their presence, absence and if present, their type should be reported.

Suggested Reading

Behr SC et al (2012) Imaging of müllerian duct anomalies. Radiographics 32(6):E233–E250

Bermejo C et al (2010) Three-dimensional ultrasound in the diagnosis of Müllerian duct anomalies and concordance with magnetic resonance imaging. Ultrasound Obstet Gynecol 35:593–601. doi:10.1002/uog.7551

Bermejo C et al (2014) Three-dimensional ultrasound and magnetic resonance imaging assessment of cervix and vagina in women with uterine malformations. Ultrasound Obstet Gynecol 43:336–345. doi:10.1002/uog.12536

Graupera B et al (2015) Accuracy of three-dimensional ultrasound compared with magnetic resonance imaging in diagnosis of Müllerian duct anomalies using ESHRE–ESGE consensus on the classification of congenital anomalies of the female genital tract. Ultrasound Obstet Gynecol 46:616–622. doi:10.1002/uog.14825

Grimbizis FG, Campo R (2012) Clinical approach for the classification of congenital uterine malformations. Gynecol Surg 9(2):119–129

Jurkovic D (2002) Three-dimensional ultrasound in gynecology: a critical evaluation. Ultrasound Obstet Gynecol 19:109–117. doi:10.1046/j.0960-7692.2001.00654

Jurkovic D et al (1995) Three-dimensional ultrasound for the assessment of uterine anatomy and detection of congenital anomalies: a comparison with hysterosalpingography and two-dimensional sonography. Ultrasound Obstet Gynecol 5:233–237. doi:10.1046/j.1469-0705.1995.05040233

Salim R et al (2003) Reproducibility of three-dimensional ultrasound diagnosis of congenital uterine anomalies. Ultrasound Obstet Gynecol 21:578–582. doi:10.1002/uog.127

Troiano RN, McCarthy SM (2004) Müllerian duct anomalies: imaging and clinical issues. Radiology 233(1):19–34

Ultrasound in Other Miscellaneous Conditions

13

Arteriovenous malformations are seen infrequently and are difficult to differentiate from vascular retained products of conception (RPOC). Proper diagnosis is essential for appropriate management of these potentially life-threatening lesions. Perforation of the uterus is also a rare condition, and a few examples have been provided. Vesicouterine fistula, a rare complication most often following a caesarean section, is covered next. Retroflexed uterus, though a common normal variant, may be an indicator of pathology or may present with symptoms. Caesarean scar defect has become important due to the rising incidence of caesarean sections. Their evaluation is gaining importance because some of these patients may be symptomatic and because of its potential for rupture in a subsequent pregnancy. Intrauterine contraceptive devices can be evaluated on ultrasound to assess whether they are in the normal position. This is best studied by three-dimensional ultrasound and has been described in this chapter. The sonographic appearances vary with the type of device and its location. Images of patients with different types of IUCD in various locations (normal and otherwise) are shown. Practical aspects of follicular tracking (that is resorted to both in natural and induced cycles), have been briefly discussed. The last part of this chapter deals with ovarian hyperstimulation syndrome, a rare but potentially life-threatening complication that is usually the result of ovulation induction.

13.1 Uterine Vascular Abnormalities (Arteriovenous Malformations)

Uterine vascular malformations are rare but potentially life threatening. They are basically multiple arteriovenous fistulous communications within the uterus without an intervening capillary network. These can be congenital or acquired. Congenital ones are very rare and a result of defective embryonic development. These congenital lesions can penetrate surrounding tissues and grow as pregnancy progresses. Most, however, are believed to be acquired secondary to uterine damage by curettage, miscarriage or termination, trophoblastic disease, neoplasia and infection.

Uterine vascular abnormalities, most often reported in the literature as arteriovenous malformations (AVM), are used to describe uterine lesions showing a hypervascular appearance with turbulent flow. Uterine vascular abnormalities would be a better terminology to use for these malformations, as not all are true AVMs. True AVMs can be confirmed histopathologically and show early venous filling on angiography. All other lesions are really non-AVM vascular abnormalities.

Typical symptoms are menorrhagia and metrorrhagia. Some complain of lower abdominal pain. Most often, there is a history of a preceding pregnancy or, in rare cases, a gestational trophoblastic disease. Though these lesions grow slowly, the onset of symptoms could be sudden when the endothelial lining of the vessels gets disrupted during menstruation or curettage. If curettage is done without prior diagnosis of the vascular lesion, the patient could bleed torrentially.

Ultrasound Features of AV Malformation (Figs. 13.1, 13.2 and 13.3)

- It appears as a focal ill-defined heterogeneous mass in the myometrium formed by multiple irregular or tubular hypoechoic cystic structures that fill with colour. That is, the mass comprises of vascular channels only.
- It is located in the area of the radial arteries of the uterus and is seen reaching up to the endometrium or even protruding into it.
- The endomyometrial junction in the corresponding area is most often poorly defined.
- On Doppler, the area shows turbulent flow which is seen as high colour filling with a mosaic pattern.
- Flows show high velocity and low resistance, with average peak systolic velocity (PSV) of 63 cm/sec and RI of 0.38.
- Vessels with a large diameter may be seen not only in the lesion but also in the related arcuate vessels and the parametrial vessels.

M. Sibal, *Ultrasound in Gynecology*, DOI 10.1007/978-981-10-2714-7_13

- During a uterine contraction, flow to the area can decrease significantly, and therefore in case the suspected area (on greyscale) is not filling with colour on Doppler, it is important to wait for a short while.
- Retained products of conception (typically seen as a heterogeneous mass in the endometrial cavity on greyscale with some flow) should be carefully looked for, because turbulent vascular flow may be seen not only in the endometrial cavity but also extending onto the adjoining myometrium in some cases with retained tissue.

The gold standard for definitive diagnosis for true AVMs is early venous filling on contrast angiography. The rest are termed non-AVM uterine vascular abnormalities. Presently, however, angiography (being invasive) is generally resorted to only for therapeutic embolisation.

The most important differential diagnoses for AVMs are retained products of conception (RPOC) and gestational trophoblastic disease (GTD).

Retained tissue may be clearly visualised in some cases, making the diagnosis simple. Greyscale ultrasound for RPOC is specific but not sensitive, and therefore ultrasound cannot rule out RPOC. Serum B hCG is useful in picking up RPOC and GTD and distinguishing them from true AVMs.

Once a uterine vascular abnormality is seen on ultrasound, if there is associated RPOC, curettage can be done. RPOC showing turbulent flow can be most often safely treated with curettage.

The rest of the AVMs (without confirming whether they are true AVMs or non-AVM vascular abnormalities) are treated based on clinical presentation. If bleeding is excessive or persistent, uterine artery embolisation or even hysterectomy may be resorted to.

In most cases, the AVM lesion subsides in 6–8 weeks, but, in certain cases, it could take up to 6 months. Conservative management with serial B hCG and ultrasound is generally sufficient. Medical management with methotrexate is also an option.

In most cases of uterine vascular lesions, serum B hCG is elevated (though often only by a small amount), and as the B hCG values decline, so does the vascularity in the uterus, until it completely disappears. Increased vascularity of the myometrium of the placental bed following pregnancy (miscarriage or delivery) is common in the first few weeks following pregnancy even in the absence of retained placental tissue on ultrasound. On follow-up, the vascularity regresses gradually over the next few weeks.

One large study has suggested that patients can be triaged into high and low risk, based on peak systolic velocity (PSV) of flows in the AVM. Those with a PSV of 83 cm/sec or more are to be considered as ‘high risk’ cases, and those with a PSV of less than 39 cm/sec are considered as ‘low risk’ cases. The cases that are not ‘low risk’ should be monitored more closely.

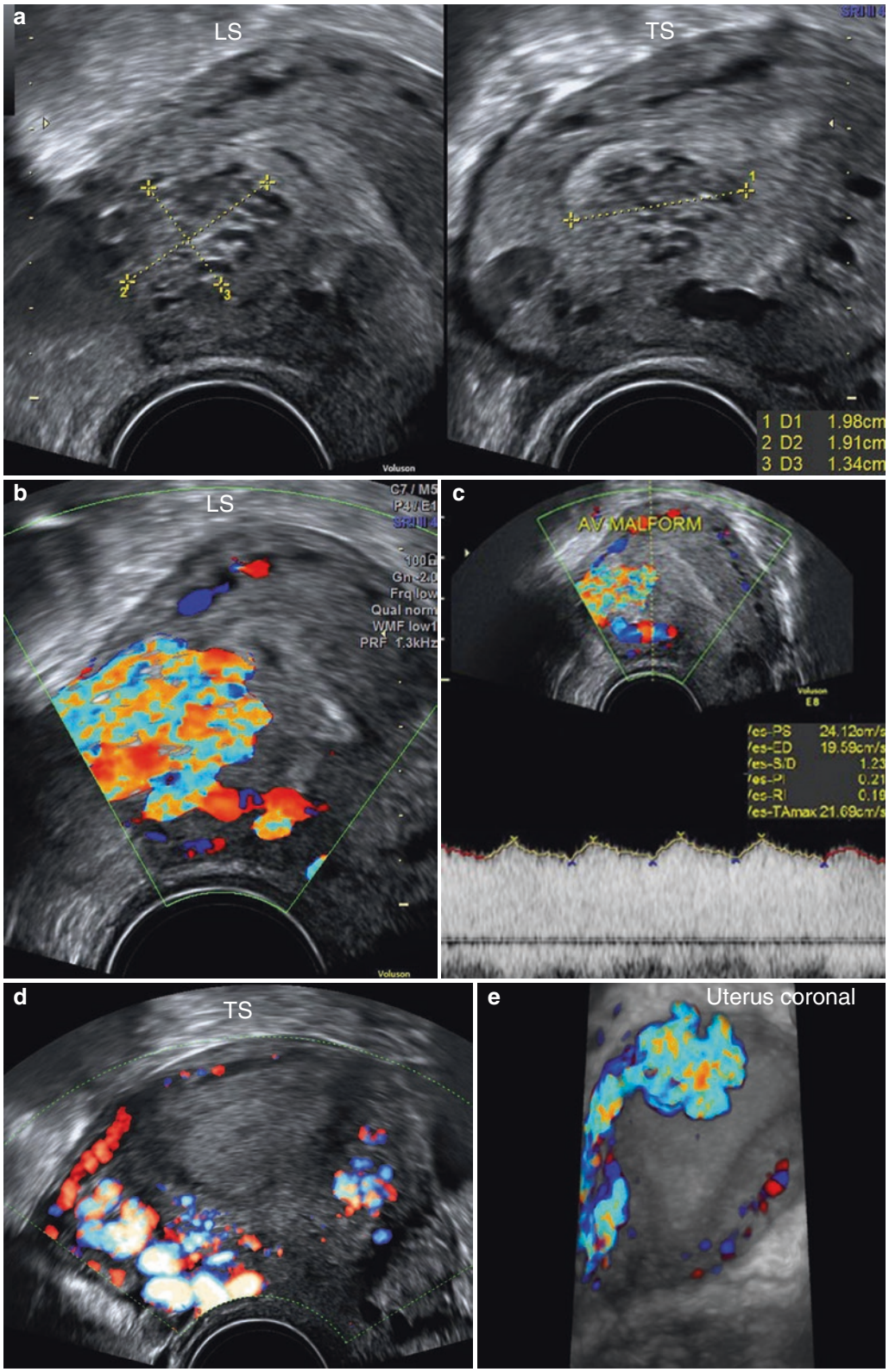

Fig. 13.1 AV malformation of the uterus with normal levels of B hCG (0.1 mIU/mL) and LCB 3 yr and 8 months ago. No history of any pregnancy or surgical intervention following LCB. Last image taken at a repeat follow-up scan done 8 weeks later, showing persistence of the lesion. This is therefore likely to be a true AV malformation. (**a**) Ill-defined heterogeneous mass comprised of multiple cystic areas is seen in the posterior myometrium of the upper corpus reaching up to the endometrium. (**b**) The area is seen filling up with colour and shows turbulent flow (high filling with mosaic pattern). (**c**) High-velocity low-resistance flow is seen. (**d**) The arcuate and parametrial vessels are seen dilated and tortuous. (**e**) 3D HD Doppler glass body image showing the lesion with turbulent flow and dilated arcuate and parametrial vessels on the side of the lesion. This image was taken during a repeat scan after 8 weeks of the earlier images

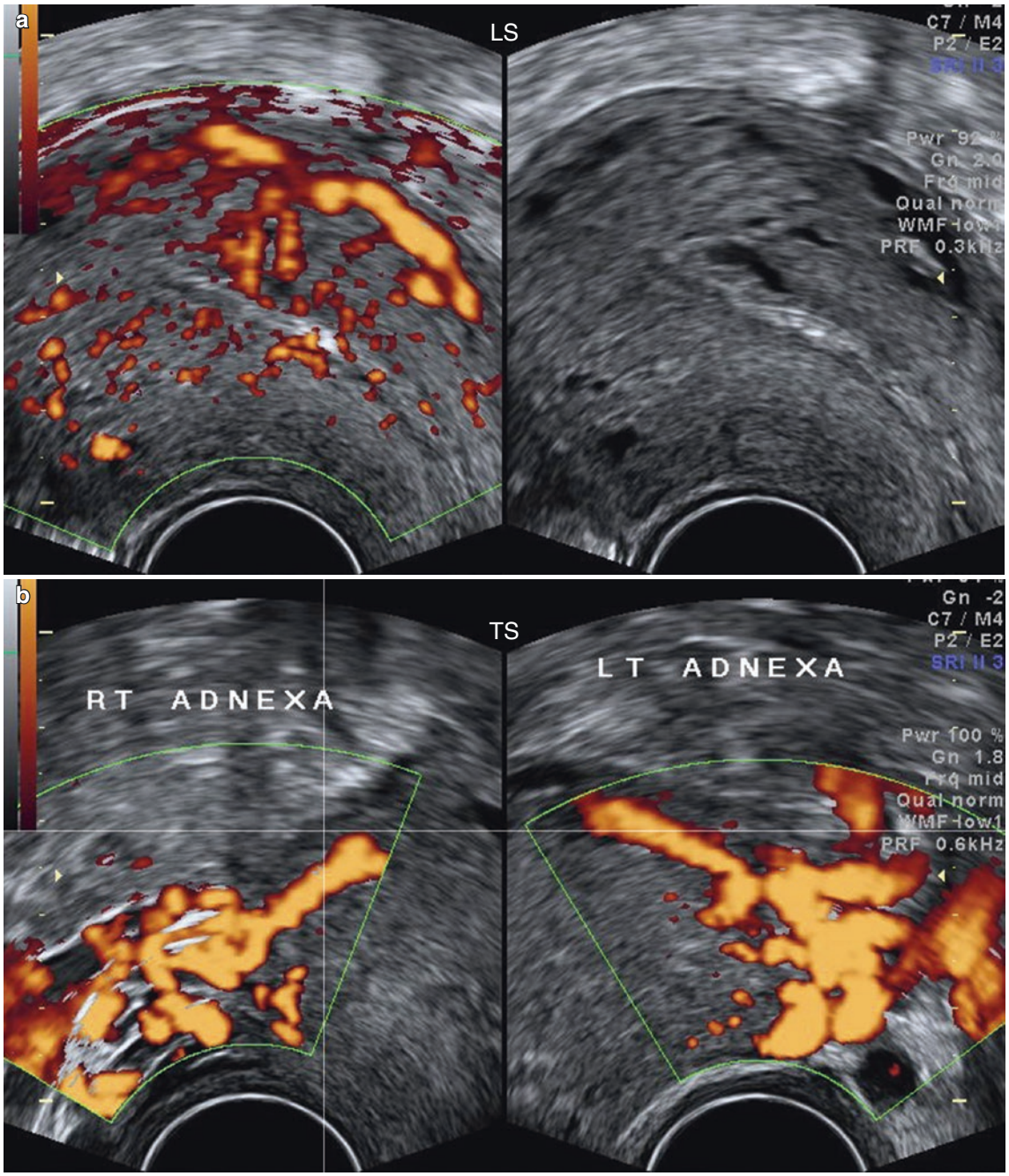

Fig. 13.2 A small AV malformation in a patient whose last child birth with tubectomy was 25 years ago. (**a**) Shows a small lesion and prominent arcuate feeding vessels on Doppler. On greyscale the lesion is less well defined. (**b**) Prominent bilateral parametrial vessels are seen

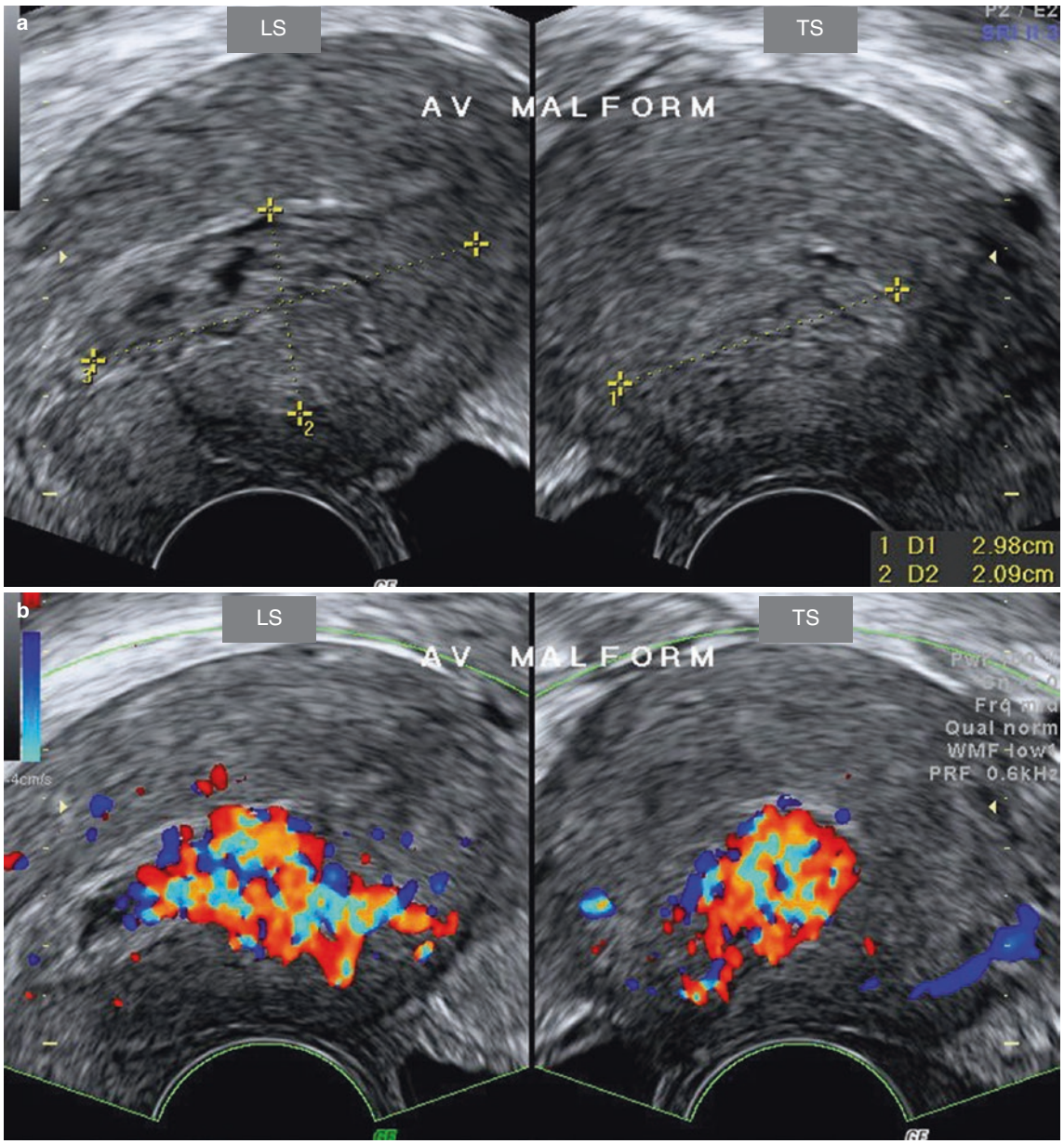

Fig. 13.3 MTP with curettage was done 4 months ago. Patient presented with profuse bleeding for which this scan was done. B hCG on the day of scan was 35 mIU/mL. Patient was treated with methotrexate, and 2 months later B hCG came down to 0.22 mIU/mL and the lesion regressed on scan. (**a**) Heterogeneous ill-defined mass seen in the anterior myometrium extending into the endometrium. The endomyometrial junction in this area is poorly defined. On greyscale, margins of the lesion are difficult to define. (**b**) The lesion is seen filling up with colour and showing turbulent flow. (**c**) On TAS, the lesion with prominent arcuate feeder vessels is noted. (**d**) Flow showing high velocity and low resistance. (**e**) Repeat scan done 2 months later, when B hCG value was normal, showed that the lesion had regressed. A faint hyperechoic area is seen in the anterior myometrium which did not show any flow on Doppler

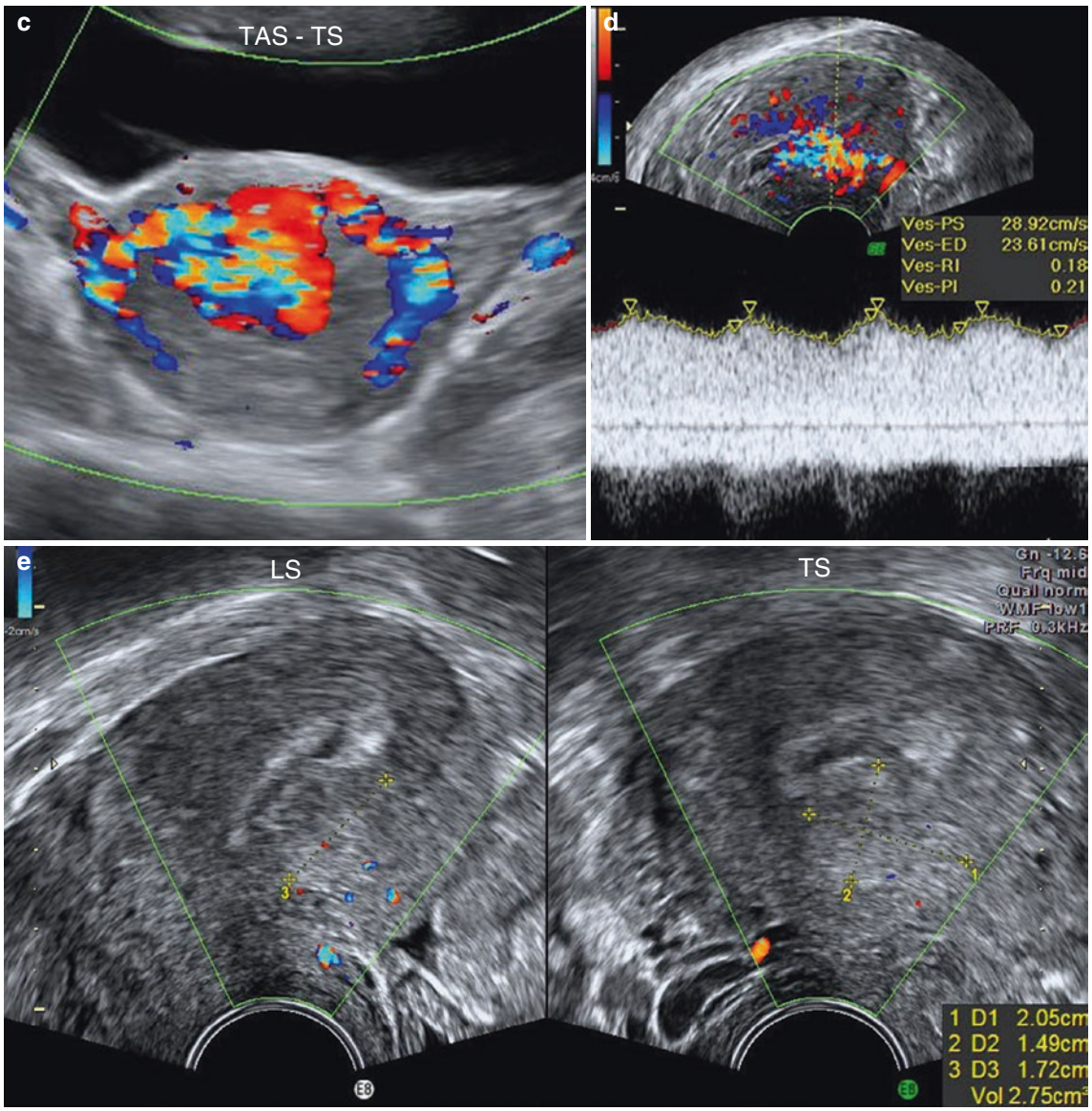

Fig. 13.3 (continued)

Summary of AV Malformation

- May present with menorrhagia or metrorrhagia. History of recent pregnancy (including molar pregnancy) and instrumentation is common.
- Ultrasound:
  - Ill-defined focal mass with cystic hypoechoic areas that fill with colour and show turbulent flow (high PSV and low RI).
  - Seen in the myometrium, extending up to or into the endometrial cavity.
  - Look for the presence of RPOC – which can also show turbulent flow at times.
  - Serum B hCG may help to differentiate true AVM from RPOC and GTD.
- Most regress on follow-up – which includes serial scans and serum B hCG (if elevated). Those with excessive or persistent bleeding will require uterine artery embolisation or rarely hysterectomy.

13.2 Perforation of the Uterus

Perforation of the uterus refers to a through and through passage in the myometrium extending from the endometrium to the serosa. It may be iatrogenic or less often of spontaneous origin. Iatrogenic causes include: perforation during dilatation and curettage (particularly in a pregnant uterus), operative hysteroscopy, endometrial ablation, insertion of intrauterine contraceptive device (IUCD) and evacuation of retained placenta. Uterine perforation is most often seen in cases of abortion with suction and curettage. Ultrasound-guided procedures decrease the risk of perforation in these cases. Spontaneous perforation is usually due to trophoblastic invasion of the myometrium in cornual and interstitial pregnancies or GTD. Iatrogenic uterine perforation usually presents at the time of injury with a history of omental or bowel fat at suction or an inability to distend the uterine cavity on hysteroscopy due to extrauterine escape of fluid or as increased intrauterine or extrauterine haemorrhage. Most often, however, they are missed and may either be diagnosed at a later time or may heal on their own. An important problem of uterine perforation is uterine rupture in a subsequent pregnancy. Routine intraoperative transabdominal ultrasound-guided procedures increase safety and expedite the procedure.

Ultrasound Features of Uterine Perforation (Figs. 13.4, 13.5 and 13.6)

- Perforation is seen as a hyperechoic tract of varying thickness in the myometrium extending from the uterine cavity up to the serosa, in cases where there is some tissue in the myometrial tract (like omentum or placental tissue). In case there are bowels within the cavity, peristalsis may be noted. The myometrium in that area is therefore deficient.
- Perforation that is recent and has no tissue within may not be visualised on ultrasound. On distension of the uterine cavity with fluid (as seen in hysteroscopy), it may show up transiently as an anechoic or hypoechoic, regular or irregular tract in the myometrium, extending from the endometrial cavity to the serosa.
- At times (particularly if sometime has lapsed following the perforation), a perforation may only appear as a hyperechoic linear area extending between the endometrium and the serosa.
- Often perforation itself is not noticed, but a diagnosis of a perforation having occurred may be implied as in finding of an intrauterine contraceptive device (IUCD) outside the uterus.

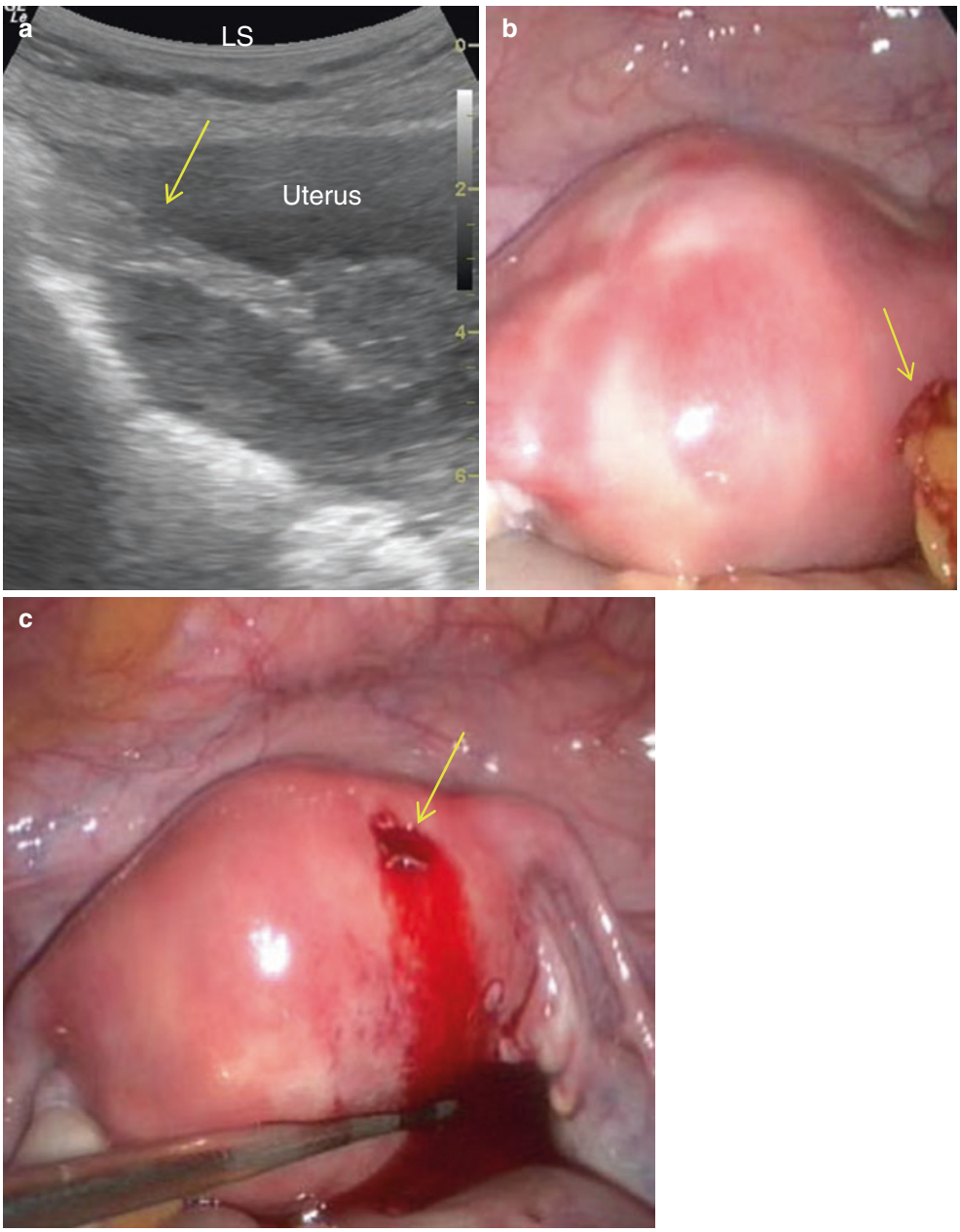

Fig. 13.4 Case of uterine perforation during surgical MTP. (**a**) Zoomed-in image of the sagittal section of the uterus. There is a hyperechoic tract (*arrow*) extending from the endometrial cavity to the serosa. (**b**) At laparoscopy, omentum is seen within the perforation (*arrow*). (**c**) Perforation is seen at the serosal surface of the uterine fundus (*arrow*) after the omentum was drawn out, which was bleeding

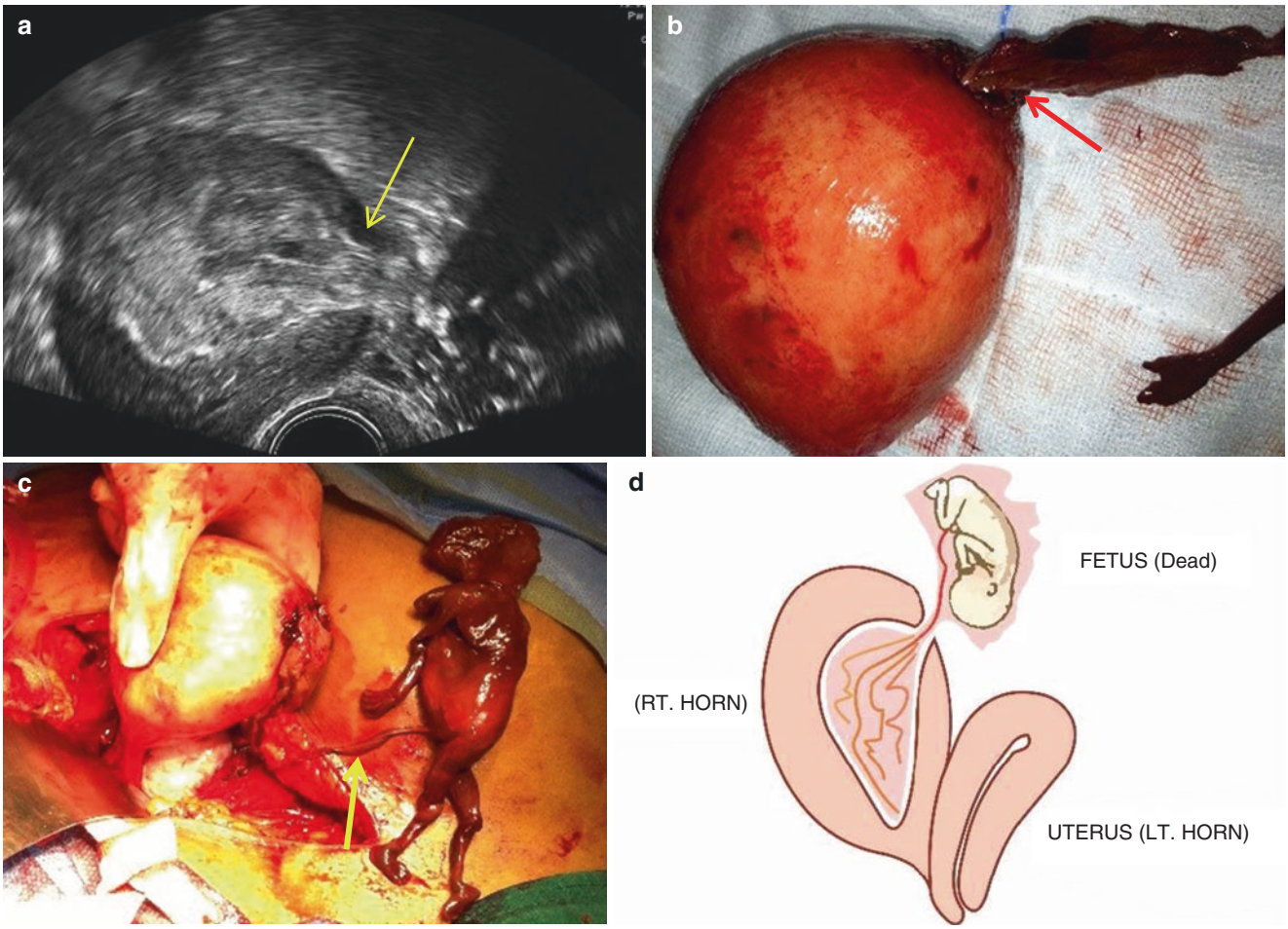

Fig. 13.5 Early trophoblastic perforation of non-communicating right-sided uterine horn (with a well-developed left horn). The placenta was seen within the endometrial cavity of the rudimentary horn. The placenta and umbilical cord were protruding out of the uterine perforation and extending up to the dead fetus. (**a**) Non-communicating right-sided horn with a hyperechoic complex tract (*arrow*) that extends from the cavity on to the serosal surface. (**b**) Post-operative specimen of the excised horn showing placental tissue extending out of the perforation (*arrow*). (**c**) Dead intra-abdominal fetus connected to the perforated uterine horn with the umbilical cord (*arrow*). (**d**) Diagrammatic representation of scan findings in the case. The uterine perforation due to invasion by trophoblastic tissue must have occurred early in pregnancy with the fetus escaping out of the rudimentary horn and continuing to grow intra-abdominally for a short period of time

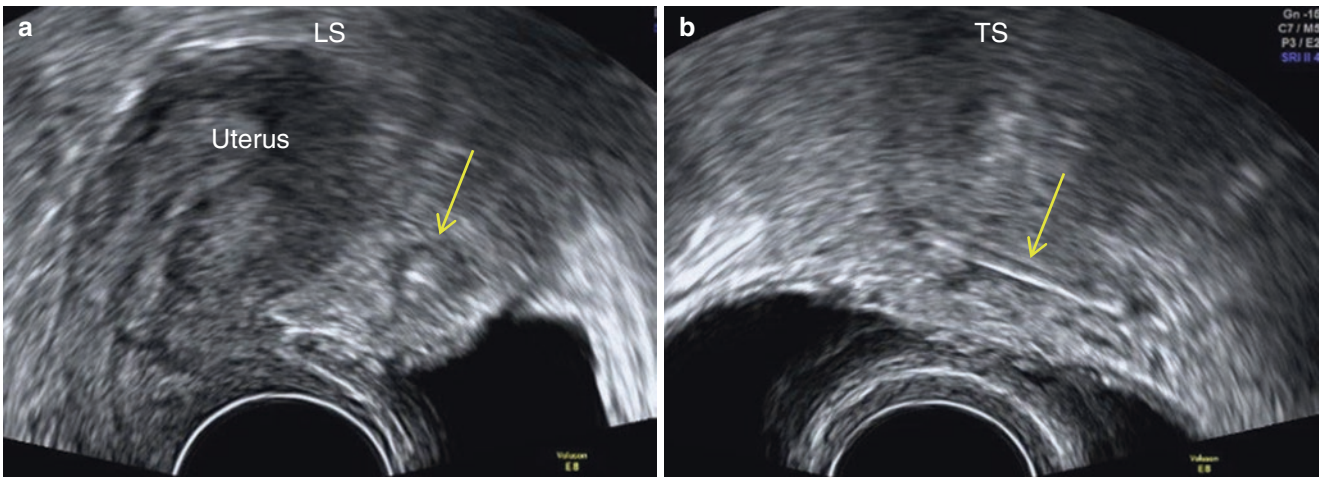

Fig. 13.6 Case of IUCD (with missing thread) that had perforated the uterine wall and was lying in the uterovesical (UV) fold. (**a**) Long section of the uterus with the cross section of the shaft of the IUCD (*arrow*) seen in the UV fold. (**b**) Transverse section of the UV fold showing the shaft of the IUCD (*arrow*)

Summary of Perforation of the Uterus

- Perforation is more often iatrogenic occurring during intrauterine procedures but it may be spontaneous due to invasion by trophoblastic tissue. Often it goes unnoticed, but those that are symptomatic present most often at the time of injury itself, commonly with haemorrhage and pain.
- On ultrasound, they may be seen either as a hyperechoic thin linear area or a hyperechoic thick tract or a transiently filling anechoic tract through the myometrium.

13.3 Vesicouterine Fistula

Vesicouterine fistula is a communication between the bladder and the uterine cavity. This may result because of previous caesarean section, particularly when followed by vaginal delivery or as a complication of a perforating IUCD. Patients with vesicouterine fistula usually have urinary incontinence in the early post-operative period. Most often they complain of bleeding per urethra, with or without associated small clots, during menstruation.

Ultrasound Features of Vesicouterine Fistula (Fig. 13.7)

- It appears as a fistulous anechoic tract extending between the endometrial cavity and the urinary bladder.
- The length, breadth and thickness of the tract can be measured, including the opening in the endometrial cavity and the bladder mucosa.
- A partially filled bladder helps in better delineation of the fistulous tract through the bladder wall.
- The bladder is seen adherent to the anterior wall of the uterus at the site of the fistulous connection (most often the site of the LSCS scar). In other words, the bladder does not slide along the uterus/vagina on pressure by the TVS probe.
- The rent in the bladder wall can be visualised well on 3D rendered images.

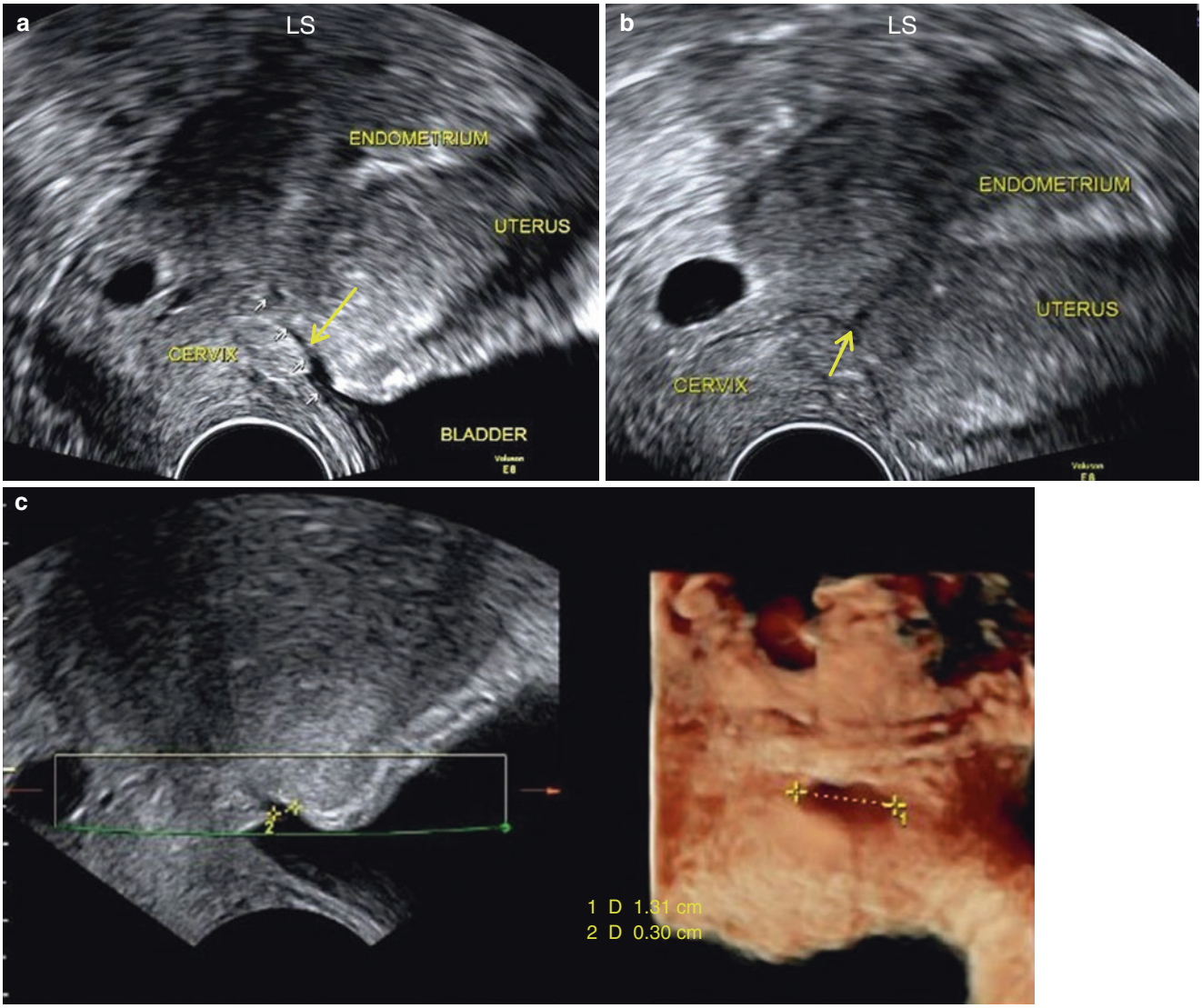

Fig. 13.7 Long-standing (13 years) uterovesical fistula following LSCS, with a history of blood-stained urine during menstruation. Patient presented with recent onset of menorrhagia with passage of clots in urine and painful micturition. (**a**) Narrow anechoic/hypoechoic tract (*arrow*) extending from the bladder into the lower corpus of the uterus. (**b**) The tract is seen communicating with the endometrial cavity (*arrow*) of the lower corpus. (**c**) 3D rendering of the bladder end of the fistula that measured about 1.3 cm transversely

13.4 Retroflexed Uterus

A retroflexed uterus is one where the axis of the uterine cavity is bent backwards as compared to that of the cervical canal. This therefore causes an angulation (retroflexion) at the level of the internal os. A retroflexed uterus is a normal variant, and most often patients are asymptomatic. In some cases, however, the patients may be symptomatic, either because of acute retroflexion itself or because of pathology causing fixed retroflexion of the uterus as seen in endometriosis and PID. The common symptoms seen in women with retroflexion are pain (due to associated PID, endometriosis or incomplete drainage of menstrual blood), postmenstrual spotting (of collected menstrual blood) or occasionally urinary retention in a gravid retroflexed uterus.

Ultrasound Features of Retroflexed Uterus (Figs. 13.8 and 13.9)

- In a midsagittal section, the endometrial cavity is seen bent backwards as compared to that of the cervical canal.
- The retroflexion typically occurs at the internal os between the cervix and the lower corpus.
- Hematometra – In an acutely retroflexed uterus at times, there may be some amount of menstrual blood seen in the uterine cavity which is believed to be because of the effect of gravity and acute angulation, impairing the drainage of normal menstrual flow.
- In patients with PID and endometriosis, the uterus is usually fixed in flexion, i.e. the posterior wall of the uterus is adherent to the bowels and or the diseased adnexa.
- Uteri that are fixed in flexion due to PID and endometriosis usually show angulation above the level of the internal os, often between the lower corpus and the mid-corpus, giving the uterus a ‘question mark’ - or ‘ear’ - shaped appearance.
- In patients with endometriosis, the posterior wall of the uterus may show coarse echoes secondary to diffuse adenomyosis.

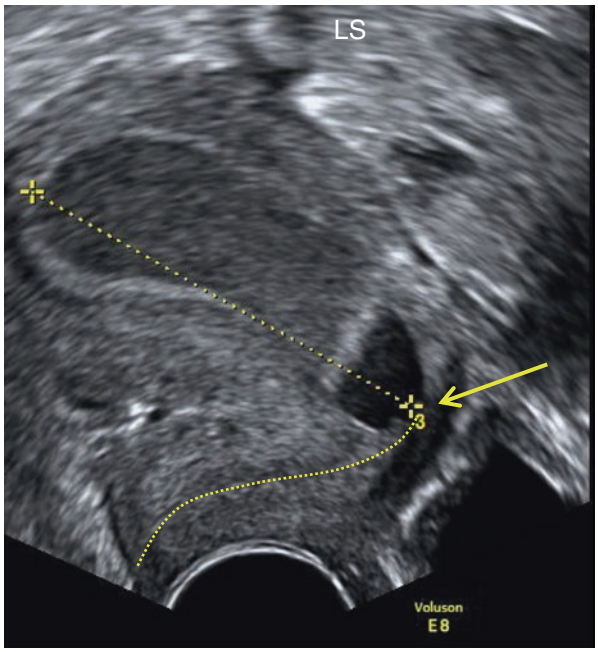

Fig. 13.8 Retroflexed uterus with hematometra showing the fluid–fluid level with the denser fluid in the dependent upper uterine cavity. Here, flexion is seen at the junction of the cervix with the uterine body (i.e. level of internal os) (*arrow*)

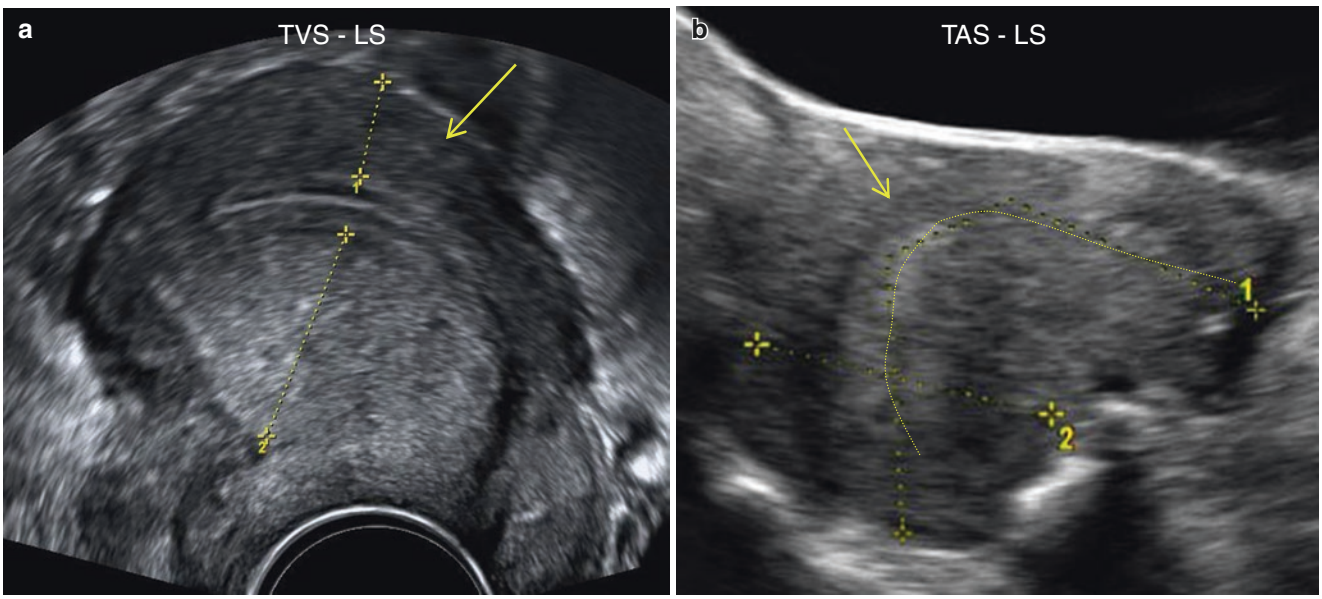

Fig. 13.9 Retroflexed uterus in a patient with DIE. (**a**) TVS – the flexion is more pronounced at the midcorpus (*arrow*). The posterior wall is thick and shows slightly coarse echoes suggestive of adenomyosis. (**b**) TAS – flexion at midcorpus (*arrow*) with an 'ear'- or 'question mark'- shaped uterus

13.5 Caesarean Scar Defect (LSCS Scar Defect)

With increasing caesarean section (CS) rates worldwide and its associated complications of late, there has been an increased interest in evaluation of the caesarean section scar defects (CSDs) and their relation to complications. Though the evaluation of a scar can be accurately done on ultrasound (TVS), the analysis of its association with complications requires in-depth studies. CSD is seen in about 70 % (on TVS) to 84 % (on SHG) of women with a previous history of cesarean section (Osser.V., *UOG* 2010, *UOG* 2011).

Multiple caesarean sections, single-layer myometrial closure and retroflexed uteri are reported in the literature to increase the risk of scar defects and are accordingly more often associated with larger scar defects. Caesarean scar defects are associated with symptoms of postmenstrual spotting (a commonly seen symptom, with typically darkish altered blood), dysmenorrhoea and chronic pelvic pain. Scar defects have also been studied with the idea to evaluate the potential risk for obstetric complications in future pregnancies like scar ectopic pregnancy, placenta previa, adherent placenta and scar dehiscence.

Ultrasound Features of Caesarean Scar Defects
(Figs. 13.10, 13.11, 13.12, 13.13, 13.14 and 13.15)

- A caesarean scar defect is diagnosed by the presence of a hypoechoic (or anechoic) cystic area within the anterior myometrium of the lower uterine segment at the site of the previous LSCS. The collection in the defect is basically retained menstrual blood. It is seen somewhere between the level of the internal os below (identified by the level of entry of the uterine arteries and the apical upper end of cervical mucosa) and the uterovesical fold of peritoneum above.
- Most often, the defect is triangular or wedge shaped with its base towards the endometrial cavity and its apex pointing towards the serosa. Some defects, however, may be 'U' shaped or irregular and are most often seen with larger defects.
- The evaluation is done on TVS, and the image should be magnified to include the cervical canal, the bladder and the lower uterine cavity. Care must be taken not to apply too much pressure with the TVS probe as that may alter the shape and measurements of the scar defect.
- The current recommendation to measure the scar is to take four measurements (Fig. 13.15):
  - Scar width (W) – is its distance along the cervico-endometrial canal taken in the sagittal section of the uterus. Increasing scar width has been found to be associated with postmenstrual spotting, dysmenorrhoea and chronic pelvic pain.
  - Scar depth (D) – is the vertical distance between the base (facing the uterine cavity) and the apex of the defect (towards the uterine serosa) taken in the sagittal section of the uterus.
  - Scar length (L) – is the length of the defect in the transverse section (this may be assessed in transverse or coronal views).
  - Residual myometrial thickness (RMT) – is the thickness of the myometrium between the apex of the scar and the overlying serosa taken in the sagittal section of the uterus.

There is no uniform definition for a large scar. Some consider a large scar to be one where there is a loss of more than 50 % of the myometrial thickness at the scar (RMT/thickness of adjacent myometrium) or an RMT of less than or equal to 2.2 mm on TVS (Osser *UOG* 2010). The thinner the residual myometrium, the higher is the chance of scar dehiscence; however, no cut-off has been established yet.

- The axis of the cervical canal to the axis of the uterine cavity should also be noted, as patients with retroflexed uterus are more likely to be symptomatic with postmenstrual spotting.
- There may be an associated small hematometra. Pressure with the TVS probe on the scar defect will often show turbid contents moving upwards from the defect into the endometrial cavity and only very occasionally into the cervical canal. On release of pressure, the turbid contents return into the defect.
- Myometrial scar tissue takes about 3 months to form, and complete involution may take 6 months. Therefore, women must be assessed in their non-pregnant state, preferably 6 months after the caesarean section.

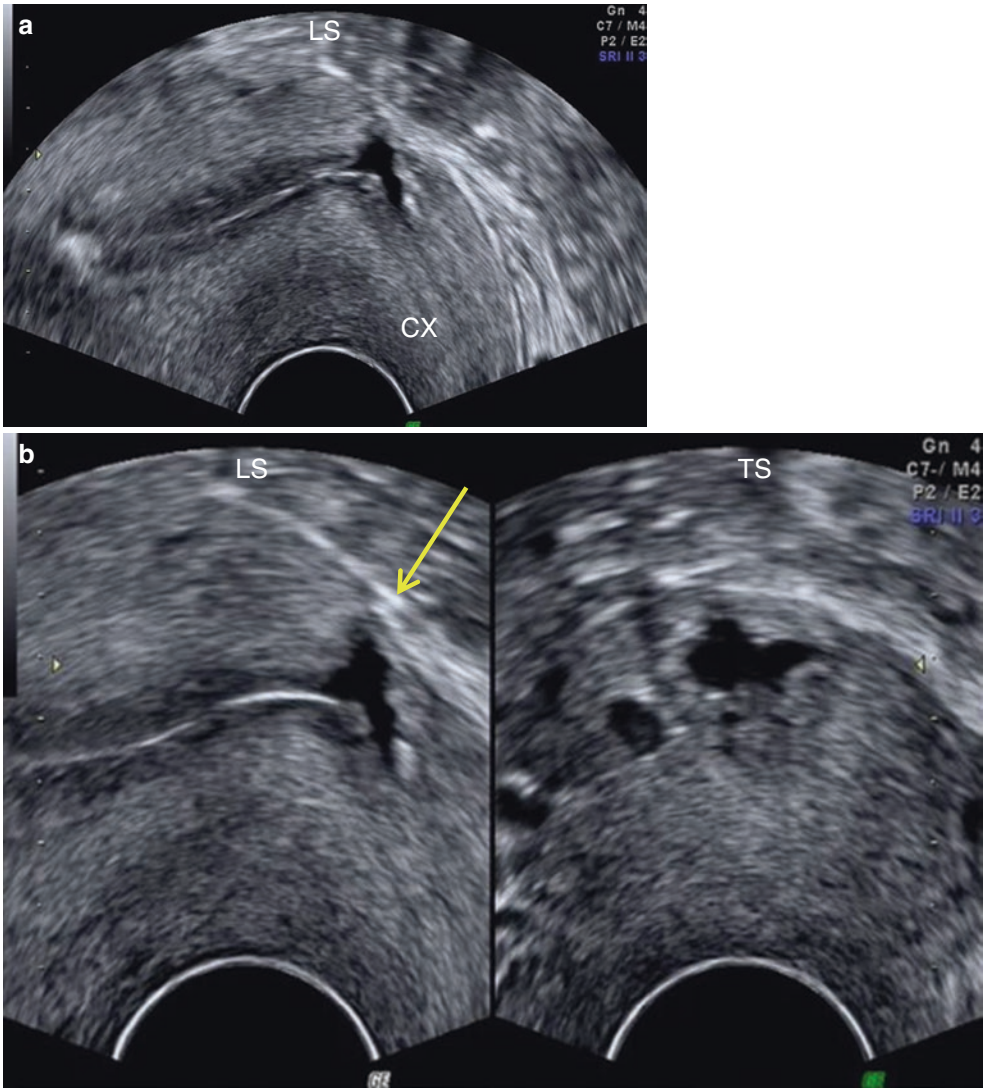

Fig. 13.10 (**a**) Defect seen as an anechoic irregular area at the site of the LSCS scar in a retroflexed uterus. (**b**) Long section and transverse section of the scar defect showing irregular margins and narrow overlying residual myometrial thickness (*arrow*)

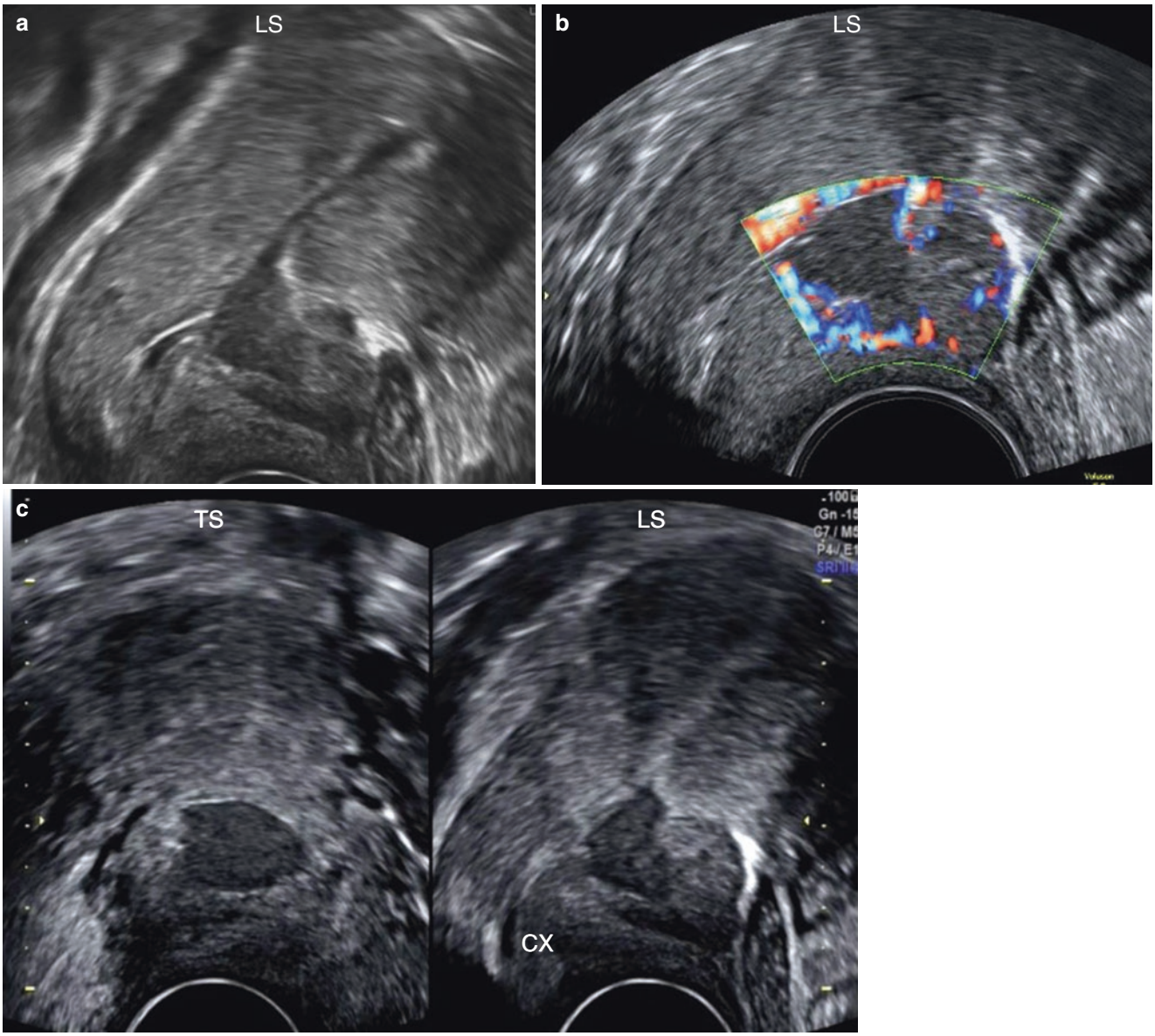

Fig. 13.11 Patient recently underwent curettage for brownish intermenstrual discharge. (**a**) Large hypoechoic triangular scar defect seen communicating with endometrial cavity above and endocervical canal below. (**b**) No flow seen in the area suggestive of fluid collection within. (**c**) Transverse and long section of the scar defect to measure the volume of collection in the defect (in this case, 1.5 cc). Thick overlying residual myometrium noted, probably as a result of some local trauma following surgical curettage

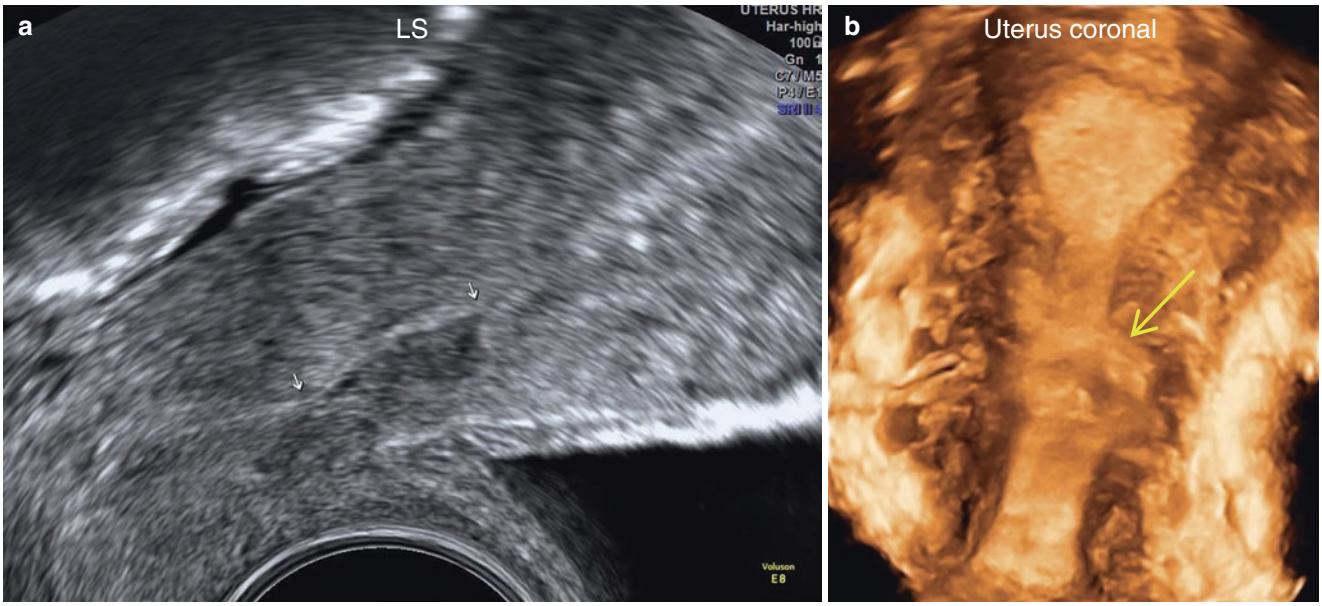

Fig. 13.12 Patient with three previous LSCS with brownish intermenstrual spotting that lasted for 10–11 days after periods. (**a**) Upper and lower end of the wedge-shaped defect showing turbid blood collection marked with tiny *arrows*. (**b**) 3D rendered image of the scar defect (*arrow*) seen in the lower corpus with hyperechoic irregular thick margins around, suggestive of surrounding fibrotic tissue

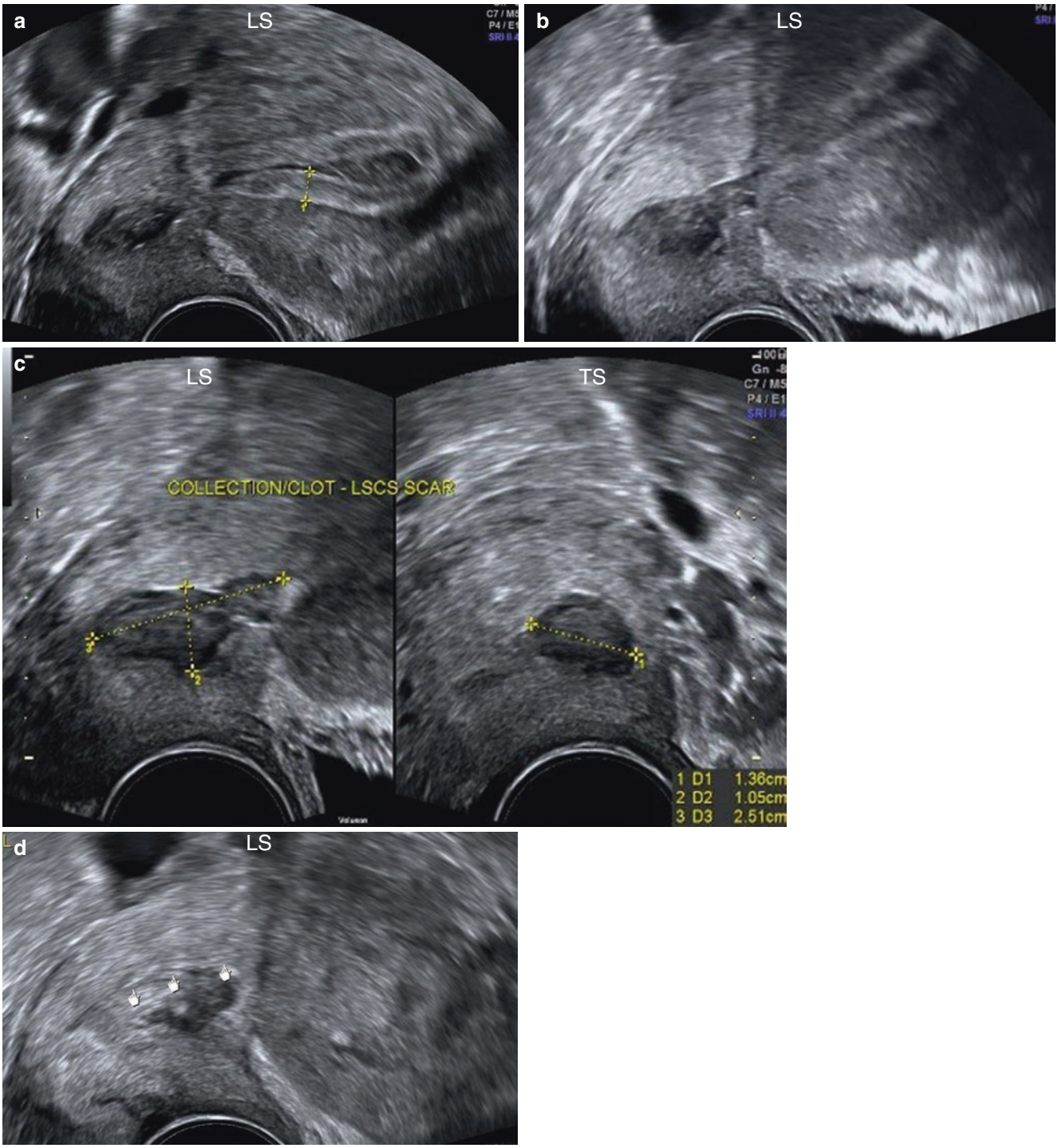

Fig. 13.13 Large irregular defect to the left of midline with hematometra. (**a**) Blood seen in the upper end of the endometrial cavity. (**b**) The defect is seen communicating with the endometrial cavity. Pressure on the defect causes the fluid to move up into the endometrial cavity, and on release of pressure it was seen trickling back into the defect. (**c**) The volume of the collection in the scar defect is measured in three perpendicular dimensions. (**d**) The defects are seen communicating with the cervical canal posterosuperiorly (*small arrows*)

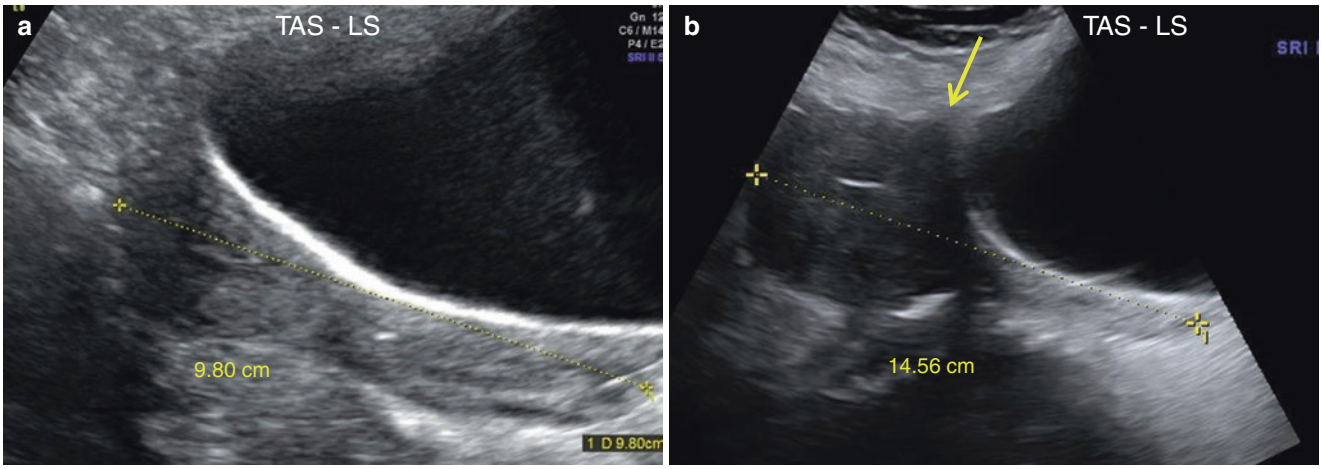

Fig. 13.14 Bladder adherent to the LSCS scar in two different cases. (**a**) With a full bladder on TAS, the uterus (particularly lower corpus and cervix) appears stretched out and elongated. The bladder usually does not extend beyond the uterine fundus and is often shadowed by the critical angle shadowing from the superior margin of the bladder wall. (**b**) A similar case where the bladder is not extending beyond the lower corpus. The anterior wall of the uterus shows a right angle (*arrow*) which is a typical feature of an adherent structure

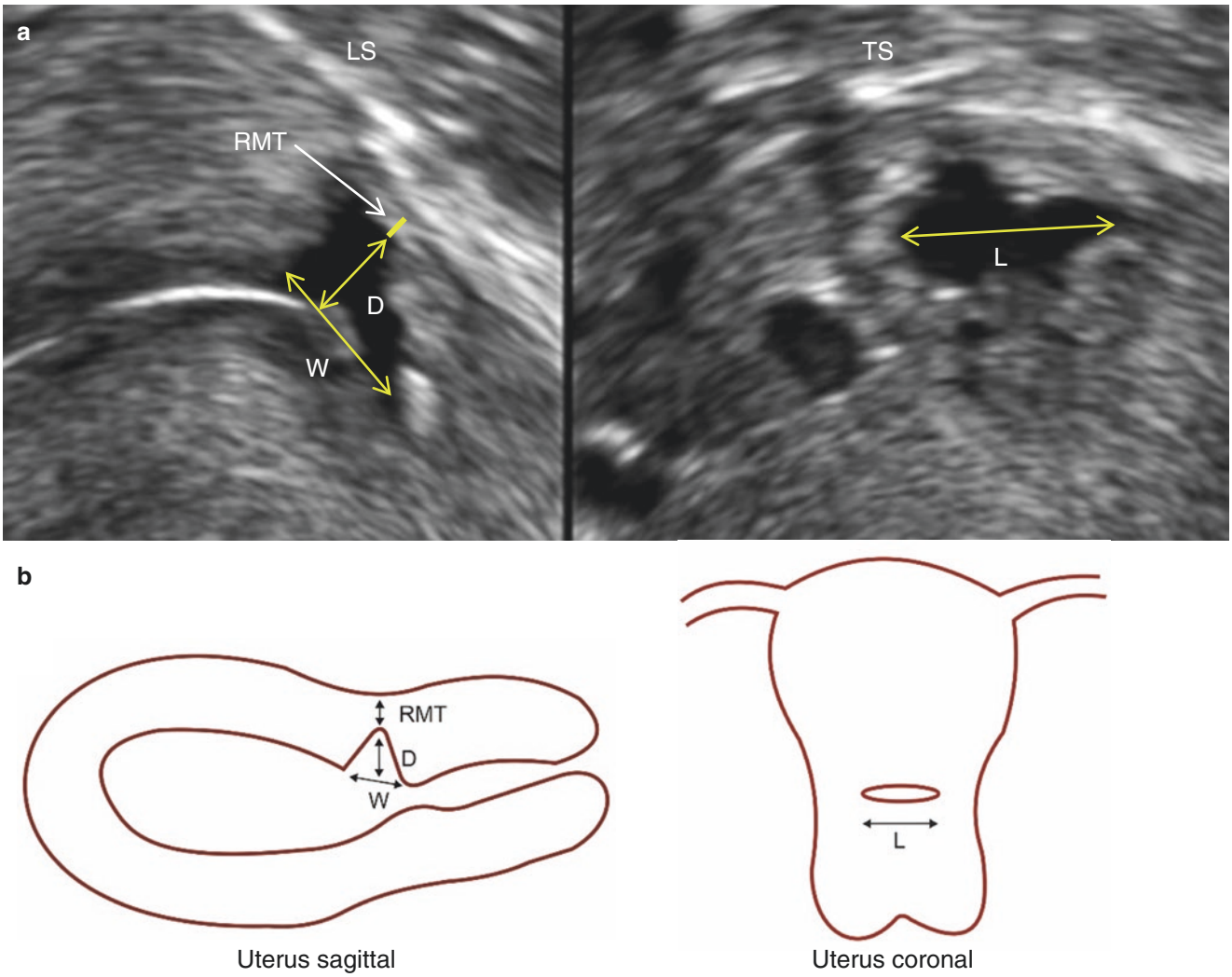

Fig. 13.15 (**a**) Sagittal section of the uterus (the image has been zoomed in to more than essential, for better understanding) showing: (*W*) scar width, (*D*) scar depth, (*RMT*) residual myometrial thickness and the transverse section of the uterus showing (*L*) scar length. (**b**) Diagrammatic representation of the same in LS and coronal views

Summary: Caesarean Scar Defect

- CSD can be evaluated on transvaginal scans accurately in non-pregnant women, but the relation of their appearance and measurement to associated symptoms and complications has not been established. Common presenting complaint is postmenstrual spotting.
- The scar is seen as a wedge-shaped defect at the site of the previous caesarean scar. The width, depth, length and residual myometrial thickness should be measured.

13.6 Intrauterine Contraceptive Device (IUCD)

The intrauterine contraceptive device is one of the most commonly used contraceptive devices in the world. In addition, the hormone-containing IUCDs are also used to decrease menstrual flow in patients with menorrhagia. Sonography is useful in assessing the location of the device and complications that may arise due to IUCD insertion. Complications include malposition, retention, fragmentation, expulsion, uterine perforation, pelvic inflammatory disease and pregnancy. Malposition of an IUCD typically occurs at the time of insertion but may be due to the migration of the IUCD through a scar. Patients with IUCDs may present with menorrhagia, pain and bleeding due to a malpositioned IUCD; pain and fever if there is associated PID; or with pregnancy (intrauterine or ectopic) in association with a normally placed, malpositioned or expelled IUCD. Patients are referred for ultrasound if there was a difficult insertion, if the threads are missing or if the patient is symptomatic.

Basically there are three types of IUCDs:

1. *Inert IUCD* – These are made of plastic polyethylene with some barium sulphate so that they can be visualised on X-rays. Examples: Lippes loop (that is not in use today) and ring-shaped IUCD (still used in China).
2. *Copper-containing IUCD* – These IUCDs have copper in them and are of different types. They typically have a straight shaft and cross bars. They are well seen on ultrasound because their copper shaft appears echogenic. Examples: Copper T, Copper 7 and Multiload.
3. *Hormone-producing IUCD* – These contain progesterone. Examples: Progestasert and Mirena. Mirena is T shaped with a 32 mm vertical shaft and 32 mm horizontal portion containing barium sulphate. Its shaft is more difficult to visualise on ultrasound.

Ultrasound Features of IUCDs (Figs. 13.16, 13.17, 13.18, 13.19, 13.20, 13.21, 13.22, 13.23, 13.24 and 13.25)

- Most IUCDs appear hyperechoic on ultrasound. Copper IUCDs have a very echogenic shaft which shows acoustic shadowing beyond it. The Mirena IUCD has a characteristic appearance with its shaft being non-echogenic, whereas the proximal and distal ends of the shaft are echogenic. On 2D, significant acoustic shadowing is noted from the shaft. The horizontal cross bars however can appear hyperechoic and can be seen on 2D. The shaft of the Mirena is, however, well seen on a 3D rendered image as a dark shadow. Sometimes, the thread of the IUCD is seen below it as a hyperechoic fine linear echo lying in the cervical canal.
- The shaft of an IUCD can most often be seen on 2D imaging of the uterus. However, to visualise the entire IUCD within the endometrial cavity, a 3D rendered coronal section of the uterus is important and is therefore done routinely. On 3D, because the entire IUCD can be visualised in addition to its location, the shape of the IUCD and type can also be deciphered.
- Normal position – The shaft is seen in the midsagittal plane extending from the upper end of the endometrial cavity downwards. Its horizontal cross bar (when present) is seen in the upper part of the endometrial cavity.
- Endometrial evaluation is difficult in the presence of an IUCD. Some amount of information and measurement may be obtained by moving just lateral to the IUCD in the sagittal plane. Endometrium and EMJ, however, can be seen on a 3D rendered image.
- Low position of IUCD – The IUCD may be displaced downwards with its upper end some distance away from the upper margin of the endometrial cavity. The IUCD may even be seen in the cervical canal. When an IUCD is displaced down, it is not considered as effective for the purpose of contraception.
- Malposition of IUCD – An IUCD is considered malpositioned if any part of it extends beyond the endomyometrial junction into the myometrium or cervix. This is seen clearly on 3D rendered coronal views of the endometrial cavity.
- Uterine perforation – IUCD may perforate the uterus and move out of the uterine cavity into the pelvis. In these cases, the thread of the IUCD will not be visible on clinical examination. Radiographic studies may be required to search for the IUCD, when it is not seen on an ultrasound examination.
- Expulsion of IUCD – Sometimes the IUCD may not be located in the uterus or the surrounding structures (clinically, the thread is also not visualised), suggesting that it is probably expelled. Radiographic studies may be required to search for the IUCD, if not seen on ultrasound.
- Associated complications – Patients with IUCD are at an increased risk for PID, features of which may be seen on ultrasound. Pregnancy may occur with an IUCD in the uterine cavity. Though the pregnancy may be intrauterine, the probability of an ectopic pregnancy is higher in patients with IUCDs because implantation is less likely in the endometrial cavity. Ultrasound may also be used for USG-guided removal of malpositioned or fragmented IUCDs.

A CT scan of the abdomen may be required for accurate localisation of the IUCD for appropriate management.

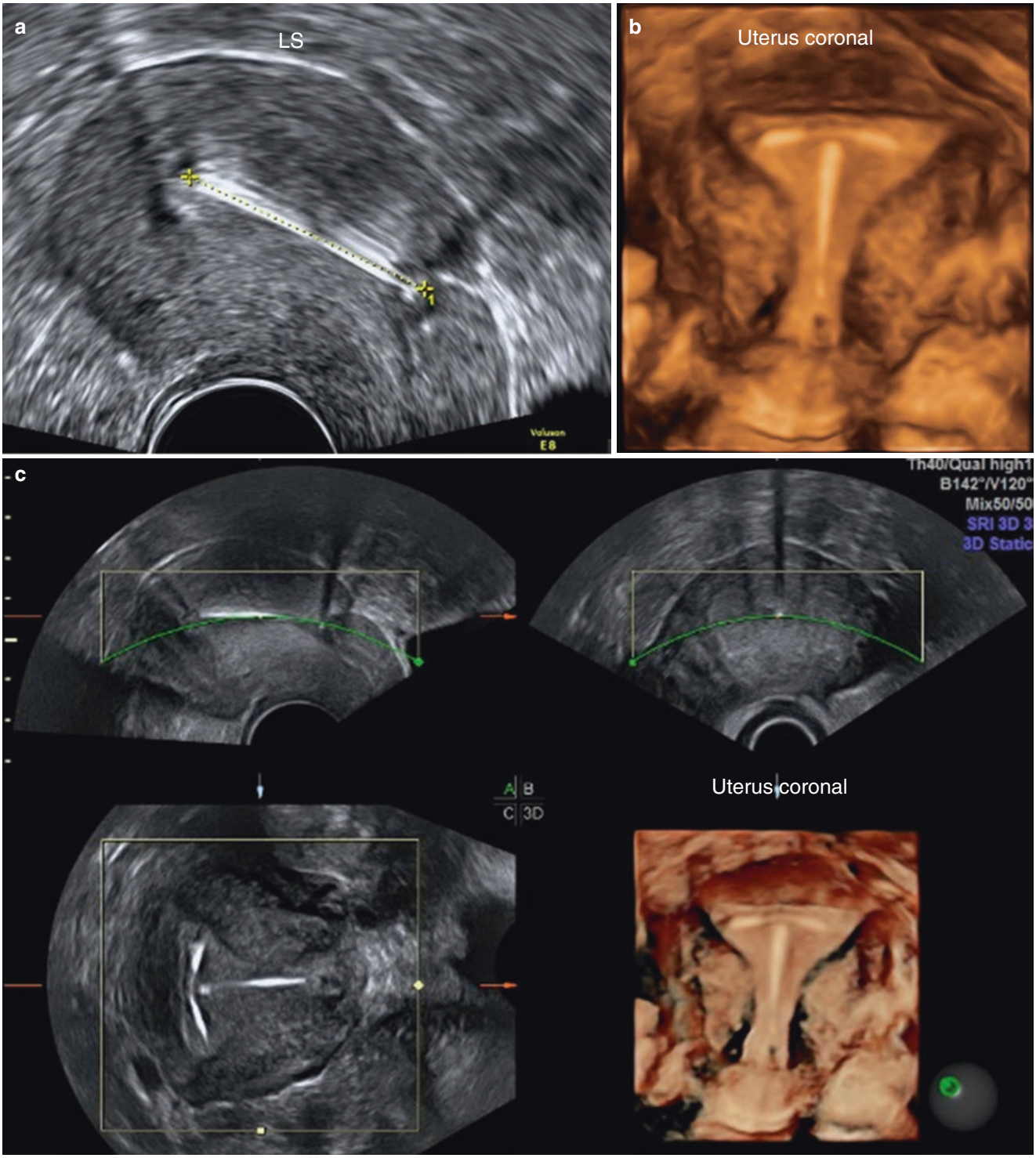

Fig. 13.16 IUCD seen in situ, well placed within the endometrial cavity. (**a**) Sagittal section of the uterus showing the vertical limb of the IUCD as a bright linear echo with acoustic shadowing. (**b**) 3D rendered image of the same showing the vertical limb of the IUCD (Cu T) in the endometrial cavity and the horizontal limbs along the upper margins of the endometrial cavity. (**c**) Image showing 3D rendering with HDI

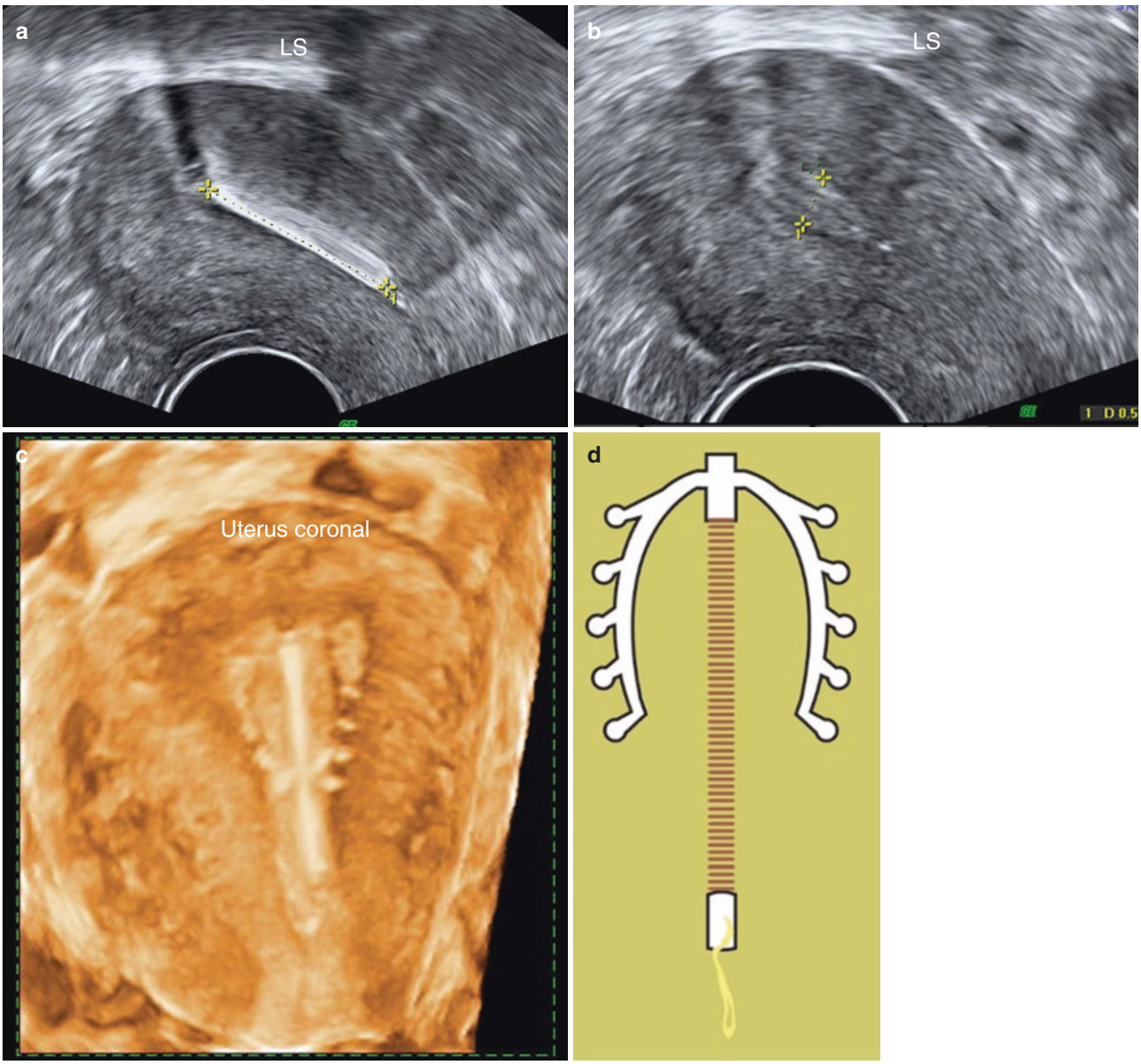

Fig. 13.17 Copper IUCD. Multiload seen in situ. (**a**) Sagittal section of the uterus showing the vertical limb of the IUCD as a bright linear echo with acoustic shadowing. (**b**) Measuring the endometrium in a patient with IUCD in situ is difficult. One may, however, move a little to the side of the IUCD in the sagittal plane to visualise the endometrium and measure it as seen in this image. (**c**) 3D rendered coronal image showing typical features of a Multiload IUCD. (**d**) Diagrammatic representation of a Multiload IUCD

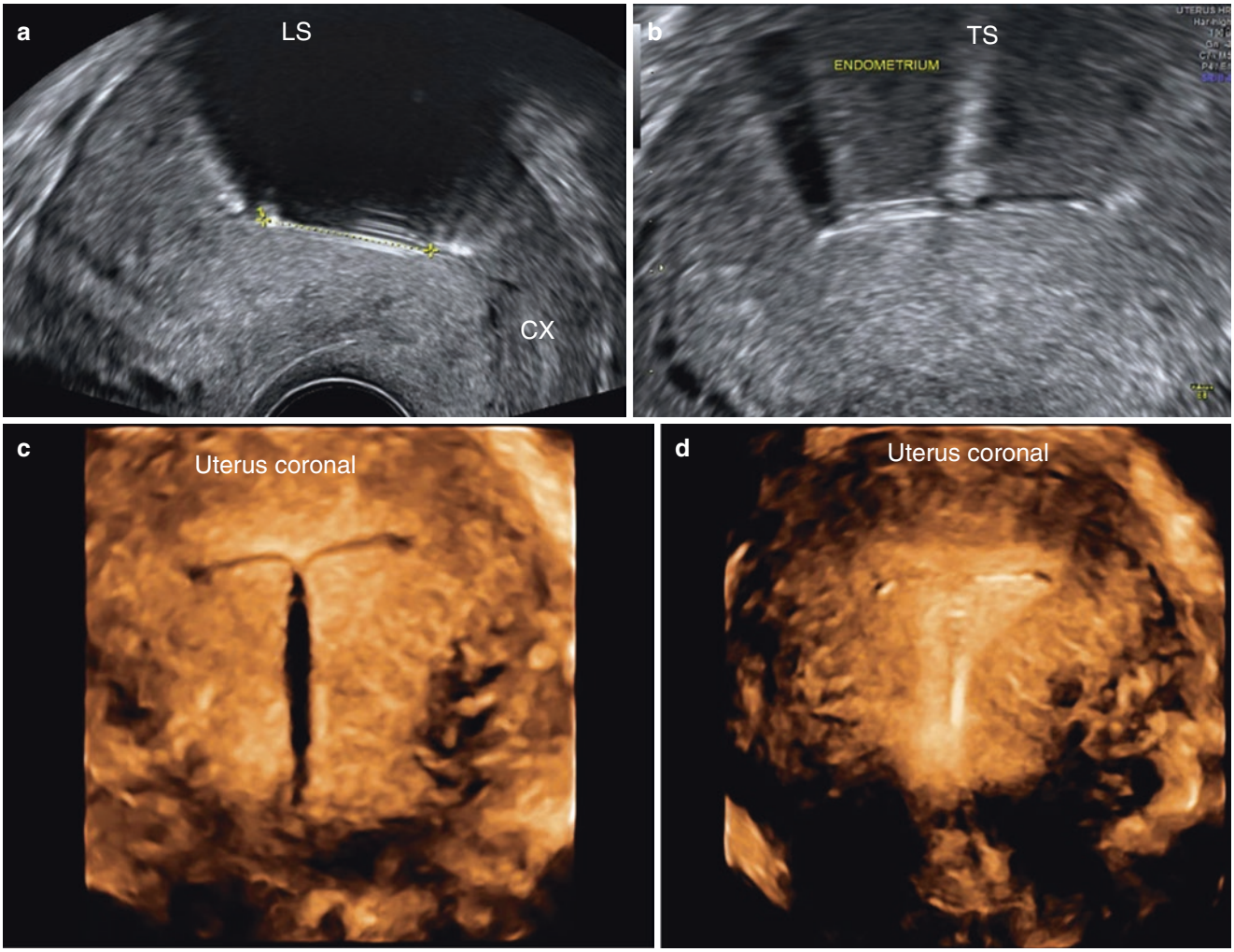

Fig. 13.18 Hormone-producing IUCD – Mirena. (a) Sagittal section of the uterus – the vertical shaft of the Mirena is not properly seen on greyscale imaging (unlike the copper IUCDs). It, however, shows significant acoustic shadowing. (**b**) Transverse section of the uterus with horizontal limbs of the Mirena seen. (**c**) In 3D rendered images, most often the Mirena is identified by the dense acoustic shadowing that it causes. (**d**) If the rendered plane is just proximal to the IUCD, one may be able to visualise the Mirena itself (instead of its more obvious acoustic shadow)

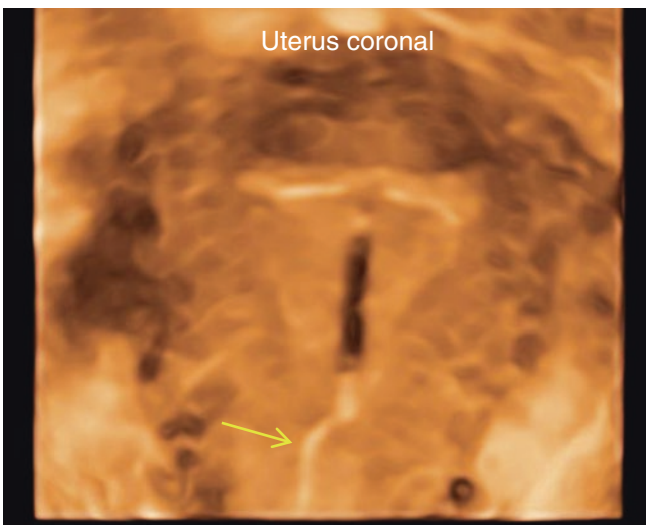

Fig. 13.19 Mirena seen in situ. Only the two ends of the vertical shaft are typically seen. The main shaft is seen as a dark area because of acoustic shadowing. The horizontal limb is seen along the upper margin of the uterine cavity. The IUCD thread (*arrow*) is seen in this rendered image, extending downwards from the lower end of the IUCD

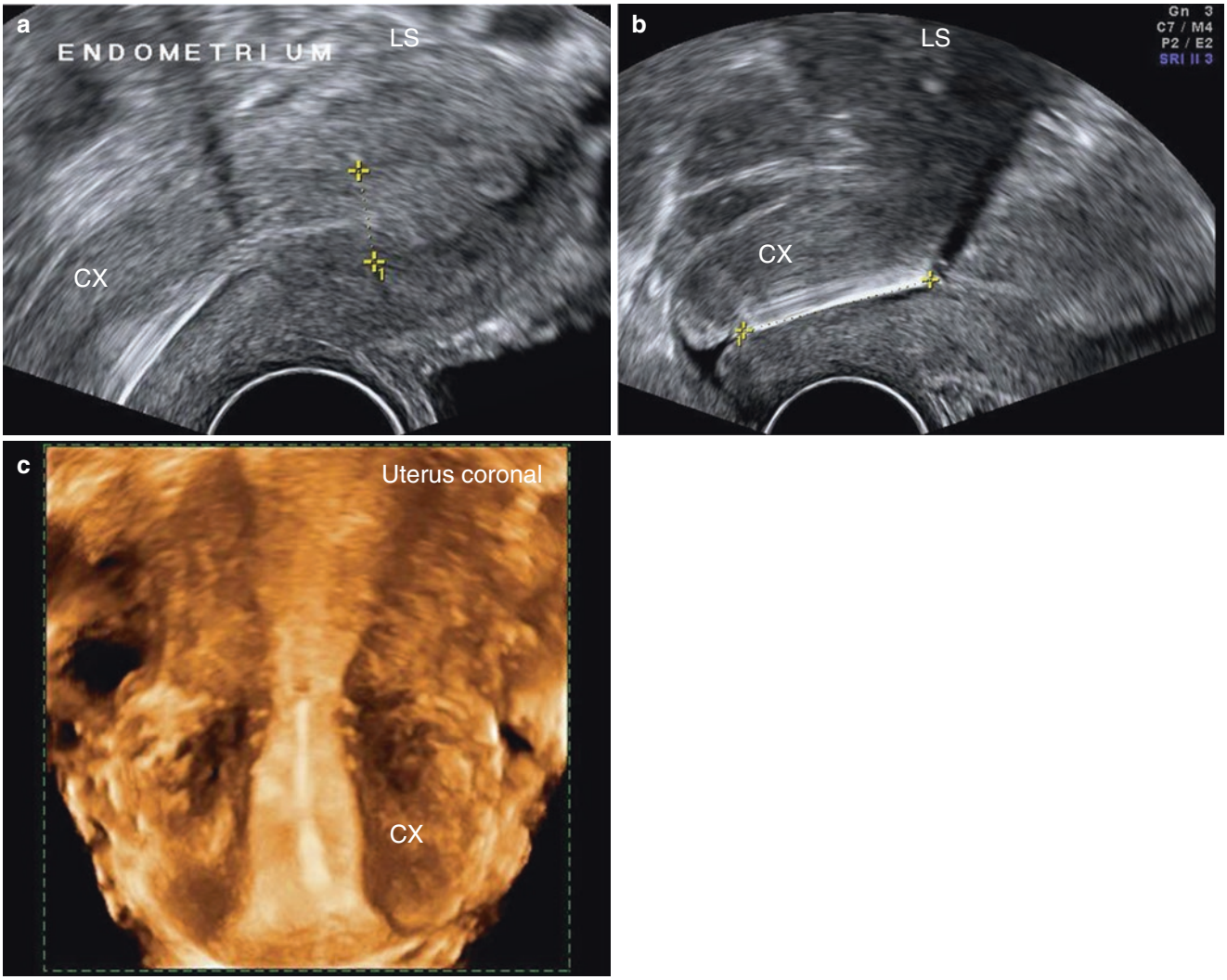

Fig. 13.20 Multiload IUCD displaced down into the cervical canal. (**a**) Endometrial cavity seen with no IUCD within. (**b**) Cervix seen with the bright echogenic shaft of the IUCD in the cervical canal. (**c**) 3D rendered image showing the Multiload IUCD in the cervical canal

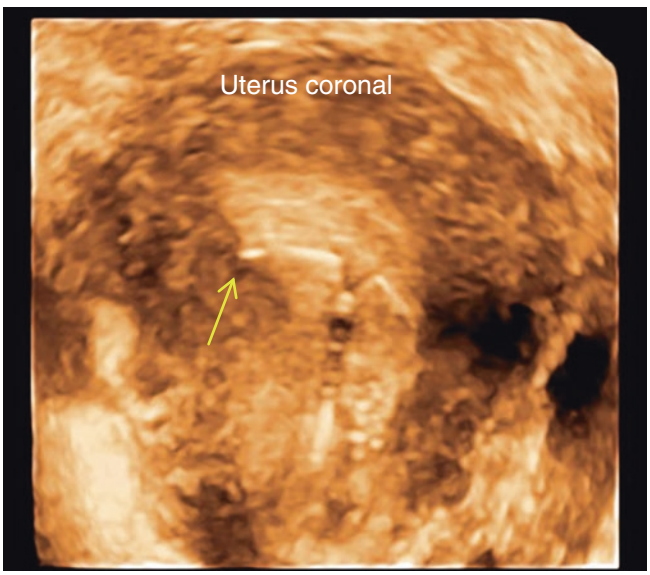

Fig. 13.21 Displaced Mirena seen in a 3D rendered image. The IUCD displaced down a little with the horizontal limbs of the Mirena some distance below the upper endometrial margin. One of its limbs is extending just beyond the EMJ (*arrow*)

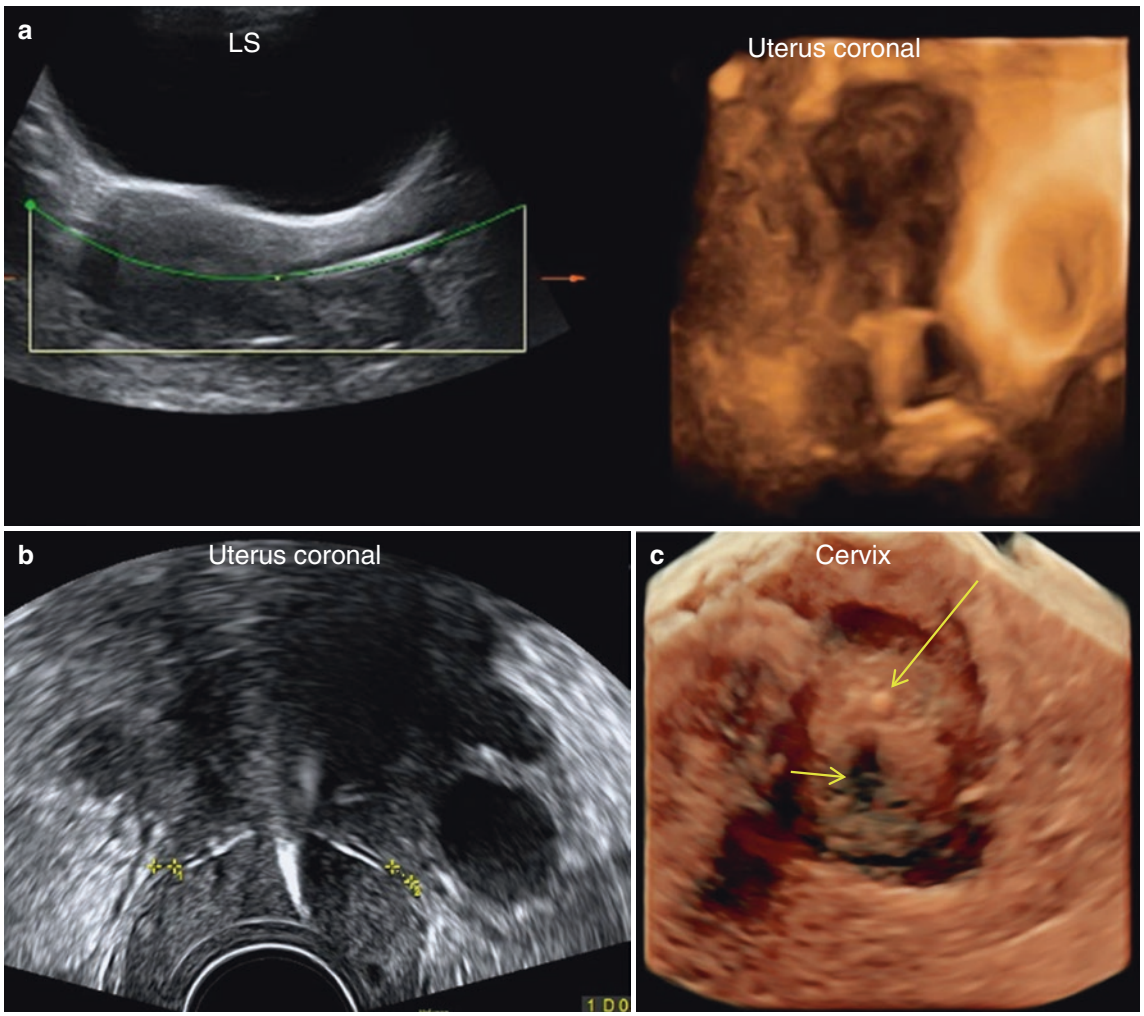

Fig. 13.22 Displaced IUCD. (**a**) TAS with rendered image showing the IUCD displaced down into the cervix. (**b**) Vertical shaft of the IUCD seen within the walls of the cervix. (**c**) 3D rendered image of the cervix showing the cervical os (*short arrow*) and lower end of the IUCD protruding out of the cervical walls (*long arrow*), above the external os

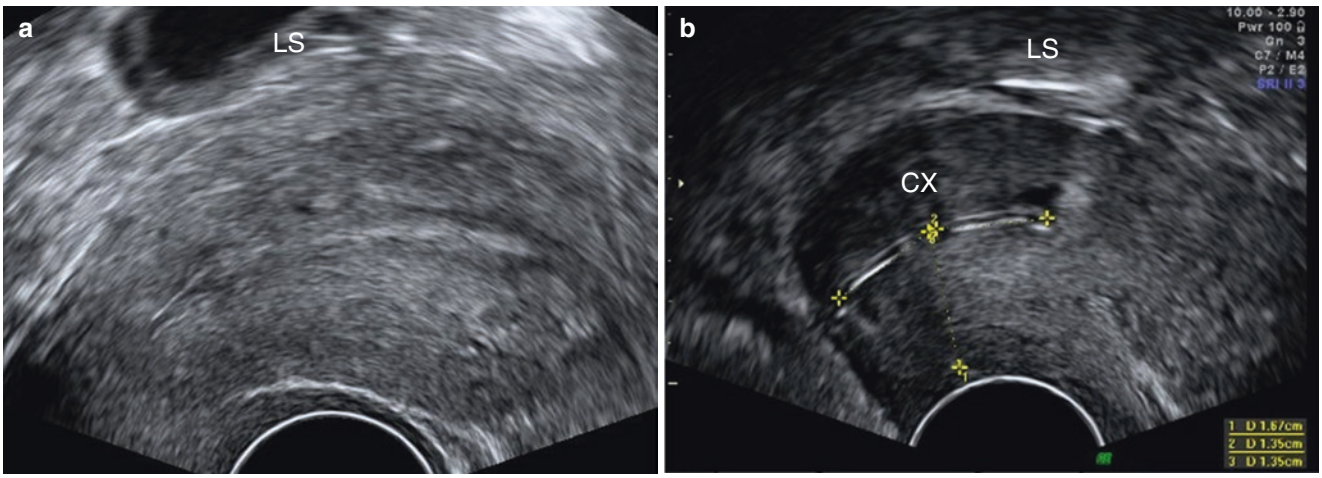

Fig. 13.23 Displaced Mirena. (**a**) IUCD not seen in the endometrial cavity. (**b**) IUCD seen in the long section of the cervix with its horizontal limbs in the cervical canal and vertical limb extending through the anterior cervical wall

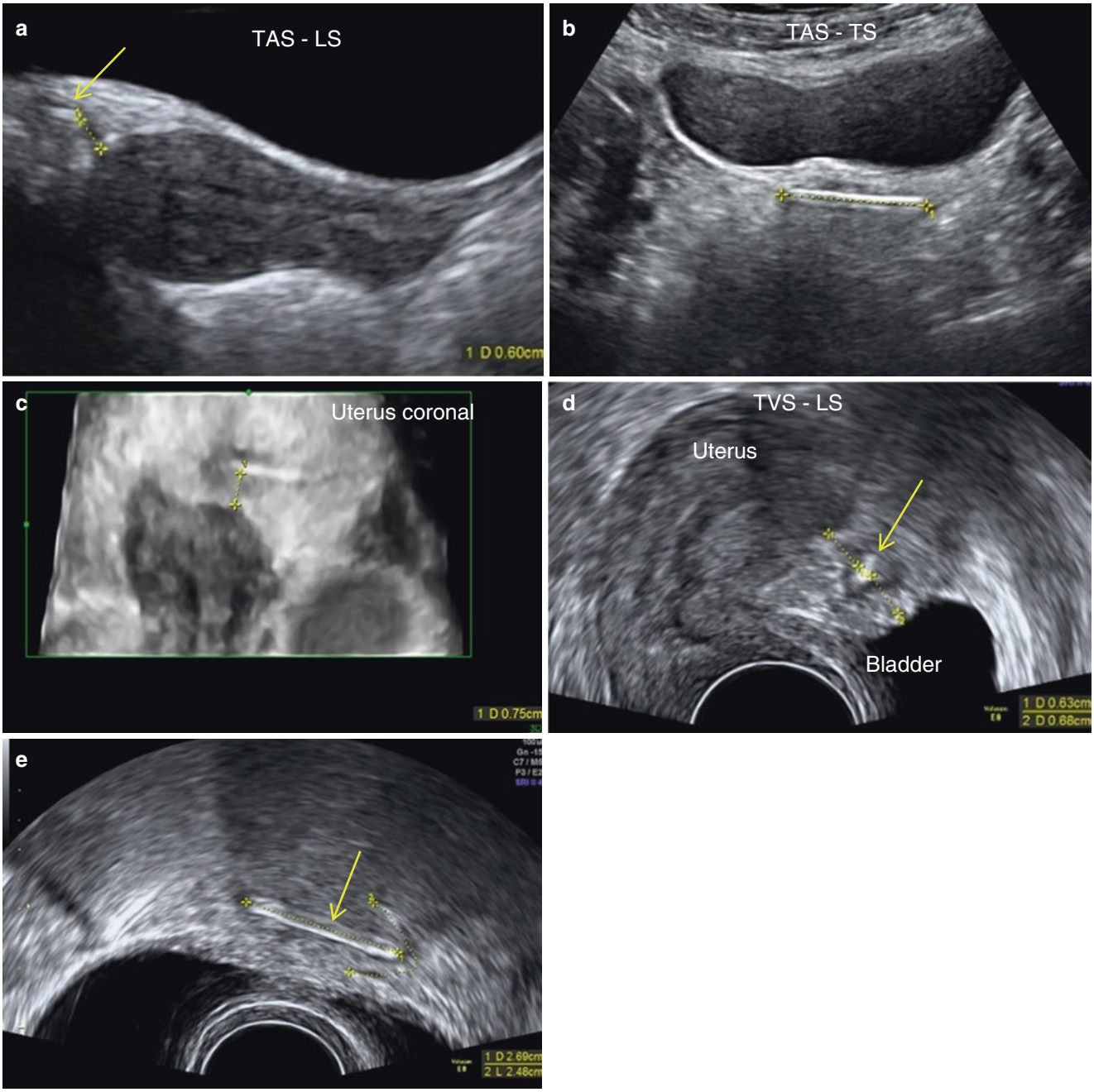

Fig. 13.24 Displaced IUCD. (**a**) TAS – cross section of the vertical limb of the IUCD seen above the uterine fundus (*arrow*). (**b**) Long section of the IUCD seen in the pelvis, posterior to the bladder in the UV fold. (**c**) 3D rendered image showing the IUCD above the uterine corpus. (**d**) TVS – sagittal section of the uterus with the cross section of the shaft of the IUCD in the UV fold between the bladder and the uterus. (**e**) TVS – shaft of the IUCD (*arrow*) seen in the UV fold on TS

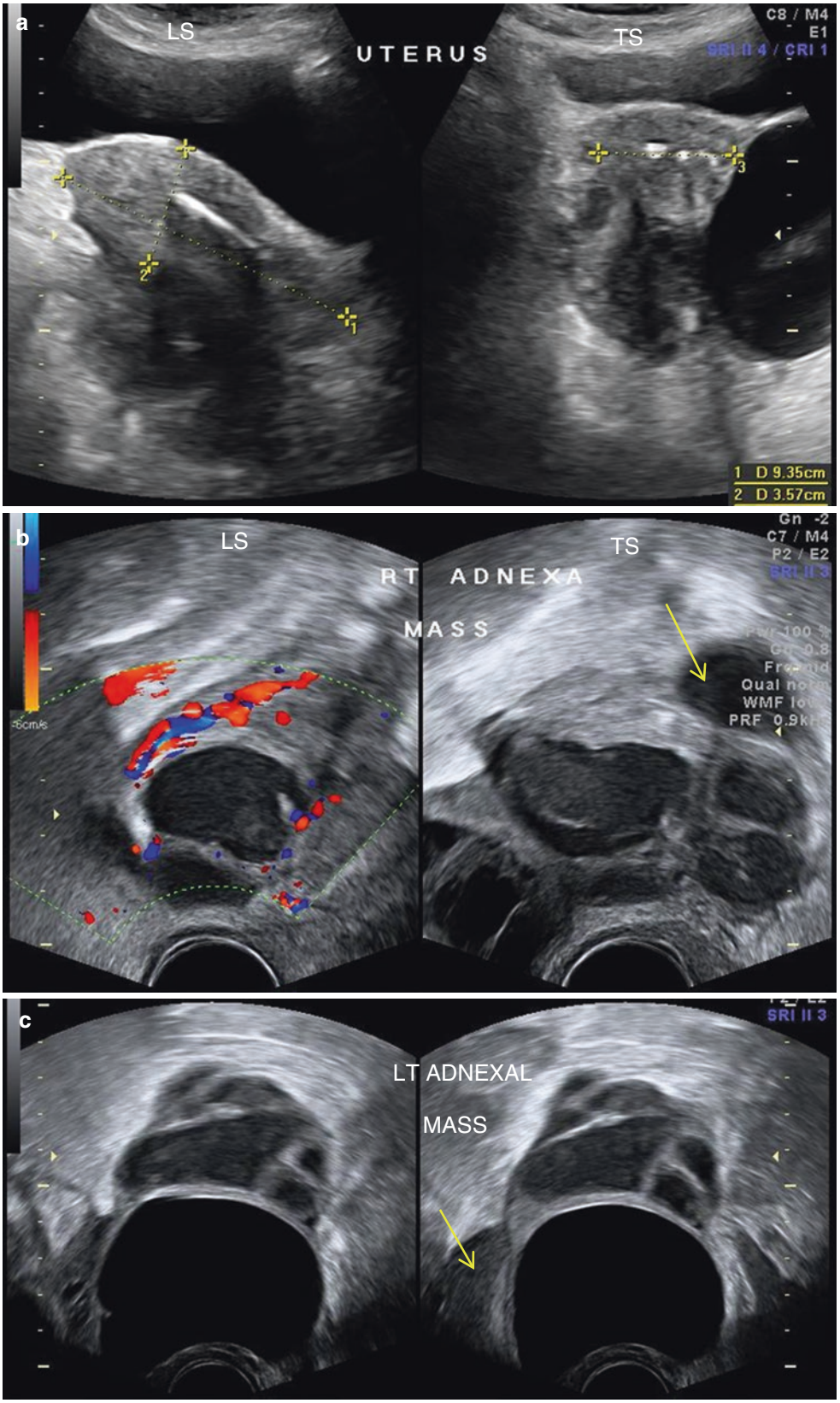

Fig. 13.25 IUCD in situ with bilateral PID. (**a**) TAS – the uterus with complex masses posterior to it, in the POD. (**b**) Right-sided TO mass with turbid contents (pus). (**c**) Left-sided TO mass with turbid contents (pus). (**b**,**c**) Pus is also seen surrounding the adnexal masses (*arrows*)

Summary: IUCD

- Patients are often referred for ultrasound location of the IUCD in cases of difficult placement, missing threads or in patients presenting with pain, bleeding, fever or pregnancy.
- On ultrasound, 3D rendered views of the coronal section of the endometrial cavity are essential to see the entire IUCD and its relationship to the endometrial cavity. If the upper end of the IUCD is below the upper margin of the endometrium or if any part of the IUCD lies outside the endometrial cavity, it is considered to be malpositioned. The shaft of the Mirena may not be seen on 2D but is well seen on 3D, because of its acoustic shadowing, as a dark imprint.
- Features of PID, an intrauterine or an ectopic pregnancy may be seen along with an IUCD.
- If an IUCD is missing, a radiograph (X-ray) or CT scan may be required to look for it elsewhere in the abdomen.

13.7 Follicular Monitoring and Ultrasonography in Patients with Infertility (Figs. 13.26 and 13.27)

Prior to ultrasonographic evaluation of patients presenting with infertility, changes during a menstrual cycle are briefly discussed.

13.7.1 Cyclical Changes During Menstrual Cycle (Both Natural and Induced) (Figs. 13.26 and 13.27)

A menstrual cycle can be divided into the menstrual phase, the follicular phase and the luteal phase. An average cycle lasts for about 28 days, with a range of 21–35 days. While the follicular phase varies in length, the luteal phase typically lasts for 14 days. Ovulation is the event that separates the follicular phase and the luteal phase.

Menstrual phase (Day 1–6 of the menstrual cycle):

- During the menstrual phase, follicular selection begins, and a small cohort of follicles are selected and begin growing. Antral follicles are seen in this phase as anechoic small cysts of 2–9 mm.
- The endometrium appears hyperechoic and complex. By the end of menstruation, it is thin – about 1–4 mm in thickness.
- The baseline scan in women on treatment for infertility is done on Day 2 or 3 of the menstrual cycle (discussed later in the section).

Proliferative phase or follicular phase (Day 6–14 of the menstrual cycle):

- By Day 6–8, a dominant follicle is selected, and the rest undergo atresia. The dominant follicle continues to grow till it reaches a size of about 22–24 mm in diameter, following which it ruptures and forms a corpus luteum.
- The endometrium gradually increases in thickness from 5 mm to about 10–12 mm. The proliferative endometrium is typically seen as a three-layer endometrium with an echogenic basal layer, a hypoechoic inner functional layer and an echogenic midline at the interphase of the two layers. Minimal intracavitary fluid may be seen in the preovulatory phase. The vascularity of the endometrium gradually increases to a maximum just prior to ovulation.
- Follicular tracking is done basically in the proliferative phase of the cycle, typically from Day 7 to ovulation. This has been discussed in detail later in this section. A primary scan in patients with infertility or subfertility is ideally done in this phase between Day 10 and 12; this is also discussed later in the section.

Ovulation

- Ovulation is the release of the ovum from a mature follicle. This is difficult to visualise on ultrasound, and ovulation is usually a retrospective diagnosis made by documenting post-ovulatory changes. Ovulation may occur naturally, following LH surge, or it may be induced by administration of HCG. This is usually done when the follicle is about 18 mm in diameter, with an endometrial thickness of at least 6 mm (ideally 7 mm). Rupture typically occurs 36–40 hours after the HCG injection, and intercourse or insemination can be timed accordingly.

Secretory phase or luteal phase (Day 14–28 of the menstrual cycle):

- Following rupture, the granulosa cells of the dominant follicle luteinise and the follicle becomes a corpus luteum. The corpus luteum may vary in appearance but is typically a thick walled structure with crenated walls, showing high vascularity around its walls (RI 0.35–0.5). The granulosa cells then produce progesterone, which produces secretory changes in the endometrium.
- The endometrial thickness may decrease minimally at ovulation, but thereafter it increases gradually (7–15 mm). The endometrium gradually becomes hyperechoic starting from the periphery towards the centre. This increased echogenicity is believed to be due to stromal edema and the presence of mucus and glycogen in the glands.
- If pregnancy does not occur, the activity of the corpus luteum declines, and when the hormone levels fall, menstruation occurs.

13.7.2 Types of Scans Done in Patients Presenting or on Treatment for Infertility

1. A *primary scan* in the opinion of the author (supported by other experts), in patients with infertility or subfertility, is ideally done between *Day 10 and 12* of a 28-day menstrual cycle. This, in some ways, would be a compromise as regards ovarian reserve assessment, which is ideally done on Day 2 or 3. It, however, has certain advantages which are as follows:
   - To determine the presence of a good dominant follicle and the ability to assess the endometrial response to follicular development, primarily in terms of endometrial thickness.
     At this time, one expects to see in one of the ovaries a dominant follicle (Fig. 13.26 c) of about 16–18 mm, with Doppler flow around more than 50% of its circumference with a PSV of about 10 cm/sec. Stromal blood flow velocity is around 6–12 cm/sec.

The absence of a dominant follicle or the presence of a functional cyst might serve as an indicator for ovulation dysfunction. The presence of a dominant follicle is however not a guarantee that the oocyte would be of good quality or that ovulation will occur. The presence of Doppler signals around more than 50% of the dominant follicle is generally associated with a good-quality oocyte. A triple-line appearance of the endometrium, with a minimum thickness of 7 mm, and a uterine artery of PI less than 3 are considered as reliable markers for good endometrial receptivity. The visualisation of spiral arteries into the endometrium has also been seen to correlate well with good receptivity (Fig. 13.26 d).

- A proliferative endometrium, normally seen on Day 10–12, is also ideal for assessing endometrial pathologies such as polyps or Asherman's syndrome. At this primary scan, in addition, other pelvic pathologies such as fibroids, endometriosis, uterine anomalies, etc., if present can also be assessed. A diagnosis of polycystic ovaries can also be made at this time.

2. *Day 2–3, baseline scan* (when hormones – FSH, LH, estrogen and progesterone – are at their baseline). This is done to study ovarian reserve and to assess the response. Some centres prefer a Day 2–3 baseline scan in patients presenting for the first time with infertility. The antral follicle count (which can be done in a faster and more accurate manner using 3D with SonoAVC software, particularly if there are a high number of antral follicles), ovarian volume and stromal flow are assessed. This helps plan stimulation protocols, especially in IVF cycles.

   Features that suggest low ovarian reserve are as follows: (1) an ovarian volume of less than 3 mL, (2) fewer than five antral follicles (between two ovaries) and (3) PSV of ovarian stromal vessels being less than 6 cm/sec.

   An antral follicle count of more than 20 increases risk for ovarian hyperstimulation syndrome (OHSS) and requires careful use of gonadotrophins.

   The menstruating endometrium at this time appears complex and hyperechoic. By the end of menstruation, it is less than 4 mm in thickness and no subendometrial flow is seen.

3. *Follicular tracking or follicular monitoring or follicular study* is done for the assessment of ovulation, both in natural cycles as well as induced cycles (with ovulation induction agents). It basically involves the assessment of ovarian follicles and the endometrium at regular intervals, typically starting on Day 7. For IVF cycles and in those patients where a functional cyst is known to exist from a previous cycle, an initial Day 2–3 scan is recommended. Follicular tracking is typically done until there is evidence of ovulation or egg retrieval.

- Follicular tracking starts from Day 7. The dominant follicle (more than 10 mm) in each ovary is measured. These may be one or more in number. The follicle is measured in three perpendicular dimensions in two perpendicular planes so that the average diameter can be obtained. The follicle is seen as an anechoic, unilocular, round, smooth-walled cyst. The two-layer endometrial thickness is also measured, and the endometrial pattern is noted (three line, echogenic, etc.).
- The patient is generally scanned on alternate days, and the size of each follicle and endometrium is noted. Once the follicle reaches an average diameter of 16 mm, a daily monitoring of the follicle is recommended.
- Once the average diameter is 18 mm, with an endometrial thickness of at least 6 mm (ideally 7 mm), the referring clinician may choose to give the patient an HCG injection to induce ovulation (likely to occur 36–40 hours after the injection is administered), and intercourse or insemination is timed accordingly.
- Ovulation on ultrasound can be determined by the following signs:
  - Sudden disappearance or reduction in the size of the follicle
  - Irregular margins
  - Presence of internal echoes within the follicle
  - Free fluid in the POD
- The endometrium, following ovulation, shows thick hyperechoic walls along the EMJ, and gradually the hyperechogenicity spreads inwards to the entire thickness of the endometrium.
- Once ovulation is documented, ultrasound is not required for follicular monitoring.

13.7.3 Luteinised Unruptured Follicle (Fig. 13.28)

In a small percentage of women, following the LH surge, the dominant follicle continues to grow and luteinise without rupture. As a result, there is an increase in progesterone secretion, and the endometrium shows secretory changes, but there is no release of oocyte from the dominant follicle. In such patients, on follicular monitoring, serial scans will show secretory changes in the endometrium without evidence of rupture of the follicle (i.e. no collapse of follicle or free fluid). The follicle itself increases in size and may either remain anechoic or may show lacy internal echoes. Some patients are known to have recurrent LUF, and treatment protocols may have to be altered accordingly.

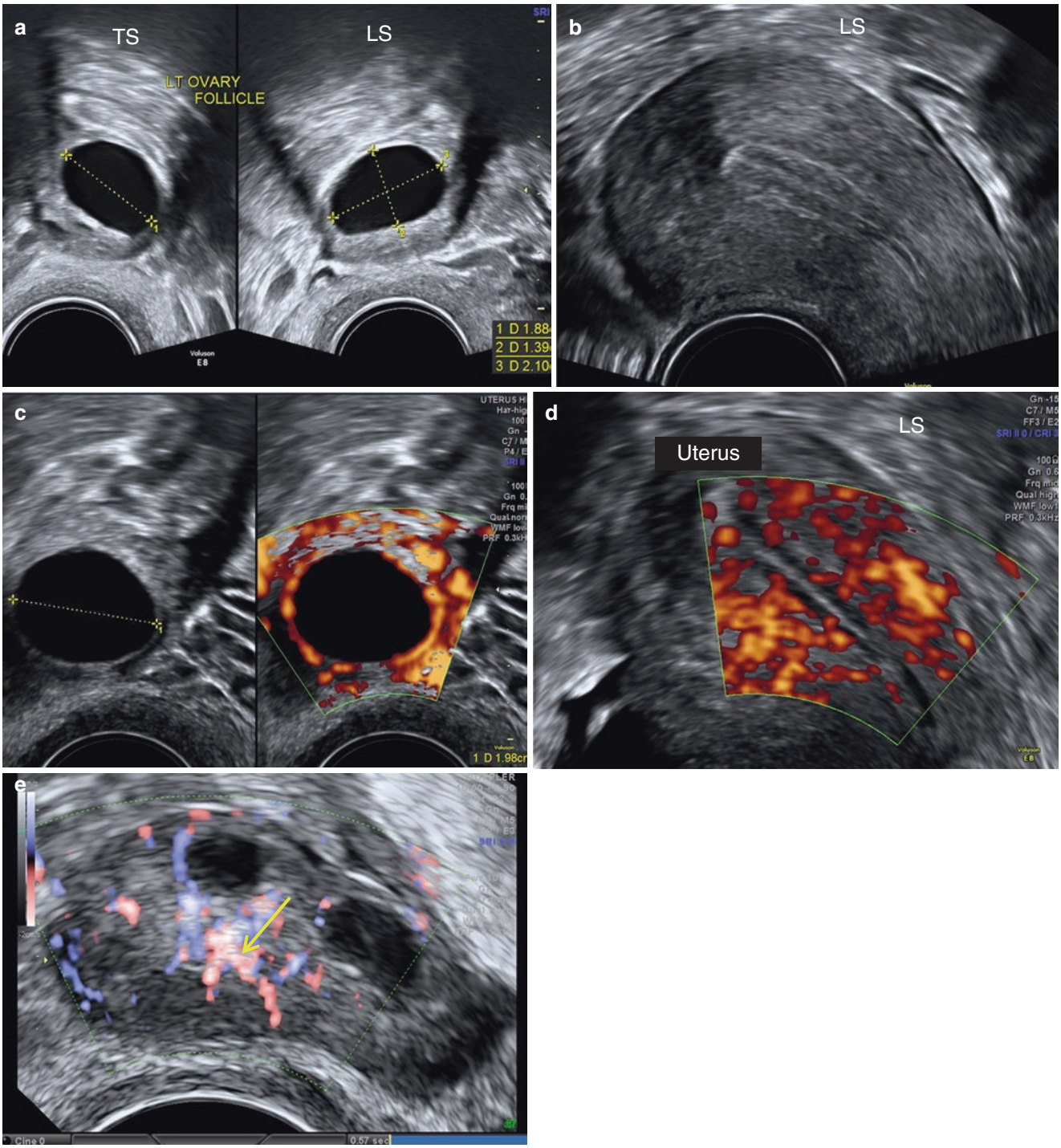

Fig. 13.26 Follicular phase. (**a**) Day 9 – proliferative (trilaminar) endometrium and (**b**) ovary showing a developing follicle (anechoic unilocular). (**c**) Day 11 – follicle showing flow around more than 50 % of its circumference and (**d**) endometrial flow in the same case with spiral vessels entering the endometrium. (**e**) Stromal flow in a different case. The most prominent vessel (*arrow*) should be sampled to assess flows

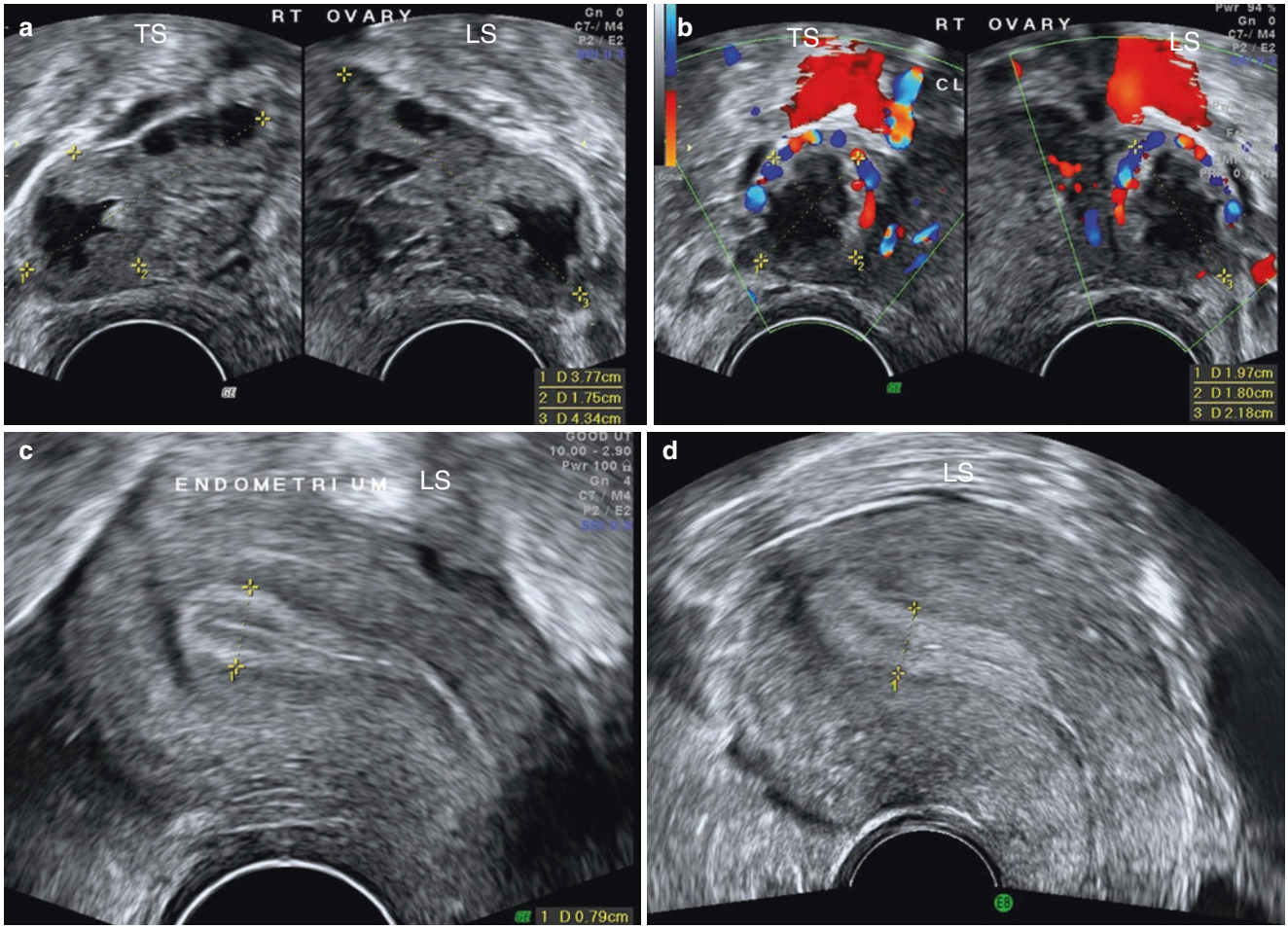

Fig. 13.27 Secretory phase. (**a**) Corpus luteum shows thick irregular walls and turbid contents. (**b**) Increased flow seen on Doppler in the walls of the corpus luteum. (**c**) Uterus with an early secretory endometrium – the outer endometrium is hyperechoic. (**d**) Uterus with a secretory endometrium – the entire endometrium is hyperechoic with a central white midline

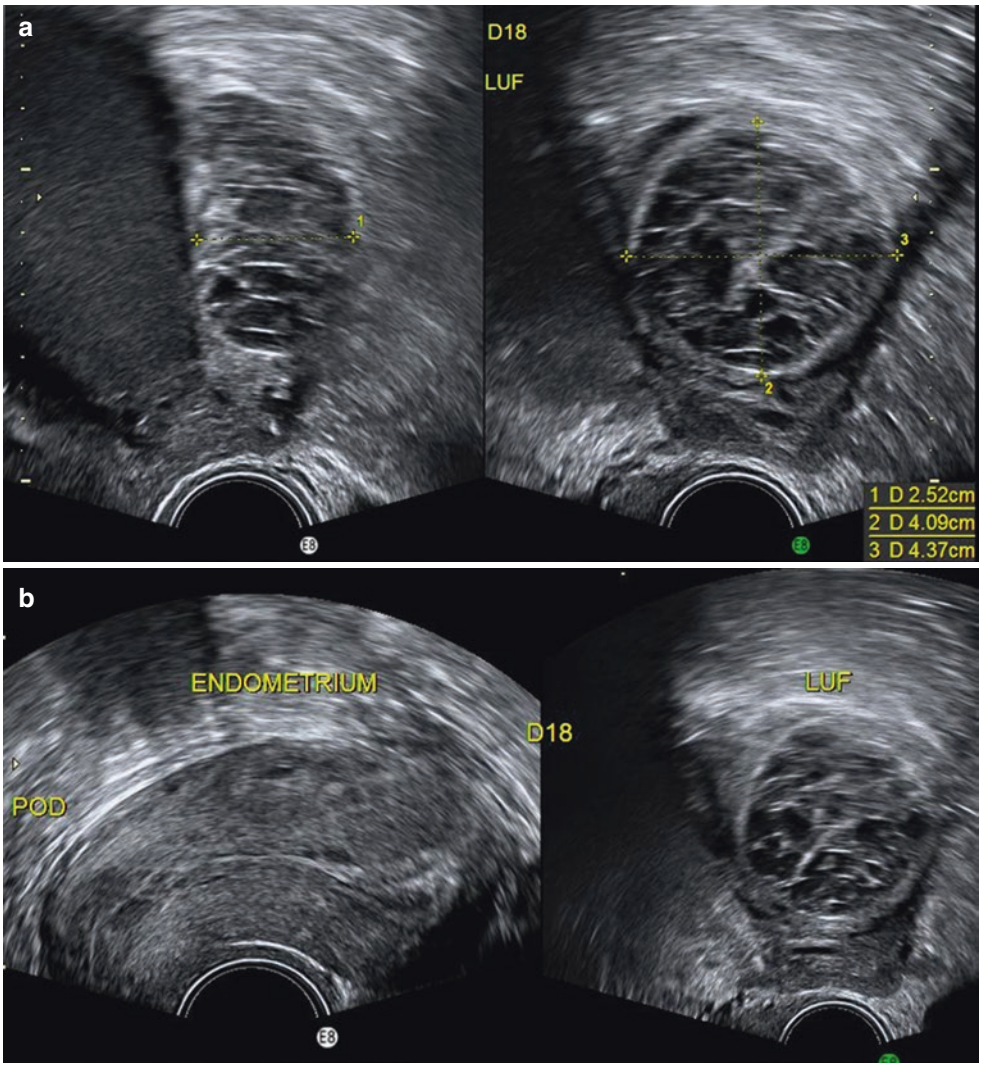

Fig. 13.28 Luteinised unruptured follicle (LUF) in a patient on Day 18 of follicular tracking. (**a**) LUF shows lacy internal echoes. An anechoic follicle was seen 48 hours earlier which now shows internal echoes and has increased in size, with no evidence of ovulation. An endometriotic cyst is seen beside it, in the same ovary. (**b**) Along with the LUF, an early secretory endometrium is seen. There is no free fluid in the POD, as ovulation has not occurred

13.8 Ovarian Hyperstimulation Syndrome (OHSS)

Ovarian hyperstimulation syndrome is an iatrogenic, potentially life-threatening complication of supraphysiological ovarian stimulation. OHSS is a systemic condition with enlarged cystic ovaries and increased vascular permeability, as a result of vasoactive peptides released from the granulosa cells of the hyperstimulated ovary. This results in the shift of fluid from the intravascular compartment to the third space compartments, resulting in hypovolemia and other complications, as seen in cases with severe OHSS.

Factors that increase risk for OHSS include polycystic ovaries, a previous history of OHSS, a high baseline antral follicle count, a large number of developing follicles, a large number of oocytes retrieved (more than 20), the use of HCG as opposed to progesterone for luteal phase support and early pregnancy (particularly in patients with multiple pregnancy).

The syndrome is most often secondary to ovarian stimulation with gonadotrophins and rarely after clomiphene citrate or spontaneous ovulation. Symptoms of OHSS may begin as early as 24 hours after the hCG injection is administered but can occur any time in the first 7–10 days after hCG. The later ones (presenting after Day 9) are usually associated with high hCG due to an early pregnancy.

The ovaries are enlarged with multiple follicular and luteal cysts. Complications like torsion and haemorrhage can rarely be seen in these enlarged ovaries. Many of these patients present in the emergency department because of abdominal pain and discomfort from the enlarged ovaries and ascites, shock due to hypovolemia, ovarian torsion or intraperitoneal haemorrhage from the ovaries.

Based on the severity, OHSS has been divided into mild, moderate and severe:

- Mild OHSS is common and usually self-limiting. These patients give a history of abdominal distention and pain and have enlarged cystic ovaries.
- Moderate OHSS, where the woman presents with abdominal pain, nausea, vomiting and ascites, and on ultrasound enlarged ovaries are noted.
- Severe OHSS, where, in addition to the above, the patient has clinical evidence of ascites and/or hydrothorax. In critical OHSS, there may be hypovolemia, hemoconcentration, coagulation abnormalities, renal failure, etc.

Patients with mild and moderate OHSS can be treated on an outpatient basis, whereas those with severe OHSS should ideally be admitted. Weight, abdominal circumference, urinary output, CBC, electrolytes and blood creatinine may require to be monitored.

Ultrasound Features of OHSS (Fig. 13.29)

- Bilateral symmetrically enlarged ovaries – Ovaries are usually more than 6 cm in size, and in severe OHSS they are usually more than 12 cm.
- The ovaries are multicystic (due to multiple follicular cysts and corpus luteal cysts) with thin septae.
- These cysts are typically arranged surrounding a central core of ovarian stroma creating a ‘spoke wheel’ appearance.
- The cyst may contain clear fluid (anechoic) or may appear turbid showing internal echoes within.
- The ovarian stroma and septae show increased vascularity.
- Ascites is seen. In mild OHSS, fluid may be seen only in the pelvis, but in severe cases, the ascites may be significant. The ascitic fluid may be clear, but if there is haemorrhage from the ovaries, it may be turbid showing internal echoes.

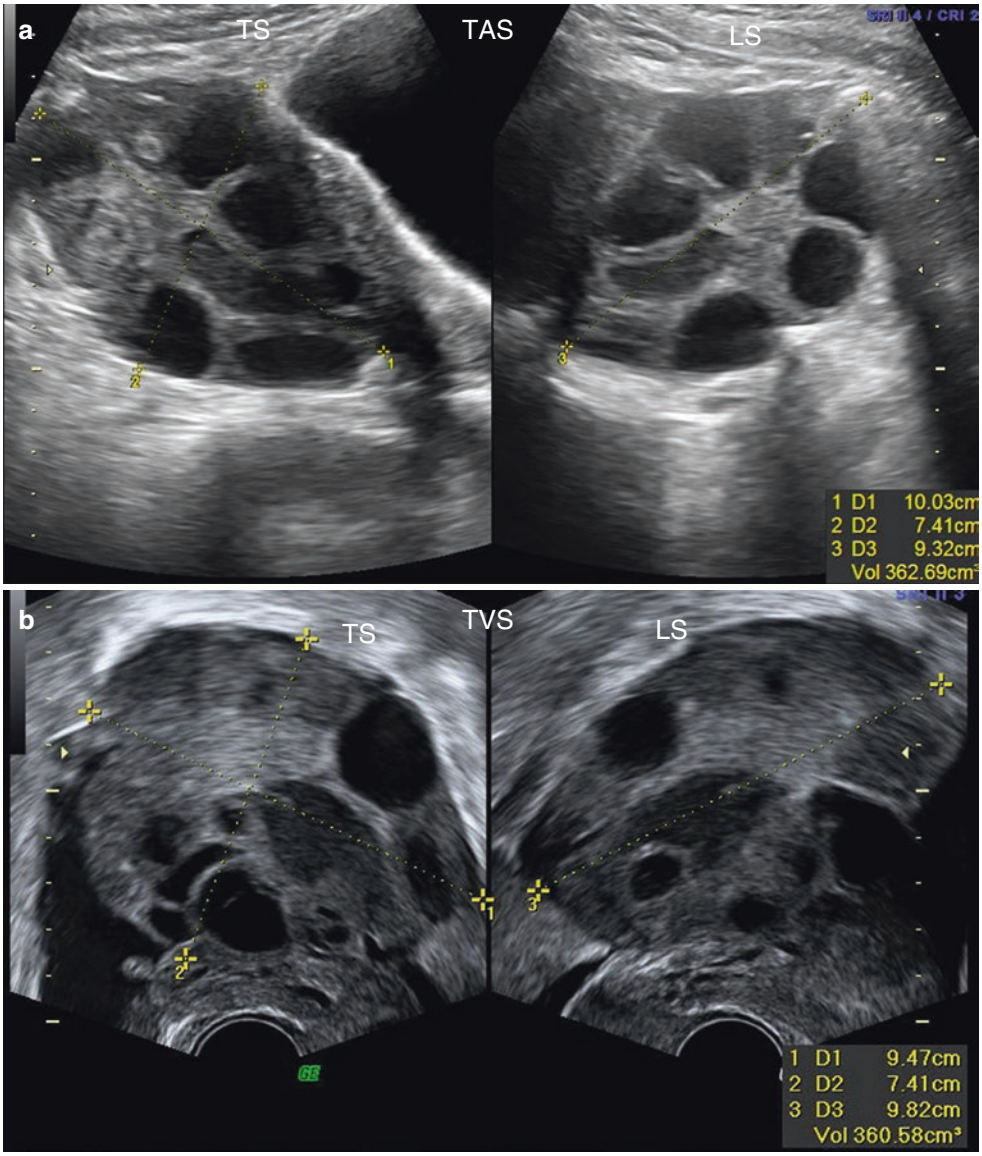

Fig. 13.29 Ovarian hyperstimulation syndrome seen in a patient with a single ovary, and IVF conception, following a cycle of ovulation induction. (**a**) Grossly enlarged ovary on TAS showing a 'spoke wheel' appearance. (**b**) TVS – enlarged ovary with a volume of about 360 cc. The ovaries show multiple cysts, mainly corpora lutea. (**c**) Ovary showing high vascularity. (**d**) Flow in the ovary shows a low RI of 0.39 (**e**, **f**) showing gross ascites. (**g**) TVS – image of the uterus surrounded by ascitic fluid and showing three tiny intrauterine gestational sacs

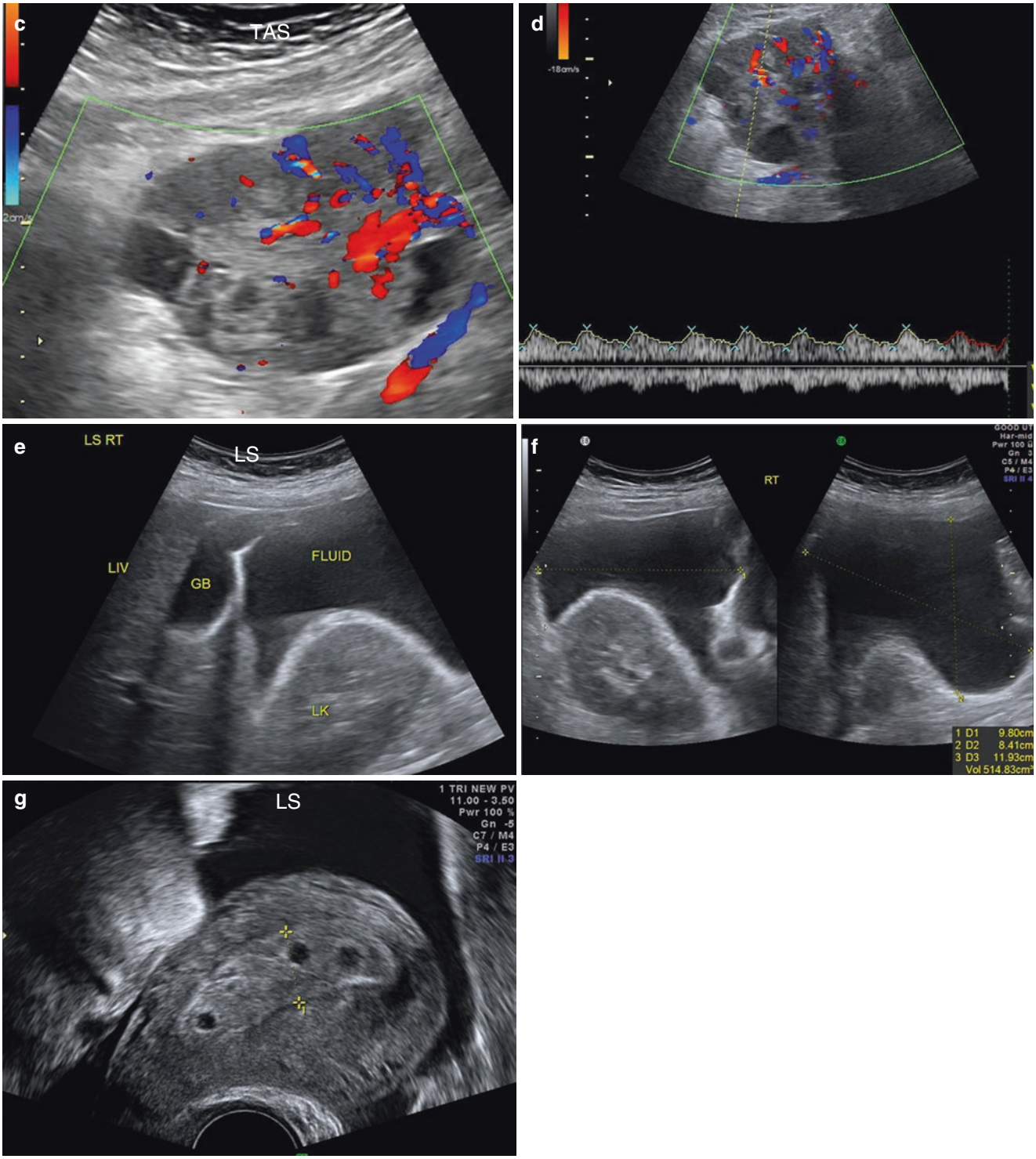

Fig. 13.29 (continued)

Summary of OHSS

- OHSS is a systemic disease resulting from the release of vasoactive substances from a hyperstimulated ovary. These substances cause increased capillary permeability with fluid leak from the intravascular to the extravascular compartment. It is commonly seen in patients with ovulation induction with gonadotrophins. It is more likely to occur in cycles that result in a conception.
- The most common presenting feature in mild to moderate OHSS is abdominal pain.
- The ovaries are grossly enlarged with multiple follicular and corpus luteal cysts with thin septae separating them. The ovarian tissue shows increased vascularity. Ascites is seen.
- Some of these patients may present with complications of OHSS like associated torsion and intraperitoneal haemorrhage.

Suggested Reading

Alkatib M, Franco AVM, Fynes MM (2005) Vesicouterine fistula following Cesarean delivery—ultrasound diagnosis and surgical management. Ultrasound Obstet Gynecol 26:183–5. doi:10.1002/uog.1925

Baron KT et al (2013) Emergent complications of assisted reproduction. Radiographics 33(1):229–44

Benacerraf BR et al (2009) Three-dimensional ultrasound detection of abnormally located intrauterine contraceptive devices which are a source of pelvic pain and abnormal bleeding. Ultrasound Obstet Gynecol 34:110–5. doi:10.1002/uog.6421

Bij de Vaate AJM et al (2011) Ultrasound evaluation of the Cesarean scar: relation between a niche and postmenstrual spotting. Ultrasound Obstet Gynecol 37:93–9. doi:10.1002/uog.8864

Boortz HE et al (2012) Migration of intrauterine devices: radiologic findings and implications for patient care. Radiographics 32(2):335–52

Caspi B et al (1996) Penetration of the bladder by a perforating intrauterine contraceptive device: a sonographic diagnosis. Ultrasound Obstet Gynecol 7:458–60. doi:10.1046/j.1469-0705.1996.07060458

De Cicco, et al (2016) Uterine perforation and small bowel incarceration 11 months after dilatation ad curettage: sonographic and surgical findings. Ultrasound Obstet Gynecol. Accepted Author Manuscript. doi:10.1002/uog.15904

Granberg S et al (1994) The use of transvaginal ultrasonography compared to routine gynecological examination to check the location of an intrauterine contraceptive device. Ultrasound Obstet Gynecol 4:316–9. doi:10.1046/j.1469-0705.1994.04040316

Huang MW et al (1998) Uterine arteriovenous malformations: gray-scale and Doppler US features with MR imaging correlation. Radiology 206(1):115–23

Langer JE et al (2012) Imaging of the female pelvis through the life cycle. Radiographics 32:1575–97

Müngen E (2003) Vascular abnormalities of the uterus: have we recently over-diagnosed them? Ultrasound Obstet Gynecol 21:529–31. doi:10.1002/uog.163

Naji O et al (2012) Standardized approach for imaging and measuring Cesarean section scars using ultrasonography. Ultrasound Obstet Gynecol 39:252–9. doi:10.1002/uog.10077

Nastri CO et al (2015) Ovarian hyperstimulation syndrome: pathophysiology, staging, prediction and prevention. Ultrasound Obstet Gynecol 45:377–93. doi:10.1002/uog.14684

Ofili-Yebovi D et al (2008) Deficient lower-segment Cesarean section scars: prevalence and risk factors. Ultrasound Obstet Gynecol 31:72–7. doi:10.1002/uog.5200

Osser OV et al (2010) Cesarean section scar defects: agreement between transvaginal sonographic findings with and without saline contrast enhancement. Ultrasound Obstet Gynecol 35(1):75–83. doi: 10.1002/uog.7496

Osser OV, Valentin L (2011) Clinical importance of appearance of cesarean hysterotomy scar at transvaginal sonography in non-pregnant women. Obstet Gynecol 117(3):525–32

Polat P et al (2002) Color Doppler US in the evaluation of uterine vascular abnormalities. Radiographics 22(1):47–53

Park O et al (2003) Sonographic diagnosis of vesicouterine fistula. Ultrasound Obstet Gynecol 22:82–4. doi:10.1002/uog.161

Parsons AK, Sanders RC (2007) OP17.07: Menometrorrhagia due to impaired uterine drainage. Ultrasound Obstet Gynecol 30:514. doi:10.1002/uog.4585

Sanders RC (2012) OP19.08: Retroverted uterine position and pelvic pain. Ultrasound Obstet Gynecol 40:113. doi:10.1002/uog.11573

Syla BH et al (2011) Transabdominal two- and three-dimensional color Doppler imaging of a uterine arteriovenous malformation. Ultrasound Obstet Gynecol 37:376–8. doi:10.1002/uog.8918

Timmerman D et al (2000) Vascular malformations in the uterus: ultrasound diagnosis and conservative management. Eur J Obstet Gynecol Reprod Biol 92:171–8

Timmerman D et al (2003) Color Doppler imaging is a valuable tool for the diagnosis and management of uterine vascular malformations. Ultrasound Obstet Gynecol 21:570–7. doi:10.1002/uog.159

Den Bosch V et al (2002) Color Doppler and gray-scale ultrasound evaluation of the postpartum uterus. Ultrasound Obstet Gynecol 20:586–91. doi:10.1046/j.1469-0705.2002.00851

Van Schoubroeck D et al (2009) Sonographic determination of the position of a levonorgestrel intrauterine device. Ultrasound Obstet Gynecol 33:121–4. doi:10.1002/uog.6288

Vikhareva Osser O et al (2009) High prevalence of defects in Cesarean section scars at transvaginal ultrasound examination. Ultrasound Obstet Gynecol 34:90–7. doi:10.1002/uog.6395

Wang C-B (2009) Cesarean scar defect: correlation between Cesarean section number, defect size, clinical symptoms and uterine position. Ultrasound Obstet Gynecol 34:85–9. doi:10.1002/uog.6405

Exploring Pathologies Based on Clinical Presentation

14

14.1 Abnormal Uterine Bleeding

To investigate abnormal uterine bleeding, one must know what 'normal' bleeding is. Features of normal menstrual bleeding are:

- Cyclical menstrual flow with cycle length varying from 21 to 35 days.
- Duration of menstrual flow or bleeding up to 7 days.
- Amount of flow is a subjective parameter (normally, patients change about 3–5 pads per day).

14.1.1 Common Forms of Abnormal Uterine Bleeding

Amenorrhoea – the absence of menstrual periods (for a period of 3 months or more)
Hypomenorrhoea – scanty flow during periods
Oligomenorrhoea – long menstrual cycles with period length of greater than 35 days
Menorrhagia – excessive flow or prolonged flow during periods
Polymenorrhoea – short menstrual cycles
Polymenorrhagia – short cycles with increased flow during periods
Metrorrhagia – acyclical bleeding which could be heavy or minimal
Intermenstrual bleeding – bleeding in between two periods
Postmenstrual bleeding – bleeding (often minimal) just after periods
Premenstrual bleeding – bleeding (often minimal) just before periods
Post-coital bleeding – bleeding following intercourse

Based on the nature of bleeding, one may be able to suspect the type of gynecological pathology leading to abnormal uterine bleeding:

- Amenorrhoea and hypomenorrhoea – These are most often due to local endometrial pathology but could be secondary to hormonal disturbances.
- Menorrhagia and polymenorrhagia – These patients usually have myometrial pathology (fibroids or adenomyosis). In some cases, endometrial pathology like hyperplasia may be noted.
- Metrorrhagia and intermenstrual bleeding – Pathology involving the surface of the uterine cavity can cause irregular bleeding from the surface of the lesion. If it is heavy, one must think of neoplasia or an AV malformation or retained products of conception. If it is minimal, it could be due to an endometrial polyp or hormonal imbalance.
- Post-coital bleeding – These patients are likely to have local pathology involving the cervix or vagina (like neoplasia, polyps or infection).

14.1.2 Abnormal Uterine Bleeding in the Reproductive Age Group

1. *Causes for decreased flow (amenorrhoea, hypomenorrhoea or oligomenorrhoea):*
   - Pregnancy – This is a frequent cause of amenorrhoea in women of reproductive age group, and a simple urine pregnancy test or serum BhCG levels will help in the diagnosis. Ultrasound may show an intrauterine or an extrauterine pregnancy, which helps to confirm the diagnosis.
   - Premature menopause – That is, menopause occurring before the age of 40 can also cause amenorrhoea or oligomenorrhoea (in the few months preceding menopause). On ultrasound, the ovaries appear atrophic. Diagnosis can be further confirmed with the help of serum FSH and LH levels.
   - Asherman's syndrome – In these cases, patients will often give history of instrumentation. On ultrasound, endometrial scarring can be seen (details in Chap. 4).

M. Sibal, *Ultrasound in Gynecology*, DOI 10.1007/978-981-10-2714-7_14

- Hormonal causes like polycystic ovaries, hyperandrogenism, hormone-producing tumours, hormonal medication, etc., can also cause amenorrhea, hypomenorrhoea or oligomenorrhoea.

2. *Causes for increased flow (menorrhagia, polymenorrhagia and metrorrhagia):*
   - Pregnancy related – This includes patients with threatened abortion (Fig. 14.1), incomplete abortion, retained products of conception, ectopic pregnancy, molar pregnancy and gestational trophoblastic disease (GTD). In these cases, ultrasound will help clinch the diagnosis (details in Chap. 10).
   - Pregnancy unrelated:
     – If the flow is cyclical (i.e. the patient complains of excessive flow during periods – menorrhagia or polymenorrhagia), possibilities include myometrial pathologies like fibroid and adenomyosis or an endometrial pathology like endometrial hyperplasia or even an endometrial malignancy. Patients with fibroids and adenomyosis are likely to complain of dysmenorrhoea. On ultrasound, the uterus may be enlarged with fibroids and adenomyosis, or there may be thickened endometrium secondary to hyperplasia or malignancy. This may also be seen in women with bleeding disorders (e.g. Von Willebrand's disease). Hormonal disorders like hormone-producing tumours or polycystic ovaries can also cause excessive bleeding.
     – If the flow is acyclical (i.e. metrorrhagia, intermenstrual bleeding or post-coital bleeding), one must think of pathologies involving the surface of the uterine cavity (polyps, malignancy and submucous fibroid) or pathologies of the cervix or vagina (polyps and malignancy). These lesions can be picked up on ultrasound (details of ultrasound diagnosis are available in Chaps. 2, 3, 4 and 5, respectively); those involving the uterine cavity may be better seen with sonohysterogram, while those involving the cervix and vagina may be better assessed with gel sonovaginography (unless the patient is actively bleeding). Sometimes in a patient with a deficient caesarean scar or an acutely retroflexed uterus, brownish postmenstrual spotting may be seen due to retention of menstrual blood in the deficient scar or upper uterine body, respectively.

Both cyclical and acyclical bleeding may coexist in a few conditions, for example, endometrial malignancy and AV malformations (this is a rare condition, and diagnosis has been discussed on Chap. 13), etc.

In patients with a thickened endometrium, possibilities include endometrial polyp, endometrial hyperplasia and endometrial carcinoma. The ultrasound features and their differentiation are discussed in Chap. 4.

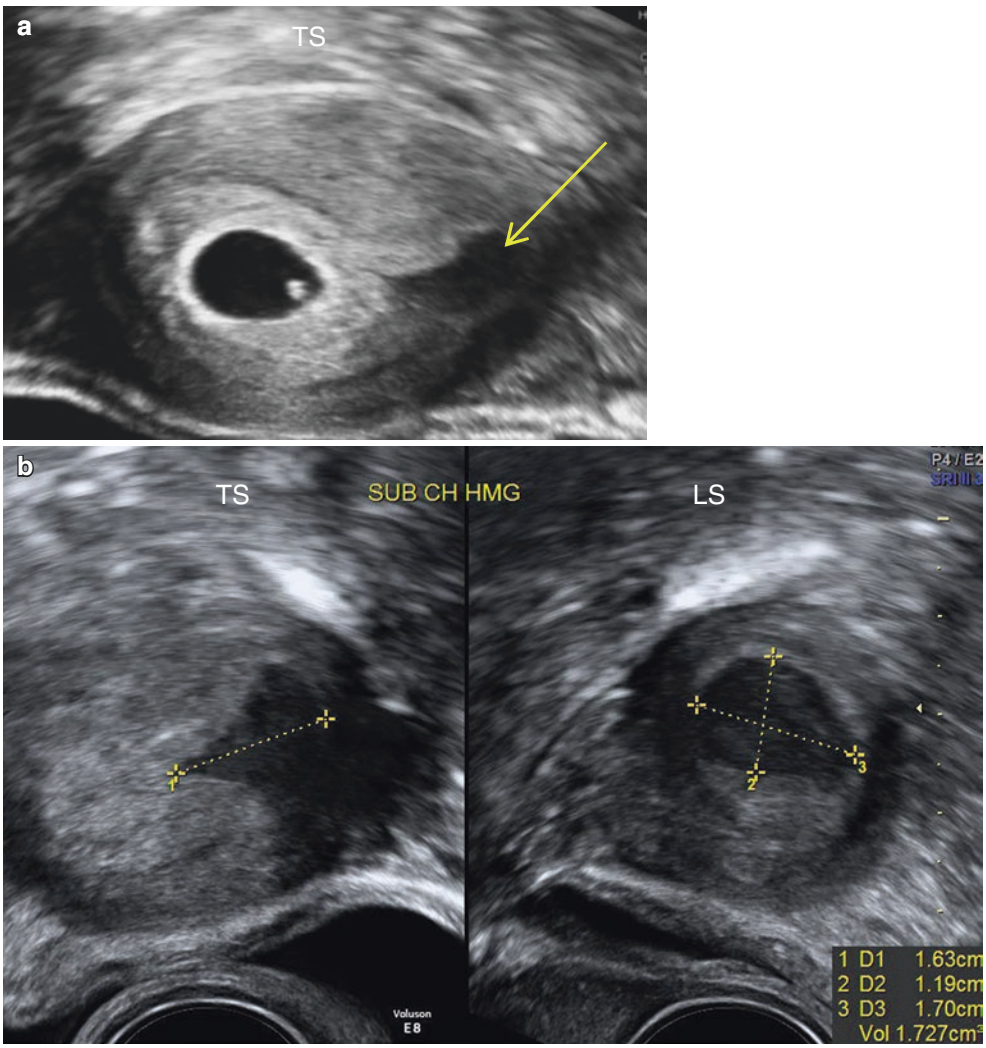

Fig. 14.1 A six-week live pregnancy, in a patient presenting with pain and bleeding. (**a**) Uterus with a gestational sac and subchorionic haemorrhage (*arrow*). (**b**) Subchorionic haemorrhage measured

Summary of Abnormal Uterine Bleeding

- History: particularly menstrual history and history of hormonal intake are important.
- Complaints: details of presenting complaint is important – whether it is cyclical or acyclical or intermenstrual or post-coital. Brownish flow indicates discharge of old collected blood.
- Rule out pregnancy: an important cause in women of reproductive age group, particularly with unscheduled bleeding.
- Per speculum examination is important in diagnosing local, cervical and vaginal pathology.
- Ultrasound is the diagnostic modality of choice, particularly TVS.
- Previous reports may be helpful in diagnosis.
- Beyond the age of 40: think of the possibility of malignancy.
- When in doubt, call the patient back for review.
- Discussing with the referring gynecologist often helps in appropriate management.

14.2 Pelvic and Adnexal Masses

Pelvic and adnexal masses may arise from the uterus, ovary, tubes and a few other structures, both gynecological and non-gynecological. These patients may at times come with a history of abdominal distention, abdominal mass or pain. Most often, however, the mass is detected or suspected by the clinician on examination of the patient. Pelvic masses which are small can be felt on bimanual examination. Large masses, however, may be felt abdominally.

Ultrasound is the modality of choice for investigating these masses. TVS is ideal and is more accurate in evaluating these masses, not only because of better assessment of their morphology and Doppler flows, but also because TVS is interactive and one can move structures, which helps in knowing their origin, the presence of adhesions, tenderness, etc. TAS is more informative for large masses extending above the true pelvis and in those cases where visualisation may be suboptimal due to fibroids in lower corpus or cervix. Ideally, as mentioned throughout the book, a TAS and TVS should both be done in all cases.

For adnexal masses, the terminology used to describe the morphology of the masses should be based on the IOTA recommendations. In addition, the IOTA consensus group has come out with methodologies to help assess the nature of the mass, particularly whether it is likely to be benign or malignant. This includes a three-step strategy, logistic regression models LR1 and LR2 and the ADNEX model (details of the LR1, LR2 and ADNEX models may be obtained from the references).

The most common of these masses (particularly an adnexal mass) is of ovarian origin. Therefore, whenever one sees an adnexal mass, the first question that one needs to consider is whether it is of ovarian origin (Fig. 14.2). This can be assessed as follows:

- Ovaries or ovarian tissue are identified very easily in women of reproductive age group by the presence of small cystic spaces within, i.e. the follicles (both developing and antral follicles). In postmenopausal women with atrophic ovaries, it is more challenging because follicles are not seen.
- If both the ovaries are visualised separate from the mass, then it is of extra-ovarian origin.
- If the mass is seen lying beside the ovary and there is intervening tissue between the ovary and the mass, or if the ovary, on pressure with the TVS probe, can be seen moving away from the mass or sliding along the mass, then the mass is not of ovarian origin.
- If, on the other hand, the mass is seen lying beside the ovary but does not move away from the ovary on pressure, then it is likely to be an exophytic ovarian mass or an extra-ovarian mass adherent to the ovary. In these cases, deciding the site of origin can be challenging.
- If the ovarian tissue is seen stretched around the mass (or cyst) as if it were hugging it, then the mass is of ovarian origin. This feature of stretched out ovarian tissue along the walls of the mass is called the ‘crescent sign’.
- Sometimes, however, the mass is extremely large, and ovarian tissue may not be seen around it even when it is of ovarian origin. But in these cases, an ovary will not be seen separate from the mass.

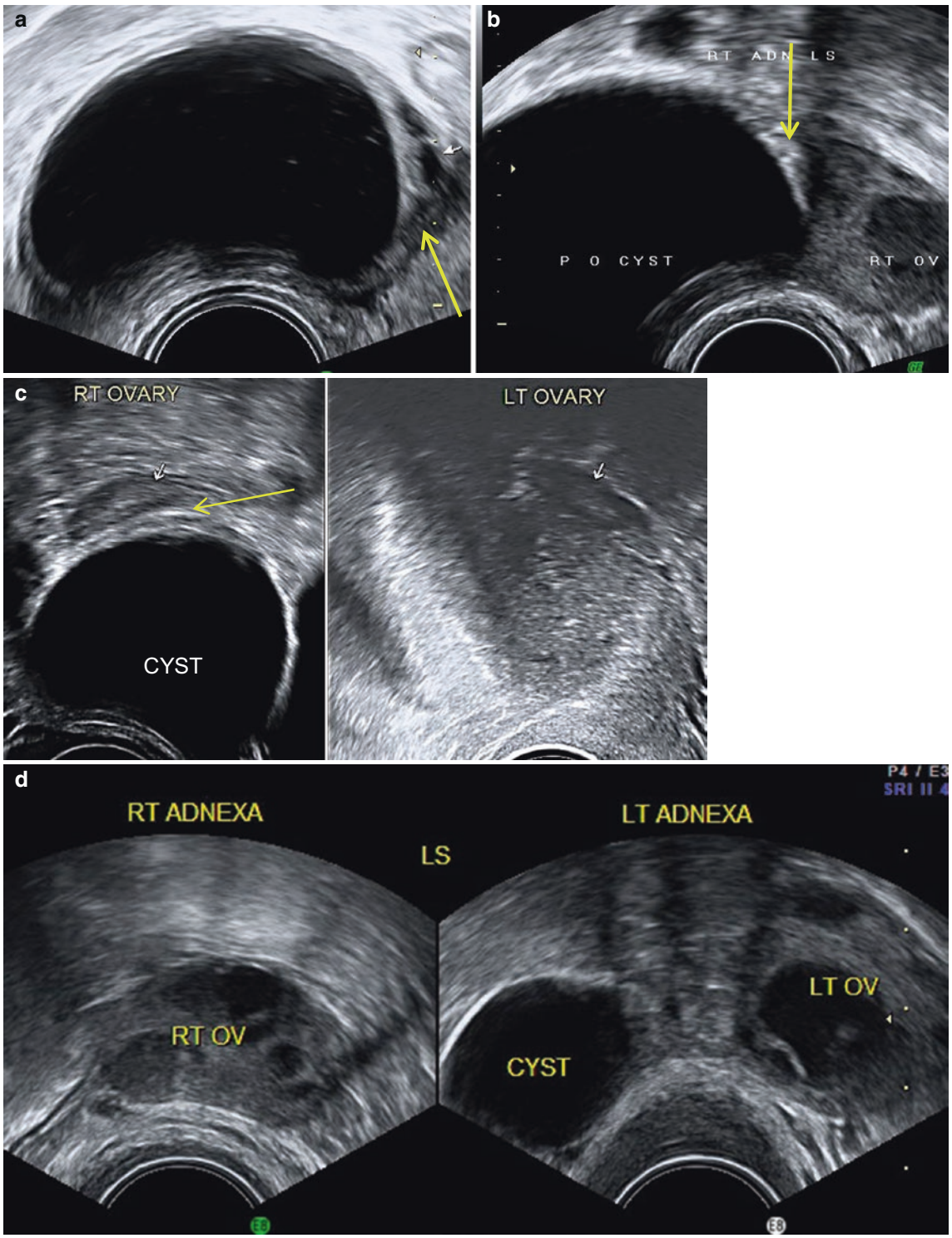

Fig. 14.2 Assessing ovarian origin. (**a**) Ovarian tissue (*arrow*) seen beside the cyst and stretched around it ('crescent sign') – suggesting ovarian origin. (**b**) Ovarian tissue seen beside the cyst, with a wedge of intervening external tissue (*arrow*) – suggesting that the cyst may not be of ovarian origin. This can be further checked by applying external pressure with the probe when one will be seen sliding along the other (positive sliding sign) or they may move apart (splitting sign). (**c**) Both ovaries (*small arrows*) seen separate from the cyst with some tissue (*long arrow*) between the right ovary and cyst – suggesting extra-ovarian origin. (**d**) Both ovaries seen distinctly with the left ovary and cyst far apart in the left adnexa – suggesting the cyst is not of ovarian origin

14.2.1 Ovarian Masses

Ovarian masses can be broadly classified into functional cysts, neoplastic masses, endometriomas and masses of inflammatory origin. The ovary may also be enlarged due to other conditions like torsion, hyperstimulation, polycystic ovaries, ovarian ectopic pregnancy, etc. All these conditions have been dealt with in detail in their respective chapters.

A rare cause for enlarged cystic ovaries is the *Van Wyk–Grumbach syndrome* (VWGS), a condition associated with juvenile hypothyroidism (of long standing duration and with high levels of TSH), delayed bone age and isosexual precocious puberty. These return to normal on thyroid hormone replacement. These patients have bilateral enlarged multicystic ovaries secondary to stimulation of the gonadal FSH receptor by TSH, resulting in multiple follicular cysts. Histopathological analysis of resected ovaries showed cystic follicles and little, if any, luteinisation. Some reports have suggested myxoedematous infiltration of the ovaries. Awareness of this condition is important because of the high probability of this being diagnosed wrongly as a case of bilateral neoplastic ovaries with inadvertent surgical excision (in a young girl and one that can be treated with simple thyroid replacement). In the case described below, preoperative blood workup picked up the high TSH levels and led to the diagnosis (Fig. 14.3).

14.2.2 Uterine Masses

An enlarged uterus presenting as a pelvic mass may be seen in both adenomyosis and fibroids. In adenomyosis, of course, the uterus is usually globular in shape, with distinctive features making diagnosis very simple. With fibroids, the uterus may be irregularly enlarged or there may at times be confusion about the origin of the mass. This is particularly so when the mass is a subserous/pedunculated fibroid. Fibroids have typical ultrasound features but can be confused with adnexal masses, particularly when they show degenerative changes. Fibroids are usually masses within the uterus, but the subserous pedunculated ones can be diagnosed to be of uterine origin by tracing their attachment to the uterus through a pedicle or blood flow. The pedicle may not be well seen unless there is surrounding fluid. Doppler flows are very helpful in assessing the origin of any mass as vessels are seen passing between the mass and the source of origin. Exceptions to this, of course, are true broad ligament fibroids or fibroids seen in cases with disseminated leiomyomatosis. In such cases, however, the ovaries will be seen separate from the mass.

Occasionally, in patients with unicornuate uterus, the adjoining rudimentary horn (particularly when non-cavitary) may present as an adnexal mass, but these masses are attached to the main uterine body and their echotexture is similar to that of the myometrium (Fig. 14.4).

14.2.3 Tubal Masses

The normal fallopian tube is difficult to identify, unless it is surrounded by fluid. It appears as an elongated undulating isoechoic or hyperechoic structure. Tubal masses may be of inflammatory or neoplastic nature or secondary to a tubal ectopic pregnancy. These have been dealt with in their respective chapters. Tubal masses may be seen continuous with the uterine cornua, but often they are not, because the pathological segment of the tube is away from its attachment to the uterus. The distal part of the tube has a broader lumen, and most collections (hydrosalpinx, pyosalpinx or haematosalpinx) are, therefore, seen at its distal end. Cystic tubal masses are generally easy to identify because of their elongated shape and incomplete septa.

14.2.4 Tubo-ovarian Masses

Tubo-ovarian masses are typically secondary to PID. At times, one may be able to differentiate between the tubal and ovarian component; however, often (like in some tubo-ovarian abscesses) this may not be possible. These have been dealt with in the section on PID in Chap. 9.

14.2.5 Paraovarian Masses

These are typically cystic masses seen in the adnexa separate from the ovary. Occasionally, they may be adherent to the ovary, when distinguishing them from an exophytic ovarian cyst can be challenging. They are usually small, unilocular and anechoic but can be large, septate and even undergo torsion. They have been dealt with in the section on paraovarian cysts in Chap. 9.

14.2.6 Pseudoperitoneal or Peritoneal Inclusion Cysts

Pseudoperitoneal cysts are nothing but areas of loculated fluid with adhesions. They may be secondary to chronic infection, endometriosis or previous surgery. They can pose a diagnostic challenge in a patient in whom ovarian cystectomy or ovariotomy has been done for a neoplastic ovarian cyst, where these may be considered as a recurrence of pathology. This has also been dealt with in Chap. 9.

14.2.7 Pelvic Hematomas and Pelvic Abscess

These may be seen to be associated with ectopic pregnancies or infection. They may present as pelvic masses when localised to an area. These are avascular masses, and correlation with other findings helps in diagnosis.

14.2.8 Non-gynecological Masses (Fig. 14.5)

These are rarely seen and most often are either appendicular masses or malignant masses arising from the small or large intestine (e.g. gastrointestinal stromal tumour of the small bowel and anorectal masses). The ovaries are seen distinct from these masses, and they do not originate from the uterus (i.e. no flow is seen between the uterus and the mass).

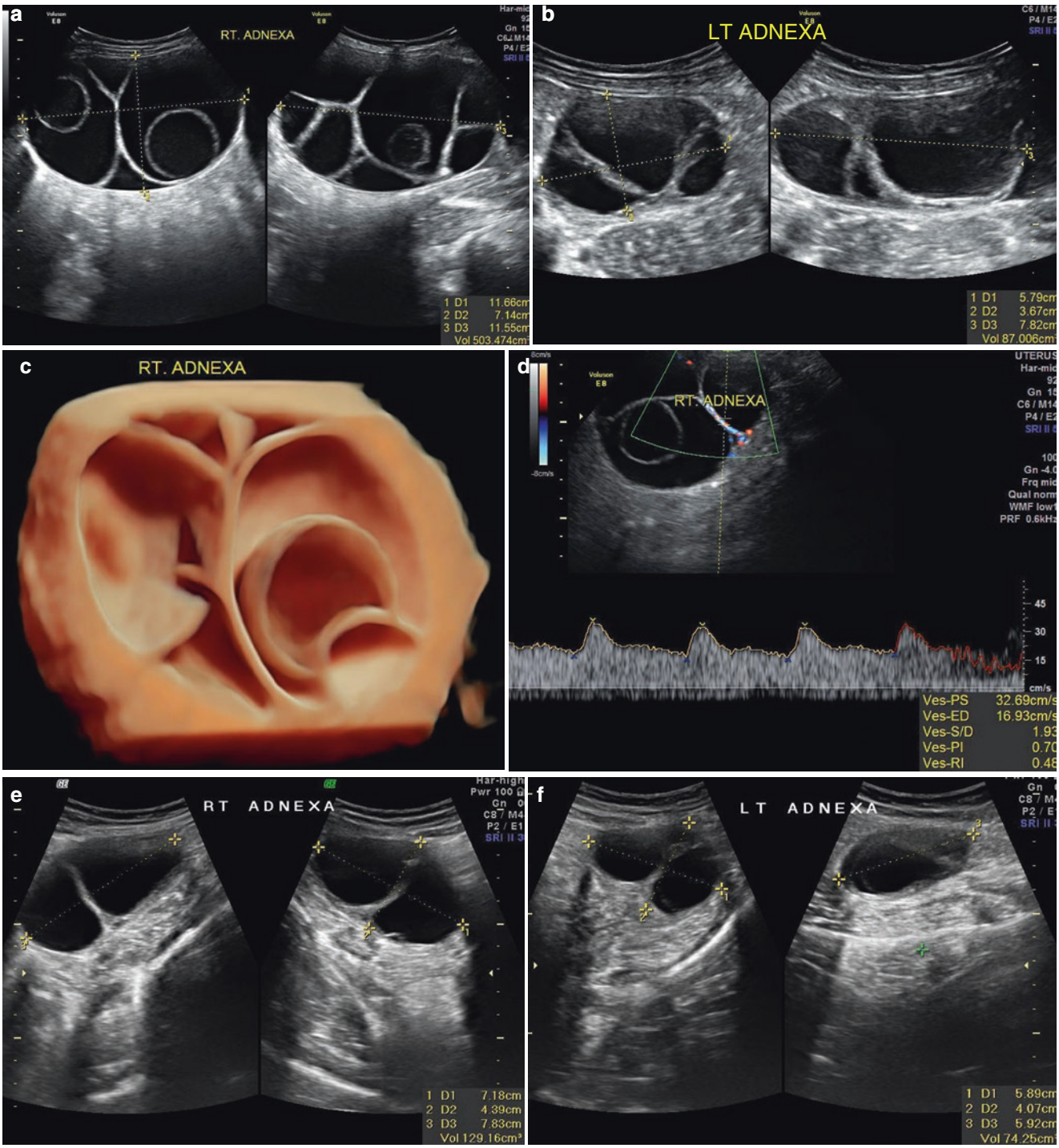

Fig. 14.3 Van Wyk–Grumbach syndrome – Bilateral multicystic enlarged ovaries with a very high TSH level of 1980 micIU/ml in a 14-year-old girl with short stature, who presented with the complaint of irregular periods. Both ovaries were enlarged and multicystic. (**a**) Right ovarian volume – 503 ml. (**b**) Left ovarian volume – 87 ml. (**c**) 3D-rendered image showing multiple locules. (**d**) Flow in septa with RI of 0.48. (**e**, **f**) Six weeks after thyroid replacement treatment, the ovaries had reduced in size with lesser number of locules – the right ovarian volume was 129 ml and the left ovarian volume was 74 ml

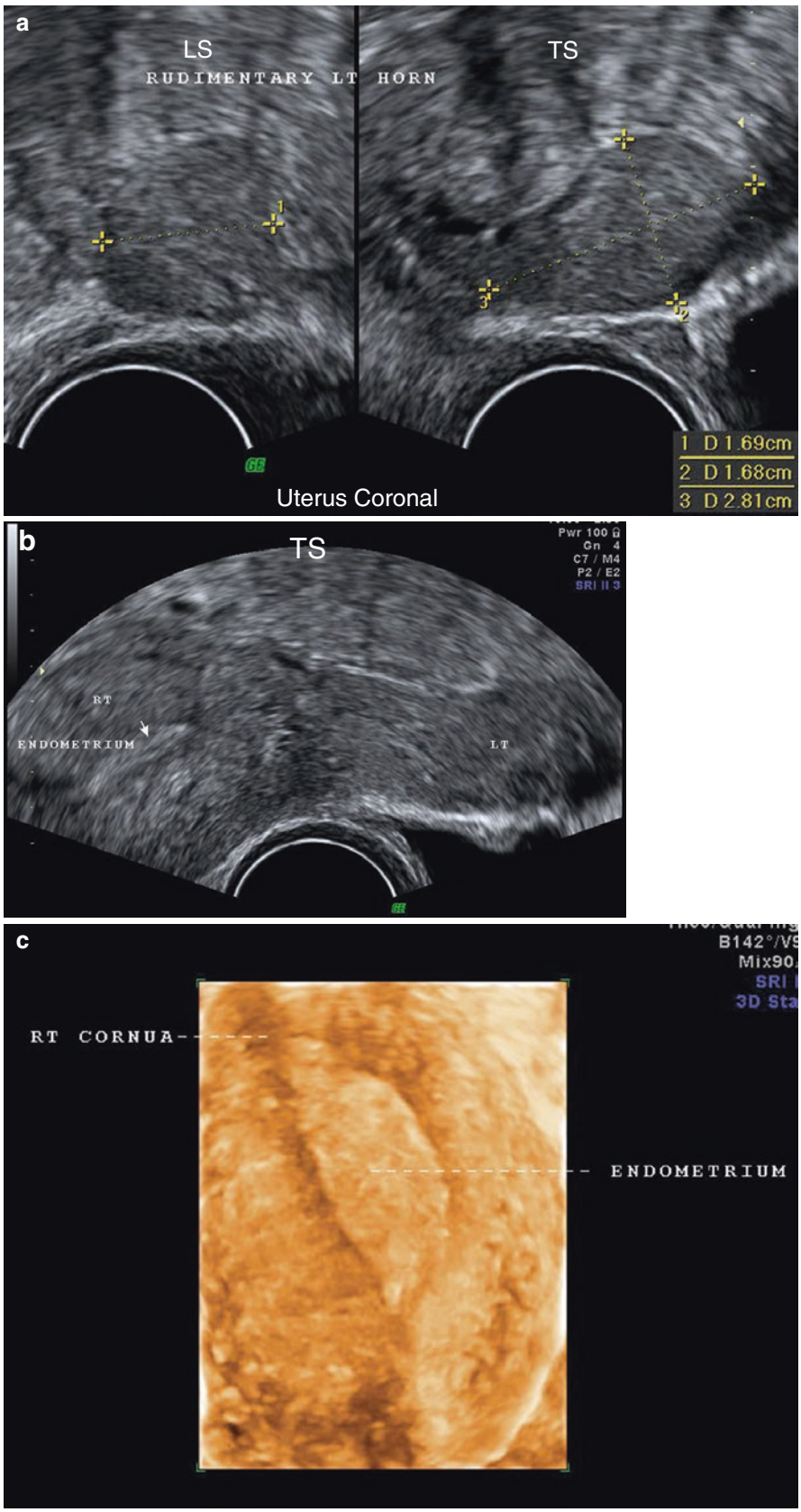

Fig. 14.4 Rudimentary horn presenting as an adnexal mass. (**a**) Well-defined, isoechoic mass seen in the left adnexa, raising the suspicion of a solid adnexal mass. (**b**) This mass, on further evaluation, was found to be connected to the main uterine body of a right-sided unicornuate uterus. (**c**) 3D-rendered image of the unicornuate right uterus

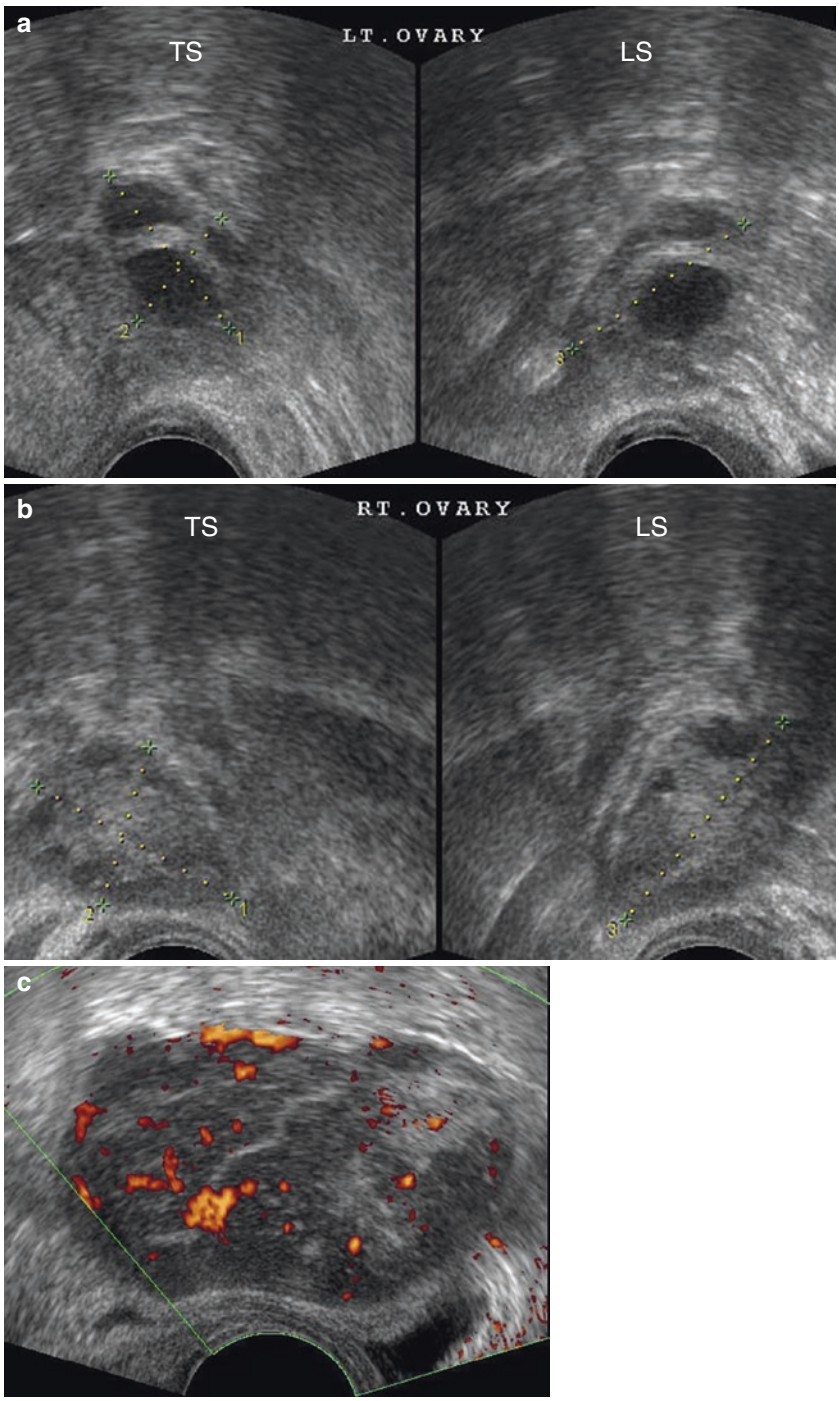

Fig. 14.5 Non-gynecological mass in a 36-year-old patient treated for papillary carcinoma of the thyroid 4 years prior to scan. Patient presented with abdominal pain. (**a**) Normal left ovary. (**b**) Normal right ovary. (**c**) Right sided adnexal mass which is solid, heterogeneous, lobulated and has septae. The mass shows high vascularity. It had no connection with the uterus or ovaries on greyscale or on Doppler. This raised suspicion of a non-gynecological malignant mass. *HPE:* gastrointestinal stromal tumour of the jejunum

14.2.9 IOTA Recommendation for Evaluation of Persistent Adnexal Masses

Chronic adnexal masses are to be described and evaluated based on the IOTA guidelines (which has been discussed in detail in the chapter on ovarian masses). The IOTA consensus group has come out with a methodology to help assess the nature of persistent adnexal masses, particularly to investigate whether they are likely to be benign or malignant. This includes a three-step strategy, logistic regression models LR1 and LR2 and the ADNEX model (details of the LR1, LR2 and ADNEX models may be obtained from the references suggested at the end of the chapter). The three-step strategy is discussed below.

Prior to the three-step strategy for evaluating the nature of adnexal masses, we need to know and understand the simple rules and simple descriptors as provided by the IOTA consensus group.

14.2.9.1 Simple Rules (Figs. 14.6 and 14.7)

The IOTA group has come up with simple rules that help in differentiating between malignant and benign masses.

Malignant

- Ascites (fluid outside POD)
- Irregular solid tumour (80 % or more appears solid)
- At least four papillary structures*
- Irregular multilocular solid with largest diameter of 10 cm or more
- Strong blood flow – colour score 4

**When in doubt about the number of papillae particularly when they appear to merge with one another, it is recommended that the worst-case scenario should be applied. For example, if there is a doubt of 3–5 papillae, it is better to consider it as 5.*

Benign

- Unilocular (no solid areas)
- Unilocular solid with the largest diameter of the solid area less than 7 mm
- Acoustic shadowing
- Smooth multiloculated mass less than 10 cm
- No blood flow – colour score 1

- If one or more malignant features are seen and no benign feature is seen, the mass is considered malignant.
- If one or more benign features are seen and no malignant feature is seen, the mass is considered benign.
- If one or more features of both benign and malignant are noted, the nature of the mass is considered inconclusive.
- If no features of either benign or malignant are noted, the nature of the mass is also considered inconclusive.

Using this method, about 77 % of masses can be categorised as benign or malignant, with a specificity of 96 % and sensitivity of 92 %. In the remaining 23 % that cannot be categorised, the options are to further evaluate with CA 125 levels or obtain a subjective opinion of an expert. Another option is to simply consider these masses as malignant since about half of them (47 %) do turn out to be malignant.

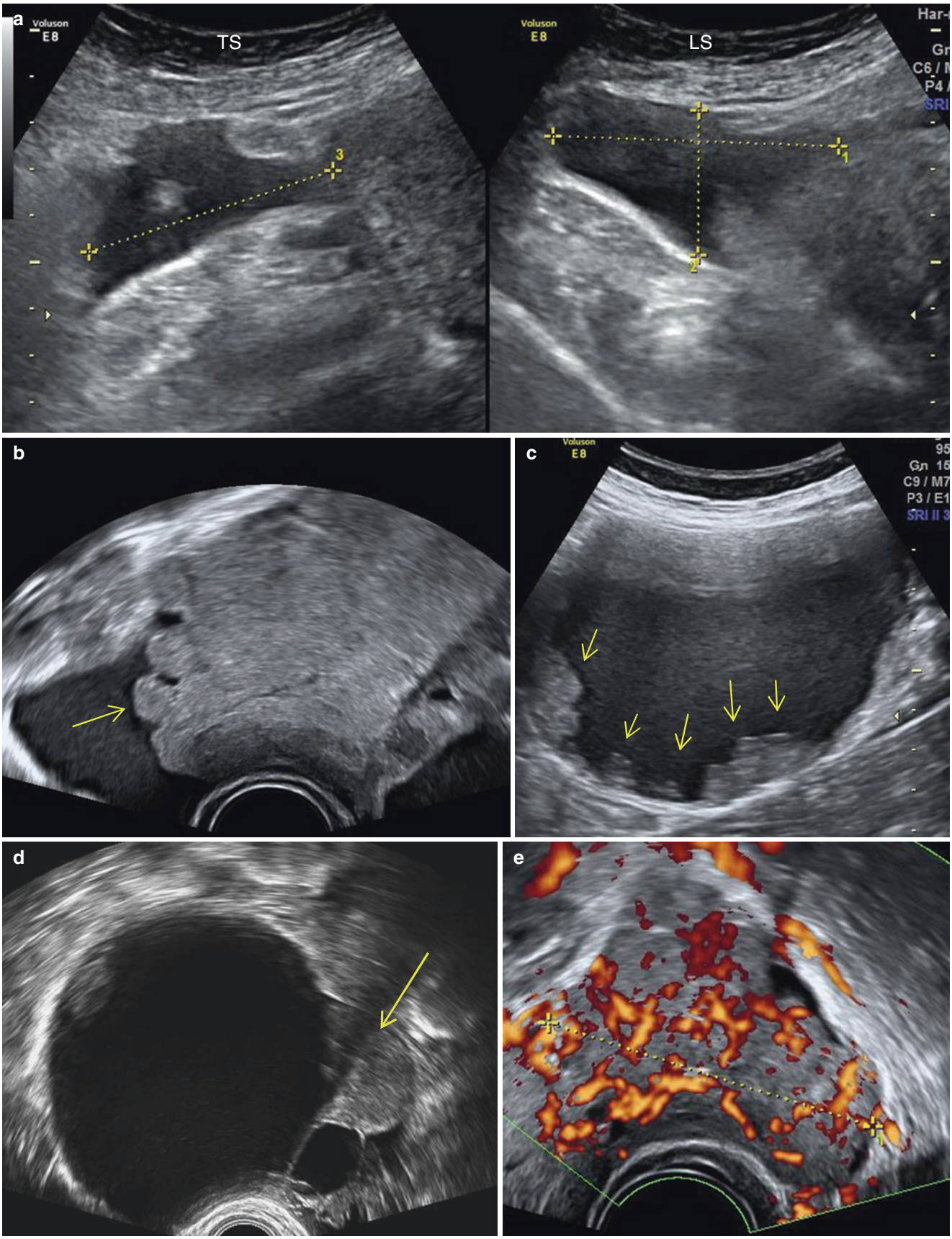

Fig. 14.6 *Simple rules for malignancy*: (**a**) Ascites (fluid outside POD) with fluid in LIF. (**b**) Irregular solid tumour (80% or more appears solid). *Arrow* showing its irregular margins. (**c**) At least four papillary structures in the mass. (**d**) Irregular multilocular solid mass with largest diameter of 10 cm or more (this tumour was 13.3×9.8×12.0 cm). The *arrow* pointing at the solid component. (**e**) Strong blood flow – colour score 4

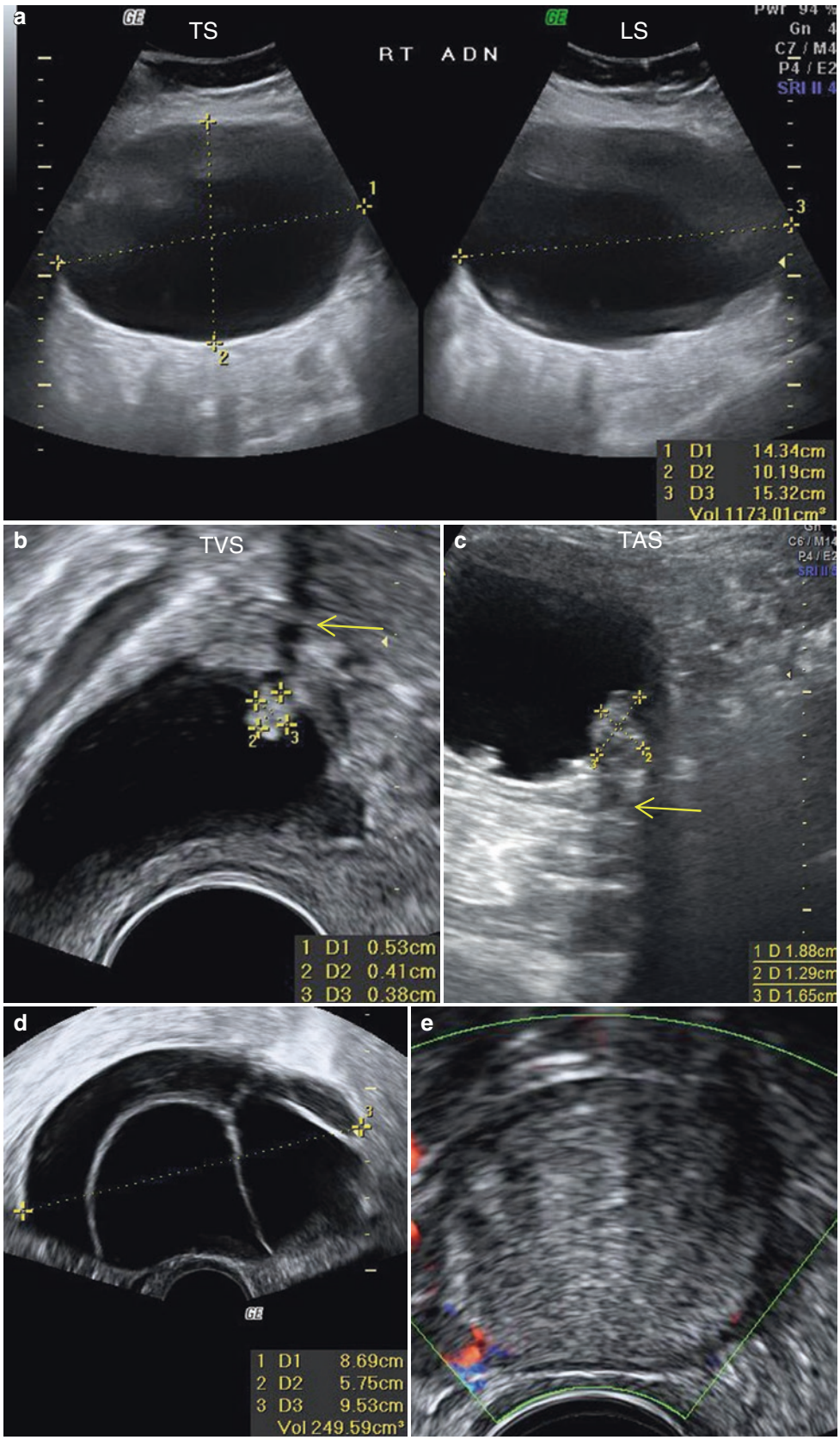

Fig. 14.7 *Simple rules for benign masses*: (**a**) Unilocular cyst (no solid areas). (**b**) Unilocular solid cyst with the largest diameter of solid area less than 7 mm. Here the solid papilla measured 5×4×3 mm and showed acoustic shadowing (*arrow*). (**c**) Presence of acoustic shadowing (*arrow*) – from a papilla of larger than 7 mm (*arrow*). (**d**) Smooth multiloculated mass less than 10 cm. (**e**) No blood flow – colour score 1

14.2.9.2 Simple Descriptors (Figs. 14.8 and 14.9)

There are, however, some masses that have such typical features that they are easy to classify and do not require the above methodology to categorise them as benign or malignant. These features have been termed 'simple descriptors' and show sensitivity and specificity of 98 % each.

Benign Simple Descriptors

- Unilocular ground glass cyst in premenopausal women (suggestive of an endometrioma)
- Unilocular cyst with mixed echogenicity and aoustic shadowing in premenopausal women (suggestive of a dermoid)
- Unilocular anechoic cyst of less than 10 cm with regular walls (suggestive of a benign cystadenoma)
- Remaining unilocular cysts with regular walls (probably physiological, e.g. a haemorrhagic cyst)

Malignant Simple Descriptors

- Postmenopausal women with ascites, and at least moderate flow (colour score of 3–4)
- Women aged more than 50 with a CA 125 level of more than 100 IU/mL

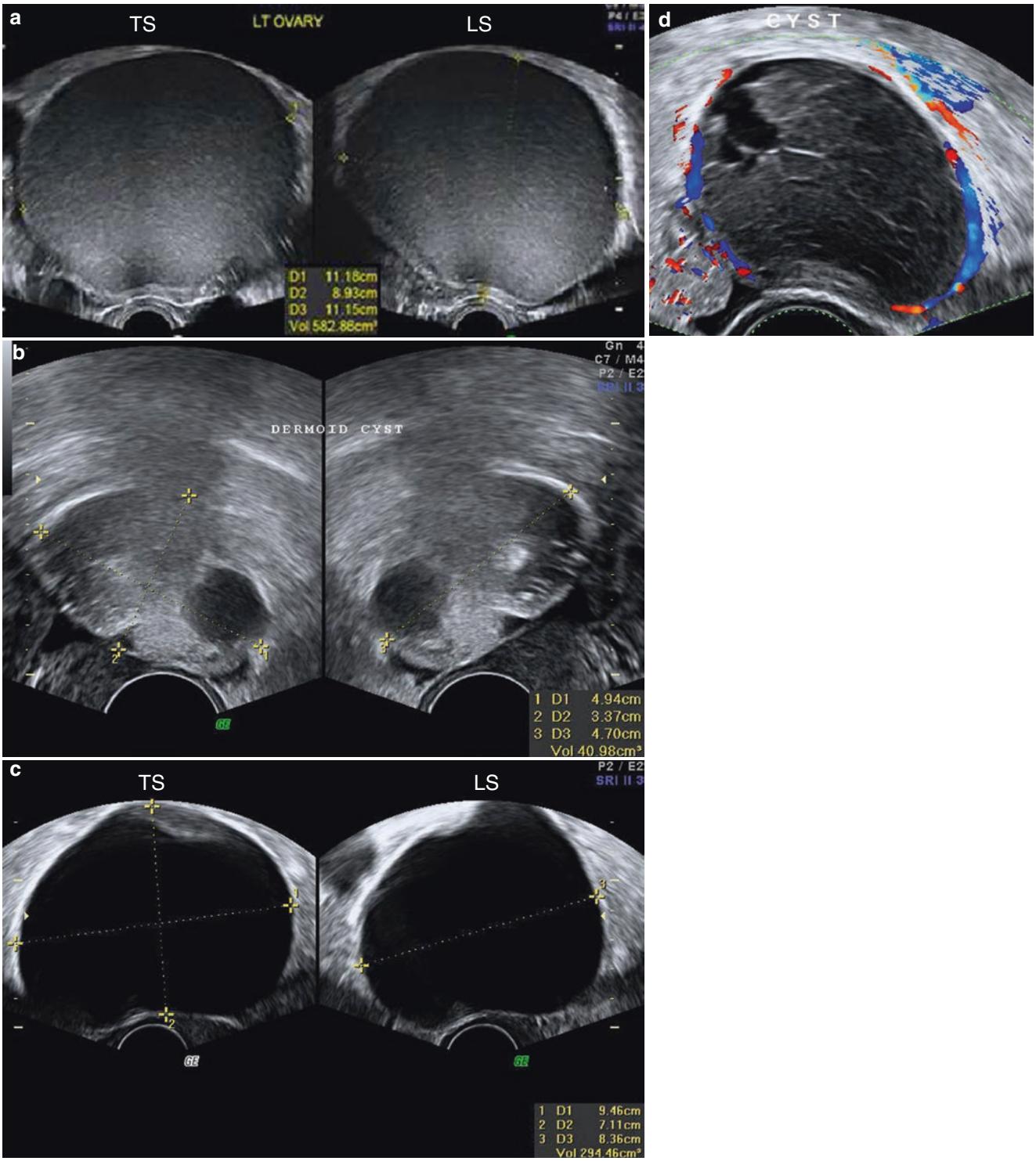

Fig. 14.8 *Benign simple descriptors*: (**a**) Unilocular ground glass cyst in premenopausal women (suggestive of an endometrioma). (**b**) Unilocular cyst with mixed echogenicity and acoustic shadowing in premenopausal women (suggestive of a dermoid). (**c**) Unilocular anechoic cyst of less than 10 cm with regular walls (suggestive of a benign cystadenoma). (**d**) Remaining unilocular cysts with regular walls (suggestive of a haemorrhagic cyst)

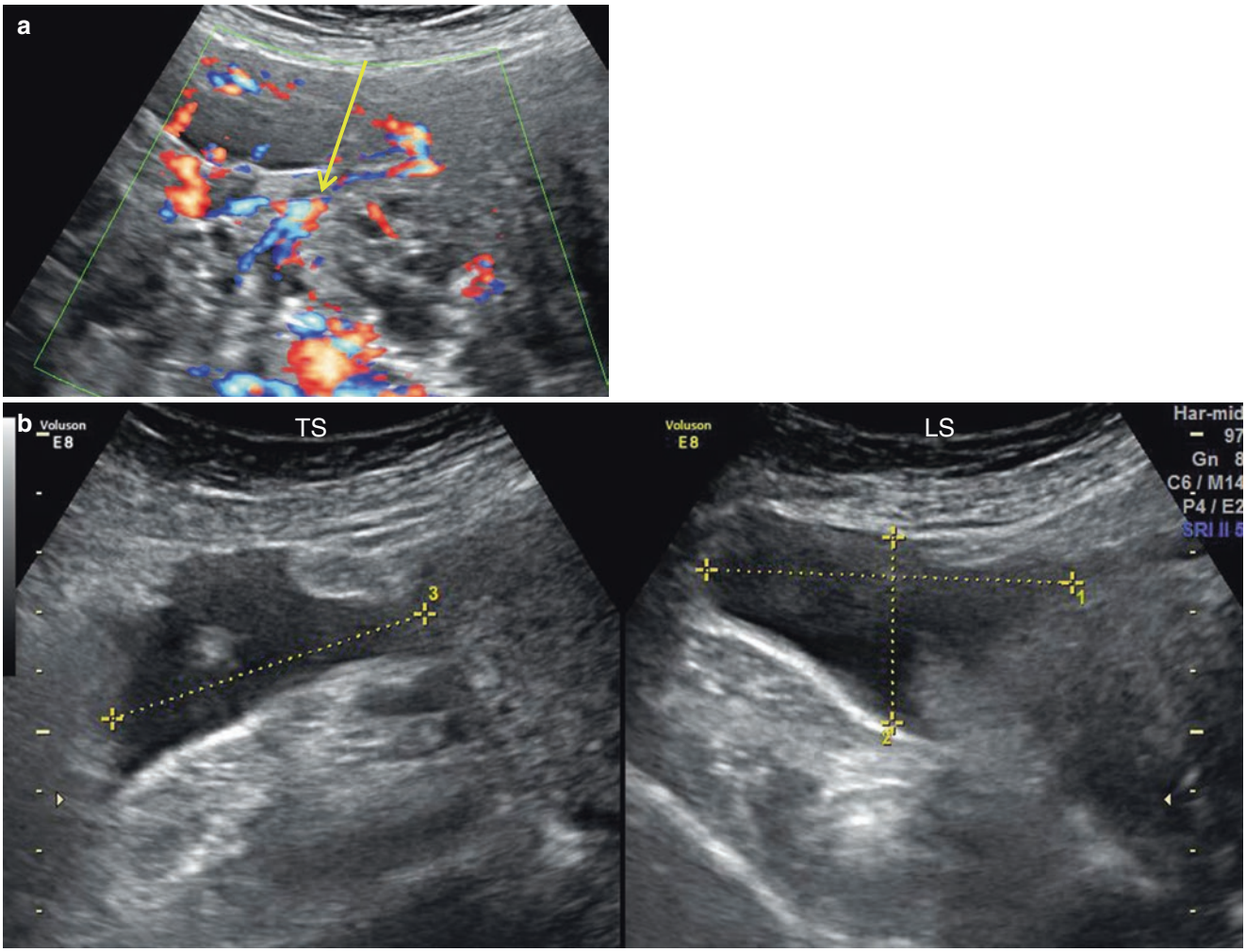

Fig. 14.9 *Malignant simple descriptors*: Postmenopausal woman (59 years) with (**a**) ascites and (**b**) at least moderate flow (colour score of 3–4) – seen in the solid component (*arrow*) of a mucinous cystadenocarcinoma

14.2.9.3 Three-Step Strategy for Evaluating the Nature of Persistent Adnexal Masses (Ameye et al. 2012)

Step 1: Simple Descriptors

Simple descriptors are used for easy, instant diagnosis. The nature of the mass can be determined using these in about 47 % of cases.

Step 2: Simple Rules

The rest of the masses are assessed using simple rules to predict whether they are benign or malignant. In this manner, another 34 % can be categorised.

Step 3: Subjective Assessment by Expert

The remaining 19 % of cases are subjected to assessment by an expert examiner (other options include CA 125 estimation or MRI, or the mass is simply assumed to be malignant).

Please Note: For all of us to improve our expertise, it is suggested that we read up journal articles for rare adnexal masses (e.g. UOG series – Imaging in Gynaecological Disease). It is also important to follow up all difficult and atypical cases with surgical findings, discharge summaries, macroscopy and histopathology.

While reporting adnexal masses, the morphology should be described using standard terminology. In some cases, the exact pathology can be ascertained, while in others our impression of the type of pathology must be provided – physiological, inflammatory, endometriotic, neoplastic (benign or malignant).

Summary: Pelvic/Adnexal Masses

- History: clinical findings and previous reports are essential, as they may help in diagnosis.
- The morphology of the mass must be described using standard terminology (as suggested by IOTA).
- Blood flow in the mass should be assessed with optimised Doppler settings.
- Structure of origin is to be assessed by looking for the ovaries, ovarian tissue along the mass or Doppler flows from the mass to its source of origin.
- Exact pathology may be possible in some conditions like a tubal ectopic pregnancy, dermoid, pedunculated fibroid, etc.
- In the others, our impression of the type of pathology must be mentioned, i.e. whether it is physiological, inflammatory or neoplastic.
- The mass should be assessed as malignant or not, if possible. If not, it should be mentioned in the report. IOTA guidelines help in assessing whether the mass is benign or malignant.
- Further investigations like BhCG, CA 125 and MRI, if required, should be suggested in the report.

14.3 Acute Pelvic Pain

Acute pelvic pain can be associated with both gynecological and non-gynecological pathologies. In this chapter, gynecological causes for acute pelvic pain have been discussed. For practical purposes, the cases with acute pelvic pain are grouped into various categories. The details of diagnosis by ultrasound features are dealt with in their respective sections:

1. *Pain associated with pregnancy* – Here the patient may give a history of amenorrhoea. UPT may be positive or serum BhCG may be elevated. In some cases, however, the patient may present without knowing that she is pregnant, and an ultrasound scan is likely to provide evidence of an intrauterine or an extrauterine pregnancy:
   (a) Threatened or inevitable abortion (intrauterine pregnancy or GS seen on scan).
   (b) Incomplete or complete abortion – The patient usually gives a history of heavy bleeding, and retained products of conception may be seen on scan.
   (c) Ectopic pregnancy – Pain here may or may not be severe. Other than the ectopic pregnancy mass, the scan may show blood in the pelvis or general abdominal cavity. The patient may present with hypovolaemic shock, if internal bleeding is heavy.
2. *Pain associated with periods* – This is also known as dysmenorrhoea. These patients typically give a history of recurrent pain occurring cyclically during periods. Common causes that can be diagnosed on ultrasound are:
   (a) Endometriosis including extra-ovarian endometriosis. The pain in endometriosis is typically congestive with associated backache. The pain tends to persist even after periods. Depending on the site of deep infiltrating endometriosis, the patient may complain of dysuria (painful micturition), dyspareunia (painful intercourse), dyschezia (painful defecation), etc. Deep infiltrating endometriosis is a condition which causes pain, but diagnosis is often missed or delayed (discussed in detail in Chap. 8).
   (b) Submucous fibroid or fibroid polyp – Along with dysmenorrhoea, these patients also complain of abnormal uterine bleeding.
   (c) Adenomyosis – These patients in addition to dysmenorrhoea may complain of menorrhagia.
   In some patients suffering from dysmenorrhoea, particularly adolescents, no pathology may be noted on ultrasound.
3. *Pain associated with ovulation* – Pain here is typically mid-cycle and more pronounced on one side:
   (a) Ovulation pain *(mittelschmerz)* – Ovulation itself could be a cause for pain. It is generally not severe, is one sided, lasts for a few hours and may be associated with mid-cycle spotting. The patient may give a history of similar mid-cycle pain in the past. On ultrasound, evidence of ovulation may be noted (corpus luteum and minimal fluid in the POD).

   The author has noticed that many of the patients with significant ovulation pain are found, on scan, to have their ovaries just under the anterior abdominal wall (not adherent, but placed in close association with the anterior abdominal wall). In such cases, often the patient can actually point to the area of pain. The ovary is seen at that site and is tender to touch on transabdominal scan. On applying pressure with the probe, the patient also mentions that it is exactly like the pain she has been experiencing.
   (b) Corpus luteal haemorrhage – Occasionally, there may be haemorrhage from a corpus luteum following ovulation. This may occur at ovulation or at some time thereafter. The pain may be severe and more pronounced on one side. On ultrasound, turbid fluid suggestive of blood is seen in the pelvis. Clots (avascular complex hyperechoic areas) may be seen suspended and floating in blood and surrounding the ovary which houses the corpus luteum, from which haemorrhage has occurred.
4. *Pain associated with infection* – These patients generally have associated fever and high white blood cell counts:
   (a) The most common gynecological cause is pelvic inflammatory disease (PID), which has been discussed in detail in Chap. 9. Here, ultrasound findings depend on the severity and the structures involved.
   (b) There are a few non-gynecological infections that could present with pain and fever – the common ones being appendicitis, cystitis, ureteric calculi and diverticulitis. The discussion and diagnosis of these are beyond the scope of this book. Briefly, however, in cystitis the patient will give a history of micturition and urine examination will give evidence of infection. In appendicitis (Fig. 14.10), the patient will have pain and tenderness in the right iliac fossa (McBurney's point), and on ultrasound an elongated tubular mass with a blunt end (inflamed appendix) may be seen in the RIF. In diverticulitis, features are similar to appendicitis, and when it is on the right side, it may be difficult to differentiate from appendicitis. In ureteric colic, the pain typically radiates from loin to groin, and an ultrasound is usually able to detect the ureteric calculus.
5. *Pain associated with pelvic or adnexal mass* – The common causes in this category include:
   (a) Torsion: Both ovarian and non-ovarian torsions (hydrosalphinx or paraovarian cysts) can present with severe acute pelvic pain or recurrent pain. Ultrasound diagnosis has been discussed in great detail in Chap. 10.

(b) Rupture of a cyst could be a rare cause of acute pelvic pain. Other than a corpus luteal cyst (Fig. 14.11), this may be seen with an endometriotic cyst (Fig. 14.12) or a malignant cyst.
(c) Degeneration of a fibroid is a rare cause of pain. In red degeneration, the fibroid is usually enlarged in size, avascular and tender.
(d) Ovarian hyperstimulation syndrome (OHSS): This is seen in patients with infertility undergoing ovulation induction. The ovaries are enlarged, are vascular and show multiple cysts. Free fluid is seen in the pelvis, or frank ascites may be noted. Occasionally, they may be associated torsion or haemorrhage.

Chronic pelvic pain is typically noted in women with endometriosis, pelvic inflammatory disease (PID) or malignant masses. In the case of malignancy, the pain is more often in the form of a chronic discomfort.

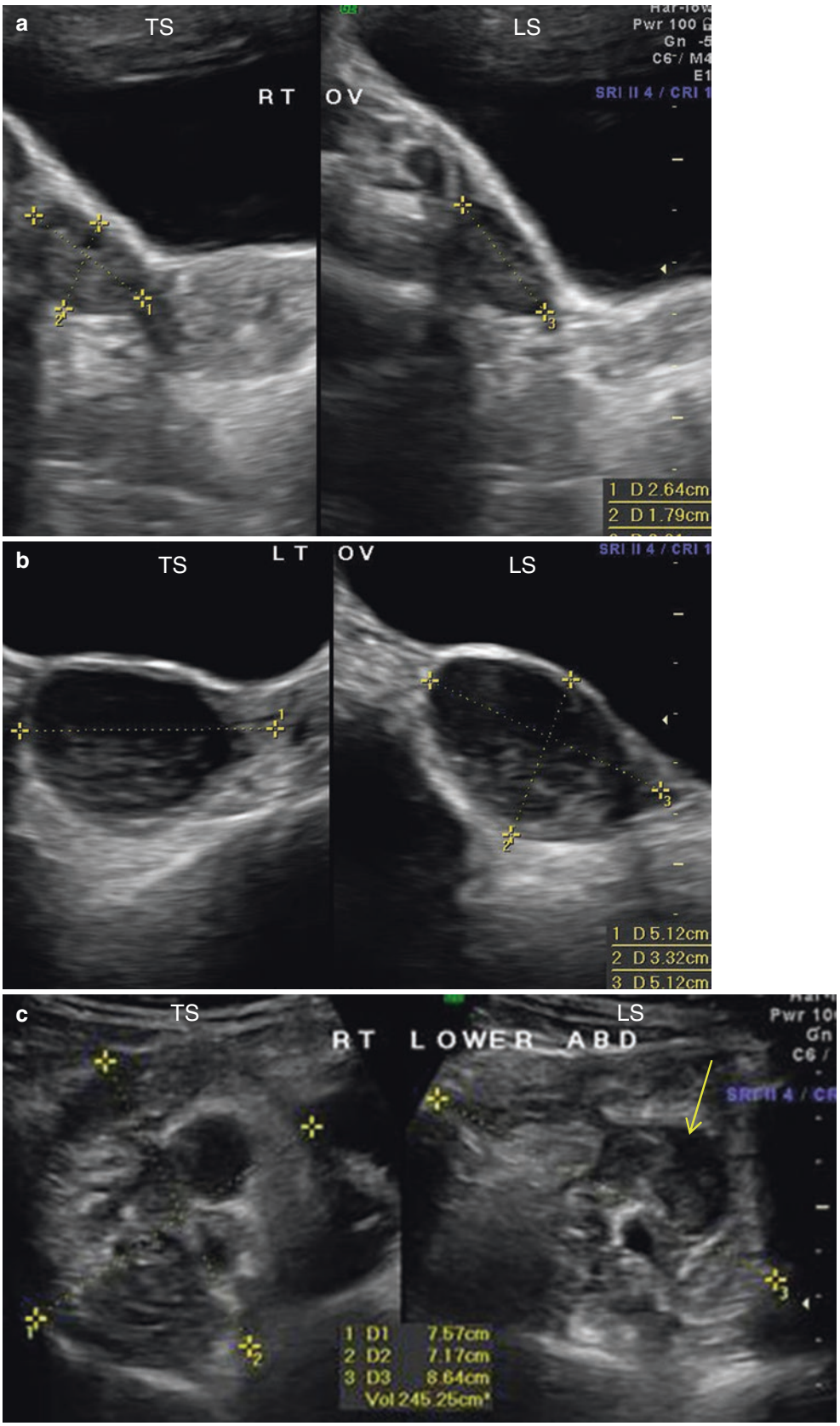

Fig. 14.10 A 15-year-old girl with 2 days of fever, lower abdominal pain and vomiting. Scan done elsewhere reported a left ovarian cyst with suspicion of torsion: (**a**) normal right ovary, (**b**) left ovary showing a haemorrhagic corpus luteum and (**c**) complex mass with turbid contents (*arrow*) seen in the right lower abdomen, which was tender. There was no evidence of torsion. *HPE:* appendicitis

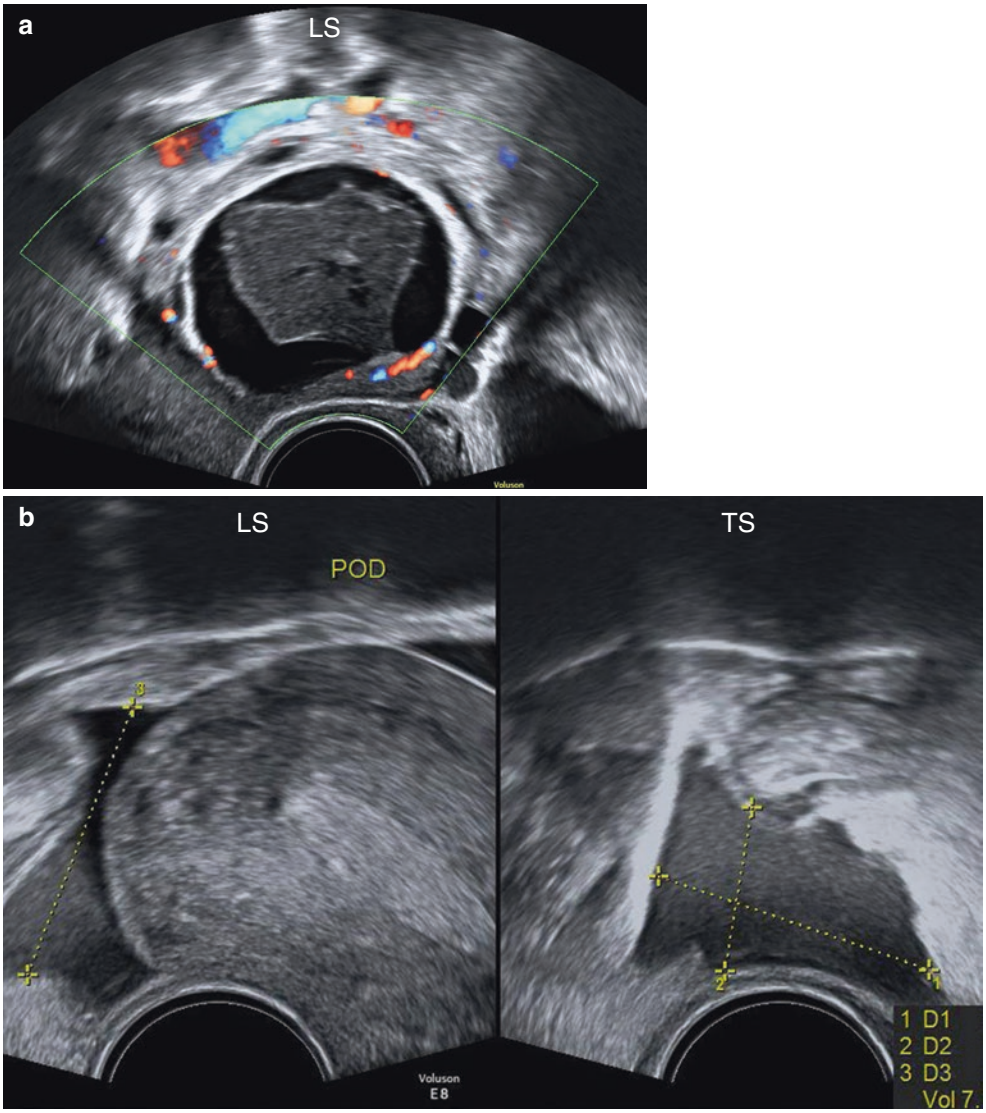

Fig. 14.11 Haemorrhage from a corpus luteum. (**a**) Haemorrhagic corpus luteum is seen showing a clot within and flow around its walls. Turbid fluid suggestive of blood is seen around the ovary. (**b**) POD on LS and TS showing turbid fluid, suggestive of blood. UPT was negative

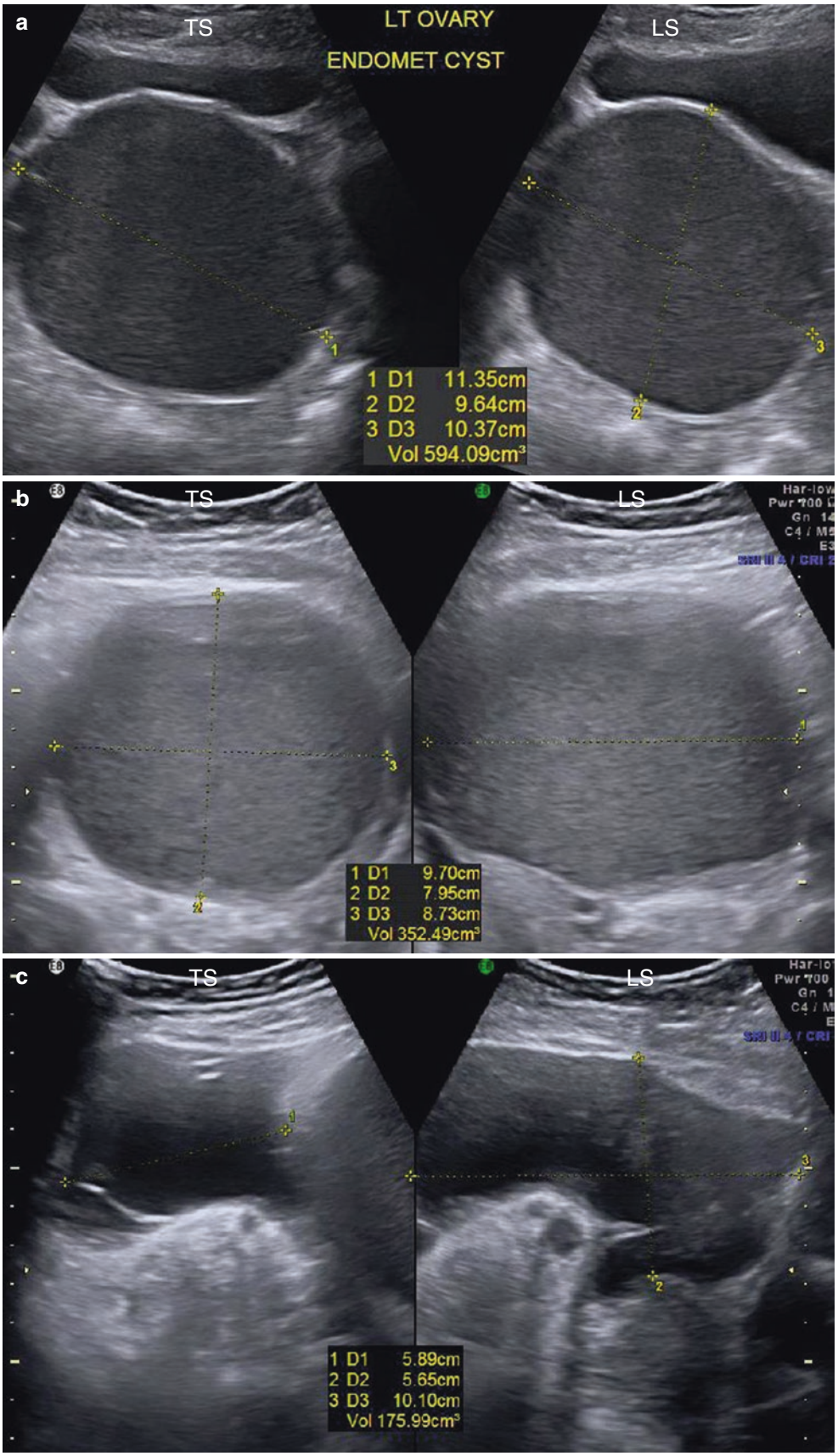

Fig. 14.12 Rupture of an endometriotic cyst. (**a**) A circumscribed left ovarian endometriotic cyst of volume 594 cc. (**b**) Patient returned 32 days later with severe abdominal pain. On examination, the cyst appeared more flaccid and the volume had reduced to 352 cc. (**c**) Turbid fluid suggestive of blood was seen in the abdomino-pelvic cavity. Rupture of the endometriotic cyst was confirmed at surgery

Summary of Pelvic Pain

- History is important in making a diagnosis, particularly menstrual history, details of pain (location, duration, intensity, triggering factors, etc.) and the presence of associated nausea, vomiting, bleeding, discharge and fever.
- Clinical examination, both abdominal and bimanual, may help in locating the site of tenderness and the presence of a mass.
- Ultrasound (TVS) is the diagnostic modality of choice, wherein one can not only see structures but also touch them to assess tenderness. In addition, it is non-invasive and easily available.
- Previous reports may help diagnosis by correlation with present findings.
- Appropriate investigations (UPT, BhCG, CBC, urine routine, etc.) should be suggested.
- Discussion with the clinician is important for appropriate and prompt management.

14.4 Locating the Pregnancy and Pregnancy of Unknown Location (PUL)

Once the patient presents with a positive pregnancy test, the next step is to confirm the pregnancy on ultrasound. The first question that arises is – when should ultrasound be done?

- If the patient is symptomatic with pain or bleeding, then an ultrasound scan is suggested at the time she presents with her symptoms.
- If the patient is a high-risk case (history of previous ectopic pregnancy, PID, infertility or IVF), then an early scan is suggested at 5–6 weeks of gestation or when BhCG is above 1000 or 1500 mIU/ml.
- In all other asymptomatic low-risk women, a scan is suggested at 7 weeks of gestation. This is because scans done prior to 5 weeks of gestation may not be able to locate an intrauterine or extrauterine pregnancy. Between 5 and 6 weeks, an intrauterine gestation may be seen, but its viability may be difficult to confirm. Even at 7 weeks, ultrasound may be inconclusive in up to 20–25 % of women (Bottomley et al. 2009).

When a scan is done, there are two types of ultrasound findings:

1. The ultrasound may be diagnostic if it is able to locate or provide evidence of an intrauterine or extrauterine pregnancy.
2. The ultrasound may be non-diagnostic if there is no evidence of an intrauterine or extrauterine pregnancy. These cases are defined as pregnancy of unknown location (PUL).

The possibilities therefore include:

- Intrauterine pregnancy (including missed abortion): The presence of an intrauterine pregnancy is reassuring that there is no extrauterine pregnancy, as heterotopic pregnancy is very rare. Once the BhCG levels reach 1000–1500 mIU/ml, an intrauterine gestation should be visualised on TVS. This level of BhCG is therefore called the 'discriminatory zone' (DZ). It is important to carefully search for an intrauterine sac, which is often missed when close to a cornua. When an intrauterine pregnancy is present with a yolk sac or fetal pole (with or without fetal heart), then the diagnosis is clear. However, if there is a tiny intrauterine sac, without a yolk sac or fetal pole, the dilemma may arise whether it is a true gestational sac or a pseudo-sac. The endometrium in the cases with ectopic pregnancy may show fluid collection, giving it the appearance of a gestational sac called the 'pseudo-gestational sac'. The differences between a true and pseudo-gestational sac are given as follows (Fig. 14.13):

True GS

- Eccentrically placed, lying within one layer of the endometrium
- Circular in shape
- Hyperechoic trophoblastic rim seen around the GS
- Doppler flow seen around the GS (Doppler studies are to be avoided in any case with suspected normal intrauterine pregnancy)

Pseudo-GS

- Located between the two layers of the endometrium
- Takes the shape of the uterine cavity
- No hyperechoic rim around it
- No Doppler flow around it

In addition, the endometrium undergoes decidualisation in an ectopic pregnancy where it appears thick and shows multiple tiny cystic spaces (Fig. 14.14). These are seen closer to the EMJ and should not be mistaken for a gestational sac:

- Retained products of conception: The patient may give history of bleeding or passing tissues. On ultrasound, retained products of conception typically appear as an area of complex echoes with flow within (details of which are available in the section on RPOC in Chap. 10). Unless one is sure of the diagnosis of RPOC, it may be safer to consider these patients as cases of PUL and follow them up.
- Complete abortion: A patient may give history of heavy bleeding with or without a history of passing tissues, but on scan there may be no evidence of intrauterine products of conception, suggestive of complete abortion. Unless there is a previous scan report suggestive of an intrauterine pregnancy, again it is safer to follow up these cases as is done in cases with PUL.
- Molar pregnancy: Here, along with the history of amenorrhoea and bleeding, the patient may give a history of passing vesicles. On ultrasound, the uterus is filled with an echogenic mass showing tiny cystic spaces. In the first trimester, findings may not be classic and may be similar to that of a case with missed abortion.
- Ectopic pregnancy: This has been discussed in great detail in Chap. 10. One must remember that not all patients are symptomatic with pain. Also, an ectopic pregnancy mass may exist with or without rupture, even with BhCG levels below the DZ. Knowledge of the spectrum of ectopic pregnancies is important in making a diagnosis. An ectopic pregnancy that is commonly missed is a cervical ectopic pregnancy. This is because most sonologists tend to search carefully primarily in the endometrial cavity and the

adnexa, neglecting the cervix. Heterotopic pregnancy can also get missed because it is rare, and visualisation of an intrauterine pregnancy is generally considered reassuring. However, in symptomatic patients and in those with ovulation induction and IVF, one must think of such a possibility and look at the adnexa carefully.

- Pregnancy of unknown location (PUL): As mentioned earlier, this implies that there is a positive biochemical pregnancy test (UPT or BhCG), but there is no evidence of any intrauterine or extrauterine gestation. Possibilities on follow-up of PUL cases are:
  - Intrauterine pregnancy – 30 to 50 %.
  - Ectopic pregnancy – 7 to 20 %. This risk of an ectopic pregnancy is the main issue that warrants close follow-up of patients with PUL.
  - Failing pregnancy (intrauterine or extrauterine) – 50 to 70 %.

Management of PUL: In haemodynamically unstable women or women with severe pain, a laparoscopy may have to be resorted to. In haemodynamically stable women with pain, one may either consider laparoscopy or monitor these patients closely with serum BhCG. In all other women, expectant management on an outpatient basis is considered adequate. These patients are however counselled about possible outcomes, need for regular follow-up and reporting, if there are any relevant symptoms. In these patients, a BhCG if not done earlier is done immediately and repeated after 48 hours. Based on the values, the patients are triaged into:

- BhCG rise of more than 66 % (high likelihood of an intrauterine pregnancy) – Scan is suggested a week later or once the BhCG is above the DZ.
- Falling BhCG levels – Any fall in BhCG suggests a failing pregnancy (intrauterine or extrauterine). This is again reassuring, and a BhCG may be repeated after a week or two.
- BhCG rise of less than 66 % – These are cases at a high risk of an ectopic pregnancy and need to be monitored closely with serial BhCG. A scan may be done a week after the initial scan or earlier if the patient is symptomatic.

Methotrexate may occasionally be considered for cases with persistent PULs, who are either not keen on pregnancy or are not compliant.

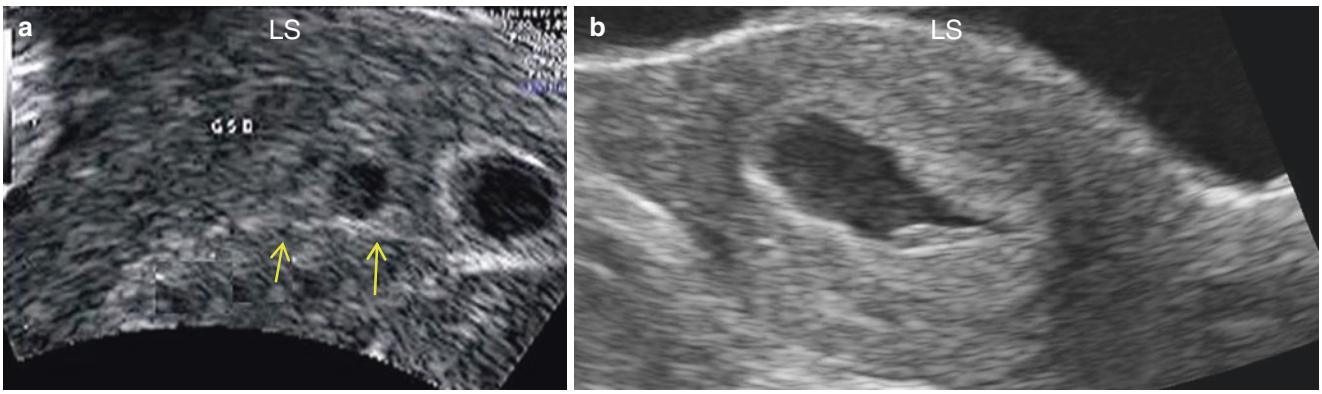

Fig. 14.13 GS: (**a**) Twin true gestational sacs in one wall of the endometrium. *Arrows* show endometrial midline. (**b**) Pseudo-gestational sac

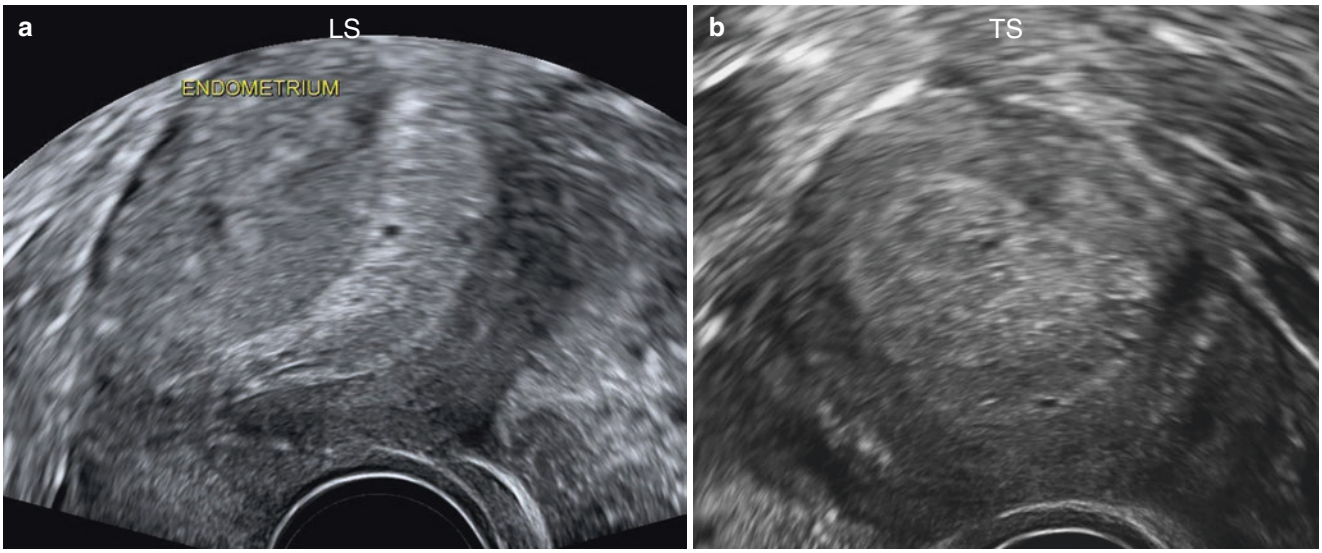

Fig. 14.14 Decidualised endometrium on (**a**) LS and (**b**) TS, showing tiny cystic spaces in the periphery of the endometrium close to the EMJ

Summary of Location the Pregnancy and PUL

- Proper attention must be given to history, symptoms and previous reports that may help in diagnosis.
- Transvaginal scan is indispensable in locating the pregnancy.
- In low-risk asymptomatic women, a scan should not be done prior to 7 weeks as it may be inconclusive.
- In patients with intrauterine pregnancy, it is important that one does not miss searching near the cornua. Missing an intrauterine pregnancy may result in medicolegal issues if the patient is treated with methotrexate, as is sometimes done in PULs or suspected ectopic pregnancies.
- To diagnose extrauterine pregnancy, a TAS prior to TVS improves pick-up. Search for an extrauterine pregnancy must be done thoroughly, and one must not forget to look at the cervix.
- In women with PUL, close follow-up with appropriate counselling is important.
- When in doubt about the location of pregnancy, surveillance should be like that of patients with PUL.
- The need for serial BhCG and follow-up must be mentioned in the report.
- Discussing the ultrasound findings with the clinician may help in appropriate management.

Suggested Reading

Ameye L et al (2012) Clinically oriented three-step strategy for assessment of adnexal pathology. Ultrasound Obstet Gynecol 40:582–591. doi:10.1002/uog.11177

Baranowski E, Hogler W (2012) An unusual presentation of acquired hypothyroidism: the Van Wyk – Grumbach syndrome. Eur J Endocrinol 166:537–542

Bottomley C et al (2009) The optimal timing of an ultrasound scan to assess the location and viability of an early pregnancy. Hum Reprod 24(8):1811–1817

Condous G et al (2007) Prediction of ectopic pregnancy in women with a pregnancy of unknown location. Ultrasound Obstet Gynecol 29:680–687. doi:10.1002/uog.4015

Epstein E et al (2016) Subjective ultrasound assessment, the ADNEX model and ultrasound-guided tru-cut biopsy to differentiate disseminated primary ovarian cancer from metastatic non-ovarian cancer. Ultrasound Obstet Gynecol 47:110–116. doi:10.1002/uog.14892

Kaijser J et al (2013) Improving strategies for diagnosing ovarian cancer: a summary of the International Ovarian Tumor Analysis (IOTA) studies. Ultrasound Obstet Gynecol 41:9–20. doi:10.1002/uog.12323

Kirk E et al (2008) Why are some ectopic pregnancies characterized as pregnancies of unknown location at the initial transvaginal ultrasound examination? Acta Obstet Gynecol Scand 87:1150–1154. doi:10.1080/00016340802443822

Lin EP et al (2008) RadioGraphics: diagnostic clues to ectopic pregnancy. Radiographics 28(6):1661–1671

Malvasi A et al (2001) Reduction of complications during first trimester abortion with the use of sonography. Ultrasound Obstet Gynecol 18:P24. doi:10.1046/j.1469-0705.2001.abs26-25

Nunes N et al (2014) Use of IOTA simple rules for diagnosis of ovarian cancer: meta-analysis. Ultrasound Obstet Gynecol 44:503–514. doi:10.1002/uog.13437

Parsons AK, Sanders RC (2007) OP17.07: Menometrorrhagia due to impaired uterine drainage. Ultrasound Obstet Gynecol 30:514. doi:10.1002/uog.4585

Potter AW, Chandrasekhar CA (2008) US and CT evaluation of acute pelvic pain of gynecologic origin in nonpregnant premenopausal patients. Radiographics 28(6):1645–1659

Sagili H, Mohamed K (2008) Pregnancy of unknown location: an evidence-based approach to management. Obstet Gynaecol 10:224–230. doi:10.1576/toag.10.4.224.27438

Saksouk FA, Johnson Samuel C (2004) Recognition of the ovaries and ovarian origin of pelvic masses with CT. Radiographics 24(Spec Issue):S133–S146

Timmerman D et al (2008) Simple ultrasound-based rules for the diagnosis of ovarian cancer. Ultrasound Obstet Gynecol 31:681–690. doi:10.1002/uog.5365

Williams PL et al (2003) US of abnormal uterine bleeding. Radiographics 23(3):703–718

Index

M. Sibal, *Ultrasound in Gynecology*, DOI 10.1007/978-981-10-2714-7